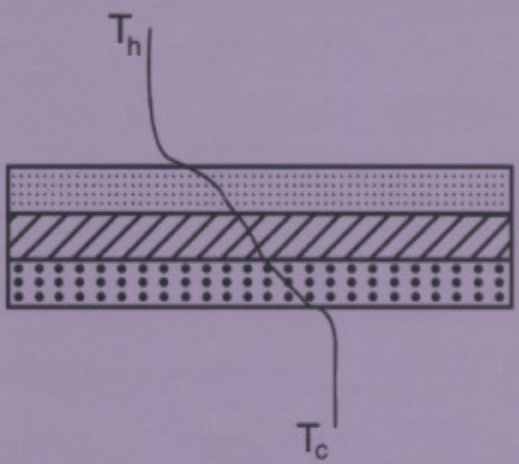
Copyrighted Material

HEAT EXCHANGER DESIGN HANDBOOK



T. KUPPAN

Copyrighted Material

HEAT EXCHANGER DESIGN HANDBOOK

MECHANICAL ENGINEERING

A Series of Textbooks and Reference Books

Founding Editor

L. L. Faulkner

Columbus Division, Battelle Memorial Institute
and Department of Mechanical Engineering
The Ohio State University
Columbus, Ohio

1. *Spring Designer's Handbook*, Harold Carlson
2. *Computer-Aided Graphics and Design*, Daniel L. Ryan
3. *Lubrication Fundamentals*, J. George Wills
4. *Solar Engineering for Domestic Buildings*, William A. Himmelman
5. *Applied Engineering Mechanics: Statics and Dynamics*, G. Boothroyd and C. Poli
6. *Centrifugal Pump Clinic*, Igor J. Karassik
7. *Computer-Aided Kinetics for Machine Design*, Daniel L. Ryan
8. *Plastics Products Design Handbook, Part A: Materials and Components; Part B: Processes and Design for Processes*, edited by Edward Miller
9. *Turbomachinery: Basic Theory and Applications*, Earl Logan, Jr.
10. *Vibrations of Shells and Plates*, Werner Soedel
11. *Flat and Corrugated Diaphragm Design Handbook*, Mario Di Giovanni
12. *Practical Stress Analysis in Engineering Design*, Alexander Blake
13. *An Introduction to the Design and Behavior of Bolted Joints*, John H. Bickford
14. *Optimal Engineering Design: Principles and Applications*, James N. Siddall
15. *Spring Manufacturing Handbook*, Harold Carlson
16. *Industrial Noise Control: Fundamentals and Applications*, edited by Lewis H. Bell
17. *Gears and Their Vibration: A Basic Approach to Understanding Gear Noise*, J. Derek Smith
18. *Chains for Power Transmission and Material Handling: Design and Applications Handbook*, American Chain Association
19. *Corrosion and Corrosion Protection Handbook*, edited by Philip A. Schweitzer
20. *Gear Drive Systems: Design and Application*, Peter Lynwander
21. *Controlling In-Plant Airborne Contaminants: Systems Design and Calculations*, John D. Constance
22. *CAD/CAM Systems Planning and Implementation*, Charles S. Knox
23. *Probabilistic Engineering Design: Principles and Applications*, James N. Siddall
24. *Traction Drives: Selection and Application*, Frederick W. Heilich III and Eugene E. Shube
25. *Finite Element Methods: An Introduction*, Ronald L. Huston and Chris E. Passerello
26. *Mechanical Fastening of Plastics: An Engineering Handbook*, Brayton Lincoln, Kenneth J. Gomes, and James F. Braden
27. *Lubrication in Practice: Second Edition*, edited by W. S. Robertson
28. *Principles of Automated Drafting*, Daniel L. Ryan
29. *Practical Seal Design*, edited by Leonard J. Martini
30. *Engineering Documentation for CAD/CAM Applications*, Charles S. Knox
31. *Design Dimensioning with Computer Graphics Applications*, Jerome C. Lange
32. *Mechanism Analysis: Simplified Graphical and Analytical Techniques*, Lyndon O. Barton
33. *CAD/CAM Systems: Justification, Implementation, Productivity Measurement*, Edward J. Preston, George W. Crawford, and Mark E. Coticchia
34. *Steam Plant Calculations Manual*, V. Ganapathy
35. *Design Assurance for Engineers and Managers*, John A. Burgess
36. *Heat Transfer Fluids and Systems for Process and Energy Applications*, Jasbir Singh

37. *Potential Flows: Computer Graphic Solutions,* Robert H. Kirchhoff
38. *Computer-Aided Graphics and Design: Second Edition,* Daniel L. Ryan
39. *Electronically Controlled Proportional Valves: Selection and Application,* Michael J. Tonyan, edited by Tobi Goldoftas
40. *Pressure Gauge Handbook,* AMETEK, U.S. Gauge Division, edited by Philip W. Harland
41. *Fabric Filtration for Combustion Sources: Fundamentals and Basic Technology,* R. P. Donovan
42. *Design of Mechanical Joints,* Alexander Blake
43. *CAD/CAM Dictionary,* Edward J. Preston, George W. Crawford, and Mark E. Coticchia
44. *Machinery Adhesives for Locking, Retaining, and Sealing,* Girard S. Haviland
45. *Couplings and Joints: Design, Selection, and Application,* Jon R. Mancuso
46. *Shaft Alignment Handbook,* John Piotrowski
47. *BASIC Programs for Steam Plant Engineers: Boilers, Combustion, Fluid Flow, and Heat Transfer,* V. Ganapathy
48. *Solving Mechanical Design Problems with Computer Graphics,* Jerome C. Lange
49. *Plastics Gearing: Selection and Application,* Clifford E. Adams
50. *Clutches and Brakes: Design and Selection,* William C. Orthwein
51. *Transducers in Mechanical and Electronic Design,* Harry L. Trietley
52. *Metallurgical Applications of Shock-Wave and High-Strain-Rate Phenomena,* edited by Lawrence E. Murr, Karl P. Staudhammer, and Marc A. Meyers
53. *Magnesium Products Design,* Robert S. Busk
54. *How to Integrate CAD/CAM Systems: Management and Technology,* William D. Engelke
55. *Cam Design and Manufacture: Second Edition; with cam design software for the IBM PC and compatibles, disk included,* Preben W. Jensen
56. *Solid-State AC Motor Controls: Selection and Application,* Sylvester Campbell
57. *Fundamentals of Robotics,* David D. Ardayfio
58. *Belt Selection and Application for Engineers,* edited by Wallace D. Erickson
59. *Developing Three-Dimensional CAD Software with the IBM PC,* C. Stan Wei
60. *Organizing Data for CIM Applications,* Charles S. Knox, with contributions by Thomas C. Boos, Ross S. Culverhouse, and Paul F. Muchnicki
61. *Computer-Aided Simulation in Railway Dynamics,* by Rao V. Dukkipati and Joseph R. Amyot
62. *Fiber-Reinforced Composites: Materials, Manufacturing, and Design,* P. K. Mallick
63. *Photoelectric Sensors and Controls: Selection and Application,* Scott M. Juds
64. *Finite Element Analysis with Personal Computers,* Edward R. Champion, Jr., and J. Michael Ensminger
65. *Ultrasonics: Fundamentals, Technology, Applications: Second Edition, Revised and Expanded,* Dale Ensminger
66. *Applied Finite Element Modeling: Practical Problem Solving for Engineers,* Jeffrey M. Steele
67. *Measurement and Instrumentation in Engineering: Principles and Basic Laboratory Experiments,* Francis S. Tse and Ivan E. Morse
68. *Centrifugal Pump Clinic: Second Edition, Revised and Expanded,* Igor J. Karassik
69. *Practical Stress Analysis in Engineering Design: Second Edition, Revised and Expanded,* Alexander Blake
70. *An Introduction to the Design and Behavior of Bolted Joints: Second Edition, Revised and Expanded,* John H. Bickford
71. *High Vacuum Technology: A Practical Guide,* Marsbed H. Hablanian
72. *Pressure Sensors: Selection and Application,* Duane Tandeske
73. *Zinc Handbook: Properties, Processing, and Use in Design,* Frank Porter
74. *Thermal Fatigue of Metals,* Andrzej Weronski and Tadeusz Hejwowski
75. *Classical and Modern Mechanisms for Engineers and Inventors,* Preben W. Jensen
76. *Handbook of Electronic Package Design,* edited by Michael Pecht
77. *Shock-Wave and High-Strain-Rate Phenomena in Materials,* edited by Marc A. Meyers, Lawrence E. Murr, and Karl P. Staudhammer
78. *Industrial Refrigeration: Principles, Design and Applications,* P. C. Koelet
79. *Applied Combustion,* Eugene L. Keating
80. *Engine Oils and Automotive Lubrication,* edited by Wilfried J. Bartz

81. *Mechanism Analysis: Simplified and Graphical Techniques, Second Edition, Revised and Expanded*, Lyndon O. Barton
82. *Fundamental Fluid Mechanics for the Practicing Engineer*, James W. Murdock
83. *Fiber-Reinforced Composites: Materials, Manufacturing, and Design, Second Edition, Revised and Expanded*, P. K. Mallick
84. *Numerical Methods for Engineering Applications*, Edward R. Champion, Jr.
85. *Turbomachinery: Basic Theory and Applications, Second Edition, Revised and Expanded*, Earl Logan, Jr.
86. *Vibrations of Shells and Plates: Second Edition, Revised and Expanded*, Werner Soedel
87. *Steam Plant Calculations Manual: Second Edition, Revised and Expanded*, V. Ganapathy
88. *Industrial Noise Control: Fundamentals and Applications, Second Edition, Revised and Expanded*, Lewis H. Bell and Douglas H. Bell
89. *Finite Elements: Their Design and Performance*, Richard H. MacNeal
90. *Mechanical Properties of Polymers and Composites: Second Edition, Revised and Expanded*, Lawrence E. Nielsen and Robert F. Landel
91. *Mechanical Wear Prediction and Prevention*, Raymond G. Bayer
92. *Mechanical Power Transmission Components*, edited by David W. South and Jon R. Mancuso
93. *Handbook of Turbomachinery*, edited by Earl Logan, Jr.
94. *Engineering Documentation Control Practices and Procedures*, Ray E. Monahan
95. *Refractory Linings: Thermomechanical Design and Applications*, Charles A. Schacht
96. *Geometric Dimensioning and Tolerancing: Applications and Techniques for Use in Design, Manufacturing, and Inspection*, James D. Meadows
97. *An Introduction to the Design and Behavior of Bolted Joints: Third Edition, Revised and Expanded*, John H. Bickford
98. *Shaft Alignment Handbook: Second Edition, Revised and Expanded*, John Piotrowski
99. *Computer-Aided Design of Polymer-Matrix Composite Structures*, edited by S. V. Hoa
100. *Friction Science and Technology*, Peter J. Blau
101. *Introduction to Plastics and Composites: Mechanical Properties and Engineering Applications*, Edward Miller
102. *Practical Fracture Mechanics in Design*, Alexander Blake
103. *Pump Characteristics and Applications*, Michael W. Volk
104. *Optical Principles and Technology for Engineers*, James E. Stewart
105. *Optimizing the Shape of Mechanical Elements and Structures*, A. A. Seireg and Jorge Rodriguez
106. *Kinematics and Dynamics of Machinery*, Vladimír Stejskal and Michael Valášek
107. *Shaft Seals for Dynamic Applications*, Les Horve
108. *Reliability-Based Mechanical Design*, edited by Thomas A. Cruse
109. *Mechanical Fastening, Joining, and Assembly*, James A. Speck
110. *Turbomachinery Fluid Dynamics and Heat Transfer*, edited by Chunill Hah
111. *High-Vacuum Technology: A Practical Guide, Second Edition, Revised and Expanded*, Marsbed H. Hablanian
112. *Geometric Dimensioning and Tolerancing: Workbook and Answerbook*, James D. Meadows
113. *Handbook of Materials Selection for Engineering Applications*, edited by G. T. Murray
114. *Handbook of Thermoplastic Piping System Design*, Thomas Sixsmith and Reinhard Hanselka
115. *Practical Guide to Finite Elements: A Solid Mechanics Approach*, Steven M. Lepi
116. *Applied Computational Fluid Dynamics*, edited by Vijay K. Garg
117. *Fluid Sealing Technology*, Heinz K. Muller and Bernard S. Nau
118. *Friction and Lubrication in Mechanical Design*, A. A. Seireg
119. *Influence Functions and Matrices*, Yuri A. Melnikov
120. *Mechanical Analysis of Electronic Packaging Systems*, Stephen A. McKeown
121. *Couplings and Joints: Design, Selection, and Application, Second Edition, Revised and Expanded*, Jon R. Mancuso
122. *Thermodynamics: Processes and Applications*, Earl Logan, Jr.
123. *Gear Noise and Vibration*, J. Derek Smith
124. *Practical Fluid Mechanics for Engineering Applications*, John J. Bloomer

125. *Handbook of Hydraulic Fluid Technology*, edited by George E. Totten
126. *Heat Exchanger Design Handbook*, T. Kuppan

Additional Volumes in Preparation

Probability Applications in Mechanical Design, Franklin E. Fisher and Joy R. Fisher

Rotating Machinery Vibration: Problem Analysis and Troubleshooting, Maurice L. Adams

Handbook of Machinery Dynamics, Lynn Faulkner and Earl Logan Jr.

Designing for Product Sound Quality, Richard H. Lyon

Mechanical Engineering Software

Spring Design with an IBM PC, Al Dietrich

Mechanical Design Failure Analysis: With Failure Analysis System Software for the IBM PC, David G. Ullman

This page intentionally left blank

HEAT EXCHANGER DESIGN HANDBOOK

T. KUPPAN
Southern Railway
Madras, India



MARCEL DEKKER, INC. NEW YORK · BASEL

ISBN: 0-8247-9787-6

This book is printed on acid-free paper.

Headquarters
Marcel Dekker, Inc.
270 Madison Avenue, New York, NY 10016
tel: 212-696-9000; fax: 212-685-4540

Eastern Hemisphere Distribution
Marcel Dekker AG
Hutgasse 4, Postfach 812, CH-4001 Basel, Switzerland
tel: 41-61-261-8482; fax: 41-61-261-8896

World Wide Web
http://www.dekker.com

The publisher offers discounts on this book when ordered in bulk quantities. For more information, write to Special Sales/Professional Marketing at the headquarters address above.

Copyright © 2000 by Marcel Dekker, Inc. All Rights Reserved.

Neither this book nor any part may be reproduced or transmitted in any form or by any means, electronic or mechanical, including photocopying, microfilming, and recording, or by any information storage and retrieval system, without permission in writing from the publisher.

Current printing (last digit):
10 9 8 7 6 5 4 3 2 1

PRINTED IN THE UNITED STATES OF AMERICA

To my parents
Thulukkanam
Senthamarai

To my mentor
Dr. Ramesh K. Shah

This page intentionally left blank

Preface

A heat exchanger is a heat transfer device that exchanges heat between two or more process fluids. Heat exchangers have widespread industrial and domestic applications. Extensive technical literature is available on heat exchangers, but it is widely scattered throughout the technical journals, industrial bulletins, codes and standards, etc. This book is intended to consolidate into one volume the basic concepts of design and theoretical relationships useful in the design of heat exchangers, material selection, fabrication, and industrial practices.

Thermal design information such as heat transfer and pressure drop data, thermal design methods, and flow-induced vibration for exchangers involving single-phase flow duties are discussed. Other books and handbooks are available that deal with the design of vaporizers and condensers in which there is two-phase flow.

The book is an excellent resource for mechanical, chemical, and petrochemical engineers; process equipment and pressure vessel designers; and upper-level undergraduate and graduate students in these disciplines.

The book is divided into 15 chapters covering most of the information required for selection, design, material selection, fabrication, inspection, and operation of heat exchangers.

Chapter 1 discusses the classification and selection of heat exchangers for the intended application. In addition to the principal types used in industry, such as compact, shell and tube exchangers, regenerators, and plate heat exchangers, other specialized types such as double pipe, heat pipe, spiral, lamella, jacketing, glass, graphite, and Teflon heat exchangers are also discussed.

To successfully carry out the thermal design of heat exchangers, knowledge of thermohydraulic fundamentals is necessary. The discussion of thermal resistance variables, overall conductance equations, temperature distribution, mean temperature difference, temperature correction factors, number of transfer units, and effectiveness formulas for various flow arrangements, pass arrangements, and compact and shell heat exchangers with thermal relation charts is presented in Chapter 2.

Heat exchanger design methodology, heat exchanger design featuring rating and sizing

problems, computer-aided thermal design, pressure drop analysis, temperature-dependent fluid properties correction, performance failures, flow maldistribution, and uncertainties involved in thermal design are covered in Chapter 3.

Compact heat exchangers are used in a wide variety of applications. The need for lightweight, space-saving, and economical heat exchangers has driven the development of compact surfaces. Basic construction types, surface geometrical parameters, j and f factors, fin efficiency, rating, and sizing are discussed in Chapter 4. Air coolers that use atmospheric air as the coolant are widely used in industry. They are also discussed in detail in Chapter 4.

Shell and tube sheet exchangers are the workhorses of process industries. The major construction features, thermal design, sizing, and rating are shown in detail in Chapter 5. Thermal design procedures for disk and doughnut and rod baffle heat exchangers are also discussed.

The drastic escalation of energy prices has made waste heat recovery more attractive over the past two decades. Recovery of waste heat from flue gas by means of heat exchangers can improve overall plant efficiency, serves to reduce national energy needs, and conserves fossil fuels. The objective of Chapter 6 is to acquaint the reader with various types of regenerators and with their construction details, their applications other than for heat recovery, and their thermal, and mechanical design. Additionally, some industrial regenerators for waste heat recovery are discussed.

In the 1930s, plate heat exchangers (PHEs) were introduced to meet the hygienic demands of the dairy industry. Today PHEs are universally used in many fields.They are used as an alternative to tube and shell exchangers for low- and medium-pressure liquid–liquid heat transfer applications. Design of PHEs, recent developments in their construction, and spiral plate heat exchangers are covered in Chapter 7.

In recent years, increasing energy and material costs have provided significant incentives for the development of various augmented heat transfer surfaces and devices. Various forms of enhancement devices are discussed in Chapter 8.

Most heat transfer processes result in the deposition of undesirable materials, commonly referred to as fouling. Fouling introduces perhaps the major uncertainty into the design and operation of heat exchangers, very often leading to extra capital and running costs, and reduces thermal performance. This necessitates a thorough understanding of the fouling phenomenon. Fouling mechanisms, prevention, and control are reviewed in Chapter 9.

One of the major considerations in the design of shell and tube heat exchangers is that it is free from flow-induced vibration problems. Flow-induced vibration can cause potential tube failures. Chapter 10 presents a review of flow-induced vibration mechanisms, their evaluation, and vibration prevention guidelines.

Chapter 11, on the mechanical design of shell and tube heat exchangers, deals with minimum thickness calculation procedures and stress analysis of various pressure parts such as tubesheets, heads, end closures, flanges, expansion joints, and nonpressure parts. Tubesheet design, as per ASME code, TEMA, BS 5500, and CODAP, is explained in detail. Important details of heat exchanger and pressure vessel construction codes and standards are also covered in detail.

Metallic corrosion is a process that causes enormous material losses annually. Thus it is necessary to examine thoroughly the material and environmental interactions that adversely affect the performance and life of equipment. Chapter 12 discusses corrosion principles, various forms of corrosion and their evaluation, corrosion control and prevention, and monitoring. With few exceptions, water is the preferred industrial medium for removing heat from process fluids. An understanding of cooling-water corrosion is important for heat exchanger designers. Most problems associated with cooling water are identified, and their control and prevention are also discussed.

Proper material selection is important for desired thermal performance, strength considerations, safe operation, and achieving the expected life and economy. Thus it is necessary to have a thorough knowledge of various heat exchanger materials and their fabricability. Chapter 13 discusses the selection criteria for a wide spectrum of heat exchanger materials and their fabrication by welding.

Quality of goods and equipment manufactured in the world market has become a matter of concern in recent years. For heat exchangers and pressure vessels, the overriding goal is to avoid the consequences of failure, which can be catastrophic in human, monetary, and environmental terms. Chapter 14 discusses various aspects of quality control and quality assurance, inspection, and nondestructive testing methods (NDT) and recent trends in NDT techniques.

After thermal design, the heat exchanger unit is fabricated by shop floor operations. Beyond the theoretical background, a knowledge of shop floor practices is required for a manufacturer to efficiently achieve the desired quality and performance. Chapter 15 discusses various shop floor practices for shell and tube heat exchangers, and brazing and soldering of compact heat exchangers.

The preparation of this book was facilitated by the great volume of existing literature contributed by many workers and scholars in this field. I have tried to acknowledge all the sources and have sought the necessary permissions. If omissions have been made, I offer my sincere apologies. Most materials manufacturers and research organizations responded to my inquiries and supplied substantial useful data and informative material. They are all acknowledged either directly or through references. Last, I make a special mention of my mentor and guide Dr. R. K. Shah, Vice President, ASME Board on Communications, Delphi Harisson Thermal Systems, Lockport, New York, who helped me throughout the preparation of the book and provided the basic literature required for the thermal design, flow-induced vibration, and thermal relations formulas for all types of arrangements.

During the preparation of this book, my parents and family were denied much of my time and interest that they rightfully deserve. I apologize to them.

T. Kuppan

This page intentionally left blank

Contents

Preface v

1. Heat Exchangers—Introduction, Classification, and Selection 1
2. Heat Exchanger Thermohydraulic Fundamentals 27
3. Heat Exchanger Thermal Design 129
4. Compact Heat Exchangers 159
5. Shell and Tube Heat Exchanger Design 229
6. Regenerators 303
7. Plate Heat Exchangers and Spiral Plate Heat Exchangers 347
8. Heat-Transfer Augmentation 373
9. Fouling 393
10. Flow-Induced Vibration of Shell and Tube Heat Exchangers 423
11. Mechanical Design of Shell and Tube Heat Exchangers 485
12. Corrosion 579

13. Material Selection and Fabrication 667

14. Quality Control and Quality Assurance, Inspection, and Nondestructive Testing 863

15. Heat Exchanger Fabrication 955

References *1035*

Index *1093*

1
Heat Exchangers—Introduction, Classification, and Selection

1 INTRODUCTION

A heat exchanger is a heat-transfer devise that is used for transfer of internal thermal energy between two or more fluids available at different temperatures. In most heat exchangers, the fluids are separated by a heat-transfer surface, and ideally they do not mix. Heat exchangers are used in the process, power, petroleum, transportation, air conditioning, refrigeration, cryogenic, heat recovery, alternate fuels, and other industries. Common examples of heat exchangers familiar to us in day-to-day use are automobile radiators, condensers, evaporators, air preheaters, and oil coolers. Heat exchangers could be classified in many different ways.

2 CONSTRUCTION OF HEAT EXCHANGERS

A heat exchanger consists of heat-exchanging elements such as a core or matrix containing the heat-transfer surface, and fluid distribution elements such as headers or tanks, inlet and outlet nozzles or pipes, etc. Usually, there are no moving parts in the heat exchanger; however, there are exceptions, such as a rotary regenerator in which the matrix is driven to rotate at some design speed. The heat-transfer surface is in direct contact with fluids through which heat is transferred by conduction. The portion of the surface that separates the fluids is referred to as the primary or direct contact surface. To increase heat-transfer area, secondary surfaces known as fins may be attached to the primary surface.

3 CLASSIFICATION OF HEAT EXCHANGERS

In general, industrial heat exchangers have been classified according to (1) construction, (2) transfer processes, (3) degrees of surface compactness, (4) flow arrangements, (5) pass arrangements, (6) phase of the process fluids, and (7) heat-transfer mechanisms. These classifications (shown in Fig. 1) are briefly discussed here. For more details on heat exchanger classification

and construction refer to Shah [1,2], Gupta [3], and Graham Walker [4]. For classification and systematic procedure for selection of heat exchangers, refer to Larowski et al. [5a,5b].

3.1 Classification According to Construction

According to constructional details, heat exchangers are classified as [1]:

1. Tubular heat exchangers—double pipe, shell and tube, coiled tube
2. Plate heat exchangers—gasketed, spiral, plate coil, lamella
3. Extended surface heat exchangers—tube-fin, plate-fin
4. Regenerators—fixed matrix, rotary

Tubular Heat Exchanger

Double Pipe Exchangers. A double pipe heat exchanger has two concentric pipes, usually in the form of a U-bend design as shown in Fig. 2. The flow arrangement is pure countercurrent. A number of double pipe heat exchangers can be connected in series or parallel as necessary. Their usual application is for small duties requiring, typically, less than 300 ft^2 and they are suitable for high pressures and temperatures, and thermally long duties [5]. This has the advantages of flexibility since units can be added or removed as required, and the design is easy to service and requires low inventory of spares because of its standardization. Either longitudinal fins or circumferential fins within the annulus on the inner pipe wall are required to enhance the heat transfer from the inner pipe fluid to the annulus fluid. Design pressures and temperatures are broadly similar to shell and tube heat exchangers. The design is straightforward, and carried out using the method of Kern [6], or proprietary programs.

Shell and Tube Heat Exchanger. In process industries, shell and tube exchangers are used in great numbers, far more than any other type of exchanger. More than 90% of heat exchangers used in industry are of the shell and tube type [7]. The shell and tube heat exchangers are the "work horses" of industrial process heat transfer [8]. They are the first choice because of well-established procedures for design and manufacture from a wide variety of materials, many years of satisfactory service, and availability of codes and standards for design and fabrication. They are produced in the widest variety of sizes and styles. There is virtually no limit on the operating temperature and pressure.

Coiled Tube Heat Exchanger.

Coiled Tube Heat Exchanger Used for Liquefaction Systems. One of the three classical heat exchangers used today for large-scale liquefaction systems is the coiled tube heat exchanger (CTHE). The construction details are explained in Refs. 5 and 9. Construction of these heat exchangers involves winding a large number of small-bore ductile tubes in helix fashion around a central core tube, with each exchanger containing many layers of tubes along both the principal and radial axes. Tubes in individual layers or groups of layers may be brought together into one or more tube plates through which different fluids may be passed in counterflow to the single shellside fluid.

The high-pressure stream flows through the small-diameter tubes, while the low-pressure return stream flows across the outside of the small-diameter tubes in the annular space between the inner central core tube and the outer shell. Pressure drops in the coiled tubes are equalized for each high-pressure stream by using tubes of equal length and varying the spacing of these in the different layers. Because of small-bore tubes on both sides, CTHEs do not permit mechanical cleaning and therefore are used to handle clean, solid-free fluids or fluids whose fouling deposits can be cleaned by chemicals. Materials are usually aluminum alloys for cryogenics, and stainless steels for high-temperature applications.

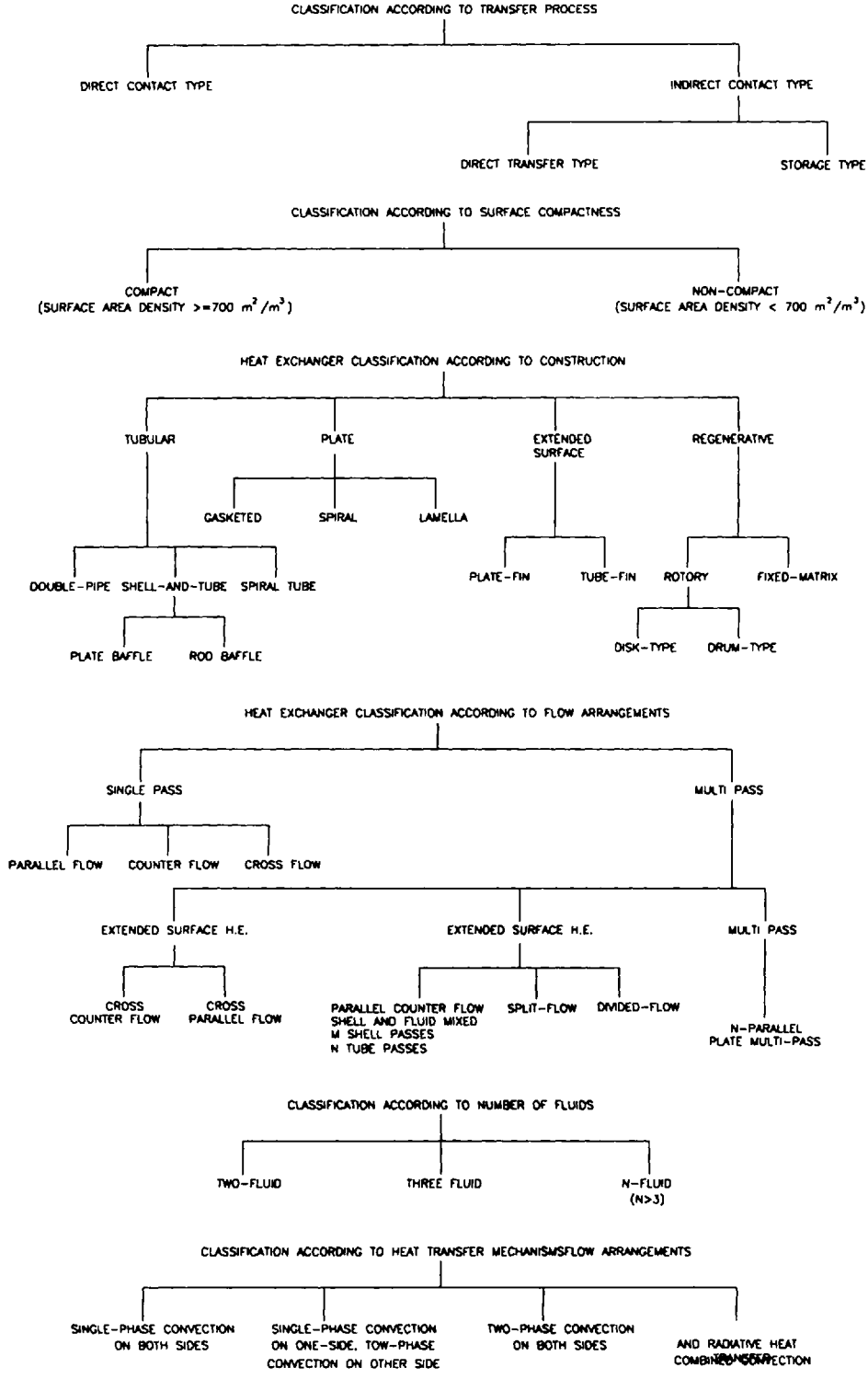


Figure 1 Classification of heat exchangers [1].

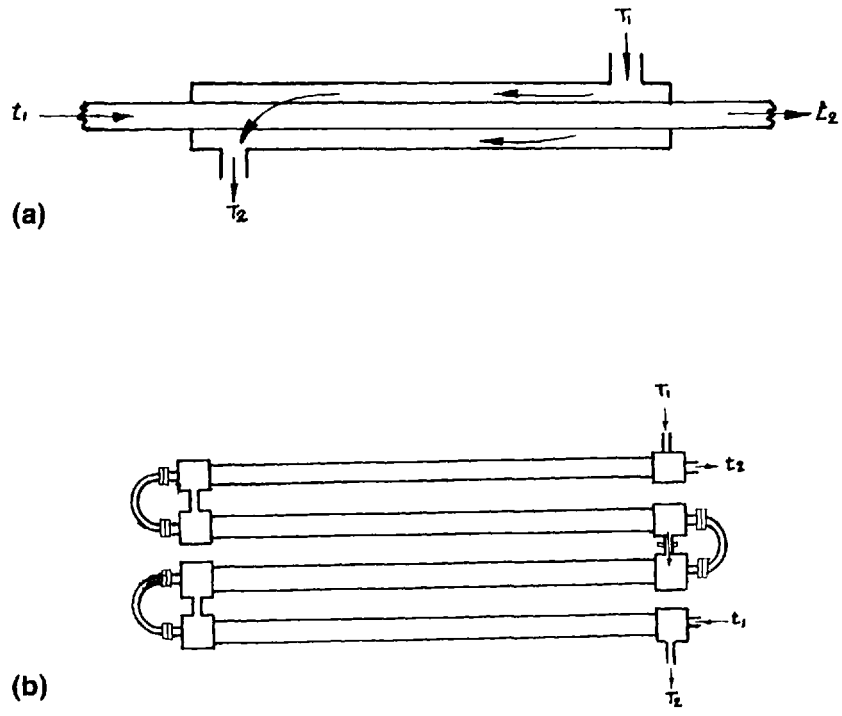


Figure 2 Double pipe heat exchanger. (a) Single pass with counterflow; and (b) multipass with counterflow [6].

The coiled tube heat exchanger offers unique advantages, especially when dealing with low-temperature applications for the following cases [9]:

1. Simultaneous heat transfer between more than two streams is desired.
2. A large number of heat-transfer units is required.
3. High operating pressures are involved.

The coiled tube heat exchanger is not cheap because of the material costs, high labor input in winding the tubes, and the central mandrel, which is not useful for heat transfer but increases the shell diameter [5].

Glass Coil Heat Exchangers. Glass coil exchangers have a coil fused to the shell to make a one-piece unit. This prohibits leakage between the coil and shell-side fluids [10]. A glass coil heat exchanger is shown schematically in Fig. 3. More details on glass heat exchangers are furnished in Chapter 13.

Plate Heat Exchangers

Plate heat exchangers are less widely used than tubular heat exchangers but offer certain important advantages. Plate heat exchangers can be classified in three principal groups:

1. Plate and frame or gasketed plate heat exchangers used as an alternative to tube and shell exchangers for low- and medium-pressure liquid–liquid heat-transfer applications.
2. Spiral heat exchanger used as an alternative to shell and tube exchangers where low maintenance is required, particularly with fluids tending to sludge or containing slurries or solids in suspension.

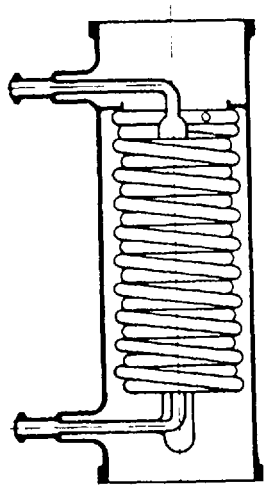


Figure 3 Glass coil heat exchanger [10].

3. Plate coil or panel heat exchangers made from embossed plates to form a conduit or coil for liquids coupled with fins.

Plate Heat Exchangers. A plate heat exchanger (PHE) essentially consists of a number of corrugated metal plates in mutual contact, each plate having four apertures serving as inlet and outlet ports, and seals designed to direct the fluids in alternate flow passages. The plates are clamped together in a frame that includes connections for the fluids. Since each plate is generally provided with peripheral gaskets to provide sealing arrangements, the plate heat exchangers are called gasketed plate heat exchangers. A plate heat exchanger is shown in Fig. 4. The PHE is covered in detail in Chapter 7, Plate Heat Exchangers.

Spiral Plate Heat Exchanger. Spiral plate heat exchangers (SPHEs) have been used since the 1930s, when they were originally developed in Sweden for heat recovery in pulp mills. Spiral plate heat exchangers are classified as a type of welded plate heat exchanger. An SPHE is fabricated by rolling a pair of relatively long strips of plate around a split mandrel to form a pair of spiral passages. Channel spacing is maintained uniformly along the length of the spiral passages by means of spacer studs welded to the plate strips prior to rolling. An SPHE is shown in Fig. 5. For most applications, both flow channels are closed by alternate channels welded at both sides of the spiral plate. In some services, one of the channels is left open, whereas the other closed at both sides of the plate. These two types of construction prevent the fluids from mixing.

The SPHE is intended especially for these applications [5]:

1. To handle slurries and liquids with suspended fibers, and mineral ore treatment where the solid content is up to 50%.
2. The SPHE is the first choice for extremely high viscosities, say up to 500,000 cp, especially in cooling duties, because of maldistribution, and hence partial blockage by local overcooling is less likely to occur in a single-channel exchanger.
3. SPHEs are finding applications in reboiling, condensing, heating or cooling of viscous fluids, slurries, and sludge [11].

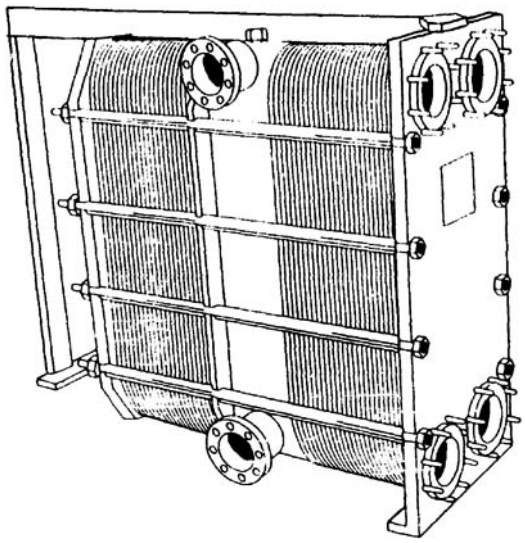


Figure 4 Plate heat exchanger. [From *Hydrocarbon Processing*, p. 123, (1996).]

More details on the SPHE are furnished in Chapter 7, Plate Heat Exchangers.

Panel Coil Heat Exchanger. These exchangers are called panel coils, plate coils, or embossed-panel or jacketing. The panel coil serves as a heat sink or a heat source, depending upon whether the fluid within the coil is being cooled or heated. Panel coil heat exchangers are relatively inexpensive and can be made into any desired shapes and thickness for heat sinks and heat sources under varied operating conditions. Hence, they have been used in many industrial applications such as cryogenics, chemicals, fibers, food, paints, pharmaceuticals, and solar absorbers.

Construction Details of a Panel Coil. Two types of panel coil designs are shown in Fig. 6. The panel coil is used in such industries as plating, metal finishing, chemical, textile, brewery, pharmaceutical, dairy, pulp and paper, food, nuclear, beverage, waste treatment, and many others. Construction details of panel coils are discussed next. The text has been provided by M/s Paul-Muller Company, Springfield, MO.

1. Single embossed surface. The single embossed heat-transfer surface (Fig. 7a) is an economical type to utilize for interior tank walls, conveyor beds, and when a flat side is required. The single embossed design uses two sheets of material of different thickness and is available in stainless steel, other alloys, and carbon steel, and in many material gauges and working pressures.
2. Double embossed surface. Inflated on both sides using two sheets of material and the same thickness, the double embossed construction (Fig. 7b) maximizes the heating and cooling process by utilizing both sides of the heat-transfer plate. The double embossed design is commonly used in immersion applications, and they are available in stainless steel, other alloys, and carbon steel, and in many material gauges and working pressures.
3. Dimpled surface. Dimpled on one side surface is shown in Fig. 7c. This surface is machine punched and swaged, prior to welding, to increase the flow area in the passages. It is available in stainless steel, other alloys, and carbon steel, in many material gauges and working pressures, and is available in both MIG plug welded and resistance spot welded forms.

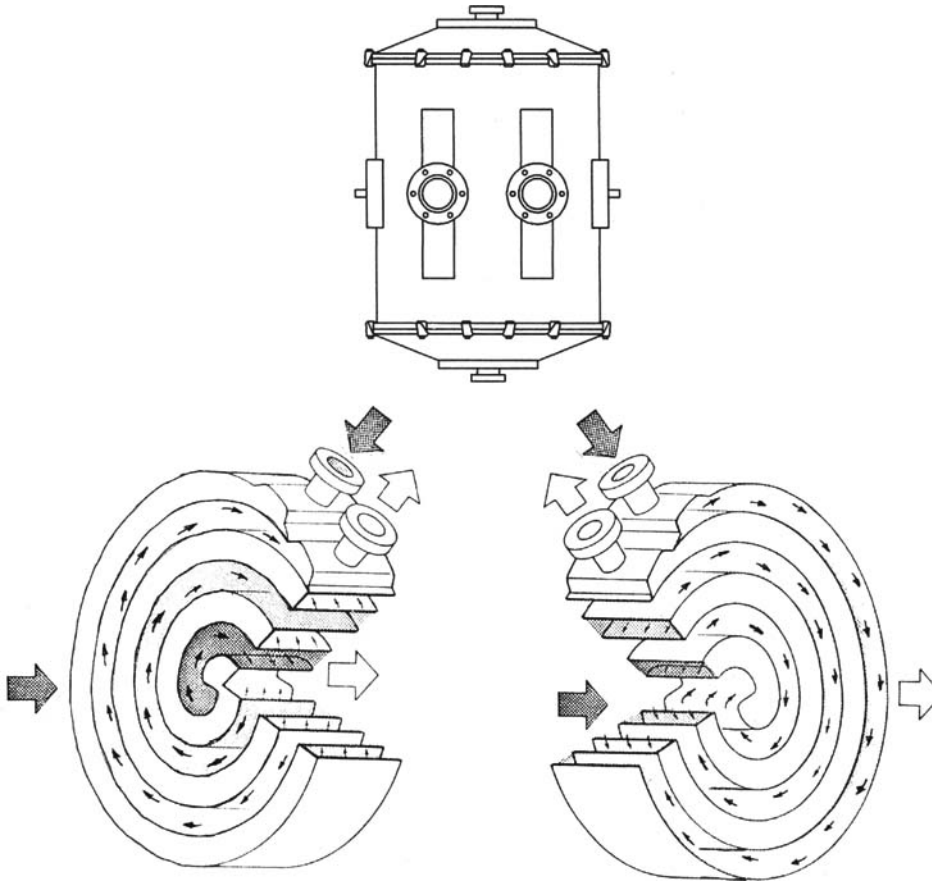


Figure 5 Alfa-Laval spiral plate heat exchanger.

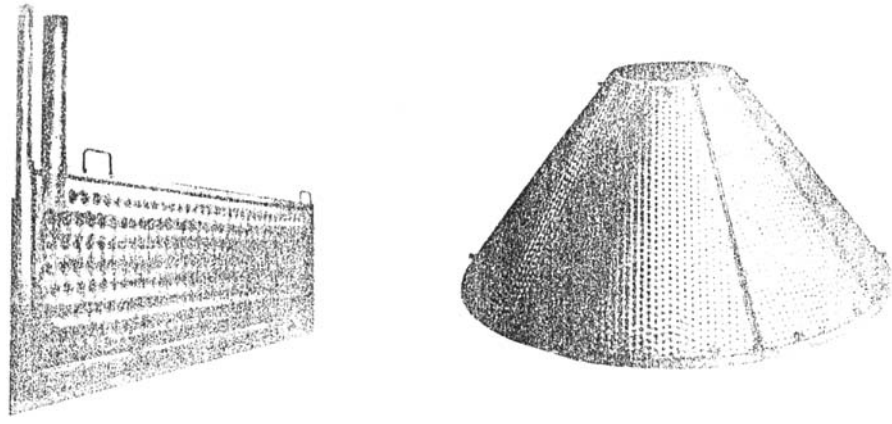


Figure 6 Panel coil heat exchanger.

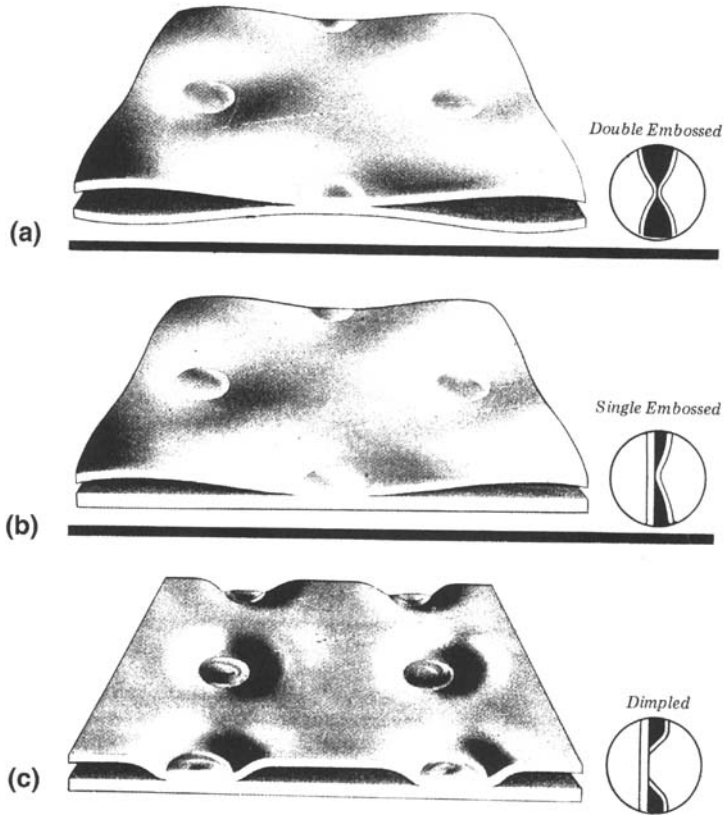


Figure 7 Embossing pattern of Paul-Muller panel coils. (a) double embossed surface; (b) single embossed surface; and (c) dimpled surface.

Methods of Manufacture of Panel Coils. Basically, three different methods have been employed to manufacture the panel coils: (1) They are usually welded by the resistance spot welding process (RSW) and/or the resistance seam welding process (RSEW). An alternate method now available offers the ability to resistance spot weld the dimpled jacket style panel coil with a perimeter weldment made with the GMAW process (Fig. 8). Other methods are (2) the die-stamping process and (3) the roll-bond process. In the die-stamping process, flow channels are die stamped on either one or two metal sheets. When one sheet is embossed and joined to a flat (unembossed sheet), it forms a single-sided embossed panel coil. When both sheets are stamped, it forms a double-sided embossed panel coil.

Types of Jackets. Jacketing of process vessels is usually accomplished by using one of the three main available types (Fig. 9): conventional jackets, dimple jackets, and half-pipe coil jackets [12].



Figure 8 Gas metal arc welding (MIG) on a Paul-Muller dimpled jacket style template.

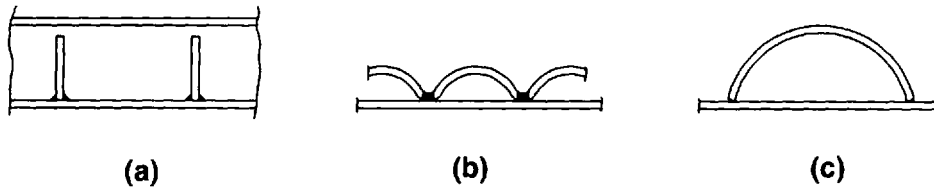


Figure 9 Jacketing construction details. (a) Conventional; (b) dimple; and (c) half-pipe [12].

Advantages of Panel Coils. Panel coils provide the optimum method of heating and cooling process vessels in terms of control, efficiency, and product quality. Using a panel as a means of heat transfer offers many advantages [12]:

All liquids can be handled, as well as steam and other high-temperature vapors.
Circulation, temperature, and velocity of heat transfer media can be accurately controlled.
Panels may often be fabricated from a much less expensive metal than the vessel itself.
Contamination, cleaning, and maintenance problems are eliminated.
Maximum efficiency, economy, and flexibility are achieved.
In designing reactors for specific process, this variety gives the chemical engineer a great deal of flexibility in the choice of heat-transfer medium.

Lamella Heat Exchanger. The lamella is a form of welded heat exchanger that combines the construction of a plate heat exchanger with that of a shell and tube exchanger. In this design, tubes are replaced by pairs of thin flat parallel metal plates, which are edge welded to provide long narrow channels, and banks of these elements of varying width are packed together to form a circular bundle and fitted within a shell. The cross section of a lamella heat exchanger is shown schematically in Fig. 10. With this design, the flow area on the shellside is a minimum

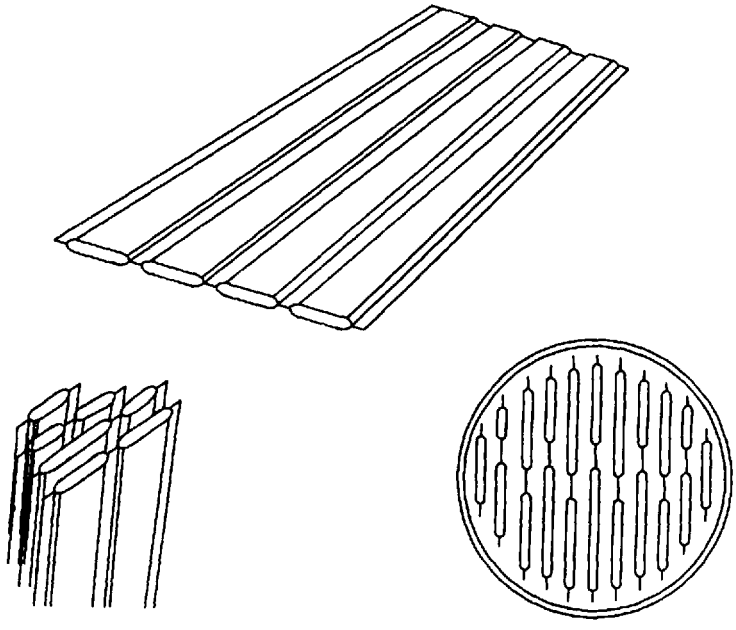


Figure 10 Cross section of an Alfa-Laval lamella heat exchanger.

and similar in magnitude to that of the inside of the bank of elements; due to this, the velocities of the two liquid media are comparable [13]. The flow is essentially longitudinal countercurrent "tubeside" flow of both tube and shell fluids [4]. Due to this, the velocities of the two liquid media are comparable. One end of the element pack is fixed and the other is floating to allow for thermal expansion and contraction. The connections fitted at either end of the shell, as in the normal shell and tube design, allow the bank of elements to be withdrawn, making the outside surface accessible.

Lamella heat exchangers can be fabricated from carbon steel, stainless steel, titanium, Incolly, and Hastelloy. They can handle most fluids, with large volume ratios between fluids. The floating nature of the bundle usually limits the working pressure to 300 psi. Lamella heat exchangers are generally less versatile than either PHEs or shell and tube exchangers but are cheaper than the latter for a given duty [5]. Design is usually left to the vendors.

Extended Surface Exchangers

In a heat exchanger with gases or some liquids, if the heat-transfer coefficient is quite low, a large heat-transfer surface area is required to increase the heat-transfer rate. This requirement is served by fins attached to the primary surface. Tube-fin and plate-fin geometries (Fig. 11) are the most common examples for extended surface heat exchanger. Their design is covered in Chapter 4, in the section on compact heat exchanger design.

Regenerative Heat Exchangers

Regeneration is an old technology dating back to the first open hearths and blast furnace stoves. Manufacturing and process industries such as glass, cement, and primary and secondary metals account for a significant fraction of all energy consumed. Much of this energy is discarded in the form of high-temperature exhaust gas. Recovery of waste heat from the exhaust gas by means of heat exchangers known as regenerators can improve the overall plant efficiency.

Types of Regenerators. Regenerators are generally classified as fixed-matrix and rotary regenerators. Further classifications of fixed and rotary regenerators are shown in Fig. 12. In the former the regeneration is achieved with periodic and alternate blowing of hot and the cold stream through a fixed matrix. During the hot flow period, the matrix receives thermal energy from the hot gas and transfers it to the cold stream during the cold stream flow. In the latter, the matrix revolves slowly with respect to two fluid streams. The rotary regenerator is commonly employed in gas turbine power plants where the waste heat in the hot exhaust gases is

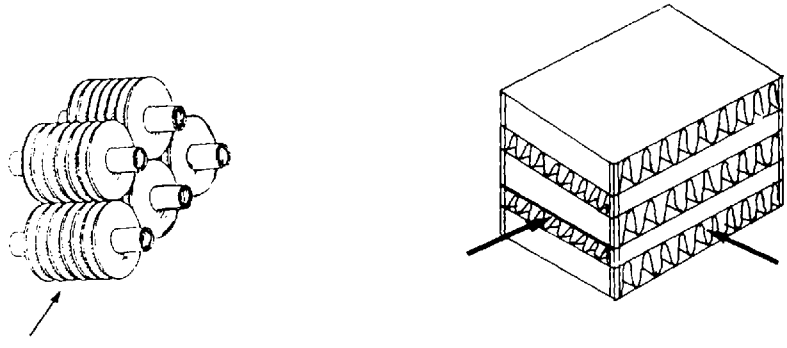


Figure 11 Extended surface heat exchanger. (a) Tube-fin; (b) plate-fin.

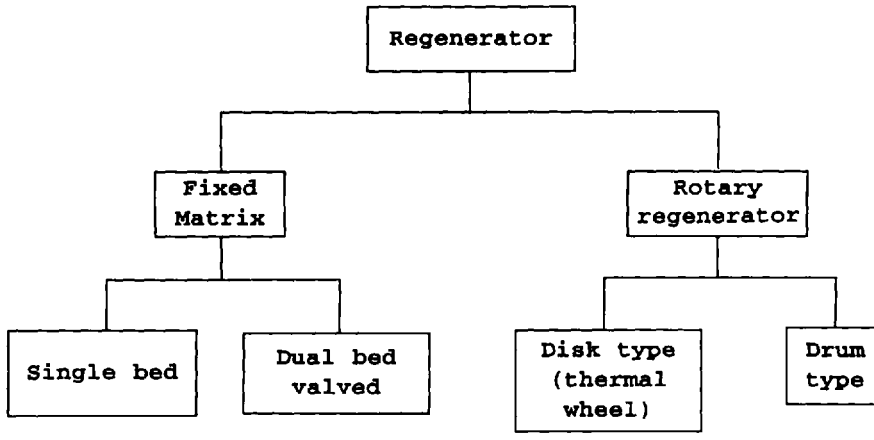


Figure 12 Classification of regenerators.

utilized for raising the temperature of compressed air before it is supplied to the combustion chamber. A rotary regenerator is shown in Fig. 13 [14] and one type of rotary regenerator is shown in Fig. 14. Rotary regenerators fall in the category of compact heat exchangers since the heat-transfer surface area to regenerator volume ratio is very high.

3.2 Classification According to Transfer Process

These classifications are:

1. Indirect contact type—direct transfer type, storage type, fluidized bed.
2. Direct contact type—cooling towers.

Indirect Contact Heat Exchangers

In an indirect contact type heat exchanger, the fluid streams remain separate, and the heat transfer takes place continuously through a dividing impervious wall. This type of heat exchanger can be further classified into the direct transfer type, storage type, and fluidized bed exchangers. Direct transfer type is dealt with next whereas the storage type and the fluidized bed type are discussed in Chapter 6, Regenerators.

Direct Transfer Type Exchangers

In this type, there is a continuous flow of the heat from the hot fluid to the cold fluid through a separating wall. There is no direct mixing of the fluids because each fluid flows in separate fluid passages. There are no moving parts. This type of exchanger is designated as a recuperator. Some examples of direct transfer type heat exchangers are tubular exchangers, plate heat exchangers, and extended surface exchangers. Recuperators are further subclassified as prime surface exchangers, which do not employ fins or extended surfaces on the prime surface. Plain tubular exchangers, shell and tube exchangers with plain tubes, and plate heat exchangers are examples of prime surface exchangers.

Direct Contact Type Heat Exchangers

In direct contact type heat exchangers, the two fluids are not separated by a wall; owing to the absence of a wall, closer temperature approaches are attained. Very often, in the direct contact type, the process of heat transfer is also accompanied by mass transfer. The cooling towers

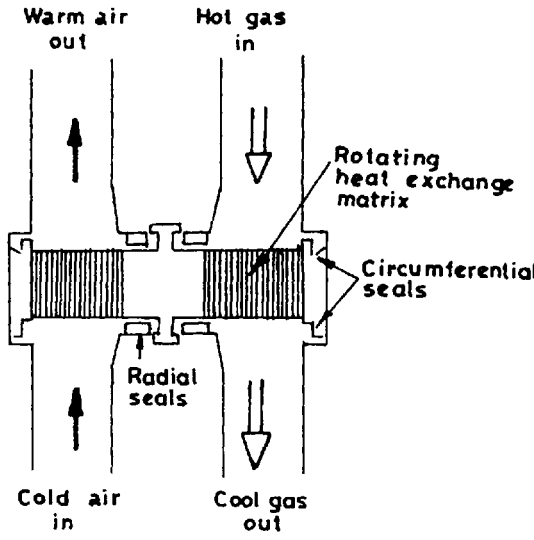


Figure 13 Rotary regenerator [14].

and scrubbers are examples of a direct contact type heat exchanger. The discussion of cooling towers and scrubbers is not within the scope of this book.

3.3 Classification According to Surface Compactness

Compact heat exchangers are important when there are restrictions on the size and weight of exchangers. A compact heat exchanger incorporates a heat-transfer surface having a high area density, β, somewhat arbitrarily 700 m^2/m^3 (200 ft^2/ft^3) and higher [1]. The area density, β, is the ratio of heat transfer area A to its volume V. A compact heat exchanger employs a compact surface on one or more sides of a two-fluid or a multifluid heat exchanger. They can often achieve higher thermal effectiveness than shell and tube exchangers (95% vs. the 60–80% typical for shell and tube heat exchangers), which makes them particularly useful in energy-intensive industries [15]. For least capital cost, the size of the unit should be minimal. There are additional advantages to small volume. Some of these are:

1. Small inventory, making them good for handling expensive or hazardous materials [15]
2. Low weight
3. Easier transport
4. Less foundation
5. Better temperature control

Some barriers to the use of compact heat exchangers include [15]:

1. The lack of standards similar to pressure vessel codes and standards, although this is now being redressed in the areas of plate-fin exchangers [16] and air-cooled exchangers [17].
2. Narrow passages in plate-fin exchangers make them susceptible for fouling and they cannot be cleaned by mechanical means. This limits their use to clean applications like handling air, light hydrocarbons, and refrigerants.

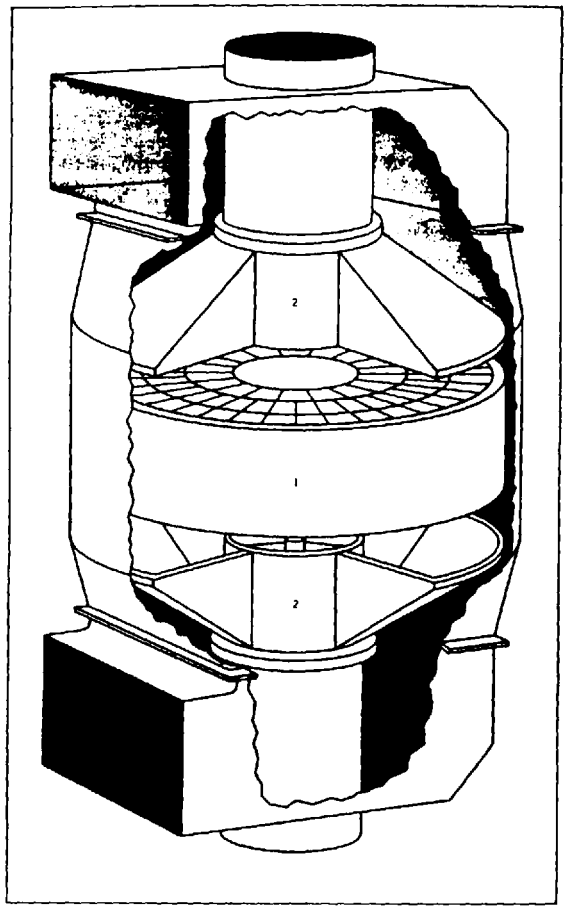


Figure 14 Rothemuhle regenerative air heater. Main parts: 1, stationary matrix; 2, revolving hoods. (Courtesy of Babcock and Wilcox Company.)

3.4 Classification According to Flow Arrangement

The basic flow arrangements of the fluids in a heat exchanger are

1. Parallel flow
2. Counterflow
3. Crossflow

The choice of a particular flow arrangement is dependent upon the required exchanger effectiveness, fluid flow paths, packaging envelope, allowable thermal stresses, temperature levels, and other design criteria. These basic flow arrangements are discussed next.

Parallel Flow Exchanger

In this type, both the fluid streams enter at the same end, flow parallel to each other in the same direction, and leave at the other end (Fig. 15). Fluid temperature variations, idealized as one-dimensional, are shown in Fig. 16. This arrangement has the lowest exchanger effectiveness among the single-pass exchangers for the same flow rates, capacity rate (mass × specific

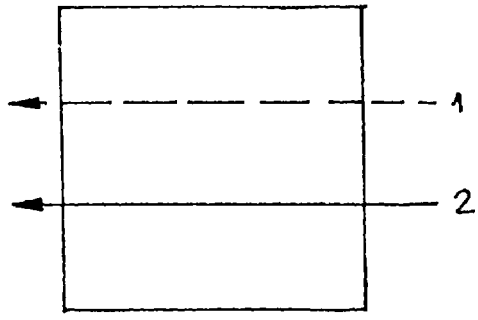


Figure 15 Parallel flow arrangement.

heat) ratio, and surface area. Moreover, the existence of large temperature differences at the inlet end may induce high thermal stresses in the exchanger wall at inlet. Although this flow arrangement is not used widely, it is preferred for the following reasons [2]:

1. Since this flow pattern produces a more uniform longitudinal tube wall temperature distribution and not as high or as low a tube wall temperature as in a counterflow arrangement, it is sometimes preferred with temperature in excess of 1100°C (2000°F).
2. It is preferred when there is a possibility that the temperature of the warmer fluid may reach its freezing point.
3. It provides early initiation of nucleate boiling for boiling applications.
4. For a balanced exchanger (i.e., heat capacity rate ratio $C^* = 1$), the desired exchanger effectiveness is low and is to be maintained approximately constant over a range of NTU values.
5. The application allows piping only suited to parallel flow.

Counterflow Exchanger

In this type, as shown in Fig. 17, the two fluids flow parallel to each other but in opposite directions, and its temperature distribution may be idealized as one-dimensional (Fig. 18). Ideally, this is the most efficient of all flow arrangements for single-pass arrangements under the same parameters. Since the temperature difference across the exchanger wall at a given cross section is the lowest, it produces minimum thermal stresses in the wall for equivalent performance compared to other flow arrangements. In certain type of heat exchangers, counterflow arrangement cannot be achieved easily, due to manufacturing difficulties associated with the separation of the fluids at each end, and the design of inlet and outlet header design is complex and difficult [2].

Crossflow Exchanger

In this type, as shown in Fig. 19, the two fluids flow normal to each other. Important types of flow arrangement combinations for a single-pass crossflow exchanger include:

1. Both fluids unmixed
2. One fluid unmixed and the other fluid mixed
3. Both fluids mixed

A fluid stream is considered "unmixed" when it passes through individual flow passage without any fluid mixing between adjacent flow passages. Mixing implies that a thermal averaging process takes place at each cross section across the full width of the flow passage. A

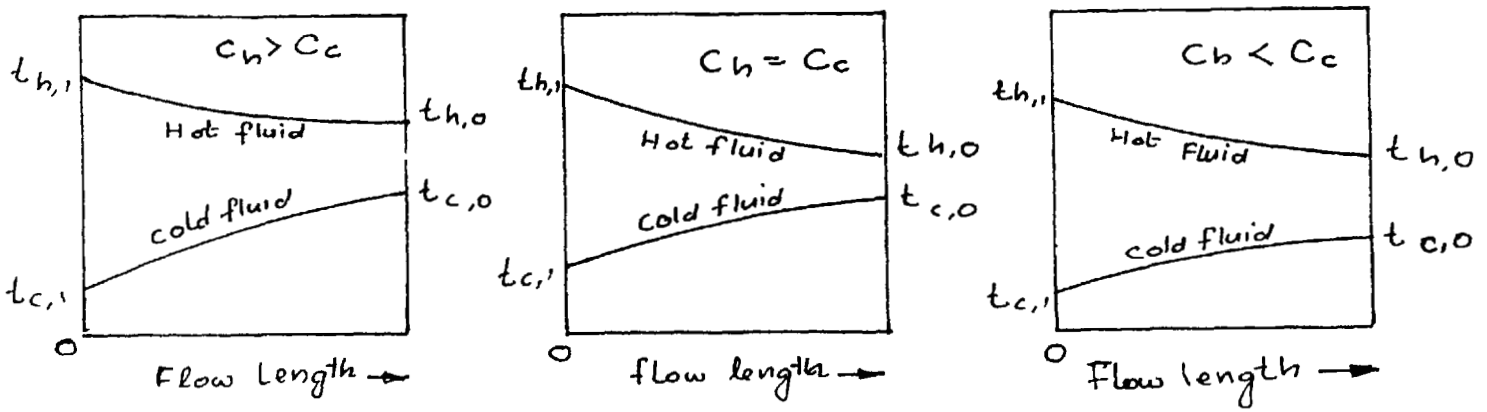


Figure 16 Temperature distribution for parallel flow arrangement.

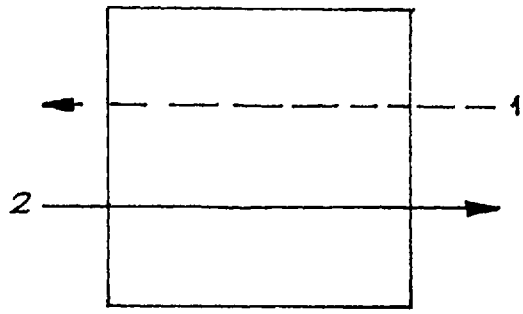


Figure 17 Counterflow arrangement.

tube-fin exchanger with flat (continuous) fins and a plate-fin exchanger wherein the two fluids flow in separate passages (e.g., wavy fin, plain continuous rectangular or triangular flow passages) represent the unmixed–unmixed case. A crossflow tubular exchanger with bare tubes on the outside would be treated as the unmixed–mixed case, that is, unmixed on the tube side and mixed on the outside. The both fluids mixed case is practically a less important case, and represents a limiting case of some multipass shell and tube exchangers (TEMA E and J shell).

For the unmixed–unmixed case, fluid temperature variations are idealized as two-dimensional only for the inlet and outlet sections, and this is shown in Fig. 20. The thermal effectiveness for the crossflow exchanger falls in between those of the parallel flow and counterflow arrangements. This is the most common flow arrangement used for extended surface heat exchangers, because it greatly simplifies the header design. If the desired heat exchanger effectiveness is generally more than 80%, the size penalty for crossflow may become excessive. In such a case, a counterflow unit is preferred [2]. In shell and tube exchangers, crossflow arrangement is used in the TEMA X shell having a single tube pass.

3.5 Classification According to Pass Arrangements

These are either single pass or multipass. A fluid is considered to have made one pass if it flows through a section of the heat exchanger through its full length once. In a multipass arrangement, a fluid is reversed and flows through the flow length two or more times.

Multipass Exchangers

When the design of a heat exchanger results in either extreme length, significantly low velocities, or low effectiveness, or due to other design criteria, a multipass heat exchanger or several single pass-exchangers in series or a combination of both is employed. Specifically, multipassing is resorted to increase the exchanger thermal effectiveness over the individual pass effectiveness. As the number of passes increases, the overall direction of the two fluids approaches that of a pure counterflow exchanger. The multipass arrangements are possible with compact, shell and tube, and plate exchangers.

3.6 Classification According to Phase of Fluids

Gas–Liquid

Gas–liquid heat exchangers are mostly tube-fin type compact heat exchangers with the liquid on the tubeside. The radiator is by far the major type of liquid–gas heat exchanger, typically cooling the engine jacket water by air. Similar units are necessary for all the other water-

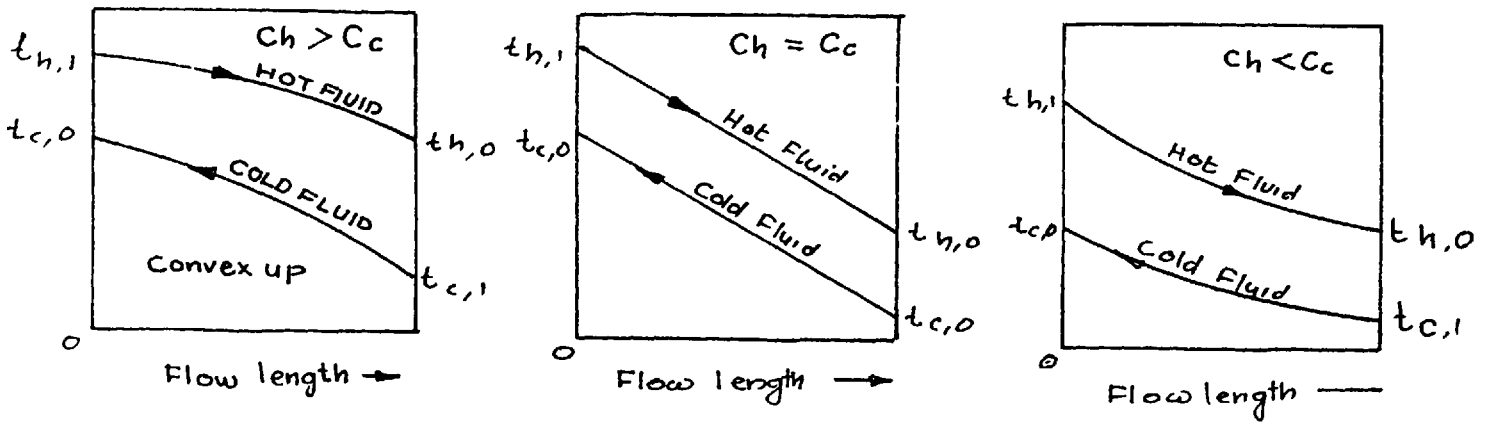


Figure 18 Temperature distribution for counterflow arrangement.

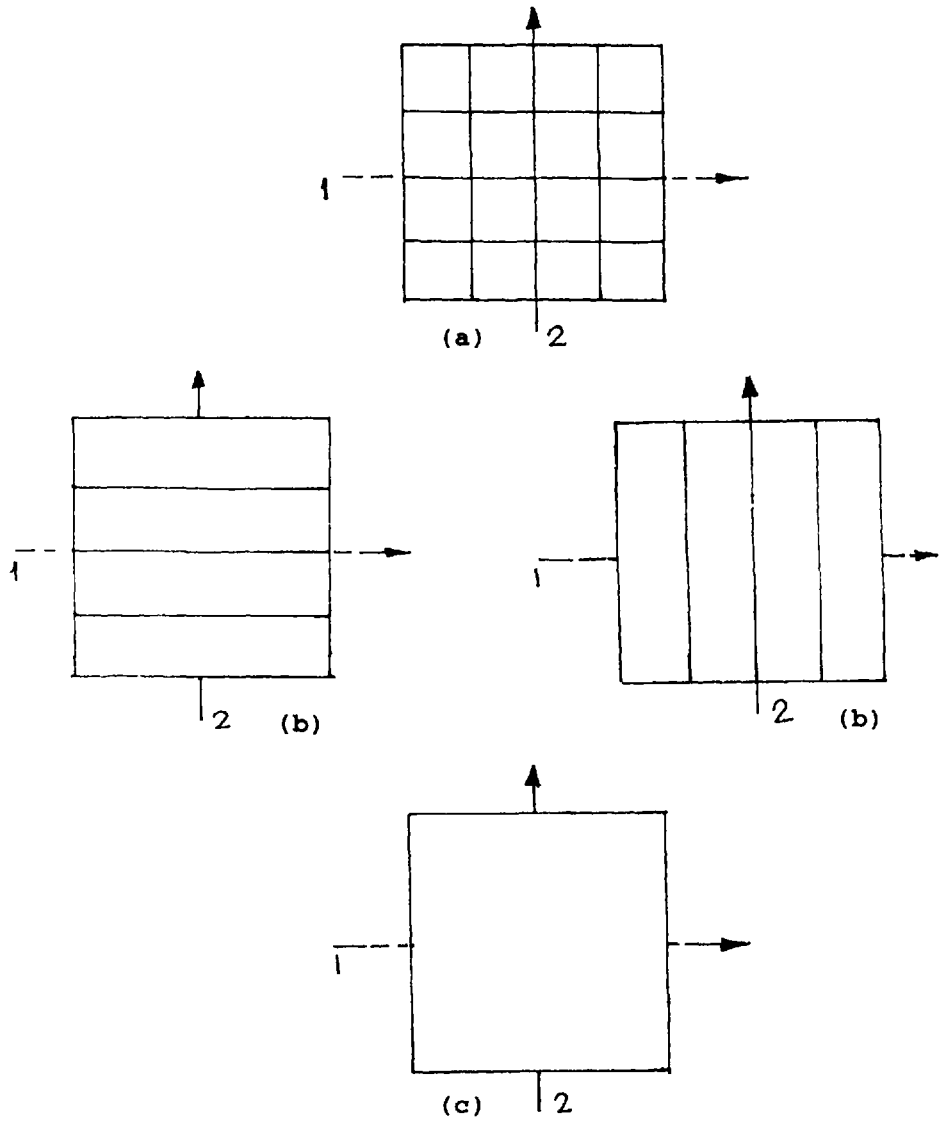


Figure 19 Crossflow arrangement. (a) Unmixed-unmixed; (b) unmixed-mixed; (c) mixed-mixed.

cooled engines used in trucks, locomotives, diesel-powered equipment, and stationery diesel power plants. Other examples are air coolers, oil coolers for aircraft, intercoolers and aftercoolers in compressors, and condensers and evaporators of room air conditioners. Normally, the liquid is pumped through the tubes, which have a very high convective heat-transfer coefficient. The air flows in crossflow over the tubes. The heat-transfer coefficient on the air side will be lower than that on the liquid side. Fins will be generally used on the outside of the tubes to enhance the heat-transfer rate.

Liquid–Liquid

Most of the liquid–liquid heat exchangers are shell and tube type, and plate heat exchangers to a lesser extent. Both fluids are pumped through the exchanger, so the principal mode of heat transfer is forced convection. The relatively high density of liquids results in very high

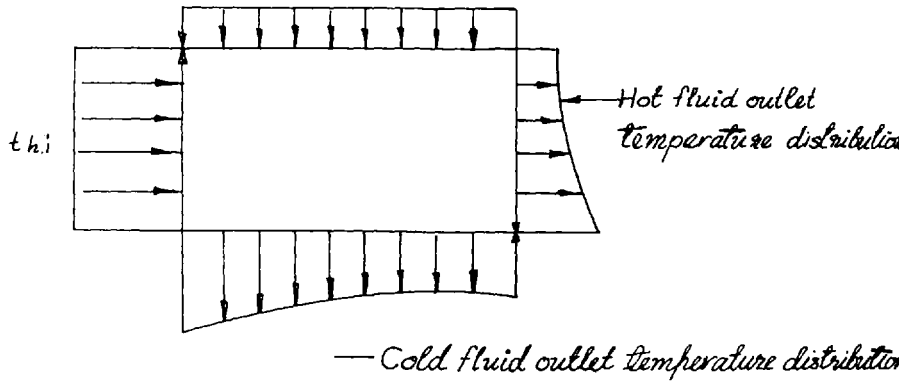


Figure 20 Temperature distribution for unmixed-unmixed crossflow arrangement.

heat-transfer rate, so normally fins or other devices are not used to enhance the heat transfer [4]. In certain applications, low finned tubes, microfin tubes, and heat-transfer augmentation devices are used to enhance the heat transfer.

Gas–Gas

This type of exchanger is found in exhaust gas–air preheating recuperators, rotary regenerators, intercoolers and/or aftercoolers to cool supercharged engine intake air of some land-based diesel power packs and diesel locomotives, and cryogenic gas liquefaction systems. In many cases, one gas is compressed so the density is high while the other is at low pressure and low density. Compared to liquid–liquid exchangers, the size of the gas–gas exchanger will be much larger, because the convective heat-transfer coefficient on the gas side is low compared to the liquid side. Therefore, secondary surfaces are mostly employed to enhance the heat-transfer rate.

3.7 Classification According to Heat-Transfer Mechanisms

The basic heat-transfer mechanisms employed for heat transfer from one fluid to the other are (1) single-phase convection, forced or free, (2) two-phase convection (condensation or evaporation) by forced or free convection, and (3) combined convection and radiation. Any of these mechanisms individually or in combination could be active on each side of the exchanger. Based on the phase change mechanisms, the heat exchangers are classified as (1) condensers and (2) evaporators.

Condensers

Condensers may be liquid (water) or gas (air) cooled. The heat from condensing streams may be used for heating fluid. Normally the condensing fluid is routed (1) outside the tubes with a water-cooled steam condenser, or (2) inside the tubes with gas cooling, that is, air-cooled condensers of refrigerators and air conditioners. Fins are normally provided to enhance heat transfer on the gas side.

Evaporators

This important group of tubular heat exchangers can be subdivided into two classes: fired systems and unfired systems.

Fired Systems. These involve the products of combustion of fossil fuels at very high temperatures but at ambient pressure (and hence low density) and generate steam under pressure. Fired systems are called boilers. A system may be a fire tube boiler (for small low-pressure applications) or a water tube boiler.

Unfired Systems. These embrace a great variety of steam generators extending over a broad temperature range from high-temperature nuclear steam generators to very-low-temperature cryogenic gasifiers for liquid natural gas evaporation. Many chemical and food processing applications involve the use of steam to evaporate solvents, concentrate solutions, distill liquors, or dehydrate compounds.

3.8 Other Classifications

Scraped Surface Exchangers

Scraped surface heat exchangers are used for processes likely to result in the substantial deposition of suspended solids on the heat-transfer surface. Chief applications are in dewaxing plants and in the food industries. Use of a scraped surface exchanger prevents the accumulation of significant buildup of solid deposits. The construction details of scraped surface heat exchangers are explained in Ref. 4. Scraped surface heat exchangers are essentially double pipe construction with the process fluid in the inner pipe and the cooling (water) or heating medium (steam) in the annulus. A rotating element is contained within the tube and is equipped with spring-loaded blades scraping the inside tube wall. For scraped surface exchangers, operating costs are high and applications are highly specific [5]. Design is mostly by vendors.

4 SELECTION OF HEAT EXCHANGERS

4.1 Introduction

Selection is the process in which the designer selects a particular type of heat exchanger for a given application from a variety of heat exchangers. There are a number of alternatives for selecting heat-transfer equipment, but only one among them is the best for the given set of conditions. Heat exchanger selection criteria are discussed in this section.

4.2 Selection Criteria

Selection criteria are many, but primary criteria are type of fluids to be handled, operating pressures and temperatures, heat duty, and cost (see Table 1). Fluids involved in heat transfer can be characterized by temperature, pressure, phase, physical properties, toxicity, corrosivity, and fouling tendency. Operating conditions for heat exchangers vary over a very wide range, and a broad spectrum of demands is imposed for their design and performance. All of these must be considered when assessing the type of unit to be used [18]. When selecting a heat exchanger for a given duty, the following points must be considered:

1. Materials of construction
2. Operating pressure and temperature, temperature program, and temperature driving force
3. Flow rates
4. Flow arrangements
5. Performance parameters—thermal effectiveness and pressure drops
6. Fouling tendencies
7. Types and phases of fluids
8. Maintenance, inspection, cleaning, extension, and repair possibilities
9. Overall economy
10. Fabrication techniques
11. Intended applications

Table 1 Heat Exchanger Selection Criteria [5]

Criteria	Air cooled	Plate	Spiral plate	Lamella	Plate fin	Coiled tube	Double pipe	Graphite	Scraped surface	Shell and tube
Pressure psi	6000	300 (4)	250 (7)	600	1000 150 (11)	1000	600	150	600 (18)	8000
Temperature °F	(1)	500 (4)	750	1000	150 (12) 750 (13)	900	1000	(16)	600	1000
Max ft^2/Unit	none	16000/frame	3000	10000	100000 (12) 500 (13)	200000	300 (14)	(17)	10	30000/shell
Compactness	*(2)	****	****	**	*****	****	*	***	*	*
Mech. cleaning	**	*****	****	**	*	*	***	*	***	***
Chem.	**	****	****	***	**	***	***	*****	****	***
Cost/ft^2	**	**** (5)	*** (8)	** (10)	*****	****	**	*	*	**
Maintenance ease	**	*****	****	***	*	*	***	*	**	**
Corrosion risk	***	****	****	****	***	****	****	*****	***	**
Fouling risk	**	*****	****	***	**	***	***	***	***** (18)	*
Fouling effect	* (3)	****	****	**	*	**	***	**	**** (18)	**
Leakage risk	**	* (6)	* (9)	**	****	***	*** (15)	*	**	** (22)
Duty changes after installation	**	****	*	*	***	**	*	***	*	*
Temp. cross	*	****	****	***	*****	*****	***	***	***	**
Viscous flow	*	****	****	**	*****	**	**	****	***	* *** (23)
Heat sensitive fluids	**	****	****	**	***	**	**	***	***** (19)	*
Solids flowing	*	**	****	**	*	*	***	*	***** (20)	*
Gases	****	*	***	***	****	****	****	***	*	****
Phase change	****	*	****	***	****	****	****	***	***** (21)	****
Multi fluid exchange	***	***	*	**	*****	****	*	***	*	**

*Very poor; **poor; ***fair; ****good; *****very good.

Notes: (1) use restricted to temperatures from ambient to around 300°F; (2) often mounted high or above pipe racks; (3) fouling on outside can reduce air flow and diminish MTD; (4) depends on gasket material; (5) low relative cost applies to non-ferrous materials; (6)plate edges can be seal welded but dismantling then very difficult; (7) for diameters up to 1 meter. For larger diameters the pressure limit is lower; (8) in all metals; (9) see (6); (10) available only in nonferrous materials; (11) applies to reversing service in aluminum; (12) in aluminum; (13) in nonferrous, nonaluminum materials; (14) above 300 ft^2 shell and tube exchangers are usually cheaper; (15) if all welded; (16) 400°F for liquids, up to 1500°F for some gases; (17) 300 ft^2 for cubic block; 2000 ft^2 for modular block; (18) applies to scraped inside; (19) high speed rotor; (20) low speed rotor; (21) liquid to solid, or liquid to vapor; (22) depends on TEMA type; and (23) applies to viscous fluids being heated on shellside.

Materials of Construction

For reliable and continuous use, the construction materials for pressure vessels and heat exchangers should have a well-defined corrosion rate in the service environments. Furthermore, the material should exhibit strength to withstand the operating temperature and pressure. Shell and tube heat exchangers can be manufactured in virtually any materials that may be required for corrosion resistance, for example, from nonmetals like glass, Teflon, and graphite to exotic metals like titanium, zirconium, tantalum, etc. Compact heat exchangers with extended surfaces are mostly manufactured from any metal that has drawability, formability, and malleability. Heat exchanger types like plate heat exchangers normally require a material that can be pressed or welded.

Operating Pressure and Temperature

Pressure. The design pressure is important to determine the thickness of the pressure retaining components. The higher the pressure, the greater will be the required thickness of the pressure-retaining membranes and the more advantage there is to placing the high-pressure fluid on the tubeside. The pressure level of the fluids has a significant effect on the type of unit selected [18].

1. At low pressures, the vapor-phase volumetric flow rate is high and the low allowable pressure drops may require a design that maximizes the area available for flow, such as crossflow or split flow with multiple nozzles.
2. At high pressures, the vapor-phase volumetric flow rates are lower and allowable pressure drops are greater. These lead to more compact units.
3. In general, higher heat-transfer rates are obtained by placing the low-pressure gas on the outside of tubular surfaces.
4. Operating pressures of the gasketed plate heat exchangers and spiral plate heat exchangers are limited because of the difficulty in pressing the required plate thickness, and by the gasket materials in the case of PHEs. The floating nature of floating-head shell and tube heat exchangers and lamella heat exchangers limits the operating pressure.

Temperature.

Design Temperature. This parameter is important as it indicates whether a material at the design temperature can withstand the operating pressure and various loads imposed on the component. For low-temperature and cryogenic applications toughness is a prime requirement, and for high-temperature applications the material has to exhibit creep resistance.

Temperature Program. Temperature program in both a single pass and multipass shell and tube heat exchanger decides (1) the mean metal temperatures of various components like shell, tube bundle, and tubesheet, and (2) the possibility of temperature cross. The mean metal temperatures affect the integrity and capability of heat exchangers and thermal stresses induced in various components.

Temperature Driving Force. The effective temperature driving force is a measure of the actual potential for heat transfer that exists at the design conditions. With a counterflow arrangement, the effective temperature difference is defined by the log mean temperature difference (LMTD). For flow arrangements other than counterflow arrangement, the LMTD must be corrected by a correction factor, F. The F factor can be determined analytically for each flow arrangement but is usually presented graphically in terms of the thermal effectiveness P and the heat capacity ratio R for each flow arrangement.

Influence of Operating Pressure and Temperature on Selection of Some Types of Heat Exchangers. The influence of operating pressure and temperature on selection of shell and tube

heat exchanger, compact heat exchanger, gasketed plate heat exchanger, and spiral exchanger is discussed next.

Shell and Tube Heat Exchanger. Shell and tube heat exchanger units can be designed for almost any combination of pressure and temperature. In extreme cases, high pressure may impose limitations by fabrication problems associated with material thickness, and by the weight of the finished unit. Differential thermal expansion under steady conditions can induce severe thermal stresses either in the tube bundle or in the shell. Damage due to flow-induced vibration on the shellside is well known. In heat-exchanger applications where high heat-transfer effectiveness (close approach temperature) is required, the standard shell and tube design may require a very large amount of heat transfer surface [19]. Depending on the fluids and operating conditions, other types of heat-exchanger design should be investigated.

Compact Heat Exchanger. Compact heat exchangers are constructed from thinner materials; they are manufactured by mechanical bonding, soldering, brazing, welding, etc. Therefore, they are limited in operating pressures and temperatures.

Gasketed Plate Heat Exchangers and Spiral Exchangers. Gasketed plate heat exchangers and spiral exchangers are limited by pressure and temperature, wherein the limitations are imposed by the capability of the gaskets.

Flow Rate

Flow rate determines the flow area: the higher the flow rate, the higher will be the crossflow area. Higher flow area is required to limit the flow velocity through the conduits and flow passages, and the higher velocity is limited by pressure drop, impingement, erosion, and, in the case of shell and tube exchanger, by shell-side flow-induced vibration. Sometimes a minimum flow velocity is necessary to improve heat transfer, to eliminate stagnant areas, and to minimize fouling.

Flow Arrangement

As defined earlier, the choice of a particular flow arrangement is dependent upon the required exchanger effectiveness, exchanger construction type, upstream and downstream ducting, packaging envelope, and other design criteria.

Performance Parameters—Thermal Effectiveness and Pressure Drops

Thermal Effectiveness. For high-performance service requiring high thermal effectiveness, use brazed plate-fin exchangers (e.g., cryogenic service) and regenerators (e.g., gas turbine applications), use tube-fin exchangers for slightly less thermal effectiveness in applications, and use shell and tube units for low thermal effectiveness service.

Pressure Drop. Pressure drop is an important parameter in heat exchanger design. Limitations may be imposed either by pumping cost or by process limitations or both. The heat exchanger should be designed in such a way that unproductive pressure drop is avoided to the maximum extent in areas like inlet and outlet bends, nozzles, and manifolds. At the same time, any pressure drop limitation that are imposed must be utilized as nearly as possible for an economic design.

Fouling Tendencies

Fouling is defined as the formation on heat exchanger surfaces of undesirable deposits that impede the heat transfer and increase the resistance to fluid flow, resulting in higher pressure drop. The growth of these deposits causes the thermohydraulic performance of heat exchanger to decline with time. Fouling affects the energy consumption of industrial processes, and it also decides the amount of extra material required to provide extra heat-transfer surface to

compensate for the effects of fouling. Compact heat exchangers are generally preferred for nonfouling applications. In a shell and tube unit the fluid with more fouling tendencies should be put on the tube side for ease of cleaning. On the shellside with cross baffles, it is sometimes difficult to achieve a good flow distribution if the baffle cut is either too high or too low. Stagnation in any regions of low velocity behind the baffles is difficult to avoid if the baffles are cut more than about 20–25%. Plate heat exchangers and spiral plate exchangers are better chosen for fouling services. The flow pattern in plate heat exchanger induces turbulence even at comparable low velocities; in the spiral units, the scrubbing action of the fluids on the curved surfaces minimizes fouling.

Types and Phases of Fluids

The phase of the fluids within a unit is an important consideration in the selection of the heat exchanger type. Various combinations of fluid phases dealt in heat exchangers are liquid–liquid, liquid–gas, and gas–gas. Liquid phase fluids are generally the simplest to deal with. The high density and the favorable values of many transport properties allow high heat-transfer coefficients to be obtained at relatively low pressure drops [4].

Maintenance, Inspection, Cleaning, Repair, and Extension Aspects

Consider the suitability of various heat exchangers as regards maintenance, inspection, cleaning, repair, and extension. For example, the pharmaceutical, dairy, and food industries require quick access to internal components for frequent cleaning. Since some of the heat exchanger types offer great variations in design, this must be kept in mind when designing for a certain application. For instance, consider inspection and manual cleaning. Spiral plate exchangers can be made with both sides open at one edge, or with one side open and one closed. They can be made with channels between 5 mm and 25 mm wide, with or without studs. The shell and tube heat exchanger can be made with fixed tubesheets or with a removable tube bundle, with small- or large-diameter tubes, or small or wide pitch. A lamella heat exchanger bundle is removable and thus fairly easy to clean on the shellside. Inside the lamella, however, cannot be drilled to remove the hard fouling deposits. Gasketed plate heat exchangers (PHEs) are easy to open, especially when all nozzles are located on the stationary end-plate side. The plate arrangement can be changed for other duties within the frame and nozzle capacity.

Repair of some of the shell and tube exchanger components is possible, but the repair of expansion joint is very difficult. Tubes can be renewed or plugged. Repair of compact heat exchangers of tube-fin type is very difficult except by plugging of the tube. Repair of the plate-fin exchanger is generally very difficult. For these two types of heat exchangers, extension of units for higher thermal duties is generally not possible. All these drawbacks are easily overcome in a PHE. It can be easily repaired, and plates and other parts can be easily replaced. Due to modular construction, PHEs possess the flexibility of enhancing or reducing the heat transfer surface area, modifying the pass arrangement, and addition of more than one duty according to the heat-transfer requirements at a future date.

Overall Economy

There are two major costs to consider in designing a heat exchanger: the manufacturing cost and the operating costs, including maintenance costs. In general, the less the heat-transfer surface area and less the complexity of the design, the lower is the manufacturing cost. The operating cost is the pumping cost due to pumping devices such as fans, blowers, pumps, etc. The maintenance costs include costs of spares that require frequent renewal due to corrosion, and costs due to corrosion/fouling prevention and control. Therefore, the heat exchanger design requires a proper balance between thermal sizing and pressure drop.

Fabrication Techniques

Fabrication techniques are likely to be the determining factor in the selection of a heat-transfer surface matrix or core. They are the major factors in the initial cost and to a large extent influence the integrity, service life, and ease of maintenance of the finished heat exchanger [20]. For example, shell and tube units are mostly fabricated by welding, plate-fin heat exchangers and automobile aluminum radiators by brazing, copper–brass radiators by soldering, most of the circular tube-fin exchangers by mechanical assembling, etc.

Choice of Unit Type for Intended Applications

According to the intended applications, the selection of heat exchangers will follow the guidelines given in Table 2.

5 REQUIREMENTS OF HEAT EXCHANGERS

Heat exchangers have to fulfill the following requirements:

1. High thermal effectiveness
2. Pressure drop as low as possible
3. Reliability and life expectancy
4. High-quality product and safe operation

Table 2 Choice of Unit Type for Intended Applications

Application	Remarks
Low-viscosity fluid to low-viscosity fluid	For high temperature/pressures, use STHE. PHE will require the smallest surface area. Where elastomeric gaskets are not suitable, use a PHE with compressed asbestos gaskets, SPHE, or LHE.
Low-viscosity liquid to steam	For noncorrosive applications, use STHE in carbon steel; for more demanding duties, and where steam pressures are moderate, use PHE.
Medium-viscosity fluids	For such fluids on both sides, use PHE; in the event of gasket problems, or with high solids content, use SPHE.
High-viscosity fluids	PHE offers the advantages of good flow distribution, and will involve the smallest surface area. For extreme viscosities, the SPHE is preferred.
Fouling liquids	Use STHE with removable tube bundle. SPHE or PHE is preferred due to good flow distribution. Use PHE if easy access is of importance.
Slurries, suspensions, and pulps	SPHE offers the best characteristics.
Heat-sensitive liquids	PHE fulfils the requirements best, but the SPHE may also be used in certain cases.
Cooling with air	Extended surface types.
Gas or air under pressure	Use STHE with extended surface on the gas side or brazed plate-fin exchanger.
Cryogenic applications	Brazed aluminum plate-fin exchanger.
Vapor condensation	STHE in carbon steel is preferred. For more demanding applications, SPHE type 2 or 3.
Vapor/gas partial condensation	SPHE type 3 is specially designed for such applications.

Note: STHE, shell and tube heat exchanger; PHE, gasketed plate heat exchanger; SPHE, spiral plate heat exchanger; LHE, lamella heat exchanger. (Information for Table 2 was furnished by m/s Alpha-Laval, India, Ltd.)

5. Material compatibility with the process fluids
6. Convenient size, easy for installation, reliable in use
7. Easy for maintenance and servicing
8. Light in weight but strong in construction to withstand the operational pressures
9. Simplicity of manufacture
10. Low cost
11. Possibility of effecting repair to maintenance problems

The heat exchanger must meet normal process requirements specified through problem specification and service conditions for combinations of the clean and fouled conditions, and uncorroded and corroded conditions. The exchanger must be maintainable, which usually means choosing a configuration that permits cleaning as required and replacement of tubes, gaskets, and any other components that are damaged by corrosion, erosion, vibration, or aging. This requirement may also place limitations on space for tube bundle pulling, to carry out maintenance around it, lifting requirements for heat exchanger components, and adaptability for in-service inspection and monitoring.

2
Heat Exchanger Thermohydraulic Fundamentals

I. HEAT EXCHANGER THERMAL CIRCUIT AND OVERALL CONDUCTANCE EQUATION

In order to develop relationships between the heat-transfer rate q, surface area A, fluid terminal temperatures, and flow rates in a heat exchanger, the basic equations used for analysis are the energy conservation and heat-transfer rate equations [1]. The energy conservation equation for an exchanger having an arbitrary flow arrangement is

$$q = C_h(t_{h,i} - t_{h,o}) = C_c(t_{c,o} - t_{c,i}) \tag{1}$$

and the heat-transfer rate equation is

$$q = UA\ \Delta t_m = \frac{\Delta t_m}{R_o} \tag{2}$$

where Δt_m is the true mean temperature difference, which depends upon the exchanger flow arrangement and the degree of fluid mixing within each fluid stream; C_c is capacity rate of the cold fluid, $(Mc_p)_c$; C_h is capacity rate of the hot fluid, $(Mc_p)_h$; $t_{c,i}$ and $t_{c,o}$ are cold fluid terminal temperatures (inlet and outlet); and $t_{h,i}$ and $t_{h,o}$ are hot fluid terminal temperatures (inlet and outlet).

The heat exchanger thermal circuit variables and overall conduction described here are based on Refs. 1 and 2.

The inverse of the overall thermal conductance UA is referred to as the overall thermal resistance R_o, and it is made up of component resistances in series as shown in Fig. 1:

$$R_o = R_h + R_i + R_w + R_2 + R_c \tag{3}$$

where the parameters of the right-hand side of Eq. 3 are R_h, hot side film convection resistance, $1/(\eta_o hA)_h$; R_i, thermal resistance due to fouling on the hot side given in terms of fouling resistance $R_{f,h}$ (i.e., values tabulated in standards or textbooks), $R_{f,h}/(\eta_o A)_h$; R_w, thermal resistance of the separating wall, expressed for a flat wall by

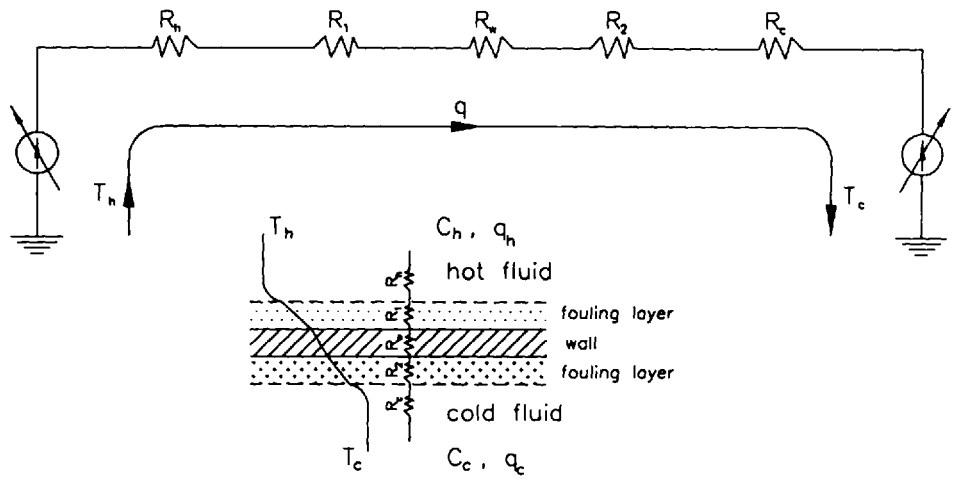


Figure 1 Elements of thermal resistance of a heat exchanger.

$$R_w = \frac{\delta}{A_w k_w} \tag{4a}$$

and for a circular wall by

$$R_w = \frac{\ln(d/d_i)}{2\pi k_w L N_t} \tag{4b}$$

where δ is the wall thickness, A_w is the total wall area for heat conduction, k_w is thermal conductivity of the wall material, d is the tube outside diameter, d_i is the tube inside diameter, L is the tube length, and N_t is the number of tubes, and total wall area for heat conduction is given by

$$A_w = L_1 L_2 N_p \tag{5}$$

where L_1, L_2, and N_p are the length, width, and total number of separating plates, respectively; R_2, thermal resistance due to fouling on the cold side, given in terms of cold side fouling resistance $R_{f,c}$ by $R_{f,c}/(\eta_o A)_c$; and R_c, cold side film convection resistance, $1/(\eta_o hA)_c$.

In these definitions, h is the heat-transfer coefficient on the side under consideration, A represents the total of the primary surface area, A_p, and the secondary (finned) surface area, A_f, on the fluid side under consideration, η_o is the overall surface effectiveness of an extended surface, and the subscripts h and c refer to the hot and cold fluid sides, respectively. The overall surface effectiveness η_o is related to the fin efficiency η_f and the ratio of fin surface area A_f to total surface area A as follows:

$$\eta_o = 1 - \frac{A_f}{A}(1 - \eta_f) \tag{6}$$

Note that η_o is unity for an all prime surface exchanger without fins. Equation 3 can be alternately expressed

$$\frac{1}{UA} = \frac{1}{(\eta_o hA)_h} + \frac{R_{f,h}}{(\eta_o A)_h} + R_w + \frac{1}{(\eta_o hA)_c} + \frac{R_{f,c}}{(\eta_o A)_c} \tag{7}$$

Since $UA = U_h A_h = U_c A_c$, the overall heat-transfer coefficient U as per Eq. 7 may be defined optionally in terms of either hot fluid surface area or cold fluid surface area. Thus the option of A_h or A_c must be specified in evaluating U from the product, UA. For plain tubular exchangers, U_o based on tube outside surface is given by

$$\frac{1}{U_o} = \frac{1}{h_o} + R_{f,o} + \frac{d \ln(d/d_i)}{2k_w} + \frac{R_{f,i} d}{d_i} + \frac{d}{h_i d_i} \tag{8}$$

The knowledge of wall temperature in a heat exchanger is essential to determine the localized hot spots, freeze points, thermal stresses, local fouling characteristics, or boiling and condensing coefficients. Based on the thermal circuit of Fig. 1, when R_w is negligible, $T_{w,h} = T_{w,c} = T_w$ is computed from [1,2]:

$$T_w = \frac{T_h + T_c[(R_h + R_1)/(R_c + R_2)]}{1 + [(R_h + R_1)/(R_c + R_2)]} \tag{9}$$

When $R_1 = R_2 = 0$, Eq. 9 further simplifies to

$$T_w = \frac{T_h/R_h + T_c/R_c}{1/R_h + 1/R_c} = \frac{(\eta_o hA)_h T_h + (\eta_o hA)_c T_c}{(\eta_o hA)_h + (\eta_o hA)_c} \tag{10}$$

2. HEAT EXCHANGER HEAT-TRANSFER ANALYSIS METHODS

2.1 Energy Balance Equation

The first law of thermodynamics must be satisfied in any heat exchanger design procedure at both the macro and micro level. The overall energy balance for any two-fluid heat exchanger is given by

$$m_h c_{p,h}(t_{h,i} - t_{h,o}) = m_c c_{p,c}(t_{c,o} - t_{c,i}) \tag{11}$$

Equation 11 satisfies the "macro" energy balance under the usual idealizations made for the basic design theory of heat exchangers [3].

2.2 Heat Transfer

For any flow arrangement, heat transfer for two fluid streams is given by

$$q = C_h(t_{h,i} - t_{h,o}) = C_c(t_{c,o} - t_{c,i}) \tag{12}$$

and the expression for maximum possible heat transfer rate q_{max} is

$$q_{max} = C_{min}(t_{h,i} - t_{c,i}) \tag{13}$$

The maximum possible heat transfer rate would be obtained in a counterflow heat exchanger with very large surface area and zero longitudinal wall heat conduction, and the actual operating conditions are same as the theoretical conditions.

2.3 Basic Methods to Calculate Thermal Effectiveness

There are four design methods to calculate the thermal effectiveness of heat exchangers:

1. ε-NTU method
2. P-NTU$_t$ method
3. LMTD method
4. ψ-P method

The basics of these methods are discussed next. For more details on these methods, refer to Refs. 1 and 2.

ε-NTU Method

The formal introduction of the ε-NTU method for the heat exchanger analysis was in 1942 by London and Seban [4]. In this method, the total heat-transfer rate from the hot fluid to the cold fluid in the exchanger is expressed as

$$q = \varepsilon C_{min}(t_{h,i} - t_{c,i}) \tag{14}$$

where ε is the heat exchanger effectiveness. It is nondimensional and for a direct transfer type heat exchanger, in general, it is dependent on NTU, C^*, and the flow arrangement:

$$\varepsilon = \phi \text{ (NTU, } C^*\text{, flow arrangement)} \tag{15}$$

These three nondimensional parameters, C^*, NTU, and ε, are defined next.

Heat Capacity Rate Ratio, C*. This is simply the ratio of the smaller to larger heat capacity rate for the two fluid streams so that $C^* \leq 1$.

$$C^* = \frac{C_{min}}{C_{max}} = \frac{(mc_p)_{min}}{(mc_p)_{max}} \tag{16}$$

Here, C refers to the product of mass and specific heat of the fluid, and the subscripts min and max refer to the C_{min} and C_{max} sides, respectively. In a two-fluid heat exchanger, one of the streams will usually undergo a greater temperature change than the other. The first stream is said to be the "weak" stream, having a lower thermal capacity rate (C_{min}), and the other with higher thermal capacity rate (C_{max}) is the "strong" stream.

Number of Transfer Units, NTU. NTU designates the nondimensional "heat-transfer size" or "thermal size" of the exchanger. It is defined as a ratio of the overall conductance to the smaller heat capacity rate.

$$\text{NTU} = \frac{UA}{C_{min}} = \frac{1}{C_{min}} \int_A U\, dA \tag{17}$$

If U is not a constant, the definition of the second equality applies. For constant U, substitution of the expression for UA results in [1,2]:

$$\text{NTU} = \frac{1}{C_{min}} \left[\frac{1}{1/(\eta_o hA)_h + R_1 + R_w + R_2 + 1/(\eta_o hA)_c} \right] \tag{18}$$

where R_1 and R_2 are the thermal resistances due to fouling on the hot side and cold side, respectively, as defined in Eq. 7. In the absence of the fouling resistances, NTU can be given by the expression

$$\frac{1}{\text{NTU}} = \frac{1}{\text{NTU}_h(C_h/C_{min})} + R_w C_{min} + \frac{1}{\text{NTU}_c(C_c/C_{min})} \tag{19}$$

and the number of heat transfer units on the hot and cold sides of the exchanger may be defined as follows:

$$\text{NUT}_h = \frac{(\eta_o hA)_h}{C_h} \qquad \text{NTU}_c = \frac{(\eta_o hA)_c}{C_c} \tag{20}$$

Heat Exchanger Effectiveness, ε. Heat exchanger effectiveness, ε, is defined as the ratio of the actual heat-transfer rate, q, to the thermodynamically possible maximum heat-transfer rate (q_{max}) by the second law of thermodynamics,

$$\varepsilon = q/q_{max} \tag{21}$$

The value of ε ranges between 0 and 1. Using the value of actual heat-transfer rate q from Eq. 12 and q_{max} from Eq. 13, the exchanger effectiveness ε of Eq. 21 is given by

$$\varepsilon = \frac{C_h(t_{h,i} - t_{h,o})}{C_{min}(t_{h,i} - t_{c,i})} = \frac{C_c(t_{c,o} - t_{c,i})}{C_{min}(t_{h,i} - t_{c,i})} \tag{22}$$

Dependence of ε *on NTU.* At low NTU, the exchanger effectiveness is generally low. With increasing values of NTU, the exchanger effectiveness generally increases, and in the limit it approaches the maximum asymptotic value. However, there are exceptions such that after reaching a maximum value, the effectiveness decreases with increasing NTU.

P-NTU$_t$ Method

This method represents a variant of the ε-NTU method. The origin of this method is related to shell and tube exchangers. In the ε-NTU method, one has to keep track of the C_{min} fluid. In order to avoid possible errors, an alternative is to present the temperature effectiveness, P, of the fluid side under consideration as a function of NTU and heat capacity rate of that side to that of the other side, R. Somewhat arbitrarily, the side chosen is the tube side regardless of whether it is the hot side or the cold side. This approach is followed in TEMA Standards [5].

General P-*NUT$_t$ Functional Relationship.* Similar to the exchanger effectiveness ε, the thermal effectiveness P is a function of NTU$_t$, R, and flow arrangement.

$$P = \phi\,(\text{NTU}_t, R, \text{flow arrangement}) \tag{23}$$

Here P, NTU$_t$, and R are defined consistently based on the tube-side fluid variables. In this method, the total heat-transfer rate from the hot fluid to the cold fluid is expressed by

$$q = PC_t(T_1 - t_1) \tag{24}$$

Thermal Effectiveness, P. For a shell and tube heat exchanger, the temperature effectiveness of the tube-side fluid, P, is referred to as the "thermal effectiveness." It is defined as the ratio of the temperature rise (drop) of the tube-side fluid (regardless of whether it is hot or cold fluid) to the difference of inlet temperature of the two fluids. According to this definition, P is given by

$$P = \frac{t_2 - t_1}{T_1 - t_1} \tag{25}$$

where t_1 and t_2 refer to tube-side inlet and outlet temperatures, respectively, and T_1 and T_2 refer to shell-side inlet and outlet temperatures, respectively.

Comparing Eqs. 25 and 22, it is found that the thermal effectiveness P and the exchanger effectiveness ε are related as

$$\begin{aligned} P &= \frac{C_{min}}{C_t}\varepsilon = \varepsilon \qquad \text{for } C_t = C_{min} \\ &= \varepsilon C^* \qquad \text{for } C_t = C_{max} \end{aligned} \tag{26}$$

Note that P is always less than or equal to ε. The thermal effectiveness of the shell-side fluid can be determined from the tube-side values by the relationship given by

$$P_s = P\frac{C_t}{C_s} = PR \tag{27}$$

Heat Capacity Ratio, R. For a shell and tube exchanger, R is the ratio of the capacity rate of the tube fluid to the shell fluid. This definition gives rise to the following relation in terms of temperature drop (rise) of the shell fluid to the temperature rise (drop) of the tube fluid:

$$R = \frac{C_t}{C_s} = \frac{T_1 - T_2}{t_2 - t_1} \tag{28}$$

where the right-hand-side expressions come from an energy balance and indicate the temperature drop/rise ratios. The value of R ranges from zero to infinity, zero being for pure vapor condensation and infinity being for pure liquid evaporation. Comparing Eqs. 28 and 16, R and C^* are related by

$$\begin{aligned} R = \frac{C_t}{C_s} &= C^* \qquad \text{for } C_t = C_{min} \\ &= 1/C^* \qquad \text{for } C_t = C_{max} \end{aligned} \tag{29}$$

Thus R is always greater than or equal to C^*.

Number of Transfer Units, NTU_t. For a shell and tube exchanger, the number of transfer units NTU_t is defined as a ratio of the overall conductance to the tube-side fluid heat capacity rate:

$$NTU_t = \frac{UA}{C_t} \tag{30}$$

Thus NTU_t is related to NTU based on C_{min} by

$$\begin{aligned} NTU_t = NTU\frac{C_{min}}{C_t} &= NTU \qquad \text{for } C_t = C_{min} \\ &= NTU\ C^* \qquad \text{for } C_t = C_{max} \end{aligned} \tag{31}$$

Thus NTU_t is always less than or equal to NTU.

Log Mean Temperature Difference Correction Factor (LMTD) Method

The maximum driving force for heat transfer is always the log mean temperature difference (LMTD) when two fluid streams are in countercurrent flow. However, the overriding importance of other design factors causes most heat exchangers to be designed in flow patterns different from true countercurrent flow. The true mean temperature difference of such flow arrangements will differ from the logarithmic mean temperature difference by a certain factor dependent on the flow pattern and the terminal temperatures. This factor is usually designated as the log mean temperature difference correction factor, F. The factor F may be defined as the ratio of the true mean temperature difference (MTD) to the logarithmic mean temperature difference. The heat transfer rate equation incorporating F is given by

$$q = UA\ \Delta t_m = UAF\ \Delta t_{lm} \tag{32}$$

where Δt_m is the true MTD and Δt_{lm} the LMTD.

The expression for LMTD for a counterflow exchanger is given by

$$LMTD = \Delta t_{lm} = \frac{\Delta t_1 - \Delta t_2}{\ln(\Delta t_1/\Delta t_2)} \tag{33a}$$

where $\Delta t_1 = t_{h,i} - t_{c,o} = T_1 - t_2$ and $\Delta t_2 = t_{h,o} - t_{c,i} = T_2 - t_1$ for all flow arrangements except for parallel flow; for parallel flow $\Delta t_1 = t_{h,i} - t_{c,i}\ (= T_1 - t_1)$ and $\Delta t_2 = t_{h,o} - t_{c,o}\ (= T_2 - t_2)$. Therefore, LMTD can be represented in terms of the terminal temperatures, that is, greater terminal temperature difference (GTTD) and smaller terminal temperature difference (STTD) for both pure parallel and counterflow arrangements. Accordingly, LMTD is given by

$$LMTD = \Delta t_{lm} = \frac{GTTD - STTD}{\ln(GTTD/STTD)} \tag{33b}$$

A chart to determine LMTD from the terminal temperature differences is presented in Refs. 5 and 6. Figure 2 shows a typical chart taken from Ref. 5. From its definition, F is expressed by

$$F = \frac{\Delta t_m}{\Delta t_{lm}} \tag{34}$$

In situations where the heat release curves are nonlinear, the approach just described is not applicable and a "weighted" temperature difference must be determined.

It can be shown that in general, F is dependent upon the thermal effectiveness P, the heat capacity rate ratio R, and the flow arrangement. Therefore, F is represented by

$$F = \phi(P, R, \text{NTU}_t, \text{flow arrangement}) \tag{35}$$

and the expression for F in terms of P, R, and NTU is given by

$$F = \frac{1}{(R-1)NTU} \ln\left[\frac{1-P}{1-PR}\right] \quad \text{for } R \neq 1$$
$$= \frac{P}{(1-P)NTU} \quad \text{for } R = 1 \tag{36a}$$

$$F = \frac{1}{(1-C^*)NTU} \ln\left[\frac{1-\varepsilon C^*}{1-\varepsilon}\right] \quad \text{for } C^* \neq 1$$
$$= \frac{\varepsilon}{(1-\varepsilon)NTU} \quad \text{for } C^* = 1 \tag{36b}$$

The factor F is dimensionless.

The value of F is unity for a true counterflow exchanger, and thus independent of P and R. For other arrangements, F is generally less than unity, and can be explicitly presented as a function of P, R, and NTU_t by Eq. 36. The value of F close to unity does not mean a highly efficient heat exchanger, but it means a close approach to the counterflow behavior for the comparable operating conditions of flow rates and inlet fluid temperatures. Because of a large capital cost involved with a shell and tube exchanger, generally it is designed in the steep region of the P-NTU_t curve (ε-NTU relation for the compact heat exchanger) (ε or $P < 60\%$), and as a rule of thumb, the F value selected is 0.80 and higher. However, a better guideline for F_{min} is provided in the next section.

Applicability of ε-NTU and LMTD Methods. Generally, the ε-NTU method is used for the design of compact heat exchangers. The LMTD method is used for the design of shell and tube heat exchangers. It should be emphasized that either method will yield the identical results within the convergence tolerances specified.

ψ-P Method

The ψ-P method was originally proposed by Smith [7] and modified by Mueller [8]. In this method, a new term ψ is introduced, which is expressed as the ratio of the true mean temperature difference to the inlet temperature difference of the two fluids:

$$\psi = \frac{\Delta t_m}{t_{h,i} - t_{c,i}} = \frac{\Delta t_m}{T_i - t_i} \tag{37}$$

and ψ is related to ε and NTU and P and NTU_t as

$$\psi = \frac{\varepsilon}{\text{NTU}} = \frac{P}{\text{NTU}_t} \tag{38}$$

$$LMTD = \frac{(GTTD - LTTD)}{ln\left(\frac{GTTD}{LTTD}\right)}$$

where GTTD = Greater Terminal Temperature Difference.
LTTD = Lesser Terminal Temperature Difference.

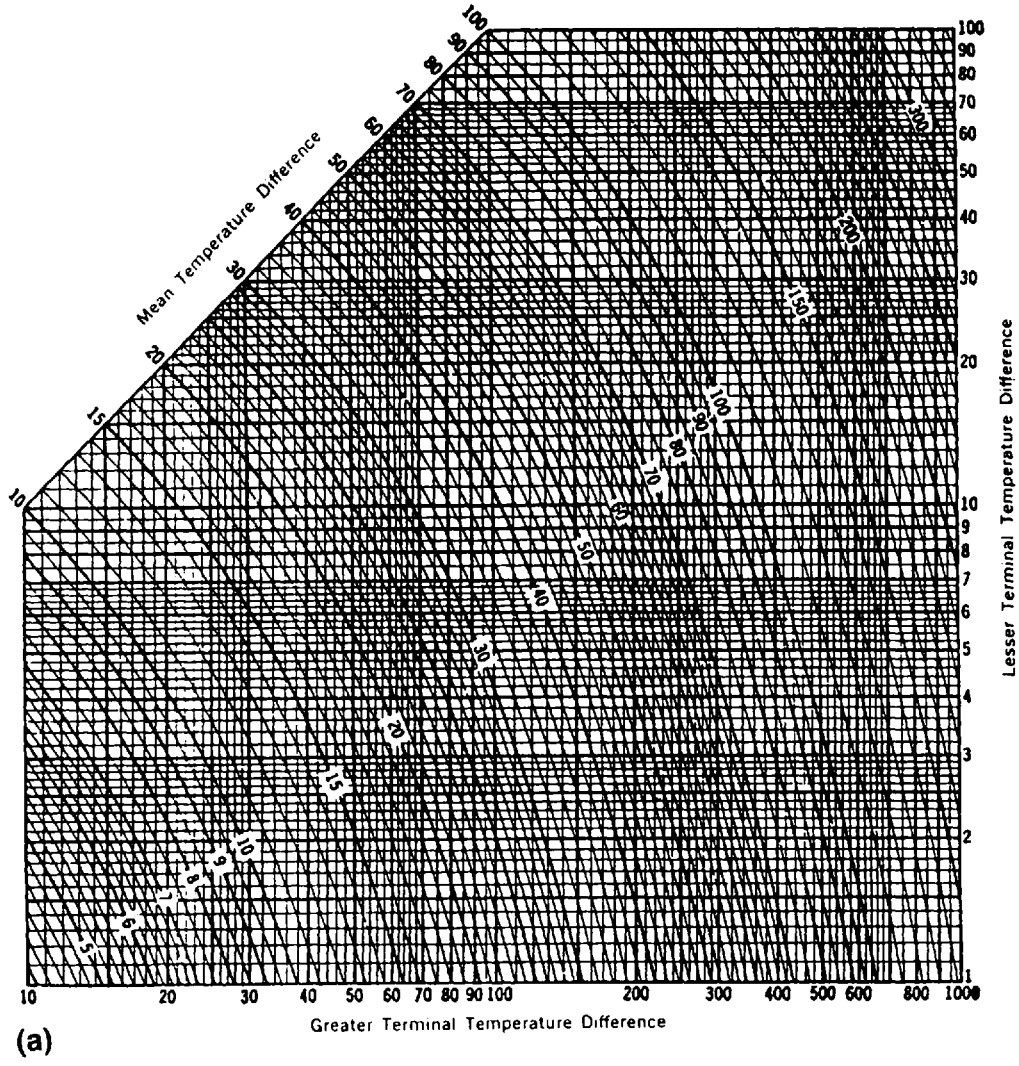
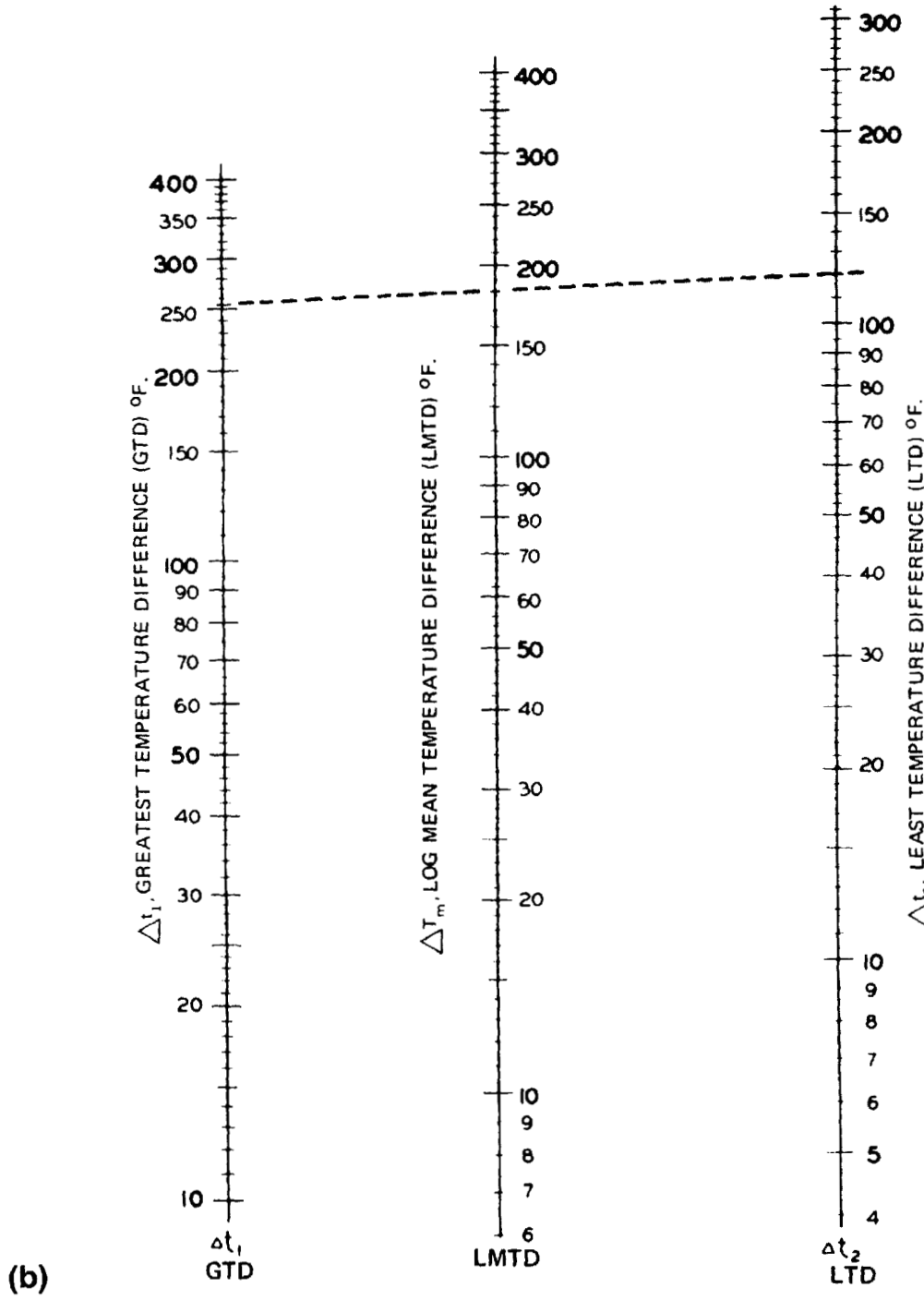


Figure 2 (a) Chart for solving LMTD formula [5]; (b) nomogram to find LMTD. For points not included on this sheet multiply greater terminal temperature difference and lesser terminal temperature difference by any multiple of 10 and divide the resulting value of curved lines by the same multiple. [Copyright Tubular Exchanger Manufacturers Assocation (1988).]



(b)

Figure 2 Continued. (Courtesy of Paul-Muller Company, Springfield, Missouri.)

and the heat-transfer rate is given by

$$q = UA\psi(t_{h,i} - t_{c,i}) \tag{39a}$$

$$= UA\psi(T_1 - t_1) \tag{39b}$$

Since ψ represents the nondimensional Δt_m, there is no need to compute Δt_{lm} in this method.

Functional Relationship Between the Various Thermal Design Methods

The general functional relationship for the ε-NTU, P-NTU$_t$, LMTD, and ψ-P methods is shown in Table 1, which as been adopted from Ref. 1, and the relationship between the dimensionless groups of these methods are given in Table 2.

Thermal Design Methods for the Design of Shell and Tube Heat Exchangers

Any of the four methods (ε-NTU, P-NTU$_t$, LMTD, and ψ-P) can be used for shell and tube exchangers.

2.4 Some Fundamental Relationships to Characterize the Exchanger for "Subdesign" Condition

The partial derivatives of the temperature efficiency P with respect to NTU and R enables complete characterization of the exchanger performance around an operating point. Thus, the exchanger performance can be readily predicted for the "subdesign" conditions [9]. Singh [9] developed derivatives of P, F, and NTU. Derivatives for P and F are discussed next.

Dependence of Thermal Effectiveness

Thermal performance P and thermal effectiveness ε can be represented through R by [9]:

Table 1 General Functional Relationship Between Dimensionless Groups of the ε-*NTU*, *P-NTU*$_t$, *LMTD*, and ψ-*P* Methods [1]

ε-NTU method	*P-NTU*$_t$ method
$C^* = \dfrac{C_{min}}{C_{max}} = \dfrac{(mc_p)_{min}}{(mc_p)_{max}}$	$R = \dfrac{C_t}{C_s} = \dfrac{T_1 - T_2}{t_2 - t_1}$
$NTU = \dfrac{UA}{C_{min}} = \dfrac{1}{C_{min}} \int_A U dA$	$NTU_t = \dfrac{UA}{C_t}$
$\varepsilon = \phi(NTU, C^*, \text{flow arrangement})$	$P = \phi(NTU_t, R, \text{flow arrangement})$
$\varepsilon = \dfrac{C_h(t_{h,i} - t_{h,o})}{C_{min}(t_{h,i} - t_{c,i})} = \dfrac{C_c(t_{c,o} - t_{c,i})}{C_{min}(t_{h,i} - t_{c,i})}$	$P = \dfrac{t_2 - t_1}{T_1 - t_1}$
$q = \varepsilon\, C_{min}(t_{h,i} - t_{c,i})$	$q = P\, C_t (T_1 - t_1)$
LMTD method	ψ-P method
$LMTD = \dfrac{\Delta t_1 - \Delta t_2}{\ln\left[\dfrac{\Delta t_1}{\Delta t_2}\right]}$	$\psi = \phi(P, R, \text{flow arrangement})$
	$\psi = \dfrac{\Delta t_m}{t_{h,i} - t_{c,i}}$
$F = \phi(P, R, NTU_t, \text{flow arrangement})$	$q = UA\psi\,(t_{h,i} - t_{c,i})$
$q = UA\Delta t_m = UAF\Delta t_{lm}$	

Source: After Ref. 1.

Table 2 Relationship Between Dimensionless Groups of the ε-*NTU*, *P*-NTU_t, *LMTD*, and ψ-*P* Methods

$$P = \frac{C_{min}}{C_t}\varepsilon = \varepsilon \qquad \text{for } C_t = C_{min}$$
$$= \varepsilon C^* \qquad \text{for } C_t = C_{max}$$

$$R = \frac{C_t}{C_s} = C^* \qquad \text{for } C_t = C_{min}$$
$$= 1/C^* \qquad \text{for } C_t = C_{max}$$

$$NTU_t = NTU\frac{C_{min}}{C_t} = NTU \qquad \text{for } C_t = C_{min}$$
$$= NTUC^* \qquad \text{for } C_t = C_{max}$$

$$F = \frac{1}{(R-1)NTU}\ln\left[\frac{1-P}{1-PR}\right] \qquad \text{for} R \neq 1$$
$$= \frac{P}{(1-P)\,NTU} \qquad \text{for } R = 1$$

$$\psi = \frac{\varepsilon}{NTU} = \frac{P}{NTU_t}$$

$$\varepsilon = P \quad R \leq 1$$
$$= PR \qquad R > 1 \tag{40}$$

$$P = f(NTU, R) \tag{41}$$

$$\varepsilon = \phi(NTU, R^*) \tag{42}$$

Thus

$$d\varepsilon = d\phi = \frac{\partial \phi}{\partial NTU}dNTU + \frac{\partial \phi}{\partial R}dR \tag{43}$$

$$d\varepsilon = dP = \frac{\partial P}{\partial NTU}dNTU + \frac{\partial P}{\partial R}dR \qquad \text{for } R \leq 1 \tag{44}$$

$$d\varepsilon = P\,dR + R\,dP \tag{45}$$

$$= P\,dR + R\left(\frac{\partial P}{\partial \mathrm{NTU}}d\mathrm{NTU} + \frac{\partial P}{\partial R}dR\right) \tag{46}$$

or

$$d\varepsilon = \left(P + R\frac{\partial P}{\partial R}\right)dR + R\frac{\partial P}{\partial \mathrm{NTU}}d\mathrm{NTU} \qquad \text{for } R \geq 1 \tag{47}$$

Dependence of LMTD Correction Factor, *F*

The derivatives of *F* with respect to ε, *P*, and *R* are given by [9]:

$$\frac{\partial F}{\partial NTU} = -\frac{1}{NTU^2(R-1)}\ln\left[\frac{1-P}{1-PR}\right] = \frac{-F}{NTU} \tag{48}$$

$$\frac{\partial F}{\partial P} = \frac{1}{NTU\,(1-P)\,(1-PR)} \tag{49}$$

$$\frac{\partial F}{\partial R} = \frac{-F}{(R-1)} + \frac{1}{NTU\,(R-1)\,(1-PR)} \tag{50}$$

and

$$dF = \frac{\partial F}{\partial P}\,dP + \frac{\partial F}{\partial \mathrm{NTU}}\,d\mathrm{NTU} + \frac{\partial F}{\partial R}\,dR \tag{51}$$

3. THERMAL EFFECTIVENESS CHARTS

Broadly speaking, there are two types of heat exchanger problems: rating and sizing. To solve either type of problem from first principles is laborious and time-consuming. However, sizing and rating of heat exchangers are solved with the use of performance charts easily. The graphical charts were introduced many years ago and have gained wide acceptance throughout the industry. Five types of heat exchanger design charts are found in the literature, and the salient features of these charts are discussed by Turton et al. [10]. These charts are shown schematically in Fig. 3(a) to (f). The dimensionless variables used in these charts (ε, P, R, C^*, F, NTU, NTU_t) were defined in Section 2.

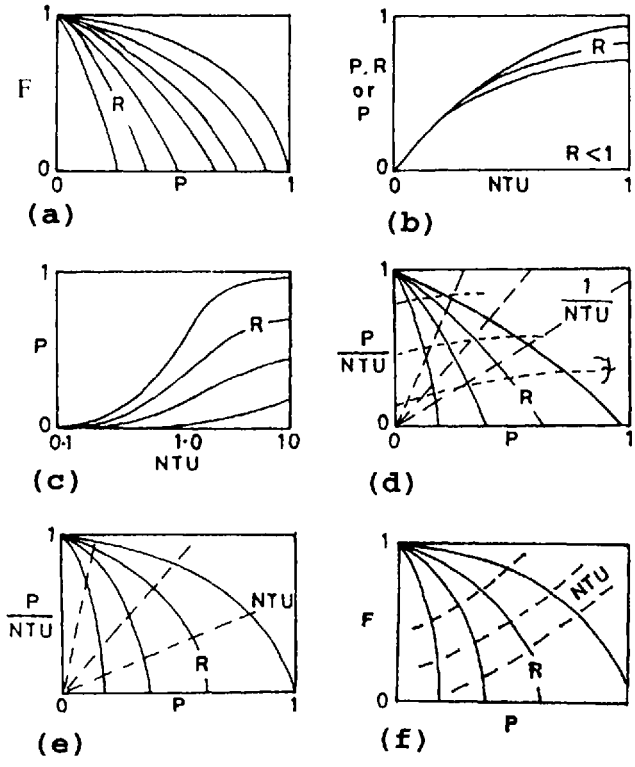
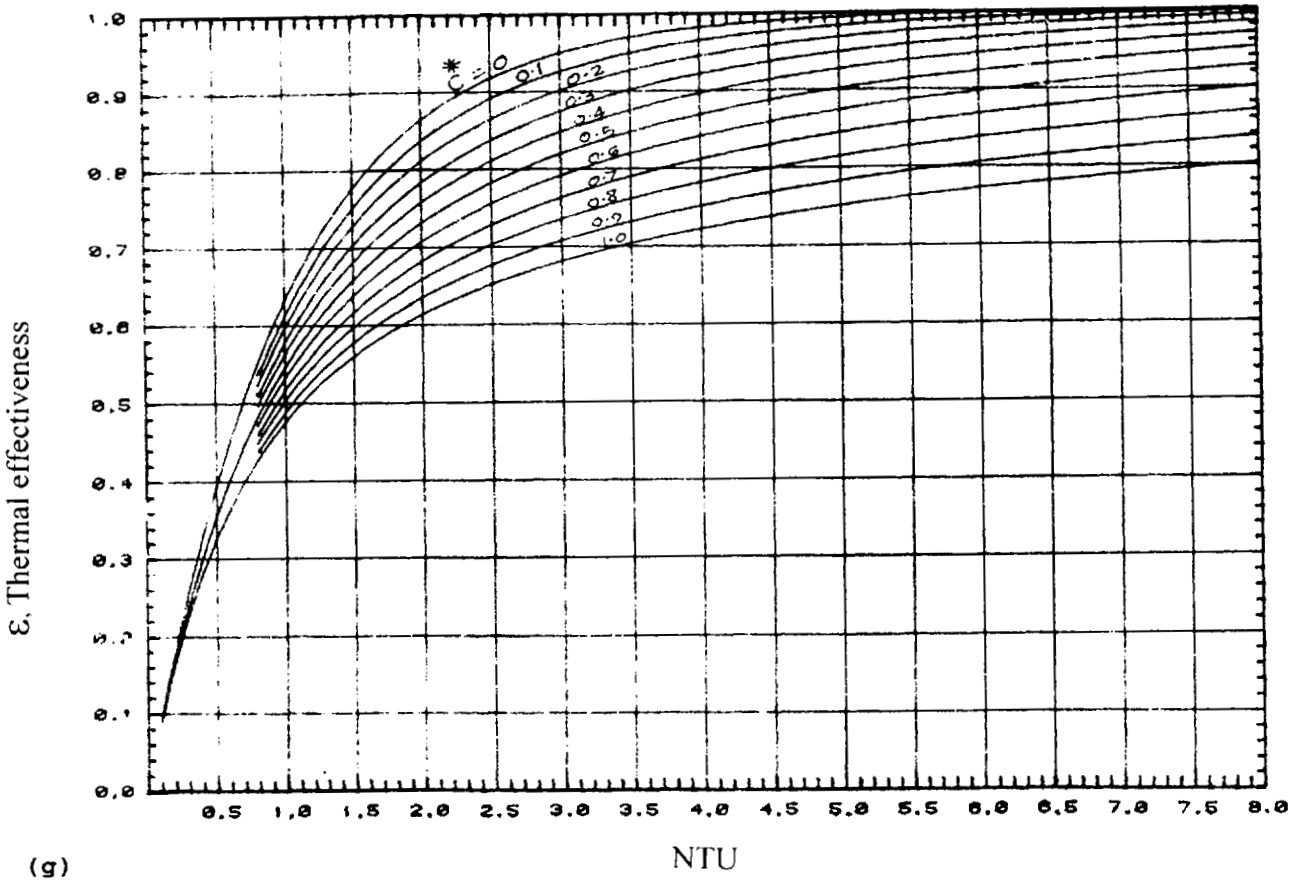


Figure 3 Thermal effectiveness charts. (a) Bowman chart; (b) Kays and London chart; (c) TEMA chart; (d) F-P-R-chart; (e) ψ chart; (f) Turton et al. chart or F-P-R-NTU chart; (g) ε-NTU chart for unmixed-unmixed crossflow [10].



(g)

Figure 3 Continued.

Figure 3(a) is the most widely used of these charts and was introduced by Bowman et al. [11] in 1940. In this chart, the LMTD correction factor, F, is presented as a function of the effectiveness, P, and the heat capacity rate ratio, R. Using this chart, the design problem where terminal temperatures and flow rates are usually specified but overall U and/or A are unknown can be solved; however, the rating problem can be solved by a trial-and-error solution. Since F compares the true mean temperature difference of a given flow arrangement with that of the counterflow arrangement, these charts provide a well-suited means of finding out the best of several possible flow arrangements. The one with the higher F will require the lower NTU, that is, the lower area if U remains constant, operating with the same R and P. Underwood [12] first derived the expression for true mean temperature difference for $E_{1\text{-}2}$, $E_{1\text{-}4}$, and $E_{2\text{-}4}$ shell and tube exchangers in 1934. Bowman et al. [11] published a summary of correction factors for exchangers of different flow arrangements. Ten Broeck [13] further constructed charts using dimensionless groups, $UA/(mc_p)_t$, $P = (t_2 - t_1)/(T_1 - t_1)$, and $R = (T_1 - T_2)/(t_2 - t_1)$ for direct calculation of terminal temperatures with known surface area of a heat exchanger. At present, F charts are available for all TEMA shells.

Figures 3(b) and 3(c) are due to Kays and London [14] and TEMA [15], respectively. Figure 3(c) is plotted on a semilog paper, since the most useful NTU and NTU_t design range for compact heat exchangers and shell and tube exchangers, respectively, are in the range of 0.2–3.0. A careful look at the linear graphical presentation of the ε-NTU results of Fig. 3(b) indicates that the NTU scale in this range is short and hence one cannot obtain the accurate values of ε or NTU from graphs. For better appreciation, this is illustrated through the thermal relation chart (ε-NTU) for crossflow heat exchanger in Fig. 3(g). An alternative is to stretch the NTU scale in the range 0.2 to 3.0 by using a logarithmic scale. Thus, the P-NTU_t results are generally presented on a semilog paper, as shown for example in Fig. 3(c), in order to obtain more accurate graphical values of P or NTU_t. Using these charts, both the sizing and rating problem can be solved. However, the LMTD correction factor F is not shown in these charts. Hence it is to be calculated additionally.

Muller [8] proposed the charts of Fig. 3(d) with its triple family of curves. This chart can be used to solve both the sizing and rating problems and in addition gives the F values. However, Fig. 3(d) is somewhat cramped and difficult to read accurately and introduces yet another parameter, P/NTU_t. The Muller charts have been redrawn recently by Taborek and included in HEDH [16]. The present form of this chart is shown in Fig. 3(e). The main difference between Figs. 3(d) and 3(e) is that the F parameter curves have been omitted in the latter, and thus the problem of having separately calculate the F values has been retained.

In a system with four variables, F, P, R, and NTU or NTU_t, any chart displays just one family of curves, such as Figs. 3(a)–(c), and does not give all the interrelationships directly. On the other hand, a chart with three families of curves, as in Fig. 3(d), has one set that is redundant. To show all the interrelationships between these four variables requires a chart with two families of curves. This is satisfied by Fig. 3(e).

In the graphical presentation, ψ is plotted against P and R as a parameter as shown in Fig. 3(e). The lines of constant R originate at $\psi = 1$ and terminate at $\psi = 0$ so that the asymptotic values of P for NTU tend to infinity. Thus the curves of constant R are similar to those for the F-P charts. In order to tie in with the P-NTU_t and LMTD methods, the lines of constant NTU_t and constant F are also superimposed on this chart. Figure 3(e) also has one limitation: it does not show directly the four parameters of interest.

Constraints due to the charts in Figs. 3(a) to 3(e) are overcome by a chart as shown in Fig. 3(f) proposed by Turton et al. [10]. The chart in Fig. 3(f) extends the easy-to-read Bowman charts of Fig. 3(a) to include a second family of curves representing the variable NTU. Both the sizing and rating problems can be solved using this form of chart, and F values can

be found directly for both types of problems. Thus to find exchanger surface area, use P and R to evaluate F and NTU. To find terminal temperature, use NTU and R to evaluate P and F. Most of the charts included in this book are of the type of Fig. 3(f).

4. SYMMETRY PROPERTY AND FLOW REVERSIBILITY AND RELATION BETWEEN THE THERMAL EFFECTIVENESS OF OVERALL PARALLEL AND COUNTERFLOW HEAT EXCHANGER GEOMETRIES

4.1 Symmetry Property

The symmetry property relates the thermal behavior of a heat exchange process to that of the reverse process, in which the directions of flow of both fluids are reversed [17]. Figure 4 shows four different flow arrangements for the TEMA $E_{1,2}$ shell and tube heat exchanger that are equivalent if complete transverse mixing of the shell fluid is satisfied.

4.2 Flow Reversibility

Flow reversibility establishes a relation between the thermal effectiveness of two heat exchanger configurations that differ from each other in the inversion of either one of the two fluids [18]. Although the inversion of both fluids often does not alter the configuration, the inversion of only one of them usually leads from one configuration to an entirely different one, as is the case in going from a pure parallel flow to a pure counterflow arrangement or vice versa. Using this relation, if the expression for the effectiveness, P, of a configuration as a function of the heat capacity rate ratio, R (or C^*), and the number of heat transfer units NTU is known, the corresponding expression for the "inverse" configuration is immediately obtained from the simple relation [18]:

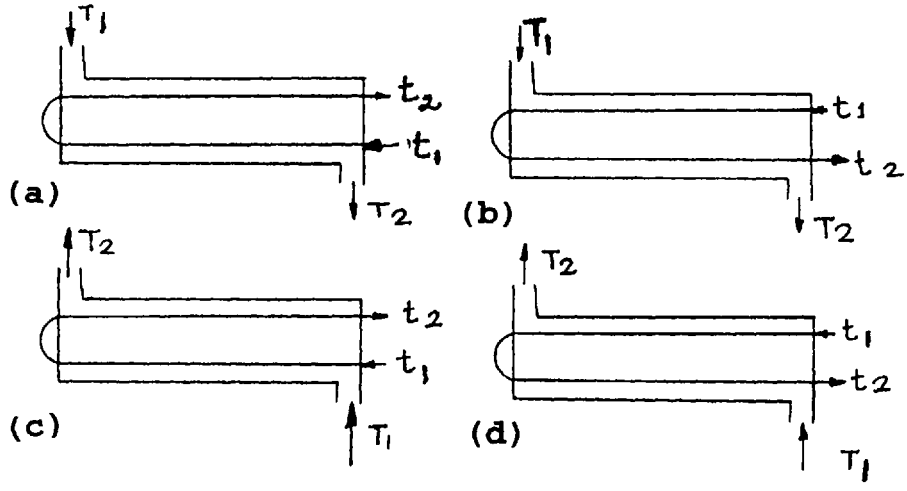


Figure 4 Flow reversibility principle. (Symmetry operations performed on the TEMA $E_{1,2}$ shell.) (Ref. 17.)

$$P_t(R, \text{NTU}) = \frac{P(-R, \text{NTU})}{1 + RP(-R, \text{NTU})} \tag{52}$$

where P denotes the effectiveness of a given arrangement, and P_t that of the same one with fluid direction reversed. The relation is valid under the assumptions of temperature independence of the heat-transfer coefficient and heat capacity rates, when one of the fluids proceeds through the exchanger in a single, mixed stream. In some cases with special symmetry the inversion of both fluids does not alter the geometry, and therefore this property is trivially satisfied. Pignotti [18] illustrates the property of flow reversibility with several examples from the available literature. An example to clarify the meaning of Eq. 52 is given next. Consider the well-known expression for the effectiveness of a parallel flow configuration:

$$P(R, \text{NTU}) = \frac{[1 - \exp[-\text{NTU}(1 + R)]}{(1 + R)} \tag{53}$$

Let us derive from it the expression for the effectiveness of a pure counterflow configuration, which we denote $P_t(R, \text{NTU})$. Equation 52 is applicable, because the counterflow geometry is obtained from parallel flow by inverting the direction of flow of one of the fluids, and the condition that at least one of the fluids should be mixed throughout the exchanger is satisfied. After replacing R by $-R$ in Eq. 53 and performing the elementary algebraic operations indicated in Eq. 52 we obtain the expression for the effectiveness of the counterflow configuration:

$$P_t(R, NTU) = \frac{\{1 - \exp[-NTU(1 - R)]\}}{\{1 - R \exp[-NTU(1 - R)]\}} \tag{54}$$

Observe also that the inversion of one fluid leads from a parallel flow connection to a counterflow one, and likewise, from the latter to the former; therefore, Eq. 52 can be used to go from parallel flow to counterflow and vice versa.

The transformation property of Eq. 52 can also be expressed in terms of the variables referred to the mixed fluid. For example if the thermal relation on the shell side or tube side is known in terms of P_s, R_s, and NTU_s, the thermal relation for the other side P_t, R_t, and NTU_t may be obtained from the relation

$$P_t = R_s P_s, \qquad R_t = \frac{1}{R_s}, \qquad \text{NTU}_t = R_s \text{NTU}_s \tag{55}$$

For example, let the tube-side values of an $H_{1,2}$ exchanger be $P = 0.752$, $R = 0.7$, and NTU = 2.5. Then the shell-side values will be $P = 0.7 \times 0.752$, $R = 1/0.7$, and NTU $= 0.7 \times 2.5$. For $R = 1.0$, both the tube-side and shell-side values are the same.

When the thermal effectiveness is the same for the original case and the invented case, it is referred to as stream symmetric. Typical examples for stream symmetric are parallel flow, counterflow, and crossflow unmixed–unmixed, and mixed–mixed cases.

5. TEMPERATURE APPROACH, MEET, AND CROSS

The meanings of temperature approach, meet, and cross are as follows. In a counterflow exchanger or a multipass exchanger, (1) if the cold fluid outlet temperature $t_{c,o}$ is less than the hot fluid outlet temperature $t_{h,o}$, then this condition is referred to as temperature approach; (2) if $t_{c,o} = t_{h,o}$, this condition is referred to as temperature meet; and (3) if $t_{c,o}$ is greater than $t_{h,o}$, the difference $(t_{c,o} - t_{h,o})$ is referred to as the temperature cross or temperature pinch. In this case, the temperature approach $(t_{h,o} - t_{c,o})$ is negative and loses its meaning. The underlying meanings of these three cases are brought out in Table 3.

Table 3 Temperature Approach, Meet, and Cross

Temperature approach	Temperature meet	Temperature cross
$t_{h,i} \rightarrow t_{h,o}$	$t_{h,i} \rightarrow t_{h,o}$	$t_{h,i} \rightarrow t_{h,o}$
$t_{c,o} \leftarrow t_{c,i}$	$t_{c,o} \leftarrow t_{c,i}$	$t_{c,o} \leftarrow t_{c,i}$
$t_{c,o} < t_{h,o}$	$t_{c,o} = t_{h,o}$	$t_{c,o} > t_{h,o}$

The temperature cross is undesirable, particularly for shell and tube exchangers, because the tube surface area is not utilized effectively and hence there is wastage of capital cost. This phenomenon is explained in detail by Shah [2] and is briefly dealt with here with reference to an $E_{1\text{-}2}$ exchanger.

Two possible shell fluid directions with respect to the tube fluid direction are shown in Fig. 5. The temperature distributions of Fig. 5(b) reveal that there is a temperature cross. In region X, the second tube pass transfers heat to the shell fluid. This is contrary to the design objective, in which ideally the heat transfer should have taken place only in one direction [from the shell fluid to the tube fluid, as shown in Fig. 5(a)] throughout the two passes. The reason for this temperature cross is as follows: Although an addition of surface area (a high value of NTU_t or a low value of F) is effective in raising the temperature of the tube fluid and rises in the second pass up to point X, beyond this point the temperature of the shell fluid is lower than that of the tube fluid, since we have considered the shell fluid mixed at a cross section and it is cooled rapidly by the first pass. Thus, the addition of the surface area in the second tube pass left of point X is useless from the thermal design point of view. A "good" design avoids the temperature cross in a shell and tube exchanger. Theoretically, the optimum design would have the temperature cross point just at the end of the second tube pass, which will satisfy the condition.

$$t_{t,o} = t_{s,o} \qquad \text{or } t_{t,o} - t_{s,o} = 0 \tag{56}$$

This condition leads to the following formula:

$$P = \frac{1}{1+R} \tag{57}$$

Thus for a given R, Eq. 57 provides the limiting (maximum) value of P. Corresponding to P and R, the limiting (maximum) value of NTU_t beyond which there will be a temperature cross can be determined from its thermal relation formula. Therefore, from P, R, and NTU, F can be calculated. This F value is known as the F_{min} value beyond which there will be a temperature cross. This is illustrated for an $E_{1\text{-}2}$ exchanger here. For a known value of R, determine the limiting value of P from Eq. 57 and NTU from the following equation:

$$\text{NTU} = \frac{1}{(1+R^2)^{0.5}} \ln\left[\frac{2 - P[R + 1 - (1+R^2)^{0.5}]}{2 - P[R + 1 + (1+R^2)^{0.5}]}\right] \tag{58}$$

For known values of P, R, and NTU, determine F from Eq. 36.

5.1 Temperature Cross for Other TEMA Shells

Temperature cross for other TEMA shells such as $G_{1\text{-}2}$, $H_{1\text{-}2}$, and $J_{1\text{-}2}$ can be evaluated from Eq. 57 [19]. The F_{min} curves for $G_{1\text{-}2}$, $H_{1\text{-}2}$, and $J_{1\text{-}2}$ cases are given in the next section.

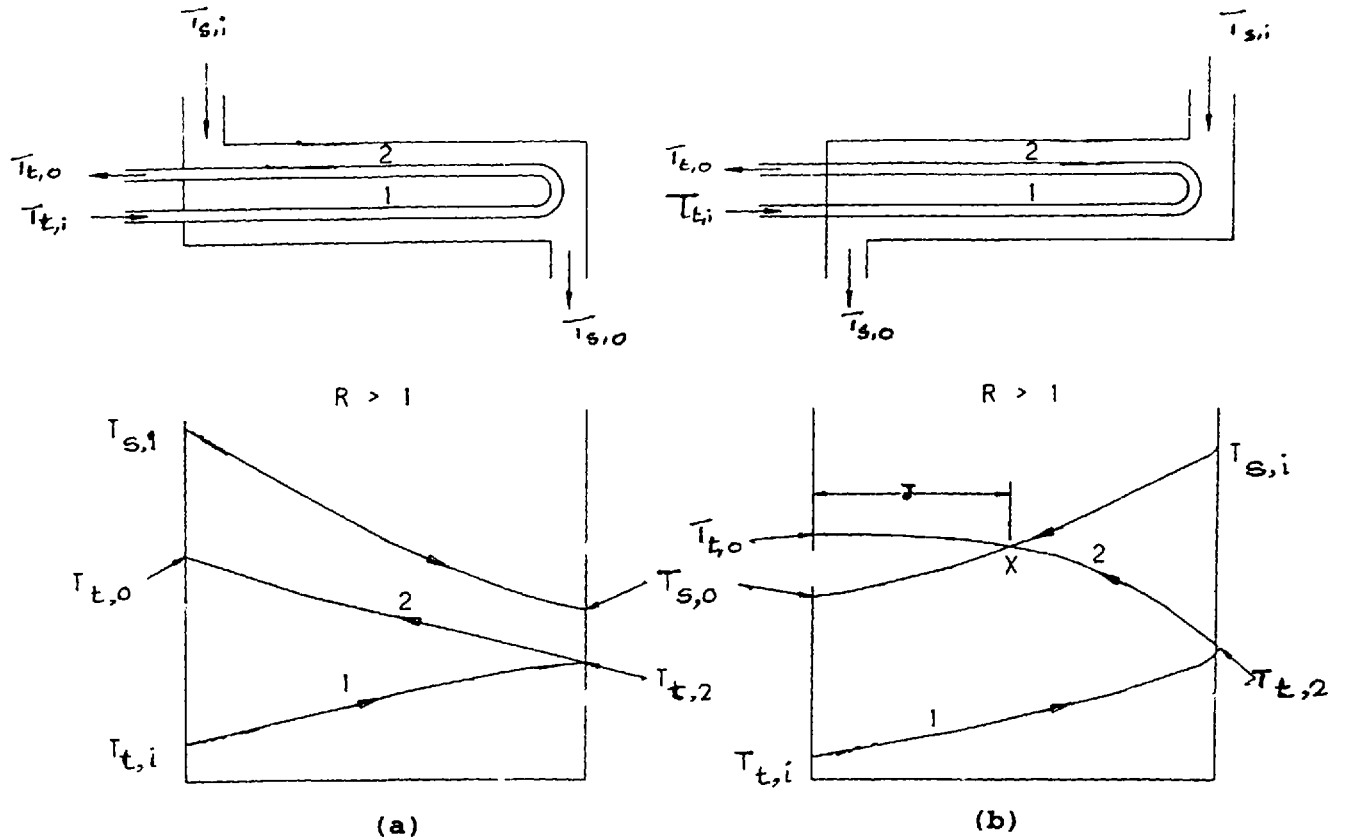


Figure 5 Temperature distribution in a $E_{1,2}$ exchanger. (a) Without temperature cross; (b) with temperature cross [1].

6. THERMAL RELATION FORMULAS FOR VARIOUS FLOW ARRANGEMENTS AND PASS ARRANGEMENTS

The heat exchanger effectiveness is defined as the ratio of the overall temperature drop of the weaker stream to the maximum possible temperature difference between the fluid inlet temperatures. The following assumptions are commonly made in deriving thermal effectiveness.

1. The overall heat-transfer coefficient is constant throughout the exchanger.
2. Each pass has the same heat-transfer area; that is, unsymmetrical pass arrangements are not considered.
3. There is no phase change.
4. The specific heat of each fluid is constant and independent of temperature.
5. The flow rates of both streams are steady.
6. The flow of both fluids is evenly distributed over both the local and the total transfer area.
7. Heat losses from the system are negligible.

In this section, thermal relation formulas for (1) various flow arrangements—parallel flow, counterflow, and crossflow, (2) various types of heat exchangers—compact and shell and tube, and (3) multipass arrangements or multiple units of both compact and shell and tube heat exchangers are presented. Most of the formulas are tabulated and the thermal effectiveness charts are given. Mostly counterflow arrangements are considered. For shell and tube exchangers, formulas are given for both parallel flow and counterflow, but thermal effectiveness charts are given only for counterflow arrangements referred to tube side (similar to TEMA Standards). Thermal effectiveness relations referred to the shell side can be derived from the "flow reversibility" principle. Wherever thermal effectiveness relations are not given for parallel flow arrangements can be easily derived (wherever applicable) from the "flow reversibility" principle. Customarily, the ε-NTU method is employed for compact heat exchangers. In this method, the capacity ratio C^* is always ≤ 1. Hence, thermal effectiveness charts are given in terms of ε–C^*–NTU, and wherever possible, the thermal effectiveness charts are given in terms of P–R–F–NTU, instead of ε–C^*–NTU.

6.1 Parallel Flow

For a given set of values of C^* or R, and NTU, (1) the thermal effectiveness is much lower for parallel flow than for counterflow arrangement, except in the limiting case $C^* = R = 0$, where it is the same for both cases and approaches unity as NTU increases to infinity, and (2) at a given value of NTU, the effectiveness increases with decreasing capacity ratio, C^* or R. The formula for thermal effectiveness is given by Eq. T1 in Table 4 and the thermal effectiveness chart is given in Fig. 6.

6.2 Counterflow

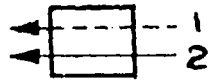
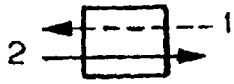
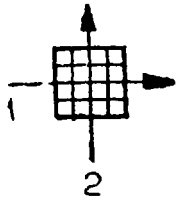
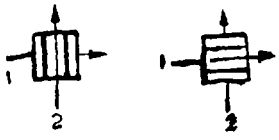
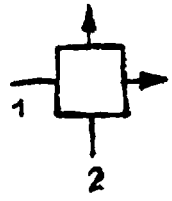
Among the various flow arrangements, counterflow has the highest thermal effectiveness. For counterflow exchangers, at a given value of NTU, the effectiveness increases with decreasing capacity ratio, C^* or R. The formula for thermal effectiveness is given by Eq. T2 in Table 4 and the thermal effectiveness chart is given in Fig. 7.

6.3 Crossflow Arrangement

Unmixed–Unmixed Crossflow

This is an industrially important arrangement representing the case of a large number of unmixed channels in both sides. The original solution was due to Nusselt [20] and was later

Table 4 Thermal Effectiveness Relations for Basic Cases

Flow arrangement	Eq. no./ Ref.	General formula	Value for R = 1 and special cases
 Parallel flow; stream symmetric.	T1	$P = \dfrac{1 - e^{-\mathrm{NTU}(1+R)}}{1+R}$	$P = \dfrac{1}{2}[1 - e^{(-2\mathrm{NTU})}]$ for $R = 1$ $= 1 - e^{-\mathrm{NTU}}$ for $R = 0$ $P_{max} = 50\%$ for $R = 1$
 Counterflow; stream symmetric	T2	$P = \dfrac{1 - e^{-\mathrm{NTU}(1-R)}}{1 - Re^{-\mathrm{NTU}(1-R)}}$	$P = \dfrac{\mathrm{NTU}}{1 + \mathrm{NTU}}$ for $R = 1$ $= 1 - e^{-\mathrm{NTU}}$ for $R = 0$
 Crossflow; Both the fluids unmixed; stream symmetric.	T3 [25]	$P = \dfrac{1}{R\mathrm{NTU}} \sum_{k=0}^{\infty} \left\{ \left[1 - e^{-\mathrm{NTU}} \sum_{m=0}^{k} \dfrac{\mathrm{NTU}^m}{m!} \right] \left[1 - e^{-R\mathrm{NTU}} \sum_{m=0}^{k} \dfrac{(R\mathrm{NTU})^m}{m!} \right] \right\}$ For $R = 1$, this equation holds.	
	T4 [22]	$\varepsilon = 1 - e^{[-(1+C^*)\mathrm{NTU}]} \left[I_0(2\,\mathrm{NTU}\sqrt{C^*}) + \sqrt{C^*}\, I_1(2\,\mathrm{NTU}\sqrt{C^*}) - \dfrac{1 - C^*}{C^*} \sum_{n=2}^{\infty} C^{*\,n/2} I_n(2\,\mathrm{NTU}\sqrt{C^*}) \right]$ For $C^* = 1$. $\varepsilon = 1 - e^{-2\mathrm{NTU}} [I_0(2\,\mathrm{NTU}) + I_1(2\,\mathrm{NTU})]$	
Crossflow; one fluid mixed and the other fluid unmixed: (1) weaker/C_{min} fluid unmixed; (2) stronger/ C_{max} fluid unmixed	T5 [23]	$\varepsilon_1 = 1 - \exp\left\{ \dfrac{\mathrm{NTU}^{0.22}}{C^*} [\exp(-C^*\mathrm{NTU}^{0.78}) - 1] \right\}$ Weaker/C_{min} fluid mixed $P_1 = [1 - \exp(-K/R)]$ $K = 1 - \exp(-R\mathrm{NTU})$	
	T6	Stronger/C_{max} fluid mixed	
	T7	$P_1 = \dfrac{[1 - \exp(-KR)]}{R}$ $K = 1 - \exp(-\mathrm{NTU})$	$P_1 = 1 - e^{-1 + e^{-\mathrm{NTU}}}$
 Crossflow; mixed–mixed flow; stream symmetric same as $J_{1-\infty}$	T8	$P = \dfrac{1}{\left(\dfrac{1}{K_1} + \dfrac{R}{K_2} - \dfrac{1}{\mathrm{NTU}} \right)}$ $K_1 = 1 - e^{(-\mathrm{NTU})}$ $K_2 = 1 - e^{(-R\mathrm{NTU})}$	$P = \dfrac{1}{\dfrac{2}{K_1} - \dfrac{1}{\mathrm{NTU}}}$

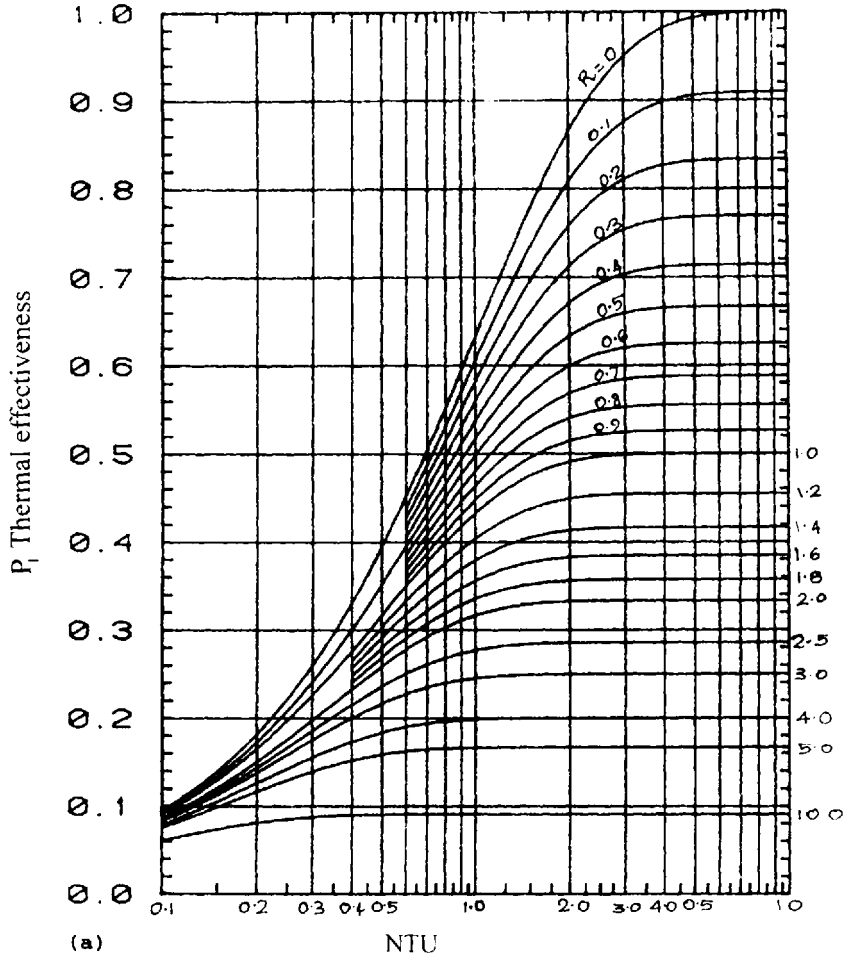


Figure 6 (a) Parallel flow; stream symmetric, R-P-NTU chart.

reformulated into a more manageable equation by Mason [21]. Mason's formula is given by Eq. T3 in Table 4, and this equation can be used for P–NTU–R relation. Baclic [22] presents Nusselt's equation in terms of a modified Bessel function of the first kind as given in Eq. T4 in Table 4; Eckert [23] provide a simplified formula without involving Bessel function as given by Eq. T5 in Table 4, and this equation predicts ε within ±1% of ε from Eq. T4 of Table 4 for $1 < \text{NTU} < 7$; Eqs. T4 and T5 can be used for formulas involving $C^* \leq 1$ only. The thermal effectiveness chart as per Eq. T3 is given in Fig. 8 and as per Eq. T4 is given in Fig. 9.

Unmixed–Mixed Crossflow

In this arrangement, one fluid is mixed and the other is unmixed. A typical example is a bare tube compact heat exchanger in which the fluid outside the tube is mixed, whereas the tube-side fluid is unmixed. There are two possible cases: (1) weaker fluid ($C_{\min}$) is mixed, and (2) stronger fluid ($C_{\max}$) is mixed. Formulas for thermal effectiveness for the weaker fluid mixed are given by Eq. T6 and for the stronger fluid mixed by Eq. T7 in Table 4. The thermal

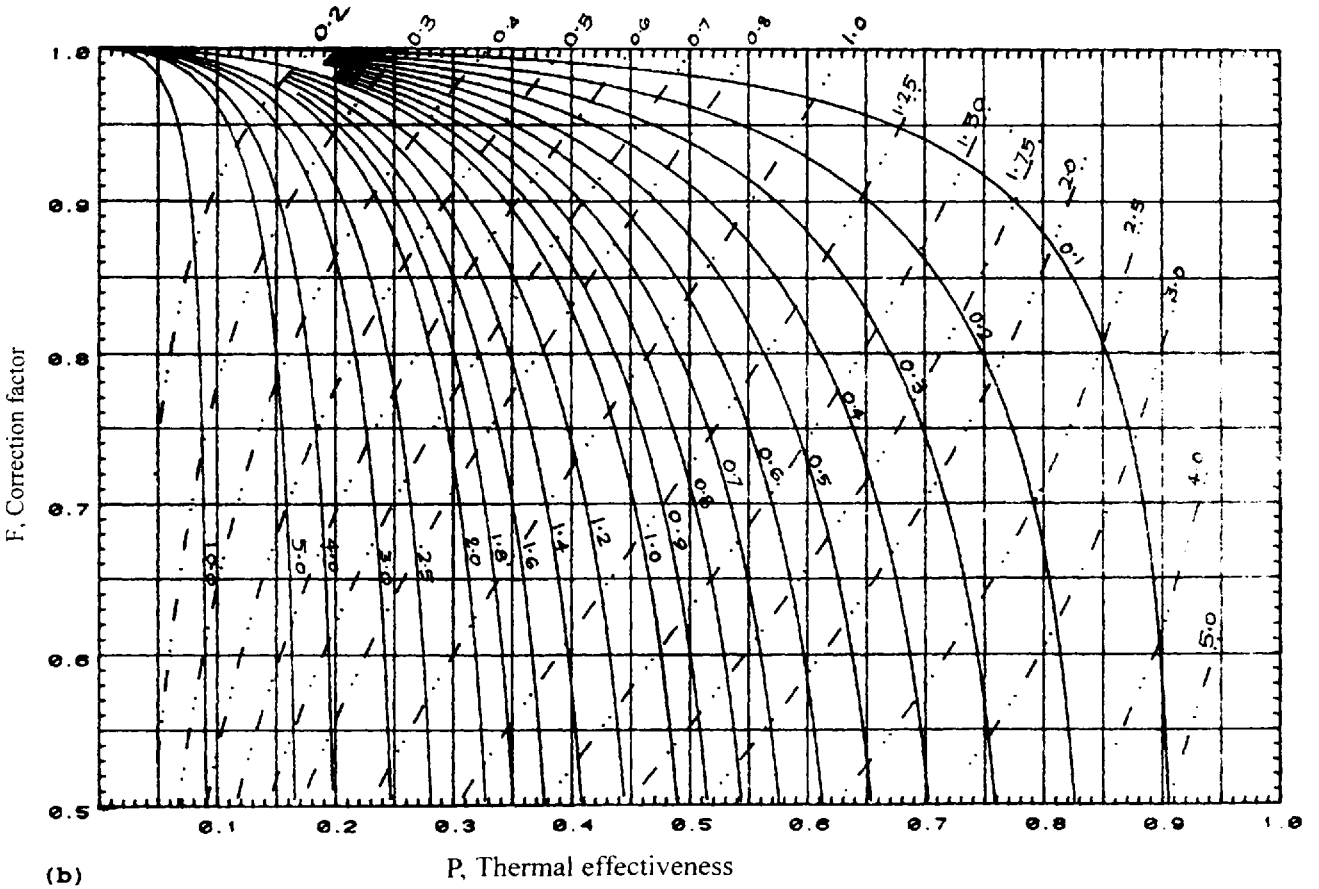


Figure 6 (b) Parallel flow; stream symmetric, F-R-P-NTU chart; F as a function of P for constant R (solid lines) and constant NTU (dashed lines).

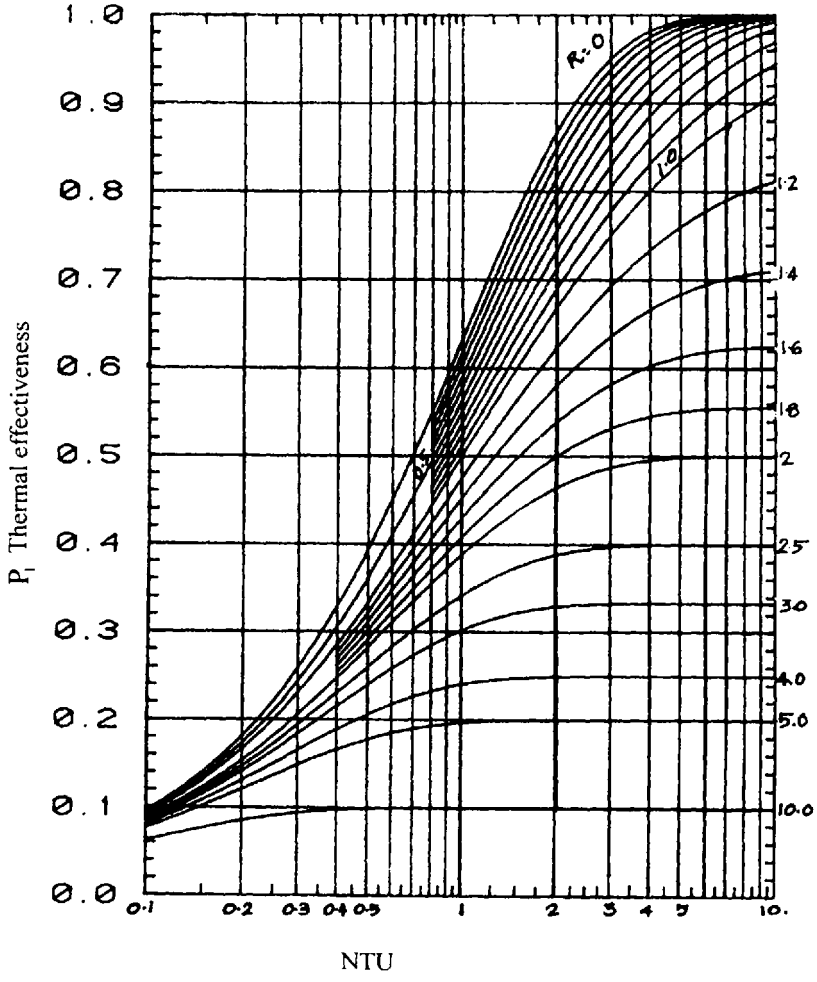


Figure 7 Counterflow; stream symmetric, R-P-NTU chart.

effectiveness charts are given in Fig. 10 for the weaker fluid mixed and Fig. 11 for the stronger fluid mixed. For $R = 1$ or $C^* = 1$, the thermal effectiveness is the same for both cases.

Mixed–Mixed Crossflow

This case has no industrial application and is shown here only as an extreme of the crossflow arrangement. The solution is identical to the TEMA J shell with infinite tube-side passes. The formula for thermal effectiveness is given by Eq. T8 in Table 4.

Single or Multiple Rows in Crossflow

Many process heat exchangers provide a crossflow arrangement between the hot (or cold) process fluid that flows through the tubes and the external coolant (or hot air such as supercharged engine intake air), usually air. Because this flow arrangement is not strictly countercurrent, the MTD must be corrected by applying a correction factor, F. The factor F depends on the terminal temperatures, the number of tube rows per pass, and the number of passes. The basic unmixed–unmixed case, shown in Fig. 12, assumes a large number of flow channels in

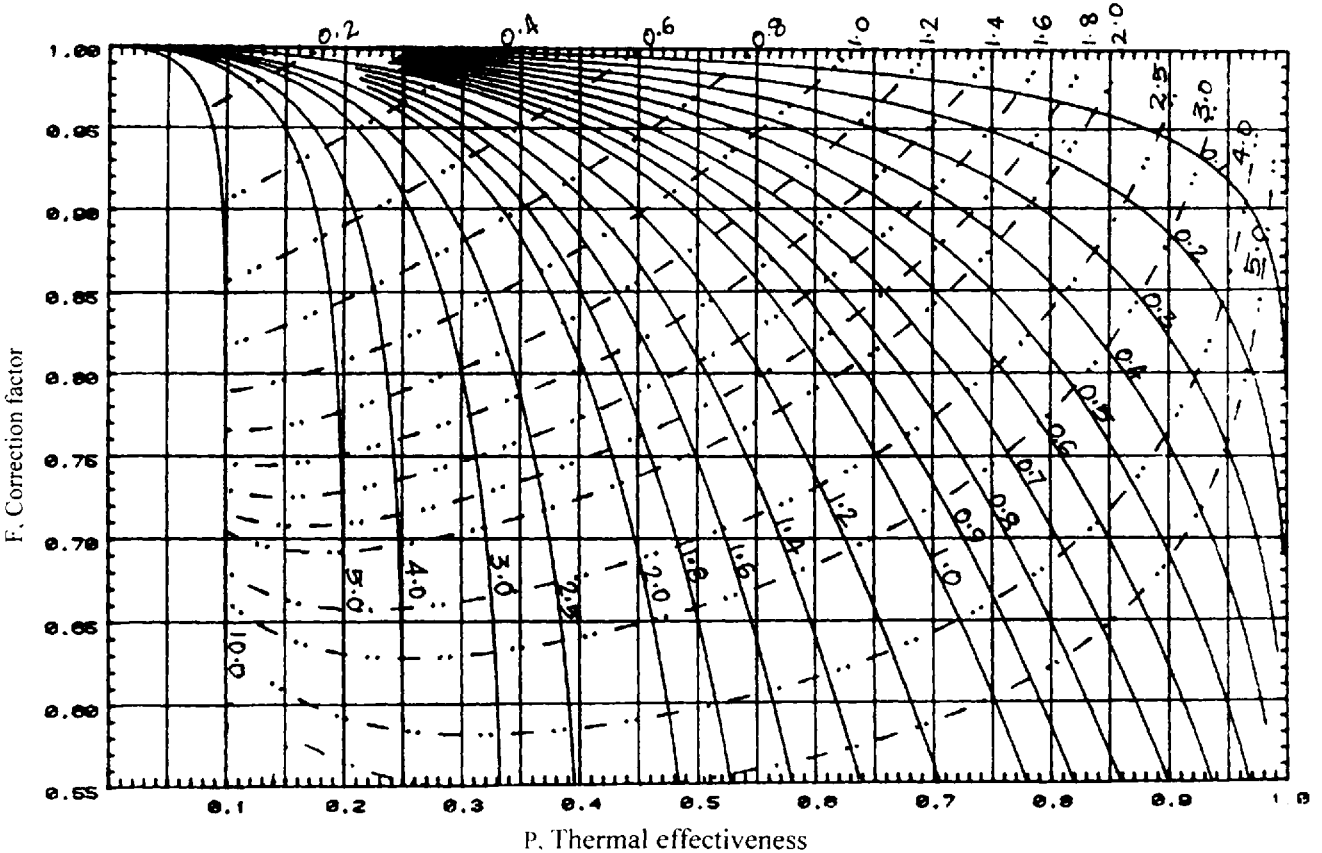


Figure 8 Crossflow; both the fluids unmixed; stream symmetric; F-R-P-NTU chart; F as a function of P for constant R (solid lines) and constant NTU (dashed lines).

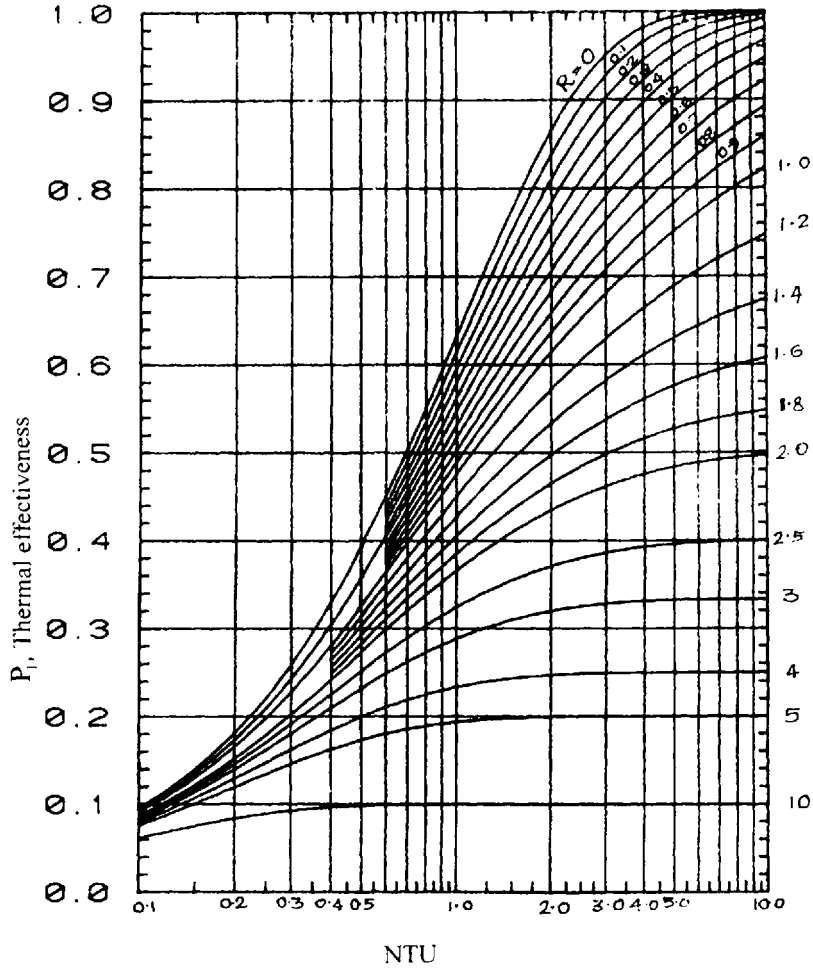


Figure 9 Crossflow; both the fluids unmixed; stream symmetric; R-P-NTU chart.

both streams. For a single tube-side pass with one or more tube rows the thermal effectiveness formula is different from that of the basic unmixed–unmixed case. Thermal relations for single-pass tube rows arrangements are discussed next.

Single Tube-Side Pass, N Rows per Pass, Both Fluids Unmixed. A common header at one end of the tubes distributes the tube-side fluid into a single pass having N rows in parallel. A similar header at the other end collects tube-side fluid. For given terminal temperatures, F increases with the number of rows per pass and the number of passes being increased and is more sensitive to the latter. Taborek [24], Pignotti and Cordero [25], and Pignotti, [26] present values of F for a variety of crossflow configurations, applicable to air-cooled heat exchangers.

Schedwill's formula for the thermal effectiveness of N rows is given by [27]:

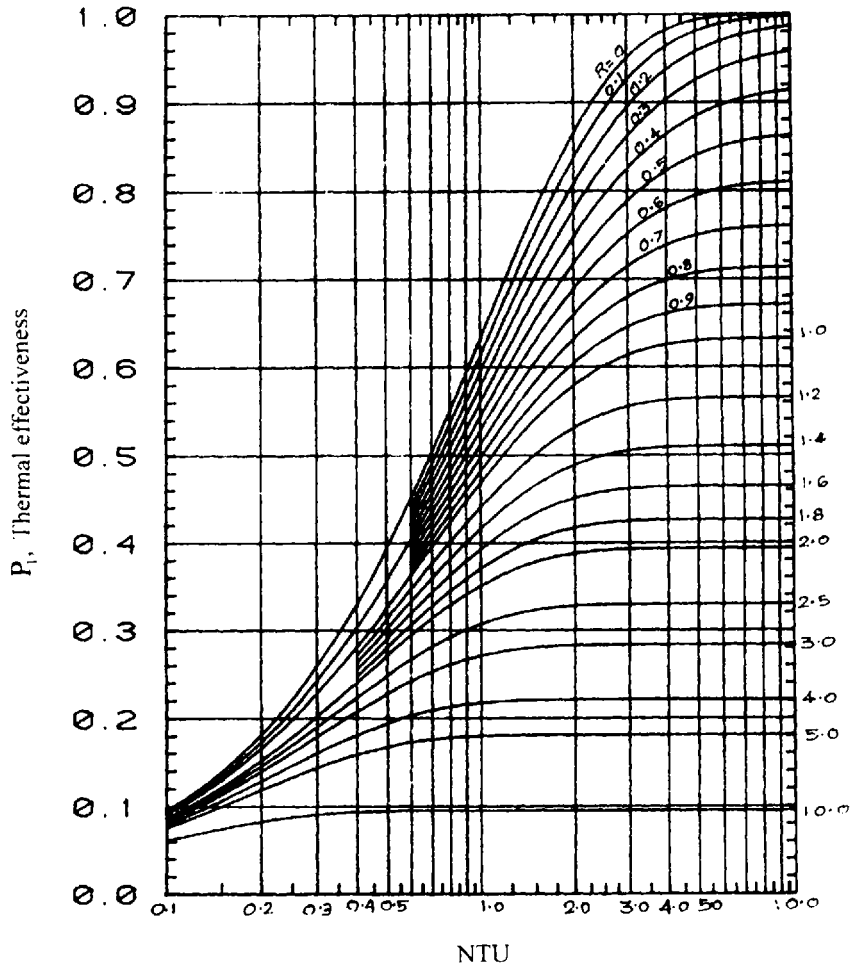


Figure 10 (a) Crossflow: unmixed-mixed-the weaker/C_{min} fluid mixed, R-P-NTU chart; (b) F-R-P-NTU chart. F as a function of P for constant R (solid lines) and constant NTU (dashed lines).

$$P = \frac{1}{R}\left\{1-\left[\frac{Ne^{NKR}}{1+\sum_{i=1}^{N-1}\sum_{j=0}^{i}\binom{i}{j}K^i e^{-(i-j)NTU/N}\sum_{k=0}^{j}\frac{(NKR)^k}{k!}}\right]\right\}^{-1} \tag{59}$$

where

$$\binom{i}{j} = \frac{i!}{(i-j)!j!} \tag{60}$$

that is, the number of combinations of i and j taken j at a time, and

$$K = 1 - \exp\left(-\frac{NTU}{N}\right) \tag{61}$$

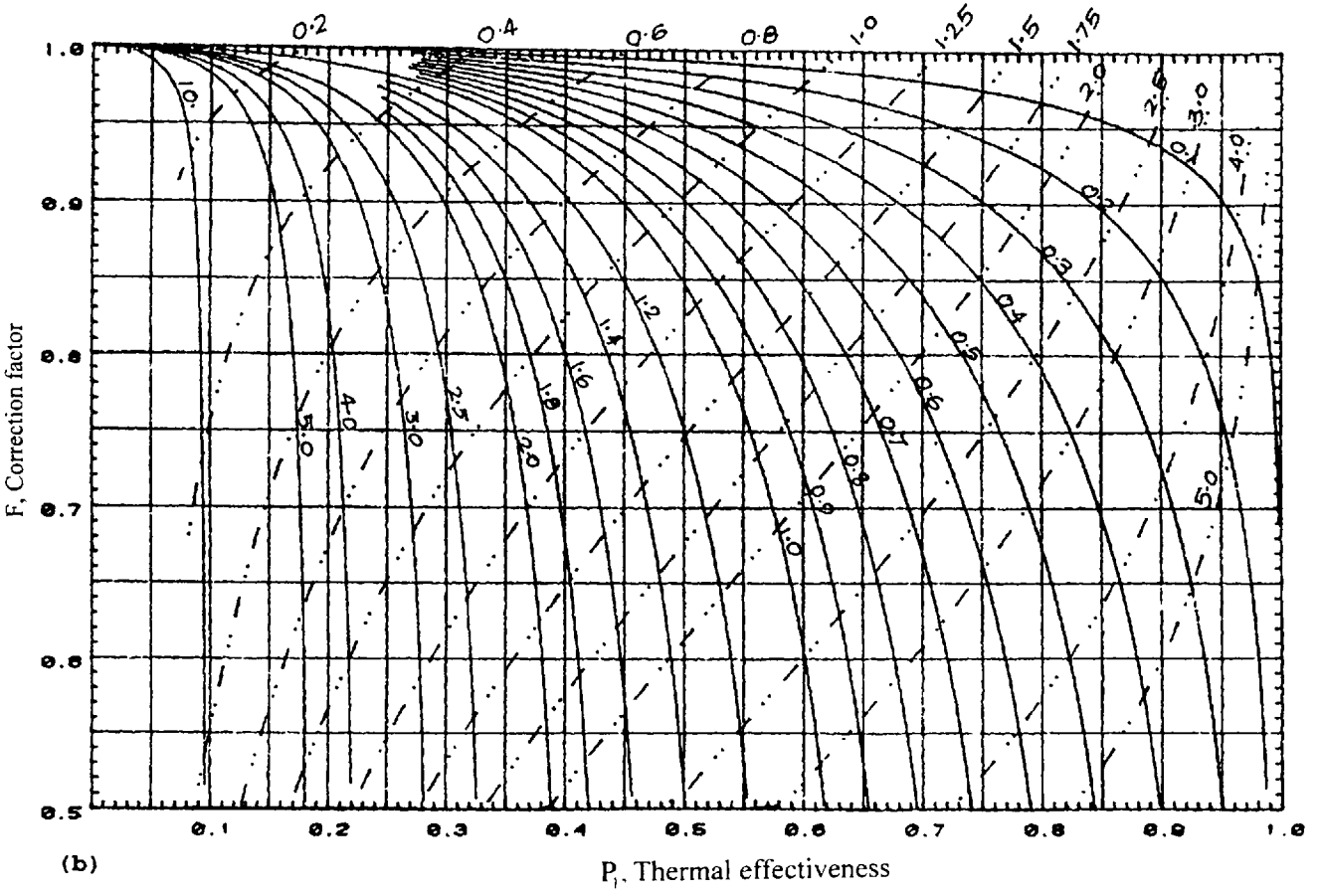


Figure 10 Continued.

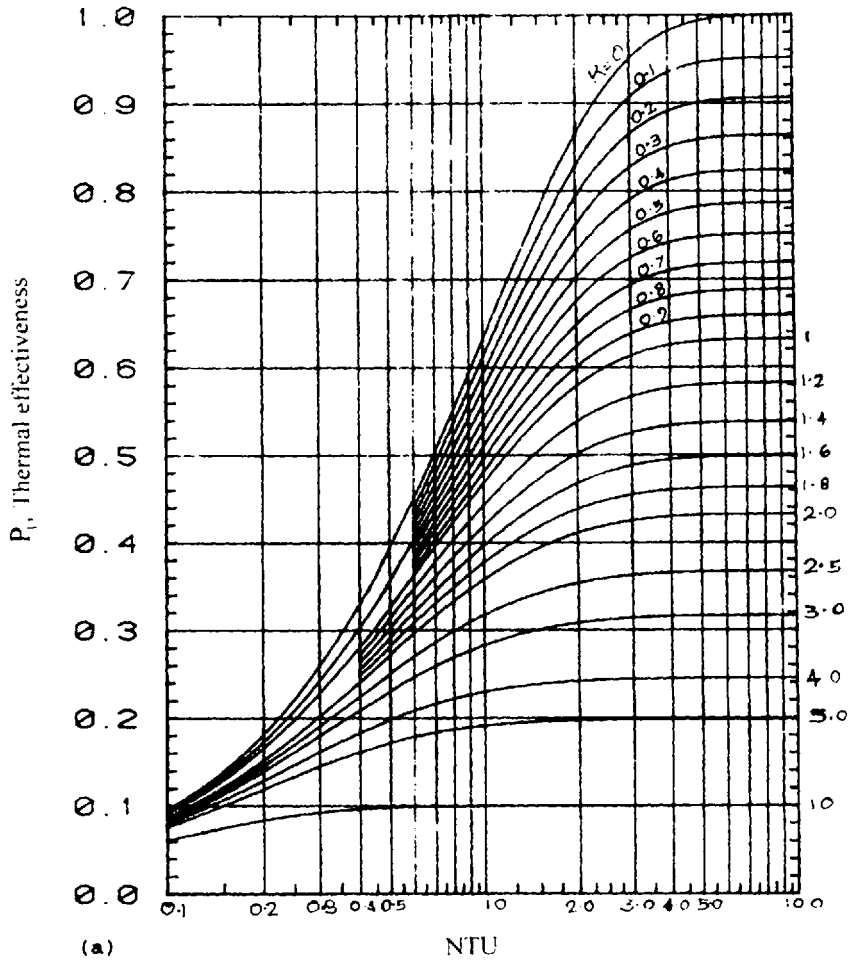


Figure 11 (a) Crossflow: unmixed-mixed-the stronger/C_{min} fluid mixed, ε-C*-NTU chart; (b) F-R-P-NTU chart; F as a function of P for constant R (solid lines) and constant NTU (dashed lines).

By substituting $N = 1,2,3,\ldots$ in Eqs. 59 and 61, equations for thermal relations are obtained for the specific arrangements by Nicole [28], and this is given in Table 5 (Eqs. T9–T12) for one row, two rows, three rows, and four rows. For a larger number of tube rows (for all practical purposes, when N exceeds 5), the solution approaches that of unmixed-unmixed crossflow arrangement. Values of F for $N = 1,2,3,4$ are shown in Figs. 13–16 and are always less than the basic case of unmixed–unmixed crossflow (Fig. 8).

Multipass Tube Rows Cross-Counterflow Arrangements, Both Fluids Unmixed, and Multiple Tube Rows in Multipass Tube Rows, Cross-Counterflow Arrangements. This would apply to a manifold-type air cooler in which the tubes in one row are connected to the next by U-bends. The solutions are based on Ref. 28. Solutions for the 2 rows–2 pass and 3 rows–3 pass cases are based on Stevens et al. [29]. The general formula for thermal effectiveness referred to the air side (fin side) is given by [28]:

$$P_1 = \frac{1}{R}\left(1 - \frac{1}{\zeta}\right) \tag{62}$$

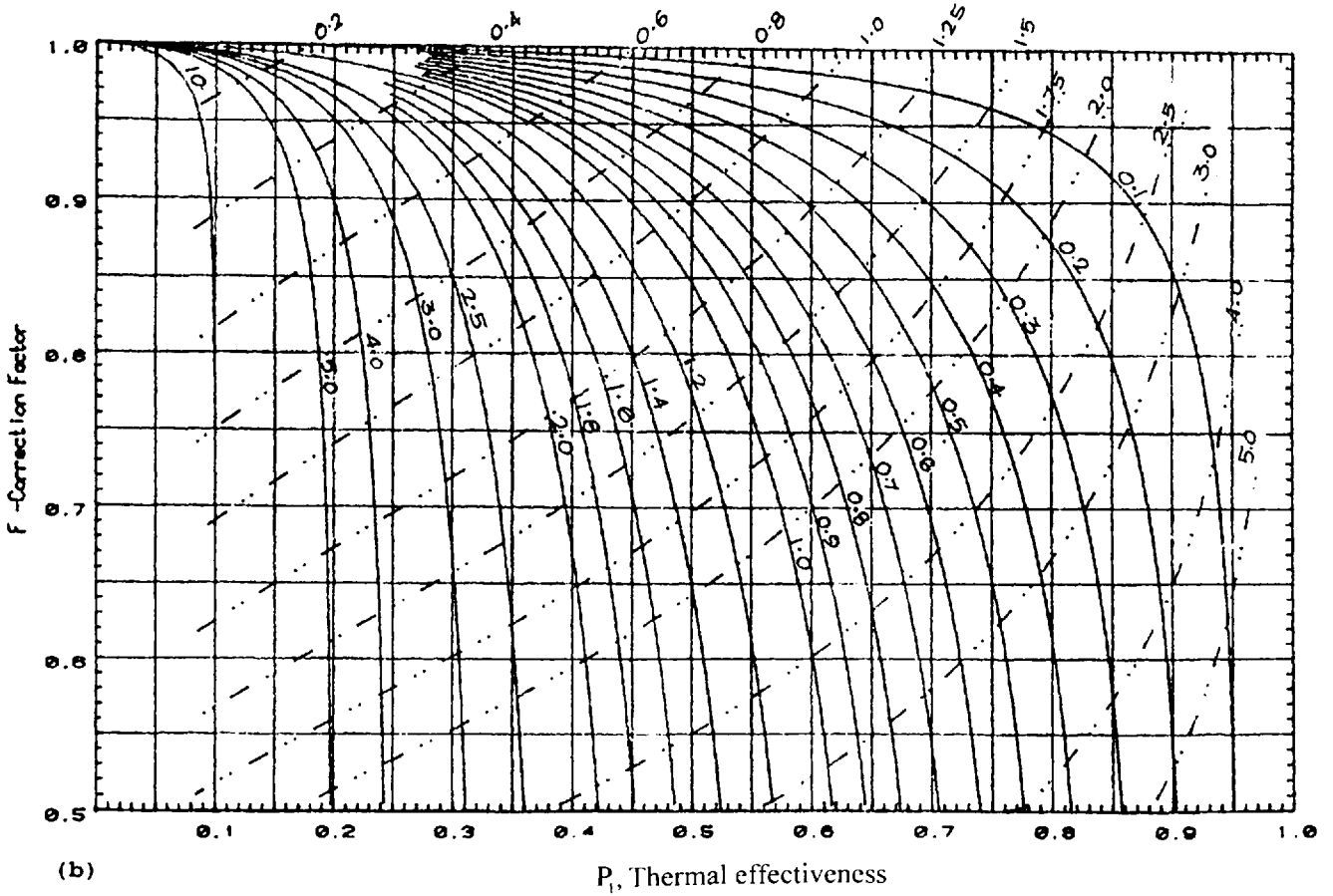


Figure 11 Continued.

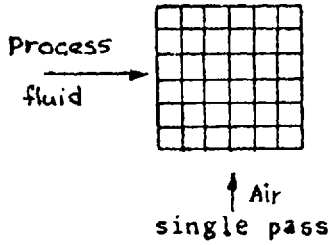


Figure 12 Unmixed-unmixed crossflow arrangement.

The expressions for ζ for various cases are as follows:

1. Two tube rows, two passes, as shown in Fig. 17a [29]:

$$\zeta = \frac{K}{2} + \left(1 - \frac{K}{2}\right)e^{2KR} \tag{63a}$$

$$K = 1 - \exp\left(-\frac{\text{NTU}}{2}\right) \tag{63b}$$

2. Three tube rows, three passes as shown in Fig. 17b [29]:

$$\zeta = K\left[1 - \frac{K}{4} - RK\left(1 - \frac{K}{2}\right)\right]e^{KR} + e^{3KR}\left(1 - \frac{K}{2}\right)^2 \tag{64a}$$

$$K = 1 - \exp\left(-\frac{\text{NTU}}{3}\right) \tag{64b}$$

3. Four tube rows, four passes as shown in Fig. 17c [28]:

$$\zeta = \frac{K}{2}\left(1 - \frac{K}{2} + \frac{K^2}{4}\right) + K\left(1 - \frac{K}{2}\right)\left[1 - \frac{R}{8}K\left(1 - \frac{K}{2}\right)e^{2KR}\right] + e^{4KR}\left(1 - \frac{K}{2}\right)^3 \tag{65a}$$

$$K = 1 - \exp\left(-\frac{\text{NTU}}{4}\right) \tag{65b}$$

4. Five tube rows, five passes [28]:

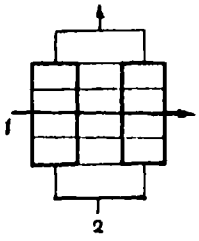
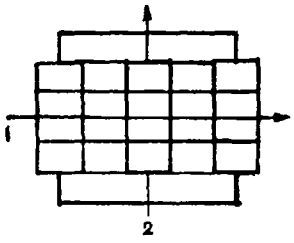
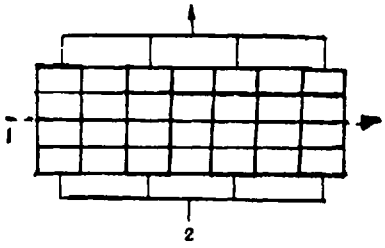
$$\zeta = \left\{K\left(1 - \frac{3}{4}K + \frac{K^2}{2} - \frac{K^3}{8}\right) - RK^2\left[1 - K + \frac{3}{4}K^2 - \frac{1}{4}K^3 - \frac{R}{2}K^2\left(1 - \frac{K}{2}\right)^2\right]\right\}e^{KR}$$
$$+ \left[K\left(1 - \frac{3}{4}K + \frac{1}{16}K^3\right) - 3RK^2\left(1 - \frac{K}{2}\right)^3\right]e^{3KR} + \left(1 - \frac{K}{2}\right)^4 e^{5KR} \tag{66a}$$

$$K = 1 - \exp\left(-\frac{\text{NTU}}{5}\right) \tag{66b}$$

5. Six tube rows, six passes [28]:

$$\zeta = \frac{K}{2}\left(1 - K + K^2 - \frac{1}{2}K^3 + \frac{1}{8}K^4\right) + K\left(1 - K + \frac{3}{4}K^2 - \frac{5}{16}K^3 + \frac{1}{32}K^4\right)e^{2KR}$$
$$- RK^2\left[2 - 3K + 3K^2 - \frac{7}{4}K^3 + \frac{3}{8}K^4 - RK^2\left(2 - 3K + \frac{3}{2}K^2 - \frac{1}{4}K^3\right)\right]e^{2KR}$$
$$+ \left[\frac{K}{2}\left(2 - 2K + \frac{1}{2}K^3 - \frac{1}{8}K^4\right) - 4KR^2\left(1 - \frac{K}{2}\right)^4\right]e^{4KR} + \left(1 - \frac{K}{2}\right)^5 e^{6KR} \qquad (67a)$$

Table 5 Thermal Effectiveness Relations for Tube Rows with Single Pass Arrangement

Flow arrangement	Eq. no.	General formula, Ref. (28) Note-These formulas are valid for R = 1.
One tube row. 	T9 [28]	$P_1 = \frac{1}{R}(1 - e^{-KR})$ $K = 1 - \exp(-\mathrm{NTU})$
Two tube rows. 	T10 [28]	$P_1 = \frac{1}{R}[1 - e^{-2KR}(1 + RK^2)]$ $K = 1 - \exp\left(-\frac{\mathrm{NTU}}{2}\right)$
Three tube rows. 	T11 [28]	$P_1 = \frac{1}{R}\left\{1 - \left[\frac{e^{3KR}}{1 + RK^2(3 - K) + (3/2)R^2K^4}\right]^{-1}\right\}$ $K = 1 - \exp\left(-\frac{\mathrm{NTU}}{3}\right)$
Four tube rows. 	T12 [28]	$P_1 = \frac{1}{R}\left\{1 - \left[\frac{e^{4KR}}{[1 + RK^2(6 - 4K + K^2) + 4R^2K^4(2 - K) + (8/3)R^3K^6}\right]^{-1}\right\}$ $K = 1 - \exp(-\mathrm{NTU}/4)$

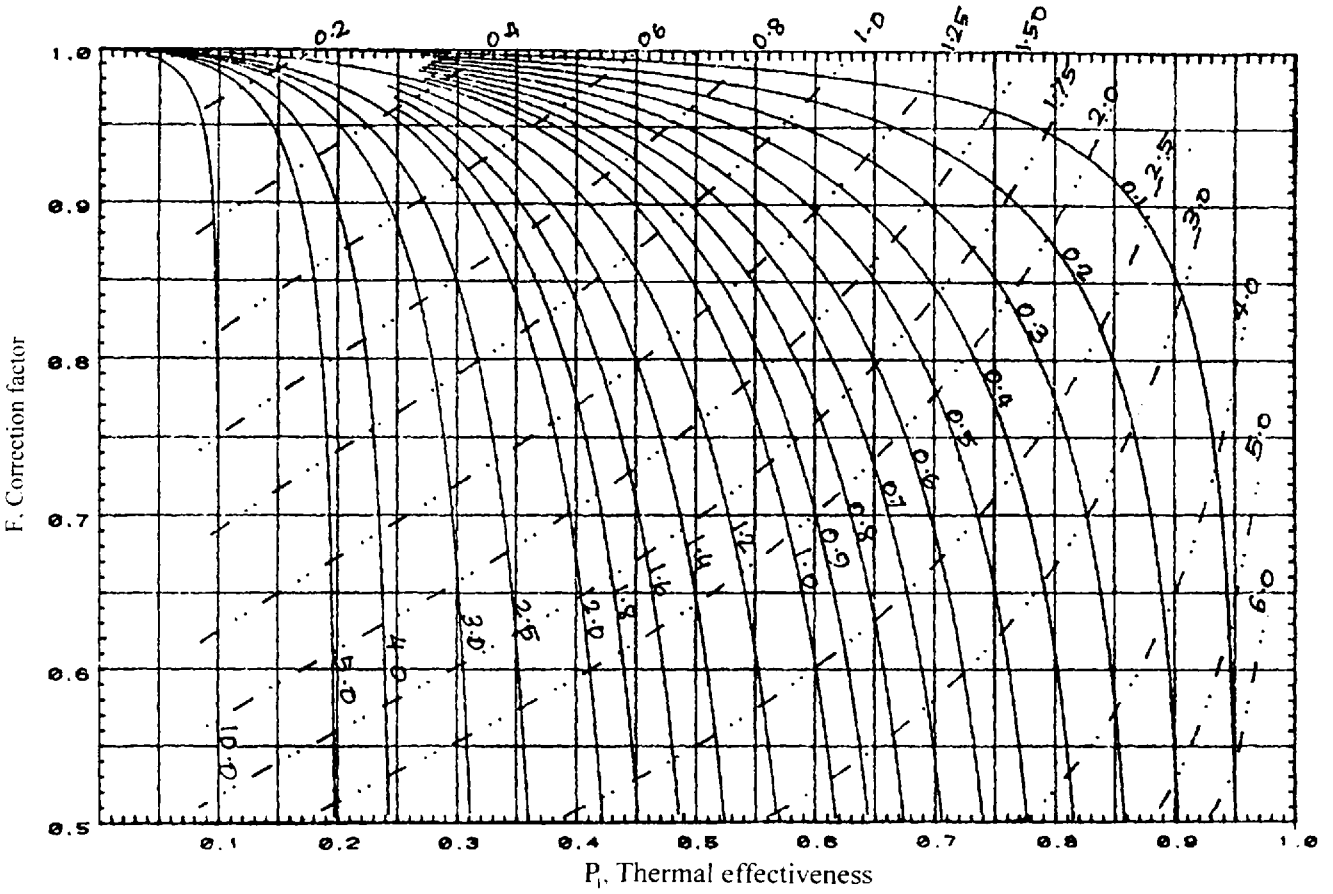


Figure 13 One tube row; F as a function of P for constant R (solid lines) and constant NTU (dashed lines).

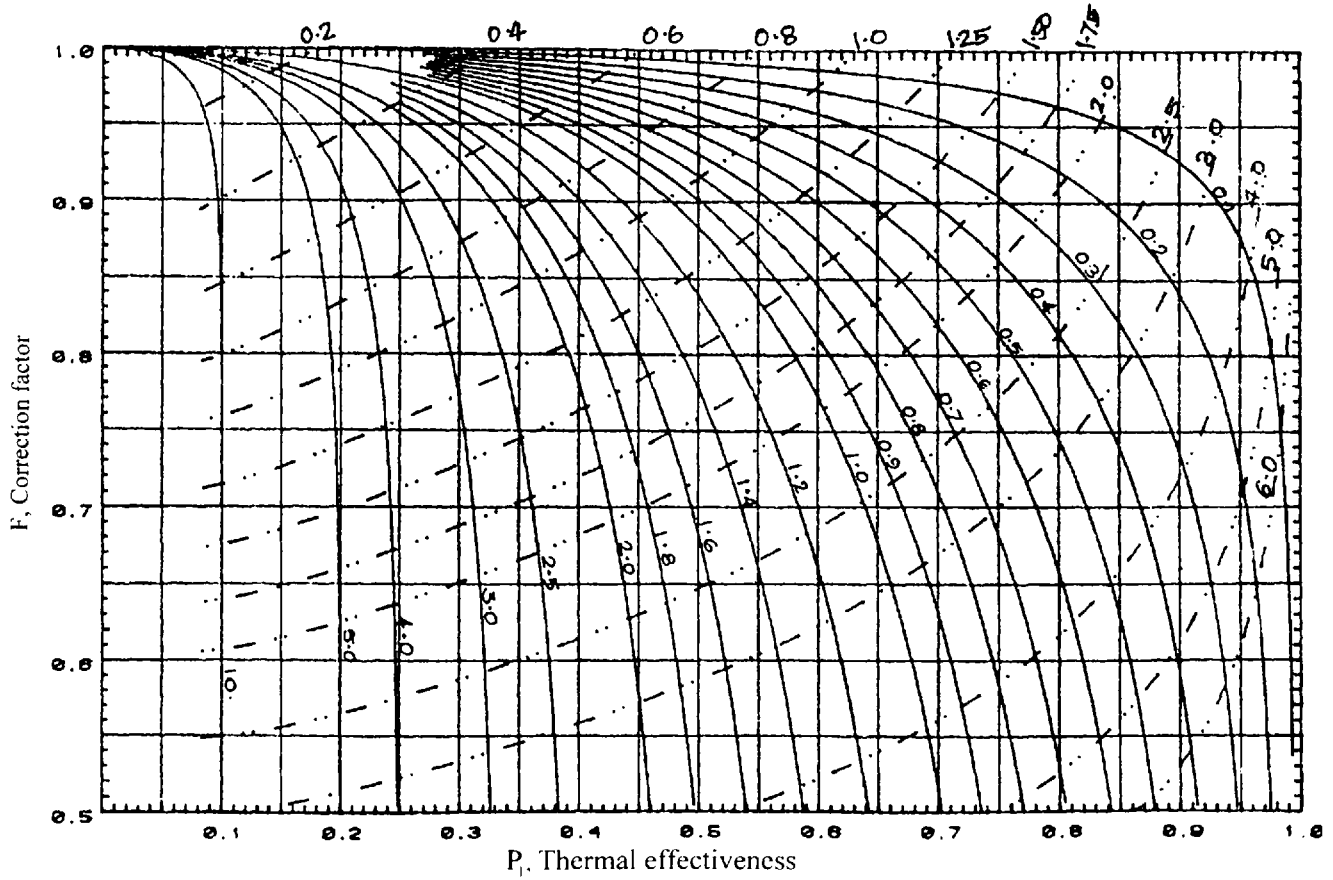


Figure 14 Two tube rows; F as a function of P for constant R (solid lines) and constant NTU (dashed lines).

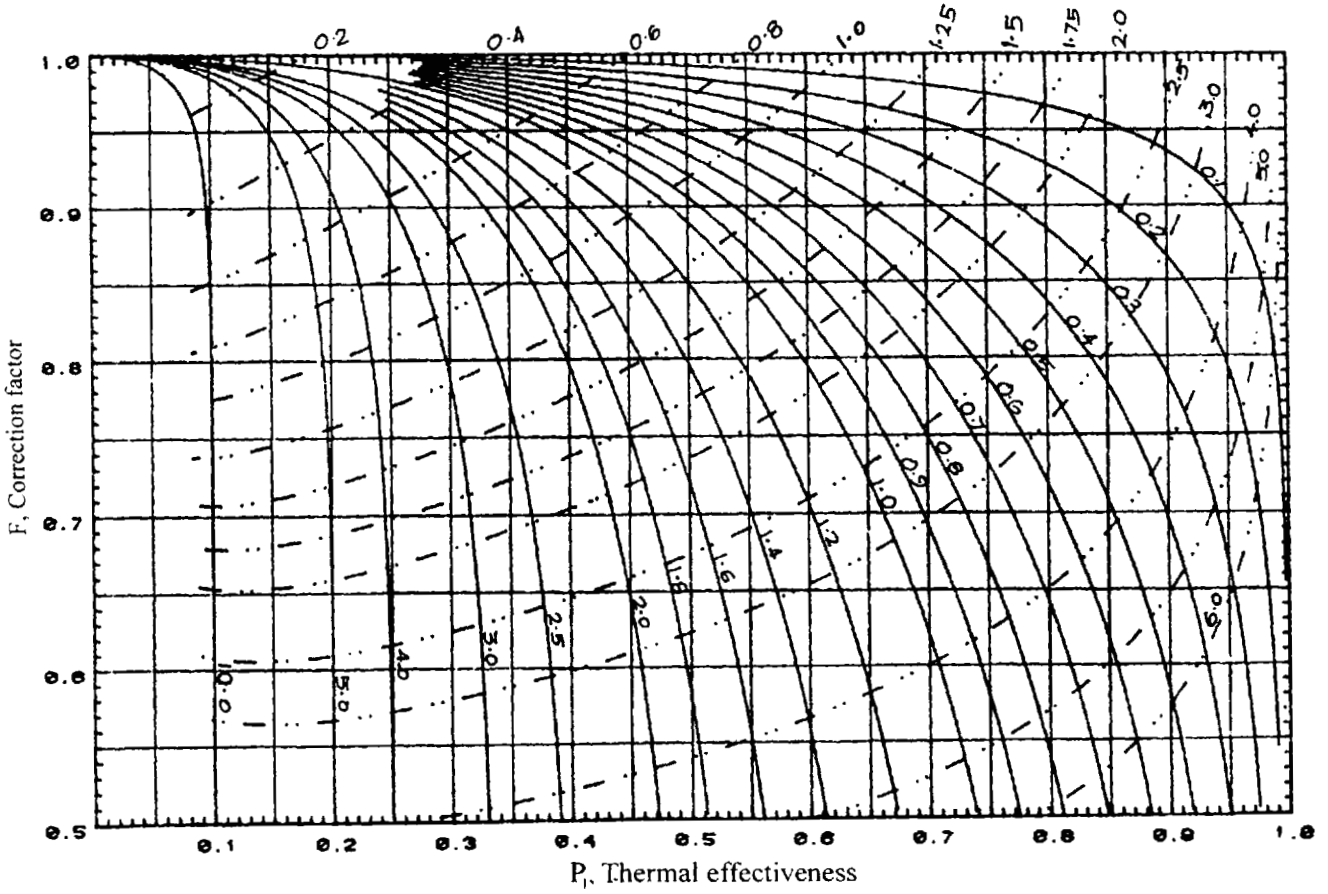


Figure 15 Three tube rows; F as a function of P for constant R (solid lines) and constant NTU (dashed lines).

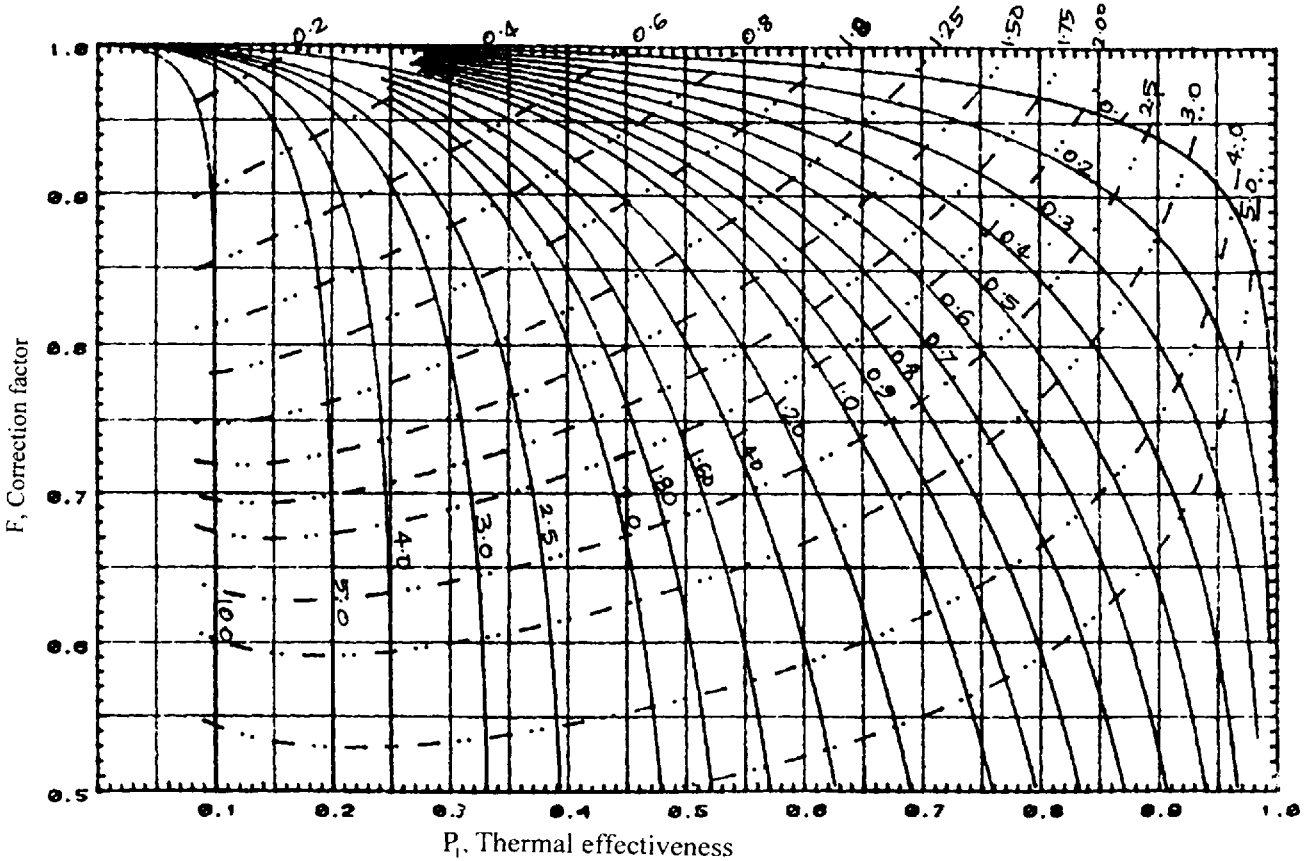


Figure 16 Four tube rows. F as a function of P for constant R (solid lines) and constant NTU (dashed lines).

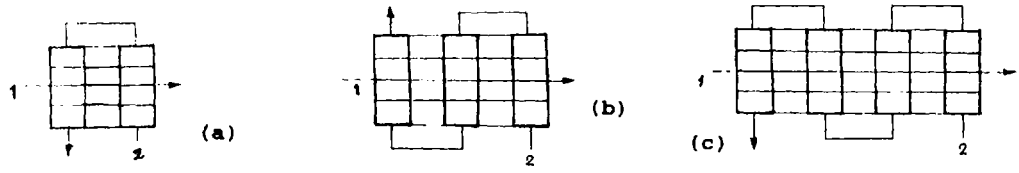


Figure 17 Multipass tube rows. (a) Two rows-two pass; (b) three rows-three pass; (c) four rows-four pass.

$$K = 1 - \exp\left(-\frac{\text{NTU}}{6}\right) \tag{67b}$$

Values of F referred to the fluid outside the tube side (air side) for $N = 2$, 3, 4, 5, and 6 are shown in Figs. 18, 19, 20, 21, and 22, respectively. The F values are always higher than the basic case (Fig. 8). When N becomes greater than 6, F approaches 1, that is, pure counter-current flow.

6. *Multiple Tube Rows in Multipass Cross-Counterflow Arrangements; One Fluid Unmixed Throughout; Other Fluid (Tube Fluid) Unmixed in Each Pass but Mixed Between Passes).*

1. Four rows, two passes, with two rows per pass. Tube-side fluid mixed at the header and the other fluid is unmixed throughout, coupling in inverted order [Fig. 23(a)] [28]:

$$\zeta = \left\{\frac{R}{2}K^3[4 - K + 2RK^2] + e^{4KR} + K\left[1 - \frac{K}{2} + \frac{K^2}{8}\right][1 - e^{4KR}]\right\}\frac{1}{(1 + RK^2)^2} \tag{68a}$$

$$K = 1 - \exp\left(-\frac{NTU}{4}\right) \tag{68b}$$

2. Six rows, two passes, with three rows per pass. Tube-side fluid is mixed between passes, that is, at the header, and the other fluid is unmixed throughout, coupling in inverted order [Fig. 23(b)] [26]:

$$P_1 = \frac{2A - RA^2 - \delta}{1 - R\delta} \tag{69a}$$

$$A = a_0C_0(3KR) + a_1C_1(3KR) + a_2C_2(3KR)$$

$$a_0 = 1 - (1 - K)^3$$

$$a_1 = 3RK^3(3 - 2K)$$

$$a_2 = \frac{9R^2K^5}{2}$$

$$\delta = a_0^2C_0(6KR) + 2a_0a_1C_1(6KR) + (a_1^2 + 2a_0a_2)C_2(6KR) + 2a_1a_2C_3(6KR) + a_2^2C_4(6KR)$$

$$C_n(z) = \frac{n!}{z^{n-1}}\left[1 - e^{-z}\left(1 + z + \frac{z}{2!} + \cdots + \frac{Z^n}{n!}\right)\right]$$

$$K = 1 - \exp\left(-\frac{\text{NTU}}{6}\right) \tag{69b}$$

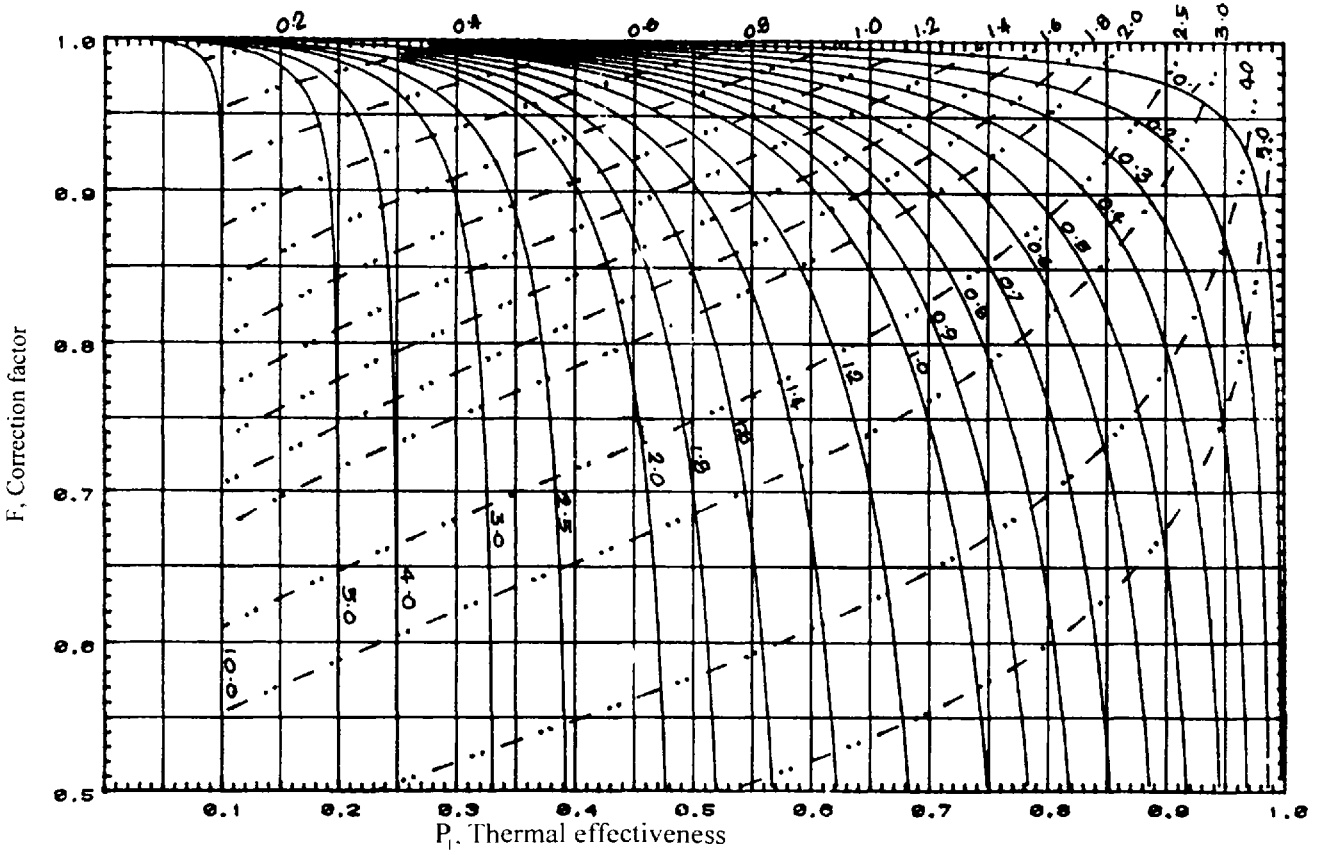


Figure 18 Two tube rows, two passes. Both fluids unmixed throughout; fluid 1 inverted coupling between passes. F as a function of P for constant R (solid lines) and constant NTU (dashed lines).

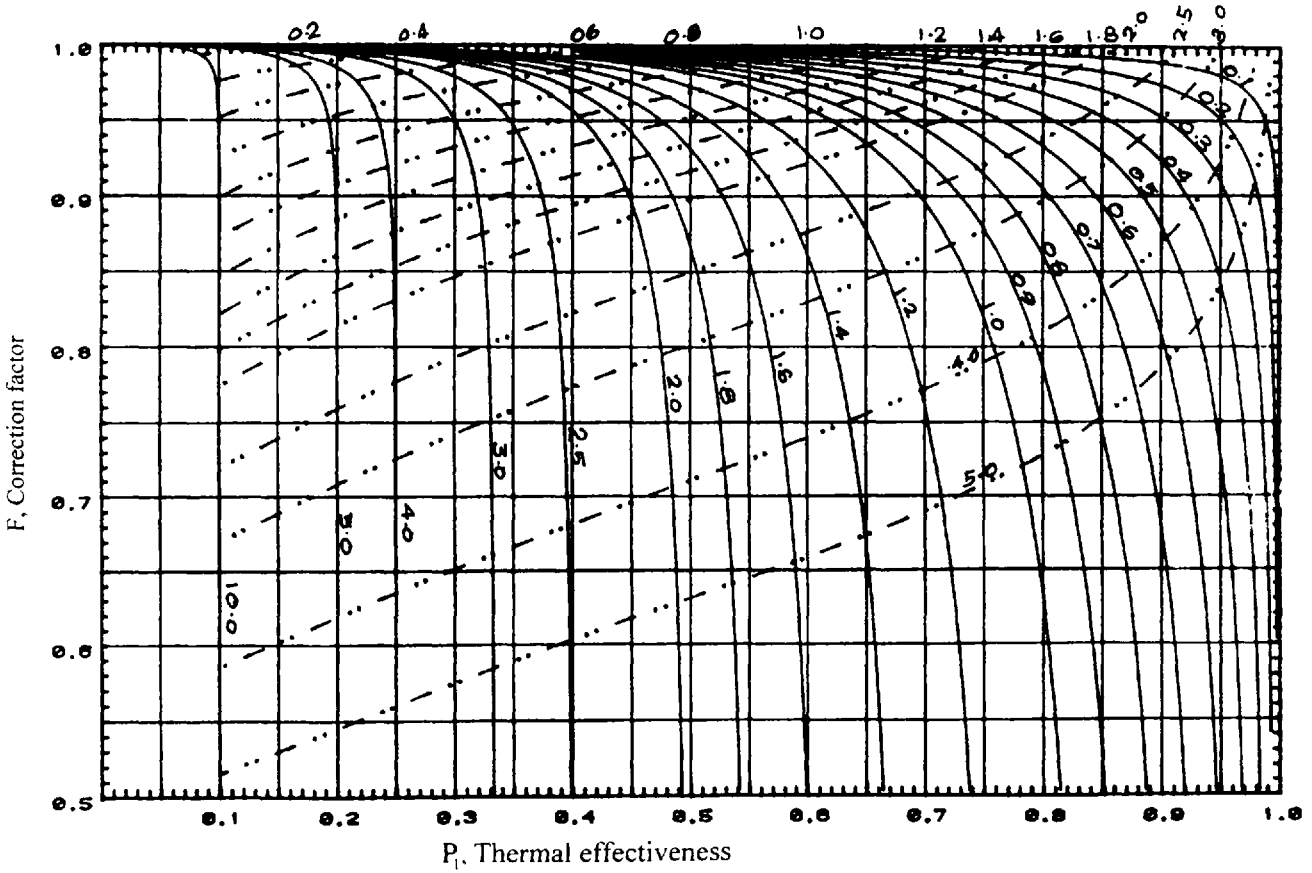


Figure 19 Three tube rows, three passes. Both fluids unmixed throughout; fluid 1 inverted coupling between passes. F as a function of P for constant R (solid lines) and constant NTU (dashed lines).

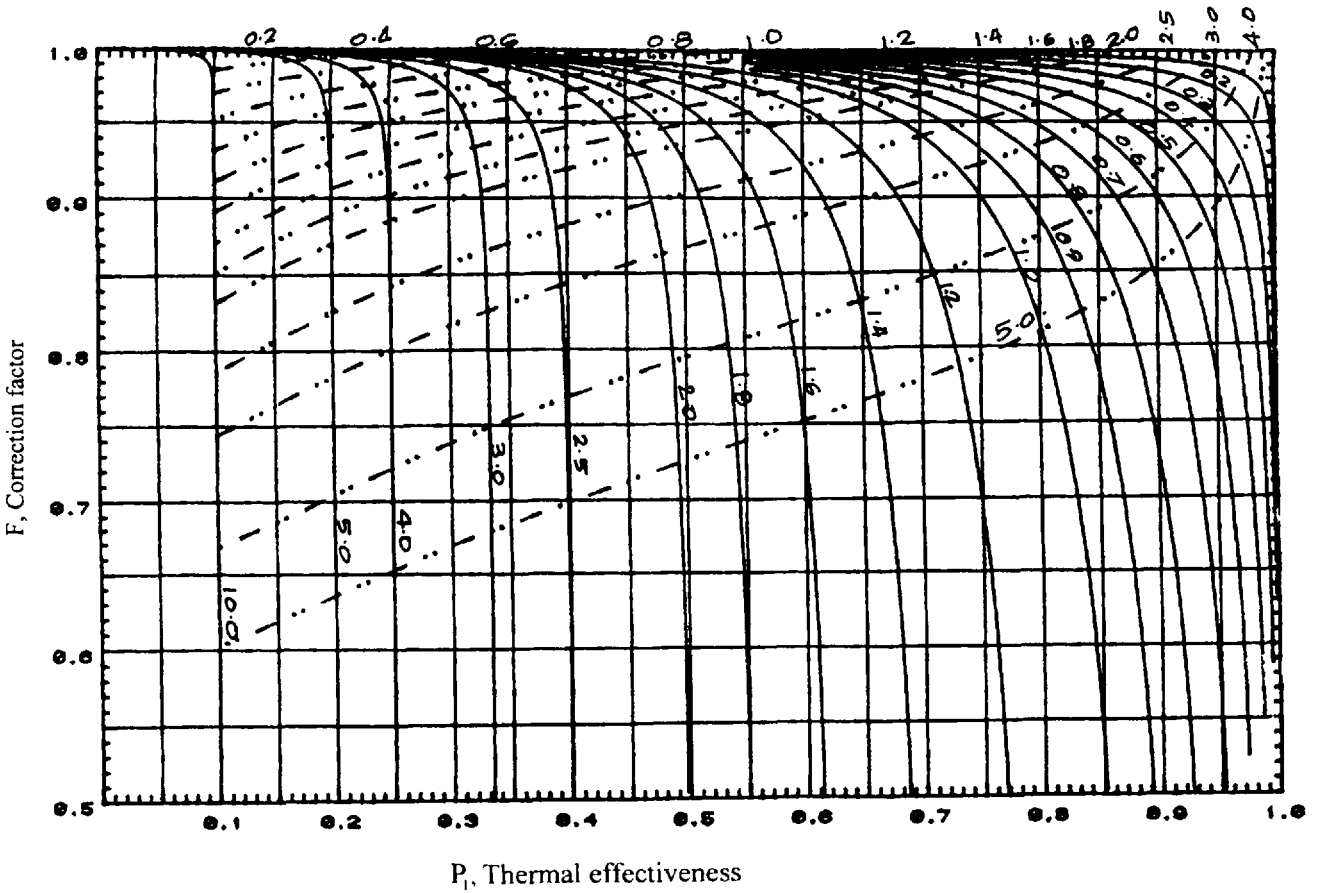


Figure 20 Four tube rows, four passes. Both fluids unmixed throughout; fluid 1 inverted coupling between passes. F as a function of P for constant R (solid lines) and constant NTU (dashed lines).

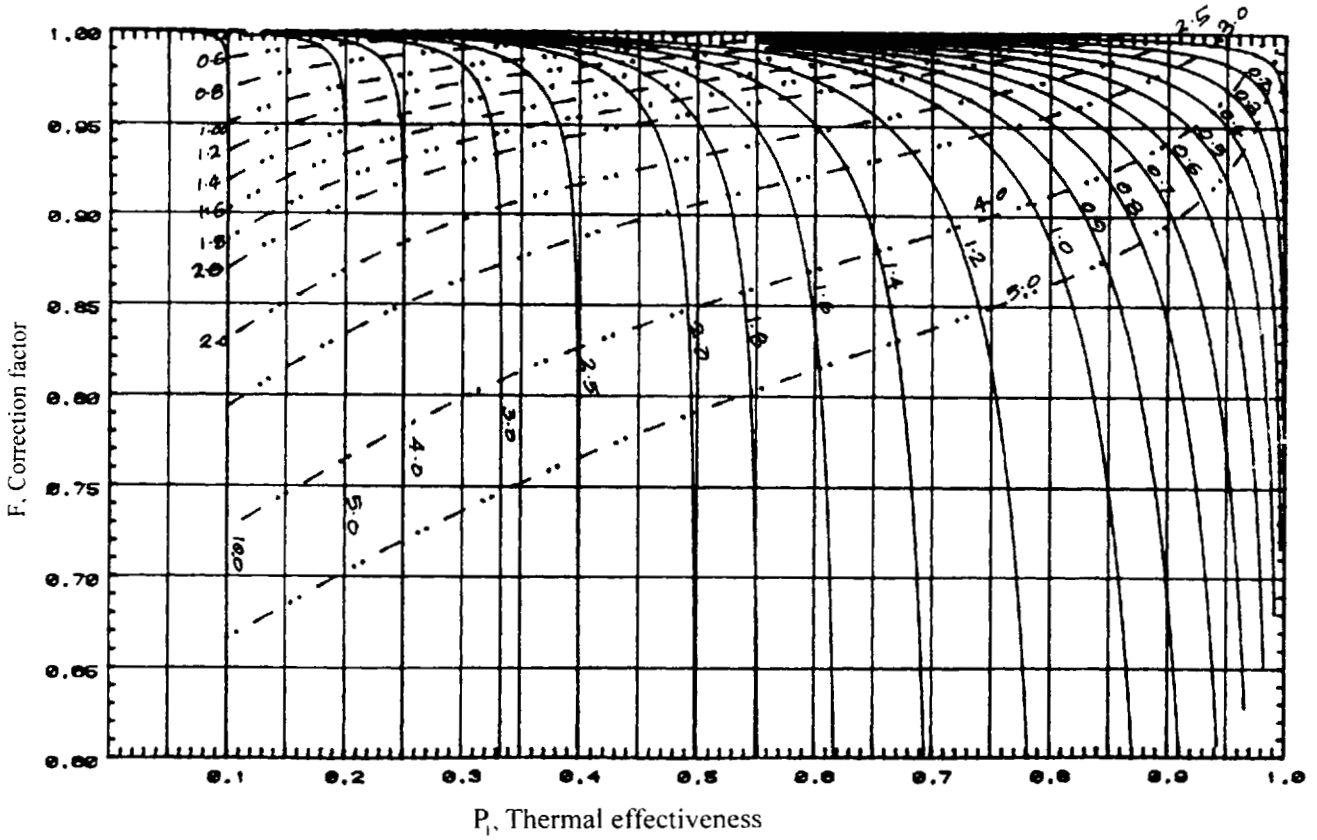


Figure 21 Five tube rows, five passes. Both fluids unmixed throughout; fluid 1 inverted coupling between passes. F as a function of P for constant R (solid lines) and constant NTU (dashed lines).

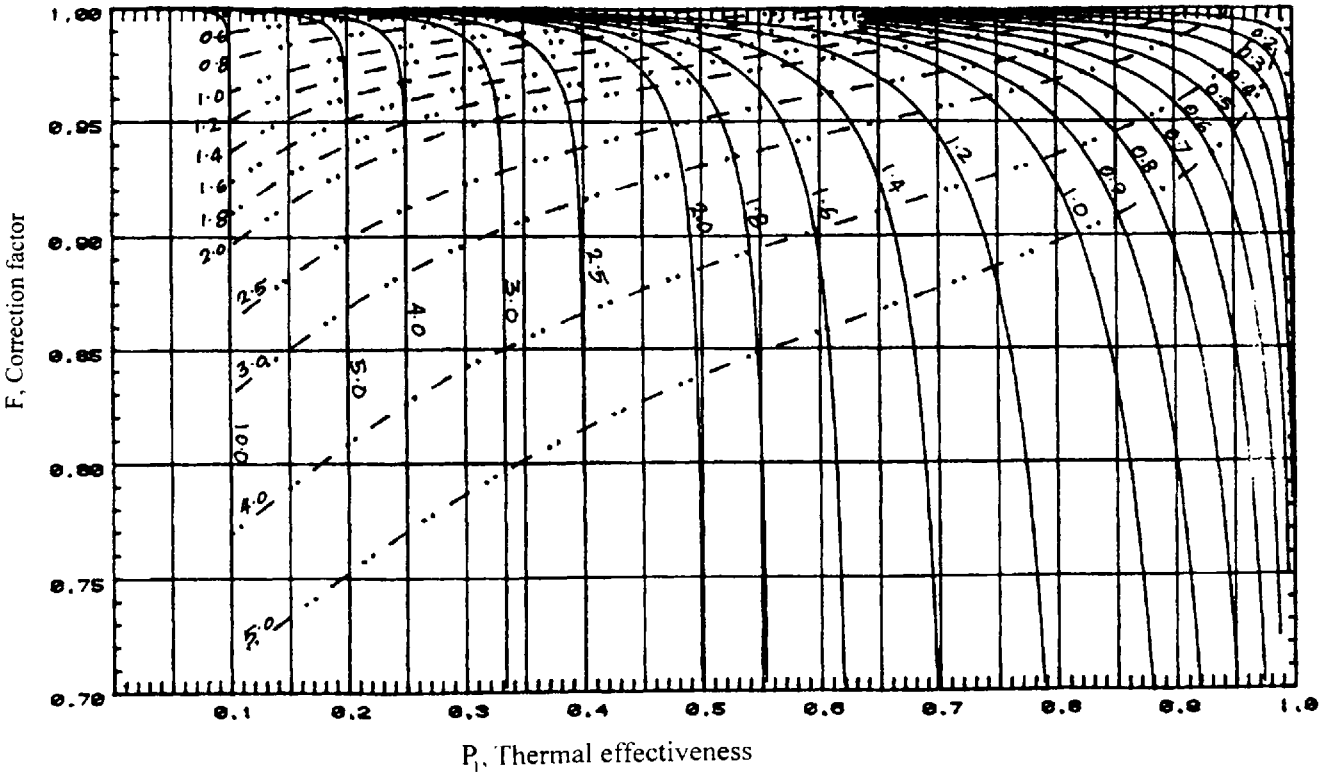


Figure 22 Six tube rows, six passes. Both fluids unmixed throughout; fluid 1 inverted coupling between passes. F as a function of P for constant R (solid lines) and constant NTU (dashed lines).

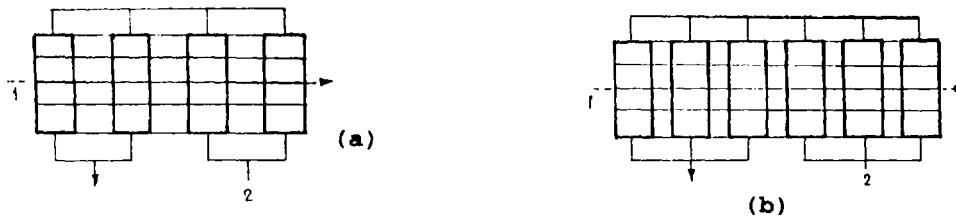


Figure 23 Tube rows multiples arrangement; (a) four rows-two pass; (b) six rows-two pass.

Values of F for four rows, two passes, and six rows, two passes are shown in Figs. 24 and 25, respectively.

6.4. Thermal Relations for Various TEMA Shells and Others

The thermal effectiveness relations for various TEMA shells and others are presented next, using the following simplifying assumptions given at the beginning of this section and the additional assumption of perfect transverse mixing of the shell fluid. Since the shell-side flow arrangement is unique with each shell type, the exchanger effectiveness is different for each shell even though the number of tube passes may be the same. The P-NTU$_t$ or LMTD method is commonly used for the thermal analysis of shell and tube exchangers. Therefore, thermal relation formulas and effectiveness charts are presented as for the P-NTU$_t$ method.

E Shell

The basic case of the E shell, one shell pass and one tube pass with parallel flow and counterflow arrangement, is shown in Fig. 26. For the counterflow case with more than five baffles, the F value can be taken as 1. Thermal effectiveness charts shown in Fig. 6 can be used for parallel flow arrangement and Fig. 7 for counterflow arrangement.

Multipassing on the Tube Side. On the tube side, any number of odd or even passes is possible. Increasing the even number of tube passes from two to four, six, etc., decreases the exchanger effectiveness slightly, and in the limit when the number of tube passes approaches infinity with one shell pass, the exchanger effectiveness approaches that for a single-pass crossflow exchanger with both fluids mixed. The odd number of tube passes per shell has slightly better effectiveness when the shell fluid flows countercurrent to the tube fluid for more than half the tube passes. However, this is an uncommon design and may result in structural and thermal problems in manufacturing and design. Common tube-side multipass arrangements for TEMA $E_{1,2}$, $E_{1,3}$, and $E_{1,4}$ shells are shown in Fig. 27.

Even Number of Tube Passes. One shell pass and two tube passes as shown in Fig. 4 using a U-tube bundle is one of the most common flow arrangements used in the single-pass TEMA E shell. The heat exchanger with this arrangement is also simply referred to as a conventional 1-2 heat exchanger. If the shell fluid is idealized as well mixed, its temperature is constant at any cross section. In this case, reversing the tube fluid flow direction will not change the idealized temperature distribution and the exchanger thermal effectiveness. Possible flow patterns of the $E_{1,2}$ shell were already shown in Fig. 4. This is referred as "stream symmetric."

The 1-2 and 1-4 cases were solved long ago by Bowman [11], Underwood [12], and Nagle [30]. The 1-N geometry for even number of passes was solved by Baclic [31]. Thermal effectiveness formula for the $E_{1,2}$ case is given by Eq. T13 in Table 6 and the thermal effectiveness chart is given in Fig. 28 along with the F_{min} curve. Thermal effectiveness formulas for 4 and N tube-side passes are given by Eqs. T14 and T15, respectively, in Table 6. The thermal

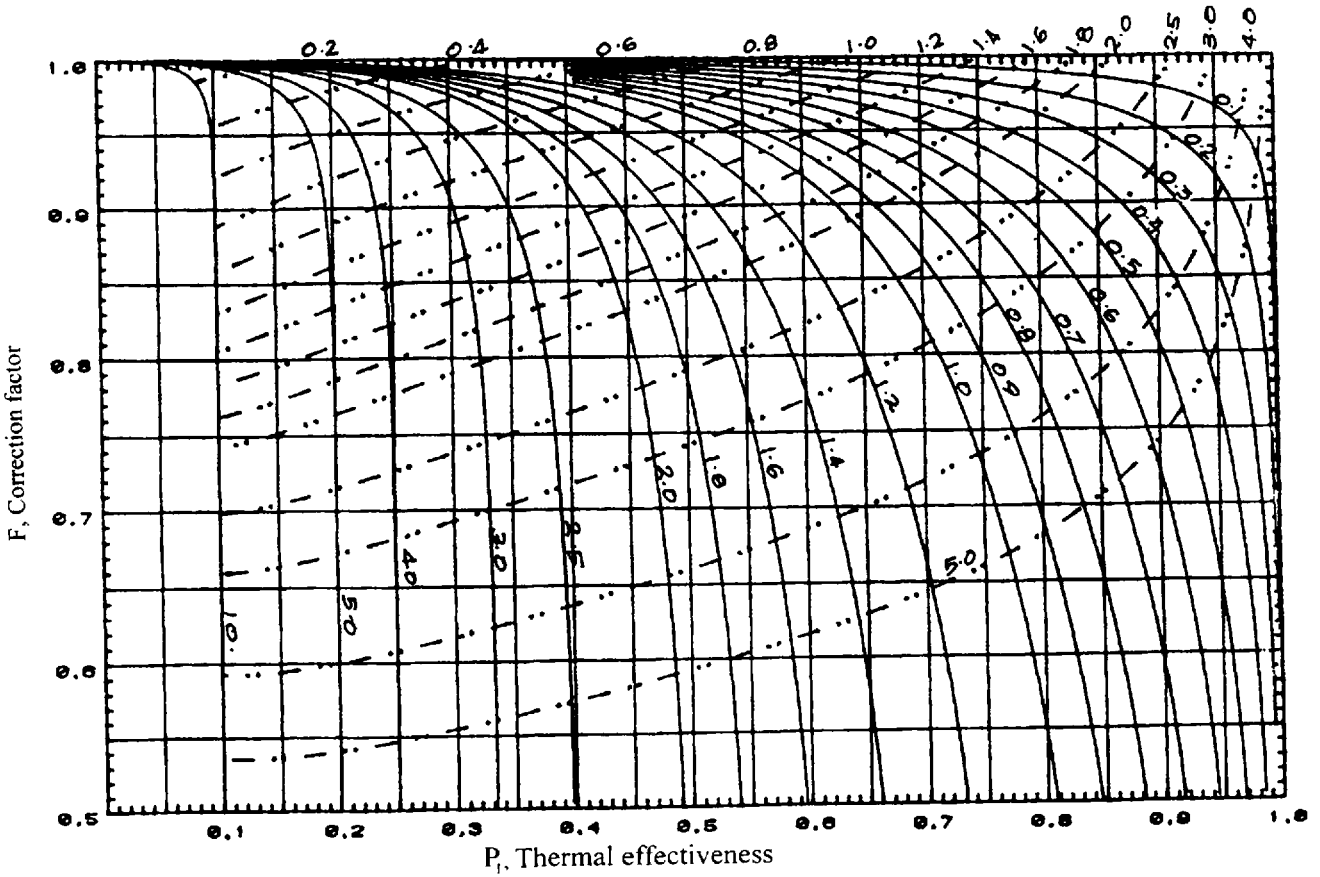


Figure 24 Four rows-two passes with two rows per pass. One fluid is unmixed throughout; Tubeside fluid mixed between passes and in each pass unmixed; fluid 1 inverted coupling between passes. F as a function of P for constant R (solid lines) and constant NTU (dashed lines).

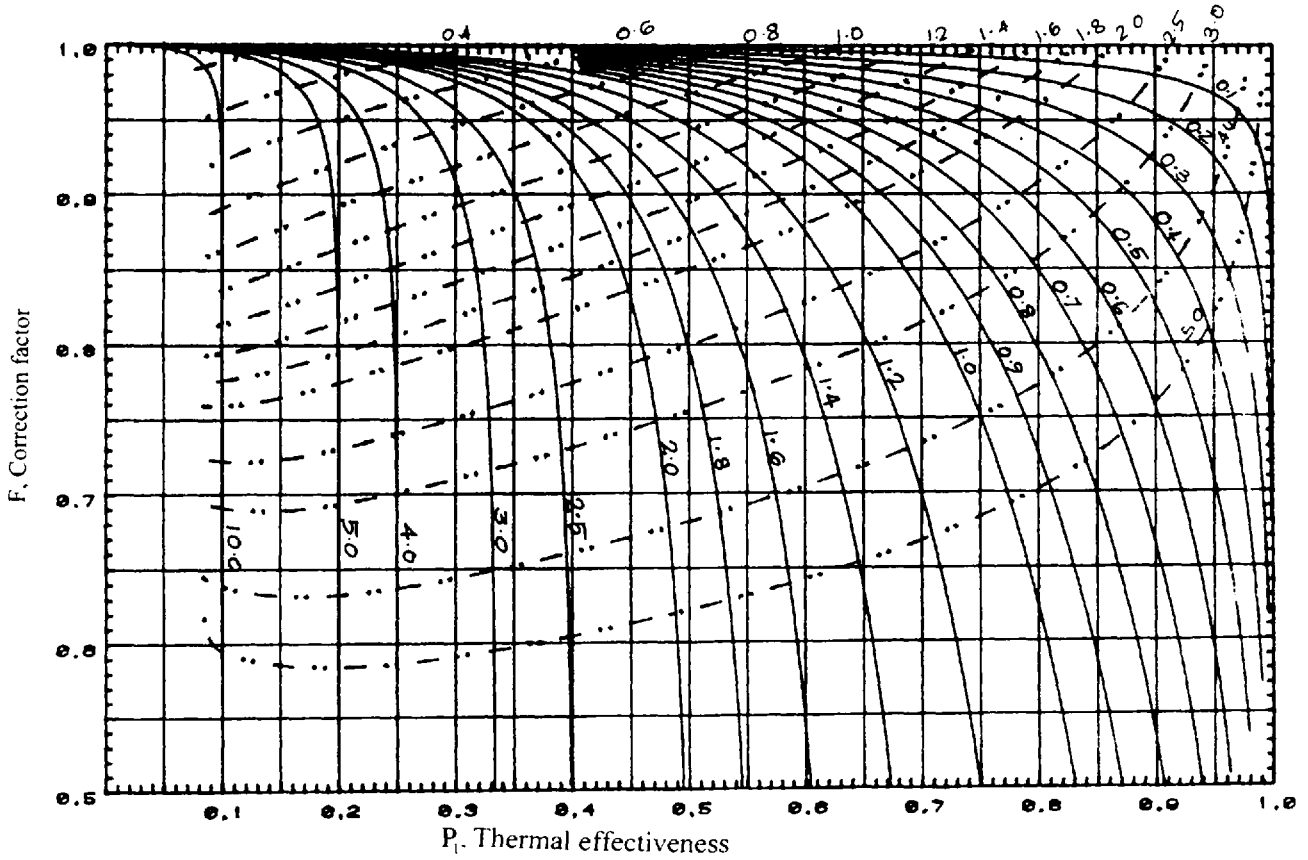


Figure 25 Six Rows-two passes with three rows per pass. One fluid is unmixed throughout; tubeside fluid mixed between passes and in each pass unmixed; fluid 1 inverted coupling between passes. F as a function of P for constant R (solid lines) and constant NTU (dashed lines).

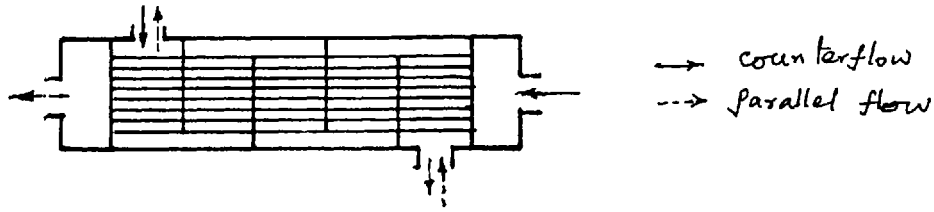


Figure 26 E shell single pass arrangement: parallel flow; counterflow. (Note: for a large number of segmental baffles, the flow approaches true parallel and counterflow.)

effectiveness chart for the $E_{1\text{-}4}$ case is shown in Fig. 29, and this figure may be used for even $N \geq 6$ cases also without loss of much accuracy.

Odd Number of Tube Passes. With the TEMA E shell, an odd number of tube passes can have both parallel flow and counterflow arrangements. Thermal effectiveness relations for overall parallel flow and counterflow arrangements are discussed next.

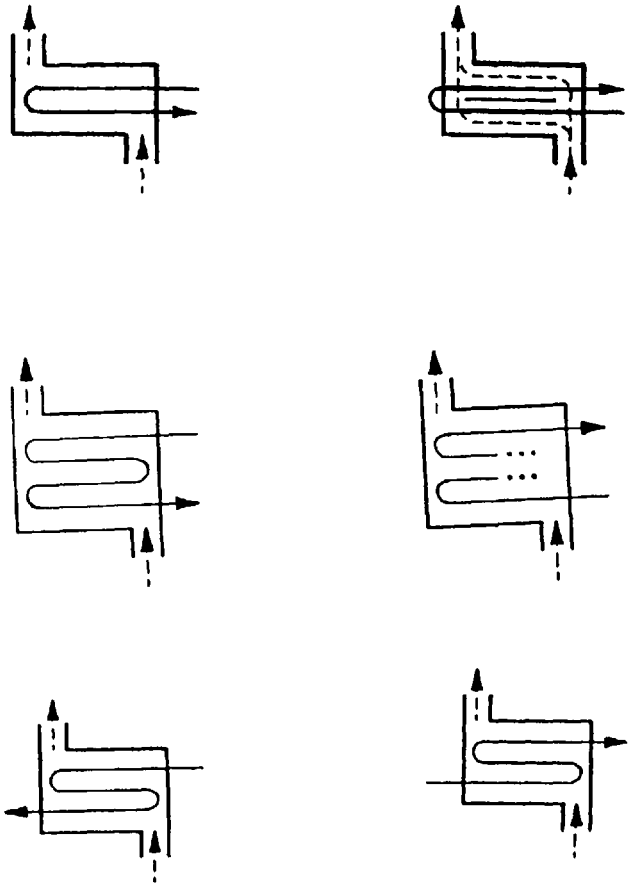
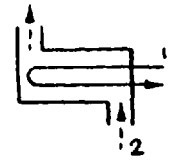
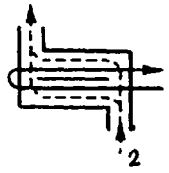
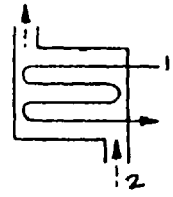
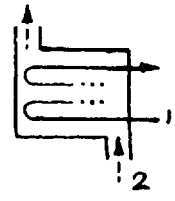


Figure 27 Common tubepass arrangement for $E_{1\text{-}2}$, $E_{1\text{-}4}$ and $E_{1\text{-}3}$ shells.

Table 6 $E_{1\text{-}2}$ Shell (N Even) (Referred to Tubeside)

Flow arrangement	Eq. no./ Ref.	General formula	Value for R = 1 and special cases
 TEMA $E_{1\text{-}2}$ shell: shell fluid mixed, tube fluid mixed between passes; stream symmetric	T13 [30]	$P = \dfrac{2}{1 + R + A \coth (A\,NTU/2)}$ $A = \sqrt{1 + R^2}$	$P = \dfrac{1}{1 + \coth (NTU/\sqrt{2})/\sqrt{2}}$
 $E_{1\text{-}2}$ shell. shell fluid divided into two streams, individually mixed; tube fluid mixed between passes		Same as $J_{1\text{-}1}$ shell	Same as $J_{1\text{-}1}$ shell
 TEMA $E_{1\text{-}4}$ shell: shell fluid mixed, tube fluid mixed between passes	T14 [30]	$P_1 = \dfrac{4}{\left[2\,(1+R) + \gamma \coth\left(\dfrac{\gamma\,NTU}{4}\right) + \tanh\left(\dfrac{NTU}{4}\right)\right]}$ $\gamma = \sqrt{(4R^2 + 1)}$	$P = \dfrac{4}{[4 + \sqrt{5}A + B]}$ $A = \coth (\sqrt{5}NTU/4)$ $B = \tanh (NTU/4)$
 TEMA $E_{1\text{-}N}$ (even N) shell: shell fluid mixed; and tube fluid mixed between passes	T15 [31]	$P_1 = \dfrac{2}{A + B + C}$ $A = 1 + R + \coth(NTU/2)$ $B = \dfrac{-1}{N_1} \coth\left(\dfrac{NTU}{2N_1}\right)$ $C = \dfrac{1}{N_1}\sqrt{1 + N_1^2 R^2} \quad \coth\left(\dfrac{NTU}{2N_1}\sqrt{1 + N_1^2 R^2}\right)$ $N_1 = \dfrac{N}{2}$ $N \to \infty$ results in well known single pass cross-flow exchanger with both fluids mixed.	Same as Eqn. T15 with $R = 1$.

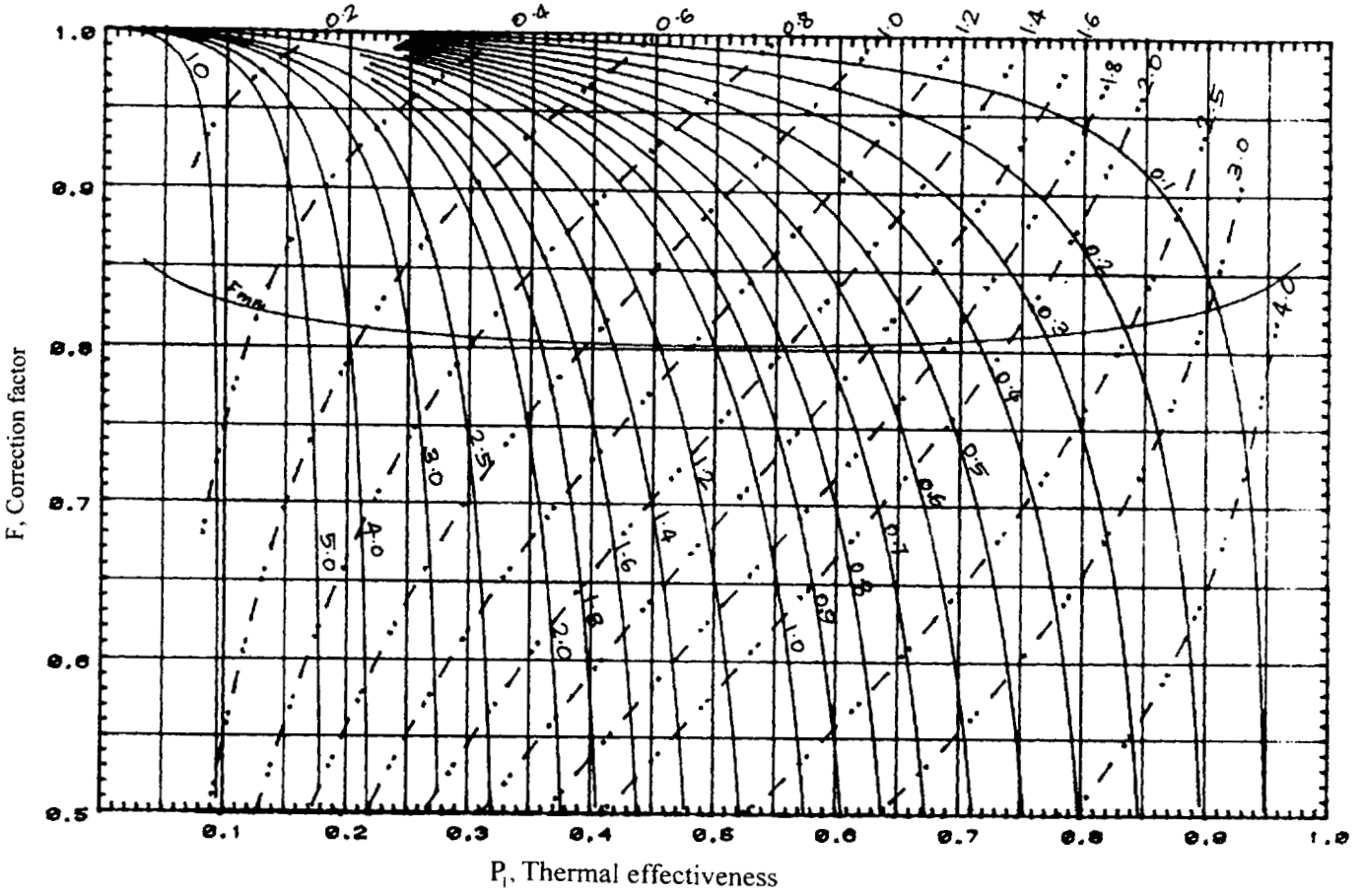


Figure 28 TEMA $E_{1\text{-}2}$ shell; shell fluid mixed, tube fluid mixed between passes. Stream symmetric. F as a function of P for constant R (solid lines) and constant NTU (dashed lines).

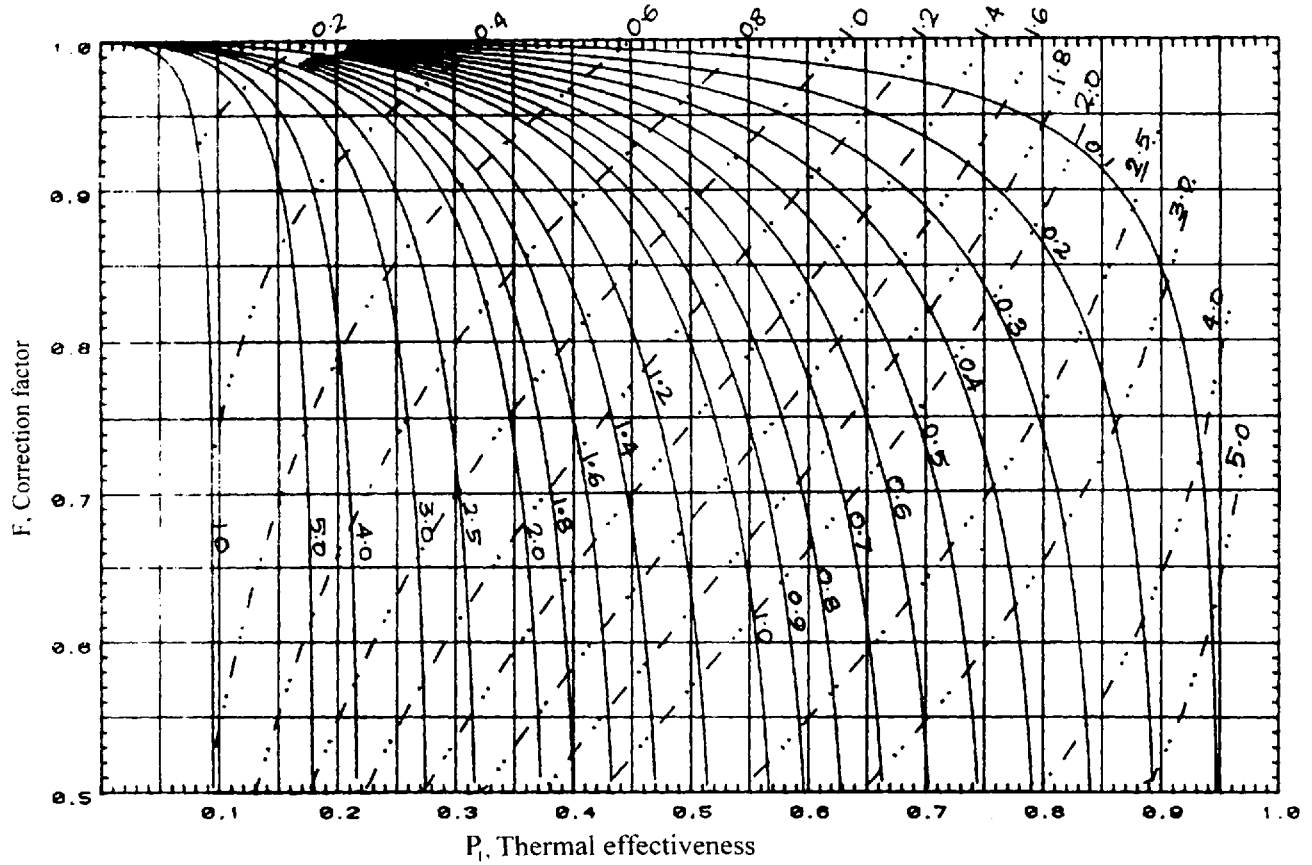


Figure 29 TEMA $E_{1,1}$ shell. Shell fluid mixed, tube fluid mixed between passes. F as a function of P for constant R (solid lines) and constant NTU (dashed lines).

In an $E_{1\text{-}3}$ overall counterflow arrangement, two tube passes are in counterflow and one tube pass is in parallel flow, whereas in an $E_{1\text{-}3}$ overall parallel flow arrangement, two tube passes are in parallel flow and one tube pass is in counterflow. Similarly, in an $E_{1\text{-}5}$ overall counterflow arrangement, three tube passes are in counterflow and two tube passes are in parallel flow. The flow arrangement for $E_{1\text{-}3}$ was already shown in Fig 27 and for $E_{1\text{-}5}$ is shown in Fig. 30. Pignotti and Tamborenea [32] obtained an analytical solution for the 1-N (odd N) case and obtained effectiveness for the 1-3 and 1-5. Explicit thermal relations are given by Pignotti [18] for $E_{1\text{-}3}$ parallel flow and counterflow cases.

For $N = 3$. Thermal effectiveness formulas for $E_{1\text{-}3}$ parallel flow arrangement are given by Eq. T16 and for $E_{1\text{-}3}$ counterflow arrangement by Eq. T17 in Table 7. The thermal effectiveness chart for $E_{1\text{-}3}$ counterflow arrangement is given in Fig. 31.

For $N = 5$. For the overall counterflow arrangement or opposite end case, the thermal effectiveness is given by Eq. T18 in Table 8 and the thermal effectiveness chart is given in Fig. 32.

For the overall parallel flow arrangement or same end case, the configuration can be obtained from that of the opposite end case (T18) by just the inversion of the direction of flow of the tube fluid, which leads to the expression [32]:

$$P_1 = (1 - X_5^*) \tag{70}$$

with

$$X_5^*(R, \text{NTU}) = \frac{1}{X_5(-R, \text{NTU})} \tag{71}$$

TEMA F Shell

For the TEMA F shell, as is usual with two tube passes, the arrangement results in pure counterflow with $F = 1$. For four tube passes, the configuration would be treated as two $E_{1\text{-}2}$ exchangers in series. As the longitudinal baffle is exposed on one side to the hot stream and on the other side to the cold stream, there is a conduction heat exchange that reduces the thermal effectiveness and hence the F factor has to be corrected. The effect of thermal leakage by conduction across the baffle has been analyzed by Whistler [33] and in nondimensional form by Rozenman and Taborek [34], with proposed baffle correction methods. The baffle correction factor based on Ref. 34 is presented in Ref. 35.

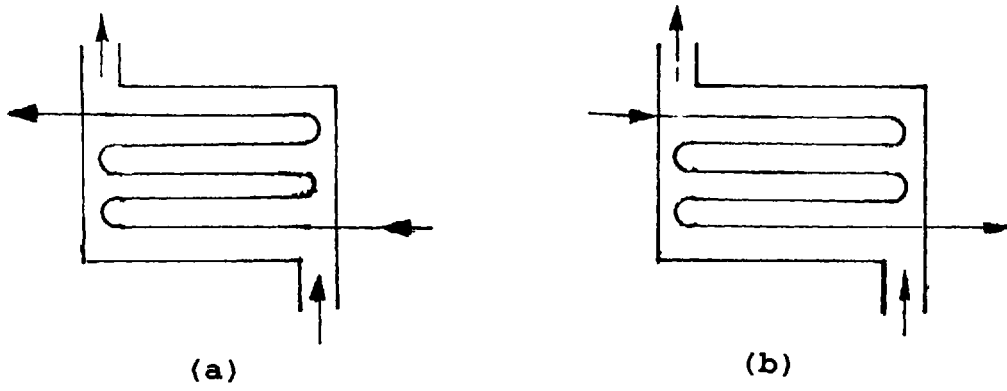
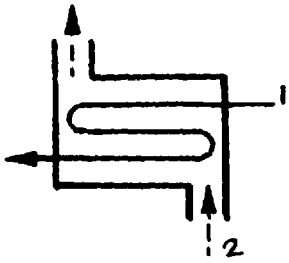
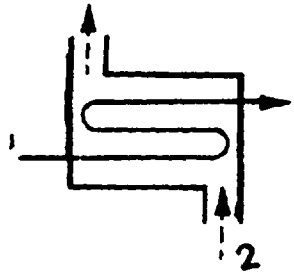


Figure 30 Flow arrangement of E shell with one shell pass and five tube passes ($E_{1\text{-}5}$). (a) Parallel flow; (b) counterflow.

Table 7 $E_{1\text{-}3}$ Shell (Referred to Tube side)

Flow arrangement	Eq. no./ Ref.	General formula	Value for R = 1
1-3 TEMA E shell: two parallel flow and one counterflow passes; shell fluid mixed, tube fluid mixed between passes 	T16 [18]	$P_1 = \left[1 - \frac{AC + B^2}{C}\right]$ $A = \chi_1 (1 - R\lambda_1)(1 + RN_2)/2R^2\lambda_1 - E$ $-\chi_2 (1 - R\lambda_2)(1 + R\lambda_1)/2R^2\lambda_2 + R/(1 + R)$ $B = \chi_2 (1 + R\lambda_1)/R - \chi_1 (1 + R\lambda_2)/R + E$ $C = \chi_1 (3 - R\lambda_2)/R - \chi_2 (3 - R\lambda_1)/R + E$ $E = 0.5e^{(-NTU/3)}$ $\lambda_{1,2} = (-3 \pm \delta)/2$ $\delta = \frac{[9R^2 + 4(R+1)]^{0.5}}{R}$ $\chi_{1,2} = \frac{e^{(\lambda_{1,2} R\, NTU/3)}}{2\delta}$	Same as Eq. T16 with $R = 1$
1-3 TEMA E Shell: one parallel flow and two counterflow passes; shell fluid mixed, tube fluid mixed between passes 	T17 [18]	$P_1 = \left[1 - \frac{C}{(AC + B^2)}\right]$ $A = \chi_1 (1 + R\lambda_1)(1 - R\lambda_2)/2R^2\lambda_1 - E$ $-\chi_2 (1 + R\lambda_2)(1 - R\lambda_1)/2R^2\lambda_2 + R/(R - 1)$ $B = \chi_1 (1 - R\lambda_2)/R - \chi_2 (1 - R\lambda_1)/R + E$ $C = -\chi_1 (3 + R\lambda_2)/R + \chi_2 (3 + R\lambda_1)/R + E$ $E = 0.5\, e^{(NTU/3)}$ $\lambda_{1,2} = (-3 \pm \delta)/2$ $\delta = \frac{[9R^2 + 4(1 - R)]^{0.5}}{R}$ $\chi_{1,2} = \frac{e^{(\lambda_{1,2} RNTU/3)}}{2\delta}$	Same as Eq. T17 with $R = 1$ and $A = -\frac{e^{-NTU}}{18} - \frac{e^{NTU/3}}{2} + \frac{(5 + NTU)}{9}$

TEMA G Shell or Split-Flow Exchanger

Possible flow arrangements for the TEMA G shell are $G_{1\text{-}1}$, $G_{1\text{-}2}$, and $G_{1\text{-}4}$. The solution of the $G_{1\text{-}2}$ counterflow case is due to Schindler and Bates [36] and that of the parallel flow case is due to Pignotti [18]. The thermal effectiveness P of this shell with two tube passes is higher than that of the conventional $E_{1\text{-}2}$ exchanger for a given NTU_1 and R. It is also possible to have only a single pass on the tube side, which is stream symmetric [37]. The thermal effectiveness formula for $G_{1\text{-}1}$ is given by Eq. T19 in Table 9 and the thermal effectiveness chart is given in Fig. 33. For the $G_{1\text{-}2}$ arrangement, the thermal relations for the parallel flow and counterflow

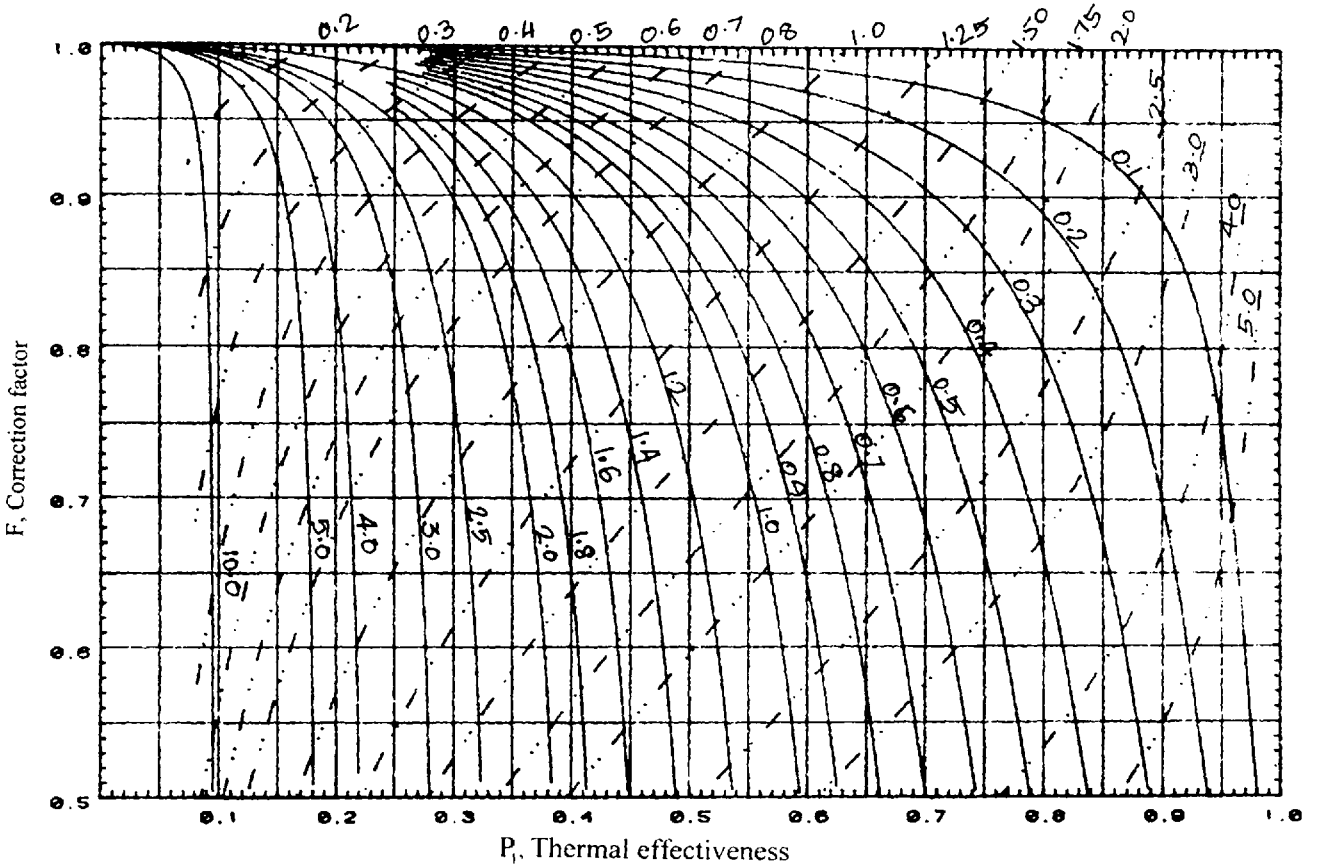
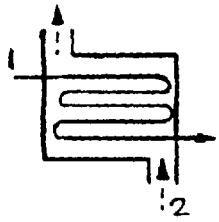


Figure 31 TEMA $E_{1\,1}$ shell. One parallel flow and two counterflow passes; shell fluid mixed, tube fluid mixed between passes. F as a function of P for constant R (solid lines) and constant NTU (dashed lines).

Table 8 Formula for $E_{1,S}$ Shell and Tube Exchanger with Three Tube Two Tube Passes in Parallel Flow Arrangement; Shell Fluid Mixed, Passes (Referred to Tube Side) [32]

where



$$P_1 = (1 - X_S) \qquad \text{for } N = J$$

$$X_S = X_5 = \frac{(\alpha\gamma - \beta^2)}{[(\alpha\gamma - \beta^2)H_{13} + \alpha\xi^2 + \gamma\eta^2 - 2\beta\xi\eta]}$$

$$\alpha = H_{24} - H_{11} - 2H_{12}$$

$$\beta = H_{22} - H_{13} - 2H_{12}$$

$$\gamma = H_{24} - H_{13} - 2H_{12}$$

$$\xi = H_{11} + H_{12}$$

$$\eta = H_{13} + H_{12}$$

T18

$$H_{11} = \frac{(1 + R\lambda_1)(1 - R\lambda_2)}{R^2(N+1)\lambda_1\delta} X_1 - \frac{(1 - R\lambda_1)(1 + R\lambda_2)}{R^2(N+1)\lambda_2\delta} X_2 + \frac{N-1}{N+1} X_3 + \frac{R}{R-1} \qquad \text{for } R \neq$$

$$= \frac{2N - 1 + \text{NTU}}{N^2} + \frac{1 - N}{(N+1)N^2} X_2 + \frac{N-1}{N+1} X_3 \qquad \text{for } R = 1$$

$$H_{12} = \frac{(1 + R\lambda_1)(1 + R\lambda_2)}{R^2(N-1)\lambda_1\delta} X_1 - \frac{(1 + R\lambda_1)(1 + R\lambda_2)}{R^2(N-1)\lambda_2\delta} X_2 - \frac{R}{R-1} \qquad \text{for } R \neq 1$$

$$= \frac{1 - \text{NTU}}{N^2} - \frac{X_2}{N^2} \qquad \text{for } R = 1$$

$$H_{13} = \frac{(1 + R\lambda_1)(1 - R\lambda_2)}{R^2(N+1)\lambda_1\delta} X_1 - \frac{(1 - R\lambda_1)(1 + R\lambda_2)}{R^2(N+1)\lambda_2\delta} X_2 - \frac{2}{N+1} X_3 + \frac{R}{R-1} \qquad \text{for } R \neq$$

$$= \frac{2N - 1 + \text{NTU}}{N^2} + \frac{1 - N}{(N+1)N^2} X_2 - \frac{2}{N+1} X_3 \qquad \text{for } R = 1$$

$$H_{22} = \frac{(1 - R\lambda_1)(1 + R\lambda_2)}{R^2(N-1)\lambda_1\delta} X_1 - \frac{(1 + R\lambda_1)(1 - R\lambda_2)}{R^2(N-1)\lambda_2\delta} X_2 + \frac{N-3}{N-1} X_4 - \frac{R}{R-1} \qquad \text{for } R \neq$$

$$= \frac{2N + 1 - \text{NTU}}{N^2} + \frac{1 + N}{(N-1)N^2} X_2 + \frac{N-3}{N-1} X_4 \qquad \text{for } R = 1$$

$$H_{24} = \frac{(1 - R\lambda_1)(1 + R\lambda_2)}{R^2(N-1)\lambda_1\delta} X_1 - \frac{(1 + R\lambda_1)(1 - R\lambda_2)}{R^2(N-1)\lambda_2\delta} X_2 - \frac{2X_4}{N-1} - \frac{R}{R-1} \qquad \text{for } R \neq 1$$

$$= \frac{2N + 1 - \text{NTU}}{N^2} + \frac{1 + N}{(N-1)N^2} X_2 - \frac{2X_4}{N-1} \qquad \text{for } R = 1$$

Note: Expressions for δ, λ_1, λ_2, X_1, X_2, X_3 and X_4 are: $\lambda_{1,2} = -\frac{N}{2} \pm \left[\frac{N^2}{4} + \frac{1}{R^2}(1 - R)\right]^{1/2}$; $\lambda_3 = 1/R$; $\lambda_4 = 1/R$; $\delta = \lambda_1 - \lambda_2$; $X_1 = e^{\lambda_1 RN}$; $X_2 = e^{(\lambda_1 RNTU)/S}$; $X_3 = e^{\lambda_3 RNTU/S}$; $X_4 = e^{(\lambda_4 RNTU)/S}$. (Ref. 32.)

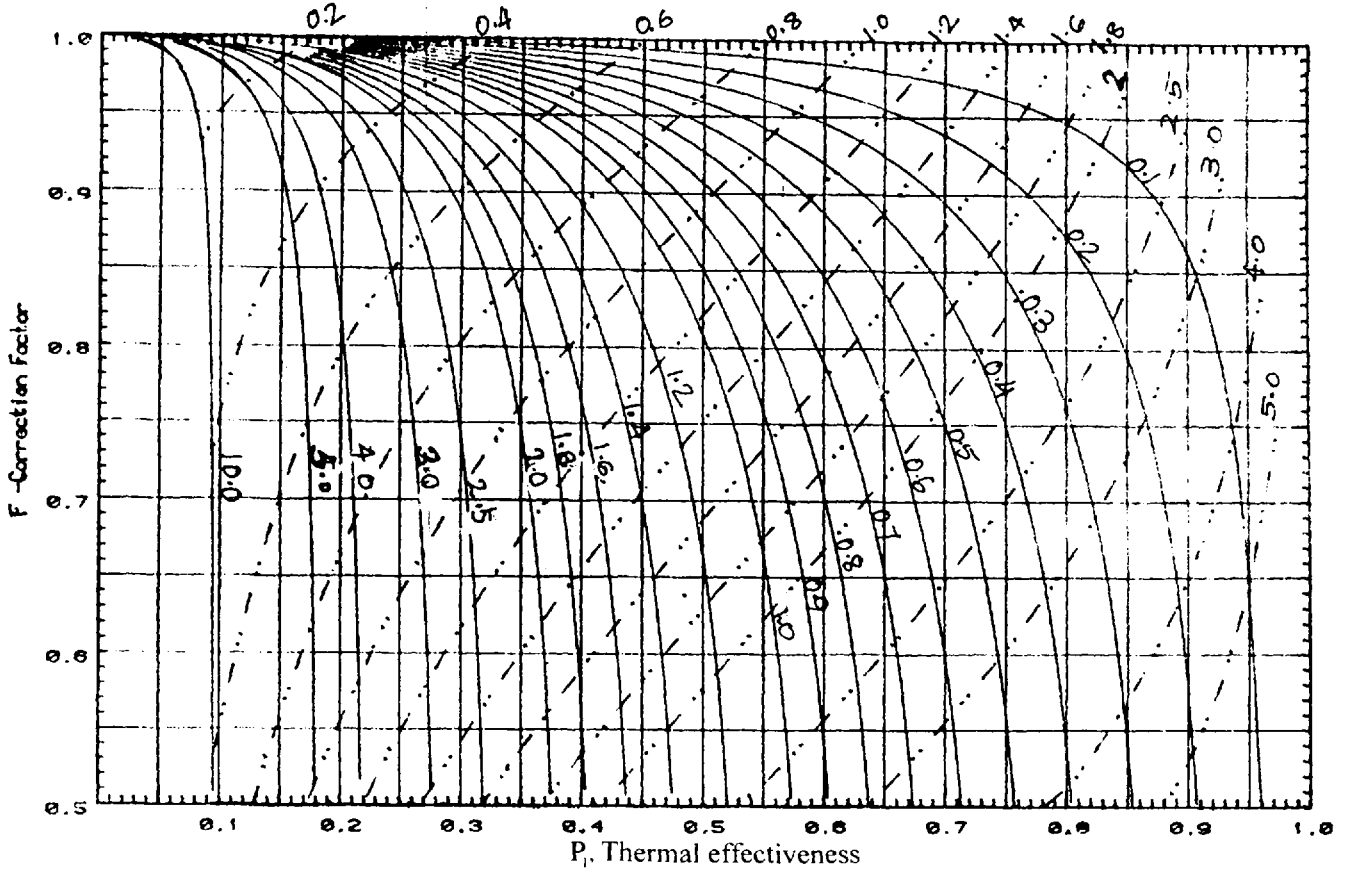
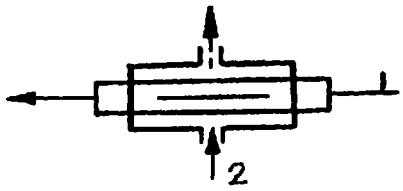
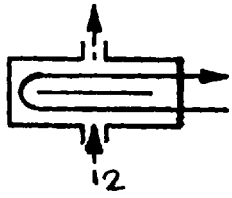
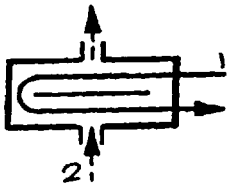


Figure 32 TEMA $E_{1,5}$ shell. Two parallel flow and three counterflow passes; shell fluid mixed, tube fluid mixed between passes. F as a function of P for constant R (solid lines) and constant NTU (dashed lines).

Table 9 G Shell (Referred to Tube Side)

Flow arrangement	Eq. no./ Ref.	General formula	Value for $R = 1$ and special cases
 1-1 G shell: tube fluid split into two streams; shell fluid mixed, stream symmetric	T19 [37]	$P = \frac{1}{R}[A + B - AB(1 + 1/R) + AB^2/R]$ $A = \frac{1 - e^{-\mathrm{NTU}(1+R)/2}}{(1+R)/R}$ $B = \frac{(1-D)}{(1-D/R)}$ $D = e^{-\mathrm{NTU}(R-1)/2}$	$B = \frac{\mathrm{NTU}}{2 + \mathrm{NTU}}$ for $R = 1$
 1-2 TEMA G shell: overall parallel flow arrangement; shell fluid mixed, tube fluid mixed between passes	T20 [18]	$P_1 = \frac{(B - \alpha^2)}{R(A - \alpha^2/R + 2)}$ $A = \frac{(1-\alpha)^2}{(R - 0.5)}$ $B = \frac{4R - \beta(2R-1)}{(2R+1)}$ $\alpha = e^{\frac{-\mathrm{NTU}(2R-1)}{4}}$ $\beta = e^{\frac{-\mathrm{NTU}(2R+1)}{2}}$	For $R = 0.5$ $P_1 = \frac{1 + 2R\ \mathrm{NTU} - \beta}{R(4 + 4R\ \mathrm{NTU} + R^2\ \mathrm{NTU}^2)}$ $\beta = e^{(-2R\ \mathrm{NTU})}$
 1-2 TEMA G shell: overall counterflow arrangement; shell fluid mixed, tube fluid mixed between passes	T21 [36]	$P_1 = \frac{(B - \alpha^2)}{R(A + 2 + B/R)}$ $A = \frac{-(1-\alpha)^2}{(R + 0.5)}$ $B = \frac{4R - \beta(2R+1)}{(2R-1)}$ $\alpha = e^{\frac{-\mathrm{NTU}(2R+1)}{4}}$ $\beta = e^{\frac{-\mathrm{NTU}(2R-1)}{2}}$	For $R = 0.5$ $P_1 = \frac{1 + 2R\ \mathrm{NTU} - \alpha^2}{R[4 + 4R\ \mathrm{NTU} - (1-\alpha)^2]}$ $\alpha = e^{(-R\ \mathrm{NTU})}$

arrangements are given by Eqs. T20 and T21, respectively in Table 9, and the thermal effectiveness chart for the counterflow arrangement is given in Fig. 34. G_{1-4} arrangement was analyzed by Singh et al. [38] and the thermal effectiveness chart is given at the end of this chapter.

TEMA H Shell

The arrangement of the TEMA H shell exchanger resembles a configuration in which two TEMA G shell exchangers are connected side by side. The solution for the TEMA H shell with 1-2 flow arrangement was analytically derived by Kohei Ishihara and Palen [39]. It is also possible to have only a single pass on the tube side [40]. The thermal effectiveness relation referred to the shell side for H_{1-1} is given by Eq. T22 in Table 10, and the thermal effectiveness

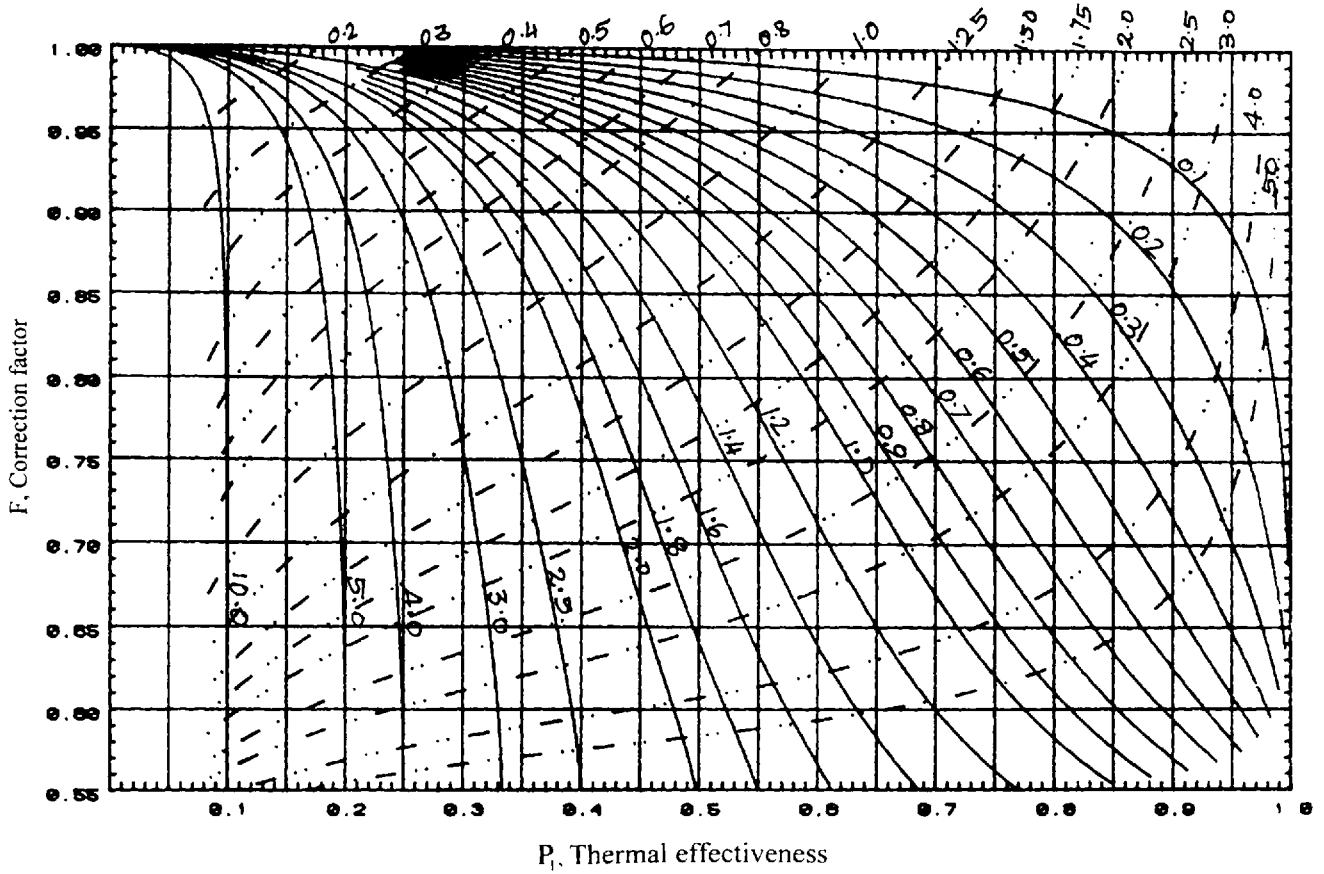


Figure 33 G_{11} shell. Tube fluid split into two streams with shell of mixed fluid. Stream symmetric. F as a function of P for constant R (solid lines) and constant NTU (dashed lines).

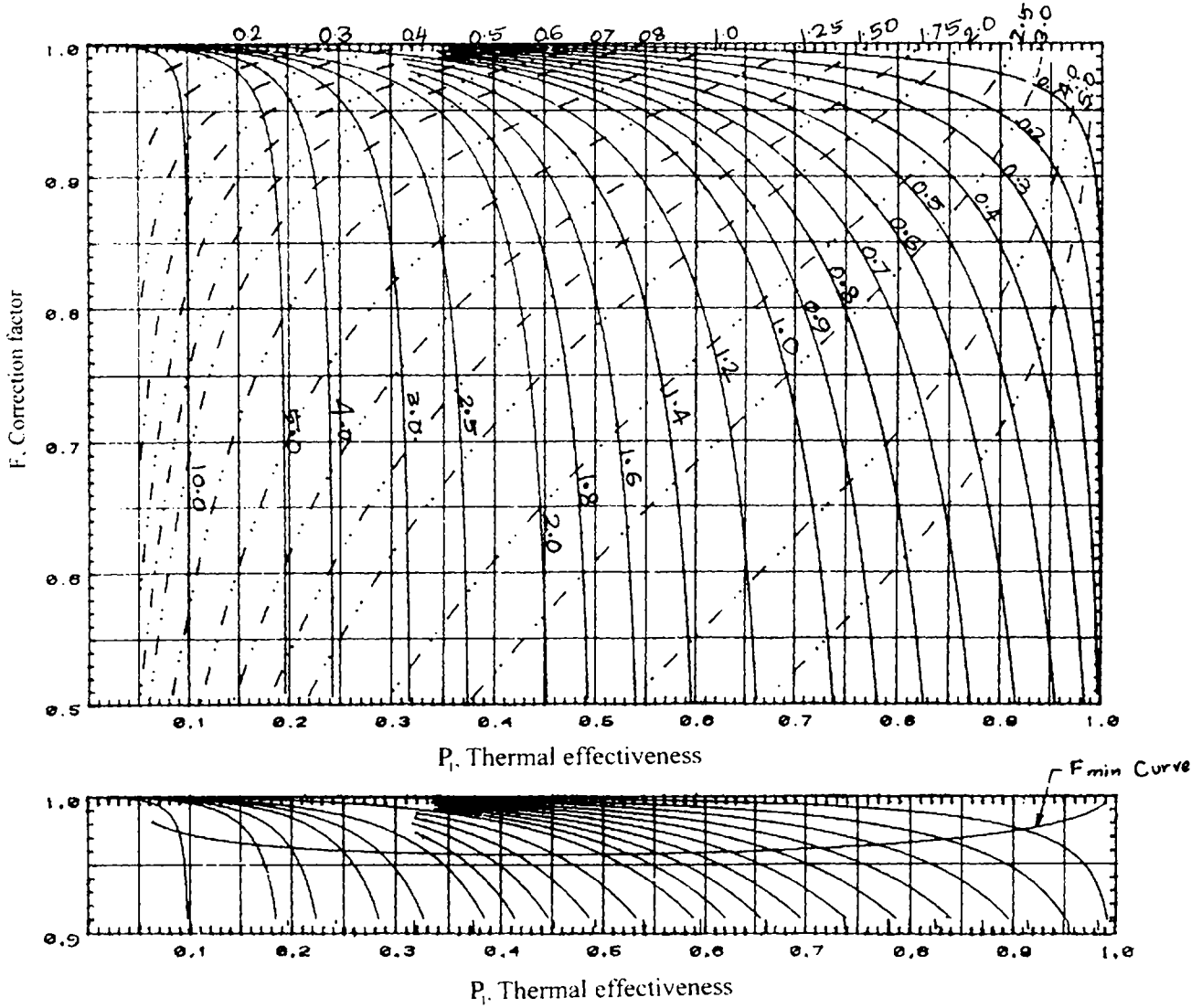


Figure 34 TEMA $G_{,}$ shell. Overall counterflow arrangement; shell fluid mixed, tube fluid mixed between passes. F as a function of P for constant R (solid lines) and constant NTU (dashed lines). *F* min curve is also shown.

Table 10 H Shell (Referred to Tube Side)

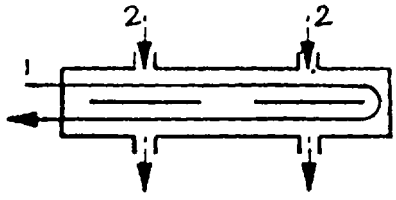
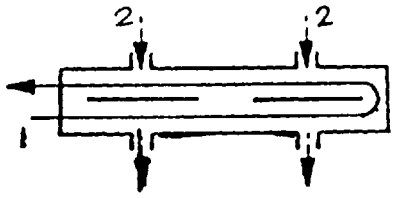
Flow arrangement	Eq. no./ Ref.	General formula	Value for $R = 1$ and special cases
 1-1 H shell: tube fluid split into two streams; shell fluid mixed	T22 [37]	$P_1 = \frac{1}{R}\{E[1 + (1 - B/2R)(1 - A/2R + AB/R)] - AB(1 - B/2R)\}$ $A = \frac{1}{1 + 1/2R}(1 - \exp[-R\,\mathrm{NTU}(1 + 1/2R)/2]$ $B = (1 - D)/(1 - D/2R)$ $D = e^{[-R\,\mathrm{NTU}(1-1/2R)/2]}$ $E = (A + B - AB/2R)/2$	Same as Eq. T22 with For $R = 0.5$ $B = \frac{R\,\mathrm{NTU}}{(2 + R\,\mathrm{NTU})}$
 1-2 TEMA H shell: overall parallel flow arrangement; shell fluid mixed, tube fluid mixed between passes	T23 [39]	$P_1 = \left[1 - \frac{B + 4GR}{(1 - D)^4}\right]$ $B = (1 + H)(1 + E)^2$ $G = (1 - D)^2(D^2 + E^2) + D^2(1 + E)^2$ $D = \frac{1 - e^{-\alpha}}{1 - 4R}$ $E = \frac{e^{-\beta} - 1}{4R + 1}$ $H = \frac{e^{-2\beta} - 1}{4R + 1}$ $\alpha = \frac{\mathrm{NTU}}{8}(4R - 1)$ $\beta = \frac{\mathrm{NTU}}{8}(4R + 1)$	For $R = 0.25$ $P_1 = \left[1 - \frac{B + 4GR}{(1 - D)^4}\right]$ $D = -\mathrm{NTU}/8$

chart referred to the shell side is given in Fig. 35. For the $H_{1\text{-}2}$ arrangement, the thermal relations for the parallel flow and counterflow arrangements are given by Eqs. T23 and T24 respectively, in Table 10, and the thermal effectiveness chart for the counterflow arrangement is given in Fig. 36.

TEMA J Shell or Divided-Flow Shell

The use of divided-flow exchangers with one shell pass and one or more tube passes is very common. If the shell-side heat-transfer resistance is not a limiting factor, and entrance and exit

Table 10 Continued

Flow arrangement	Eq. no./ Ref.	General formula	Value for $R = 1$ and special cases
 1-2 TEMA H shell: overall counterflow arrangement; shell fluid mixed, tube fluid mixed between passes	T24 [39]	$P_1 = \left[1 - \frac{(1-D)^4}{(B-4RG)}\right]$ $B = (1+H)(1+E)^2$ $G = (1-D)^2(D^2+E^2)$ $+D^2(1+E)^2$ $D = \frac{1-e^{-\alpha}}{4R+1}$ $E = \frac{1-e^{-\beta}}{4R-1}$ $H = \frac{1-e^{-2\beta}}{4R-1}$ $\alpha = \frac{NTU}{8}(4R+1)$ $\beta = \frac{NTU}{8}(4R-1)$	For $R = 0.25$ $P_1 = \left[1 - \frac{(1-D)^4}{(B-G)}\right]$ $B = (1+\alpha)(1+\alpha/2)^2$ $G = (1-D)^2 x$ $(D^2 + \alpha^2/4) + D^2(1+\alpha/2)^2$

losses are neglected, the shell-side pressure loss is approximately one-eighth of that same heat exchanger arranged as the conventional $E_{1\text{-}2}$ or $E_{1\text{-}4}$ exchanger. The possible flow arrangements are

1. Divided-flow shell with one tube pass. This arrangement is equivalent to the $E_{1\text{-}2}$ exchanger with unmixed shell fluid.
2. Divided-flow shell with two tube passes.
3. Divided-flow shell with four tube passes.
4. Divided-flow shell with infinite number of tube passes.

Jaw [41] analyzed the cases with two and four tube passes. Extending the number of tube passes to infinity, the case becomes identical to that of mixed–mixed crossflow, as derived by Gardner [42a]. Divided flow shell with one tube pass arrangement is equivalent to $E_{1\text{-}2}$ exchanger with unmixed shell fluid as presented by Gardner [42b]. The difference in P is negligible for four or more passes compared to the two passes arrangement in the region of interest, i.e., $F > 0.5$. The thermal effectiveness relations for $J_{1\text{-}1}$, $J_{1\text{-}2}$, $J_{1\text{-}4}$, and $J_{1\text{-}\infty}$ arrangements are given by Eqs. T25, T26, T27, and T28, respectively, in Table 11. The thermal effectiveness charts for $J_{1\text{-}1}$, $J_{1\text{-}2}$, and $J_{1\text{-}4}$ are given in Figs. 37, 38, and 39, respectively.

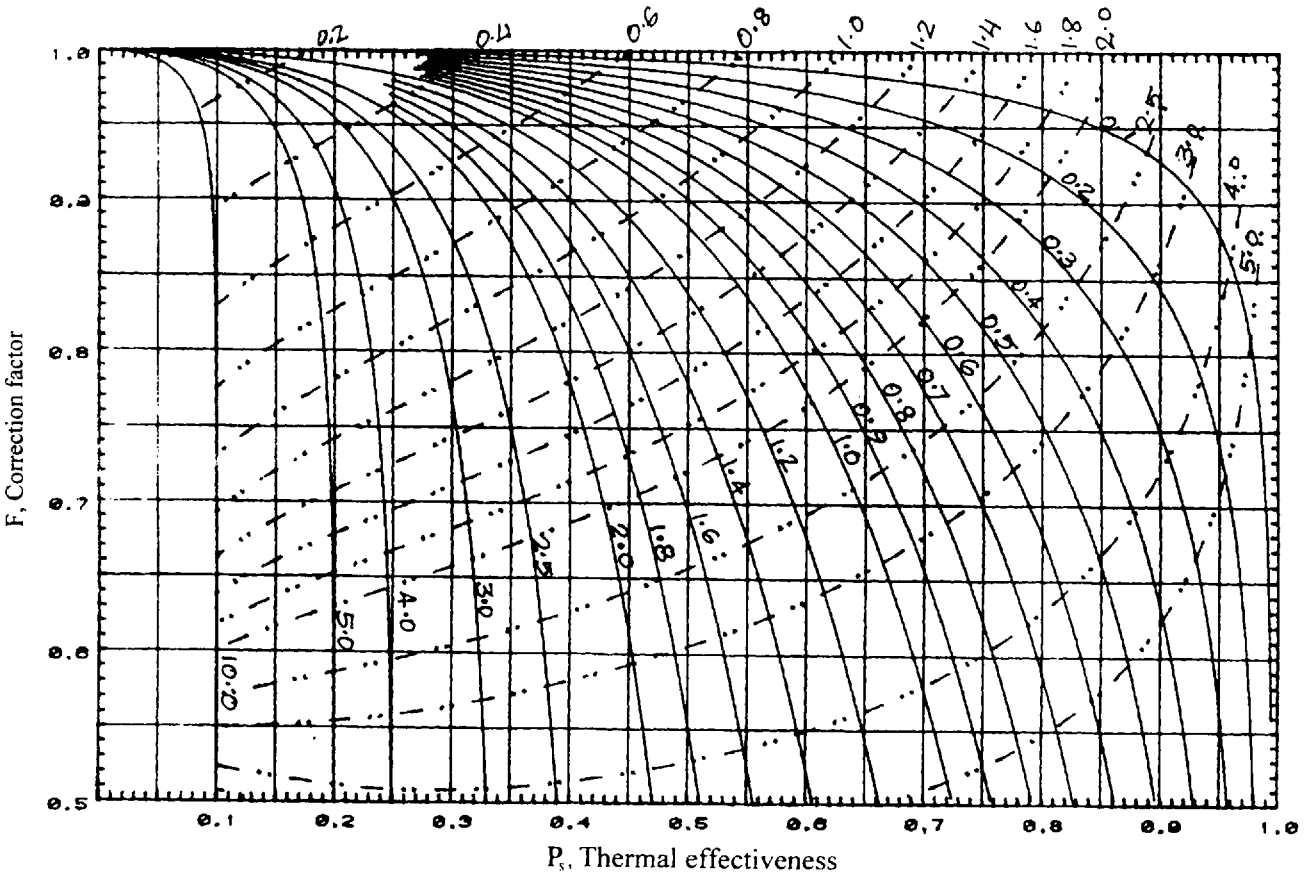


Figure 35 $H_{1,1}$ shell. Tube fluid split into two streams. Shell fluid mixed. F as a function of P for constant R (solid lines) and constant NTU (dashed lines) referred to shellside.

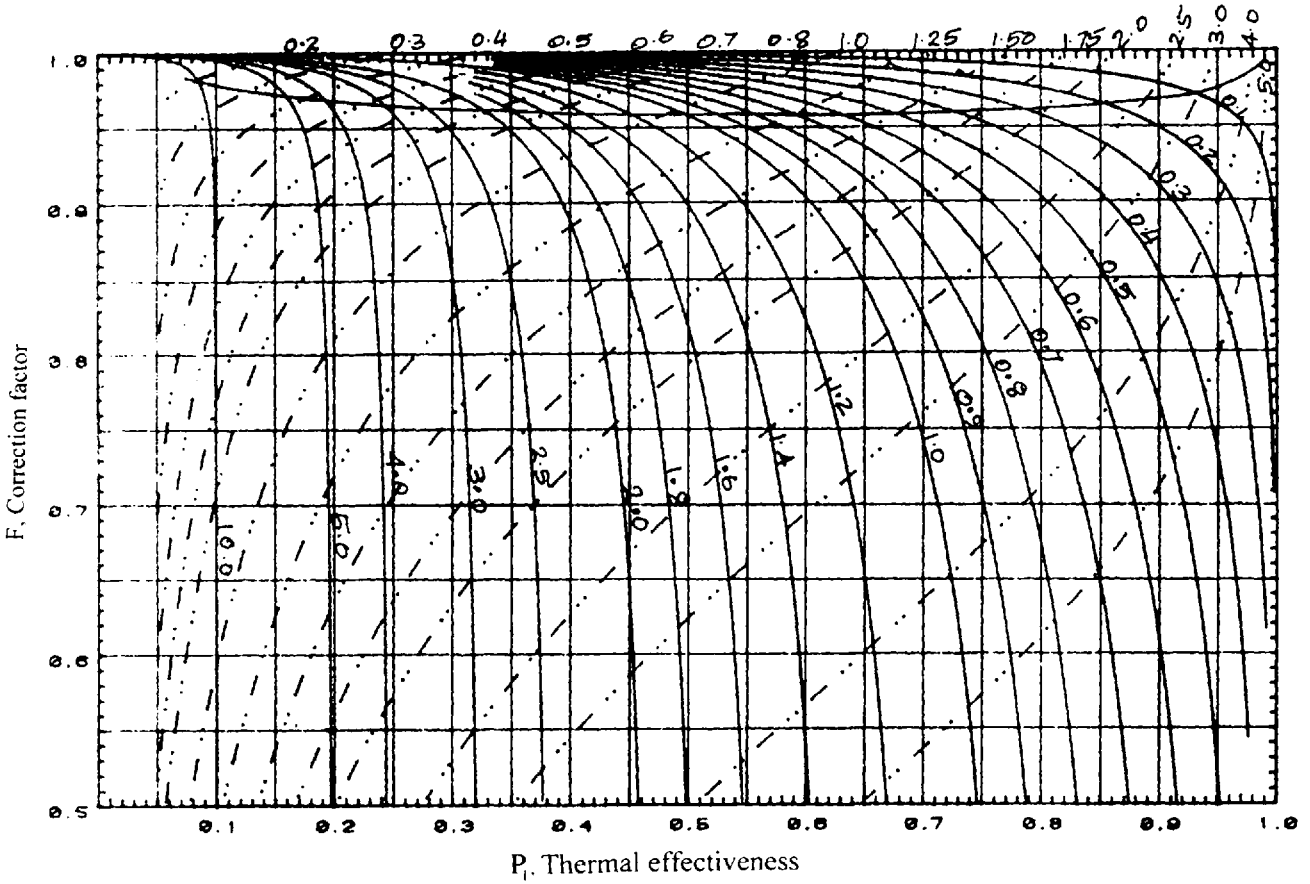


Figure 36 TEMA H_1 shell. Overall counterflow arrangement; shell fluid mixed, tube fluid mixed between passes. F as a function of P for constant R (solid lines) and constant NTU (dashed lines).

TEMA X Shell

This exchanger is for very-low-pressure applications. For an X_{1-1} exchanger, the thermal effectiveness is same as single-pass crossflow with both fluids unmixed, that is, the unmixed–unmixed case [1]. An X_{1-2} crossflow shell and tube exchanger is equivalent to Fig. 40(a) for both fluids unmixed throughout with overall parallel flow (shell fluid entering at the tube inlet pass end) and Fig. 40(b) for overall counterflow (shell fluid entering at the tube exit pass end), respectively. The thermal relation formulas are discussed in Section 6.6.

6.5 Thermal Effectiveness of Multiple Heat Exchangers

Since the thermal effectiveness of a basic heat exchanger is sometimes low, to enhance the exchanger effectiveness multipassing in the same unit or connecting multiple exchangers is resorted to. Sometimes, to utilize the allowable pressure drop effectively, multipassing is also employed; this in turn enhance the thermal effectiveness. Multipassing by multiple units is possible both with compact exchangers and shell and tube exchangers. With multipassing, two or more exchangers can be coupled either in an overall parallel or in an overall countercurrent scheme as shown in Fig. 41. Multipassing is also possible in a single unit of a compact exchanger (Fig. 42).

Fundamental formulas for the global effectiveness of multiple units are given next. These equations are not valid for multiple tubeside passes of various TEMA shells. The following idealizations are employed, in addition to those already listed at the beginning of this section:

1. Each pass has the same effectiveness, although any basic flow arrangement may be employed in any pass. If each pass has the same flow arrangement, then NTU is equally distributed between N passes, and NTU per pass (NTU_p) is given by NTU/N.
2. The fluid properties are idealized as constant so that C^* or R is the same for each pass. The final results of this analysis are valid regardless of which fluid is being C_{max} or C_{min}.

Two-Pass Exchangers

The expression for the global effectiveness for the parallel flow case is given by Pignotti [43]:

$$P_2 = P_A + P_B - P_A P_B(1 + R) \tag{72}$$

and for the counterflow case by

$$P_2 = \frac{P_A + P_B - P_A P_B(1 + 4)}{(1 - RP_A P_B)} \tag{73}$$

where P_A and P_B are the thermal effectiveness of individual heat exchangers and R is the capacity rate ratio.

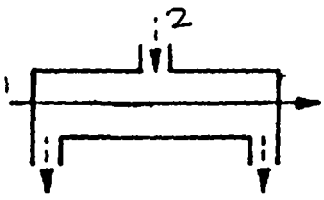
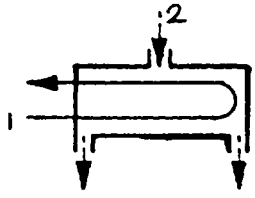
N-Pass Exchangers

Counterflow Arrangement. The effectiveness P_N of an N-pass assembly, in terms of the efectiveness P_1 of each unit, which is equal for all units, has been described by Domingos [44]. For overall countercurrent connection, the effectiveness is given by

$$P_N = \frac{1 - \left[\dfrac{(1 - P_1 R)}{(1 - P_1)}\right]^N}{R - \left[\dfrac{(1 - P_1 R)}{(1 - P_1)}\right]^N} \qquad \text{for } R \neq 1 \tag{74a}$$

$$= \frac{NP_1}{1 + (N - 1)P_1} \qquad \text{for } R = 1 \tag{74b}$$

Table 11 J Shell (Referred to Tube Side)

Flow arrangement	Eq. no./ Ref.	General formula	Value for $R = 1$ and special cases
 1-1 TEMA J shell: shell fluid mixed	T25 [40]	$P_1 = 1 - \frac{(2R-1)}{(2R+1)}\left[\frac{2R+\phi^{-(R+0.5)}}{2R-\phi^{-(R-0.5)}}\right]G$ $\phi = e^{NTU}$	For $R = 0.5$, $P_1 = 1 - \frac{1+\phi^{-1}}{2+NTU}$
 1-2 TEMA J shell: shell fluid mixed and tube fluid mixed between passes	T26 [41]	$P_1 = \frac{2}{1+2R\,[1+\lambda A-2B\lambda\,(1+C)]}$ $A = \frac{\phi^{R\lambda}+1}{\phi^{R\lambda}-1}$ $B = \frac{\frac{\phi^{R(1+\lambda)/2}}{\phi^{R\lambda}-1}}{1+\lambda\left(\frac{\phi^{R\lambda}+1}{\phi^{R\lambda}-1}\right)}$ $C = 1 + \frac{\lambda\phi^{R(\lambda-1)/2}}{\phi^{R\lambda}-1}$ $\phi = e^{NTU}$ $\lambda = \frac{\sqrt{1+4R^2}}{2R}$	Same as Eq. T26

Here, R is the heat capacity rate ratio, which is the same for the individual unit, as for the overall assembly. Alternately, if P_N is known, then the individual component effectiveness can be determined from the following formulas:

$$P_1 = \frac{1 - \left[\frac{(1-P_N R)}{(1-P_N)}\right]^{1/N}}{R - \left[\frac{(1-P_N R)}{(1-P_N)}\right]^{1/N}} \quad \text{for } R \neq 1 \tag{75a}$$

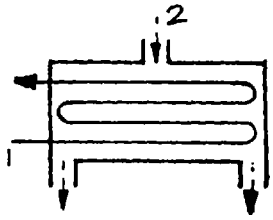
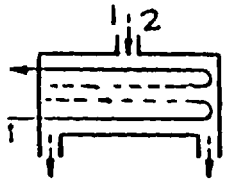
$$= \frac{P_N}{N - P_N(N-1)} \quad \text{for } R = 1 \tag{75b}$$

Parallel Flow Arrangement. Refer to Table 12 for thermal relation formulas.

6.6 Multipass Crossflow Exchangers

Two or more crossflow units can be coupled in two or more passes either in an overall parallel flow or in an overall counterflow arrangement. When both fluids are mixed in the interpass,

Table 11 Continued

	Eq. no./ Ref.	General formula	Value for $R = 1$ and special cases
 1-4 J Shell: shell fluid mixed and tube fluid mixed between passes	T27 [41]	$P_1 = \dfrac{4}{1 + A + 4R\,[1 + \lambda B - 2\,C\lambda\,(1 + D)]}$ $A = \dfrac{2\sqrt{\phi}}{1 + \sqrt{\phi}}$ $B = \dfrac{\phi^{R\lambda} + 1}{\phi^{R\lambda} - 1}$ $C = \dfrac{\dfrac{\phi^{R(1+\lambda)/2}}{\phi^{R\lambda} - 1}}{1 + \lambda\left(\dfrac{\phi^{R\lambda} + 1}{\phi^{R\lambda} - 1}\right)}$ $D = 1 + \dfrac{\lambda\phi^{R(\lambda-1)/2}}{\phi^{R\lambda} - 1}$ $\phi = e^{NTU}$ $\lambda = \dfrac{\sqrt{1 + 16\,R^2}}{4R}$	Same as Eq. T27
 Lime of 1-N J Shell for $N \to \infty$: shell fluid mixed and tube fluid mixed between passes; stream symmetric	T28 [42]	$P = \dfrac{1}{\dfrac{R\phi^R}{(\phi^R - 1)} + \dfrac{\phi}{\phi - 1} - \dfrac{1}{NTU}}$ $\phi = e^{NTU}$	Same as Eq. T28

the resulting flow arrangement can be differentiated only by the flow arrangements in each pass (unmixed–mixed or mixed–mixed). However, if one fluid is unmixed throughout, the order in which the streams enter the next pass must be differentiated. The coupling of the unmixed fluid from one pass to the other pass can be two types as shown in Fig. 43: (1) identical order coupling, and (2) inverted order coupling. The coupling is referred to an identical order if the stream leaving one pass enters the next pass from the same side as in the previous pass, as in Fig. 43(a), whereas a coupling is considered to be in an inverted order if the stream leaving one pass enters the next pass from the opposite side of the previous pass, as in Fig. 43(b). Inverted-order coupling is very convenient for manufacturing and installation of heat exchangers. Thermal effectiveness must decrease for constant NTU whenever irreversibilities take place, which may be due to mixing between passes, or due to higher local temper-

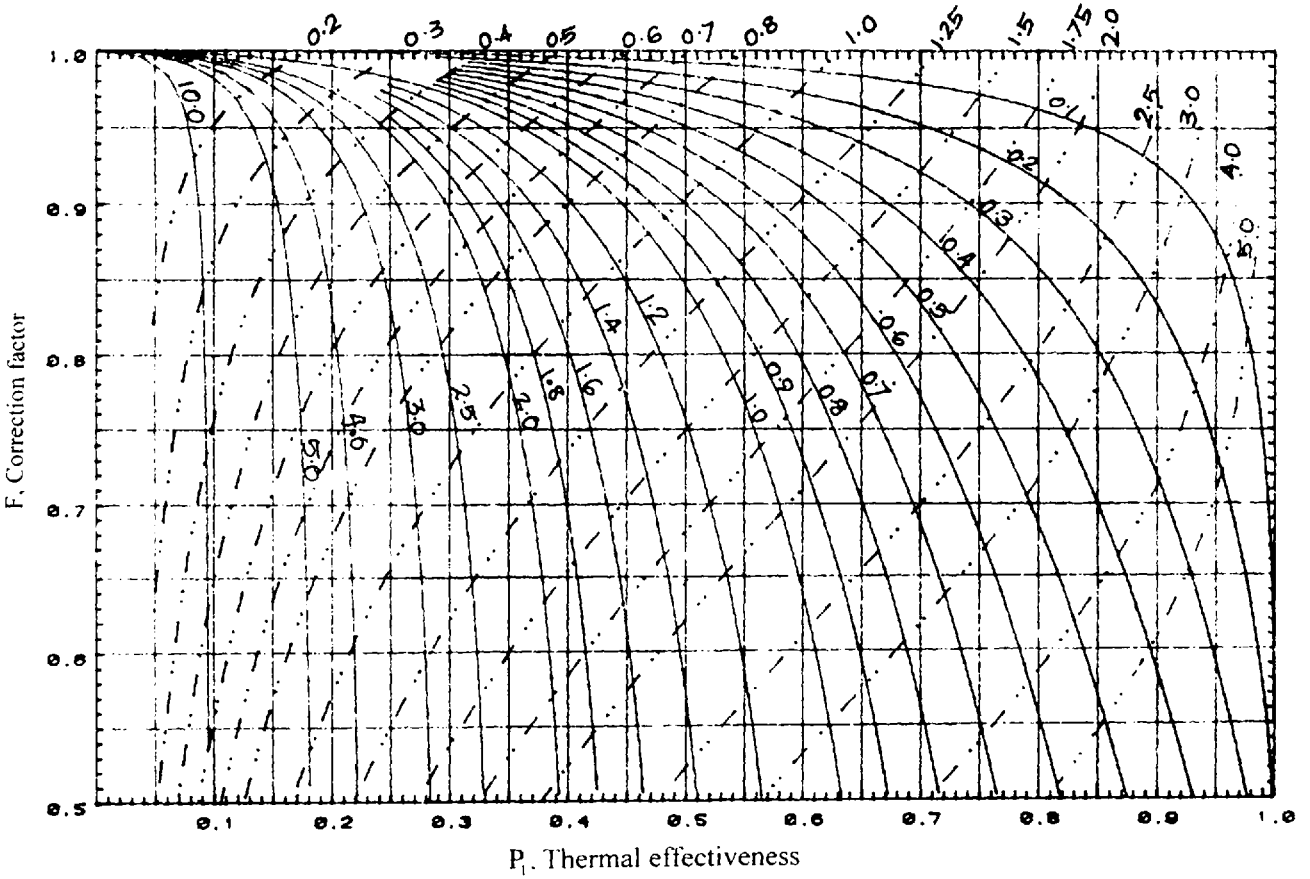


Figure 37 TEMA J_{11} shell. Shell fluid mixed. F as a function of P for constant R (solid lines) and constant NTU (dashed lines).

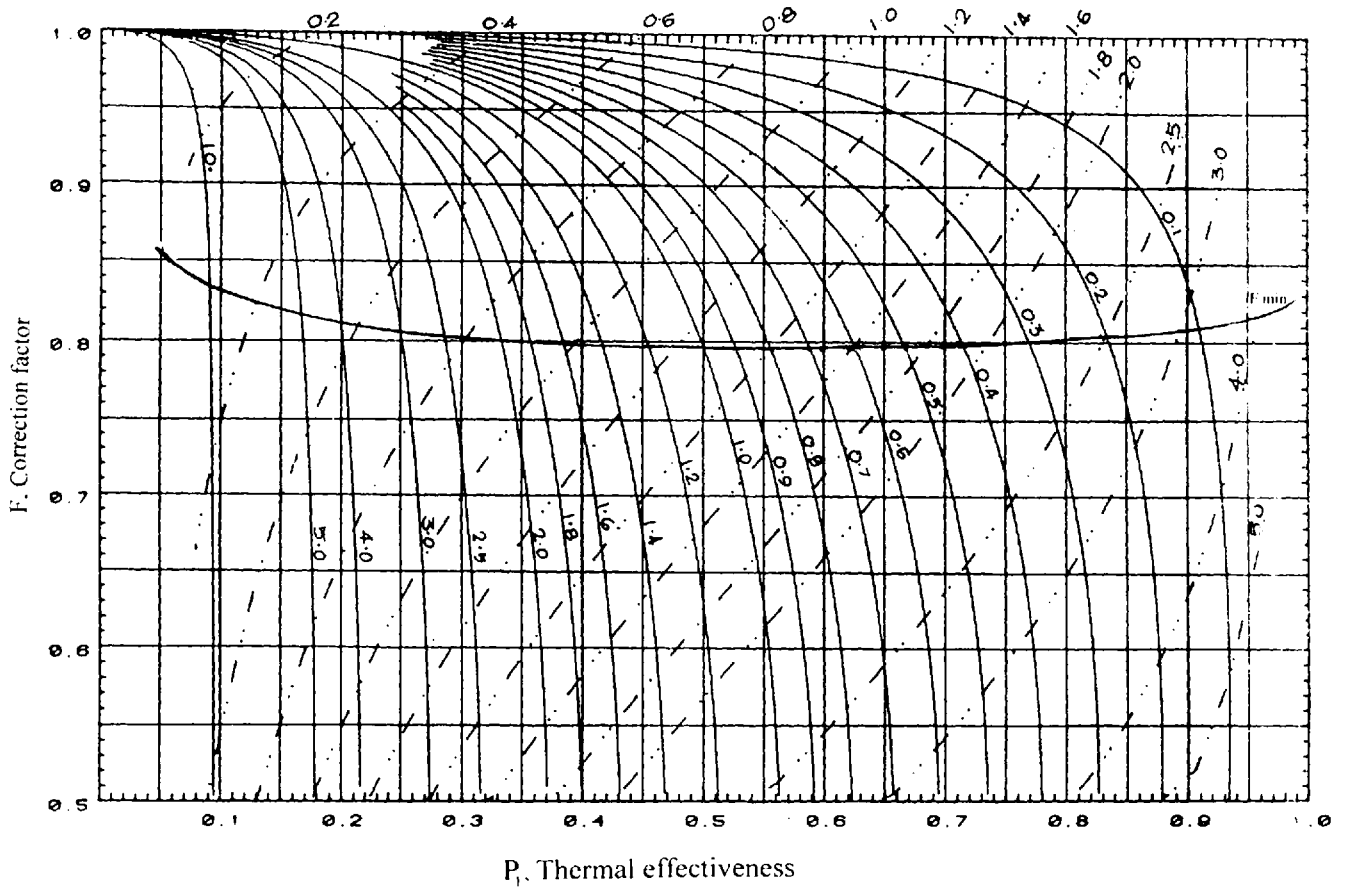


Figure 38 TEMA $J_{1,2}$ shell. Shell fluid mixed and tube fluid mixed between passes. F as a function of P for constant R (solid lines) and constant NTU (dashed lines), with *F* min to avoid temperature cross (horizontal bowl-shaped curve).

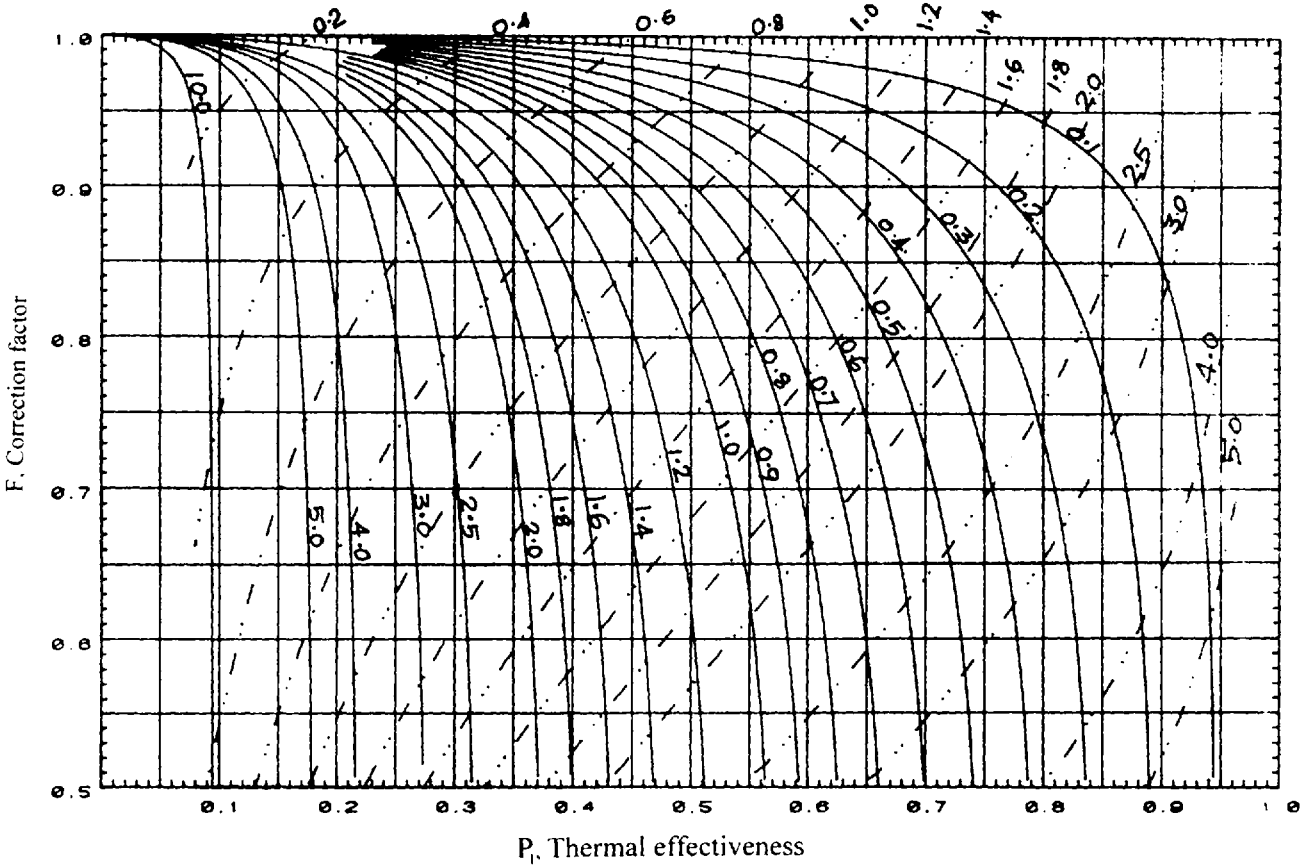


Figure 39 TEMA $J_{1,4}$ shell. Shell fluid mixed and tube fluid mixed between passes. F as a function of P for constant R (solid lines) and constant NTU (dashed lines).

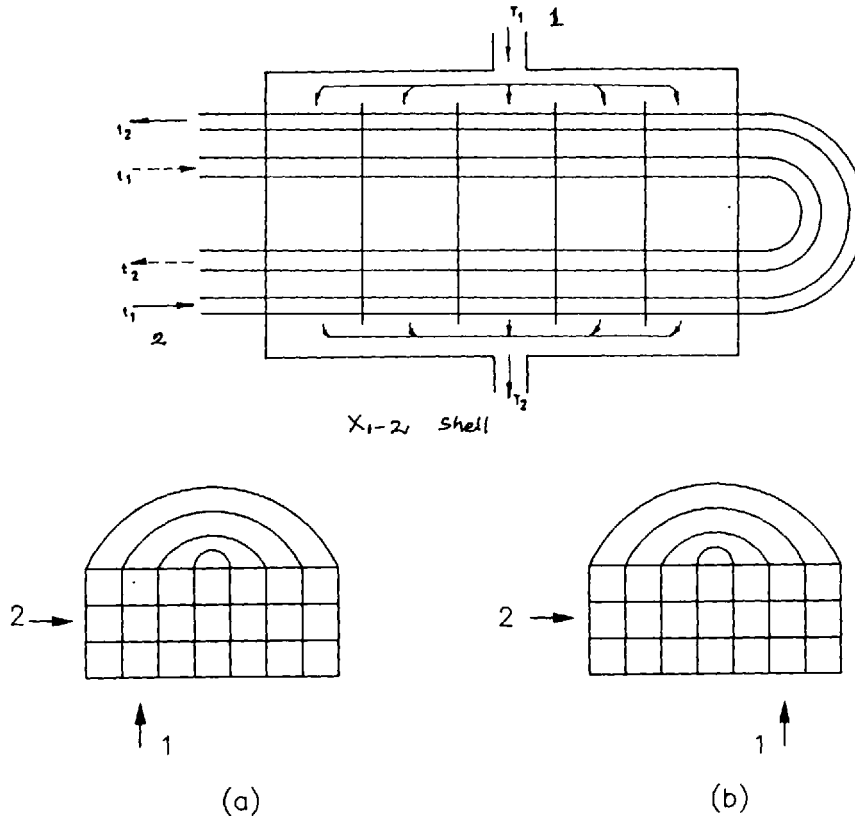


Figure 40 $X_{1,2}$ shell arrangement equivalent with two pass crossflow heat exchanger. (a) Parallel flow; (b) counterflow.

ature difference between the fluids, which occurs when the order of the flow arrangement is inverted [28]. Some of the possible cases of two-pass heat exchangers are shown in Fig. 44. All these cases were analyzed by Stevens et al. [29], some analytically and others by numerical integration, whereas Baclic [3] solved all possible flow arrangements of two passes units analytically. Multipass crossflow arrangements with complete mixing between passes were analyzed by Domingos [44], and the formulas are also presented in Ref. 2.

Multipassing with Complete Mixing Between Passes. Equations T29 to T33 in Table 12 define thermal relation formulas for various multipass crossflow arrangements with complete mixing between passes. Thermal effectiveness charts are given for the following cases of two- and three-pass cross-counterflow arrangements with complete mixing between passes:

1. Weaker fluid is mixed in all the passes: For the two-pass arrangement (IV-a or I-d of Fig. 44) the thermal effectiveness chart is given in Fig. 45, and in Fig. 46 for the three-pass arrangements.
2. Stronger fluid is mixed in all the passes: For the two-pass arrangement (IV-a or I-d of Fig. 44), the thermal effectiveness chart is given in Fig. 47, and in Fig. 48 for the three-pass arrangements.
3. Both the fluids unmixed–unmixed in all the passes: For the two-pass arrangements (IV-d

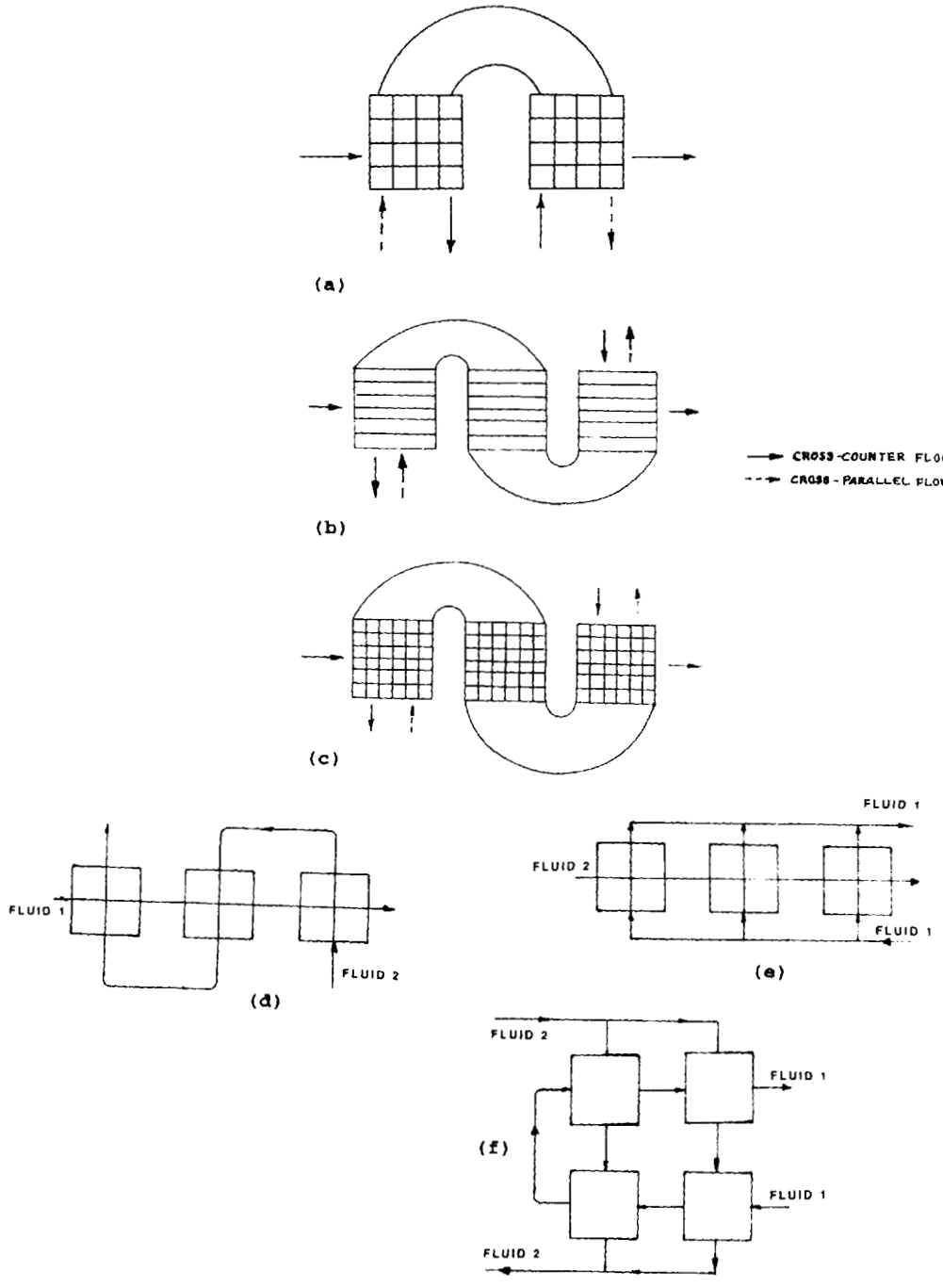


Figure 41 Multipass assemblies.

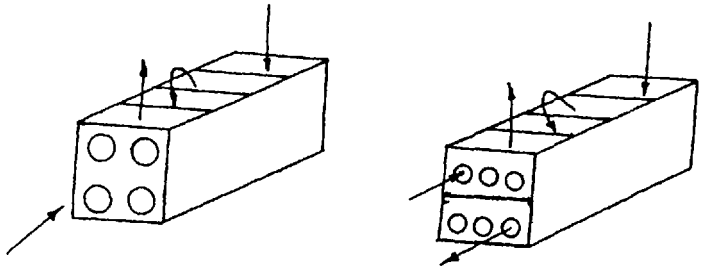


Figure 42 Multipassing in the same unit.

Table 12 Multiple Assemblies of Heat Exchangers

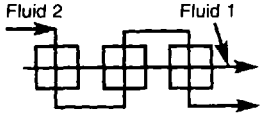
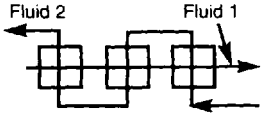
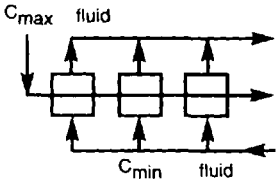
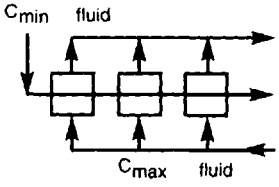
Flow arrangement	Eq. no./ Ref.	General formula	Value for $C^* = 1$ and $C = 0$
 N-pass exchanger (N = 3 as shown): parallel-cross-flow arrangement; fluids mixed between passes; each pass having the same effectiveness ε_p	T29 [44]	$\varepsilon_N = \dfrac{1 - \sum_{i=1}^{N}[1 - \varepsilon_i(1 + C^*)]}{1 + C^*}$ $\varepsilon_N = \dfrac{1 - [1 - \varepsilon_p(1 + C^*)]^N}{1 + C^*}$ Note $C^* = C_p^*$, and NTU = N NTU_p $\varepsilon_p = \dfrac{1}{1 + C^*}[1 - \{1 - \varepsilon_N(1 + C^*)\}^{1/N}]$	$\varepsilon_N = 0.5\,[1 - (1 - 2\varepsilon_p)^N]$ for $C^* = 1$ $= 1 - (1 - \varepsilon_p)^N$ for $C^* = 0$ $\varepsilon_p = 0.5\,[1 - (1 - 2\,\varepsilon_N)^{1/N}]$ for $C^* = 1$ $= 1 - (1 - \varepsilon_N)^{1/N}$ for $C^* = 0$
 N-pass exchanger, (N = 3 as shown): counter-cross-flow arrangement; fluids mixed between passes, and each pass having the same effectiveness ε_p	T30 [44]	$\varepsilon_N = \dfrac{1 - \sum_{i=1}^{N}\left(\dfrac{1 - \varepsilon_i C^*}{1 - \varepsilon_i}\right)}{C^* - \sum_{i=1}^{N}\left(\dfrac{1 - \varepsilon_i C^*}{1 - \varepsilon_i}\right)}$ $\varepsilon_N = \dfrac{1 - \left(\dfrac{1 - \varepsilon_p C^*}{1 - \varepsilon_p}\right)^N}{C^* - \left(\dfrac{1 - \varepsilon_p C^*}{1 - \varepsilon_p}\right)^N}$ Note $C^* = C_p^*$, and NTU = N NTU_p $\varepsilon_p = \dfrac{1 - \left(\dfrac{1 - \varepsilon_N C^*}{1 - \varepsilon_N}\right)^{1/N}}{C^* - \left(\dfrac{1 - \varepsilon_N C^*}{1 - \varepsilon_N}\right)^{1/N}}$	$\varepsilon_N = \dfrac{N\varepsilon_p}{1 + (N-1)\,\varepsilon_p}$ for $C^* = 1$ $= 1 - (1 - \varepsilon_p)^N$ for $C^* = 0$ $\varepsilon_p = \dfrac{\varepsilon_N}{N - (N-1)\,\varepsilon_N}$ for $C^* = 1$ $= 1 - (1 - \varepsilon_N)^{1/N}$ for $C^* = 0$

Table 12 Continued

Flow arrangement	Eq. no./ Ref.	General formula	Value for $C^* = 1$ and $C = 0$
 N-pass exchanger (N = 3 as shown): C_{min} stream is in parallel, C_{max} stream is in series; series fluid mixed between passes, and each pass having the same effectiveness ε_p	T31 [44]	$\varepsilon_N = \frac{1}{C^*}\left[1 - \left(1 - \frac{C^*\varepsilon_p}{N}\right)^N\right]$ Note $C^* = NC_p^*$, and NTU = NTU_p $\varepsilon_p = \frac{1}{C_p^*}[1 - (1 - NC_p^*\varepsilon_N)^{1/N}]$	$\varepsilon_N = 1 - (1 - \varepsilon_p/N)^N$ for $C^* = 1$ $= \varepsilon_p$ for $C^* = 0$ $\varepsilon_p = N[1 - (1 - \varepsilon_N)^{1/N}]$ for $C^* =$ $= \varepsilon_N$ for $C^* = 0$
 N-pass exchanger ($N = 3$ as shown): C_{max} stream in parallel, C_{min} stream is in series; series fluid is mixed between passes, and each pass having the same effectiveness ε_p	T32 [44]	Parallel stream as C_{max} stream and $C_{max}/N \le C_{min}$, $C \ge 1/N$ $\varepsilon_N = 1 - \left(1 - \frac{\varepsilon_p}{NC^*}\right)^N$ $C^* = 1/NC_p^*$, NTU = NTU_p/C^* $\varepsilon_p = \frac{1}{C_p^*}[1 - (1 - \varepsilon_N)^{1/N}]$	$\varepsilon_N = 1 - (1 - \varepsilon_p)^N$ for $C_p^* = 1 - \frac{1}{NC^*}$ $= 1 - e^{-NTU}$ for $N \to \infty$, $C^* = 0$ $\varepsilon_p = 1 - (1 - \varepsilon_N)^{1/N}$ for $C_p^* = 1 - \frac{1}{NC^*}$ $= 1$ for $N \to \infty$, $C_p^* = 0$
	T33 [44]	Parallel stream as C_{max} stream and $C_{max}/N > C_{min}$, and $C^* \le 1/N$ $\varepsilon_N = 1 - (1 - \varepsilon_p)^N$ $C^* = C_p^*/N$, NTU = $NTU_p N$ $\varepsilon_p = 1 - (1 - \varepsilon_N)^{1/N}$	$C^* = 1$ only when $N = 1$ $\varepsilon_N = 1 - (1 - \varepsilon_p)^N$ for $C_p^* = 1 - \frac{C}{1}$ $= 1 - e^{-NTU}$ for $C^* = 0$ $\varepsilon_p = 1 - (1 - \varepsilon_N)^{1/N}$ for $C_p^* = 1$ $= 1 - e^{-NTU_p}$ for $C_p^* = 0$

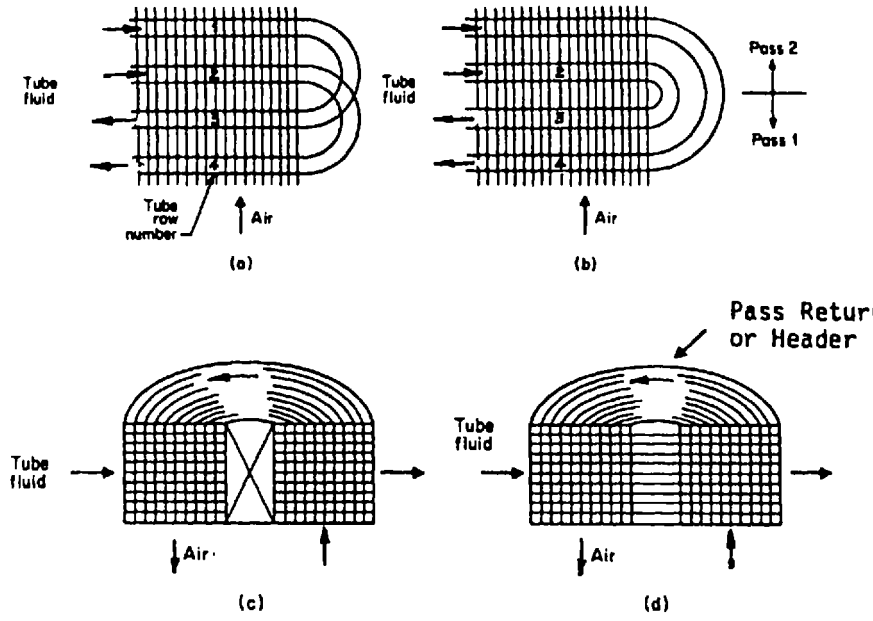


Figure 43 Two pass parallel-cross flow with both fluids unmixed throughout; coupling of tubefluid between passes. (a) Identical order coupling; (b) inverted order coupling. The cases (c) and (d) are symbolic representations of cases (a) and (b), respectively [1].

of Fig. 44), the thermal effectiveness chart is given in Fig. 49, and in Fig. 50 for the three-pass arrangements.

Two Passes with One Fluid Unmixed Throughout, Cross-Counterflow Arrangement. Some of the possible cases of two passes with one fluid unmixed throughout with cross-counterflow arrangements are given here, and these cases were solved by Stevens et al. [29]:

1. Two-pass cross-counterflow arrangement. Fluid 1 unmixed throughout, inverted-order coupling; fluid 2 mixed throughout (II-a of Fig. 44).
2. Two-pass cross-counterflow arangement. Fluid 1 mixed throughout; fluid 2 unmixed throughout, inverted-order coupling (I-b of Fig. 44).
3. Two-pass cross-counterflow arrangement. Fluid 1 unmixed throughout, identical-order coupling; fluid 2 mixed throughout (III-a of Fig. 44).
4. Two-pass cross-counterflow arrangement. Fluid 1 mixed throughout; fluid 2 unmixed throughout, identical-order coupling (I-c of Fig. 44).

Thermal relation formulas (T34–T37) for these cases are given in Table 13, and thermal effectiveness charts are given in Figs. 51, 52, 53, and 54, respectively.

Two Passes with Both Fluids Unmixed–Unmixed in Each Pass and One Fluid Unmixed Throughout, Cross-Counterflow Arrangement. Possible cases of two passes with both fluids unmixed–unmixed in each pass and one fluid unmixed throughout with cross-counterflow arrangements are:

1. Two-pass cross-counterflow arrangement. Fluid 1 unmixed throughout, inverted-order coupling; fluid 2 unmixed in each pass and mixed between passes (II-d of Fig. 44).
2. Two-pass cross-counterflow arrangement. Fluid 1 unmixed in each pass and mixed between passes; fluid 2 unmixed throughout, inverted-order coupling (IV-b of Fig. 44).

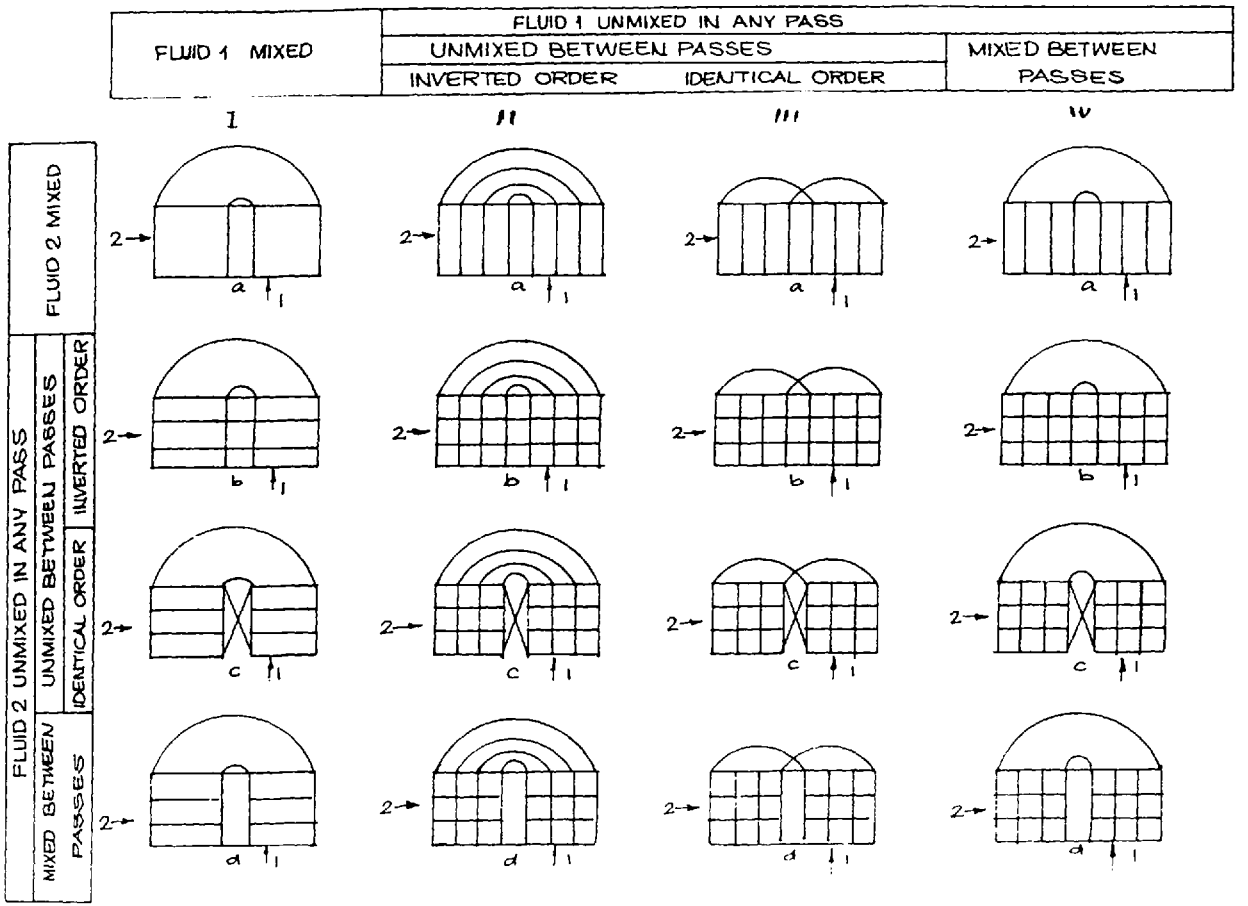


Figure 44 Some of the possible cases of two pass heat exchangers [29].

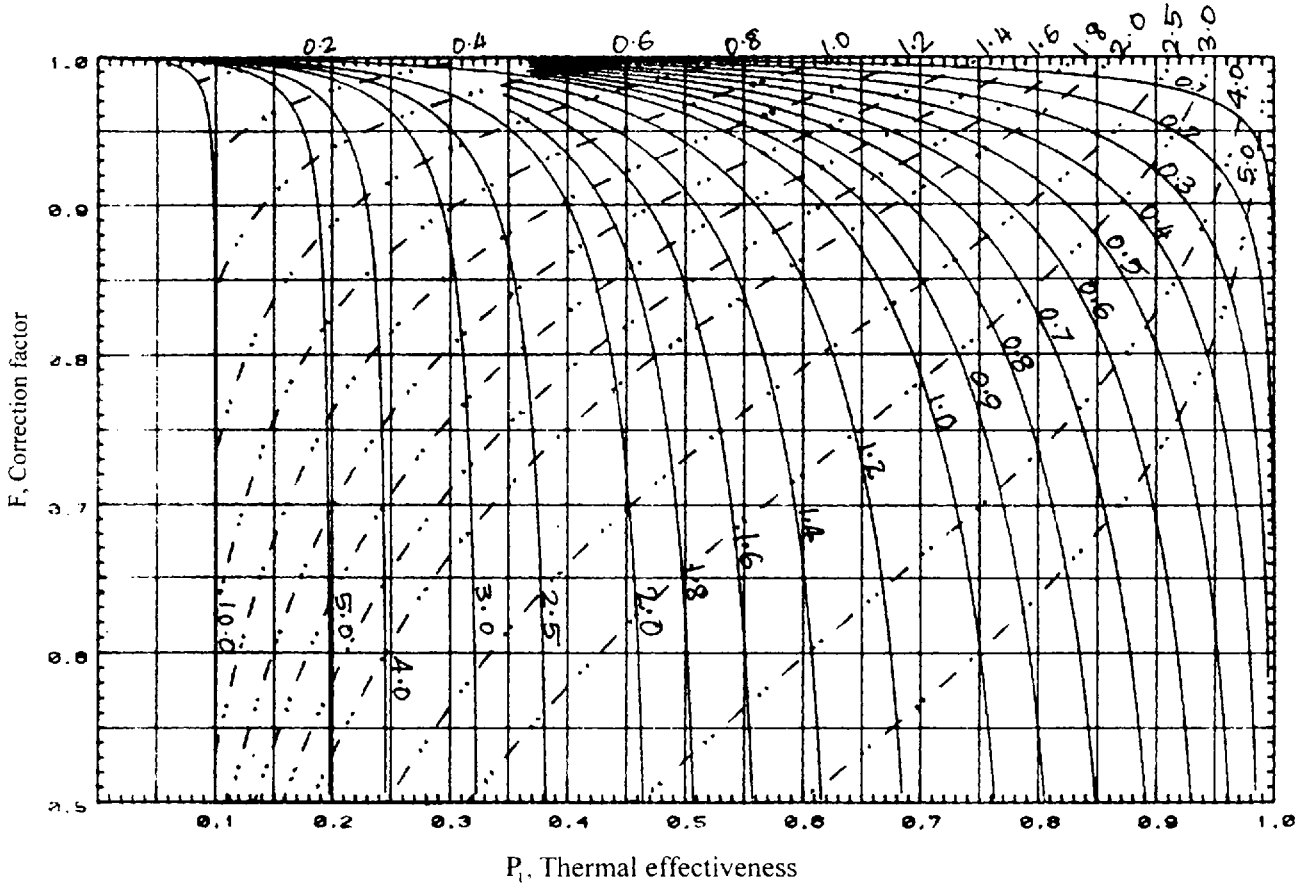


Figure 45 Two pass cross-counterflow arrangement with complete mixing between passes. Each pass is unmixed-mixed arrangement with weaker fluid mixed (iv-a or I-d of Fig. 44); F-R-P-NTU chart; F as a function of P for constant R (solid lines) and constant NTU (dashed lines).

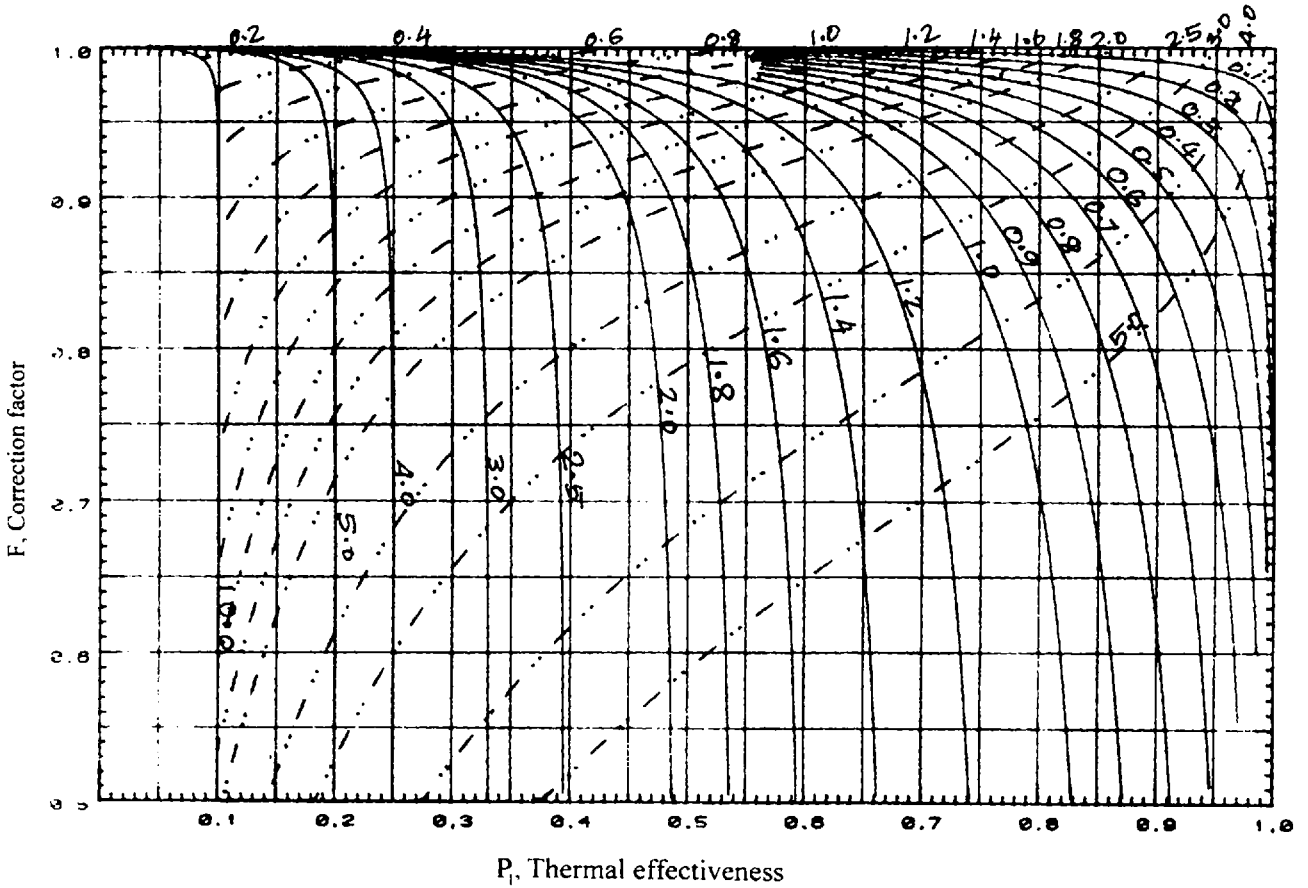


Figure 46 Three pass cross-counterflow arrangement with complete mixing between passes. Each pass is unmixed-mixed arrangement with weaker fluid mixed; F-R-P-NTU chart; F as a function of P for constant R (solid lines) and constant NTU (dashed lines).

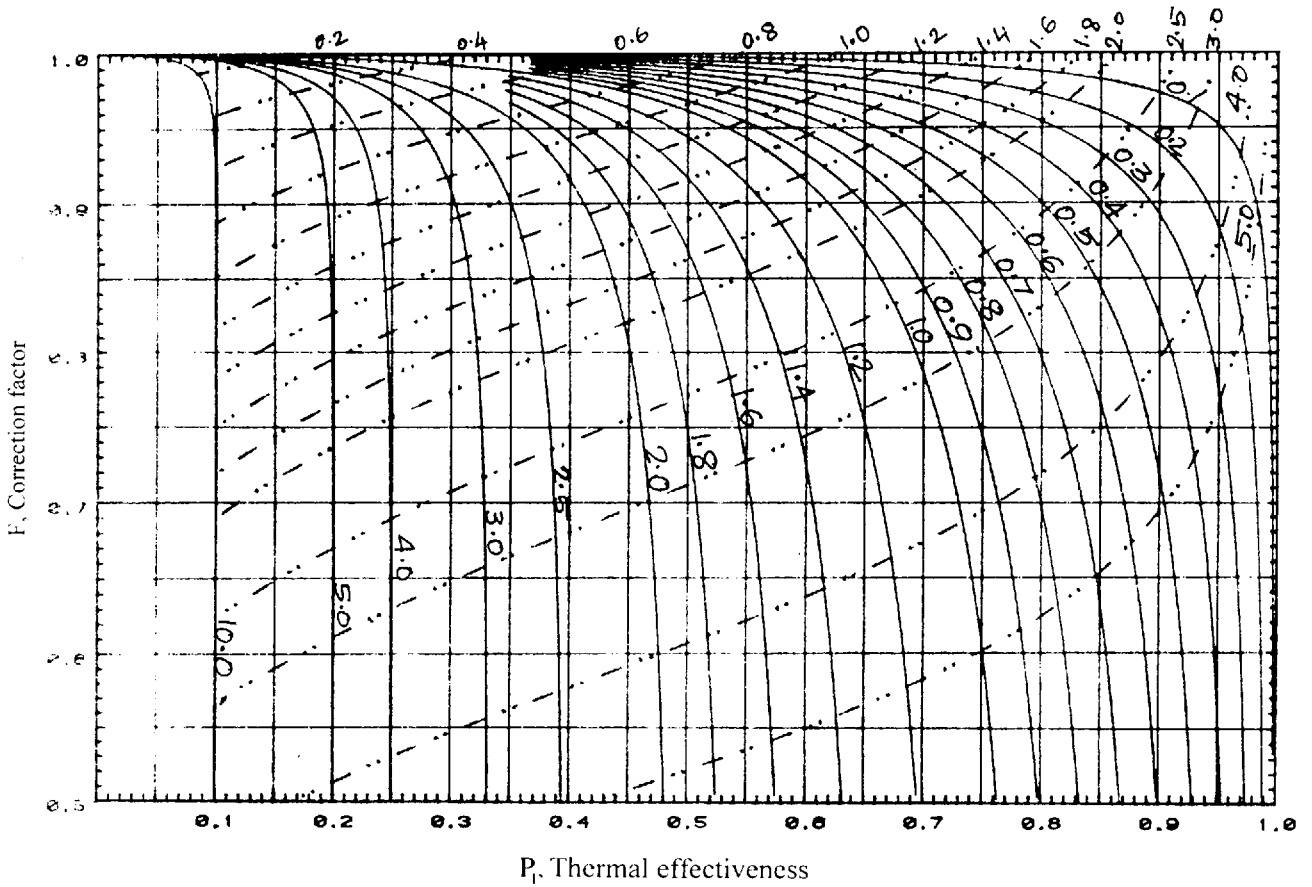


Figure 47 Two pass cross-counterflow arrangement with complete mixing between passes. Each pass is unmixed-mixed arrangement with stronger fluid mixed (iv-a or I-d of Fig. 44); F-R-P-NTU chart; F as a function of P for constant R (solid lines) and constant NTU (dashed lines).

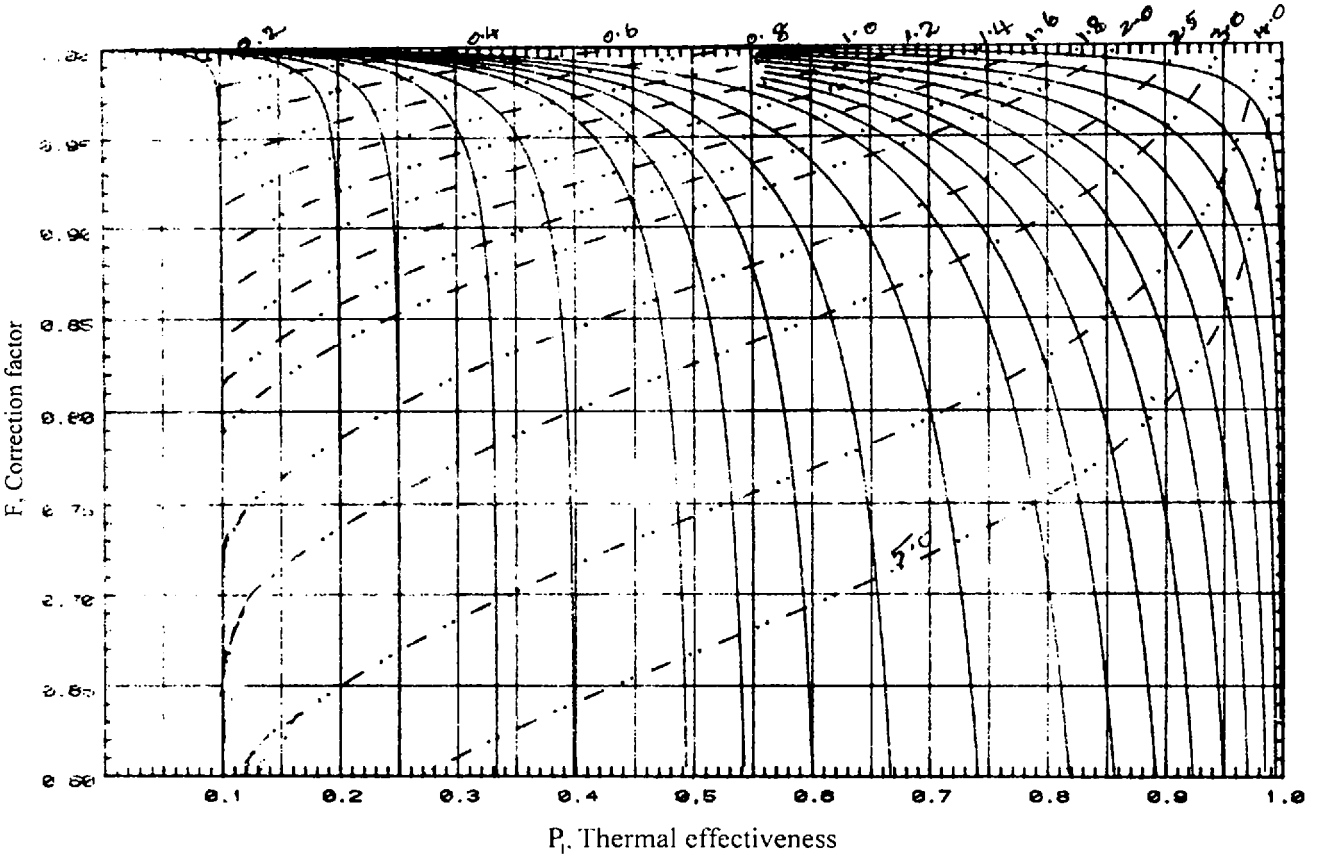


Figure 48 Three pass cross-counterflow arrangement with complete mixing between passes. Each pass is unmixed-mixed arrangement with stronger fluid mixed; F-R-P-NTU chart; F as a function of P for constant R (solid lines) and constant NTU (dashed lines).

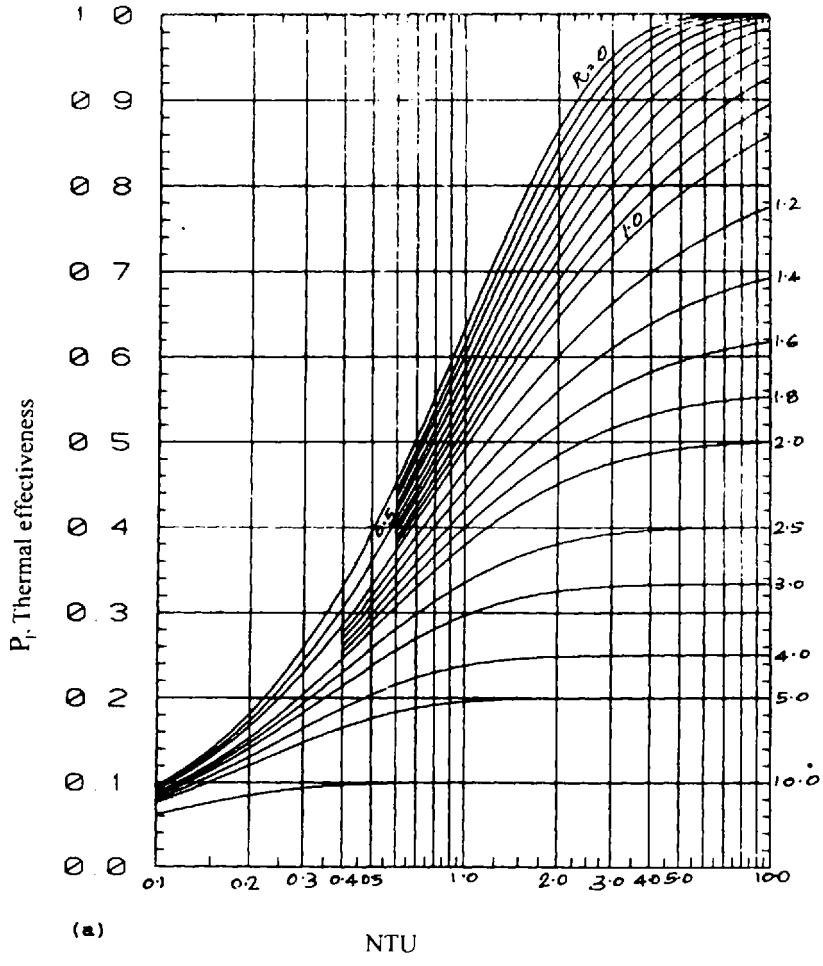


Figure 49 (a) Two pass cross-counterflow arrangement with complete mixing between passes. In each pass both the fluids unmixed (iv-d of Fig. 44); R-P-NTU chart. (b) F-R-P-NTU chart; F as a function of P for constant R (solid lines) and constant NTU (dashed lines).

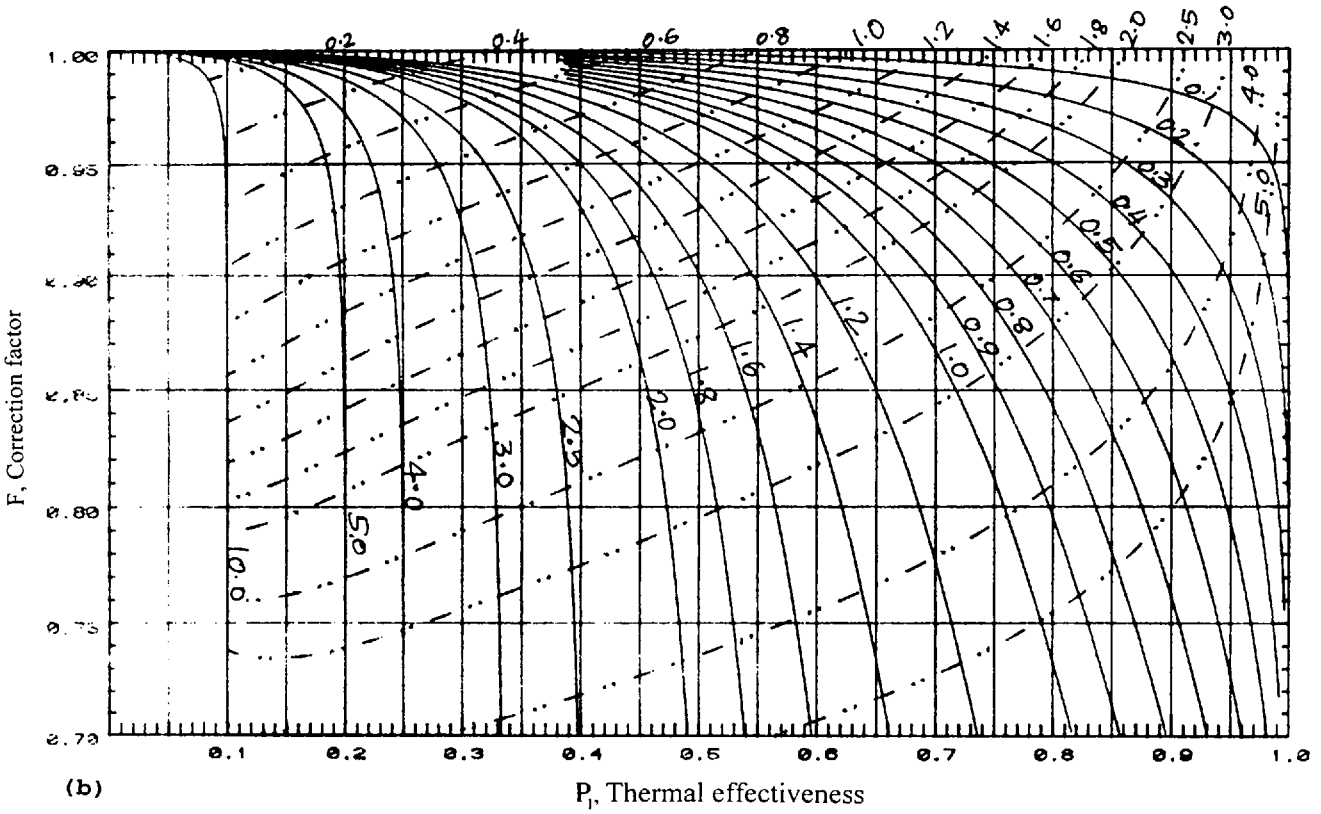


Figure 49 Continued.

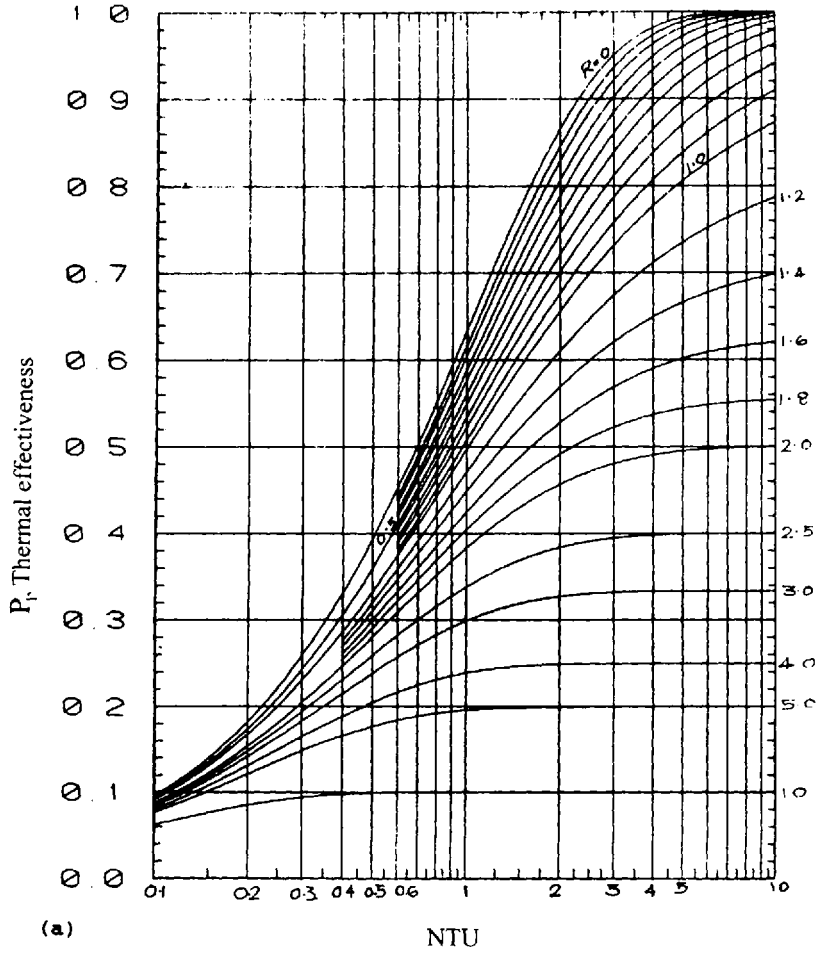
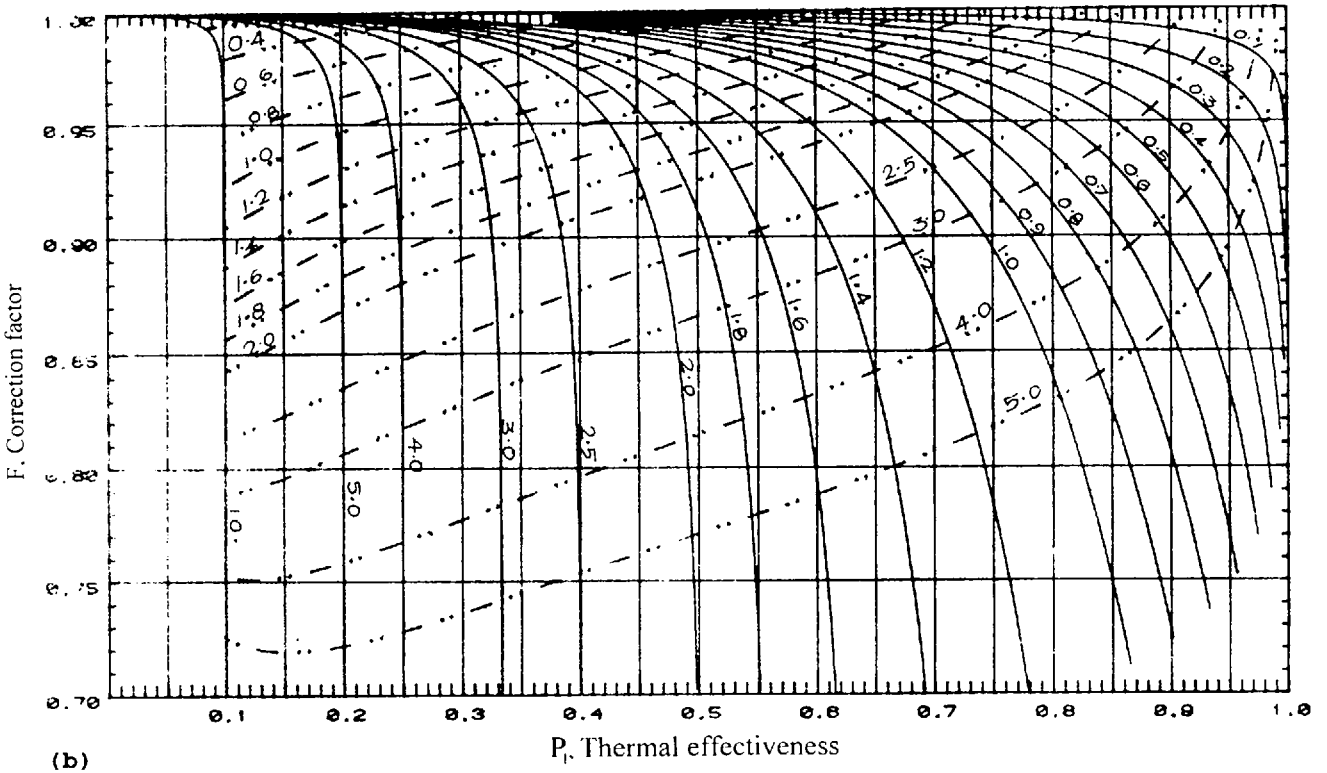


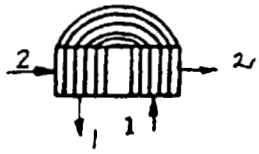
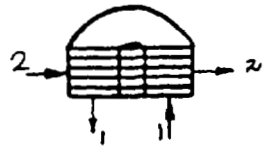
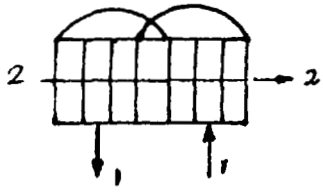
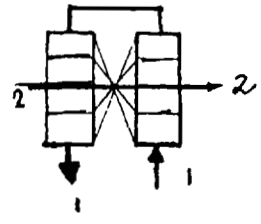
Figure 50 (a) Three pass cross-counterflow arrangement with complete mixing between passes. In each pass both the fluids unmixed; R-P-NTU chart. (b) F-R-P-NTU chart; F as a function of P for constant R (solid lines) and constant NTU (dashed lines).



(b)

Figure 50 Continued.

Table 13 Thermal Effectiveness Relations for Two-Pass Assemblies of Heat Exchangers Arrangement with One Fluid Unmixed Throughout [29]

Flow arrangement	Eq. no./ Ref.	Formula for overall cross-counterflow exchangers
 Fluid 1 unmixed throughout; fluid 2 mixed throughout	T34 [28]	$P_1 = \frac{1}{R}\left[1 - \frac{1}{\frac{K}{2} + \left(1 - \frac{K}{2}\right)e^{2KR}}\right]$ $K = 1 - e^{(-NTU/2)}$ Eq. for P_2 = Eq. T35
 Fluid 1 mixed throughout; fluid 2 unmixed throughout	T35 [28]	$P_1 = \left[1 - \frac{1}{\frac{K}{2} + \left(1 - \frac{K}{2}\right)e^{(2K/R)}}\right]$ $K = 1 - e^{(-RNTU/2)}$ Eq. for P_2 = Eq. T34
 Fluid 1 unmixed throughout, identical order; fluid 2 mixed throughout	T36 [28]	$P_1 = \frac{1}{R}\left[1 - \frac{e^{-KR}}{e^{KR} - K^2 R}\right]$ $K = 1 - e^{(-NTU/2)}$ Eq. for P_2 = Eq. T37
 Fluid 1 mixed throughout; fluid 2 unmixed throughout, identical order	T37 [28]	$P_1 = \left[1 - \frac{e^{-K/R}}{e^{K/R} - K^2/R}\right]$ $K = 1 - e^{(-RNTU/2)}$ Eq. for P_2 = Eq. 36

Note: for an individual case, at $R = 1$, $P_1 = P_2$.

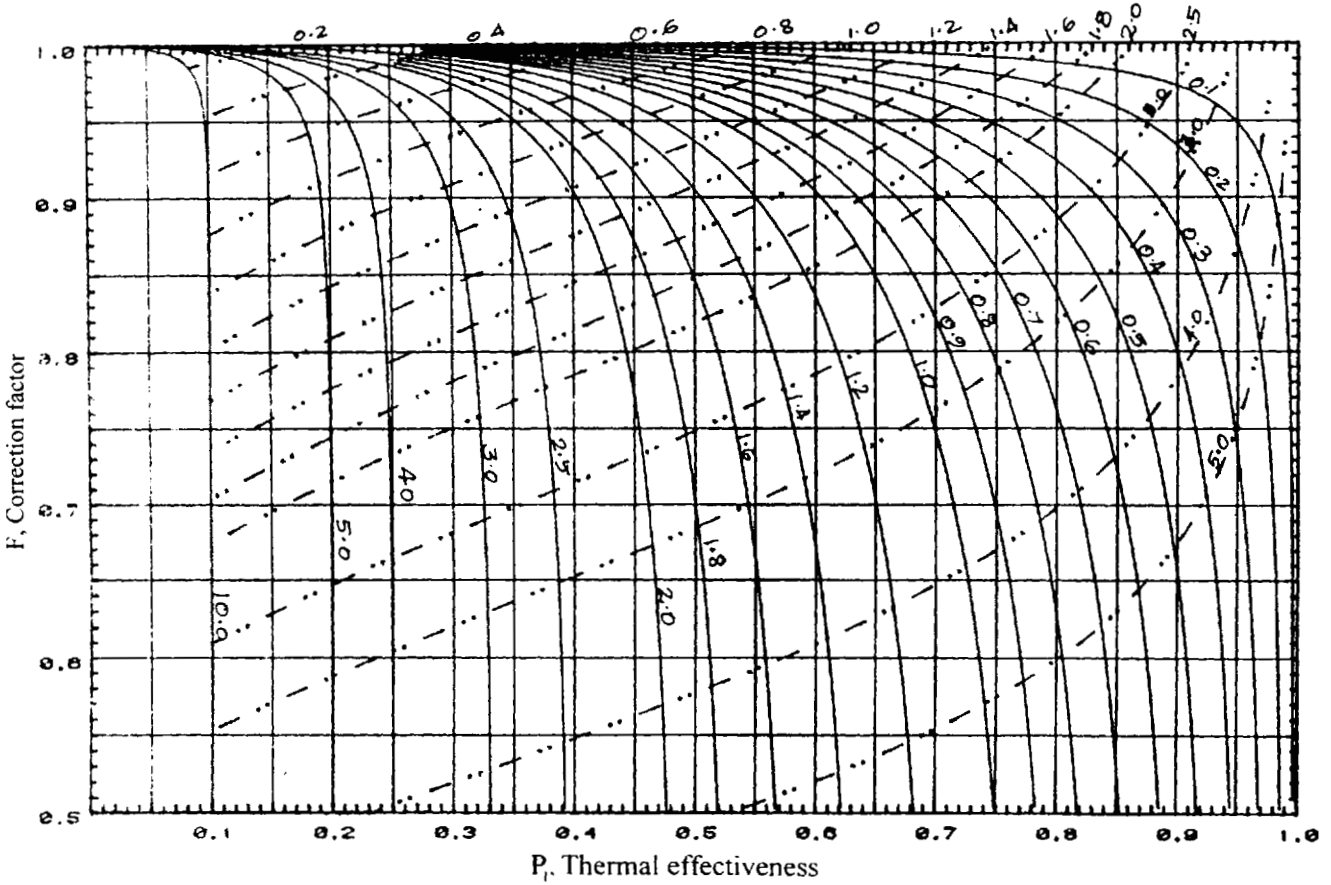


Figure 51 Two pass cross-counterflow arrangement. Fluid 1 unmixed throughout, inverted order coupling; fluid 2 mixed throughout. F as a function of P for constant R (solid lines) and constant NTU (dashed lines).

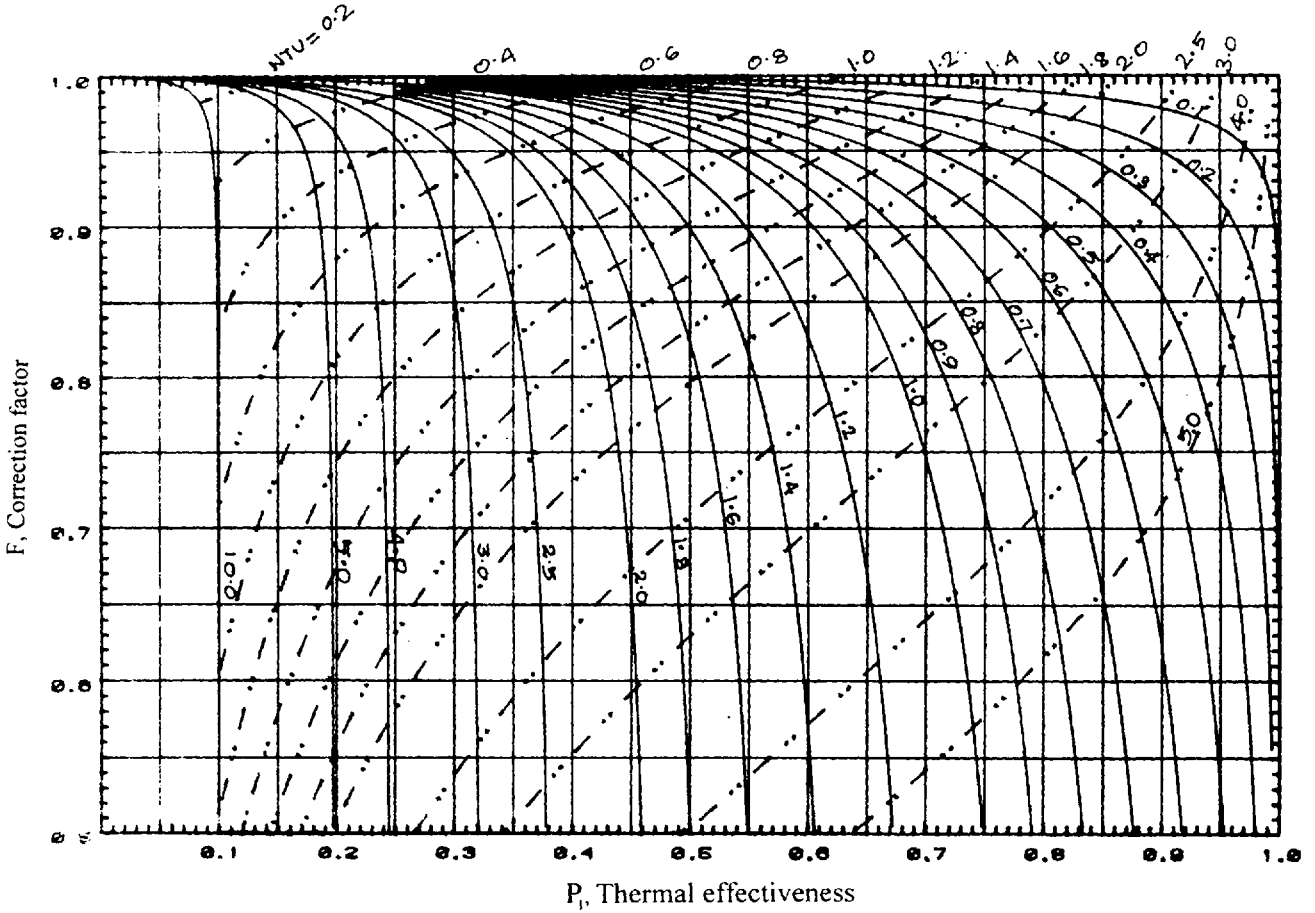


Figure 52 Two pass cross-counterflow arrangement. Fluid 1 mixed throughout; fluid 2 unmixed throughout, inverted order coupling. F as a function of P for constant R (solid lines) and constant NTU (dashed lines).

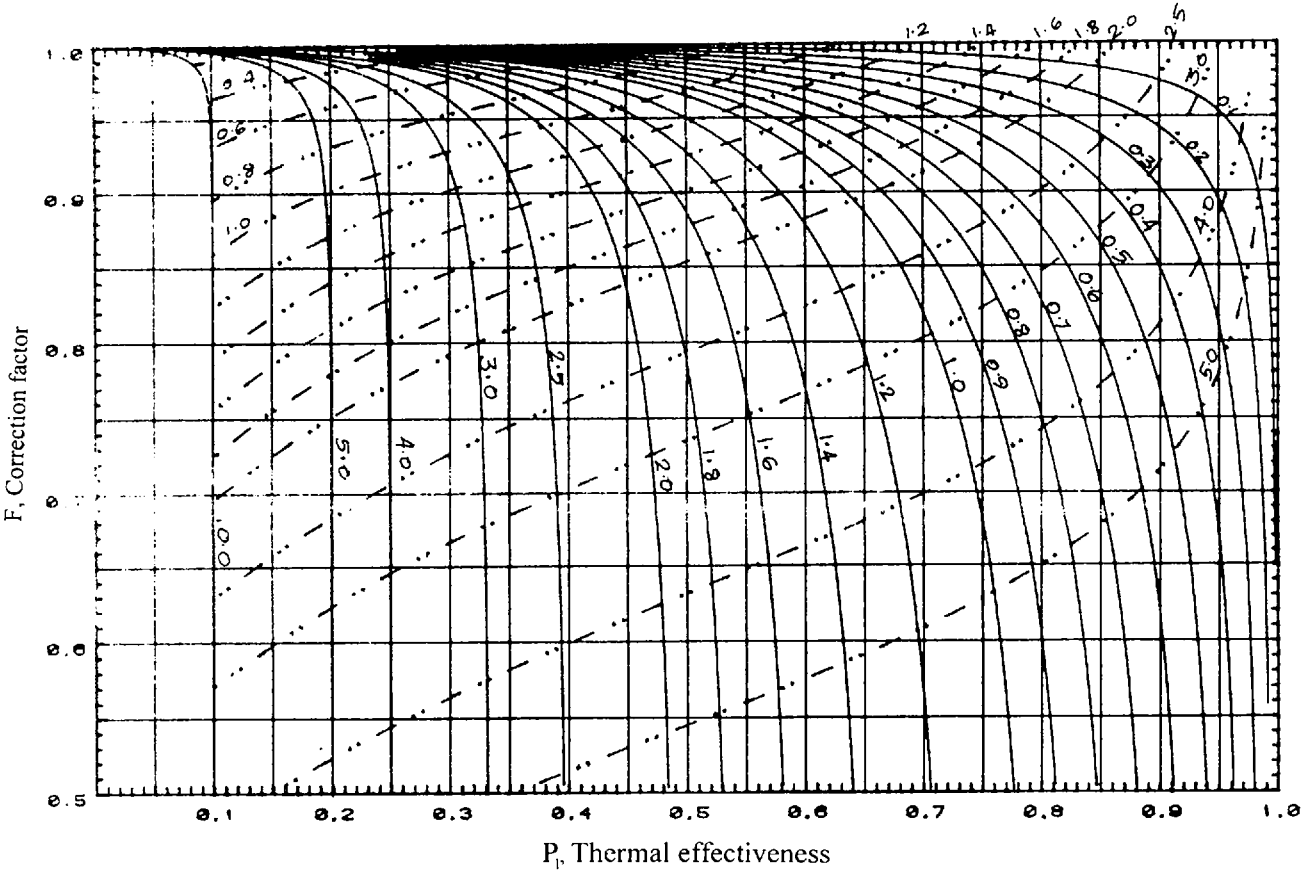


Figure 53 Two pass cross-counterflow arrangement. Fluid 1 unmixed throughout, identical order coupling; fluid 2 mixed throughout. F as a function of P for constant R (solid lines) and constant NTU (dashed lines).

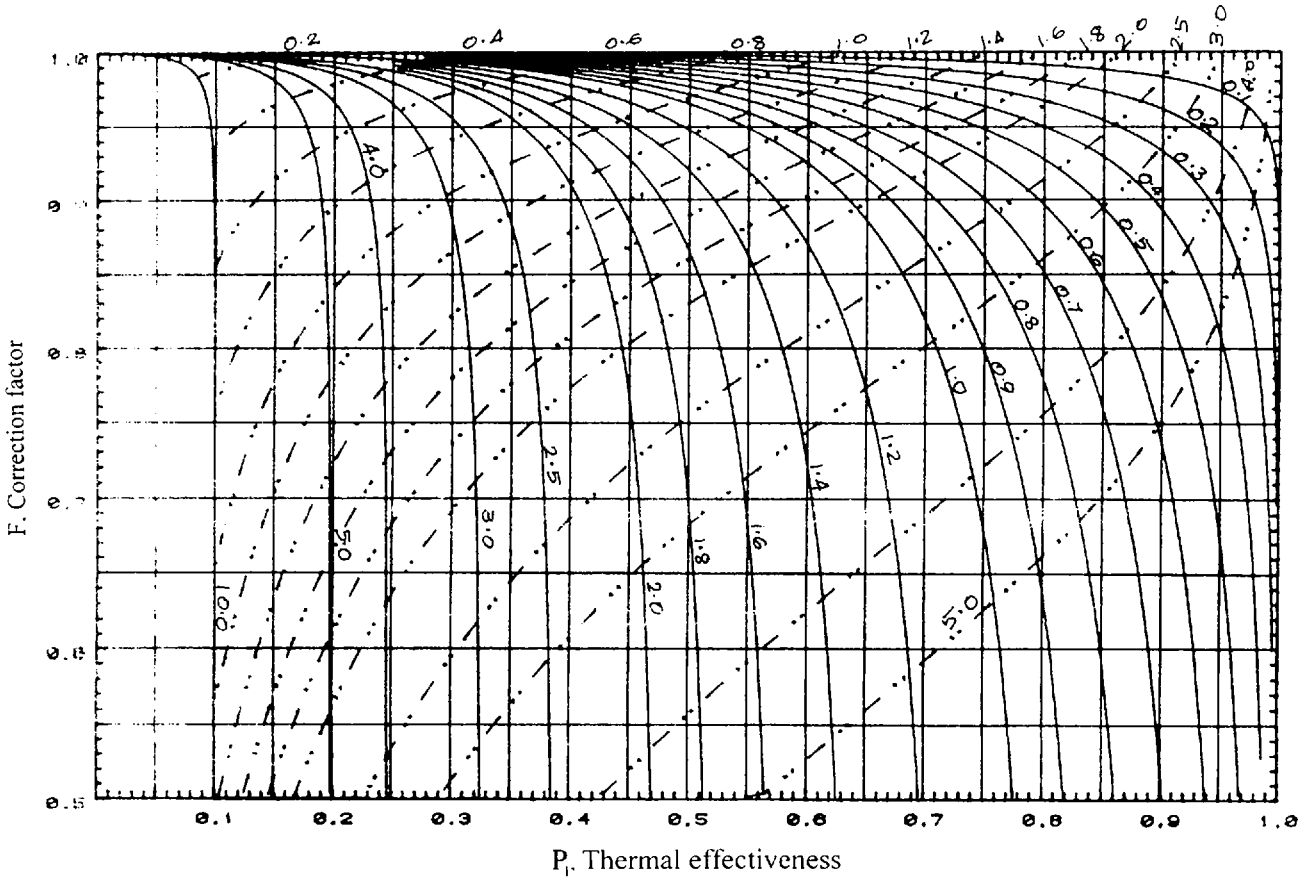
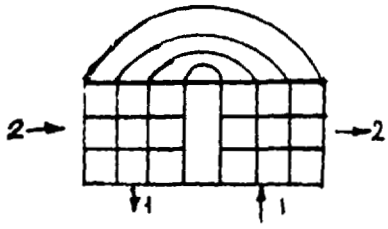
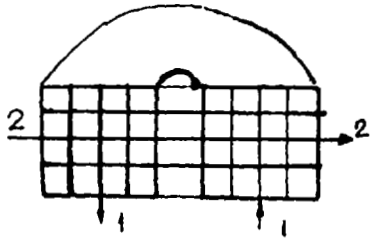
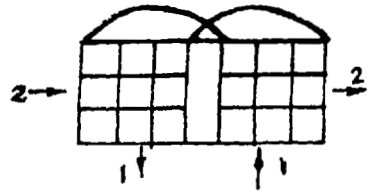
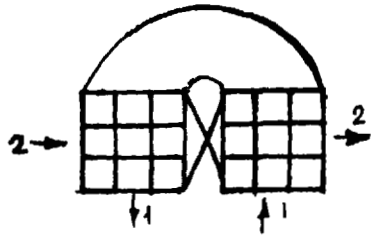


Figure 54 Two pass cross-counterflow arrangement. Fluid 1 mixed throughout; fluid 2 unmixed throughout, identical order coupling. F as a function of P for constant R (solid lines) and constant NTU (dashed lines).

Table 14 Thermal Effectiveness Relations for Two-Pass Assemblies of Heat Exchangers Arrangement with Both Fluids Unmixed in the Passes [1,45,46]

Flow arrangement	Eq. no./ Ref.	Formula for overall cross-counterflow exchangers
	T38 [45]	$\varepsilon_1 = \frac{1}{C^*}\left[1 - \frac{\bar{v}_{1/2}^2}{\bar{v}_{1/2} + \bar{\mu}_{1/2}}\right]$ Eq. for ε_2 = T39
Fluid 1 unmixed throughout; fluid 2 unmixed in each pass and mixed between passes		
	T39 [45]	$\varepsilon_1 = 1 - \frac{v_{1/2}^2}{v_{1/2} + \mu_{1/2}}$ Eq. for ε_2 = T38
Fluid 1 unmixed in each pass and mixed between passes; fluid 2 unmixed throughout		
	T40 [46]	$\varepsilon_1 = \frac{1}{C^*}\left[1 - \frac{\bar{v}_{1/2}^2}{1 + 2\bar{v}_{1/2} - 2\bar{v}_{2/2}}\right]$ Eq. for ε_2 = T41
Fluid 1 unmixed throughout, identical order; fluid 2 mixed between passes and unmixed in each pass		
	T41 [46]	$\varepsilon_1 = 1 - \frac{v_{1/2}^2}{1 + 2v_{1/2} - 2v_{2/2}}$ Eq. for ε_2 = T40
Fluid 1 mixed between passes and unmixed in each pass; fluid 2 unmixed throughout, identical order		

Note: for individual case at $C^* = 1$, $\varepsilon_1 = \varepsilon_2$.

3. Two-pass cross-counterflow arrangement. Fluid 1 unmixed throughout, identical-order coupling; fluid 2 mixed between passes and unmixed in each pass (III-d of Fig. 44).
4. Two-pass cross-counterflow arrangement. Fluid 1 mixed between passes and unmixed in each pass; fluid 2 unmixed throughout, identical-order coupling (IV-c of Fig. 44).

Thermal relation formulas (T38–T41) for these cases are given in Table 14. The thermal effectiveness chart for case 2 is given in Fig. 55 and for case 3 in Fig. 56.

Two Passes with Both Fluids Unmixed Throughout, Cross-Counterflow Arrangement.

1. Fluid 1 unmixed throughout; fluid 2 unmixed throughout. Both fluids coupling in inverted order (II-b of Fig. 44). The thermal effectiveness chart is given in Fig. 57. This is also equivalent to the TEMA X-shell, two passes on the tube side with counterflow arrangement.

   For cross-parallel flow, the thermal effectiveness is given by [45]:

$$\varepsilon = \mu_{1/2} + \frac{1}{C^*}\bar{\mu}_{1/2} \tag{76}$$

   where the terms of the equation were defined earlier. This is also equivalent to the TEMA X-shell, two passes on the tubeside with parallel flow arrangement.

Table 14 Continued (Footnotes)

Terms of the equations:

$$\mu_{1/2} = \frac{2}{C^*NTU}\sum_{m=0}^{\infty}\sum_{n=0}^{\infty}\frac{(-1)^n(n+m)!}{n!m!}V_{m+2}\left(\frac{C^*NTU}{2}, \frac{NTU}{2}\right)V_{n+2}\left(\frac{NTU}{2}, \frac{C^*NTU}{2}\right) \tag{A}$$

Set $C^* = 1/C^*$, $NTU = C^*NTU$ and $C^*NTU = NTU$ in Eq. (A), then, Eq. (B) is obtained by

$$\bar{\mu}_{1/2} = \frac{2}{NTU}\sum_{m=0}^{\infty}\sum_{n=0}^{\infty}\frac{(-1)^n(n+m)!}{n!m!}V_{m+2}\left(\frac{NTU}{2}, \frac{C^*NTU}{2}\right)V_{n+2}\left(\frac{C^*NTU}{2}, \frac{NTU}{2}\right) \tag{B}$$

in which

$$V_0(\xi, \eta) = e^{-(\xi+\eta)}I_0(2\sqrt{\xi\,\eta}) \tag{C}$$

$$V_m(\xi, \eta) = e^{-(\xi+\eta)}\sum_{n=m-1}^{\infty}\binom{n}{m-1}\left(\frac{\eta}{\xi}\right)^{m/2}I_n(2\sqrt{\xi\,\eta}) \qquad m \geq 1 \tag{D}$$

$$U(a,b) = e^{-(a+b)}[I_0(2\sqrt{a\,b}) + \sqrt{(b/a)}I_1(2\sqrt{a\,b}) - \left(\frac{a}{b} - 1\right)\sum_{n=2}^{\infty}\left(\frac{b}{a}\right)^{n/2}I_n(2\sqrt{a\,b})] \tag{E}$$

The expressions for $U_{1/2}$ and $\bar{U}_{1/2}$ are given by,

$$U_{1/2} = \exp\left[-(1+C^*)\frac{NTU}{2}\right]\left[I_o\,(NTU\sqrt{C^*}) + \sqrt{C^*}\,I_1\,(NTU\sqrt{C^*}) - \frac{1-C^*}{C^*}\sum_{n=2}^{\infty}(C^*)^{n/2}\,I_n(NTU\sqrt{C^*})\right] \tag{F}$$

$$\bar{U}_{1/2} = \exp\left[-\frac{1+C^*}{C^*}\frac{C^*\,NTU}{2}\right]\left[I_0(NTU\sqrt{C^*}) + \sqrt{\frac{1}{C^*}}\,I_1(NTU\sqrt{C^*}) - C^* - 1)\sum_{n=2}^{\infty}(C^*)^{-n/2}\,I_n(NTU\sqrt{C^*})\right] \tag{G}$$

Various forms Eq. (E): $U = U_{1/1} = U(NTU, C^*NTU)$; $U_{1/2} = U(NTU/2, C^*NTU/2)$; $U_{2/2} = U(NTU/2, C^*NTU)$; $\bar{U} = \bar{U}_{1/1} = U(C^*NTU, NTU)$; $\bar{U}_{1/2} = U(C^*NTU/2, NTU/2)$; $\bar{U}_{2/2}U(C^*NTU/2,NTU)$.

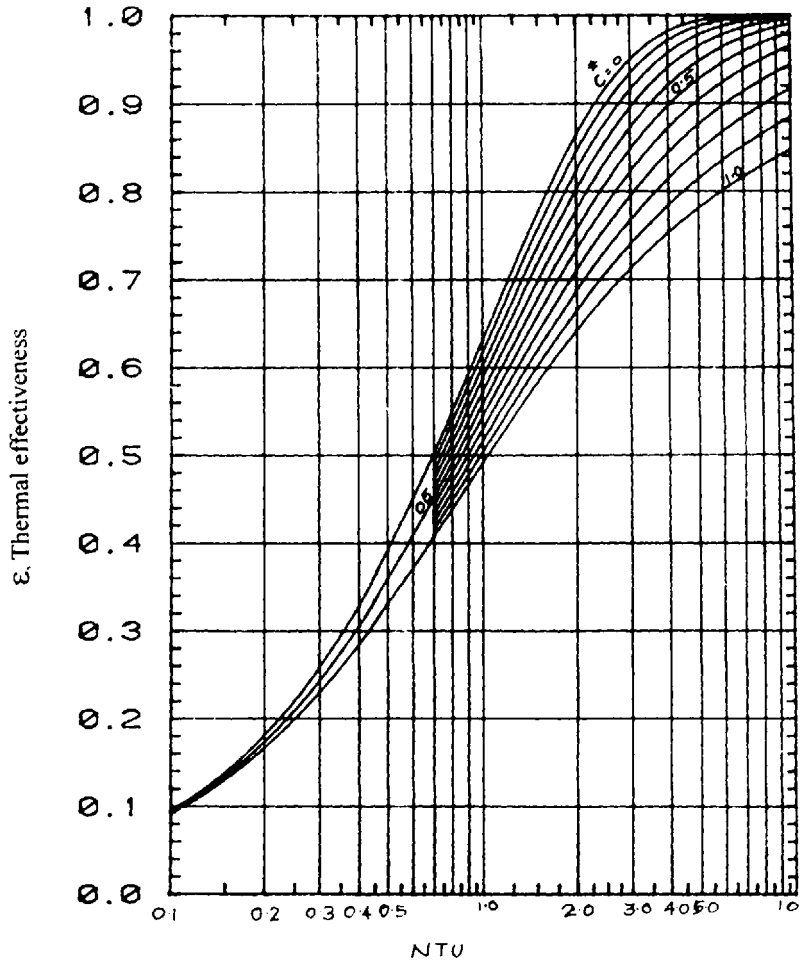


Figure 55 Two pass cross-counterflow arrangement. Fluid 1 unmixed in each pass and mixed between passes; fluid 2 unmixed throughout, inverted order coupling.

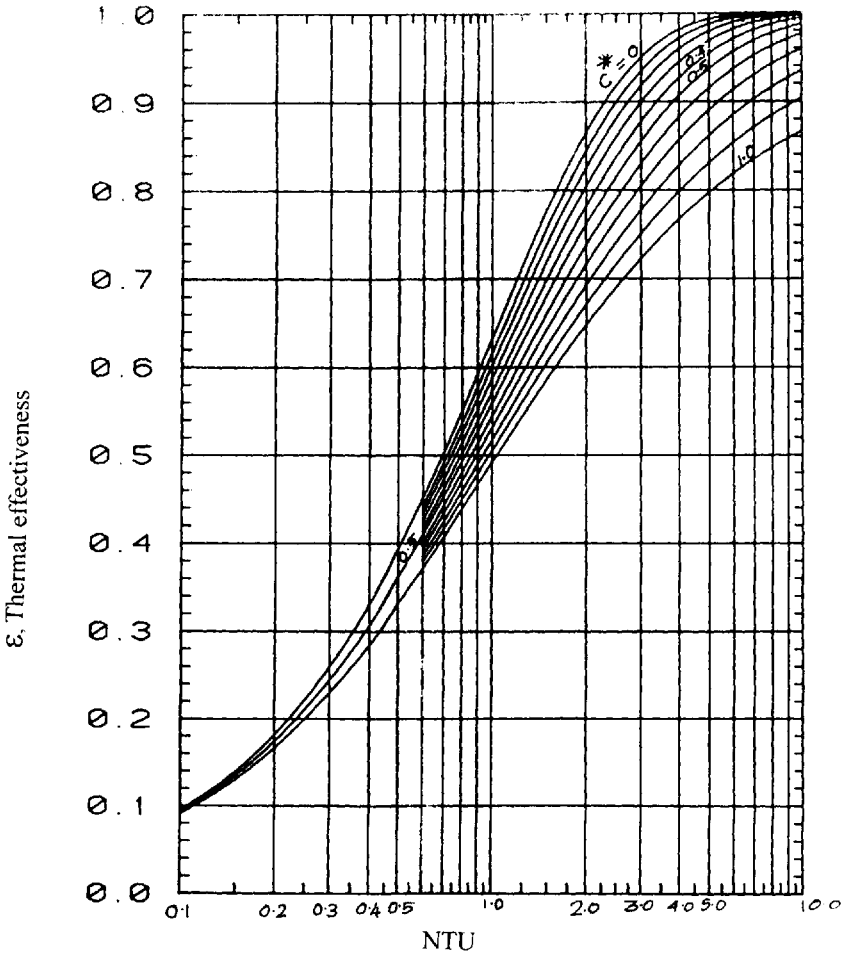


Figure 56 Two pass cross-counterflow arrangement. Fluid 1 unmixed throughout, identical order coupling; fluid 2 mixed between passes and unmixed in each pass.

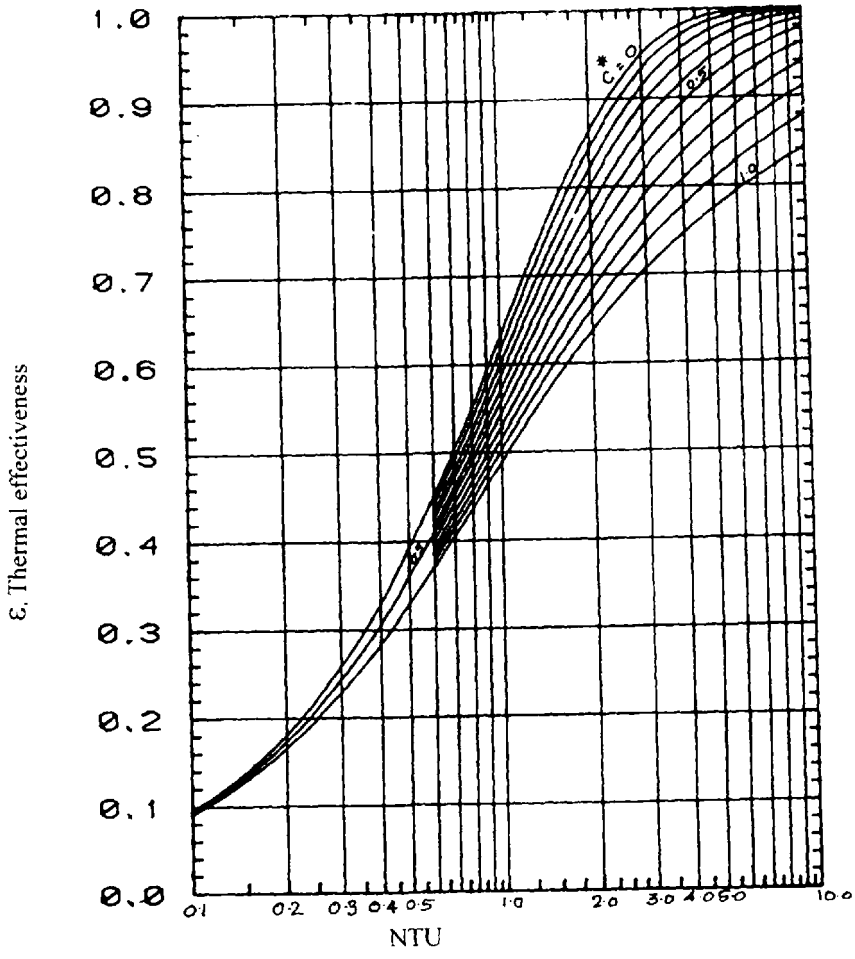


Figure 57 Two pass cross-counterflow arrangement. Fluid 1 unmixed throughout; fluid 2 unmixed throughout, both the fluids coupling in inverted order (equivalent to TEMA $X_{1\,2}$ shell with two passes on the tube side, counterflow arrangement).

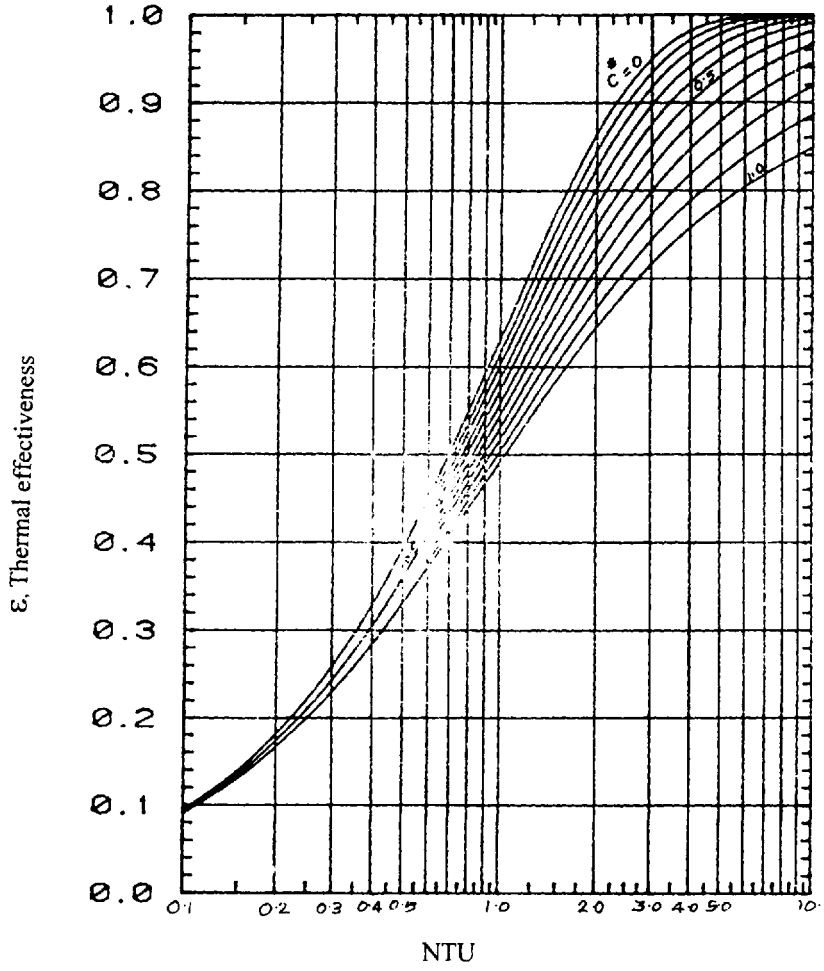


Figure 58 Two pass cross-counterflow arrangement. Fluid 1 unmixed throughout; fluid 2 unmixed throughout, coupling in identical order.

Table 15 Comparison of Thermal Effectiveness for $C^* = 1$ [29]

NTU	$\varepsilon_{III\text{-}c}/\varepsilon_{I\text{-}a}$	$\varepsilon_{III\text{-}c}/\varepsilon_{I\text{-}b}$	$\varepsilon_{III\text{-}c}/\varepsilon_{I\text{-}d}$
1.0	1.008	1.007	1.006
4.0	1.093	1.073	1.060
7.0	1.181	1.128	1.111
NTU	$\varepsilon_{III\text{-}c}/\varepsilon_{I\text{-}c}$	$\varepsilon_{III\text{-}c}/\varepsilon_{II\text{-}b}$	$\varepsilon_{III\text{-}c}/\varepsilon_{II\text{-}d}$
1.0	1.004	1.006	1.004
4.0	1.049	1.038	1.031
7.0	1.096	1.049	1.042
NTU	$\varepsilon_{III\text{-}c}/\varepsilon_{II\text{-}c}$	$\varepsilon_{III\text{-}c}/\varepsilon_{IV\text{-}d}$	$\varepsilon_{III\text{-}c}/\varepsilon_{III\text{-}d}$
1.0	1.003	1.003	1.001
4.0	1.025	1.021	1.012
7.0	1.037	1.030	1.019

2. Fluid 1 unmixed throughout, coupling in identical order; fluid 2 unmixed throughout, coupling in inverted order (III-b of Fig. 44).
3. Fluid 1 unmixed throughout, coupling in inverted order; fluid 2 unmixed throughout, coupling in identical order (II-c of Fig. 44). The thermal effectiveness chart is shown in Fig. 58.
4. Fluid 1 unmixed throughout; fluid 2 unmixed throughout. Both fluids coupling in identical order (III-c of Fig. 44).

The thermal effectiveness charts shown in Figs. 57 and 58 were arrived at by a numerical method as described by Stevens et al. [29]. For all these four cases, a closed-form solution is given by Baclic [3].

For the flow arrangement of III-c of Fig. 44, the most efficient case, the thermal effectiveness for $C^* = 0.5$ is less by 1.8% (approx.) compared to the corresponding counterflow case. The maximum difference is in the *NTU* range 3.5–4.0, and for other values of NTU, the difference is fast decreasing and approaches zero. Also, for $0.0 < C^* < 0.5$, the difference is decreasing with C^* and it is zero for $C^* = 0.0$. For $C^* = 1.0$, the thermal effectiveness is less by 2.9% (approx.) compared to the corresponding counterflow case. The maximum difference is in the NTU range 4–6, and for other values of *NTU*, the difference is fast decreasing and approaches to zero. Also, for $0.5 < C^* < 1$, the difference is decreasing with decrease in C^*.

Comparison of Thermal Effectiveness of Two-Pass Crossflow Cases for $C^* = 1$. Table 15 shows all of the arrangements compared with arrangement III-c in increasing order of efficiency.

Thermal Effectiveness of Multiple-Pass Shell and Tube Heat Exchangers

Since the 1-*N* exchanger has lower effectiveness, multipassing on the shell side may be employed to approach the counterflow effectiveness. With this concept, the heat exchanger would have *M* shell passes and *N* tube passes. Figure 59 represents few such multipassing arrangements for $E_{1,2}$ and $E_{1,3}$ shells [32]. But multipassing on the shell side decreases the transfer area on the shell side, it is very difficult to fit the partition walls, and the possibility of leakage

(*text continues on p. 127*)

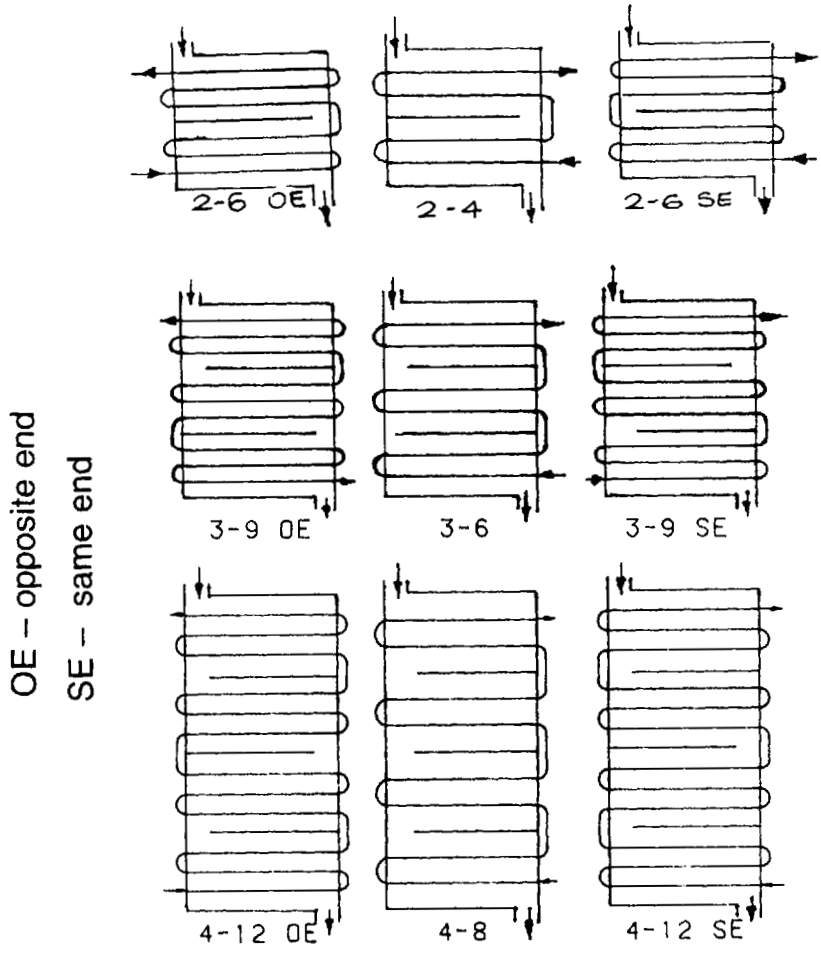


Figure 59 Shell side multipass arrangement for E shell.

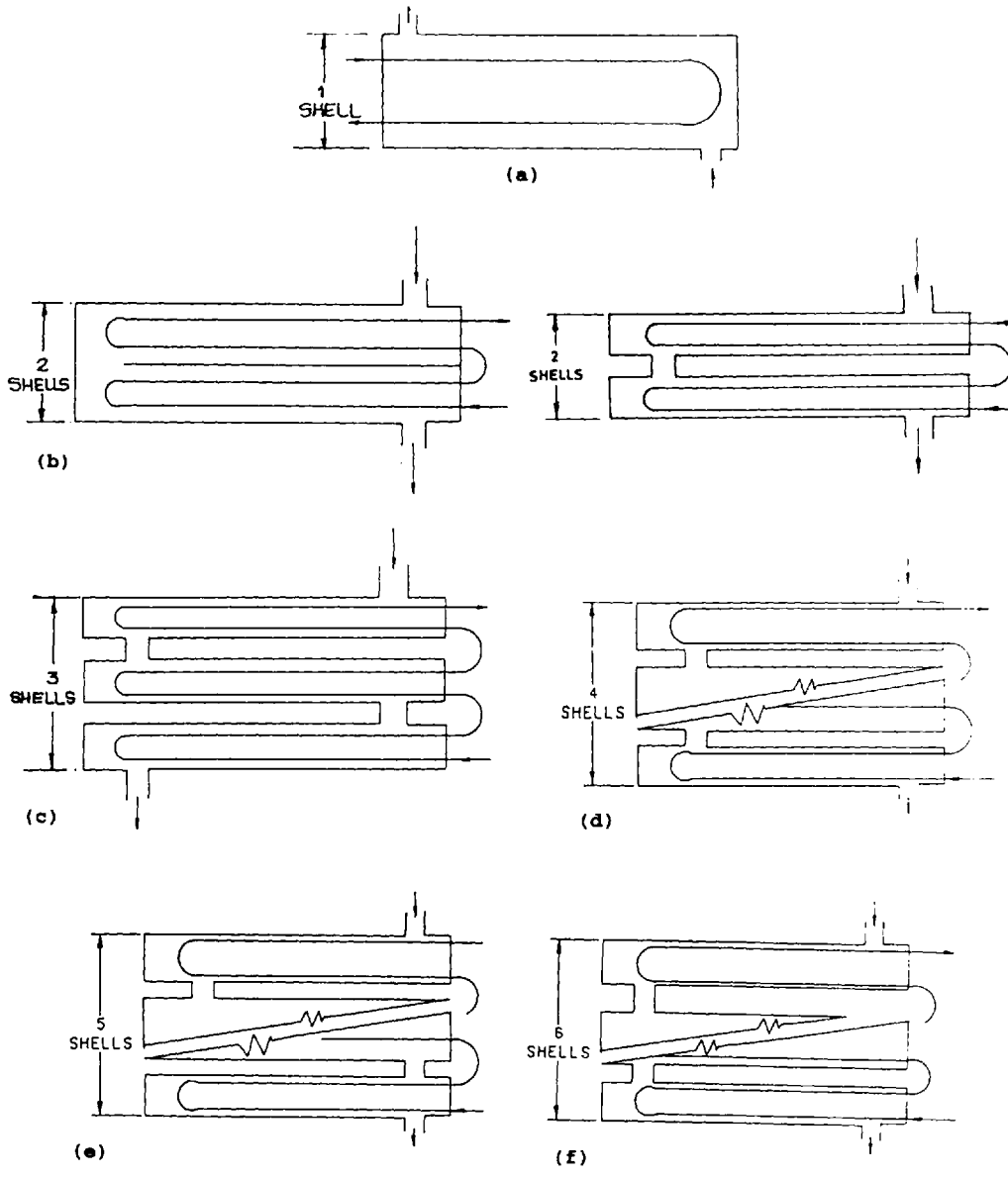


Figure 60 M-shell side passes. Each N-tube pass is equivalent to M-shells in series, each with N-tube passes.

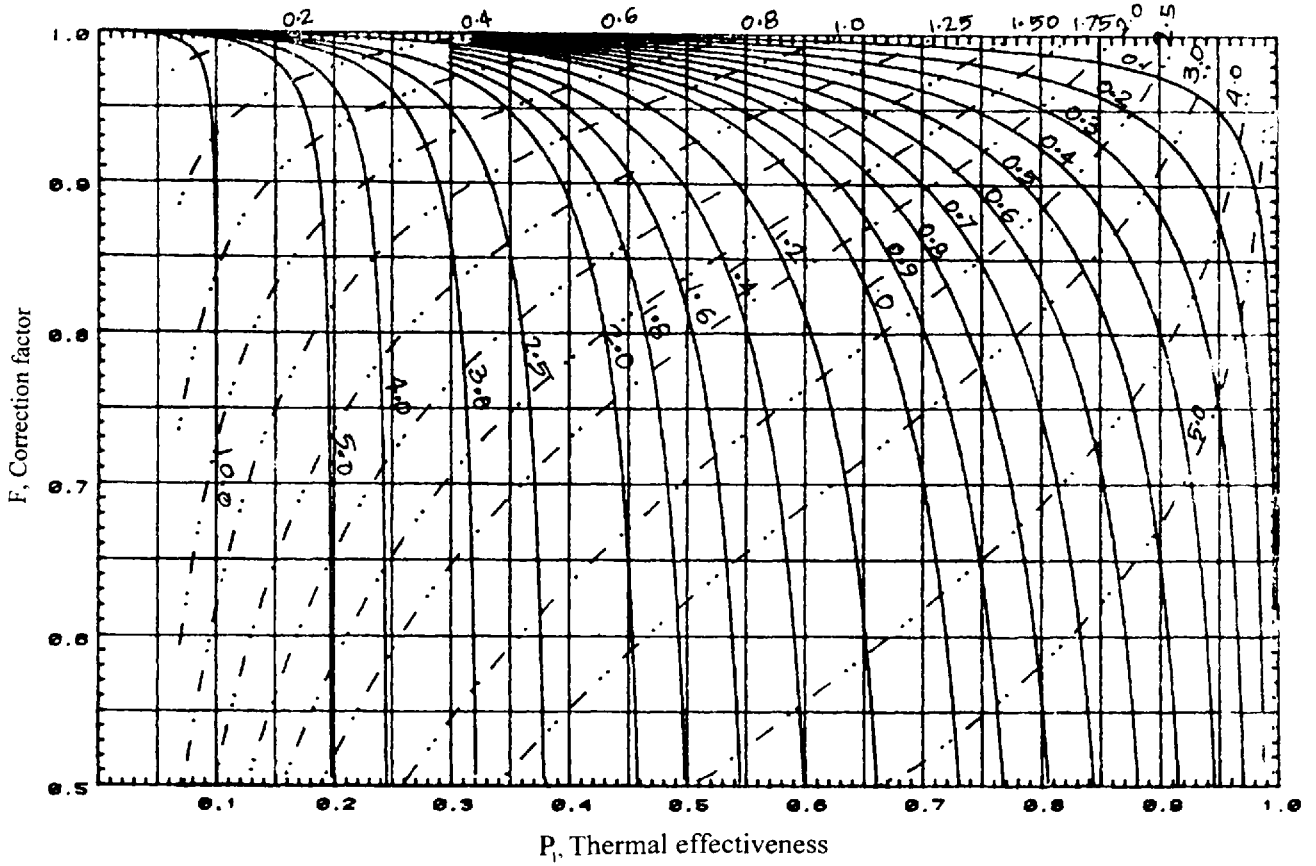


Figure 61 Two $E_{1\text{-}2}$ shells in series; shell fluid mixed, tube fluid mixed between passes with stream symmetric. F as a function of P for constant R (solid lines) and constant NTU (dashed lines).

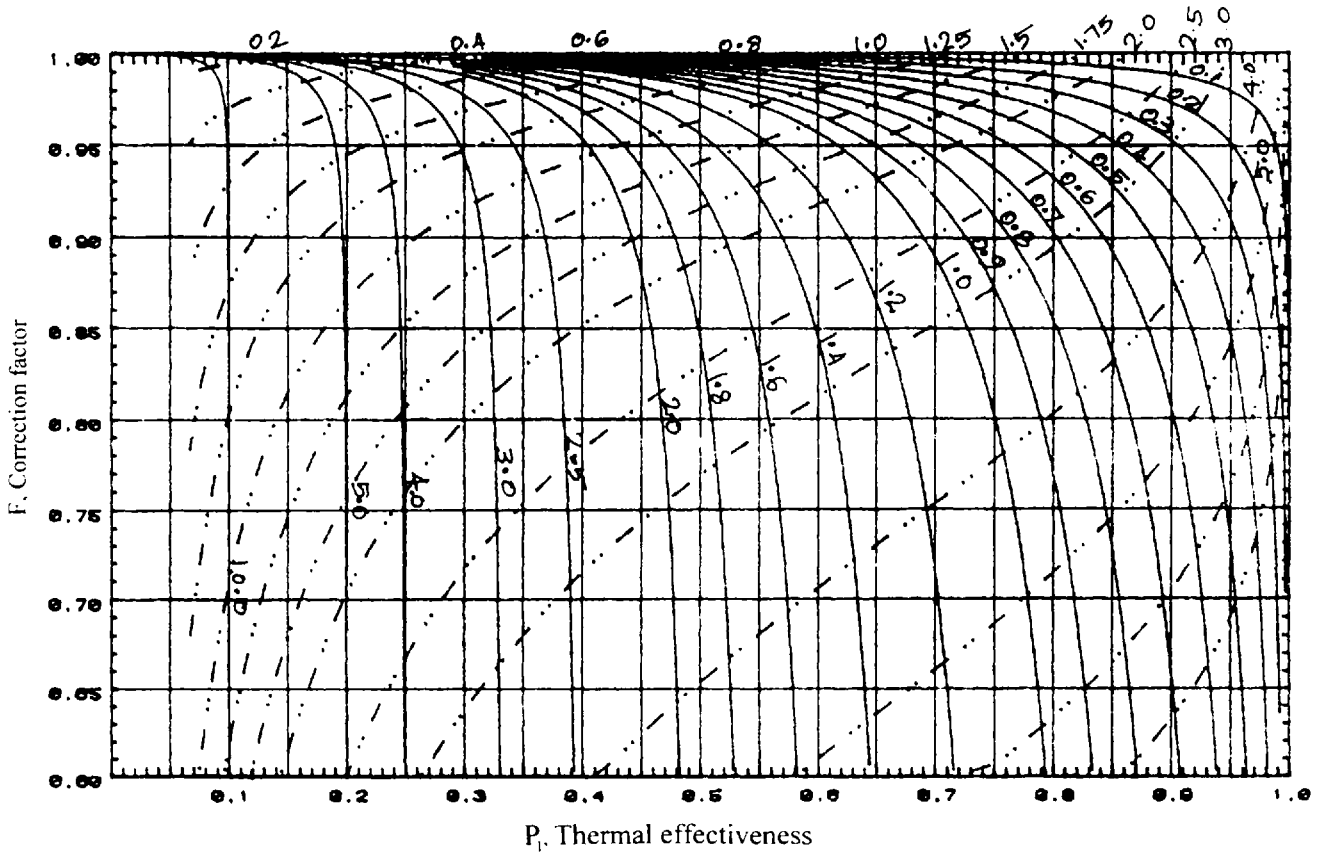


Figure 62 Three $E_{1,2}$ shells in series; shell fluid mixed, tube fluid mixed between passes with stream symmetric. F as a function of P for constant R (solid lines) and constant NTU (dashed lines).

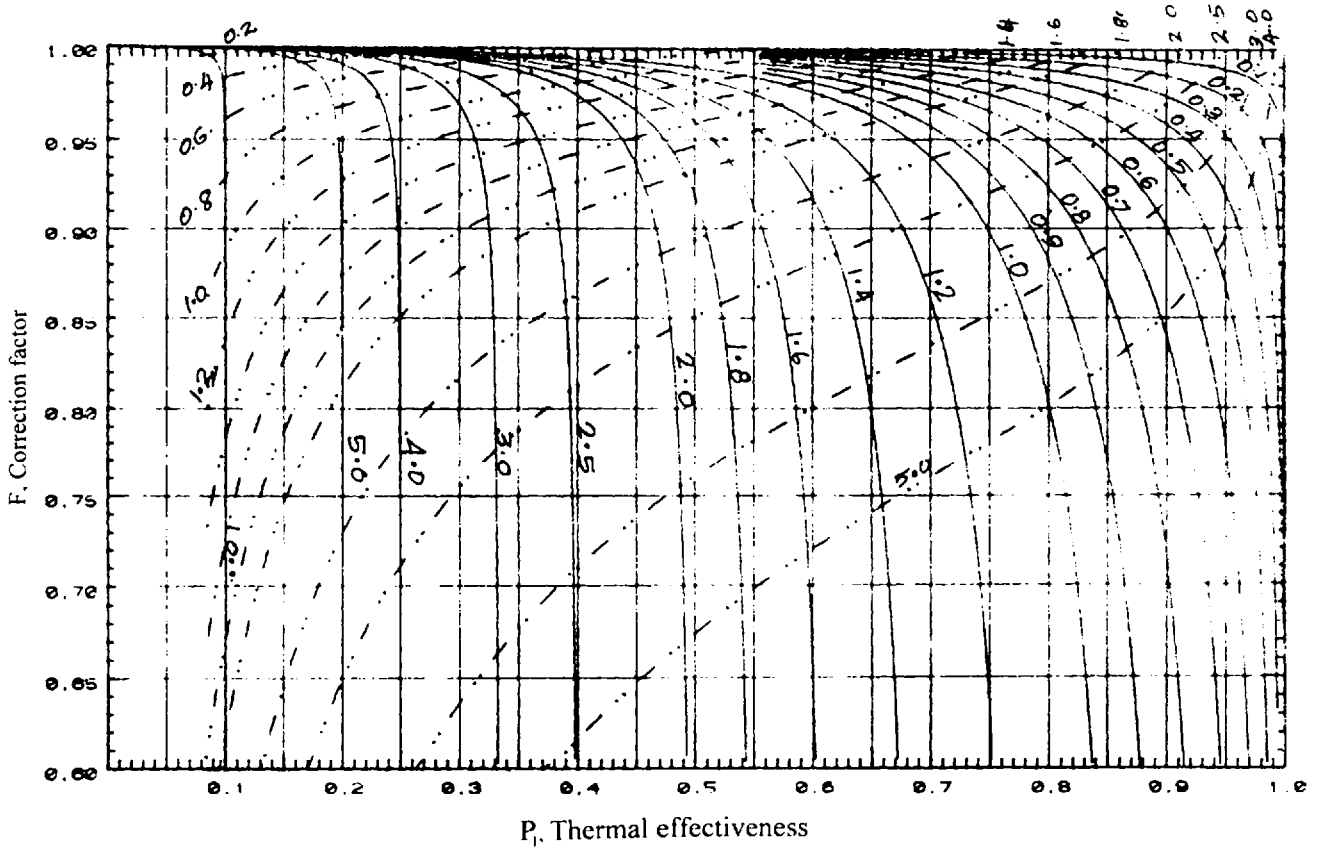


Figure 63 Four $E_{1,2}$ shells in series; shell fluid mixed, tube fluid mixed between passes with stream symmetric. F as a function of P for constant R (solid lines) and constant NTU (dashed lines).

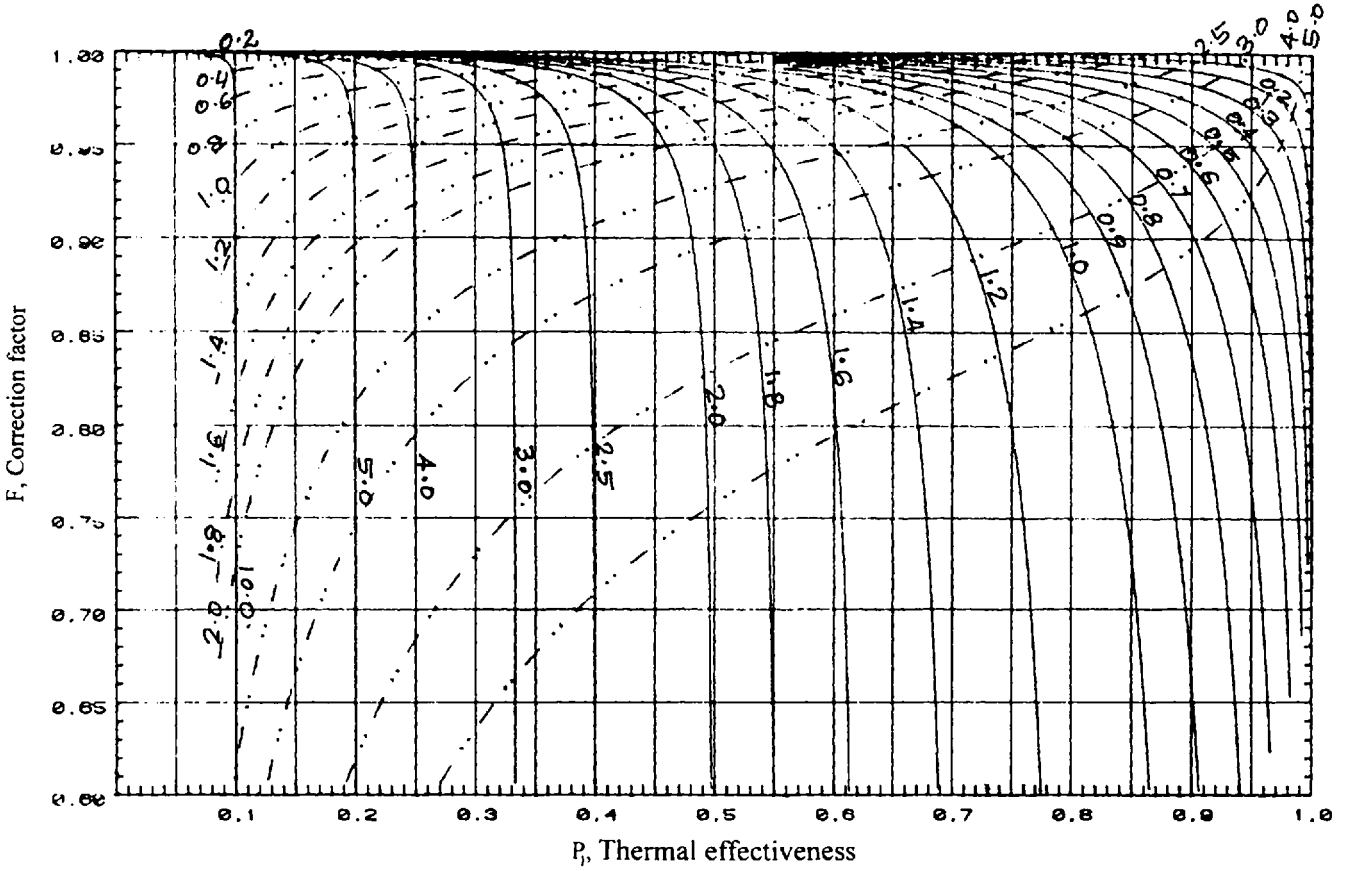


Figure 64 Five $E_{1,2}$ shells in series; shell fluid mixed, tube fluid mixed between passes with stream symmetric. F as a function of P for constant R (solid lines) and constant NTU (dashed lines).

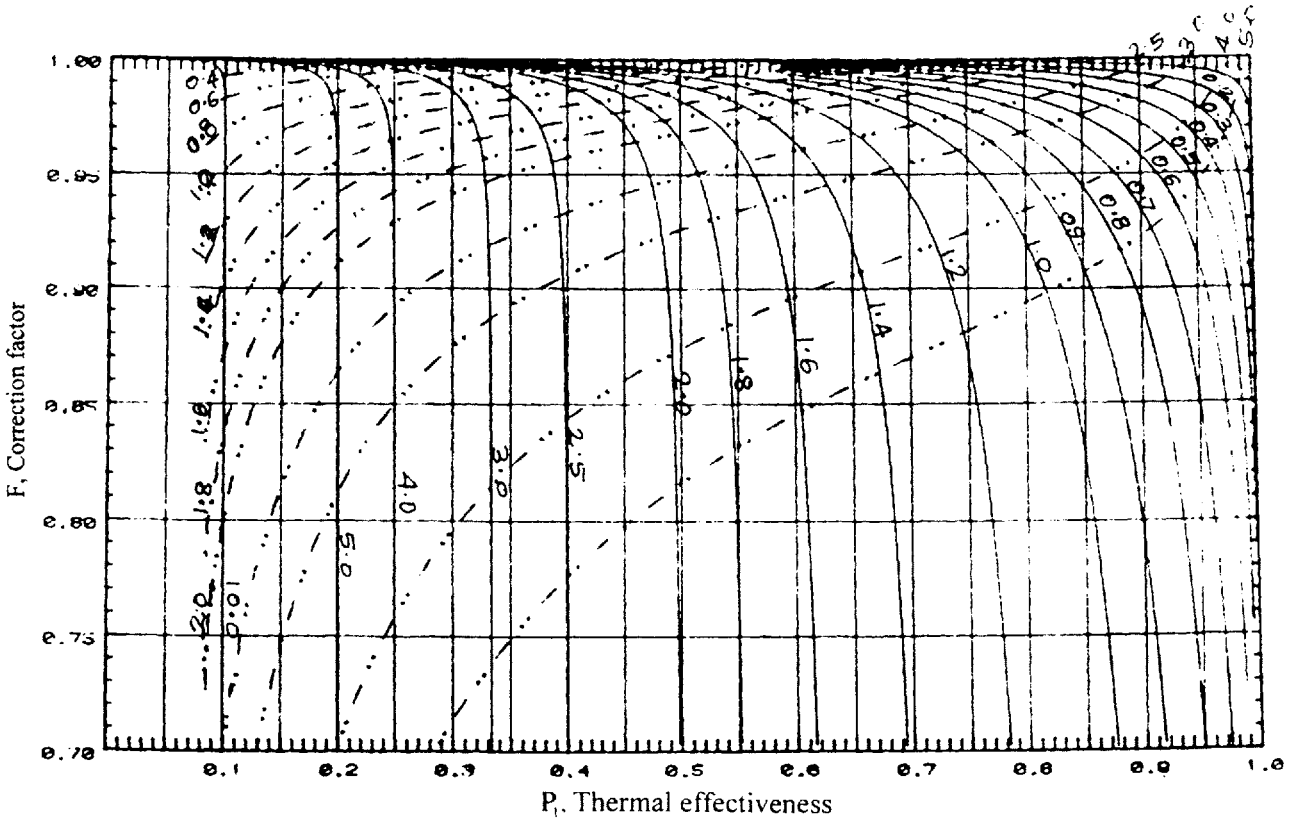
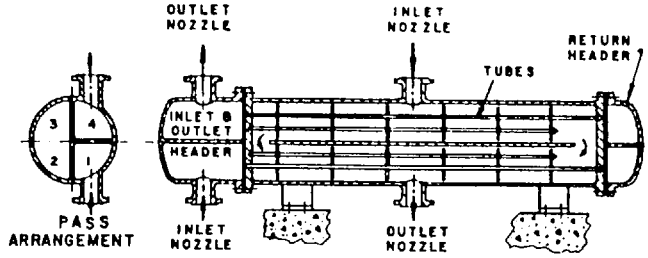
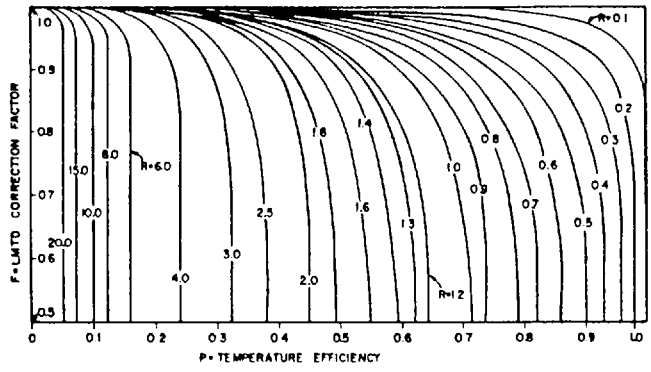
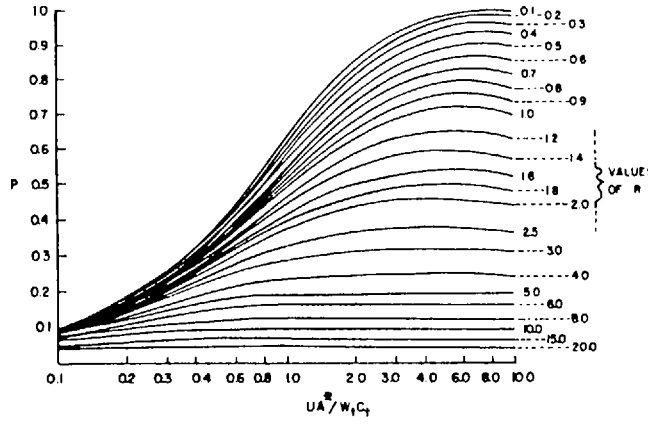


Figure 65 Six $E_{1,2}$ shells in series; shell fluid mixed, tube fluid mixed between passes with stream symmetric. F as a function of P for constant R (solid lines) and constant NTU (dashed lines).





P_1, Thermal effectiveness



NTU_1

Figure 66 G_{1-4} split flow heat exchanger [38]. Thermal effectiveness referred to tubeside.

through the partition plates cannot be ruled out. Therefore, this difficulty is overcome by with multiple shells with basic shell arrangements. A configuration with M shell passes, each one with N tube passes (similar to Fig. 59), is equivalent to a series assembly of M shells each with N tube passes. This is illustrated in Fig. 60 for $E_{1\text{-}2}$.

Multiple E Shells in Series, Each with Two Tube Passes, $E_{1\text{-}2}$. Thermal effectiveness charts for $2E_{1\text{-}2}$, $3E_{1\text{-}2}$, $4E_{1\text{-}2}$, $5E_{1\text{-}2}$, and $6E_{1\text{-}2}$ are given in Figs. 61, 62, 63, 64, and 65.

Thermal relation chart for TEMA $G_{1\text{-}4}$. Figure 66 gives details about (i) schematic of $G_{1\text{-}4}$ exchanger, (ii) temperature correction factor for $G_{1\text{-}4}$ exchanger, and (iii) thermal effectiveness for $G^{1\text{-}4}$ exchanger (38).

ACKNOWLEDGEMENT

The author acknowledges Dr. R. K. Shah, Technical Director of Research, Delphi-Harrison Thermal Systems, for providing the thermal relation formulas for various cases of crossflow arrangements and shell and tube heat exchangers.

This page intentionally left blank

3
Heat Exchanger Thermal Design

1 FUNDAMENTALS OF HEAT EXCHANGER DESIGN METHODOLOGY

Heat exchanger design methodology, shown in Fig. 1, involves the following major design considerations [1]:

1. Process/design specifications
2. Thermohydraulic design
3. Flow-induced vibration in the case of shell and tube heat exchanger and individual fin-tube and bare tube bank compact heat exchanger
4. Mechanical design
5. Cost and manufacturing considerations
6. Trade-off factors and system-based optimization

Most of these considerations are dependent on each other and should be considered simultaneously to arrive at the optimum exchanger design. Of these design considerations, items 1 and 2 are discussed in this chapter, flow-induced vibration and mechanical design are discussed in Chapters 10 and 11, respectively, and item 5 was discussed earlier. The remaining item, trade-off factors and system-based optimization, is not within the scope of this book.

1.1 Process/Design Specifications

Process or design specifications include all the necessary information to design and optimize the exchanger for a specific application. It includes the following information [1]: (1) problem specification, (2) exchanger construction type, (3) flow arrangement, (4) construction materials, (5) design/operation/manufacturing constraints, (6) construction code, and (7) safety and protection. Items 1 and 2 are discussed next, and the others have been covered elsewhere.

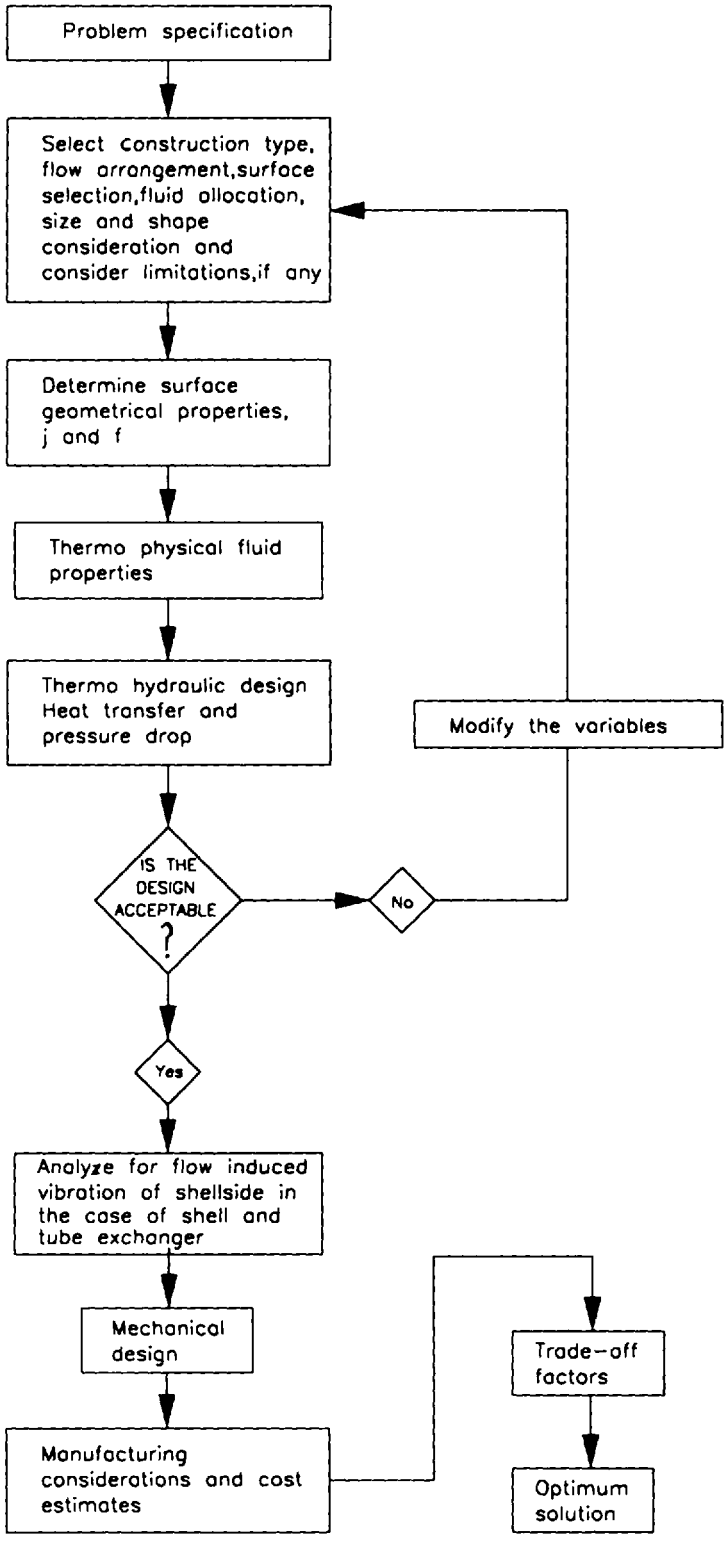


Figure 1 Heat exchanger design methodology.

Problem Specification

The problem specification involves the process parameters, operating conditions, and environment in which the heat exchanger is going to be operated. Typical details pertaining to problem specification include design parameters such as inlet temperatures and pressures, flow rates (including composition for mixtures), vapor quality, heat duty, allowable pressure drops, and fluctuations in the process parameters; overall size, layout, weight, etc.; and corrosiveness and fouling characteristics of fluid. Other factors that must be considered are

1. Climatic conditions—minimum ambient, frost, snow, hail, and humidity
2. Operating environment—maritime, desert, tropical, seismic, cyclonic, and dust
3. Site layout—proximity to buildings or other cooling equipment, prevailing wind directions, duct allowances, length of pipe runs, and access

Exchanger Construction

Based on the problem specifications and experience, the exchanger construction type and flow arrangement are first selected. Selection of the construction type depends upon the following parameters [1]:

1. Fluids (gas, liquids, or condensing/evaporating) used on each side of a two-fluid exchanger
2. Operating pressures and temperatures
3. Fouling
4. Whether leakage or contamination of one fluid to the other is allowed or not
5. Cost and available heat exchanger manufacturing technology

Surface Selection

Compact Heat Exchanger. Factors that influence the surface selection include the operating pressures, fouling, maintenance requirements, erosion, fabricability, cost, etc.

Shell and Tube Heat Exchanger. For shell and tube exchangers, the criteria for selecting core geometry or configurations are the desired heat-transfer performance within specified pressure drops, fouling, corrosion, maintenance, repair, cleanability by mechanical means, minimal operational problems (flow-induced vibrations), safety, and cost; additionally, the allocation of fluids on the shell side and the tube side is an important consideration.

1.2 Thermohydraulic Design

Heat exchanger thermohydraulic design involves quantitative heat transfer and pressure drop evaluation or exchanger sizing. Basic thermohydraulic design methods and inputs to these analyses are as follows.

Basic Thermohydraulic Design Methods

As discussed in Chapter 2, the ε-NTU, P-NTU$_t$, LMTD, or ψ-P method can be used for solving the thermal design problem.

Thermophysical Properties

For heat-transfer and pressure-drop analysis, the following thermophysical properties of the fluids are needed: dynamic viscosity μ, density, specific heat c_p, surface tension, and thermal conductivity k. For the conduction wall, thermal conductivity is needed.

Surface Geometrical Properties

For heat transfer and pressure drop analyses, at least the following surface geometrical properties are needed on each side of a two-fluid compact heat exchanger:

Heat-transfer area, A, which includes both primary and secondary surface area if any
Core frontal area, A_{fr}
Minimum free flow area, A_o
Hydraulic diameter, D_h
Flow length, L
Fin thickness and fin conduction length
Core volume, V and core dimensions L_1, L_2 and L_3

These quantities are computed from the basic dimensions of the core and heat-transfer surface. On the shell side of a shell and tube heat exchanger, various leakage and bypass flow areas are also needed. The procedure to compute these quantities is presented elsewhere.

Surface Characteristics

Surface characteristics for heat transfer, j, and flow friction, f, are key inputs for the exchanger heat transfer and pressure drop analysis, respectively. Experimental results for a variety of exchanger surfaces are presented in Kays and London [2], and correlations in Shah and Bhatti [3]. More references on j and f factors are furnished in Chapter 4.

Heat Exchanger Specification Sheet

Heat exchanger specification sheet for shell and tube heat exchangers is shown in Fig. 2 and for plate-fin heat exchangers in Fig. 3.

2 DESIGN PROCEDURE

The design of heat exchangers requires the consideration of the factors just outlined. It is unlikely that any two designers will arrive at exactly the same design for a given set of conditions, as the design process involves many judgments while carrying out the design [4]. Gollin [4] describes the step-by-step design procedure for a heat exchanger. Important steps in the heat exchanger design procedure include the following:

1. Assess the heat transfer mechanisms involved.
2. Select the heat exchanger class.
3. Determine the construction details and select the surface geometry.
4. Determine size and layout parameters keeping in mind the constraints imposed by the purchaser/client.
5. Perform preliminary thermal design known as approximate sizing.
6. Perform the detailed design.
7. Check the design.
8. Optimize the design.
9. Perform the check for flow-induced vibration in the case of shell and tube heat exchanger, individually finned tube, and bare tube bank compact heat exchangers.
10. Perform mechanical design.
11. Estimate cost and finalize the design as per trade considerations.

3. THERMOHYDRAULIC DESIGN PROGRAM STRUCTURE

One of the pioneers in developing computer software for thermal and mechanical design of shell and tube exchangers and air coolers is M/s B-Jac International, Inc., Midlothian, VA. An insight into the logic of their programs for the design of shell and tube exchangers, and air coolers is discussed next.

Table 1 B-Jac HETRAN Technical Specifications

Specification	Description
TEMA exchanger types	Front head: A, B, C, N
	Shell: E,F,G,H,J,K,X
	Rear head: L,M,N,P,S,T,U,W
Special types	Vapor belts
	Double tubesheets
Tube types	Plain
	Integral low finned tubes
Baffle types	Single segmental
	Double segmental
	Triple segmental
	Full supports
	No tubes in window
	Strip baffles
	Rod baffles
Baffle cuts	Horizontal, vertical, rotated
Tube patterns	Triangular
	Rotated triangular
	Square
	Rotated square
Tube passes	1 to 16 (odd or even)
Pass layout types	Quadrant, mixed, ribbon

3.1 Thermal Design Program for Shell and Tube Heat Exchanger

The salient features of the B-Jac HETRAN program for the thermal design of shell and tube exchanger are given in Tables 1 and Table 2.

Additionally, the following features are available:

Table 2 B-Jac HETRAN Output

Design summary	A comprehensive overview of the most important variables: shell- and tube-side temperatures, flow rates, coefficients, velocities, and pressure drops, plus a concise description of key heat exchanger dimensions and geometry
Performance evaluation	Required area and distribution of resistances in clean, specified fouling, and maximum fouling conditions
Coefficients	Film coefficients and their components
MTD and flux	LMTD, correction factors, heat fluxes, and heat flux limitations
Pressure drop	Clean and dirty pressure drops, velocity and pressure drop distribution from inlet to outlet
Shell-side flow	Stream analysis flow fractions and ρV^2 analysis (per TEMA)
Construction of tube bundle	Baffle and tube layout specifications
Vibration analysis	Fluid elastic critical velocity and frequency matching for acoustic, natural, and vortex shedding at inlet, bundle, outlet, and user-specified spans
Recap of design cases	Concise summary of alternative solutions that have been explored and their costs

Enhanced version of TEMA specification sheet
Condensing details
Vaporization details
Warning and messages on any design, fabrication, or operation considerations or problems

3.2 Thermal Design Program—AEROTRAN

The salient features of the AEROTRAN program for the thermal design of air coolers are given in Tables 3 and 4.

4 HEAT EXCHANGER DESIGN PROBLEMS

In a broad sense, the design of a new heat exchanger means the selection of exchanger construction type, flow arrangement, tube and fin material, and the physical size of an exchanger to meet the specified heat-transfer and pressure-drop requirements. Two most common heat exchanger design problems are the rating and sizing. For an existing exchanger, the performance evaluation problem is referred to as the rating problem. The sizing problem is also referred to as the design problem. Rating and sizing problems are discussed here. For more details on the rating and sizing problems, refer to Refs. 2 and 5 and Bell [6].

4.1 Rating

Determination of heat-transfer and pressure-drop performance of either an existing exchanger or an already sized exchanger is referred to as a rating problem. Inputs to the rating problem include [1]: (1) heat exchanger construction details, (2) flow arrangement, (3) overall dimensions, (4) material details, (5) surface geometries and surface characteristics (j and f factors), (6) fluid flow rates, (7) inlet temperatures, and (8) fouling factors. The designers's task is to predict the fluid outlet temperatures, total heat-transfer rate, and pressure drop on each side.

Rating of a Compact Exchanger

The rating problems for a two-fluid direct-transfer type compact heat exchanger that has gas as a working fluid at least on one side is discussed briefly here, and the detailed rating of a

Table 3 B-Jac AEROTRAN Technical Specifications for Air-Cooled Heat Exchanger

Code	ASME Code, Section VIII, Div. 1.
Standards	API 661.
Header types	Plug, studded cover, flanged confined cover, flanged full face cover, bonnet, U-tube, pipe
Tube size	No practical limitation
Fin size	High-profile fin
Fin configuration	Circular, segmented, plate
Fin types	Extruded, L-type weld, U-type weld, I-type weld, L-type tension, embedded sleeve, metal-coated, plate
Tube pass arrangement	Horizontal, vertical
Fan size	Any commercially available fan size
Draft types	Forced, induced
Plenums	Transition, panel

Table 4 B-Jac AEROTRAN Output

Optimization path
Design summary
Performance evaluation
Heat-transfer coefficients
MTD/LMTD, heat flux
Pressure drop
Construction of bundle
Fan details
Heat exchanger specification sheet
Recap of designs
Condensing details
Warnings and messages

crossflow and counter-crossflow exchanger is described separately. Customarily, the ε-NTU method is employed for compact heat exchangers. Hence, the solution procedure is outlined here using the ε-NTU method. The basic steps involved in the analysis of a rating problem are the determination of:

1. Surface geometrical parameters
2. Thermophysical fluid properties
3. Reynolds numbers
4. Surface characteristics, j and f
5. Corrections to the temperature-dependent fluid properties
6. Heat-transfer coefficients
7. Fin effectiveness and overall surface effectiveness
8. Thermal resistance due to conduction wall
9. Overall heat-transfer coefficient
10. NTU, C^*, and exchanger effectiveness ε
11. Heat transfer rate, outlet temperatures, and pressure drop on each side

Rating of a Shell and Tube Exchanger

"Rating" implies that a specific heat exchanger is fairly completely described geometrically (with the possible exception of the length) and the process specifications for the two streams are given. The Bell–Delaware method is a rating method. The basic rating program of the Bell–Delaware method is shown in Fig. 2, and the method is described in detail in Chapter 5.

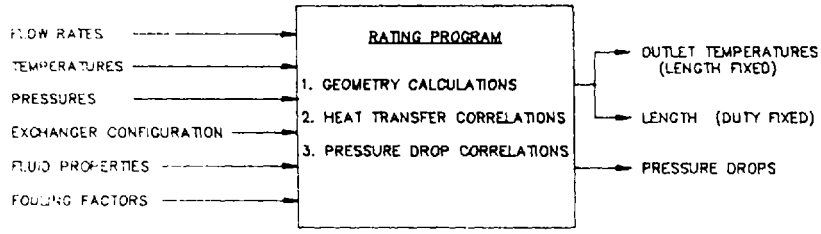
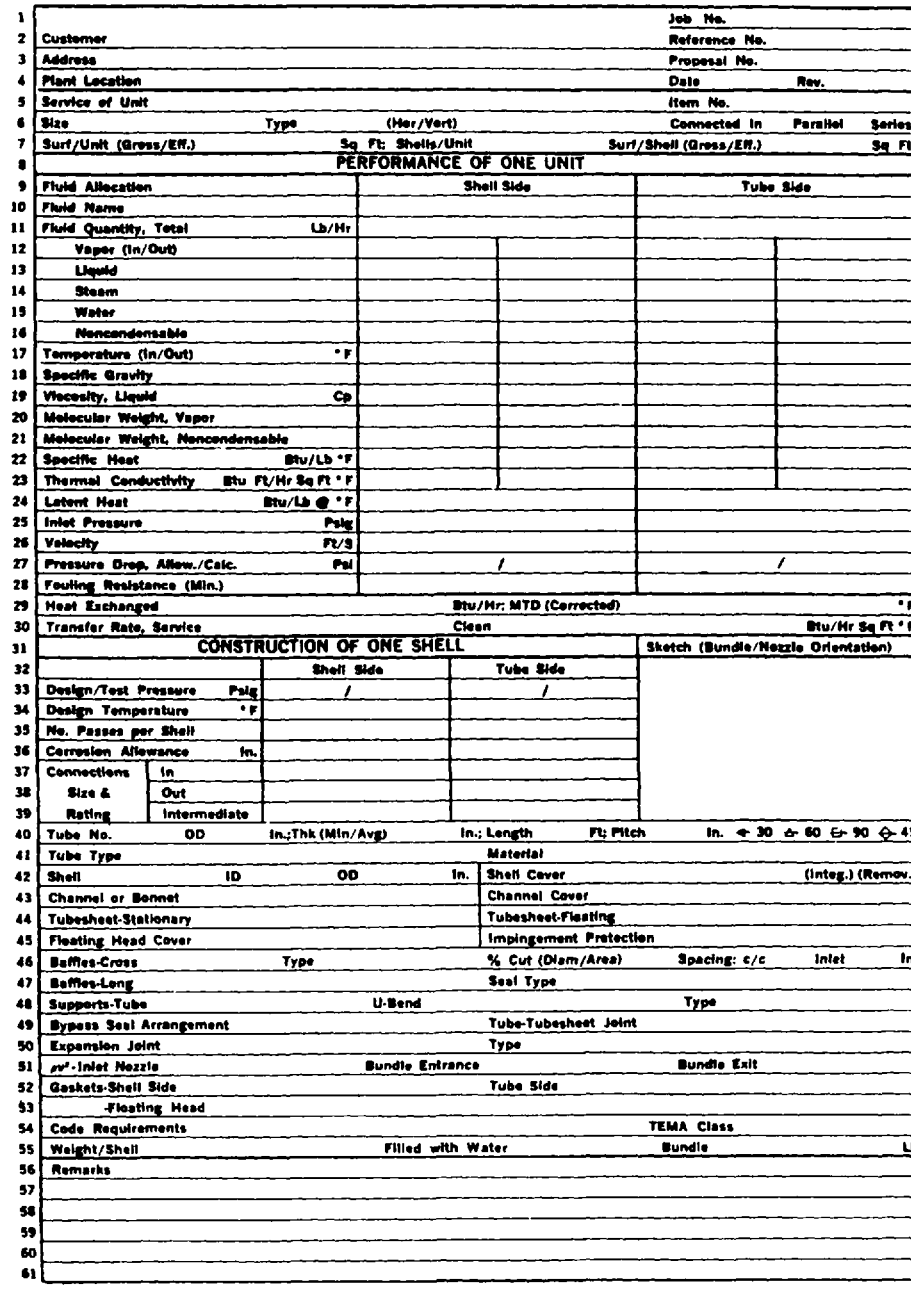


Figure 2 Rating of shell and tube heat exchanger. From Heat Exchanger Design Handbook, Vol. 3, 1983, pp. 3.1.3–1—3.1.3–4, Bell, K. J., Editor-in-Chief, E. V. Schlunder, Hemisphere Publishing Corporation, Washington, D.C. Reproduced with permission. All right reserved.



| | | |

CLIENT						JOB. NO.			
LOCATION		Design Data Sheet Plate Fin Heat Exchanger				ITEM NO.			
1	Service					No. of trains/service			
2	No. of process streams/block		Flow: cross/counter/cross-counter			No. blocks ser/par per train			
3	DATA FOR ONE TRAIN								
4	Stream Identification	Units	A	B	C	D	E	F	
5	Fluid Name								
6	Quality: w/w in/out								
7	Total Flowrate								
8	Operating Pressure								
9	Design Pressure								
10	Test Pressure								
11	Allowable Pressure Drop								
12	Temperature: in/out								
13	Design Temp. Max/Min								
14	Heat Load: Gas								
15	Latent								
16	Liquid								
17	Total								
18	Fouling Factor								
19	Design Code		Approval Authority			Inspection Organisation			
20	External Environment		External Protection			Insulation			
21	DESIGN OF ONE TRAIN								
22	Total Pressure Drop/Train								
23	Corrugation Code								
24	No. of Layers/Block								
25	Free Flow Area/Block								
26	Thermal Surface/Block								
27	Thermal Length/Block								
28	Inlet Distributor Code								
29	Type/Position on Block								
30	Outlet Distributor Code								
31	Type/Position on Block								
32	Nozzle in dia/sch/type								
33	out dia/sch/type								
34	Header Tank dia. in/out								
35	Manifold dia. in/out								
36	Stacking Arrangement (including dummies)								
37	Total Surface/Block	Thermal Margin				Sketch:			
38	Mat'ls/Block - fins	- headers							
39	- parting sheets	- cap sheets							
40	Width of spacer bars	Total X sect metal							
41	W×H×L of block	Free Volume/Block							
42	W×H×L of train								
43	Weight/Block - dry	- operating							
44	Weight/Train - operating	- max for shipping							
45	Notes:								

Rev	Alterations	Date	By	Checked	Approved
0					
1					
2					
				Sheet	of

Figure 4 Heat exchanger specification sheet for plate-fin heat exchanger. Reproduced from Taylor, M.A., Editor, Plate-Fin Heat Exchangers, Guide to Their Specification and Use, HTFS (Harwell Laboratory), Oxon, UK, 1980.

4.2 Sizing

In a sizing problem, we determine the physical size (length, width, height, and surface area on each side) of an exchanger. Inputs to the sizing problem are the fluid inlet and outlet temperatures, flow rates, fouling factors, and the pressure drop on each side. The designer's task is to select construction type, flow arrangement, materials, and surface geometry on each side. With the selection of construction types and surface geometries on each side, the problem then reduces to the determination of the core dimensions for the specified heat-transfer and pressure-drop performance. However, one can reduce the sizing problem to the rating problem by tentatively specifying the dimensions, then predict the performance [1]. If the computed results do not agree with the specified values, a new size is assumed and the calculations are repeated.

Size of a Heat Exchanger

For a given heat duty, the size of the heat exchanger is a function of the following parameters:

1. Thermal effectiveness
2. Fluid flow rate
3. Secondary surface area per unit volume
4. Heat-transfer surface performance parameters
5. Heat-transfer augmentation devices, if any
6. Conductance ratio of the process fluids

Sensitivity Analysis

In a sizing problem, sometimes one is interested in determining the sensitivity of certain variables individually. For example, how does the heat transfer vary when changing the fin density in a compact heat exchanger with secondary surface? In such a case, one inputs a series of values of fin densities at one time, runs the performance (rating) calculations, obtains a series of results, and analyzes them.

Sizing of a Compact Heat Exchanger

The principle of compact heat exchanger sizing is discussed in Chapter 4, Compact Heat Exchanger Design.

Sizing of a Shell and Tube Heat Exchanger

Shell and tube heat exchanger design or sizing is based upon (1) design conditions, that is, fluid flow rates, terminal temperatures, thermophysical fluid properties, and allowable pressure drop; (2) assumptions, heat-transfer surface area, overall heat-transfer coefficient, or size, length, or number of tubes; and (3) pressure drop across the heat exchanger [7]. The design conditions are fixed by overall plant design and determine the expected performance of the exchanger. Trial-and-error calculations of the film coefficients area used to check the assumptions, which are also checked by an overall heat balance. Finally, the pressure drop is calculated and compared with the allowable values. If the calculated pressure drop is too high, a new set of assumptions is made and rechecked as before.

Heat Exchanger Optimization

The solution to the sizing problem in general is not adequate for the design of a new exchanger, since other constraints in addition to pressure drop are imposed on the design, and the objective of the design is to minimize the weight, volume, and heat-transfer surface, and minimum pumping power, pressure drop, or other considerations in addition to meeting the required heat transfer. This is achieved by heat exchanger optimization. Shah et al. [8] reviewed various methods used in the literature for heat exchanger optimization and described numerical nonlinear programming techniques.

4.3 Solution to the Rating and Sizing Problem

Now let us discuss the basic steps involved in the solution of the two design problems, the rating and sizing.

Rating

The basic steps involved in the solution to the rating problem are as follows [9].

ε-NTU Method.

1. Compute C^* and NTU from the input specifications.
2. Determine ε for known NTU, C^*, and the flow arrangement.
3. Compute q from

$$q = \varepsilon C_{min} (t_{h,i} - t_{c,i})$$

and outlet temperatures from

$$t_{h,o} = t_{h,i} - q/C_h$$

$$t_{c,o} = t_{c,i} + q/C_c$$

and compare with those of step 2.

LMTD Method.

1. Compute R from $R = C_i/C_c$.
2. Assume the outlet temperatures to determine P, or assume P and calculate outlet temperatures. Also calculate LMTD.
3. Determine LMTD correction factor, F.
4. Determine q from $q = UAF(\text{LMTD})$.
5. Evaluate the outlet temperatures from known q, C_c, and C_h, and compare with those of step 2.
6. Repeat steps 2–5 until the desired convergence is achieved.

Solution to the Sizing Problem

In a sizing problem, U, C_c, C_h, and the terminal temperatures are specified, and the surface area A is to be determined. Or U may be calculated from the specified convective film coefficients and the fouling resistances. The basic steps involved in sizing by the ε-NTU and LMTD methods are as follows [9].

ε-NTU Method.

1. Compute ε from the specified inlet and outlet temperatures and calculate C^*.
2. Determine NTU from known ε, C^*, and the flow arrangement.
3. Calculate the required surface area A from $A = (\text{NTU})C_{min}/U$ and from terminal temperatures.

LMTD Method.

1. Compute P and R from the specified inlet and outlet temperatures.
2. Determine F from F-P curves for known P, R, and the flow arrangement.
3. Calculate the heat transfer rate q and LMTD.
4. Calculate A from $A = q/[U\,F(\text{LMTD})]$.

A trial-and-error approach is needed for the solution of the rating problem by the LMTD method.

5 COMPUTER-AIDED THERMAL DESIGN

In the present computer era, thermal design is almost exclusively performed by industry using computers. Chenoweth et al. [10], Bell [11], and Palen [12] discuss computer-aided design methods for shell and tube exchangers. Shah [13] discusses in detail the computer-aided thermal design methodology for both compact and shell and tube exchangers. Although there are similarities in the overall structure of the computer programs, the details vary significantly between compact and shell and tube exchangers. In the following subsections, we discuss the structure of a computer design method for thermal design of (1) compact heat exchangers and (2) shell and tube heat exchangers. Salient features of this computer program are discussed.

5.1 Overall Structure of a Thermal Design Computer Program

The overall structure of a thermal design computer program for a compact heat exchanger (Fig. 5), consists at a minimum of these subroutines [13]: (1) input subroutines, (2) geometry subroutine, (3) fluid properties subroutine, (4) surface characteristics subroutine, (5) fin efficiency subroutine, (6) ε-NTU subroutine, (7) pressure drop subroutine, (8) rating problem subroutine, (9) sizing problem subroutine, (10) optimization subroutines, and (11) output subroutines.

Input Subroutines. These serve (1) to feed the problem specifications/process data, and (2) to convert the given unit from one system to other. The input subroutine should be structured to verify whether the input data is within normal ranges and to give a warning message if any inconsistency is found.

Geometry Subroutine. The geometry subroutine calculates the various surface geometrical parameters for commonly used surfaces. For uncommon surfaces, calculated values are fed through the input subroutine or the terminal.

Fluid Properties Subroutine. This subroutine provides fluid properties for commonly used fluids in the form of specific or generalized correlations together with heat release/added curve. For others, they may be transferred through input data. Methods or correlations should be incorporated for evaluating properties of fluid mixtures.

Surface Characteristics Subroutine. For common surfaces, j and f versus Reynolds number data may be stored in the subroutine, or correlations may be built in. For uncommon surfaces, such information may be transferred through the input subroutine or through the terminal.

Fin Efficiency Subroutine. This subroutine calculates the fin efficiency and overall surface effectiveness for various types of extended surfaces.

ε-NTU Subroutine. ε-NTU formulas for all flow arrangements of interest are built into this subroutine. The subroutine could be used for solving both the rating and sizing problems. That means, for a rating problem, it computes ε when NTU and C^* are given, and for a sizing problem it computes NTU when ε and C^* are given.

Pressure Drop Subroutine. The friction factor f is fed through the surface characteristic subroutine. Provisions must be made to compute the pressure drop in manifolds, headers, turns, or sudden area changes at manifold/header inlet/outlet sections.

Rating Problem Subroutine. Since outlet temperatures are not known initially, they are therefore guessed, and the solution to the rating problem is iterated on the fluid properties once or twice until the desired convergence is achieved.

Sizing Problem Subroutine. All of the subroutines (except the rating problem subroutine) discussed so far are used in sizing problem. The sizing problem is solved by first determining

an approximate mass velocity G that accounts for both specified heat transfer and pressure drop. The sizing problem is iterated on G until the desired convergence is met.

Optimization Subroutines. In a sophisticated computer program, not only are the options of solving straightforward rating and sizing problems available, but also optimization procedures are incorporated. Such a program logically searches among feasible solutions and arrives at an optimum objective function.

Output Subroutines. These serve to print all the output results in the desired units along with the desired input data and error messages. All important output results should be verified for their basic validity.

Guidelines on Program Logic

Shah [13] lists several points that should be taken into account in the initial organization and writing of the program:

1. The program should be written in a modular form containing many subroutines rather than one big main program. This allows flexibility in thorough debugging and modification of the program while running the program.
2. Error messages subroutines should be inbuilt that monitor the warning and minor and major errors for the input data and throughout the problem execution.
3. All of the iterative calculations should have a maximum number of iterations specified.
4. For a sophisticated computer program to be good, it must satisfy the requirements of individuals with diverse yet specific interests. The program should provide correct answers and ease of use, and it will be viable only as long its developers provide user support [10].

5.2 Program Structure for a Shell and Tube Exchanger

For a shell and tube exchanger, most of the structure of the subroutines mentioned so far are common but the contents slightly vary as follows:

1. Geometry subroutine: This should include the auxiliary calculations on the shell side and a range of geometries including the shell type, number of shells in series, number of shells in parallel, shell diameter, tube length, baffles and baffle cut, various shell-side clearances, tube count, and nozzles.
2. Various shell-side correction factors calculated for heat transfer and pressure drop.
3. The thermal effectiveness subroutine: P-NTU_t relations should be built in for all possible flow arrangements and TEMA shells, including the check for "temperature cross."

6 PRESSURE-DROP ANALYSIS, TEMPERATURE-DEPENDENT FLUID PROPERTIES, PERFORMANCE FAILURES, FLOW MALDISTRIBUTION, FOULING, AND CORROSION

6.1 Heat Exchanger Pressure-Drop Analysis

The term "pressure drop" refers to the pressure loss that is not recoverable in the circuit. The determination of pressure drop in a heat exchanger is essential for many applications for at least two reasons [9]:

1. The operating cost of a heat exchanger is primarily the cost of the power to run fluid-moving devices such as pumps, fans, and blowers. This pumping power, P_p, is proportional to the exchanger pressure drop as given by

$$P_p = \frac{M \Delta p}{\rho} \tag{1}$$

where M is the mass flow rate, Δp is the pressure drop, and ρ is the fluid density.

2. The heat-transfer rate can be significantly influenced by the saturation temperature change for a condensing/evaporating fluid for a large pressure drop.

The principle of pressure-drop analysis for a heat exchanger is described by Kays [14] and is extended to all types of heat exchangers. In this section, pressure-drop analysis for various types of heat exchangers as per Ref. 9 is discussed.

Pressure Drop Evaluation for Heat Exchangers

The pressure drop associated with a heat exchanger may be considered as having two major components: (1) pressure drop associated with the core or matrix, and (2) pressure drop in inlet and outlet headers, manifolds, nozzles, or ducting due to change in flow area, flow turning, etc. In this section, core pressure drop for extended surface exchangers, regenerators, and tubular exchangers is presented, followed by the pressure drop associated with bends and flow turnings.

Pressure Drop Through a Heat Exchanger

The pressure drop on any one side consists of pressure losses due to sudden contraction at the core inlet, $\Delta p_{1\text{-}2}$, core pressure drop, $\Delta p_{2\text{-}3}$, and the pressure rise due to sudden expansion at the core outlet, $\Delta p_{3\text{-}4}$. Therefore, the total pressure drop on any one side of the exchanger is given by

$$\Delta p = \Delta p_{1\text{-}2} + \Delta p_{2\text{-}3} - \Delta p_{3\text{-}4} \tag{2}$$

Pressure drop through a heat exchanger is schematically shown in Fig. 6. This figure is based on Ref. 14.

Pressure Drop for Various Compact Heat Exchangers. Pressure drop for various compact heat exchangers on the fin side is given in Table 5. Generally the core frictional pressure drop is a dominating term, accounting for about 90% or more of the pressure drop. The entrance

Table 5 Pressure Drop for Various Compact Heat Exchangers*

Heat exchanger type	Pressure drop	
1. Plate-fin heat exchangers	$\frac{\Delta p}{p_1} = \frac{G^2}{2 g_c p_1 \rho_1}\left[(1-\sigma^2+K_c) + 2\left(\frac{\rho_1}{\rho_o}-1\right) + f\frac{L}{r_h}\rho_1\left(\frac{1}{\rho}\right)\right]$	(3)
2a. Tube-fin heat exchangers (individually finned)	$\frac{\Delta p}{p_1} = \frac{G^2}{2 g_c p_1 \rho_1}\left[2\left(\frac{\rho_1}{\rho_o}-1\right) + f\frac{L}{r_h}\rho_1\left(\frac{1}{\rho}\right)\right]$	(4)
2b. Tube-fin heat exchangers (continuously finned)	$\frac{\Delta p}{p_1} = \frac{G^2}{2g_c p_1 \rho_1}\left[2\left(\frac{\rho_1}{\rho_0}-1\right) + f\frac{AL}{D_h}\rho_1\left(\frac{1}{\rho}\right)_m\right] + \frac{G'^2}{2g_c p_1 \rho_1}\left[(1-\sigma'^2+K_c) - (1-\sigma'^2-K_e)\frac{\rho_1}{\rho_0}\right]$	(5)
	Note: $G\sigma = G'\sigma'$	
3. Regenerator		
i. Plate-fin type	Same as Eq. 3	
ii. Randomly staked matrix	Same as Eq. 4	

Source: This table has been compiled from Ref. 9.

and exit losses are important at low values of σ (short flow length) L (i.e., short core), and high values of Reynolds number. For gases they are negligible and for liquids, the values of K_c and K_e are presented in Fig. 7 [14].

Important terms of correlations given in Table 5 are:

1. K_c is the contraction loss coefficient. Values of K_c are given in Ref. 14 for four different entrance flow passage geometries, which are presented in Fig. 7.
2. $1/\rho_m$ is defined as

$$\left(\frac{1}{\rho}\right)_m = v_m = \frac{v_i + v_o}{2} = \frac{1}{2}\left(\frac{1}{\rho_i} + \frac{1}{\rho_o}\right) \tag{6}$$

where v denotes specific volume. For a perfect gas,

$$\left(\frac{1}{\rho}\right)_m = \frac{R_c T_{lm}}{P_{ave}} \tag{7}$$

where R_c is the gas constant, $P_{ave} = (p_i + p_o)/2$, and $T_{lm} = T_m \pm \text{LMTD}$. Here, T_m is the average temperature of the fluid on the other side of the exchanger.

3. K_e is the expansion coefficient. Values of K_e for four different flow passage geometries are presented in Fig. 7.
4. Mass velocity G is given by

$$G = \frac{M}{A_o} \tag{8}$$

where A_o is the minimum free flow area.

5. σ' for continuously tinned tube-fin heat exchangers (Fig. 19 of Chapter 4) is given by [15]:

$$\sigma' = \frac{L_3 L_1 - L_3 \delta N_f L_1}{L_3 L_1} \tag{9a}$$

and $$G\sigma = G\sigma' \tag{9b}$$

Shell and Tube Heat Exchangers

The pressure drop on the tube side is determined from Eq. 3 with proper values of f, K_c, and K_e. However, in shell and tube exchangers K_c and K_e for the tube flow are generally neglected since their contribution is small compared to the losses associated with inlet and outlet headers/channels. If U-tubes or hairpins are used in a multipass unit, additional pressure drop due to a 180° bend needs to be included. The pressure drop associated with such a bend is discussed next.

Pressure Drop Due to Flow Turning

The pressure drop associated with flow turning is expressed in the general form

$$\Delta p_r = K\left(\frac{1}{2}\rho U^2\right) \tag{10}$$

where K is the turning loss coefficient and U is the upstream velocity based on unaffected flow area. For a 180° turning, $-p_r$ is expressed in terms of mass velocity G by:

$$\Delta p_r = \frac{4G^2}{2g_c\rho}$$
$$= 4\text{xVeloci} \tag{11}$$

Pressure Drop in the Nozzles

Pressure drop in the inlet nozzle, $-p_{n,i}$, is given by

$$\Delta p_{n,i} = \frac{1.0G_n^2}{2g_c\rho_i}$$
$$= 1.0\text{xVelocity head} \tag{12}$$

Pressure drop in the outlet nozzle, $\Delta p_{n,e}$, is given by

$$\Delta p_{n,e} = \frac{0.5G_n^2}{2g_c\rho_i} \tag{13}$$
$$= 0.5\text{xVelocity head}$$

Total pressure drop associated with the inlet and outlet nozzles, Δp_n, is given by

$$\Delta p_n = \frac{1.5G_n^2}{2g_c\rho_i} \tag{14}$$
$$= 1.5\text{xVelocity head}$$

where G_n is mass velocity through nozzle.

6.2 Temperature-Dependent Fluid Properties Correction

One of the basic idealizations made in the theoretical solutions for j and f is that the fluid properties are constant. Most of the experimental j and f data obtained involve small temperature differences so that the fluid properties do not vary significantly. For those problems that involve large temperature differences, the constant-property results would deviate substantially and need to be modified [2,5]. Two schemes for such correction commonly used are:

1. The property ratio method, which is extensively used for the internal flow problem
2. The reference temperature method, which is most common for the external flow problem

One of the two methods, the property ratio method, is described next. In the property ratio method, all properties are evaluated at the bulk mean temperature, and then all of the variable properties effects are lumped into a function. Shah's approach [5] to temperature-dependent fluid properties correction via the property ratio method is discussed here.

Gases

For gases, the viscosity, thermal conductivity, and density are functions of the absolute temperature T; they generally increase with temperature. The temperature-dependent property effects for gases are correlated by the following equations:

$$\frac{Nu}{Nu_{cp}} = \frac{St}{St_{cp}} = \left(\frac{T_w}{T_m}\right)^n \tag{15}$$

$$\frac{f}{f_{cp}} = \left(\frac{T_w}{T_m}\right)^m \tag{16}$$

where the subscript cp refers to the constant property variable and all temperatures are absolute. All of the properties in dimensionless groups of Eqs. 15 and 16 are evaluated at the bulk mean temperature. The values of the exponents n and m depend upon the flow regime, namely, laminar or turbulent.

Laminar Flow. For laminar flow, the exponents n and m are given by [16]:

$$n = 0.0, \quad m = 1.00 \qquad \text{for } 1 < \frac{T_w}{T_m} < 3 \qquad \text{(heating)} \tag{17}$$

$$n = 0.0, \quad m = 0.81 \qquad \text{for } 0.5 < \frac{T_w}{T_m} < 1 \qquad \text{(cooling)} \tag{18}$$

Turbulent Flow.

Gas Heating. For gas heating, Sleicher and Rouse [17] recommend the following correlations:

$$\text{Nu} = 5 + 0.012\ \text{Re}^{0.83}\ (\text{Pr} + 0.29)(T_w/T_m)^n \tag{19}$$

where

$$n = -[\log_{10}(T_w/T_m)]^{0.25} + 0.3 \tag{20}$$

Equations 19 and 20 are valid for $0.6 < \text{Pr} < 0.9$, $10^4 < \text{Re} < 10^6$, $1 < T_w/T_m < 5$, $L/D_h > 40$. All the fluid properties in Nu, Re, and Pr are evaluated at the bulk mean temperature.

Further, $m = -0.10$ for $1 < T_w/T_m < 2.4$.

Gas Cooling. Kays and Crawford [18] recommend $n = 0.0$ and $m = -0.10$.

Liquids

For liquids, only the viscosity varies greatly with temperature. Thus, the temperature-dependent effects for liquids are correlated by the following equations:

$$\frac{Nu}{Nu_{cp}} = \left(\frac{\mu_w}{\mu_m}\right)^n \tag{21}$$

$$\frac{f}{f_{cp}} = \left(\frac{\mu_w}{\mu_m}\right)^m \tag{22}$$

Laminar Flow. For laminar flow through a circular tube, the exponents n and m are given by Deissler [19] for heating and by Shannon and Depew [20] for cooling as

$$n = -0.14, \quad m = 0.58 \qquad \text{for } \frac{\mu_w}{\mu_m} < 1 \qquad \text{(heating)} \tag{23}$$

$$n = -0.14, \quad m = +0.54 \qquad \text{for } \frac{\mu_w}{\mu_m} > 1 \qquad \text{(cooling)} \tag{24}$$

Turbulent Flow. Petukhov [21] recommends the following values for the exponents n and m:

$$n = -0.11 \qquad \text{for } 0.08 < \mu_w/\mu_m < 1 \qquad \text{(heating)} \tag{25}$$

$$n = -0.25 \qquad \text{for } 40 > \mu_w/\mu_m > 1 \qquad \text{(cooling)} \tag{26}$$

which are valid for $2 \le \text{Pr} \le 140$, $10^4 \le \text{Re} \le 1.25 \times 10^5$. Also,

$$m = 0.25 \qquad \text{for } 0.35 < \mu_w/\mu_m < 1 \qquad \text{(heating)} \tag{27}$$

$$m = 0.24 \qquad \text{for } 2 > \mu_w/\mu_m > 1 \qquad \text{(cooling)} \tag{28}$$

which are valid for $1.3 \le \text{Pr} \le 10$, $10^4 \le \text{Re} \le 2.3 \times 10^5$.

For liquid heating, Petukhov [21] correlates the variable property friction data in the following forms:

$$\frac{f}{f_{cp}} = \frac{1}{6}\left(7 - \frac{\mu_m}{\mu_w}\right) \qquad \text{for } 0.35 < \frac{\mu_w}{\mu_m} < 1 \tag{29}$$

Equation 29 is based on the following data: $1.3 \le Pr \le 10$, $10^4 \le Re \le 2.3 \times 10^5$, and 0.35–2 for μ_w/μ_m. Tables 6a and 6b show property ratio method exponents of Equations (15), (16) or of Equations (21) and (22) for laminar flow and turbulent flow, respectively, both for gases and liquids.

6.3 Performance Failures

Satisfactory performance of heat exchangers can be obtained only from units that are properly designed and have built-in quality. Correct installation and preventive maintenance are user responsibilities. The failure of heat exchanger equipment to perform satisfactorily may be caused by one or more factors:

1. Improper thermal design
2. Operating conditions differing from design conditions
3. Uncertainties in the design parameters
4. Excessive fouling
5. Air or gas blanketing
6. Flow maldistribution
7. Deterioration in the geometrical parameters that cause bypassing the main fluids

6.4 Maldistribution

A serious deterioration in performance results for a heat exchanger when the flow through the core is not uniformly distributed. This is known as maldistribution. Maldistribution of flow takes place when the flow is not uniformly distributed over the frontal area of the core. This is due to inherent design constraints in accommodating the distributor. Due to maldistribution, the flow passages nearer to the distributor will be flush with more fluids, whereas the passages further away will have lean flow or starve for want of fluids. Maldistribution causes the following:

1. Thermal performance deterioration
2. Enhanced pressure drop
3. Erosive wear of flow passages with high mass velocity

Typical causes of maldistribution are

1. Poor header design; for example, too small header or distributor located in one end of the core; flow commences from one end of the core and flows perpendicular to the core.
2. Blocking of fin passages due to fouling, mechanical damage of core passages.
3. Damage of flow passages either at the entrance or at the exit.

Maldistribution due to unfavorable nozzle location can be corrected either by relocating the nozzles (Fig. 8) or using deflecting vanes (for side entry nozzle), or baffle plates or perforated plates in the header to direct the fluid uniformly through the tubes [22]. The baffle plate/perforated plate should be installed parallel to the tubesheet.

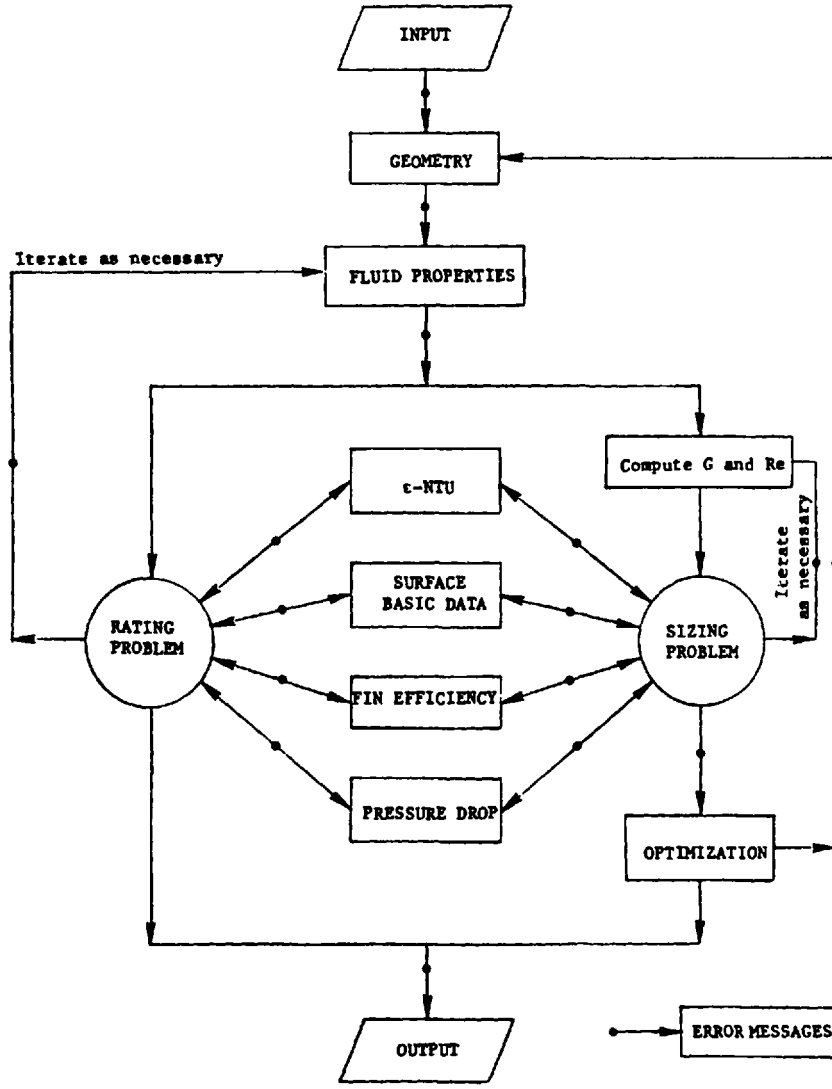


Figure 5 Overall structure of a thermal design computer program for a compact heat exchanger. From Low Reynolds Number Flow Heat Exchangers, 1983, pp. 983–998, Shah, R. K., Hemisphere Publishing Corporation, Washington, D.C. Reproduced with permission. All rights reserved.

6.5 Fouling

Fouling of the shell-side heat-transfer surfaces is common. Generally the effects of fouling are to reduce the leakage of fluid between baffles and tubes by blocking these gaps, and it also results in less leakage paths [23]. Industrial practice is generally to evaluate the heat transfer in the clean condition and apply appropriate fouling resistances (Table 1 of Chapter 9 gives a partial list) to arrive at the heat-transfer surface area required in the fouled condition. Pressure drop is lower during commissioning and startup after cleaning and gradually increases to values those predicted in the fouled condition.

Table 6a Property Ratio Method Exponents of Eqs. (15) and (16), or of Eqs. (21) and (22) for Laminar Flow

Fluid	Heating	Cooling
Gases	$n = 0.0$, $m = 1.00$ for $1 < T_w/T_m < 3$ [16]	$n = 0.0$, $m = 0.81$ for $0.5 < T_w/T_m < 1$ [16]
Liquids	$n = -0.14$, $m = 0.58$ for $\mu_w/\mu_m < 1$ [19]	$n = -0.14$, $m = 0.54$ for $\mu_w/\mu_m > 1$ [20]

Table 6b Property Ratio Method Correlations Or Exponents of Eqs. (15) and (16), or of Eqs. (21) and (22) for Turbulent Flow

Fluid	Heating	Cooling
Gases	$Nu = 5 + 0.012\ Re^{0.83}\ (Pr + 0.29)\ (T_w/T_m)^n$ $n = -[\log_{10}(T_w/T_m)]^{1/4} + 0.3$ for $1 < T_w/T_m < 5$, $0.6 < Pr < 0.9$, $10^4 < Re < 10^6$ and $L/D_h > 40$ [17] $m = -0.1$ for $1 < T_w/T_m < 2.4$	$n = 0$ [18] $m = -0.1$ (tentative) [18]
Liquids [21]	$n = -0.11$† for $0.08 < \mu_w/\mu_m < 1$ $f/f_{cp} = (7 - \mu_m/\mu_w)/6$‡ or $m \approx 0.25$ for $0.35 < \mu_w/\mu_m < 1$	$n = -0.25$† for $1 < \mu_w/\mu_m < 40$ $m = 0.24$‡ for $1 < \mu_w/\mu_m < 2$

†Valid for $2 \le Pr \le 140$, $10^4 \le Re \le 1.25 \times 10^5$
‡Valid for $1.3 \le Pr \le 10$, $10^4 \le Re \le 2.3 \times 10^5$

6.6 Corrosion Allowance

Corrosion allowances are required for the various heat exchanger components to allow for the material loss due to corrosion in service. Corrosion allowances are specified according to the severity of corrosion and the corrosion resistance property of the material. Corrosion allowance is usually specified by the purchaser and goes hand-in-hand with the material selection.

7 COOPERATIVE RESEARCH PROGRAMS ON HEAT EXCHANGER DESIGN

A text on thermal design of heat exchangers would not be considered complete unless mention is made about HTRI and HTFS.

7.1 HTRI

Heat Transfer Research, Inc. (HTRI), Alhambra, CA, is a cooperative research organization whose membership includes many of the leading users of heat exchangers, engineering contractors, and heat exchanger manufacturers. One of the major activities of HTRI is the development of computer programs that enable its members to design and rate heat exchangers.

7.2 HTFS

Heat Transfer and Fluid Flow Service (HTFS) is a cooperative venture between industry and the United Kingdom and Canadian governments. HTFS carries out its work at three facilities: Harwell Laboratory (its headquarters) in England, NEL (formerly the National Engineering Laboratory) in Scotland, and Chalk River Laboratories in Ontario, Canada. HTFS has over 200 members worldwide, in over 20 countries. Industries covered include chemical processing, engineering contracting, heat exchanger fabrication, petroleum refining, pharmaceuticals, electric and gas utilities, petrochemicals, and plastics. HTFS products and services such as com-

puter programs, design handbook, and research papers are available only to members. HTFS also provides technical advice and consultancy and other information services, including educational courses. For more information, contact Marketing Manager, Heat Transfer and Fluid Flow Service, Chalk River Laboratories, Chalk River, Ontario, Canada, KOJ 1 JO.

8 UNCERTAINTIES IN THERMAL DESIGN OF HEAT EXCHANGERS

A major problem constantly faced by heat exchanger designers is to predict accurately the performance of a given heat exchanger or a system of heat exchangers for a given set of service conditions. The problem is complicated by the fact that uncertainties exist in most of the design parameters and in the design procedures themselves [24]. The design parameters that are used in the basic thermal design calculations of a heat exchanger include process parameters, heat-transfer coefficients, tube dimensions (e.g., tube diameter, wall thickness), thermal conductivity of the tube material, and thermophysical properties of the fluids. Nominal or mean values of these parameters are used in the design calculations. However, uncertainties in these parameters prevent us from predicting the exact performance of the unit. The effect of the uncertainties is mostly in the performance degradation in service. Hence, there is an imperative need to consider all the uncertainties and to critically evaluate them and correctly predict the thermal performance of a heat exchanger. This is particularly true for critical applications. In this section, various uncertainties that influence the thermal performance and a method to account for these uncertainties in the design calculations are presented.

8.1 Uncertainties in Heat Exchanger Design

Uncertainties in the design parameters are summarised by Al-Zakri et al. [24], Cho [25], and Mahbub Uddin and Bell [26]. Various uncertainties and their reasons are:

1. Fluid flow rates, temperatures, pressures, and compositions vary from the design conditions.
2. Temperatures of cooling water and air used to cool process fluids vary with seasonal temperature changes.
3. Physical properties of the process fluids are often poorly known, especially for mixtures.
4. Heat-transfer and pressure-drop correlations from which one computes convective heat-transfer coefficients and pressure drop have data spreads around the mean values.
5. Manufacturing of heat-transfer tubes and other component dimensions influencing thermal performance does not produce precise tube dimensions.
6. Manufacturing tolerances in equipment lead to significant differences in thermohydraulic performance between nominally identical units.
7. Fouling of heat-transfer surface is poorly predictable.
8. Miscellaneous factors influence the thermal performance.

In this section, the following uncertainties are discussed.

1. Uncertainty in process conditions
2. Uncertainty in the physical properties of the process fluids
3. Flow nonuniformity
4. Nonuniform flow passages
5. Uncertainty in the basic design correlations
6. Uncertainty due to thermodynamically defined mixed or unmixed flows for crossflow heat exchangers
7. Bypass path on the air side of compact fin-tube exchangers

8. Nonuniform heat-transfer coefficient
9. Uncertainties in fouling
10. Miscellaneous effects

Items 1–3, 5, and 8–10 are common both for shell and tube exchangers and compact heat exchangers. Items 4, 6, and 7 pertain to compact heat exchangers only.

Uncertainty in Process Conditions

Heat exchangers are designed for a nominal set of operating conditions chosen to represent a relatively ideal state of a system. In general, a heat exchanger will not operate under the ideal design conditions. Process stream flow rates, compositions, and temperatures can all be expected to vary during the lifetime of the exchanger, and seasonal changes in weather constantly change cooling water and air temperatures.

Uncertainty in the Physical Properties of the Process Fluids

Correlations for heat-transfer coefficients and pressure drops, and the heat-transfer rate equation, require values of one or more of the following physical properties: density, specific heat, viscosity, thermal conductivity, latent heat, etc. There are substantial uncertainties in the physical properties of all but a few fluids. Uncertainties in these physical properties are due to the following reasons [27]:

1. Measure error.
2. Extrapolation and interpolation errors—interpolation errors may be very small, whereas extrapolation errors may substantial.
3. Estimation errors.
4. Errors in estimated temperatures and pressures.
5. Mixture properties calculated from component properties.
6. Physical properties closer to the critical temperature and pressure change rapidly and significantly. Any attempt to get mixture properties via individual properties of components around their critical points needs great care.
7. If the fluid is a mixture, the uncertainties will normally be larger than those for a pure component.

Flow Nonuniformity

To obtain maximum thermal performance, the flow should be uniform across the entire frontal area of the core. However, the flow may not be uniform due to unfavorable header design, nozzle location, and nonuniform flow passages in the case of tube-fin and plate-fin heat exchangers. For example, automobile radiators are usually designed with the assumptions that the cooling air is uniformly distributed over the radiator core, and the cooling water is uniformly distributed over the radiator tubes [28]. According to Chiou [28], these assumptions are normally not met due to these reasons: Flow nonuniformity on the cooling airside is usually due to unfavorable location of fan with respect to the radiators and due to crowded radiator compartment. The flow nonuniformity on the engine coolant side is the result of the unfavorable arrangement and configuration of the inlet manifold of the coolant to the radiator. Nonuniform flow distribution adversely affects the thermal performance and also could produce high-velocity regions leading to erosion–corrosion of flow passages. Chiou presents a mathematical method to determine the thermal effectiveness of the engine radiator accounting for two-dimensional nonuniform fluid flow distribution on both cooling air and engine coolant sides. Flow nonuniformity due to header design and due to unfavorable location of radiator fan of a diesel electric locomotive are discussed next.

Flow Nonuniformity Due to Header Design. Normally the frontal area of a compact heat exchanger is very large compared to the dimensions of the nozzles and the core depth. The

large frontal area requires turning the streams in a system of headers. The turnings have marked area changes through the headers, leading to nonuniform flow through the core (Fig. 9), even though there may be uniform flow passages. Therefore, the header design has a profound effect on the thermal performance of the core. The main objective in designing the header is to ensure uniform distribution of fluids over the entire frontal area of the core and to have minimum pressure drop due to flow turning. Maldistribution due to unfavorable nozzle location can be corrected as discussed earlier. The thermal performance degradation due to unfavorable nozzle location on the tubeside can be evaluated as discussed by Muller [29]. If the tube-side film coefficient is not controlling the overall thermal resistance, the effect of maldistribution on the overall heat-transfer coefficient will be negligible.

Maldistribution Due to Unfavorable Location of Radiator Fan in a Diesel Electric Locomotive. Flow nonuniformity on diesel locomotive radiators is usually due to inherent problems on the air side due to unfavorable location of the fan with respect to the radiators. In diesel locomotives, the left and right radiators are mounted vertically; the radiator fan is mounted at the top but at the center of the radiators, which results in nonuniform flow distribution over the radiators. Other reason for flow nonuniformity are crowded radiator compartment fitted with lube oil cooler and filter, and radiator fan drives.

Nonuniform Flow Passages

For high-surface-density compact heat exchangers like tube-fin and plate-fin units with parallel fins, the identified nonuniform flow passages are due to [30] (1) nonuniform fin spacing, (2) recurved fin, and (3) open fin. For mechanically bonded tube-fin cores, there is ample scope for bunching of fins due to deficiency in bullet expansion, thermal fatigue, and cracking of fin collars. Maldistribution due to nonuniform flow passages as shown in Fig. 10 does not adversely affect the thermal performance in the case of either turbulent flow or highly interrupted laminar flow surfaces like offset strip fins and louvred fins, but can have a marked effect in fully developed laminar flow in continuous cylindrical passage geometries, such as those employed in disk-type rotary regenerators [31]. As a result, the reduction in Colburn j factor is substantial, with a slight reduction in friction factor f. The theoretical analysis of this problem

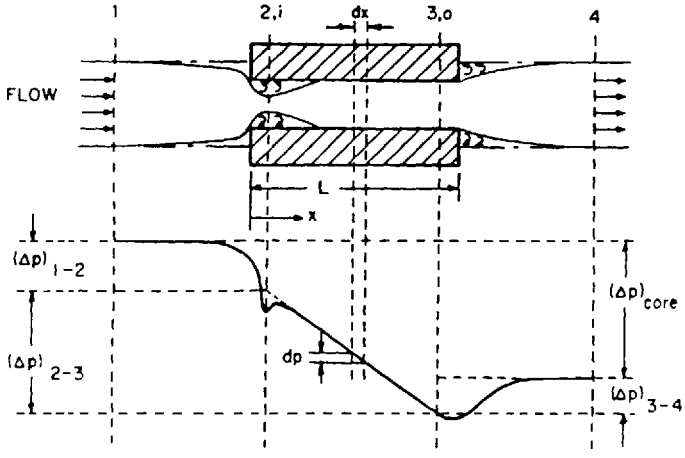


Figure 6 Pressure drop through a heat exchanger on one side (schematic representation). From Low Reynolds Number Flow Heat Exchangers, 1983, pp. 21–71, Shah, R. K., Hemisphere Publishing Corporation, Washington, D.C. Reproduced with permission. All rights reserved.

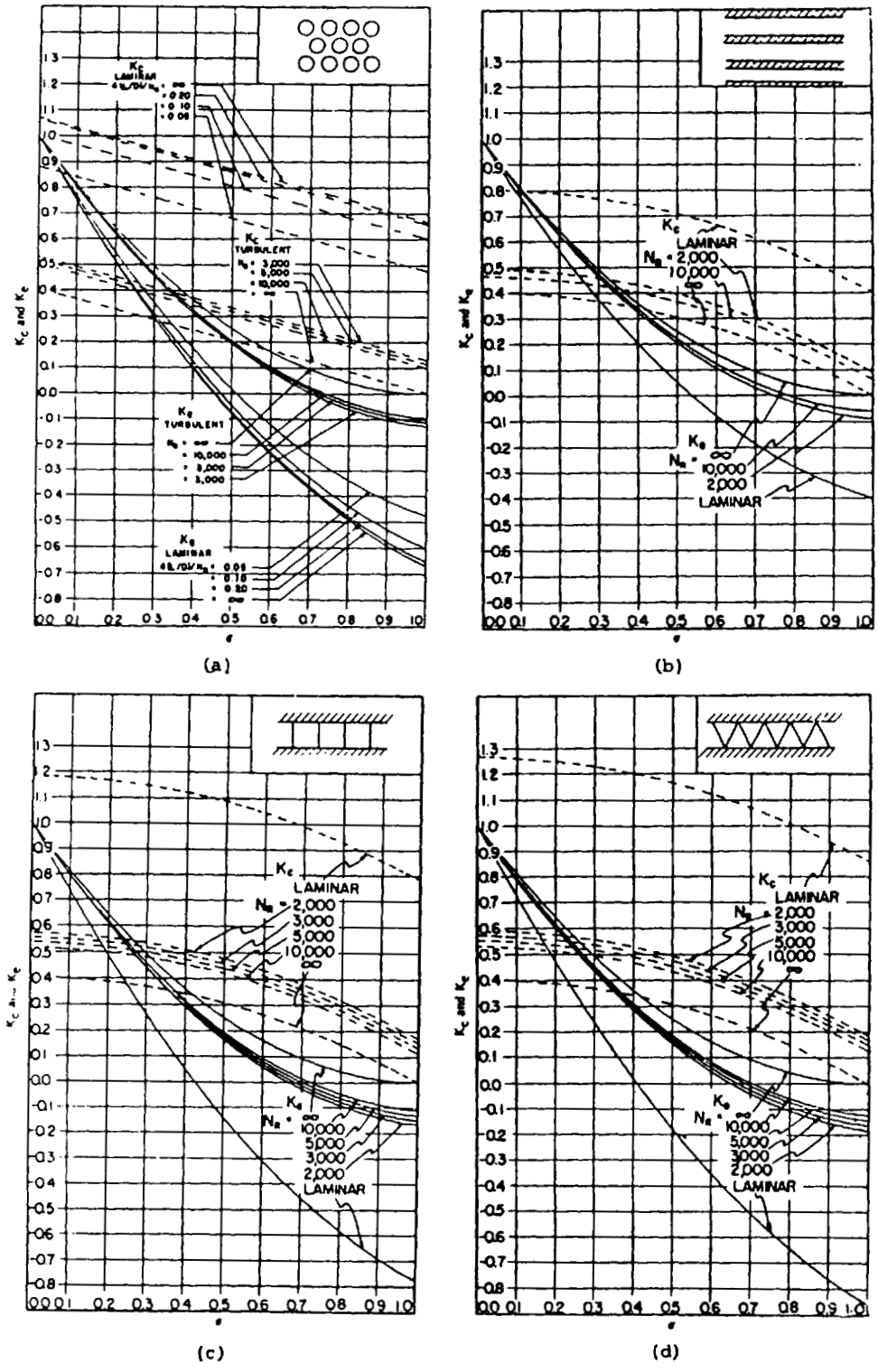


Figure 7 Entrance and exit pressure loss coefficients for (a) a multiple circular tube core, (b) multiple flat tube core, (c) a multiple square tube core, and (d) a multiple triangular tube core, Kays[14].

for low Reynolds number laminar flow surfaces is discussed in Refs. 30a, 30b, and 31. To a certain extent, nonuniform flow passages due to fin bunching of mechanically bonded cores or soldered radiator cores can be overcome by combing of fins during maintenance schedules.

Uncertainty in the Basic Design Correlations

All of the correlations for the basic fluid flow and heat-transfer mechanisms in heat exchangers show scatter when compared to experimental data. Some processes, such as, nucleate boiling, are only very crudely predictable a priori [24].

Uncertainty Due to Thermodynamically Defined Mixed or Unmixed Flows for Crossflow Heat Exchangers, After Digiovanni and Webb [32]

The thermal effectiveness of cross-flow heat exchangers is evaluated for known values of NTU and capacity rate ratio C^*, from the thermodynamically defined fluid mixedness and unmixedness and/or both through the core. The typical patterns of flow mixedness across the core are:

1. Unmixed–unmixed; e.g., brazed plate-fin exchanger with plain fins and continuously finned tube compact heat exchanger
2. Unmixed–mixed
3. Mixed–mixed

However, the thermodynamic definitions do not tell whether a specific geometry will provide mixed or unmixed flow. For any values of NTU and C^*, the unmixed–unmixed arrangement yields the highest thermal effectiveness and the mixed–mixed arrangement has the lowest, and the unmixed–mixed case offers the intermediate values.

Generally there is always some mixedness on the air side in the cases of individually finned tube banks and offset strip fins. During the design stage if these cases are assumed to act as a thermodynamically unmixed case, the actual thermal effectiveness will be less than the predicted value. For a tube bank, the level of mixedness depends on the tube layout patterns, pitch ratios, Reynolds number, size of the eddies in the transverse direction, etc.

Correction for Partial Mixing. Digiovanni and Webb [32] developed a procedure to calculate the effectiveness of cross flow heat exchangers for partially mixed flow. To calculate the correction factor, it is necessary to provide a quantitative definition of the "percent mixing," which is designated as $100y$. The partially mixed condition is defined by linear interpolation between the unmixed and the mixed flow effectiveness values. If $y = 0$, the flow stream is unmixed, and $y = 1$ represents the fully mixed stream. There are three possible cases of interest for the partially mixed condition:

1. Partially mixed flow on one stream and unmixed in the other stream
2. One stream partially mixed and the other stream mixed
3. Both streams partially mixed

They presented equations to define y for the three cases of interest. For case 1, y has been defined; for the other two cases refer to Ref. 32.

Case 1. If the measured effectiveness of the partially mixed exchangers is $\varepsilon_{pm,u}$, then

$$y = \frac{\varepsilon_{u,u} - \varepsilon_{pm,u}}{\varepsilon_{u,u} - \varepsilon_{m,u}} \tag{30}$$

From the above equation, for $y\%$ mixedness, $\varepsilon_{pm,u}$ is given by

$$\varepsilon_{pm,u} = \varepsilon_{u,u} - y\,(\varepsilon_{u,u} - \varepsilon_{m,u}) \tag{31}$$

Nonuniform Heat-Transfer Coefficient

The idealization that the heat transfer coefficient, h, is constant throughout its flow length is not correct. It varies with location, the entrance length effect (due to the boundary layer devel-

opment), surface temperature, maldistribution, fouling, manufacturing imperfections, fluid physical properties, etc. [34]. Thermal performance degradation due to uncertainties in heat transfer will be felt more in the case of highly viscous fluids and units in which phase change takes place. Temperature effects and thermal entry length effect are significant in laminar flows; the latter effect is generally not significant in turbulent flow except for low Prandtl number fluids. Approximate methods to account for specific variations in heat-transfer coefficient for counterflow are analyzed by Colburn [35] and Butterworth [36], for crossflow by Sider-Tate [37] and Roetzel [38], and for 1-2N shell flow by Bowman et al. [39]. These methods are summarised in Refs. 33 and 34. The state of the art on nonuniform heat transfer coefficient is reviewed in Ref. 34.

Bypass Path on the Air Side of Compact Tube-Fin Exchangers

Owing to the construction requirements, there are various clearances on the shell side of a shell and tube exchanger leading to various bypass paths. Modern procedures for shell-side heat-transfer calculations do take care of various leakages and bypass streams while evaluating shell-side performance. In the case of finned-tube banks, the bypass paths are inevitable between (1) the sidesheet assembly and the outermost tubes, and (2) the core assembly and the housing in which the core is housed. The thermal performance deterioration due to these clearances can be overcome by the following means:

1. Attach seals to the sidesheet assembly to block the clearance between the sidesheet assembly and the outermost tubes.
2. Permanently weld strips to the housing (without hindering the fitment of the core), which will block the bypass path between the core assembly and the housing in which the core is housed.

These measures will be discussed in Chapter 4.

Uncertainty in Fouling

The influence of uncertainties inherent in fouling factors is generally greater than that of uncertainties in physical properties, flow rates, or temperatures, such as in heat exchange between dirty aqueous fluids, in which fouling resistances can completely dominate the thermal design [40]. Planned fouling prevention, maintenance, and cleaning schedules make it possible to allow lower resistance values.

Miscellaneous Effects

Depending upon the individual design/constructional features, there exist certain miscellaneous effects that add uncertainties on thermal performance. Such effects include stagnant regions, radiation effects, allowance for in-service tube plugging due to leakages that cannot be corrected, influence of brazing/soldering, etc. Compact soldered finned-tube cores and brazed PFHEs will suffer from soldering/brazing-induced surface roughness/partial blockage due to melting of brazing filler metal. This may reduce the j factor slightly but increase the f factor substantially.

8.2 Determination of Uncertainties

The method usually used by heat exchanger designers is to ignore in the original calculations uncertainties in the design parameters. After the area has been calculated, it is multiplied by a safety factor assigned by the designer to ensure that the exchanger will perform adequately. The safety factor is based mostly upon the designer's experience and judgment and can vary from 15 to 100%. Such methods can unnecessarily add to the cost of the equipment in capital investment [24].

Computational Procedures

Buckley [41] was the first to use a statistical approach to the sizing of process equipment. His approach was to first size the unit with nominal values of design parameters. Then, based on the assumption that uncertainties follow the normal distribution, he determined the standard deviation for each variable. From the individual uncertainty (standard deviation), its effect on the overall uncertainty of the area was determined. Once the effects of all uncertain parameters on the overall heat transfer area are known, the oversizing can be determined according to the desired confidence level.

Mahbub Uddin and Bell [26] presents a Monte Carlo procedure for dealing with the effect of uncertainties on the design, performance, and operation of systems of process heat exchangers.

Cho [25] presents a simple method of assessing the uncertainties in the design of heat exchangers assuming a Gaussian form of data distribution for "uncertain" parameters, which leads to the root sum square (RSS) method of establishing the probability, or confidence level, that the heat exchanger design will meet its performance requirements. This method is briefly discussed next.

Cho's Method of Uncertainty Analysis [25]. The degree of data spread around the mean value may be quantified using the concept of standard deviation, σ. Suppose that the distribution of data points for a certain parameter has a Gaussian or normal distribution. Then the procedure to incorporate the effect of data spread into the design of a heat exchanger is as follows. For example, consider the convective heat-transfer coefficient, h, which has a data spread as shown in Fig. 11(a). The probability of the value of h falling below the mean value is of concern. Therefore, if one takes

$$X_1 = \bar{h} - Z\sigma_h \qquad \text{and} \qquad X_2 = \infty \tag{32a}$$

or

$$Z_1 = -Z \qquad \text{and} \qquad Z_2 = \infty \tag{32b}$$

then the probability that h will attain a value greater than $\bar{h} - Z\,\sigma_h$ is

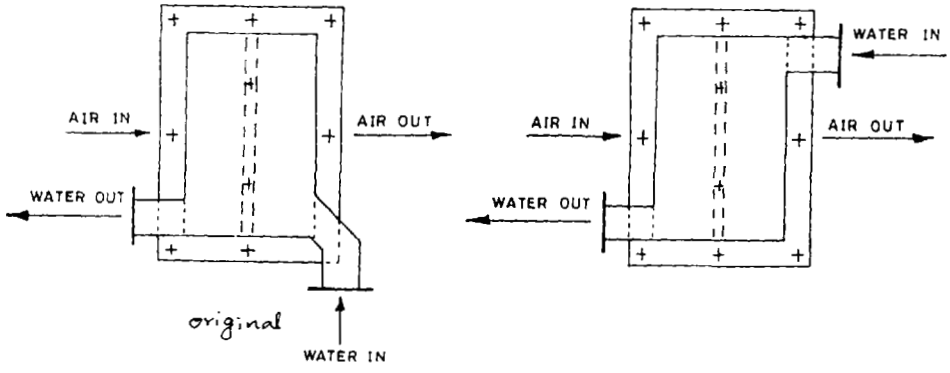


Figure 8 Maldistribution due to nozzle location is corrected by relocating the nozzles.

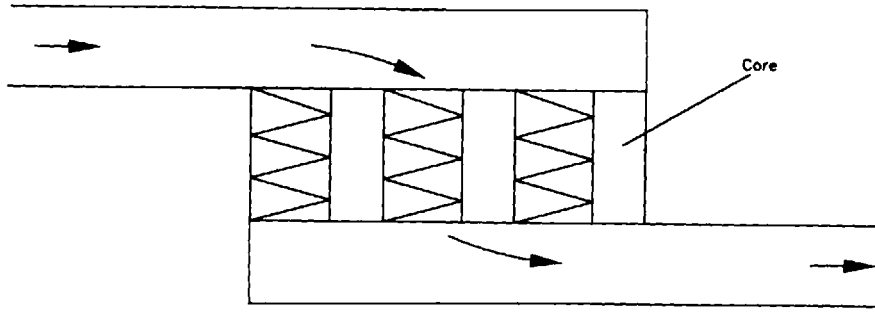


Figure 9 Nonuniform flow due to flow turning in a header.

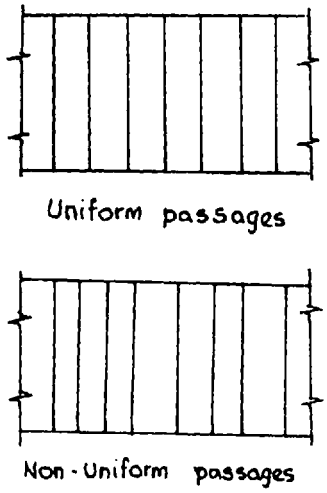


Figure 10 Nonuniform flow passages of a compact heat exchanger.

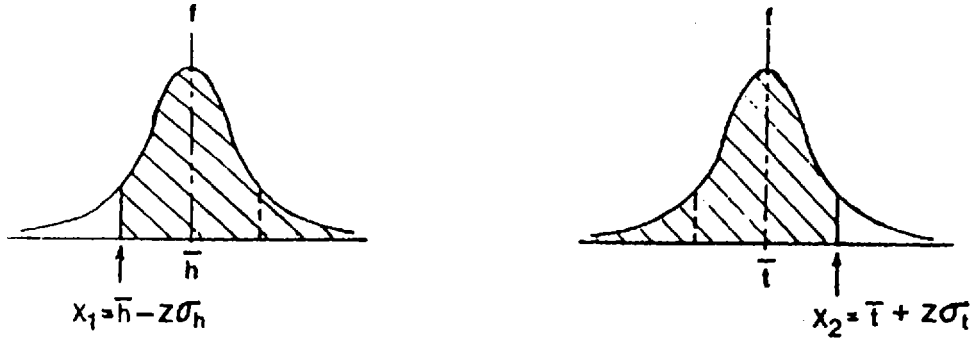


Figure 11 Normal distribution of (a) heat transfer coefficient, h; and (b) tube wall thickness, t.

$$P(X_1 = \bar{h} - Z\sigma_h, X_2 = \infty) = \frac{1}{\sqrt{2\pi}} \int_{-Z}^{\infty} e^{-Z^2/2}\, dZ \tag{33}$$

where

$$Z = \left(\frac{Z - \bar{X}}{\sigma} \right) \tag{34}$$

This probability is known as the cumulative probability or one-sided confidence level and the numerical values are given in Table 7. Here, Z indicates the degree of the design confidence level; for example, if one desires a 90% confidence level, the value of Z becomes 1.282. This means the value of h should be reduced to $\bar{h} - 1.282\ \sigma_h$ to obtain a 90% level of design confidence. Due to the reduction in the heat-transfer coefficient, the surface area is to be increased to get the desired thermal performance. These equations (32 and 33) are applicable to uncertain parameters whose lower values are of design concern, like heat-transfer coefficients and tube-wall thermal conductivity.

Now consider the effect of tube wall thickness, t, which has a data spread as shown in Fig. 11(b). The value of t greater than the mean value is of concern here. Therefore, if one takes

$$X_1 = -\infty^* \quad \text{and} \quad X_2 = \bar{t} + Z\,\sigma_t \tag{35a}$$

or

$$Z_1 = -\infty \quad \text{and} \quad Z_2 = +Z \tag{35b}$$

then the probability that $\bar{t}$ will attain a value less than $\bar{t} + Z\,\sigma_t$ is

$$P(X_1 = -\infty, X_2 = \bar{t} + Z\sigma_t) = \frac{1}{\sqrt{2\pi}} \int_{-Z}^{\infty} e^{-Z^2/2}\, dZ \tag{36}$$

Again, Z indicates the degree of the design confidence level. The numerical values are given in Table 7. A 90% level of design confidence requires the use of an increased thickness, $\bar{t} + 1.282\sigma_t$ in the sizing calculation. The reduction in heat-transfer rate due to increased thickness is to be compensated by increase in heat-transfer surface area. These equations (35 and 36) are applicable to uncertain parameters whose upper values are of design concern, like tube-wall thickness and fouling resistance.

The effects of data spreads have been discussed for individual parameters. These individual effects usually take place simultaneously, and the combined effect can be assessed for normally distributed parameters, using the root sum square (RSS) method [25]:

$$\Delta X = \sqrt{\sum_{i=1}^{N} (\Delta X_i)^2} \tag{37}$$

Additional Surface Area Required Due to Uncertainty

The effects of data spread have been discussed for individual parameters. These individual effects usually take place simultaneously and the combined effect is assessed using the RSS method. The total additional surface area ΔA_i required to obtain a certain level of design confidence is calculated from [25]:

$$\Delta A = \sqrt{\sum_{i=1}^{N} (\Delta A_i)^2} \tag{38}$$

Additional Pressure Drop Due to Uncertainty

Equation 37 can also be applied to determine the additional pressure drop, $\Delta(\Delta p)$ required to obtain a certain level of design confidence, as given by the following equation [25]:

$$\Delta(\Delta p) = \sqrt{\sum_{i=1}^{N} [\Delta(\Delta p)_i]^2} \tag{39}$$

Table 7 Cumulative Probability Function [25]

$$1[Z] = \frac{1}{\sqrt{2\,\Pi}} \int_{-\infty}^{Z} e^{-z^2/2}\, dZ = \frac{1}{\sqrt{2\,\Pi}} \int_{z}^{\infty} e^{-z^2/2}\, dz$$

z	0	1	2	3	4	5	6	7	8	9
0.0	0.5000	0.5040	0.5080	0.5120	0.5160	0.5199	0.5239	0.5279	0.5319	0.5359
0.1	0.5398	0.5438	0.5478	0.5517	0.5557	0.5596	0.5636	0.5675	0.5714	0.5753
0.2	0.5793	0.5832	0.5871	0.5910	0.5948	0.5987	0.6026	0.6064	0.6103	0.6141
0.3	0.6179	0.6217	0.6255	0.6293	0.6331	0.6368	0.6406	0.6443	0.6480	0.6517
0.4	0.6554	0.6591	0.6628	0.6664	0.6700	0.6736	0.6772	0.6808	0.6844	0.6879
0.5	0.6915	0.6950	0.6985	0.7019	0.7054	0.7088	0.7123	0.7157	0.7190	0.7224
0.6	0.7257	0.7291	0.7324	0.7357	0.7389	0.7422	0.7454	0.7486	0.7517	0.7549
0.7	0.7580	0.7611	0.7642	0.7673	0.7703	0.7734	0.7764	0.7794	0.7823	0.7852
0.8	0.7881	0.7910	0.7939	0.7967	0.7995	0.8023	0.8051	0.8078	0.8106	0.8133
0.9	0.8159	0.8186	0.8212	0.8238	0.8264	0.8289	0.8315	0.8340	0.8365	0.8389
1.0	0.8413	0.8438	0.8461	0.8485	0.8508	0.8531	0.8554	0.8577	0.8599	0.8621
1.1	0.8643	0.8665	0.8686	0.8708	0.8729	0.8749	0.8770	0.8790	0.8810	0.8830
1.2	0.8849	0.8869	0.8888	0.8907	0.8925	0.8944	0.8962	0.8980	0.8997	0.9015
1.3	0.9032	0.9049	0.9066	0.9082	0.9099	0.9115	0.9131	0.9147	0.9162	0.9177
1.4	0.9192	0.9207	0.9222	0.9236	0.9251	0.9265	0.9278	0.9292	0.9306	0.9319
1.5	0.9332	0.9345	0.9357	0.9370	0.9382	0.9394	0.9406	0.9418	0.9430	0.9441
1.6	0.9452	0.9463	0.9474	0.9484	0.9495	0.9505	0.9515	0.9525	0.9535	0.9545
1.7	0.9554	0.9564	0.9573	0.9582	0.9591	0.9599	0.9608	0.9616	0.9625	0.9633
1.8	0.9641	0.9648	0.9656	0.9664	0.9671	0.9678	0.9686	0.9693	0.9700	0.9706
1.9	0.9713	0.9719	0.9726	0.9732	0.9738	0.9744	0.9750	0.9756	0.9762	0.9767
2.0	0.9772	0.9778	0.9783	0.9788	0.9793	0.9798	0.9803	0.9808	0.9812	0.9817
2.1	0.9821	0.9826	0.9830	0.9834	0.9838	0.9842	0.9846	0.9850	0.9854	0.9857
2.2	0.9861	0.9864	0.9868	0.9871	0.9874	0.9878	0.9881	0.9884	0.9887	0.9890
2.3	0.9893	0.9896	0.9898	0.9901	0.9904	0.9906	0.9909	0.9911	0.9913	0.9916
2.4	0.9918	0.9920	0.9922	0.9925	0.9927	0.9929	0.9931	0.9932	0.9934	0.9936
2.5	0.9938	0.9940	0.9941	0.9943	0.9945	0.9946	0.9948	0.9949	0.9951	0.9952
2.6	0.9953	0.9955	0.9956	0.9957	0.9959	0.9960	0.9961	0.9962	0.9963	0.9964
2.7	0.9965	0.9966	0.9967	0.9968	0.9969	0.9970	0.9971	0.9972	0.9973	0.9974
2.8	0.9974	0.9975	0.9976	0.9977	0.9977	0.9978	0.9979	0.9979	0.9980	0.9981
2.9	0.9981	0.9982	0.9982	0.9983	0.9984	0.9984	0.9985	0.9985	0.9986	0.9986
3.0	0.9987	0.9990	0.9993	0.9995	0.9997	0.9998	0.9998	0.9999	0.9999	0.1000

4
Compact Heat Exchangers

1 CLASSIFICATION AND CONSTRUCTION DETAILS OF TUBE-FIN COMPACT HEAT EXCHANGERS

Compact heat exchangers are used in a wide variety of applications. Typical among them are the heat exchangers used in automobiles, air conditioning, electronics cooling, waste and process heat recovery, cryogenics, aircraft and spacecraft, ocean thermal energy conservation, solar, and geothermal systems. The need for light-weight, space-saving, and economical heat exchangers has driven the development of compact surfaces.

1.1 Characteristics of Compact Heat Exchangers

Specific characteristics of compact heat exchangers are discussed by Shah [1–4] and include the following:

1. Usually with extended surfaces.
2. A high heat-transfer surface area per unit volume of the core, usually in excess of 700 m^2/m^3 on at least one of the fluid sides, which usually has gas flow.
3. Small hydraulic diameter.
4. Usually at least one of the fluids is a gas.
5. Fluids must be clean and relatively nonfouling because of small hydraulic diameter (D_h) flow passages and difficulty in cleaning; plain uninterrupted fins are used when "moderate" fouling is expected.
6. The fluid pumping power (i.e., pressure drop) consideration is as important as the heat-transfer rate.
7. Operating pressures and temperatures are limited to a certain extent compared to shell and tube exchangers due to thin fins and/or joining of the fins to plates or tubes by brazing, mechanical expansion, etc.
8. The use of highly compact surfaces results in an exchanger with a large frontal area and

a short flow length; therefore, the header design of a compact heat exchanger is important for a uniform flow distribution.
9. Fluid contamination is generally not a problem.
10. Variety of surfaces are available having different order of magnitudes of surface area density.
11. Flexibility in distributing surface area on the hot or cold side as desired by the designer.

Other features of compact heat exchangers are:

Materials for the manufacture of fins are limited by the operating temperature of certain applications. For low- to moderate-temperature applications, fins can be made from aluminum, copper, or brass and thus maintain high fin efficiency. For high-temperature applications, stainless steel and heat-resistant alloys may be used with possibly a reduction in the fin efficiency. Consequently, suitable high-performance surfaces may be selected to offset the reduction in fin efficiency or the fin thickness should be reduced.

Manufacture is by brazing or welding. For low- or moderate-temperature applications, the fins can be mechanically bonded. Low-fin tubes are extruded.

Flow arrangements: Compact exchangers are mostly used as single-pass crossflow or multipass cross-counterflow exchangers.

1.2 Construction Types of Compact Heat Exchangers

Basic construction types of compact heat exchangers are

1. Tube-fin
2. Plate-fin
3. Regenerators

Tube-fin and plate-fin heat exchangers are discussed in this chapter. Regenerators, exclusively used in gas-to-gas applications, could have more compact surface area density compared to plate-fin or tube-fin surfaces. They are covered in detail in a separate chapter. The unique characteristics of compact extended-surface plate-fin and tube-fin exchangers that favor them as compared with the conventional shell and tube exchangers include the following [1,3,4]:

1. Many surfaces are available having different orders of magnitude of surface area density.
2. Flexibility in distributing surface area on the hot and cold sides as warranted by design considerations.
3. Generally substantial cost, weight, or volume savings.

The following factors mainly determine the choice among the three types of compact heat exchangers:

1. Operating pressure and temperature
2. Phases of the fluids dealt with
3. Fouling characteristics of the fluid
4. Allowable pressure drop
5. Strength and ruggedness
6. Restrictions on size and/or weight
7. Acceptable intermixing of the fluids dealt with

1.3 Tube-Fin Heat Exchangers

Tube-fin heat exchangers are widely used throughout the industry in a variety of applications. They are employed when one fluid stream is at a higher pressure and/or has a significantly

higher heat-transfer coefficient compared to the other fluid stream. For example, in a gas-to-liquid exchanger, the heat-transfer coefficient on the liquid side is generally very high compared to the gas side. Fins are used on the gas side to increase surface area. In a tube-fin exchanger, round and rectangular tubes are most commonly used (although elliptical tubes are also used), and fins are employed either on the outside or on the inside, or on both sides of the tubes, depending upon the application. Fins on the outside of the tubes (Fig. 1) may be categorized as follows:

1. Normal fins on individual tubes (Fig. 1a), referred to as individually finned tubes.
2. Longitudinal fins on individual tubes (Fig. 1b), which are generally used in condensing applications and for viscous fluids in double-pipe heat exchangers.
3. Flat or continuous (plain, wavy, or interrupted) external fins on an array of tubes (Fig. 1c). Since interrupted fins are more prone to fouling, many users prefer plain continuous fins in situations where fouling, particularly by fibrous matter, is a serious problem.

Specific Qualitative Considerations for Tube-Fin Surfaces

Specific qualitative considerations for the tube-fin surfaces include the following:

Tube-fin exchangers usually have lower compactness than plate-fin units.

A tube-fin exchanger may be designed for a wide range of tube fluid operating pressures, with the other fluid being at low pressure.

Reasonable fouling can be tolerated on the tube side if the tubes can be cleaned.

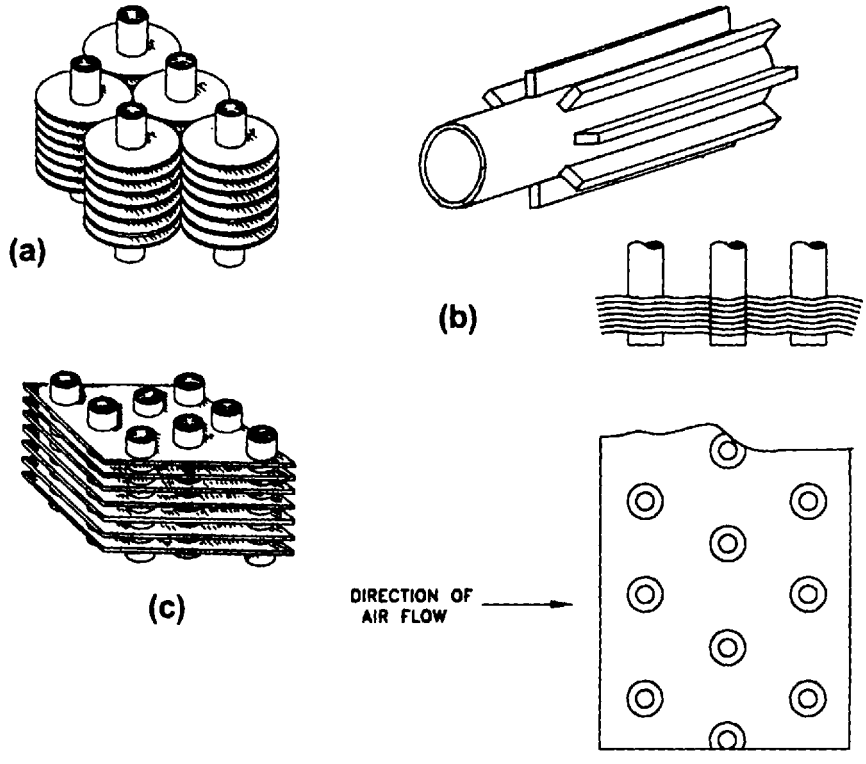


Figure 1 Tube-fin exchanger: (a) normal fin; (b) longitudinal fin; (c) continuous fins on an array of straight tubes fin; and (d) continuous fins on an array of wavy tubes fin.

Applications

Tube-fin exchangers are extensively used as condensers and evaporators in air-conditioning and refrigeration applications, for cooling of water or oil of vehicular or stationary internal combustion engines, and as air-cooled exchangers in the process and power industries. The ususal arrangement is that water, oil, or refrigerant flows in the tubes, while air flows across the finned tubes.

Individually Finned Tubes

Individually finned tube geometry is much more rugged than the continuous fin geometry, but has lower compactness. The most common individual finned tubes are with plain circular, helical, or annular enhanced fin geometries like segmented, spine, studded, slotted, or wire-loop fins [5]. Figure 2 shows some of the fin geometries that have been used on circular tubes. They are attached to the tubes by a tight mechanical fit, tension winding, adhesive bonding, soldering, brazing, welding, or extrusion. Figure 3 shows common circular tube-fin classification and manufacturing techniques. Details of various geometries are discussed next.

Plain Circular Fins. Plain circular fins are the simplest and most common. They are manufactured by tension wrapping the fin strip around a tube, forming a continuous helical fin, or by mounting circular fin disks on the tube. Helically wrapped and extruded fins on circular tubes are frequently used in the process industries and in heat recovery applications. Classification of plain circular fin tubes in terms of fin height is discussed next.

Fin Height and Classification of Finned Tubes. Fin height and classification of finned tubes are discussed by Wen-Jei Yan [6]. According to fin height, the finned tubes are called low-fin tubes, medium-fin tubes, and high-fin tubes, as follows:

1. In low-fin tubes, fins are extruded from the tube material with fin heights on the order of 1–2 mm. Fins of nominal 1.6 mm ($\frac{1}{16}$ in) height have become standard for the low-fin type of duty usually required in shell and tube exchangers. The integral type eliminates all the uncertainty concerning the tube-fin bond contact resistance.
2. Fins of approximately 3.2 mm ($\frac{1}{8}$ in) are referred to as medium fins and are usually employed in shell and tube exchangers.
3. Air-cooled exchangers require high fins, which have the height of 6.4–25 mm ($\frac{1}{4}$–1.0 in). Heat recovery systems prefer medium to high fins in tube banks of in-line arrangement.

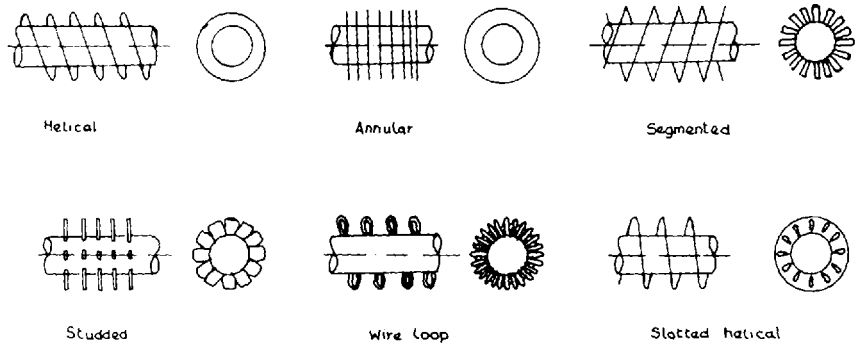


Figure 2 Forms of individually finned tubes.

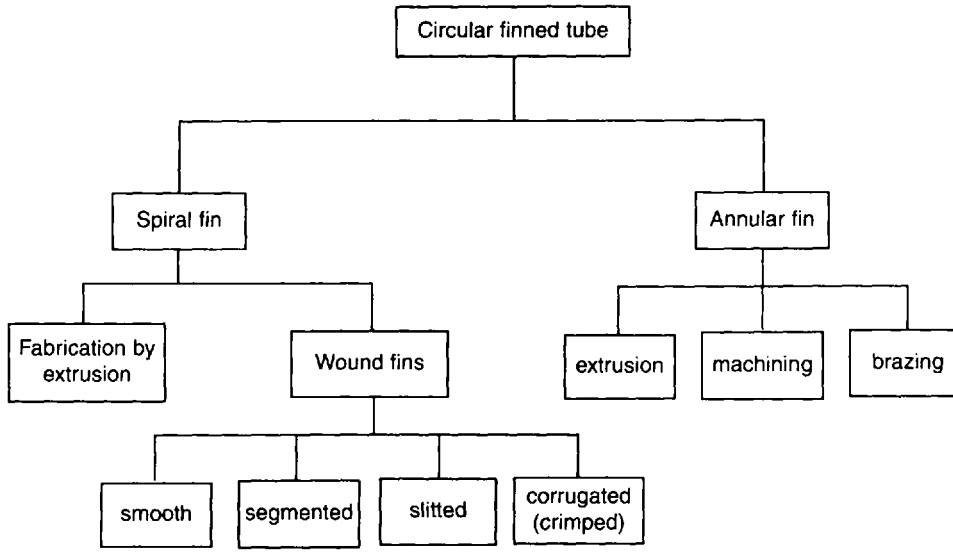


Figure 3 Tube-fin manufacturing techniques.

However, Rabas and Taborek [7] low-fin tubes as having a fin height less than 6.35 mm (0.25 in). The major reasons for using low-finned tubes in various types of heat exchangers are [7]:

1. To balance heat-transfer resistance
2. To maintain fin bond integrity
3. To reduce fouling
4. To satisfy the tube material specification

Enhanced Fin Geometries.

Segmented or Spine Fins. Segmented or spine fins are made by helically winding a continuous strip of metal that has been partially cut into narrow sections. Upon winding, the narrow sections separate and form the narrow strip fins that are connected at the base.

Studded Fins. A studded fin is similar to the segmented fin, but individual studs are welded to the tubes.

Slotted Fins. Slotted fins have slots in the radial direction; when radially slitted material is wound on a tube, the slits open.

Wire Loops Around the Tube. The wire loops are held in the tube by a tensioned wire within the helix or by soldering. The enhancement characteristic of small-diameter wires is important at low flows where the enhancement of other interrupted fins diminishes.

All of these geometries provide enhancement by the periodic development of thin boundary layers on small-diameter wires or flat strips, followed by their dissipation in the wake region between elements [8].

Construction Materials. The materials to be used for the tubes, headers, and water tanks depend on the specific requirements of the application. The most common materials for tubes and fins are copper, aluminum, and steel. For open-circuit installations, the tubes are made from copper, phosphorus-deoxidized copper, aluminum, brass, and copper–nickel–iron alloys, that is, cupronickels, and carbon steel for heat recovery applications. Fins are mostly from

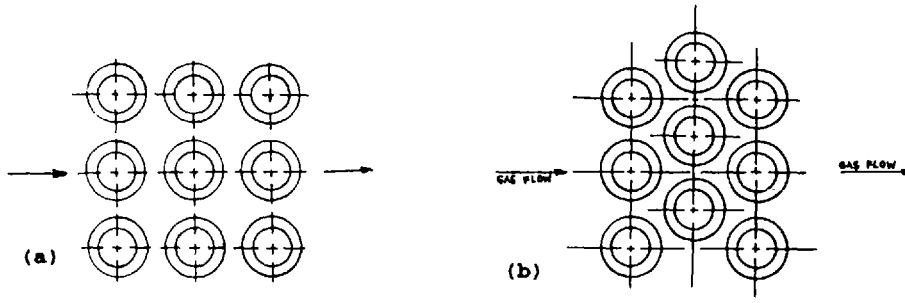


Figure 4 Tube-fin layout: (a) inline; and (b) staggered.

aluminum and copper; for heat recovery applications they are made from carbon steel. Headers and tube plates are made of carbon steel.

Tube Layout. The two basic arrangements of the tubes in a tube bank are staggered and in-line. These arrangements are shown in Fig. 4. The only construction difference between these two is that in the staggered arrangement each alternate row is shifted half a transverse pitch, and the two arrangements differ in flow dynamics. Due to compactness and higher heat transfer, the staggered layouts are mostly used. However, if the air stream is laden with dust and abrasive particles etc., in-line layout is preferred, being less affected and having ease of cleaning.

1.4 Continuous Fins on a Tube Array

This type of tube-fin geometry (Fig. 1c) is most commonly used in (1) air conditioning and refrigeration exchangers in which high-pressure refrigerant is contained on the tube side, (2) as radiators for internal combustion engines, and (3) for charge air coolers and intercoolers for cooling supercharged engine intake air of diesel locomotives. The tube layout pattern is mostly staggered.

Tube Details

Round or flat tubes (rectangular tubes with rounded corners) usually with a staggered tube arrangement are used. Elliptical tubes are also being used. Round tubes are used for high-pressure applications and also when considerable fouling is anticipated. The use of flat tubes is limited to low-pressure applications, such as vehicular radiators. Flat or elliptical tubes, instead of round tubes, are used for increased heat transfer in the tube and reduced pressure drop outside the tubes [2,9]. High-parasitic-form drag is associated with flow normal to the round tubes. In contrast, the flat tubes yield lower pressure loss for flow normal to the tubes due to lower form drag and avoid the low-performance wake region behind the tubes.

Fin Details

Continuous fin exchangers use flat, continuous, plain, wavy, louvered fins. The plain continuous fins are used in those applications in which the pressure drop is critical, although a larger amount of surface area is required for the specified heat transfer compared to the wavy or interrupted fins.

Exchangers for Air Conditioning and Refrigeration

Evaporators and condensers for air conditioning and refrigeration are usually the tube-fin type when air is one of the fluids. These exchangers are referred to as coils when air is one of the

fluids. Tube-fin geometry is becoming widespread in the current energy conservation era, because the bond between the fin and tube is made by mechanically or hydraulically expanding the tube against the fin, instead of employing welding, brazing, or soldering [2]. Formation of a mechanical bond requires very little energy compared to the energy required to solder, braze, or weld the fin to the tube. Because of the mechanical bond, the operating temperature is limited.

Tube-fin details for air conditioning and refrigeration applications are furnished by Shah [2]: Evaporator coils for small-capacity systems (less than 20 tons) use 7.9, 9.5, and 12.7 mm ($\frac{5}{16}$, $\frac{3}{8}$, and $\frac{1}{2}$ in) tubes and fin densities in the range of 315–551 fins/m (8–14 fins/in). For refrigeration applications, lower fin densities (157–315 fins/m or 4–8 fins/in) are used due to the possibility of frosting and blockage. For condenser coils, tube diameters used are 7.9, 9.5, and 12.7 mm ($\frac{5}{16}$, $\frac{3}{8}$, and $\frac{1}{2}$ in), and fin densities range from 394 to 787 fins/m (10–20 fins/in) and fin thickness from 0.09 to 0.25 mm (0.0035–0.10 in).

Radiators

Radiators are compact liquid-to-gas heat exchangers widely used in automotive vehicles. Major construction types used for radiators include (1) soldered design with flat brass tubes with flat plain or louvered copper fins—tubes and header sheets are made from brass and the water tank from brass or plastics—and (2) brazed aluminum design with flat tube and corrugated fins, usually louvered fins or flat tube continuous fins. These two construction types are shown in Fig. 5. Louvered cores are preferred as they allow a lower fin density than a nonlouvered core of the same area for the same thermal performance. The soldered brass tubes and copper fins (Fig. 6) were primarily used before the 1980s. Because of light weight and significantly better durability and operating life, brazed aluminum tubes and aluminum corrugated multilouver fin radiators have almost replaced the copper–brass radiators [2]. Typical fin density ranges from 400 to 1000 fins/m (10–25 fins/in), and the surface area density (β) ranges from 900 to 1650 m^2/m^3 (275–500 ft^2/ft^3).

Effect of Fin Density on Fouling

A major question in the choice of detailed dimensions for a core is the appropriate fin spacing. As the number of fins per inch (or per meter) is increased, the unit can be made progressively more compact. At the same time, it becomes more sensitive to clogging by dirt, soot, airborne dirts, insects, and the like, and more sensitive to nonuniformity in the fin spacing. In practice it has been found that for most automotive applications, radiators can have 10–12 fins/in. Fourteen fins per inch can be fabricated with little increase in cost per unit surface area, and

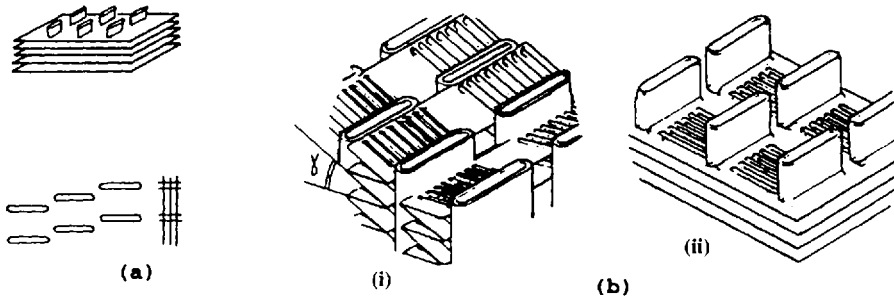


Figure 5 Forms of radiators: (a) soldered flat fin-tube; and (b) flat tube louvred fin design: (i) corrugated fin, (ii) flat continuous fin.

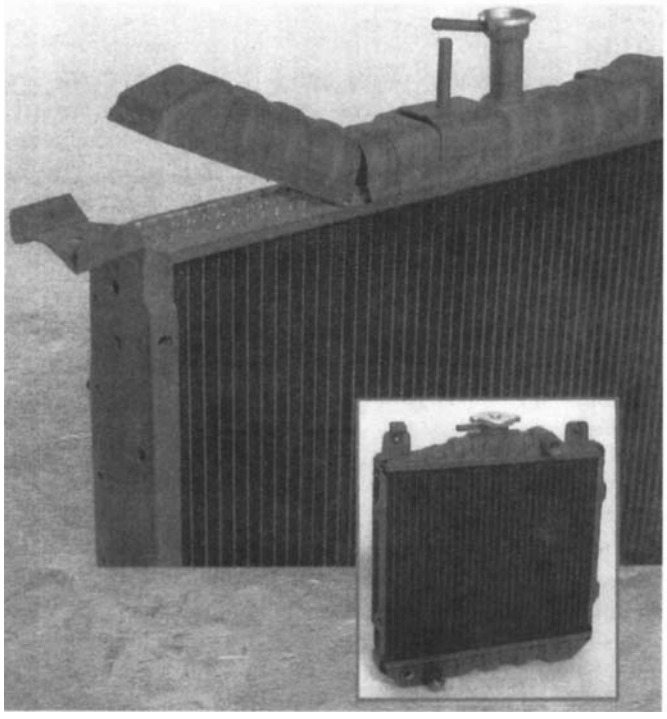


Figure 6 Soldered radiator. (Courtesy of Banco Products, Vadodara, India.)

this closer fin spacing may be justified for installations where space is a constraint and fouling of the surfaces is not a problem [9].

One-Row Radiators [10]

In conventional multirow radiators, the fin array is not in contact with the tubes over the full fin depth. The region of no contact occurs between the tube rows and is illustrated in Fig. 7. This hinders heat conduction from the tubes to the fin region between the tube rows. If the fins are louvered in this region, the conduction path is further impaired. Hence the thermal

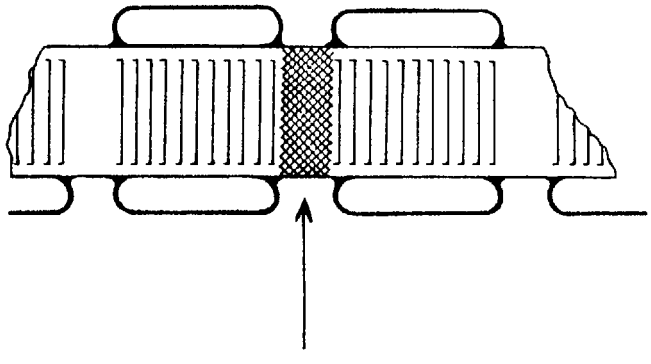


Figure 7 Region of no contact between tube rows of a radiator.

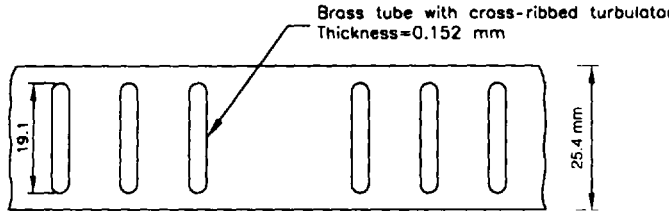


Figure 8 Single tube row radiator design.

performance per unit fin depth is low compared to the fin region in contact with the tubes. Remedies for this problem follow:

1. Use a one-row core in place of the multirow design (Fig. 8). This design eliminates the low-performance fin area between tube rows, and offers either material savings and lower air pressure drop, or increased thermal performance. In the United States, manufacturers usually make 19.1 mm ($\frac{3}{4}$ in) tubes in 0.152 mm (0.006 in) thick brass. To prevent the tube wall from becoming concave during core assembly, heavier wall thickness is usually adopted. Another method followed to prevent the tube wall from becoming concave during assembly is to use cross-ribbed turbulator tubes. The indented cross ribs increase the cross-sectional moment of inertia of the tube wall, increasing its stiffness. The indentations in the wall of turbulator tubes may be beneficial for low-flow-rate applications, where the flow may be laminar. For turbulent flow, the increase in coolant-side heat-transfer coefficient will be marginal, because the dominant thermal resistance is typically on the air side, and the ribs or indentations produce large increase in pressure drop.

2. An alternative method of eliminating the ineffective fin area is to eliminate the space between the tube rows. In other words, have the tubes touching in the axial direction (Fig. 8). This is referred to as the "tubes-touching" design. To achieve tubes-touching design, the ends of the tubes must be shaped to provide the requirement of minimum ligament between the tubes in the header plate. For the same fin depth in the air flow direction, the tubes-touching design should provide the same thermal performance as a one-row design.

Manufacture of Continuous Finned Tube Heat Exchangers

The manufacturing procedure for continuous finned tube heat exchanger is discussed next. Detailed manufacturing practices are further described in the chapter on Heat Exchanger Fabrication: Brazing and Soldering.

Mechanically Bonded Core. In a rounded hole design, the flat fins are formed with holes larger than the tubes to be inserted. Tubes are assembled in a fixture and fins are inserted. The fin gap (i.e., the fin density) is controlled by the ferrule height (Fig. 9). After assembly, the tubes are expanded so that metal-to-metal contact is being achieved. The tube ends are gener-

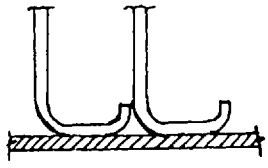


Figure 9 Ferrule height of a tube-fin heat exchanger.

ally expanded into the header plates. Sometimes, on thinner tube plates, the tubes are brazed. The tubes, fins, and headers together form the core, which is then attached to the side sheet assembly and the header for the tube-side fluid or water tank, as the case may be, and tightly sealed with gaskets.

Soldered Core. In a soldered design, which is mostly followed for flat tube-fin exchangers, the radiator cores are built from tinned brass tubes and copper fin sheets. The fins are punched with holes slightly larger than the tube dimension, and tubes are inserted through the holes. The tube outer surfaces and fin surfaces are solder coated for achieving bonding. After the header plates are assembled, the core is baked in an oven. During baking the solder metal on the tube outer surface and on the fin surface melts and give perfect metal-to-metal contact. Alternately, a fluxed core assembly is dip soldered.

1.5 Surface Selection

Various surfaces are being used in compact heat exchanger applications. A proper selection of a surface is one of the most important considerations in compact heat exchanger design. The selection criteria for these surfaces are dependent upon (1) the qualitative and (2) the quantitative considerations [11].

Qualitative Considerations

The qualitative considerations include the following:

1. Heat-transfer requirements
2. Operating temperature and pressure
3. Flow resistance
4. Size or compactness and weight
5. Mechanical integrity
6. Fouling characteristics
7. Availability of surfaces, manufacturing considerations
8. Low capital cost, and low operating cost, especially low pumping cost
9. Designer's experience and judgment
10. Maintenance requirements, reliability, and safety

Heat-transfer requirements with low flow resistance to minimize the pumping cost and a compact, low-weight unit are the important criteria for selecting a surface for a compact heat exchanger. These aspects are common for all types of heat exchangers and have been covered earlier. Surface selection influenced by fouling, manufacturing considerations, and cost are discussed next with additional details.

Fouling of Compact Exchangers. Fouling is one of the major problems in compact heat exchangers, particularly with various fin geometries and fine flow passages that cannot be cleaned mechanically. Hence, compact heat exchangers may not be applicable in highly fouling applications. There is a belief and some evidence that integral and low-finned tubes foul either at essentially the same rate or in some cases at a lower rate than plain tubes and also they are easier to clean the most types of fouling [7]. Other than low-finned tubes, if fouling is a problem, with the understanding of the problem and applying innovative means to prevent/minimize fouling, compact heat exchangers may be used in at least low to moderate fouling applications. Methods to reduce fouling are discussed in Chapter 9.

Manufacturing Considerations. Most of the heat exchanger manufacturing industries make only a limited number of surfaces due to limited availability of tools and to market potential.

Select a surface that a company can manufacture, even though theory and analysis can be used to arrive at some high-performance surfaces that may pose problems to manufacture.

Cost. Cost is one of the most important factors in the selection of surfaces, such that the overall heat exchanger is least expensive either in initial cost or in both initial and operating costs. If a plain fin surface can do the job for an application, a plain surface is preferrable to expensive complicated surface geometries.

Quantitative Considerations

The quantitative considerations include performance comparison of surfaces with some simple "yardsticks." Surface selection by a quantitative method is made by comparing performance of various heat exchanger surfaces and choosing the best under some specified criteria for a given heat exchanger application. Various methods have been proposed in the literature for such comparisons for compact heat exchanger surfaces and for other heat-transfer devices. Some of them have been reviewed by Bergles et al. [12] from the viewpoint of performance enhancement. Shah [11] categorizes the surface selection method as follows:

1. Comparisons based on j and f factors
2. Comparison of heat transfer as a function of fluid pumping power
3. Miscellaneous direct comparison methods
4. Performance comparisons with a reference surface

These methods are discussed in Chapter 8.

2 PLATE-FIN HEAT EXCHANGERS

The definition given in the Plate-Fin Heat Exchangers Guide to Their Specification and Use [13] is as follows: Plate-fin heat exchangers (PFHE) are a form of compact heat exchanger consisting of a stack of alternate flat plates called "parting sheets" and fin corrugations, brazed together as a block. The basic elements of PFHE and the brazed unit are shown in Fig. 10. Fluid streams flow along the passages made by the corrugations between the parting sheets. The corrugations serve as both secondary heat-transfer surfaces and mechanical supports for the internal pressures between layers. In liquid or phase-change (to gas) applications, the parting sheets may be replaced by flat tubes on the liquid or phase-change side. Plate-fin heat exchangers are widely used in various industrial applications because of their compactness. For many years, PFHEs have been widely used for gas separation in cryogenic applications and for aircraft cooling duties. In aerospace applications weight saving is of paramount importance. An important guidebook on PFHE specification and use is Ref. 13. This guidebook covers construction, thermal design, mechanical design, manufacture by brazing, inspection and quality control, packing, and despatch.

2.1 Essential Features

Salient features of PFHE are discussed by Shah and include the following [1,2]:

1. Plate-fin surfaces are commonly used in gas-to-gas exchanger applications. They offer high area densities (up to about 6000 m^2/m^3 or 1800 ft^2/ft^3).
2. The passage height on each side could be easily varied. Different fins (such as the plain triangular, louver, perforated, or wavy fin) can be used between plates for different applications.
3. Plate-fin exchangers are generally designed for low-pressure applications, which operating pressures limited to about 1000 kPag (150 psig).
4. The maximum operating temperatures are limited by the type of fin-to-plate bonding and

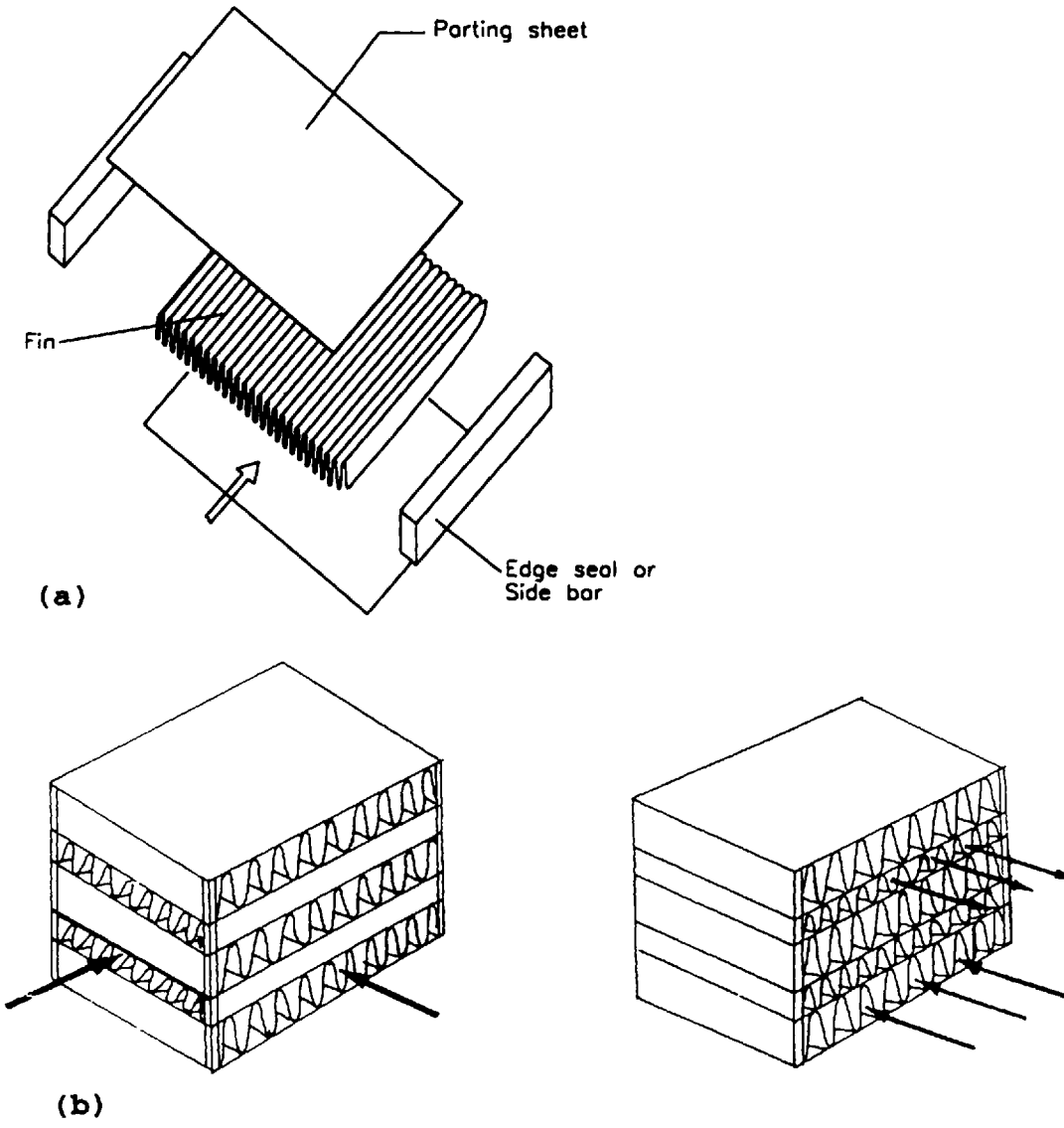


Figure 10 Plate-fin heat exchanger: (a) basic elements; and (b) Two designs of PFHE.

the materials employed. Plate-fin exchangers have been designed from low cryogenic operating temperatures (all-aluminum PFHE) to about 800°C (1500°F) (made of heat-resistant alloys).

5. Fluid contamination (mixing) is generally not a problem since there is practically zero fluid leakage from one side to the other of the exchanger.

2.2 Application for Fouling Service

The PFHE is limited in application to relatively clean streams because of its small flow passages. It is generally not designed for applications involving heavy fouling since there is no

easy method of cleaning the exchanger. If there is a risk of fouling, use wavy fins and avoid serrated fins. Upstream strainers should be employed where there is any doubt about solids in the feed. Measures to overcome fouling problems with PFHE are described by Shah [2].

2.3 Size

Maximum size is limited by the brazing furnace dimensions, and by the furnace lifting capacity. The heating characteristics of denser blocks also impose limitations on the maximum size which can be brazed. Typical maximum dimensions for low-pressure aluminum PFHEs are 1.2 m × 1.2 m in cross section × 6.2 m along the direction of flow [1,2,13], and 1.0 m × 1.0 m × 1.5 m for nonaluminum PFHEs [13]. Higher pressure units, being heavier per volume, make both handling and brazing more difficult, thus reducing the economic maximum size. Duties that call for larger units are met by welding together several blocks, or by manifolding pipework.

2.4 Advantages of PFHEs

The principal advantages of PFHEs over other forms of heat exchangers are summarized in Ref. 13 and include the following:

1. Plate fin heat exchangers, in general, are superior in thermal performance to those of the other type of heat exchangers employing extended surfaces.
2. PFHE can achieve temperature approaches as low as 1°C between single-phase streams and 3°C between multiphase streams. Typically, overall mean temperature differences of 3–6°C are employed in aluminum PFHE applications [13].
3. With their high surface compactness, ability to handle multiple streams, and with aluminum's highly desirable low temperature properties, brazed aluminum plate-fins are an obvious choice for cryogenic applications.
4. Very high thermal effectiveness can be achieved; for cryogenic applications, effectiveness of the order of 95% and above is common.
5. Provided the streams are reasonably clean, PFHEs can be used to exchange heat in most processes, for the wide range of stream compositions and pressure/temperature envelopes [13].
6. Large heat-transfer surface per unit volume is possible.
7. Low weight per unit heat transfer.
8. Possibility of heat exchange between many process streams.
9. Provided correct materials are selected, the PFHE can be specified for temperatures ranging from near absolute zero to more than 800°C, and for pressures up to at least 140 bar [1]. According to Shah [1], usually PFHEs do not involve both high temperature and high pressure together.
10. PFHE offers about 25 times more surface area per equipment weight than the shell and tube heat exchanger [13].

2.5 Limitations of PFHEs

Limitations other than fouling and size include the following [1]:

1. With a high-effectiveness heat exchanger and/or large frontal area, flow maldistribution becomes important.
2. Due to short transient times, a careful design of controls is required for startup compared with shell and tube exchangers.
3. Flow oscillations could be a problem.

2.6 Applications

Current areas of application include [13]:

1. Cryogenics/air separation
2. Petrochemical production
3. Syngas production
4. Aerospace
5. Land transport (automotive, locomotive)
6. Oil and natural gas processing

PFHEs are used in all modes of heat duty, including [13]:

1. Heat exchange between gases, liquids, or both
2. Condensing
3. Boiling
4. Sublimation ("reversing" heat exchangers)
5. Heat or cold storage

2.7 Economics

The PFHE is not necessarily cheaper for a given heat duty than other forms of heat exchangers, because the method used for constructing PFHEs is complex and energy-intensive [13].

2.8 Flow Arrangements

The fins on each side can be easily arranged such that overall flow arrangement of the two fluids can result in crossflow, counterflow, cross-counterflow, or parallel flow, though parallel flow is mostly not used. Properly designed, the PFHE can be made to exchange heat in perfect counterflow, which permits PFHEs to satisfy duties requiring a high thermal effectiveness. Crossflow, counterflow, and cross-counterflow arrangements are shown in Fig. 11. The construction of a multifluid plate-fin exchanger is relatively straightforward except for the inlet and outlet headers for each fluid.

2.9 Fin Geometry Selection and Performance Factors

Plate-fin surfaces have plain triangular, plain rectangular, wavy, offset-strip, louver, perforated, or pin fin geometries. These fin geometries are shown in Fig. 12 [8]. Plate-fin heat exchangers are superior to tube-fin heat exchangers from heat-transfer and pressure-drop points of view for the given total packaging space. Fin density varies from 120 to 700 fins/m (3–18 fins/in), thickness from 0.05 to 0.25 mm (0.002–0.01 in), and fin heights may range from 2 to 25 mm (0.08–1.0 in) [2].

Plain Fin

Plain fin corrugation is the simplest type of finning. These surfaces are straight fins that are uninterrupted (uncut) in the fluid flow direction. Triangular and rectangular passages are more common. The triangular fin is generally not structurally as strong as the rectangular fin for the same passage size and fin thickness. When the fins are straight along the flow length, the boundary layers tend to be thick resulting in lower values of the heat transfer coefficient. When they are wavy or off-set strip fin along the flow length, the boundary layers are thinner or the growth of boundary layers is disrupted periodically, respectively, resulting in a higher heat transfer coefficient.

Plain fin surfaces have pressure-drop and heat-transfer characteristics similar to flow

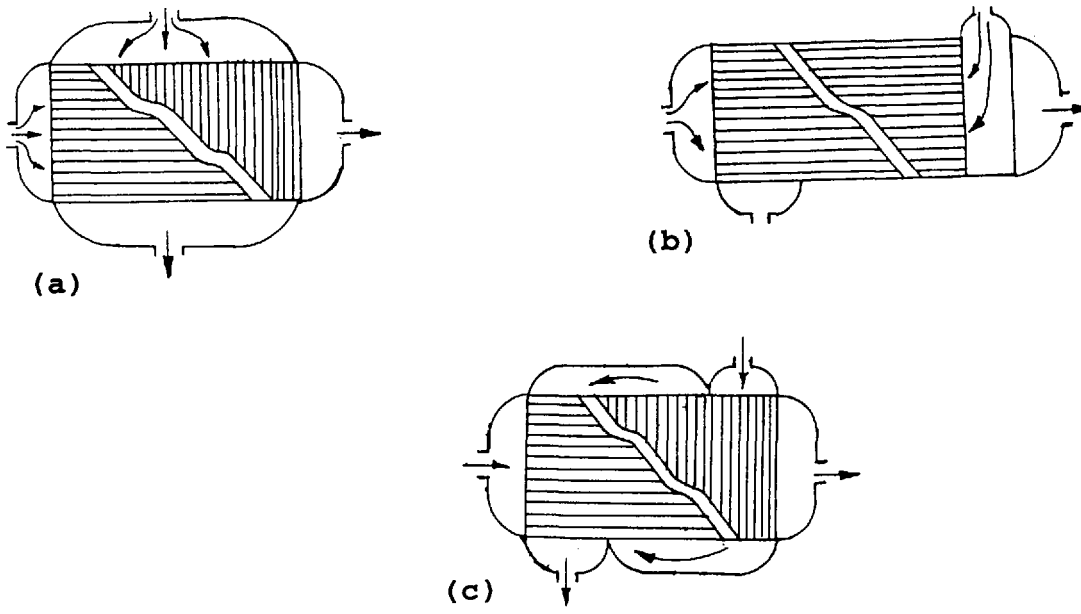


Figure 11 PFHE flow arrangement: (a) crossflow; (b) counterflow; and (c) cross-counter flow, Taylor[13].

through small-bore tubes, i.e., relatively low pressure drop and heat transfer, but a high ratio of heat transfer to pressure drop [13]. For a flow channel with rectangular or triangular cross section, under turbulent flow conditions, standard equations for turbulent flow in circular tubes may be used to calculate j and f, provided the Reynolds number (Re) is based on the hydraulic diameter, D_h. If the Re based on hydraulic diameter is less than 2000, one may use theoretical laminar flow solutions for j and f.

Plain fins are preferred for very low Reynolds number applications and in applications where the pressure drop is very critical. Condensing duties require minimal pressure drop or else the heat release curve can significantly alter and the overall duty may not be met. Therefore for condensation, plain fins are normally specified.

Plain-Perforated Fin

Perforated fins have either round or rectangular perforations, having the size and longitudinal and transverse spacings as major perforation variables. The flow passages are either triangular or rectangular. A metal strip is first perforated, then corrugated. Perforated areas vary from about 5 to 25% of the sheet area [13]. When the corrugations are laid across the flow, the stream is forced to pass through these small holes. Salient performance features include:

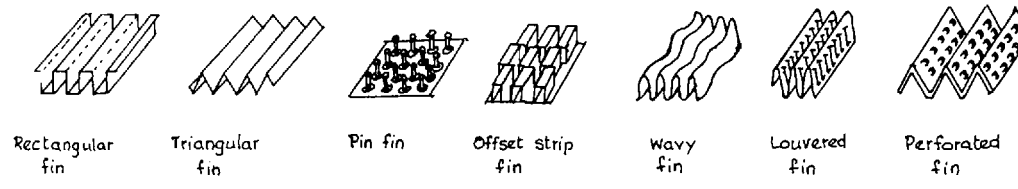


Figure 12 PFHE fin geometries.

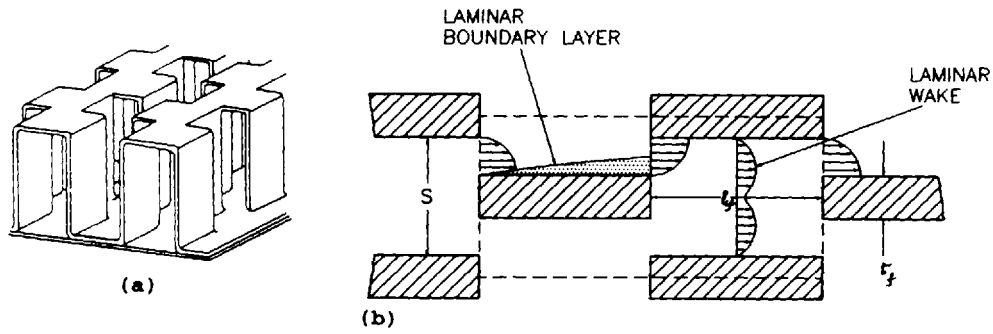


Figure 13 Offset strip fin: (a) schematic; and (b) laminar flow on the fins and in the wakes.

1. The perforated holes promote turbulence, which increases the local heat-transfer coefficient compared to plain fins, but as the percentage of perforated holes increase, the loss of heat transfer surface offsets this advantage [13].
2. The perforated surface is prone to flow-induced noise and vibration.

Applications. Perforated fins are now used in only a limited number of applications [14]. Typical applications include:

1. "Turbulators" in oil coolers.
2. In boiling applications to maintain a wetted surface and minimize depositions/concentrations [13]. Perforated corrugations permit interchannel fluid migration, which evens out surges and vibration and avoids localized concentrations or depositions.
3. Perforated fins were once used in two-phase cryogenic air separation exchangers, but now they have been replaced by offset strip fins.

Shah [15] provides a very detailed evaluation of the perforated fin geometries.

Offset Strip Fin

The offset strip fin (OSF) is commonly used geometry in plate-fin heat exchangers. The offset strip fin is designated as the serrated fin in Ref. 13. The fin has a rectangular cross section; it is cut into small strips of length l, and every alternate strip is offset by about 50% of the fin pitch in the transverse direction as schematically shown in Fig. 13. Fin spacing, fin height, fin thickness, and strip length in the flow direction are the major variables of offset strip fins.

Offset strip fin geometry is characterized by high heat-transfer area per unit volume, and high heat-transfer coefficients. The heat-transfer mechanism in offset strip fins is described by Joshi and Webb [16] and is as follows. The heat-transfer enhancement is obtained by periodic growth of laminar boundary layers on the fin length, and their dissipation in the fin wakes as shown schematically in Fig. 13b. This enhancement is accompanied by an increase in pressure drop because of increased friction factor. A form drag force, due to the finite thickness of the fins, also contributes to the pressure drop. Fluid interchange between channels is possible. Offset strip fins are used in the approximate Reynolds number range of 500–10,000 [14]. Salient features pertaining to thermal performance include the following [13]:

1. Commonly used in air separation plants where high thermal effectiveness at low mass velocities is required [13].
2. The heat-transfer performance of offset strip fins is increased by a factor of about 1.5 to 4 over plain fins of similar geometry, but at the expense of higher pressure drop [14].

3. At high Reynolds numbers, the j factor decreases, while the friction factor remains constant because of the high form drag. Therefore offset fins are used less frequently for very high Reynolds number applications.
4. They are used at low Reynolds number applications calling for accurate performance predictions, such as some aerospace applications; other fin performance data are not as repeatable.

Herringbone or Wavy Fin

Since wavy fins have noninterrupted walls in each flow channel, they are less likely to catch particulates and foul than are offset strip fins. Their performance is competitive with that of the offset strip fin, but the friction factor continues to fall with increasing Reynolds numbers [13]. The waveform in the flow direction provides effective interruptions to flow and induces very complex flows. The augmentation is due to Goertler vortices, which form as the fluid passes over the concave wave surfaces. These are counterrotating vortices, which produce a corkscrew-like pattern and probable local flow separation that will occur on the downstream side of the convex surface [8,14]. In the low-turbulence regime (Re of about 6000 to 8000), the wall corrugations increase the heat transfer by about nearly three times compared with the smooth wall channel. Therefore, wavy fins are often a better choice at the higher Reynolds numbers typical of the hydrocarbon industry; the smooth surface allows the friction factor to fall with increasing Reynolds number. Kays and London [17] provide curves of j and f versus Re for two wavy-fin geometries.

Louver Fins

The louvers are essentially formed by cutting the sheet metal of the fin at intervals and by rotating the strips of metal thus formed out of the plane of the fin. Louvers can be made in many different geometries, some of which is shown in Fig. 14. Note that the parallel louver fin and offset strip fin both have small strips aligned parallel to the flow. The louvered fin geometry of Fig. 14 bears a similarity to the offset strip. Rather than offsetting slit strips, the entire slit fin is rotated 20–60° relative to the airflow direction. As such, they are similar in principle to the offset strip fin. Louvered fins enhance heat transfer by providing multiple flat plate leading edges with their associated high values of heat-transfer coefficient. Salient features of louver fins are:

The louvered fin strip length is usually longer than the OSF, e.g., 6–18 mm, versus 3–9 mm for the OSF [8]; the louvered fin gage is generally thinner than that of an offset strip of the fin.

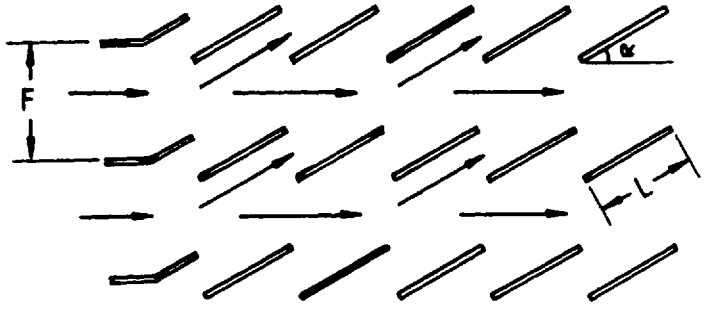


Figure 14 Flow pattern through a typical louvred fin showing limiting flow directions where F is louvre pitch, L, louvre length and α the louvre angle.

The fin corrugations normally form a triangular passage. Hence, it is generally not as strong as an offset strip fin, since the latter has a "large" flat area for brazing, thus providing strength [14].

The louver fins may have a slightly higher potential of fouling compared to the offset strip fins [14].

The louvered fin can provide heat-transfer coefficients comparable to the OSF. However, the ratio of j/f tends to be lower because of the considerable form drag on the bent fins [8].

Louver fins can enhance heat transfer by a factor of two or three compared with the equivalent unlouvered surfaces [13].

A wide range in performance can be achieved by varying the louver angle, louver width, and louver form.

The operating Reynolds number range is 100–5000, depending upon the type of louver geometry employed [14].

Applications. Their attractive thermal performance characteristics in terms of compactness, light weight and low pumping power for a given heat-transfer duty make louver fins a potential candidate for aerospace applications [18]. They are recognized as very effective heat-transfer surfaces, leading to compact solutions to cooling problems. Louvered fin surfaces are now used widely for engine cooling equipment, air-conditioning heat exchangers (evaporators and condensers), and aircraft oil and air coolers. They share this quality with the offset strip fin surfaces [19]. The louvered surface is the standard geometry for automotive radiators. For the same strip width the louvered fin geometry provides heat-transfer coefficients comparable to the OSF.

Pin Fins

An array of wall-attached cylinders (e.g., rods, wires) mounted perpendicular to the wall is known as pin fins. They can be manufactured at a very high speed continuously from a thin wire. After the wire is formed into rectangular passages, the top and bottom horizontal wire portions are flattened for brazing or soldering with the plates. Pins can be of circular or elliptical shapes. The enhancement mechanism due to a pin array is the same as that of the offset strip fin, namely, repeated boundary layer growth and wake dissipation [8]. The potential application for pin fins is at very low Reynolds number ($Re < 500$) for which the pressure drop is of no major concern. Present applications for pin fins include [14]: (1) electronic cooling devices with generally free convective flows over the pin fins and (2) to cool turbine blades.

Limitations of Pin Fins.

1. The surface compactness achieved by the pin fin geometry is much lower than that achieved by the strip fin or louver fin surfaces.
2. Due to vortex shedding behind the circular pins, noise and flow-induced vibrations can take place.

2.9.1 FIN Corrugation Code

A commonly encountered code for fin corrugation is [13]: 350S1808. The first three digits give the fin height in thousandths of an inch (350 = 0.35 inches). The letter gives the type of corrugation (S = serrated). Other types are P = plain, R = perforated, H = herringbone. The next two digits give the fins per inch (18 = 18 fpi). The following two digits give the fin thickness in thousandths of an inch (08 = 0.008 in). The time following the oblique stroke (if any) is used only for perforated fin and it is the porosity, σ.

2.10 Corrugation Selection

Corrugations, edge bars, and parting sheets are chosen primarily to contain the appropriate pressure. Corrugation selection depends on factors such as [13] compactness, pressure, mechanical integrity, manufacture, performance, velocity limits, and fouling.

2.11 Materials of Construction

PFHEs are made in a variety of materials to suit a wide range of process streams, temperatures and pressures. Material specifications should comply with the appropriate section of the ASME or to other applicable codes.

Aluminum

Aluminum is preferred for cryogenic duties, because of its relatively high thermal conductivity, strength at low temperatures, and low cost. For cryogenic services, aluminum alloy 3003 is generally used for the parting sheets, fins, and edge bars that form the rectangular PFHE block. Headers and nozzles are made from aluminum alloy 3003, 5154, 5083, 5086, or 5454 [13]. Above ambient temperature, with increase in temperature, most aluminum alloys rapidly lose their strength. For land-based transport vehicles, aluminum PFHEs are used up to 170–180°C to cool supercharged engine intake air.

Nonaluminum

Stainless steels and most nickel alloys are used for PFHEs, particularly for high-temperature services. Stainless steels have poor thermal conductivity, but their higher strength allows thinner parting plates and fins than with aluminum, which offsets some of the reduction in heat transfer.

2.12 Mechanical Design

The PFHE is a pressure vessel. It is required to be designed and constructed in accordance with a recognized Pressure Vessel Code. The mechanical design of a PFHE can be divided into the conventional pressure vessel area of header tanks, nozzle, nozzle reinforcements, lifting devices, pipe loads, etc., and the less familiar area of the block itself.

2.13 Manufacture, Inspection, and Quality Control

PFHEs are manufactured by brazing. Heat exchanger manufacture by brazing is described in Chapter 15. The manufacturer is responsible for the mechanical design and for the thermal design where the latter is not specified by the purchaser. Salient features of quality control and inspection of PFHE are detailed in Ref. 13.

3 SURFACE GEOMETRICAL RELATIONS

3.1 Surface Geometrical Parameters—General

The following are some of the basic relationships between the surface and core geometries on one side of the compact heat exchangers.

Hydraulic Diameter, D_h

The generalized relation for hydraulic diameter is given by

$$D_h = \frac{4A_o L}{A} \tag{1}$$

where A is total heat transfer area, A_o is free flow area, and L is flow length. The hydraulic radius r_h is given by $D_h/4$.

Surface Area Density α and σ

For a compact heat exchanger with secondary surface on one side, it is customary to designate the ratio of the total heat-transfer surface area on one side of the exchanger to total volume of the exchanger by α, and the ratio of the free flow area to the frontal area by σ. Thus,

$$\alpha_1 = \frac{A_1}{V} \quad \text{and} \quad \alpha_2 = \frac{A_2}{V} \tag{2}$$

$$\sigma_1 = \frac{A_{o,1}}{A_{fr,1}} = \left(\frac{AD_h/4}{A_{fr}L}\right)_1 = \frac{(AD_h/4)_1}{V} \tag{3a}$$

$$\sigma_2 = \frac{A_{o,2}}{A_{fr,2}} = \left(\frac{AD_h/4}{A_{fr}L}\right)_2 = \frac{(AD_h/4)_2}{V} \tag{3b}$$

From the definition of hydraulic diameter D_h, the relation between hydraulic diameter, surface area density α, and σ is given by

$$\left(\frac{D_h}{4L}\right)_1 = \left(\frac{A_o}{A}\right)_1 = \left(\frac{\sigma}{L\alpha}\right)_1 \tag{4a}$$

$$\left(\frac{D_h}{4L}\right)_2 = \left(\frac{A_o}{A}\right)_2 = \left(\frac{\sigma}{L\alpha}\right)_2 \tag{4b}$$

and

$$D_{h,1} = 4\frac{\sigma_1}{\alpha_1}, \qquad D_{h,2} = 4\frac{\sigma_2}{\alpha_2} \tag{5}$$

3.2 Tubular Heat Exchangers

Geometrical relations are derived for the in-line and staggered tube arrangements with bare tubes, individually finned circular tubes, and circular tubes with plain continuous fins. The header dimensions for the tube bank is $L_2 \times L_3$, the core length for flow normal to the tube bank is L_2, and the no-flow dimension is L_3. The lateral pitch is given by P_t and longitudinal pitch by P_l. Flow is idealized as being normal to the tube bank on the outside. Surface geometrical relations for tube-fin heat exchangers are derived from first principles by Shah [20,21], and for individually finned tubes by Idem et al. [22]. The surface geometrical relations given here are based on Shah [20].

Tube Inside

Tubes have inside diameter d_i, length between headers L_1, header thickness T_h, and total length including header plates thickness as $L_1 + 2T_h$. The total number of tubes, N_t, is given by

$$N_t = \frac{L_2 L_3}{P_t P_l} \tag{6}$$

The geometrical properties of interest for analysis are

Total heat transfer area $A = \pi d_i L_1 N_t$ (7)

Minimum free flow area $A_o = (\pi/4) d_i^2 N_t$ (8)

Hydraulic diameter $D_h = d_i$ (9)

Tube length for heat transfer = L_1 (10)

Tube length for pressure drop = $L_1 + 2T_h$ (11)

The geometrical properties given by Eqs. (7) to (11) also hold good for other types of arrangements discussed next.

Tube Outside

Bare Tube Bank.

In-Line Arrangement. The geometrical properties of the in-line tube bank as shown in Fig. 15 are summarized here. The number of tubes in one row (in the flow direction) are

$$N_t' = L_3/P_t \tag{12}$$

The total heat-transfer area consists of the area consists of the area associated with the tube outside surface, given by

$$A = \pi d_o L_1 N_t \tag{13}$$

The minimum free flow area A_o, frontal area A_{fr}, the ratio of free flow area to frontal area σ, and hydraulic diameter D_h are given by

$$A_o = (P_t - d_o)N_t' L_1 \tag{14}$$

$$A_{Fr} = L_1 L_3 \tag{15}$$

$$\sigma = \frac{(P_t - d_o)}{P_t} \tag{16}$$

$$D_h = \frac{4\,A_o L_2}{A} \tag{17}$$

Flow length for pressure drop calculation = L_2 (18)

Heat exchanger volume $V = L_1 L_2 L_3$

It must be emphasized that the foregoing definition of the hydraulic diameter is used by Kays and London [17] for tube banks. However, many correlations use the tube outside diame-

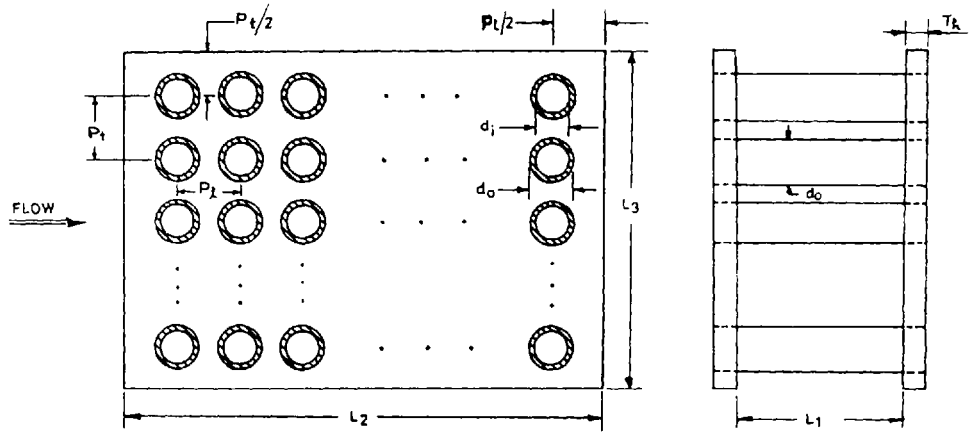


Figure 15 Inline tube bank geometry.

ter or fin root diameter as the characteristic dimension in the heat-transfer and pressure-drop correlations. So it is essential to find out first the specific definition of the characteristic length before using a particular correlation.

The geometrical properties given by Eqs. 14 to 18 also hold good for other types of arrangements discussed later.

Staggered Arrangement. A staggered tube bank and its unit cell are shown in Fig. 16. The total number of tubes with half tubes in the alternate row is given by Eq. 6. If the half tubes are eliminated from the alternate intermediate tube rows, then the number of tubes in the first row will be L_3/X_t and in the second row $L_3/X_t - 1$. The minimum free flow area occurs either at the front or through the diagonals (refer to Fig. 16b). The minimum free flow area is then given by [20]:

$$A_o = \left[\left(\frac{L_3}{P_t} - 1\right) z + (P_t - d_o)\right] L_1 \tag{19a}$$

where

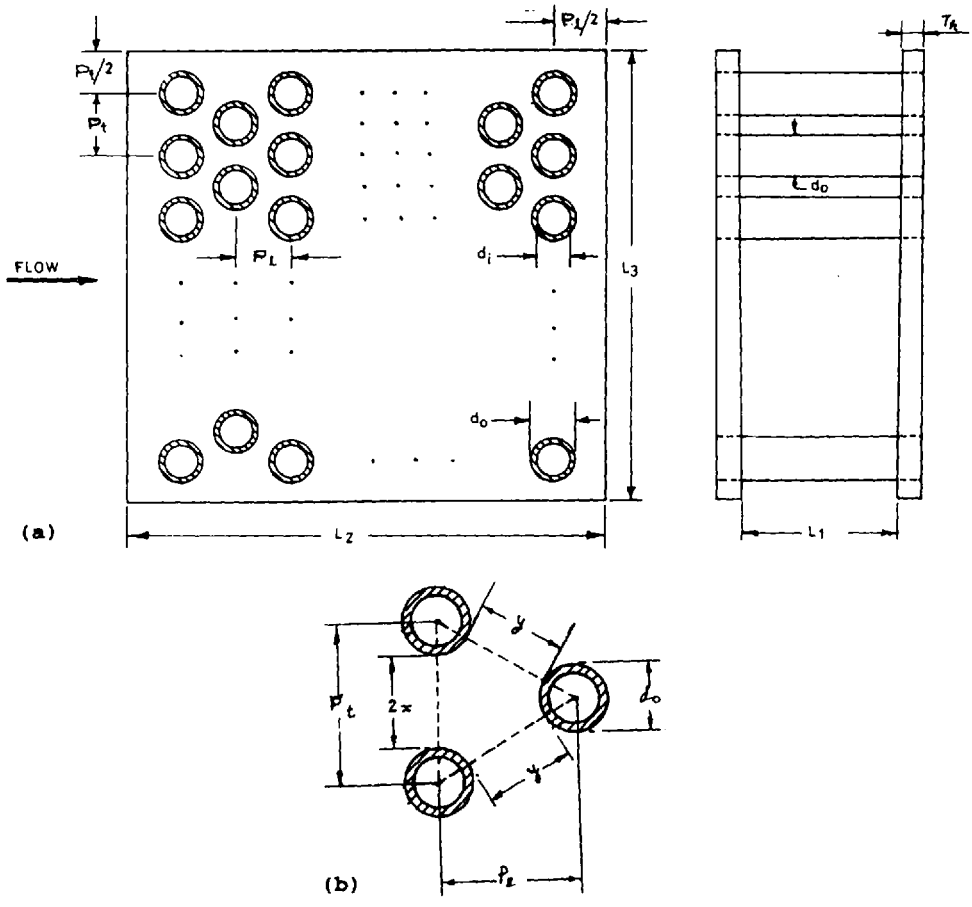


Figure 16 Staggered tube bank: (a) layout; and (b) unit cell.

$$z = 2x \quad \text{if} \quad 2x < 2y \tag{19b}$$

$$z = 2y \quad \text{if} \quad 2y < 2x \tag{19c}$$

in which $2x$ and y are defined as

$$2x = (P_t - d_o) \tag{20a}$$

$$y = [(P_t/2)^2 + (P_l)^2]^{0.5} - d_o \tag{20b}$$

In Eq. (19a), the last term $(P_t - d)L_1$ corresponds to the free flow area between the last tube at each end in the first row and the exchanger wall.

Circular Fins on Circular Tubes. The basic core geometry of an idealized single-pass cross-flow exchanger for an inline arrangement is shown in Fig. 17. The total number of tubes in this exchanger is given by Eq. 6. It is idealized that the root of a circular fin has an effective

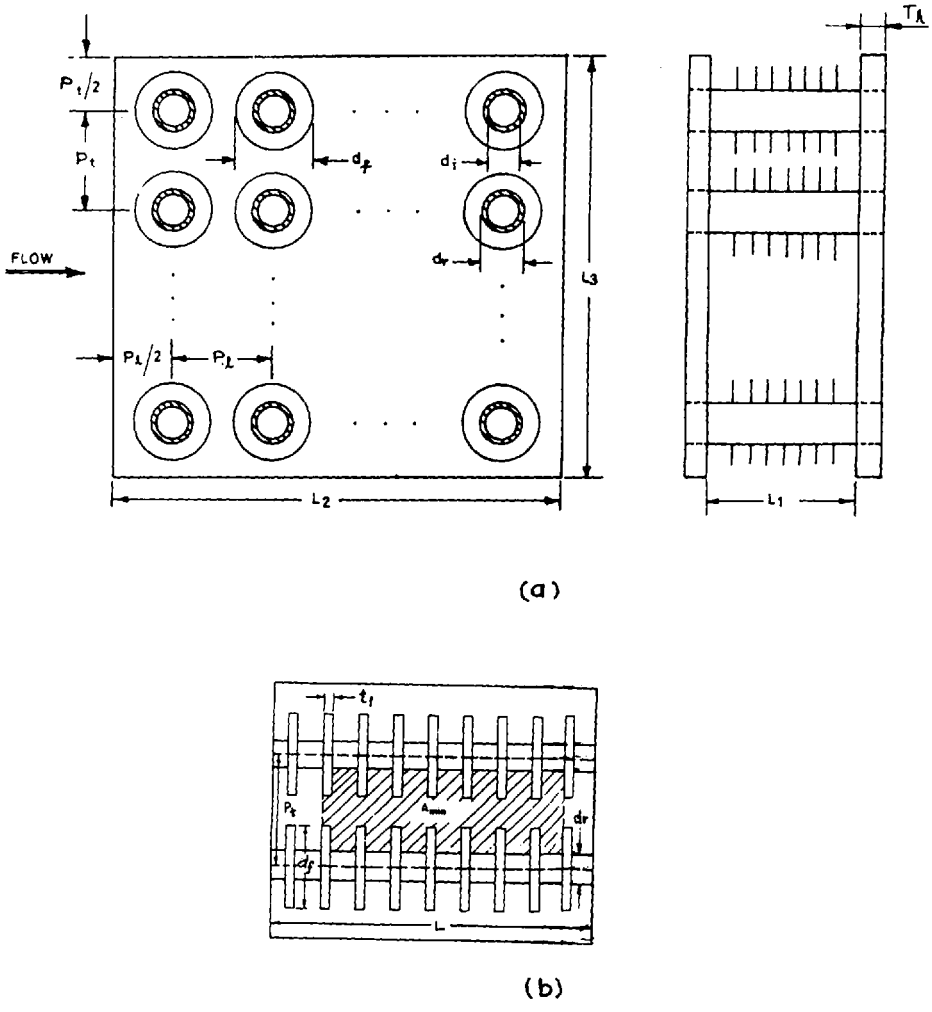


Figure 17 Individually finned circular fin tube. (a) Layout; and (b) diagram showing frontal area (dotted lines) and free flow area (hatched area).

diameter d_r and the fin tip has a diameter d_f. Depending upon the manufacturing techniques, d_r may be the tube outside diameter or tube outside diameter plus two fin collar thickness. The total heat transfer area consists of the area associated with the exposed tubes (primary area) and fins (secondary area). The primary area, A_p is the tube surface area minus the area blocked by the fins. It is given by

$$A_p = \Pi d_r(L_1 - t_f N_t L_1)N_t \tag{21}$$

where t_f is fin thickness and N_t is number of fins per unit length.

The fin surface area, A_f, is given by

$$A_f = [2\pi(d_f^2 - d_r^2)/4 + \pi d_f t_f]N_t L_1 N_t \tag{22}$$

and therefore, the total heat-transfer surface area A is equal to $A_p + A_f$, given by:

$$A = \pi d_r(L_1 - t_f N_t L_1)N_t + [2\pi(d_f^2 - d_r^2)/4 + \pi d_f t_f]N_t L_1 N_t \tag{23}$$

Minimum Free Flow Area for Circular Fins on Circular Tubes—In-Line Arrangement. The minimum free flow area for the in-line arrangement is that area for a tube bank, Eq. 13, minus the area blocked by the fins:

$$A_o = [(P_t - d_r)L_1 - (d_f - d_r)t_f N_t L_1](L_3/P_t) \tag{24}$$

Minimum Free Flow Area for Circular Fins on Circular Tubes—Staggered Arrangement. The basic core geometry of an idealized single-pass crossflow exchanger for staggered arrangement is given in Fig. 18. The total number of tubes in this exchanger is given by Eq. 6. For the staggered tube arrangement, the minimum free flow area could occur either through the transverse pitch or through the diagonals similar to those of the unit cell shown in Fig. 4.18b. The minimum free flow area is given by [19,20]:

$$A_o = [(L_3/P_t - 1)z' + (P_t - d_r) - (d_f - d_r)t_f N_t]L_1 \tag{25}$$

where

$$z' = 2x' \quad \text{if} \quad 2x' < 2y' \tag{26a}$$

$$z' = 2y' \quad \text{if} \quad 2y' < 2x' \tag{26b}$$

in which $2x'$ and y' are given by

$$2x' = (P_t - d_r) - (d_f - d_r)t_f N_t \tag{27a}$$

$$y' = [(P_t/2)^2 + (P_l)^2]^{0.5} - d_r - (d_f - d_r)t_f N_t \tag{27b}$$

Dimensions $2x'$ and y' cannot be depicted in the figure.

Continuous Plain Fins on Circular Tubes. The tube-fin arrangement is shown in Fig. 19. The total heat-transfer area consists of the area associated with the exposed tubes (primary area) and the fins (secondary area). The primary area is the same as that given by Eq. 13, minus the area blocked by the fins. Therefore, A_p is given by [14,20]:

$$A_p = \pi d_r(L_1 - t_f N_t L_1)N_t \tag{28}$$

The total fin surface area, A_f, consists of (1) the fin surface area, d_r, and (2) the area with leading and trailing edges, d_r^2, given by:

$$A_f = 2[L_2 L_3 - \pi d_r^2 N_t/4]N_t L_1 + 2L_3 t_f N_t L_1 \tag{29}$$

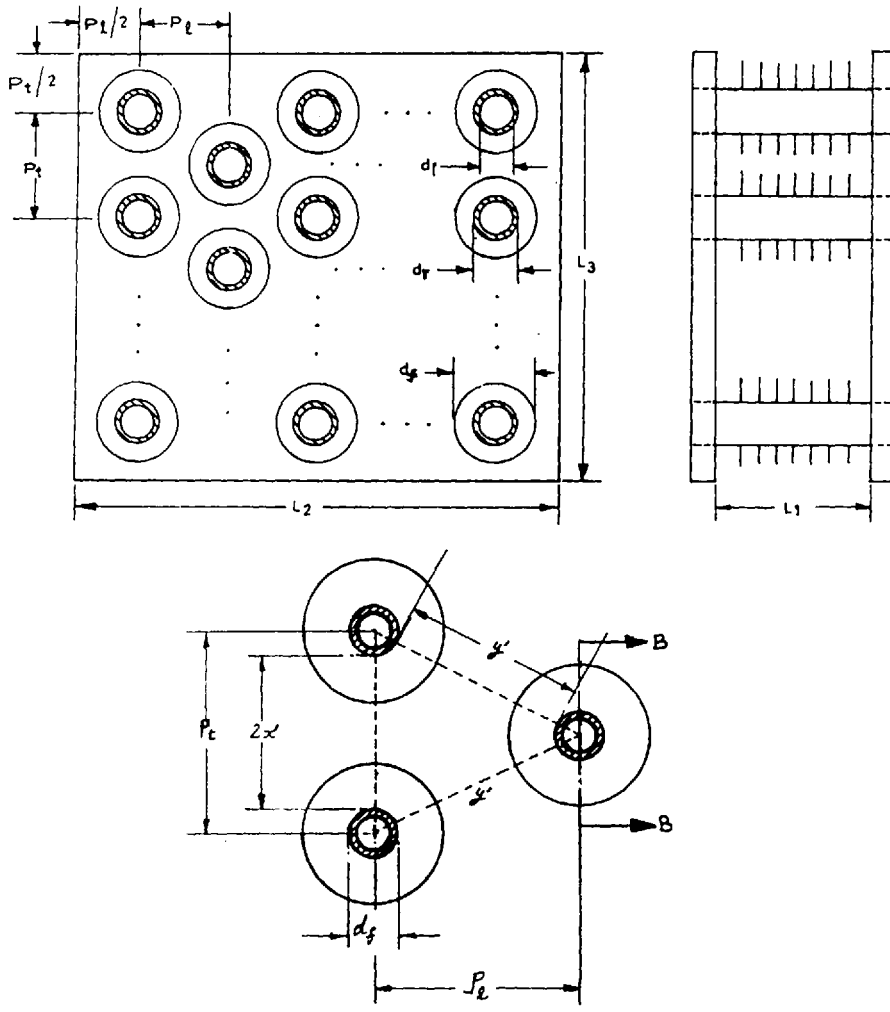


Figure 18 Individually finned tube staggered arrangement. (a) Geometry; and (b) unit cell [after Ref (21)].

and

$$\text{Total heat transfer surface area } A = A_p + A_f \tag{30}$$

Minimum Free Flow Area for the In-Line Arrangement. The minimum free flow area for an in-line arrangement is that area for a tube, Eq. 13, minus the area blocked by the fins [14,20]:

$$A_o = [(P_t - d_r)L_1 - (P_t - d_r)t_f N_f L_1](L_3/P_t) \tag{31}$$

Minimum Free Flow Area for the Staggered Arrangement. For the staggered tube arrangement as shown in Fig. 20, the minimum free flow area could occur either through the transverse pitch or through the diagonals. The minimum free flow area is given by [20]:

$$A_o = \{(L_3/P_t - l)z'' + [(P_t - d_r) - (P_t - d_o)t_f N_f]\}L_1 \tag{32}$$

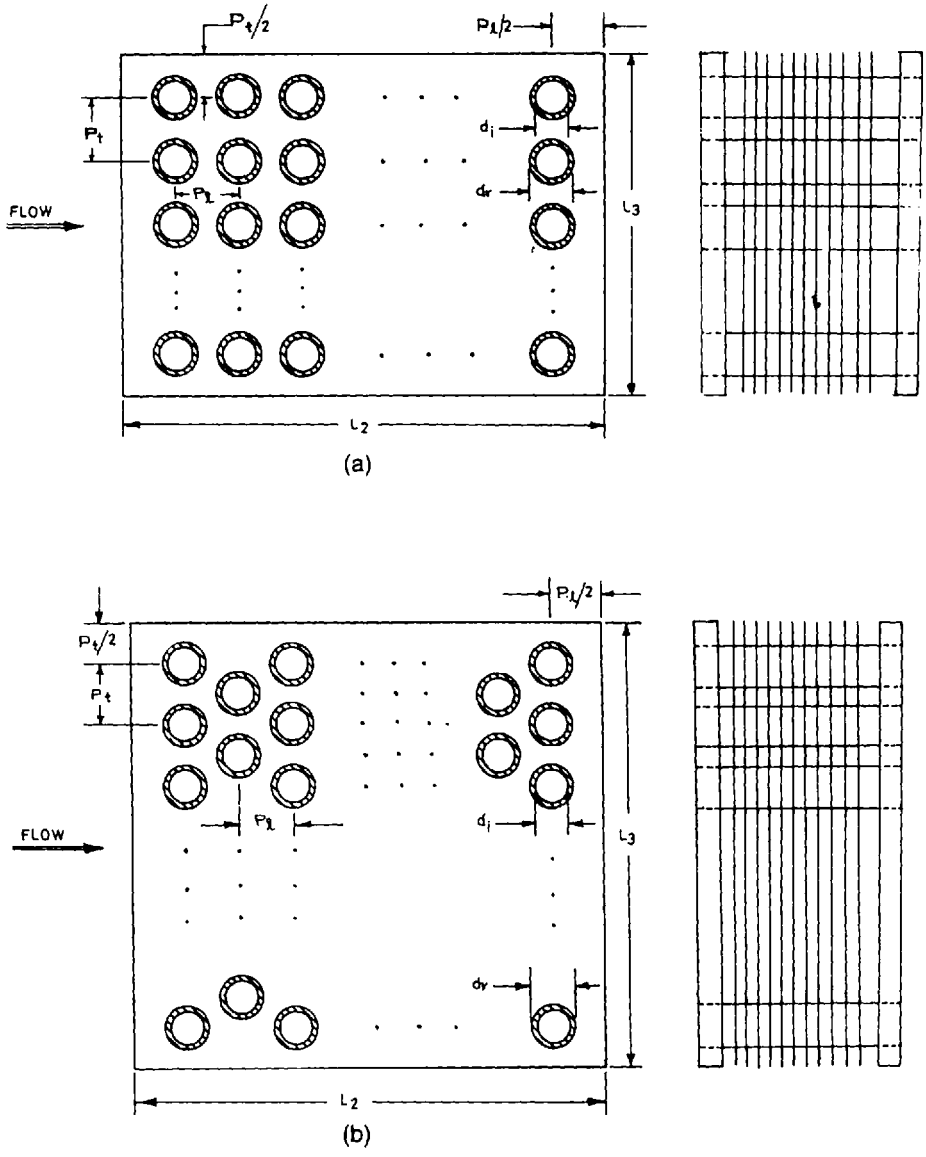


Figure 19 Continuous flat fin-tube heat exchanger: (a) inline layout; and (b) staggered layout.

In Eq. 32 z'' is defined as

$$z'' = 2x'' \quad \text{if} \quad 2x'' < 2y'' \tag{33a}$$

$$z'' = 2y'' \quad \text{if} \quad 2y'' < 2x'' \tag{33b}$$

where $2x''$ and y'' are given by

$$2x'' = (P_t - d_r) - (P_t - d_r)t_f N_f \tag{34a}$$

$$y'' = [(P_t/2)^2 + (P_l)^2]^{0.5} - d_r - (P_t - d_r)t_f N_f \tag{34b}$$

Minimum Free Flow Area for Pressure Drop

For the determination of entrance and exit pressure losses, the area contraction and expansion ratio σ' is needed at the leading and trailing fin edges (Fig. 19). It is given by [14,20]:

$$\sigma' = \frac{L_3 L_1 - L_3 t_f N_f L_1}{L_3 L_1} \tag{35}$$

3.3 Compact Plate-Fin Exchangers

The following geometrical properties on each side are needed for the heat-transfer and pressure-drop analysis of plate-fin heat exchanger (PFHE):

1. The primary and secondary surface area (if any) A_p and A_s, respectively
2. Minimum free flow area A_o
3. Frontal area A_{fr}
4. Hydraulic diameter D_h and
5. Flow length L
6. Fin dimensions—thickness and length (height)

The information not specified directly is computed based on the specified surface geometries and core dimensions. Consider a PFHE as shown in Fig. 20 in which L_1 and L_2 are the flow lengths, N_p and $N_p + 1$ are the number of flow passages on sides 1 and 2, respectively, and V is the total core volume. The following formulas define some of the geometrical properties on any one side of the PFHE. These geometrical relations are derived in Refs. 17, 23, and 24.

The volume between plates on each side is given by

$$V_{p,1} = L_1 L_2 (b_1 N_p) \qquad V_{p,2} = L_1 L_2 b_2 (N_p + 1) \tag{36}$$

Heat transfer area on each side is given by

$$A_1 = \beta_1 V_{p,1} \qquad A_2 = \beta_2 V_{p,2} \tag{37}$$

where β_1 and β_2 are the surface area density on each side per unit volume between plates.

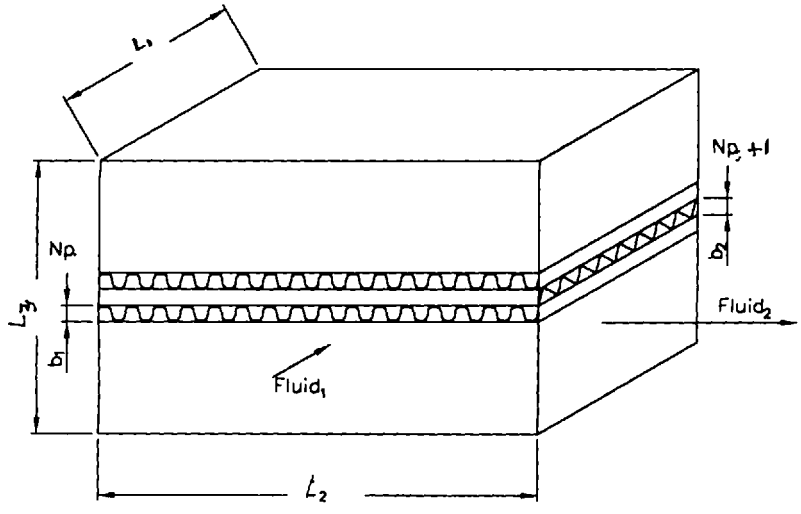


Figure 20 Crossflow plate-fin heat exchanger.

The ratio of minimum free flow area to frontal area (σ) on side 1 is given by

$$\sigma_1 = \frac{A_{0,1}}{A_{fr,1}} = \frac{A_{0,1}L_1}{A_{fr,1}L_1} = \frac{A_1 D_{h,1}/4}{V} = \frac{V_{p,1}\beta_1 D_{h,1}/4}{V} \tag{38a}$$

$$= \frac{b_1 N_p \beta_1 D_{h,1}/4}{b_1 N_p + b_2(N_p + 1) + 2a(N_p + 1)} \approx \frac{b_1\beta_1 D_{h,1}/4}{b_1 + b_2 + 2a} \tag{38b}$$

$$\sigma_2 = \frac{b_2(N_p + 1)\beta_2 D_{h,2}/4}{b_1 N_p + b_2(N_p + 1) + 2a(N_p + 1)} \approx \frac{b_2\beta_2 D_{h,2}/4}{b_1 + b_2 + 2a} \tag{39}$$

where a is the thickness of parting plates. The ratio is given similarly for side 2. Here, the last approximate equality is for the case when $N_p \gg 1$ or the numbers of passages on the two sides are the same.

The heat-transfer surface area on one side divided by the total volume V of the exchanger, designated as α_1, is

$$\alpha_1 = \frac{A_1}{V} = \frac{4\sigma_1}{D_{h,1}} = \frac{b_1\beta_1}{b_1 + b_2 + 2a} \tag{40}$$

Similarly, α_2 is given by

$$\alpha_2 = \frac{A_2}{V} = \frac{4\sigma_2}{D_{h,2}} = \frac{b_2\beta_2}{b_1 + b_2 + 2a} \tag{41}$$

4 FACTORS INFLUENCING TUBE-FIN HEAT EXCHANGER PERFORMANCE

Important factors that influence the heat-transfer performance of tube-fin heat exchangers include the following:

1. Tube layout (staggered vs. in-line arrangement)
2. Equilateral layout versus equivelocity layout
3. Number of rows
4. Tube pitch
5. Finned tube variables (fin height, spacing, thickness)
6. Fin tubes with surface modifications
7. Side leakage
8. Boundary-layer disturbances and characteristic flow length
9. Contact resistance in finned tube heat exchangers
10. Induced draft versus forced draft

Johnson [5] and Rabas and Taborek [7] discuss the effect of various tube-fin parameters on thermohydraulic performance.

4.1 Tube Layout

The two basic arrangements of the tubes in a tube bank are (1) staggered arrangement with equilateral triangular pitch, and (2) in-line arrangement. The extent of transverse flow in the inline layout is small in comparison to the staggered arrangement. The most commonly used is the staggered layout. There are very few applications of low-finned tubes with the in-line arrangement. It may be used when air-side fouling problems are encountered. For identical operating conditions, the in-line arrangement has low heat transfer, of the order of 70%, and pressure drop is also of this order.

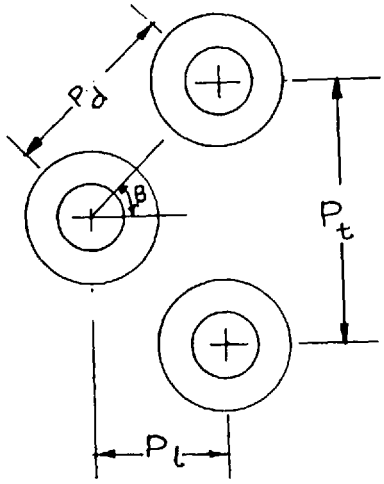


Figure 21 Equivelocity layout of a heat exchanger [25]. A_1 is transverse area available for flow; A_2 is diagonal area available for flow.

4.2 Equilateral Layout versus Equivelocity Layout [25]

In the conventional equilateral staggered layout, the area available for air flow in the transverse direction is half of that available in the diagonal direction; therefore, energy is lost in accelerating and decelerating the air stream as it flows through the bank. In the equivelocity layout (shown in Fig. 21), these two areas are made equal by adjusting the transverse (P_t) and longitudinal (P_l) pitches, thus minimizing these losses. For the tube bank examined in Ref. 25, the transverse pitch increases from 2.5 to 3.625 in (63.5 to 92.1 mm), while the longitudinal pitch decreases from 2.165 to 1.6 in (55.0 to 40.60 mm). The layout angle for the equilateral case is 30°, and it becomes around 50° for high-finned tubes in the equivelocity arrangement (the exact value of this angle depends on the specific fin geometry).

The thermal hydraulic performance of the equivelocity layout (Fig. 22) has been compared

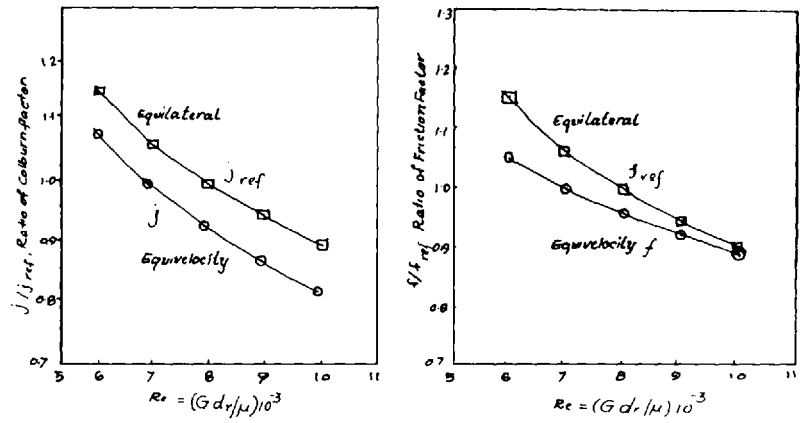


Figure 22 Performance of an equivelocity unit [25].

with that of an equilateral bank of high-finned tubes typical of air-cooler heat exchanger (ACHE) design with the following results [25]:

At the same Reynolds number, the equivelocity layout shows, on the average, a 7% lower j factor and a 4% lower Fanning friction factor than the equilateral factor.

At the same face velocity, the equivelocity layout shows average reductions of 19% in pressure drop per row over the equilateral layout.

In each of the layouts, the j and f factors for a three-row bundle have essentially the same value (95–98%) of that for a five-row bundle, indicating that only three rows of tubes are necessary to obtain uniform surface characteristics for high finned tubes.

In general, for applications where horsepower is evaluated at a high premium and a reduced pressure drop is attractive, even at the expense of some loss of thermal performance, an expanded pitch layout type should be strongly considered.

4.3 Number of Tube Rows

The addition of tube rows in the crossflow direction is the common way of increasing heat-transfer area when the frontal area of the tube bank is fixed. Such an addition of tube rows increases the flow length for the air and may affect the fluid dynamics with a possible effect on heat transfer and pressure drop. Pressure drop through the tube bundle increases with the number of tube rows. The temperature drop through the tube bundle also increases with the number of tube rows, though the effect is very large with the first few tube rows and for a very large number of tube rows the effect is small. Temperature drop through a multirow tube bank is shown in Fig. 23 [26]. The row effect on heat transfer coefficient is discussed by Johnson [5]. A basic difference exists between the row effects for the in-line and the staggered arrangements. For an in-line arrangement, the heat-transfer coefficient decreases with an in-

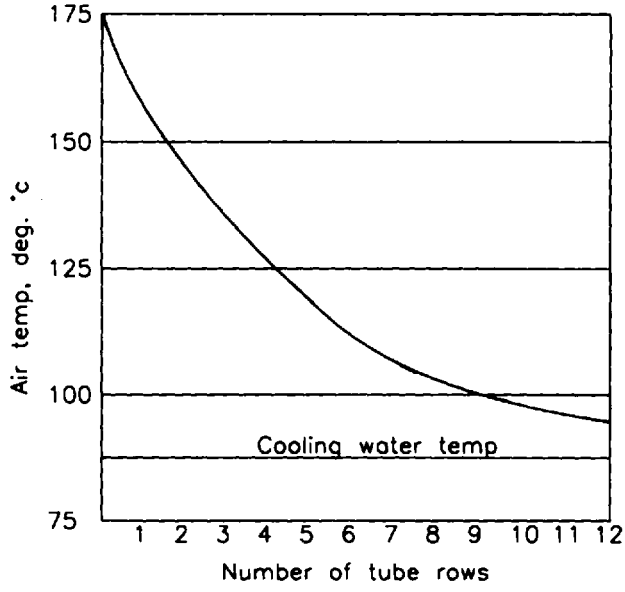


Figure 23 Temperature drop through a multi-tube row heat exchanger.

crease in the number of rows. Brauer [27] shows that the one-row tube bank heat-transfer coefficient is approximately 50–80% higher than the average for four rows, whereas for a staggered arrangement the four-row tube bank has approximately 30% higher heat-transfer coefficient (average) than a one-row tube bank.

4.4 Tube Pitch

Tube pitch is commonly used in heat-exchanger design to affect compactness of the core and flow conditions. The hydraulic diameter increases with the pitch. Based on comparable air velocities, the pitch has no effect on the heat-transfer coefficient. However, increasing the pitch strongly affects the pressure drop, as it decreases the pressure drop through the bundle [5].

4.5 Fin-Tube Variables

The fin-tube variables that affect the thermal performance include fin height, fin spacing, and thickness and thermal conductivity of the fin material. Surface area of the tube bank can be increased by employing fin tubes with high (longer) fins and denser spacing. However, increasing the fin height will decrease the fin effectiveness, and may lower heat transfer compared with the short fins. Denser fins may lower the heat transfer because of laminarization of the flow conditions between the fins [5]. Fin efficiency increases with a reduction in fin height and an increase in fin thickness. Thermal conductivity is usually not a problem in selecting the material of a primary surface, but it is important in extended surfaces because of the relatively long and narrow heat flow path, which affects their heat-transfer performance [6].

Fin Height and Fin Pitch

The fin height and fin pitch that can be used effectively are fundamentally related to the boundary-layer thickness [6]. Wen-Jei Yang [6] states the rule of thumb: (1) For large thermal boundary layer thickness, the heat-transfer coefficient, h, is low and thus high fins are employed; (2) low fins are employed in the case of a thin boundary layer where h is high; and (3) if the fin spacing is too small, the main stream cannot penetrate the spaces between the fins, resulting in no increase in thermal boundary area and an excessive pressure drop.

4.6 Finned Tubes with Surface Modifications

The term "surface modification" refers to fin tubes that have extended surfaces that are mechanically deformed to various shapes by crimping, corrugating, cutting, slotting, or serrating the fins; for continuous plate fins, surface interruptions constitute surface modification [5]. Any surface modification will increase the heat transfer and pressure drop as compared with the identical smooth fin. Common surface modifications for circular fins are discussed further in Chapter 8.

4.7 Side Leakage

The heat-transfer and pressure-drop performance of a tube bank is affected by the leakage flow between the outermost tube and the side walls. This is equivalent to the bundle-to-shell bypass stream (C-stream) leakage in a shell and tube exchanger. The effect of bypass flow can be minimized by attaching side seals to the exchanger in every even row as shown in Fig. 24a. Clearance between the core and the housing can be minimized by welding metal strips to the housing or attaching metal strips to the header as shown in Fig. 24b.

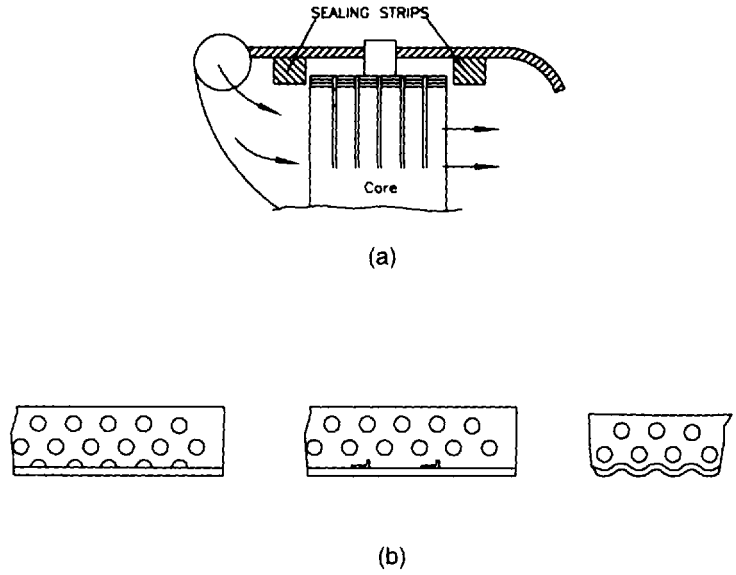


Figure 24 Sealing strips to arrest bypass flow: (a) between the core and the housing; and (b) between the tubes and side sheets.

4.8 Boundary-Layer Disturbances and Characteristic Flow Length

Periodic interruption of the boundary layer is achieved by breaking the total flow length into many characteristic lengths by means of offset strip fins, louvered fins, wavy fins, etc. [28]. The characteristic flow length, l is illustrated in Fig. 25. The characteristic flow length and the hydraulic diameter, D_h, are responsible for the numerical merits of a surface geometry. The representative length of finned heat exchangers as parameters to represent their performance suggests that it would be possible to enhance their performance by shortening the representative length of the fin and using finer segmentation than the regions of louvered or offset strip fins [29]. The application of the pin finned surface can be considered one of the best candidates.

4.9 Contact Resistance in Finned Tube Heat Exchangers

Continuous Finned Tube Exchanger

In the design of finned tube heat exchangers, the contribution of contact resistance at the interface between the tube and fin collar is not always negligible compared with the total heat transfer resistance (Fig. 26). This is particularly true for mechanically bonded tube-fin exchangers used in low-pressure applications such as air-conditioning industries and air coolers for supercharged engine intake air. In the heat exchanger assembly process, the initial interference, the microhardness of the softer material at the interface, contact area, and contact pressure are parameters that determine the contact resistance [30]. Selection of the proper bullet size can optimize the degree of contact at the interface. During the last three decades, many researchers have developed experimental methods to measure thermal contact resistance accurately. An experimental method to measure contact resistance in a vacuum environment is described by Nho et al. [30]. In a typical experimental setup, they found that the contact resistance at the tube and fin interface was 17.6–31.5% of the overall resistance in a vacuum environment.

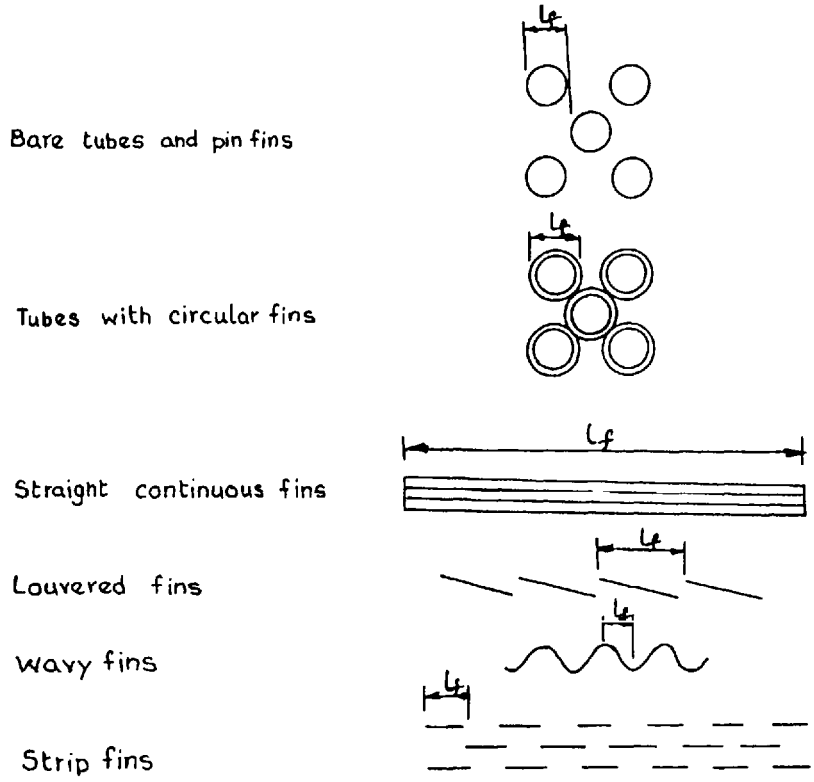


Figure 25 Characteristic flow length between major boundary layer disturbance for various heat exchanger surfaces. [From Ref. 28.]

Tension-Wound Fins on Circular Tubes

For round-fin tubes with aluminum fins wrapped on steel tubes under tension, the contact resistance increases quickly with the operating temperature so that their application is limited to temperatures of 100°C or less [31]. Otherwise, the tension would be reduced, leading to fin loosening, due to the higher thermal expansion of aluminum.

Integral Finned Tube

With an integral finned tube, there is no concern at the fin bond about heat-transfer resistance and the integrity of tubing, regardless of temperature and pressure levels. However, only certain fin geometries can be obtained with an extrusion process.

4.10 Induced Draft Versus Forced Draft

The heat transfer and pressure drop depend on the method used to generate the flow on the tube bank, namely, induced draft or forced draft. When a fluid enters the tube bank, the level of turbulence can change with penetration into the bundle. The tube bundle heat-transfer coefficient and pressure-drop performance vary for each additional row for a shallow exchanger, and become independent of the number of rows only for the deep bundles with a very large number of tube rows [7]. Common practice is to apply a row correction multiplier to the deep bundle correlations (ideal bundle) to account for these variations. Recommendations by Rabas et al. [7] for the mode of flow are discussed next.

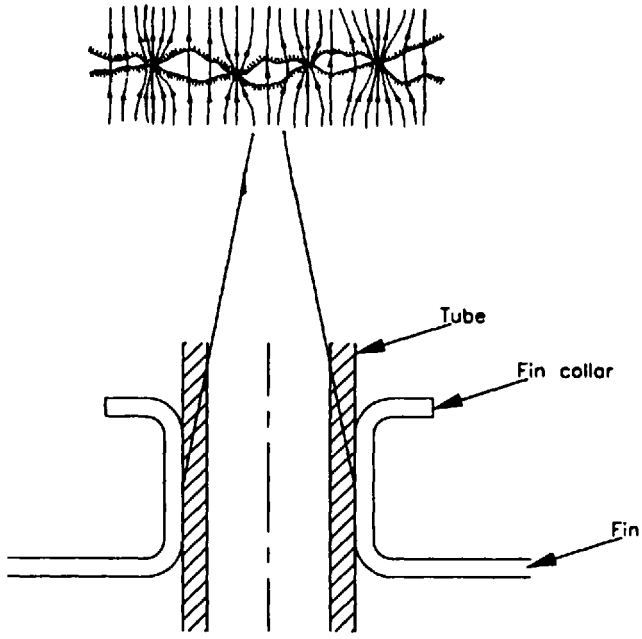


Figure 26 Metal-to-metal contact between tube and fin.

Induced Draft

For induced draft, the recommended approach is to use the heat-transfer row correction for plain tube banks. Table 1 presents the plain tube bundle row corrections from two different sources, Giedt [32] and ESDU [33] with values for more than five-tube rows. The bundle pressure drop variation with row number is smaller than the heat-transfer coefficient variation and hence the row effect is usually ignored.

Forced Draft

A conservative approach suggested is to neglect the row correction for the forced draft mode of operation for low-finned tube banks [7].

5 THERMOHYDRAULIC FUNDAMENTALS OF FINNED TUBE HEAT EXCHANGERS

It is a common practice to use the Colburn j factor to characterize the heat-transfer performance and the Fanning friction factor f to characterize the pressure drop of the tube banks as functions

Table 1 Tube Bundle Heat Transfer Row Corrections

	Number of rows							
	1	2	3	4	5	6	7	8
Giedt	0.65	0.71	0.80	0.85	0.90	0.94	0.96	0.98
ESDU	0.65	0.77	0.84	0.90	0.94	0.97	0.99	1.00

Source: Ref. 7.

of Reynolds number. This section provides empirical correlations for j and f factors. With these correlations, the performance of geometrically similar heat exchangers can be predicted, within the parameter range of the correlations.

5.1 Heat Transfer and Friction Factor Correlations for Crossflow over Staggered Finned Tube Banks

During the last 50 years many investigations have been carried out to determine the heat transfer and pressure drop over the tube banks. One of the first correlations was established by Grimson [34] for bare tube banks. A standard reference for the heat-transfer and fraction data of plate-fin heat exchanger surfaces is the book by Kays and London [17]. This book presents j and f versus Reynolds number plots for tube banks, tube-fin heat exchangers, and 52 different plate-fin surface geometries. Some of these data were published in *Transactions of the ASME*. Shah and Bhatti [35] summarize important theoretical solutions and correlations for simple geometries that are common in compact heat exchangers. Most of the experimental data have been obtained with air as the test fluid. The j factor and fanning f factor are defined rather consistently in the literature by the following equations.

$$j = \frac{h(\mathrm{Pr})^{2/3}}{Gc_p} \tag{42a}$$

$$= \frac{h}{Gc_p}\left(\frac{\mu c_p}{k}\right)^{2/3} \tag{42b}$$

$$h = jGc_p\left(\frac{\mu c_p}{k}\right)^{-2/3} \quad \text{or} \quad h = \frac{\mathrm{Nu}k}{D_h} \tag{43}$$

$$\Delta p = 4f\frac{L}{D_h}\left(\frac{G_{max}^2}{2g_c\rho}\right) \tag{44}$$

where G_{max} is given by

$$G_{max} = \rho U_f\left(\frac{A_{fr}}{A_o}\right) \tag{45}$$

and is based on the minimum free flow area within the tube bundle. This minimum free flow area includes the gaps between the outermost tubes and the side walls of the tube bundle. In Eq. 44, contraction and expansion losses and momentum losses are neglected; only flow friction effect is taken into account.

The Reynolds number is defined as

$$\mathrm{Re} = \frac{Gd_r}{\mu} \quad \text{or} \quad \mathrm{Re} = \frac{Gd_o}{\mu} \quad \text{or} \quad \mathrm{Re} = \frac{GD_h}{\mu} \tag{46}$$

where d_r is the fin root diameter or the tube outside diameter, which depends on the tube manufacturing techniques, and D_h is the hydraulic diameter. The j factor is related to Stanton number and Prandtl number by

$$j = \mathrm{St}(\mathrm{Pr})^{2/3} \tag{47}$$

where the Stanton number is given by

$$\mathrm{St} = \frac{\mathrm{Nu}}{\mathrm{Re(Pr)}} \tag{48}$$

From Eqs. 47 and 48, the expression for j is given by

$$j = \frac{\mathrm{Nu}}{\mathrm{Re(Pr)}^{1/3}} \tag{49}$$

5.2 The *j* and *f* Factors

Bare Tube Bank

Experimental heat-transfer and fluid-friction data for six staggered circular tube patterns and one in-line arrangement are given in Ref. 36. The results of Ref. 36 have been presented in Kays and London [17].

The Giedt [32] correlation states that the thermal performance of a bare tube bank is given by

$$j = \frac{0.376}{\mathrm{Re}^{0.4}} \tag{50}$$

In-Line Tube Bank. For a 10-row-deep in-line tube bank, the correlation for j is given by [37]:

$$j = \frac{0.33}{\mathrm{Re}^{0.4}} \tag{51}$$

This correlation is valid for tube diameter from $\frac{1}{4}$ in to 2 in, and Reynolds number range 100–80,000.

Circular Tube-Fin Arrangement

The basic geometry is shown in Fig. 27.

Experimental heat-transfer and fluid-friction data for three circular finned tube surfaces are given in London et al. [38]. The results of Ref. 38 have been presented in Kays and London [17].

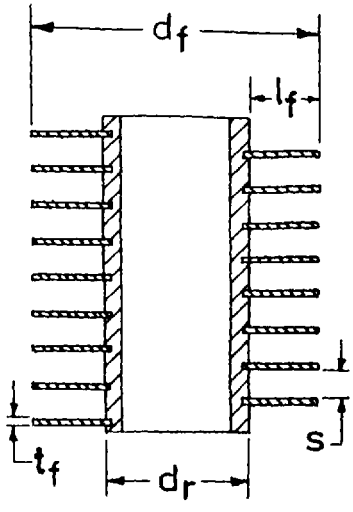


Figure 27 Tube-fin details.

Briggs and Young Correlations [*39*]. For low-fin tube banks, the correlation based on experimental heat-transfer data is

$$\mathrm{Nu} = 0.1507\mathrm{Re}_d^{0.667}\mathrm{Pr}^{1/3}\left(\frac{s}{l_f}\right)^{0.164}\left(\frac{s}{t_f}\right)^{0.075} \tag{52}$$

where $[s = (l - N_t t_f)/N_t]$ with a standard deviation of 3.1%. This is applicable for a circular finned tube with low fin height and high fin density, Re = 1000–20,000, $N_r \geq 6$, and equilateral triangular pitch.

For high-fin tube banks the correlation based on experimental heat-transfer data is

$$\mathrm{Nu} = 0.1378\mathrm{Re}_d^{0.718}\mathrm{Pr}^{1/3}\left(\frac{s}{l_f}\right)^{0.296} \tag{53}$$

with a standard deviation of 5.1%.

For all tube banks, the correlation based on regression analysis is

$$\mathrm{Nu} = 0.134\mathrm{Re}_d^{0.681}\mathrm{Pr}^{1/3}\left(\frac{s}{l_f}\right)^{0.200}\left(\frac{s}{t_f}\right)^{0.1134} \tag{54}$$

$$j = 0.134\mathrm{Re}_d^{-0.319}\left(\frac{s}{l_f}\right)^{0.200}\left(\frac{s}{t_f}\right)^{0.1134} \tag{55}$$

with a standard deviation of 5.1%.

Robinson and Briggs Correlations [*40*].

For Equilateral Triangular Pitch with High Finned Tubes.

$$f = 9.465\mathrm{Re}_d^{-0.316}\left(\frac{P_t}{d_o}\right)^{-0.927} \tag{56}$$

with a standard deviation of 7.8%. This is applicable for the following parameter definitions:

Re = 2000–50,000

d_f = 1.562–2.750

P_t = 1.687–4.50

For Isosceles Triangular Layout.

$$f = 9.465\mathrm{Re}_d^{-0.316}\left(\frac{P_t}{d_r}\right)^{-0.927}\left(\frac{P_t}{P_l}\right)^{0.515} \tag{57}$$

This is applicable for

d_o(mm) = 18.6–40.9

h/d_o = 0.35–0.56

h/p = 4.5–5.3

σ = 13.3–17.4

P_t/d = 1.8–4.6

P_l/d = 1.8–4.6

$N_r \geq 6$

Rabas, Eckels, and Sabatino Correlation [*41*]. For tube banks arranged on an equilateral triangular pitch with low-finned tubes,

$$j = 0.292\ Re_d^{-m}\left(\frac{s}{d_f}\right)^{1.116}\left(\frac{s}{l_f}\right)^{0.257}\left(\frac{t_f}{s}\right)^{0.666}$$

$$x\left(\frac{d_f}{d_r}\right)^{0.473}\left(\frac{d_f}{t_f}\right)^{0.7717}\alpha_h\alpha_n \tag{58a}$$

$$m = 0.415 - 0.0346\ln\left(\frac{d_f}{s}\right) \tag{58b}$$

$$f = 3.805Re_d^{-0.234}\left(\frac{s}{d_f}\right)^{0.251}\left(\frac{l_f}{s}\right)^{0.759}$$

$$x\left(\frac{d_r}{d_f}\right)^{0.729}\left(\frac{d_r}{P_t}\right)^{0.709}\left(\frac{P_l}{P_l}\right)^{0.379} \tag{59}$$

where α_h and α_n are a temperature-dependent fluid properties correction factor and a row correction factor respectively. The row correction factor has been covered earlier. Rabas and Taborek [7] recommend the following correlations for α_h:

$$\alpha_h = \left(\frac{T_b + 273}{T_w + 273}\right)^{0.25} \tag{60a}$$

$$\alpha_h = \left(\frac{Pr(T_b)}{Pr(T_w)}\right)^{0.26} \tag{60b}$$

Equation 60a is from Weierman [42], and Eq. 60b is from ESDU [33]. However, the Prandtl number format is recommended by Rabas and Taborek [7] for liquids and there is no fluid property correction term for the friction factor f. These are applicable for $l_f < 6.35$ mm, $1000 < \mathrm{Re} < 25{,}000$, 4.76 mm $\le d \le$ 31.75 mm, $246 \le N_f \le 1181$ fins/m, 15.08 mm $\le P_t \le 111$ mm, 10.32 mm $\le P_l \le$ 96.11 mm, $P_l \le P_t$, $d_f/s < 40$, and $N_r > 6$.

ESDU Correlation [33].

$$j = 0.183\mathrm{Re}_d^{-0.3}\mathrm{Pr}^{0.027}\left(\frac{s}{l_f}\right)^{0.36}\left(\frac{l_f}{d_f}\right)^{0.11}\left(\frac{P_t}{d_f}\right)^{0.06}\alpha_h\alpha_n \tag{61a}$$

$$\mathrm{f} = 4.71\mathrm{R}^{(-0.286)}(\mathrm{X_t/d_r} - 1)^{(-0.361)}(\mathrm{l_f/s})^{0.51}\left(\frac{\mathrm{X_t} - \mathrm{d_r}}{\mathrm{X_l} - \mathrm{d_r}}\right)^{0.536} \tag{61b}$$

This is applicable for $1000 < \mathrm{Re} < 80{,}000$ or 100,000 and $N_t > 10$.

Ganguly et al. [43] Correlation.

$$j = 0.255\mathrm{Re}_d^{-0.3}\left(\frac{d_f}{s}\right)^{-0.3} \tag{62}$$

$$f = F_s f_p \tag{63a}$$

where

$$F_s = 2.5 + \frac{3}{\pi}\tan^{-1}[0.5(A/A_p - 5)] \tag{63b}$$

$$f_p = 0.25\beta(\mathrm{Re}_d^{-0.25}) \tag{63c}$$

$$\beta = 2.5 + 1.2(X_t - 0.85)^{-1.06} + 0.4\left(\frac{X_l}{X_t} - 1\right)^3 - 0.01\left(\frac{X_t}{X_l} - 1\right)^3 \tag{63d}$$

For both j and f factors, 95% of the data correlated within 15% and 100% of the data correlated within 20%. This is applicable for $l_f \leq 6.35$ mm, $800 \leq \mathrm{Re} \leq 800{,}000$, $20 \leq \theta \leq 40$, $X_t \leq 4$, and $N_r \geq 4$.

Elmahdy and Biggs Correlation [44]. For a multirow staggered circular or continuous fin tube arrangement:

$$j = C_1 \mathrm{Re}_h^{C_2} \tag{64a}$$

where

$$C_1 = 0.159\left(\frac{t_f}{l_f}\right)^{0.141}\left(\frac{D_h}{t_f}\right)^{0.065} \tag{64b}$$

$$C_2 = -0.323\left(\frac{t_f}{l_f}\right)^{0.049}\left(\frac{s}{t_f}\right)^{0.077} \tag{64c}$$

This correlation is also valid for circular fin-tube arrangement. The experimentally determined j factor is 3–5% lower than that predicted analytically.

This correlation is applicable for:

$\mathrm{Re} = 200$–2000
$D_h/t_f = 3.00$–33.0
$t_f/l_f = 0.01$–0.45
$d_f/P_l = 0.87$–1.27
$s/t_f = 2.00$–25.0
$d_f/P_t = 0.76$–1.40
$d/d_f = 0.37$–0.85
$\sigma = 0.35$–0.62

Continuous Fin on Circular Tube

Gray and Webb Correlation [45].

Four-Row Array.

$$j_4 = 0.14\mathrm{Re}_d^{-0.328}\left(\frac{P_t}{P_l}\right)^{-0.502}\left(\frac{s}{d_o}\right)^{0.0312} \tag{65}$$

For this form, 89% of data were correlated within ±10%.

Up to Three Rows.

$$\frac{j_N}{j_4} = 0.991\left[2.24\mathrm{Re}_d^{-0.092}\left(\frac{N_r}{4}\right)^{-0.031}\right]^{0.607(4-N_r)} \tag{66}$$

This is used for $N_r = 1$–3 (for $N_r > 4$ the row effect is negligible). The standard deviation is −4% to +8%.

Pressure Drop Correlation. Gray and Webb correlation is based on a superposition model that was initially proposed by Rich [46]. The basic model is written as

$$\Delta p = \Delta p_f + \Delta p_t \tag{67}$$

where Δp_t is the pressure-drop component due to the drag force on the tubes, and Δp_f is the pressure-drop component due to the friction factor on the fins. Accordingly, the expressions for Δp_t and Δp_f are given by

$$\Delta p_t = f_t \frac{A_f}{A_c} \frac{G^2}{2g_c\rho} \tag{68a}$$

$$\Delta P_t = f_t \frac{A_t}{A_{ci}} \frac{G^2}{2g_c\rho} \tag{68b}$$

$$f = f_f \frac{A_f}{A} + f_t \left(1 - \frac{A_f}{A}\right)\left(1 - \frac{t}{p_f}\right) \tag{69a}$$

$$f_f = 0.508 Re_d^{-0.521} \left(\frac{P_t}{d_o}\right)^{0.318} \tag{69b}$$

The mass velocity G used in Eqs. (68a) and (68b) is evaluated as the same G that exists in the finned-tube exchanger. Several correlations are available for the friction factor of flow normal to tube banks [32,36,47]. Parameters are:

$N_r = 1 - 8$ or more

$\mathrm{Re} = 500–24{,}700$

$P_t/d = 1.97–2.55$

$P_l/d = 1.70–2.58$

$s/d = 0.08–0.64$

$\mathrm{Re} = Gd/\mu$

McQuistion Correlation [48].

Continuous-Fin Tube Heat Exchanger with Four Rows.

$$j_4 = 0.0014 + 0.2618 \mathrm{Re}_d^{-0.4} \left(\frac{A}{A_t}\right)^{-0.15} \tag{70}$$

where A/A_t is the ratio of the total surface area to the area of the bone tube. Here, 90% of data were correlated within ±10%.

Less Than Four Rows.

$$\frac{j_N}{j_4} = \frac{1.0 - 1280 N_r \mathrm{Re}_L^{-1.2}}{1.0 - 5120 \mathrm{Re}_L^{-1.2}} \tag{71}$$

for $N_r = 1–3$ with a standard deviation of −9% to +18%.

$$f = 4.904 \times 10^{-3} + 1.382\alpha^2 \tag{72a}$$

$$\alpha = \mathrm{Re}_d^{-0.25} \left(\frac{R}{R^*}\right)^{0.25} \left[\frac{(X_d - 2R)N_f}{4(1 - n_f t_f)}\right]^{-0.4} \left(\frac{P_t}{2R^*} - 1\right)^{-0.5} \tag{72b}$$

$$\left(\frac{R^*}{R}\right) = \frac{A/A_t}{(P_t - 2R)n_f + 1} \tag{72c}$$

$$\frac{A}{A_t} = \frac{4}{\pi} \frac{P_l}{D_h} \frac{P_t}{d_o} \sigma \tag{72d}$$

$R = d_o/2$

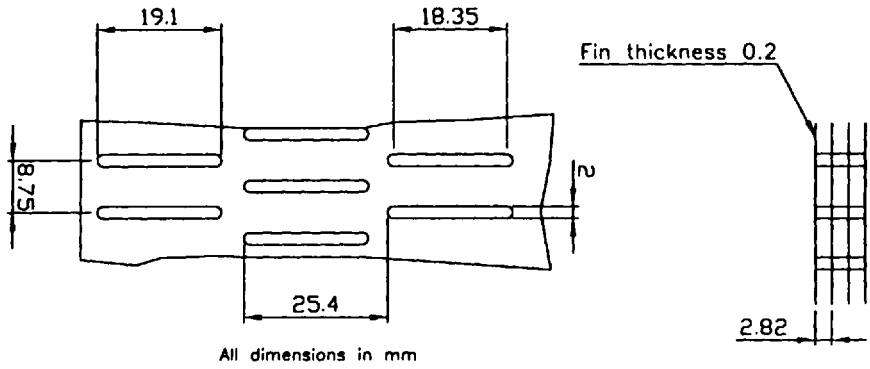


Figure 28 Geometrical details of a flat tube-fin radiator to calculate j and f factors as per Eq. (73). [Adopted from Ref. (50).]

Parameters are:

$$Pe,\ P_t = 1 - 2 \text{ in}$$

$$\alpha = 0.08\text{–}0.24$$

$$d_o = \frac{3}{8} - \frac{5}{8} \text{ in}$$

Tube spacing = 1–2 in

$$N_f = 4\text{–}14 \text{ fin/in}$$

$$t_f = 0.006\text{–}0.010 \text{ in}$$

Continuous Fin on Flat Tube Array

Performance figures for three geometries are given in Kays and London [17]. New data are presented for two new types of rippled fin by Maltson et al. [49]. For these types of layouts, fin length for calculating fin efficiency is half the spanwise length of fin between tubes. Kroger [50] presented performance characteristics for a six rows deep (3×2) core geometry given in Fig. 28, whose j and f factors are given by

$$j = \frac{0.174}{\mathrm{Re}_h^{0.387}}, \qquad f = \frac{0.3778}{\mathrm{Re}_h^{0.3565}} \tag{73}$$

These equations were also found to correlate the data for having eight rows deep (4×2).

5 CORRELATIONS FOR *J* AND *F* OF PLATE-FIN HEAT EXCHANGERS

5.1 Offset Strip Fin Heat Exchanger

Wieting correlations [51] consist of power-law curve fits of the j and f values for 22 heat exchanger surface geometries over two Reynolds number ranges: $\mathrm{Re}_h \le 1000$, which is primarily laminar, and $\mathrm{Re}_h \ge 2000$, which is primarily turbulent.

For $\mathrm{Re}_h \le 1000$,

$$j = 0.483(l_f/D_h)^{-0.162}\xi^{-0.184}\mathrm{Re}_h^{-0.536} \tag{74}$$

$$f = 7.661(l_f/D_h)^{-0.384}\xi^{-0.092}\mathrm{Re}_h^{-0.712} \tag{75}$$

For $\mathrm{Re}_h \geq 2000$,

$$j = 0.242(l_f/D_h)^{-0.322}(t_f/D_h)^{0.089}\mathrm{Re}_h^{-0.368} \tag{76}$$

$$f = 1.136(l_f/D_h)^{-0.781}(t_f/D_h)^{0.534}\mathrm{Re}_h^{-0.198} \tag{77}$$

where Re_h is the Reynolds number based on hydraulic diameter D_h given by

$$D_h = \frac{2sh_f}{s + h_f} \tag{78}$$

and α is the aspect ratio, s/h_f (Fig. 29).

Joshi and Webb [16] have developed a more sophisticated theoretical model to predict the characteristics of j and f versus Reynolds number for the offset strip fin. This model preferably includes all geometrical factors of the array (s/d, t_f/l_f, t_f/s) and heat transfer to the base surface area to which the fins are attached.

Manglik and Bergles [52] reviewed the available j and f data and developed improved correlations for j and f, with a single predictive equation representing the data continuously from laminar to turbulent flow. Their correlations for j and f are as follows:

$$j = 0.6522\ \mathrm{Re}_h^{-0.5403}\,\xi^{-0.1541}\,\delta^{0.1499}\,\eta^{-0.0678} \{1 + 5.269 \times 10^{-5}\ \mathrm{Re}_h^{1.340}\,\xi^{0.504}\,\delta^{0.456}\,\eta^{-1.055}\}^{0.1} \tag{79}$$

and

$$f = 9.6243\ \mathrm{Re}_h^{-0.7422}\,\xi^{-0.1856}\,\delta^{0.3053}\,\eta^{0.2659} \{1 + 7.6669 \times 10^{-8}\ \mathrm{Re}_h^{4.429}\,\xi^{0.92}\,\delta^{3.767}\,\eta^{0.236}\}^{0.1} \tag{80}$$

where ξ = aspect ratio = s/h_f; $\delta = t_f/l_f$; $\eta = t_f/s$ and Re_h is based on the hydraulic diameter D_h given by the following equation:

$$D_h = \frac{4sh_f l_f}{2(sl_f + h_f l_f + t_f h_f) + t_f s} \tag{81}$$

These equations correlate the experimental data for the 18 cores within ±20%.

5.2 Louvered Fin

Based on tests of 32 louvered-fin geometries, Davenport [19] developed multiple regression correlations for j and f versus Re as follows:

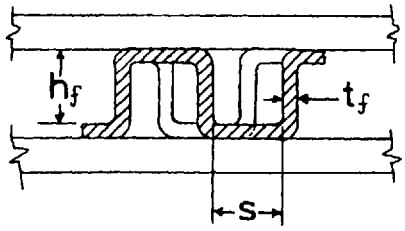


Figure 29 Details of offset strip fin. (From Ref. 16.)

$$j = 0.249\mathrm{Re}_{lp}^{-0.42} l_h^{0.33} H_l^{0.26} \left(\frac{l_l}{H_l}\right)^{1.1} \qquad 300 < \mathrm{Re} < 4000 \tag{82}$$

$$f = 5.47\mathrm{Re}_{lp}^{-0.72} l_h^{0.37} H_l^{0.23} l_p^{0.2} \left(\frac{l_l}{H_l}\right)^{0.89} \qquad 70 < \mathrm{Re} < 1000 \tag{83a}$$

$$f = 0.494\mathrm{Re}_{lp}^{-0.39} H_l^{0.46} \left(\frac{l_h}{H_l}\right)^{0.33} \left(\frac{l_l}{H_l}\right)^{1.1} \qquad 1000 < \mathrm{Re} < 4000 \tag{83b}$$

where Re_{lp} is the Reynolds number based on louver pitch, l_h is louver height, l_l is louver length, l_p is the louver pitch, and H is the fin height. Here 95% of the data could be correlated within ±6% for heat transfer, and within ±10% for the friction factor. The required dimensions are millimeters. Figure 30 defines the terms in the equations. The characteristic dimension in the Reynolds number is louver pitch, l_p, and not D_h.

5.3 Pin Fin Heat Exchangers

For the heat-transfer characteristics of pin-finned surfaces, see Kanzaka et al. [29], Kays [53], Norris et al. [54], and Bengt Sunden et al. [55], among others. The results of Ref. 53 were presented in Kays and London [17]. The works of Kays [53] and Norris [54] are limited to the heat-transfer characteristics of pin fins having their representative length comparable to those of louvered or offset fins currently used [29]. To materialize a heat exchanger that has thermal performance superior to those of offset or louvered fins requires a more finely segmented surface of less than 1 mm at maximum. Kanzaka et al. [29] studied the heat-transfer and fluid dynamic characteristics of pin finned surfaces of various profiles, namely, circular, square, and rectangular, and both in-line and staggered arrangements.

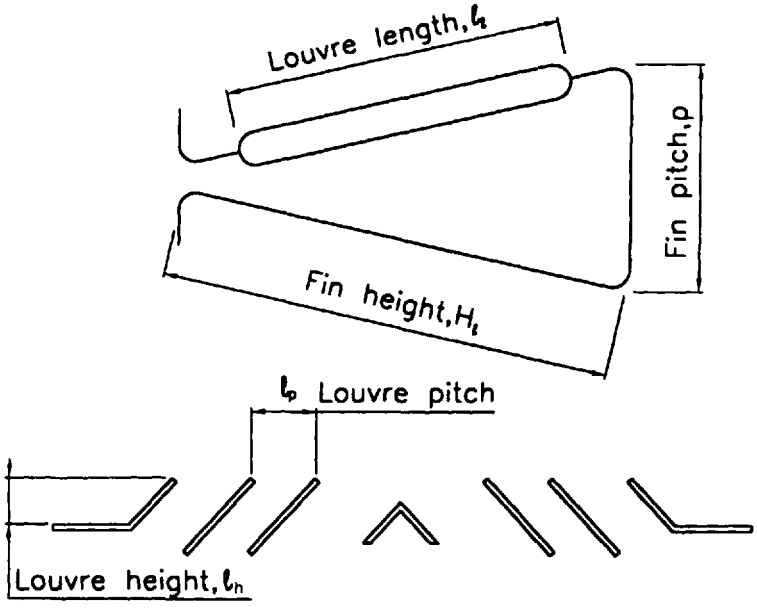


Figure 30 Definitions of geometrical parameters of a louvred fin. [From Ref. 19.]

Staggered Arrangements

For their test element, the expression for the Nusselt number is

$$\mathrm{Nu}_\phi = 0.662\mathrm{Re}_\phi^{0.5}\mathrm{Pr}^{1/3} \tag{84}$$

In-Line Arrangements

The expression for the Nusselt number is

$$\mathrm{Nu}_\phi = 0.440\mathrm{Re}_\phi^{0.5}\mathrm{Pr}^{1/3} \tag{85}$$

where ϕ is the characteristic length. The expressions for Nusselt number and ϕ are

$$\mathrm{Nu}_\phi = \frac{hd_\phi}{k} \qquad \mathrm{Re}_\phi = \frac{Gd_\phi}{\mu} \tag{86}$$

$$d_\phi = \frac{\pi d_p}{2} \qquad \text{for circular fins} \tag{87a}$$

$$d_\phi = \frac{a_p + b_p}{2} \qquad \text{for rectangular fins} \tag{87b}$$

where a_p and b_p are the rectangular pin fin dimensions (i.e., cross section is $a_p \times b_p$) and d_p is the circular fin diameter.

6 FIN EFFICIENCY

Fins are primarily used to increase the surface area and consequently to enhance the total heat-transfer rate. Both conduction through the fin cross section and convection from the surface area take place. Hence, the fin surface temperature is generally lower than the base (prime surface) temperature if the fin convects heat to the fluid. Due to this, the fin transfers less heat than if it had been at the base temperature. This is described by the fin temperature effectiveness or fin efficiency η_f. The fin temperature effectiveness is defined as the ratio of the actual heat transfer, q, through the fin to that which would be obtained, q_i, if the entire fin were at the base metal temperature:

$$\eta_f = \frac{q}{q_i} \tag{88}$$

The fin efficiency for plate-fin surfaces in heat exchanger design can be determined from Gardner [56], Kern and Kraus [57], Scott and Goldschmidt [58], Schmidt [59], Zabronsky [60], Lin and Sparrow [61], Shah [19,62], and others. Fin efficiency of a plain rectangular profile cross section is discussed in this section.

6.1 Fin Length for Some Plate-Fin Heat Exchanger Fin Configurations

The two most commonly used plate-fin geometries are rectangular and triangular passages, shown in Fig. 31. From a review of Fig. 31, the fin length l_f for a rectangular passage is

$$l_f = \frac{h_f - t_f}{2} \approx \frac{h_f}{2} \tag{89}$$

Note that no effect of the fin inclination is taken into account in Eq. 89 for the triangular fin. Numerous fin geometries and corresponding fin lengths for various flow passage configuration are presented by Shah [24].

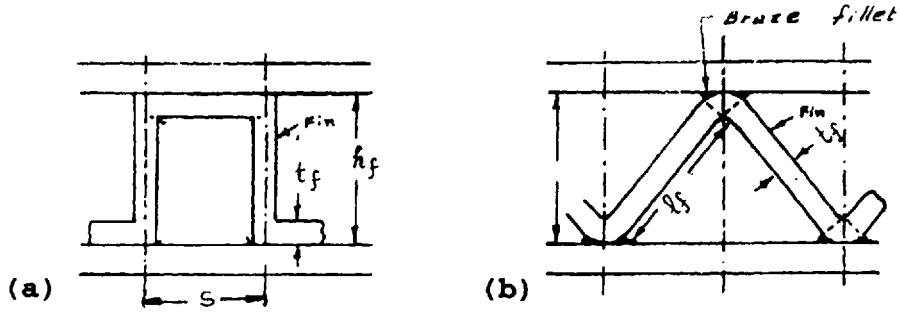


Figure 31 Fin length. (a) Rectangular passage; (b) triangular passage. [24]

6.2 Fin Efficiency

Circular Fin

Kern and Kraus [57] Formula for Rectangular-Profile Circular Fin. For circular fins (Fig. 32), the fin efficiency is given by

$$\eta_f = \frac{2r_o}{m(r_e^2 - r_o^2)} \left[\frac{I_1(mr_e)K_1(mr_o) - K_1(mr_e)I_1(mr_o)}{I_0(mr_o)K_1(mr_e) + I_1(mr_e)K_0(mr_o)} \right] \tag{90}$$

where $m = (2h/k_f t_f)^{0.5}$, I_n is the modified Bessel function of the first kind (nth order), K_n is the modified Bessel function of the second kind (nth order), k_f is the fin material thermal conductivity, r_e is the fin radius, r_o is the tube outer radius, and t_f is the fin thickness.

The fin efficiency expressed by Eq. 90 does not lend itself to comparison with the efficiencies of fins of other radial profiles but can be adjusted by expressing the efficiency in terms of the radius ratio r_o/r_e and a parameter ϕ:

$$\rho = \frac{r_o}{r_e} \tag{91}$$

$$\phi = (r_e - r_o)^{3/2} \left(\frac{2h}{k_f A_p} \right)^{0.5} \tag{92}$$

where A_p is the profile area of the fin:

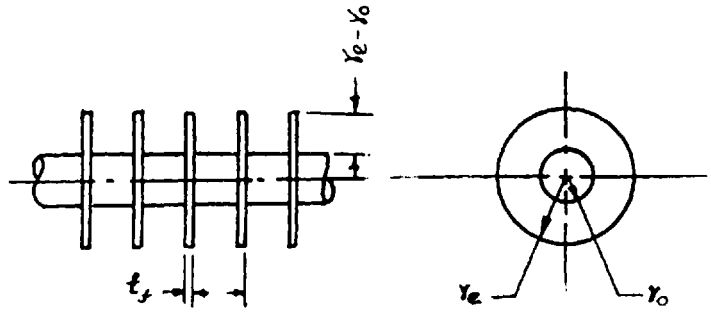


Figure 32 Circular fin details.

$$A_p = t_f(r_e - r_o) \tag{93}$$

Substituting the values of ρ and ϕ in Eq. 90, the resulting formula for fin efficiency is given by

$$\eta_f = \frac{2\rho}{\phi(1+\rho)} \left[\frac{I_1[\phi/(1-\rho)]K_1[\rho\phi/(1-\rho)] - K_1[\phi/(1-\rho)]I_1[\rho\phi/(1-\rho)]}{I_o[\rho\phi/(1-\rho)]K_1[\phi/(1-\rho)] + I_1[\phi/(1-\rho)]K_o[\rho\phi/(1-\rho)]} \right] \tag{94}$$

The efficiencies of radial fins with rectangular profile are plotted in Fig. 33 for values of $\rho = 0.8$ and $= 0.4$, using Eq. 94.

Scott and Goldschmidt. An excellent approximation of Eq. 94 has been provided by Scott and Goldschmidt [58] as follows:

$$\eta_f = x(ml_c)^{-y} \qquad \text{for } \varphi > 0.6 + 2.257(r^*)^{-0.445} \tag{95a}$$

$$\eta_f = (\tanh \varphi)/\varphi \qquad \text{for } \varphi \le 0.6 + 2.257(r^*)^{-0.445} \tag{95b}$$

where

$$x_1 = (r^*)^{-0.246} \tag{96}$$

$$\varphi = m\, l_e\, (r^*)^{\exp(0.13ml_e - 1.3863)} \tag{97}$$

$$y_1 = 0.9107 + 0.0893r^* \qquad \text{for } r^* \le 2 \tag{98a}$$

$$= 0.9706 + 0.17125\ln r^* \qquad \text{for } r^* > 2 \tag{98b}$$

$$r^* = r_e/r_o, \tag{99}$$

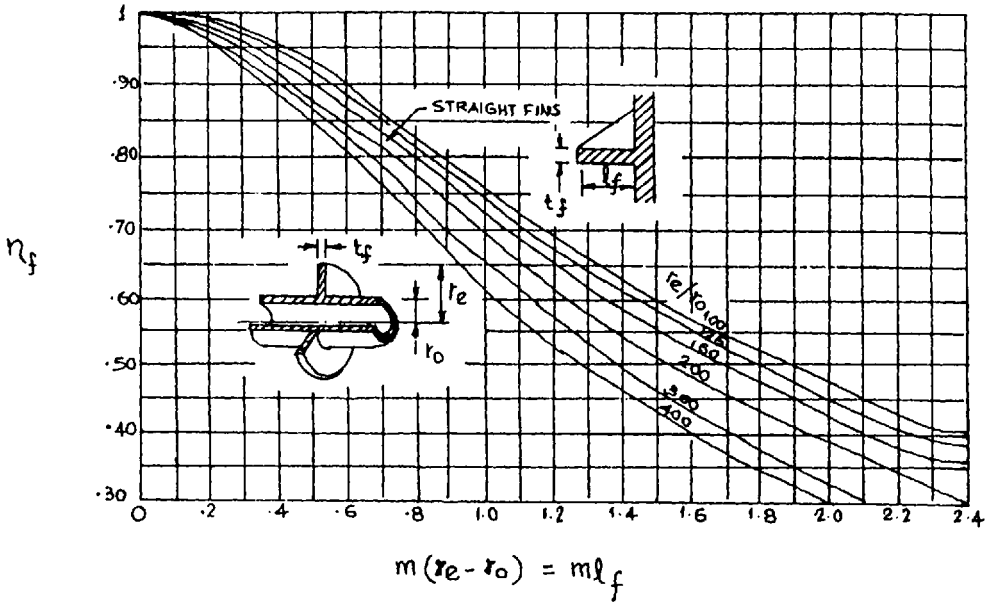


Figure 33 Fin efficiency of a radical fin with rectangular profile. (Personal communication with R. K. Shah.)

$$l_c = l_f + t_f/2 \tag{100}$$

Schmidt Method. The Schmidt [59] formula for the efficiency of a plane circular fin is given by

$$\eta = \frac{\tanh ml^*}{ml^*} \tag{101}$$

where l^* is given by

$$l^* = (r_e - r_o)\left[1 + \frac{t_f}{2(r_e - r_o)}\right][1 + 0.35 \ln(\rho)] \tag{102}$$

in which $\rho = r_e/r_o$. It was shown that for $0.5 \leq \rho \leq 1$ and $1 \leq \rho \leq 8$, the error using Eq. 101 is less than 1% of the exact value of the fin efficiency. Because the fin efficiency is very close to unity for typical low-finned tube geometries, Rabas and Taborek [7] do not recommend any corrections to this method to account for departure from a rectangular profile and for the nonuniformity of the heat-transfer coefficient over the height of the fin.

Plain Continuous Fin on Circular Tubes

A recurring arrangement of extended surface is that of a single sheet of metal pierced by round tubes in either a square or equilateral triangular array. For polygonal fins, methods suggested in Refs. 19, 59, 60, and 61 can be used.

Schmidt Method. Schmidt [59] extended the circular fin efficiency formula expressed in Eq. 101 to rectangular and hexagonal layout fin surfaces as shown in Fig. 34. The extension was made by analyzing these surfaces on the basis of equivalent circular fins. The expression for the ratio of the equivalent fin radius to the tube radius, ρ_e, is expressed as follows:

For rectangular fins,

$$\rho_e = 1.28\lambda_1(\beta_1 - 0.2)^{0.5} \tag{103}$$

For hexagonal fins,

$$\rho_e = 1.27\lambda_1(\beta_1 - 0.3)^{0.5} \tag{104}$$

where

$$\lambda_1 = \frac{M}{r_o} \tag{105}$$

$$\beta_1 = \frac{L}{M} \tag{106}$$

and where L and M are defined in Fig. 34. Of these two, L must always be the larger dimension. The fin efficiencies calculated in this way always fall within the known upper and lower limits defined by the inner and outer circumscribing circles and are very close to that of a circular fin of equal area. The accuracy of this method is especially good for square or regular hexagonal fins, where $L = M$.

Sparrow and Lin Method. The Sparrow and Lin method [61] considered both the square fin and hexagonal fin formed by tubes on equilateral triangular pitch as shown in Fig. 35. For the fins shown in Fig. 35, the fin efficiency is obtained from the numerical temperature solution and is conveniently represented in terms of a fictitious edge radius r_e^* that corresponds to a

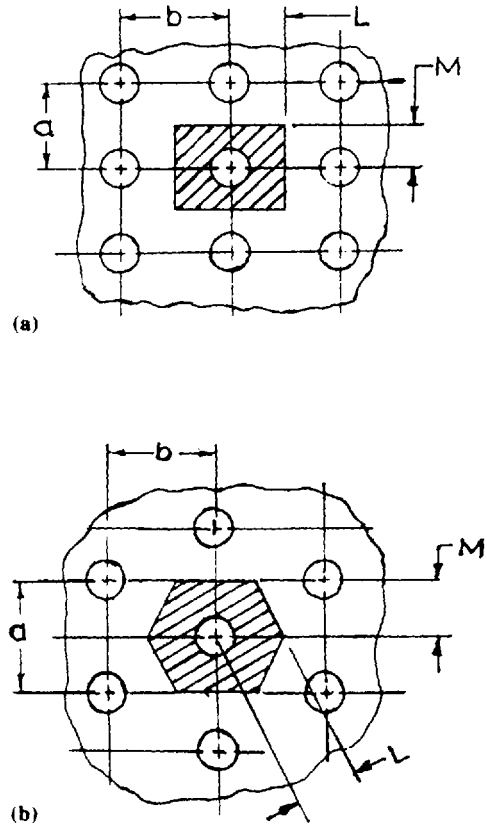


Figure 34 Geometrical details of continuous fin-tube heat exchanger layouts. (a) Rectangular tube array; (b) hexagonal tube array. (After Ref. 59.)

radial fin having the same surface area as the square and hexagonal fins under consideration. This fictitious edge radius for the square fin is given by

$$r_e^* = \left(\frac{2}{\sqrt{\pi}} \right) s \tag{107}$$

and for the hexagonal fin

$$r_e^* = \left(\frac{2\sqrt{3}}{\pi} \right)^{1/2} s \tag{108}$$

The Sparrow and Lin method satisfies exactly the isothermal boundary condition at the fin base and fulfills approximately to any desired accuracy the adiabatic boundary condition at the fin edge. The fin efficiencies for the square and hexagonal fins are given in Fig. 36.

Sector Method. The fin efficiency of the polygonal fin is obtained by an approximate method referred to as the "sector method" [19]. The flat fin is broken down into n sectors bounded by idealized adiabatic planes as indicated by the dotted lines for the in-line and staggered tube arrangements in Fig. 37. The radius of each circular sector is determined by the length of a construction line originating from the tube centre and passing through the midpoint of each

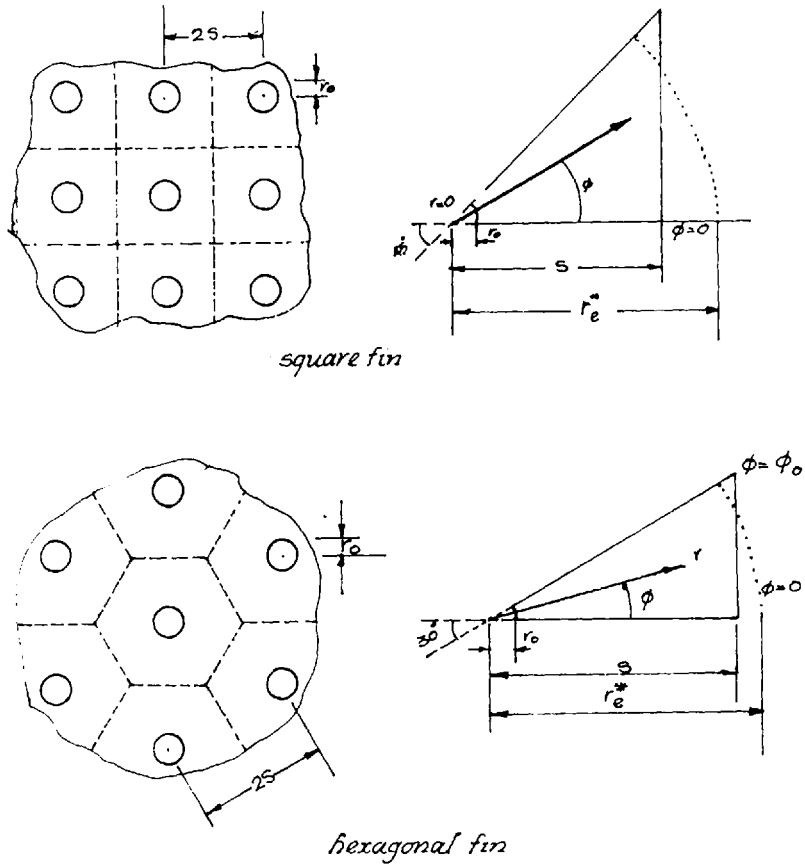


Figure 35 Fictitious edge radius for unit fin surface of continuous fin with circular tube. (a) Square layout (i.e., square fin); (b) staggered layout (30°) (i.e., hexagonal fin).

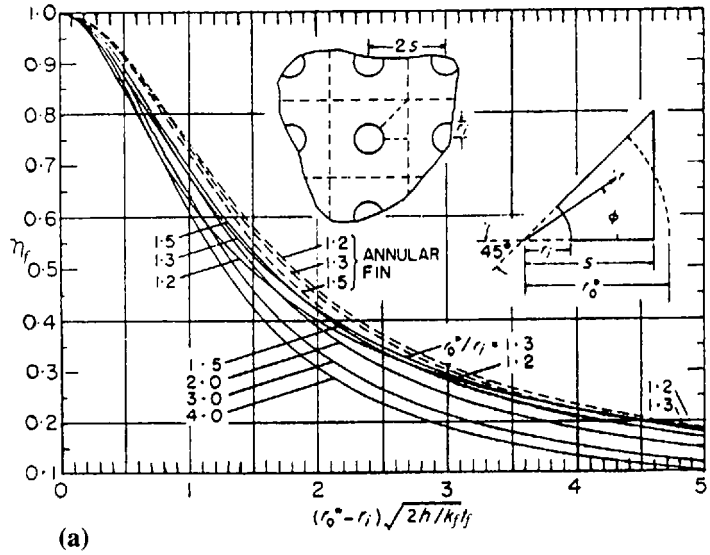
line segment. The fin efficiency of each sector is then determined by use of Eq. 94, 95, or 101. The fin efficiency for the entire surface can then be determined by the summation as

$$\eta_f = \frac{\Sigma_{i=1}^{n} \eta_{f,i} A_{f,i}}{\Sigma_{i=1}^{n} A_{f,i}} \tag{109}$$

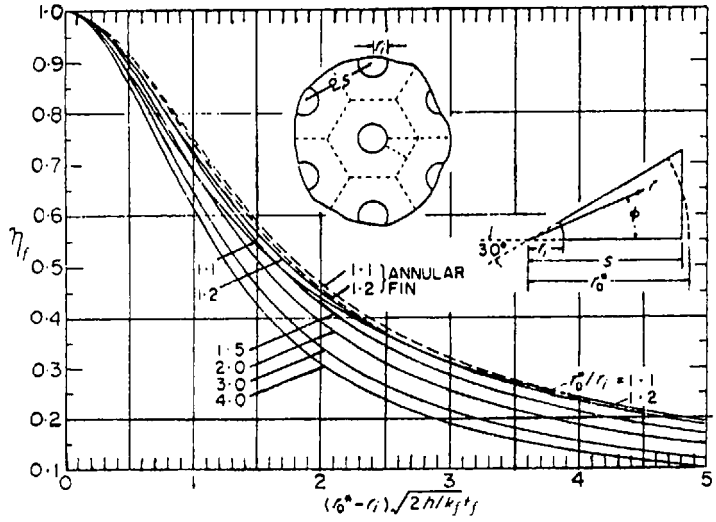
where $A_{f,i}$ is the area of each fin sector. The approximation improves as n becomes very large, but for practical purposes, only a few segments will suffice to provide O_f within a desired accuracy of 0.1%. The fin efficiency calculated by the sector method is lower than that for the actual flat fin, whereas the equivalent annulus method yields O_f values that are higher than those by the sector method for highly rectangular fin geometry around the tubes [19].

7 RATING OF A COMPACT EXCHANGER

The rating problems for a two-fluid direct transfer type compact crossflow and counterflow exchanger with gas as a working fluid at least on one side is discussed in this section. The surface employed on the gas side of this exchanger has a high surface area density and low hydraulic diameter. Customarily, the ε-NTU method is employed for compact heat exchangers.



(a)



(b)

Figure 36 Fin efficiency for a continuous finned tube heat exchanger. (a) Square fin; (b) hexagonal fin.

Hence, the solution procedure is outlined using the ε-NTU method. The rating procedure given here is as in Refs. 24 and 63.

7.1 Rating of Single-Pass Counterflow and Crossflow Exchangers

The basic steps of the rating problem are shown in Fig. 38 and involve the determination of the following parameters.

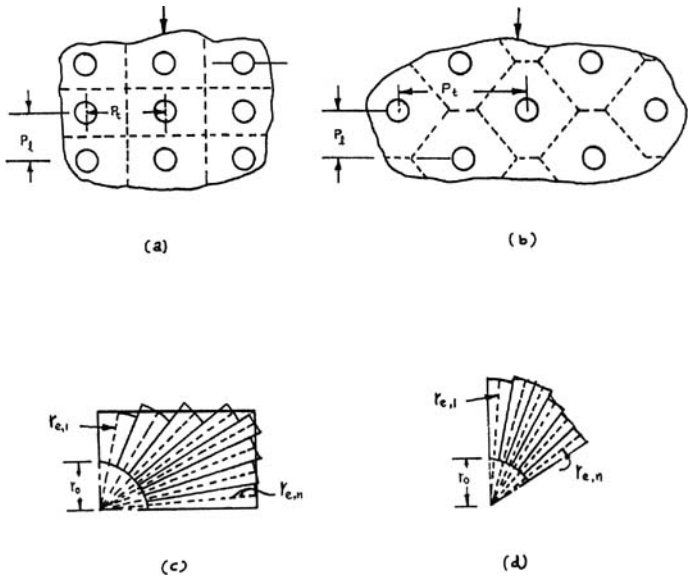


Figure 37 Fin sectors to determine fin efficiency of continuous finned tube heat exchanger.

1. Surface geometrical properties. These include

   A_c, minimum free flow area
   A, heat-transfer surface area (total of primary surface area, A_p, and secondary surface area, A_f)
   L, flow length
   D_h, hydraulic diameter
   β, heat-transfer surface area density
   σ, ratio of minimum free flow area to frontal area
   l_f, fin length
   t_f, fin thickness

   Also included are specialized dimensions used for heat-transfer and pressure-drop correlations.
2. Fluid physical properties. Determine the thermophysical properties at bulk mean temperature for each fluid, namely, hot and cold fluids. The properties needed for the rating problem are μ, c_p, k, and Pr. Since the outlet temperatures are not known for the rating problem, they are guessed initially. Unless it is known from the past experience, assume an exchanger effectiveness as 60–75% for most single-pass crossflow exchangers, and 80–85% for single-pass counterflow and two-pass cross-counterflow exchangers. For the assumed effectiveness, calculate the fluid outlet temperatures by

$$t_{h,o} = t_{h,i} - \varepsilon \frac{C_{min}}{C_h}(t_{h,i} - t_{c,i}) \tag{110}$$

$$t_{c,o} = t_{c,i} + \varepsilon \frac{C_{min}}{C_c}(t_{h,i} - t_{c,i}) \tag{111}$$

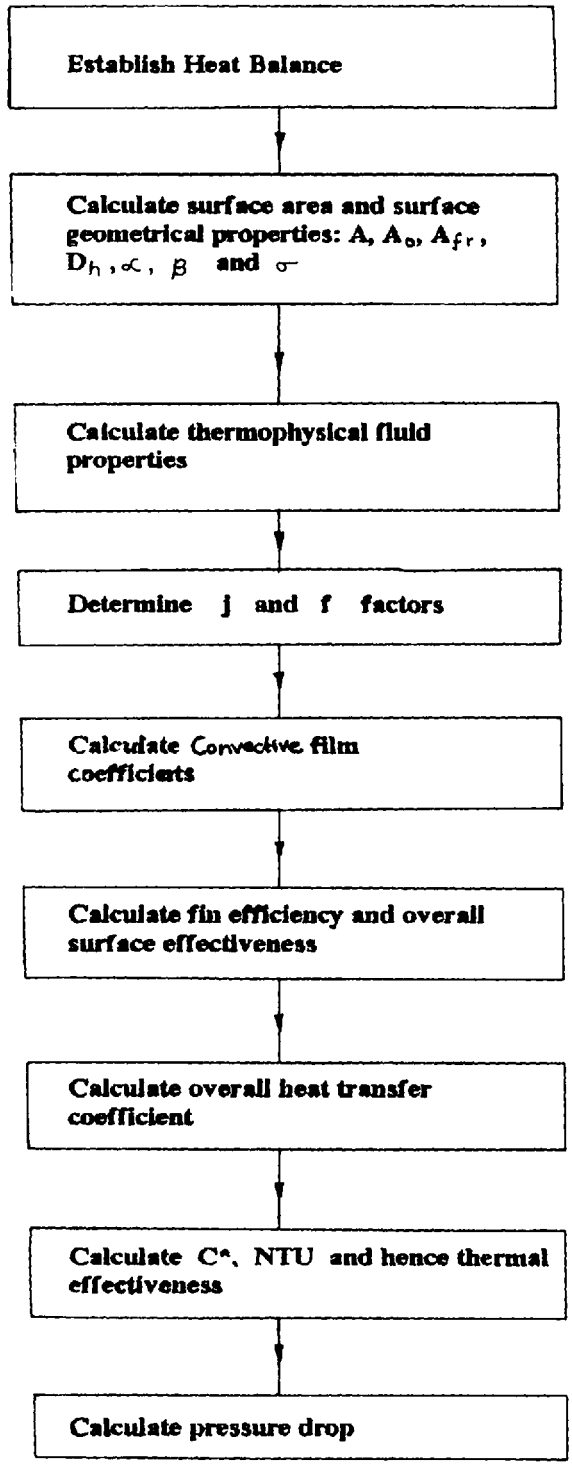


Figure 38 Rating of a compact heat exchanger.

Initially, assume $C_c/C_h \approx M_c/M_h$ for a gas-to-gas exchangers, or $C_c/C_h = (Mc_p)_c/(Mc_p)_h$ for a gas-to-liquid exchanger with approximate values of c_ps. For exchangers with $C^* \geq 0.5$ (usually gas-to-gas exchangers), the bulk mean temperature on each side will be the arithmetic mean of the inlet and outlet temperatures on each side. For exchangers with $C^* < 0.5$ (usually gas-to-liquid exchangers), the bulk mean temperature is calculated as given in Table 2.

Once the bulk mean temperatures are obtained on each side, obtain the fluid properties from thermophysical property tables or from standard thermal engineering books.

3. Reynolds numbers. Calculate the Reynolds number and/or any other pertinent dimensionless groups needed to determine j or Nu and f of heat-transfer surfaces on each side of the exchanger.
4. Compute j or Nu and f factors.
5. Correct Nu (or j) and f for variable fluid property effects in the second and subsequent iterations.
6. From Nu or j, determine heat-transfer coefficient for both the fluid streams.

$$h = \frac{\mathrm{Nu}k}{D_h} \tag{112a}$$

or

$$h = jG\ C_p Pr^{-2/3} \tag{112b}$$

7. Determine the fin efficiency η_f and the overall surface efficiency η_o given by

$$\eta_f = \frac{\tanh ml}{ml} \tag{113}$$

$$\eta_o = 1 - \frac{A_f}{A}(1 - \eta_f) \tag{114}$$

8. Overall conductance. Calculate the wall thermal resistance, R_w. Knowing the fouling resistances $R_{f,h}$ and $R_{f,c}$ on the hot and cold fluid sides, respectively, calculate the overall thermal conductance UA from

$$\frac{1}{\mathrm{UA}} = \frac{1}{(\eta_o hA)_h} + \frac{R_{f,h}}{(\eta_o A)_h} + R_w + \frac{1}{(\eta_o hA)_c} + \frac{R_{f,c}}{(\eta_o A)_c} \tag{115a}$$

$$= R_h + R_1 + R_w + R_2 + R_c \tag{115b}$$

Table 2 Approximate Bulk Mean Temperature on the Hot and Cold Side of a Two-Fluid Heat Exchanger for $c^* < 0.5$ [24,63]

C_{max} = hot fluid C_{min} = cold fluid	C_{max} = cold fluid C_{min} = hot fluid
$t_{h,m} = \frac{t_{h,i} + t_{h,o}}{2}$	$t_{c,m} = \frac{t_{c,i} + t_{c,o}}{2}$
$t_{c,m} = t_{h,m} - \Delta t_{lm}$	$t_{h,m} = t_{c,m} + \Delta t_{lm}$
$\Delta t_{lm} = \frac{(t_{h,m} - t_{c,i}) - (t_{h,m} - t_{c,o})}{\ln\left(\frac{t_{h,m} - t_{c,i}}{t_{h,m} - t_{c,o}}\right)}$	$\Delta t_{lm} = \frac{(t_{h,i} - t_{c,m}) - (t_{h,o} - t_{c,m})}{\ln\left(\frac{t_{h,i} - t_{c,m}}{t_{h,o} - t_{c,m}}\right)}$

9. Calculate NTU, C^*, and exchanger effectiveness, ε. If the thermal effectiveness is above 80%, correct for wall longitudinal conduction effect.
10. Compute the outlet temperature from Eqs. 110 and 111. If these outlet temperatures differs significantly from those assumed in step 2, use these outlet temperatures in step 2 and continue iterating steps 2–9 until the assumed and computed outlet temperatures converge within the desired degree of accuracy. For a gas-to-gas exchanger probably one or two iterations will be sufficient.
11. Compute the heat duty from

$$q = \varepsilon C_{\min}(t_{h,i} - t_{c,i}) \tag{116}$$

12. Calculate the core pressure drip. The friction factor f on each side is corrected for the variable fluid properties as discussed in Chapter 3. The wall temperature T_w is computed from

$$T_{w,h} = t_{m,h} - q(R_h + R_1) \tag{117}$$

$$T_{w,c} = t_{m,c} + q(R_c + R_2) \tag{118}$$

7.2 Shah's Method for Rating of Multipass Counterflow and Crossflow Heat Exchangers

The rating procedure for multipass crossflow exchangers with fluids mixed between passes is described by Shah [63]. The solution procedure for rating problem for the two-pass crossflow exchangers with flows unmixed in the passes but mixed between passes is also very similar to the sizing of single-pass crossflow. Only some of the calculations on the two pass side need to be modified, and only those points are summarized here.

1. In order to compute fluid bulk mean temperature and thermophysical properties of fluids, first guess the overall thermal effectiveness, ε_N. Assume it to be 80–85% unless it is known from the past experience. .Assume that the NTU per pass is same. The individual pass effectiveness ε_p is related to overall effectiveness ε_N for the case of fluids mixed between passes. Compute approximate values of C_c and C_h since we don't know yet the accurate values of the specific heats.
2. Determine the intermediate and outlet temperature by solving the following individual pass effectiveness and overall effectiveness equations:

$$\varepsilon_{p1} = \frac{C_c(t_{c,o} - t_{c,int})}{C_{\min}(t_{h,i} - t_{c,int})} \tag{120}$$

$$\varepsilon_{p2} = \frac{C_c(t_{c,int} - t_{c,i})}{C_{\min}(t_{h,int} - t_{c,i})} \tag{121}$$

$$\varepsilon = \frac{C_c(t_{c,o} - t_{c,i})}{C_{\min}(t_{h,i} - t_{c,i})} \tag{122}$$

In the foregoing three equations there are three unknowns: $t_{c,o}$, $t_{c,int}$, and $t_{h,int}$. Hence, they can be evaluated exactly and then from the overall energy balance $t_{h,o}$ is calculated.

$$C_c(t_{c,o} - t_{c,i}) = C_h(t_{h,i} - t_{h,o}) \tag{123}$$

Since we know all terminal temperatures for each pass, we can determine the bulk mean temperature for each fluid in each pass and subsequently the fluid properties separately for each pass.

8 SIZING OF A COMPACT HEAT EXCHANGER

The basis of sizing involves coupling of heat transfer and flow friction in the derivation of the core mass velocity G on each side of a two fluid exchanger. Subsequently, the sizing problem is carried out in a manner similar to the rating problem.

8.1 Core Mass Velocity Equation (after Shah [24])

The dominant term in the expression for the pressure drop is the core friction term. The entrance and exit effects are generally relatively small and are of the opposite sign. Similarly, the flow acceleration term is relatively small in most heat exchangers, being generally less than 10% of the core friction term [24], so their elimination is usually warranted in a first approximation. With these approximations and $L/r_h = A/A_o$, the expression for pressure drop may be written after rearrangement as

$$\frac{G^2}{2g_c p_i \rho_i} = \frac{\Delta p}{p_i} \frac{A_o}{A} \frac{1}{\rho_i (1/\rho)_m} \frac{1}{f} \tag{124}$$

In the absence of fouling resistances, the overall NTU is related to NTU_h, NTU_c, and the wall resistance, R_w, by

$$\frac{1}{NTU} = \frac{1}{NTU_h(C_h/C_{min})} + C_{min}R_w + \frac{1}{NTU_c(C_c/C_{min})} \tag{125}$$

The wall resistance term is generally small and hence neglected in the first-approximation calculation. Hence, the number of transfer units on one side of interest (either hot or cold), designated as NTU_1, may be estimated from the known overall NTU as given next.

If both fluids are gases, one can start with the estimate that the design is "balanced" by a selection of the hot and cold side surfaces so that $R_h = R_c = R_o/2$, that is, $NTU_h = NTU_c = 2NTU$. Then

$$NTU_1 = NTU_2 = 2NTU \tag{126}$$

For a gas-liquid heat exchanger, one might estimate

$$NTU_{\text{gas side}} = 1.1(NTU) \tag{127}$$

The term NTU_1 is related to the Colburn factor j on side 1 by

$$NTU_1 = \left(\frac{\eta_o hA}{Mc_p}\right)_1 = \left(\eta_o \frac{hA}{Gc_p A_o}\right)_1 = \left(\eta_o j \mathrm{Pr}^{-2/3} \frac{A}{A_o}\right)_1 \tag{128}$$

Eliminating (A/A_o) from Eqs. 124 and 128, and simplifying the expression, we get the core mass velocity G for one side:

The feature that makes this equation so useful is that the ratio j/f is a relatively flat function of the Reynolds number. Thus one can readily estimate an accurate magnitude of j/f based on a "ballpark" estimate of Re. If there are no fins, overall surface efficiency $\eta_o = 1$. For a "good design," the fin geometry is chosen such that η_o is in the range 70–90%. Therefore $\eta_o = 0.8$ is suggested as a first approximation to determine G from Eq. 129.

8.2 Procedure for Sizing a Compact Heat Exchanger

The procedure for sizing any of the compact heat exchangers (Fig. 39) is almost inevitably an iterative one and thus lends itself very conveniently to computer calculations. Kays and London

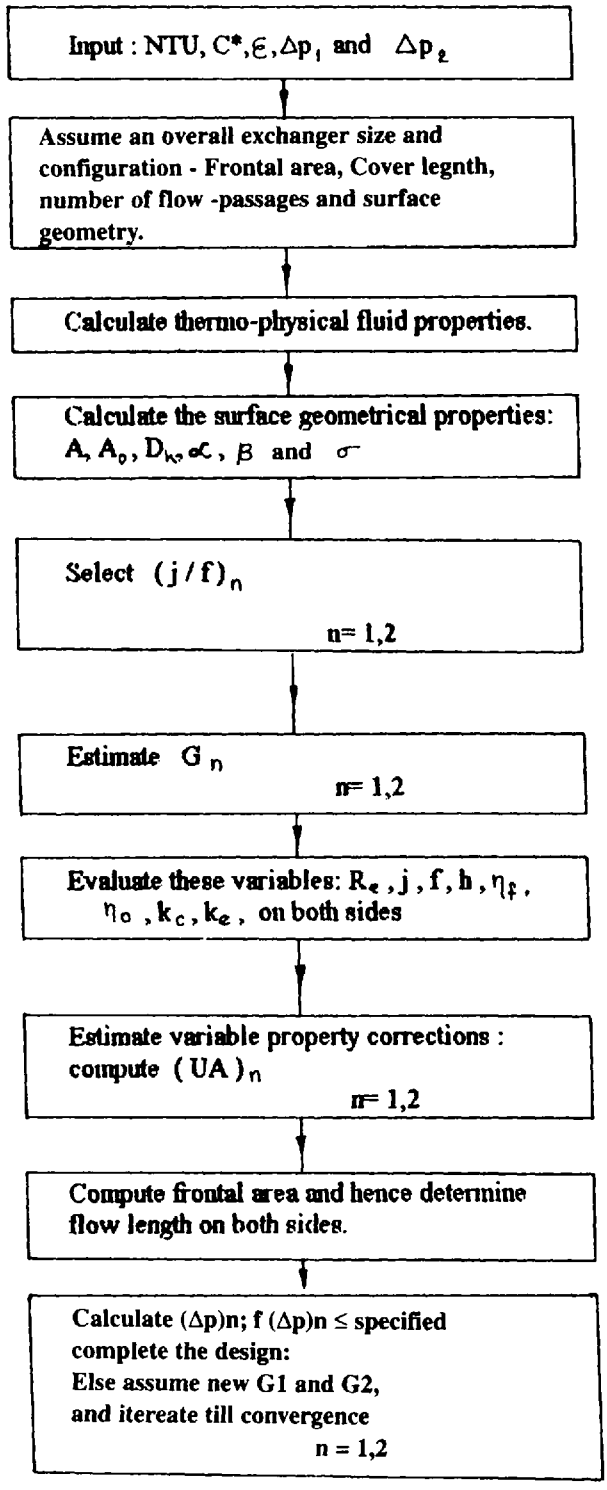


Figure 39 Sizing of a compact heat exchanger.

Table 3 Geometric Characteristics [17]

Hot side (fluid 1)	Cold side (fluid 2)
$D_{h,h}$	$D_{h,c}$
σ_h	σ_c
α_h	α_c
$\left(\frac{A_f}{A}\right)_h$	$\left(\frac{A_f}{A}\right)_c$
$\left(\frac{A_w}{A}\right)_h$	$\left(\frac{A_w}{A}\right)_c$
$(t_f)_h$	$(t_f)_c$

[17] illustrate the procedure for sizing a crossflow heat exchanger. To illustrate this, a simple crossflow heat exchanger is considered as shown in Fig. 20. It is assumed that each fluid is unmixed throughout. The two fluids are designated by h and c. The problem is to determine the three dimensions L_1, L_2, and L_3. The first step after chosen the two surfaces is to assemble the geometric characteristics of the surface as given in Table 3.

A first estimate of G_h and G_c can be made using the following approximation relation

$$G = \left[\left(\frac{2g_c\eta_o}{(1/\rho_m)\mathrm{Pr}^{2/3}}\right)\left(\frac{\Delta p}{\mathrm{NTU}}\right)\left(\frac{j}{f}\right)\right]^{0.5} \tag{130}$$

After the determination of mass velocity, carry out the calculations similar to a rating problem. The sequence of parameters to be calculated after determination of mass velocity is given in Table 4.

The pressure drop results are then compared with those specified for the design, and the procedure is repeated until the two pressure drops are within the specified value.

Table 4 Sequence of Parameters to Be Calculated for Sizing Problem After Calculating Mass Velocity [17]

Hot side (fluid 1)	Cold side (fluid 2)
Re_h	Re_c
j_h	j_c
f_h	f_c
h_h	h_c
$\eta_{f,h}$	$\eta_{f,c}$
$\eta_{o,h}$	$\eta_{o,c}$
$(\mathrm{UA})_h$	$(\mathrm{UA})_c$
A_h	A_c
$A_{o,h}$	$A_{o,c}$
$A_{fr,h}$ or L_2L_3	$A_{fr,c}$ or L_1L_3
L_1	L_2
L_1, L_2, L_3	—
$(K_c, K_e)_h$	$(K_c, K_e)_c$
$(\Delta p/p)_h$	$(\Delta p/p)_c$

8.3 Optimization of Plate Fin Exchangers and Constraints on Weight Minimization [64]

Minimizing the material volume, or weight, of the plate-fin heat exchanger core does not necessarily represents the optimum solution, even for weight-sensitive aerospace applications; size and shape can be important design considerations [64]. Minimum weight core could be longer than is desirable because of the low fin efficiency implied. If the fin is too thin, its efficiency will be low, and to compensate both core length and flow area will be high, giving an excessively high weight. On the other hand, a very thick fin giving high fin efficiency will yield a low core length but with low porosity (free flow area) and weight. Minimizing the components' thickness can also contribute for low weight. But there are limitations in reducing components beyond certain limits as follows:

The thicknesses of fin material and separating plates have lower limits set by pressure-retaining capability.

Plate fin cores are usually made from sheet stock of a fixed range of thickness; rolling finstock to a special "optimum" thickness could be uneconomic.

It may not be possible to form fins of sufficient dimensional accuracy if they are too thin; if they can be made, they might deform unsatisfactorily on brazing.

There may also be lower thickness limits set by erosion and corrosion problems.

9 EFFECT OF LONGITUDINAL HEAT CONDUCTION ON THERMAL EFFECTIVENESS

The ε-NTU and LMTD methods discussed are based on the idealization of zero longitudinal heat conduction in the wall in the fluid flow direction. If a temperature gradient is established in the wall in the fluid flow direction, heat transfer by conduction takes place from the hotter to the colder region of the wall in the longitudinal direction. This longitudinal conduction in the wall flattens the temperature distributions, reduces the mean outlet temperature of the cold fluid, increases the mean outlet temperature of the hot fluid, and thus reduces the thermal effectiveness [63,65]. The reduction in the effectiveness at a specified NTU may be quite significant for a compact exchanger designed for high thermal effectiveness (above ~80%) and a short flow length, L. The shell and tube exchangers and plate exchangers are usually designed for effectiveness of 60% or less per pass. Therefore, the influence of heat conduction in the wall in the flow direction is negligible for these effectiveness levels. The presence of longitudinal heat conduction in the wall is incorporated into the thermal effectiveness formula by an additional parameter, λ, referred to as the longitudinal conduction parameter. Another parameter that influences the longitudinal wall heat conduction is the convection conduction ratio, $\eta_o hA$. Thus, in the presence of longitudinal heat conduction in the wall, the exchanger thermal effectiveness is expressed in a functional form [65]:

$$\varepsilon = \phi\{\text{NTU}, C^*, \eta_o hA, \lambda\} \tag{131}$$

9.1 Longitudinal Conduction Influence on Various Flow Arrangements

The influence of longitudinal conduction in the case of parallel flow is not discussed because high-performance exchangers are not designed as for parallel flow arrangements. For high-performance exchangers, the effect is discussed in Chapter 7, Regenerators. In a crossflow arrangement, the wall temperature distributions are different in the two perpendicular flow

directions. This results in a two dimensional longitudinal conduction effect, and is accounted for by the cold-side and hot-side Σ parameters defined as [65]:

$$\lambda_c = \left(\frac{k_w A_k}{LC}\right)_c \quad \text{and} \quad \lambda_h = \left(\frac{k_w A_k}{LC}\right)_h \tag{132}$$

Note that the flow lengths L_c and L_h are independent in a crossflow exchanger. If the separating wall thickness is a, and the total number of parting sheets is N_p, then the transfer area for longitudinal conduction is given by [65]:

$$A_{k,c} = 2N_p L_h a \quad \text{and} \quad A_{k,h} = 2N_p L_c a \tag{133}$$

Chiou [66] analyzed the problem for a single-pass crossflow heat exchanger with both fluid unmixed and tabulated values for the reduction in thermal effectiveness due to longitudinal wall heat conduction.

10 AIR COOLERS

Air-cooled heat exchangers (ACHE), or "fin-fans," (Fig. 40) are an alternate heat rejection method that is used frequently in place of the conventional water-cooled shell and tube heat exchanger to cool a process fluid. They can be used in all climates. Generally they are not compact heat exchangers [1]. ACHE are increasingly found in a wide spectrum of applications including chemical, process, petroleum refining, and other industries. Recently very large air-cooled condensers and dry-cooling towers have been constructed at power plants located in areas where cooling water is unavailable or costly [67]. A fan located below the tube bundle forces air up through the bundle, or a fan above draws the air through the bundle. The fans are axial-flow fans varying from 4 to 12 ft diameter and having four to six blades. The fan blades may be of aluminum, plastic, or, in the case of corrosive atmospheres, stainless steel [68]. The drive can be an electric motor with gears or V-belts. Before discussing the construction details and design aspects, the factors that favor air cooling over water cooling are discussed.

10.1 Air Versus Water Cooling

Two primary methods of process cooling are (1) water cooling and (2) air cooling. The choice between air or water as coolant depends on many factors, like (1) cooler location, (2) space for cooling system, (3) effect of weather, (4) design pressure and temperature, (5) danger of contamination, (6) fouling, cleaning, and maintenance, and (7) capital costs. Environmental concerns such as shortage of makeup water, blowdown disposal, and thermal pollution have become an additional factor in cooling system selection.

Air Cooling

Air cooling is increasing in use, particularly where water is in short supply. Factors that favor air cooling include the following:

1. Air is available free in abundant quantity with no preparation costs.
2. Air cooler design is well established, and can perform well with a reasonable degree of reliability.
3. Water is corrosive and requires treatment to control both scaling and deposition of dirt, whereas air is mostly noncorrosive. Therefore, material selection is governed by process fluids routed through the tube side.

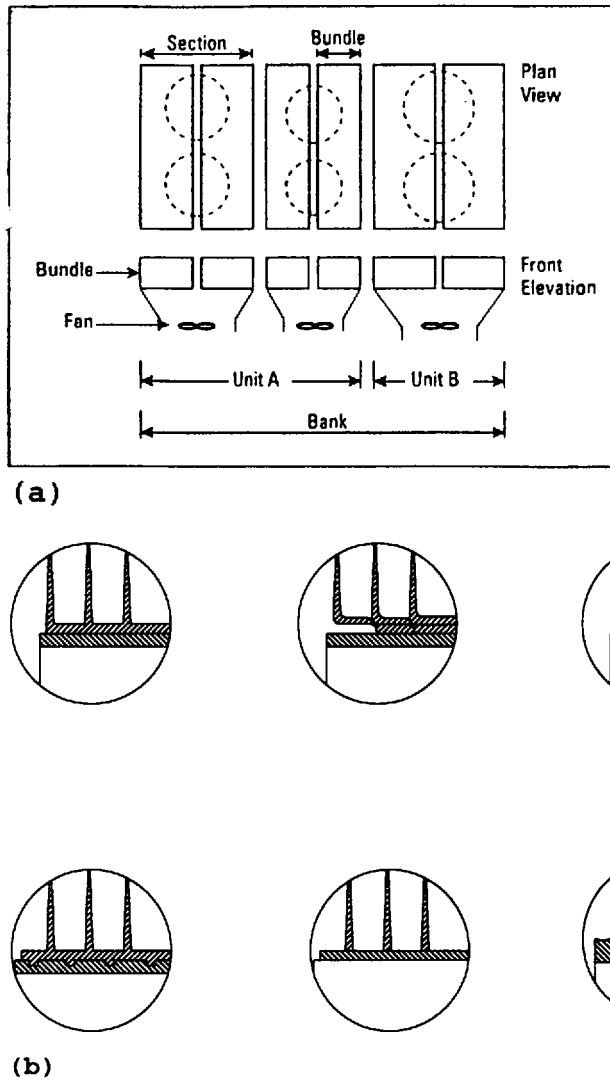


Figure 40 Details of aircooled heat exchanger (ACHE). (a) ACHEs consists of bundles combined into bays combined into units and units combined into banks; (b) details of fin tube; and (c) typical headers for air coolers offer flexibility.

4. Mechanical design problems are eased with air coolers since the process fluid is always on the tube side.
5. Danger of process fluid contamination is much greater with water cooled system.
6. Air-side fouling can be periodically cleaned by air blowing, and chemical cleaning can be carried out either during half-yearly or yearly attention. Water-cooled systems may require frequent cleaning.
7. Maintenance costs for air coolers are about 20–30% of those for water cooled system [68].

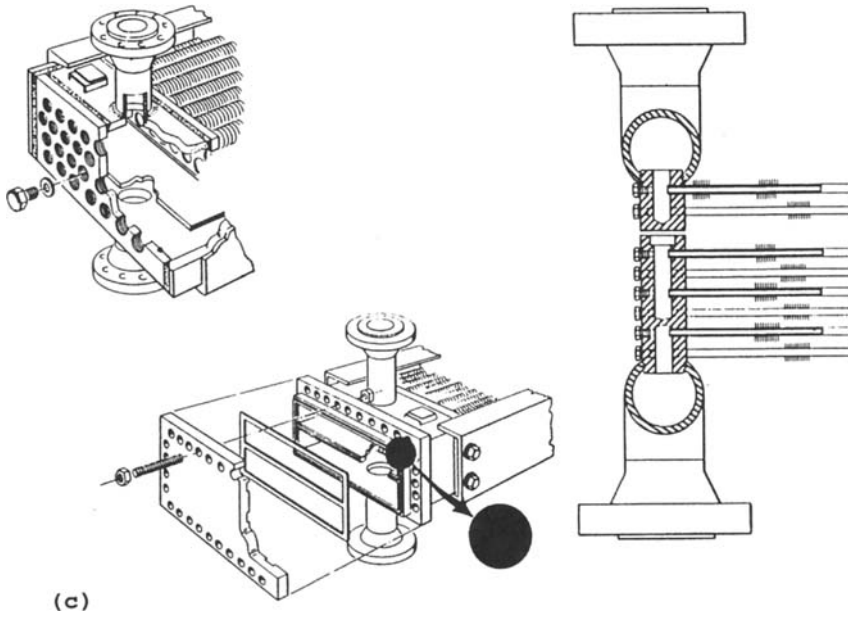


Figure 40 Continued.

Operating costs for water coolers are higher, because of higher cooling water circulation pump horsepower and water treatment costs.

8. Air cooling eliminates the environmental problems like heating up of lakes, rivers, etc., blowdown, and washout.

Air cooling has the following disadvantages:

1. Air coolers require large surfaces because of their low heat-transfer coefficient on the air side and the low specific heat of air. Water coolers require much less heat-transfer surface.
2. Air coolers cannot be located next to large obstructions if air recirculation is to be avoided.
3. Because of air's low specific heat, and dependence on the dry-bulb temperature, air cannot usually cool a process fluid to low temperatures. Water can usually cool a process fluid from 10°F to 5°F lower than air, and recycled water can be cooled to near the wet-bulb temperature of the site in a cooling tower [68].
4. The seasonal variation in air temperatures can affect performance and make temperature control more difficult. Low winter temperatures may cause process fluids to freeze.
5. Air coolers are affected by hailstorms and may be affected by cyclonic winds.
6. Noise is a factor with air coolers.

10.1 Tube Bundle Construction

An air cooler tube bundle consists of a series of finned tubes set between side frames, passing between header boxes at either end. The number of passes on the tube side (the process fluid side) is made possible by internal baffling of the header boxes. For horizontal bundles, vertical baffles result in a side-by-side crossflow arrangement, whereas horizontal baffles result in a

counter-crossflow arrangement relative to airflow. Inlet and outlet nozzles may or may not be on the same header box. Tubes are attached to the tube sheet by expansion or welding.

Tube Bundle Fin Geometry

The finned tube (Fig. 40b) specifications include extruded, embedded, welded single footed, and double footed. These fins can be solid or serrated, tension wound or welded, and of a variety of metals. The fin most commonly used for air coolers is aluminum, tension wound and footed. Embedded fins have less contact resistance to heat transfer than do tension-wound fins, but corrosion is likely to be induced at the groove between fin and tube [68].

The tubes are usually 1 in (25.4 mm) diameter; fin density varies from 7 to 16 fins/in (276–630 fins/m), fin height from $\frac{3}{8}$ to $\frac{5}{8}$ in (9.53–15.88 mm), and fin thickness from 0.012 to 0.02 in (0.3–0.51 mm). The tubes are arranged in standard bundles ranging from 4 to 40 ft (1.22–12.20 m) long and from 4 to 20 ft (1.22–6.10 m) wide, but usually limited to 9.90–10.8 ft (3.2–3.5 m).

Fin Materials

Aluminum fins are used because of high thermal conductivity, light weight, and formability, but their use is limited to low-temperature applications. Either SO_2-containing or marine atmo-

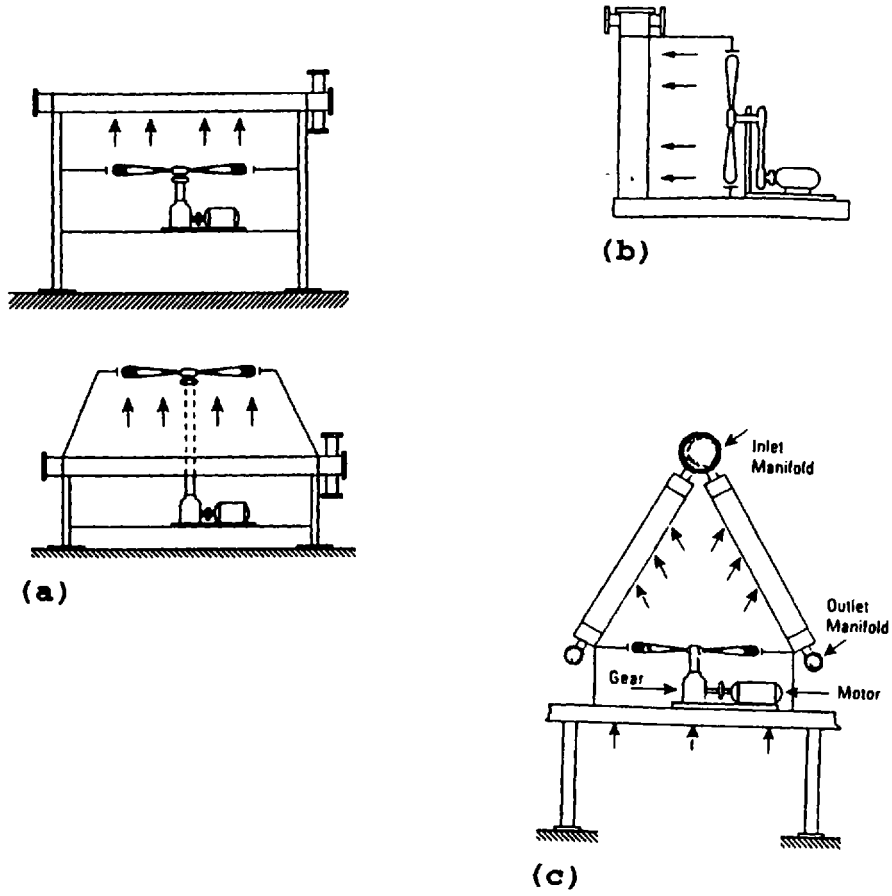


Figure 41 Orientation of ACHE.

spheres may corrode aluminum fins, so carbon steel might be preferred for such conditions. As the base tube is usually carbon or low-alloy steel, galvanic corrosion at the fin/tube junction is expected. Hence, finned tubes of carbon steel can be hot-dip galvanized to protect against galvanic corrosion and also to provide a metallic bond between the fin and the bare tube [68]. Carbon steel tubes with carbon steel or alloy steel fins are used in boiler and fired heater applications.

Header Boxes

Many types of header boxes are offered by industry. They can be grouped into three general classifications [69]:

1. Plug type boxes
2. Removable cover plate boxes for high-fouling services
3. All welded construction

See North [69] for header boxes design.

Orientation of Tube Bundle

Air-cooled exchanger bundles can be installed either vertically or horizontally. The most common orientation is in the horizontal plane. A considerable reduction in ground area can be made if bundles are vertically mounted, but the performance of the unit is greatly influenced by the prevailing wind direction. In general, the use of vertically mounted bundles is confined to small, packaged units. A compromise, which requires about half the ground area of the horizontal unit, is the A- or V-frame unit. In this type, two bundles sloped at 45–60° from the horizontal are joined by their headers at top or bottom to form the sloping side of the A (i.e., roof type) or V, respectively. The A-frame type with forced draft fans below (Fig. 42) is the more common and is used in steam condensing applications.

10.2 American Petroleum Institute Standard 661

American Petroleum Institute Standard 661 [70] is meant for air-cooled heat exchangers for general refinery service. The scope of the standard includes minimum requirements for design, materials selection, fabrication, inspection, testing, and preparation for shipment of refinery process air-cooled heat exchangers. The standard specifies that the pressure parts shall be designed in accordance with ASME Code, Section VIII, Division 1 [71]. API Standard 661 should be specified and used as a guide in preparing the requisition/specification. When the customer's requirements deviate from API 661, the exceptions or special requirements should be listed as "Specific Requirements" [72].

10.3 Problems with Heat Exchangers in Low-Temperature Environments

Air-cooled exchangers are designed to perform at ambient temperatures ranging from 130°F to –60°F. In extremely cold environments, overcooling of the process fluid may cause freezing. This may lead to tube burst, and hence freeze protection is required to prevent plugging or damage to the tubes. The minimum temperature also affects material selection for construction of the cooler.

Temperature Control

Several methods are used to control the performance of air-cooled heat exchangers to meet variations in weather and process requirements. The current practice for air cooler design in cold climates for problem services include (1) Recirculation of hot air through the tube bundle;

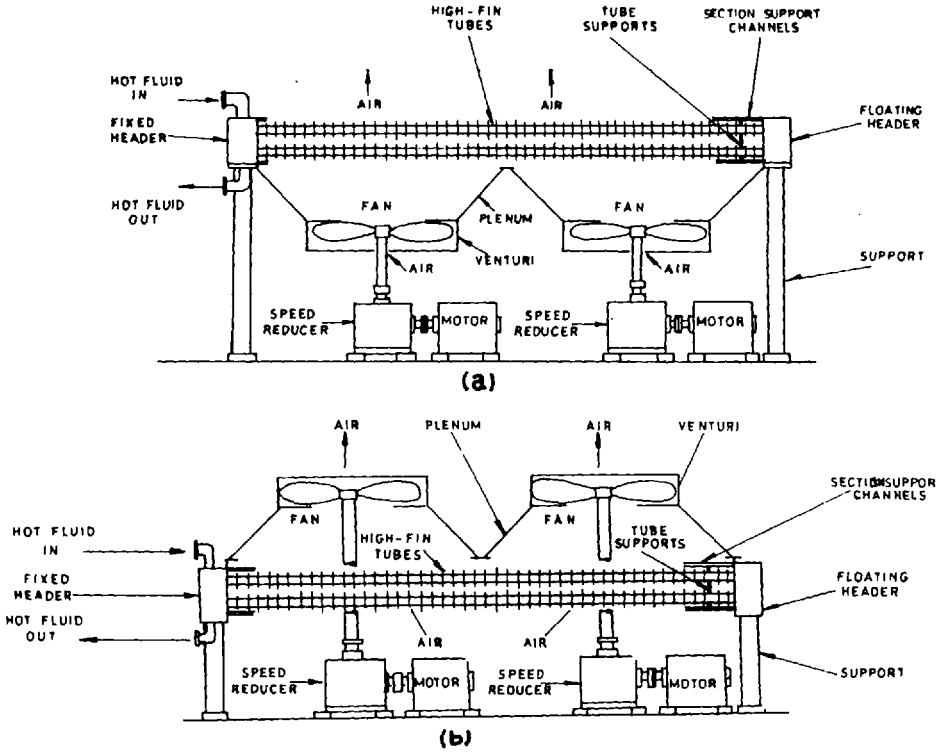


Figure 42 Air flow through ACHE: (a) forced draft, and (b) induced draft.

(2) steam coils provided to preheat air for start-up conditions—these may be mounted at the cooler base to warm up the inlet air, and according to the recommendation of API 661, this steam coil should be separate from the main cooler bundle; (3) control devices that enable part of the process fluid to bypass the unit; (4) for some units, particularly viscous oil coolers, cocurrent design is appropriate, where the hot fluid enters nearest the cold ambient wall, and the outlet where wall temperature is critical is in the warm air stream [69]; and (5) in certain cases, simply controlling the process outlet temperature with fan switching, two-speed fan drives, variable-speed motor automatic louvers, variable-pitch fans, or autovariable-pitch fans is sufficient. Each case must be considered on its merits to decide on the best method of control.

10.4 Forced Draft Versus Induced Draft

One of the design criteria affecting the performance of air coolers is the type of draft: forced draft or induced draft. Both these arrangements are shown in Fig. 43.

Forced Draft

Forced draft fans have the advantage of handling cold air entering the exchanger, requiring smaller volumes of air and less horsepower. They generally offer better arrangements for maintenance and they are easily accessible. They are best adapted for cold-climate operation with warm-air recirculation. Also, forced draft fans afford a higher heat-transfer coefficient relative to induced draft, because forced draft fans cause turbulence across the tube bundle [68].

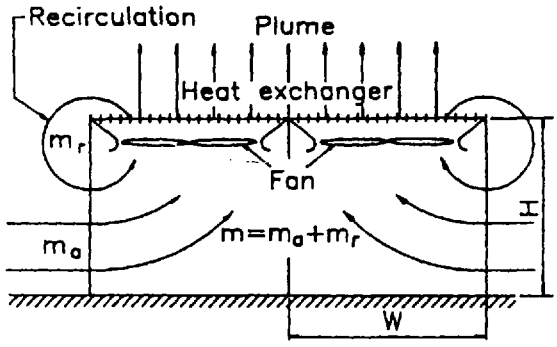


Figure 43 Air recirculation through an ACHE. H, height from ground level; w, half width; m_a, fresh air; and m_r, recirculated air.

Induced Draft

Compared with the forced draft design, induced draft design has the following advantages:

1. Easier to shop assemble, ship, and install.
2. The hoods offer protection from weather and hailstone protection.
3. Easier to clean the underside when covered with lint, bugs, and debris.
4. Better air distribution over the tube bundle.
5. Less likely to be affected by hot air recirculation.

The disadvantages of induced draft design are:

1. More difficult to remove bundles for maintenance.
2. High-temperature service limited due to effect of hot air on the fans.
3. More difficult to work on the fan assembly, due to heat from the bundle and due to their location.

10.5 Recirculation

Recirculation of hot plume air (Fig. 44) occurs in most forced draft air-cooled heat exchangers. The resultant increase in inlet cooling air reduces the effectiveness of the heat exchanger. To

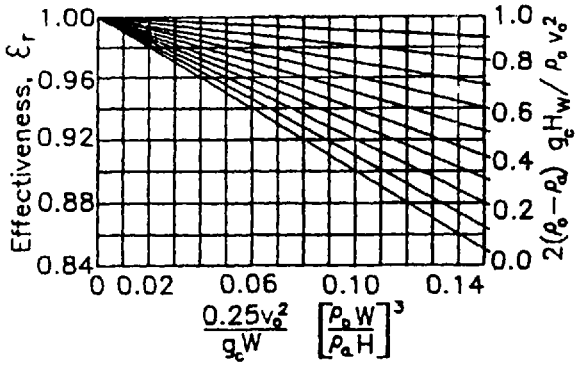


Figure 44 Effectiveness of ACHE with air circulation.

reduce the amount of recirculation, windwalls may be erected along the periphery of the heat exchanger. This problem has been analyzed experimentally and numerically by Kroger [67]. Analysis shows that the effectiveness of heat exchanger can be expressed approximately by [67]:

$$\varepsilon = 1 - 0.25\left[\frac{\rho_o W}{\rho_a H_w}\right]^3 \frac{V_o^2}{g_c W}\left[1 - \frac{2(\rho_i - \rho_o)g_c H_w}{\rho_o V_o^2}\right] \tag{134}$$

where H and W are shown in Fig. 44, H_w is the windwall height, V_o is the plume velocity immediately after the heat exchanger, and ρ_a and ρ_o are the inlet and outlet air densities respectively. To reduce the amount of recirculation, high windwalls may be erected along the periphery of the heat exchanger.

10.6 Design Aspects

Proper design of air-cooled heat exchangers for cold climate service requires a well-balanced consideration of fluid flow, heat transfer, structural design, air movement, wind effects, temperature control in cold climate, and economics [73]. Design of air-cooled heat exchangers is detailed by Paikert [31], Ganapathy [68], Brown [74], and Sunders [75], and Mukherjee [76,77].

Design Variables

Modern air-cooled heat exchanges are designed thermally by computers, which are capable of examining all design variables to produce the optimum unit. In view of the increased size and cost of these units in large plants and the competitive nature of the industry, improved and more sophisticated designs are essential to satisfy the needs of the industry and the society [67]. Important design variables pertaining to the tube bundle include

Tube (diameter, length and wall thickness, number of tube rows)
Fins (height, spacing, thickness)
Space (length, width, and depth)

Designers usually optimize criteria such as [78]:

Capital versus running cost
Forced versus induced draft fan
Type and spacing of fins
Number of tube rows
Fan design and noise level

Air Velocity

If the air flow rate is known, the tentative air velocity may be chosen, which establishes the cooler face area. In air-cooled heat exchanges, face velocity is usually in the range of 1.5–4 m/s [75]. Face velocity is based on the gross cross-sectional area for air flow (face area), as though the tubes were absent. Variation of airside heat to coefficient, pressure drop, and power consumption with air mass velocity is shown in Fig. 45.

Air-Side Pressure Losses, Fan Power, and Noise

The total air-side pressure loss is the sum of pressure loss through the finned-tube bundle and the pressure loss due to the fan and plenum. Bundle pressure loss is calculated from makers' test data or correlations.

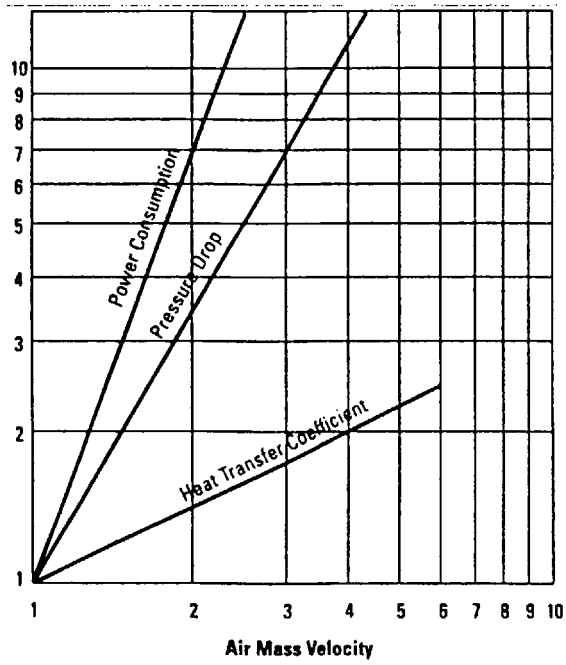


Figure 45 Variation of airside heat transfer coefficient, pressure drop, and power consumption with air mass velocity.

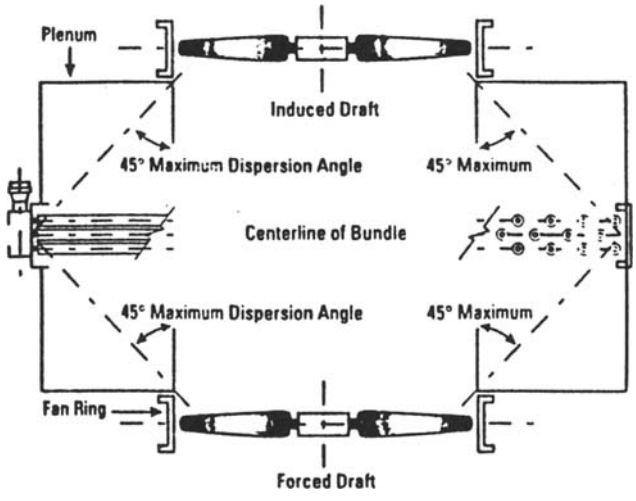


Figure 46 Condition for dispersion angle of the fan.

Capital Versus Running Cost

A total cost evaluation usually consists of the following four elements [79]:

1. Project equipment cost
2. Field installation cost
3. Electrical distribution cost
4. Operating cost

Air cooler costs are influenced by the type of air-side flow and the temperature control requirements. Those process fluids that do not require controlled outlet temperature and do not have freeze problems require minimal air flow control [77]. Consider the preferred drive and cost of horsepower, and the payback time for balancing capital investment for adding surface area, against operating costs of fan horsepower.

Design Air Temperature

The following data are needed for realistic estimates of the design air temperature [68]:

An annual temperature probability curve
Typical daily temperature curves
Duration frequency curves for the occurrence of the maximum dry-bulb temperature

Air Cooler Design Procedure

Preliminary Sizing by Brown's Method. Once the inlet temperature is known, a reliable first approximation of the cooler design may be obtained. There are several short-cut manual methods available in the literature. One such method is that of Brown [74]. Brown considers his method will establish a size within 25% of optimum. The method can be stated by the following simple steps:

First, an overall heat-transfer coefficient is assumed, depending on the process fluid and its temperature range. Approximate overall heat transfer coefficient, for air cooled heat exchangers are tabulated in Ref. 74.

Second, the air temperature rise $(t_2 - t_1)$ is calculated by the following empirical formula:

$$t_2 - t_1 = 0.005U\left(\frac{T_1 + T_2}{2} - t_1\right) \tag{135}$$

where T_1 and T_2 are hot process fluid terminal temperatures.

Third, the estimate is based on bare tubes, with a layout and fan horsepower estimated from that, so as to avoid the complexity of fin types. Approximate bare tube surface versus unit sizes are tabulated in Ref. 74.

Sizing. The procedure to follow in air cooler design includes the following steps:

1. Specify process data and identify site data.
2. Assume the layout of the tube bundle (from preliminary sizing), fin geometry, and air temperature rise.
3. Calculate film coefficients and overall heat-transfer coefficient, mean temperature difference and correction F, and surface area. Check this surface against the assumed layout.
4. If the required surface matches with the assumed layout, calculate the tube-side pressure drop and verify with the specified value.
5. If the surface area and tube-side pressure drop are verified, calculate the air-side pressure drop and fan horsepower.

Air Cooler Data Sheet

An air-cooled heat exchanger data sheet is shown in Fig. 47. It should be submitted to the vendor along with the job "specific requirements" as follows [72]:

1. Location of the plant and elevation above sea level
2. Location of the unit in the plant
3. Temperature variation due to weather conditions
4. Seismic and wind loads
5. Variations in operation
6. Process control instrumentation
7. Fire protection

DATA SHEET – AIR COOLED HEAT EXCHANGER Sheet of

1	CUSTOMER			EQUIPMENT TAG NO.		
2	PLANT LOCATION			MANUFACTURER:		
3	SERVICE					
4	SIZE			TYPE: INDUCED/FORCED DRAFT		NO. OF BAYS
5	SURFACE PER UNIT - FINNED TUBE			FT^2: BARE TUBE		FT^2
6	HEAT EXCHANGED			BTU/HR	MTD (EFF.)	°F
7	TRANSFER RATE - FINNED TUBE			BARE TUBE, SERVICE	CLEAN	BTU/HR. FT^2/°F
8	PERFORMANCE DATA					
9	TUBE SIDE					
10	FLUID CIRCULATED				GRAVITY, LIQ.	°API/SG@ 60°F
11	TOTAL FLUID ENTERING			LBS/HR	POUR POINT	°F
12		IN	OUT		BUBBLE POINT	°F
13	TEMPERATURE °F				DEW POINT	°F
14	LIQUID LBS/HR				SPECIFIC HEAT	BTU/LB °F @ °F
15	VAPOR LBS/HR, MW				LATENT HEAT	BTU/LB @ °F
16	NONCOND. LBS/HR, MW				COND. (vap./liq.)	BTU-FT/HR · FT^2 °F @ °F
17	STEAM LBS/HR				OUTLET PRESSURE	PSIG/PSIA
18	WATER LBS/HR				ALLOWABLE PRESSURE DROP	PSI
19	VISCOSITY (LIQ/VAP) cP				CALC. PRESSURE DROP	PSI
20					FOULING RESISTANCE, INSIDE	
21	AIR SIDE					
22	AIR QUANTITY		(LBS/HR) (SCFM)		ALTITUDE	FT.
23	AIR QUANTITY/FAN		ACFM		TEMPERATURE IN	°F
24	STATIC PRESSURE		INCHES OF WATER		TEMPERATURE OUT	°F
25	FACE VEL. FPM (STD)	MASS VEL.	LBS/HR FT^2		MINIMUM AMBIENT	°F
26	DESIGN · MATERIALS · CONSTRUCTION					
27	DESIGN PRESSURE PSIG		TEST PRESSURE PSIG		DESIGN TEMP.	°F
28	TUBE BUNDLE		HEADER		TUBE	
29	SIZE NO. TUBE ROWS		TYPE		MATERIAL	
30	NO./BAY		MATERIAL		ASTM SEAMLESS/WELDED	
31	ARRANGEMENT-		PASSES-NO. ARR'GMENT*		OD IN. MIN. THKNS.	IN.
32	BUNDLES IN PARALLEL IN SER.		PLUG DESIGN		NO. BUNDLE LENGTH	FT.
33	BAYS IN PARALLEL IN SER.		MATERIAL		PITCH	IN. △
34	BUNDLE FRAME		GASKET MATERIAL		FIN	
35	MISCELLANEOUS		CORROSION ALLOW. IN.		TYPE	
36	STRUCTURE MTG-PIPERACK/GRADE		SIZE INLET NOZZLE IN.		MATERIAL	
37	SURFACE PREPARATION		SIZE OUTLET NOZZLE IN.		OD IN. STOCK THKNS.	IN.
38	LOUVERS AUTO/MANUAL		RATING & FACING		NO./IN.	
39	CODE - ASME VIII STAMP - YES/NO					
40	MECHANICAL EQUIPMENT					
41	FAN		DRIVER		SPEED REDUCER	
42	MFR. & MODEL		TYPE		TYPE	
43	NO./BAY HP/FAN		NO./BAY HP/DRIVER		NO./BAY	
44	DIAMETER, FT. RPM		RPM		MODEL	
45	NO. BLADES PITCH ADJ. AUTO		ENCLOSURE		AGMA HP RATING	
46	BLADE MATERIAL ANGLE		V/PHASE/Hz		RATIO	/1
47	HUB MATERIAL		MFR.		MFR.	
48	CONTROL ACTION ON AIR FAILURE - FAN PITCH MIN./MAX.				LOUVERS OPEN/CLOSED	
49	NOTES: *GIVE TUBE COUNT OF EACH PASS WHEN IRREGULAR					
50						
51						
52	PLOT AREA PROPOSAL DWG. NO.					
53	Prepared:	Approved:	Date:	Rev.	Rev.	Rev.

Figure 47 ACHE data sheet.

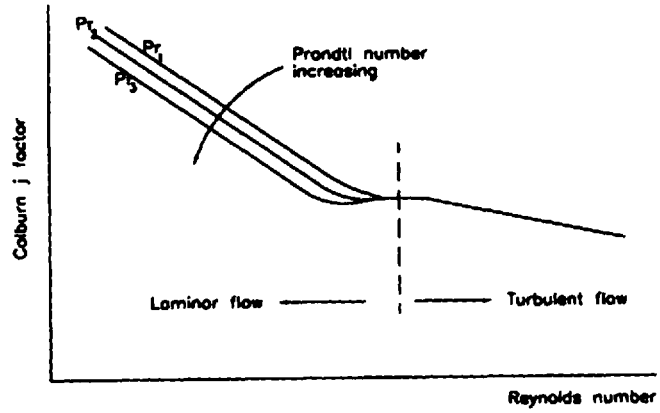


Figure 48 Typical relationship between Colburn *j* factor and Reynolds number.

8. Pumping power
9. Special surface finish

The variation of airside heat transfer coefficient, pressure drop, and power consumption with air mass velocity is shown in Fig. 45. The condition for dispersion angle of the fan is shown in Fig. 46.

Typical relationship between Colburn *j* factors and Reynolds number is shown in Fig. 48.

5
Shell and Tube Heat Exchanger Design

The most commonly used heat exchanger is the shell and tube type. It is the "workhorse" of industrial process heat transfer. It has many applications in the power generation, chemical, and process industries. Other types of heat exchangers are used when economical. Though the application of other types of heat exchangers is increasing, the shell and tube heat exchanger will continue its popularity for a long time, largely because of its versatility [1].

1 CONSTRUCTION DETAILS FOR SHELL AND TUBE EXCHANGERS

The major components of a shell and tube exchanger are tubes, baffles, shell, front head, rear head, tube sheet(s), and nozzles. Expansion joint is an important component in the case of fixed tube-sheet exchanger for certain design conditions. The selection criteria for a proper combination of these components are dependent upon the operating pressures, temperatures, thermal stresses, corrosion characteristics of fluids, fouling, cleanability, and cost. Other components include nozzles and supports. Expansion joints, nozzles, and supports are discussed in Chapter 11, Mechanical Design of Shell and Tube Heat Exchangers. A large number of geometrical variables are associated with each component and they are discussed in detail in this chapter. Major components of shell and tube heat exchangers are shown in Fig. 1.

2 TUBES

Tubes of circular cross section are exclusively used in exchangers. Since the desired heat transfer in the exchanger takes place across the tube surface, the selection of tube geometrical variables is important from the performance point of view [2]. Important tube geometrical variables include tube outside diameter, tube wall thickness, tube pitch, and tube layout patterns (Fig. 2). Tubes should be able to withstand the following:

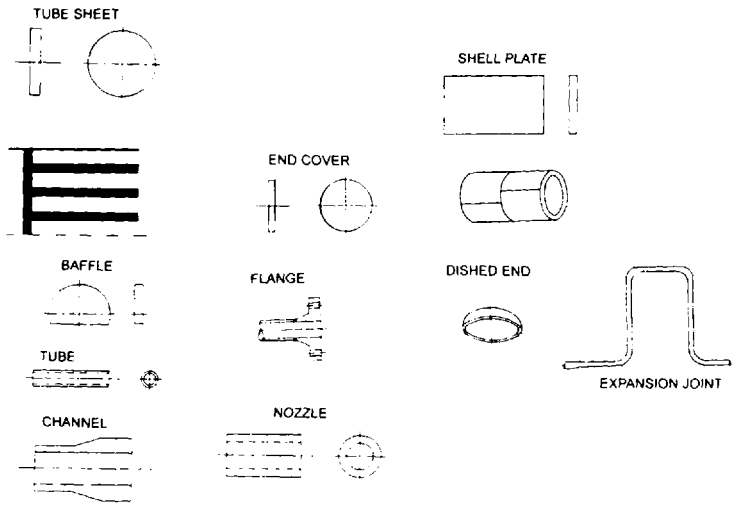


Figure 1 Major components of a shell and tube heat exchanger.

1. Operating temperature and pressure on both sides
2. Thermal stresses due to the differential thermal expansion between the shell and the tube bundle
3. Corrosive nature of both the shell-side and the tube-side fluids

There are two types of tubes: straight tubes and U-tubes. The tubes are further classified as

1. Plain tubes
2. Finned tubes
3. Duplex or bimetallic tubes
4. Enhanced surface tubes

2.1 Tube Diameter

Tube size is specified by outside diameter and wall thickness. From the heat-transfer point of view, smaller diameter tubes yield higher heat-transfer coefficients and result in a compact exchanger. However, larger diameter tubes are easier to clean, more rugged, and they are necessary when the allowable tube-side pressure drop is small. Almost all heat exchanger tubes fall within the range of $\frac{1}{4}$ in (6.35 mm)) to 2 in (5.8 mm) outside diameter. TEMA [3] tube sizes in terms of outside diameter are $\frac{1}{4}$, $\frac{3}{8}$, $\frac{1}{2}$, $\frac{5}{8}$, $\frac{3}{4}$, $\frac{7}{9}$, 1, 1.25, 1.5, and 2 in (6.35, 9.53, 12.70, 15.88, 19.05, 22.23, 25.40, 31.75, 38.10, and 50.80 mm). Standard tube sizes and gages for

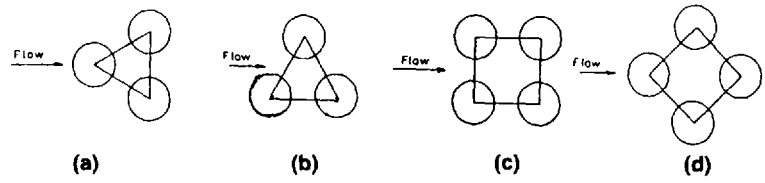


Figure 2 Tube layout patterns. (a) 30°; (b) 60°; (c) 90°; and (d) 45°.

various metals are given in TEMA Table RCB-2.21. These sizes give the best performance and are most economical in many applications. Most popular are the $\frac{3}{8}$-in and $\frac{1}{4}$-in sizes, and these sizes give the best all-around performance and are most economical in most applications [4]. Use $\frac{1}{4}$ in (6.35 mm) diameter tubes for clean fluids. For mechanical cleaning, the smallest practical size is $\frac{3}{4}$ in (19.05 mm). Tubes of diameter 1 in are normally used when fouling is expected because smaller ones are not suitable for mechanical cleaning, and falling film exchangers and vaporizers generally are supplied with 1.5- and 2-in tubes [5].

2.2 Tube Wall Thickness

The tube wall thickness is generally identified by the Birmingham wire gage (BWG). Standard tube sizes and tube wall thickness in inches are presented in TEMA Table RCB-2.21. Tube wall thickness must be checked against the internal and external pressure separately, or maximum pressure differential across the wall. However, in many cases the pressure is not the governing factor in determining the wall thickness. Except when pressure governs, the wall thickness is selected on these bases [6]: (1) providing an adequate margin against corrosion, (2) fretting and wear due to flow induced vibration, (3) axial strength, particularly in fixed tube-sheet exchangers, (4) standardized dimensions, and (5) cost.

2.3 Low-Finned Tubes

Shell and tube exchangers employ low-finned tubes (Fig. 3) to increase the surface area on the shell side when the shell-side heat-transfer coefficient is low compared to the tube-side coefficient—for example, when shell-side fluid is highly viscous liquids, gases, or condensing vapors. The low-finned tubes are generally helical or annular fins on individual tubes.

Fin tubes for a shell and tube exchanger are generally "low-fin" type with fin height slightly less than $\frac{1}{16}$ in (1.59 mm). The most common fin density range is 19–40 fins/in (748–1575 fins/m). The surface area of such a fin tube is about 2.5–3.5 times that of a bare tube [2]. The finned tube has bare ends having conventional diameters of bare tubing; the diameter of the fin is either slightly lower than or the same as the diameter of the bare ends, depending upon the manufacturer. In addition to the geometrical variables associated with bare tubes, the additional geometrical dimensions associated with a fin tube are root diameter, fin height, and fin pitch.

2.4 Tube Length

For a given surface area, the most economical exchanger is possible with a small shell diameter and long tubes, consistent with the space and the availability of handling facilities at site and in the fabricator's shop [6]. Therefore, minimum restrictions on length should be observed.

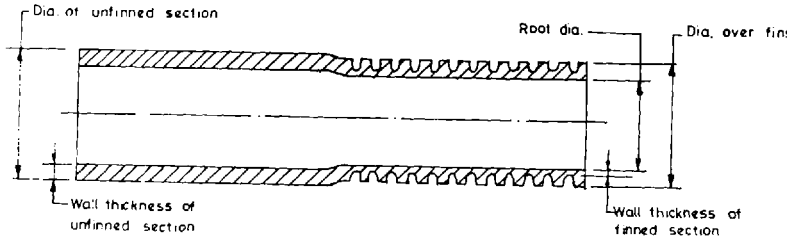


Figure 3 Low finned tube.

However, for offshore applications, long exchangers, especially with removable bundles, are often very difficult to install and maintain economically because of space limitations [7]. In this case, shorter and larger shells are preferred despite their higher price per unit heat-transfer surface. Standard lengths as per TEMA standard RCB-2.1 are 96, 120, 144, 196, and 240 in. Other lengths may be used.

2.5 Means of Fabricating Tubes

Tubing used for heat exchanger service may be either welded or seamless. The welded tube is rolled into cylindrical shape from strip material and is welded automatically by a precise joining process. A seamless tube may be extruded or hot pierced and drawn. Copper and copper alloys are available only as seamless products, whereas most commercial metals are offered in both welded and seamless. More details on tubing are given in the Chapter 13, Material Selection and Fabrication.

2.6 Duplex or Bimetallic Tubes

Duplex or bimetallic tubes are available to meet the specific process problem pertaining to either the shell side or the tube side. For example, if the tube material is compatible with the shell-side fluid, but not compatible with the tube-side fluid, a bimetallic tube allows it to satisfy both the corrosive conditions.

2.7 Number of Tubes

The number of tubes depends upon the fluid flow rate and the available pressure drop. The number of tubes is selected such that the tube-side velocity for water and similar liquids range from 3 to 8 ft/s (0.9–2.4 m/s) and the shell-side velocity from 2 to 5 ft/s (0.6–1.5 m/s) [2]. The lower velocity limit is desired to limit fouling; the higher velocity is limited to avoid erosion–corrosion on the tube side, and impingement attack and flow-induced vibration on the shell side. When sand, silt, and particulates are present, the velocity is kept high enough to prevent settling down.

2.8 Tube Count

To design a shell and tube exchanger, one must know the total number of tubes that can fit into the shell of a given inside diameter. This is known as tube count. Factors on which the tube count depends are discussed in Ref. 6 and in Phadke [8] and Whitley et al. [9]. Such factors include the following:

Shell diameter
Outside diameter of the tubes
Tube pitch
Tube layout pattern—square, triangular, rotated square, or rotated triangular
Clearance between the shell inside diameter and the tube bundle diameter
Type of exchanger, i.e., fixed tube sheet, floating head, or U-tube
Number of tube-side passes
Design pressure
Nozzle diameter
Tie rods and sealing devices that block space
Type of channel baffle, i.e., ribbon, pie shape, vertical, etc. [9].

The conventional method of obtaining tube count by plotting the layout and counting the tubes (thus the tube count) is cumbersome, time-consuming, and prone to error. Tables of tube count are available in references like Ref. 10, and Saunders [11], Escoe [12], and others, which often cover only certain standard combinations of pitch, tube diameter, and layout parameters. A mathematical approach using number theory is suggested by Phadke [8] to predict the tube count and presented tube count for various combinations of tube layout parameters. His method eliminates the disadvantages of drawing the tube layout pattern and can accommodate any configuration.

2.9 U-Bend Requirements as per TEMA

When U-bends are formed, it is normal for the tube wall at the outer radius to thin. As per TEMA section RCB-2.33, the minimum tube wall thickness in the bent portion before bending shall be [3]:

$$t_o = t_1 \left(1 + \frac{d}{4R_b}\right) \tag{1}$$

where t_o is the original tube wall thickness, t_1 the minimum tube wall thickness calculated by Code rules for a straight tube subjected to the same pressure and metal temperature, d the tube outer diameter, and R_b the mean radius of bend.

3 TUBE ARRANGEMENT

3.1 Tube Pitch

The selection of tube pitch is a compromise between a close pitch for increased shell-side heat transfer and surface compactness, and a larger pitch for decreased shell-side pressure drop and fouling, and ease in cleaning. In most shell and tube exchangers, the minimum ratio of tube pitch to tube outside diameter (pitch ratio) is 1.25. The minimum value is restricted to 1.25 because the tube-sheet ligament (a ligament is the portion of material between two neighboring tube holes) may become too weak for proper rolling of the tubes into the tubesheet. The ligament width is defined as the tube pitch minus the tube hole diameter; this is shown in Fig. 4.

3.2 Tube Layout

Tube layout arrangements are designed so as to include as many tubes as possible within the shell to achieve maximum heat transfer area. Sometimes a layout is selected that also permits

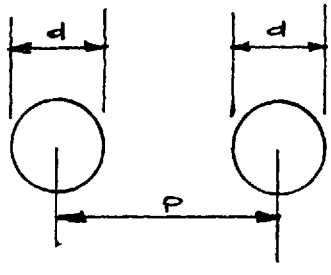


Figure 4 Tube pitch and ligament width.

access to the tubes for cleaning as required by process conditions. Four standard types of tube layout patterns are triangular (30°), rotated triangular (60°), square (90°), and rotated square (45°). (Note that the tube layout angle is defined in relation to the flow direction and is not related to the horizontal or vertical reference line arrangement, and that the 30°, 60°, and 45° arrangements are "staggered," and 90° is "in-line.") For identical tube pitch and flow rates, the tube layouts in decreasing order of shell-side heat-transfer coefficient and pressure drop are 30°, 45°, 60°, and 90°. Thus the 90° layout will have the lowest heat-transfer coefficient and pressure drop. The selection of the tube layout pattern depends on the following parameters, which influence the shell-side performance and hence the overall performance:

1. Compactness
2. Heat transfer
3. Pressure drop
4. Accessibility for mechanical cleaning
5. Phase change if any on the shell side

Triangular and Rotated Triangular Arrangements

Triangular and rotated triangular layouts (30° and 60°) provide a compact arrangement, better shell-side heat-transfer coefficients, and stronger tube sheets for a specified shell-side flow area. For a given tube pitch/outside diameter ratio, about 15% more tubes can be accommodated within a given shell diameter using these layouts [6]. These layout patterns are satisfactory for clean services, but have the disadvantage of making the lanes between tubes rather inaccessible for mechanical cleaning. It is difficult to insert a rigid tool between the tubes. Only chemical cleaning or water jet cleaning is possible.

Square and Rotated Square Arrangements

When mechanical cleaning is necessary on the shell side, 45° and 90° layouts must be used with a minimum gap between tubes of 6.35 mm. There is no theoretical limit to tube outer diameter for mechanical cleaning, but the 6.35 mm clearance limits the tubes to a minimum of $\frac{5}{8}$ or $\frac{3}{4}$ in outer diameter in practice [7]. The square pitch is generally not used in the fixed tube-sheet design because of no need of mechanical cleaning on the shell side. These layout patterns offer lower pressure drops and lower heat-transfer coefficients than triangular pitch. The 45° layout is preferred for single-phase laminar flow or fouling service, and for condensing fluid on the shell side. Shah [2] suggests a square layout for the following applications:

1. If the pressure drop is a constraint on the shell side, the 90° layout is used for turbulent flow, since in turbulent flow the 90° has superior heat-transfer rate and less pressure drop.
2. For reboilers, a square layout will be preferred for stability reasons. The 90° layout provides vapor escape lanes.

4 BAFFLES

Baffles must generally be employed on the shell-side to support the tubes, to maintain the tube spacing, and to direct the shell-side fluid across or along the tube bundle in a specified manner. There are a number of different types of baffles and these may be installed in different ways to provide the flow pattern required for a given application.

4.1 Classification of Baffles

Baffles are either normal or parallel to the tubes. Accordingly, baffles may be classified as transverse or longitudinal. The transverse baffles direct the shell-side fluid into the tube bundle

at approximately right angles to the tubes, and increase the turbulence of the shell fluid. Every shell and tube exchanger has transverse baffles except the X and K shells, which have only support plates. The longitudinal baffles are used to control the direction of the shell side flow. For example, F, G, and H shells have longitudinal baffles. In the F shell, an overall counterflow is achieved.

4.2 Transverse Baffles

Transverse baffles are of two types: (1) plate baffles and (2) rod baffles. Three types of plate baffles are (1) segmental, (2) disk and doughnut, and (3) orifice baffles.

Segmental Baffles

The segmental baffle is a circular disk (with baffle holes) having a segment removed. Predominantly, a large number of shell and tube exchangers employ segmental baffles. This cutting is denoted as the baffle cut and it is commonly expressed as a percentage of the shell inside diameter as shown in Fig. 5. Here the percent baffle cut is the height, H, given as a percentage of the shell inside diameter, D_s. The segmental baffle is also referred to as a single segmental baffle. The heat transfer and pressure drop of crossflow bundles are greatly affected by the baffle cut. The baffle cuts vary from 20 to 49% with the most common being 20–25%, and the optimum baffle cut is generally 20%, as it affords the highest heat transfer for a given pressure drop. Baffle cuts smaller than 20% can result in high pressure drop. As the baffle cut increases beyond 20%, the flow pattern deviates more and more from crossflow [5] and can result in stagnant regions or areas with lower flow velocities; both of these reduce the thermal effectiveness of the bundle [1].

Baffle Spacing. The practical range of single-segmental baffle spacing is $\frac{1}{5}$ to 1 shell diameter [1], though optimum could be 40–50% [2]. TEMA Table RCB-4.52 [3] provides maximum baffle spacing for various tube outer diameters, tube materials, and the corresponding maximum allowable temperature limit. The baffles are generally spaced between the nozzles. The inlet and outlet baffle spacings are in general larger than the "central" baffle spacing to accommodate the nozzles, since the nozzle dimensions frequently require that the nozzle should be located far enough from the tube sheets.

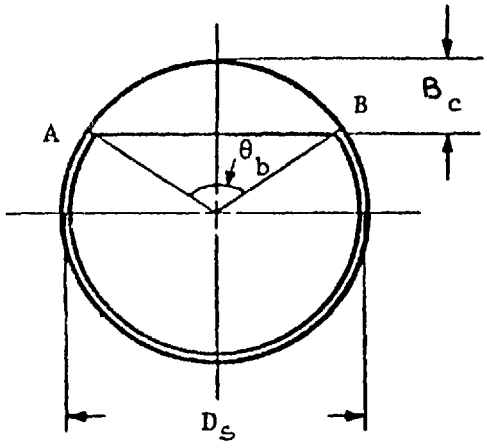


Figure 5 Baffle cut.

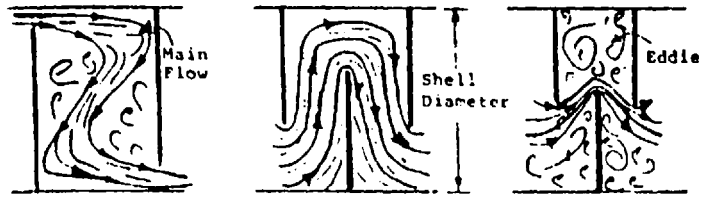


Figure 6 Shellside flow distribution influenced by baffle cut, Ref. (13).

Baffle Thickness. TEMA Tables R-4.41 and CB-4.41 [3] provide the minimum thickness of transverse baffles applying to all materials for various shell diameters and plate spacings.

Shell-Side Flow Distribution. Segmental baffles have a tendency to poor flow distribution if spacing or baffle cut ratio is not in correct proportion, as shown in Fig. 6 [13]. Too low or too high a ratio results in maldistribution and produces inefficient heat transfer and also favors fouling. For low-pressure-drop designs, choose baffles that ensure a more uniform flow such as multisegmental, disc and doughnuts, and rod baffles.

Orientation of Baffles. Alternate segmental baffles are arranged at 180° to each other, which cause shell-side flow to approach crossflow through the bundle and axial flow in the baffle window zone. All segmental baffles shown in Fig. 7a have horizontal baffle cuts. Unless the shell-side fluid is condensed, the horizontal baffle cut should be used for single-phase application, to reduce accumulation of deposits on the bottom of the shell and to prevent stratification of the shell-side fluid [5]. The direction of the baffle cut is selected as vertical (Fig. 7b) for the following shell-side applications [6]: (1) for condensation, to allow the condensate to flow freely to the outlet without covering an excessive amount of tubes [2,5]; (2) for boiling or condensing fluids, to promote more uniform flow; and (3) for solids entrained in liquid (to provide least interference for the solids to fall out).

Double Segmental and Multiple Segmental Baffles

Various multisegmental baffles can be used to reduce baffle spacing, or to reduce crossflow because of pressure limitations. The multisegmental baffles are characterized by large open areas and some allow the fluid to flow nearly parallel to the tubes, offering a much lower pressure drop [14].

Segmental baffle layout is shown in Fig. 8 and flow distribution in Fig. 9. In an exchanger with single segmental baffles the total flow, except for leakages and bypass streams, passes through the tube bank between baffles in crossflow as shown in Fig. 9a, whereas with double

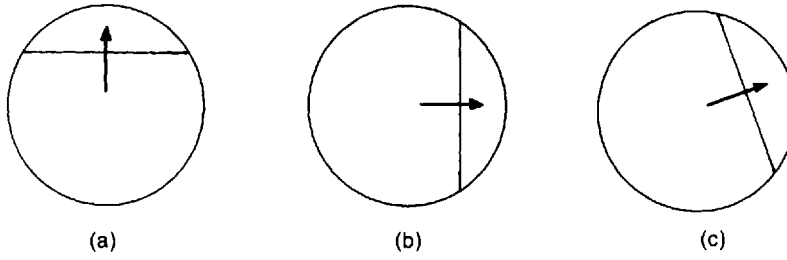


Figure 7 Baffle cut orientation: (a) horizontal; (b) vertical; and (c) rotated.

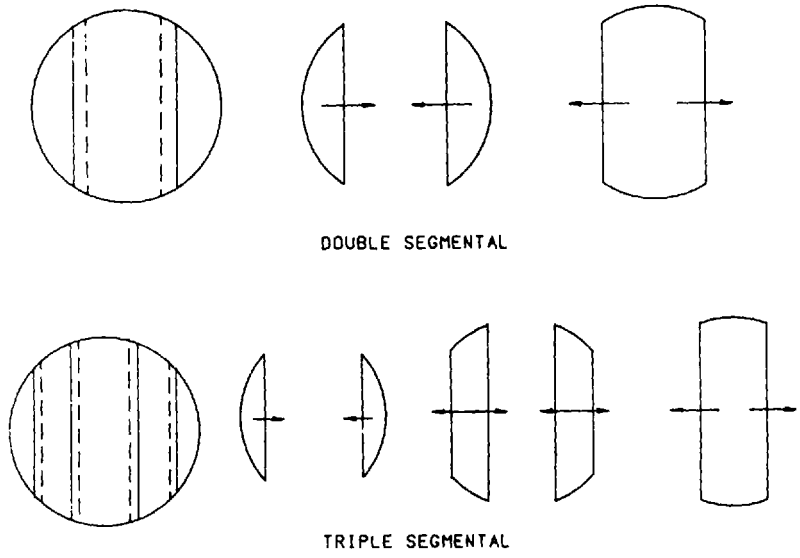


Figure 8 Segmental baffles layout: double and triple segmental with end view flow pattern.

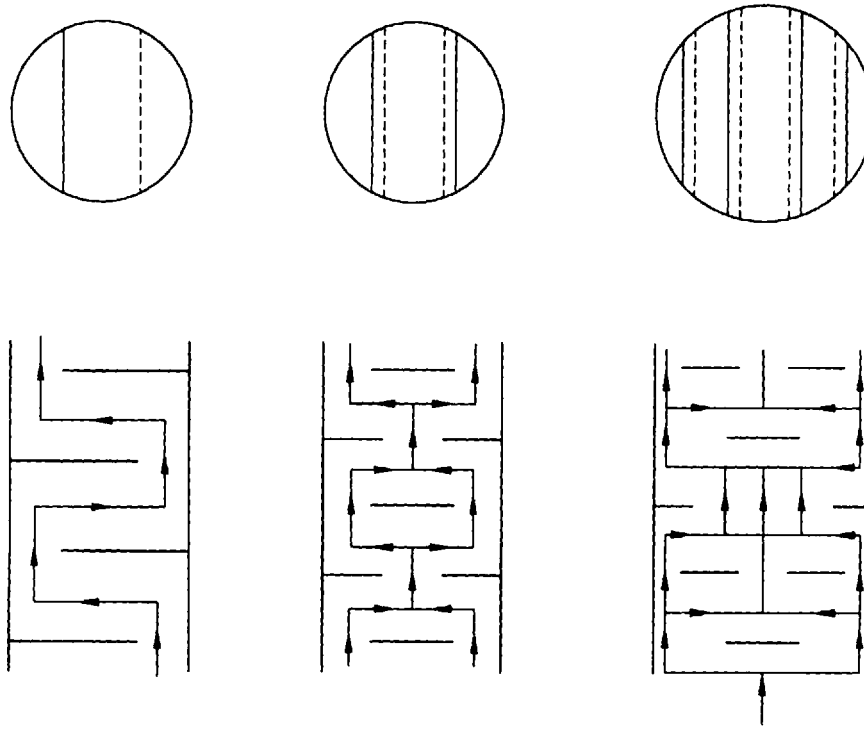


Figure 9 Flow pattern with segmental baffles.

segmental baffles barring the leakages, the flow divides into two streams on either side of the shell (Fig. 9b), and in triple segmental baffles, the flow divides into three streams (Fig. 9c). Due to this, heat exchangers with double or multiple segmental baffles can handle larger fluid flows on the shell side. Other features of double segmental or multiple segmental baffles are as follows [2]:

1. The flow on the shell side is split into two or more streams as per the number of baffle segments, namely, double, triple, multiple, etc.; hence, the danger of shell-side flow-induced vibration is minimal.
2. The baffle spacing should not be too small; otherwise it results in a more parallel (longitudinal) flow with significant low stagnant areas.

Window Baffles

These are considered when crossflow is not practical because of pressure drop limitations. Window baffles (Fig. 10) allow the fluid to flow parallel to the tubes, offering much lower pressure drop [5].

4.3 Disk and Doughnut Baffle

The disk and doughnut baffle is made up of alternate "disks" and "doughnut" baffles as shown in Fig. 11a. Disk and doughnut baffle heat exchangers are primarily used in nuclear heat exchangers [2]. This baffle design provides a lower pressure drop compared to a single segmental baffle for the same unsupported tube span, and eliminates the tube bundle to shell bypass stream.

4.4 Orifice Baffle

In an orifice baffle, the tube-to-baffle hole clearance is large so that it acts as an orifice for the shell-side flow (Fig. 11b). These baffles do not provide support to tubes, and, due to fouling, the annular orifices plug easily and cannot be cleaned. This baffle design is rarely used.

4.5 NTIW

The baffle cut area, or baffle window region, is generally filled with tubes. Since the tubes in the window zone are supported at a distance of two times the central baffle spacing, they are most susceptible to vibration. To eliminate the susceptibility of tube vibrations, the tubes in the window zone are removed and therefore all tubes pass through all baffles. Additional support plates are introduced between main baffles to reduce the unsupported span of the tubes

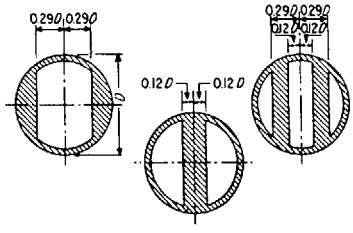


Figure 10 Window baffles [5].

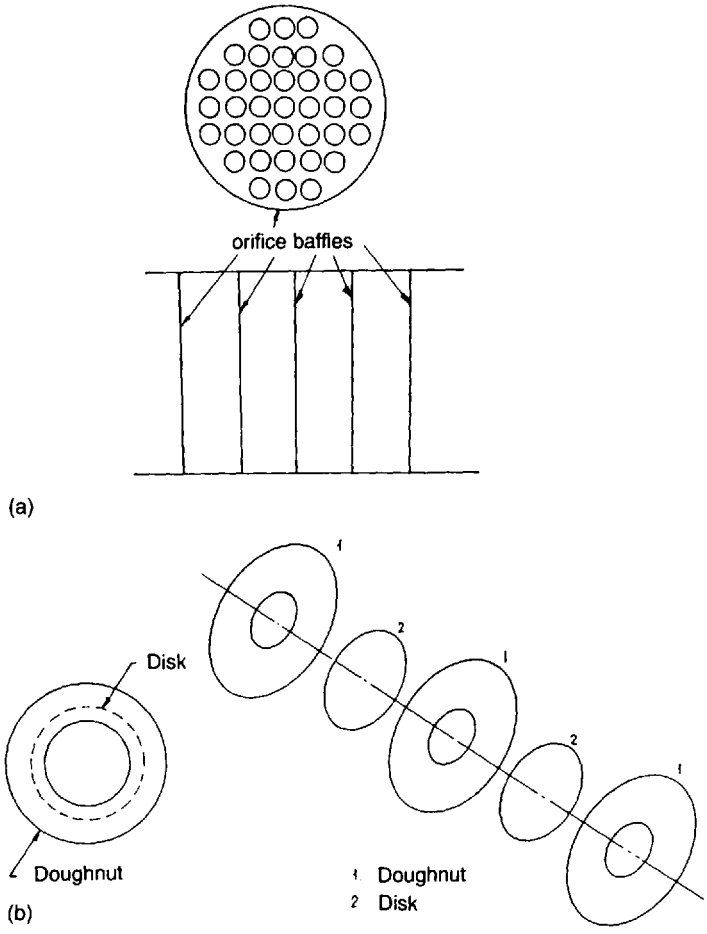


Figure 11 Nonsegmental circular baffles. (a) Orifice baffle, and (b) disk and doughnut baffles.

as shown in Fig. 12, thus providing an increase in the natural frequency of the tubes. The resultant design is referred to as the segmental baffle with no-tubes-in-window (NTIW) design. NTIW design has the following characteristics [15]:

1. Pressure drop about one-third that of single segmental baffle design.
2. Uniform shell-side flow pattern resembling that of an ideal tube bank, which offers high shell-side heat-transfer coefficient and low fouling tendency.

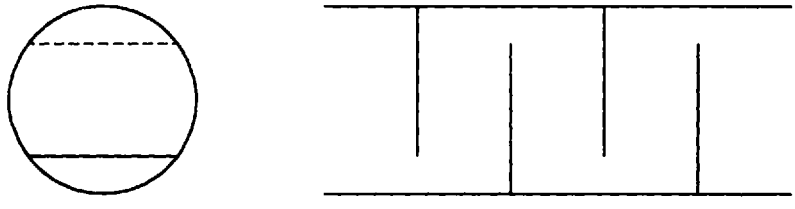


Figure 12 No tube in window design (NTIW).

3. The baffle cut and number of tubes removed varies from 15 to 25%.
4. Very low pressure drop in the window and correspondingly lower bypass and leakage streams.

Since the loss in heat transfer surface is considerable in an NTIW design, this can be minimized by having small baffle cuts and possibly by an increase in the shell-side fluid velocity or larger shell diameter to contain the same number of tubes.

4.6 Longitudinal Baffles

Longitudinal baffles divide the shell into two or more sections, providing multipass on the shellside. But this type should not be used unless the baffle is welded to the shell and tube sheet. Nevertheless, several sealing devices have been tried to seal the baffle and the shell, but none has been very effective [5]. Gupta [16] lists some sealing devices that are used to seal the baffle and shell. They are:

Sealing strips or multiflex arrangement
Packing arrangement
Slide-in or tongue-and-groove arrangement

If the baffle is not welded, bypassing occurs from one side to the other, which adversely affects the heat-transfer coefficient and makes its accurate prediction rather difficult. Hence, it is better to weld than to prefer this design. Common methods to weld the longitudinal baffle to the shell side are shown in Fig. 13 [17]. When multipass shells are required, it is economical to use a separate shell, unless the shell diameter is large enough to easily weld a longitudinal baffle to the shell [5].

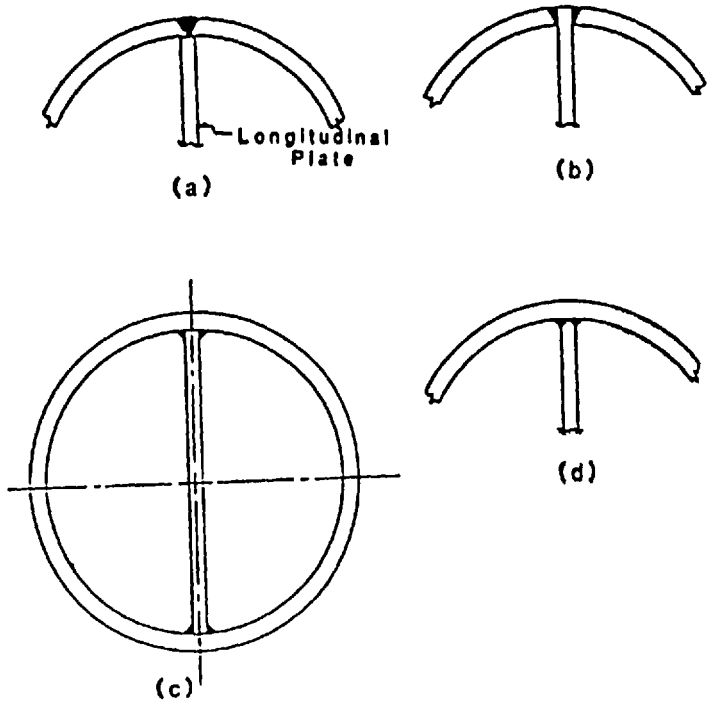


Figure 13 Longitudinal baffle weld joint. [From Ref. 17.]

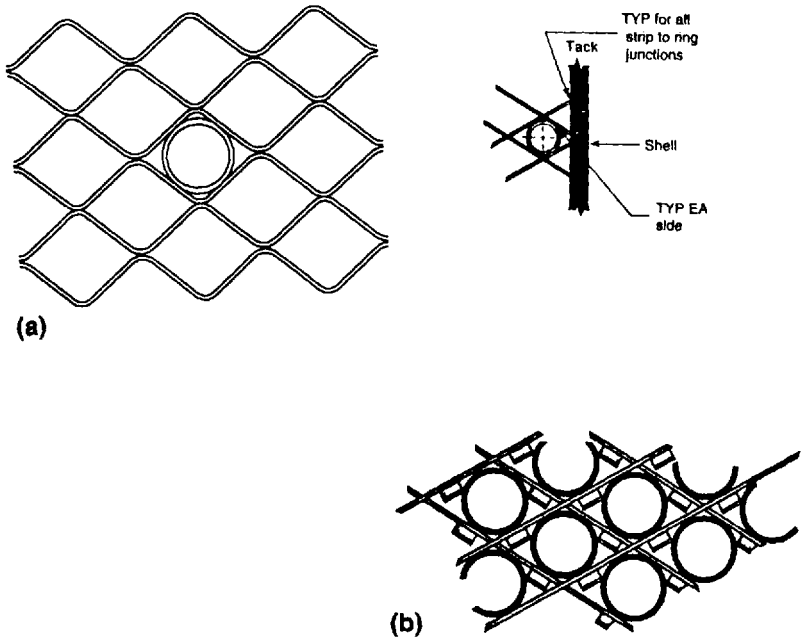


Figure 14 Special types of plate baffles. (a) NEST™; and (b) egg-crate baffle support.

4.7 Rod Baffles

Phillips RODbaffle design uses alternate sets of rod grids instead of plate baffles, enabling the tubes to be supported at shorter intervals without resulting in a large pressure drop. Flow-induced vibration is virtually eliminated by this design. The flow is essentially parallel to tube axis; as a result of the longitudinal flow, it has low pressure drop to heat transfer conversion characteristics. The tube layout is usually 45° or 90°. Design of rod baffle heat exchanger is covered separately.

4.8 NEST Baffles and Egg-crate Tube Support

This is a patented design intended to overcome the danger of flow-induced vibration of tubes. In this design, each tube rests in a V-shaped cradle and is supported at line segments (Fig. 14). These elements are preformed to the desired tube pitch and ligament size. The flow is parallel to the tube bundle, and hence the vibration problem is greatly reduced [18]. It is claimed that the pressure drop is lower for the same amount of heat transfer compared to a segmentally baffled exchanger.

EGG-CRATE-GRID™ support (Fig. 14b) is a simple and economical support for heat exchanger tubes, which can droop or collapse under stress and elevated temperature. This support is fabricated from commercial flat strip material, typically of stainless steel; strip ends are tack welded to the heat exchanger shell and tubes are welded to strips at specified intervals. This design eliminates conventional tubesheets, which require tube insertion through drilled holes.

4.9 Grimmas Baffle

The Grimmas baffle is a patented version of the plate baffle, which ensures an axial flow and improves heat transfer [19]. The design is shown in Fig. 15.

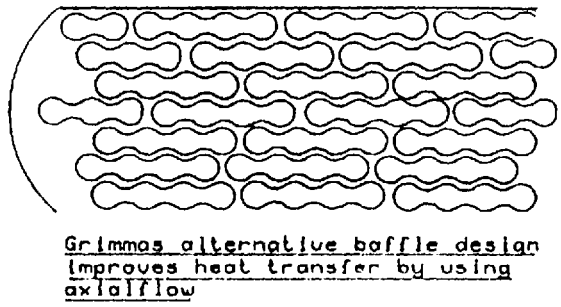


Figure 15 Grimmas baffle. (From Ref. 19.)

5 TUBE SHEET

A tube sheet is an important component of a heat exchanger. It is the principal barrier between the shell-side and tube-side fluids. Proper design of a tube sheet is important for safety and reliability of the heat exchanger. Tube sheets are mostly circular with uniform pattern of drilled holes. Tube sheets of surface condensers are rectangular shape. Tube sheets are connected to the shell and the channels either by welds (integral) or with bolts (gasketed joints) or with a combination thereof. Tube-sheet connection with the shell and channel for fixed tube-sheet exchanger can be categorized into two types:

1. Both sides integral construction,
2. Shell-side integral and tube-side gasketed construction

Tube-sheet connection with the shell and channel for floating heat exchanger and U-tube heat exchangers can be categorized into three types:

1. Both sides integral construction
2. One side integral and the other side gasketed construction
3. Both sides gasketed construction

Possible tube-sheet connections with the shell and the channel are shown in Fig. 16 [20].

5.1 Tube to Tube-Sheet Attachment

Tubes are attached to the tube sheet by (1) rolling, (2) welding, (3) rolling and welding, (4) explosive welding, and (5) brazing. Schematic sketches of tube to tube-sheet attachment are given in Chapter 15. Expansion of the tubes into the tube sheet is most widely used and is satisfactory for many services. However, when stresses are higher, or where pressures are such that significant leakage could occur, or where contamination between fluids is not permitted, the tubes are welded to the tube sheet. Explosion welding can be used instead of conventional welding where there is incompatibility between tube and tube-sheet materials and for tube plugging under hazardous conditions.

5.2 Double Tube Sheets

No known method of making tube to tube-sheet joints can completely eliminate the possibility of mixing of shell-side and tube-side fluids due to leakage. When the possibility of intermixing

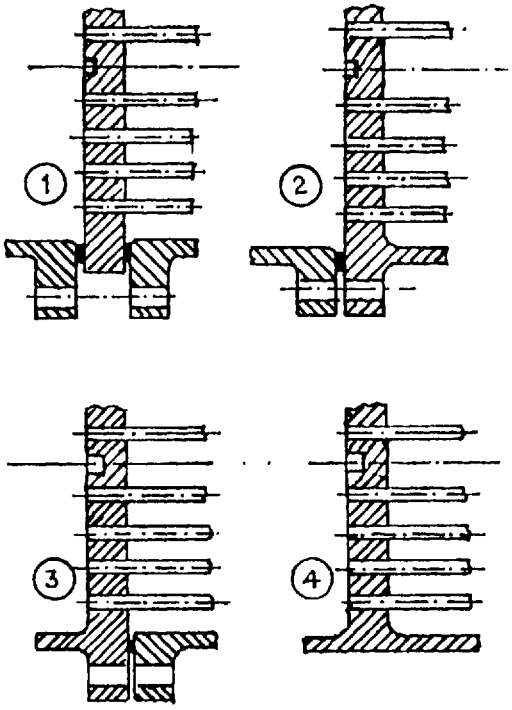


Figure 16 Tubesheet connection with shell and channel. (Note: 2 and 4 refer to fixed tubesheet design.)

of the shell-side and tube-side fluids cannot be tolerated, double tube-sheet construction will offer positive assurance against one fluid leaking into the other at a tube to tube-sheet joint.

Types of Double Tube-Sheets Designs

Two designs of double tube sheets are available: (1) the conventional double tube sheet design, which consists of two individual tube sheets at each end of the tubes, and (2) the integral double tube-sheet design [21].

Conventional Double Tube Sheet Design

In a conventional double tube-sheet design, the tube sheets are installed with a small space between them. The space is usually open to the atmosphere. Sometimes a thin strip is welded to avoid ingress of dusts and dirt, or an expansion joint is welded with vent at the top and a drain at the bottom. These patterns are shown in Fig. 17. While selecting material for double tubesheet design, the outer tubesheet should be compatible with the tubeside fluid and the inner tubesheet should be compatible with the shellside fluid. The most important consideration is the differential radial expansion of the two tubesheets which will stress the tubes. The double tube sheet can be installed only in the U-tube, fixed tube sheet, and floating head, outside packed stuffing box exchangers. It is not feasible to use the double tube sheet in heat exchanger types such as [4] (1) floating head, pull-through bundle, (2) floating head with split backing ring, and (3) floating head, outside packed lantern ring exchangers. An expression for the space between the tubesheets pairs, l_g, which is widely used in the industry is a special case of the more complex analysis of Urgami et al. [22]. The expression is given by [21]:

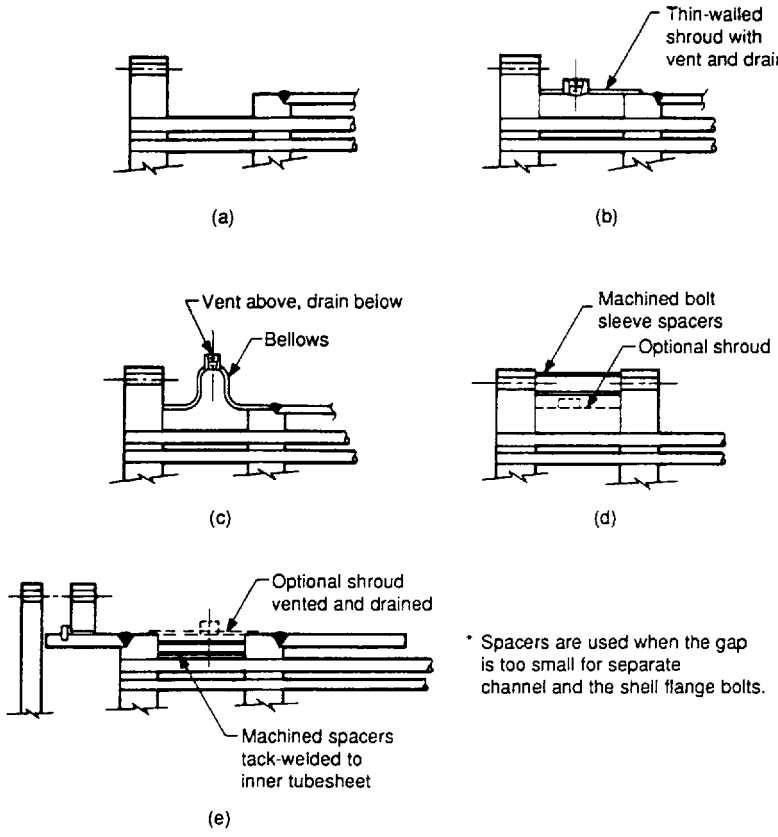


Figure 17 Conventional double tubesheet constructions. (a) Fixed tube sheet with open gap; (b) fixed tube sheet with light gauge vented and drained, and shroud around gap; (c) fixed tube sheet with bellows in light gauge shroud, vent and drain in bellows; (d) stationary-end removable bundle preferred construction; and (e) packed floating head end. (From Ref. 21.)

$$l_g = \sqrt{\frac{1.5E_t d\delta}{S_t}} \tag{2}$$

where δ is the free differential in-plane movement in inches (mm) given by

$$\delta = D_{otl/2}[\alpha_h(T_h - T_{amb}) - \alpha_c(T_c - T_{amb})] \tag{3}$$

and where d is the tube outer diameter, inches (mm); E_t is Young's modulus for the tube, psi (Pa); D_{otl} is the tube outer limit, inches (mm); T_{amb} the ambient (assembly) temperature, °F (°C); T_c the temperature of the colder tube sheet, °F (°C); T_h the temperature of the hotter tube sheet, °F(°C); α_c the coefficient of thermal expansion of the colder tube sheet between the assembly temperature and temperature T_c, in/(in · °F) [mm/(mm · °C)]; α_h the coefficient of thermal expansion of the hotter tube sheet between the assembly temperature and temperature T_h, in/(in · °F) [mm/(mm · °C)]; and S_t the allowable stress in the tubes, psi (Pa).

The provision of a double tube sheet has been mandatory for United Kingdom power-station condensers in past years to eliminate any possibility of cooling water entering the steam space of the condenser [23]. The tube-sheet interspace is drained to a low-level vessel, which

is maintained at the condenser absolute pressure by means of a connection to the air pump suction line.

5.3 Integral Double Tube Sheets

The patented integral double tube-sheet design consists of a single tube sheet made from a single plate or forging, drilled to the desired tube layout pattern. Then the annular grooves are machined into the tube holes about midway between the faces to interconnect the adjacent tubes (Fig. 18). This construction in effect minimizes differential expansion problems, but it is expensive and not effective like conventional double tube sheets to avoid fluid mixing [24].

5.4 Demerits of Double Tube Sheets

If at all practical, double tube sheets should be avoided. However, some conditions dictate their use along with the problems such as [24]:

1. Wasted tube surface.
2. Increased fabrication cost due to additional drilling and rolling requiring special equipment.
3. Differential radial expansion. This limits the length of the gap between the tube sheets to prevent over stressing the tubes in bending or shear. Very short gaps can result in outer tubes being sheared off at the tubesheet face.
4. Differential longitudinal expansion. (This is a problem if the tube sheets are restrained across the gap and increases as the gap increases.)
5. All conditions of startup, shutdown, and steam out (in the case of condenser) must be considered since they will generally be more severe on the double tube-sheet section than in the operating condition.

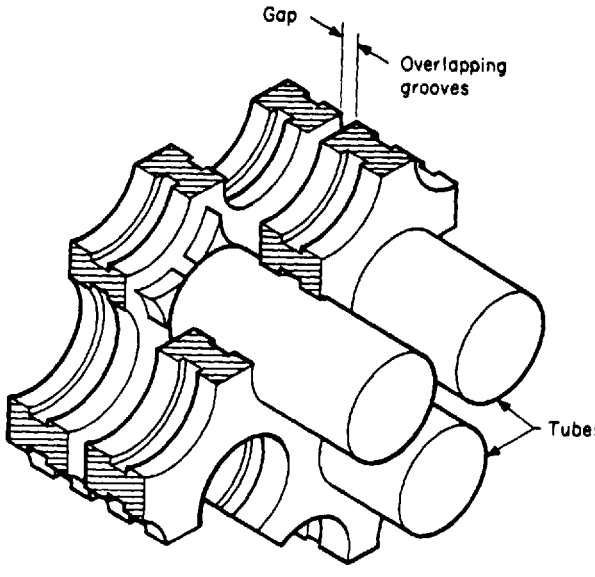


Figure 18 Integral double tubesheet. (From Ref. 21.)

6 TUBE BUNDLE

A tube bundle is an assembly of tubes, baffles, tube sheets, spacers and tie rods, and longitudinal baffles, if any. Spacers and tie rods are required for maintaining the space between baffles. Refer to TEMA for details on spacers and tie rods.

6.1 Bundle Weight

The maximum bundle weight that can conveniently be pulled should be specified and should allow for the buildup of fouling and scaling deposits. Offshore applications are particularly sensitive to weight.

6.2 Spacers, Tie Rods, and Sealing Devices

The tube bundle is held together and the baffles located in their correct positions by a number of tie rods and spacers. The tie rods are screwed into the stationary tube sheet and extend the length of the bundle up to the last baffle, where they are secured by lock nuts. Between baffles, tie rods have spacers fitted over them. Tie rods and spacers may also be used as a sealing device to block bypass paths due to pass partition lanes or the clearance between the shell and the tube bundle.

6.3 Outer Tube Limit

The outer tube limit (OTL) is the diameter of the largest circle, drawn around the tube-sheet center, beyond which no tube may encroach.

7 SHELLS

Heat exchanger shells are manufactured in a large range of standard sizes, materials, and thickness. Smaller sizes are usually fabricated from standard size pipes. Larger sizes are fabricated from plate by rolling. The cost of the shell is much more than the cost of the tubes; hence a designer tries to accommodate the required heat-transfer surface in one shell. It is found that a more economical heat exchanger can usually be designed by using a small diameter shell and the maximum shell length permitted by such practical factors as plant layout, installation, servicing, etc. [4]. Nominal shell diameter and shell thickness are furnished in TEMA Tables R-3.13 and CB-3.13 [3].

8 PASS ARRANGEMENTS FOR FLOW THROUGH TUBES

The simplest flow pattern through the tubes is for the fluid to enter at one end and exit at the other. This is a single-pass tube arrangement. To improve the heat-transfer rate, higher velocities are preferred. This is achieved by increasing the number of tube-side passes. The number of tube passes depends upon the available pressure drop, since higher velocity in the tube results in higher heat-transfer coefficient, at the cost of increased pressure drop. Larowski et al. [7] suggests the following guidelines for tube-side passes:

1. Two-phase flow on the tube side, whether condensing or boiling, is best kept in a single straight tube run or in a U-tube.
2. If the shell-side heat-transfer coefficient is significantly lower than on the tube side, it is not advisable to increase the film coefficient on the tube side at the cost of higher tube-side pressure drop, since this situation will lead to a marginal improvement in overall heat-transfer coefficient.

8.1 Number of Tube Passes

The number of tube-side passes generally ranges from one to eight. The standard design has one, two, or four tube passes. The practical upper limit is 16. Maximum number of tubeside passes are limited by workers' abilities to fit the pass partitions into the available space and the bolting and flange design to avoid interpass leakages on the tubeside. In multipass designs, an even number of passes is generally used; odd numbers of passes are uncommon, and may result in mechanical and thermal problems in fabrication and operation. Partitions built into heads known as partition plates control tube-side passes. This is shown schematically in Fig. 19. The pass partitions may be straight or wavy rib design.

There are some limitations on how the different types of heat exchangers can be partitioned to provide various number of passes. They are summarized here.

1. Fixed tube-sheet exchanger—any practical number of passes, odd or even. For multipass arrangements, partitions are built into both front and rear heads.
2. U-tube exchanger—minimum two passes; any practical even number of tube passes can be obtained by building partition plates in the front head.
3. Floating head exchangers:

   With pull through floating head (T head) type and split backing ring exchanger (S head), any practical even number of passes is possible. For single-pass operation, however, a packed joint must be installed on the floating head.

   With outside packed floating head type (P head), the number of passes is limited to one or two.

   With externally sealed floating tubesheet (W head), no practical tube pass limitation.

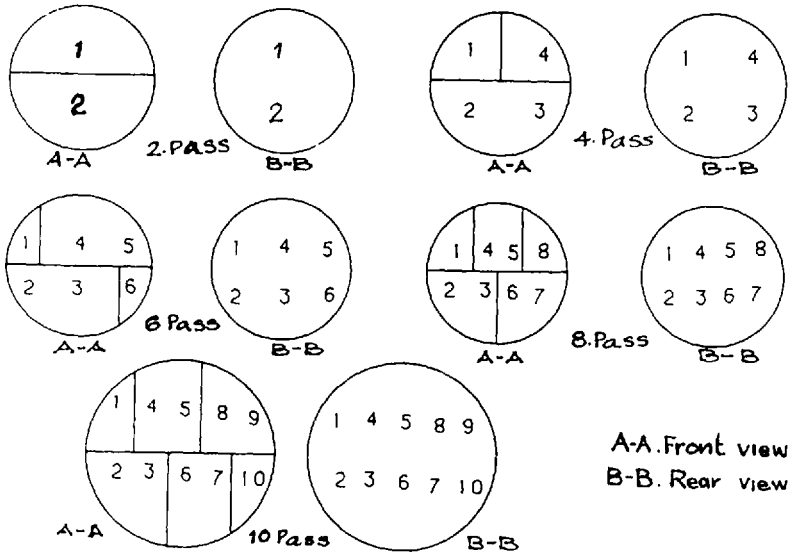
4. Two-phase flow on the tube side, whether condensing or boiling, is best kept within a single pass or in U-tubes to avoid uneven distribution and hence uneven heat transfer.

8.2 Shell-Side Passes

For exchangers requiring high effectiveness, multipassing is the only alternative. Shell-side passes could be made by the use of longitudinal baffles. However, multipassing on the shell with longitudinal baffles will reduce the flow area per pass compared to a single pass on the shell side. This drawback is overcome by shells is series, which is also equivalent to multipassing on the shell side. For the case of the overall direction of two fluids in counterflow, as the number of shell-side passes is increased to infinity (practically above four), its effectiveness approaches that of a pure counterflow exchanger. In heat recovery trains and some other applications, up to six shells in series are commonly used.

9 OTHER COMPONENTS

Since the shell-side fluid is at a different temperature than the tube-side fluid, there will be a corresponding difference in the expansion of shell and tube. If the temperature difference is high, the differential thermal expansion will be excessive, and hence the thermal stresses induced in the shell and the tube bundle will be high. This is particularly true for fixed tube-sheet exchangers. In fixed tube-sheet exchangers, the differential thermal expansion problem is overcome by incorporating an expansion joint into the shell. For U-tube exchangers and floating head exchangers, this is taken care of by the inherent design. Types of expansion joints, selection procedure, and design aspects are discussed in Chapter 11, Mechanical Design of Shell and Tube Heat Exchangers.



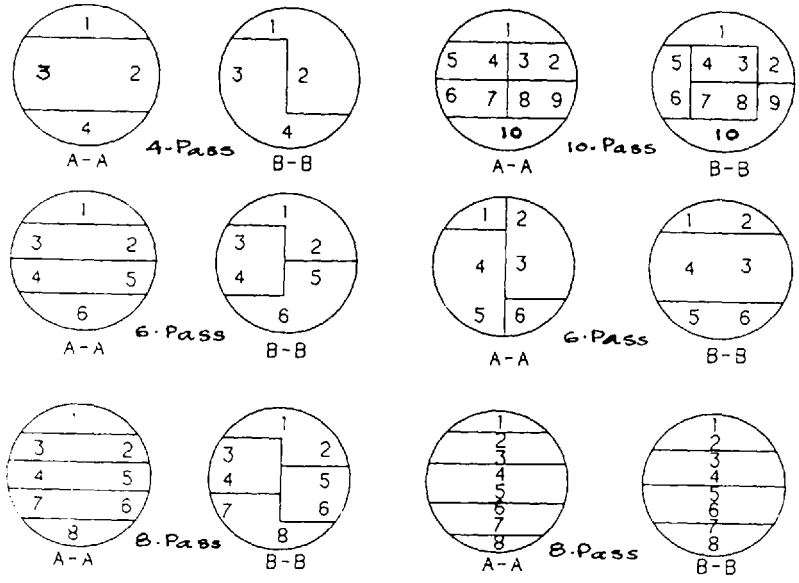


Figure 19 Typical tubeside partitions for multipass arrangement. (a) U-tube; and (b) straight tubes.

9.1 Drains and Vents

All exchangers need to be drained and vented; therefore, care should be taken to properly locate and size drains and vents. Additional openings may be required for instruments such as pressure gages and thermocouples.

9.2 Nozzles and Impingement Protection

Nozzles are used to convey fluids into and out of the exchanger. These nozzles are pipes of constant cross section welded to the shell and the channels. The nozzles must be sized with the understanding that the tube bundle will partially block the opening. Whenever a high-velocity fluid is entering the shell some type of impingement protection is required to avoid tube erosion and vibration. Some forms of impingement protection include (1) impingement plate (Fig. 20), (2) impingement rods, and (3) annular distributors. Criteria for requirement of the impingement protection is covered in Chapter 12, Corrosion.

Minimum Nozzle Size

Gollin [25] presents a methodology for determining the minimum inside diameter of a nozzle for various types of fluid entering or leaving the unit. The actual size of nozzle used will depend on the pressure, material, corrosion allowance, and pipe schedule.

The minimum inside diameter, d_{min}, is calculated from

$$d_{min} = \sqrt[4]{\frac{M^2}{3.54 \times 10^6 \times Vh\rho}} \tag{4}$$

where M is the mass flow rate of fluid through nozzle (lb/h), ρ the density of fluid (lb/ft^3), and Vh the velocity head loss through the nozzle, psi.

10 FLUID PROPERTIES AND ALLOCATION

To determine which fluid should be routed through the shell side and which fluid on the tube side, consider the following factors. These factors are discussed in detail in Refs. 5, 26, and 27.

Corrosion: Fewer corrosion resistant alloys or clad components are needed if the corrosive fluid is placed on the tube side.

Fouling: This can be minimized by placing the fouling fluid in the tubes to allow better velocity control; increased velocities tend to reduce fouling.

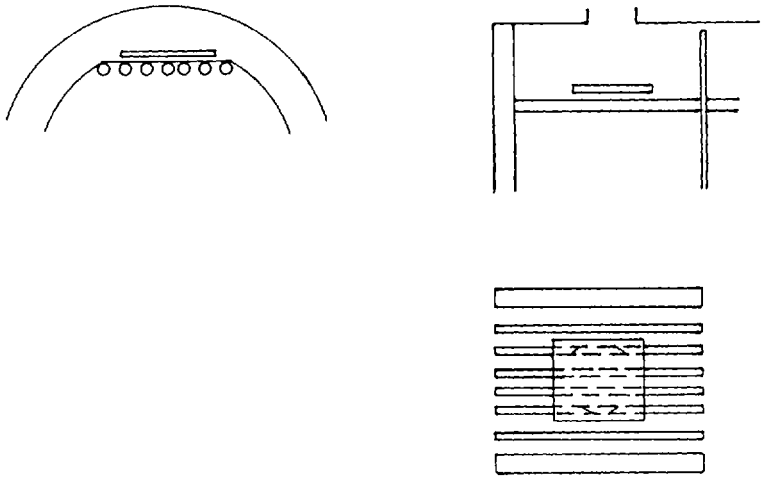


Figure 20 Impingement plate protection. (After Ref. 3.)

Table 1 Design Features of Shell-and-Tube Heat Exchangers [5]

Design features	Fixed tubesheet	Return bend (U-tube)	Outside-packed stuffing box	Outside-packed Lantern ring	Pull-through bundle	Inside split backing ring
Is tube bundle removable?	No	Yes	Yes	Yes	Yes	Yes
Can spare bundles be used?	No	Yes	Yes	Yes	Yes	Yes
How is differential thermal expansion relieved?	Expansion joint in shell	Individual tubes free to expand	Floating head	Floating head	Floating head	Floating head
Can individual tubes be replaced?	Yes	Only those in outside rows without special designs	Yes	Yes	Yes	Yes
Can tubes be chemically cleaned, both inside and outside?	Yes	Yes	Yes	Yes	Yes	Yes
Can tubes be physically cleaned on inside?	Yes	With special tools	Yes	Yes	Yes	Yes
Can tubes be physically cleaned on outside?	No	With square or wide triangular pitch	With square or wide triangular pitch	With square or wide triangular pitch	With square or wide triangular pitch	With square or wide triangular pitch
Are internal gaskets and bolting required?	No	No	No	No	Yes	Yes
Are double tubesheets practical?	Yes	Yes	Yes	No	No	No
What number of tubeside passes are available?	Number limited by number of tubes	Number limited by number of U-tubes	Number limited by number of tubes	One or two	Number limited by number of tubes. Odd number of passes requires packed joint or expansion joint	Number limited by number of tubes. Odd number of passes requires packed joint or expansion joint
Relative coat in ascending order, least expensive = 1	2	1	4	3	5	6

Cleanability: The shell side is difficult to clean; chemical cleaning is usually not effective on the shell side because of bypassing, and requires the cleaner fluid. Straight tubes can be physically cleaned without removing the tube bundle; chemical cleaning can usually be done better on the tube side.

Temperature: For high-temperature services requiring expensive alloy materials, fewer alloy components are needed when the hot fluid is placed on the tube side.

Pressure: Placing a high-pressure fluid in the tubes will require fewer costly high-pressure components and the shell thickness will be less.

Pressure drop: If the pressure drop of one fluid is critical and must be accurately predicted, then that fluid should generally be placed on the tube side.

Viscosity: Higher heat-transfer rates are generally obtained by placing a viscous fluid on the shell side. The critical Reynolds number for turbulent flow in the shell is about 200; hence, when the flow in the tubes is laminar, it may be turbulent if the same fluid is placed on the shell side. However, if the flow is still laminar when in the shell, it is better to place the viscous fluid only on the tube side since it is somewhat easier to predict both heat transfer and flow distribution [27].

Toxic and lethal fluids: Generally, the toxic fluid should be placed on the tubeside, using a double tube sheet to minimize the possibility of leakage. Construction code requirements for lethal service must be followed.

Flow rate: Placing the fluid with the lower flow rate on the shell side usually results in a more economical design and a design safe from flow-induced vibration. Turbulence exists on the shell side at much lower velocities than on the tube side.

11 CLASSIFICATION OF SHELL AND TUBE HEAT EXCHANGERS

There are four basic considerations in choosing a mechanical arrangement that provides for efficient heat transfer between the two fluids while taking care of such practical matters as preventing leakage from one into the other [4]:

1. Consideration for differential thermal expansion of tubes and shell.
2. Means of directing fluid through the tubes.
3. Means of controlling fluid flow through the shell.
4. Consideration for ease of maintenance and servicing.

Heat exchangers have been developed with different approaches to these four fundamental design factors. Three principal types of heat exchangers—(1) fixed tube-sheet exchangers, (2) U-tube exchangers, and (3) floating head exchangers—satisfy these design requirements.

11.1 Fixed Tube-Sheet Exchangers

This is the most popular type of shell and tube heat exchanger (Fig. 21). The fixed tube-sheet heat exchanger uses straight tubes secured at both ends into tube sheets, which are firmly welded to the shell. Hence, gasketed joints are minimized in this type, and thereby least maintenance is required. Fixed tube-sheet heat exchangers are used where [28]:

1. It is desired to minimize the number of joints.
2. Temperature conditions do not represent a problem for thermal stress.
3. The shell-side fluid is clean and tube bundle removal is not required.

Provision is to be made to accommodate the differential thermal expansion of the shell and the tubes when the thermal expansion is excessive. Fixed tube-sheet exchangers can be designed with removable channel covers, "bonnet" type channels, integral tube sheets on both

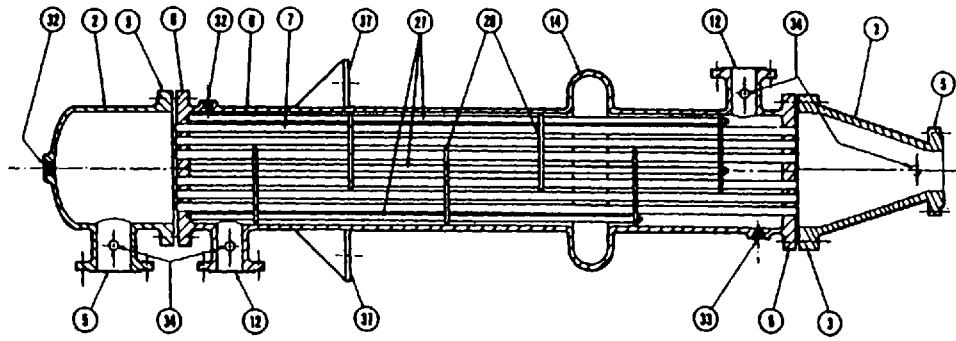


Figure 21 TEMA fixed tubesheet heat exchanger. (1) Stationary head-channel; (2) stationary head-bonnet; (3) stationary head flange-channel or bonnet; (4) channel cover; (5) stationary head nozzle; (6) stationary tubesheet; (7) tubes; (8) shell; (9) shell cover; (10) shell flange-stationary head end; (11) shell flange-rear head end; (12) shell nozzle; (13) shell cover flange; (14) expansion joint; (15) floating tubesheet; (16) floating head cover; (17) floating head cover flange; (18) floating head backing device; (19) split shear ring; (20) slip-on backing flange; (21) floating head cover-external; (22) floating tubesheet skirt; (23) packing box; (24) packing; (25) packing gland; (26) lantern ring; (27) tierods and spacers; (28) transverse baffles or support plates; (29) impingement plate; (30) longitudinal baffle; (31) pass partition; (32) vent connection; (33) drain connection; (34) instrument connection; (35) support saddle; (36) lifting lug; (37) support bracket; (38) weir; and (39) liquid level connection. (Copyright, Tubular Exchanger Manufacturers Association, 1988.)

sides, and tube sheets extended as shell flanges. They can be designed as counterflow one-to-one exchangers (i.e., single pass on the tube side and on the shell side) or with multipasses on the tube side. Where three or five passes have been specified for the tube side, the inlet and outlet connections will be on opposite sides. For fixed tube sheet exchangers, a temperature analysis must be made considering all phases of operation (i.e., startup, normal, upset, abnormal) to determine if thermal stress is a problem and how to relieve it [28].

11.2 U-Tube Exchangers

In this type of construction, tube bundle as well as individual tubes are free to expand and the tube bundle is removable. A U-tube exchanger is shown in Fig. 22. U-tube exchangers can be used for the following services [28]:

1. Clean fluid on the tube side
2. Extreme high pressure on one side
3. Temperature conditions requiring thermal relief by expansion
4. For H_2 service in extreme pressures, utilizing an all welded construction with a nonremovable bundle
5. To allow the shell inlet nozzle to be located beyond the bundle

Shortcomings of U-Tube Exchangers

Some of the demerits associated with U-tube exchangers are:

1. Mechanical cleaning from inside tubes is difficult, the chemical cleaning is possible.
2. Flow-induced vibration can also be a problem in the U-bend region for the tubes in the outermost row because of long unsupported span.
3. Individual tubes cannot be replaced.

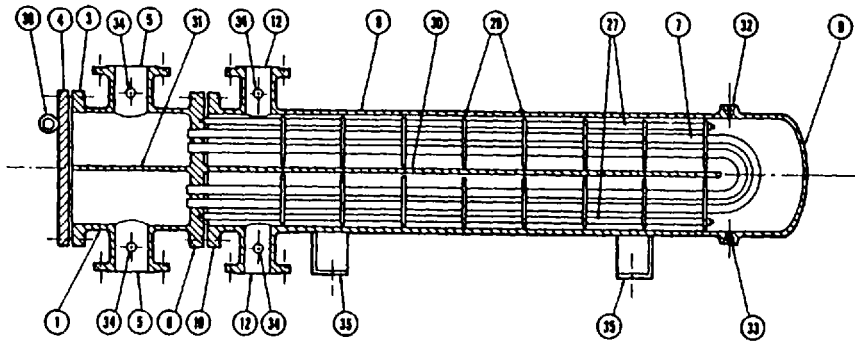


Figure 22 TEMA U-tube heat exchanger. (See Fig. 21 for key.) (Copyright, Tubular Exchanger Manufacturers Association, 1988.)

11.3 Floating Head Exchangers

The floating head exchanger consists of a stationary tube sheet and one floating tube sheet that is free to accommodate the thermal expansion of the tube bundle. A floating head exchanger with TEMA designation AES is shown in Fig. 23. There are four basic types of floating head exchangers. They are discussed next.

Floating Head, Outside Packed Floating Head

The floating head (P head), outside packed stuffing box heat exchanger uses the outer skirt of the floating tube sheet as part of the floating head. The packed stuffing box seals the shell-side fluid while allowing the floating head to move. The tube bundle is removable. Maintenance is also very easy since all bolting is from outside only. With this floating head, any leak (from either the shell side or the tube side) at the gaskets is to the outside and there is no possibility of contamination of fluids. Since the bundle-to-shell clearance is large (about 1.5 in or 38 mm), sealing strips are usually required.

Floating Head, Externally Sealed Floating Tube Sheet

The floating head (W head), externally sealed floating tube sheet or outside packed lantern ring heat exchanger uses a lantern ring around the floating tube sheet to seal the two fluids as

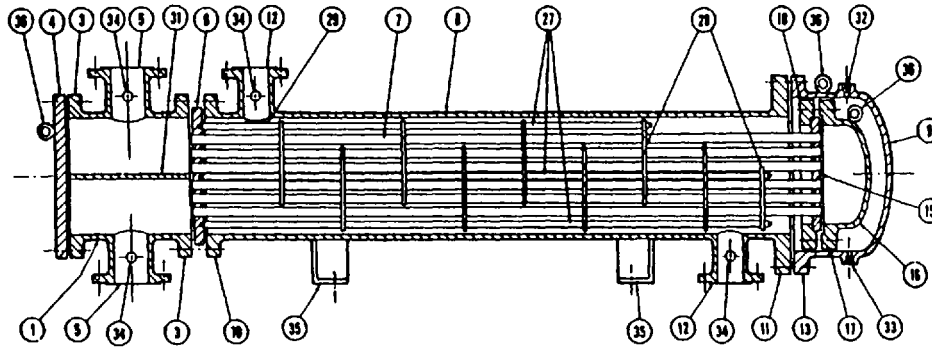


Figure 23 TEMA floating head heat exchanger. (See Fig. 21 for key.) (Copyright, Tubular Exchanger Manufacturers Association, 1988.)

the floating tube sheet moves back and forth. The lantern ring is packed on both sides, and is provided with vent or weep holes so that leakage through either should be to the outside. Number of tube passes is limited to one or two. The tube bundle is removable.

Floating Head, Pull Through Floating Head

In the floating head (T head), pull through head exchanger, a separate head or cover is bolted to the floating tube sheet within the shell. In this design, the tube bundle can be removed without dismantling the joints at the floating end. Due to the floating head bonnet flange and bolt circle, many tubes are omitted from the tube bundle at the tube bundle periphery and hence it accommodates the smallest number of tubes for a given shell diameter. This results in the largest bundle-to-shell clearance or a significant bundle-to-shell bypass stream C. To overcome the reduction in thermal performance, sealing devices are normally required and the shell diameter is somewhat increased to accommodate a required amount of surface area. An ideal application for the T head design is as the kettle reboiler, in which there is ample space on the shell side and the flow bypass stream C is of no concern.

Floating Head with Backing Device

In the floating head (S head) with backing device, the floating head cover (instead of being bolted directly to the floating tube sheet as in the pull through type) is bolted to a split backing ring. The shell cover over the floating head has a diameter larger than the shell. As a result, the bundle to shell clearance is reasonable and sealing strips are generally not required. The tube bundle is not removable. Both ends of the heat exchanger must be disassembled for cleaning and maintenance.

11.4 Differential Thermal Expansion

Means should be identified to accommodate the thermal expansion or contraction between the shell and the tube bundle due to high mean metal temperature differentials between the shell and the tube bundle. This is particularly true for fixed tube-sheet exchangers. Differential thermal expansion is overcome by the following means in the shell and tube heat exchangers:

U-Tube Design. The U-bend design allows each tube to expand and contract independently.

Fixed Tube-Sheet Design. For fixed tube-sheet exchangers, when the difference between shell and tube mean metal temperatures becomes large (greater than approximately 50°C for carbon steel), the tube-sheet thickness and tube end loads become excessive [29]. When a thermal expansion problems exists, an expansion joint is incorporated in the shell. This permits the shell to expand and contract.

Floating Head Designs. The floating head exchangers solve the expansion problem by having one stationary tube sheet, and one floating tube sheet that is free to accommodate the thermal expansion of the tube bundle.

12 TEMA CLASSIFICATION OF HEAT EXCHANGERS

TEMA has set up mechanical standards for three classes of shell and tube heat exchangers: R, C, and B [3]. Class R heat exchangers specify design and fabrication of unfired shell and tube heat exchangers for the generally severe requirements of petroleum and related processing applications, class C for the generally moderate requirements of commercial and general process applications, and class B for chemical process service. Salient features of TEMA standards are discussed in Chapter 11. Table 2 shows some major differences between TEMA classes R, C, and B.

Table 2 Major Differences Between TEMA Classes R, C, and B [3]

Item	Description	Classes	Remarks
RCB 1.5	Corrosion allowances	R,C + B	$\frac{1}{8}$ and $\frac{1}{16}$ in
RCB 2.5	Tube pitch	R,C,B	1.25 or 1.2 times tube OD
RCB 4.7	Tie rods size	R,C + B	$\frac{3}{8}$ vs. $\frac{1}{4}$ in
RCB 5.1	Floating head covers	R,C + B	Depth vs. tube area
RCB 5.3	Lantern ring design	C,R + B	Maximum pressure limits
RCB 6.2	Gasket materials	R,C + B	Pressure limits
RCB 6.3	Minimum width of gaskets	R + C,B	Full-face gasket
RCB 6.32	Gasket surface flatness	R,C + B	Tolerances
RCB 6.5	Pass partition gasket	R,C + B	Confined (or unconfined)
RCB 7.13	Minimum tube-sheet thickness	R,C,B	Function of tube diameter
RCB 7.44	Tube hole grooving	C,R + B	*C* only above 300 psi
RCB 7.51	Tube/tube-sheet joints	C,R + B	Length of expansion
RCB 7.6	Pass partition grooves	R,C + B	Pressure limit for C, B
RCB 7.8	Clad tube-sheets	C,R + B	$\frac{3}{16}$, $\frac{5}{16}$ in
RCB 9.11	Channels and bonnets	R,C + B	Minimum thickness
RCB 9.22	Channel cover grooves	R,C,B	Pass partition, minor
RCB 11.1	End-flange minimum bolt size	R,C,B	$\frac{3}{4}$, $\frac{1}{2}$, $\frac{5}{8}$ in

Source: Ref. 30.

13 SHELL AND TUBE HEAT EXCHANGER SELECTION

The fixed tube-sheet exchanger is usually the cheapest. If, however an expansion joint has to be used, then a U-tube exchanger may prove cheaper. If the bundle has to be removable, a U-tube will be the cheapest.

14 TEMA SYSTEM FOR DESCRIBING HEAT EXCHANGER TYPES

Major components of a shell and tube heat exchanger are the front head, shell section, and rear head. Each of these components is available in a number of standard designs. In TEMA standards, they are identified by an alphabetic character. A heat exchanger unit is designated using the designations of front head, shell, and rear head. It consist of three alphabetic characters, such as AES, AKT, AJW, BEM, AEP, and CFU. Seven major types of shells, five types of front heads, and eight types of rear heads are shown in Fig. 24. In addition to these types, special types of shells and heads are also available depending upon the applications and customer needs.

14.1 Shell Type

Seven types of shells are standardized by TEMA [3]. They are:

E One-pass shell
F Two-pass shell with longitudinal baffle
G Split flow
H Double split flow
J Divided flow
K Kettle type reboiler
X Crossflow

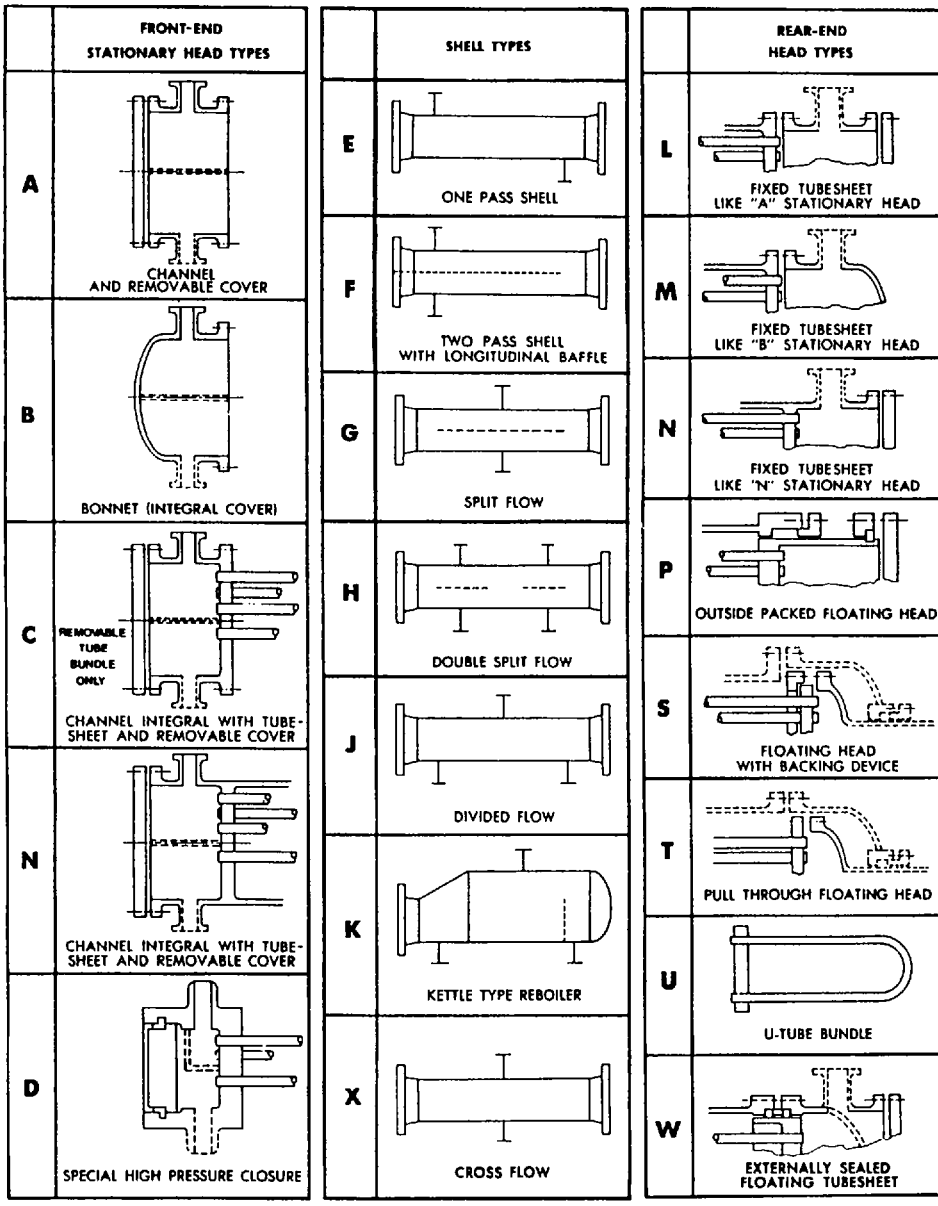


Figure 24 TEMA designation for shells and heads. (Copyright, Tubular Exchanger Manufacturers Association, 1988.)

A brief description of each type is provided next.

TEMA E Shell

The E shell is the most common due to its cheapness, simplicity, and ease of manufacture. It has one shell pass, with the shell-side fluid entry and exit nozzles attached at the two opposite ends of the shell. The tube side may have a single pass or multiple passes. The tubes are

supported by transverse baffles. This shell is the most common for single-phase shell fluid applications. Multiple passes on the tube side reduce the exchanger effectiveness or LMTD correction factor F over a single pass arrangement. If F is too low, two E shells in series may be used to increase the effective temperature difference and thermal effectiveness. Possible flow arrangements are $E_{1\text{-}1}$, $E_{1\text{-}2}$, $E_{1\text{-}3}$, and $E_{1\text{-}N}$ (Fig. 25).

TEMA F Shell

The F shell with two passes on the shell side is commonly used with two passes on the tube side as shown in Fig. 26 so that the flow arrangement is countercurrent, resulting in *F* factor 1.0. This is achieved by the use of an E shell having a longitudinal baffle on the shell side. The entry and exit nozzles are located at the same end. The amount of heat transferred is more than in an E shell but at the cost of an increased pressure drop. Although ideally this is a desirable flow arrangement, it is rarely used because of many problems associated with the shell-side longitudinal baffle. They include the following:

1. There will be a conduction heat transfer through the longitudinal baffle because of the temperature gradient between the shell-side passes.
2. If the longitudinal baffle is not continuously welded to the shell, or if seals are not provided

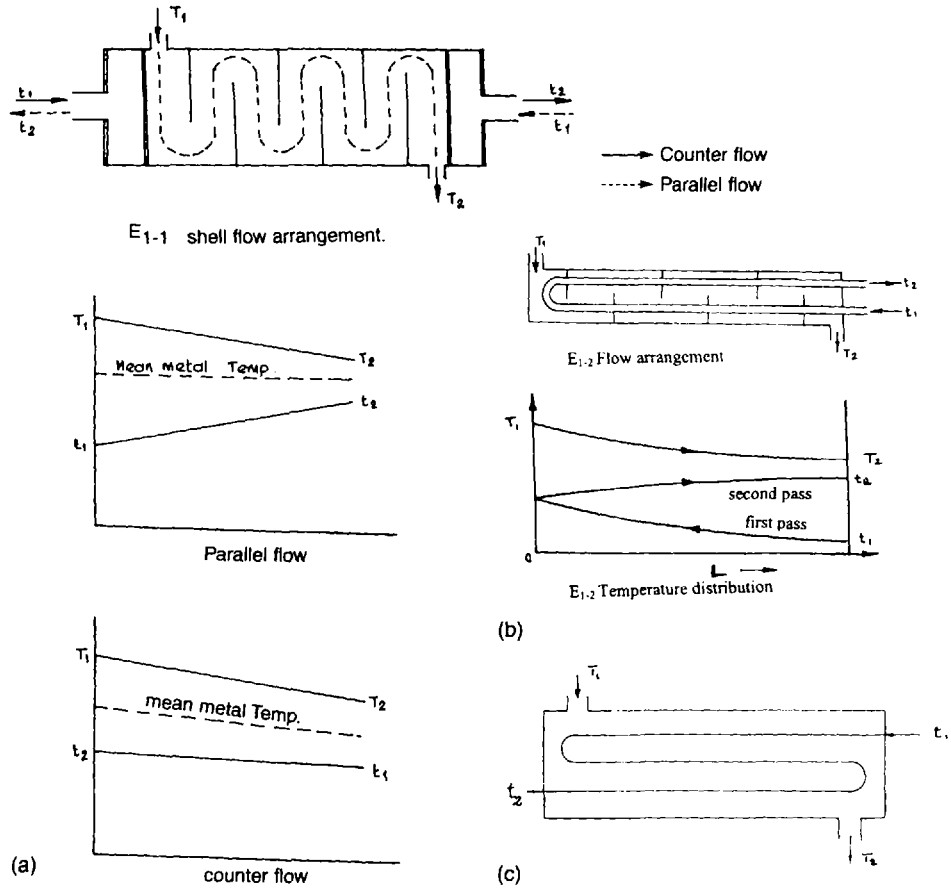


Figure 25 TEMA E-shell flow arrangement and temperature distribution. (a) $E_{1\text{-}1}$; (b) $E_{1\text{-}2}$; and (c) $E_{1\text{-}3}$ (temperature distribution not given).

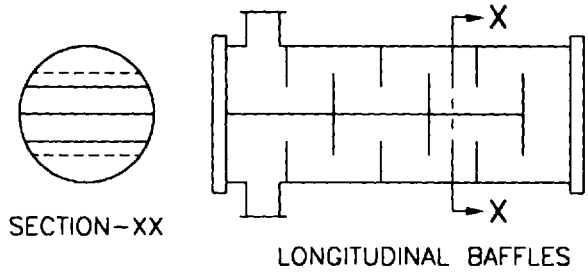


Figure 26 TEMA F shell.

effectively between the longitudinal baffle and the shell, there will be fluid leakage from the high pressure to low pressure side.

Both the factors will reduce the mean temperature difference and the exchanger effectiveness more than the gain by achieving the pure counterflow arrangement. The welded baffle construction has a drawback: It does not permit the withdrawal of the tube bundle for inspection or cleaning. Hence, if one needs to increase the mean temperature difference, multiple shells in series are preferred over the F shell.

TEMA G Shell or Split Flow Exchanger

In this exchanger, there is one central inlet and one central outlet nozzle with a longitudinal baffle. The shell fluid enters at the center of the exchanger and divides into two streams. Hence, it is also known as a split flow unit. Possible flow arrangements ($G_{1\text{-}1}$, $G_{1\text{-}2}$, and $G_{1\text{-}4}$) are shown in Fig. 27. G shells are quite popular with heat exchanger designers for several reasons. One important reason is their ability to produce "temperature correction factors" comparable to those in an F shell with only a fraction of the shell-side pressure loss in the latter type [31].

TEMA H Shell or Double Split Flow Exchanger

This is similar to the G shell, but with two inlet nozzles and two outlet nozzles and two horizontal baffles resulting in a double split flow unit. It is used when the available pressure drop is very limited. Possible pass arrangements are $H_{1\text{-}1}$ and $H_{1\text{-}2}$ (Fig. 28). The H shell approaches the crossflow arrangement of the X shell, and it usually has low shell-side pressure drop compared to E, F, and G shells [2].

TEMA J Shell or Divided Flow Exchanger

The divided flow J shell has two inlets and one outlet or one inlet and two outlet nozzles (i.e., a single nozzle at the midpoint of shell and two nozzles near the tube ends). With a single inlet nozzle at the middle, the shell fluid enters at the center of the exchanger and divides into two streams. These streams flow in longitudinal directions along the exchanger length and exit from two nozzles, one at each end of the exchanger. The possible pass arrangements are one shell pass, and one, two, four, N (even) or infinite tube passes. J shell pass arrangements with temperature distribution are shown in Fig. 29 [32]. With a TEMA J shell, the shell-side velocity will be one-half that of the TEMA E shell and hence the pressure drop will be approximately one-eighth that of a comparable E shell. Due to this reason, it is used for low pressure-drop applications like condensing in vacuum [2]. For a condensing shell fluid, the J shell is used with two inlets for the gas phase and one central outlet for the condensates and leftover gases.

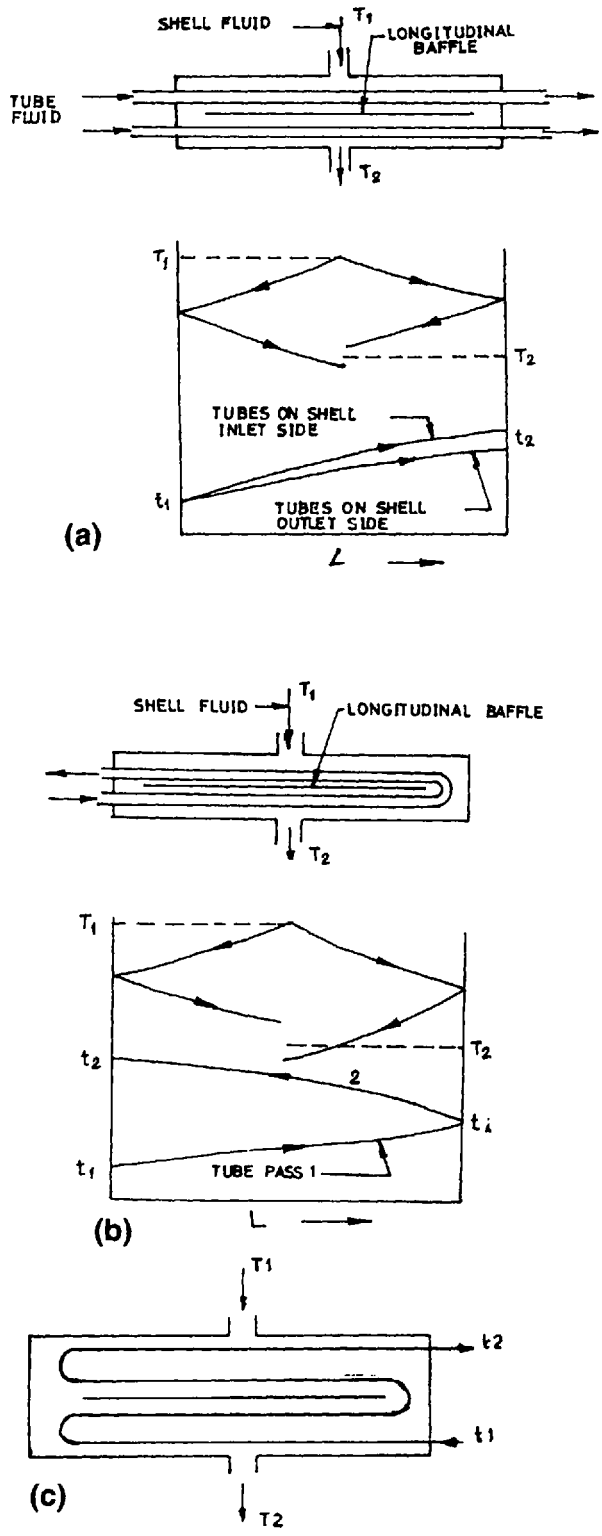


Figure 27 G shell flow arrangement and temperature distribution. (a) $G_{1,1}$; (b) $G_{1,2}$; and (c) $G_{1,4}$ (for temperature distribution refer to Ref. (38) of Chapter 2).

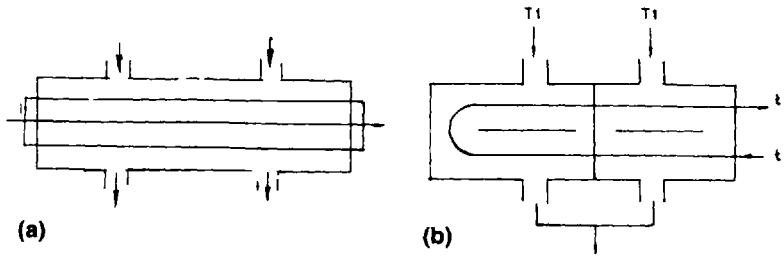


Figure 28 H shell flow arrangement. (a) $H_{1\text{-}1}$; and (b) $H_{1\text{-}2}$.

TEMA K Shell or Kettle Type Reboiler

The K shell is used for partially vaporizing the shell fluid. It is used as a kettle reboiler in the process industry and as a flooded chiller in the refrigeration industry [2]. Usually, it consists of a horizontal bundle of heated U tubes or floating head placed in an oversized shell (Fig. 30). The tube bundle is free to move and it is removable. Its diameter is about 50–70% of the shell diameter. The large empty space above the tube bundle acts as a vapor disengaging space. The liquid to be vaporized enters at the bottom, near the tube sheet, and covers the tube bundle; the vapor occupies the upper space in the shell, and the dry vapor exits from the top nozzle(s), while a weir (the vertical unperforated baffle shown in Fig. 30) helps to maintain the liquid level over the tube bundle. The bottom nozzle in this space is used to drain the excess liquid.

TEM X Shell

The X shell (Fig. 31) is characterized by pure shell-side crossflow. No transverse baffles are used in the X shell; however, support plates are used to suppress the flow-induced vibrations. It has nozzles in the middle as in the G shell. The shell-side fluid is divided into many substreams, and each substream flows over the tube bundle and leaves through the bottom nozzle. Flow maldistributions on the shell side can be a problem unless a proper provision has been made to feed the fluid uniformly at the inlet. Uniform flow distribution can be achieved by a

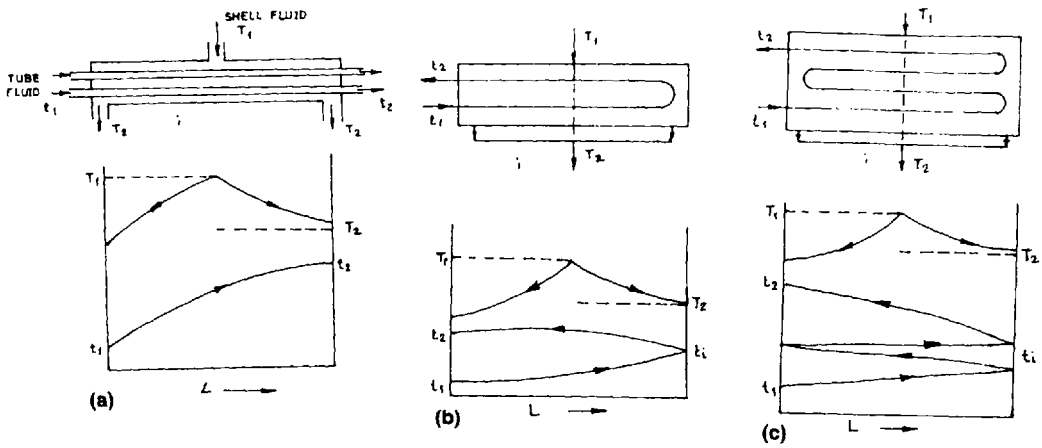


Figure 29 TEMA J shell flow arrangement and temperature distribution, (a) $J_{1\text{-}1}$; (b) $J_{1\text{-}2}$; and (c) $J_{1\text{-}4}$. (From Ref. 32.)

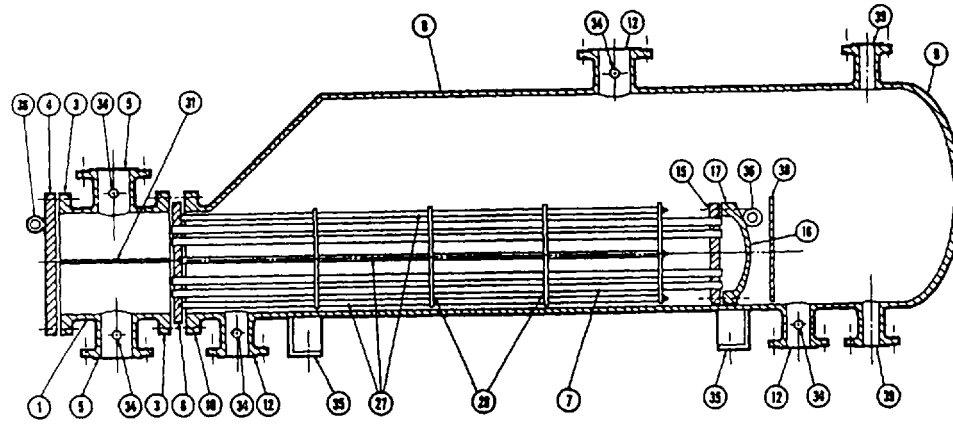


Figure 30 TEMA K-shell. (Copyright, Tubular Exchanger Manufacturers Association, 1988.)

bathtub nozzle, multiple nozzles, or keeping a clear lane along the length of the shell near the nozzle inlet [2]. The tube side can be single pass, or two passes, either parallel crossflow or counter-crossflow. For a given set of conditions, the X shell has the lowest shell-side pressure drop compared to all other shell types (except the K shell). Hence, it is used for gas heating and cooling applications and for condensing under vacuum.

Comparison of Various TEMA Shells

In general, E and F type shells are suited to single-phase fluids because of the many different baffle arrangements possible and the relatively long flow path [7]. When the shell-side pressure drop is a limiting factor, G and H shells can be used. The G and H shells are not used for shell-side single-phase applications, since there is no edge over the E or X shells. They are used as horizontal thermosyphon reboilers, condensers, and in other phase-change applications. The longitudinal baffle serves to prevent flashing out of the lighter components of the shell fluid, helps flushing out noncondensables, provides increased mixing, and helps flow distribution [2]. Velocity head and pressure drop for various TEMA shells are given in Table 3 [33].

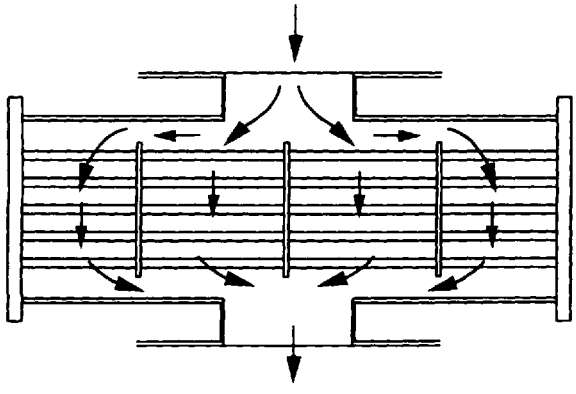


Figure 31 TEMA X shell.

Table 3 Shellside Velocity Head and Pressure Drop for Some TEMA Shells [33]

TEMA shell type	Velocity head	Pressure drop
E shell	V	$\alpha V^2 L$
F shell	2V	$\alpha 8V^2 L$
G shell	V	$\alpha V^2 L$
H shell	V/2	$\alpha V^2 L/8$
J shell	V/2	$\alpha V^2 L/8$

Source: Ref. 33.

14.2 Front and Rear Head Designs

Head designs can vary from plain standard castings to fabricated assemblies with many special features. Two of the major considerations in the choice of heads are [4] (1) accessibility to the tubes, and (2) piping convenience. Where fouling conditions are encountered or where frequent access for inspection is desired, a head or cover plate that can be easily removed is an obvious choice. In this head, connections are located on the sides, not on the ends of removable heads. Typical open end heads used for this purpose are called channels. They are fabricated from cylindrical shells and fitted with easily removable cover plates so that the tubes can be cleaned without disturbing piping.

Designations for Head Types

Front Head. For the variable front head, the constants and their meanings are:

A Channel with removable cover
B Bonnet with integral cover
C Channel integral with the tube sheet and removable cover when the tube bundle is removable
N Channel integral with the tube sheet and having a removable cover but the tube bundle is not removable
D Special high-pressure closure

Rear Head.

L Fixed tube sheet like A stationary head
M Fixed tube sheet like B stationary head
N Fixed tube sheet like N stationary head
P Outside packed floating head
S Floating head with backing device
T Pull through floating head
U U-tube bundle
W Externally sealed floating tube sheet

Salient features of these heads are discussed and tabulated by Larowski et al. [7].

15 SHELLSIDE CLEARANCES

Even though one of the major functions of the plate baffle is to induce crossflow over the tube bundle, this objective is achieved partially. Various clearances on the shell side partially bypass the fluid. Bypassing is defined as a leakage flow where fluid from the crossflow stream, in-

tended to flow through the tube bundle, avoids flowing through it by passing through an alternative, low-resistance flow path [34]. A major source of bypassing is the shell-side clearances. Clearances are required for heat exchanger fabrication. Fabrication clearances and tolerances have been established by the Tubular Exchanger Manufacturers Association (TEMA) [3], and these have become widely accepted around the world and are enforced through inspection during fabrication. Three clearances are normally associated with a plate baffle exchanger. They are (1) tube to baffle hole, (2) baffle to shell, and (3) bundle to shell. Additionally, in a multipass unit, the tube layout partitions may create open passages for the bypass of the crossflow stream. Since bypassing reduces heat transfer on the shell side, to achieve good shell-side heat transfer, bypassing of the fluid must be reduced. These clearances and their effect on the shell-side performance are discussed in detail next.

15.1 Tube-to-Baffle-Hole Clearance

The holes in the baffles must be slightly larger than the tube outer diameter to ensure easy tube insertion. The resultant clearance is referred to as the tube-to-baffle-hole clearance. It should be kept at a minimum (1) to reduce the flow-induced vibration and (2) to minimize the A leakage stream (various shellside bypass streams are discussed next). As per TEMA RCB-4.2, where the maximum unsupported tube length is 36 in (914.4 mm) or less, or for tubes larger than 1.25 in (31.8 mm) outer diameter, the clearance is $\frac{1}{32}$ in (0.80 mm); where the unsupported tube length exceeds 36 in for tube outer diameter 1.25 in or smaller, the clearance is $\frac{1}{64}$ in (0.40 mm).

15.2 Shell-to-Baffle Clearance

The clearance between the shell inner diameter and baffle outer diameter is referred to as the baffle-to-shell clearance. It should be kept to a minimum to minimize the E leakage stream. TEMA recommend maximum clearance as per RCB-4.3 [3] varies from 0.125 in (3.175 mm) for 6 in (152.4 mm) shell inner diameter to 0.315 in (7.94 mm) for 60 in (1524 mm) shell inner diameter.

15.3 Shell-to-Bundle Clearance

Since the tube bundle does not fill the shell, there is a shell-to-bundle clearance. This allows the so-called bypass stream C flowing around the bundle. Sealing strips are used to block this space and force the bypass stream to flow across the tubes. The use of sealing strips is recommended every five to seven rows of tubes in the bypass stream direction.

15.4 Bypass Lanes

The lanes provided for the tubeside partition ribs is a source of bypass on the shell side. The pass partition lanes (Fig. 32) are, however, placed perpendicular to the crossflow whenever possible, or the bypass lanes are usually blocked by tie rods, which act similar to the sealing strips. Hence, the effect of the bypass lanes on thermal performance is usually can be neglected.

16 DESIGN METHODOLOGY

16.1 Shell-Side Flow Pattern

Shell Fluid Bypassing and Leakage

In shell and tube exchangers with segmental plate baffles, the shell-side flow is very complex due to a substantial portion of the fluid bypassing the tube bundle through various shell-side

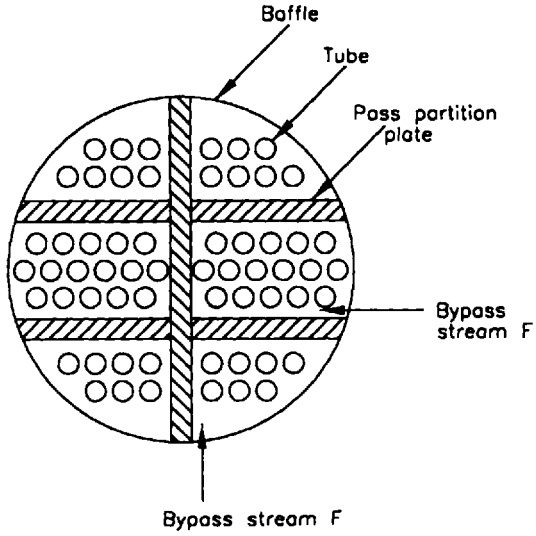


Figure 32 Bypass lane.

constructional clearances defined earlier. Another contributing factor for bypassing is due to notches made in the bottom portion of the baffles for draining purposes. Notches are usually not required for draining because the necessary fabrication tolerances provide ample draining [2]. To achieve good shell-side heat transfer, bypassing of the fluid must be reduced.

Bypass Prevention and Sealing Devices

Sealing devices can be employed to minimize the bypassing of fluid around the bundle or through pass partition lanes. If tube bundle-to-shell bypass clearance becomes large, such as for pull through bundles, resulting in decreased heat-transfer efficiency, the effectiveness can be restored by fitting "sealing strips." As a rule of thumb, sealing strips should be considered if the tube bundle-to-shell diameter clearance exceeds approximately 2.25 in (30 mm). Fixed tube-sheet and U-tube heat exchangers usually do not require sealing strips, but split ring and pull through floating head designs usually require sealing strips.

Types of Sealing Devices. Sealing devices are strips that prevent bypass around a bundle by "sealing" or blocking the clearance area between the outermost tubes and the inside of the shell. Some common types include [5] tie rods, sealing devices, and tie rods.

1. Tie rods and spacers hold the baffles in place but can be located at the periphery of the baffle to prevent bypassing.
2. Sealing strips. These are typically longitudinal strips of metal between the outside of the bundle and the shell and fastened to the baffles (Fig. 33a); they force the bypass flow back into the tube field. A typical flow pattern with sealing strips in an effective penetration area is shown in Fig. 33b.

Number of Sealing Strips Pair in Between Two Baffles. Bypassing of the shell-side fluid can be adequately controlled by providing one sealing device for every four tube rows on the bundle periphery and by providing one sealing device for every two tube rows at bypass lanes internal to the bundle such as pass partition lanes [1]. The use of sealing strips to divert flow

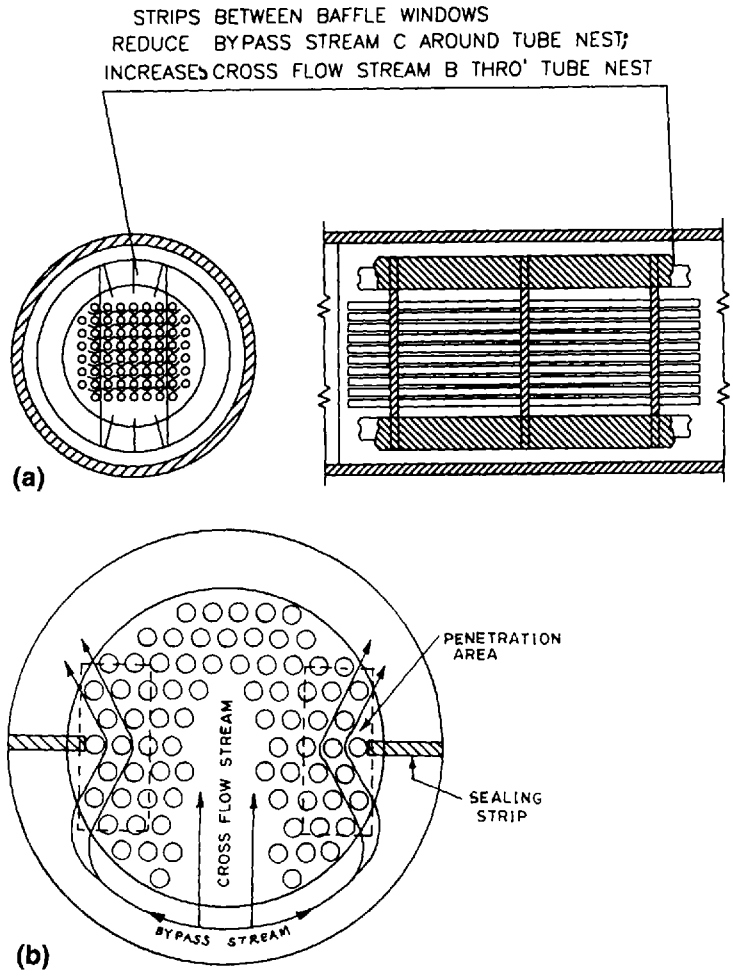


Figure 33 Sealing strips. (a) Typical sealing strip attachment to the tube bundle [37]; and (b) typical flow pattern with sealing strips [13].

within heat exchangers was studied by Taylor et al. [35]. They examined the variation of sealing strip shape, location, and gap size, that is, the distance between the sealing device and the nearest tube (Fig. 34). According to their study, (1) rectangular shape sealing strips are preferred, (2) sealing strips placed close together (3.6 rows apart) will provide optimum heat transfer characteristics, and (3) most significant results were obtained when the gap size = $p - d$.

3. Tie rods with "winged" spacers. The wings are extended longitudinal strips attached to the spacers.

Dummy Tubes. Usually closed at one end, dummy tubes are used to prevent bypassing through lanes parallel to the direction of fluid flow on the shell side (Fig. 35). They do not pass through the tube sheet. In moderate to large exchangers, one dummy tube is as effective in promoting heat transfer as 50 process tubes [5].

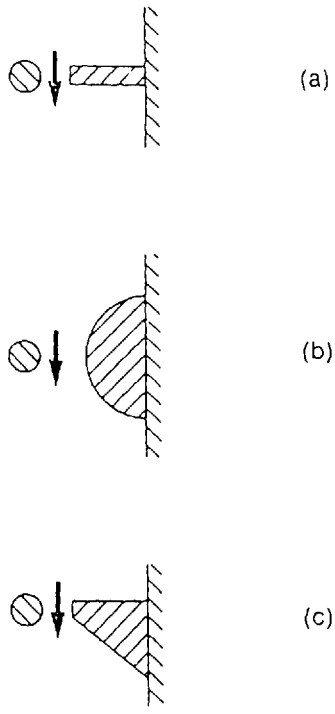


Figure 34 Forms of sealing strips. (a) Rectangular; (b) semicircular; and (c) triangular. (From Ref. 35.)

Shell-Side Flow Pattern

An ideal tube bundle (the term introduced by HTRI) refers to segmentally baffled circular bundles with no clearance between tubes and baffles, baffles and shell, or outer tubes and the shell, so that all fluid must flow across the tube bundle [13]. In a practical tube bundle, the total shell-side flow distributes itself into a number of distinct partial streams due to varying flow resistances through the shell-side clearances. This stream distribution pattern is now well established and is shown schematically in Fig. 36. This flow model was originally proposed by Tinker [36] and later modified by Palen et al. [13] for a segmentally baffled exchanger. Various streams in order of decreasing thermal effectiveness are discussed next.

A Stream. This is a tube-to-baffle-hole leakage stream through the clearance between the tubes and tube holes in the baffles (Fig. 37a). This stream is created by the pressure difference on the sides of the baffle. As heat-transfer coefficients are very high in the annular spaces, this stream is considered fully effective.

B Stream. This is a crossflow stream through tube bundle. This stream is considered fully effective for both heat transfer and pressure drop.

C Stream. This is a bundle-to-shell bypass stream through the annular spaces between the tube bundle and shell. It flows between successive baffle windows. This stream is only partially effective for heat transfer as it contacts the tubes near the tube bundle periphery.

E Stream. This is a shell-to-baffle leakage stream through the clearance between the edge of a baffle and the shell (Fig. 37b). This stream is the least effective for heat transfer, particularly in laminar flow, because it may not come in contact with any tubes.

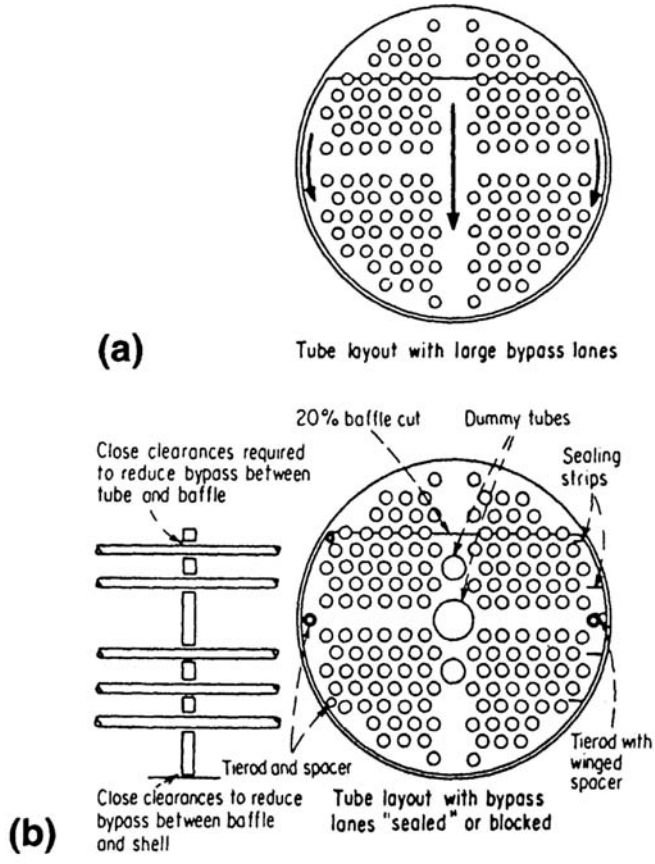


Figure 35 Tube layout: (a) with bypass lanes, and (b) bypass lanes blocked [5].

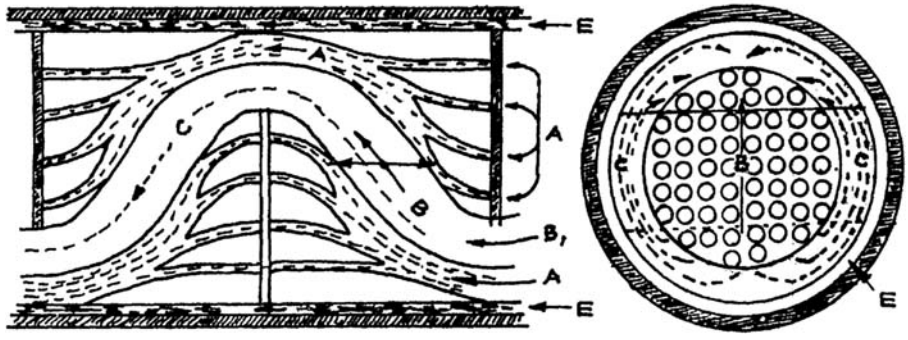


Figure 36 Shell side flow distribution. (From Ref. 37.)

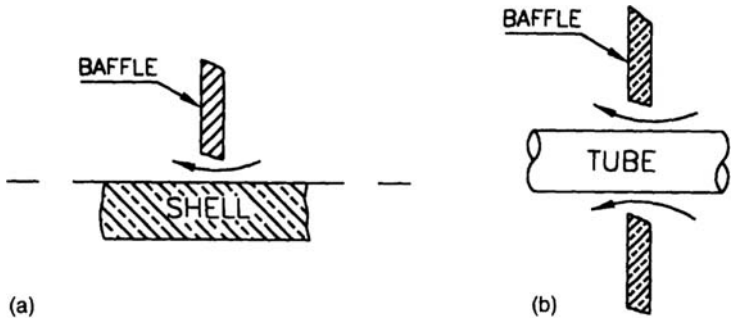


Figure 37 Leakage streams: (a) shell-to-baffle leakage stream ('E' stream); and (b) tube-to-baffle leakage stream ('A' stream). (After Ref. 13.)

F Stream. This is a tube pass partition bypass stream through open passages created by tube layout partition lanes (when placed in the direction of the main crossflow stream) in a multipass unit. This stream is less effective than the A stream because it comes into contact with less heat-transfer area per unit volume; however, it is slightly more effective than the C stream.

Flow Fractions for Each Stream

Each of the streams has a certain flow fraction of the total flow such that the total pressure drop for each stream is the same. Each stream undergoes different frictional processes and has different heat-transfer effectiveness as discussed earlier. The design of the plate baffle shell and tube exchanger should be such that most of the flow (ideally about 80%) represents the crossflow B stream. However, this is rarely achieved in practice. Narrow baffle spacing will result in higher pressure drop for the B stream and forces more flow into the A, C, and E streams.

Based on extensive test data, Palen et al. [13] arrived at the flow fractions for various streams shown in Table 4. Even for a good design, the crossflow stream represents only 65% of the total flow in turbulent flow. Hence, the predicted performance based on the conventional LMTD method will not be accurate in general. As a result, there is no need to compute very accurate F factors for the various exchanger configurations [13]. If the computed values of the B stream are lower than those indicated, the baffle geometry and various clearances should be checked.

Shell-Side Performance

Many investigators have studied the shell-side thermal performance. One of the earliest was Tinker [36,37]. Perhaps the most widely accepted and recognized study is known as the Bell–

Table 4 Flow Fractions for Various Shell-Side Flow Streams

Flow stream	Turbulent flow	Laminar flow
Crossflow stream B	30–65%	10–50%
Tube-to-baffle leakage stream A	9–23%	0–10%
Bundle-to-shell bypass stream C	15–35%	30–80%
Baffle-to-shell leakage stream E	6–21%	6–48%

Source: Ref. 13.

Delaware method [38]. The original method has been further refined by Bell [39] and presented also in Ref. 40, and other modifications and improvements have been made by Taborek [41]. The Bell–Delaware approach is to present heat-transfer and pressure-drop performance for an ideal tube bundle, one without any leakage or bypassing. The effects of the various leakages and bypassing are then evaluated and corrections are applied to the heat transfer and pressure drop for ideal bundles. Proprietary methods have also been developed by consortia such as Heat Transfer Research, Incorporated (HTRI), and Heat Transfer and Fluid Flow Services (HTFS). These methods are generally restricted for use by members of the organizations. Private programs like B-Jac [42] are also available.

16.2 Sizing of Shell and Tube Heat Exchangers

The design of shell and tube heat exchanger involves the determination of the heat-transfer coefficient and pressure drop on both the tube side and the shell side. A large number of methods [37,43,44,45] are available for determining the shell-side performance. Since the Bell–Delaware method is considered the most suitable open-literature method for evaluating shell-side performance, the method is described here. Before discussing the design procedure, some guidelines for shell-side design and points to be raised while specifying a heat exchanger are listed, followed by preliminary sizing of a shell and tube heat exchanger.

Guidelines for Shell-Side Design

Recommended guidelines for shellside design include the following [1]:

1. Accept TEMA [3] fabrication clearances and tolerances, and enforce these standards during fabrication.
2. For segmental baffles employ 20% battle cuts.
3. Employ no-tubes-in-window design to eliminate the damage from flow-induced vibration.
4. Evaluate heat transfer in the clean condition and pressure drop in the maximum fouled condition.
5. Employ sealing devices to minimize bypassing between the bundle and shell for pull through floating heat exchanger, and through pass partition lanes.
6. Ratio of baffle spacing to shell diameter may be restricted to values between 0.2 and 1.0. Baffle spacing much greater than the shell diameter must be carefully evaluated.
7. Avoid shell longitudinal baffles that are not welded to the shell; all other sealing methods are inadequate.

Specify the Right Heat Exchanger

When specifying an exchanger for design, various factors to be considered or questions that should be raised are listed by Gutterman [28]. A partial list include the following:

1. Type of heat transfer, i.e., boiling, condensing, or single-phase heat transfer.
2. Since the heat exchanger has two pressure chambers, which chamber should receive the cold fluid?
3. More viscous fluid shall be routed on the shell side to obtain better heat transfer.
4. It is customary to assign the higher pressure to the tube side to minimize shell thickness.
5. Consider various potential and possible upset conditions in assigning the design pressure and/or design temperature.
6. Pass arrangements on the shellside and tubeside to obtain maximum heat transfer?
7. Have you considered the tube size and thickness?
8. What is the acceptable pressure drop on the tube side and shell side? Is the sum of the pumping cost and the initial equipment cost minimized?

9. Have you considered the maximum allowable pressure drop to obtain the maximum heat transfer?
10. Are the tube-side and shell-side velocities are high enough for good heat transfer and to minimize fouling but well below the limits that can cause erosion–corrosion on the tube side, and impingement attack and flow-induced vibration on the shell side?
11. Have you considered the nozzle sizes and adequate shell escape area? Are the nozzle orientations consistent with tube layout pattern?
12. Is the baffle arrangement designed to promote good flow distribution on the shell side and hence good heat transfer, and to minimize fouling and flow-induced vibration?
13. Does the design provide for efficient expulsion of noncondensables that may degrade the performance? (A prime example in this category is surface condensers.)
14. Is the service corrosive or dirty? If so, have you specified corrosion-resistant materials and reasonable fouling factors?
15. Does the design minimize fouling?
16. Do you want to remove the bundle? If so, are adequate space and handling facilities available for tube bundle removal?
17. Is leakage a factor to be considered? If so, did you specify: (a) seal welded tube joint, (b) rolled joint, (c) strength welded joint? Is the tube wall thickness adequate for welding? (d) Are you specifying tube holes with grooves or without grooves?
18. What kind of tests do you specify to prove the tube-to-tube-sheet joint integrity?

All of these and numerous other factors determine the type of exchanger to be specified.

Design Considerations for a Shell and Tube Heat Exchanger

The basic criterion that a given or designed heat exchanger should satisfy is that it should perform the given heat duty within the allowable pressure drop. The design is also to satisfy additional criteria such as [46]:

1. Withstand operating conditions, startup, shutdown, and upset conditions that influence the thermal and mechanical design.
2. Maintenance and servicing.
3. Multiple shell arrangement.
4. Cost.
5. Size limitations.

In terms of the five factors just mentioned, multishell arrangement needs some comments on it. Consider the advantages of a multishell arrangement to allow one unit to be taken out of service for maintenance without severely upsetting the rest of the plant. For part load operations, multiple shells will result into an economical operation. Shipping and handling may dictate restrictions on the overall size or weight of the unit, resulting in multiple shells for an application.

Thermal Design Procedure

The overall design procedure of a shell and tube heat exchanger is quite lengthy, and hence it is necessary to break down this procedure into distinct steps:

1. Approximate sizing of shell and tub heat exchanger.
2. Evaluation of geometric parameters also known as auxiliary calculations.
3. Correction factors for heat transfer and pressure drop.
4. Shell-side heat-transfer coefficient and pressure drop.
5. Tube-side heat-transfer coefficient and pressure drop.
6. Evaluation of the design, i.e., comparison of the results with the design specification.

In this section, approximate sizing of the shell and tube exchanger by Bell's method is discussed first; then this is extended to size estimation, and subsequently the rating is carried out as per the Bell–Delaware method. Finally, the rated unit is evaluated.

Bell's Method [46] for Approximate Sizing of a Shell and Tube Heat Exchanger

The approximate design involves arriving at a tentative set of heat exchanger parameters, and if the design is accepted after rating then this becomes the final design. Various stages of approximate design include the following:

1. Compute overall heat-transfer coefficient.
2. Compute heat-transfer rate required.
3. Compute the heat-transfer area required.
4. Design the geometry.

A flow chart for approximate sizing is given in Fig. 38.

Estimation of Heat Load. The heat load is calculated in the general case from

$$q = M_h c_{p,h}(T_{h,i} - T_{h,o}) = M_c c_{p,c}(T_{c,o} - T_{c,i}) \tag{5}$$

where $c_{p,h}$ and $c_{p,c}$ are the specific heats of the hot and cold fluids, $T_{h,i}$ and $T_{h,o}$ are the inlet and outlet temperatures of the hot stream, and $T_{c,i}$ and $T_{c,o}$ are the inlet and outlet temperatures of the cold stream.

Estimation of Log Mean Temperature Difference. Determine the logarithmic mean temperature difference for countercurrent flow using the temperatures as defined earlier:

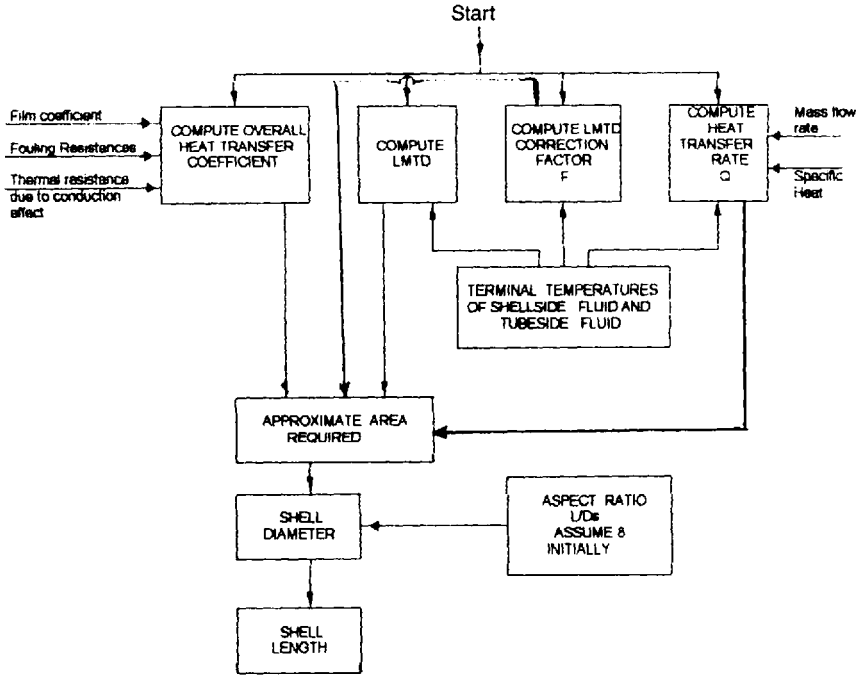


Figure 38 Flow chart for approximate sizing of STHE.

$$\text{LMTD} = \frac{(T_{h,i} - T_{c,o}) - (T_{h,o} - T_{c,i})}{\ln[(T_{h,i} - T_{c,o})/(T_{h,o} - T_{c,i})]} \tag{6}$$

LMTD Correction Factor. Values of F can be found from the thermal relation charts given in Chapter 2 for a variety of heat exchanger flow configurations. However, for estimation purposes, a reasonable estimate may often be obtained without restoring to the charts.

1. For a single tube pass, purely countercurrent heat exchanger, $F = 1.0$.
2. For a single shell with any even number of tube-side passes, F should be between 0.8 and 1.0.

Method to Determine Number of Shells. Quickly check the limits:

$2T_{h,o} \geq T_{c,i} + T_{c,o}$ hot fluid on the shell side

$2T_{c,o} \leq T_{h,i} + T_{h,o}$ cold fluid on the shell side

If these limits are approached, it is necessary to use multiple 1-2N shells in series. There is a rapid graphical technique for estimating a sufficient number of 1-2N shells in series. The procedure is discussed here. The terminal temperatures of the two streams are plotted on the ordinates of an arithmetic graph paper sheet as shown in Fig. 39. The distance between the ordinates is arbitrary. Starting with the cold fluid outlet temperature, a horizontal line is laid off until it intercepts the hot fluid line. From that point a vertical line is drawn to the cold fluid temperature. The process is repeated until a vertical line intercepts the cold fluid operating line at or below the cold fluid inlet temperature. The number of horizontal lines (including the one that intersects the right-hand ordinate) is equal to the number of shells in series that is clearly sufficient to perform the duty. Following this procedure will usually result in a number of shells having an overall F close to 0.8.

Estimation of U. The greatest uncertainty in preliminary calculations is estimating the overall heat-transfer coefficient. Approximate film coefficients for different type of fluids are given by Bell [43]. Thus, U can be calculated from the individual values of heat-transfer coefficient on the shell side and tube side, wall resistance, and fouling resistance (R_{fo} and R_{fi}), using the following equation:

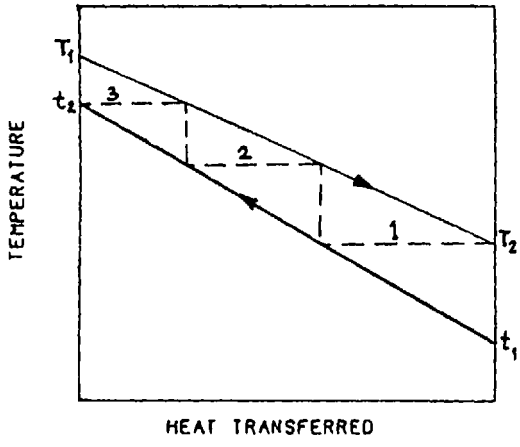


Figure 39 Procedure to determine number of shells. Note: T_1 and T_2 are shell side terminal temperatures and t_1 and t_2 are tube side terminal temperatures. [After Ref. 46.]

$$U = \frac{1}{\left[\frac{1}{h_s} + R_{fo} + \frac{t_w}{k_w}\frac{A_o}{A_m} + \left(R_{fi} + \frac{1}{h_t}\right)\frac{A_o}{A_i}\right]} \tag{7}$$

where t_w is the wall thickness and A_m is the effective mean wall heat-transfer area, which is approximated by the arithmetic mean, using the outside and inside radii, r_o and r_i:

$$A_m = \pi L(r_o + r_i) \tag{8a}$$

For a bare tube $$\frac{A_o}{A_i} \rightarrow \frac{r_o}{r_i} \tag{8b}$$

$$\frac{A_o}{A_m} \rightarrow \frac{r_o}{r_o + r_i} \tag{8c}$$

Heat-Transfer Coefficient for Finned Tubes. Bell [46] suggests that the values given for plain tubes can be usually be used with caution for low-finned tubes if the controlling resistance is placed on the shell side; the values should be reduced by 10–30% if the shell-side fluid is of medium or high viscosity, and by 50% if the shell-side fluid is of high viscosity and is being cooled. Whitley et al. [9] suggest reducing the value for finned tubes to 90% of those of plain tubes.

Fouling Resistance. Fouling resistance values may be chosen from TEMA Table RGP-T-2.4 [3]. A partial list is furnished in Chapter 9.

Calculation of A_o. Once q, U, LMTD, and F are known, the total outside heat transfer area (including fin area) A_o is readily found from the following equation:

$$A_o = \frac{q}{UF(\text{LMTD})} \tag{9}$$

Determination of Shell Size and Tube Length from Heat Transfer Area, A_o (*after Taborek* [26]). The problem now arises of how to interpret the value of A in terms of tube length and shell diameter, when both values are not known. If the problem specification specifies the limitation on shell length and diameter, the problem can be simplified. In the absence of these values, A_o is given by

$$A_o = \pi d L_{ta} N_t \tag{10}$$

and for estimation purposes, the tube count N_t is given in terms of tube pitch, L_{tp} by

$$N_t = \frac{0.78 D_{ctl}^2}{C_l L_{tp}^2} \tag{11}$$

where C_l is the tube layout constant given by

$$\begin{aligned} C_l &= 0.86 \quad \text{for} \quad \theta_{tp} = 30° \\ C_l &= 1.0 \quad \text{for} \quad \theta_{tp} = 45° \text{ and } 90° \end{aligned} \tag{12}$$

Substituting Eq. 11 into Eq. 10, the resulting equation is given by

$$A_o = (0.78\pi)\frac{d}{C_l L_{tp}^2}[L_{ta} D_{ctl}^2] \tag{13}$$

In Eq. 13, the first term is a constant; the second term reflects the tube size and tube layout geometry; and the third term includes the values of tube length and shell diameter (known as

aspect ratio), which are the items to be determined. Heat-transfer surface A_o can be obtained by various combinations of the parameter L_{ta} and D_{otl} for any given tube layout pattern. An initially assumed aspect ratio of 8 is suggested. Some tube count tables are available in Refs. 8, 10, 11, 12, and 21, and there is a tube count chart in Ref. 46 for various tube layout patterns, tube diameters, and shell diameters. This helps to calculate A_o easily. If such a source is not available, the designer must assume a rational tube length, and calculate the corresponding diameter D_{otl} and finally the shell inside diameter D_s.

Detailed Design Method: Bell–Delaware Method

Designing a shell and tube heat exchanger with the Bell–Delaware method is explained here. A flow chart for designing with the Bell–Delaware method is shown in Fig. 40.

Evaluation of Geometric Parameters. After the determination of shell inside diameter and tube length, the next step is the evaluation of geometric parameters, such as:

1. Baffle and bundle geometry
2. Flow areas
3. Various flow areas for calculating various correction factors

The calculation of various geometric parameters is known as auxiliary calculations in the Bell–Delaware method [41]. These calculations are required for the determination of shell-side heat-transfer coefficient and pressure drop. The auxiliary calculations are defined in the following steps.

Input Data. The Bell–Delaware method assumes that the flow rate and the inlet and the outlet temperatures (also pressures for a gas or vapor) of the shell-side fluid are specified and that the density, viscosity, thermal conductivity, and specific heat of the shell-side fluid are known. The method also assumes that the following minimum set of shell-side geometry data is known or specified:

Tube outside diameter, d
Tube layout pattern, θ_{tp}
Shell inside diameter, D_s
Tube bank outer tube limit diameter, D_{otl}
Effective tube length (between tubesheets), L_{tl}
Baffle cut, B_c, as a percent of D_s
Central baffle spacing, L_{bc} (also the inlet and outlet baffle spacing, L_{bi} and L_{bo}, if different from L_{bc})
Number of sealing strips per side, N_{ss}

From this geometrical information, all remaining geometrical parameters pertaining to the shell side can be calculated or estimated by methods given here, assuming that the standards of TEMA [3] are met with respect to various shell-side constructional details.

Shell-Side Parameters.

Bundle-To-Shell Clearance, L_{bb}. A suitable tube bundle is selected based on the user's requirement, and the bundle-to-shell clearance is calculated based upon these equations:

For a fixed tube-sheet heat exchanger,

$$L_{bb} = 12.0 + 0.005D_s \quad \text{(mm)}$$

For a U-tube exchanger,

$$L_{bb} = 12.0 + 0.005D_s \quad \text{(mm)}$$

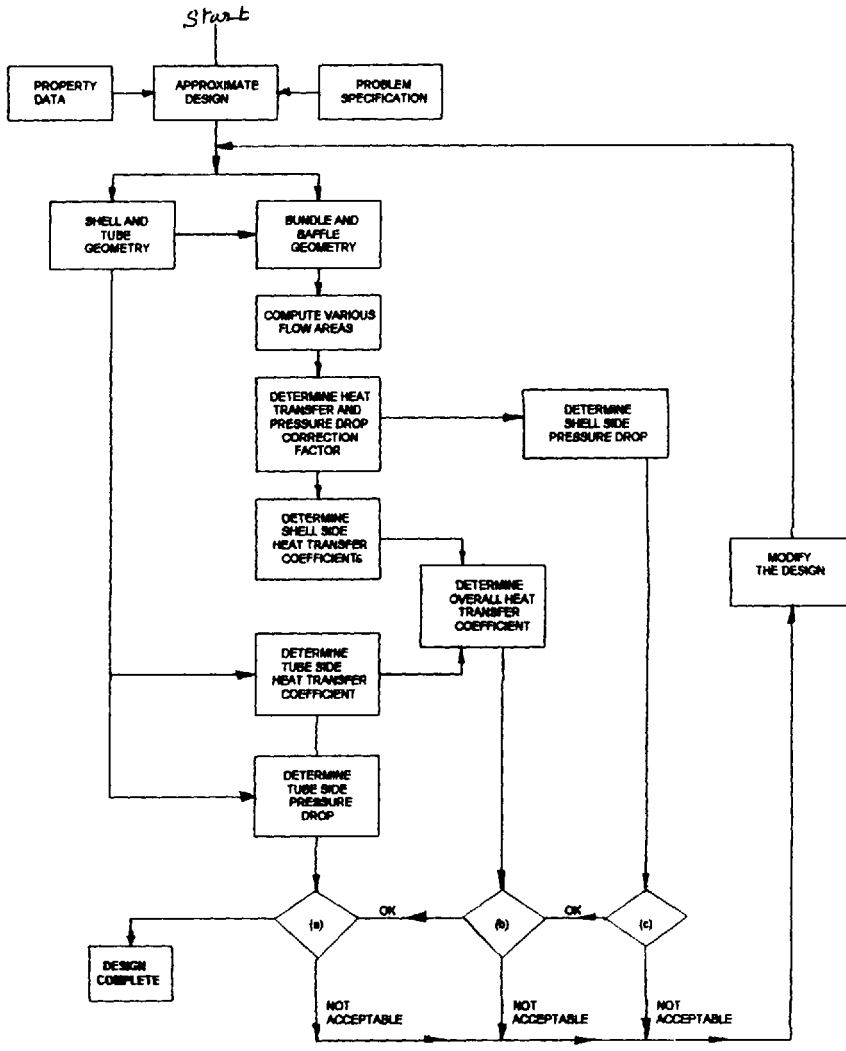


Figure 40 Flow chart for detailed design of STHE. (a) $\Delta P_t \leq$ allowed pressure drop; (b) compare area required with area available for heat transfer; and (c) $\Delta P_s \leq$ allowable pressure drop.

Bundle Diameter (D_{ctl}). This is computed from the equation

$$D_{otl} = D_s - L_{bb}$$
$$= D_{ctl} + d$$

Shell Length. This is taken as the overall nominal tube length, L_{to}, given by

$$L_{to} = L_{ta} + 2L_{ts}$$

where L_{ts} is tube sheet thickness. Its value may be assumed initially as 1 in (25.4 mm) for calculation purposes.

Central Baffle Spacing, L_{bc}. The number of baffles N_b is required for calculation of the total number of cross passes and window turnarounds. It is expressed as

$$N_b = \frac{L_{tl}}{L_{bc}} - 1 \tag{14}$$

where L_{tl} and L_{bc} are the tube length and central baffle spacing, respectively. Tube length L_{tl} is defined in Fig. 41. A uniform baffle spacing (L_{bc}) is assumed initially, equal to the shell diameter, D_s. To determine L_{tl}, we must know the tube sheet thickness. If drawings are not available, the tube-sheet thickness, L_{ts}, can be roughly estimated as $L_{ts} = 0.1D_s$ with limit $L_{ts} =$ 25 mm. Otherwise assume the minimum TEMA tubesheet thickness [3]. For all bundle types except U-tubes, $L_{tl} = L_{to} - L_{ts}$, whereas for U-tube bundles L_{to} is nominal tube length.

The number of baffles is rounded off to the lower integer value and the exact central spacing is then calculated by

$$L_{bc} = \frac{L_{ta}}{N_b + 1} \tag{15}$$

Auxiliary Calculations, Step-by-Step Procedure.

Step 1: Sequential Baffle Window Calculations. Refer to Fig. 42, which reveals the basic segmental baffle geometry in relation to the tube field. Calculate the centriangle of baffle cut, θ_{ds}, and upper centriangle of baffle cut, θ_{ctl}.

The centriangle of baffle cut, θ_{ds}, is the angle subtended at the center by the intersection of the baffle cut and the inner shell wall as shown in Fig. 42. It is given by

$$\theta_{ds} = 2 \cos^{-1}\left(1 - \frac{2B_c}{100}\right) \tag{16}$$

The upper centriangle of baffle cut, θ_{ctl}, is the angle subtended at the center by the intersection of the baffle cut and the tube bundle diameter, as shown in Fig. 42. It is given by

$$\theta_{ctl} = 2 \cos^{-1}\left[\frac{D_s}{D_{ctl}}\left(1 - \frac{2B_c}{100}\right)\right] \tag{17}$$

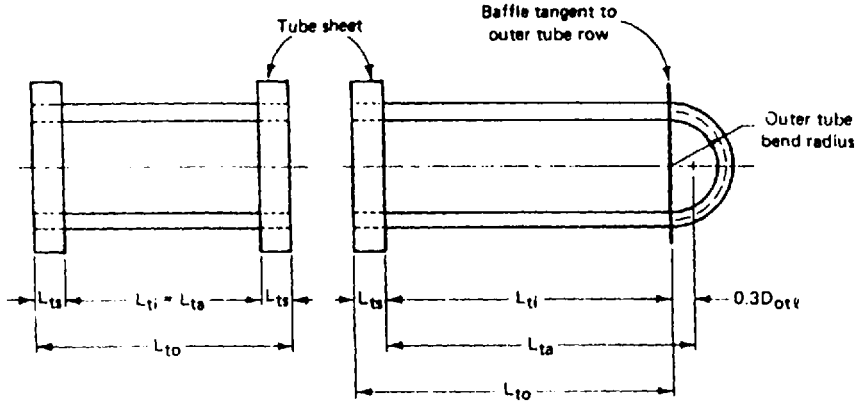


Figure 41 Tube length definition.

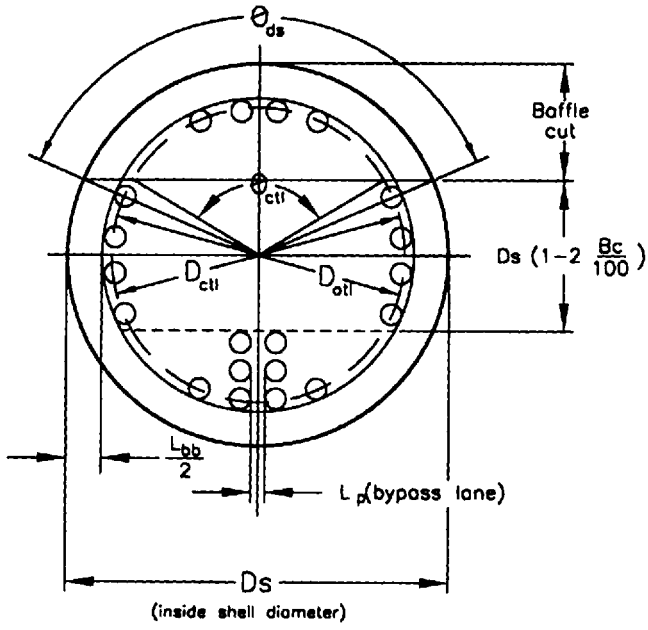


Figure 42 Basic segmental baffle geometry.

Step 2: Shell-Side Crossflow Area. The shell-side crossflow area, S_m, is given by

$$S_m = L_{bc}\left[L_{bb} + \frac{D_{ctl}}{L_{tp,eff}}(L_{tp} - d)\right] \tag{18}$$

where

$$L_{bb} = D_s - D_{otl}$$
$$D_{ctl} = D_{otl} - d$$
$$L_{tp,eff} = L_{tp} \quad \text{for } 30° \text{ and } 90° \text{ layouts}$$
$$= 0.707L_{tp} \quad \text{for } 45° \text{ staggered layouts}$$
$$L_{tp} = \text{tube pitch}$$

Basic tube layout parameters are given in Table 5.

Step 3: Baffle Window Flow Areas. The gross window flow area, i.e., without tubes in the window, S_{wg}, is given by

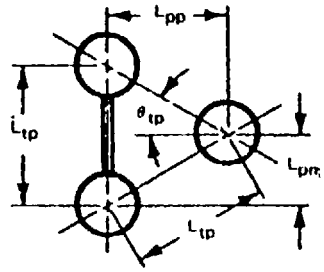
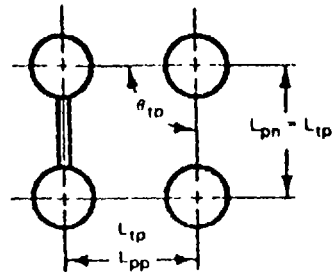
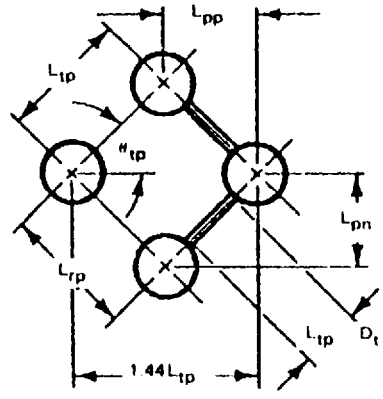
$$S_{wg} = \frac{\pi}{4} D_s^2 \left(\frac{\theta_{ds}}{2\pi} - \frac{\sin \theta_{ds}}{2\pi}\right) \tag{19}$$

From the calculations of centriangle and gross window flow area, calculate the fraction of tubes in baffle window, F_w, and in pure crossflow, F_c, that is, between the baffle cut tips as indicated in Fig. 42 by distance $D_s[1 - 2(B_c/100)]$:

$$F_c = 1 - 2F_w \tag{20}$$

where F_w is the fraction of number of tubes in the baffle window, given by

Table 5 Tube Layout Basic Parameters [38]

Cross flow →	θ_{tp}	L_{pn}	L_{op}
	30°	0.5 L_{tp}	0.866 L_{tp}
	90°	L_{tp}	L_{tp}
	45°	0.707 L_{tp}	0.707 L_{tp}

$$F_w = \frac{\theta_{ctl}}{2\pi} - \frac{\sin\ \theta_{ctl}}{2\pi} \tag{21}$$

The segmental baffle window area occupied by the tubes, S_{wt}, can be expressed as

$$S_{wt} = N_{tw}\frac{\pi}{4}d^2 \tag{22a}$$

$$= N_t F_w \frac{\pi}{4} d^2 \tag{22b}$$

The number of tubes in the window, N_{tw}, is expressed as

$$N_{tw} = N_t F_w \tag{23}$$

The net crossflow area through one baffle window, S_w, is the difference between the gross flow area, S_{wg}, and the area occupied by the tubes, S_{wt}. Net crossflow area through one baffle window, S_w, is given by

$$S_w = S_{wg} - S_{wt} \tag{24}$$

Step 4: Equivalent Hydraulic Diameter of a Segmental Baffle Window, D_w. The equivalent hydraulic diameter of a segmental baffle window, D_w, is required only for pressure-drop calculations in laminar flow, i.e., if $Re_s < 100$. It is calculated by classical definition of hydraulic diameter, i.e., four times the window crossflow area S_w divided by the periphery length in contact with the flow. This is expressed in the following equation:

$$D_w = \frac{4S_w}{\pi d N_{tw} + \pi D_s \theta_{ds}/2\pi} \tag{25}$$

Step 5: Number of Effective Tube Rows in Crossflow, N_{tcc}, and Baffle Window, N_{tcw}. The number of effective tube rows crossed in one crossflow section, i.e., between the baffle tips, is expressed as N_{tcc}:

$$N_{tcc} = \frac{D_s}{L_{pp}}\left(1 - \frac{2B_c}{100}\right) \tag{26}$$

where L_{pp} is the effective tube row distance in the flow direction, which is given in Table 5. The effective number of tube rows crossed in the baffle window, N_{tcw}, is given by

$$N_{tcw} = \frac{0.8}{L_{pp}}\left[\frac{D_s B_c}{100} - \frac{D_s - D_{otl}}{2}\right] \tag{27}$$

Step 6: Bundle-to-Shell Bypass Area Parameters, S_b and F_{sbp}. The bypass area between the shell and the tube bundle within one baffle, S_b, is given by

$$S_b = L_{bc}(D_s - D_{otl} + L_{pl}) \tag{28}$$

where L_{pl} expresses the effect of the tube lane partition bypass width (between tube walls) as follows: L_{pl} is 0 for all standard calculations; L_{pl} is half the dimension of the tube lane partition L_p. For estimation purposes, assume that $L_p = d$.

For calculations of the correction factors J_l and R_l, the ratio of the bypass area, S_b, to the overall crossflow area, S_m, designated as F_{sbp}, is calculated from the expression

$$F_{sbp} = \frac{S_b}{S_m} \tag{29}$$

Step 7: Shell-to-Baffle Leakage Area for One Baffle, S_{sb}. The shell-to-baffle leakage area, S_{sb}, is a factor for calculating baffle leakage effect parameters J_l and R_l. The diametral clearance between the shell diameter D_s and the baffle diameter D_b is designated as L_{sb} and given by

$$L_{sb} = 3.1 + 0.004 D_s \tag{30}$$

The shell-to-baffle leakage area within the circle segment occupied by the baffle is calculated as:

$$S_{sb} = \pi D_s \frac{L_{sb}}{2} \left(\frac{2\pi - \theta_{ds}}{2\pi} \right) \tag{31}$$

Step 8: Tube-to-Baffle-Hole Leakage Area for One Baffle, S_{tb}. The tube-to-baffle-hole leakage area for one baffle, S_{tb}, is required for calculation of the correction factors J_l and R_l. The total tube-to-baffle leakage area is given by

$$S_{tb} = \frac{\pi}{4}[(d + L_{tb})^2 - d^2]N_t(1 - F_w) \tag{32}$$

where L_{tb} is diametral clearance between tube outside diameter and baffle hole. TEMA standards specify recommended clearances as a function of tube diameter and baffle spacing. Its value is either 0.8 or 0.4.

Step 9: Calculate Shell-Side Crossflow Velocity, U_s. The shell-side crossflow velocity U_s from shell-side mass flow rate M_s is given by

$$U_s = \frac{M_s}{\rho_s S_m} \tag{33}$$

where ρ_s is the mass density of the shell-side fluid. Equation 33 gives shell-side crossflow velocity as per the Bell–Delaware method. Since flow-induced vibration guidelines given in the TEMA Standards [3] are based on crossflow velocity as per Tinker [34], the procedure to calculate crossflow velocity is given in Appendix 1.

Shell-Side Heat Transfer and Pressure Drop Correction Factors.

Heat Transfer Correction Factors. In the Bell–Delaware method, the flow fraction for each stream is found by knowing the corresponding flow areas and flow resistances. The heat-transfer coefficient for ideal crossflow is then modified for the presence of each stream through correction factors. The shell-side heat-transfer coefficient, h_s, is given by

$$h_s = h_i J_c J_l J_b J_s J_r \tag{34}$$

where h_i is the heat transfer coefficient for pure crossflow of an ideal tube bank. The correction factors in Eq. 34 are:

J_c is the correction factor for baffle cut and spacing. This correction factor is used to express the effects of the baffle window flow on the shell-side ideal heat-transfer coefficient h_i, which is based on crossflow.

J_l is the correction factor for baffle leakage effects, including both shell-to-baffle and tube-to-baffle leakage.

J_b is the correction factor for the bundle bypass flow (C and F streams).

J_s is the correction factor for variable baffle spacing in the inlet and outlet sections.

J_r is the correction factor for adverse temperature gradient buildup in laminar flow.

The combined effect of all of these correction factors for a reasonably well-designed shell and tube heat exchanger is typically of the order of 0.6; i.e., the effective mean shell-side heat-transfer coefficient for the exchanger is of the order of 60% of that calculated if the flow took place across an ideal tube bank corresponding in geometry to one crossflow section. It is interesting to note that this value was suggested by McAdams [47] in 1933 and has been used as a rule of thumb [1].

Pressure Drop Correction Factors. The following three correction factors are applied for pressure drop:

1. Correction factor for bundle bypass effects, R_b
2. Correction factor for baffle leakage effects, R_l
3. Correction factor for unequal baffle spacing at inlet and/or outlet, R_s

Step-by-Step Procedure to Determine Heat Transfer and Pressure Drop Correction Factors.

Step 10: Segmental Baffle Window Correction Factor, J_c. For the baffle cut range 15–45%, J_c is expressed by

$$J_c = 0.55 + 0.72F_c \tag{35}$$

This value is equal to 1.0 for NTIW design, increases to a value as high as 1.15 for small baffle cut, and decreases to a value of about 0.52 for very large baffle cuts. A typical value for a well-designed heat exchanger with liquid on the shell side is about 1.0.

Step 11: Correction Factors for Baffle Leakage Effects for Heat Transfer, J_l, and Pressure Drop, R_l. The correction factor J_l penalizes the design if the baffles are put too close together, leading to an excessive fraction of the flow being in the leakage streams compared to the crossflow stream. R_l is the correction factor for baffle leakage effects. For computer applications, the correction factors are curve-fitted as follows:

$$J_l = 0.44\ (1 - r_s) + [1 - 0.44(1 - r_s)]e^{-2.2r_{lm}} \tag{36}$$

$$R_l = \exp[-1.33(1 + r_s)]r_{lm}^{\ x} \tag{37}$$

where

$$x = [-0.15(1 + r_s) + 0.8] \tag{38}$$

The correlational parameters used are

$$r_s = \frac{S_{sb}}{S_{sb} + S_{tb}} \tag{39}$$

$$r_{lm} = \frac{S_{sb} + S_{tb}}{S_m} \tag{40}$$

where S_{sb} is the shell-to-baffle leakage area, S_{tb} the tube-to-baffle leakage area, and S_m the crossflow area at bundle centerline.

A well-designed exchanger should have a valve of J_l not less than 0.6, preferably in the range 0.7–0.9. If a low J_l value is obtained, modify the design with wider baffle spacing, increase tube pitch, or change the tube layout to 90° or 45°. More drastic measures include change to double or triple segmental baffles, TEMA J shell type, or both. A typical value for R_l is in the range of 0.4–0.5, though lower values may be found in exchangers with closely spaced baffles.

Step 12: Correction Factors for Bundle Bypass Effects for Heat Transfer, J_b, and Pressure Drop, R_b. To determine J_b and R_b, the following parameters must be known:

1. N_{ss}, the number of sealing strips (pairs) in one baffle
2. N_{tcc}, the number of tube rows crossed between baffle tips in one baffle section

The expression for J_b is correlated as

$$J_b = \exp\{-C_{bh}F_{sbp}[1 - (2r_s)^{1/3}]\} \tag{41}$$

where

C_{bh} = 1.25 for laminar flow, $Re_s \leq 100$, with the limit of $J_h = 1$, at $r_{ss} \geq 0.5$
= 1.35 for turbulent and transition flow, $Re_s > 100$

The expression for R_h is given by

$$R_h = e^{[-C_{hp}F_{sbp}(1-(r_{ss})^{1/3})]} \tag{42}$$

where

$$\gamma_{ss} = \frac{N_{ss}}{N_{tcc}} \tag{43}$$

with the limits of

$R_h = 1$ at $r_{ss} \geq 0.5$
C_{hp} = 4.5 for laminar flow, $Re_s \leq 100$
= 3.7 for turbulent and transition flow, $Re_s > 100$

For the relatively small clearance between the shell and the tube bundle, J_h is about 0.9: for the much larger clearance required by pull through floating head construction, it is about 0.7. J_h can be improved using sealing strips.

A typical value for R_h ranges from 0.5 to 0.8, depending upon the construction type and number of sealing strips. The lower value would be typical of a pull through floating head with only one or two pairs of sealing strips, and the higher value typical of a fully tubed fixed tube-sheet exchanger.

Step 13: Heat-Transfer Correction Factor for Adverse Temperature Gradient in Laminar Flow, J_r. J_r applies only if the shell-side Reynolds number is less than 100 and is fully effective only in deep laminar flow characterized by Re_s less than 20. For $Re_s < 20$, J_r can be expressed as:

$$J_r = \frac{1.51}{N_c^{0.18}} \tag{44}$$

where N_c is the total number of tube rows crossed in the entire exchanger. N_c is given by

$$N_c = (N_{tcc} + N_{tcw})(N_b + 1) \tag{45}$$

For Re_s between 20 and 100, a linear proportion is applied resulting in

$$J_r = \frac{1.51}{N_c^{0.18}} + \left(\frac{20 - Re_s}{80}\right)\left(\frac{1.51}{N_c^{0.18}} - 1\right) \tag{46}$$

with the limit

$J_r = 0.400$ for $Re_s \leq 100$
$J_r = 1$ for $Re_s > 100$

Step 14: Heat-Transfer Correction for Unequal Baffle Spacing at Inlet and/or Outlet, J_s. Figure 43 shows a schematic sketch of an exchanger where the inlet and outlet baffle spacing L_{bi} and L_{bo} are shown in comparison to the central baffle spacing, L_{bc}:

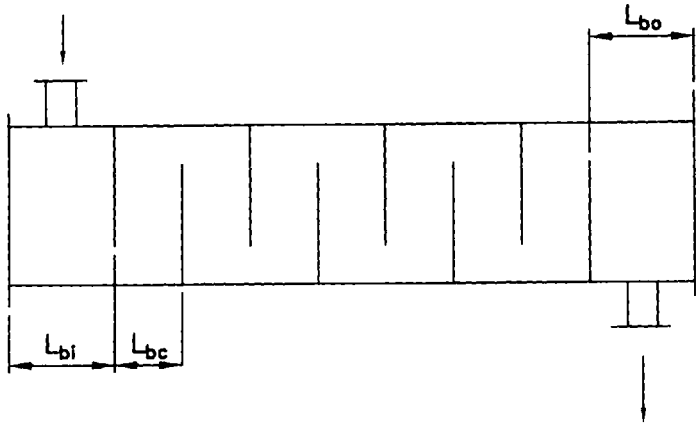


Figure 43 Typical layout of baffle spacings.

$$J_s = \frac{(N_b - 1) + (L_i^*)^{1-n} + (L_o^*)^{1-n}}{(N_b - 1) + (L_i^* - 1) + (L_o^* - 1)} \tag{47}$$

where

$$L_i^* = \frac{L_{bi}}{L_{bc}} \qquad L_o^* = \frac{L_{bo}}{L_{bc}} \tag{48}$$

J_s will usually be between 0.85 and 1.0. If $L_{bi} = L_{bo} = L_{bc}$ or $L^* = L_i^* = L_o^* = 1.0$, $J_s = 1.0$. For turbulent flow, $n = 0.6$ and values of L^* larger than 2 would be considered poor design, especially if combined with a few baffles only, i.e., low N_b. In such a case an annular distributor or other measures should be used. Typical arrangements for increasing effectiveness of end zones are presented by Tinker [33]. For laminar flow, the correction factor is about halfway between 1 and J_s computed for turbulent conditions.

Step 15: Pressure-Drop Correction for Unequal Baffle Spacing at Inlet and/or Outlet, R_s. R_s is given by

$$R_s = \left(\frac{1}{L_i^*}\right)^{2-n} + \left(\frac{1}{L_o^*}\right)^{2-n} \tag{49}$$

with $n = 1$ for laminar flow, $\mathrm{Re}_s \le 100$, and $n = 0.2$ for turbulent flow.

1. For $L_{bc} = L_{bo} = L_{bi}$, $R_s = 2$.
2. For the reasonable extreme case $L_{bo} = L_{bi} = 2L_{bc}$, $R_s = 1.0$ for laminar flow, and $R_s = 0.57$ for turbulent flow.
3. For a typical U-tube, $L_{bi} = L_{bc}$ and $L_{bo} = 2L_{bc}$, $R_s = 1.5$ for laminar flow, and $R_s = 3.0$ for turbulent flow.

Shell-Side Heat-Transfer Coefficient and Pressure Drop.

Shell-Side Heat-Transfer Coefficient.

1. Calculate the shell-side mass velocity G_s, Reynolds number Re_s, and Prandtl number Pr_s:

$$G_s = \frac{M_s}{S_m} \quad \mathrm{kg/(m^2 \cdot s)} \text{ or } \mathrm{lb_m/(h \cdot ft^2)} \tag{50}$$

$$\mathrm{Re}_s = \frac{dG_s}{\mu} \qquad \mathrm{Pr}_s = \frac{\mu_s C_{ps}}{k_s} \tag{51}$$

2. Calculate the ideal heat transfer coefficient h_i given by

$$h_i = \frac{j_i C_{ps} G_s (\phi_s)^n}{\mathrm{Pr}_s^{2/3}} \tag{52}$$

where j_i and $(\phi_s)^n$ are defined next.

The term j_i is the ideal Coulburn j factor for the shell side and can be determined from the appropriate Bell–Delaware curve for the tube layout and pitch and a typical curve. For example, $d = 0.75$ in (19.05 mm), pitch = 1.0 in (25.4 mm), and $\theta_{tp} = 30°$, curve fits for j_i are given by Bell [40]:

$$j_i = 1.73\mathrm{Re}_s^{(-0.694)} \qquad 1 \le \mathrm{Re}_s < 100 \tag{53a}$$

$$= 0.717\mathrm{Re}_s^{(-0.574)} \qquad 100 \le \mathrm{Re}_s < 1000 \tag{53b}$$

$$= 0.236\mathrm{Re}_s^{(-0.346)} \qquad 1000 \le \mathrm{Re}_s \tag{53c}$$

The term $(\phi_s)^n$ is the viscosity correction factor, which accounts for the viscosity gradient at the tube wall versus the viscosity at the bulk mean temperature of the fluid, and is given by [48]:

$$(\phi_s)^n = \left(\frac{\mu_s}{\mu_w}\right)^{0.14} \tag{54}$$

For liquids, ϕ_s is greater than 1 if the shell-side fluid is heated, and less than 1 for shell-side fluid is cooled. In order to determine μ_w, it is essential to determine T_w, which is estimated as follows using the approximate values of h_i and h_s [48]:

$$T_w = T_{t,av} + \frac{T_{s,av} - T_{t,av}}{1 + h_i h_s} \tag{55}$$

where $T_{s,av}$ and $T_{t,av}$ denote the average mean metal temperatures of shell and tube, both of them being the arithmetic means of inlet and outlet fluid temperatures on the shell side and tube side, respectively. An accurate equation to calculate tube mean metal temperature is given by TEMA [3]. For gases, the viscosity is a weak function of temperature. The correction factor ϕ_s is formulated as follows

For gases being cooled: $(\phi_s)^n = 1.0$ (56)

For gases being heated: $$(\phi_s)^n = \left[\frac{(T_{s,av} + 273.15)}{(T_w + 273.15)}\right]^{0.25} \tag{57}$$

For a gas being heated, T_w is always higher than $T_{s,av}$ and hence the correction factor is less than 1.0. Calculate the shell-side heat-transfer coefficient, given by

$$h_s = h_i J_c J_l J_s J_b J_r \tag{58}$$

Shell-Side Pressure Drop. The shell-side pressure drop is calculated in the Delaware method by summing the pressure drop for the inlet and exit sections, and the internal sections after applying various correction factors. The total shell-side pressure drop Δp_s consists of the pressure drop due to (1) crossflow Δp_c, (2) window regions Δp_w, and (3) entrance and exit sections Δp_e as given by Refs. 39 and 40:

$$\Delta p_s = \Delta p_c + \Delta p_w + \Delta p_e \tag{59}$$

The elements of shell-side pressure drop are shown schematically in Fig. 44. The crossflow pressure drop and the entrance and exit region pressure drop depend on the ideal tube bank pressure drop, given by

$$\Delta p_{b,i} = 2 f_s N_{tcc} \frac{G_s^2}{g_c \rho_s} (\phi_s)^{-n} \tag{60}$$

The friction factor f can be determined from the appropriate Bell–Delaware curve for the tube layout and pitch under consideration. For example, for $d = 0.75$ in (19.05 mm), pitch = 1.0 in (25.4 mm), and $\theta_{tp} = 30°$, curve fits for f_s are given by Bell [40]:

$$f_s = \frac{52}{\mathrm{Re}_s} + 0.17 \qquad 1 \le \mathrm{Re}_s < 500 \tag{61a}$$

$$= 0.56 \mathrm{Re}_s^{(-0.14)} \qquad 500 \le \mathrm{Re}_s \tag{61b}$$

Calculate the various terms of shell-side pressure drop as given next, and finally calculate the overall heat-transfer coefficient.

1. The pressure drop in the interior crossflow sections is affected by both bypass and leakage. Therefore, the combined pressure drop of all the interior crossflow sections is given by:

$$\Delta p_c = (N_b - 1)(\Delta p_{b,i} R_b R_l) \tag{62}$$

2. The pressure drop in the entrance and exit sections is affected by bypass but not by leakage, and by variable baffle spacing. Therefore, the combined pressure drop for the entrance and exit sections is

$$\Delta p_e = 2(\Delta p_{b,i}) \left(1 + \frac{N_{tcw}}{N_{tcc}}\right) R_b R_s \tag{63}$$

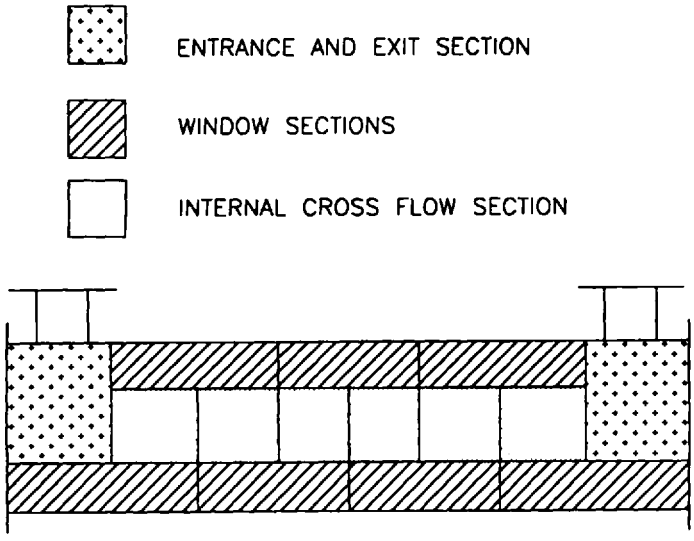


Figure 44 Elements of shellside pressure drop of a TEMA E-shell.

3. The pressure drop in the windows is affected by leakage but not by bypass. Therefore, the combined pressure drop of all the window sections is given by

$$\Delta p_w N_b R_l \tag{64}$$

where Δp_w is given as follows:

For $Re_s \geq 100$,

$$\Delta p_w = \frac{(2 + 0.6N_{tcw})G_w^2}{2g_c\rho_s} \tag{65}$$

For $Re_s < 100$,

$$\Delta p_w = 26\frac{G_w\mu_s}{g_c\rho_s}\left(\frac{N_{tcw}}{L_{tp} - d} + \frac{L_{bc}}{D_w^2}\right) + 2\frac{G_w^2}{g_c\rho_s} \tag{66}$$

in which the window mass velocity G_w is given by

$$G_w = \frac{M_s}{\sqrt{S_m S_w}} \tag{67}$$

Summing these individual effects, we obtain the equation for the total nozzle-to-nozzle shell-side pressure drop:

$$\Delta p_s = [(N_b - 1)(\Delta p_{b,i}R_b) + N_b(\Delta p_w)]R_l + 2(\Delta p_{b,i})\left(1 + \frac{N_{tcw}}{N_{tcc}}\right)R_b R_s \tag{68}$$

The total shell-side pressure drop of a typical shell and tube exchanger is of the order of 20–30% of the pressure drop that would be calculated for flow through the corresponding heat exchanger without baffle leakage and without tube bundle bypass effects [39].

Tube-Side Heat-Transfer Coefficient and Pressure Drop.

Tube-Side Heat-Transfer Coefficient.

1. Calculate the tube-side mass velocity G_t, Reynolds number Re_t, and Prandtl number, Pr_t:

$$G_t = \frac{M_t}{A_t} \quad \text{for single pass} \tag{69a}$$

$$= \frac{M_t}{A_t/N_p} \quad \text{for } N_p \text{ passes} \tag{69b}$$

where

$$A_t = \frac{\pi}{4}d_i^2 N_t$$

and where A_t is the tube-side flow area, N_p the number of tube-side passes, N_t the number of tubes, and

$$Re_t = \frac{G_t d_i}{\mu_t} \qquad Pr_t = \frac{\mu_t C_{pt}}{k_t} \tag{70}$$

2. Calculate the tube-side heat-transfer coefficient, h: For laminar flow with Re_t of 2100 and less, the heat-transfer coefficient is determined from the Sider–Tate (1936) empirical equation for both heating and cooling of viscous liquids:

$$\frac{h_i d_i}{k_t} = 1.86\left[\mathrm{Re}_t Pr \frac{d_i}{L}\right]^{0.5} Pr_t^{1/3} \left(\frac{\mu_t}{\mu_w}\right)^{0.14} \tag{71}$$

For those cases where the Grashof number Na_r exceeds 25,000 the value of h obtained from Eq. (71) must be corrected for the increase in heat transfer due to natural convection effects by multiplying by the term

$$0.8(1 + 0.015 Na_r^{1/3}) \tag{71a}$$

$$Na_r = \frac{\beta \Delta t\, d_i^2 \rho_i^2 g_c}{\mu_t^2} \tag{71b}$$

where β = thermal coefficient of cubical expansion, 1/°F; Δt = temperature difference, °F; Na_r = Grashof number; ρ_i = tubeside fluid density, lb/ft^3; g_c = acceleration of gravity, 4.17×10^8 ft/hr^2; μ_t = viscosity at bulk mean temperature, lb/hr.ft.

At values above 10,000 turbulent flow occurs and the heat transfer coefficient is determined from the following correlation:

Sider–Tate equation modified by McAdams:

$$\frac{h_i d_i}{k_t} = 0.027 \mathrm{Re}_t^{0.8}\, \mathrm{Pr}_t^{1/3} \left(\frac{\mu_t}{\mu_w}\right)^{0.14} \tag{72}$$

In the intermediate region where Reynolds number varies from 2100 to 10,000 the relation does not follow a straight line. Fig. 45 can be used to find the tube side heat transfer coefficient using Sider-Tate relation.

Colburn equation:

$$\frac{h_i d_i}{k_t} = 0.023 \mathrm{Re}_t^{0.8}\, \mathrm{Pr}_t^{0.4} \left(\frac{\mu_t}{\mu_w}\right)^{0.14} \tag{73a}$$

Dittus–Boelter equation

$$\frac{h_i d_i}{k_t} = 0.023 \mathrm{Re}_t^{0.8}\, \mathrm{Pr}_t^{n} \tag{73b}$$

where

$n = 0.4$ for heating
$= 0.3$ for cooling

In the intermediate region where Re_t varies between 2100 and 10,000, the relation does not follow a straight line. In this region, Kern [40] recommends the following formula:

$$\frac{h_i d_i}{k_t} = 0.116[\mathrm{Re}_t^{2/3} - 125]\left[1 + \left(\frac{d_i}{L}\right)^{2/3}\right] \mathrm{Pr}_t^{1/3} \left(\frac{\mu_t}{\mu_w}\right)^{0.14} \tag{74}$$

Pressure Drop in Tubes and Pipes—General. For tubes and pipes, the pressure drop in steady flow between any two points may be expressed by the following Weisbach–Darcy equation:

$$\Delta p_t = f_t \left(\frac{L}{d_i} \right) \frac{G_t^2}{2g_c \rho_t} \frac{1}{(\phi_t)^r} \tag{75}$$

where

$$(\phi_t)^r = \left(\frac{\mu_t}{\mu_w} \right)^{0.14} \quad \text{for } \mathrm{Re}_t > 2100 \tag{76a}$$

$$= \left(\frac{\mu_t}{\mu_w} \right)^{0.25} \quad \text{for } \mathrm{Re}_t < 2100 \tag{76b}$$

and where L is the length of pipe between two points, d_i the inside diameter of the pipe, ρ_t the mass density of the tube-side fluid, G_t the mass velocity of the fluid inside the pipe, and f the friction factor. To determine the pressure drop through the tube bundle, multiply the pressure drop by the number of tubes. For multipass arrangements, multiply by the number of tube-side passes.

Tubeside Pressure Drop. The total pressure drop for a single pass consists of the following items:

1. Pressure drop in the nozzles, Δp_n, which is the sum of pressure drop in the inlet ($\Delta p_{n,i}$) and outlet nozzle ($\Delta p_{n,o}$):

$$\Delta p_n = \frac{1.5 G_n^2}{2g_c \rho_t} \tag{77}$$

2. Sudden contraction and expansion losses at the tube entry and exit, $\Delta p_{c,e}$, is given by

$$\Delta p_{c,e} = \frac{G_t^2}{2g_c \rho_t} (K_c + K_e) N_p \tag{78}$$

where K_c and K_e are the contraction and expansion loss coefficients (Fig. 4 of Chapter 3).

3. Pressure drop through the tube bundle, Δp_t:

$$\Delta p_t = \frac{f L_{tp} G_t^2 N_p}{2g_c \rho_t d_i} \frac{1}{\phi_t^r} \tag{79}$$

4. Pressure drop associated with the turning losses, Δp_r, given by:

$$\Delta p_r = \frac{4 N_p G_t^2}{2g_c \rho_t}$$

$$= 4N_p \times \text{Velocity head per pass} \tag{80}$$

Total tube-side pressure drop, Δp_t, is given by

$$\Delta p_t = \frac{G_t^2}{2g_c \rho_t} \left[\frac{1.5}{N_p} + \frac{f L_{tp}}{d_i} \frac{1}{(\phi_t)^r} + K_c + K_e + 4 \right] N_p \tag{81}$$

Determination of Fanning Friction Factor f on the Tube Side. The friction factor f has been found to depend upon Reynolds numbers only. For laminar flow in smooth pipes, the value of f can be derived from the well-known Hagen–Poiseuille equation.

Accordingly, f for laminar flow is given by:

$$f = \frac{64}{\mathrm{Re}_t} \tag{82}$$

For turbulent flow in smooth pipes, f can be determined from the Blasius empirical formula given by:

$$f = \frac{0.3164}{\mathrm{Re}_t^{0.25}} \tag{83}$$

This equation is valid for Reynolds numbers up to 1000,000. Another formula to determine f for smooth walled conduits in the Reynolds number range 10,000–120,000 is given by [49]:

$$f = \frac{0.184}{\mathrm{Re}_t^{0.2}} \tag{84}$$

Calculate the overall heat transfer coefficient, U, as per Eq. 7 using the values of h_s and h_t from Eq. 53 and Eq. 71, respectively.

Calculate heat transfer area, A_o, required using Eq. 9 using the U value calculated earlier.

Evaluation and Comparison of the Results with the Specified Values

In the evaluation stage, the calculated values of the film coefficients and the pressure drop, for both the streams, are compared with the specified values. If the values match, the design is complete. If the calculated values and the specified values do not match, repeat the design with new design variables. Sometimes, even after many iterations, the design may not meet the specified performance limits in the following parameters [26]:

1. Heat-transfer coefficient
2. Pressure drop
3. Temperature driving force
4. Fouling factors

Taborek [26] describes various measures to overcome limitations in these parameters. For the heat-transfer-limited cases, utilize the permissible pressure drop effectively. The film coefficients can be increased by increasing the flow velocities, changing the baffle spacing, changing the number of the tube-side passes, etc. Attempts to increase the heat-transfer coefficient also results in pressure-drop increase. Designs with inherently low heat-transfer coefficients, such as laminar flow or low-pressure gases, may deserve special attention. For pressure-drop-limited cases, try alternate designs such as [26]:

Double or multiple segmental baffles
Use TEMA J or X shell
Reduce tube length
Increase tube pitch
Change tube layout pattern.

For the temperature-driving-force-limited cases, methods to improve the LMTD correction factor have been discussed while describing various shell types and pass arrangements. Fouling-limited cases are dealt with during the design stage by making sure that the factors promoting fouling are suppressed and/or designed for periodic cleaning.

Accuracy of the Bell–Delaware Method

It should be remembered that this method, though apparently generally the best in the open literature, it is not extremely accurate [13]. Palen et al. [13] compare the thermohydraulic

performance prediction error of Bell–Delaware methods [38,39], stream analysis methods [13], and Tinker [37].

Extension of the Delaware Method to Other Geometries

The Delaware method, as originally developed and as it exists in the open literature, is more or less explicitly confined to the design of fully tubed E shell configurations using plain tubes. Extension of this method to other geometries are discussed in Refs. 15 and 27, and these are discussed in this subsection.

Applications to Low-Finned Tubes. It is possible to apply the Delaware method to the design of such heat exchangers in a fairly straightforward way by making use of the results of Brigs and Young [50] and Briggs, Katz, and Young [51]. As shown by Briggs et al. [51], the Colburn j factor for low-finned tubes is slightly less than for a plain tube in the Reynolds number range about 2–1000; the difference is larger in the lower Reynolds number range. The fin-tube j factor j_f can be represented in terms of plain-tube-bank j factor as j_f as [15]:

$$j_f = K_f j_i \tag{85}$$

where K_f is the correction factor whose values, taken from Ref. 50, are presented in Ref. 15. Its approximate values at discrete points are:

Re	20	70	100	200	400	600	800–1000
K_f	0.575	0.65	0.675	0.75	0.885	0.975	1.0

For the fin tube friction factor, Bell [39,40] suggests a conservative value that is 1.5 times those for the corresponding plain tube bank, whereas Taborek [15] recommends 1.4 times the friction factor of the plain tube bank. The adaptation of the Bell–Delaware method to finned tubes is explained in Refs. 15 and 27.

Application to the No-Tubes-in-Window Configuration. In calculations, use $N_{cw} = 0$ and the baffle configuration correction factor $J_c = 1$. Otherwise the calculation is essentially identical to a fully tubed bundle. It is suggested that one choose a smaller baffle cut so that the free flow area through the window corresponds reasonably closely to the free crossflow area through the tube bank itself.

Application to F Shells. Since the shell side is essentially split in two, it is possible to adopt the Delaware method by reducing all of the areas for flow by half compared to the case for a single shell side pass. It is assumed that the flow leakage and conduction across the longitudinal baffle are minimized.

Application to J Shells. The adaptation of the method to a J shell is straightforward. Take one-half the length of the exchanger as a "unit" equivalent to an E shell and take one-half the mass flow rate.

Application to Double Segmental and Disk and Doughnut Exchangers. According to Taborek [15], the Bell–Delaware method cannot be easily adapted to these baffle types, as the driving forces for bypass and leakage flow are much smaller than for segmental baffles.

APPENDIX 1

A1.1 Reference Crossflow Velocity as per Tinker [37]

Reference crossflow velocity as per Tinker is given by:

$$U_s = \frac{F_h M_s}{M A_s \rho_s} \tag{86}$$

where A_s is the crossflow area within the limits of the tube bundle, F_h is the fraction of total fluid flowing through A_s of clean unit, M is the A_s multiplication factor, M_s is the mass flow rate of shell-side fluid, and ρ_s is the mass density of shell-side fluid.

$$A_s = a_s L_{bc} D_s \tag{87}$$

$$F_h = \frac{1}{1 + N_h\sqrt{S}} \tag{88}$$

$$M = \frac{1}{1 + \dfrac{0.7L_{bc}}{D_1}\left[\dfrac{1}{M_w^{0.6}} - 1\right]} \tag{89}$$

The list of expressions required to evaluate N_h, M_w are

$$a_1 = \frac{D_1}{D_s} \tag{90}$$

For units with sealing strips, a_1 is given by

$$a_1 = 1 + \left[\frac{D_1/D_s - 1}{4}\right] + 1.5\left[\frac{D_1 - D_2}{D_1}\right] \tag{91}$$

$$a_2 = \frac{d_B - d}{d} \tag{92}$$

$$a_3 = \frac{D_1 - D_2}{D_1} \tag{93}$$

$$b_1 = \frac{(a_1 - 1)^{1.5}}{a_1} \tag{94}$$

$$b_2 = \frac{a_2}{a_1^{1.5}} \tag{95}$$

$$b_3 = a_3\sqrt{a_1} \tag{96}$$

The terms a_s, a_4, a_5, a_6, and m are dependent on the tube layout pattern and they are given in Table 6.

The expression for a_7 is:

Table 6 Terms to Find Crossflow Velocity

	30°	90°	45°	60°
a_s	$\dfrac{0.97\ (p-d)}{p}$	$\dfrac{0.97(p-d)}{p}$	$\dfrac{1.372(p-d)}{p}$	$\dfrac{0.97(p-d)}{p}$
a_4	1.26	1.26	0.90	1.09
a_5	0.82	0.66	0.56	0.61
a_6	1.48	1.38	1.17	1.28
m	0.85	0.93	0.80	0.87

Note: Values for 60° have been taken from TEMA [3].

$$a_7 = a_4 \left(\frac{p}{p-d} \right)^{1.5} \tag{97}$$

Values for a_8 are given in Table 7.

$$A = a_5 a_8 \left(\frac{D_1}{L_{bc}} \right) \left(\frac{d}{p} \right)^2 \left(\frac{p}{p-d} \right) \tag{98}$$

$$E = a_6 \left(\frac{p}{p-d} \right) \left(\frac{D_1}{L_{bc}} \right) \left(1 - \frac{h}{D_1} \right) \tag{99}$$

$$N_h = a_7 b_1 + A b_2 + b_3 E \tag{100}$$

$$M_w = m a_1^{0.5} \tag{101}$$

Nomenclature

A_h crossflow area within limits of tube bundle
A_w area of one baffle window
a_1 bypass clearance constant
a_2 baffle hole clearance constant
a_3 baffle edge clearance constant
a_1–a_8 factors required to determine F_h
b_1,b_2,b_3 factors required to determine F_h
D_1 shell inside diameter (D_s)
D_2 baffle diameter
D_3 diameter of outer tube limit (D_{otl})
d_B baffle hole diameter
d tube outer diameter (for finned tubes, equal to fin root diameter)
F_h fraction of total fluid flowing within limits of tube bundle
p tube pitch
L_{bc} baffle spacing
M_s mass flow rate of shell-side fluid
M_w A_x multiplier to obtain geometric mean of A_x and A_w
p tube pitch
h baffle cut
S exchanger size ratio = D_1/p
ρ_s density of shell side fluid

A1.2 Design of Disk and Doughnut Heat Exchanger

In shell and tube heat exchangers with baffle disks and rings, known as disk and doughnut heat exchanger (Fig. 45), the flow inside the shell is made to alternate between longitudinal and transverse (or crossflow) direction in relation to the tube bundle. This type of heat exchanger is used in some European countries. Occasionally, oil coolers at thermal power stations are of

Table 7 Baffle Cut Ratio and the Term a_8 for Cross Flow Velocity

h/D_1	0.10	0.15	0.20	0.25	0.30	0.35	0.40	0.45	0.50
a_8	0.94	0.90	0.85	0.80	0.74	0.68	0.62	0.54	0.49

this type. It has been reported that for the same pressure drop in shell-side fluid, the heat-transfer coefficient obtained with disk and doughnut baffles is approximately 15% more than that obtained with segmental baffles [52]. Exchangers are fabricated for horizontal or vertical installation.

Design Method

The effect of clearance between segmental baffles and the shell on the performance of a heat exchanger has been reasonably well studied, but there is hardly any corresponding published literature available for the disk and doughnut type heat exchangers. Very few open literature methods are available for the thermal design of disk and doughnut heat exchangers. Notable among them are Donohue [53], Slipcevic [54,55], and Goyal et al. [56]. Donohue's thermal design method was recently discussed by Ratnasamy [57]. In this section, the Slipcevic and Donohue's method are discussed.

Slipcevic Method

Design Considerations. Follow these design guidelines on the shell side [54]:

1. The spacing between the baffle disks and rings usually amounts to 20–45% of the inside shell diameter. Less than 15% is not advisable.
2. Since the heat-transfer coefficient for flow parallel with the tubes is lower than that for flow normal to the tubes, space the baffle plates so that the velocity in the baffle spacing opening is higher than that of the flow normal to the tubes.
3. It is advisable to make the annular area between the disk and the shell, S_{k1}, the same as the area inside the ring, S_{k2}, such that

$$S_{k1} = \frac{\pi}{4}(D_s^2 - D_1^2) \tag{102}$$

$$S_{k2} = \frac{\pi}{4}D_2^2 \tag{103}$$

$$S_{k1} = S_{k2} \rightarrow D_s^2 = D_1^2 + D_2^2 \tag{104}$$

Heat Transfer.

Step 1. Calculate the individual flow area for longitudinal flow:

1. Flow area in the annular region between the disk and the shell, S_1:

$$S_1 = \frac{\pi}{4}(D_s^2 - D_1^2 - N_{t1}d^2) \tag{105}$$

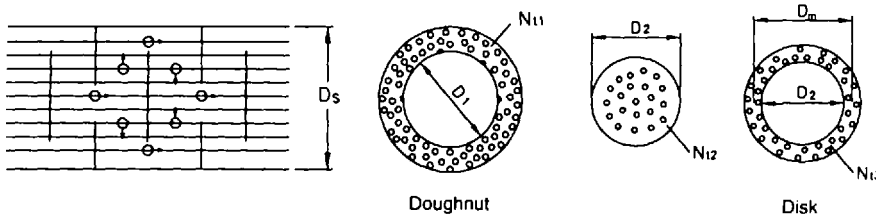


Figure 45 Disk and doughnut heat exchanger with tubes in various flow areas. Note: $D_m = 0.5(D_1 + D_2)$, where D_1 is disk diameter. (From Ref. 54.)

2. Flow area in the ring opening, S_2:

$$S_2 = \frac{\pi}{4}(D_2^2 - N_{t2}d^2) \tag{106}$$

Step 2. Calculate the effective crossflow area, S_q:

$$S_q = L_c \Sigma x \tag{107}$$

where Σx is the sum of the clear distances between the neighboring tubes closest to the mean diameter, $D_m = 0.5\ (D_1 + D_2)$. Determine the sum of clear distances between neighboring tubes closest to D_m, either from a drawing (as shown in Fig. 46) or by computational methods.

The number of tubes in the flow areas S_1, S_2, and crossflow area S_3 (to be defined later) are N_{t1}, N_{t2}, and N_{t3}, respectively. They are shown in Fig. 45.

Step 3. Calculate the hydraulic diameter for the longitudinal flow in the annulus, D_{h1}, and in the ring opening, D_{h2}:

$$D_{h1} = \frac{4S_1}{\pi(N_{t1}d + D_c + D_1)} \tag{108}$$

$$D_{h2} = \frac{4S_2}{\pi(N_{t2}d + D_2)} \tag{109}$$

Step 4. Calculate the heat-transfer coefficients h_1 and h_2 for the longitudinal flow through the cross section S_1 and S_2 from the equation of Hausen [58]:

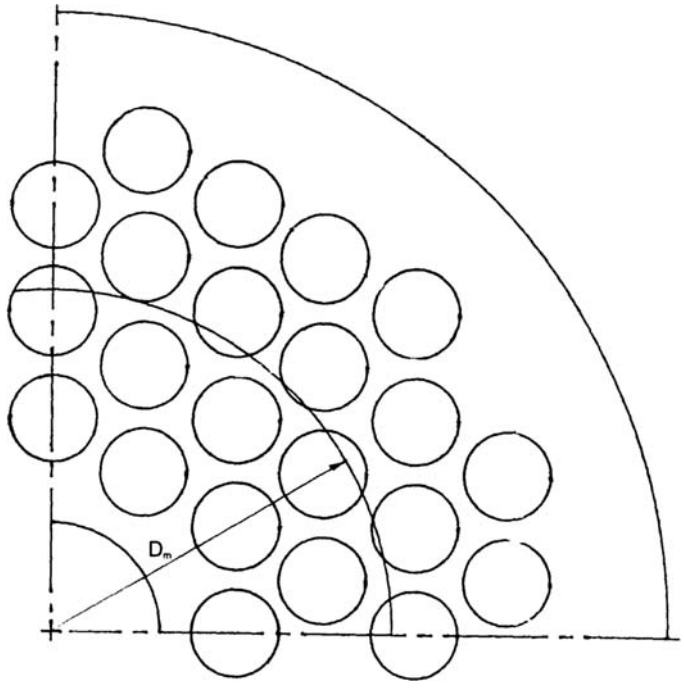


Figure 46 Mean diameter to calculate effective crossflow area of a disk and doughnut heat exchanger.

$$\mathrm{Nu}_1 = 0.024\mathrm{Re}_1^{0.8}\mathrm{Pr}^{0.33}\left(\frac{\mu_b}{\mu_w}\right)^{0.14} \tag{110}$$

$$\mathrm{Nu}_2 = 0.024\mathrm{Re}_2^{0.8}\mathrm{Pr}^{0.33}\left(\frac{\mu_b}{\mu_w}\right)^{0.14} \tag{111}$$

where

$$Nu_1 = \frac{h_1 D_{h1}}{k} \tag{112}$$

$$Nu_2 = \frac{h_2 D_{h2}}{k}$$

$$Re_1 = \frac{U_1 D_{h1}}{\mu_b} \tag{113a}$$

$$\mathrm{Re}_2 = \frac{U_2 D_{h2}}{\mu_b} \tag{113b}$$

and U_1 and U_2 are based on S_1 and S_2, respectively.

Step 5. Calculate the heat-transfer coefficient h_3 for crossflow across the bundle from McAdams [47] for the turbulent range:

$$\mathrm{Nu}_3 = K\ \mathrm{Re}_3^{0.6}\ \mathrm{Pr}^{0.33}\left(\frac{T_b}{T_w}\right)^{0.14} \tag{114}$$

where $K = 0.33$ for the staggered tube arrangement and $K = 0.26$ for the in-line tube arrangement.

To calculate Re_3, use U_3 calculated using the crossflow area S_4:

$$\mathrm{Re}_3 = \frac{U_3 d}{\mu_b} \tag{115}$$

Alternately, Slipcevic recommends calculating the heat-transfer coefficient of the individual tube row with the corresponding flow cross section. From these heat-transfer coefficients, calculate the weighted mean average of heat-transfer coefficients.

Step 6. Calculate the heat-transfer area in the longitudinal flow section A_1, A_2, crossflow section A_3, and total heat-transfer area, A:

$$A_1 = \pi d L N_{t1} \tag{116a}$$

$$A_2 = \pi d L N_{t2} \tag{116b}$$

$$A_3 = \pi d L N_{t3} \tag{116c}$$

where

$$N_{t3} = N_{t2} - (N_{t1} + N_{t2}) \tag{117}$$

$$A = A_1 + A_2 + A_3 \tag{118a}$$

$$= \pi d N_t L \tag{118b}$$

Step 7. Calculate the heat-transfer coefficient h referred to the entire heat-transfer surface A:

$$h = \frac{h_1 A_1 + h_2 A_2 + h_3 A_3}{A} \tag{119}$$

Shell-Side Pressure Drop. Refer to Slipcevic [55] for pressure drop calculation.

Shortcomings of Disk and Doughnut Heat Exchanger. The disadvantages of this design include the following [2]: (1) All the tie rods to hold baffles are within the tube bundle, and (2) the central tubes are supported by the disk baffles, which in turn are supported only by tubes in the overlap of the larger diameter disk over the doughnut hole.

Nomenclature

A total heat-transfer area on the shell side
A_1 heat-transfer area for longitudinal flow in the annulus between the shell and the disk
A_2 heat-transfer area for longitudinal flow through the ring opening
A_3 heat-transfer area for crossflow
D_1 disc diameter
D_2 diameter of ring opening
D_m mean diameter for calculating the crossflow area = 0.5 $(D_1 + D_2)$
D_s shell inside diameter
d tube outer diameter
g_c acceleration due to gravity
h_1 heat-transfer coefficient for the longitudinal flow corresponding to Nu_1
h_2 heat-transfer coefficient for the longitudinal flow corresponding to Nu_2
h_3 heat-transfer coefficient for the crossflow corresponding to Nu_3
K heat-transfer correlation coefficient
L tube length
M multiplication factor in Eq. 86
M_s mass flow rate on the shell side
N_t total number of tubes
N_{t1} number of tubes in annulus between the shell and disk
N_{t2} number of tubes in the ring opening
N_{t3} number of tubes in crossflow
Nu_1 Nusselt number to calculate h_1
Nu_2 Nusselt number to calculate h_2
Nu_3 Nusselt number to calculate h_3
Pr Prandtl number
Re_1 Reynolds number in the longitudinal flow area S_1
Re_2 Reynolds number in the longitudinal flow area S_2
Re_3 Reynolds number in the longitudinal flow area S_3
S_1 cross-sectional area for longitudinal flow through the annulus between the shell and the disk
S_2 cross-sectional area for longitudinal flow through the ring opening
S_{b1} annular area between the disk and the shell
S_{b2} area inside the ring
S_b crossflow area through tube bundle
S_s mean longitudinal flow area = 0.5 $(S_1 + S_2)$
T_b bulk mean temperature of the shell-side fluid
T_w tube wall temperature
U_1 shell-side velocity through the cross-sectional area S_1
U_2 shell-side velocity through the cross-sectional area S_2
U_3 shell-side velocity through the cross-sectional area S_3
μ_b viscosity at bulk mean temperature of the shell side fluid (kg/m · s)
μ_w viscosity at tube wall temperature of the shell side fluid (kg/m · s)

A1.3 Phillips RODbaffle Heat Exchanger

Phillips RODbaffle Heat Exchanger

The RODbaffle exchanger is a shell and tube heat exchanger that uses an improved support system for the tubes. It consists of rods located in a predisposed manner such that they confine tube movement. RODbaffle heat exchangers are used in process industries to enhance thermohydraulic performance, eliminate flow-induced tube vibration occurrence, minimize shell-side pressure losses, increase shell-side flow-field uniformity, and reduce shell-side fouling [59]. The RODbaffle concept and design came about as a result of tube vibration failures in three shell and tube exchanger bundles resulting in frequent plant shutdowns in a Phillips Petroleum plant in 1970. The emergency repairs made included the substitution of rod tube supports for the plate baffles, resulting in significantly improved operating characteristics. This was the starting point of the RODbaffle concept. References 59–64 provide general and specific information on RODbaffle heat exchanger design.

RODbaffle Exchanger Concepts

The RODbaffle exchangers (Fig. 47) use rods, with a diameter equal to the clearance between tube rows, inserted between alternate tube rows in the bundle in both the horizontal and vertical directions. The support rods are laid out on a square pitch with no nominal clearance between tubes and support rods. Support rods are welded at each end to a fabricated circumferential baffle ring. Major components of each individual RODbaffle are support rods, baffle ring, cross-support strips, partition blockage plate, and longitudinal slide bars, as shown in Fig. 47a. Four different RODbaffle configurations (*W,X,Y,Z*) are welded to longitudinal slide bars to form the RODbaffle cage assembly as shown in Fig. 47c. Tube and rod layout is shown in Fig. 47d.

Important Benefit—Elimination of Shell-Side Flow-Induced Vibration

Although RODbaffle heat exchangers are being increasingly used because of thermohydraulic advantages, flow-induced vibration protection of tubes remains one of the major design considerations. The RODbaffle bundle eliminates harmful flow-induced vibration by using these major design innovations:

1. Each tube is supported in all four directions.
2. Positive four-point confinement of the tubes.
3. Minimum convex point contact between rods and tubes.

Since these exchangers have longitudinal flow fields, vortex shedding and fluid elastic instability mechanisms (which lead to flow-induced tube vibration in crossflow exchangers) are not present [60]. Similarly, because zero nominal clearance exists between tubes and support rods, fretting wear and collision damage that may occur in plate baffle units is not evident in RODbaffle exchangers. Under design conditions where plate baffles are required and positive tube support is critical, combination RODbaffle–plate–baffle exchangers may be used [60].

Proven RODbaffle Applications

Typical applications for RODbaffle exchangers include gas–gas exchangers, compressor aftercoolers, gas–oil coolers, reactor feed–effluent exchangers, condensers, kettle reboilers, waste heat boilers, HF acid coolers, and carbon black air preheaters.

Operational Characteristics

The unobstructed flow path created by the support rod matrix makes the flow field in a RODbaffle heat exchanger predominantly longitudinal. Longitudinal flow fields produce the highest

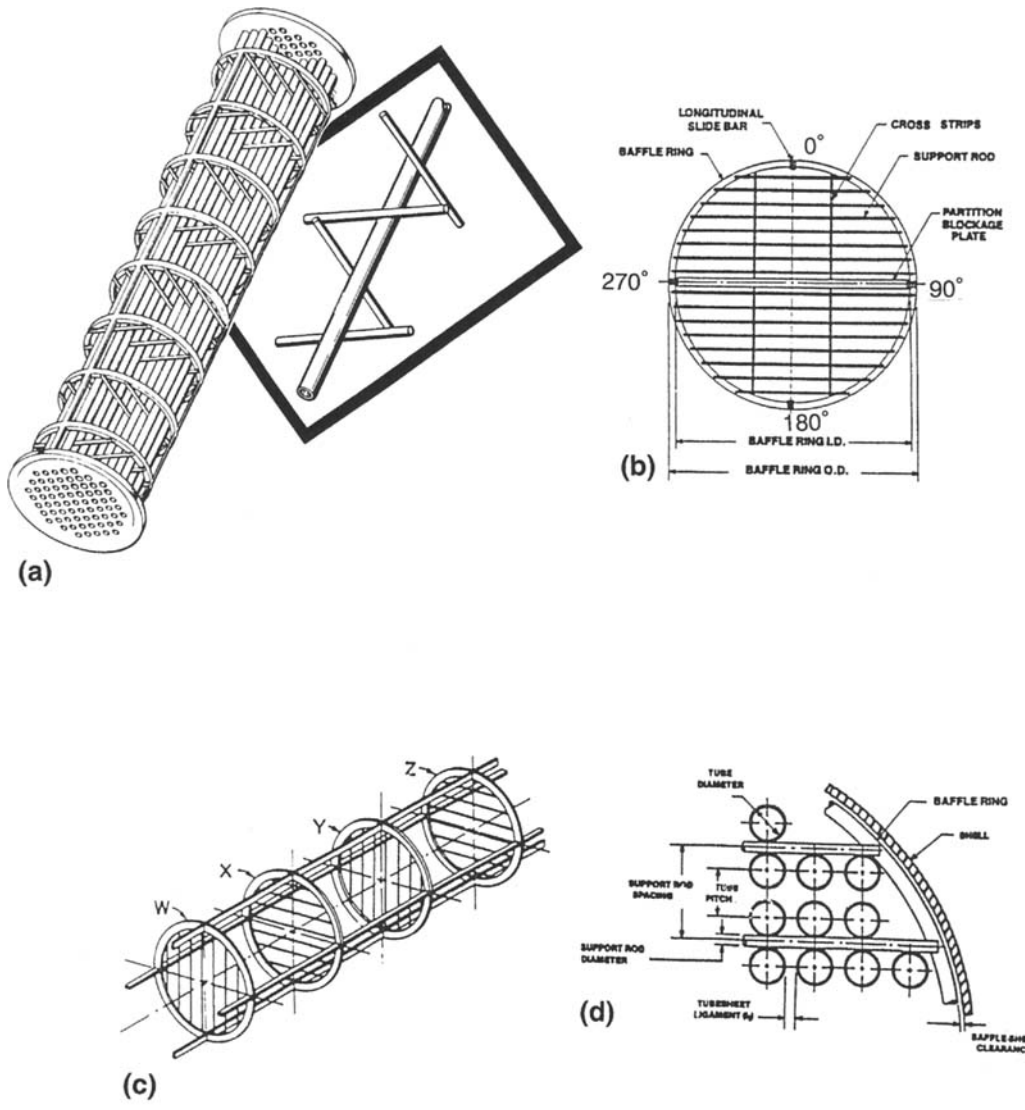


Figure 47 Rod baffle heat exchanger and support. (a) Schematic; (b) details; (c) cage assembly; and (d) tube and support rod layout. (From Ref. 59.)

thermohydraulic effectiveness of any commercial heat exchanger geometry. The main characteristics of longitudinal flow on the outside of tube bundles include the following [65]:

1. Extremely low pressure drop and a very high effectiveness of pressure drop to heat-transfer conversion, compared to baffled crossflow pattern. In longitudinal flow, the friction occurs directly at the heat-transfer surface, and there are no parasitic pressure losses due to window turnarounds.
2. Uniformity of flow distribution, without any stagnant areas characteristic of segmental baffle exchangers, results in uniform local heat-transfer rates and less fouling.

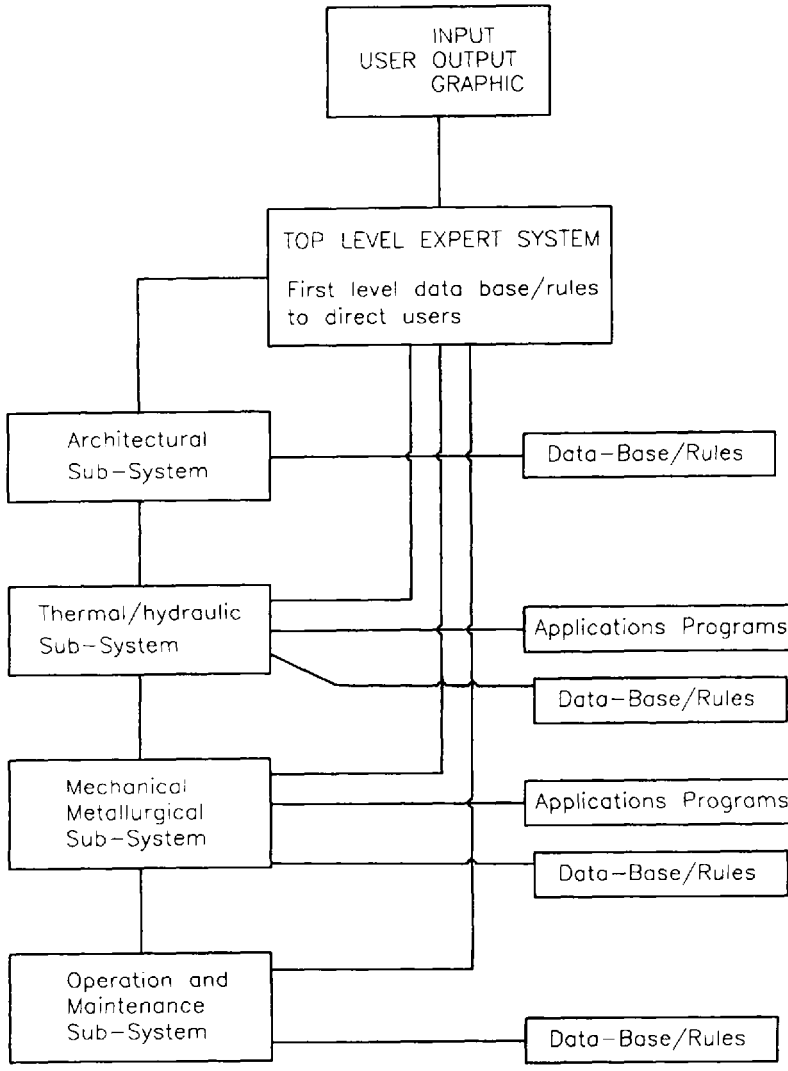


Figure 48 Schematic of integrated expert system for heat exchangers [66].

3. The grid baffles increase pressure drop through the flow contraction process, but also enhance heat transfer.

As reported in Refs. 60 and 61, RODbaffle exchanger heat-transfer rates compare favorably with double segmental plate baffle exchangers and are generally higher than in comparable triple segmental plate baffle and "no-tube-in window" designs. Shell-side pressure losses in RODbaffle exchangers are lower because neither bundle crossflow form drag nor repeated flow reversal effects are present.

Thermal Performance

For shell side, the expressions for Nusselt number, Nu, for laminar flow and turbulent flow are given by [59]:

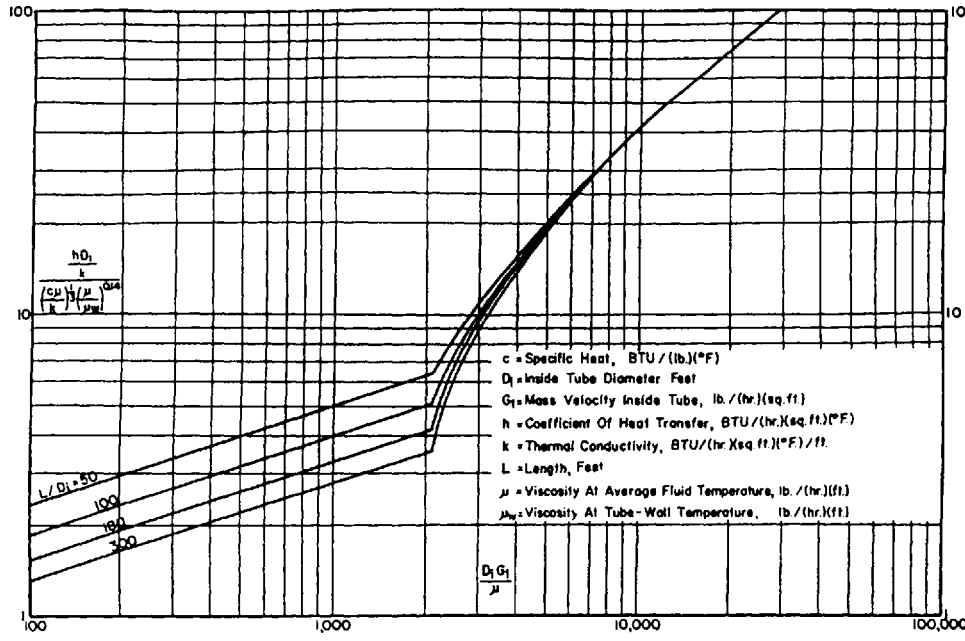


Figure 49 Coefficient of heat transfer, fluids inside tubes [44].

$$\text{Nu} = C_L \text{Re}_h^{0.6}\, \text{Pr}^{0.4} (\phi_s)^n \qquad \text{for laminar flow} \tag{120a}$$

$$\text{Nu} = C_T \text{Re}_h^{0.8}\, \text{Pr}^{0.4} (\phi_s)^n \qquad \text{for turbulent flow} \tag{120b}$$

where C_L and C_T are RODbaffle exchanger geometric coefficient functions for laminar flow and turbulent flow, respectively.

Pressure Drop. Shell-side pressure loss for flow through a RODbaffle heat exchanger bundle, excluding inlet and exit nozzles, is defined as the sum of an unbaffled frictional component, Δp_L, and a baffle flow contribution Δp_b as [59]:

$$\Delta p = \Delta p_L + \Delta p_b \tag{121}$$

According to Gentry [59], shell-side pressure losses in RODbaffle exchangers are generally less than 25% of shell-side losses produced in comparable double segmental plate baffle exchangers.

Design and Rating Program Available

Phillips Petroleum engineers have an ongoing development and testing program on RODbaffle exchangers from which they have developed basic correlations to predict heat transfer and pressure drop. The correlations are based on experimental data obtained from different bare and low-finned tube test bundles using water, light oil, and air as test fluids. The program is available for use on an IBM mainframe or IBM PC or equivalent.

Nomenclature

C_L laminar heat-transfer bundle geometry function
C_T turbulent heat-transfer bundle geometry function
Nu Nusselt number

Pr Prandtl number
Re_h Reynolds number
Δp_L pressure drop due to unbaffled frictional component
Δp_h pressure drop due to baffle flow contribution
μ_w viscosity of shell side fluid at wall temperature (kg/m • s)
$(\phi_s)^n$ bulk-to-wall viscosity correction, $(\mu_s/\mu_w)^{0.14}$

This page intentionally left blank

6
Regenerators

1 INTRODUCTION

Regeneration is an old technology dating back to the first open hearths and blast furnace stoves. The drastic escalation of energy prices has made waste heat recovery more attractive over the past two decades. Manufacturing and process industries such as glass, cement, primary and secondary metals, etc. account for a significant fraction of all energy consumed. Much of this energy is discarded in the form of high-temperature flue gas exhaust streams. Recovery of waste heat from flue gas by means of heat exchangers can improve the overall plant efficiency and serves to reduce the national energy needs and conserve fossil fuels. Figure 1 shows the cross section of a side-port regenerative furnance used in the container and flat glass industry [1]. Currently, interest in storage-type regenerators has been renewed due to their applications of heat recovery, heat storage, and general energy related problems [2]. The objective of this chapter is to acquaint the readers with various types of regenerators, construction details, and thermal and mechanical design. Additionally, some industrial heat recovery devices for waste heat recovery are discussed.

1.1 Regeneration Principle

For many years the regeneration principle has been applied to waste heat recovery by preheating the air for blast furnaces and steam generation. In the former the regeneration is achieved with periodic and alternate blowing of the hot and the cold stream through a fixed matrix of checkered brick. During the hot flow period, the matrix receives thermal energy from the hot gas and transfers it to the cold stream during the cold stream flow. In the latter, the metal matrix revolves slowly with respect to two fluid streams. The two gas streams may flow either in parallel directions or in opposite directions. However, counterflow is mostly preferred because of high thermal effectiveness. The inclusion of an air preheater in a steam power plant improves the boiler efficiency and overall performance of the power plant.

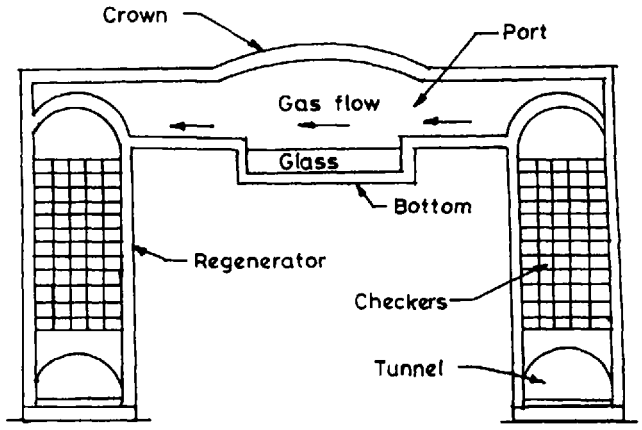


Figure 1 Regenerative furnace used in the container and flat glass industry (From Ref. 1.)

1.2 Regenerators in Thermodynamic Systems and Others

The addition of regeneration as a thermodynamic principle improves the overall performance of the gas turbine power plants, steam power plants, and the heat exchangers embodying the thermodynamic cycle of Stirling, Ericcssion, Gifford, McMohan, and Vuillemier [3]. Regenerators are also used as a dehumidifier for air-conditioning applications, cryogenic separation processes, and in noncatalytic chemical reactors such as the Wisconsin process for the fixation of nitrogen and the Wulff process for pyrolysis of hydrocarbon feedstocks to produce acetylene and ehtylene. The principle of regeneration applied to a gas turbine plant is described next.

1.3 Gas Turbine Cycle with Regeneration

The simple gas turbine plant consisting only of compressor, combustion chamber, and turbine has the advantages of light weight and compactness. However, it is known for high specific fuel consumption compared to the modern steam power plant and reciprocating internal combustion engines. The single improvement that gives the greatest increase in thermal efficiency is the addition of a regenerator for transferring thermal energy from the hot turbine exhaust gas to the air leaving the compressor, especially when it is employed in conjunction with intercooling during compression. The addition of a regenerator results in a flat fuel economy versus load characteristic, which is highly desirable for the transportation type prime movers like the gas turbine locomotives, marine gas turbine plant, and the aircraft turboprop.

1.4 Waste Heat Recovery Application

Substantial gains in fuel efficiency can be made by recovering the heat contained in the flue gas by these three means [4]:

1. Reheating process feedstock
2. Generating steam
3. Preheating the combustion air.

Each of the three methods of heat recovery has its own mertis. According to Liang et al. [4], feedstock preheating is often best suited for continuous counterflow furnaces. Applications of this method, however, are often limited by high capital costs and large space requirements.

Steam generation is an effective means for heat recovery when the demand for steam corresponds well to the availability of flue gas. Typical methods of steam generation include simple forced recirculation cycle, exhaust heat recovery with economizer, and exhaust heat recovery with superheater and economizer. Combustion air preheating is the most adaptable of heat recovery systems because it requires minimum modification to the existing system. This improves the system efficiency, and preheating the cold combustion air reduces the fuel requirement.

1.5 Fuel Savings Due to Preheating Combustion Air

Recuperators of high-temperature furnaces can provide and increase the process efficiency. This is illustrated in Fig. 2, where the theoretical fuel savings is plotted as a function of three parameters [5]:

1. Exhaust gas temperature
2. Preheat combustion air temperature
3. Effectiveness of the recuperator

It can be seen from Fig. 2 that the higher is the percentage of exhaust gas temperature, the higher the percentage fuel that can be saved. For a flue gas temperature of 1350°C and an air preheated temperature of 1100°C, the theoretical fuel savings achievable is approximately 65% of fuel consumption of an unrecuperated furnace operating at the same temperature levels.

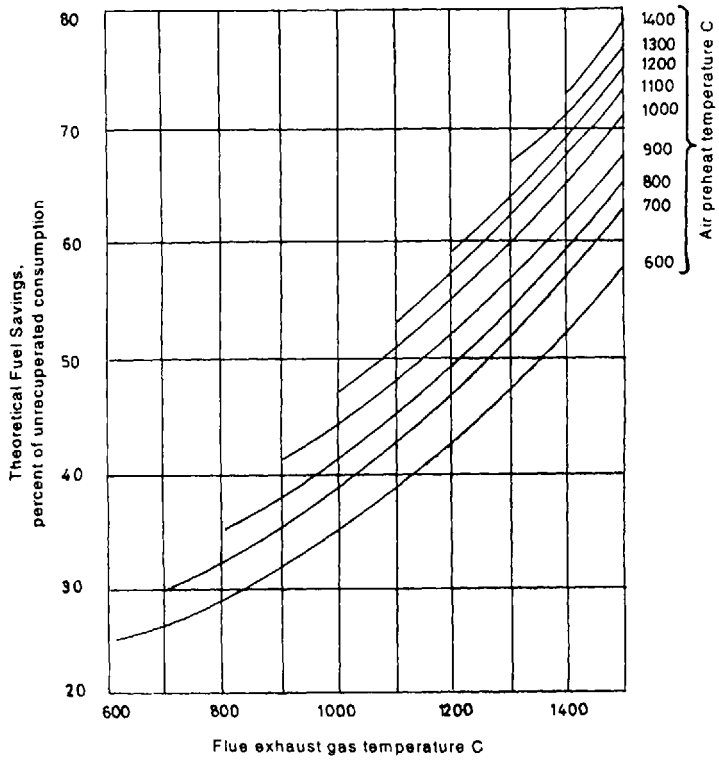


Figure 2 Fuel saving due to preheating combustion air (From Ref. 5.)

2 HEAT EXCHANGERS USED FOR REGENERATION

The heat exchanger used to preheat combustion air is called either a recuperator or a regenerator. Thermodynamically the exhaust gas thermal energy is in part recuperated or regenerated, and this same thermodynamic function is served regardless of the type of heat exchanger employed. The thermodynamic principle of regeneration is discussed in the following paragraphs.

2.1 Recuperator

A recuperator is a direct transfer type heat exchanger where the two fluids are separated by a conduction wall through which heat transfer takes place. The fluids flow simultaneously and remain unmixed. There are no moving parts in the recuperator. Some examples of recuperators are tubular, plate-fin, and extended surface heat exchangers. Recuperators are used when the flue gas is clean and uncontaminated.

Merits of Recuperators

The recuperators have the advantages of (1) ease of manufacture, (2) stationary nature, (3) uniform temperature distribution and hence less thermal shock, and (4) absence of sealing problem. However, their use is limited due to the requirement of temperature-resistant material to withstand the high-temperature flue gas and to retain its shape under operating temperature and pressure. Also, recuperators are subject to degradation in heat recovery performance by fouling from exhaust-gas-borne volatiles and dust.

2.2 Regenerator

A regenerator consists of a matrix through which the hot stream and cold stream flow periodically and alternatively. First the hot fluid gives up its heat to the regenerator. Then the cold fluid flows through the same passage, picking up the stored heat. The passing of hot fluid stream through a matrix is called the hot blow and the cold flow is called the cold blow. Thus, by regular reversals, the matrix is alternatively exposed to the hot and cold gas streams, and the temperature of the packing, and the gas, at each position fluctuates with time. Under steady-state operating conditions, a number of cycles after the startup of the regenerator, a condition of cyclic equilibrium is reached where the variations of temperature with time are the same during successive cycles and the period of hot blow and the cold blow should ensure sufficient time to absorb and release heat. From this, the regenerators can be distinguished from recuperators. In the case of recuperators, heat is transferred between two fluid streams across some fixed boundary, and conditions at any point depend, during steady-state operation, only on the position of that point, whereas in the case of regenerators, the heat transport is transient and conditions depend both on position and time.

Figure 3 shows the temperature field in a regenerator, for both the fluid and matrix at the instant of flow reversal. The upper curve represents the temperature of the fluid and matrix at the end of the hot blow and start of the cold blow. The lower curves represent temperature conditions at the end of the cold blow and the start of hot blow. At any particular station along the length of the matrix, the temperatures may fluctuate between the upper and lower curves in a time-dependent relationship.

2.3 Types of Regenerators

Since the matrix is alternatively heated by hot fluid and cooled by the cold fluid, either the matrix must remain stationary and the gas streams must be passed alternatively, or the matrix

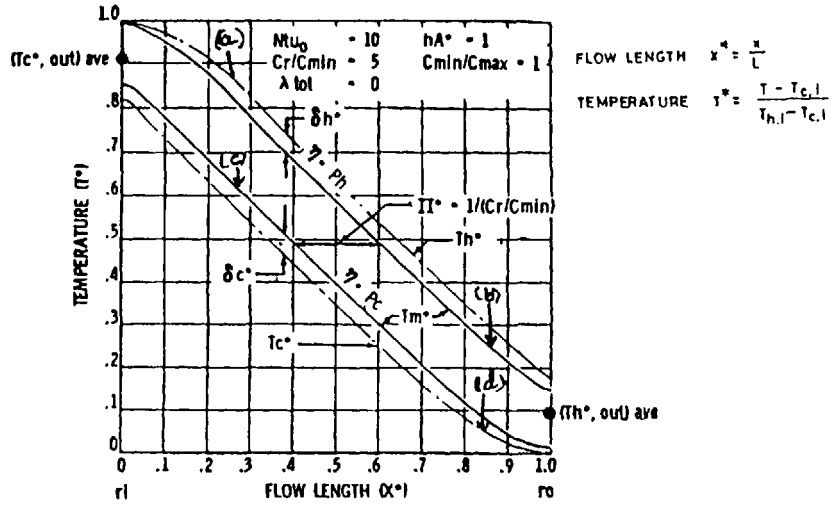


Figure 3 Balanced regenerator temperature distribution at switching instants. (a) Hot fluid temperature at end of the hot blow; (b) matrix temperature at end of the hot blow and start of the cold blow; (c) matrix temperature at the end of the cold blow; and (d) cold fluid temperature at the end of cold blow. (From Ref. 23.)

must be rotated between the passages of the hot and cold gases. Hence the regenerator may be classified according to its position with respect to time as (1) fixed-matrix or fixed-bed and (2) rotary regenerators.

2.4 Fixed-Matrix or Fixed-Bed Type Regenerator

The fixed-matrix or fixed-bed or storage-type regenerator is a periodic-flow heat-transfer device with high thermal capacity matrix through which the hot fluid stream and cold fluid stream pass alternatively. To achieve continuous flow, at least two matrices are necessary as shown in Fig. 1. The flow through the matrix is controlled by valves. According to the number of beds employed, the fixed matrix regenerators are classified into two categories: (1) single bed, and (2) dual bed valved. In a dual-bed valved type, shown in Fig. 4, initially matrix A is heated by the hot fluid and matrix B is cooled by the cold fluid. After a certain interval of time, the valves are operated so that the hot fluid flows through B and transfers heat to it. Cold fluid, however, flows through A and the fluid is being heated. The switching process continues periodically. Some examples of storage type heat exchangers are fixed bed air preheaters for blast furnace stoves, glass furnaces, and open hearth furnaces.

Shape. The shape of matrix used for the construction of a fixed-matrix regenerator is dependent upon the application. For example, in the glass-making industry, the matrix is often constructed from ceramic bricks arranged in patterns such as pigeonhole setting, closed basket weave setting, and open basket weave setting. In the steel-making industry, the gases are much cleaner and a variety of proprietary configurations such as Andco checkers, McKee checkers, Kopper checkers, and Mohr checkers are used in place of the brick arrangements. Most of these types of checkers employ tongue-and-grove shapes, which provide a bonded structure of higher stability, because regenerators in the steel-making industry are normally much taller than in the glass industry.

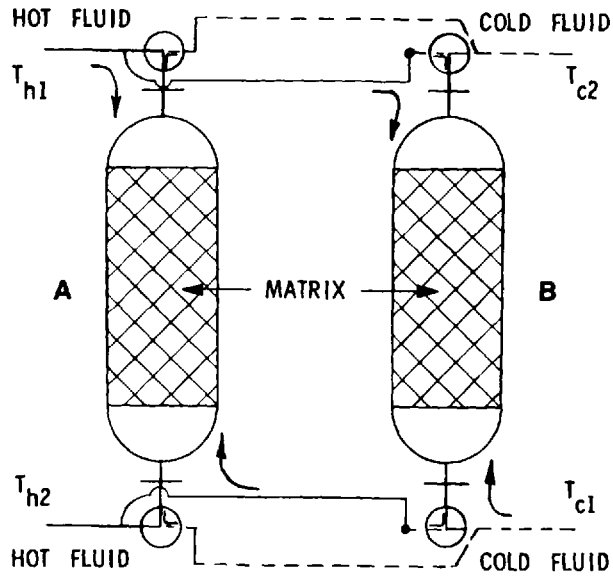


Figure 4 Dual bed valved type regenerator. (From Ref. 2.)

Construction Features. A fixed regenerator is generally constructed of either a porous matrix or checkers. The porous matrix forms a long, tortuous path for the flowing fluid in order to provide the largest possible contact surface between the regenerator matrix and the fluid. Checkers are blocks with holes pierced through them. Additional details on checkers and settings are given next.

Checkers. Checkers are the tools of heat recovery; they consist of a large quantity of bricks properly arranged in an orderly setting creating many small flues and offering a large surface area for heat absorption and release. The design of the brick, their proper setting, and flow of turbulent gases in the flues are the keys to efficient heat recovery.

Settings. The development of special strapped bricks and their setting in checkers potentially yield higher efficiencies through improved heat-transfer features. The open basket weave setting has been popular in the glass industry. The brick checkers geometry commonly used in the valved type glass furnace regenerator is essentially an offset strip fin having a large fin thickness.

Fixed-Matrix Surface Geometries

Noncompact Surface Geometry. The commonly used checker shapes have a surface area density range of 25–42 m^2/m^3 (8–13 ft^2/ft^3). The checker flow passage (referred to as flue) size is relatively large primarily due to the fouling problem. A typical heat transfer coefficient in such a passage is about 5 $W/m^2 \cdot K$ (1 $Btu/hr \cdot ft^2 \cdot °F$) [3].

Compact Surface Geometry. The surface geometries used for the compact fixed-matrix regenerator are similar to those used for rotary regenerators, but in addition quartz pebbles, steel, copper, or lead shots, copper wool, packed fibers, powders, randomly packed woven screens, and crossed rods are used.

Size

The fixed-bed regenerators are usually very large heat exchangers, some having spatial dimensions up to 50 m height and having unidirectional flow periods of many hours.

Merits of Fixed-Bed Regenerators

Fixed-bed regenerators consisting of a packed bed of refractory offer the following inherent advantages:

1. If loosely packed, the bed material is free to expand thermally; hence, thermal stresses are low.
2. Regenerators of this type are easily equipped so that the bed materials can be removed, cleaned, and replaced.
3. Unlike a recuperator, accumulated fouling does not reduce the heat exchanger capability of a regenerator; it merely increases the resistance to flow [6].

The major disadvantages of fixed-bed regenerators are the additional complexity and cost associated with the flow-switching mechanisms.

2.5 Rotary Regenerators

A rotary regenerator [Fig. 5] consists of a rotating matrix, through which the hot and cold fluid streams flow continuously. The rotary regenerator is also called a periodic-flow heat exchanger since each part of the matrix, because of its continuous rotation, is exposed to a regular periodic flow of hot and cold gas streams. The rotary regeneration principle is achieved by two means: (1) the flow through the matrix is periodically reversed by rotating the matrix, and (2) the matrix is held strationary whereas the headers are rotated continuously. Both the approaches are rotary because for either design approach, heat-transfer performance, pressure drop, and leakage considerations are the same, and rotary components must be designed for either system. The examples for rotary regenerators are (1) the Rothemuhle type and (2) the Ljungstrom type. In the Rothemuhle type, the connecting hood rotates while the heat transfer matrix is stationary, whereas in Ljungstrom type the matrix rotates and connecting hood is stationary. The rotary regenerator is used in vehicular gas turbine engines and as a dehumidifier in air-conditioning applications.

Salient Features of Rotary Regenerators

The periodic flow rotary regenerator is characterized by the features like:

1. A more compact size ($\beta = 8800$ m^2/m^3 for rotating type and 1600 m^2/m^3 for fixed matrix type), shape, desired density, porosity, and low hydraulic diameter can be achieved by pressing the metal strips, wire mesh, or sintered ceramic and hence less expensive surface per unit transfer area.
2. The porous matrix provides a long, tortuous path and hence large area of contact for the flowing fluids.
3. The absence of a separate flow path like tubes or plate walls but the presence of seals to separate the gas stream in order to avoid mixing due to pressure differential.
4. The presence of moving parts, like the rotary core in rotary regenerators and alternate closing and opening of valves in a fixed regenerator.
5. With rotary regenerators, high effectiveness can be obtained since the matrix can be heated up to nearly the full exhaust gas temperature.
6. To achieve very high thermal effectiveness approaching unity, the thermal capacity of

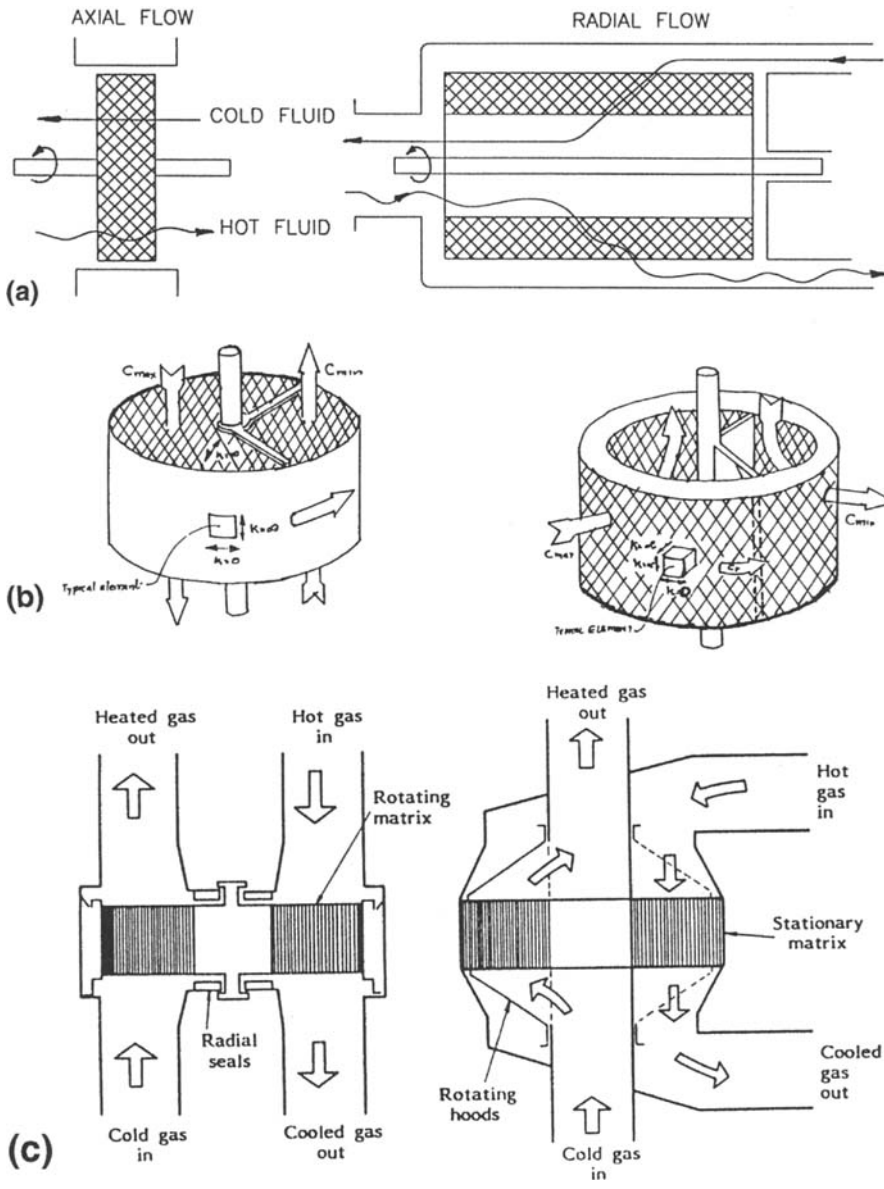


Figure 5 Rotary regenerator. (a) Disk and drum type [20]; (b) illustrative arrangement of matrix [22]; and (c) two alternative forms of disc type rotary regenerator [30].

the matrix should be very large compared to the working fluids. This requirement restricts the use of regenerators exclusively to gaseous applications.

7. Bypass leakage from the high-pressure cold stream to the low-pressure hot stream and carryover loss from one stream to the other with flow reversal or rotary nature of the matrix. However, the bypass leakage problem is less in a dehumidifier for an air-conditioning application.
8. Application to both high temperatures (800–1100°C) for metal matrix, and 2000°C for

ceramic regenerators for services like gas turbine applications, melting furnaces or steam power plant heat recovery and cryogenic applications (−20°).

9. Operating pressure of 5–7 bar for gas turbine applications and low pressure of 1–1.5 bar for air dehumidifier and waste heat recovery applications.
10. Regenerators have self-cleaning characteristics because the hot and clod gases flow in the opposite directions periodically through the same passage. As a result, compact regenerators have minimal fouling. If heavy fouling is anticipated, regenerators are not used.
11. Normally a laminar flow condition prevails, due to the small hydaulic diameter.

Rotary Regenerators for Gas Turbine Applications

One of the important areas of rotary regenerator applications is in vehicular gas turbine engines. Starting in the 1950s, the vehicle industry intensively researched gas turbine power plants, which included rotary regenerators. Both disk and drum regenerators were developed by General Motors and other vehicle builders for gas turbine engines. Their engine programs significantly advanced all facets of regenerator technology such as improved modeling, heat transfer surfaces for the matrix, sealing designs, and materials, both metals and ceramics [2].

Types of Rotary Regenerators

The two most commonly used configurations of rotary regenerators are (1) disk and (2) drum types (shown in Fig. 5a and 5b). The disk type matrix consists of alternate layers of corrugated, flat, thin metal strips wrapped around a central hub or ceramic pressing in a disk shape. Gases flow normal to the disk. In an ideal circumstance without maldistribution, the single-disk design is favored due to less seal length and lower seal leakage. Depending upon the applications, disk-type regenerators are variously referred to as heat wheel, thermal wheel, Munter wheel, or Ljungstrom wheel. Two alternative forms of disk type rotary regenerator is shown in Fig. 5c. The drum type matrix consists of heat-exchanger material in a hollow drum shape. Gases flow radially through the drum. The cost of fabricating a drum-type regenerator is much higher than that for a disk-type regenerator, and hence the drum is not used in any applications.

Drive to Rotary Regenerators

The matrix in the regenerator is rotated by a hub shaft or a peripheral ring gear drive. Most ceramic regenerators have been driven at the periphery, probably because of their brittleness.

Operating Temperature and Pressure

The regenerators are designed to cover an operating temperature range from cryogenic to very high temperatures. Metal regenerators are used for operating temperatures up to about 870°C (1600°F). Ceramic regenerators are used for higher temperature, up to about 2000°C (3600°F). Regenerators are usually designed for a low-pressure application. Rotary regenerators are limited to operating pressures about 615 kPa or 90 psi and even lower pressures for fixed-matrix regenerators.

Surface Geometries for Rotary Regenerators

The rotary regenerator surfaces consist of many uninterrupted passages in parallel. The most common are triangular, rectangular, circular, or hexagonal smooth continuous passages. Details on the foregoing surface geometries are provided in reference 2. Interrupted passage surfaces (such as strip fins, louvre fins) are not used because a transverse flow leakage will be present if the two fluids are at different pressures. Hence, the matrix generally has continuous, uninterrupted flow passages and the fluid is unmixed at any cross section for these surfaces. Some surface geometries for rotary regenerator are shown in Fig. 6.

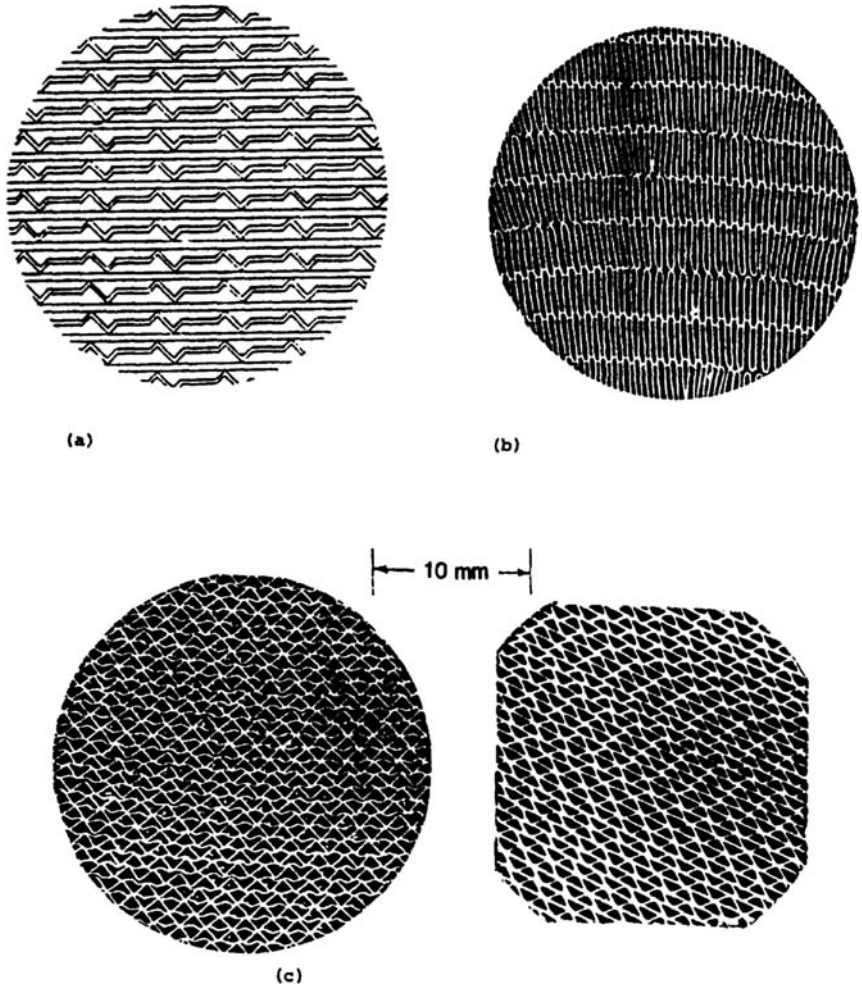


Figure 6 Surface geometries for rotary regenerator. (From Ref. 2.)

Influence of Hydraulic Diameter on Performance

Packings having small hydraulic diameter will provide the highest heat transfer coefficients; for laminar flow, $h \propto 1/D_h$. However, the associated fouling by the hot gas may limit the size of the flow passages. Very small passage size may be used in air ventilation heat recovery regenerators compared to in those used for exhaust gas heat recovery, particularly from coal fired exhaust gases or glass furnace exhausts. As passage size is reduced the number of passages required increases, while the passage length must decrease if the pressure drop is to be maintained constant. The conventional shell and tube heat exchanger cannot exploit this characteristic very far as a large number of small tubes introduce fabrication difficulties and short tube lengths prevent the use of counterflow.

Size

Typical power-plant regenerators have the rotor diameter up to 10 m (33 ft) and rotational speeds in the range of 0.5–3 rpm. The air ventilating regenerators have the rotors with 0.25–3

m (0.8–9.8 ft) diameters and rotational speeds up to 10 rpm. The vehicular regenerators have diameters up to 0.6 m (24 in) and rotational speeds up to 18 rpm [3].

Desirable Characteristics for a Regenerative Matrix

Desirable characteristics of a regenerator matrix include the following [7]:

1. A large and solid matrix, for maximum heat capacity.
2. A porous matrix without obstruction, to minimize the possible blocking and contamination.
3. A large, finely divided matrix, to achieve maximum heat-transfer rate,
4. A small, highly porous matrix, for minimum flow losses.
5. A small, dense matrix, for minimum dead space.

Other desirable matrix properties include negligible thermal conduction in the direction of fluid flow, to minimize longitudinal conduction, and maximum specific heat, for high thermal capacity.

Total Heat Regenerators

Up to this point, consideration has only been given to the transfer of sensible heat between two fluid streams and the intermittant storage of thermal energy, as sensible heat, in a solid matrix. A number of variations on these conditions are possible; for example, rotary regenerators are designed to transfer both sensible heat and latent heat of vapors mixed with the gas stream, known as total regenerators. They are intended mainly for air-conditioning applications and can employ both absorbent fibrous materials and nonabsorbent materials like plastics.

Merits of Regenerators

Among their advantages, regenerators

1. Can use compact heat transfer materials.
2. Can use less expensive heat transfer surfaces.
3. Are self-cleaning because of periodic flow reversals.
4. Can use simpler header designs.

In contrast, there are several major disadvantages of the periodic flow regenerators. They are as follows:

1. Seals suitable for pressure differentials of 4–7 bar represent a major problem; the necessity of provision of seals between the hot fluids due to high pressure differential, and the leakage problem enhanced due to the thermal expansion and contraction of the matrix.
2. Many more changes of flow direction are required as compared to the recuperators, resulting in flow losses and requiring expensive ducting.
3. Restrictions in pressure drop make necessary a large flow area with the usual matrix surface. As a consequence, the advantage of small matrix volume is somewhat nullified by the requirement of bulky approach ducting.
4. Carryover and leakage losses, especially for the high-pressure compressed air that has absorbed the compressor work.
5. Always some amount of mixing of the two fluids due to carryover and bypass leakages. Where this leakage and subsequent fluid contamination is not permissible (e.g., cryogenic systems), the regenerator is not used.
6. The high thermal effectiveness, approaching unity, provided by the regenerator demands a heat capacity of the matrix considerably larger than that of the working fluid. This requirement restricts the use of regenerators to gases only.
7. The rotary designs require a drive and support system.

2.6 Comparison of Recuperators and Regenerators

1. A recuperator is easier to build and rugged in design. For a given size, the recuperator is less effective than the regenerator due to lower overall mean temperature difference. The regenerator, on the other hand, is smaller and, for its size, a much more efficient heat exchanger. Much higher surface area, higher heat-transfer coefficients because of random nature of flow through the packing, and a higher oveall temperature difference as the top of the packing is heated to the exhaust gas temperature [7] are found.
2. Because a recuperator is not rotating and is at a constant temperature, there is less thermal shock and many normal materials can be used. Because of periodic flow, regenerators are subjected to thermal shock.
3. A recuperator does not have the problem of sealing between the hot and cold gas streams.

3 CONSIDERATIONS IN ESTABLISHING A HEAT RECOVERY SYSTEM

Although the addition of a regenerator is highly attractive from a thermodynamic point of view, its bulk, shape, mass, or cost may be such as to nullify the thermodynamic advantages. Optimum design therefore will call for a careful consideration of the following factors [4]:

1. Compatibility with the existing process [8].
2. Initial capital cost.
3. Economic benefits.
4. Life of the equipment.
5. Maintenance and cleaning requirement.
6. Controllability and production scheduling.

Other limitations include manufacturing limitations, and weight, space, and shape limitations.

3.1 Compatibility with the Existing Process System

In order for a heat exchanger to be integrated into a process, the system design must be compatible with the process design parameters. One key area of compatibility is pressure drop. Many combustion processes are designed to use the natural draft of a stack to remove the products of combustion from the process. The heat recovery equipment designed for such a process either must be designed within the pressure drop limitations imposed by natural draft or must incorporate an educator to overcome these pressure drop restrictions [8].

3.2 Economic Benefits

Economic considerations in establishing the need for heat exchanger should include initial capital costs, and fuel savings.

Capital Costs

The capital costs include the heat exchanger costs and the ancillary equipments required for the functioning of the system. Such ancillary equipment includes the following:

Blowers. Both the flue gas and the preheat air streams would require blowers to overcome pressure losses in the system.

Ducting. Ducting is between the furnace and the heat exchanger to conduit the flue gas and the preheat air.

Controls. The proposed heat recovery system would be operated in conjunction with the demand of the furnace. A control mechanism would be established for this purpose.

Energy Savings. The benefits of energy savings due to the heat recovery system should offset the capital costs on heat exchanger, blowers, ducting and control mechanisms, and maintenance cost. A break-even analysis (capital costs vs. fuel savings) will help in this regard. The desired economic benetifs can be accomplished by designing a heat exchanger to [8]:

1. Maximize the equipment life.
2. Maximize the energy cost savings.
3. Minimize the equipment capital costs.

3.3 Life of the Exchanger

The success of waste heat recovery depends on the maximum equipment life against the hostile environment of exhaust gases. The factors that affect the heat exchanger life are [8]:

1. Excessive thermal stress.
2. Creep.
3. Thermal fatigue and thermal shock.
4. High-temperature gaseous corrosion.

Corrosion and stress cause accelerated failure in both metal and ceramic recuperators, resulting in leakage, which degrades the performance.

3.4 Maintainability

Ideally, a heat exchanger should provide long service life and the equipment installation should facilitate easy maintenance. Where necessary, the design should incorporate provisions to isolate the heat exchanger from the system so that inspection, maintenance, repairs, and replacement can be made without interrupting the process, and the ability to clean the fouling deposits from the heat transfer surfaces should be provided for those processes in which fouling will take place, Ref. (8).

4 REGENERATOR CONSTRUCTION MATERIAL

An important requirement of a regenerator for waste heat recovery is life and extended durability. Regenerators are to work under hostile environments including (1) elevated temperatures, (2) fouling particulates, (3) corrosive gases and particulates, and (4) thermal cycling [9]. To achieve this requirement, proper material selection is vital. Much of the waste heat is in the form of high temperature (1900–3000°F), and the exhaust gases are corrosive in nature. Therefore, the two important considerations for selecting material for heat exchangers of a heat recovery system are (1) strength and stability at the operating temperature, and (2) corrosion resistance. Other parameters include low cost, formability, and availability.

4.1 Strength and Stability at the Operating Temperature

Metals are ideal for recuperator and regenerator construction because of their ductility and ease of fabrication. But the metallic units lack the ability to withstand high temperatures and are susceptible to corrosion from exhaust gases. Stainless steels and certain nickel- and iron-based alloys are the conventionally preferred materials. Generally, carbon steel at temperatures above 425°C (800°F) and stainless steel at temperatures above 650°C (1200°F) begin to rapidly oxidize, and if the exhaust stream contains corosive constituents, there will be a severe corrosion attack [10]. Approximate temperature ranges for various heat exchanger materials are shown in Fig. 7 [11]. In general, above 1600°F, metal heat exchangers have limitations due to

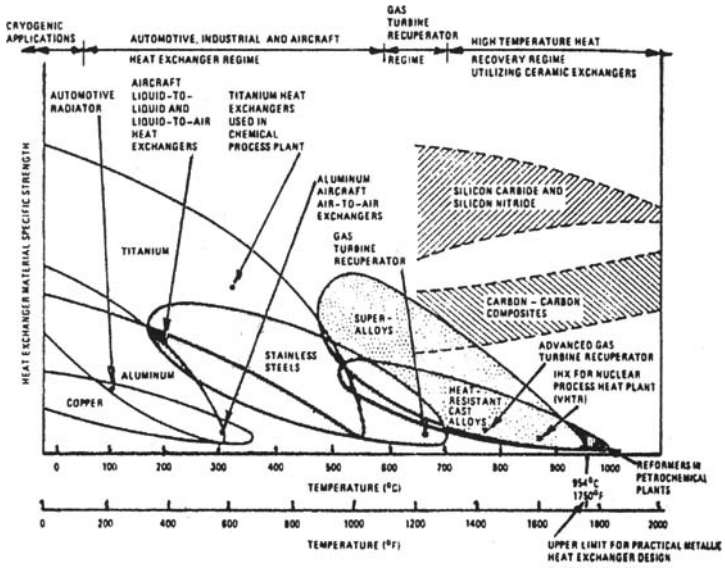


Figure 7 Approximate temperature range for various heat exchanger materials. (From Ref. 11.)

excessive costs from the expensive alloys required, requirements of temperature control devices or loss of effectiveness due to air dilution, and maintenance problems due to high thermal stresses [12]. In some cases, the high temperature problem is overcome by diluting the flue gas with a portion of cold air to be preheated. However, dilution lowers the heat transfer from the flue gas stream.

4.2 Corrosion Resistance

Materials for high-temperature heat exchangers should exhibit high-temperature gaseous and liquid corrosion resistance to the carburizing, sulfidizing, oxidizing, etc. effects of combustion products, and to the coal ash slags and fuel impurities. Regenerators used for heat recovery from the gases generated by boiler, furnaces, heaters, etc. should be protected against "cold end corrosion" caused by condensation of sulfuric acid and water on the heat-transfer surface and the volatiles and corrosive fluxes in the exhaust gas. This problem is overcome either by ceramic units or with the use of the porcelain enameled exchanger.

4.3 Ceramic Heat Exchangers

Ceramic units can be very cost-effective above 1600°F since they have the potential for greater resistance to creep and oxidation at very high temperatures, and do not require temperature controls or air dilution because of their high melting points [12]. At present, a ceramic heat exchanger is probably the most economical solution for high temperature in excess of 800°C (1475°F) applications where the specific strength of metallic materials decreases very rapidly. The ceramic recuperators are available as plate-fin and bayonet tube exchangers. Material properties that favor ceramic as regenerator materials are:

Moderate strength.
Generally inexpensive.
High thermal shock resistance and lower high-temperature creep.

Good corrosion resistance and excellent erosion resistance properties.
Low thermal expansion characteristics; this simplifies the sealing problem.
About one-fifth the density of steel, high specific heats, and higher thermal conductivity.
Low gas permeability.

The inability to join ceramic shapes reliably, once the parts have been densified, is a serious impediment to the design of large assemblies such as heat exchangers. Among the other drawbacks, the application of ceramic materials in recuperators is limited by the inherent brittleness, the higher fabrication costs associated with producing ceramic heat exchangers, and the low thermal conductivity of many oxide ceramics [13]. According to McNallan et al. [13], because of their higher thermal conductivities and corrosion resistance compared with other ceramics, silicon carbide-based ceramics have received the most attention as heat exchanger materials.

4.4 Ceramic–Metallic Hybrid Recuperator

To overcome the high-temperature heat recovery problem a ceramic–metallic hybrid recuperator is used. It consists of a ceramic recuperator operating in series with a conventional plate-fin metallic recuperator. An air diluton system is employed between the two recuperators to overcome the high-temperature oxidation problem of the metallic recuperator. This system is capable of handling flue gas temperatures up to 1370°C (2520°F).

4.5 Regenerator Materials for Other Than Waste Heat Recovery

The regenerator construction materials used for applications other than waste heat recovery are discussed by Shah [3]. They include the following:

1. In the air-conditioning and industrial process heat recovery applications, rotary regenerators are made from knitted aluminum or stainless steel wire matrix.
2. For cryogenic applications, ordinary carbon steels become brittle, so materials such as austenitic stainless steels, copper alloys, certain aluminum alloys, nickel, titanium, and a few other metals that retain ductility at cryogenic temperatures must be used. Cryogenic materials are covered in the chapter on material selection and fabrication (Chapter 13).
3. Plastics, paper, and wool are used for regenerators operating below 65°C (150°F).

5 THERMAL DESIGN: HYDRAULIC FUNDAMENTALS

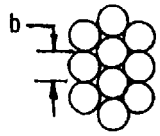
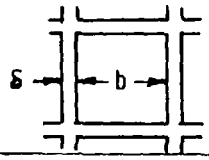
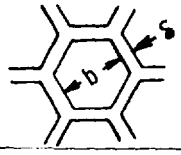
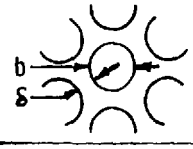
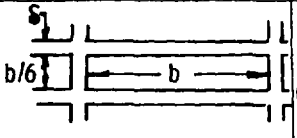
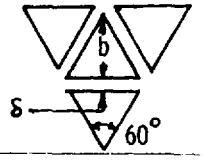
5.1 Surface Geometrical Properties

A consistent set of geometry-related symbols and factors facilitates comparative studies. The following factors can be used for all geometries, either bluff or laminar [2].

1. Porosity, σ = void volume/total volume.
2. Area density, β = surface area/total volume.
3. Hydraulic radius, r_h = flow area/wetted perimeter = σ/β.
4. Flow area, A_c = porosity × frontal area = σA_{fr}.
5. Cell density, N_c = number of holes or cells per unit frontal area.

Reference 2 presents these surface geometrical factors for several surface geometries—square, hexagonal, circular, rectangular, and triangular—which are reproduced in Table 1. The surface geometrical properties, D_h ($4r_h$), L (flow length), σ, and β are the same on both fluid sides. They related to each other as follows:

Table 1 Surface Geometrical Properties for Rotary Regenerators [2]

	cell density N_c cells/in^2	porosity p_{or} —	area density β 1/m	hydraulic radius r_h m
	-	0.37 - 0.39	$\frac{6(1-p_{or})}{b}$	$\frac{b(p_{or})}{6(1-p_{or})}$
	$\frac{1}{(b+\delta)^2}$	$\frac{b^2}{(b+\delta)^2}$	$\frac{4b}{(b+\delta)^2}$	$\frac{b}{4}$
	$\frac{2}{\sqrt{3}(b+\delta)^2}$	$\frac{b^2}{(b+\delta)^2}$	$\frac{4b}{(b+\delta)^2}$	$\frac{b}{4}$
	$\frac{2}{\sqrt{3}(b+\delta)^2}$	$\frac{\pi b^2}{2\sqrt{3}(b+\delta)^2}$	$\frac{2\pi b}{\sqrt{3}(b+\delta)^2}$	$\frac{b}{4}$
	$\frac{1}{(\frac{b}{6}+\delta)(b+\delta)}$	$\frac{b^2/6}{(\frac{b}{6}+\delta)(b+\delta)}$	$\frac{7b/3}{(\frac{b}{6}+\delta)(b+\delta)}$	$\frac{b}{14}$
	$\frac{4\sqrt{3}}{(2b+3\delta)^2}$	$\frac{4b^2}{(2b+3\delta)^2}$	$\frac{24b}{(2b+3\delta)^2}$	$\frac{b}{6}$

$$D_h = \frac{4A_oL}{A} = \frac{4\sigma}{\beta} \qquad \sigma = \frac{A_o}{A_{fr}}, \qquad \beta = \frac{4\sigma}{D_h} \tag{1}$$

If the frontal area is not 50% for each fluid, the disk frontal area, minimum free flow area, and heat transfer area on each side will not be the same. The method to calculate frontal area and heat-transfer surface area on the hot and cold sides, area for longitudinal conduction, and mass is described by Shah [14], and various parameters are explained as per Shah's method. If the flow area ratio split for both fluids is in the ratio $x:y$, where $x + y = 1$, and if the face seal and hub coverage are specified as a% of the total face area $A_{fr,t}$, then the frontal areas on each side, namely, $A_{fr,h}$ and $A_{fr,c}$, are given by

$$A_{fr,t} = \frac{\pi}{4}(D^2 - d^2) \qquad A_{fr} = A_{fr,t}(1 - a/100) \tag{2}$$

Table 2 Surface Geometrical Properties for Triangular Geometry Glass Ceramic Heat Exchangers [16]

Core description/Case no.	505A	503A	504A
Passage count, N_c Number/in^2	526	1008	2215
Porosity, σ	0.794	0.708	0.644
Hyd. diam., D_h, 10^{-1} ft	2.47	1.675	1.074
Area density, α, ft^2/ft^3	1285	1692	2397
Cell height/width, d^*	0.731	0.709	0.708
L/D_h	101	149.5	233

$$A_{fr,h} = \frac{x}{x+y}A_{fr} \qquad A_{fr,c} = \frac{y}{x+y}A_{fr} \tag{3}$$

where

$A_{fr} = A_{fr,h} + A_{fr,c}$

D = the regenerator disk outer diameter at the end of the heat transfer surface

d = the hub diameter

The effective total volume of the regenerator is given by

$$V = (A_{fr,h} + A_{fr,c})L \tag{4}$$

With the known porosity σ, the minimum free flow area on each side is calculated from $A_c = \sigma A_{fr}$. The heat-transfer surface areas on the hot and cold sides are given by

$$A_h = \frac{x}{x+y}\beta V \qquad A_c = \frac{y}{x+y}\beta V \tag{5}$$

The matrix mass M_r is calculated from the following equation for known matrix material density, ρ_r:

$$M_r = \rho_r V(1-\sigma) = \rho_r (1-\sigma)A_{fr,t}L \tag{6}$$

5.2 Correlation for *j* and *f*

For j and f values of commonly used surface geometries, refer to Mondt [2] and Kays and London [15]. Basic heat transfer and flow friction design data are presented for three straight, triangular-passage, glass ceramic heat exchanger surfaces in London et al. [16]. These surfaces have heat-transfer area density ratios ranging from 1300 to 2400 ft^2/ft^3, corresponding to a passage count of 526–2215 passages/in^2. Table 2 provides a comparison of the surface geometrical characteristics. Figure 8 provides a description of the idealized triangular geometry used

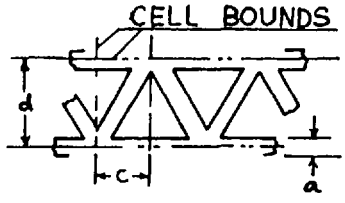


Figure 8 Idealised triangular geometry for glass ceramic heat exchanger. (From Ref. 16.)

to calculate D_h and α. Glass ceramic heat exchangers are of importance to vehicular gas turbine technology as they give promise of allowing low mass production costs for the high-effectiveness rotary regenerator required for most of the vehicular turbine engine concepts now under development.

If manufacturing tolerances are controlled as specified, the recommended j factor for Re < 1000 is given by

$$j = \frac{3.0}{\mathrm{Re}} \tag{7}$$

This is approximately 10% lower than the theory to allow for some passage nonuniformity (±20% of flow area).

The recommended j factor for Re < 1000 is given by

$$j = \frac{14.0}{\mathrm{Re}} \tag{8}$$

This is 5% higher than the theory to allow a small margin for the walls and the variation of passage cross section along flow length.

6 THERMAL DESIGN THEORY

The thermal design theory of recuperators is simple and quite straightforward. The effectiveness-number of transfer units (ε-NTU) method is used to analyze heat transfer in recuperators. In contrast, the theory of the periodic-flow type regenerator is much more difficult. Despite the simplicy of the differential equations under classical assumptions, their solution has proved to be challenging, and performances of counterflow regenerators have been widely investigated numerically as well as analytically [17]. Various solution techniques have been tried for solving the thermal design problem, and they are discussed here.

6.1 Regenerator Solution Techniques

For the steady-state behaviour of a regenerator, Nusselt [18] has given an exact solution, which conists of an infinite series of integrals. However, this solution is complicated for practical purposes, and hence several solution techniques were developed. They are:

1. Approximate solution methods by simplifying the parameters defining the regenerator behaviour; examples include Hausen's [19] heat pole method, which approximates the integral equation for the initial temperature distribution of the matrix. Hausen expressed the performance result in terms of two dimensionless parameter called the *reduced length* and the *reduced period.*
2. Empirical effectiveness relation correlated by treating the regenerator by an equivalent recuperator, e.g., that of Coppage and London [20].

Open Methods—Numerical Finite-Difference Method

Prior to the availability of general-purpose digital computers, regenerator thermal behavior was analyzed by restricting the range of parameters. With the availability of digital computers, Lamberston [21], Bahnke and Howard [22], Mondt [23], and Chung-Hsiung Li [24], among others, used a numerical finite-difference method for the calculation of the regenerator thermal effectiveness. In this approach, the regenerator and the gas streams are represented by two separate but dependent heat exchangers with the matrix stream in cross-flow with each gas stream as shown in Fig. 9.

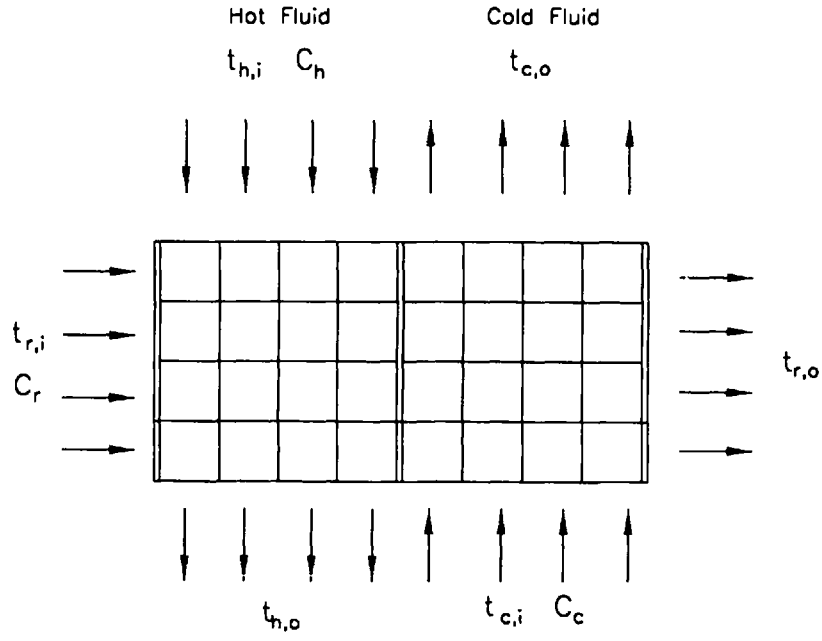


Figure 9 Regenerator matrix as the third stream. (From Ref. 21.)

Closed Methods

In the closed methods, the reversal condition is implicitly incorporated in the mathematical model for solving the differential equations both for the hot period and cold period. The closed methods used to solve the Nusselt integral equation are

1. Collocation method of Nahavandi and Weinstin [25] and Willmott and Duggan [26].
2. Galerkin method of Baclic [17] and Baclic et al. [27].
3. Successive integral method (SIM) of Romie and Baclic [28].

6.2 Basic Thermal Design Methods

For design purposes, a regenerator is usually considered to have attained regular periodic flow conditions. The solution to the governing differential equations is presented in terms of the regenerator effectiveness as a function of the pertinent dimensionless groups. The specific form of these dimensionless groups is to some extent optional, and the two most common forms are (1) the effectiveness and number of transfer units (ε-NTU_o) method (generally used for rotary regenerators), whereby

$$\varepsilon = \phi[NTU_o, C^*, C_r^*, (hA)^*] \tag{9}$$

and (2) the reduced length-reduced period (Λ–Π) method (generally used for fixed matrix regenerators) in which

$$\varepsilon = \phi[\Lambda_h, \Lambda_c, \Pi_h, \Pi_c] \tag{10}$$

These two methods are equivalent as shown in Ref. (20) and Shah [29]; that is, the thermal effectiveness of a single fixed regenerator is equal to that of the rotary regenerator with the same values of the four parameters. This one-to-one correspondence between the two dimen-

Table 3 Equivalence Between the ε-NTU_0 and Λ–Π Design Methods

ε-NTU_0 method	Λ–Π method
$NTU_0 = \dfrac{\Lambda_c/\Pi_c}{1/\Pi_c + 1/\Pi_h}$	$\Lambda_h = C^*\left[1 + \dfrac{1}{(hA)^*}\right] NTU_0$
$C^* = \dfrac{\Pi_c/\Lambda_c}{\Pi_h/\Lambda_h}$	$\Lambda_c = [1 + (hA)^*]\, NTU_0$
$C_r^* = \dfrac{\Lambda_c}{\Pi_c}$	$\Pi_h = \dfrac{1}{C_r^*}\left[1 + \dfrac{1}{(hA)^*}\right] NTU_0$
$(hA)^* = \dfrac{\Pi_c}{\Pi_h}$	$\Pi_c = \dfrac{1}{C_r^*}[1 + (hA)^*]\, NTU_0$

sionless methodologies, as shown in Table 3, allows the results obtained in the form of either Eq. (9) or (10) to be used for both types of regenerators.

The ε-NTU_0 method is mainly used for rotary regenerator design and analysis, and was first developed by Coppage and London [20]. Their model is explained next.

6.3 Coppage and Longon [20] Model for a Rotary Regenerator

The ε-NTU_0 method was used for the rotary regenerator design and analysis by Coppage and London [20] with the following idealizations.

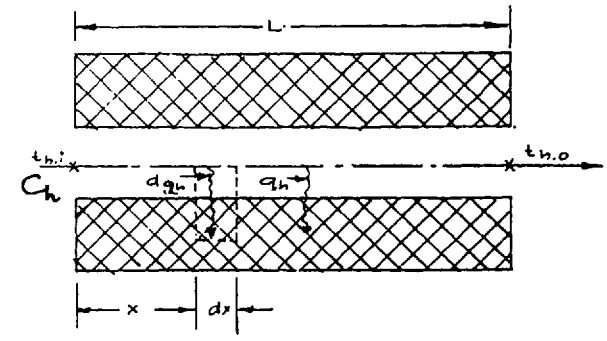
1. The thermal conductivity of the matrix is zero in the gas and air flow directions, and infinite in the direction normal to the flow.
2. The specific heats of the fluids and the matrix material are constant with temperature.
3. No mixing of the fluids occurs during the switch over from hot to cold flow.
4. The convective conductances between the fluids and the matrix are constant with flow length.
5. The fluids flow in counterflow directions.
6. Entering fluid temperatures are uniform over the flow cross section and constant with time.
7. Regular periodic conditions are established for all matrix elements, and heat losses to the surroundings are negligible.
8. Fluid carryover during the switching operation and the pressure leakage effects are negligible.

On the basis of these idealizations the following differential equations and boundary conditions may be expressed. For the hot gas flow, energy balance on the element dx as shown in Fig. 10, is given by

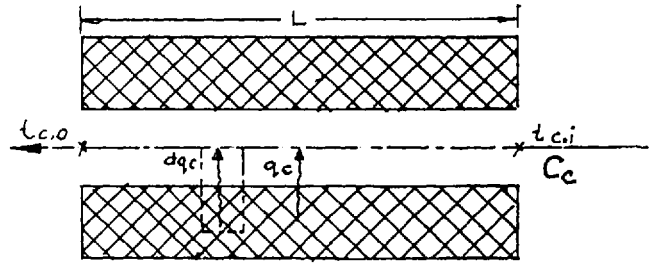
$$\frac{dq_h}{dx} = \frac{M_r c_r}{L}\frac{\partial t_r}{\partial \tau} \tag{11}$$

$$\frac{dq_h}{dx} = -\left(M_h c_{p,h}\frac{\partial t_h}{\partial x} + \frac{m_h' c_{p,h}}{L}\frac{\partial t_h}{\partial \tau}\right) \tag{12}$$

Equation 11 represents the energy received by the matrix in terms of its thermal capacitance. The right-hand side of Eq. 12 represents the energy given up by the hot gas, and m_h'/L represents



Regenerator elemental flow passage and associated matrix during hot gas flow period



Regenerator elemental flow passage and associated matrix during cold gas flow period

Figure 10 Regenerator basic heat transfer model. (From Ref. 20.)

the mass of the hot gas retained in a flow length dx. The convective heat-transfer rate equation is

$$dq_h = \frac{h_h A_h}{L}(t_h - t_r)\,dx \tag{13}$$

Elimination of dq_h yields the equation

$$M_h c_{p,h}\frac{\partial t_h}{\partial x} + \frac{m_h c_{p,h}}{L}\frac{\partial t_h}{\partial \tau} = -\frac{M_r c_r}{L}\frac{\partial t_r}{\partial \tau} = \frac{-h_h A_h}{L}(t_h - t_r) \tag{14}$$

For the cold gas flow, a similar equation results:

$$M_c c_{p,c}\frac{\partial t_c}{\partial x} + \frac{m'_c c_{p,c}}{L}\frac{\partial t_c}{\partial \tau} = -\frac{M_r c_r}{L}\frac{\partial t_r}{\partial \tau} = \frac{-h_c A_h}{L}(t_c - t_r) \tag{15}$$

The boundary conditions are as follows:

For interval of hot flow: $t_{h,i}$ = constant at $x = 0$

For interval of cold flow: $t_{c,i}$ = constant at $x = L$

Thermal Effectiveness

The overall heat-transfer performance of the regenerator is most conveniently expressed as the heat-transfer "effectiveness" ε, which compares the actual heat-transfer rate to the thermodynamically limited maximum possible heat-transfer rate. With this definition, the regenerator thermal effectiveness is simply the dimensionless time-average cold fluid outlet temperature. This is true under the condition that the cold stream is weaker, that is, has the lower heat capacity rate. This definition (for $C_c \leq C_h$ as is the case for the recuperator) results in

$$\varepsilon = \frac{t_{c,o} - t_{c,i}}{t_{h,i} - t_{c,i}} \tag{16}$$

where $t_{c,o}$ is the bulk average temperature of the cold air stream after passage through the regenerator. The effectiveness is expressed as a function of four nondimensional parameters given by

$$\varepsilon = \phi[C^*, C_r^*, (hA)^*, \mathrm{NTU_o}] \tag{17}$$

Definition of $\mathrm{NTU_o}$, C^*, C_r^*, (hA)*

$\mathrm{NTU_o}$ is the modified number of transfer units, defined as

$$\mathrm{NTU_o} = \mathrm{NTU_c}\left[\frac{1}{1 + (\mathrm{hA})^*}\right] \tag{18}$$

The heat capacity rate ratio C^* is simply the ratio of the smaller to larger heat capacity rate of the fluid steams so that C^* should be less than or equal to 1.

$$C^* = \frac{C_{min}}{C_{max}} = \frac{(Mc_p)_{min}}{(Mc_p)_{max}} = \frac{C_c}{C_h} \tag{19}$$

C_r^* is the matrix heat capacity rate C_r normalized with respect to C_{min}:

$$C_r^* = \frac{C_r}{C_{min}} = \frac{M_r c_r N}{(Mc_p)_{min}} \tag{20}$$

where M_r is the mass of the matrix, c_r is the specific heat of the matrix material, and N is the speed of the matrix in revolution per unit time.

(hA)* is the ratio of the convective conductance on the C_{min} side to that on the C_{max} side.

$$(\mathrm{hA})^* = \frac{(\mathrm{hA}) \text{ on the } C_{min} \text{ side}}{(\mathrm{hA}) \text{ on the } C_{max} \text{ side}} = \frac{(\mathrm{hA})_c}{(\mathrm{hA})_h} \tag{21}$$

Various terms used here are defined as follows:

A_c = matrix transfer area on cold side
A_h = matrix transfer area on hot side
C_c = fluid stream capacity rate (Mc_p) for cold gas flow
C_h = fluid stream capacity rate (Mc_p) for hot gas flow
C_r = capacity rate of the rotor matrix ($M_r c_r N$)
(hA)* = thermal conductance
h_c = convective conductance for cold gas
h_h = convective conductance for hot gas
M_c = mass flow rate of cold gas
M_h = mass flow rate of hot gas
M_r = matrix mass
$(Mc_p)_c$ = capacity rate of cold gas

$(Mc_p)_h$ = capacity rate of hot gas
$M_r c_r$ = thermal capacitance of matrix
m'_c = mass of cold gas retained in the matrix length L
m'_h = mass of hot gas retained in the matrix length L
L = matrix flow length
N = rpm of the matrix
t_c = temperature of the cold gas
t_h = temperature of the hot gas
t_r = temperature of the matrix
$t_{c,i}$, $t_{c,o}$ = cold fluid terminal temperatures
$t_{h,i}$, $t_{h,o}$ = hot fluid terminal temperatures
τ = flow period

For the special case of $C_r/C_c = \infty$, the behavior becomes identical in form to that of a counterflow direct-type exchanger and its effectiveness is given by

$$\varepsilon_{cf} = \frac{1 - e^{[-NTU_o(1-C^*)]}}{1 - C^* e^{[-NTU_o(1-C^*)]}} \qquad \text{for } C^* < 1 \tag{22a}$$

$$= \frac{NTU_o}{(1 + NTU_o)} \qquad \text{for } C^* = 1 \tag{22b}$$

The following formula for thermal effectiveness was first empirically correlated by Lambertson [21] and later modified by Kays and London [15]:

$$\varepsilon = \varepsilon_{cf}\left[1 - \frac{1}{9\, C_r^{*1.93}}\right] \tag{23}$$

Equation 23 agrees with accurate numerical results within ±1% for the following ranges: (1) $3 \le NTU_o \le 9$, $0.90 \le C^* \le 1$, $1.25 \le C_r^* \le 5$; (2) $2 < NTU_o < 14$, $C^* = 1$, $C_r^* \ge 1.5$; (3) $NTU_o \le 20$, $C^* = 1$, $C_r^* 2$; and (4) the complete range of NTU_o, $C^* = 1$, $C_r^* \ge 5$. In all cases, $0.25 \le (hA)^* \le 4$. Note that the value of C^* is limited to between 0.9 and 1.0.

The regenerator effectiveness increases with NTU_o asymptotically and approaches unity for specified values of C^* and C_r^*. Thus, in this case, the periodic-flow type regenerator would have the same performance as a counterflow direct-type unit possessing the same hot-side and cold-side transfer areas and the same convection heat-transfer coefficients, providing only negligible thermal resistance offered by the wall structure. To provide a sense of magnitudes for these parameters, the following tabulations were presented by these authors to indicate extreme ranges of values to be expected in gas turbine design work:

ε = 50–90%
C_c/C_h = 0.90–1.00
C_r/C_c = 1 to 10
$(hA)^* = (hA)_c/(hA)_h$ = 0.2–1
NTU_c = 2–20 (≈ twice NTU_o)
NTU_o = 1–10

Heat Transfer

For rotary regenerators, the magnitude of the heat transfer rate between the gas and matrix during a flow period is necessarily the same for both flow periods, and therefore

$$q = \varepsilon\, (Mc_p)_c (t_{h,i} - t_{c,i}) \tag{24}$$

Table 4 Parameter Definitions and Equivalents for Stationary and Rotary Regenerators

	Stationary	Rotary
NTU_o	$\frac{\Lambda_c}{1 + (hA)^*}$	$NTU_c\left[\frac{1}{1 + hA^*}\right]$
C^*	$\frac{(Mc_p\tau)_c}{(Mc_p\tau)_h}$	$\frac{(Mc_p)_c}{(Mc_p)_h}$
C_r^*	$\frac{M_r c_r}{(Mc_p\tau)_c}$	$\frac{M_r c_r N}{(Mc_p)_c}$
$(hA)^*$	$\frac{(hA\tau)_c}{(hA\tau)_h}$	$\frac{(hA)_c}{(hA)_h}$

in which $t_{h,i}$ and $t_{c,i}$ are constant inlet temperatures of the hot and cold gases. For stationary regenerators, the heat-transfer rate is

$$q = \varepsilon\,(Mc_p\tau)_c(t_{h,i} - t_{c,i}) \tag{25}$$

6.4 Parameter Definitions

Various parameters definitions and their equivalents for the stationary and rotary regenerators are given in Table 4.

Note: While defining various parameters, throughout this chapter, it is assumed that the cold fluid is the C_{min} fluid and accordingly, subscripts c for cold fluid and h for hot fluid are allotted. However, parameter definition can be gneralized to subcripts a and b such that the term

$$C_a\ C_b \le 1 \text{ or } \Lambda_b\Pi_a/\Lambda_a\Pi_b \le 1 \tag{26}$$

6.5 Classification of Regenerator Operation

Based on the values of C^* and $(hA)^*$, or Λ–Π, regenerators are classified into eight types [29]: (1) balanced regenerator, (2) unbalanced regenerator, (3) symmetric regenerator, (4) unsymmetric regenerator, (5) symmetric and balanced regenerator, (6) unsymmetric and balanced regenerator, (7) symmetric and unbalanced regenerator, and (8) unsymmetric and unbalanced regenerator. For a balanced regenerator the heat capacity of the fluids blown through the regenerator is equal and a regenerator is termed symmetric if the reduced length of each period is equal. The unsymmetric and unbalanced regenerator operation is the most general one, and the others are merely subsets [30]. These designations are shown in Table 5.

6.6 Additional Formulas for Regenerator Effectiveness

Tables of thermal effectiveness are given by many sources: Kays and London [15], Baclic [17], Lamberston [21], Bhanke and Howard [22], and Romie [31], among others. Methods of computing the thermal effectiveness are described by, for example, Baclic [17], Willmott and Duggan [26], Baclic et al. [27], Romie and Baclic [28], reference 32, and many others. Additional formulas and closed form solutions from a few of these references are given next.

Table 5 Designation of Regenerators [29, 30]

Terminology	Λ–Π method	ε-NTU$_o$ method
Balanced regenerator	$\Lambda_h/\Pi_h = \Lambda_c/\Pi_c$	$C^* = 1$
Unbalanced regenerator	$\Lambda_h/\Pi_h \neq \Lambda_c/\Pi_c$	$C^* \neq 1$
Symmetric regenerator	$\Lambda_h = \Lambda_c$	$(hA)^* = 1$
Unsymmetric regenerator	$\Lambda_h \neq \Lambda_c$	$(hA)^* \neq 1$
Symmetric and balanced regenerator	$\Lambda_h = \Lambda_c$, $\Pi_h = \Pi_c$	$(hA)^* = 1$
	$\Lambda_h/\Pi_h = \Lambda_c/\Pi_c$	$C^* = 1$
Unsymmetric and balanced regenerator	$\Lambda_h \neq \Lambda_c$	$(hA)^* \neq 1$
	$\Lambda_h/\Pi_h = \Lambda_c/\Pi_c$	$C^* = 1$
Symmetric and unbalanced regenerator	$\Lambda_h = \Lambda_c$	$(hA)^* = 1$
	$\Lambda_h/\Pi_h \neq \Lambda_c/\Pi_c$	$C^* \neq 1$
Unsymmetric and unbalanced regenerator	$\Lambda_h \neq \Lambda_c$	$(hA)^* \neq 1$
	$\Lambda_h/\Pi_h \neq \Lambda_c/\Pi_c$	$C^* \neq 1$

Balanced and Symmetric Counterflow Regenerator

Baclic [17] obtained a highly accurate closed form expression for the counterflow regenerator effectiveness for the balanced and symmetric regenerator; that is, for $C^* = 1$ and $(hA)^* = 1$ by the Galerkin method,

$$\varepsilon = \frac{\Lambda}{\Pi}\left[\left(2\sum_{j=0}^{N} B_j - 1\right)\right] \tag{27}$$

where B_j is determined by solving the set of equations of the form

$$\Sigma_{j=0}^{N} a_{jk} B_j = 1 \tag{28}$$

where

$$a_{jk} = \frac{(k+1)!(j+1)!}{(k+j+1)!}\left[1 + (k+j+1)!\,\Sigma_{m=0}^{k}\frac{(-1)^m}{(k-m)!}\,V_{j+m+2}(\Pi,\ \Lambda/\Lambda^{j+m+1})\right] \tag{29}$$

$$V_m(x, y) = e^{|-(x+y)|}\,\Sigma_{n=m-1}^{\infty}\binom{n}{m-1}(y/x)^{n/2}\,I_n(2\sqrt{xy}) \qquad m \geq 1 \tag{30a}$$

$$\binom{n}{m-1} = \frac{n!}{(m-1)!(n-m+1)!} \tag{30b}$$

For $N = 2$, the equation for ε simplifies to the following equation:

$$\varepsilon = C_r^* \frac{1 + 7\beta_2 - 24\{B - 2[R_1 - A_1 - 90\,(N_1 + 2E)]\}}{1 + 9\beta_2 - 24\{B - 6[R - A - 20\,(N - 3E)]\}} \tag{31}$$

where

$$B = 3\beta_3 - 13\beta_4 + 30\,(\beta_5 - \beta_6) \tag{32}$$

and

$$R = \beta_2[3\beta_4 - 5(3\beta_5 - 4\beta_6)] \tag{33}$$

$$A = \beta_3[3\beta_3 - 5(3\beta_4 + 4\beta_5 - 12\beta_6)] \tag{34}$$

$$N = \beta_4[2\beta_4 - 3(\beta_5 + \beta_6)] + 3\beta_5^2 \tag{35}$$

$$E = \beta_2\beta_4\beta_6 - \beta_2\beta_5^2 - \beta_3^2\beta_6 + 2\beta_3\beta_4\beta_5 - \beta_4^3 \tag{36}$$

$$N_1 = \beta_4[\beta_4 - 2(\beta_5 + \beta_6)] + 2\beta_5^2 \tag{37}$$

$$A_1 = \beta_3[\beta_3 - 15(\beta_4 + 4\beta_5 - 12\beta_6)] \tag{38}$$

$$R_1 = \beta_2[\beta_4 - 15(\beta_5 - 2\beta_6)] \tag{39}$$

$$\beta_i = V_i(2\mathrm{NTU}_o, 2\mathrm{NTU}_o/C_r^*)/(2\mathrm{NTU}_o)^{i-1}$$
$$= V_i(\Pi,\Lambda)/\Lambda^{i-1} \qquad \text{for} \quad i = 2,3,\ldots,6 \tag{40}$$

$$V_i(x,y) = e^{[-(x+y)]} \sum_{n=i-1}^{\infty} \binom{n}{i-1} (y/x)^{n/2} I_n(2\sqrt{xy}) \qquad i \geq 1 \tag{41}$$

Regenerator effectiveness ε, computed from Eq. 31, as a function of NTU_o and C_r^* is presented in Table 6. Note that the results are valid for $C^* = 1$ and $(hA)^* = 1$. It is emphasized again that the regenerator effectiveness ε by Eq. 23 is valid for $0.9 \leq C^* \leq 1$ and $C_r^* > 1.25$ while that of Eq. 31 is valid for $C^* = 1$ but for all values of C_r^*. Exact asymptotic values of ε for $\Lambda \to \infty$ and $\Pi/\Lambda \to 0$, when $\varepsilon = \Lambda/(2 + \Lambda)$ holds are also included in this table.

6.7 Reduced Length–Reduced Period (Λ–Π) Method

Galerkin Method of Baclic et al. [27] for Asymmetric–Unbalanced Counterflow Regenerator

The asymmetric–unbalanced counterflow regenerator problem described by the classical idealizations is solved by the Galerkin method by Baclic et al. [27]. Based on these assumptions, an energy balance provides two equaitons applicable during the hot gas flow period and two equaitons during the cold gas flow period:

$$\frac{1}{\Lambda_h}\frac{\partial t_h}{\partial \xi} = -\frac{1}{\Pi_h}\frac{\partial t_r}{\partial \eta} = t_r - t_h \tag{42}$$

$$\pm\frac{1}{\Lambda_c}\frac{\partial t_c}{\partial \xi} = -\frac{1}{\Pi_c}\frac{\partial t_r}{\partial \eta} = t_r - t_c \tag{43}$$

The regenerator can operate with either parallel flow (plus sign in Eq. 43) or counterflow arrangement (minus sign in Eq. 43). In Eq. 42 and Eq. 43, ξ is the fractional distance along the flow path in the regenerator matrix of length L and η is the fractional completion of a respective gas flow period. Temperatures of the hotter gas, colder gas, and the solid matrix are denoted by t_h, t_c, and t_r, respectively. The four parameters Λ_h and Λ_c (reduced lengths), Π_h and Π_c (reduced periods), and their expressions are given in Table 7, and their equivalent parameters for the rotary regenerators are given in Table 8.

The differential equations 42 and 43 describe the regenerator operation when the appropriate boundary conditions are specified. These are constant gas inlet temperature $t_{h,i}$ and $t_{c,i}$ at the opposite ends ($\xi = 0$ and 1) of the regenerator matrix, and the condition stating that the matrix temperature field at the end of one gas flow period is the initial matrix temperature distribution for the subsequent gas flow period.

The subscript 1 is assigned to the weaker gas flow period such that the respective $U_1 = (\Lambda/\Pi)_1$ ratio is smaller of the two ratios $U_h = (\Lambda/\Pi)_h$ and $U_C = (\Lambda/\Pi)_C$. The ratio (Λ/Π) is termed the *utilization factor*. The main advantage of the utilization factors is the fact that these parame-

Table 6 Symmetric and Balanced Counterflow Regenerator Effectiveness $\varepsilon = \phi(\Lambda,\Pi)$ (as calculated from Eq. 31) [17]

$\Lambda\backslash\Pi/\Lambda$	0.0	0.1	0.2	0.3	0.4	0.5	0.6	0.7	0.8	0.9	1.0
1.0	1/3	0.3332	0.3329	0.3323	0.3315	0.3304	0.3292	0.3277	0.3260	0.3241	0.3221
1.5	3/7	0.4283	0.4276	0.4264	0.4248	0.4227	0.4202	0.4173	0.4139	0.4102	0.4061
2.0	1/2	0.4996	0.4986	0.4968	0.4943	0.4912	0.4874	0.4830	0.4780	0.4725	0.4665
2.5	5/9	0.5551	0.5537	0.5513	0.5481	0.5440	0.5391	0.5333	0.5269	0.5197	0.5120
3.0	3/5	0.5994	0.5977	0.5949	0.5910	0.5861	0.5802	0.5733	0.5655	0.5570	0.5477
3.5	7/11	0.6357	0.6338	0.6305	0.6261	0.6204	0.6137	0.6058	0.5970	0.5872	0.5766
4.0	2/3	0.6659	0.6638	0.6602	0.6553	0.6490	0.6416	0.6329	0.6232	0.6124	0.6006
4.5	9/13	0.6915	0.6892	0.6853	0.6800	0.6732	0.6652	0.6559	0.6454	0.6337	0.6210
5.0	5/7	0.7134	0.7109	0.7068	0.7011	0.6940	0.6855	0.6756	0.6645	0.6521	0.6385
5.5	11/15	0.7324	0.7293	0.7255	0.7195	0.7121	0.7032	0.6928	0.6811	0.6681	0.6537
6.0	3/4	0.7491	0.7463	0.7418	0.7356	0.7279	0.7187	0.7080	0.6958	0.6822	0.6672
6.5	13/17	0.7637	0.7609	0.7562	0.7498	0.7419	0.7324	0.7215	0.7089	0.6948	0.6792
7.0	7/9	0.7768	0.7738	0.7690	0.7625	0.7544	0.7447	0.7335	0.7206	0.7061	0.6900
7.5	15/19	0.7884	0.7854	0.7804	0.7738	0.7656	0.7558	0.7444	0.7313	0.7164	0.6997
8.0	4/5	0.7989	0.7958	0.7908	0.7840	0.7757	0.7658	0.7543	0.7409	0.7257	0.7036
8.5	17/21	0.8084	0.8052	0.8001	0.7933	0.7849	0.7749	0.7633	0.7497	0.7342	0.7167
9.0	9/11	0.8171	0.8138	0.8086	0.8017	0.7933	0.7833	0.7715	0.7578	0.7421	0.7242
9.5	19/23	0.8250	0.8216	0.8164	0.8094	0.8010	0.7909	0.7791	0.7653	0.7493	0.7311
10.0	5/6	0.8322	0.8288	0.8235	0.8165	0.8080	0.7980	0.7862	0.7722	0.7560	0.7375
10.5	21/25	0.8388	0.8354	0.8300	0.8230	0.8146	0.8046	0.7927	0.7787	0.7623	0.7435
11.0	11/13	0.8450	0.8415	0.8361	0.8290	0.8206	0.8106	0.7988	0.7847	0.7681	0.7491
11.5	23/27	0.8506	0.8471	0.8417	0.8346	0.8262	0.8163	0.8044	0.7903	0.7736	0.7543
12.0	6/7	0.8559	0.8524	0.8469	0.8398	0.8315	0.8216	0.8098	0.7956	0.7788	0.7592
12.5	25/29	0.8603	0.8573	0.8517	0.8447	0.8364	0.8266	0.8147	0.8005	0.7836	0.7638
13.0	13/15	0.8654	0.8618	0.8562	0.8492	0.8410	0.8312	0.8194	0.8052	0.7882	0.7682
13.5	27/31	0.8697	0.8661	0.8605	0.8535	0.8453	0.8356	0.8239	0.8096	0.7925	0.7723
14.0	7/8	0.8737	0.8701	0.8644	0.8575	0.8494	0.8397	0.8280	0.8138	0.7966	0.7762
14.5	29/33	0.8775	0.8738	0.8682	0.8612	0.8532	0.8436	0.8320	0.8177	0.8004	0.7799
15.0	15/17	0.8811	0.8773	0.8717	0.8648	0.8568	0.8473	0.8358	0.8215	0.8041	0.7834
15.5	31/35	0.8844	0.8807	0.8750	0.8681	0.8602	0.8508	0.8393	0.8251	0.8076	0.7868
16.0	8/9	0.8876	0.8838	0.8781	0.8713	0.8635	0.8542	0.8427	0.8285	0.8110	0.7900
17.0	17/19	0.8934	0.8896	0.8839	0.8771	0.8695	0.8604	0.8490	0.8348	0.8172	0.7959
18.0	9/10	0.8967	0.8948	0.8891	0.8824	0.8749	0.8660	0.8548	0.8406	0.8229	0.8014
19.0	19/21	0.9034	0.8995	0.8938	0.8872	0.8799	0.8711	0.8601	0.8459	0.8282	0.8065
20.0	10/11	0.9077	0.9038	0.8981	0.8916	0.8844	0.8758	0.8649	0.8509	0.8331	0.8111
25	25/27	0.9245	0.9205	0.9148	0.9087	0.9024	0.8947	0.8844	0.8707	0.8528	0.8302
30	15/16	0.9360	0.9319	0.9263	0.9207	0.9151	0.9081	0.8984	0.8851	0.8673	0.8442
35	35/37	0.9445	0.9403	0.9347	0.9295	0.9246	0.9182	0.9090	0.8961	0.8785	0.8552
40	20/21	0.9509	0.9467	0.9411	0.9363	0.9320	0.9261	0.9174	0.9048	0.8875	0.8640
45	45/47	0.9559	0.9517	0.9462	0.9417	0.9379	0.9325	0.9241	0.9119	0.8948	0.8713
50	25/26	0.9600	0.9557	0.9503	0.9461	0.9427	0.9378	0.9297	0.9177	0.9009	0.8775
60	30/31	0.9662	0.9619	0.9565	0.9529	0.9502	0.9459	0.9383	0.9269	0.9106	0.8874
70	35/36	0.9707	0.9663	0.9611	0.9578	0.9558	0.9519	0.9447	0.9337	0.9180	0.8951
80	40/41	0.9740	0.9697	0.9645	0.9616	0.9600	0.9565	0.9497	0.9390	0.9239	0.9014
90	45/46	0.9767	0.9723	0.9672	0.9646	0.9634	0.9602	0.9536	0.9432	0.9236	0.9065

(*continued*)

Table 6 Continued

$\Lambda\backslash\Pi/\Lambda$	0.0	0.1	0.2	0.3	0.4	0.5	0.6	0.7	0.8	0.9	1.0
100	50/51	0.9788	0.9744	0.9693	0.9670	0.9662	0.9632	0.9568	0.9467	0.9325	0.9109
150	75/76	0.9852	0.9808	0.9759	0.9744	0.9747	0.9726	0.9667	0.9574	0.9452	0.9258
200	100/101	0.9835	0.9840	0.9792	0.9782	0.9791	0.9774	0.9719	0.9629	0.9520	0.9348
300	150/151	0.9917	0.9873	0.9826	0.9821	0.9837	0.9824	0.9772	0.9686	0.9592	0.9456
400	200/201	0.9934	0.9889	0.9843	0.9841	0.9860	0.9850	0.9799	0.9714	0.9629	0.9522
500	250/251	0.9944	0.9899	0.9853	0.9853	0.9874	0.9865	0.9815	0.9731	0.9651	0.9568
600	300/301	0.9950	0.9905	0.9860	0.9861	0.9884	0.9876	0.9826	0.9743	0.9665	0.9602
800	400/401	0.9959	0.9914	0.9869	0.9871	0.9896	0.9889	0.9840	0.9758	0.9682	0.9650
1000	500/501	0.9964	0.9919	0.9874	0.9877	0.9903	0.9897	0.9848	0.9766	0.9692	0.9634
2000	1000/1001	0.9974	0.9928	0.9884	0.9890	0.9917	0.9912	0.9865	0.9784	0.9711	0.9770
∞	1.0000	1.0000	1.0000	1.0000	1.0000	1.0000	1.0000	1.0000	1.0000	1.0000	1.0000

Note:For the ε-NTU method, $\Pi/\Lambda = \dfrac{1}{C_r^*}$ and $\Lambda = 2\mathrm{NTU}_o$.

ters do not contain the fluid to matrix heat-transfer coefficients of the respective flow periods. Thus, U_1 is defined as

$$U_1 = \min\{U_c, U_h\} \tag{44}$$

The effectiveness is given by

$$\varepsilon = \frac{1}{U_1} \Sigma_{m=0}^{M} \frac{x_{2m} - x_{1m}}{(m+1)!} \qquad \text{for } m = 0,1,2,3, \ldots, M \tag{45}$$

The unknown coefficients x_{1m} and x_{2m} are determined from the following set of algebraic equations:

$$\Sigma_{m=0}^{M} [-A_{mk}(\Pi_1,\Lambda_1)\, x_{1m} + B_{mk}\, x_{2m}] = C_k \qquad k = 0,1,2,3, \ldots, M \tag{46}$$

$$\Sigma_{m=0}^{M} [B_{mk} x_{1m} - A_{mk}(\Pi_2,\Lambda_2) x_{2m}] = 0 \qquad k = 0,1,2,3, \ldots, M \tag{47}$$

where

$$A_{mk}(\Pi_j,\Lambda_j) = \Sigma_{i=0}^{M} \frac{(-1)^i}{(k-i)!}\, V_{i+m+2}(\Pi_j,\Lambda_j)/\Lambda_j^{i+m+1} \qquad j = 1,2 \tag{48}$$

$$B_{mk} = \frac{1}{(m+k+1)!} \tag{49}$$

$$C_k = \frac{1}{(k+1)!} - \Sigma_{i=0}^{k} \frac{(-1)^i}{(k-i)!} \frac{V_{i+2}(\Pi_1,\Lambda_1)}{\Lambda_1^{i+1}} \tag{50}$$

Table 7 Expressions for Λ_h, Λ_c, Π_c, and Π_h

$\Pi_c = \dfrac{(hA\tau)_c}{M_r c_r}$	$\Pi_h = \dfrac{(hA\tau)_h}{M_r c_r}$	$\Lambda_c = \dfrac{(hA)_c}{(Mc_p)_c}$	$\Lambda_h = \dfrac{(hA)_h}{(Mc_p)_h}$

For any fixed M, one needs $2(M+1)$ equations for $M+1$ unknowns x_{1m} and for $M+1$ unknowns x_{2m}. For any practical purpose $M = 2$ will be adequate.

6.8 Razelos Method for Asymmetric–Unbalanced Counterflow Regenerator

The forms produced by the Galerkin method of Baclic et al. [27] are not amenable for hand calculation methods. They can be solved by either a computer or a programmable calculator. A hand calculation method was presented by Razelos [33]. In this approach, the unsymmetric regenerator is approximated using an "equivalent" symmetric regenerator. The Razelos approximate method can be used to calculate the counterflow regenerator effectiveness for the complete range of C^* and NTU_o, and $C_r^* \geq 1$, $0.25 \leq (hA)^* \leq 4$. The method follows these steps.

1. For the ε-NTU_o method, compute the range of $NTU_{o,m}$ and $C_{r,m}^*$ for an equivalent balanced regenerator as follows from the specified values of NTU_o, C_r^*, and C^*.

$$NTU_{o,m} = \frac{2\,NTU_o(C^*)}{1 + C^*} \tag{51}$$

$$C_{r,m}^* = \frac{2\,C_r^*\,C^*}{1 + C^*} \tag{52}$$

2. For the Λ–Π method, calculate Λ_m and Π_m as

$$\Pi_m = \frac{2}{(\Pi_h^{-1} + \Pi_c^{-1})} \qquad \Lambda_m = \frac{2\,\Pi_m}{[(\Pi/\Lambda)_h + (\Pi/\Lambda)_c]} \tag{53}$$

3. The equivalent balanced regenerator effectiveness ε_r is evaluated from Eq. 23 or Eq. 31 for $NTU_{o,m}$ and $C_{r,m}^*$ or from Table 6 for Λ_m and Π_m. For example, the equivalent form of Eq. 23 is given by

$$\varepsilon_r = \frac{NTU_{o,m}}{1 + NTU_{o,m}}\left[1 - \frac{1}{9\,(C_{r,m}^*)^{1.93}}\right] \tag{54}$$

4. The acutal regenerator effectiveness ε is then given by

Table 8 Reduced Length and Reduced Period Parameters: Definitions [20]

Term	Equivalent in the two thermal design models	
Reduced length	$\Lambda_c = NTU_c$	$\Lambda_h = NTU_h$
Reduced period	$\Pi_c = \dfrac{NTU_c}{C_r/C_c}$	$\Pi_h = \dfrac{NTU_h}{C_r/C_h}$
Utilization factor	$U_c = \left(\dfrac{\Pi}{\Lambda}\right)_c = \dfrac{C_c}{C_r}$	
	$U_h = \left(\dfrac{\Pi}{\Lambda}\right)_h = \dfrac{C_h}{C_r}$	

$$\varepsilon = \frac{1 - e^{\{\varepsilon_r(C^{*2}-1)/[2C^*(1-\varepsilon_r)]\}}}{1 - C^* e^{\{\varepsilon_r(C^{*2}-1)/[2C^*(1-\varepsilon_r)]\}}} \tag{55}$$

or

$$\varepsilon = \frac{1 - e^{[\phi\varepsilon_r/(1-\varepsilon_r)]}}{1 - [(\Lambda/\Pi)_h/(\Lambda/\Pi)_c]\, e^{\phi\varepsilon_r/(1-\varepsilon_r)}} \tag{56}$$

where

$$\phi = \frac{[(\Lambda/\Pi)_h^2 - (\Lambda/\Pi)_C^2]}{2\,(\Lambda/\Pi)_h\,(\Lambda/\Pi)_c} \tag{57}$$

where C^* is the original specified value, which is less than unity.

A sample calculation [17] for $\Lambda_h = 18$, $\Lambda_C = 15.5$, $\Pi_h = 16$, and $(\Lambda/\Pi)_C = 1.2$ yields $\Pi_m = 4960/347$ and $\Lambda_m = 5760/347$. From Table 6, by linear interpolation, one obtains $\varepsilon_r = 0.8215$, since $(\Pi/\Lambda)_m = 31/36$ for this case, while $\phi = -0.0645833$ from the equation. With these values, $\varepsilon = 0.847047$ from the equation. The exact value of the effectiveness for this example is 0.847311, which is just 0.03% higher than the result obtained from this approximate procedure.

6.9 Influence of Longitudinal Heat Conduction in the Wall

In the foregoing analysis, the influence of longitudinal heat conduction was neglected. For a high-thermal-effectiveness regenerator with a large axial temperature gradient in the wall, longitudinal heat conduction reduces the regenerator effectiveness and the overall heat-transfer rate. Bahnke and Howard [22] showed that an additional parameter λ, the longitudinal conduction parameter, would account for the influence of longitudinal heat conduction in the wall. Here λ is defined as

$$\lambda = \frac{k_w A_{k,t}}{L C_{min}} \tag{58}$$

where k_w is the thermal conductivity of the matrix wall, and $A_{k,t}$ is the total solid area available for longitudinal conduction; $A_{k,t}$ is given by [14]:

$$A_{k,t} = A_{k,h} + A_{k,c} = A_{fr} - A_o = A_{fr}\,(1 - \sigma) \tag{59}$$

Introducing the longitudinal conduction parameter, a generalized expression for thermal effectiveness in the functional form is given by

$$\varepsilon = \{NTU_o,\ C^*,\ C_r^*,\ (hA)^*,\ \lambda\} \tag{60}$$

Lowered effectiveness because of longitudinal conduction, $\Delta\varepsilon$, can be calculated in several ways. Parameter definitions for λ and its equivalents for the stationary and rotary regenerators are given in Table 9.

Table 9 Parameter Definitions for λ

	Stationary	Rotary
λ	$\dfrac{k_w A_{k,t}}{L(MC_p)_c}\left(\dfrac{\tau_c + \tau_h}{\tau_c}\right)$	$\dfrac{k_w A_{k,t}}{L(Mc_p)_c}$

Bahnke and Howard Method

Bahnke and Howard [22] illustrated the influence of the thermal conductivity on thermal effectiveness by a factor called the *conduction effect*. The conduction effect is defined as the ratio of the difference between effectiveness with no conduction effect and with conduction effect to the no conduction effectivness, as given by

$$\frac{\Delta\varepsilon}{\varepsilon} = \frac{\varepsilon_{\lambda=0} - \varepsilon_{\lambda}}{\varepsilon_{\lambda=0}} \tag{61}$$

Bahnke and Howard tabulated results for ε for a wide range of NTU_o, C_r^*, C_r, and λ. their results are valid over the following range of dimensionless parameters:

$$1 \geq C_{min}/C_{max} \geq 0.90$$
$$1.0 \leq C_r/C_{min} \leq \infty$$
$$1 \leq NTU_o \leq 100$$
$$1.0 \geq (hA)^* \geq 0.25$$
$$1.0 \geq A^* \geq 0.25$$
$$0.01 \leq \lambda \leq 0.32$$

Bahnke and Howard's results for $C^* = 1$ can be accurately expressed by [29]:

$$\varepsilon = C_{\lambda}\varepsilon_{\lambda=0} \tag{62}$$

where $\varepsilon_{\lambda=0}$ is given by Eq. 23 or 31, and C_{λ} is given by

$$C_{\lambda} = \frac{1 + NTU_o}{NTU_o}\left[1 - \frac{1}{1 + NTU_o\,(1 + \lambda\psi)/(1 + \lambda NTU_o)}\right] \tag{63}$$

in which

$$\psi = \left(\frac{\lambda NTU_o}{1 + \lambda NTU_o}\right)^{0.5} \tanh\left[\frac{NTU_o}{[\lambda NTU_o/(1 + \lambda NTU_o)]^{0.5}}\right] \tag{64a}$$

$$\approx \left(\frac{\lambda NTU_o}{1 + \lambda NTU_o}\right)^{0.5} \qquad \text{for} \quad NTU_o \geq 3 \tag{64b}$$

Romie's Solution

Romie [34] expressed the effects of longitudinal heat conduction on thermal effectiveness in terms of a parameter G_L. The factor G_L is derived from the analysis of axial conduction in counterflow recuperators by Hahnemann [35]. G_L is given by

$$G_L = 1 - [1 - \tanh(b)/b]\,(NTU/b)^2 \qquad \text{for} \quad C^* = 1,\ (hA)^* = 1 \tag{65}$$

where

$$b = NTU_o\left[1 + 1/(\lambda NTU_o)\right]^{0.5} \tag{66}$$

The expression for $\varepsilon_{\lambda\neq 0}$ is given by

$$\varepsilon_{\lambda\neq 0} = \frac{1 - e^{-G_L NTU_o(1-C^*)}}{1 - C^* e^{-G_L NTU_o(1-C^*)}} \qquad C^* < 1 \tag{67a}$$

$$= \frac{G_L NTU_o}{(1 + G_L NTU_o)} \qquad C^* = 1 \tag{67b}$$

Figure 11 shows G_L as a function of the product NTU_o for several values of NTU_o. The curves are for $(hA)^* = 1$ and $C^* = 0.9$ and 1. The same curves were obtained using $(hA)^* = 0.5$, thus indicating that G_L is a very weak function of $(hA)^*$ [34].

Shah's Solution to Account for the Longitudinal Conduction Effect

For $0.9 \le C^* \le 1$, Shah [36] has provided a closed-form formula to take into account the longitudinal conduction effect. However, the following more general method is recommended for $C^* < 1$, by Shah [14].

1. Use the Razelos method to compute $\varepsilon_{r,\lambda=0}$ for an equivalent balanced regenerator using the procedure from Eqs. 51, 52, and 54.
2. Compute C_λ from Eq. 63 using $NTU_{o,m}$ and λ.
3. Calculate $\varepsilon_{r,\lambda\neq 0} = C_\lambda \varepsilon_{r,\lambda=0}$.
4. Finally ε is determined from Eq. 55 or 56 with ε_r replaced by $\varepsilon_{r,\lambda\neq 0}$.

This procedure yields a value of ε accurate within 1% for $1 \le NTU_o \le 20$ and $C_r^* \ge 1$ when compared to Bahnke and Howard's results.

6.10 Fluid Bypass and Carryover on Thermal Effectiveness

Fluid bypass and carryover on thermal effectiveness are discussed in references 14 and 37.

6.11 Regenerator Design Methodology

To design a successful regenerator, the engineer must consider many design factors including the following [2]:

1. Describe different types of regenerative heat exchangers.
2. Discuss basic heat-transfer process and the correlation of cyclic temperature distributions resulting from storage of thermal energy.

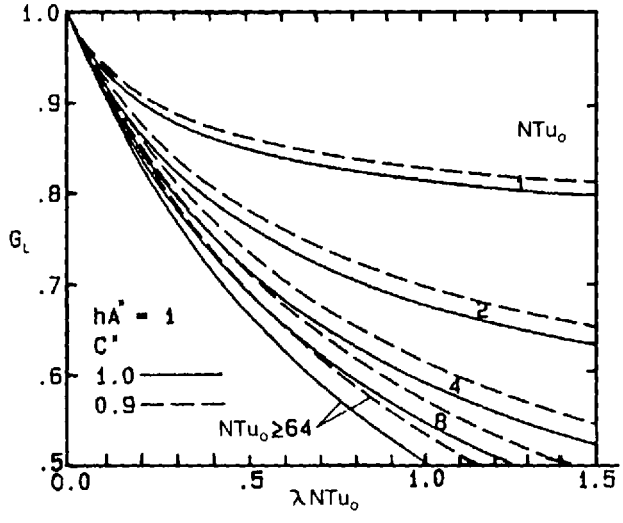


Figure 11 G_L for longitudinal conduction. (From Ref. 34.)

3. Relate the regenerator to classical counterflow arrangements to enable trade-offs of heat transfer, pressure drop, size, and alternative surfaces.
4. Discuss effects of leakage on both performance and design.
5. Consider effects of pressure loads, leakage control, and rotation on mechanical design.

6.12 Primary Considerations Influencing Design

Primary considerations influencing the design of a regenerator especially for aircraft/vehicular gas turbine applications may be summarized as follows [38]:

1. Manufacturing limitations.
2. Cost limitations.
3. Maintenance and cleaning requirements.
4. Mechanical design problems.
5. Weight, shape, and size limitations.
6. Limitations on flow friction-power expenditure.
7. Desired exchanger heat-transfer effectiveness.

6.13 Rating of Rotary Regenerators

The basic steps involved in the analysis of a rating problem are the determination of surface geometrical properties, matrix wall properties, fluid physical properties, Reynolds numbers, j (or Nu) and f factors corrected for property variations, heat-transfer coefficients, NTU_o, C^*, C_r^*, and pressure drops. The procedure presented for regenerators parallels that for a compact heat exchanger. Therefore, the rating procedure is not repeated here. However, for details on a rating procedure from first principles consult Shah [14].

6.14 Sizing of Rotary Regenerators

The sizing problem for a rotary regenerator is more difficult. Similar to recuperator design, the sizing of a regenerator involves decisions on material, surface geometry selection, and mechanical design considerations. Once these are decided, the problem reduces to the determination of the disk diameter, division of flow area, disk depth, and disk rotational speed to meet the specified heat transfer and pressure drops [14]. Sometimes a limitation on the size is also imposed. One method for a new design would be to assume a regenerator size, consider it as a rating problem, and evaluate the performance as outlined for compact recuperators. Iterate on the size until the computed performance matches the specified performance. A detailed sizing procedure is outline in reference 14.

7 MECHANICAL DESIGN

After the heat-transfere surface has been chosen, sizing studies completed, and the regenerator selected to be compatible with the overall system requirements, the next step involves mechanical design. Mechanical designs must consider items such as [2](1) thermal distortions, (2) leakages, (3) pressure loadings, and in the case of the rotary types, (4) a drive system and (5) sealing. An important source book on regenerator mechanical design is Mondt [2].

7.1 Single-Bed and Dual-Bed Fixed Regenerators

Single-bed and dual-bed regenerators can be relatively simple to design. If the bed is composed of loose pellets, grids or screens are necessary to retain the pellets within a container. The grid

mesh must be fine enough to retain the smallest pellet in the bed, yet the mesh must be porous enough to keep pressure drops low. If the retaining grids are not strong enough at the operating temperature, the bed will "sag" and loosen the packing.

Leakages. Both the single-bed and dual-bed valved regenerators have displacement leakage, that is, displacement of the fluid entrained in the matrix voids at the switching instant. This fluid is trapped and "displaced" into the other fluid stream and hence is known as displacement leakage. In addition to displacement leakage, fixed-bed regenerators may have small primary leakage of one fluid into the other through leaks in closed switching valves.

7.2 Rotary Regenerators

The mechanical design of a rotary regenerator requires (additionally to the recuperator) the following items [39]:

1. A subdividion of the casing into a rotor and a stator.
2. Leakage and an effective seal between the two gases.
3. Means for supporting the rotor in the stator.
4. A drive for the rotor.

Items (2) and (4) are discussed next.

Leakages

Primary leakages in a rotary regenerator can be classified as (1) labyrinth leakage, (2) carryover or displacement leakage, and (3) structural leakage.

Labyrinth or Seal Leakage. This is leakage through the seal stem from the fact that the cold gases are at much higher pressures than the hot gases. This is especially true in the case of gas turbine with high pressure ratio.

Carryover or Displacement Leakage. In addition to direct leakage through seals, there is inevitably a "carryover" or displacement leakage due to air trapped in the matrix as it passes through the gas side.

Structural Primary Leakage. Structural leakages take place through any gaps existing in the matrix and the housing.

Any leakage is a serious loss, because it is the air that has absorbed compressor work but escapes to the atmosphere without passing through the turbine. It is more important than pressure loss, as it affects the net work severely [40]. Leakage is dependent mainly on pressure ratio and carryover on matrix rpm. Leakage due to seal leakage and displacement leakage can amount to 3–4% of the airflow out of the compressor [41]. The effect of a given fractional leakage depends on the values of exchanger effectiveness and cycle pressure ratio. As an example, for a cycle with typical temperatures, component efficiencies, and regenerator effectiveness of 90%, a leakage of 5% will reduce the net output by about 11% while a leakage of 10% will reduce it by twice that amount [40].

Seal Design

In a rotary regenerator, the stationary seal locations control the desired frontal areas for each fluid and also serve to minimize the primary leakage from the high pressure side to the low pressure side. The sealing arrangement must adequately prevent leakage flow, and at the same time not introduce high frictional resistance for rotation. Because, the matrix is alternately exposed to hot and cold gases, thermal expansion and contraction add to the sealing problem. Sealing arrangements will be of two general types [42]: (1) continuous cylindrical seals similar to a shaft seal, and (2) main seals, which divide the high and low pressure sides. The main

seals present a more difficult problem because of the effect of the displacement or carryover loss, the pressure forces under the seal faces, which must be balanced, and allowances to be made for the thermal distortion of the rotor. Two possible classes of main seal arrangements are illustrated diagrammatically in Fig. 12. Figure 12a shows the case where the seal bears directly upon the regenerator matrix. Figure 12b shows the case where the seal bears against a system of rotor compartments. Certain considerations for seal design are [43]:

1. The seals must be efficient at very high temperature and pressures but still allow freedom of movement.
2. The seals must accommodate the expansion and contraction accompanying temperature variations and stll prevent leakage.

Drive for the Rotor

A design probem encountered with the regenerator is that of supporting and driving the matrix at low speed. The regenerator usually rotates at a speed of approximately 20–30 rpm [41]. An electric drive will be ideal, because of its low rpm and small power requirement.

Thermal Distortion and Transients

A regenerator is subjected to thermal shock and thermal distortion due to unsteady thermal conditions. However, this can be minimized by the use of ceramic material. A regenerator cannot be designed assuming that all operations will be at steady-state conditions. In vehicular gas turbines system, transients are common. Even industrial regenerators are occasionally exposed to starting and stopping transients. Gentle or long-duration transients are desirable to minimize thermal distortions and potential thermal stresses [2]. More problems are usually faced during the warm-up of a regenerator than during stopping because on starting, the matrix and rotor respond much faster than the surrounding housing. If the housing does not accommodate the matrix and the rotor to expand during warm-up, the housing may constrain the matrix growth and cause thermal stresses.

Pressure Forces

Pressures in the regenerator system exert forces on the matrix or structure. There are two sources of pressure forces in a rotary regenerator, [2]: One source of pressure forces is due to pressure difference between the high-pressure cold air and the low-pressure hot gases. This pressure force depends on the seal arrangement. The seals for a disk can be arranged so that the net force on the support is essentially zero. The second source results from pressure drop of the fluids flowing through the matrix. This pressure force is the product of the total pressure drop and the frontal area.

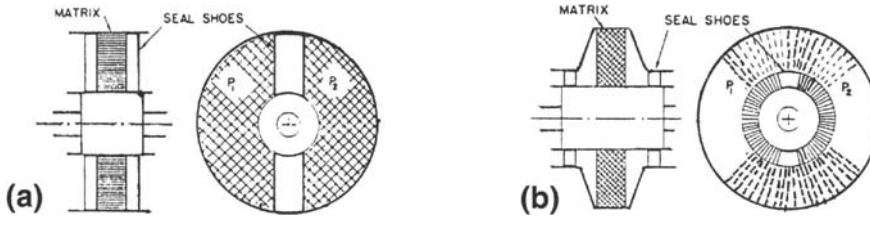


Figure 12 Seals for rotary regenerator. (From Ref. 42.)

8 INDUSTRIAL REGENERATORS AND HEAT RECOVERY DEVICES

Apart from recuperators and regenerators, various types of heat recovery devices are available for many years. Commercially available heat recovery devices for combustion air preheaters include the following [44]:

1. Fluid-bed regenerative heat exchanger.
2. Fluidized-bed waste heat recovery system.
3. Vortex-flow direct-contact heat exchanger.
4. Ceramic bayonet tube heat exchanger or high-temperature burner duct recuperators.
5. Regenerative burner.
6. Porcelain-enameled flat-plate heat exchanger.
7. Radiation recuperators.
8. Heat-pipe exhangers.

Because of the multitude of different industrial heating processes and exhaust system designs, there is no one universal type of heat-transfer device best suited for all applications. The following discussion on various types of industrial air preheaters (except heat-pipe exchangers) working on the regeneration principle is based on reference 44.

8.1 Fluid-Bed Regenerative Heat Exchangers

In fluid-bed regenerative heat exchangers, fluidized beds of pellets recover heat from hot exhaust gas and transfer this heat to cold combustion air [45]. The basic fluid-bed heat exchanger consists of an insulated cylindrical tower incorporating an upper and a lower chamber as shown Figure 13. Each chamber is fitted with several horizontal perforated trays. Hot exhaust gases

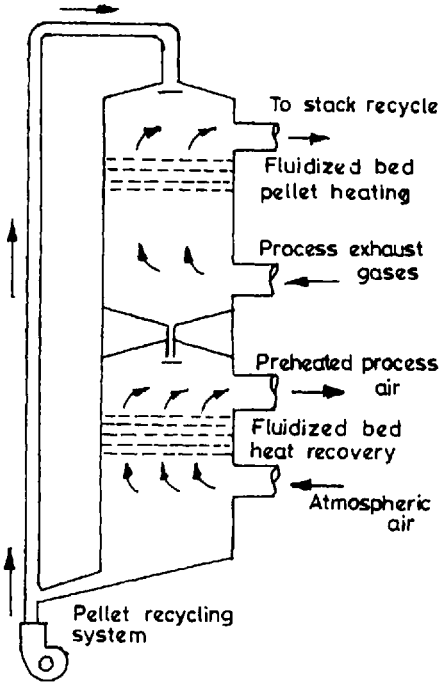


Figure 13 Fluid bed regenerator. (From Ref. 45.)

enter the upper chamber near its base and rise to the outlet near the top, heating counterflowing alumina pellets as they fall. The heated pellets pass through an aperture into the lower chamber, where they give up their heat to the cold air. Air enters the lower chamber near the base and exits near the top. Direct contact of gas and air streams with the heat exchange media, namely, the alumina pellets, coupled with controlled dwell time at the trays, results in high heat-transfer rates. By controlling the rate of pellet recycling, the temperature of the air being heated can be held constant within wide variations of gas inlet temperature and volume. As a part of this heat exchange system, an auxiliary pneumatic system is incorporated for recycling alumina pellets.

8.2 Fluidized-Bed Waste Heat Recovery

Fluidized-bed waste heat recovery (FBWHR) systems are being developed to preheat combustion air for industrial furnaces. FBWHR systems employ a heat-transfer particulate media, which is heated as it falls through the upward-flowing flue gases in a raining bed heat exchanger [9,46]. This type of heat exchanger is known as a fluidized-bed heat exchanger. Fluidized-bed heat exchangers (FBHE) offer the potential for economic recovery of high-temperature (2000–3000°F) heat from the flue gases of industrial processes such as steel soaking pits, aluminum remelt furnaces, and glass melting furnaces.

A fluidized-bed heat exchanger (Fig. 14) consists of horizontal finned heat exchanger tubes with a shallow bed of fine inert particles, which move upward with gas flow and give up the heat to the finned tubes, which in turn transfer heat to cold air passing through them. A thin steel plate with small perforations supports the bed and distributes the hot gas evenly. The perforations are uniform with a hole size of 1.5 mm diameter or less, and the holes are spaced to provide a free flow area of 3–10%. For many applications only ceramic distributor plates will withstand the temperatures and corrosive environments of flue gases. Among the FBHE advantages are enduring the hostile environments such as elevated temperature, fouling particulates, corrosive gases, corrosive particulates, and thermal cycling [9]. Most surfaces are kept clean by fluidizing action.

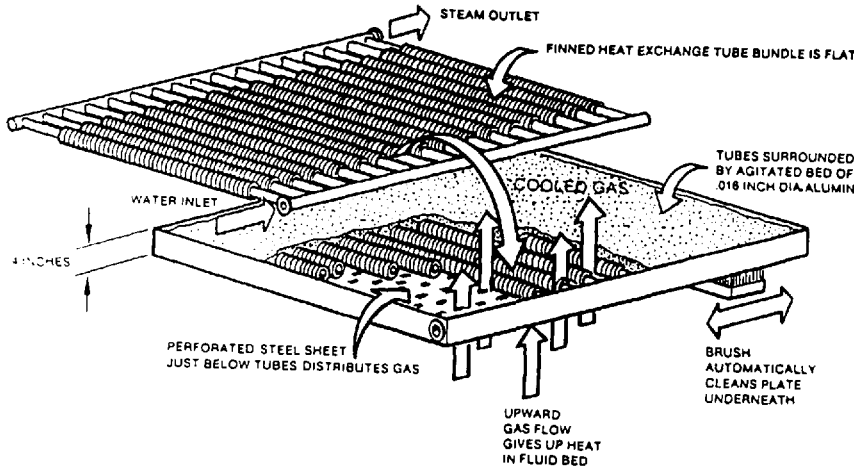


Figure 14 Fluidized bed regenerator. (From Ref. 19.)

8.3 Vortex-Flow Direct-Contact Heat Exchangers

The vortex-flow direct-contact heat exchanger represents a new approach for high-temperature (2500°F) heat recovery from industrial waste heat flue gas with a simple payback period. In the vortex-flow direct-contact heat exchanger, the heat conduction material wall of conventional metal or high-temperature ceramic material is replaced by a vortex-induced fluid dynamic gas boundary, which separates the tangentially rotating hot and cold gas flows between which heat exchange is desired [47].

The VFHE shown in Fig. 15 is a cylindrical cavity into which separate hot flue gas and cold preheat air gas flows are injected. Injection of the gases is such that a vortex-flow pattern is established in the cavity, providing confinement of hot fluid to the central region of the cavity surrounded by cold air stream. Solid particles of size 20–200 μm diameters as a medium to exchange heat between hot and cold streams are injected into the hot spiraling gas stream. Due to centrifugal action these particles pass into the surrounding cold gas rotating flow, to which the particles transfer heat. Figure 16 shows the particles' trajectory projections. Upon reaching the outside cavity surface, the particles are entrained in the outermost region of the vortex flow and removed with a portionof the cold flow, which exits at the periphery (exhaust end wall) as shown in Fig. 16. The VFHE requires a particle injection and separation subsystem to collect and recycle the particle to the vortex chamber for continued heating and cooling cycles.

8.4 Ceramic Bayonet Tube Heat Exchangers

Babcock and Wilcox (B&W) and the Department of Energy (DOE) developed high-temperature burner duct recuperator (HTBDR) systems capable of recovering waste heat from high-temperature flue gas using ceramic bayonet elements [48,49]. The high-temperature burner duct recuperators consist of silicon carbide ceramic bayonet tubes suspended into the exhaust

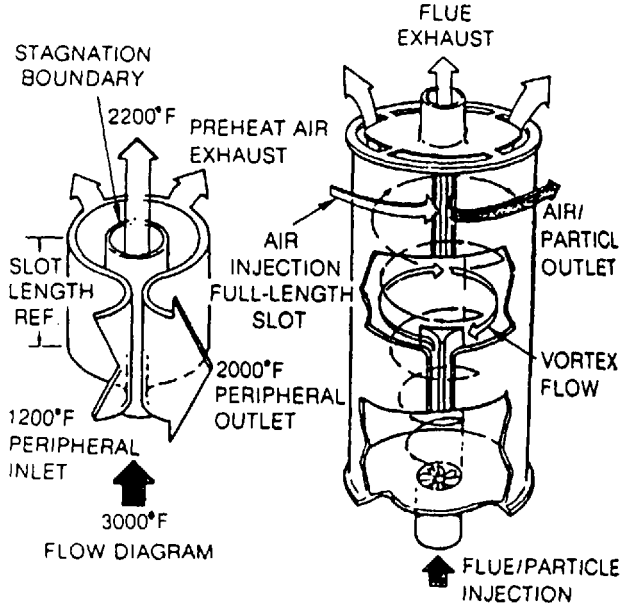


Figure 15 Vortex flow direct contact regenerator. (From Ref. 47.)

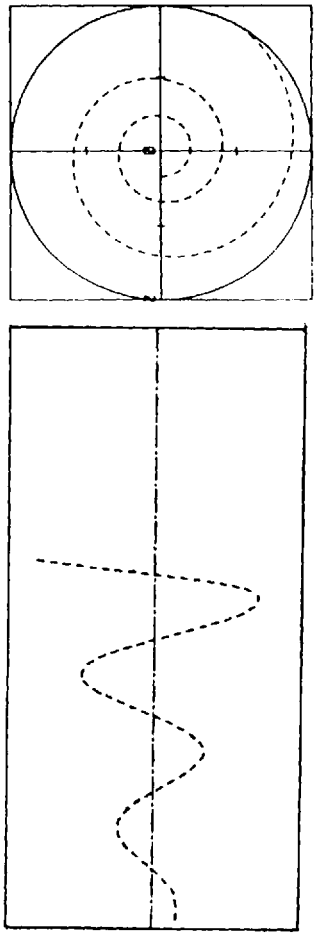


Figure 16 Particles trajectory projections in a vortex flow direct contact regenerator. (From Ref. 47.)

gas flow stream, where they recover the heat from the exhaust and preheat the combustion air up to a temperature of 1090°C (2000°F). The ceramic bayonet elements shown in Fig. 17 consist of an assembly of two concentric tubes of each bayonet element suspended from metallic, air-cooled tube sheets at the top end of the element. Combustion air is directed through the elements at the inner tube or the annulus from heavily insulated plena located

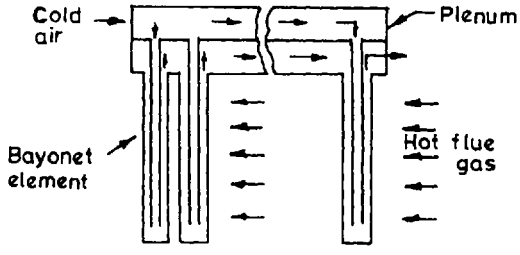


Figure 17 Ceramic bayonet tube regenerator. (From Ref. 48.)

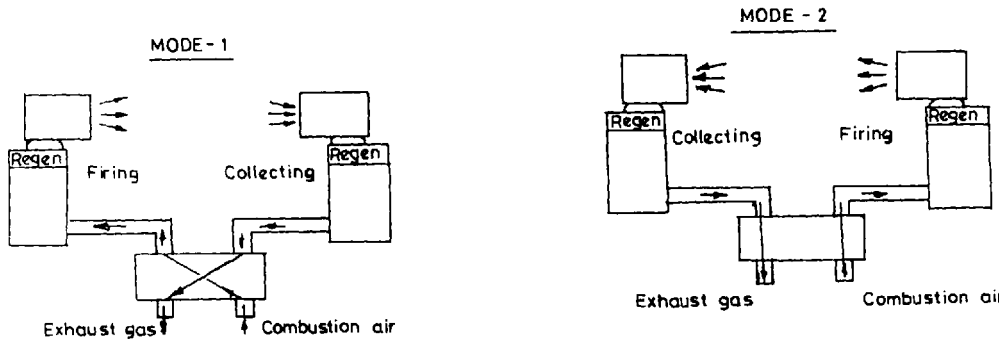


Figure 18 Regenerative burner. (From Ref. 7.)

above the tube sheets. The tubes of each element are free to expand or contract under the influence of temperature variations. The ceramic bayonet elements are also expected to ease maintenance and to best deal with problems associated with thermal stress, leakage, and stress-related corrosion.

8.5 Regenerative Burners

The reGen regenerative burner, an all-ceramic high-temperature burner, close coupled to a compact, fast-cycle, ceramic regenerator, provides air preheats in excess of 85% of the process temperature in fuel-fired applications up to 1399°C (2550°F) [7]. Figure 18 shows one complete regenerative unit comprised of two burners, two regenerators, a reversing valve, and the related pipings. While one of the burners fires, drawing the preheated air fed through its regenerator, exhaust gas is drawn through the other burner and down into its associated regenerator, then discharged to the atmosphere. After a sufficient interval the reversing operation takes place.

8.6 Porcelain-Enameled Flat-Plate Heat Exchangers

Porcelain-enameled heat exchangers offer cost-effective solutions to problems of heat recovery from extremely corrosive gases that preclude the use of carbon steel or common types of stainless steels [50]. Porcelain enamel is a glass coating material that is applied to a metal substrate to protect the base metal. The base metal gives strength and rigidity; the metal can be steel, cast iron, aluminum, or copper, but mostly steel is used on a larger scale. The glass coating offers significant corrosion resistance to the corrosive flue gas. The porcelain-enameled coating finds application in flat-plate heat exchangers of the open channel air preheater (OCAP) type for advanced heat recovery. The OCAP is a plate-type exchanger characterized by a nonweld construction of the heat transfer core. The enameled plates are assembled into a floating construction. Elastic springs are used between all adjacent plates to ensure a uniform distribution of the dead weights and to allow for the thermal expansion and contraction in operation. This floating core is enclosed in a rigid frame, again without any welding or any damage to the porcelain enamel layer.

8.7 Radiation Recuperators

Metallic recuperator for industrial furnaces are generally of the following types [51]:

1. Convective units, operating at flue gas temperatures up to a maximum of 1100°C (2000°F).
2. Radiation-type units, that is, the heat-transfer mode is by radiation, operating at temperature ranges of nearly 900°C to 1500°C (2700°F). In radiation-type recuperators, parallel flow is essential to control the operating temperatures of the heating surface. A combination of parallel flow and counterflow is required to reach the highest recuperator efficiencies of air temperature of above 800°C (1500°F). Typical radiation recuperators include a double-shell parallel-flow radiation recuperator consisting of two concentric cylinders—through the inner shell the flue gas flows and through the annulus the cold air flows in a parallel direction—as well as cage-type radiation recuperators for very large high-temperature furnaces, with a combination of parallel flow and counterflow units.

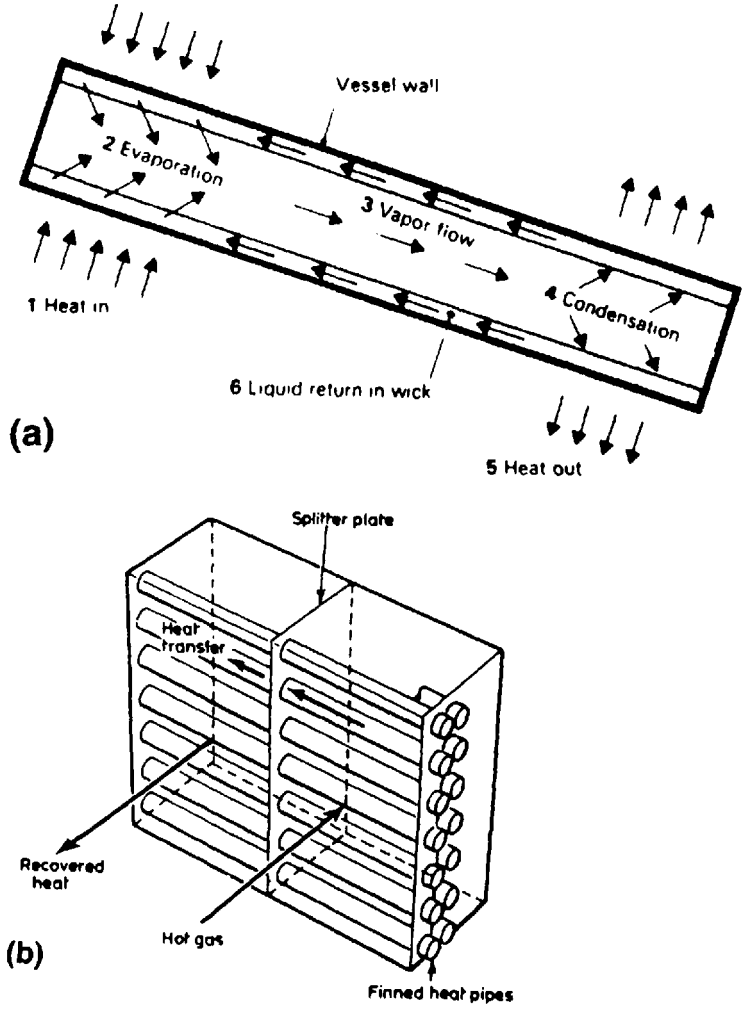


Figure 19 Heat pipe heat exchanger. (From Ref. 52.)

8.8 Heat-Pipe Heat Exchangers

The heat-pipe heat exchanger used for gas-gas heat recovery is essentially bundle of finned heat pipes assembled like a conventional air-cooled heat exchanger. The heat pipe consists of a working fluid inside the tubes and a wick lining inside the wall. The purpose of the wick is to transport the working fluid contained within the heat pipe, from one end to the other by capillary action.

The heat-pipe heat exchanger consists of an evaporative section through which the hot exhaust gas flows and a condensaton section through which the cold air flows. These two sections are separated by a separating wall as shown in Fig. 19 [52]. The working of a heat-pipe heat exchanger is as follows. Heat transfer by the hot flue gas at the evaporative section causes the working fluid contained within the wick to evaporate and the increase in pressure causes the vapor to flow along the central vapor region to the condensation section, where it condenses, and gives up the latent heat to the cold air. The condensate then drains back to the evaporative section by capillary action in the wick. In cases where gravity aids return of the condensate to the evaporative section, it is possible to operate without a wick; the device then becomes a simple two-phase thermosyphon.

NOMENCLATURE

A_C = matrix transfer area on cold side, m^2 (ft^2)
A_{fr} = frontal area, m^2 (ft^2) = $A_{fr,h} + A_{fr,c}$
$A_{fr,c}$ = frontal area on cold side, m^2 (ft^2)
$A_{fr,h}$ = frontal area on hot side, m^2 (ft^2)
$A_{fr,t}$ = total face area, m^2 (ft^2)
A_h = matrix transfer area on hot side, m^2 (ft^2)
$A_{k,t}$ = total solid area for longitudinal conduction, m^2 (ft^2)
A_{mk} = constants defined by Eq. 48
a_{jk} = constants defined by Eq. 29
A_o = minimum free flow area, m^2 (ft^2) = σA_{fr}
$\%a$ = face seal and hub coverage
B_j = constants defined by Eq. 28
B_{mk} = constants defined by Eq. 49
b = cell geometry dimension, m (ft); or function defined by Eq. 66
C = heat capacity rate (Mc_p), J/°C (Btu/hr • °F)
C^* = heat capacity rate ratio (it should be less than or equal to 1) = C_{min}/C_{max}
C_c = fluid stream capacity rate (Mc_p) for cold gas, W/°C (Btu/hr • °F)
C_h = fluid stream capacity rate (Mc_p) for hot gas, W/°C (Btu/hr • °F)
C_k = constant defined by Eq. 50
C_{max} = maximum of C_c or C_h, W/°C (Btu/hr • °F)
C_{min} = minimum of C_c or C_h, W/°C (Btu/hr • °F)
$c_{p,c}$ = specific heat of cold gas, J/kg • °C (Btu/lbm • °F)
$c_{p,h}$ = specific heat of hot gas, J/kg • °C (Btu/lbm • °F)
C_r = capacity rate of the rotor matrix ($M_r c_r$), W/°C (Btu/hr • °F)
= $M_r c_r N$ for rotary regenerator, W/°C (Btu/hr • °F)
c_r = specific heat of the matrix material, J/kg • °C (Btu/lbm • °F)
C_r^* = matrix heat capcity rate ratio
= $(M_r c_r)/C_{min}$
$C_{r,m}^*$ = C_r^* for equivalent balanced regenerator

C_λ = longitudinal conduction correction factor
D = regenerator disk outer diameter at the end of the heat transfer surface, m (ft)
D_h = hydraulic diameter, $(4r_h)$, m (ft)
d = hub diameter, m (ft)
d^* = cell height/width
f = Fanning friction factor
G_L = parameter to account the effects of longitudinal heat conduction on thermal effectiveness as defined in Eq. 65
hA = thermal conductance W/°C (Btu/hr · °F)
$(hA)^*$ = ratio of the convective conductance on the C_{min} side to C_{max} side = $(hA)_c/(hA)_h$
h_c = convective conductance for cold gas, W/m^2 · °C (Btu/hr · ft^2 · °F)
h_h = convective conductance for hot gas, W/m^2 · °C (Btu/hr ·ft^2 · °F)
$I_n(\cdot)$ = modified Bessel function of the first kind and nth order
j = Colburn factor for heat transfer
i, j, k, n = integers
k_w = thermal conductivity of the matrix wall
L = matrix flow length, m (ft)
M = order of the trial solution, Eq. 45
M_c = mass flow rate of cold gas, kg/s (lbm/hr)
m_c = mass of the cold gas retained in the matrix flow length dx, kg (lbm)
$(Mc_p)_c$ = capacity rate of cold gas, W/°C (Btu/hr · °F)
$(Mc_p)_h$ = capacity rate of hot gas, W/°C (Btu/hr · °F)
M_h = mass flow rate of hot gas, kg/s (lbm/hr)
m_h = mass of the hot gas retained in the matrix flow length dx, kg (lbm)
M_r = matrix mass, kg (lbm)
M_rc_r = thermal capacitance of matrix, W/°C (Btu/hr · °F)
N = rpm of the matrix
N_c = cell density
Nu = Nusselt number, hD_h/k
NTU = number of transfer units, hA/C
NTU_c = number of transfer units on the cold side (≈ twice NTU_o)
NTU_h = number of transfer units on the hot side (≈ twice NTU $_o$)
NTU_o = modified number of transfer units
$NTU_{o,m}$ = NTU_o for an equivalent balanced regenerator
Q = total heat duty of the exchanger, W · s (Btu)
q = heat transfer rate, W (Btu/hr)
Re = Reynolds number
r_h = hyraulic radius, m (ft) = $D_h/4$
t_c = temperature of the cold gas, °C (°F)
t_h = temperature of the hot gas, °C (°F)
t_r = temperature of the matrix, °C (°F)
$t_{c,i}$, $t_{c,o}$ = cold fluid terminal temperatures, °C (°F)
$t_{h,i}$, $t_{h,o}$ = hot fluid terminal temperatures, °C (°F)
U_C = utilization factor on the cold side $(\Lambda/\Pi)_C$
U_h = utilization factor on the cold side $(\Lambda/\Pi)_h$
U_1 = $(\Lambda/\Pi)_1$, the smaller of the two ratios U_C and U_h
x_{1m}, x_{2m} = unknown coefficients defined by Eq. 45
x, y = variables as defined in Eq. 2
V = $(A_{fr,h} + A_{fr,c})L$, m^3 (ft^3)

$V_i(x,y)$ = special functions defined by Eq. 41
β = area density, m^2/m^3 (ft^2/ft^3)
δ = matrix stock thickness, m (ft)
ε = thermal effectiveness
ε_{cf} = counterflow regenerator thermal effectiveness
ε_r = thermal effectiveness of reference regenerator
$\Delta\varepsilon$ = lowered effectiveness because of longitudinal conduction
$\varepsilon_{r,\lambda=0}$ = equivalent balanced regenerator neglecting longitudinal heat conduction
$\varepsilon_{r,\lambda\neq 0}$ = $C_\lambda \varepsilon_{r,\lambda=0}$
ξ = fractional distance along the flow path in the regenerator matrix of length L
η = fractional completion of a respective gas flow period
Λ = reduced length
Λ_m = mean reduced length
λ = longitudinal conduction parameter
λ_c = longitudinal conduction on the cold side
λ_h = longitudinal conduction on the hot side
Π = reduced period
Π_m = mean reduced period
ρ_r = matrix material density
ϕ = function defined by Eq. 57
ψ = function defined by Eq. 64
σ = porosity = A_f/A_{fr}
τ = flow period, s
τ_c = duration of cold flow period, s
τ_h = duration of hot flow period, s
τ_t = time for one revolution, $\tau_c + \tau_h$, s

Subscripts

c = cold
h = hot
i = in
m = mean
o = hot
r = matrix

7
Plate Heat Exchangers and Spiral Plate Heat Exchangers

Dr. Richard Seligman, the founder of APV International, introduced the first commercially successful gasketed plate heat exchanger design in 1923. A plate heat exchanger essentially consists of a number of corrugated metal plates provided with gaskets and corner ports to achieve the desired flow arrangement. Each fluid passes through alternate channels. The plates are clamped together in a frame that includes connections for the fluids. Since each plate is generally provided with peripheral gaskets to provide sealing arrangements, the plate heat exchangers are called gasketed plate heat exchangers. Extensive information on the plate heat exchanger has been summarized by Focke [1], Cooper et al. [2], Raju et al. [3,4], and Shah et al. [5].

1 PLATE HEAT EXCHANGER CONSTRUCTION—GENERAL

A plate heat exchanger (PHE), as shown in Fig. 1, is usually comprised of a stack of corrugated or embossed metal plates in mutual contact, each plate having four apertures serving as inlet and outlet ports, and seals designed so as to direct the fluids in alternate flow passages. The flow passages are formed by adjacent plates so that the two streams exchange heat while passing through alternate channels. When assembled, the spacing between adjacent plates ranges from 1.3 to 6.4 mm. The number and size of the plates are determined by the flow rate, physical properties of the fluids, pressure drop, and temperature program. The plate corrugations promote fluid turbulence and support the plates against differential pressure. The stack of plates is held together in a frame by a pressure arrangement.

The periphery of each plate is grooved to house a molded gasket, each open to the atmosphere. Gaskets are generally cemented in, but snap-on gaskets are available that do not require cement. Gasket failure cannot result in fluid intermixing but merely in leakage to the atmosphere. Proper selection of gasket material and operating conditions will eliminate the leakage risk.

Frame assembly tightly holds the plates pack. It ensures optimum compression and leak

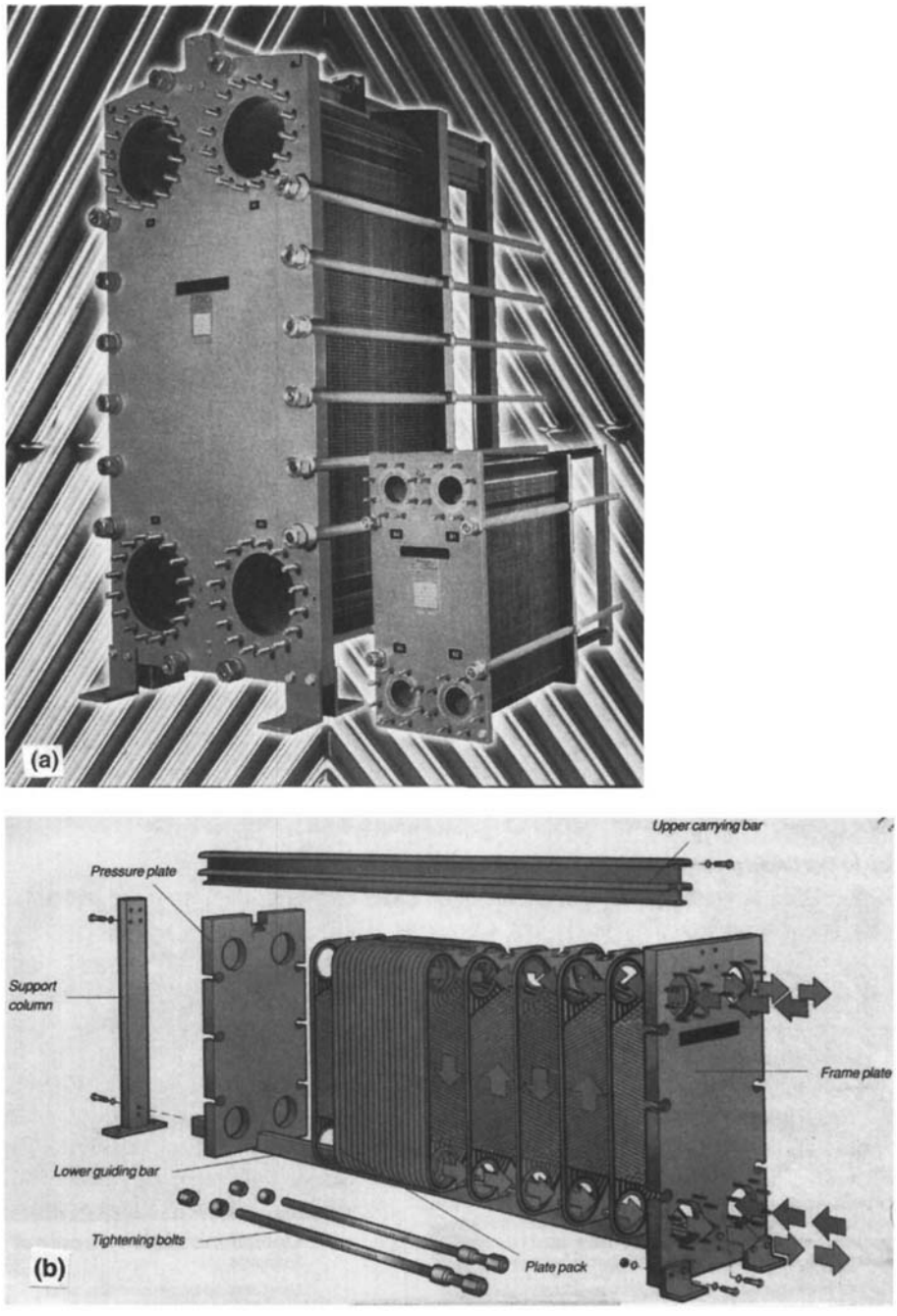


Figure 1 Plate heat exchanger construction details.

tightness. The elements of the frame are a fixed plate, compression plate, pressing equipment, and connecting ports. Every plate is notched at the center of its top and bottom edges so that it may be suspended from the top carrier bar and guided by the bottom guide bar, and the plates are free to slide along the bars. The movable head plate is similarly notched and free to slide along both bars. Both the upper carrying bar and the lower guiding bar are fixed to the support columns. The plate pack is tightened by means of either a mechanical or hydraulic tightening device. Connections are located in the frame cover or, if either or both fluids make more than a single pass within the unit, the frame and pressure plates. By including intermediate separating/connecting plates, three or more separate fluid streams can be handled. Frames are usually free standing; for smaller units, they are attached to structural steel work. Salient constructional features of PHE and the resulting advantages and benefits are given in Table 1.

1.1 Flow Patterns and Pass Arrangement

In a plate heat exchanger, several types of flow patterns can be achieved:

1. Series flow arrangement, in which a stream is continuous and changes direction after each vertical path, that is, *n* pass–*n* pass with individual passes per channel as shown in Fig. 2a.
2. Single-pass looped arrangement: U-arrangement, Z-arrangement. Both fluids flow countercurrently through parallel passages that make up a single pass as shown in Fig. 2b.
3. Multipass with equal passes (series flow pattern), wherein the stream divides into a number of parallel flow channels and then recombines to flow through the exit in a single stream, that is, *n* pass–*n* pass as shown in Fig. 2c.
4. Multipass with unequal pass, such as 2 pass–1 pass, and 3 pass–1 pass, as shown in Fig. 2d.

Table 1 Construction Features of Plate Heat Exchangers [6]

Feature	Advantage	Benefit
PHE concept	Efficient heat transfer, low weight	Reduced capital cost, smaller foundations (lower investment cost)
Modular construction	Flexibility	Easy to modify for altered duties
Fixed frame and movable pressure plates	Easily accessible heat-transfer area	Reduced shutdown time, i.e., lower plates maintenance and operating costs
Metallic contact between plates	Minimized vibrations	Longer lifetime; great reliability
Bearing boxes on tightening bolts	Reduced friction	Easy opening and closing, reduced maintenance
One-step plate pressing	High dimensional tolerances	Improved performance
Glue-free gaskets	Simplified regasketing while still in frame	Reduced shut-down time, reduced maintenance costs
Two-component oven-cured epoxy on glued gaskets	Superior bonding	Greater reliability

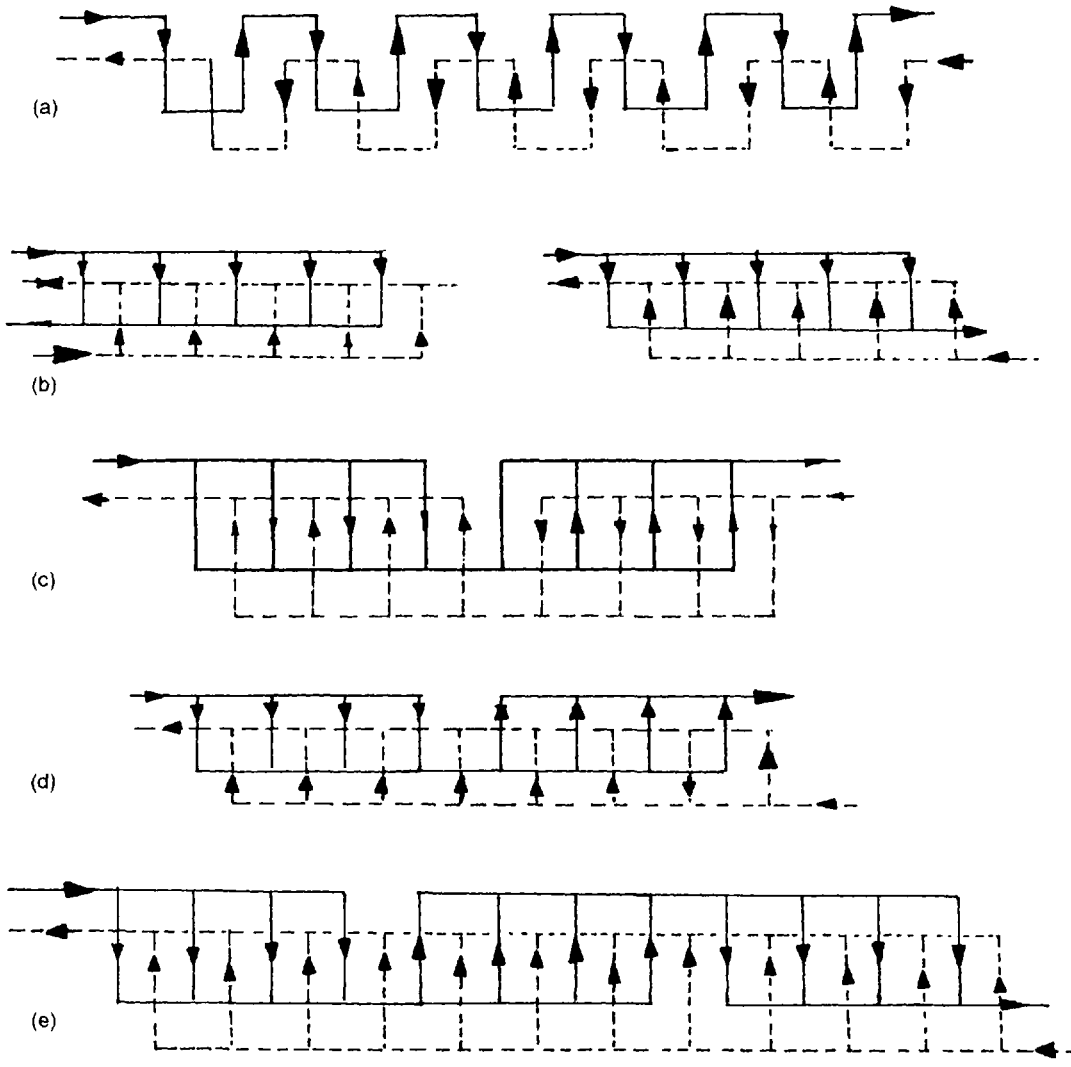


Figure 2 PHE Flow arrangements. (a) Series flow *n* pass-*n* pass; (b) single pass looped: U arrangement arrangement; (c) multipass with equal pass (*n* pass-*n* pass); and (d) multipass with unequal pass, 2 pass-1 pa and 3 pass-1 pass.

Table 2 Useful Data on PHE

Unit		Plates	
Size	1540–2500 m^2	Thickness	0.5–1.2 mm
Number of plates	up to 700	Size	0.03–2.2 m
Port size	up to 39 cm	Spacing	1.5–5.0 mm
		Corrugation depth	3–5 mm

1.2 Useful Data on PHE

Useful data on plate exchangers are given in Table 2.

1.3 Standard Performance Limits

Standard performance limits for Alpha-Laval PHE are [6]:

Maximum operating pressure	25 bar (360 psi)
With special construction	30 bar (435 psi)
Maximum temperature	160°C (320°F)
With special gaskets	200°C (390°F)
Maximum flow rate	3600 m^3/h (950,000 USG/min)
Heat-transfer coefficient	3500–7500 $W/m^2 \cdot °C$
	(600–1300) BTU/ft^2 hr·°F)
Heat-transfer area	0.1–2200 m^2 (1–24,000 ft^2)
Maximum connection size	450 mm (18 in)
Thermohydraulic Data	
Temperature approach	as low as 1°C
Heat recovery	as high as 93%
Heat-transfer coefficient	3000–7000 $W/m^2 \cdot °C$
	(water–water duties with normal fouling resistance)
NTU	0.3–4.0
Pressure drop	30 kPa per NTU

2 BENEFITS OFFERED BY PLATE HEAT EXCHANGERS

High Turbulence and High Heat-Transfer Performance. The embossed plate patterns promotes high turbulence at low fluid velocities (Fig. 3). On plates with the washboard pattern, turbulence is promoted by the continuously changing flow direction and velocity [7]. Plates with the herringbone pattern are assembled with the corrugations pointing in alternate direc-

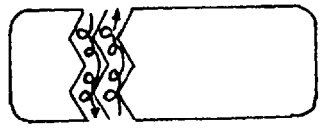


Figure 3 Turbulence promoted by embossed plate pattern. (From Ref. 7.)

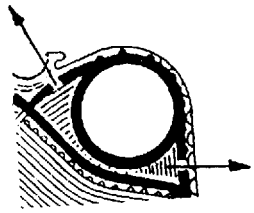


Figure 4 Elimination of cross contamination by venting of gasket space. (From Ref. 7.)

tions, which imparts a swirling motion to the fluids. This high turbulence results in very high heat-transfer coefficients.

Reduced Fouling. High turbulence, absence of stagnant areas, uniform fluid flow, and the smooth plate surface reduce fouling and the need for frequent cleaning.

Cross-Contamination Eliminated. In PHE, each medium is individually gasketed. The space between gasket is vented to atmosphere, eliminating the possibility of any cross-contamination of fluids (Fig. 4).

True Counterflow. In PHE, fluids can be made to flow in opposite directions, resulting in greater effective temperature difference.

Close Approach Temperature. In PHE, very close approach temperatures of 1–2°F are possible because of the true counterflow, advantageous flow rate characteristics, and high heat-transfer efficiency of the plates.

Multiple Duties With a Single Unit. It is possible to heat or cool two or more fluids within the same unit by simply installing intermediate divider sections between the heat transfer plates (Fig. 5).

Expandable. Due to modular construction, true flexibility is unique to the PHE both in initial design and after installation (Fig. 6).

Easy to Inspect and Clean, and Less Maintenance. A PHE can be easily opened for inspection, cleaning, and gasket replacement. By simply removing the compression bolts and sliding away the movable end frame, one can visually inspect the entire heat-transfer surface. Easy cleanability and thin layer of product to ensure a good bacteriological effect during pasteurization are advantages in the dairy industry, where PHE are cleaned once a day.

Lightweight. The PHE unit is lighter in total weight than other types of heat exchangers because of reduced liquid volume space and less surface area for a given application.

High-Viscosity Applications. Because the PHE induces turbulence at low fluid velocities, it has practical application for high-viscosity fluids. Note that a fluid sufficiently viscous to produce laminar flow in a shell and tube heat exchanger may well be in turbulent flow in PHE.

Saves Space and Servicing Time. The PHE fits into an area one-fifth to one-half that required for a comparable shell and tube heat exchanger. The plate heat exchanger can be opened for inspection, maintenance, or rebuilding all within the length of the frame, while the shell and



Figure 5 Handling of multiple duties. (From Ref. 7.)

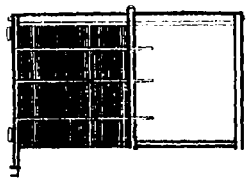


Figure 6 Flexibility to expand. (From Ref. 7.)

tube heat exchanger with removable tube bundle requires double its length to remove the tube bundle.

Less Operational Problems. In plate heat exchangers, flow-induced vibration, noise, and erosion–corrosion due to impingement attack are not present as in shell and tube heat exchangers.

Lower Cost. Plate heat exchangers are generally more economical than other types of equivalent duty heat exchangers, due to the higher thermal efficiency and lower manufacturing costs of plate heat exchangers.

Quick Process Control. Owing to the thin channels created between the two adjacent plates, the volume of fluid contained in PHE is small; it quickly reacts to the new process condition and is thereby easier to control.

3 COMPARISON BETWEEN A PLATE HEAT EXCHANGER AND A SHELL AND TUBE HEAT EXCHANGER

In many cases the plate heat exchanger has replaced the shell and tube exchanger (STHE) for services within the latter's operational limits. For identical duties (liquid–liquid service) and in those cases when the working limits of the gaskets are not exceeded, the merits of the PHE over the STHE are given in Table 3.

4 PLATE HEAT EXCHANGER—DETAILED CONSTRUCTION FEATURES

With a brief discussion of PHE construction, additional construction features and materials of construction for components such as plates, gaskets, frame, and connectors are discussed next.

4.1 Plate

Plate Pattern

Plates are available in a variety of corrugated or embossed patterns. The basic objective of providing corrugation to the plates is to impart high turbulence to the fluids, which results in a very high heat-transfer coefficient compared to those obtainable in a shell and tube heat exchanger for similar duties. These embossing patterns also result in increased effective surface areas and provide additional strength to the plates by means of many contact points over the plates to withstand differential pressure that exists between the adjacent plates. Plate thickness as low as 0.6 mm (0.024 in) can therefore be used for working pressures as high as 230 psig, particularly when using the cross-corrugated, herringbone pattern [8].

Types of Plate Corrugation

Over 60 different plate patterns have been developed worldwide. The pattern and geometry are proprietary. The most widely used corrugation types are the *intermating troughs* or *wash-*

Table 3 Comparison Between PHE and Shell and Tube Heat Exchanger [6]

Features	Traditional PHE	STHE
Multiple duty	Possible	Impossible
Piping connections	From one direction (on frame plate)	From several directions
Heat-transfer ratio	3–5	1
Operating weight ratio	1	3–10
Hold-up volume	Low	High
Space ratio	1	2–5
Welds	None	Welded
Sensitivity to vibrations	Not sensitive	Sensitive
Gaskets	On every plate	On each flanged joint
Detection of leakage	Easy to detect on exterior	Difficult to detect
Access for inspection	On each side of plate	Limited
Time required for opening	15 min with pneumatic tightener	60–90 min
Repair	Easy to replace plate and/or gasket	Requires tube plugging (decreased capacity)
Modification	Easy by adding or removing plates	Impossible
Fouling	10–25% that of STHE	—

board and the *chevron* or *herringbone* pattern. Figure 7 shows both types. The construction features of the these two patterns are discussed next.

Intermating Troughs Pattern

In the intermating troughs or washboard pattern, the corrugations are usually pressed deeper than the plate spacing. The plates nestle into one another when the plate pack is assembled

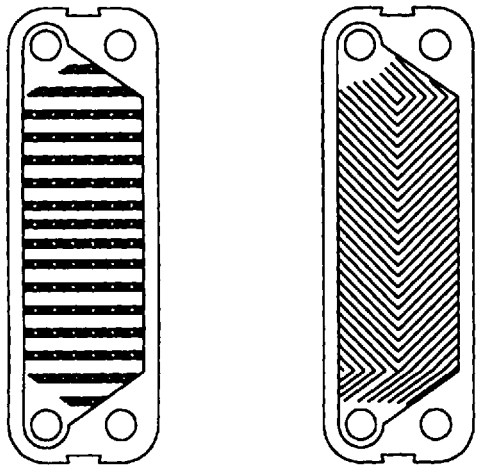


Figure 7 Two most widely used corrugation types. (a) Intermating troughs or washboard pattern; and (b) chevron or herringbone pattern.

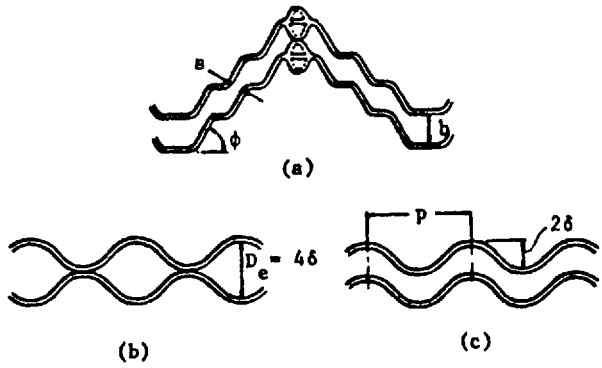


Figure 8 Cross-section of two neighboring plates (contact). (a) Intermating troughs; and (b) and (c) chevron troughs. (From Ref. 5.)

(Fig. 8a). The plate spacing is maintained by dimples, which are pressed into the crests and troughs and contact one another on adjacent plates. Since the washboard type has fewer contact points, and due to its greater corrugation depth than the herringbone type, it operates at lower pressures. The maximum channel gap, b (shown in Fig. 8a), varies from 3 to 5 mm and the minimum channel gap varies from 1.5 to 3 mm. Typical liquid velocity range in turbulent flow is from 0.2 to 3 m/s, depending upon the required pressure drop [5].

Chevron or Herringbone Trough Pattern

In the herringbone pattern, the corrugations are pressed to the same depth as the plate spacing. The chevron angle is reversed on adjacent plates so that when the plates are clamped together the corrugations cross one another to provide numerous contract points. The herringbone type therefore has greater strength than the washboard type, which enables it to withstand higher pressures with smaller plate thickness [9]. It is the most common type in use today. The contact arrangements of the plates are shown in Fig. 8b. The corrugation depth generally varies from 3 to 5 mm. Typical liquid velocities (in turbulent flow) range from 0.1 to 1 m/s [5].

Plate Materials

Materials that are suitable for cold pressing and corrosion resistant are the standard materials of construction. Table 4 gives a list of most common materials used for fabrication of plates. Carbon steel is rarely used due to its poor corrosion resistance.

Table 4 Common PHE Materials

Stainless steel AISI 304	Incoloy 825
Stainless steel AISI 316	Monel 400
Avesta SMO 254	Hastelloy B
Titanium, titanium–0.2% palladium stabilized	Hastelloy C-276
	Aluminum brass 76/22/2
Tantalum	Cupronickel (70/30)
Inconel 600	Cupronickel (90/10)
Inconel 625	Diabon F 100

4.2 Gasket Selection

When selecting the gasket material, the important requirements to be met are chemical and temperature resistance coupled with good sealing properties and shape over an acceptable period of life [3]. Much work has been done to develop elastomer formulations that increase the temperature range and chemical resistance of gaskets. Typical gasket materials and their maximum operating temperature are given in Table 5.

4.3 Frames

Frames are classified [7] as (1) B frame, suspension-type frame used with larger PHEs, (2) C frame, compact cantilever-type frame used with smaller PHEs, and (3) F frame, an intermediate size suspension-type frame. The frame is usually constructed in carbon steel and painted for corrosion resistance. Where stringent cleanliness requirements apply, such as in pharmaceuticals and in dairy, food, and soft drinks industries, the frame may be supplied in stainless steel. Stainless-steel-clad frames are available for highly corrosive environments. The units are normally floor mounted, but small units may be wall mounted.

4.4 Nozzles

Nozzles are located in one or both end plates. In single-pass arrangement, both the inlet and outlet ports for both fluids are located in the fixed head end, and hence, the unit may be opened up without disturbing the external piping. But with multipass arrangements the ports must always be located on both heads. This means that the unit cannot be opened up without disturbing the external piping at the movable head end. To be corrosion resistant, nozzles are usually same as plate material. Typical nozzle materials include stainless steel type 316, rubber clad, titanium, Incoloy 825, and Hastelloy C-276.

4.5 Tie Bolts

The tie bolts are usually made of 1% Cr–0.5% Mo low-alloy steel. The packing of large units may be compressed by hydraulic, pneumatic, or electric tightening devices.

4.6 Connector Plates

It is possible to process three or more fluids in a single gasketed PHE. This is being achieved by means of connector plates. This practice is widely used in food processing and permits heating, cooling, and heat recovery of the fluids in a single unit [9].

Table 5 Gasket Materials and Maximum Operating Temperature

Styrene butadiene rubber (80°C)
Nitrile rubber (140°C)
Ethylene propylene rubber, EPDM (150°C)
Resin-cured butyl rubber (140°C)
Fluorocarbon rubbers (180°C)
Fluoroelastomer (Viton) (100°C)
Compressed asbestos fiber (CAF) (260°C)
Silicon elastomers (low-temperature applications)

4.7 Connections

Connections are usually made of the same material as the plates to avoid the galvanic corrosion damage. Rubber-lined connections can be used for some duties.

5 OTHER FORMS OF PLATE HEAT EXCHANGERS

Continued developments and product innovations are taking place among various manufacturers to overcome limitations of pressure and temperatures, and to handle products of high viscosity, high fibrous contents, and high corrosivity. As a result, various forms of PHEs have come into the market. Some new forms of PHEs are discussed next. Text for items 5.1 to 5.7 has been taken from product literature of Alfa Laval, Pune, India [6].

5.1 Brazed Plate Heat Exchanger, Based on Reference 6

The brazed plate heat exchanger evolved from the conventional plate heat exchanger in answer to the need for a compact plate heat exchanger for high-pressure and high-temperature duties. Like the gasketed plate heat exchanger, the brazed plate heat exchanger is constructed of a series of corrugated metal plates but without the gaskets, tightening bolts, frame, or carrying and guide bars. It consists simply of stainless steel plates and two end plates. The plates are brazed together in a vacuum oven to form a complete pressure-resistant unit. The two fluids flow in separate channels. This compact design can easily be mounted directly on piping without brackets and foundations. Brazed plate heat exchangers accommodate a wide range of temperatures, from cryogenic to more than 200°C. Because of the brazed construction, the units are not expandable, but get their reputation from their relatively tiny size.

5.2 Wide-Gap Plate Heat Exchanger, Based on Reference 6

The wide-gap—about 16 mm (5/8 in)—plate heat exchanger provides a free-flow channel for liquids and products containing fibers or coarse particles or high-viscosity liquids that normally clog or cannot be satisfactorily treated in shell and tube heat exchangers.

5.3 Flow-Flex Tubular Plate Heat Exchanger, Based on Reference 6

In Flow-Flex, the tubular plate heat exchanger, the plate pattern builds the tube channels with a free cross section on one side and conventional plate channels on the other. This allows Flow-Flex to handle asymmetrical duties, that is, dissimilar flow rates at a ratio of at least two to one (for the same fluid properties and pressure drop). This vibration-free construction is also suitable for low-pressure condensing and vaporizing duties and for fibrous and particle-laden fluids.

5.4 Twin-Plate Heat Exchanger, Based on Reference 6

The twin-plate heat exchanger is a welded plate heat exchanger designed especially for handling aggressive media. The twin-plate pack consists of welded channels that alternate with traditional gasketed channels. The aggressive medium flows in the welded channels, and the only gaskets in contact with the aggressive medium are two circular porthole gaskets between the welded plate pair. The porthole gaskets are available in highly resistant elastomers and nonelastomer materials. The channels for the nonaggressive medium are sealed by traditional elastomer gaskets. Use of semiwelded units is increasing in the chemical, petroleum refining, and refrigeration industries [10].

5.5 Double-Wall Plate Heat Exchanger, Based on Reference 6

The double-wall plate heat exchanger is designed for use with media between which contamination or a hostile reaction can occur if the two media should mix. Double plates replace the single plates normally between the two media. The channels formed by assembling the double plates are sealed by conventional gaskets. In the unlikely event of leakage, the media will be easily visible on the outside of heat exchanger. A hole in one of the double plates results in leakage between them. A gasket defect causes an external leak, either directly from the peripheral gasket or from between the plates at the site of the failure.

5.6 Diabon F Graphite Plate Heat Exchanger, Based on Reference 6

The Diabon F graphite plate heat exchanger is a heat exchanger with graphite plates developed for use with media normally too corrosive for exotic metals and alloys. The Diabon F 100 graphite plates are made of a composite material composed of graphite and fluoroplastics. The material is compressed into corrugated plates fitted with thin, flat, corrosion-resistant gaskets. The graphite plates offer excellent corrosion resistance and good heat-transfer properties in combination with low thermal expansion and high pressure.

5.7 Glue-Free Gaskets (Clip-On Snap-On Gaskets), Based on Reference 6

The clip-on snap-on gaskets are glue-free gaskets designed to perform in heavy industrial applications in the same manner as traditional glued gaskets. The glue-free gaskets are attached to the plate by fasteners situated at regular intervals around the plate periphery. The gaskets simply slip into place during fitting and slip out for regasketing procedures, eliminating gluing procedures. Both operations can be performed on site without removing the plate from the frame. All these contribute to reduced service costs and downtime.

5.8 All Welded Plate Exchangers, After Larry Trom [10]

This design entirely eliminates the gaskets and by developing a fully welded plate exchanger further enhances the reliability as well as the temperature and pressure limits of the gasketed plate exchanger. Welded plate exchangers, unlike gasketed and semiwelded models, can neither be expanded in surface area nor be cleaned readily by mechanical methods. Only chemical cleaning is possible.

6 WHERE TO USE PLATE HEAT EXCHANGERS

The characteristics of plate heat exchangers are such that they are particularly well suited to liquid–liquid duties in turbulent flow [8]. Incidentally, a fluid sufficiently viscous to produce laminar flow in a shell and tube heat exchanger may be in turbulent flow in a PHE. In the 1930s, PHEs were introduced to meet the hygienic demands of the dairy industry. Today the plate heat exchanger is universally used in many fields: heating and ventilating, breweries, dairy, food processing, pharmaceuticals and fine chemicals, petroleum and chemical industries, power generation, offshore oil and gas production, onboard ships, pulp and paper production, etc. Plate heat exchangers also find applications in water-to-water closed-circuit cooling-water systems using a potentially corrosive primary cooling water drawn from sea, river, lake, or

cooling tower, to cool a clean, noncorrosive secondary liquid flowing in a closed circuit [8]. In this application, titanium (99.8%)–palladium (0.2%) stabilized titanium is used because of its outstanding corrosion resistance.

6.1 Applications for Which Plate Heat Exchangers Are Not Recommended

PHEs are not recommended for the following services [3]:

1. Gas-to-gas applications.
2. Fluids with very high viscosity may pose flow distribution problems, particularly when cooling is taking place; flow velocities less than 0.1 m/s are not used because they give low heat-transfer coefficients and low heat exchanger efficiency.
3. Less suitable for vapors condensing under vacuum.

7 THERMOHYDRAULIC FUNDAMENTALS OF PLATE HEAT EXCHANGERS

The design of plate heat exchangers is highly specialized in nature, considering the variety of plate corrugations (there are more than 60 different plate) available to suit varied duties. The plate design varies from manufacturer to manufacturer, and hence the thermohydraulic performance. Unlike tubular heat exchangers, for which design data and methods are easily available, plate heat exchanger design continues to be proprietary in nature. Manufacturers have developed their own empirical correlations for the prediction of thermal performance applicable to the exchangers marketed by them. Therefore, specific and accurate characteristics of specific plate patterns are not available in the open literature. In recent years, some correlations have been reported in many references. These correlations are mostly approximate in nature, to suit preliminary sizing of the units for a given duty. No published information is available on accurate heat-transfer correlations. Hence, it is better to leave the thermal and also mechanical design aspects to a plate manufacturer who offers an optimum design for the process parameters submitted by the consignee. In the following paragraphs, the salient features of the thermal design methods for approximate sizing are presented.

7.1 High- and Low-Theta Plates

A plate having a low chevron angle, β (Fig. 9) (about 25–30°), provides high heat transfer combined with high pressure drop, whereas a plate having a high chevron angle (about 60°–65°) provides a low heat transfer combined with low pressure drop, [8]. Manufacturers specify the plates having low values of chevron angle as *high-theta plates* and plates having high values of chevron angle as *low-theta plates*. Theta is used by manufacturers to denote the number of heat transfer units (NTU). The expression for theta is given by

$$\theta_c = \mathrm{NTU}_c = \frac{(UA)_c}{(mc_p)_c} \tag{1a}$$

$$\theta_h = \mathrm{NTU}_h = \frac{(UA)_h}{(mc_p)_h} \tag{1b}$$

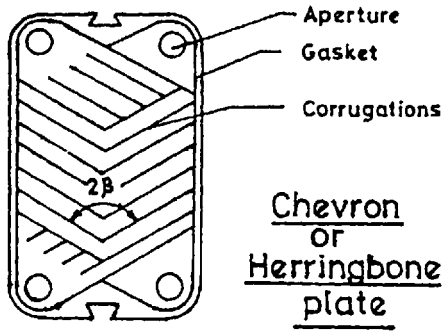


Figure 9 Chevron angle.

The values of θ achieved per pass for various plate types vary enormously (1.15 to about 4), and NTU for high-theta plates is of the order of 3.0 and for low-theta plates 0.50.

7.2 Thermal Mixing

One of the thermal design problems associated with PHE is the exact matching of the thermal duties; it is very difficult to achieve the required thermal duty and at the same time utilize the available pressure drop fully [3]. This problem is overcome through a procedure known as thermal mixing. Thermal mixing provides the designers with a better opportunity to utilize the available pressure drop without excessive surface, and with fewer standard plate patterns [9]. Thermal mixing is achieved by two methods:

1. Using high- and low-theta plates.
2. Using horizontal and vertical plates.

Thermal Mixing Using High- and Low-Theta Plates

In this method, the pack of plates may be composed of all high-theta plates (say, $\beta = 30°$), or all low-theta plates (say, $\beta = 60°$), or a combination of high- and low-theta plates arranged alternatively in the pack to provide an intermediate level of performance. Thus two plate configurations provide three levels of performance plates, as shown in Fig. 10.

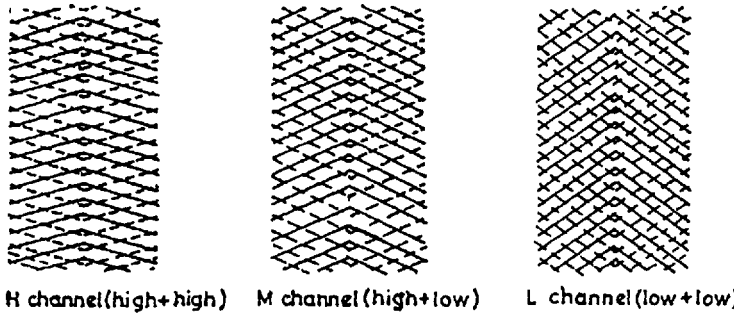


Figure 10 Thermal mixing using a combination of high theta and low theta plates.

Thermal Mixing Using Horizontal and Vertical Plates

In this method, two combinations of geometric patterns are selected to provide three levels of performance plates (Fig. 11) [7]:

1. Horizontal-style plates: Accu-Therm™ "H" style plates have a horizontal herringbone embossing. These plates have higher heat-transfer coefficients and slightly larger pressure drop.
2. Vertical-style plates: Accu-Therm™ "V" style plates have a vertical herringbone embossing. These plates have lower pressure drop and slightly lower heat transfer coefficients.
3. Combination-style plates: Accu-Therm™ "H" and "V" style plates have been combined to obtain an intermediate thermal and pressure drop performance.

7.3 Flow Area

Close spacing of the plates with nominal gaps ranging from 2 to 5 mm (0.08–0.02 in), gives hydraulic mean diameters in the range of 4–10 mm (0.15–0.4 in) [9]. The plates are embossed so that very high degrees of turbulence are achieved. Critical Reynolds numbers are in the range of 10–400, depending on the geometry. These factors contribute to produce very high

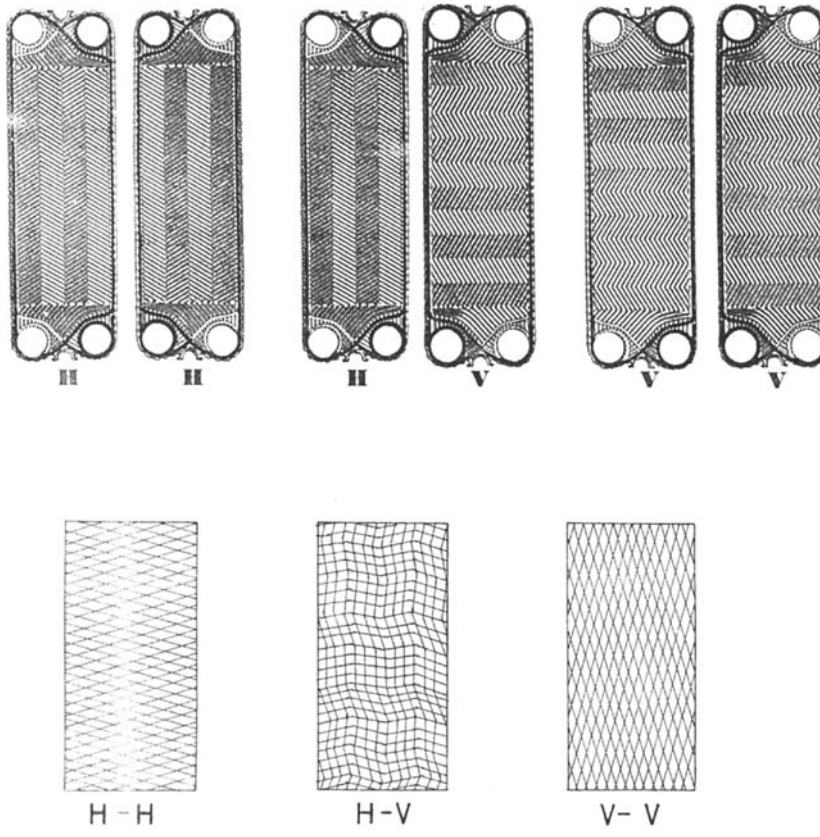


Figure 11 Thermal mixing using combination of plate geometries. (a) Horizontal-horizontal; (b) horizontal-vertical; and (c) vertical-vertical. (Courtesy of M/S Paul Muller Company, Springfield, Missouri.)

heat-transfer coefficients. Nominal velocities for "waterlike" liquids in turbulent flow are usually in the range 0.3–1.0 m/s (1–3.1 ft/s), but true velocities may be higher by a factor three or four due to the effect of the corrugations [8]. All heat-transfer and pressure drop relationships are, normally, based on channel velocity. The channel velocity is calculated by dividing the flow per channel by the channel cross sectional area [11]. The channel cross-sectional area, A_c is given by

$$A_c = Wb \tag{2}$$

where b is the mean plate gap and W is the effective plate width (gasket to gasket). Dimension W is shown schematically in Fig. 12.

7.4 Heat-Transfer and Pressure-Drop Correlations

Heat-Transfer Correlations

A general correlation for turbulent flow is given by [8]:

$$\mathrm{Nu} = C\,\mathrm{Re}^{n}\mathrm{Pr}^{m}(\mu_b/\mu_w)^{x} \tag{3}$$

Typical reported values are

$C = 0.15$–0.40

$n = 0.65$–0.85

$m = 0.30$–0.45 (usually 0.333)

$x = 0.05$–0.20

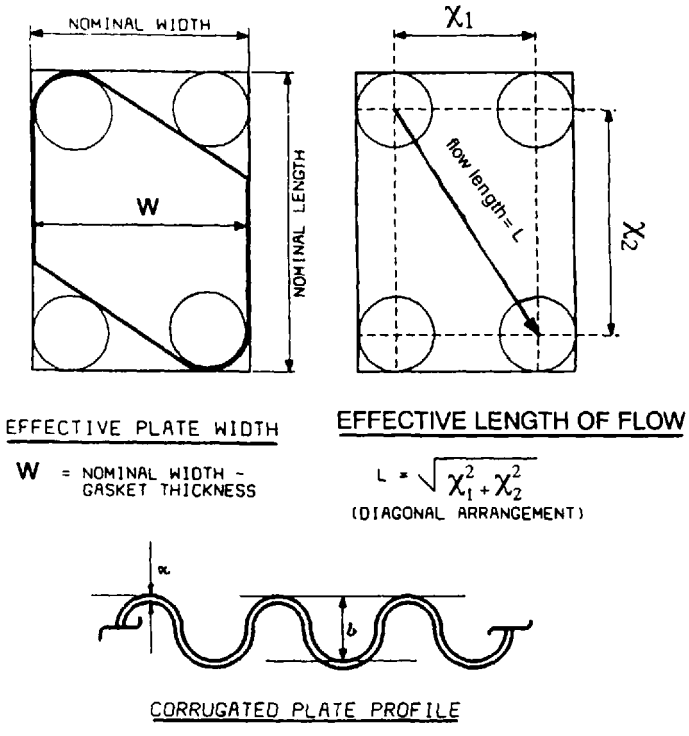


Figure 12 Major plate dimensions, W-Plate width and L-Effective flow length. (From Ref. 11.)

One of the most widely used plates has the following relationship [8]:

$$\mathrm{Nu} = 0.374\mathrm{Re}^{0.668}\mathrm{Pr}^{0.33}(\mu_b/\mu_w)^{0.15} \tag{4}$$

where the Reynolds number is based on equivalent diameter, D_e, defined by

$$D_e = \frac{4Wb}{2(W+b)} \tag{5a}$$

$$= 2b \qquad \text{since } b \text{ is very small compared to } W \tag{5b}$$

The expression for hydraulic diameter D_h for PHE is given by:

$$D_h = \frac{4 \times \text{minimum free flow area}}{\text{wetted perimeter}} \tag{6a}$$

$$\approx \frac{2b}{\phi^*} \tag{6b}$$

where ϕ^* is the ratio of actual (developed) surface area to projected surface area.

But to calculate Reynolds number, the hydraulic diameter expressed by Eq. 6 is not used because it is difficult to measure the parameter ϕ^* [5].

Buonopane and Troupe [12] present generalized relationships for a number of geometries for laminar flow. It seems that the following Sieder-Tate type relationship applies [8]:

$$\mathrm{Nu} = C_1(\mathrm{RePr}D_h/L)^{0.333}(\mu_b/\mu_w)^{0.14} \tag{7}$$

where $C_1 = 1.86$–4.50 depending on geometry, replace D_h by D_e, and L is the effective plate length (as shown in Fig. 12). More correlations are summarised in references 4, 5, 7, and 11.

Pressure Drop

Friction Factor, f. The fanning friction factor, f, is of the form [13]:

$$f = \frac{C_2}{\mathrm{Re}^y} \tag{8}$$

where C_2 is a constant characterizing each type of plate, and y covers different ranges. For a typical plate, the f factor is given by [13]:

$$f = \frac{2.5}{\mathrm{Re}^{0.3}} \tag{9}$$

Usher [14] reported that the friction factor for plate exchangers is 10–60 times that developed inside tubular exchangers at similar Reynolds numbers for turbulent flow. Marriott [8] observed that this value can be up to 400 times. Though the friction factors are high compared to that of the tubular units, the pressure drop will be less due to the following reasons [8]:

1. The nominal velocities are low, and nominal plate lengths do not exceed about 6 ft (1829 mm), so that the term $(G^2/2g_c)L$ in the pressure-drop equation is very much smaller than would be the case in a tubular unit,
2. Only a few passes will achieve the required NTU value, so that the pressure drop is effectively utilized for heat transfer and losses due to unfruitful flow reversals are minimized.

Expression for Pressure Drop.

Generalized Equation for Pressure Drop. The pressure drop in a plate heat exchanger consists of the following components [5]:

1. Empirically, pressure drop associated with the inlet and outlet manifolds and ports, Δp_m is approximately 1.5 times the inlet velocity head per pass,

$$\Delta p_m = 1.5\left(\frac{\rho U_m^2}{2g_c}\right)N_p \tag{10}$$

where N_p is the number of fluid ports and U_m the velocity through the ports.

2. Pressure drop associated within the plate passages is given by

$$\Delta p_c = \underbrace{\frac{4fLG^2}{2g_cD_e}\left(\frac{1}{\rho}\right)_m}_{\text{friction effect}} + \underbrace{\left(\frac{1}{\rho_o}-\frac{1}{\rho_i}\right)\frac{G^2}{g_c}}_{\text{momentum effect}} \tag{11}$$

where

$$\left(\frac{1}{\rho}\right)_m = \frac{1}{2}\left(\frac{1}{\rho_o}+\frac{1}{\rho_i}\right) \tag{12}$$

and where G is the mass velocity and L is the flow passage length. The flow passage length is equal to the distance (diagonal) between the centers of inlet and outlet ports [11]. For liquids, the momentum effect is negligible, and $(1/\rho)_m \approx 1/\rho_m$.

3. Pressure drop due to an elevation change is given by

$$\Delta p_n = \pm\frac{\rho_m g L}{g_c} \tag{13}$$

where the + stands for vertical upward flow, the − stands for vertical downward flow, g is the gravitational acceleration, g_c the proportionality constant in Newton's second law of motion, $g_c = 1$ and dimensionless in SI units, or $g_c = 32.174$ lbm ft/lbf s^2.

The total pressure drop on one side of the plate exchanger is the sum of Δp's of Eqs. 10, 11 and 13.

Approximate Equation for Pressure Drop. The general correlation for calculating pressure drop in a plate exchanger after accounting for Sieder–Tate viscosity correction factor has the general form

$$\Delta p = \frac{4fLG^2}{2g_c\rho D_e}\left(\frac{\mu_w}{\mu_b}\right)^{0.14} \tag{14}$$

7.5 Specific Pressure Drop or Jensen Number

In assessing the performance of any heat exchanger, the *specific pressure drop* (J) can be used [15]. This is defined as the pressure drop per NTU, that is,

$$J = \Delta p/\text{NTU} = \Delta p/\theta \tag{15}$$

Jensen [15] reports that optimum values for J for water–water duties of commercially available plates are close to 4.5 psi/NTU.

8 PHE THERMAL DESIGN METHODS

There are two different aspects of PHE design [2]:

1. The design of individual plate types so that they conform to specific performance and operational characteristics.
2. The calculation of the number and arrangement of such plates in order to satisfy the thermal and pressure drop requirements.

The thermal design method can be based on either the LMTD or ε-NTU method. Buonopane et al. [16] described the LMTD design method, and Jackson and Troupe [17] described the ε-NTU method, and both the methods are described in reference 4 and the ε-NTU method in reference 5.

8.1 LMTD Method, Due to Buonopane et al. [16]

This method gives the heat-transfer area needed in a PHE for both looped and series flow arrangements, given the temperature program, flow rates, and physical characteristics of the plates. The steps involved in the method are given next.

For series flow (Fig. 2a):

1. Determine the inlet and outlet temperatures for both the fluids.
2. Estimate LMTD for counterflow arrangement.
3. Estimate Reynolds number for the each stream, assuming an exchanger containing one thermal plate, one pass for each stream, as given:

$$\mathrm{Re} = \frac{(G/n_s)D_e}{\mu} \tag{16}$$

   where n_s is the number of substreams. For series flow, $n_s = 1$.
4. Estimate heat-transfer coefficient on both sides
5. Estimate overall heat-transfer coefficient taking into account the wall thermal resistance.
6. Estimate the total heat-transfer area from $A = q/U$ LMTDF.
7. Estimate the number of plates from, $N = A/A_p$, where A_p is the area of a plate and $2A_p$ is the area per channel.

For parallel flow or looped flow (Fig. 2b):

1–7. Repeat steps 1 to 7 already given.

8. From the number of thermal plates calculated in step 7, n_s is determined for both the fluids. For odd N, values of n_s will be equal for both fluids, whereas for even N, n_s will be different for both the fluids, and one fluid will have an additional substream compared to the other.
9. The values of n_s determined in step 8 are compared with the corresponding values assumed in step 3. If the calculated values do not agree with the assumed values, steps 3–9 are to be repeated, replacing the assumed values with the values calculated from step 8 until there is agreement between the two.

8.2 ε-NTU Approach

Jackson and Troupe [17] presented an ε-NTU method for the design of PHEs. The following steps illustrate the method:

1. Calculate the heat load, q, and from it determine the inlet and outlet temperatures for both the fluids.
2. Calculate the bulk mean temperature and determine the thermo physical fluid properties. Estimate the heat capacity rate ratio, C^*.
3. Estimate the heat-transfer effectiveness, ε, using the relation

$$\varepsilon = \frac{C_h(t_{h,i} - t_{h,o})}{C_{min}(t_{h,i} - t_{c,i})} = \frac{C_c(t_{c,o} - t_{c,i})}{C_{min}(t_{h,i} - t_{c,i})} \tag{17}$$

4. Assume an exchanger containing an infinite number of channels and find the required NTU using the appropriate ε-NTU relation.
5. Estimate Reynolds number for the each stream, assuming an exchanger containing one thermal plate, and one pass for each stream.
6. Calculate the heat-transfer coefficient on both sides. Estimate the overall heat-transfer coefficient, taking into account the wall thermal resistance.

For series flow (Fig. 2a):

7. Estimate the approximate number of thermal plates using the equation

$$N = \frac{\text{NTU}(mc_p)_{min}}{UA_p\Delta t_m} \tag{18}$$

where Δt_m is the mean temperature difference.

8. Assuming an exchanger of $N + 1$ channels, determine NTU from the appropriate ε-NTU relationship.
9. Recalculate N from Eq. 18.
10. Repeat calculations in steps 8 and 9 until the calculated value of N in step 9 matches the assumed value in step 8.

For parallel flow or looped flow (Fig. 2b): In a design involving looped flow patterns, the overall coefficient requires recalculation during each iteration because the channel flow rates become less with the addition of channels in parallel. The calculation procedure for looped flow is as follows:

7. Assuming an exchanger of N thermal plates, calculate the overall heat-transfer coefficient as in step 6.
8. Estimate the approximate number of thermal plates using Eq. 18.
9. Assuming an exchanger of $N + 1$ channels, determine NTU from the appropriate ε-NTU relationship for looped flow.
10. Recalculate the overall heat-transfer coefficient as per step 6 and recalculate N with Eq. 18.
11. Repeat calculations in steps 9 and 10 until the calculated value of N matches with the assumed value.

8.3 Specification Sheet for PHE

Table 6 is a specification sheet for PHE.

9 CORROSION OF PLATE HEAT EXCHANGERS

It is general practice for plate exchanger manufacturers to use only corrosion-resistant materials for a PHE, dictated by factors such as product purity and to minimize corrosion fouling. Ero-

Table 6 Specification Sheet for PHE

Description	Hot side	Cold side
Fluid circulated		
Flow rate		
Temperature in		
Temperature out		
Maximum pressure drop		
Operating pressure		
Specific heat		
Specific gravity or density		
Thermal conductivity		
Viscosity in		
Viscosity out		
Required gasket material		
Required plate material		
ASME code requirement		

sion is not a governing factor, since pressure drop limitations will generally determine the maximum permissible fluid velocities. As the plates are very thin (0.6–1.2 mm) compared to the tube thickness (maximum permitted up to 4.2 mm in the case of 19.5 mm diameter tube dimensions, conforming to TEMA Standards [18]), corrosion allowances normally recommended for tubular units are not relevant for plate units. In the design of a tubular unit, a corrosion allowance of 0.125 mm/year is used; for plate units the corrosion rate should not exceed 0.05 mm/year [3].

10 FOULING

High degrees of turbulence, uniform fluid flow and the smooth plate surface, and application of corrosion-resistant material for manufacture of plates reduce fouling and the need for frequent cleaning. Hence, the fouling factors required in plate heat exchangers are small compared with those commonly used in shell and tube designs [8]. They should be normally 20–25% of those used in shell and tube exchangers. For design purposes, fouling values not greater than one-fifth of the published tubular figures are recommended by Cooper et al. [2]. Fouling factors for plate heat exchangers are tabulated by Marriott [8]. Marriott states that in no circumstances, even under low pressure-drop conditions, is a total fouling resistance exceeding 0.00012 $m^2 \cdot °C/W$ or 0.0006 $ft^2/°f \cdot hr/Btu$ recommended.

11 LIMITATIONS OF PLATE HEAT EXCHANGERS

While plate exchangers have pressure drops comparable to those found in shell and tube units, they are generally confined to operation at lower pressures and temperatures due to the use of elastomer gaskets for sealing. Commonly stated limits have been 300°F (149°C) and 300 psi [14]. Maximum allowable working pressure is also limited by the frame strength and plate deformation resistance. Manufacturers produce a low-cost frame for low-pressure duties, say up to 85 psig (6 atmg) and a more substantial frame for higher pressures, for a given plate size. All PHEs used in the chemical and allied industries are capable of operating at 85 psig, most at 142 psig, many at 230 spig, and some at pressures as high as 300 psig [8]. The

limitations of temperature and pressure are overcome in heat exchangers with the lamella heat exchanger or by brazed plate exchanger. Other limitations of plate heat exchangers include:

1. Upper plate size is limited by the available press capacity to stamp out the plates from the sheet metal [3].
2. Because of the narrow gap (or the flow passages) between the plates, high liquid rates will involve excessive pressure drops, thus limiting the capacity.
3. Frequent gasket removal (gaskets are numerous) during cleaning of plates can lower the gasket life.
4. Large differences in fluid flow rates of two streams cannot be handled.

Acknowledgments

The author acknowledge the assistance received from Alpha Laval, Pune, India and Paul Muller Company, Springfield, MO, USA, which provided literature.

12 SPIRAL PLATE HEAT EXCHANGERS

A spiral plate heat exchanger (SPHE) is fabricated by rolling a pair of relatively long strips of plate around a split mandrel to form a pair of spiral passages (Fig. 13). Channel spacing is maintained uniformly along the length of the spiral passages by means of spacer studs welded to the plate strips prior to rolling. It can be made with channels 5–25 mm wide, with or without studs. The spiral channels are welded shut on their ends in order to contain respective fluids. An overall gasket is applied to the cover. The covers are attached to the spiral element by means of forged hook bolts and adapters. The hook bolt engages the bevel at the back of the flange ring and the adapter engages the rim at the edge of the cover. A header is welded on the outer end of each passage to accommodate the respective peripheral nozzle. For most services, both fluid flow channels are closed by alternate channels welded at both sides of the spiral plate. In some applications, one of the channels is left completely open, and the other closed at both sides of the plate. These two types of construction prevent the fluids from mixing.

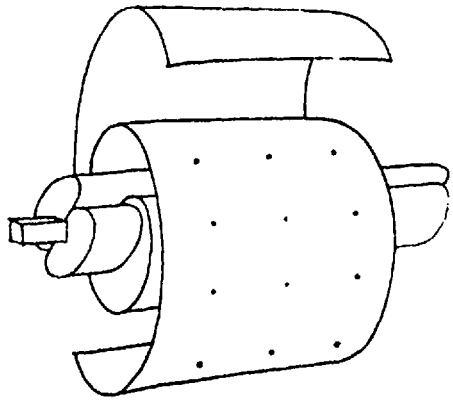


Figure 13 SPHE fabricated from long strips.

12.1 Flow Arrangements and Applications

The spiral assembly can be fitted with covers to provide three flow pattern types:

1. Both fluids in spiral flows; this arrangement can accommodate the media in full counterflow. General uses are for liquid to liquid, condensers, and gas coolers.
2. One fluid in spiral flow and the other in axial flow across the spiral; general uses are as condensers, reboilers, and gas coolers and heaters.
3. One fluid in spiral flow and the other in a combination of axial and spiral flow; general uses are as condensers (with built-in aftercoolers) and vaporizers.

These flow arrangements are shown schematically in Fig. 14.

12.2 Construction Material

Spiral plate exchangers are fabricated from any material that can be cold worked and welded. Typical construction materials include carbon steel, stainless steels, Hastelloy B and C, nickel and nickel alloys, aluminum alloys, titanium, and copper alloys. To protect against corrosion from cooling water, the surface is given baked phenolic resin coatings, among others. Anodic elements may also be wound into the assembly to anodically protect surfaces against corrosion [19].

12.3 Thermal Design of Spiral Plate Heat Exchangers

Thermal design procedures of spiral plate heat exchangers are covered by Minton [19]. The system of ordinary differential equations for the temperature distribution in spiral plate heat exchangers has been solved numerically by Chaudhury et al. [20] to obtain the efficiency, LMTD correction factor F as a function of number of transfer units, number of turns n, and the heat capacity rate ratio. They found that the LMTD correction factors, when plotted versus NTU per turn, fall approximately on a single curve and that curve can be represented by the simple formula [20]:

$$F = \frac{n}{\text{NTU}} \tanh(\text{NTU}/n) \tag{19}$$

12.4 Mechanical Design of Spiral Plate Heat Exchangers

Spiral exchangers can be furnished in accordance with most pressure vessel codes. Sizes range from 0.5 to 350 m^2 of heat-transfer surface in one single spiral body. The maximum design

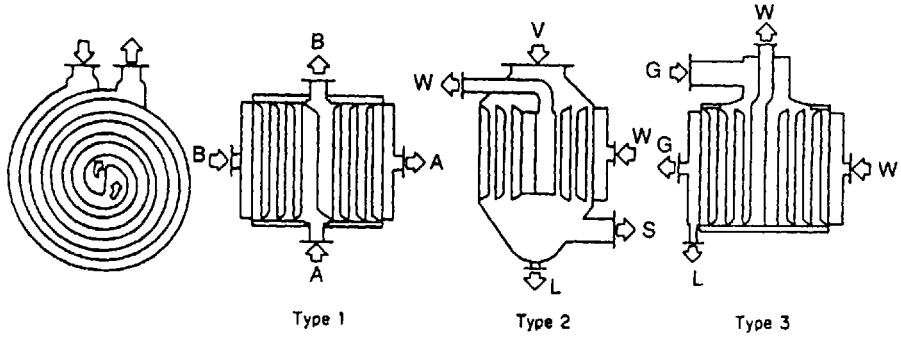


Figure 14 Alfa-Laval SPHE flow arrangements. (A, fluid 1; B, fluid 2; L, condensate; G, gas; W, liquid; V, vapor; and S, noncondensables.)

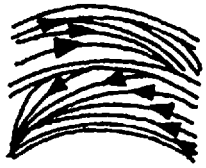


Figure 16 Turbulence induced in SPHE.

pressure is normally limited to 150 psi due to the following reasons, although for smaller diameters the pressure may sometimes be higher [19]:

1. They are normally designed for the full pressure of each passage.
2. Because the turns of the spiral are of relatively large diameter, each turn must contain its design pressure,
3. The plate thickness is somewhat restricted.

Limitations of materials of constructions govern design temperature.

12.5 Advantages of the Spiral Plate Exchangers

Spiral plate heat exchangers have a number of advantages over conventional shell and tube exchangers.

1. The spiral heat exchanger approaches the ideal in heat exchanger design. Media can be arranged in full counterflow (Fig. 15). Flow characteristics are the same for each medium. The long passages on each side permit close temperature approaches. Radiation losses are negligible.
2. The exchanger is well suited for heating or cooling viscous fluids because its *L/D* ratio is lower than that of tubular exchangers [19].
3. At a velocity that would be marginal and approaching streamline flow in straight tubes, good turbulence (Fig. 16) is realized because of the continuously curving passages.
4. The scrubbing action of the fluids in each side of the passage tends to flush away deposits as they form and hence permits the use of low fouling resistance values.
5. Media cannot intermix; they are isolated by the welded closing on one side of each passage.
6. The spiral exchanger is compact and requires less installation and servicing space than conventional exchangers of equivalent surface.
7. They are easily maintainable. By removing the covers of the spiral exchanger, the entire lengths of the passages are easily accessible for inspection or mechanical cleaning, if necessary. Similarly, because of the single passage on each side, the spiral heat exchanger is readily cleaned with cleaning solutions without opening the unit.

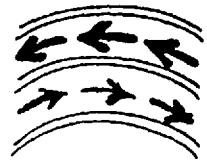


Figure 15 Counterflow arrangements in SPHE.

8. Spiral plate exchangers avoid problems associated with differential thermal expansion in non cyclic service [19].
9. In axial flow, a large flow area affords a low pressure drop, which becomes especially important when condensing under vacuum [19].

12.6 Limitations

Besides the pressure limitation noted earlier, the spiral plate exchanger also has the following disadvantages [19]:

1. Repairing an SPHE in the field is difficult; however, the possibility of leakage in a spiral is less because it is generally fabricated from much thicker plate than tube walls.
2. Spiral plate exchangers are not recommended for service in which thermal cycling is frequent. When used for such services, the unit sometimes must be designed for higher stresses.
3. The SPHE usually should not be used when a hard deposit forms during operation, because the spacer studs prevent such deposits from being easily removed by drilling.

Acknowledgments

The author acknowledges the assistance received from Alpha Laval, Pune, India, which provided literature.

NOMENCLATURE

A = total heat transfer area, m^2 (ft^2)
A_p = heat transfer area of a plate, m^2 (ft^2)
b = mean plate gap, m (ft)
C = constant in Eq. 3
C_1 = constant in Eq. 7
C_2 = constant in Eq. 8
C_{min} = minimum of $(mc_p)_h$, and $(mc_p)c$, W/°C (Btu/hr·°F)
c_p = specific heat, J/kg·°C (Btu/lbm.°F)
C^* = heat capacity rate ratio = $(mc_p)_{min}/(mc_p)_{max}$
D_e = equivalent diameter of flow passages, m (ft)
D_h = hydraulic diameter, m (ft)
F = LMTD correction factor
f = Fanning friction factor
G = mass velocity based on minimum flow area, $kg/m^2 \cdot s$ ($lbm/hr \cdot ft^2$)
g_c = acceleration due to gravity or proportionality constant 9.81 m/s^2 (32.17 ft/s^2)
= 1 and dimensionless in SI units
h = convective heat transfer coefficient, $W/m^2 \cdot °C$ ($Btu/ft^2 \cdot hr \cdot °F$)
J = Jenson number (of specific pressure drop), Pa/NTU (lbf/ft^2/NTU)
j = Colburn heat transfer factor
k = thermal conductivity, W/m·°C (Btu/hr·ft·°F)
L = effective flow passage length, m (ft)
LMTD = log mean temperature difference, °C (°F)
m, n = exponents in Eq. 3
N = number of plates
n = number of turns of spiral plate heat exchanger, Eq. 19

Nu = Nusselt number
N_p = number of fluid ports, Eq. 10
n_s = number of substreams
Pr = Prandtl number
p = pressure, Pa (lbf/ft^2)
Q = total heat duty of the exchanger, W·s (Btu)
q = heat transfer rate, W (Btu/hr)
Re = Reynolds number
R_f = Fouling resistance, m^2·°C/W (ft^2·°F·hr/Btu)
t = fluid static temperature, °C (°F)
U = overall heat transfer coefficient, W/m^2·°C (Btu/hr·ft^2·°F)
U_m = fluid velocity through port or manifold, m/s (ft/hr)
W = width of the plate (gasket to gasket), m (ft)
x = exponent in Eq. 3
y = exponent in Eq. 8

β = chevron angle
Δ_p = pressure drop, Pa (lbf/ft^2)
Δp_c = pressure drop within the plate passages, Pa (lbf/ft^2)
Δp_h = pressure drop due to elevation, Pa (lbf/ft^2)
Δp_m = pressure drop associated with the inlet and outlet manifolds and ports, Pa (lbf/ft^2)
Δt_{lm} = log mean temperature difference, °C (°F)
Δt_m = mean temperature difference, °C (°F)
ε = thermal effectiveness
μ_b = viscosity at bulk mean temperature, Pa·s (lbm/hr·ft)
μ_w = viscosity at wall temperature, Pa·s (lbm/hr·ft)
ϕ^* = ratio of actual (developed) surface area to projected surface area.
ρ = fluid density, kg/m^3 (lbm/ft^3)
θ = number of transfer units (NTU)

Subscripts

c cold
h hot
i inlet
m mean
o outlet
1 inlet or outlet of the exchanger
2 outlet or inlet of the exchanger
min minimum
max maximum

8
Heat-Transfer Augmentation

1 INTRODUCTION

The study of improved heat-transfer performance is referred to as heat-transfer enhancement or augmentation. The enhancement of heat transfer has concerned researchers and practitioners since the earliest documented studies of heat transfer [1]. In recent years increasing energy and material costs have provided significant incentives for development of energy efficient heat exchangers. As a result, considerable emphasis has been placed on the development of various augmented heat-transfer surfaces and devices [2,3]. Heat-transfer enhancement today is characterized by vigorous activity in both research and industrial practice. This can be seen from the exponential increase in world technical literature published in heat-transfer augmentation devices, growing patents, and hundreds of manufacturers offering products ranging from enhanced tubes to entire thermal systems incorporating enhancement technology [1]. In this chapter, single-phase heat-transfer augmentation devices are discussed in detail without specific correlations for j and f factors and two-phase heat-transfer augmentation devices are briefly dealt. An important reference source on heat-transfer augmentation devices is Bergles [4].

1.1 Benefits of Heat-Transfer Augmentation Devices

An enhanced surface is more efficient in transferring heat than what might be called the standard surface. The application of enhancement device can result in benefits such as:

1. A decrease in heat-transfer surface area, size, and hence weight of a heat exchanger for a given heat duty and pressure drop.
2. An increase in heat transfer for a given size, flow rate, and pressure drop.
3. A reduction in pumping power for a given size and heat duty.
4. A reduction in the approach temperature difference.
5. An appropriate combination of the above.

While considering these benefits, the associated flow friction changes is also to be taken into account [2].

2 APPLICATION OF AUGMENTED SURFACES

For a two-fluid exchanger, augmentation should be considered for the fluid stream that has the controlling thermal resistance. If both resistances are approximately equal, augmentation may be considered for both sides of the exchanger. The majority of two-fluid exchanger applications are served by four basic exchanger types [5]: (1) shell and tube, (2) tube-fin, (3) brazed plate-fin, and (4) plate heat exchangers (PHE). If enhancement is employed, it must be applied to three basic flow geometries [5]:

1. Internal flow in circular tubes.
2. External flow normal to tubes and tube banks.
3. Channel flow in closely spaced parallel plate channels, e.g., brazed plate-fin heat exchangers and plate heat exchangers.

3 PRINCIPLE OF SINGLE-PHASE HEAT-TRANSFER ENHANCEMENT

Single-phase flow can be classified as internal flow or external flow. It can be further classified as turbulent or laminar flow. The principal mechanisms of enhancement in turbulent of laminar flow are the use of a secondary heat transfer surface and the disruption of the unenhanced fluid velocity and temperature profile [6]. The rate of heat transfer between a fluid and finned surface can be expressed in a general form as [7]:

$$q = h(\eta_o A)\,\Delta T \tag{1}$$

where h is the heat-transfer coefficient, η_o the overall surface efficiency, A the total heat transfer area, and ΔT the surface–fluid temperature difference.

In Eq. 1, $h\eta_o A$ represents the surface conductance. Obviously, high performance may be achieved by using a heat-transfer surface with high value of $\eta_o A$, h, or both. Special surface geometries provide enhancement by establishing a higher $h\eta_o A$ per unit surface area. Three basic principles are employed to increase $h\eta_o A$ or hA [5,7,8]:

1. Increase of A without appreciably changing h; e.g., finned tubes.
2. Increase in h without an appreciable area A increase; e.g., surface roughness or turbulence promoters. This principle is further explained in the next section.
3. Increase of both h and A; for example, extended surfaces in compact heat exchangers have increased heat transfer coefficient by means of surface promoters, such as perforations, louvres, and corrugations or displaced promoters such as canted tubes.

3.1 Increase in Convection Coefficient Without an Appreciable Area Increase

A surface that results in performance enhancement due to increase in the heat transfer coefficient h without an appreciable transfer area is known as an enhanced heat-transfer (EHT) surface. EHT surfaces are vital to the development of heat-transfer augmentation devices. The underlying principle of the enhanced heat-transfer surface is as follows. As a reasonable approximation, the heat-transfer coefficient is given by [7]:

$$h = k/\Delta \tag{2}$$

where k is the thermal conductivity of the fluid and Δ the thermal boundary layer thickness.

From Eq. 2, it can be seen that h can be increased by altering the flow pattern near the surface in order to reduce the thermal boundary layer thickness.

3.2 Enhancement in Turbulent Flow

Turbulent flow in a tube [after 6] exhibits a low-velocity flow region known as the laminar sublayer immediately adjacent to the wall, with velocity approaching zero at the wall. Most of the thermal resistance occurs in this low-velocity region. Any roughness or enhancement technique (e.g., swirl flow devices such as wire coil inserts, spiral inserts, and protrusions) that disturbs the laminar sublayer will enhance the heat transfer. For fully developed flow in a smooth tube, the dimensionless laminar sublayer thickness is given by:

$$y^* = \frac{y\sqrt{G_c \tau_0 / \rho}}{\nu} = 5 \tag{3}$$

Using the shear stress τ_0 for a smooth tube, the ratio of laminar sublayer thickness y to tube diameter d is given by:

$$\frac{y}{d} = 25\ \mathrm{Re}^{-0.875} \tag{4}$$

For example, if Re = 30,000 and d = 1.0 in (25.4 mm), the laminar sublayer thickness is 0.003 in (0.0762 mm). Any roughness or enhancement technique that disturbs the laminar sublayer will enhance the heat transfer.

3.3 Enhancement in Laminar Flow

Laminar flow generally results in low heat-transfer coefficients. The fluid velocity and temperature vary across the entire flow channel width so that the thermal resistance is not just in the region near the wall as in turbulent flow. Hence, small-scale surface roughness is not effective in enhancing heat transfer in laminar flow; the enhancement techniques employ some method of swirling the flow or creating turbulence [6].

4 ENHANCEMENT TECHNIQUES

Enhancement techniques may be (1) passive methods, which require no direct application of external power, and (2) active methods, which require external power. These methods are discussed in Ref. 1. Table 1 gives a list of passive and active methods. Two or more of the methods may be used to provide a "compound enhancement" greater than that of the individual method. Each method has its own merits and demerits. According to Bergles [4], the effectiveness of these methods depends strongly on the mode of heat transfer, which might range from single-phase free convection to dispersed-flow film boiling.

Although many enhancement techniques have been proposed and tested, only a small number are currently used in heat exchangers [1]. Of these, passively enhanced tubes are relatively easy to manufacture, cost-effective for many applications, and can be used for retrofitting existing units, whereas active methods, such as vibrating tubes, are costly and complex [9].

Table 1 Enhancement Techniques [4]

Passive techniques (No external power needed)	Active techniques (External power required)
Extended surfaces	Mechanical aids
Treated surfaces	Surface vibration
Rough surfaces	Fluid vibration
Displaced enhancement devices	Electric or magnetic fields
Swirl flow devices	Injection or suction
Surface tension devices	
Additives for fluids	
Additives for gases	

5 HEAT-TRANSFER MODE

The heat-transfer augmentation techniques can be applied for various heat transfer modes such as

1. Single-phase natural convection
2. Single-phase forced convection
3. Pool boiling
4. Forced convection boiling
5. Condensation

6 PASSIVE TECHNIQUES

6.1 Extended Surfaces

Extended surfaces are routinely employed in compact heat exchangers and shell and tube exchangers either for liquids or for gases. The application of extended surfaces for liquid and gas service are discussed next.

Extended Surfaces for Gases

In forced convection heat transfer between a gas and a liquid, the heat transfer coefficient of the gas may be of the order of 1/50 to 1/10 that of the liquid, Ref. (8). The use of extended surfaces will reduce the gas side thermal resistance. However, the resulting gas side resistance may still exceed that of the liquid.

Enhanced Surface Geometries on Tube-Fin Exchangers. Enhanced surface geometries that have been used on circular tube-fin heat exchangers include [8]: (1) plain circular fin, (2) slotted fin, (3) punched and bent triangular projections, (4) segmented fin, and (5) wire loop extended surface. Some of the enhanced fin geometries of individual fins are shown in Fig. 1.



Figure 1 Enhanced circular fin geometries. (a) Plain circular fin; (b) slotted fin; (c) punched and triangular projections; (d) segmented fin; and (e) wire-loop extended surface.

All of these geometries provide enhancement by the periodic development of thin boundary layers on small-diameter wires or flat strips, followed by their dissipation in the wake region between elements.

Enhanced Surface Geometries for Plate-Fin Exchangers. Many enhanced surface geometries are used on plate-fin exchangers. To be effective, the enhancement technique must be applicable to low Reynolds number flows. Two basic concepts have been extensively employed to provide enhancement [5,8]:

Special channel shapes, such as the wavy channel, which provide mixing due to secondary flows or boundary layer separation within the channel.

Repeated growth and wake destruction of boundary layers; e.g., offset strip fin, louvred fin, pin fin, and to some extent the perforated fin.

Extended Surfaces for Liquids

Extended surfaces used with liquids may be on the inner or outer surface of the tubes. Because liquids have higher heat-transfer coefficients than gases, fin efficiency considerations require shorter fins with liquids than with gases.

Internally Extended Surfaces. Widely varied integral internally finned tubes (Fig. 2) have been developed for tube-side heat-transfer augmentation, and they are commercially available in copper and aluminum. Most of them are for single-phase flows. In recent years, tubes with special internal geometries for augmentation of boiling in refrigeration systems have been developed. Typical, commercial names includes Thermofin tubes A, B, EX, and HEX. Other possible methods for tube-side augmentation include internal roughness geometries, inserts such as twisted tape inserts, and wire coil inserts.

The current trend for enhancement of intube evaporation of refrigerants is toward the use of *internal microfin tubes*. The reasons for their popularity are the fact that (1) they increase heat transfer significantly while only slightly increasing pressure drop and (2) the amount of extra material required for microfin tubing is much less than that required for other types of internally finned tubes [10]. Cross-sectional views of typical microfin tubes are shown in Fig. 3 [11]. These are made from copper tubes and the popular ones are 9.525 mm (3/8 in) outer diameter and have 60 to 70 spiral fins/inch, fin height from 0.10 to 0.19 mm, and spiral angles from 15 to 25° [1,11]. These dimensions are in contrast to other types of internal finning that seldom exceed 30 fins/inch and fin heights that range from several factors higher than the microfin tube height. The heat-transfer coefficients, based on area of an equivalent smooth

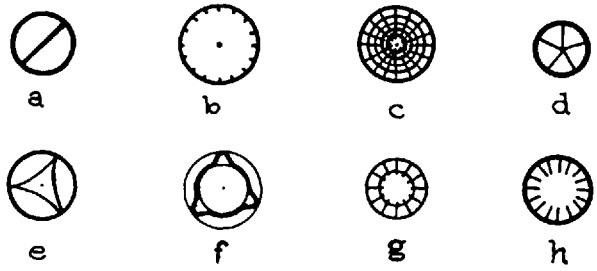


Figure 2 Representative commercially available tubes with internal enhancement. (a) Twisted tape insert in plain tube; (b) spiral internally finned tube; (c) quintuplex finned tube; (d) star shaped insert in plain tube; (e) amatron internally finned tube; (f) corrugated tube; (g) duplex internally finned tube; and (h) straight internally finned tube. (From Ref. 3.)

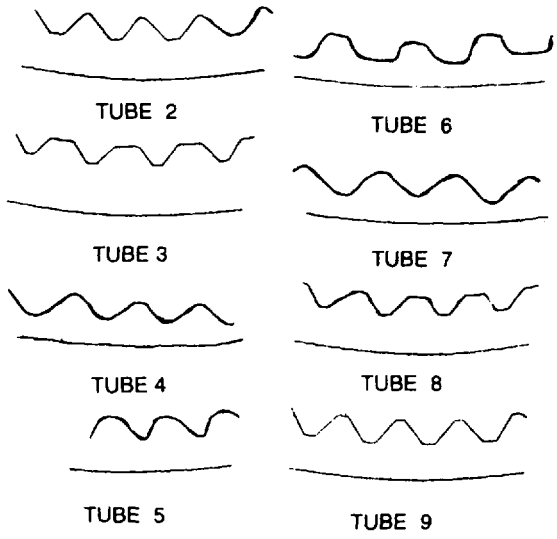


Figure 3 Fin profiles for micro-fin tubes used in refrigerant evaporators and condensers. (From Ref. 11.)

tube, are increased 30 to 80% above the smooth tube values, depending on the vapor quality and fin profile [1].

External Low-Fin Tubes. Low-fin tubes are generally 0.75–1 in (19.2–25.4 mm) OD with fins of 1/16 or 1/8 in (1.6 or 3.2 mm) height [12], and standard fin densities are 11, 19, 26, 30, and 40 fins/in (433–748 fins/m). A low-fin tube is ideally suited for a shell and tube exchanger. The outside surface of the low-fin tube is typically three times that of a plain tube. Tube diameters are the same as plain tubes; which permits low-fin and plain tubes to be interchangeable. External low-fin tube surfaces are generally economical if the outside heat-transfer coefficient is less than one-third of the inside heat-transfer coefficient [13]. The low-fin tube is also effective with compressed gases, namely, in intercoolers and aftercoolers and they are employed in condensing and evaporating duties, particularly with refrigerants and hydrocarbons [7]. Low-fin tubes are used for applications such as [13]:

1. Sensible heat applications like cooling of gases or viscous fluids.
2. Condensing fluids with relatively low surface tension; low-fin tubes can enhance condensing heat transfer typically by about 30%.
3. Boiling—Low-fin tubes permit nucleate boiling at lower temperature differences than can be achieved with plain tubes.
4. Fouling fluids—Fouling is not accelerated with low-fin tubes; it is often reduced. Low-fin tubes are more easily cleaned by chemical or mechanical means than are plain tubes.

6.2 Treated Surfaces

Treated surfaces involve fine-scale alternation of the surface finish or provision of either continuous or discontinuous coating. Treated surfaces such as hydrophobic coatings and porous coatings (Fig. 4) are most effective for phase changes but are not applicable to single-phase convection. The roughness height is below that which affects single-phase heat transfer [1].

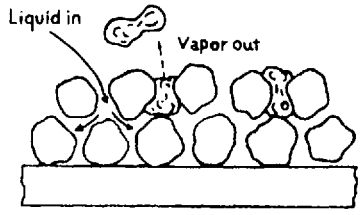


Figure 4 Treated surface.

6.3 Rough Surfaces

Rough surfaces refer to tubes and channels having roughness elements in the form of regularly repeated ridge-like protrusions perpendicular to the stream direction. The configuration is generally chosen to promote turbulence rather than to increase the heat-transfer surface area. The surface roughness may be applied to any of the usual prime or extended heat exchange surfaces [1,8]:

1. Flat plates
2. Circular tubes
3. Annuli having roughness on the outer surface of the inner tube
4. Fins

Rough surfaces are produced in many configurations, ranging from random sand-grain type roughness to discrete protuberances. Helical repeated-rib roughness is readily manufactured and results in good heat-transfer performance in single-phase turbulent flow without severe pressure drop. The main effect is that the ribs cause flow separation and reattachment [1]. The principal parameters are ridge height e and pitch p. Examples of repeated-rib roughness are shown in Fig. 5 [14]. Both two-and three-dimensional integral roughness elements are also possible. Within the category of surface roughness, a three-dimensional roughness of the sand-grain type appears to offer the highest performance [15]. Roughness elements have been produced by the traditional processes of machining, forming, casting, or welding [7]. Various inserts or wrap-around structures can also provide surface proturbances [1].

Applications. Surface roughness is attractive for turbulent-flow applications with high Prandtl number fluids for which the increase in heat-transfer coefficient is greater than the friction factor increase [15]. In laminar-flow applications, small-scale roughness is not effective, but twisted tape inserts and internally finned tubes appear to be the favored augmentation techniques [5].

6.4 Tube Inserts and Displaced Enhancement Devices

This class refers to devices that are inserted inside a smooth tube. The tube inserts are relatively low in cost, relatively easy to insert and to take out of the tubes for cleaning operations.

Enhancement Mechanism

Tube inserts can create one of or some combinations of the following conditions, which are favorable for enhancing the heat transfer with a consequent increase in the flow friction [16]:

1. Interrupting the development of boundary layer of the fluid flow and increasing the degree of flow turbulence.

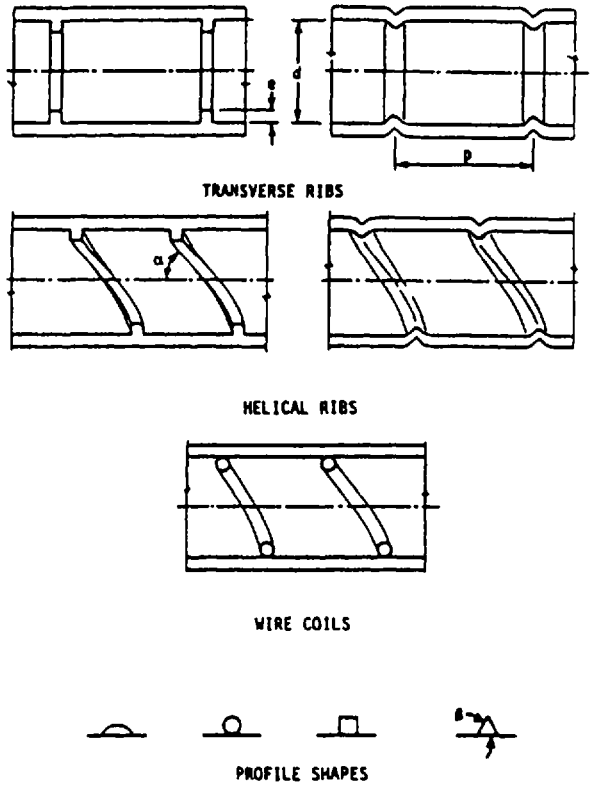


Figure 5 Examples of repeated rib roughness. (Ravigururajan and Bergles, 1985.)

2. Increasing the effective heat-transfer area if the contact between the tube inserts and the tube wall is excellent.
3. Generating rotating and/or secondary flow.

Forms of Insert Device

Various forms of insert devices are [8]:

1. Devices that cause the flow to swirl along the flow length, e.g., swirl strips and twisted tapes.
2. Extended surface insert devices that provide thermal contact with the tube wall (this may also swirl the flow), e.g., star inserts.
3. Wall-attached insert devices that mix the fluid at the tube wall.
4. Displaced insert devices that are displaced from the tube wall and cause periodic mixing of the gross flow.

Displaced Enhancement Devices

Displaced enhancement devices are inserted into the flow channel so as to improve the fluid flow near the heat-transfer surface [17]. These devices include [8] streamline shape, disks, static mixer, and meshes or brushes, and wire coil inserts.

Coil Inserts. Coil inserts provide an efficient and inexpensive way to enhance the heat transfer inside heat-exchanger tubes [18]. In applications that require frequent cleaning, their easy-

to-retrofit characteristic offers a significant advantage over integrally enhanced tube types; however, the coil inserts can have an inherent disadvantage if imperfect contact exists between the coil and the tube wall. For inserts, the parameters that affect the enhancement are the disruption height, the disruption spacing or pitch, the helix angle, and the disruption shape [9]. Spiral spring inserts are shown in Fig. 6.

Inserts for Heating/Cooling Mode Operation. In the heating mode operation, the rotating flow is noted to have favorable centrifugal convection effect, which can increase the heat-transfer coefficient, whereas in the cooling mode operation, the rotating flow may have an adverse centrifugal convection effect, which even may decrease the convection heat-transfer coefficient [16]. Thus tube inserts that can generate rotating flow, such as swirl strips or twisted tapes, are generally not used in oil coolers; instead, coil or spiral springs are used, since spiral springs usually do not generate rotating flow.

6.5 Swirl Flow Devices

Swirl flow devices include a number of geometric arrangements or tube inserts for forced flow that create rotating and/or secondary flow inside tube. Such devices include inlet vortex generators, twisted tape inserts, and axial core inserts with screw type windings [1,16]. The augmentation is attributable to several effects [1]: increased path length of flow, secondary flow effects, and, in the case of tapes, fin effects.

Twisted Tape Insert

The twisted tap insert shown in Fig. 7 has been extensively investigated. Variants of the twisted tape that have been evaluated include mechanically rotated twisted tapes, short sections of twisted tape at the tube inlet or periodically spaced along the tube length, and periodically spaced "propeller" inserts that are mechanically rotated by the flowing fluid [8].

Corrugated Surfaces

Corrugated tubes are associated with circumferential or spiral indentations (spirally fluted) as shown in Fig. 8. Flows in corrugated channels are associated with secondary flows, suppression of the secondary flow by counteracting centrifugal forces, and destruction of the secondary flow by the onset of turbulence [7]. In condensing services, corrugated tubes increase the heat-transfer coefficient because only a thin film of the liquid condensate is left on the crests, while most of it drains into the troughs due to the surface tension and gravity effects. The thin film offers very little resistance, and hence the condensing coefficient is very high.

Among the corrugated tubes, spirally corrugated tubes provide several advantages over other rough surfaces. They have easier fabrication, limited fouling, and higher enhancement in the heat-transfer rate compared to increase in the friction factor [19]. The tube parameters that affect enhancement of corrugated surfaces are the pitch, the depth and type of the grooves, and number of groove starts.

Doubly Enhanced Surfaces

If enhancement is applied to the inner and outer tube surfaces, a doubly enhanced tube results. Applications for such doubly enhanced tubes include condenser and evaporator tubes. Typical forms of doubly enhanced tubes include [8]: (1) helical rib roughness on inner surface and integral fins on outer surface, (2) internal fins on inner surface and porous boiling coating on outer surface, (3) twisted tape insert on inner surface and integral fins on outer surface, (4) corrugated roughness on inner and outer surfaces, and (5) corrugated tubes. The aluminum, spirally fluted tube of GA Technologies is an example. Figure 9 illustrates five basic approaches that may be employed to provide doubly enhanced tubes.

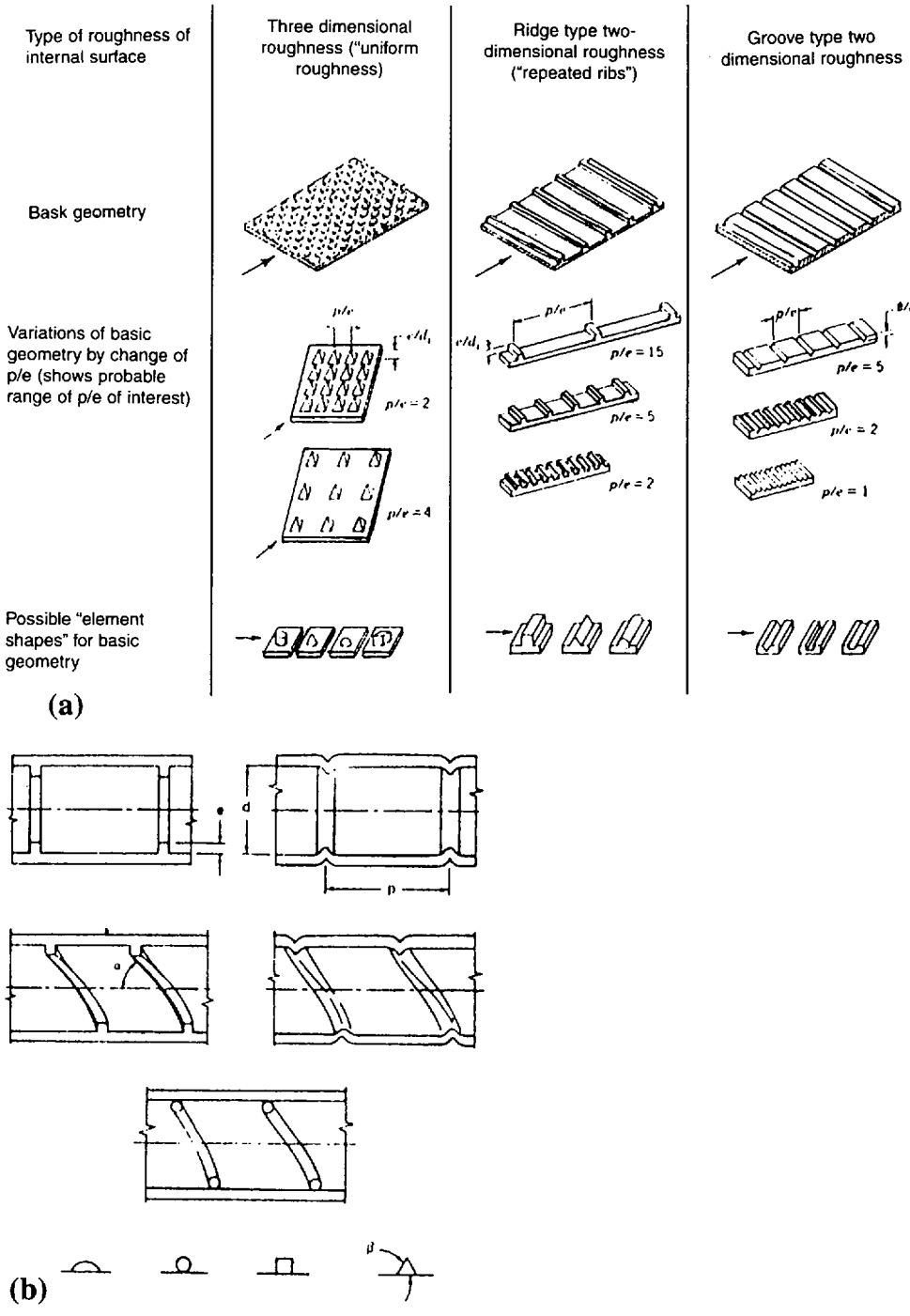


Figure 6 (a) Catalog of roughness geometries and (b) internal roughness.

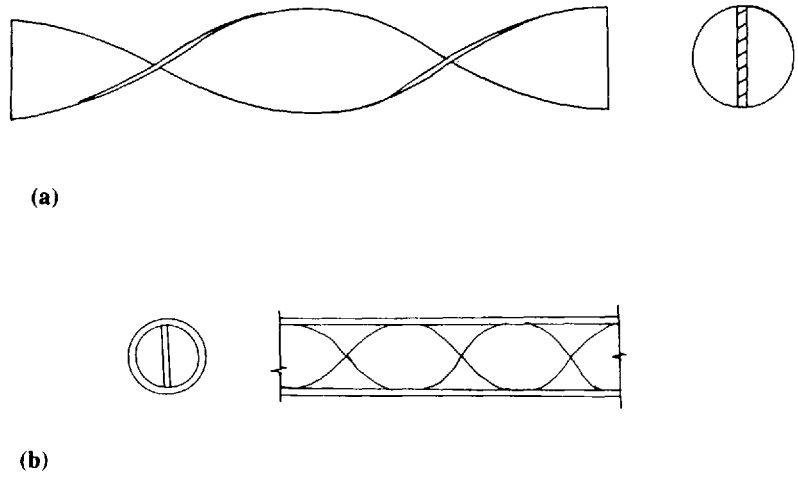


Figure 7 Twisted tape insert. (a) Insert; and (b) insert in a plain tube.

Turbulators for Fire Tube Boilers

A popular technique for enhancement of heat transfer in fire tube boilers is to introduce turbulators into the boiler tubes to increase the gas-side heat-transfer coefficients, thereby increasing heat recovery from flue gases [20]. This will reduce fuel consumption and improve boiler efficiency. Turbulators are made from a narrow, thin metal strip bent and twisted in zig-zag fashion to allow periodic contact with the tube wall.

6.6 Surface Tension Devices

Surface tension devices consist of relatively thick wicking material or grooved surfaces on heat-transfer devices to direct the flow of liquid in boiling and condensing.

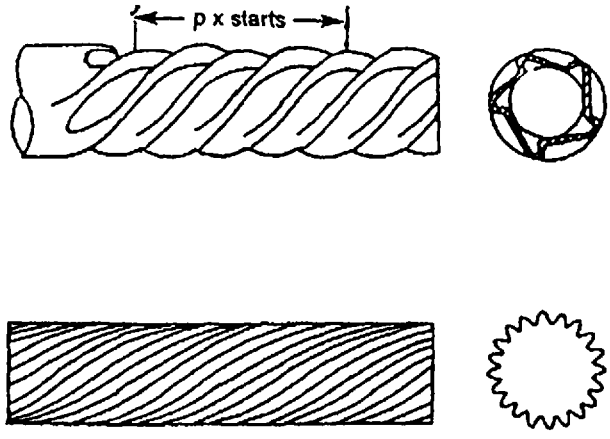


Figure 8 Spirally fluted tubes.

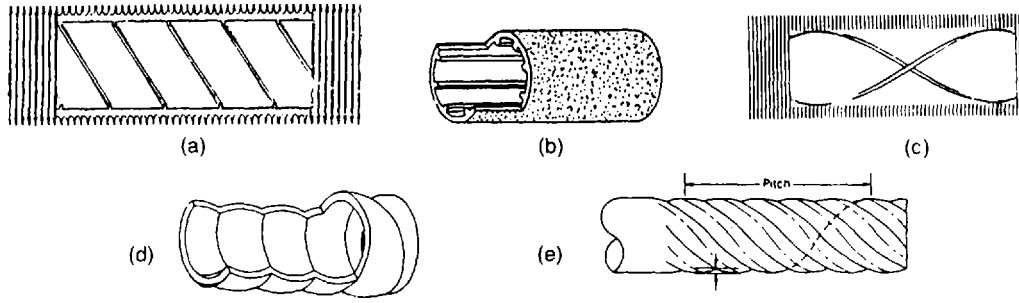


Figure 9 Doubly enhanced tubes. (a) Helical rib roughness on inner surface and integral fins on outer surface; (b) internal fins on inner surface and porous boiling coating on outer surface; (c) twisted tape insert on inner surface and integral fins on outer surface; (d) corrugated roughness on inner and outer surfaces; and (e) corrugated tube, i.e., corrugated strip rolled in a cylinder form and seam welded. (From Ref. 8.)

6.7 Additives for Liquids

Additives for liquids are liquid droplets for boiling, solid particles in single-phase flow, and gas bubbles for boiling.

6.8 Additives for Gases

Additives for gases are liquid droplets or solid particles, either dilute phase (gas-solid suspensions) or dense phase (fluidized beds).

7 ACTIVE TECHNIQUES

The active techniques are (after Bergles [1]) described next.

1. *Mechanical aids* stir the fluid by mechanical means or by rotating the surface or by surface scraping. Surface scraping is widely used for viscous liquids in the chemical process industry.
2. *Surface vibration* at either low or high frequency has been used primarily to improve single-phase heat transfer. Possible modes of heat-transfer applications are single-phase flow, boiling, and condensing.
3. *Fluid vibration* is the most practical type of vibration enhancement, given the mass of most heat exchangers. The vibrations range from pulsations of about 1 Hz to ultrasound. Single-phase fluids are primary concern. Possible modes of heat-transfer applications are single-phase flow, boiling, and condensing.
4. *Electrostatic fields* (dc or ac) are applied in many different ways to dielectrics to cause greater bulk mixing of fluid in the vicinity of the heat-transfer surface. An electrical field and a magnetic field may be combined to provide forced convection via electromagnetic pumping.
5. *Injection* involves supplying gas to a flowing liquid through a porous heat-transfer surface or injecting similar fluid upstream of the heat-transfer section.
6. *Suction* involves either vapor removal through a porous heated surface in nucleate or film boiling, or fluid withdrawal through a porous heated surface in single-phase flow.

The active techniques have not found commercial interest because of the capital and operating cost of the enhancement devices, complex nature, and problems associated with vibration or noise [9].

8 FRICTION FACTOR

Due to the form drag and increased turbulence caused by the disruption, the pressure drop with flow inside an enhanced tube always exceeds that obtained with a plain tube for the same length, flow rate, and diameter (after [18]). In most cases, the increase over that of plain tube is about 70–500%, and usually exceeds the increase in heat transfer, which is about 50–200%. However, for Reynolds number in the range of 5000 to 10,000 and for fluids with Prandtl numbers greater than about 2, the heat-transfer enhancement can exceed the pressure drop increase.

9 PERTINENT PROBLEMS

Three problems are intimately related to enhanced surfaces [7]: (1) testing methods, (2) performance evaluation criteria, and (3) fouling.

9.1 Testing Methods

The basis for selecting an "optimum" heat-transfer surface is easy, provided generalized heat-transfer and friction correlations and quantitative relations for performance evaluation are available. The multitude of augmentation devices with various surface geometries made it impossible to generalize specific correlations for j and f factors. However, this can be overcome, by devising a reliable experimental technique to determine the performance. A common method for determining turbulent-flow, single-phase coefficients from heat-exchanger tests is the Wilson method [6]. In this method, the coefficient on one side is held constant while the coefficient to be determined is varied by making a series of tests at different flow rates. The equation for Nusselt number describing the coefficient to be measured is of the form

$$\mathrm{Nu} = k_1 \mathrm{Re}^{k_2} \mathrm{Pr}^{k_3} \tag{5}$$

where the constants k_2 and k_3 are known in advance. The objective of the test is to determine k_1. As shown next, the total resistance R_T is composed of a constant resistance R_C and a variable resistance R_V, which is to be determined:

$$R_T = R_c + R_v = R_c + \frac{1}{k_1}\left(\frac{1}{k\mathrm{Re}^{k_2}\mathrm{Pr}^{k_3}/D_h} \right) \tag{6}$$

where D_h is the tube hydraulic diameter and k is the thermal conductivity of the fluid. Equation 6 is that of a straight line with slope $1/k_1$ and an intercept R_C when the equation is plotted graphically (Fig. 10).

9.2 Fouling

An important consideration for whether enhanced surfaces should be used is the effect of fouling on the heat exchanger performance. Many research programs are ongoing to study the fouling of enhanced surfaces. There are some techniques that are not affected by fouling; in some applications, fouling can be reduced by using enhanced surfaces. In general, the same factors that influence fouling on unenhanced surfaces will influence fouling of high-performance surfaces [6].

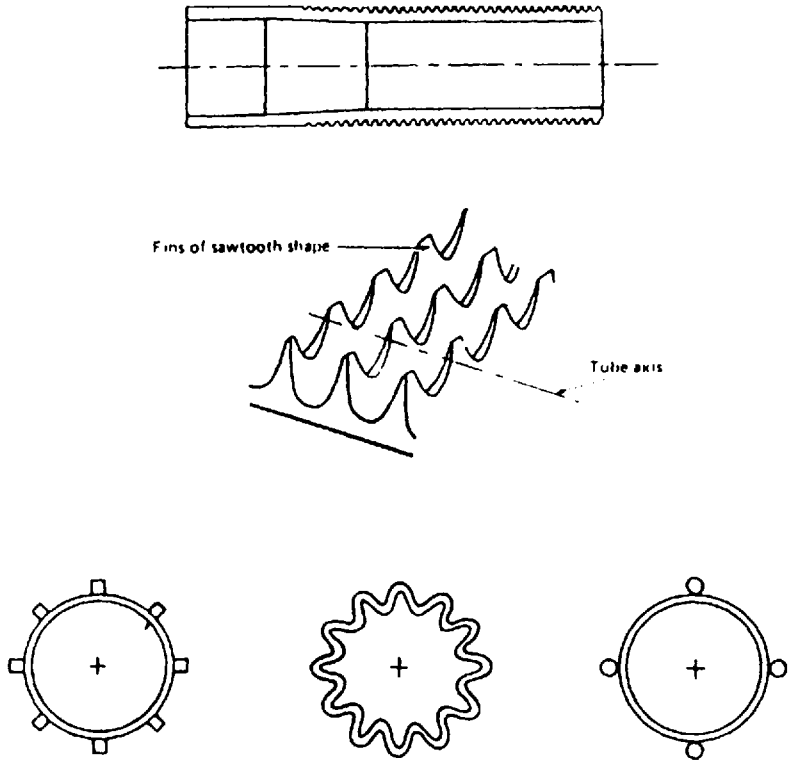


Figure 10 Example of Nelson plot for turbulent flow.

9.3 Performance Evaluation Criteria (PECs)

The basic thermohydraulic characteristic of an enhanced surface is defined by curves of the j and f vs. Reynolds number. Numerous factors decide the merit of enhanced surfaces developed for augmentation of heat transfer. A performance evaluation criterion (PEC) establishes a quantitative statement to account for the heat transfer enhancement, taking into account the pressure-drop characteristics of the enhanced surface. Possible performance objectives of interest include [5,8]:

1. Reduced heat-transfer size and hence low material requirement for fixed heat duty and pressure drop.
2. Increased UA; this may be exploited in two ways: to obtain increased heat duty, or to secure reduced LMTD for fixed heat duty.
3. Reduced pumping power for fixed heat duty.

A PEC is established by selecting one of the operational variables, namely, geometry, flow rate, heat transfer rate, and fluid inlet temperature, for the performance objective subject to design constraints on the remaining variables. So far, there is no universally accepted criterion for evaluating performance, although numerous criteria have been in practice. Bergles et al. [21] reviewed these criteria, which were classified into three objectives: (1) increase in heat transfer, (2) reduced pumping power for fixed heat duty, and (3) reduce exchanger size for fixed heat duty and pressure drop. Shah [22] also critically reviewed more than 30 dimensional or nondimensional comparison methods.

Webb's PECs: Performance Comparison with a Reference

Webb [23] developed a number of PECs of interest with flow inside enhanced and smooth tubes of the same envelope diameter. Generally, these PECs are defined by three different geometry constraints:

1. *FG criteria*: The cross-sectional envelope area and tube length are held constant.
2. *FN criteria*: These criteria maintain fixed-flow frontal area and allow the length of the heat exchange to be a variable. These criteria seek reduced surface area or reduced pumping power for constant heat duty.
3. *VG criteria*: These criteria maintain constant exchanger flow rate.

The concepts of PEC analysis are explained for the case of a prescribed wall temperature or a prescribed heat flux in Ref. 8. The heat transfer enhancement, $hA/h_pA_p = K/K_p$, is given by [8]:

$$\frac{K}{K_p} = \frac{\mathrm{St}}{\mathrm{St}_p}\frac{A}{A_p}\frac{G}{G_p} \tag{7}$$

or

$$\frac{K}{K_p} = \frac{j}{j_p}\frac{A}{A_p}\frac{G}{G_p} \tag{8}$$

where the subscript p refers to the reference, or plain smooth surface. The relative friction power is

$$\frac{p}{P_p} = \frac{f}{f_p}\frac{A}{A_p}\left(\frac{G}{G_p}\right)^3 \tag{9}$$

It is assumed that the smooth tube operating conditions (G_p, f_p, and $j_p\mathrm{St}_p$) are known.

The advantages of this comparison method for compact heat exchangers include [22]: (1) the designer can select his or her own criteria for comparison, (2) then the performance of a surface can be compared with the reference surface, and (3) there is no need to evaluate the fluid properties since they drop out in computing the comparison ratios.

Shah's [22] Recommendation for Surface Selection of Compact Heat Exchanger With Gas on One Side

Four of the criteria recommended by Shah [22] are discussed here. These criteria require the j and f factors, and Reynolds number, together with the geometry specification. These criteria are employed for comparison of flat-tube radiators with plain fin and ruffled fin performances by Maltson et al. [24].

1. *Flow area goodness factor comparison*: The ratio of j factor to the friction factor f, against Reynolds number, generally known as the "flow area goodness factor," was suggested by London [25]:

$$\frac{j}{f} = \frac{\mathrm{Nu}\,\mathrm{Pr}^{-1/3}}{f\,\mathrm{Re}} = \frac{1}{A_c^2}\left[\frac{\mathrm{Pr}^{1/3}\mathrm{NTU}\,M^2}{2g_c\quad\Delta p}\right] \tag{10}$$

   A surface having a higher j/f factor is "good" because it will require a lower free flow area and hence a lower frontal area for the exchanger.
2. *Volume goodness factor comparison*: This is the standardized heat-transfer coefficient against the pumping power per unit of heat-transfer surface area, suggested by London

and Ferguson [26]. Two types of comparison are suggested: (1) h_{std} versus E_{std}, and (2) $\eta_o h_{std}\beta$ versus $E_{std}\beta$ as given:

$$h_{std} = \frac{j\,\mathrm{Re}\mu_{std}C_{p,std}}{D_h\,\mathrm{Pr}_{std}^{2/3}} \tag{11}$$

and

$$E_{std} = \frac{P_p}{A} = \frac{f\,\mathrm{Re}^3\mu_{std}^3}{2g_c\rho_{std}^2 D_h^3} \tag{12}$$

3. The performance of the heat exchanger per unit volume, the criterion suggested by Shah [22]. This method includes the effect of the fin effectiveness. A good performance using this criterion gives the best heat exchanger to use where the size of the unit is an important consideration. Two types of comparison are suggested: (1) h_{std} versus E_{std}, and (2) $\eta_o h_{std}\beta$ versus $E_{std}\beta$ as given:

$$\eta_o h_{std}\beta = \frac{j\,\mathrm{Re}(4\sigma)\eta_o C_{p\,std}\mu_{std}}{\mathrm{Pr}_{std}^{2/3}D_h^2} \tag{13}$$

and

$$E_{std}\beta = \frac{f\,\mathrm{Re}^3(4\sigma)\mu_{std}^3}{2g_c\rho_{std}^2 D_h^4} \tag{14}$$

4. The actual heat-transfer rate performance versus the gas side fan power, suggested by Bergles et al. [27].

10 PHASE CHANGE

Even though heat transfer with phase change is not within the scope of this book, for sake of completion, enhanced heat-transfer surfaces used for condensation and evaporation are mentioned. Enhanced surfaces used for phase change applications other than microfin tubes are shown in Fig. 11. References 1, 5, and 6 detail heat-transfer enhancement techniques for phase change. One major area of application of enhanced heat-transfer surfaces for phase change-applications is in refrigeration and air conditioning. Pate et al. [10] and Bergles [1] detail the application of heat-transfer enhancement techniques in refrigeration and air conditioning industry.

10.1 Condensation Enhancement

The heat-transfer resistance in condensation of pure components is primarily due to conduction across the condensate film thickness. Condensation enhancement is generally obtained by tak-

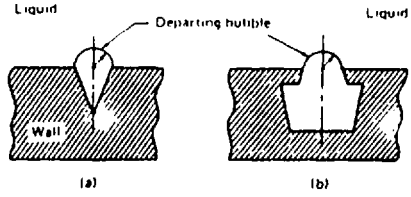


Figure 11 Shellside enhancement devices for phase change (condensation and evaporation). (From Ref. 2.)

ing advantages of surface tension forces to obtain thin condensate film or to strip condensate from the heat-transfer surface. Special surface geometries or treated surfaces are effective in attaining this goal. Heat-transfer enhancement is possible on either the shell side or tube side of a condenser. Since the tube orientation will affect its condensate drainage characteristics, one must distinguish between horizontal and vertical orientations.

Horizontal Orientation

Shell Side.

1. Short radial fins, fluted tubes, wires attached to tubes, modified annular fins with sharp tips on tubes [6].
2. Surfaces of doubly augmented tube geometries like helically corrugated tubes, helically deformed tubes having spiral ridges on outer surface and grooves on inner surface, or corrugated tubes formed by rolling in helical shape followed by seam welding are used [5].
3. Recent developments in extended surfaces for film condensation on horizontal tubes include Hitachi Thermoeexcel-C, and the spine-fin surface.

Tube Side. Closely spaced helical internal fin, twisted tape insert, repeated rib roughness, and sand-grain type roughness may be used.

Shell-Side Condensation on Vertical Tubes

Shell-side condensation enhancement on a vertical surface can be achieved by finned tubes, fluted surfaces, and loosely attached spaced vertical wires [5].

10.2 Evaporation Enhancement

The mechanisms important for evaporation enhancement are thin film evaporation, convective boiling, and nucleate boiling [6]. Nucleate and transition pool boiling are usually dependent on the surface condition as characterized by the material, the surface finish, and the surface chemistry. Certain types of roughness have been shown to reduce wall superheats, increase peak critical heat flux, and destabilize film boiling [1]. Heat-transfer augmentation techniques for thin film evaporation and nucleation are:

1. Thin film vaporization: fluted vertical tubes.
2. Nucleation: For nucleation enhancement, structured surfaces are used. Structured surface refers to fine-scale alteration of the surface finish. A coating may be applied to the plain tube, or the surface may be deformed to produce subsurface channels or pores [1]. Typical structured surfaces are *enhanced surface cavities*—a pore or reentrant cavity within a critical size range, interconnected cavities, and nucleation sites of a re-entrant shape; and *integral roughness*—the three commercially used boiling surface of this type are Trane bent fins, Hitachi bent sawtooth fins, and Weiland flattened fins (T-shaped fin forming) [5].
3. Convective boiling: On the shell side, use integral fins, and enhanced boiling surfaces. On the tube side, there are internal ridges, and axial and helical fins.
4. Flow boiling inside tubes: Linde porous coating, and special internal roughness geometries.

10.3 Heat-Transfer Augmentation Devices for the Air Conditioning and Refrigeration Industry

Shell-Side Evaporation of Refrigerants

Enhanced tubes and their commercial names include (1) modified structured surfaces with porous coatings—High Flux (Union Carbide), and (2) modified low-fin tubes such as are used for shell-side evaporation of refrigerants: GEWA-T (Weilaand Werke), GEWA-TX, GEWA-

TXY, Thermoexcel-E (Hitachi), Turbo-B (Wolverine) [10], EverFin-40 (Furukawa Electric), and Thermoexcel-HE.

Shell-Side Condensation of Refrigerants

Recognition of surface tension as the dominant force for determining condensate thickness has led to the development of surfaces designed to produce thin films, and to remove condensate from the heat-transfer surface. The profiles such as Thermoexcel-C (Hitachi) and Turbo-V shaped fin with a steep angle help in maintaining a thin refrigerant film.

In-Tube Evaporation of Refrigerants

In-tube enhancement devices for evaporation of refrigerants include (1) rough surfaces like helical wire inserts, internal thread, and corrugated tubes, (2) extended surfaces like microfin tubes and high-profile fins, and (3) swirl flow devices such as twisted tape inserts. Examples of all three types of enhancement are shown in Fig. 12.

In-Tube Condensation

The same enhancement techniques described for in-tube evaporation and microfin tubes (Fig. 12) are used.

11 MAJOR AREAS OF APPLICATIONS

Heat-transfer augmentation devices used in major areas of applications are discussed in detail by Bergles [1]. In the following paragraphs they are briefly mentioned.

Heating, Ventilating, and Refrigeration and Air Conditioning. In the common evaporator or condenser coil, airside heat transfer is improved with louvered, corrugated, or serrated fins. Microfin configurations are usually found in evaporator or condenser applications. The structured boiling surfaces are being adopted more frequently for flooded refrigerant evaporators. For condensing and boiling applications, tubes are now provided with tubeside enhancements of the spiral repeated rib type.

Automotive Industries. Radiators, charge air coolers, and intercoolers of automobiles have been provided with various forms of extended surfaces: louvred fin, offset strip fin, and low-fin tubes. Twisted tape inserts have received considerable attention for oil cooler applications. In these applications enhanced air-side surfaces have contributed to the dramatic reduction in size and weight found in modern vehicles.

Power Sector. High-performance enhanced surfaces on the air side have been developed for dry cooling towers used for fossil power plant heat rejection and turbulators on the tube side

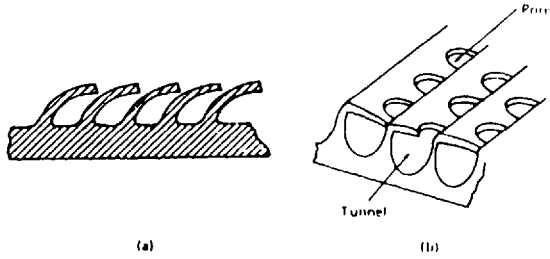


Figure 12 Intube enhancement techniques for evaporating and condensing refrigerants. (a) Extended surface; and (b) swirl flow device.

of fire tube boilers and structured boiling surfaces in the intermediate heat exchangers in dispersed-flow film boiling.

Process Industries. The chemical process industry has sparingly adopted enhancement technology because of concerns about fouling. Wire loop inserts and vapor sphere matrix fluted spheres (tube side), or solid spheres (shell side) not only improve heat transfer but reduce fouling with typical process fluids.

Industrial Heat Recovery. Ceramic tubes that are enhanced externally and/or internally for high-temperature waste heat recovery are used.

Electronics Cooling. Enhanced extended surfaces are used for air cooling of electronic devices ranging from radar tubes to microelectronic chips used in computers.

Aerospace. Improved gas turbine blade cooling is achieved by transverse repeated ribs and pin fins cast into the blade, thereby reducing the wall temperature.

This page intentionally left blank

9
Fouling

Fouling is defined as the formation on heat transfer surfaces of undesired deposits, which impede the heat transfer and increase the resistance to fluid flow, resulting in higher pressure drop. Industrial heat exchangers rarely operate with nonfouling fluids. Low-temperature cryogenic heat exchangers are perhaps the only exception [1]. The growth of the deposits causes the thermohydraulic performance of heat exchanger to degrade with time. Fouling affects the energy consumption of industrial processes, and it can also decide the amount of extra material required to provide extra heat-transfer surface employed in heat exchangers to compensate for the effects of fouling. In addition, where the heat flux is high, as in steam generators, fouling can lead to local hot spots and ultimately it may result in mechanical failure of the heat-transfer surface. The progression of fouling with time and its effect on thermal performance are shown schematically in Fig. 1 [2]. Bott [3] and Chenoweth [4] give general and specific information on fouling.

1 EFFECT OF FOULING ON THE THERMOHYDRAULIC PERFORMANCE OF HEAT EXCHANGERS

Effects can include:

1. The fouling layers on the inside and the outside surfaces are known generally to increase with time as the heat exchanger is operated. Since the fouling layers normally have lower thermal conductivity than the fluids or the conduction wall, they increase the overall thermal resistance. For the common case of a cylindrical tube with flow and fouling at both the inside and outside surface represented in Fig. 2, the total resistance R_t to heat transfer between the two streams is given by

$$R_T = \frac{1}{U_o A_o} = \frac{1}{h_i A_i} + \frac{R_i}{A_i} + \frac{\Delta t_w}{k_w A_m} + \frac{R_o}{A_o} + \frac{1}{h_o A_o} \tag{1}$$

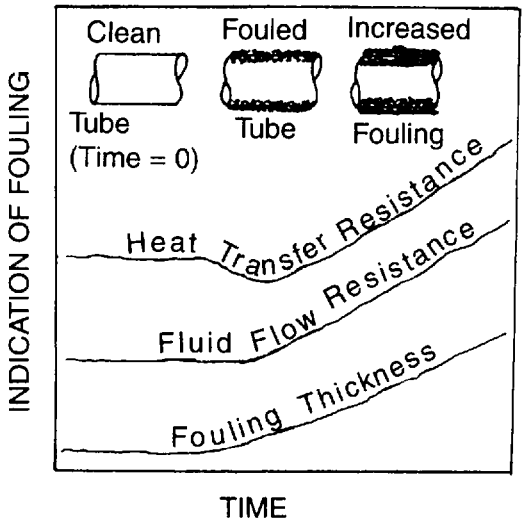


Figure 1 Effect of fouling. (From Ref. 2.)

where the symbols have the usual meaning, and R_i and R_o are fouling resistance on the inside and outside surfaces respectively. The overall heat-transfer coefficient in fouled conditions may be expressed in terms of the overall heat-transfer coefficient in clean condition and an overall fouling resistance R_f involving the terms related to fouling:

$$\frac{1}{U_{o,f}} = \left[\frac{1}{h_i}\frac{A_o}{A_i} + \frac{\Delta t_w}{k_w}\frac{A_o}{A_m} + \frac{1}{h_o}\right] + \left[R_i\frac{A_o}{A_i} + R_o\right] \tag{2a}$$

$$= \frac{1}{U_{o,c}} + R_F \tag{2b}$$

or

$$R_F = \frac{1}{U_{o,f}} - \frac{1}{U_{o,c}} \tag{3}$$

2. There is an increase of the surface roughness, thus increasing frictional resistance to flow, and fouling blocks flow passages; due to these effects, the pressure drop across the heat exchanger increases.

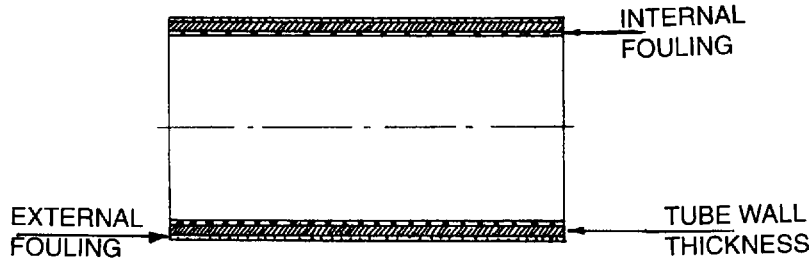


Figure 2 Fouling deposit build up on heat transfer surface.

3. Fouling may create a localized environment where corrosion is promoted.
4. Fouling will reduce the thermal effectiveness of heat exchangers, which in turn affect the subsequent processes or will increase the thermal load on the system.
5. An additional goal become prevention of contamination of a process fluid or product.

2 COSTS OF HEAT EXCHANGER FOULING

Fouling of heat exchangers has been estimated to represent an annual expense in the United States of somewhere between $4.2 and $10 billion [4]. Fouling is something that is unwanted and counterproductive. The presence of fouling on heat exchange surfaces causes additional costs due to the following reasons:

1. Increased capital expenditure due to oversizing.
2. Energy losses associated with poor performance of the equipment.
3. Treatment cost to lessen corrosion and fouling.
4. Lost production due to maintenance schedules.

Economic considerations should be among the most influential parameters for determining appropriate allowances for fouling. It is important to determine a strategy as to whether first cost, operating and maintenance cost, or total cost over a period of years is the objective.

2.1 Oversizing

While sizing a heat exchanger it is a normal practice to oversize the heat-transfer surface area to account for fouling, and the oversizing is normally of the order of 20–40%.

2.2 Additional Energy Costs

Since fouling reduces the heat-transfer rates, additional energy is expended to increase the heat-transfer rate; fouling also increases the pressure drop across the core and hence more pumping power is required to meet the heat load.

2.3 Treatment Cost to Lessen Corrosion and Fouling

The formation of fouling deposits on heat-transfer surfaces necessitates periodical cleaning, which costs money for cleaning materials and process, personnel required, and recently environmental problems to discharge the effluents.

2.4 Lost Production Due to Maintenance Schedules and Down Time for Maintenance

Periodical cleaning requires plant shutdown and hence the unavailability of system for productive purposes. Critical industries that cannot afford for downtime and loss in production will maintain standby units, which again raises additional capital costs for spares.

3 PARAMETERS THAT INFLUENCE FOULING RESISTANCES

Many operational and design variables have been identified as having most pronounced and well-defined effects on fouling. These variables are reviewed here in principle to clarify the fouling problems and because the designer has an influence on their modification. Those parameters include the following:

1. Properties of fluids and their propensity for fouling
2. Surface temperature
3. Velocity and hydrodynamic effects
4. Tube material
5. Fluid purity and freedom from contamination
6. Surface roughness
7. Suspended solids
8. Placing the more fouling fluid on the tube side
9. Shell-side flow
10. Type of heat exchanger
11. Heat exchanger geometry and orientation
12. Equipment design
13. Seasonal temperate changes
14. Heat-transfer processes like sensible heating, cooling, condensation, vaporization, etc.

3.1 Properties of Fluids and Usual Propensity for Fouling

The most important consideration is the fluid and the conditions conducive for fouling. At times a process modification can result in conditions that are less likely to cause fouling.

3.2 Temperature

A good practical rule to follow is to expect more fouling as the temperature rises. This is due to a "baking on" effect, scaling tendencies, increased corrosion rate, faster reactions, crystal formation and polymerization, and loss in activity by some antifoulants [5]. Lower temperatures produce slower fouling buildup, and usually deposits that are easily removable [4]. However, for some process fluids, low surface temperature promotes crystallization and solidification fouling. For those applications, it is better to use an optimum surface temperature to overcome these problems. For cooling water with a potential to scaling, the desired maximum surface temperature is about 140°F (60°C). Biological fouling is a strong function of temperature. At higher temperatures, chemical and enzyme reactions proceed at a higher rate with a consequent increase in cell growth rate [6]. According to Mukherjee [6], for any biological organism, there is a temperature below which reproduction and growth rate are arrested and a temperature above which the organism becomes damaged or killed. If, however, the temperature rises to an even higher level, some heat-sensitive cells may die.

3.3 Velocity and Hydrodynamic Effects

Hydrodynamic effects such as flow velocity and shear stress at the surface influence fouling. Within the pressure drop considerations, the higher the velocity, higher will be the thermal performance of the exchanger and less will be the fouling. Uniform and constant flow of process fluids past the heat exchanger favors less fouling. Foulants suspended in the process fluids will deposit in low-velocity regions, particularly where the velocity changes quickly, as in heat exchanger water boxes and on the shell side [5]. Higher shear stress promotes dislodging of deposits from surfaces. Maintain relatively uniform velocities across the heat exchanger to reduce the incidence of sedimentation and accumulation of deposits.

3.4 Tube Material

The selection of tube material is significant to deal with corrosion fouling.

Carbon steel is corrosive but least expensive.

Copper exhibits biocidal effects in water. However, its use is limited in certain applications:

(1) Copper is attacked by biological organisms including sulfate-reducing bacteria; this

increases fouling. (2) Copper alloys are prohibited in high-pressure steam power plant heat exchangers, since the corrosion deposits of copper alloys are transported and deposited in high-pressure steam generators and subsequently block the turbine blades. (3) Environmental protection limits the use of copper in river, lake, and ocean waters, since copper is poisonous to aquatic life.

Noncorrosive materials such as titanium and nickel will prevent corrosion, but they are expensive and have no biocidal effects.

Glass, graphite, and Teflon tubes often resist fouling and/or improve cleaning.

Although the construction material is more important to resist fouling, surface treatment by plastics, vitreous enamel, glass, and some polymers will minimize the accumulation of deposits [3].

3.5 Impurities

Seldom are fluids pure. Intrusion of minute amounts of impurities can initiate or substantially increase fouling. They can either deposit as a fouling layer or acts as catalysts to the fouling processes [4]. For example, chemical reaction fouling or polymerization of refinery hydrocarbon streams is due to oxygen ingress and/or trace elements such as Va and Mo. In crystallization fouling, the presence of small particles of impurities may initiate the deposition process by seeding. The properties of the impurities form the basis of many antifoulant chemicals. Sometimes impurities such as sand or other suspended particles in a cooling water may have a scouring action, which will reduce or remove deposits [3].

3.6 Surface Roughness

The surface roughness is supposed to have the following effects [3]:

1. The provision of "nucleation sites" that encourage the laying down of the initial deposits.
2. The creation of turbulence effects within the flowing fluid and, probably, instabilities in the viscous sublayer.

Better surface finish has been shown to influence the delay of fouling and ease cleaning. Similarly, nonwetting surfaces delay fouling. Rough surfaces encourage particulate deposition. After the initiation of fouling, the persistence of the roughness effects will be more a function of the deposit itself [3]. Even smooth tubes may become rough in due course due to scale formation, formation of corrosion products, or erosion.

3.7 Suspended Solids

Suspended solids promote particulate fouling by sedimentation or settling under gravitation onto the heat-transfer surfaces. Since particulate fouling is velocity dependent, prevention is achieved if stagnant areas are avoided. For water, high velocities (above 1 m/s) help prevent particulate fouling. Often it is economical to install an upstream filtration.

3.8 Placing the More Fouling Fluid on the Tube Side

As a general guideline, the fouling fluid is preferably placed on the tube side for ease of cleaning. Also, there is less probability for low-velocity or stagnant regions on the tube side.

3.9 Shell-Side Flow

Velocities are generally lower on the shell side than on the tube side, less uniform throughout the bundle, and limited by flow-induced vibration. Zero-or low-velocity regions on the shell

side serve as ideal locations for the accumulation of foulants. If fouling is expected on the shell side, then attention should be paid to the selection of baffle design. Segmental baffles have the tendency for poor flow distribution if spacing or baffle cut ratio is not in correct proportions. Too low or too high a ratio results in an unfavorable flow regime that favors fouling (Fig. 3).

3.10 Type of Heat Exchanger

Low-Finned Tube Heat Exchanger

There is a general apprehension that low Reynolds number flow heat exchangers with low-finned tubes will be more susceptible to fouling than plain tubes. Fouling is of little concern for finned surfaces operating with moderately clean gases. According to Silvestrini [7], fin type does not affect the fouling rate, but the fouling pattern is affected for waste heat recovery exchangers. Plain and serrated fin modules with identical densities and heights have the same fouling thickness increases in the same period of time. As far as fouling pattern is concerned, for plain fin tubes soot deposits are equally distributed between fin and tube surfaces when buildup first begins. Subsequently, the distribution becomes uneven, as the fin fouling thickness reach a maximum and the fin gaps are filled with soot that builds up from the tube walls. This pattern also occurs in certain areas of the serrated fin tubes, but another pattern evident is localized bridging of the serrated fin tips across both the fin gaps and serrations.

Heat-Transfer Augmentation Devices

Fouling is an important consideration in whether enhanced surfaces tubes should be used on heat exchangers to enhance the performance. Experimental evidence favors most of the heat-transfer augmentation devices for improved heat transfer without penalty due to fouling. Fouling aspects of heat-transfer augmentation devices are covered in the chapter on heat transfer augmentation (Chapter 8).

Gasketed Plate Heat Exchangers

High turbulence, absence of stagnant areas, uniform fluid flow, and the smooth plate surface reduce fouling and the need for frequent cleaning. Hence the fouling factors required in plate heat exchangers are normally 10–25% of those used in shell and tube heat exchangers.

Spiral Plate Exchangers

High turbulence and scrubbing action minimize fouling on the spiral plate exchanger. This permits the use of low fouling factors.

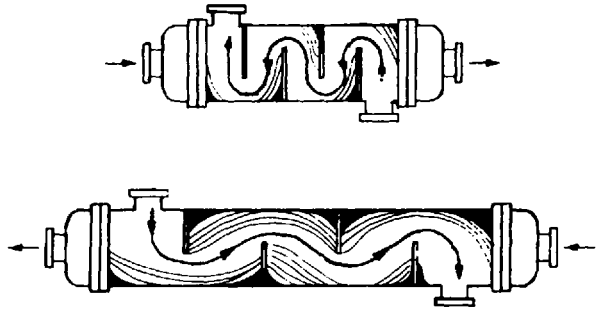


Figure 3 Effect of baffle spacing and cut on fouling. Top: Moderate baffle spacing and baffle cut; bottom, wide baffle spacing and large baffle cut. Note: dark areas represent stagnant areas with heavy fouling. (From Ref. 6.)

3.11 Seasonal Temperature Changes

When cooling tower water is used as coolant, considerations are to be given for winter conditions where the ambient temperature may be near zero or below zero on the Celsius scale. The increased temperature driving force during the cold season contributes to more substantial overdesign and hence overperformance problems, unless a control mechanism has been instituted to vary the water/air flow rate as per the ambient temperature.

3.12 Equipment Design

Equipment design can contribute to increased fouling. Heat exchanger tubes that extend beyond tube sheet, for example, can cause rapid fouling.

3.13 Heat Exchanger Geometry and Orientation

Heat exchanger geometry influences the uniformity of flows on the shell side and tube side. Orientation of heat exchangers eases cleaning [4]. Finned tube heat exchanger geometry and surface characteristics like tube layout, tube pitch, secondary surface density, etc. influence fouling. The influences of surface modification and fin density on fouling were discussed in Chapter 4.

3.14 Heat-Transfer Processes Like Sensible Heating, Cooling, Condensation, and Vaporization

The fouling resistances for the same fluid can be considerably different depending upon whether heat is being transferred through sensible heating or cooling, boiling, or condensing [4].

4 FOULING CURVES/MODES OF FOULING

The amount of material deposited per unit area, m_f is related to the fouling resistance R_f and the density of the foulant ρ_f, thermal conductivity k_f, and thickness of the deposit x_f by the following equation [1]:

$$m_f = \rho_f x_f = \rho_f k_f R_f \tag{4}$$

The incidence of fouling with reference to time is normally defined by the following three modes [1]:

1. Linear mode—Increase of m_f (or R_f) with time t.
2. Falling rate mode—The rate of deposition decreases with increasing time.
3. Asymptotic mode—The value of m_f (or R_f) is not time variant after initial fouling.

The representation of various modes of fouling with reference to time is known as a fouling curve. Typical fouling curves are shown in Fig. 4. The linear modes and falling rate modes may be the incidence of fouling in the early stages of asymptotic behavior. The asymptotic mode is of particular interest to heat exchangers, since the incidence of fouling raises the possibility of continued operation of the equipments without additional fouling. The time delay period, t_d, is time required for the formation of initial fouling substrata. Smooth and nonwetting surfaces like glass and Teflon will extend the delay period.

5 STAGES OF FOULING

For all the categories of fouling, the successive events that commonly occur in most situations are up to five in number. They are initiation of fouling, transport to surface, attachment to surfaces, removal from surfaces, and aging of deposit [8].

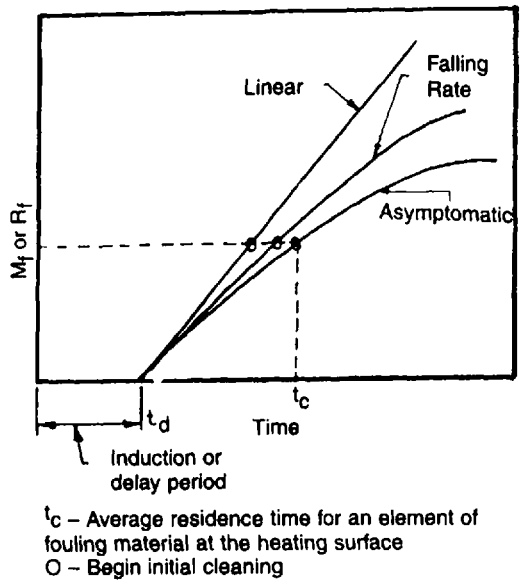


Figure 4 Fouling curves.

6 FOULING MODEL

Fouling is usually considered to be the net result of two simultaneous processes: a deposition process and a removal (reentrainment process) [9]. A schematic representation of fouling process is given in Fig. 5. The net rate of fouling can be expressed in terms of the rate of deposition of fouling mass ($\dot{m}_d$) and the rate of removal ($\dot{m}_r$) from the heat-transfer surface. Thus,

$$\frac{dm_f}{dt} = \dot{m}_d - \dot{m}_r \tag{5}$$

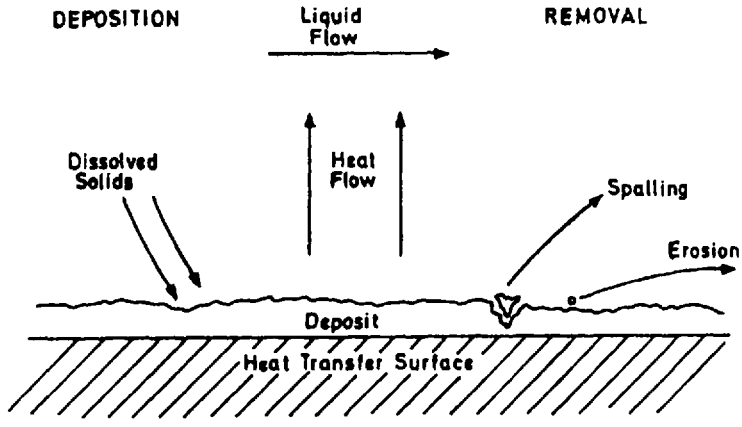


Figure 5 Schematic representation of fouling process. (From Ref. 9.)

One of the earliest models of fouling was that by Kern and Seaton [10]. In this model, it was assumed that $\dot{m}_d$ remained constant with time t but that $\dot{m}_r$ was proportional to m_f and therefore increased with time to approach $\dot{m}_d$ asymptotically. Thus $\dot{m}_d = \beta m_f$; then integration of Eq. 5 from the initial condition $m_f = 0$ at $t = 0$ gives

$$m_f = m_f^*(1 - e^{-\beta t}) \tag{6}$$

where m_f^* is the asymptotic value of m_f and $\beta = 1/t_c$. The time constant t_c represents the average residence time for an element of fouling material at the heating surface. Equation 6 can be expressed in terms of fouling resistance R_f at time t in terms of the asymptotic value R_f^* by

$$R_f = R_f^*(1 - e^{-\beta t}) \tag{7}$$

Modeling efforts in the past 25 years have centered on evaluating the functions m_d and m_r for specific fouling situations.

7 MECHANISMS OF FOULING

It is of great importance to understand the fouling mechanisms in principle, as they will indicate the causes and conditions of fouling and hence give clues how fouling can be minimized. Based on the mechanism of fouling, Epstein [8] classifies fouling into six types:

1. Particulate fouling
2. Reaction fouling
3. Corrosion fouling
4. Precipitation fouling
5. Biological fouling
6. Solidification fouling

7.1 Particulate Fouling

Particulate fouling may be defined as the accumulation of particles suspended in the process streams onto the heat-transfer surfaces. This type of fouling includes sedimentation of settling under gravitation as well as deposition of colloidal particles by other deposition mechanisms on to the heat transfer surfaces. Various forms of particulate fouling are:

1. Fouling that occurs in once-through cooling-water systems using sea, river, and lake water containing mud, silt, and sediments. They are capable of depositing in low-flow areas, forming a physical barrier, and preventing oxygen from reaching the metal/solution interface. The deposit buildup will promote localized corrosion.
2. Gas-side fouling: Gas-side fouling is mostly by particulate fouling by dirty gas streams, airborne contaminants, and the leakage and mixing of one process stream with the other, in addition to its own contaminants—carbon soot in the case of combustion gases and exhaust gases. In some cases, gas-side fouling may also be accompanied by corrosion, particularly when condensation of corrosive acids take place from combustion gases. Level of gas-side fouling depends on features such as

   Tube layout pattern—in-line or staggered
   Tube pitch
   Fin density
   Fin surface characteristic such as plain fin, surface-modified fin

3. Another important area of particulate fouling is due to the aluminum transport phenomenon. The problem consists of corrosion of heat-rejecting aluminum surfaces (engine block) followed by deposition of insoluble aluminum salts in the radiator. The corrosion process can be prevented by the inclusion of silicate inhibitors in the coolant formulation.

7.2 Chemical Reaction Fouling (Polymerization)

Deposits formed by chemical reactions at the heat-transfer surface in which the surface material itself is not a reactant are known as chemical reaction fouling. Polymerization, cracking, and coking of hydrocarbons are prime examples of reaction fouling. The factors likely to affect reaction fouling include the following [3,11]:

Temperature is the most sensitive variable. It is usual that below a certain surface temperature polymerization does not initiate, but increases rapidly above that. The reaction rate is related to the temperature by the Arrhenius law:

$$K_r = A_{cr} e^{-E/RT_s} \tag{8}$$

where E is the activation energy, R the gas constant, A_{cr} the rate constant, and T_s the heat transfer surface temperature.

The presence of most sulfur compounds, nitrogen compounds, and the presence of trace elements (metallic impurities) such as Mo and Va in hydrocarbon streams significantly increases the fouling rates.

Composition of the process stream, including contaminants and, especially, oxygen ingress will affect reaction fouling.

Sound prevention measures for chemical reaction fouling should include the following [3,11]:

1. Avoidance of feed contact with air or oxygen by nitrogen blanketing.
2. Elimination or reduction of unsaturates, which are particularly high in cracked stocks.
3. Caustic scrubbing to remove sulfur compounds.
4. Desalting, which reduces trace metal contamination.
5. The use of antioxidation additives that inhibit the polymerization reaction, along with steps taken to minimize oxygen ingress.
6. Use of additives known as metal coordinators, which react with the trace elements and prevent them from functioning as fouling catalysts. Other additives recommended are corrosion inhibitors and dispersion agents [3].

7.3 Corrosion Fouling

Corrosion fouling is due to the deposition of corrosion products on heat-transfer surfaces. In this category of fouling process, the heat-transfer surface material itself reacts to produce corrosion products, which foul the heat-transfer surface. The most common forms of this type of fouling are material loss due to general thinning, iron oxide on carbon steel tubes in cooling-water systems, and fouling of soldered radiator tube ends on the water side by solder bloom corrosion. Corrosion fouling is highly dependent upon the choice of material of construction and the environment. Hence, it is possible to overcome corrosion fouling if the right choice of material has been made to resist the environment. Measures such as the use of inhibitors, cathodic protection, and surface treatment such as passivation of stainless steel will minimize corrosion and hence corrosion fouling.

7.4 Crystallization or Precipitation Fouling

This type of fouling mostly takes place in cooling-water systems, when water-soluble salts, predominantly calcium carbonates, become supersaturated and crystallize on the tube wall to form scaling. Such scaling occurs because many of the dissolved salts in water exhibit inverse solubility effects, a condition that reverses the normal solubility (increasing with temperature) into one that decreases with temperature. Thus an inverse solubility solution will crystallize when heated (e.g., cooling water), while normal solubility salts will crystallize when cooled. Chemical additives can be helpful to reduce fouling problems due to crystallization and freezing in a number of ways. Broadly there are four groups of chemicals to control crystallization [3]: distortion agents, dispersants, sequestering agents, and threshold chemicals.

Modeling for Scaling

According to Hasson [12], scaling is due to diffusion of calcium and carbonate ions from the bulk of the fluid, followed by crystallization of $CaCO_3$ on the hot wall surfaces. Their model for predicting $CaCO_3$ scaling rates is given by

$$m_s = K_R[(Ca^{2+})_i(CO_3^{2-})_i - K_{sp}] \tag{9}$$

where m_s is the scale deposition rate ($kg/m^2 \cdot s$), K_R the constant for crystallization rate, and K_{sp} the solubility product of $CaCO_3$ $(mol/m^3)^2$.

The principle of fouling and the factors promoting scaling are discussed in the section on cooling water corrosion are discussed at the end of this chapter.

7.5 Biological Fouling

The attachment of microorganisms (bacteria, algae, and fungi) and macroorganisms (barnacles, sponges, fishes, seaweed, etc.) on heat-transfer surfaces where the cooling water is used in as-drawn condition from river, lake, sea and coastal water, etc., is commonly referred to as biological fouling. On contact with heat-transfer surfaces, these organisms can attach and breed, sometimes completely clogging the fluid passages, as well as entrapping silt or other suspended solids and giving rise to deposit corrosion. Concentration of microorganisms in cooling-water systems may be relatively low before problems of biofouling are initiated. For open recirculating systems, bacteria concentrations of the order of 1×10^5 cells/ml and fungi of 1×10^3 cells/ml may be regarded as limiting values [3]. Corrosion due to biological attachment to heat-transfer surfaces is known as microbiologically influenced corrosion (MIC). MIC is discussed in detail in Chapter 12 on corrosion. The techniques that can be effective in controlling biological fouling include the following:

1. Select materials that posses good biocidal properties.
2. Mechanical cleaning techniques like upstream filtration, air bumping, back flushing, passing brushes, sponge rubber balls, grit coated rubber balls, and scrapers [4].
3. Chemical cleaning techniques that employ biocides such as chlorine, chlorine dioxide, bromine, ozone, surfactants, pH changes, and/or salt additions.
4. Thermal shock treatment by application of heat, or deslugging with steam or hot water.
5. Some less well-known techniques like ultraviolet radiation.

7.6 Solidification Fouling or Freezing Fouling

The freezing of a liquid or of higher-melting constituents of a multicomponent solution on a subcooled heat-transfer surface is known as solidification fouling. Notable examples include frosting of moisture in the air, freezing of cooling water in low-temperature processes, and

paraffin wax deposition during cooling of hydrocarbon streams. There are various remedies for dealing with duties where solidification occurs on the product side:

1. Do not include very large fouling resistances in the design. This will result in an oversized unit, which presents problems in the clean condition.
2. Use concurrent flow instead of counterflow.

8 FOULING DATA

In choosing the fouling resistances to be used in a given heat exchanger, the designer has three main sources [13]:

1. Past experience of heat exchanger performance in the same or similar environments.
2. Results from portable test rigs.
3. TEMA values, which are overall values for a very limited number of environments.

8.1 Instruments for Monitoring of Fouling

Instruments have been developed to monitor conditions on a tube surface to indicate accumulation of fouling deposits and, in some cases, to indicate the effect on heat exchanger performance. Various fouling monitors are described in Ref. 14. The following is a summary of the different fouling monitors [2].

1. Removable sections of the fouled surface, which may be used for microscopic examination, mass measurements, and chemical and biological analysis of the deposits.
2. Increase in pressure drop across the heat exchanger length. This method provides a measure of fluid frictional resistance, which usually increases with buildup of fouling deposits. This device is relatively inexpensive and is easy to operate.
3. Thermal resistance monitors, which are used to determine the effect of the deposit on overall heat transfer resistance. The thermal method of monitoring has the advantage over the others of giving directly information that is required for predicting or assessing heat-transfer performance.

8.2 Gas-Side Fouling Measuring Devices

Marner and Henslee [15] carried out a comprehensive review of gas-side fouling measuring devices. They classified the devices into the five groups: heat flux meters, mass accumulation probes, optical devices, deposition probes, and acid condensation probes. A heat flux meter uses the local heat transfer per unit area to monitor the fouling. The decrease in heat flux as a function of time is thus a measure of the fouling buildup. A mass accumulation device measures the fouling deposit under controlled conditions. Optical measuring devices use optical method to determine the deposition rate. Acid condensation probes are used to collect liquid acid that accumulates on a surface that is at a temperature below the acid dew point of the gas stream.

9 HOW FOULING IS DEALT WHILE DESIGNING HEAT EXCHANGERS

At present, fouling is usually treated in a very elementary way in design by this measure [16]: adding an extra thermal resistance, known as fouling factors, or providing extra surface area to accommodate fouling.

9.1 Specifying the Fouling Resistances

Values of the fouling resistances are specified that are intended to reflect the values at the point in time just before the exchanger is to be cleaned. This implies that the exchanger is oversized for clean condition and barely adequate for conditions just before it should be cleaned. The fouling resistances result in higher heat-transfer surface area. Planned fouling prevention, maintenance, and cleaning can justify lower fouling resistances, but at higher ongoing costs [4].

9.2 Oversizing

Another approach to heat exchanger design is to arbitrarily increase the heat-transfer surface area to allow for fouling. This approach usually assumes zero fouling resistance in the fundamental overall heat-transfer equation. The overall heat-transfer coefficient is determined for clean conditions, and subsequently, the surface area required for clean condition is increased by a certain percentage. Based upon experience, the oversurface specified can range from 15 to 50% depending on the service [4]. In effect, the fouling for the exchanger is combined and no longer can be identified as belonging to one side or another.

10 TEMA FOULING RESISTANCE VALUES

The influence of the TEMA Fouling Resistance values [17] on design of heat exchangers has been enormous. In practice some thought the TEMA values too high, others too low, since the tendency to fouling in a heat exchanger is dependent upon parameters such as local flow velocities, heat fluxes, etc., rather than overall values or point values as given for most cases in TEMA. Fouling types and effects of fouling are included in the RGP section of the seventh edition. The data contained in the new section are the results of studies by Heat Transfer Research, Inc. (HTRI), and TEMA jointly for several years. TEMA fouling resistance values for water are given in Table 1.

10.1 Research in Fouling

Much research is in underway for fouling. This research will some day enable us to understand the parameters responsible for fouling and hence to devise means to control or eliminate fouling. Today, however, we largely rely upon experience.

Important cooperative research is being done by groups such as Heat Transfer Research, Inc. (USA), and the Heat Transfer and Fluid Flow Service (UK). By the year 2000, it is likely that a number of usable models will be available that are somewhat better than the TEMA fouling resistances [16].

11 FOULING MONITORING

Exchangers subject to fouling or scaling should be monitored for their efficient functioning. A light fouling on the tube greatly reduces its efficiency. A marked increase in pressure drop and/or reduction in performance usually indicates fouling. The unit should first be checked for air or vapor binding to confirm that this is not the cause for the reduction in performance.

12 EXPERT SYSTEM

A computerized, consultative expert system has been developed that can simulate human reasoning, perform water treatment diagnoses, and recommend procedures to minimize corrosion

Table 1 Fouling Resistances for Water

Temperature of Heating Medium	Up to 240°F		240 to 400°F	
Temperature of water	125° (water velocity ft/sec)		Over 125° (water velocity ft/sec)	
	3 and Less	Over 3	3 and Less	Over 3
Sea water	0.0005	0.0005	0.001	0.001
Brackish water	0.002	0.001	0.003	0.002
Cooling tower and artificial spray pond				
treated make up	0.001	0.001	0.002	0.002
untreated	0.003	0.003	0.005	0.004
City or well water	0.001	0.001	0.002	0.002
River water				
minimum	0.002	0.001	0.003	0.002
average	0.003	0.002	0.004	0.003
Muddy or silty	0.003	0.002	0.004	0.003
Hard (over 15 grains/gal.)	0.003	0.003	0.005	0.005
Engine jacket	0.001	0.001	0.001	0.001
Distilled or closed cycle				
Condensate	0.0005	0.0005	0.0005	0.0005
Treated boiler feedwater	0.001	0.0005	0.001	0.001
Boiler blowdown	0.002	0.002	0.002	0.002

Note: If the heating medium temperature is over 400°F and the cooling medium is known to scale, these ratings should be modified accordingly. (Copyright Tubular Exchanger Manufacturers Association, 1988.)

and fouling in cooling water system [18]. In this work, a basic model adopted for knowledge representation is in the form of a fault tree. The expert system has been developed as a useful tool to accomplish the following:

1. Integrate myriad data from monitoring programs
2. Provide a diagnosis
3. Organize a logical stepwise approach to problem solving
4. Serve as a valuable tool for training

13 FOULING PREVENTION AND CONTROL

Specifying the fouling resistances or oversizing result in added heat-transfer surface. The excess surface area can result in problems during startup and bring about conditions that can, in fact, encourage excess fouling due to low velocity [19]. There are a number of techniques that can overcome or mitigate the effects of fouling in heat exchangers, and they include:

1. Designing the plant or process in such a way that the condition leading to the fouling is limited or reduced.
2. Instituting an on-line mechanical cleaning system, or cleaning the equipment when the effects of the fouling can no longer be tolerated to restore its effectiveness by various off-line cleaning techniques.
3. The use of chemical additives or antifoulants in the fouling stream.

These aspects are discussed in detail next.

13.1 Measures to Be Taken During the Design Stages

No hard and fast rules can be applied for heat exchanger design in relation to fouling, but the following points should be kept in mind during the conception and design of a heat exchanger:

1. Make the design simple.
2. Select the heat exchanger type with point 1 in mind. Heat exchangers other than shell and tube units may be better suited to fouling applications. Gasketed plate exchangers and spiral plate exchangers offer better resistance to fouling because of increased turbulence, higher shear, or other factors. Before commissioning a heat exchanger, carry out design checks and ensure that all constructional details and clearances conform to specification.
3. Prevent the possibility of corrosion and fouling during and subsequent to hydrostatic testing.
4. Startup conditions should avoid temperatures higher or velocities lower than the design values [3].
5. Maximize the flow velocities of process fluids to enhance the removal of the fouling deposits, provided that the fluid velocity is not high enough to cause excessive pressure drop or flow-induced vibration on the shell side. Ensure that velocities in tubes are in general above 2 m/s and about 1 m/s on the shell side [3]. Avoid stagnant areas where the flow velocities are less than those in the bulk of the core.
6. Assume nominal fouling resistance either from past experience or from published standards and design the heat exchanger with nominal oversizing. The oversizing may be of the order of 20–40%. It is generally prudent to avoid large fouling factors, which result in larger equipment. Larger equipment generally results in lower velocities and hence may accelerate fouling.
7. To minimize fouling of finned tube or plate fin heat exchangers, use optimum fin density. Otherwise the initial benefit of increased heat transfer will be offset by fouling in the long run. This is most appropriate for industrial air coolers, radiators of automobiles, and diesel locomotives. Compact heat exchangers functioning in outdoor unit are most prone to fouling due to airborne dirt, flying objects, leaves, and fibrous objects. Other considerations are in-line layouts to provide cleaning lanes for soot blowers, and wide pitches for dirty flue gases.
8. Fouling fluid on the tube side: When the fouling fluid is on the tube side, Mukherjee [6] recommends measures such as (1) using larger diameter tubes (a minimum of 25 mm OD), (2) maintaining high velocity (for cooling water, a minimum velocity of 1.5 m/s for mild steel, 1.2 m/s for nonferrous tubes, and as high as 5 m/s for titanium tubes is recommended), (3) leaving sufficient margin in pressure drop (for high fouling services, leave a margin of 30–40% between the allowable and calculated pressure drop), (4) using a spare tube bundle or spare exchanger, (5) using two shells in parallel (each with 60–70% of total capacity), (6) using wire-fin tube inserts, and (7) using on-line cleaning methods.
9. Fouling fluid on the shell side: When the fouling fluid is on the shell side, use a square or rotated square tube layout, minimize dead spaces by optimum baffle design, and maintain high velocity [6].
10. If severe fouling is inevitable, it is frequently better to install spare units. Installed spares will permit cleaning while the other unit is in service.
11. Proper selection of cooling medium can frequently avoid problems associated with foul-

ing. For example, air cooling in place of cooling water solves many of the corrosion and fouling problems such as scaling, biological growth, and many of the aqueous corrosion. The cleaning of bare tube or finned tube surfaces fouled by air is easier than surfaces fouled by water.

12. Particulate fouling, scaling, and trace-metal-catalyzed hydrocarbon reaction fouling can often be prevented by pretreatment of the feed streams to a heat exchanger by filtration, softening, and desalting, respectively [20].
13. Once the unit is onstream, operate at the design conditions of velocity and temperature.

14 CLEANING OF HEAT EXCHANGERS

In most applications, fouling is known to occur in spite of good design, effective operation, and maintenance. Hence, heat exchangers and associated equipment must be cleaned. The time between cleaning operations will depend upon the severity of the fouling problem. In some instances, cleaning can be carried out during periodical maintenance programs—say, twice yearly or annually—but in other cases frequent cleaning will be required, perhaps as frequently as monthly or quarterly. For example, locomotive radiators are air blown during their fortnightly schedules.

14.1 Cleaning Techniques

In general, the techniques used to remove the foulants from the heat exchanger surfaces, both on the shell side and on the tube side, can be broadly classified into two categories: mechanical and chemical. The cleaning process may be employed while the plant is still operating, that is, *on line*, but in most situations it will be necessary to shutdown the plant to clean the heat exchangers, known as *off-line* cleaning. In some instances combinations of these cleaning methods may be necessary. Each method of cleaning has advantages and disadvantages with specific equipment types and materials of construction.

14.2 Deposit Analysis

Information about the composition of fouling deposits through deposit analysis is extremely helpful to identify the source of the major foulants, to develop proper treatment, and as an aid in developing a cleaning method for a fouling control program [5]. The sample should represent the most critical fouling area. For heat exchangers and boilers, this is the highest heat transfer area [21]. Many analytical techniques are used to characterize deposit analysis. Typical methods include x-ray diffraction analysis, x-ray spectrometry, and optical emission spectroscopy.

14.3 Selection of Appropriate Cleaning Methods

Before attempting to clean a heat exchanger, the need should be carefully examined. Consider the following factors for selecting a cleaning method:

Degree of fouling.
Nature of the foulant, known through deposit analysis.
Chemical cleaning is associated with pumping hot corrosives through temporary connections and therefore the compatibility of the heat exchanger material and system components in contact with the cleaning chemicals.
Regulations against environmental discharges.
Accessability of the surfaces for cleaning.
Cost factors.

Precautions to Be Taken While Undertaking a Cleaning Operation

Precautions to be taken while undertaking a cleaning operation are listed in TEMA [17] paragraph E-4.32 and in Ref. 21:

1. Individual tubes should not be steam blown because this heats the tube and may result in severe thermal strain and deformation of the tube, or loosening of the tube to tube sheet joint.
2. When mechanically cleaning a tube bundle, care should be exercised to avoid damaging the tubes. Tubes should not be hammered with a metallic tool.

Various cleaning methods are discussed next.

14.4 Off-Line Mechanical Cleaning

Techniques using mechanical means for the removal of deposits are common throughout the industry. The various off-line mechanical cleaning methods are

1. Manual cleaning
2. Jet cleaning
3. Drilling and roding of tubes
4. Blasting
5. Soot blowing
6. Thermal cleaning

Manual Cleaning

Where there is good access, as with a plate or spiral heat exchanger, or a removable tube bundle, and the deposit is soft, hand scrubbing and washing may be employed, although the labor costs are high.

Jet Cleaning

Jet cleaning or hydraulic cleaning with high-pressure water jets can be used mostly on external surfaces where there is an easy accessability for passing the high pressure jet. Jet washing can be used to clean foulants such as [22]: (1) airborne contaminants of air-cooled exchangers at a pressure of 2–4 bar, (2) soft deposits, mud, loose rust, and biological growths in shell and tube exchangers at a pressure of 40–120 bar, (3) heavy organic deposits, polymers, tars in condensers and other heat exchangers at a pressure of 300–400 bar, and (4) scales on the tube side and fire side of boilers, preheaters, and economizers at a pressure of 300–700 bar. This method consists of directing powerful water jets at fouled surfaces through special guns or lances. A variety of nozzles and tips is used to make most effective use of the hydraulic force. The effectiveness of this cleaning procedure depends on accessibility, and care is needed in application to prevent damage to the tubes and injury to the personnel. Similar to water jet cleaning, pneumatic descaling is employed on the fire side of coal-fired boiler tubes.

Drilling and Roding of Tubes

Drilling is employed for tightly plugged tubes and roding for lightly plugged tubes. Drilling of tightly plugged tubes is known as bulleting. For removing deposits, good access is required, and care is again required to prevent damage to the equipment. A typical example is roding of radiator tubes plugged by solder bloom corrosion products.

Turbining

Turbining is a tube-side cleaning method that uses air, steam, or water to send motor-driven cutters, brushes, or knockers in order to remove deposits.

Blast Cleaning

Blast cleaning involves propelling suitable abrasive material at high velocity by a blast of air or water (hydroblasting) to impinge on the fouled surface. Hydroblasting is seldom used to clean tube bundles because the tubes are very thin. However, the technique is suitable to descale and clean tube-sheet faces, shells, channel covers, bonnets, and return covers inside and outside.

Soot Blowing

Soot blowing is a technique employed for boiler plants, and the combustion or flue gas heat exchangers of fired equipment. The removal of particles is achieved by the use of air or steam blasts directed on the fin side. Water washing may also be used to remove carbonaceous deposits from boiler plants. A similar cleaning procedure is followed for air blowing of radiators on the fin side during periodical schedule attention.

Thermal Cleaning

Thermal cleaning involves steam cleaning, with or without chemicals. This method is also known as hydrosteaming. It can be used to clean waxes and greases in condensers and other heat exchangers.

14.5 Merits of Mechanical Cleaning

The merits of mechanical cleaning methods include simplicity and ease of operation, and capability to clean even completely blocked tubes. However, this method may damage the equipment, particularly tubes, it does not produce a chemically clean surface, and the use of high pressure water jet or air jet may cause injury and/or accidents to personnel engaged in the cleaning operation—hence the personnel are to be well protected against injuries.

14.6 Chemical Cleaning

The usual practice is to resort to chemical cleaning of heat exchangers only when other methods are not satisfactory. Chemical cleaning involves the use of chemicals to dissolve or loosen deposits. The chemical cleaning methods are mostly off-line.

Choosing a Chemical Cleaning Method

Chemical cleaning methods must take into account a number of factors such as:

1. Compatibility of the system components with the chemical cleaning solutions. If required, inhibitors are added to the cleaning solutions.
2. Information relating to the deposit must be known beforehand.
3. Chemical cleaning solvents must be assessed by a corrosion test before beginning cleaning operation.
4. Adequate protection of personnel employed in the cleaning of the equipment must be provided.
5. Chemical cleaning poses the real possibility of equipment damage from corrosion. Precautions may be taken to reduce the corrosion rate to acceptable levels. On-line corrosion monitoring during cleaning is necessary [21]. Postcleaning inspection is extremely important to check for corrosion damage due to cleaning solvents and to gauge the cleaning effectiveness.
6. Disposal of the spent solution.

Chemical Cleaning Solutions

Chemical cleaning solutions include mineral acids, organic acids, alkaline bases, complexing agents, oxidizing agents, reducing agents, and organic solvents. Inhibitors and surfactant are

Table 2 Foulants and Common Solvents [22]

Foulant	Cleaning solvent
Iron oxides	Inhibited hydrofluoric acid, hydrochloric acid, monoammoniated citric acid or sulfamic acid, EDTA
Calcium and magnesium scale	Inhibited hydrochloric acid, citric acid, EDTA
Oils or light greases	Sodium hydroxide, trisodium phosphate with or without detergents, water-oil emulsion
Heavy organic deposits such as tars, asphalts, polymers	Chlorinated or aromatic solvents followed by a thorough rinsing
Coke/carbonaceous deposits	Alkaline solutions of potassium permanganate or steam air decoking

added to reduce corrosion and to improve cleaning efficiency [21]. Common foulants and cleaning solvents are given in Table 2 and common solvents and the compatible base materials are given in Table 3.

14.7 General Procedure for Chemical Cleaning

The majority of chemical cleaning procedures follow these steps [22]:

1. Flush to remove loose debris.
2. Heating and circulation of water.
3. Injection of cleaning chemical and inhibitor if necessary in the circulating water.
4. After sufficient time, discharge cleaning solution and flush the system thoroughly.

Table 3 Solvent and Compatible Base Metals [21]

Solvent	Base metal/foulant
Hydrochloric acid	Water-side deposits on steels. Inhibited acid can be used for cleaning carbon steels, cast iron, brasses, bronzes, copper-nickels, and Monel 400. This acid is not recommended for austenitic stainless steels, Inconel 600, Incoloy 800, and aluminum.
Hydrofluoric acid	To remove mill scale.
Inhibited sulfuric acid	Carbon steel, austenitic stainless steels, copper-nickels, admirality brass, aluminum bronze, and Monel 400. It should not be used on aluminum.
Nitric acid	Stainless steel, titanium, and zirconium.
Sulfamic acid	To remove calcium and other carbonate scales and iron oxides. Inhibited acid can be used on carbon steel, copper, admiralty brass, cast iron, and Monel 400.
Formic acid with citric acid or HCl.	To remove iron oxide deposit. Can be used on stainless steels.
Acetic acid	To remove calcium carbonate scale.
Citric acid	To clean iron oxide deposit from aluminum or titanium.
Chromic acid	To remove iron pyrite and certain carbonaceous deposits that are insoluble in HCl on carbon steel and stainless steels. It should not be used on copper, brass, bronze, aluminum, and cast iron.

5. Passivate the metal surfaces.
6. Flush to remove all traces of cleaning chemicals.

It is suggested that one employ qualified personnel or a qualified organization for cleaning services.

14.8 Off-Line Chemical Cleaning

Major off-line chemical cleaning methods are

1. Circulation
2. Acid cleaning
3. Fill and soak cleaning
4. Vapor-phase organic cleaning
5. Steam injection cleaning

Circulation. This method involves the filling of the equipment with cleaning solution and circulating it by a pump. While cleaning is in progress, the concentration and temperature of the solution are monitored.

Acid Cleaning. Scales due to cooling water are removed by circulating a dilute hydrochloric acid solution. This is discussed in detail with the discussion of cooling-water fouling.

Fill and Soak Cleaning. In this method, the equipment is filled with a chemical cleaning solution and drained after a period of time. This may be repeated several times until satisfactory results are achieved. However, this method is limited to small units only.

Vapor-Phase Organic Cleaning. This method is used to remove deposits that are organic in nature.

Steam Injection Cleaning. This method involves an injection of a concentrated mix of cleaning solution and steam into a fast-moving stream. The steam atomizes the chemicals, increasing their effectiveness and ensuring good contact with metal surfaces.

14.9 Merits of Chemical Cleaning

Chemical cleaning offers the following advantages over the mechanical cleaning:

1. Uniform cleaning and sometimes complete cleaning.
2. Sometimes chemical cleaning is the only possible method.
3. No need to dismantle the unit, but it must be isolated from the system.
4. Capable of cleaning inaccessible areas.
5. Moderate cleaning cost and longer intervals between cleaning.

14.10 Disadvantages of Chemical Cleaning Methods

Chemicals used for cleaning are often hazardous to use and require elaborate disposal procedures. Noxious gases can be emitted from the cleaning solution from unexpected reactions. Chemical cleaning corrodes the base metal and the possibility of excess corrosion cannot be ruled out. Complete washing of the equipment is a must to eliminate corrosion due to residual chemicals.

14.11 On-Line Cleaning Methods

There is an obvious need for an industrial on-line cleaning procedure that can remove fouling deposits without interfering with a plant's normal operation. On-line cleaning methods can be

either mechanical or chemical. On-line chemical cleaning is normally achieved by dosing with chemical additives.

14.12 On-Line Mechanical Cleaning Methods

Various on-line mechanical cleaning methods to control fouling in practice are:

1. Upstream filtration
2. Flow excursion
3. Air bumping of heat exchangers
4. Reversing flow in heat exchangers
5. Passing brushes through exchanger tubes
6. Sponge rubber balls cleaning system
7. Brush and cage system
8. SPIRELF system
9. Grit cleaning
10. Use of inserts
11. Self-cleaning fluidized-bed exchangers

Upstream Filtration (Debris Filter)

Cooling-water fouling can be controlled, and in some cases eliminated, by adequately filtering the intake water. Power-station condensers are more vulnerable to the intake of debris and biological organisms. One solution to prevent the blockage of condenser tubes is the installation of an upstream filtration system. All particles in the cooling water larger than 10 mm are kept in the filter and rinsed away through the debris discharge [23].

Flow Excursion

In this method the instantaneous flow is increased to remove the fouling deposits. This method is particularly applicable to a heat exchanger fouled badly due to the effects of low velocity either on the shell side or the tube side.

Air Bumping

This technique involves the creation of slugs of air, thereby creating localized turbulence as slugs pass through the equipment. The technique has been applied to the liquid system on the shell side of heat exchangers. Care has to be taken to avoid the possibility of producing explosive mixtures of gases if the process fluid is volatile and flammable [3].

Reversing Flow in Heat Exchangers

This is followed on the water side of the cooling-water system by intermittent reversal of flow and intermittent air injection.

Passing Brushes Through Exchanger Tubes

CTI developed the ram brush to clean fouled heat exchanger tubes [16]. The unit consists of a 2.5-in-long plastic dowel wrapped with 1.5-in nylon bristles. The brushes are propelled through the tube by an air and water gun and shot right through the tube. Water pressure of 40–60 psi and air pressure of 90–100 psi are sufficient to send the ram brush through standard heat exchanger tubes.

Sponge Rubber Ball Cleaning System

A large number of sponge rubber balls, slightly larger in diameter than the inner diameter of the tubes and having about the same specific gravity as sea water, are passed continuously into the inlet water box as shown in Fig. 6 (for instance, the Taprogge system) [23]. The cooling-

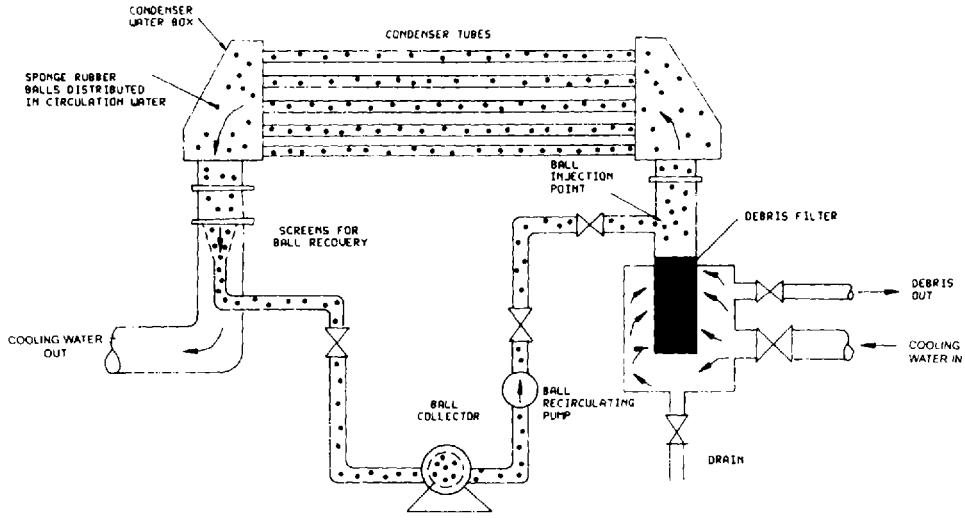


Figure 6 Sponge rubber ball cleaning system of a water cooled condenser. (From Ref. 23.)

water flow forces the balls through the tubes and the deposits on the tube walls are wiped out. The method may not be effective on longer runs once hard deposits are formed, or pitted. The balls used for normal operation should have the right surface roughness to gently clean the tubes, without scoring the tube surface. To remove heavy deposits, special abrasive balls that have a coating of carborundum are available [24].

Brush and Cage System or the Mesroc Automatic On-Load Tube Cleaning System

The brush and cage or the Mesroc automatic on-load tube cleaning system used for cleaning heat exchangers consists of cleaning sets each containing two baskets and a brush, all within the tubes of the heat exchanger, as shown in Fig. 7. The baskets are fixed to the ends of the heat exchanger tubes and every tube has its own brush. By reversing the flow direction, every brush is being moved from one end of the tube to the other, where it is retained by the basket. It remains there until the next cleaning cycle. The brushes moving to and fro keep the inner

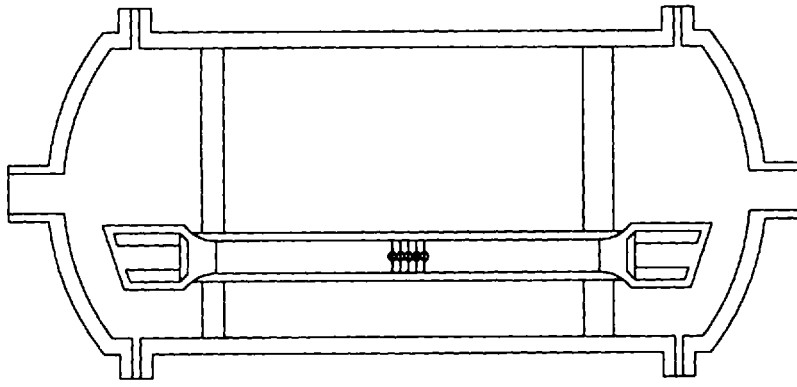


Figure 7 Brush and cage or Mesroc™ tube cleaning system.

walls clean. An actuator and a control system initiate the cleaning cycles. A major advantage of the system is that it does not require a recirculation system as for rubber ball system and an important disadvantage is the interruption of the flow in the heat exchanger and consequent disturbance of steady state conditions. Unlike the rubber ball circulation system, the brush and cage system has not been used to any extent in power plant condensers. However, it has been applied to single exchangers in process industries [3].

SPIRELF System

In the SPIRELF system (after Butterworth et al. [16]), Fig. 8, developed by Elf aquitaine (Paris La Defense, France), fine wire springs are threaded through the tubes and held in place by straight wires at the ends of the tubes as fluid flows through the tubes. Loose springs are located inside the tubes. The springs vibrate radially and axially under the influence of fluid flow. This action reduces buildup of fouling inside the tube walls.

Grit Cleaning

In this method, abrasive materials, such as sand, glass, or metal spheres, is passed through the tubes. The scouring action removes the deposits from the inside of the tubes. The method has found application in cooling-water systems, but it could be used in conjunction with any fouling fluids. A special grit blasting nozzle accelerates the grit and causes it to follow a sinusoidal path through the tube, dislodging the deposits [23]. Velocities more than 3 m/s are probably required for the technique to be effective. The demerits of this method are [3]:

1. The risk of settlement of particles in the low-velocity regions, as in the water boxes of exchangers where the local velocities are much lower than in the tubes.
2. The possibility of erosion–corrosion.
3. It is also necessary to filter out the particles from the liquid stream effectively, to avoid problems downstream from the exchanger.

Use of Inserts

Inserts, as a means of heat-transfer augmentation device, located on the inside of tubes, often reduce the incidence of fouling. Wire-wound inserts and twisted tape turbulence promoters have been found to reduce fouling by vibrating axially and radially under the influence of the fluid motion. However, in some instances with the use of wire-wound inserts, the fouling rate has increased with excessive pressure drop due to accumulation of deposits on wire inserts.

Self-Cleaning Fluidized-Bed Exchangers

A variation of the abrasive cleaning method is to use a fluidized bed of particles to control fouling on the outside or inside of tubular exchangers, known as self-cleaning exchangers. A

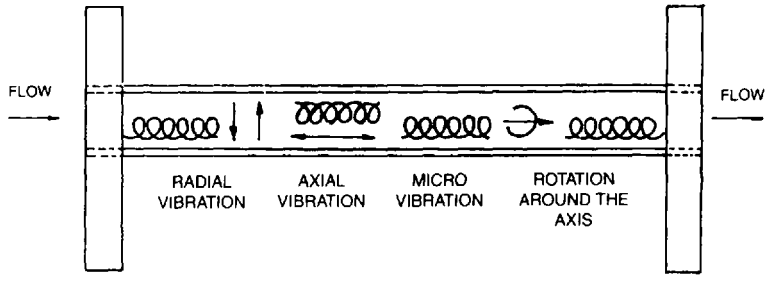


Figure 8 SPIRELF™ tube cleaning system. (From Ref. 16.)

fluidized-bed exchanger consists of a large number of parallel vertical tubes, in which small solid particles are kept in a fluidized condition by the liquid velocities. The particles have a slightly abrasive effect on the tube walls, so that they remove the deposits [25]. A typical example for fin-side foulant control is the fluidized-bed waste heat recovery (FBWHR) heat exchanger used to preheat combustion air for industrial furnaces. Fluidized-bed heat exchangers consists of horizontal finned heat exchanger tubes with a shallow bed of fine inert particles, which move upward with gas flow and give up heat to the finned tubes. Similarly on the tube side, the fine particles scrub the tube surfaces to minimize fouling deposit.

14.13 Merits of On-Line Cleaning

The merits of on-line cleaning are that it

1. Is more convenient.
2. Does not require any plant shutdown.
3. Can save time and labor.

However, the initial cost may be very high in certain cases.

15 FOULANT CONTROL BY CHEMICAL ADDITIVES

If fouling cannot be tackled adequately either by process design or equipment design, it can be further reduced by periodical on-line injection of additives into the process stream [20]. Chemical additives find wider use in cooling-water systems and to control fouling due to crystallization and freezing, chemical reaction or polymerization, precipitation, particulate, and scaling. The use of additives to prevent chemical reaction or polymerization fouling in liquids is well known in the petroleum refining industry, where a particular feedstock is a complex mixture of hydrocarbon and other organic materials [3]. Various types of additives and their functions are:

1. Alkali or acid dosing: By dosing either alkali or acid, pH may be controlled. This may be effective to control precipitation fouling. Acid dosing controls the hardness of hard or brackish water.
2. Complexing agents: Agents such as chelants complex the metallic ion into a ring structure that is difficult to ionize.
3. Chemical reactants: These are used to complex or tie up the active foulants. They can solubilize or condition the foulants to prevent deposition.
4. Sequestrant: This additive complexes the metallic ions into a water-soluble structure, thus preventing its adhesion to the heat exchanger surface. A sequestrator physically surrounds and isolates particles (e.g., EDTA).
5. Oxidizing agents: These oxidize the deposits, making them suitable for dissolution (e.g., chromic acid, sodium nitrite, potassium permanganate).
6. Reducing agents: Reduce the compounds in deposits and make them suitable for dissolution and to prevent the formation of hazardous by-products.
7. Inhibitors: Control cooling-water corrosion. Corrosion inhibitors such as filming amines stifle chemical reaction fouling [3].
8. Surfactant: Added to chemical cleaning solution to improve the wetting characteristics.
9. Antiscalants: In aqueous system, these additives chemically combine the scales to form soluble compounds.
10. Distortion agents: These interfere with the crystal structure so that it becomes more difficult for coherent crystal structures to form on surfaces.

11. Dispersants: Dispersants impart an electrical charge to the particles so that they are held in suspension in the bulk of the liquid and the particles pass through the equipment without deposition on heat transfer surfaces. Dispersants are helpful to control chemical reaction fouling.
12. Depressants: Depressants lower the freezing point of the solution such that the potential forming solids is brought down (e.g., glycols, alcohols).
13. Flocculating agent: Causes the particles to agglomerate so that they may be settled out of the cooling water or suitably filtered.
14. Threshold agents that prevent the creation of crystal nuclei around which the larger crystals form. They also arrest the growth of nuclei (e.g., polyphosphates). In cooling-water systems, threshold agents retard the precipitation of scale-forming salts.
15. Stabilizers: On reaching the solubility limit, stabilizers are able to retard the nucleation of individual low-solubility compounds and prevent any existing crystals from forming adhesive deposits.
16. Metal coordinators react with the trace metals and prevent them from functioning as fouling catalysts in the case of chemical reaction or polymerization fouling.
17. Biocides kills the micro-or macroorganism. Biostats arrest the growth of microorganisms.

16 CONTROL OF FOULING FROM SUSPENDED SOLIDS

Methods of control of fouling from suspended solids include [3]:

1. Pretreatment of process fluids by means such as filtration, softening, and desalting to control precipitation fouling, particulate fouling, and scaling.
2. Chemical treatment using dispersants and flocculating agents.

17 COOLING-WATER MANAGEMENT FOR REDUCED FOULING

Many industries use cooling water for one purpose or another. It is appropriate to include a section devoted to cooling-water management for fouling control. Traditionally, the treatment of cooling water has often been oriented toward corrosion control followed by foulant control. However, it is impossible to separate these twin problems in any treatment program, since one can lead to the other, and since both can occur simultaneously [5]. In addition to some of the on-line foulant control measures discussed already, specific features of cooling-water fouling control are discussed here. Cooling-water corrosion control measures are discussed in Chapter 12 on corrosion.

17.1 Forms of Water-Side Fouling

Water is by far the most common fluid subject to fouling. The quality of water used in the cooling system varies depending on its sources, like sea, river, ocean, lake, etc., and on the three forms of cooling water systems: once through, open recirculating, and closed systems. Cooling-water quality factors that contribute to fouling include turbidity, salinity, dissolved solids and hardness, biological organisms, airborne contaminants, etc. The quality of raw water changes according to weather conditions also. In general, fouling associated with cooling water can be classified under the following headings [3]:

Scaling due to crystallization of inverse solubility salts, mainly in cooling-tower water and sometimes in water drawn from a river, lake, or well.

Biological fouling of water drawn from a river, lake, sea, or the ocean; algae growth in open recirculating water.

Particulate fouling—Deposition of silts, sediments and suspended solids when water is drawn from a lake, river, or nearby seashore and due to airborne objects when water is exposed to the atmosphere.

Corrosion fouling due to cooling-water quality.

17.2 Influence of Surface Temperature on Fouling

The maximum tube surface temperature (the average between the temperature of the inlet fluid and the exchanger outlet water) on the water side at the tube–water interface is usually the critical concern. The recommended design surface temperature is 145°F (63°C) with 160°F (71°C) as a practical maximum. Heat exchangers with surface temperature above 160°F are prone to localized boiling. Boiling allows concentration of even the most soluble salts, with the threat of severe deposition and subsequent corrosion. For such a situation, water quality is to be improved by full softening or demineralization. (This material is based on Chenoweth [4].)

17.3 Foulant Control Versus Type of Cooling-Water System

Fouling problems and their control in each of the three basic types of cooling systems (once-through, open recirculating, and closed) are often quite different and thus require different techniques. Cooling-system operation and specific characteristics should be analyzed constantly as a continuing part of the foulant control program.

Once-Through System

In once-through cooling-water systems, usually the major foulants are biological organisms, mud, silt, debris, or other suspended matter, and pollutants [5]. This type of cooling-water system generally needs only upstream filtration and a mechanical on-line cleaning method of passing plugs or sponge rubber balls as in condensers cooled by seawater. Generally, economics favor the chemical treatment. The chemical additives most generally used are mud fluidizers, dispersants, and biocides, particularly chlorination. Environmental regulations may restrict certain chemical additives.

Open Recirculating System

In open recirculating systems with cooling towers or spray ponds, foulants originate in the makeup water, air or process contamination, and from lack of good corrosion control [5]. Hence, this system is frequently treated for foulant control. Both mechanical and chemical methods are used singly or jointly to overcome fouling problems. Remove solid particles through sedimentation ponds and/or continuous filtration. Mud fluidizers, dispersants, flocculating chemicals and foulant solubilizers, biocides, and other chemicals are added to control fouling.

Closed Recirculating Systems

The source of foulants is usually the corrosion products from heat exchangers and piping components. Corrosion control is mostly by inhibitors.

On-Line Chemical Control of Cooling-Water Foulants

Foulant control through some of the chemical additives include the following:

Threshold chemicals

Sequestrant and chelating chemicals, such as ethylenediamine tetraacetic acid (EDTA) and derivatives, nitrilotriacetic acid (NTA), organic phosphate esters, and organic phosphonates [5]

Dispersants (e.g., lignins, tannins, alginates, cellulose, starch products, sodium polymethacrylate, and polyvinyl pyridinium butyl bromide) [5]
Sludge fluidizers
Biocides

17.4 Control of Scale Formation and Fouling Resistances for Treated Cooling Water

The following values for cooling water assume that corrosion is under control and that biological growth does not represent a significant portion of fouling [4]:

1. Since scaling in cooling water system is due to inverse solubility phenomena, which normally take place about 140°F (60°C), keep the surface temperature below this temperature.
2. The cooling-water velocity is at least 4 ft/s on the tube side for most nonferrous alloy tubes and 6 ft/s for carbon steel tubes. Velocities as high as 15 ft/s have been used inside titanium tubes.
3. The velocity of cooling water on the shell side is at least 2 ft/s. Higher velocities are permitted if erosion can be tolerated or flow-induced vibration is not possible.
4. Under the preceding conditions, a reasonable design value for the cooling-water-side fouling resistance is 0.001 $hr \cdot ft^2 \cdot °F/Btu$.
5. The fouling resistance for a clean heat exchanger should be taken as 0.0005 $hr \cdot ft^2 \cdot °F/Btu$.

Chemical Means to Control Scaling

Calcium carbonate formation can be controlled by adding acids or specific chemicals, including sulfuric acid, polymeric inorganic phosphates, phosphonates, and organic polymers like polycarboxylates [26].

Removal of the Hardness Salts. Removal of the scaling chemical species such as magnesium and calcium from water prior to use in the system, by ion exchange and lime softening procedures, is effective in scaling control. The large volumes of water usually encountered in many cooling-water systems are likely to make the treatment costs of these methods very high. The modern trend toward very small volumes and high recirculation rates may offer cost restrictions [3].

Conversion of Hardness Salts to a More Soluble Form. Control of scale formation involves conversion of hardness salts to a more soluble form. Since the solubility of scale-forming species in cooling water generally increases with decreasing pH, the addition of acid to maintain the pH in the range 6.5–7.5 (with 6.5 as the recommended minimum) may reduce the scaling. These effects are shown schematically in Fig. 9. However, corrosion may be involved if the treatment is not carried out carefully. If large concentrations of sulfate are present, the use of sulphuric acid may cause sulfate scale to appear. Hydrochloric acid may be preferable under these circumstances [3].

Alkaline Cooling Water Operation for Scale Control. Alkaline cooling water treatment can also help in scale control. When the organic phosphorous compounds, including the well-known phosphates and polyol esters, and low-molecular-weight acrylic-acid-based polymers and copolymers are used properly, they completely prevent calcium carbonate deposition under alkaline conditions [27].

Electrostatic Scale Controller and Preventer

This is on-line equipment designed as a one-time fitment that performs the dual function of scale prevention and scale removal without using chemical additives. The equipment enables

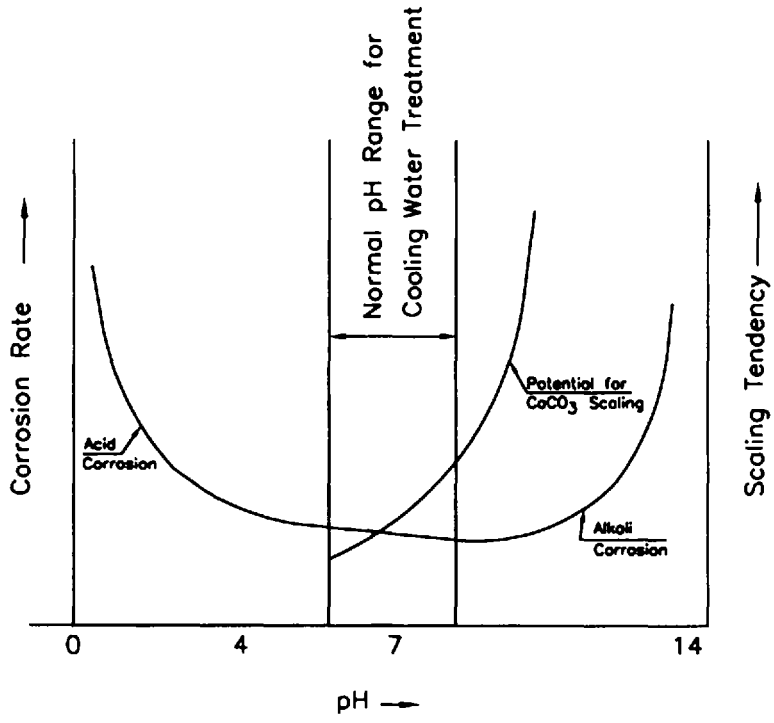


Figure 9 Cooling water corrosion and scaling control.

the use of untreated water. By subjecting the hard water to a carefully controlled electrostatic field, hardness ions are kept in suspension and prevented from depositing onto heat transfer surfaces. The merits of this system include (1) elimination of the use of expensive chemicals for descaling, (2) absence of corrosion of heat-transfer surfaces from the use of chemicals for cleaning, and (3) eliminating the need to shut down the equipment for scale cleaning.

17.5 Cleaning of Scales

Chemical Cleaning

Chemical cleaning has been the most common method of scale removal. Condensers are normally acid cleaned; sometimes alkaline cleaning is also employed. Various acid cleaning and alkaline cleaning methods are discussed in Ref. 28. Some of these methods are discussed next.

Chemical Cleaning Solvents for Scale Removal

Mineral acids such as hydrochloric, ammonium bifluoride, sulfamic acid, phosphoric acid, and sulfuric acid are strong scale dissolvers. Organic acids are much weaker. They are often used in combination with other chemicals to complex scales. Typical organic acids include formic, hydroxyacetic-formic, acetic, and citric acid. An advantage of organic acids is that they can be disposed of by incineration.

Hydrochloric Acid Cleaning. Since most of the scales formed are either calcium carbonate deposited by hard waters or rust, the most popular solvent is inhibited hydrochloric acid solution varying in concentration from 0.5 to 25.0%.

Lactic Acid Cleaning. Lactic acid solutions (20%) are also used for scale removal.

Sulfuric Acid. This is unsatisfactory for the removal of lime scale due to the formation of insoluble calcium sulfate. It is generally suitable for removing oxide scales such as rust.

Alkaline Cleaning. Some waters deposit scales that are very difficult to remove by acid cleaning methods. For example, thin scales containing a high percentage of silicate may be removed in a few hours by hot alkaline solutions such as sodium hydroxide. However, thick silicate films are difficult to remove.

Mechanical Cleaning. Calcium sulfate scales are not easily removed by chemical means but are generally dislodged by mechanical means such as steam shock blasting, rotary cutting, or sand blasting. Other mechanical methods include the use of bulleting with rubber, nylon, or twisted wire bristle.

Water Jet Cleaning. High-pressure water jet cleaning at about 9000 psi has been used in many situations. It is a time-consuming process and is therefore of little value.

Iron Oxide Removal

Conventional Cleaning Methods. Two common procedures generally followed in the industries for iron deposit removal are mechanical cleaning and chemical cleaning [29]:

1. Mechanical cleaning methods include water hydroblasting, lancing, and passing abrasive sponges, which remove most of the soft deposits but can leave hard, baked-on deposits.
2. Chemical cleaning with strong mineral acids or high concentrations of chelants up to 10% is used for temperatures up to 180°F (82°C).

With the chemical cleaning methods, the possibility of corrosion of underlying metal surfaces as they dissolve away from the iron deposits cannot be ruled out. To overcome this problem, a new on-line procedure for removing iron-based deposits from cooling water systems has been developed. This is explained next.

On-Line Removal of Iron Deposits [29]. The first step of the on-line cleaning process is the addition of a tannin-based, iron conditioning agent, which penetrates and softens the deposits. Later, a mild organic acid and dispersants are added and cause sloughing of the conditioned deposits. Postcleaning passivation of all metal surfaces can be accomplished by the normal corrosion inhibitor or by addition of on-line passivators to prevent flash corrosion. The process cleans transfer lines as well as heat exchangers and usually can be completed in 3 to 5 days.

NOMENCLATURE

A_{cr} = rate constant
A_i = surface area on the tube inside, m^2 (ft^2)
A_m = tube wall surface at the mid plane, m^2 (ft^2)
A_o = surface area on the tube outside, m^2 (ft^2)
A_r = chemical reaction fouling rate constant
A_w = total wall area for heat conduction, m^2 (ft^2)
d = tube outside diameter, m (ft)
d_i = tube inside diameter, m (ft)
E = activation energy for chemical reaction fouling
h_i = heat-transfer coefficient on the tube inside, $W/m^2 \cdot °C$ ($Btu/hr \cdot ft^2 \cdot °F$)
h_o = heat-transfer coefficient on the tube outside, $W/m^2 \cdot °C$ ($Btu/hr \cdot ft^2 \cdot °F$)
L = tube length, m (ft)
k_f = thermal conductivity of fouling deposit, $W/m \cdot °C$ ($Btu/hr \cdot ft \cdot °F$)

K_R = constant for crystallization rate
K_r = chemical reaction fouling (polymerizaton) rate
K_{sp} = solubility product of $CaCO_3$, $(mol/m^3)^2$
k_w = thermal conductivity of the conduction wall material, W/m • °C (Btu/hr • ft • °F)
$\dot{m}_d$ = rate of deposition of fouling mass on the heat-transfer surface, kg/m^2 • s (lbm/ft^2 • hr)
m_f = net rate of fouling mass deposition per unit area, kg/m^2 • s (lbm/ft^2 • hr)
m_f^* = asymptotic value of m_f
$\dot{m}_r$ = rate of removal of fouling mass from the heat-transfer surface, kg/m^2 • s (lbm/ft^2 • hr)
m_s = $CaCO_3$ scaling rate, kg/m^2 • s (lbm/ft^2 • hr)
R = gas constant
R_f = thermal resistance due to fouling on both sides of a heat exchanger surface, °C/W (°F • hr/Btu)
R_f = thermal resistance of fouling deposit for a unit surface area, m^2 • /W (ft^2 • °F • hr/Btu)
R_f^* = asymptotic value of thermal resistance due to fouling, °C/W (°F • hr/Btu)
R_i = fouling resistance on tube inside surface, m^2 • °C/W (ft^2 • °F • hr/Btu)
R_o = fouling resistance on tube outside surface, m^2 • °C/W (ft^2 • °F • hr/Btu)
R_T = total thermal resistance to heat transfer, °C/W (hr • °F/Btu)
R_w = thermal resistance of the separating wall, °C/W (hr • °F/Btu)
t = time, s
t_c = time constant
t_d = time delay period, s
T_s = heat-transfer temperature, °C (°F)
T_w = conduction wall temperature, °C (°F)
U_o = overall heat-transfer coefficient based on tube outside surface, W/m^2 • °C (Btu/hr • ft^2 • °F)
$U_{o,c}$ = overall heat-transfer coefficient based on tube outside surface in clean condition, W/m^2 • °C (Btu/hr • ft^2 • °F)
$U_{o,f}$ = overall heat-transfer coefficient based on tube outside surface in fouled condition, W/m^2 • °C (Btu/hr • ft^2 • °F)
x_f = thickness of fouling deposit, m (ft)
β = constant = $1/t_c$
Δt_w = tube wall thickness, m (ft)
ρ_f = density of the foulant, kg/m^3 (lbm/ft^3)

10
Flow-Induced Vibration of Shell and Tube Heat Exchangers

1 PRINCIPLES OF FLOW-INDUCED VIBRATION

Flow-induced vibration (FIV) of shell and tube heat exchangers (STHE) has been known for a long time. Heat exchanger tubes tend to vibrate under the influence of crossflow velocities, and if the amplitude of vibration becomes large enough, the tubes can be damaged by one or more of several mechanisms: (1) thinning due to repeated mid-span collision, (2) impact and fretting wear at baffle plate and tube interface, and (3) fatigue or corrosion fatigue due to high wear rate. Tube failures are costly because they result in plant shutdown to effect expensive repairs. These problems can be very serious in nuclear heat exchangers. Therefore, it is important to ensure that the modern shell and tube heat exchangers are free from flow-induced vibration problems at all operating conditions.

In the past heat exchangers were designed conservatively. With the success of the state-of-the art computer programs the trend is to design an efficient and compact heat exchanger. Higher thermal performance and the desirability of low fouling generally require higher flow velocities, while fewer baffle plates are desirable to minimize pressure drop. Higher flow velocities and reduced structural supports can lead to severe flow-induced vibration problems. In addition to these, the incorporation of new materials and processes without adequate considerations of the effects on the structural dynamics contributed to more flow-induced vibration problems, many of which led to tube failures [1]. It is essential to avoid such costly tube failures by a detailed flow-induced vibration analysis, preferably at the design stage after thermal design is over.

The flow-induced vibration phenomenon and the mechanism responsible have been studied extensively over the past 25–30 years. As a result, considerable literature has been developed and there have been efforts to define guidelines for vibration prevention. The subject continues to receive increasing attention because of its significance in heat exchanger applications, since as much as 60% of the heat exchangers in process industries are shell and tube type. References 1–18 brought about a better understanding of the flow-induced vibration phenomenon in shell and tube heat exchangers. In this chapter, the mechanisms that cause FIV and their evaluation, acceptance criteria, and design guidelines for vibration prevention are presented. Design guide-

lines included in TEMA Standards [19] and ASME Code Section III [20] are presented at appropriate places.

1.1 Principles of Flow-Induced Vibration

To excite vibration, energy must be fed to the tubes. The shell-side flow represents a source of energy that can induce and sustain tube vibration. The tubes, which are slender elastic beams among the heat exchanger components, are disturbed from their equilibrium position and undergo vibratory motion. Tube vibration is manifested by the periodic movement of the tube from its equilibrium position. With increasing crossflow velocity the tube movement has the following three manifestations [1]:

1. At low crossflow velocities, the tubes vibrate with low-amplitude random motion.
2. As the flow velocity is increased, rattling of tubes within the baffle holes takes place.
3. As the flow velocity exceeds a threshold value, high-amplitude motion takes place.

When the natural frequencies of the tubes are closer to the exciting frequency, resonance takes place. The relative motion between the tubes and the rigid structures like baffle supports and shell boundary can cause impact and fretting wear of tubes.

1.2 Possible Damaging Effects of the FIV on Heat Exchangers

Flow-induced vibration can cause severe damage to the tubes and other structural components of the heat exchanger. Mechanical failure as a result of tube vibration can occur from fatigue, collision damage, baffle damage, or tube joint failures [11,12]. These failures are discussed next.

Midspan collision: If the amplitude of response at the midspan is greater enough, collision with adjacent tubes takes place. The resulting wear causes failure of the tube wall under pressure.

Wear damage at the tube interface with the baffle support: Heat exchangers are generally designed with a clearance between the tube and the baffle plates. This clearance is required for ease of manufacture and design considerations. Tubes that suffer lower amplitude vibration close to baffle plates may fail by impact and fretting wear or fatigue.

Fatigue failures: If the contact stress due to impact or collision is greater than the allowable fatigue stress, fretting wear takes place.

Excessive operating noise level: When the shell-side medium is a gas, steam, or air, acoustic vibration will be induced within the tube bank containment. The acoustic vibration is characterised by pure-tone, low-frequency intense noise.

Severe pressure drop: Since the vibration of tube requires the energy from the shell-side fluid, the shell-side pressure drop increases. If the vibration is severe, destructive pressure fluctuations take place.

Intensified stress corrosion: Due to repeated impact with the baffle supports, intensive tensile stresses are induced on the tube surface. Susceptible tube material can fail due to the accelerated stress corrosion cracking in the shell-side medium. However, corrosion due to FIV is second to the failure of tube material due to the corrosive nature of shell-side fluid and/or tube-side fluid.

1.3 Most Probable Regions of Tube Failure

Although the tubes can fail anywhere in the exchanger, the regions more susceptible for flow-induced vibration are the high-velocity regions such as:

Largest unsupported midspan between two baffles.
Tubes located in the baffle window region at periphery of the tube bundle.
U-Bend regions of U-tube bundle.
Tubes located beneath the inlet nozzle.
Tubes located in the tube bundle bypass area, next to pass partition lanes.
Regions/interfaces where there is a relative movement between the tube and the heat exchanger structural components. Such regions include tube and baffle support interfaces and tube and tube-sheet interfaces.

1.4 Failure Mechanisms

The primary failure mechanisms which cause tube failure are [1]:

1. Impact wear (tube-to-tube and tube-to-baffle)
2. Fretting wear at the tube–baffle interfaces as a result of impact and/or sliding motion at the support
3. Combination of impact and fretting wear

1.5 Flow-Induced Vibration Mechanisms

The excitation mechanisms generally regarded as responsible for flow-induced vibration are

1. Vortex shedding or flow periodicity
2. Turbulent buffeting
3. Fluid elastic instability (FEI)
4. Acoustic resonance

Vortex shedding, turbulent buffeting, and acoustic excitation are due to resonance phenomena. Resonance occurs when the excitation frequency synchronizes with a natural frequency of the tubes. Fluid elastic instability sets in for tubes in a crossflow at a critical flow velocity or threshold velocity resulting in amplitude of tube response large enough to collide with the adjacent tubes and cause failure. Below the critical velocity FEI will not take place. Instability attains when the energy input to the tube mass-damping system exceeds the energy dissipated by the system.

1.6 Tube Response Curve

Figure 1 shows the tube response due to flow-induced vibration of tubes in tube bundles as a result of the three excitation mechanisms, namely, vortex shedding, turbulent buffeting, and fluid elastic instability. Each of them manifests itself only over a given range of flow parameters. However, it is believed that turbulent buffeting is operative in the entire range of flow parameters.

1.7 Dynamical Behavior of Tube Arrays in Crossflow

Flow of fluid over an array of elastic tubes results in (1) hydrodynamic effects or fluid oscillation (acoustic vibration) and (2) fluid–structure coupling. These effects caus hydrodynamic forces and fluid structure coupling forces. The dynamical behavior of an array of cylinders in increasing cross flow velocity (U) is considered to have three distinct manifestations as follows [3]:

1. At low flow velocities the cylinder respond principally to turbulent buffeting; with increasing flow velocity the amplitude of tube vibration goes up roughly as U^2.
2. At higher flow velocities, various kinds of resonance conditions may arise, such as vortex shedding, turbulent buffeting, and acoustical oscillation of gas column.

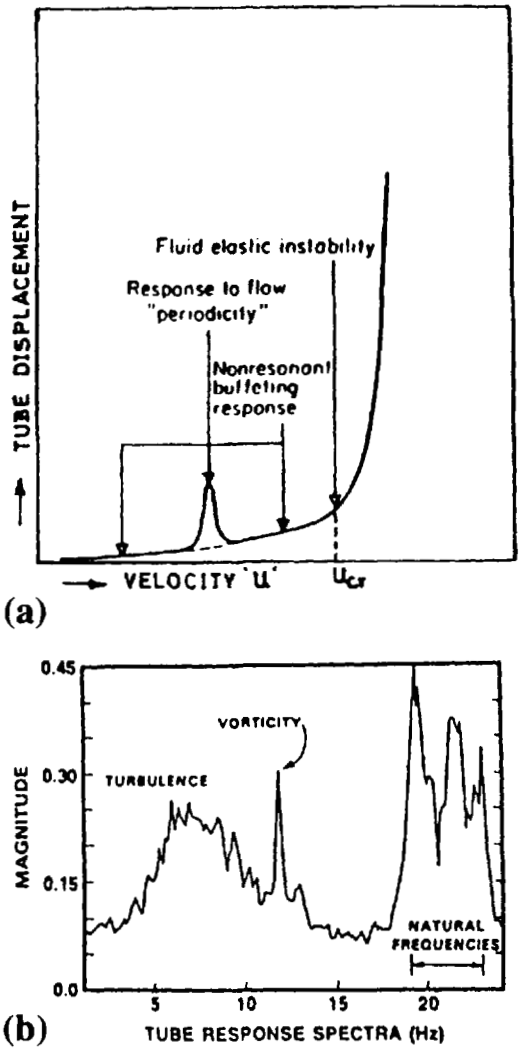


Figure 1 Tube response due to FIV mechanism. (a) Ideal diagram; (b) response spectrum of a tube in a 1.5 pitch ratio rotated square array with water crossflow and Aluminum tubes, $U_\infty = 0.117$ m/s. (From Ref. 3.)

3. At sufficient high flow velocities, fluid elastic instability will generally develop, and the amplitude of vibration increases rapidly with the flow velocity without a limit.

1.8 Hydrodynamic Forces

The hydrodynamic forces that contribute to FIV mainly fall into three groups:

1. Forces arising due to turbulent fluctuations of the pressure field
2. Forces resulting from periodic vortex shedding from tubes and formation of Von Karman's streets in their wakes
3. Motion-dependent fluid forces arising when the tubes are shifted elastically from their equilibrium within the bundle due to interaction with the flow

1.9 FIV Mechanisms Versus Flow Mediums

Of the different excitation mechanisms of flow induced vibration, only fluid elastic instability is a primary concern in all flow mediums. Other mechanisms have less importance in certain flow media. For example, turbulent buffeting is not of primary concern in gas flows since the low density of the gas does not result in a very high hydrodynamic force.

Hence, design restrictions are imposed to limit acoustic resonance and FEI [9]. Table 1 shows a breakdown of the importance of FIV mechanisms for each of the flow mediums in a tube bundle.

1.10 Approaches to FIV Analysis

Two approaches are normally followed to predict FIV effects of shell and tube heat exchangers:

1. Finite element modeling technique. This model simulates the time-dependent motion of a multispan heat exchanger tube in the presence of tube and baffle plate clearance, and the resulting wear is determined. This approach is normally followed for heat exchangers and steam generators used in very critical services such as nuclear energy generation.
2. Limiting amplitude of vibration. This approach linearizes the structural model by assuming tubes as classical beams with support plates offering simple support at the intermediate points and clamped at the tube-sheet ends. The designer then predicts the amplitude of vibration or instability thresholds and selects an acceptance criterion that will conservatively limit the vibration. This approach is used in this chapter. This procedure can be used to provide conservative designs or troubleshoot an existing heat exchanger and is widely accepted in the field.

1.11 Empirical Nature of Flow-Induced Vibration Analysis

Before discussing flow-induced vibration excitation mechanisms in detail, it is important to note that flow-induced vibration of shell and tube heat exchangers is a physical phenomenon that cannot be explained by simple empirical correlations [9,13]. It is most difficult to analyze [1,7] due to reasons like:

1. Tube bank dynamics is a multibody problem. The tubes are supported by multiple baffles with holes slightly larger than the tube diameter.
2. The interaction between the tube and the support plates is characterized by impacting as well as sliding motion. This makes the system nonlinear in nature.
3. The tubes and the surrounding fluid form a fluid–structure coupling that results in motion-dependent fluid forces that give rise to added mass, coupled modes, and damping,
4. Generally the flow field is quite complex, nonuniform, and quite unsteady, and the incidence of flow on the tubes is at variable angles to the longitudinal axis [21].
5. Structural complexity arises due to time-variant flow-dependent boundary conditions. Me-

Table 1 Vibration Excitation Mechanisms Versus Flow Medium for Crossflow [9]

Flow situations	Vortex shedding	Turbulent buffeting	FEI	Acoustic resonance
Liquid	Possible	Possible	Important	—
Gas	Possible	Possible	Important	Important
Two-phase	Unlikely	Important	Important	Unlikely

chanical tolerances, initial straightness, fit-up, and tube buckling due to manufacturing process add complexities in defining boundary conditions [22].

6. Effects of tube bundle parameters such as transverse and longitudinal pitches, tube layout pattern, pass partition lanes, shell to tube bundle clearance, number of tube rows, etc. on the occurrence of FIV cannot be correctly evaluated. The effects of some parameters have been studied by Gorman [23].

For these reasons, most of the methods in the analysis of tube bank dynamics are semiempirical in nature. To render the problem amenable for most analytical studies and experimental investigations, the flow conditions are idealized as:

1. The flow is uniform and steady
2. The incident of the flow is either axial or normal to the tubes.
3. The tube motion is linearized and it is assumed that the frequencies are well defined.
4. The baffle supports provide a simply supported condition.

2 DISCUSSION OF FLOW-INDUCED VIBRATION MECHANISMS

2.1 Vortex Shedding

Single tube

Consider a bluff body such as a circular cylinder in crossflow with the tube axis perpendicular to the flow. As the fluid flows past the tube, the wake behind the tube is no longer regular, but contains distinct vortices of the pattern shown in Fig. 2. The periodic shedding of vortices alternately from each side of the body in a regular manner gives rise to alternating lift and drag forces. This causes periodic movement of the tube. The familiar example is the von Korman vortex street behind a circular cylinder in crossflow.

Strouhal Number

The vortex shedding phenomenon can be characterized by a nondimensional parameter known as the Strouhal number S_u, and it is related to vortex shedding frequency f_v by

$$S_u = \frac{f_v D}{U_\infty} \tag{1}$$

where D is the tube outer diameter and U_∞ the upstream velocity. When the vortex shedding frequency f_v is sufficiently close to the natural frequency of the tubes f_n, the following will occur [4]:

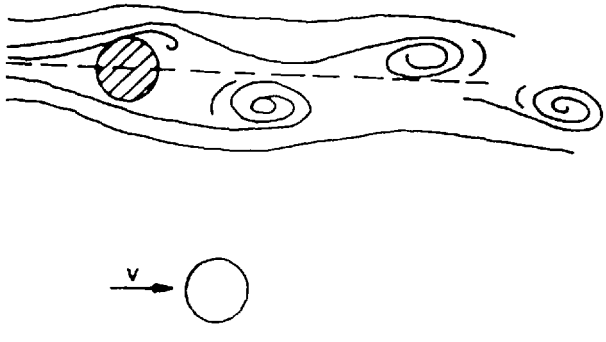


Figure 2 Vortex shedding past a single cylinder. (From Ref. 4.)

1. The vortex shedding frequency shifts to the structural natural frequency, developing the condition called "lock-in" or "synchronization." The lock-in phenomena leads to high-amplitude vibration with substantial energy input to the tube.
2. The lift force becomes a function of structural amplitude.
3. The drag force on the structure increases. However, the magnitude of the oscillating drag force is smaller than the oscillating lift force. Also the drag force occurs at twice the vortex shedding frequency.
4. The strength of the shed vortices increases

When the vortex shedding frequency coincides with the tube natural frequency or close to the natural frequency, resonance takes place. Resonance is characterized by large amplitudes of tube motion with possible damage to the tube. This mechanism has been variously referred to as vortex shedding, periodic wake shedding, Strouhal periodicity, or Strouhal excitation.

Since the vortex shedding drag force in the streamwise direction (drag) occurs at twice the vortex shedding frequency and the magnitude of drag force is smaller than the oscillating lift force, normally the analysis is carried out for lift forces only.

The vortex shedding phenomenon for a single cylinder with a peak response is well defined and has been dealt with by various researchers. Information on the lift and drag force coefficients and the Strouhal number over the complete range of Reynolds numbers of interest has been reviewed and presented by Chen and Weber [24]. For crossflow over a single tube the Strouhal number is an almost constant value of 0.2 for Reynolds numbers starting from 300 to the lower critical Reynolds number of 2×10^5 as shown in Fig. 3. After this point the Strouhal number seems to increase due to the narrowing of the wake. But as the Reynolds number exceeds the value of 3.5×10^5 and when the supercritical range is reached, the wakes become completely turbulent. No regular vortex shedding exists any more. This exceptional case lasts only to a Reynolds number of 3.5×10^6. After exceeding this value, a Von Korman vortex can be formed again. In the transcritical range the Strouhal number is about 0.27 [25].

Vortex Shedding for Tube Bundles

Traditionally it has been thought that for multiple tube arrays or ideal tube banks subjected to crossflow, vortex shedding will occur similar to that of a single isolated cylinder. However, research to date shows vortex shedding produces a peak response similar to that observed for isolated cylinders for the first few tube rows in a tube array, and a clear resonant peak does not occur for most of the tube arrays. Vortex shedding past a tube bank is shown in Fig. 4. Owen [26] disputed the existence of vortices deep within a tube bank. Deep within the tube bank, the dominant spectral frequency for both lift and drag forces of vortex shedding and turbulent buffeting coincides. According to Blevins [8] and Zukauskas [13], within a closely

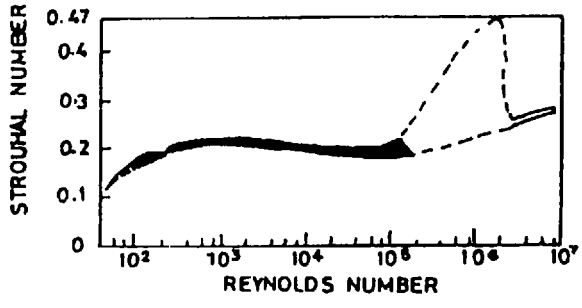


Figure 3 Strouhal number for a single cylinder. (From Ref. 24.)

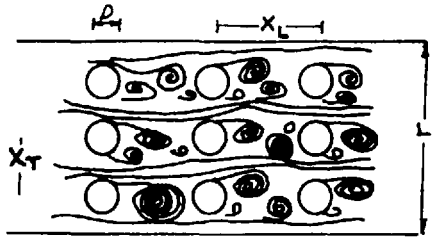


Figure 4 Vortex shedding in a tube array.

spaced tube arrays with pitch ratio less than 2.0, the vortex shedding degenerates into broadband turbulent eddies rather than a single distinct frequency. Such a mechanism is referred to as turbulent buffeting and is described in the next section. In the light of this discussion, it may be concluded that vortex shedding is a potential design problem in the front tube rows of a tube bank in liquid flows or may be a source of acoustic noise in gas flows [6]. Hence the possibility of the first few tube rows being excited by vortex shedding must be determined. Within the array, vortex shedding can be regarded as a special case of turbulent buffeting and analyzed by the method of random vibration, as explained in the next section.

The expression for the Strouhal number for a tube bank is same as Eq. 1, but the velocity term U_∞ should be replaced by the crossflow velocity. Even though many researchers used either pitch velocity or row velocity to account for crossflow velocity for their row models, in all these sections the velocity term is the crossflow velocity calculated by Tinker's method [27] or Bell's method [28] or the stream analysis method [29] or by proprietary programs such as HTFS [30], HTRI [31], B-Jac [32], or by any other standard programs. This is similar to the TEMA [19] approach—that is, for all excitation mechanisms, E-shell crossflow velocity is calculated by Tinker's method.

Avoiding Resonance

The design criterion for the possibility of vortex shedding as an excitation source involves the parameter of reduced frequency ($f_n D/U$) and/or the determination of Strouhal number, S_u. Determination of the Strouhal number is discussed next.

Calculation of Strouhal Number for Tube Arrays

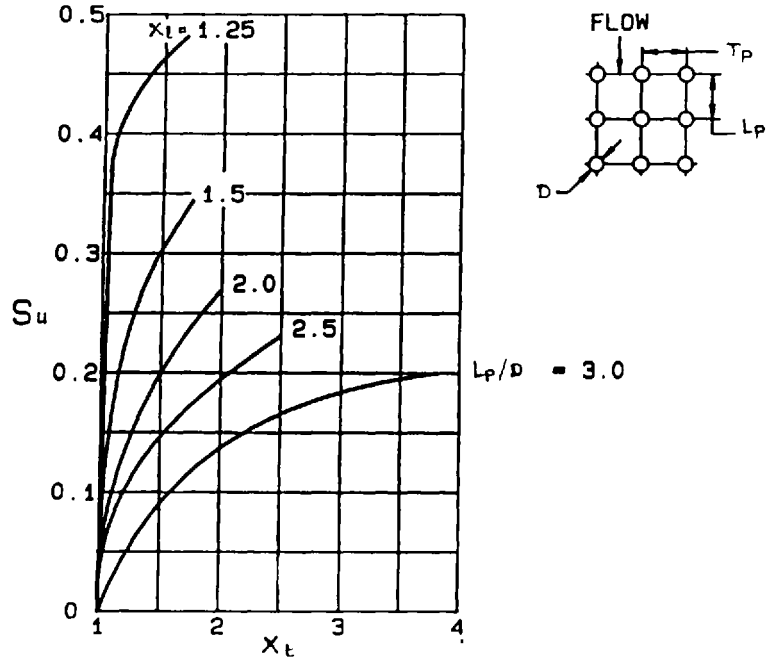
The Strouhal number may be determined from Chen's Strouhal maps [25] shown in Fig. 5 and Fitz-Hugh [33]. These maps are plotted with various pitch ratios. Alternately, it can be determined from correlations of Zukauskas [13] or Zukauskas and Katinas [34] and Weaver et al. [35]. The correlation of Weaver et al. is given next. Blevins [8] presents Fitz-Hugh's map and TEMA presents Chen's map.

Correlations of Weaver et al. [35]. The expressions for Strouhal number S_u for various tube layout patterns (Fig. 6) are given by

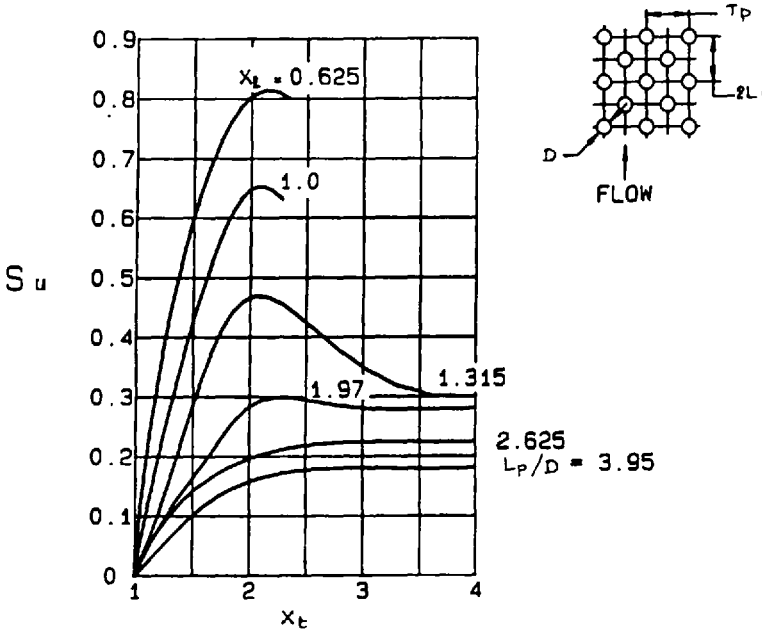
$$S_u = \frac{1}{1.73X_p} \quad \text{for } 30^\circ \text{ layout} \tag{2a}$$

$$= \frac{1}{1.16X_p} \quad \text{for } 60^\circ \text{ layout} \tag{2b}$$

$$= \frac{1}{2X_p} \quad \text{for } 90^\circ \text{ and } 45^\circ \text{ layout} \tag{2c}$$



(a) $X_l = \frac{L_P}{D}$; $X_t = \frac{T_P}{D}$



$X_l = \frac{L_P}{D}$; $X_t = \frac{T_P}{D}$

(b)

Figure 5 Strouhal maps. (a) Inline array; and (b) staggered array. (Copyright Tubular Heat Exchanger Manufacturers Association, 1988.)

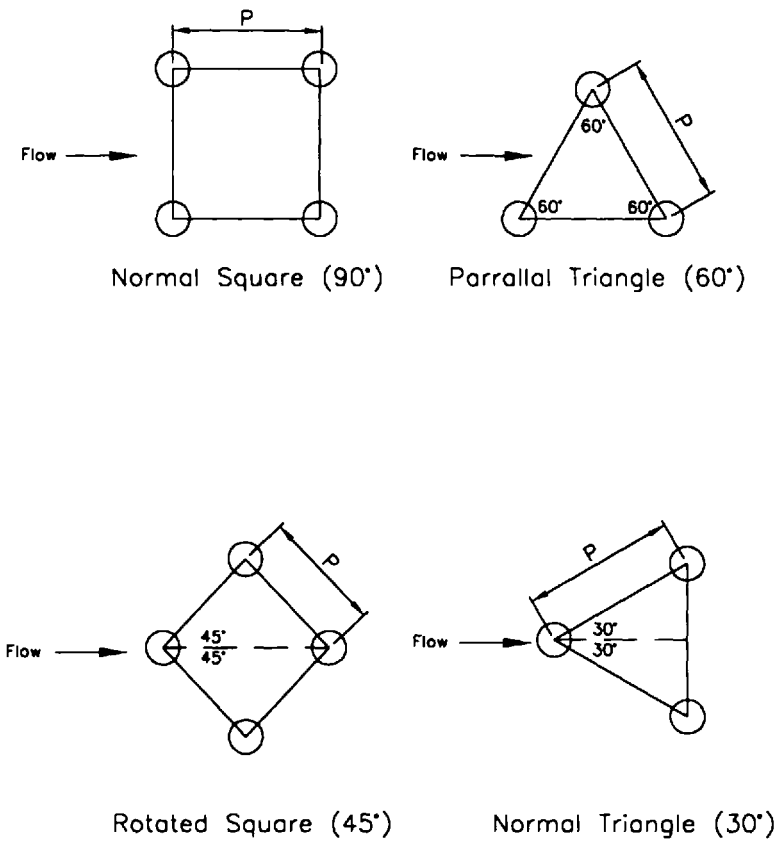


Figure 6 Tube layout patterns.

where X_p is the pitch ratio, p/D. The original expressions were in terms of upstream velocity. They were corrected for gap velocity by multiplying the expressions by $(p - D)/p$.

Criteria to Avoid Vortex Shedding

Criterion of Pettigrew and Gorman. The criterion to avoid resonance due to vortex shedding is expressed in terms of reduced frequency, $(f_n D/U)$ by Pettigrew and Gorman [36] as

$$\frac{f_n D}{U} > 2S_u \tag{3}$$

Criterion of Au-Yang [4]. To avoid resonance, the Strouhal number S_u must be less than 20% of the reduced frequency [7]:

$$\frac{f_n D}{U} < 0.2S_u \tag{4}$$

Criteria of Au-Yang et al. [4]. The criteria for avoiding lock-in due to vortex shedding in the first two to three rows in a tube bank are given by Au-Yang et al. [4]. They are:

1. If the reduced velocity for the fundamental vibration mode $(n = 1)$ is satisfied by the relation

$$\frac{U}{f_n D} < 1 \qquad \text{for} \quad n = 1 \tag{5}$$

both lift and drag direction lock-in are avoided.

2. For a given vibration mode if the reduced damping C_n is large enough,

$$C_n > 64 \tag{6}$$

then lock-in will be suppressed in that vibration mode.

3. If for a given vibration mode

$$\frac{U}{f_n D} < 3.3 \tag{7}$$

and $C_n > 1.2$, then lift direction lock-in is avoided and drag direction lock-in is suppressed. The reduced damping C_n is calculated by the equation

$$C_n = \frac{4\pi\xi_n M_n}{\rho_s D^2 \int_0^{L_e} \phi_n^2(x)\, dx} \tag{8}$$

where M_n is the modal mass, Le is the tube length subject to vortex shedding, and $\phi_n(x)$ is the mode shape. The expression for M_n is given by

$$M_n = \int_0^{L_e} m(x)\phi_n^2(u)\, du \tag{9}$$

where $m(x)$ is the tube mass per unit length. Substituting the expression for the modal mass and normalizing the mode shape, the expression for reduced damping C_n is given by

$$C_n = \frac{4\pi\xi_n m}{\rho_s D^2} \qquad \text{when } M_n = m(x) = m \tag{10}$$

These guidelines are included in ASME Code Section III.

In the preceding equations, f_n is the tube natural frequency, m is the effective tube mass per unit length, and ξ_n is the critical damping ratio. The effective tube mass is the sum of structural mass, fluid added mass due to the contribution of shell-side fluid displaced by the vibrating tube, and the mass of the contained fluid per unit length. In simple terms,

$$m = \text{structural mass} + \text{added mass} + \text{contained fluid mass}$$

$$= m_a + m_i + m_t \tag{11}$$

$$= \frac{\Pi D^2 C_m \rho_s}{4} + \frac{\Pi D_i^2 \rho_i}{4} + \frac{\Pi(D^2 - D_i^2)\rho}{4} \tag{12}$$

where m_a is the added mass per unit length, m_i the contained fluid mass per unit length, and m_t the structural mass per unit length. The terms ρ_i, ρ_s, and ρ are density of tube-side fluid, shell-side fluid, and tube metal, respectively. The added mass involves a term called added mass coefficient, C_m. The determination of f_n, C_m, and critical damping ratio ξ_n are discussed at the end of this section.

Response Due to Vortex Shedding Vibration Prediction by Dynamic Analysis

If resonance occurs, the maximum tube response can be obtained by a forced response analysis as described in refs. 4 and 36. Sandifer [9] describes this from first principles. The generalized equation for the tube response $y(x)$ for any mode number j is given by [36]:

$$y(x) = \frac{C_L \rho D}{16\pi^2 \xi_{nj} f_{nj}^2 M_j} \phi_j(x) \int_0^{L_t} U^2(x) \phi_j(x)\, dx \tag{13}$$

The mode shape in Eq. 13 is normalized by

$$\int_0^{L_t} \phi^2(x)\, dx = 1 \tag{14a}$$

and evaluation of this integral gives

$$\phi(x) = \sqrt{\frac{2}{L_t}} \sin(\pi x / L_t) \tag{14b}$$

$$= \sqrt{\frac{2}{L_t}} \quad \text{(maximum value)}$$

After normalizing the modal mass, the maximum response y_{max} is given by

$$y_{max} = \frac{C_L \rho D U^2}{4\pi^3 \xi_n f_n^2 M} \quad \text{where } M = m \tag{15}$$

The peak lift coefficients C_L(peak) for various tube layout patterns are tabulated in Refs. 9 and 37 and are given in Table 2. A conservative design can be obtained with C_L(peak) = 0.091. According to these, as long as the peak amplitude of tube response is less than 2% of the tube diameter D, it is unlikely that the tube motion would be sufficient to control and correlate wake shedding along the tube. Accordingly, the acceptance criterion is given by

$$y_{max} < 0.02D \tag{16}$$

This procedure is included in ASME Code Section III.

Table 2 Lift Coefficient C_L(peak)

		Lift coefficient C_L		
Tube layout pattern	p/D	C_L(rms)	C_L(peak)	C_L(peak) conservative
Triangular (30°)	1.33	0.046	0.065	0.091
	1.36	0.064	0.091	
	1.54	0.018	0.025	
	1.57	0.028	0.040	
Rotated triangular (60°)	1.23	0.064	0.091	
	1.36	0.012	0.017	0.091
	1.54	0.033	0.047	
	1.57	0.057	0.081	
Square (90°)	1.47	0.048	0.068	0.091
Rotated square (45°)	1.3	0.007	0.010	0.091
	1.5	0.035	0.049	

Source: Ref. 9.

3 TURBULENCE-INDUCED EXCITATION MECHANISM

3.1 Turbulence

In general, higher flow rates promote and maintain high turbulence in the fluid, which is desirable for enhanced heat transfer, but the high turbulence is a source of structural excitation. Heat exchanger tubes respond in a random manner to turbulence in the flow field. In addition to structural excitation, turbulence in the flow can affect the existence and strength of other excitation mechanism, namely, vortex shedding.

3.2 Turbulent Buffeting

Turbulent buffeting in a tube bank, sometimes called subcritical vibration, refers to the low-amplitude response before the critical velocity is reached and away from the vortex lock-in velocity region due to unsteady forces developed on a body exposed to a high turbulence in the flow field.

The turbulent flow has been characterised by random velocity perturbations associated with turbulent eddies spread over a wide range of frequencies distributed around a central dominant frequency. When the dominant central frequency in the flow field coincides with the lowest natural frequency of the tube, a considerable amount of energy transfer takes place, leading to resonance and high-amplitude tube vibration. Even in the absence of resonance, turbulent buffeting can cause fretting wear and fatigue failure. With a design objective of 40 years codal life for nuclear power plant steam generators and heat exchangers, even relatively small tube wear rates cannot be acceptable [6,38]. Hence, turbulence excitation becomes an important design consideration in the design of reliable heat exchangers.

3.3 Owen's [26] Expression for Turbulent Buffeting Frequency

Based on experimental study of gas flow normal to a tube bank, Owen [26] correlated an expression for the central dominant frequency of the turbulent buffeting, f_{tb}, as

$$f_{tb} = \frac{U}{DX_l X_t}\left[3.05\left(1 - \frac{1}{X_t}\right)^2 + 0.28\right] \tag{17}$$

where

X_l = longitudinal pitch ratio = L_p/D (L_p is longitudinal pitch)

X_t = transverse pitch ratio = T_p/D (T_p is transverse pitch)

Weaver and Grover [39] reviewed various works and observed that Owen's approach is most reliable for predicting the peak frequency in the turbulence, provided the minimum gap velocity is used in the expression. The preceding correlation is applicable for a tube bank with transverse pitch ratio more than 1.25. Since this correlation has not been tested for liquids, it should be restricted to gases only. TEMA has included this expression.

3.4 Turbulent Buffeting Excitation as a Random Phenomenon

By assuming that the tube vibrations represent steady-state random process, expression for rms amplitude of tube response have been developed by Au-Yang et al. [4], Au-Yang [7], and Pettigrew and Gorman [36]. Sandifer [9] describes the equation for tube response from first principles. The mean square resonant response of a lightly damped structure is given by:

$$\bar{y}^2(x) = \frac{\rho^2 D^2 L_i}{256\pi^3} \sum_j \frac{[C_R(f_j)U_j^2\phi_j(x)]^2}{\xi_{n,j} f_{n,j}^3 M_j^2} \tag{18}$$

After normalizing the mode shape over the span length and for the first mode of vibration, the maximum mean square response is given by

$$\bar{y}^2_{\max} = \frac{L_i[C_R(f)\rho_c U^2 D\sqrt{2/L_i}]^2}{256\pi^3 \xi_n f_n^3 M^2} \qquad \text{where } M = m \tag{19a}$$

$$\bar{y}^2_{\max} = \frac{[C_R(f)\rho_c U^2 D]^2}{128\pi^3 \xi_n f_n^3 M^2} \qquad \text{where } M = m \tag{19b}$$

$$y_{rms} = \sqrt{\bar{y}^2_{\max}} \tag{19c}$$

A recommended acceptance criterion is

$$y_{rms} \leq 0.010 \text{ in or } 0.254 \text{ mm} \tag{20}$$

The parameter $C_R(f)$ can be determined from the Fig. 7 [36].

These guidelines are included in ASME Code Sec. III.

4 FLUID ELASTIC INSTABILITY

A group of circular cylinders submerged in crossflow can be subjected to dynamic instability, typically referred to as fluid elastic instability. Fluid elastic vibration sets in at a critical flow velocity and can become of large amplitude if the flow is increased further. The familiar examples of FEI vibration are aircraft wing flutter, transmission line galloping, and vibration of tube arrays in heat exchangers.

A sudden change in vibration pattern within the tube array indicates instability and is attained when the energy input to the tube mass-damping system exceeds the energy dissipated by the system. Fluid elastic instability has been recognized as a mechanism that will almost

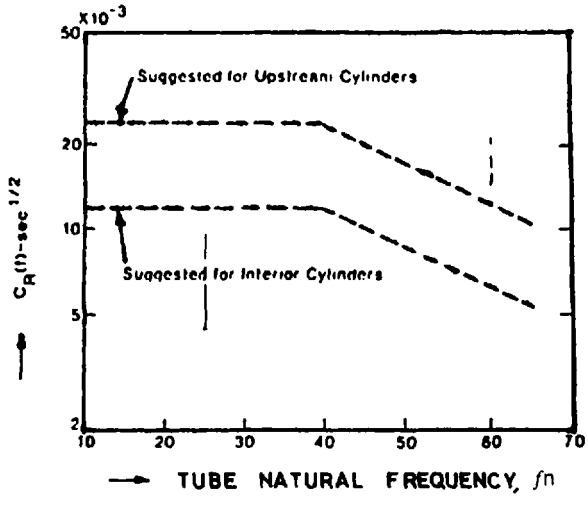


Figure 7 Random excitation force co-efficient, C_R. (From Ref. 36.)

lead to tube failure in a relatively short period of time, and this is to be avoided at any cost by limiting the crossflow velocity [40]. However, some tube response due to turbulent buffeting or vortex shedding cannot be avoided, and this may lead to long-term fretting failure [41]. If vortex shedding resonances are predicted at velocities above the fluid elastic critical velocity, then vortex shedding is not a concern and it is not necessary to predict the associated amplitudes of vibration.

4.1 Fluid Elastic Forces

Flow of fluid over an array of elastic tubes results in the following fluid elastic forces or fluid damping forces with or without fluid–structure coupling. The forces induced on the tube fall into the following three major groups [4,5]:

1. Forces that vary approximately linearly with displacement of a tube from its equilibrium position. The resulting instability mechanism is known as displacement mechanism.
2. Velocity-dependent fluid forces such as fluid inertia, fluid damping, and fluid stiffness forces. The resulting instability mechanism is known as velocity mechanism.
3. The combination of the foregoing forces.

Instability may result from any or all of these fluid forces, which are functions of the tube motion.

4.2 General Characteristics of Instability

Before understanding the fluid elastic instability mechanism it is pertinent to the know the features of instability. A sudden change in vibration pattern within the tube array is indicative of instability. The general characteristics of tube vibrations during instability include

1. Large vibration amplitude
2. Synchronization between adjacent tubes
3. Fluid structure coupling

Typical trajectories of tube motion during instability of a tube array are given in Fig. 8.

4.3 Connors Fluid Elastic Instability Analysis

The pioneering work on FEI was initiated by Connors [42]. In 1970, Connors studied a tube row in a wind tunnel using a quasi-static model. The Connors single-row tube model is shown schematically in Fig. 9. The model, using fluid dynamic coefficients obtained from tests on a stationary body to determine the fluid dynamic forces acting on a vibrating body, is generally called a quasi-static model. According to Connors, the FEI results when the amount of energy input to tubes in crossflow exceeds the amount of energy that can be dissipated by the system damping. As a result of energy imbalance, the tube vibration will intensify to the point that clashing with adjacent tubes takes place. From his model, he measured quasi-steady force coefficients and developed a semi-empirical stability criterion for predicting the onset of fluid elastic instability of tube arrays. The stability criterion relates the critical flow velocity U_{cr} to the properties of the fluid and structures of the form

$$\frac{U_{cr}}{f_n D} = K\left(\frac{m\delta}{\rho_s D^2}\right)^a \tag{21}$$

where U_{cr} is the critical velocity and δ is equal to $2\pi\xi_n$.

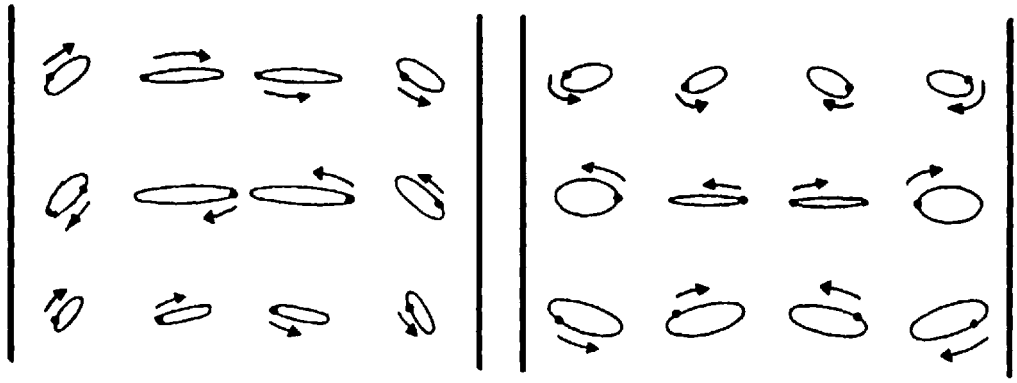


Figure 8 Tube motion during instability. (From Ref. 46.)

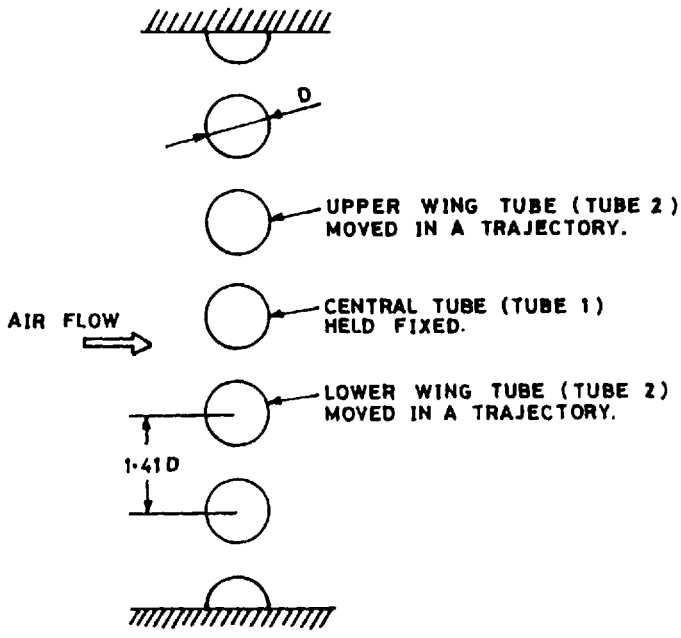


Figure 9 Connors single row FEI model. (From Ref. 42.)

For his single-row experimental model with $p/D = 1.41$, the value of K is 9.9 and $a = 0.5$. Accordingly, the expression for instability is given by

$$\frac{U_{cr}}{f_n D} = 9.9 \left(\frac{m\delta}{\rho_s D^2} \right)^{0.5} \tag{22}$$

In this expression, the two main parameters are $U_{cr}/f_n D$, the reduced velocity, and $m\delta/\rho_s D^2$, the mass damping parameter. The Connors vibration mechanism was later referred to as a displacement mechanism and the model is known as a quasi-static model.

For tube bundles, the parameter $K = 9.9$ does not hold good, and hence numerous investi-

gators conducted extensive experiments to form a more appropriate instability parameter K. Several new models—the analytical model [43–45] and the unsteady model [15,16,46,47]—have been proposed. A few researchers [48–50] refined the quasi-static model. A mechanism called the velocity mechanism was suggested by Blevins [8]. Many reviews [3,6,14] and the state of the art [6] have been presented. However, most of the researchers proposed a stability criterion similar to the Connors stability equation form. In the following sections, various instability models are discussed briefly. Subsequently the design guidelines and acceptance criteria are presented. Wherever these criteria are common with TEMA and ASME Code, this is specified.

4.4 Analytical Model

The analytical model was proposed by Lever and Weaver [43–45]. From a series of flow visualization experiments conducted in air flow to investigate the underlying mechanism responsible for the fluid elastic instability of tube arrays in crossflow, the authors assumed that a single elastic tube surrendered by rigid tubes becomes independently unstable; the effect of neighboring tubes is primarily to define the flow field unique to each array pattern. The model is known as tube-in-channel model.

4.5 Unsteady Model

Prior to 1980, the mechanism thought to cause FEI was a displacement mechanism and the dominant force causing instability was referred as fluid elastic stiffness force. From the unsteady fluid dynamic forces of Tanaka and Takkhara [46,47] and refs. 15, 16, and 51–53, it is known that the instability is caused not only by a displacement mechanism but also by an additional mechanism called the velocity mechanism. This instability model is called the unsteady model. The existence of velocity mechanism was demonstrated analytically and verified experimentally by Chen et al. [54,55]. In this model, the fluid elastic instability is caused by the following mechanisms:

1. Position-dependent FEI, which occurs at relatively high flow velocities. The instability mechanism is called displacement mechanism.
2. Fluid damping type instability occurring at low flow velocities. The instability mechanism is called velocity mechanism.

In most cases, either the velocity mechanism or the displacement mechanism or a combination of both will be dominant. The displacement mechanism and velocity mechanism are discussed in detail in refs. 5, 16, and 55. They are briefly explained next.

Displacement Mechanism

According to this mechanism, the instability is due to fluid elastic force, which is proportional to the displacement of tubes. This mechanism is dominant for high values of reduced flow velocity corresponding to gas flows. The instability criterion is given by [5]:

$$\frac{U_{cr}}{f_n D} = \alpha_d \left(\frac{m\delta}{\rho_s D^2} \right)^{0.5} \tag{23}$$

where α_d is a function of fluid elastic stiffness coefficients.

Velocity Mechanism

According to this mechanism, the dominant fluid force is a flow-velocity-dependent damping force that is proportional to the velocity of the tubes. At low reduced velocity, the fluid damp-

ing force may act as an energy dissipation mechanism, whereas at high reduced velocities it acts as an excitation mechanism. When it acts as an excitation mechanism, the system damping is reduced. The tube loses stability once the modal damping of a mode becomes negative. This type of instability is called fluid damping controlled instability, and it is dominant for low values of reduced velocities that correspond to liquid flow. The instability criterion is given by [5]:

$$\frac{U_{cr}}{f_n D} = \alpha_s \left(\frac{m\delta}{\rho_s D^2} \right)^{0.5} \tag{24}$$

where α_s is a function of fluid damping coefficients.

Unsteady Model

Based on the displacement mechanism and velocity mechanism, the dynamics of the tube array in simple form is written as [16]:

$$[M_s + M_f]\{\ddot{q}\} + [C_s + C_f + C_v]\{\dot{q}\} + [K_s + K_f]\{q\} = [F] \tag{25}$$

where

$[M_s]$ = structural mass

$[M_f]$ = added mass of the fluid

$[C_s]$ = structural damping of the system

$[C_f]$ = viscous damping of the still fluid

$[C_v]$ = velocity-dependent damping of the fluid

$[K_s]$ = structural stiffness

$[K_f]$ = fluid elastic stiffness

$[F]$ = fluid forces independent of the tube motion

$\{q\}$ = structural displacement

$\{\dot{q}\}$ = structural velocity

$\{\ddot{q}\}$ = structural acceleration

In the preceding expression the terms in square brackets are matrices and those in braces are vectors. The constituents of fluid dynamic forces are

1. $[M_f]\{\ddot{q}\}$, fluid inertia force
2. $[C_f + C_v]\{\dot{q}\}$, fluid damping force
3. $[K_f]\{q\}$, fluid elastic force

The major obstacle in the analysis of the instability mechanism by the unsteady model is to determine the flow-velocity-dependent damping $[C_v]$ and fluid stiffness $[K_f]$ for every tube layout pattern and for the entire range of reduced flow velocity of interest, either analytically or experimentally. These forces were measured experimentally by Tanaka and Takkahara [47].

4.6 Design Recommendations

Chen's Criterion

From the data of many investigators, Chen [5] recommended a criterion for the lower bound of critical velocity. Later, Chen [56] revised the criteria as shown in Table 3 where the expression for χ is given. TEMA included this criterion. The notable feature of Chen's criterion is the presence of pitch ratio (p/D) in the equation:

Table 3 TEMA Criteria for FEI [19]

Tube pattern	Parameter range for χ	Reduced velocity $U_{cr}/f_n D$
30°	$0.1 \le \chi \le 1.0$	$8.86(p/D - 0.9)\chi^{0.34}$
	$1 < \chi \le 300$	$8.86(p/D - 0.9)\chi^{0.5}$
60°	$0.01 \le \chi \le 1.0$	$2.80\chi^{0.17}$
	$1.0 < \chi \le 300$	$2.80\chi^{0.5}$
90°	$0.03 \le \chi \le 7$	$2.10\chi^{0.15}$
	$7 < \chi \le 300$	$2.35\chi^{0.5}$
45°	$0.1 \le \chi \le 300$	$4.13(p/D - 0.5)\chi^{0.5}$

$$\chi = \frac{m\delta}{\rho_s D^2} \tag{26}$$

Au-Yang et al. [4] Criteria

From the instability database of ref. [5], Au-Yang et al. [4] developed the following criteria:

1. For the displacement mechanism where $m\delta/\rho_s D^2 > 0.7$, the stability equation is similar to Connors equation with $a = 0.5$. The values for K are given in Table 4.
2. For the velocity mechanism where $m\delta/\rho D^2 < 0.7$, the criteria of displacement mechanism may be used. However, this will give a conservative value.

These guidelines are included in ASME Code, Section III.

Conservative Guideline. If the crossflow velocity is less than the critical velocity calculated using $K = 2.1$ and $a = 0.5$ with $\xi_n = 0.5\%$ in gas flow and 1.5% in liquid flow, instability is almost certainly not a problem.

Guidelines of Pettigrew and Taylor

From a parametric study of nearly 300 data points on FEI of the flexible tube bundles subjected to single-phase crossflow, a design criterion was evolved by Pettigrew and Taylor [14]. The criterion is

$$\frac{U_{cr}}{f_n D} = 3.0\left(\frac{m\delta}{\rho_s D^2}\right)^{0.5} \tag{27}$$

The reasons for variation among the various acceptance criteria are discussed in ref. 14.

Table 4 Au-Yang et al. [4] Criteria for FEI

Pitch angle	30°	60°	45°	90°	All arrays
K_{mean}	4.5	4.0	5.8	3.4	4.0

4.7 Acceptance Criteria

To avoid FEI, the acceptance criteria are:

1. Normal criterion:

$$U_{cr} > U \tag{28}$$

2. Conservative criterion, [9]:

$$\frac{U}{U_{cr}} = <0.5 \tag{29}$$

4.8 Stability Diagrams

The presentation of the stability criteria in a graphical form (log-log plot) with mass damping parameter on the x-axis and reduced velocity on the y-axis is referred to as a stability diagram. It shows relatively distinct "stable" and "unstable" regions [48]. A typical stability diagram is shown in Fig. 10.

5 ACOUSTIC RESONANCE

Acoustic resonance is excited by the crossflow of air, gas, or steam. It is due to the vibration of the standing waves surrounding the tubes. The existence of standing waves is described as follows. The gas flow across the tube bank has, in addition to its mean velocity in the flow direction, a fluctuating velocity transverse to the mean flow direction. This fluctuating velocity is associated with the standing waves (gas column). Standing waves (Fig. 11) occur transverse to both the tube axis and flow direction. The resonant vibration of the standing waves surrounding the tubes is commonly called acoustic resonance or acoustic vibration. It is usually characterized with intense, low-frequency, pure-tone noise. When the excitation frequency is closer to the standing wave frequency or both coincide in a heat exchanger, there is a possibility of acoustic vibration. Also, if the standing wave frequency coincides with natural frequencies of structural components such as casing, tubes, etc., it may be structurally harmful [57] and it can

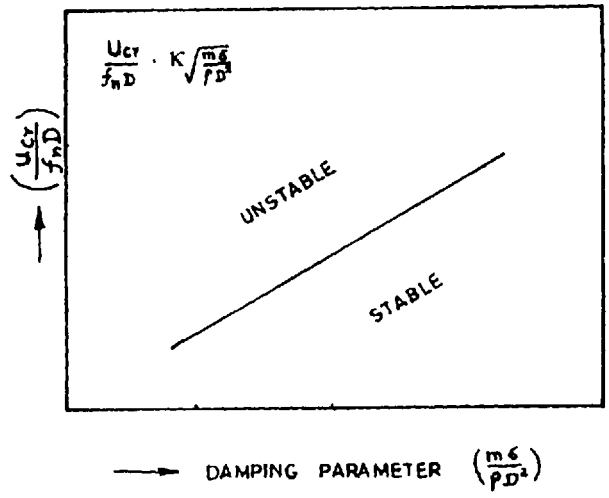


Figure 10 Stability diagram.

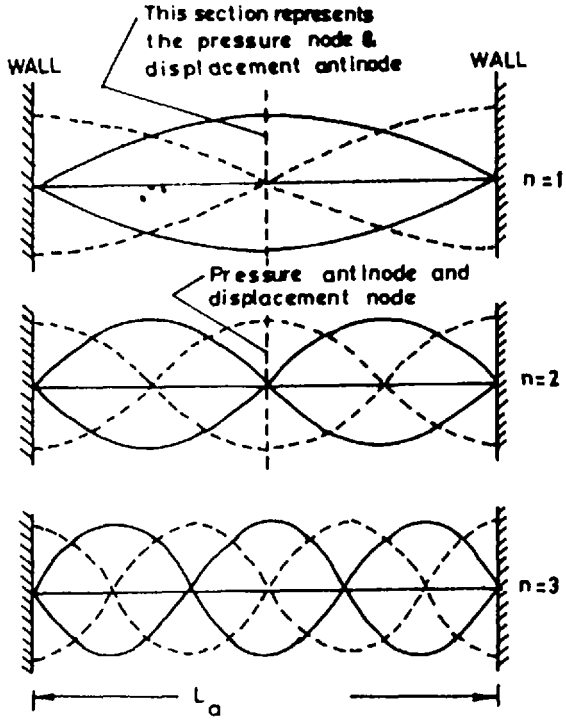


Figure 11 Variation of the fluctuating transverse velocity and fluctuating pressure associated with standing waves with one, two, and three half waves. (Solid lines are velocity and dashed lines are pressure.) (From Ref. 70.)

affect the performance characteristics of the heat exchanger by increasing the pressure drop. Acoustic resonance occurred in-line and staggered tube banks, single rows of tubes, helically coiled tubular heat exchangers, air heater economizers, superheaters, ducts of rectangular and circular shells, and others [58–61].

5.1 Principle of Standing Waves

Standing waves will develop if the distance L between the bounding walls is $\lambda/2$ or a multiple of $\lambda/2$, that is, $L = n\lambda/2$ where $n = 1,2,3, \ldots$ and λ is the wavelength of the standing wave. The standing wave frequencies are given by

$$f_a = \left(\frac{nC}{2L_a} \right) \qquad \text{for } n = 1,2,3, \ldots \tag{30}$$

where C is the velocity of sound in the shell-side medium, L is the characteristic dimension (normally the enclosing walls of the flow passages), and n is the mode number.

The velocity of sound C in the shell-side medium is given by

$$C = \sqrt{g_c Z \gamma R_c T / M_g} \tag{31}$$

where

g = acceleration due to gravity (32.174 ft/sec^2 or 9.81 m/sec^2)

Z = gas compressibility factor

R_c = universal gas constant, 1545.32 lbf · ft/lb mole or 847.6 kgf · m/kg mole °K

T = absolute temperature of the gas, °R/°K

= °F + 459.69°F or °C + 273.16

M_g = molecular weight of the gas, lb mole or kg mole

γ = ratio of specific heat of gas at constant pressure to constant volume

The value of M_g (molecular weight of the gas) for air or flue gas is 28.97 lb mole and for steam 18.02 lb mole, and γ, the ratio of the specific heat of the gas at constant pressure to that at constant volume, is 1.4 for air or flue gas and 1.328 for steam [62].

Typical standing waves with fundamental, second, and third modes are shown in Fig. 11. Normally the standing wave will form in open lanes of 45° or 90° layout angle geometries, since the least exciting energy is required to form in these tube layout patterns. According to Barrington [63], acoustic vibration occurs most frequently with a rotated square (45°) tube layout compared to other tube layouts. Although the rotated square geometry exhibited the greatest resistance to FEI, this was marred by the presence of intense acoustic standing waves. Hence they may not be suitable for shell-side gaseous medium [40].

Effect of Tube Solidity on Sound Velocity

For shell and tube heat exchangers, Parker [64] and Burton [65] have shown that the actual speed of sound C in the shell-side fluid is reduced due to the presence of the tubes. The rate of decrease of the sound speed is mainly dependent on the solidity ratio σ of the tube layout and a weak function of added mass coefficient, C_m. Accordingly, formulas for effective speed of sound C_{eff} through the tube bundle are given by

$$C_{eff} = \frac{C}{\sqrt{(1+\sigma)}} \quad \text{Parker} \tag{32a}$$

$$C_{eff} = \frac{C}{\sqrt{(1+C_m\sigma)}} \quad \text{Burton} \tag{32b}$$

For widely spaced arrays $C_m = 1$ (approximately).

The solidity ratio σ is defined as the ratio of free flow area to the frontal area of the tube layout. The expression for σ for the various tube layout patterns shown in Fig. 12 is given by Blevins [8]:

$$\sigma = 0.9069\left(\frac{D}{p}\right)^2 \quad \text{for 30 or 60° layout}$$

$$= 0.7853\left(\frac{D}{p}\right)^2 \quad \text{for 90° layout}$$

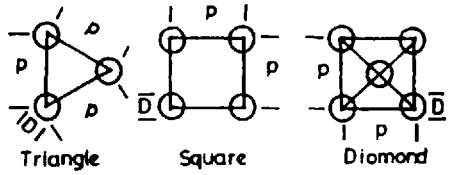


Figure 12 Solidity factor. (From Ref. 60.)

$$= 1.5707 \left(\frac{D}{p} \right)^2 \qquad \text{for } 45° \text{ layout} \tag{33}$$

In heat exchangers of normal size, either the fundamental mode or the second mode is most likely to occur. However, in large exchangers with shell diameter of the order of 20–30 m the acoustic vibration can be excited up to fifth or sixth mode.

Principles of acoustic vibration, their evaluation, and prediction methods are discussed by Grotz and Arnold [66], in refs. 24, 25, and 57–62, by Barrington [63,67], and by Fitzpatrick [68]. The better understanding of acoustic resonance is mostly due to Dr. Blevins. In this section, the excitation mechanisms are discussed and acceptance criteria are defined.

5.2 Expressions for Acoustic Resonance Frequency

Two versions of expression, one in terms of shell-side pressure and shell-side fluid density (TEMA) and the other in terms velocity of sound through shell-side medium and shell dimensions, are given next for calculating the acoustic vibration frequency f_a.

TEMA Expression

$$f_a = \frac{483.2}{L_a} \left(\frac{p_s}{\rho_s} \right)^{0.5} \qquad \text{(use TEMA dimensional units)} \tag{34}$$

Blevins Expression

Circular Shell. For a circular shell of radius R, the expression for standing wave frequency is given by [8,62]:

$$f_a = \frac{C_{\text{eff}} \lambda_i}{2\pi R} \tag{35}$$

where $\lambda_1 = 1.84$ and $\lambda_2 = 3.054$.

Rectangular Shell. Consider a closed rectangular volume of dimension L_x, L_y, and L_z with tubes as shown in Fig. 13. The indices i, j, and k give the number of acoustic waves in the flow direction (x), transverse direction (y), and tube axial (z) direction respectively. The acoustic modes typically excited by crossflow are the transverse modes (modes $j = 1, 2, 3, \ldots$) in the y direction, which are perpendicular to the flow direction and tube axis. Longitudinal modes i in the flow direction x and transverse modes k in the direction of the tube axis z are rarely excited by crossflow. Assuming that both the tubes and the duct are rigid structures and the dimension of the wavelength of the standing waves is of comparable size to the duct width and much higher than the tube diameters, the expression for acoustical frequency of the duct is given by [8]:

$$f_a = \frac{C_{\text{eff}}}{2} \left[\left(\frac{i}{L_x} \right)^2 + \left(\frac{j}{L_y} \right)^2 + \left(\frac{k}{L_z} \right)^2 \right]^{0.5} \tag{36}$$

In the absence of any standing waves in x and z directions ($i = k = 0$) the equation simplify to the following [62]:

$$f_a = \frac{jC_{\text{eff}}}{2L_y} \tag{37}$$

where L_y is the chamber dimension in the y direction, which is equal to the shell width.

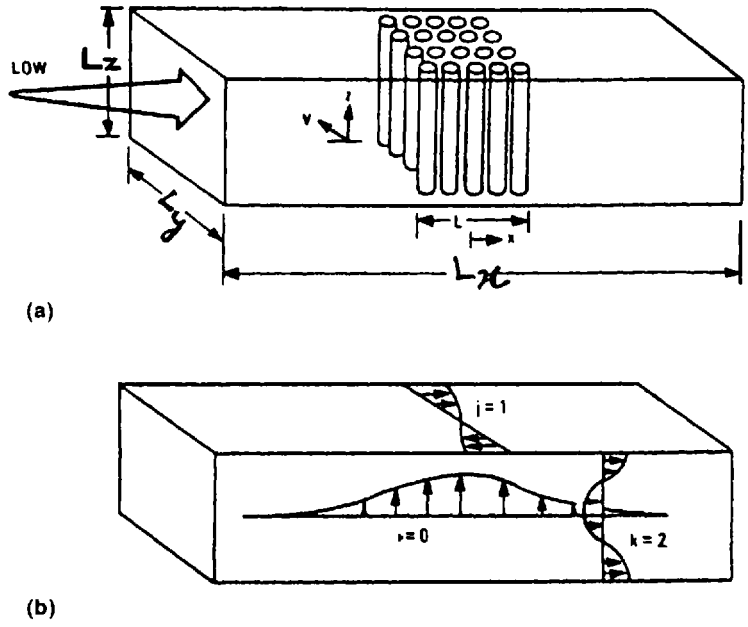


Figure 13 Acoustic modes in a closed rectangular chamber with tubes. (a) Tube bundle in duct; (b) typical mode shape of pressure in cutoff mode. (From Ref. 60.)

5.3 Excitation Mechanisms

The occurrence of acoustic resonance in tubular heat exchangers is caused by either a vortex shedding mechanism or turbulent buffeting.

Vortex Shedding Mechanism

According to vortex shedding theory, if the frequency of vortex shedding coincides with the standing wave frequency, a strong acoustic oscillation of the gas column is possible and resonance is said to occur. Thus the resonance criterion is

$$f_a = f_v \tag{38}$$

The mechanism of vortex shedding is shown schematically in Fig. 14, which shows an in-line heat exchanger tube bank with its containment; f_{a1} and f_{a2} represent the frequencies of the first and second acoustical modes of the containment [69]. Normally it is considered that for the lock-in phenomenon to occur, the acoustic resonance should be within ±20% of vortex shedding frequency.

Turbulent Buffeting Mechanism

According to this theory, acoustic resonance takes place if the dominant frequency of the turbulent eddies coincides with the standing wave frequency of the gas column. Thus the criteria for resonance is given by

$$f_a = f_{tb} \tag{39}$$

The turbulent buffeting frequency f_{tb} for fundamental mode is determined using the criteria of Owen [26] or Fitzpatrick [68]. TEMA included Owen's buffeting frequency criteria.

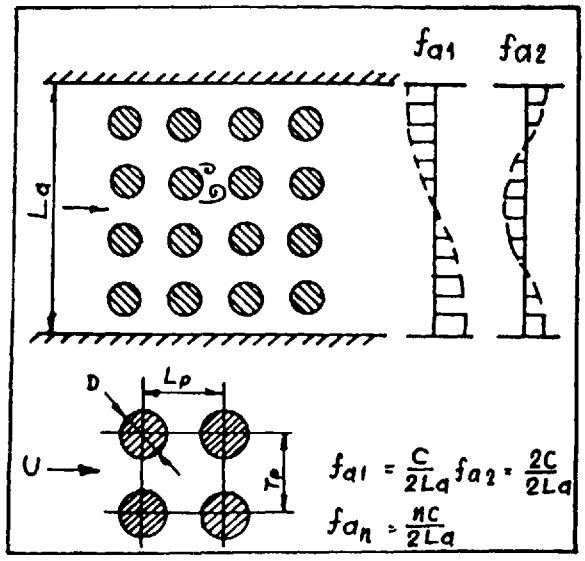


Figure 14 Acoustic resonance due to vortex shedding.

5.4 Acceptance Criteria for Occurrence of Acoustic Resonance

Vortex Shedding

Eisinger criterion [25,57]. Eisinger expressed a criterion in terms of the Chen number, ψ, for in-line arrays (Fig. 15a). The Chen number is a function of the Reynolds number, Strouhal number, and longitudinal and transverse pitch ratios. The expression for the Chen number is

$$\psi = \frac{\mathrm{Re}}{S_u} \frac{(2X_l - 1)^2}{4X_l^2 X_t} \tag{40}$$

where the Reynolds number is given by

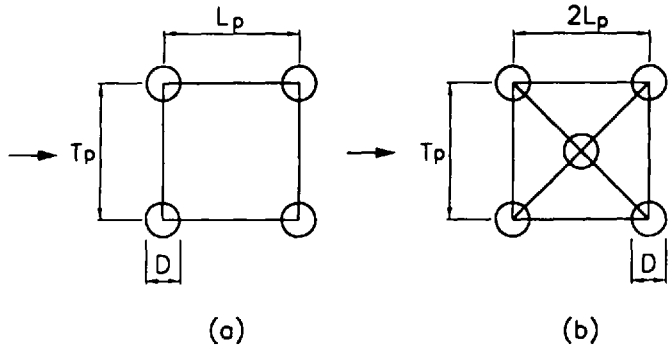


Figure 15 Tube layout parameters for calculating sound pressure level. (a) Inline array; and (b) staggered array.

$$\mathrm{Re} = \frac{UD}{\nu} \tag{41}$$

Acoustic resonance criteria are as follows:

$\psi < 2000$ No vibration

$\psi = 2000\text{–}4000$ Low likelihood of vibration

$\psi > 4000$ High likelihood of vibration

The TEMA condition is: Acoustic resonance is possible if $\psi > 2000$.

For staggered arrays as shown in Fig. 15b, replace L_p by $2L_p$ [60].

Blevins Criterion. Acoustic resonance is possible if [8]:

$$\frac{(1-\alpha)S_u U}{D} < f_a < \frac{(1+\beta)S_u U}{D} \tag{42}$$

where the parameters α and β take their values as follows.

Normal Criterion. For normal design criteria, $\alpha = \beta = 0.2$, and the resulting expression for the Blevins criterion is

$$\frac{0.8S_u U}{D} < f_a < \frac{1.2S_u U}{D} \tag{43}$$

Conservative Criterion. For the conservative criterion, $\alpha_{max} = 0.40$ and $\beta_{max} = 0.48$, and the resulting expression for the Blevins criterion is

$$\frac{0.6S_u U}{D} < f_a < \frac{1.48S_u U}{D} \tag{44}$$

TEMA prescribes $\alpha = \beta = 0.2$ in the conditionality equation.

The acoustical Strouhal number due to vortex shedding is determined either from Chen's plot [25] or from the Fitz-Hugh [33] map or from the correlations of Weaver et al. [35]. TEMA included Chen's plot.

Blevins [8] Sound Pressure Level (SPL) at Resonance. If resonance is predicted, calculate SPL from the following equation [8]:

$$\mathrm{SPL} = 20 \log_{10}(p_{rms}/0.00002) \tag{45}$$

or determine from the sound pressure level maps of Blevins [8] shown in Fig. 16. These maps are valid for Reynolds number up to 95.1×10^3.

Check: If SPL < 140 dB, there is no damage either to the structural components or harmful to the surroundings.

The typical lock-in phenomenon, frequency of vortex shedding, f_v, and sound pressure level (SPL) as a function of crossflow velocity are shown in Fig. 17.

Turbulent Buffeting

Owen [26] Criterion for Resonance.

$$0.8f_{tb} < f_a < 1.2f_{tb} \tag{46}$$

Criterion of Rae and Murray [70]. Resonance will not occur for

$$\frac{U}{f_a D} < 2(X_1 - 0.5) \tag{47}$$

This criterion is included in TEMA.

Grotz and Arnold [66] Criterion for In-Line Arrays. Calculate the slenderness ratio τ from the following equation:

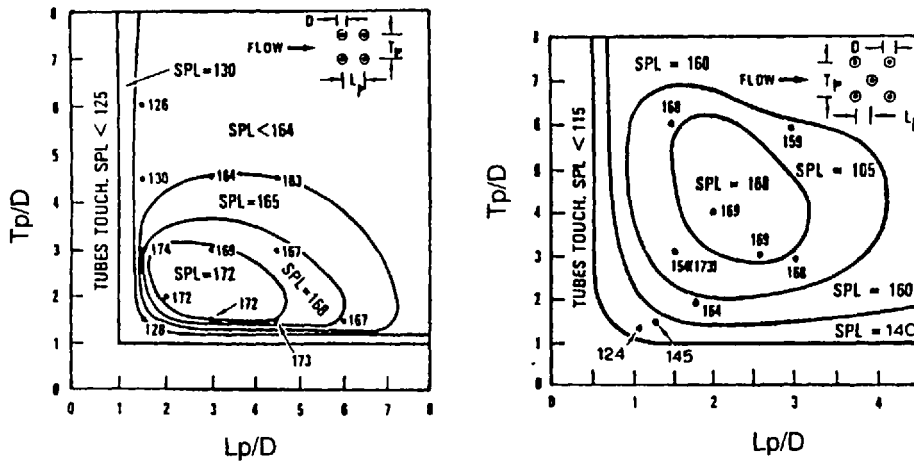


Figure 16 Sound pressure level map (SPL). Blevins [62]. Also Blevins[8].

$$\tau = \frac{L_a}{Dn(X_1 - 1)} \tag{48}$$

where L_a is the duct width and n is the mode number. Resonance will occur for $\tau = 62$–80. Application to staggered arrays is questionable [62].

Other methods for prediction of acoustic resonance have been suggested by Fitzpatrick et al. [71] and Zaida et al. [72].

6 VIBRATION EVALUATION PROCEDURE

Basically the vibration evaluation procedure involves an estimation of certain parameters for various flow-induced excitation mechanisms. The estimated parameters are compared with

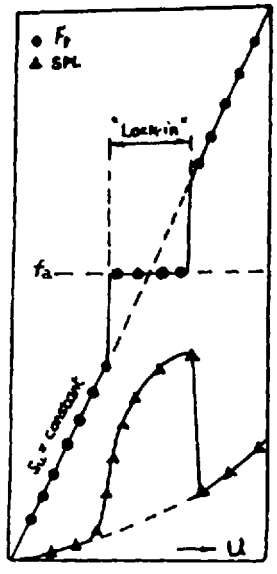


Figure 17 Acoustic lock-in phenomenon and sound pressure level. Ziada et al.[69].

their respective limiting values to check whether or not vibrations from such excitation mechanisms can cause potential damage to the tubes and the shell. There is a need to individually examine various zones of interest, namely, the nozzle inlet zone, U-bend region, and baffle window region, since there is a likelihood of high turbulence and high crossflow velocity in these regions and the variations of span lengths between baffle supports compared to the central baffle region.

6.1 Steps of Vibration Evaluation

1. Calculate the effective mass per unit length.
2. Identify the zones of interest (inlet, baffle window, central baffle zones, U-bend, etc.) to calculate the natural frequency.
3. Calculate the natural frequency for spans in various regions of interest.
4. Calculate the damping parameter.
5. Calculate crossflow velocity for the TEMA shell under consideration.

Step 6 for Liquid Flow

Vortex Shedding.

a. Calculate vortex shedding frequency. Check for the acceptance criteria.
b. If resonance takes place, calculate tube response and check whether it is not exceeding the limiting value.

Turbulent Buffeting. If resonance is predicted, calculate tube response due to random excitation and check for the acceptance criterion.

Fluid Elastic Instability. Calculate the critical velocity and compare with crossflow velocity. Keep the maximum crossflow velocity below the critical velocity.

Fill these values into the flow-induced vibration specification sheet in Table 5.

Step 6 for Gas Flow

In addition to the criteria given for liquid flow, the following check for acoustic resonance due to standing waves may be carried out.

a. Calculate acoustic resonance frequency
b. Calculate vortex shedding frequency. Check for various vortex shedding criteria.
c. Calculate turbulent buffeting frequency. Check for various turbulent buffeting criteria.

Fill these values into the flow-induced vibration specification sheet for acoustic resonance given in Table 6.

6.2 Caution in Applying Experimentally Derived Values for Vibration Evaluation

The vibration prediction methods are mostly based on linearized models that require input data reflecting a particular flow pattern and a structural configuration. The guidelines are derived from simplified test conditions and they cannot be generalized for actual heat exchangers. The parameters such as damping, Strouhal number, fluid elastic instability constant, etc. are mostly known for idealized test conditions and may be different in the real environment of the heat exchanger due to interaction between various mechanisms of excitation [57]. If the outcome of the experimentally derived design criteria is applied to specific heat exchangers, it may lead to conservative or marginal designs.

Accurately predicting the critical velocity requires testing a single-tube mockup with end conditions and supports as nearly identical as possible to the actual heat exchanger unit, or a

Table 5 Flow Induced Vibration Specification Sheet for Liquids

C_m		m =	δ		U		
TEMA	Blevins	f_n =	TEMA	Pettigrew et al.	Bell	Tinker	Others

I. Vortex shedding

i) Check for vortex shedding lock-in

Condition	Chen/TEMA S_u =	Weaver S_u =	Others
a. $f_n D/U > 2 S_u$			
b. $f_n D/U < 0.2 S_u$			

ii) Au-yang et al. criteria (safe) $U/f_nD < 1$ $C_n > 64$ $U/f_nD \leq 3.3$ & $C_n > 1.2$ $n = 1$

iii) Check for peak response at resonance

a. Normal criterion y_{max} = mm < 0.1905 mm (limit)

b. Conservative criterion with $C_L = 0.091$ y_{max} = mm < 0.1905 mm (limit)

II. Turbulance excitation: amplitude of response

$\tilde{y}_{rms} = \sqrt{\tilde{y}^2_{rms}} =$ < 0.254 mm (limit)

III. Fluid elastic instability

$\chi = \frac{m\delta}{\rho_i D^2}$	K	U_{cr}	U/U_{cr}	If Ucr > U safe	If $U/U_{cr} \leq 0.5$, safe
	TEMA				
	ASME K_{mean}				
	K_{all}				
	K_{comb}				
	Pettigrew et al.				

part scale model [73] or a full scale model if it is economically feasible. Hence, it can be concluded that the judgment of the designer, precautions taken by the heat exchanger fabricator, and model test conducted by the researchers are the means available to provide reasonable assurance that a design will not fail due to FIV [73].

7 DESIGN GUIDELINES FOR VIBRATION PREVENTION

FIV problems are better prevented rather than corrected. After the thermal design stage, a check for FIV is carried out and if the tubes are susceptible to FIV, excitation sources are identified and corrective action is taken. Tube vibration can be reduced to within limits by either increasing the tube natural frequency or reducing the crossflow velocity or suppressing the source of excitation as discussed next.

7.1 Methods to Increase Tube Natural Frequency

Tube natural frequency is represented by

$$f_n \propto \frac{1}{L_t^2}\left(\frac{EIg_c}{m}\right)^{0.5} \tag{49}$$

A careful review of this natural frequency equation indicates that the tube natural frequency can be increased by reducing the tube span L_t, increasing the ratio I/m, or increasing Young's

Table 6 Flow Induced Vibration Specification Sheet for Gases—Acoustic Resonance

1. Effective sound velocity
   i. Sound velocity
   $$C = \sqrt{g_c Z \gamma R T / M_c}$$
   ii. Solidity ratio
   $$\sigma = 0.9060\left(\frac{D}{p}\right)^2 \quad \text{for 30 or 60° layout}$$
   $$= 0.7853\left(\frac{D}{p}\right)^2 \quad \text{for 90° layout}$$
   $$= 1.5707\left(\frac{D}{p}\right)^2 \quad \text{for 45° layout}$$
   ii. Effective sound velocity
   $$C_{\text{eff}} = \frac{C}{\sqrt{(1+\sigma)}}$$
   or
   $$C_{\text{eff}} = \frac{C}{\sqrt{(1 + C_n\sigma)}}$$

2. Acouatic resonance frequency
   a. Belvins
      i. For circular shell
      $$f_a = \frac{C_{\text{eff}}\lambda_1}{2\pi R} \qquad (\lambda_1 = 1.84,\ \lambda_2 = 3.054)$$
      ii. For rectangular shell
      $$f_a = \frac{jC_{\text{eff}}}{2L_t} \qquad j = 1,2,3\ldots$$
   b. $f_a = \dfrac{483.2\ (p_s/\rho_s)^{0.5}}{L_a}$ (TEMA units)

3. Check for vortex shedding

Lock-in	SPL	Chen No. Ψ and Eisinger critiera
i. Normal criteria $0.8\dfrac{S_u U}{D} < f_a < 1.2\dfrac{S_u U}{D}$	If SPL < 140, safe	$Re = \dfrac{UD\rho_s}{\mu}$, $\Psi = \dfrac{Re}{S_u}\dfrac{(2X_1 - 1)^2}{4X_1^2 X_t}$
ii. Conservative criteria $0.6\dfrac{S_u U}{D} < f_a < 1.48\dfrac{S_u U}{D}$		$\Psi < 2000$ no vibration $\Psi < 2000$–4000 low likelihood of vibration $\Psi > 4000$ high likelihood of vibration

4. Check for turbulent excitation

Own	Bryce	Arnold's slenderness ratio
$f_{th} = \dfrac{U}{DX_1X_t}\left[3.05\left(1 - \dfrac{1}{X_t}\right)^2 + 0.28\right]$ for resonance: $0.8f_{th} < f_a < 1.2f_{th}$	$\dfrac{U}{f_a D} < 2(X_1 - 0.5)$ No resonance Blevins for $U/f_a D > 2$ resonance will occur	$\tau = \dfrac{L_a}{Dn(X_1 - 1)}$ If, $\tau < 62$-80, resonance will occur

modulus E. Since the moment of inertia and tube mass are limited by the standard tube dimensions and E is limited by the material chosen, in most of the cases the only option available to increase the natural frequency is to reduce the tube span L_t [11]. For single-segmental baffles, reducing the tube span will increase the natural frequency proportionally to $1/L_t^2$ and increase the crossflow velocity proportionally to $1/L_t$. Hence the tube span may be reduced to an optimum level [17]. The influence of E and thin tubing on FIV is explained next with reference to a retubed unit.

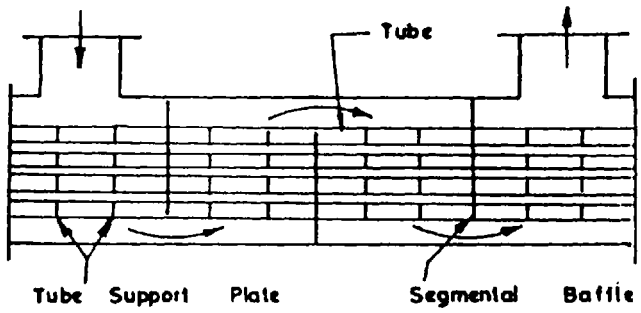


Figure 18 Support plates in NTIW to divert fluid across the tube bundle.

FIV of Retubed Units

The importance of tube support spacing and young's modulus has often come to light when a condenser that was initially fitted with copper alloy tubes, is retubed with thin titanium tubes, which have a relatively low modulus of elasticity. The thin-wall titanium tubing is not as stiff as the copper tubing it replaces, so that it usually requires supplementary support to avoid flow-induced vibration problems.

1. If the tube vibration problem is anticipated in the window zone due to longer tube span between baffles ($2L_{bc}$) and higher velocity than the tubes at central zone, eliminate the tubes in the window zone, resulting in a no-tubes-in window design (NTIW). To offset any loss in heat transfer, introduce support plates as shown in Fig. 18, to divert the fluid across the bundle.
2. An alternative to the NTIW design is to employ strip baffles as shown in the Fig. 19, in the window zone. This additional supports given to the tubes in this zone increases the stiffness of the tubes and hence increases the natural frequency.
3. Increase the structural damping of the tube bundle by means of thicker baffle plates and reduce the fretting wear by employing softer baffle material.
4. Lace the tube bundle using wire laces to increase the tube bundle stiffness.
5. U-bend support: The natural frequency of the U-bend is considerably increased by providing to the U-bend a support known as antivibration bars (AVB). Principal types of U-bend

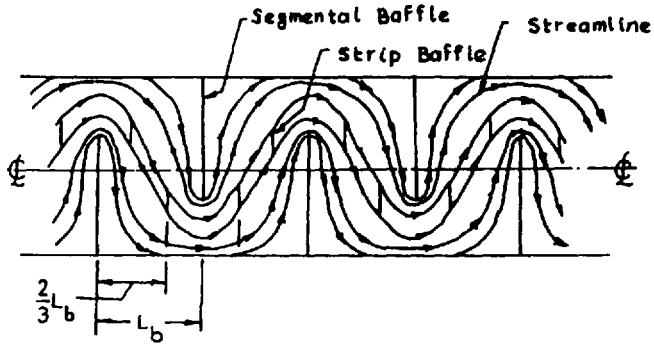


Figure 19 Placement of strip baffles. Ref. (41).

support configurations are (a) scalloped bars, (b) wiggle bars, (c) lattice bars, and (d) flat bars, and they are as shown in Fig. 20 [41].

6. Tubes are likely to be under some axial loading as a result of fabrication and operation. Tensile stresses increase the natural frequency, whereas compressive stress decreases the natural frequency. Since axial compressive stress in the tube decreases the tube natural frequency, rolling-in of the tubes in to the tubesheet should be done carefully. Care should be also taken to allow for the free thermal expansion of the tubes. When significant compressive axial loads are induced on the tubes in a multipass exchanger, these tubes shall be located in the baffle overlap regions to minimise the unsupported span length [11].
7. When only few tubes are exposed to high localized velocities, sealing strips may be applied to provide flow resistance and reduce flow in critical areas [74].

Plugging of Tubes. The affected tubes may be omitted or plugged if proper precautions are taken to ensure that collision will not endanger the adjacent tubes [74].

Detuning of Tubes. Detuning is defined as the method of producing differences among the natural frequencies of the neighboring tubes in a tube array. The tubes are detuned by installation of additional supports such as clips, wedges, flat bars, helical spacers, strip baffles, or any other means of increasing the tube fixity. Detuned tube arrays lose stability at a higher flow velocity; the incidence of instability is more gradual in a tube bank with differences in tube-to-tube frequency than in a bank with identical tube frequency [8].

Detuning Effect. For the displacement mechanism associated with the coupled motion of adjacent tubes, detuning will have a significant effect, whereas for the velocity mechanism the effect is little since the individual tube motion is independent of neighboring tubes and the instability is controlled by fluid damping forces [55]. Lever and Weaver [43] found that for air flow, detuning of neighbouring tubes produced a maximum increase in critical velocity about 40% at a frequency difference of 3%. For frequency differences greater than about 10%, there was no significant improvement in threshold instability. Tanaka et al. [46] report detuning has increased the critical velocities for air flow by about 60%.

Avoid longer unsupported tube spans. Follow maximum unsupported tube length as specified in TEMA, RCB-4.52 [19].



Figure 20 U-bend supports. Weaver et al. [41].



Figure 21 Impingement plate protection. After Ref. (19).

7.2 Methods to Decrease Crossflow Velocity

The following methods may be employed to reduce the crossflow velocity, which in turn will decrease the vibration excitation potential.

1. Reduce the crossflow velocity either by decreasing the flow rate or by increasing the shell diameter. However, this will reduce the heat transfer rate. Even though testing has indicated that controlling an instability usually requires lowering of the flow rate below its initial threshold value, hysteresis suggests that instability may be initiated by flow pulses that are caused by operational transients. Hence, while evaluating the critical velocity, if such operational transients are anticipated, it may be desirable to reduce the allowable flow rate significantly below the instability threshold [74].
2. Increase the tube pitch such that crossflow area is increased. However, this will be at the cost of lower shell-side heat transfer.
3. If vibration damage to the tubes located beneath the nozzle is predicted, increase the nozzle openings to decrease the mass velocity or install impingement plates as shown in the Fig. 21.
4. If the vibration potential is predicted in the middle zone of an E shell, change the shell design into either an X shell or J shell. Theoretically speaking, for the same mass flow rate, the crossflow velocity on the shell side of a J shell will be half that of the E shell [75].
5. Use double or multiple segmental baffles as shown in Fig. 22 to divide the flow into two or more streams. In an exchanger with single segmental baffles the total flow, except for leakages and bypass streams, passes through the tube bank between baffles (Fig. 23), whereas in an exchanger with double segmental baffles barring the leakages, the flow divides into two streams on either side of the shell, and into three streams in triple segmental baffles. Under ideal conditions the crossflow velocity in a double segmental baffles unit is half that of a comparable single segmental baffles units and one third with triple segmental baffles. Hence, it is expected that double segmental baffles will double the critical velocity compared to single segmental baffles. However, experiments on an

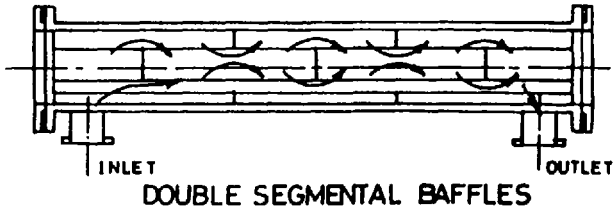


Figure 22 Double segmental baffle design.

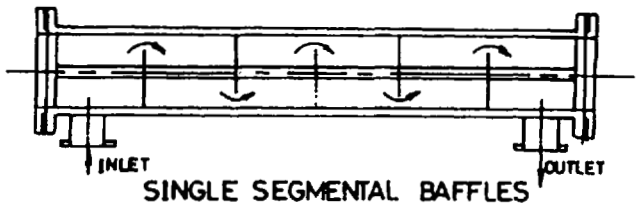


Figure 23 Fluid flow through single segmental baffle unit.

industrial size heat exchanger at Argonne National Laboratory [76] show that the threshold velocity increased by 24–67%. The full theoretical potential of approximately doubled threshold velocities was not realized. This was attributed to the effects of localized end zone conditions, which were probably not eliminated.

6. Since the crossflow velocity is the major cause of FIV, one of the design alternatives is to substitute the existing window baffle supports to Grid baffle or Rod baffle supports [77] as shown in Fig. 24. In a rod baffle exchanger the shell-side fluid is parallel to the tubes and the Rod baffles offer very high stiffness to the tube bundle.
7. Like rod baffle supports, another tube support arrangement that produces axial flow over the tubes is referred to as NESTS [78] as shown in Fig. 25. In this baffle design, the tubes are supported by a very rigid honeycomb structure, which replaces the conventional plate baffles.
8. Limit the high localized velocities in the bundle bypass flow region or in the pass partition lanes by carefully selecting the sealing strips and pass portion lane widths, respectively, without introducing a penalty on heat transfer on the shell side.
9. Avoid too small or too large baffle cuts, since both yield poor velocity distribution and high localized velocities.
10. To reduce the incidence of vibration of tubes in the window region, increase the longitudinal pitch near the baffle cuts as shown in Fig. 26. Increased longitudinal pitch has the benefit of straight baffle cut edge rather than half moon cut holes.

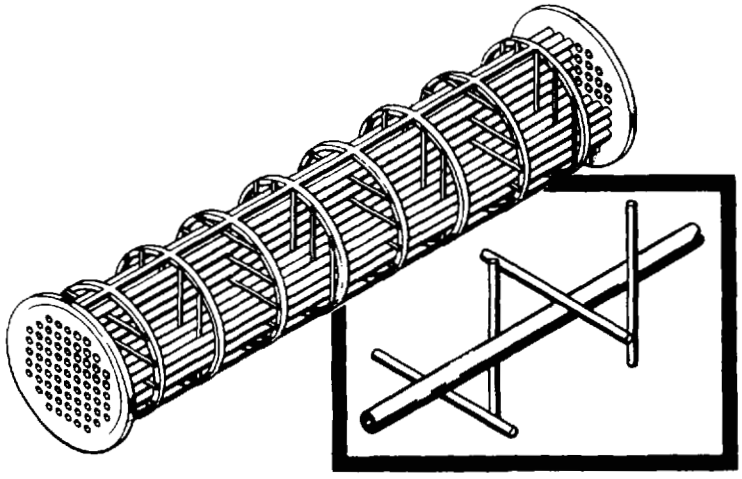


Figure 24 Phillips Rodbaffle support.

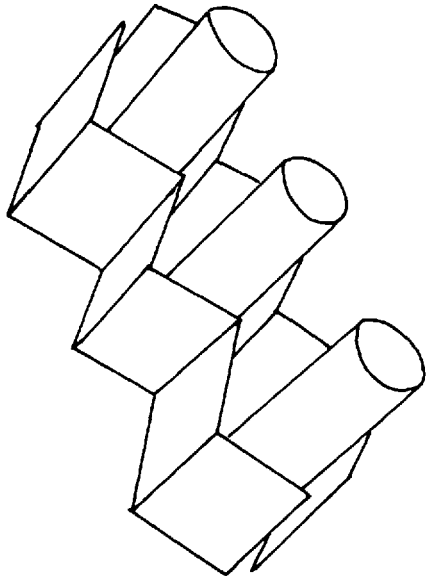


Figure 25 NEST™ tube support arrangement. After Boyer et al.[79].

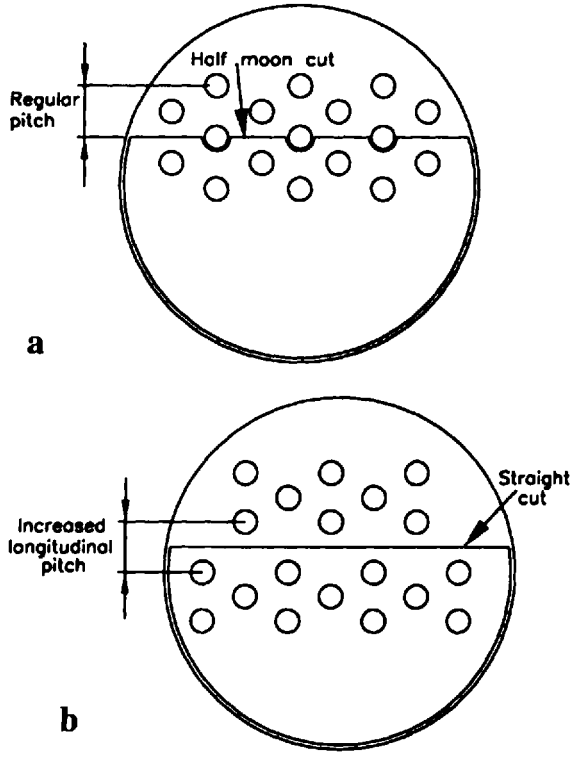


Figure 26 Baffle cut schemes. (a) Typical baffle cut (half moon); and (b) discontinuous longitudinal pitch at baffle cut. (From Ref. 11.)

11. Maintain small tube to baffle hole clearances; follow TEMA Standard RCB-4.2 [19].
12. Ensure uniform baffle spacings.

7.3 Suppression of Standing Wave Vibration

The acoustic standing waves can be suppressed by any of the following devices or methods:

1. Antivibration baffles (AVB), solid or porous baffle
2. Resonators
3. Fin barriers
4. Helical spacers
5. Detuning or structural modification
6. Removal of tubes
7. Surface modification
8. Irregular lateral spacing of tubes
9. Changing the mass flow rate

Antivibration Baffles

Solid Baffle. The occurrence of acoustic resonance in a crossflow heat exchanger is related to the development of standing waves. If the standing waves are inhibited from developing, then the associated acoustic resonance will not take place. This is achieved by incorporation of either a solid baffle or porous baffle inside the heat exchanger, in a direction parallel to the flow and perpendicular to the direction of standing waves. The baffles are also called detuning baffles. The placement of solid baffles is shown schematically in Fig. 27.

Number of Solid Baffles. As per theory, if solid baffles are to be installed in a tubular heat exchanger in which the maximum number of half-waves that can occur between the walls is N_a, then N_a solid baffles should be installed to prevent the acoustic vibration. The major drawback associated with the solid baffles is that the number of baffles required is very high for a heat exchanger of spatial size of 20–30 m used in the fossil fuel utilities, like an economizer, reheater, etc. However, the number of baffles requirement can be minimised by following Chen's method [25]. The method consists of placing solid baffles in preferred locations as shown in Fig. 28. The distances b_1, b_2, b_3, b_4, b_5, and b_6 are all to be kept different from each other and their ratios b_2/b_1, b_4/b_3, and b_6/b_5 should deviate much from the integers correspond-

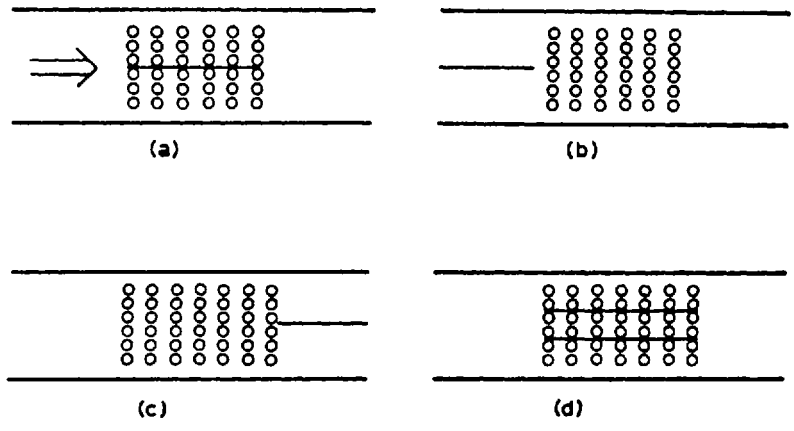


Figure 27 Detuning solid baffle arrangement. (a) Central baffle; (b) upstream baffle; (c) downstream baffle; and (d) two baffles at 1/3 and 2/3 transverse locations. (From Ref. 61.)

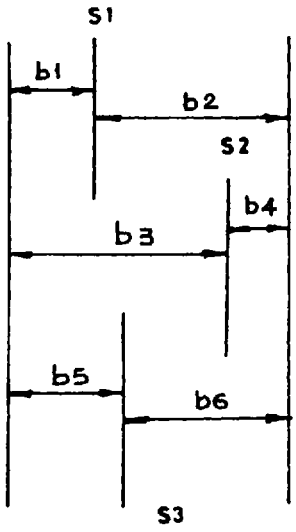


Figure 28 Chen's method of solid baffle arrangement. Insertion of the slightly overlapped detuning baffles into the heat exchanger to make the natural frequencies of the transverse gas columns in the spaces, b_1, b_2, b_3, b_4, b_5, and b_6 as different as possible from one another. (From Ref. 25.)

ing to the modes of the vibrations to be expected. While placing the baffles the length of the baffle should be large in comparison with the wavelength of the standing waves to be expected in the heat exchanger. The shortcomings associated with the solid baffles are discussed by Eisinger [57]. They include these:

1. Expensive for retrofitting
2. Inhibition of periodical inspection and maintenance operations
3. Limited life if the medium of flow is corrosive in nature
4. Tendency to vibrate and susceptible to thermal distortion in service

Porous Baffle. The porous baffle concept consists of a single flow-resistive element inserted between the tubes so that it is parallel to the flow direction [79]. Byrne [79] has shown that, in general, if the maximum number of half-waves between the walls is N_w, then a single porous baffle should be located at a distance from one wall equal to the wall-to-wall span divided by $2N_w$. The advantage of a porous baffle over that of solid baffles is that a single porous baffle can be used to inhibit the development of a number of standing waves, whereas the number of solid baffles required is equal to the maximum number of half-waves that can develop between the walls.

Helmhotz Cavity Resonator

Installation of an acoustic damper such as a tuned Helmhotz cavity resonator on the shell side will suppress the acoustic vibration. A simple Helmhotz resonator is shown in Fig. 29. The damping is maximum when the resonator is tuned with the acoustic mode of interest [62]. When tuned, there is a large oscillating mass flow through the resonator neck which expends energy by passing through the neck and/or the screen placed in the neck. An approximate formula for the resonator natural frequency is given by [62]:

$$f = \frac{C}{2\pi}\left(\frac{A}{V_h l_h}\right)^{0.5} \tag{50}$$

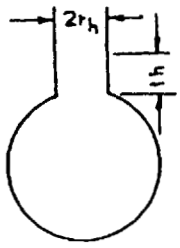


Figure 29 Helmotz's resonator.

where A is the area of cross section of opening in the resonator, V_h the volume of the cavity resonator, and l_h the length of the opening in the resonator.

The Concept of Fin Barrier

To overcome the drawbacks associated with solid baffles, a new method of solving standing wave vibration was suggested by Eisinger [57]. The method consists of using fin barriers welded to the heat exchanger tubes, forming a thin wall parallel to the flow direction and perpendicular to the direction of propagation of standing waves. The various forms of fin barriers are shown schematically in Fig. 30.

The Concept of Helical Spacers

A novel idea for overcoming FIV in a closely spaced tube array is to introduce helical spacers inside the tube bank area [57]. This method is well suited to the initial design stage or for use

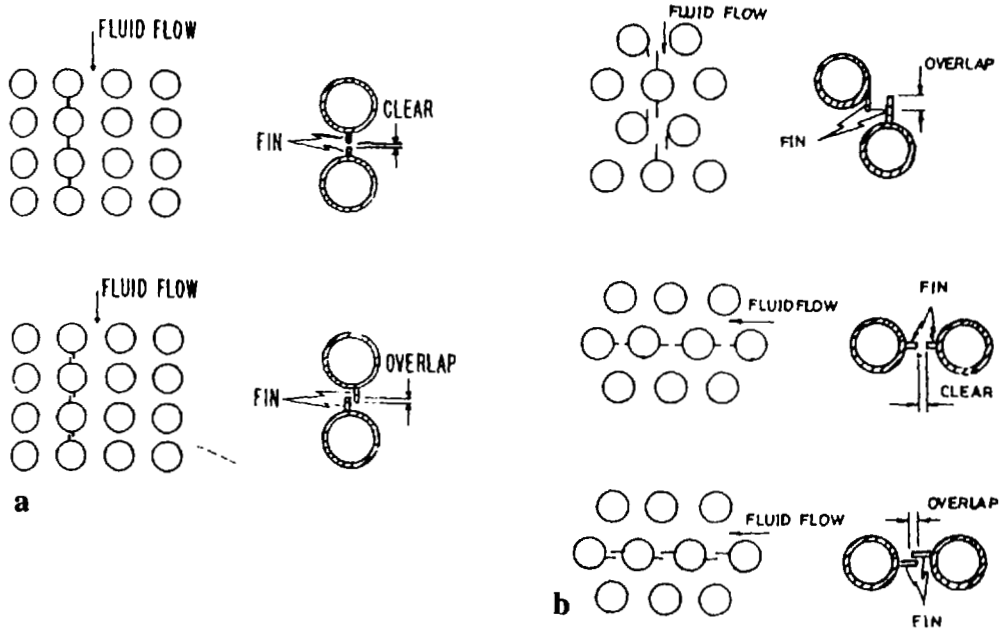


Figure 30 Two types of arrangements of fin barriers. (a) Inline array; and (b) staggered array. (From Ref. 57.)

in field modifications. The method is applicable both for staggered and in-line tube layout, and spacer placement is shown schematically in Fig. 31.

Detuning

This has been already discussed.

Removal of Tubes

Selective removal of a few tubes at the displacement antinodes of the standing waves will eliminate the vortex shedding and thus avoid the coupling between vortex shedding and acoustic resonance. This also upsets the vortex shedding regularity at pressure nodes. Walker and Reising [80] and Barrington [63,67] have observed that by removing 3–10% of tubes near the centre of the tube bank, acoustic resonance can be diminished or eliminated.

Surface Modification

Fouling of heat exchanger tubes by dirt and carbon soot has been associated with the reduction in sound level, and hence the deposition increases the acoustic damping [8,81].

Irregular Spacing of Tubes

Destroy the phasing of vortex streets by having irregular spacing of tubes. This will scramble the vortex shedding frequency. Zdravkovich and Nuttal [82] found the nonoccurrence of standing waves by displacing the susceptible tubes either laterally or longitudinally as shown in Fig. 26(b). However, this method is only attractive if the thermal performance is not affected.

Change the Mass Flow Rate

Modify vortex shedding frequency by changing the mass flow rate. This may not be very attractive from a thermal performance point of view.

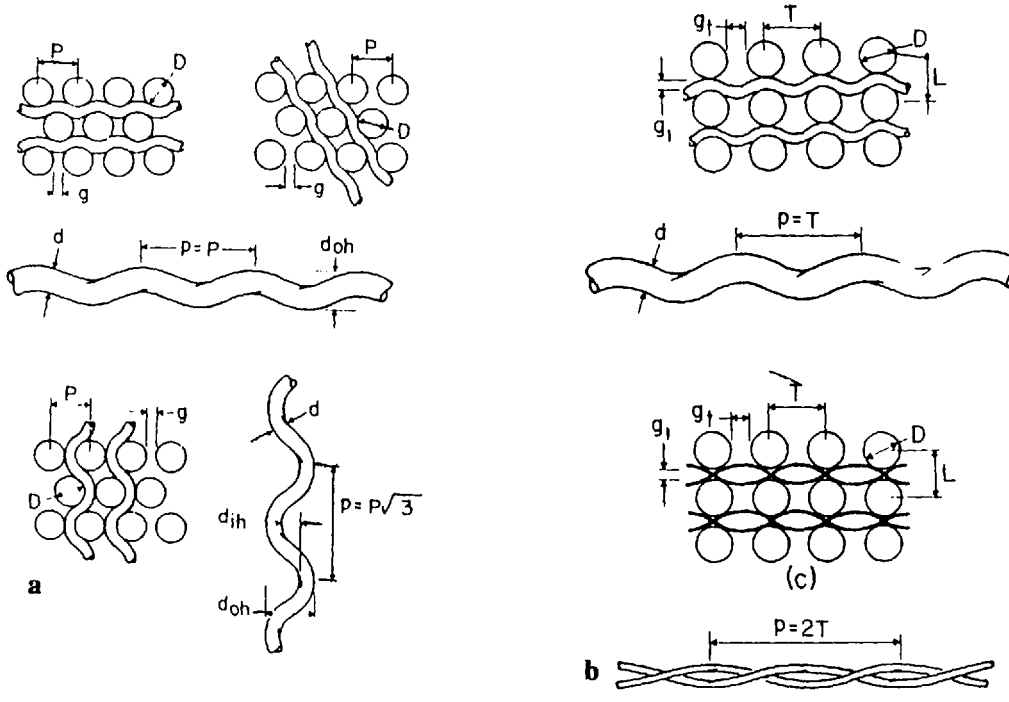


Figure 31 Helical spacers in (a) staggered tube array; and (b) inline tube array. (From Ref. 57.)

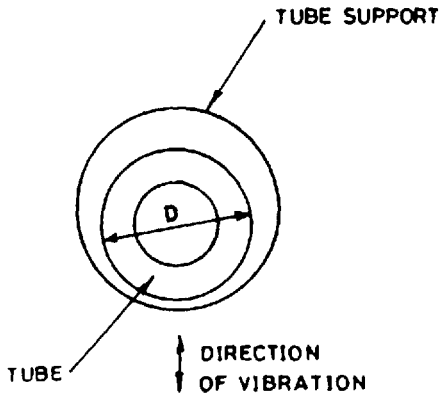


Figure 32 Vibrating tube in baffle hole. (From Ref. 94.)

8 BAFFLE DAMAGE AND COLLISION DAMAGE

Empirical Checks for Vibration Severity

From the prevalent pattern of tube failures occurring at the baffle supports and at the midspan, Thorngren [83] has attributed tube failures mainly to (1) baffle type damage and (2) collision type damage. He proposed two empirical correlations, called baffle damage number, N_{BD}, and collision damage number, N_{CD}, to check the severity of tube damage due to FIV. The expressions for these damage numbers can be easily deduced similar to Connor's instability equation. Therefore they are not discussed here.

9 IMPACT AND FRETTING WEAR

Heat exchanger tubes are supported at regular intervals by passing through oversized holes in baffle plates (Fig. 32). As the tubes vibrate against the support plates, material can be fretting away from both the tube and the support plate as shown in Fig. 33. If the fretting wear of tube is sufficiently large, the tubes will eventually rupture due to the fluid pressure [38]. When one considers that a design objective for a nuclear power plant steam generator or a heat exchanger is a 40 years codal life, even relatively small tube wear rates cannot be tolerated [6,38]. Hence in recent years significant attention has been given to study the effect of tube-to-tube support plate clearances on tube vibration and wear, by (1) laboratory experiments, (2) theoretical

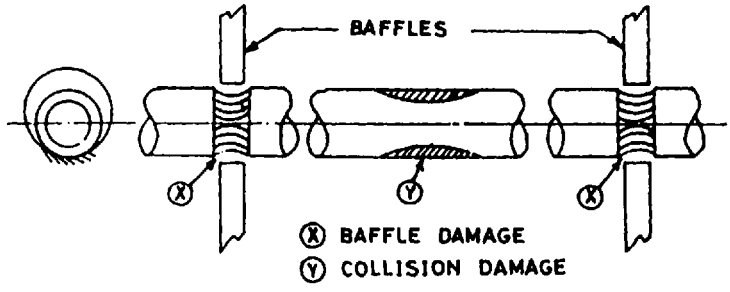


Figure 33 Fretting wear of tubes.

simulations, and (3) analytical models. Vibration excitation mechanisms responsible for fretting wear are (1) vortex shedding, (2) turbulent buffeting, and (3) fluid elastic instability. References 38 and 84–93 brought about a greater understanding of the tube-to-tube support plate interaction characteristics and resultant tube wear.

9.1 Tube Wear Prediction by Experimental Techniques

Among the experimental techniques, the notable are that of Blevins [84,85], and Haslinger et al. [86]. The fundamental assumption of the Blevins [84] experimental fretting wear model is that fretting wear is the result of relative motion between the tube and the support plates. Blevins assumed that the fretting wear is a function of parameters such as (1) tube geometry, (2) baffle plates geometry, (3) tube and baffle plate material properties, (4) amplitude, frequency and mode shape of tube vibration, (5) preload between the tube and support plate, and (6) nature of environment and operating temperature.

Recently, Blevins [94] conducted experiments to predict wear induced by vibration on a heat exchanger model with alloy 800H and 2.25Cr–1Mo steel heat exchanger tubes loosely held supports in a helium environment at temperatures up to 650°C (1200°F). From the conclusions derived from his experiments, it is seen that (1) impact wear can be minimized by reducing the impact contact stresses below the fatigue allowable stress, (2) decreasing the vibration amplitude or baffle hole clearance markedly decreases wear rate and subsurface deformation at all temperatures, and (3) application of chromium coating both to the tube and the plate specimens greatly reduces the surface self-adhesion and surface deformation that would otherwise occur above 500°C (930°F). Below this temperature, a coating is probably not required.

9.2 Theoretical Model

Nonlinear finite-element modeling techniques to predict tube wear due to turbulence excitation, fluid elastic instability, or vortex shedding are discussed in refs. 38 and 89–93. The wear parameters central for the theoretical models are (1) sliding distance, (2) contact time, (3) average contact time, (4) threshold crossings, and (5) work rate.

10 DETERMINATION OF HYDRODYNAMIC MASS, NATURAL FREQUENCY, AND DAMPING

Flow-induced vibration analysis of heat exchangers require the knowledge of damping, hydrodynamic mass, and natural frequency of tube bundle. Their determination is discussed next.

10.1 Added Mass or Hydrodynamic Mass

During flow-induced vibration, the vibrant tubes displace the shell-side fluid. When the fluids involved are liquids or very dense gases, the inertia of the fluid will have substantial effect on natural frequency of the tubes. Hence, while calculating the natural frequency of the tube, the influence of the displaced fluid is taken care of by augmenting the mass of the vibrating tube by including hydrodynamic mass or added mass. The added mass is defined as the displaced fluid mass times an added mass coefficient C_m. Since the added mass augments the vibrating tube mass, the natural frequency of the tube will be reduced compared to when the tube is vibrating in vacuum or very low density gas.

10.2 Determination of Added Mass Coefficient, C_m, for Single-Phase Flow

The added mass coefficient is estimated either by the analytical method of Blevins [8] or from the experimental database of Moretti et al. [95].

Blevins Correlation

Blevins [8] gave an analytical formula to determine added mass coefficient of a single flexible tube surrounded by an array of rigid tubes as shown in Fig. 34a. This is a reasonable approximation of the more complex case of all flexible cylinders. The expression for added mass coefficient C_m is given as

$$C_m = \frac{(D_e/D)^2 + 1}{(D_e/D)^2 - 1} \tag{51}$$

where $D_e/D = (1 + 0.5\ \text{p/D})p/D$ in which D_e is the equivalent diameter of a tube array. The equivalent diameter D_e is used to represent the confinement due to surrounding tubes.

Experimental Data of Moretti et al. [95]

The experimental results of Moretti et al. [95] for a single flexible tube surrounded by rigid tubes in a hexangular array or in a square array as shown in Fig. 34b with a pitch-to-diameter ratio from 1.25 to 1.50 is given in Fig. 35. Their test results for C_m for four pitch-to-diameter ratios are given in Table 7. TEMA included this figure (Fig. 35) for determination of added mass coefficient [19].

10.3 Natural Frequencies of Tube Bundles

The tubes in a heat exchanger are slender beams and the most flexible members. They vibrate at discrete frequencies when they are excited. The natural frequency depends on their geometry, material properties like Young's modulus, density and material damping, tube-to-support inter-

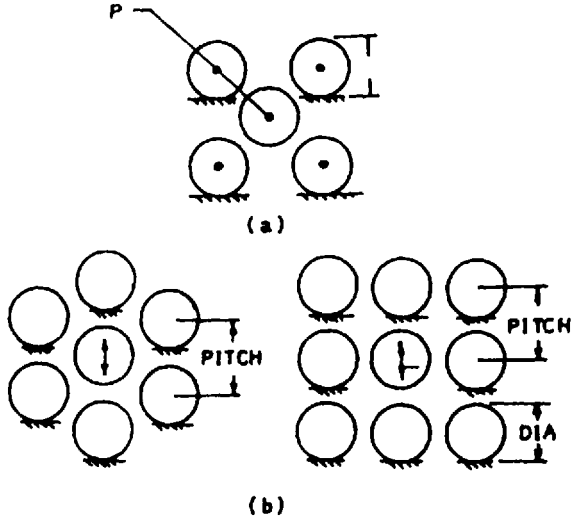


Figure 34 Tube arrangement for determining added mass coefficient, (a) Blevins model [8]; and (b) Morretti model. (From Ref. 95.)

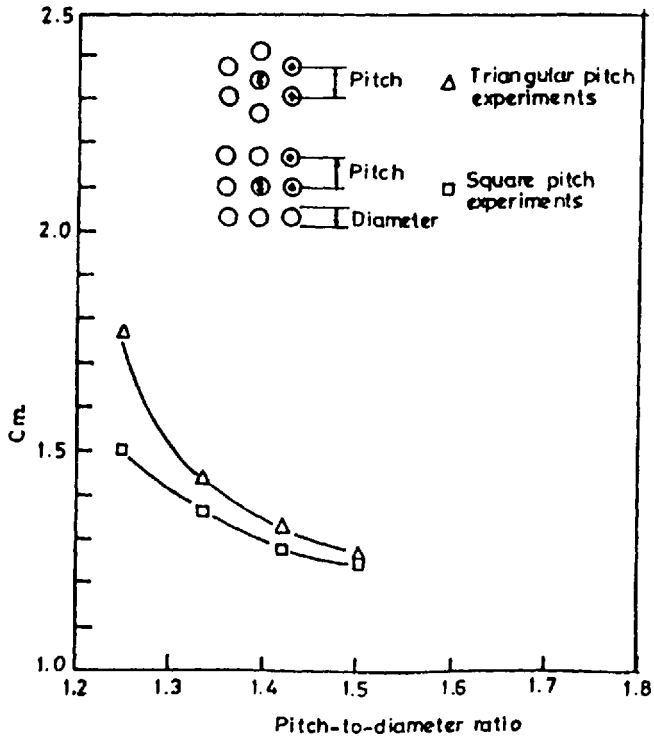


Figure 35 Added mass coefficient. (From Ref. 95.)

actions, etc. The lowest frequency at which the tubes vibrate is known as the natural frequency. The coincidence of the exciting frequency with the natural frequency is called resonance. The conventional shell and tube heat exchangers have either straight tubes or U-tubes with baffle supports at intermediate points and fixed at their ends. The determination of the natural frequencies of the straight tubes and U-tubes is dealt with next.

Estimation of Natural Frequencies of Straight Tubes

Hand Calculation Method. Though a rigorous analysis considering the multispan (Fig. 36) modeling is possible, the state of the art on vibration prediction method recommends a simpler but a slightly conservative approach treating the individual spans separately [11]. For example, the simpler hand calculations method of Timoshenko and Young [96] basically consider a tube

Table 7 Added Mass Coefficient, C_m

Pitch-to-diameter ratio	C_m	
	Triangular pitch	Square pitch
1.25	1.756	1.519
1.33	1.429	1.381
1.42	1.347	1.286
1.50	1.274	1.272

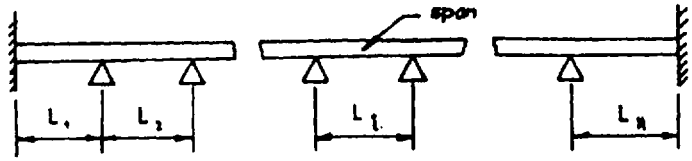


Figure 36 Multispan uniform beam with fixed ends.

as a continuous elastic beam on multiple supports with fixed end conditions and simply supported at the intermediate points (baffle locations). The individual spans (Fig. 37) are each treated as a separate beam with its own end conditions (fixed-pinned, pinned-pinned, etc.). Natural frequencies of the individual spans are calculated and the lowest frequency of the spans is taken as the representative figure for the whole tube and hence for the tube bundle.

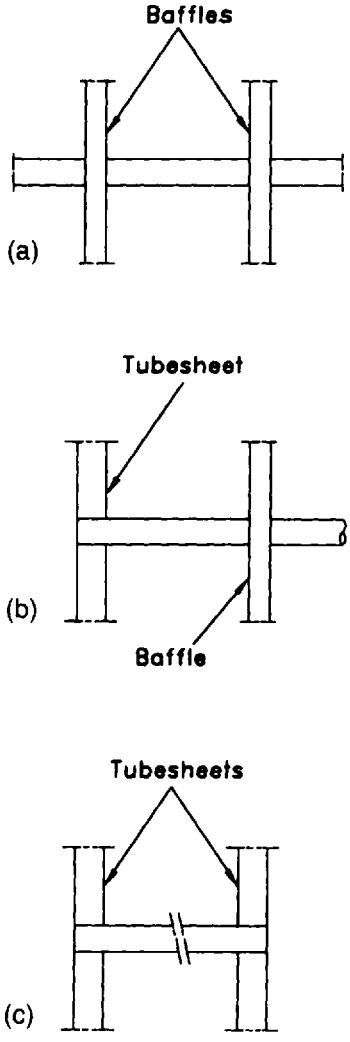


Figure 37 Individual tube span. (a) Pinned-pinned; (b) fixed-pinned; (c) fixed-fixed.

Table 8 Frequency Constant, λ_n and Euler Buckling Load, F_{cr}

	Pinned-pinned	Fixed-pinned	Fixed-fixed
λ_n	$n\pi$	$0.25(4n + 1)\pi$	$0.5(2n + 1)\pi$
F_{cr}	$\pi^2 EI/L^2$	$2\pi^2 EI/L^2$	$4\pi^2 EI/L^2$

The Timoshenko and Young method of treating the individual spans separately to find the natural frequency is recommended by Singh and Soler [11], Zukaskus [13], TEMA, and others. The frequency equation in a generalized form including the effect of axial stress is given by:

$$f_n = \frac{1}{2\pi} \frac{\chi_\beta \lambda_n^2}{L_i^2} \left(\frac{EIg_c}{m} \right)^{0.5} \qquad n = 1,2,3, \ldots \tag{52}$$

The expression for axial stress factor χ_B in terms of tube axial load F and Euler's critical buckling load F_{cr} is given by

$$\chi_B = \sqrt{1 \pm \frac{F_a}{F_{cr}}} \tag{53}$$

where

$$F_a = A_t \sigma_t \tag{54}$$

In Eq. 54, F_a is tube axial load, A_t is tube metal cross sectional area, and σ_t is tube longitudinal stress. In Eq. 53, the plus sign is for tensile load and the negative sign is for compressive load included in the tubes. The expression for frequency constant λ_n for the nth mode and for Euler's buckling load for various end conditions are given in Table 8, and the values of λ_n up to fifth mode are given in Table 9.

Rigorous Approaches to Calculate Straight Tube Natural Frequencies. These include the methods of Timoshenko and Young [96] and ABAQUS [97].

Natural Frequencies of Low Finned Tubes. These may be calculated by the TEMA method.

U-Tube Natural Frequency

The expression for the lower bound of the natural frequency of U-tubes included in TEMA for various forms of tube symmetry and U-bend support configuration (Fig. 38) is of the form

$$f_{n,u} = 68.06 \frac{C_u}{R^2} \left(\frac{EI}{m} \right)^{0.5} \tag{55}$$

Table 9 Numerical Values for Frequency Constant λ_n up to Fifth Mode

End conditions	First mode	Second mode	Third mode	Fourth mode	Fifth mode
Pinned-pinned	3.1416	6.2832	9.4248	12.5664	15.7080
Fixed-pinned	3.9269	7.0686	10.2102	13.3518	16.4934
Fixed-fixed	4.7124	7.8540	10.9956	14.1372	17.2788

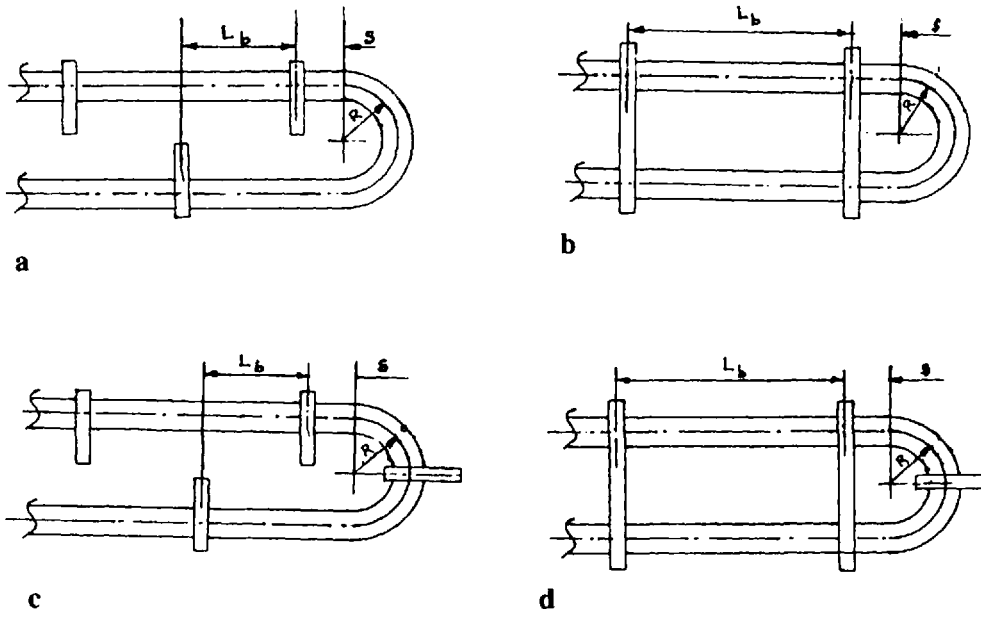


Figure 38 TEMA U-bend support configuration. Edge conditions have both ends simply supported. (Copyright Tubular Heat Exchanger Manufacturers Association, 1988.)

Detailed charts are given in TEMA [19] to determine C_u for various U-bend support geometries.

10.4 Damping

Damping plays an important role on the stability of the tube array. Damping limits the tube response when the tube is excited by any one of the excitation mechanisms. The higher the damping, the lower will be the tube response. Damping determines the critical flow velocity for FEI. The critical velocity increases with increasing damping. Damping in a vibrating system is due to several possible energy dissipation mechanisms. According to Pettigrew et al. [98], various energy dissipation mechanisms are

Internal or material damping
Viscous damping
Squeeze film damping in the baffle hole clearance
Flow dependent damping
Frictional damping
Joint damping at the tube and tube-sheet interface.
Energy dissipated by tube impact on the support and by the traveling waves

Determination of Damping

Determination of damping by experimental methods is very difficult. Empirical correlations for determining damping for gases and liquids are given next.

Gases. From the review and analysis of the available data on damping of multispan heat exchanger tubes in gases, Pettigrew, Goyder, Quio, and Axisa [98] recommended empirical correlations to calculate damping ratio ξ_n. The damping ratio is defined as the ratio of actual

damping over critical damping. The logarithmic decrement of damping δ is equal to $2\pi\xi_n$. According to these authors for gas flow, frictional damping and impacting are the dominant energy dissipation mechanisms, with baffle thickness a dominant parameter, whereas diametral clearance between the tube and baffle support is much less significant.

Liquids. According to Pettigrew, Rogers, and Axisa [99] the most important damping mechanisms in liquid flow are viscous damping (tube to fluid), squeeze film damping, and friction damping. They fitted experimental data with an empirical model considering viscous and squeeze film damping resulting in the following empirical correlation. The semi-empirical expressions recommended to estimate damping for design purposes in single-phase fluids, gases, and liquids are given.

Gas Flow on the Shell Side [98].

$$\xi_n = \frac{0.7}{100}\,\frac{N-1}{N}\,\frac{t_b}{12.7} \qquad \text{for } t_b < 12.7 \tag{56}$$

$$\therefore\ \delta = 3.463 \times 10^{-3}\,\frac{N-1}{N}\,t_b \tag{57}$$

$$\xi_n = \frac{5}{100}\,\frac{N-1}{N}\left(\frac{t_b}{L_i}\right)^{0.5} \qquad \text{for } t_b \geq 12.7 \tag{58}$$

$$\therefore\ \delta = 0.314\,\frac{N-1}{N}\left(\frac{t_b}{L_i}\right)^{0.5} \tag{59}$$

where t_b is the tube support thickness, L_m the characteristic span length, and N the number of tube supports for the tube under consideration. These expressions are valid for $D = 12$–15 mm, $t_b = 6$–25 mm, $f = 20$–600 Hz, and baffle hole clearances 0.4–0.8 mm.

TEMA included Eq. 58 for all baffle thicknesses.

Liquid Flow on the Shell Side. The determination of δ involves either dynamic (absolute) viscosity μ in the expression suggested in TEMA or kinematic viscosity ν in the expression of Pettigrew et al. [99]. The relation between them is:

$$\text{Kinematic viscosity } \nu = \frac{\text{absolute viscosity } \mu}{\text{specific gravity}}$$

$$\therefore\ \mu = \nu \times \text{specific gravity}$$

The units are centistokes for ν and centipoise for μ. Note: TEMA uses the symbol ν instead of μ.

Pettigrew, Rogers, and Axisa [99] give the equation

$$\xi_n = \frac{\pi}{\sqrt{8}}\,\frac{1 + (D/D_e)^3}{[1 - (D/D_e)^2]^2}\left(\frac{\rho_s D^2}{m}\right)\left(\frac{2\nu}{\pi f_n D^2}\right)^{0.5} + \left(\frac{N-1}{N}\right)\left(\frac{22}{f_n}\right)\left(\frac{\rho_s D^2}{m}\right)\left(\frac{t_b}{L_i}\right)^{0.6} \tag{60}$$

where

$$\frac{D_e}{D} = 1.7\,\frac{p}{D} \qquad \text{for triangular arrays} \tag{61a}$$

$$= 1.9\,\frac{p}{D} \qquad \text{for square arrays} \tag{61b}$$

Note: If ξ_n is less than 0.006, assume $\xi_n = 0.006$ [9] to account for friction damping.

TEMA included the following expressions for liquid flow, but the reference source is not given. The damping parameter δ is the greater of δ_1 and δ_2:

Table 10 Hydrodynamic Mass Coefficient, Mass Per Unit Length, and Damping Parameter

1. Hydrodynamic mass coefficient, C_m

Blevins correlation

$$\frac{D_e}{d} = \left(1. + 0.5\,\frac{p}{D}\right)\frac{p}{D}$$

$$C_m = \frac{(D_a/D)^2 + 1}{(D_{cr}/D)^2 - 1}$$

Moretti et al.

Read from Fig. 35 or from Table 7

2. Mass per unit length

$$m = \frac{\Pi D^2 C_m \rho_m}{4} + \frac{\Pi D_i^2 \rho_i}{4} + \frac{\Pi(D^2 - D_i^2)\rho}{4}$$

3. Tube natural frequency

i. Straight tube

$L =$ $A_t =$ $\sigma_t =$ $F = \sigma_t A_t$ $F_{cr} =$ $I_B =$ $I =$ $\lambda_n =$

$$f_n = \frac{1}{2\Pi}\,\frac{X_B \lambda_n^2}{L_t^2}\left[\frac{EIg_c}{m}\right]^{0.5}$$

ii. U-tube

$l_b/r =$ $C_u =$

$s/r =$

$R =$

$I =$

$$f_{n,u} = \frac{68.06 C_u}{R^2}\left[\frac{EI}{m}\right]^{0.5}$$ (use TEMA dimensional units)

4. Damping parameter

TEMA

$$\delta_1 = \frac{3.41\ D}{m\ f_n}$$

$$\delta_2 = \frac{0.012\ D}{m}\left(\frac{\rho_a \mu}{f_a}\right)^{0.5}$$

$\delta = \max\{\delta_1, \delta_2\}$(use TEMA dimensional units)

Others

Gases

$$\delta = 3.463 \times 10^{-3}\,\frac{N-1}{N}\,t_b \qquad \text{for } t_b < 12.7$$

$$\delta = 0.314\,\frac{N-1}{N}\left(\frac{t_b}{L_t}\right)^{0.5} \qquad \text{for } t_b \geq 12.7$$

Liquid

i. $\dfrac{D}{D_e} = (1.7\ p/D)^{-1}$ for triangular array

$=(1.9\ p/D)^{-1}$ for square array

ii. $$\xi_n = \frac{\Pi}{\sqrt{8}}\,\frac{1 + (D/D_a)^4}{[1 - (D/D_e)^2]^2}\left(\frac{\rho_a D^2}{m}\right)\left(\frac{2U}{\Pi f_n D^2}\right)^{0.5} + \left(\frac{N-1}{N}\right)\left(\frac{22}{f_n}\right)\left(\frac{\rho_t D^2}{m}\right)\left(\frac{t_b}{L_t}\right)^{0.5}$$

iii. $\delta = 2\Pi\xi_n$

Note: If δ is less than 0.0377, then assume $\delta = 0.0377$.

$$\delta_1 = \frac{3.41D}{m f_n} \tag{62a}$$

$$\delta_2 = \frac{0.012D}{m}\left(\frac{\rho_s \mu}{f_n}\right)^{0.5} \tag{62b}$$

$$\therefore\ \delta = \max\{\delta_1, \delta_2\} \tag{63}$$

Note: use TEMA dimensional units, D = in., ρ_s = lbm/ft^3, μ = centipoise, and m = lbm/ft.

10.5 Other Values

Fill the values of added mass coefficient, natural frequency, and damping parameter into the format given in Table 10.

10.6 Two-Phase Flow

Determination of damping for two-phase flow is detailed in Welding Research Bulletin No. 389 [62].

NOMENCLATURE

A	= area of cross section of opening in the Helmhotz cavity resonator
A_t	= tube cross sectional area, m^2(in.^{2})
C	= speed of sound in the shellside medium
C_{eff}	= effective speed of sound in the shellside fluid
C_L	= lift coefficient for vortex shedding
C_m	= added mass coefficient
C_n	= reduced damping in nth mode
$C_R(f)$	= turbulence force coefficient
C_u	= constant to determine U-tube natural frequency
D	= tube outside diameter
D_B	= baffle diameter
D_c	= equivalent confinement diameter in a tube array
	= $(1 + 0.5p/D)$p to calculate C_m
D_c/D	= $1.7p/D$ for triangular array to calculate ξ_n
	= $1.9p/D$ for square array to calculate ξ_n
D_i	= tube inside diameter
E	= modulus of elasticity of the tube material
F_a	= axial load on tubes
F_{cr}	= critical buckling load of the tube span analyzed
f	= Helmhotz cavity resonator resonance frequency, s^{-1}
f_a	= acoustic resonance frequency, s^{-1}
f_n	= tube natural frequency, s^{-1}
$f_{n,u}$	= frequency of U-bend region
f_s	= vortex shedding frequency, s^{-1}
f_{tb}	= turbulent buffeting frequency in a tube array, s^{-1}
g_c	= proportionality constant,
	= 9.81 m/s^2
	= 1.0 in SI units and dimensionless
	= 32.174 lbm · ft/lbf · s

I = moment of inertia of the cross section
j, n = vibration mode number; $j = n = 1$ is fundamental mode
i, j, k = acoustic modal indices
K = fluid elastic instability constant
L_a = characteristic dimension for acoustic standing wave
L = unsupported tube span length for flow-induced vibration
L_i = unsupported tube span for flow-induced vibration or characteristic tubespan length, m (in.)
L_{BC} = central baffle spacing
L_{BI} = baffle spacing inlet
L_{BO} = baffle spacing outlet
L_c = characteristic tube length
L_p = longitudinal tube pitch, mm (in.)
L_t = total tube length
L_x, L_y, L_z = acoustic chamber dimensions
l_h = length of Helmhotz cavity resonator neck
M, M_n = modal mass
M_g = molecular weight of shell-side gas or vapor
m = mass per unit length of tube,
$= m_a + m_c + m_s$
$m(x)$ = mass per unit length of tube at a distance x along the tube axis
m_a = fluid added mass per unit length
m_i = contained fluid mass per unit length
m_s = structural mass per unit length
N = number of tube spans for the tube being analyzed
N_w = number of solid baffles
p_s = shell-side pressure, Pa(psi)
P_{rms} = rms value of shellside pressure Pa(psi)
p = tube pitch, m(in.)
Q_g = volume flow rate of gas phase in two-phase flow
Q_L = volume flow rate of liquid phase in two-phase flow
R = U-tube bend radius, shell radius, m(in.)
R_c = universal gas constant
Re = Reynolds number based on the tube outside diameter, dimensionless, UD/v
r,s = U-bend dimensions
r_h = Helmhtoz cavity resonator neck radius, m(ft)
SPL = sound pressure level, dB
S_u = Strouhal number, dimensionless
T = absolute temperature of shellside gas, (°R/°K)
T_p = transverse tube pitch
t = time
t_b = baffle support plate thickness
U, U_{Bell}, U_{Tinker},
U_{others} = reference crossflow velocity
U_{cr} = critical fluid velocity for fluid elastic excitation
$U(x)$ = crossflow velocity distribution
U_∞ = upstream velocity
V_h = volume of Helmhtoz cavity resonator
v = kinematic viscosity of the fluid, centistokes

X_l = longitudinal pitch ratio, L_p/D
X_p = pitch ratio = p/D
X_t = transverse pitch ratio, T_p/D
x = axial distance
$y(x)$ = amplitude of vibration
y_{rms} = rms amplitude of tube vibration
$\bar{y}^2_{rms}$ = mean square amplitude of vibration
y_{max} = maximum tube response due to resonance due to vortex shedding
Z = shell-side gas or vapour compressibility factor
λ_n, λ_i = frequency constant
σ = tube bank solidity, dimensionless
δ = logarithmic decrement of damping = $2\pi\xi_n$
ψ = Chen number
χ = nondimensional parameter
χ_B = factor to account for tube axial load on tube natural frequency
$\phi_n(x)$ = mode constant for tube natural frequency, dimensionless
ξ_n = critical damping ratio
ρ = density of tube material
ρ_i = density of tube-side fluid
ρ_s = density of shell-side fluid
σ_T = shell longitudinal stress, + for tensile stress, − for compressive stress
τ = Arnold's slenderness ratio
γ = ratio of specific heat of gas at constant pressure to constant volume
μ = absolute viscocity, centipoise

REFERENCES

1. Wambsganss, M. W., Tube vibration and flow distribution in shell and tube heat exchangers, *Heat Transfer Eng.*, *8*(3) 62–71 (1987).
2. Paidoussis, M. P., Flow induced vibrations in nuclear reactors and heat exchangers: Practical experiences and state of knowledge, in *Practical Experiences with Flow Induced Vibration* (Nandascher and D. Rockwell, eds.); Springer-Verlag, Berlin, 1980, pp. 1–18.
3. Paidoussis, M. P., Fluid elastic vibration of cylinder arrays in axial and crossflow: State of art, *J. Sound Vibration*, *76*, 329–359 (1981).
4. Au-Yang, M. K., Blevins, R. D., and Mulcahy, T. M., Flow induced vibration analysis of tube bundles—A proposed Section III Appendix N nonmandatory code, *Trans. ASME, J. Pressure Vessel Technol.*, *113*, 257–267 (1991).
5. Chen, S. S., Guidelines for the instability flow velocity tube arrays in crossflow, *J. Sound Vibration*, *93*(3), 439–455 (1984).
6. Weaver, D. S., and Fitzpatrick, J. A., A review of flow induced vibration in heat exchangers, *Int. Conf. Flow Induced Vibration*, sponsored by BHRA, Bowness-on-Windermere, England, 12–14 May 1987.
7. Au-Yang, M. K., Flow induced vibration: Guidelines for design, diagnosis and trouble shooting of common power plant components, *Trans. ASME, J. Pressure Vessel Technol.*, *107*, 326–334 (1985).
8. Blevins, R. D., *Flow Induced Vibration*, 2nd ed., Van Nostrand Reinhold, New York, 1990.
9. Sandifer, J. B., Guidelines for flow induced vibration prevention in heat exchangers, Welding Research Council Bulletin 372, May 1992.
10. Chen, S. S., *Flow Induced Vibration of Circular Cylindrical Structures*, Hemisphere; New York, 1987.

11. Singh, K. P., and Soler, S. I., *Mechanical Design of Heat Exchangers and Pressure and Pressure Vessel Components*, Arcturus, Cherry Hill, NJ, 1984.
12. Gupta, J. P., *Fundamentals of Heat Exchanger and Pressure Vessel Technology*, Hemisphere, Washington, DC, 1984.
13. Zukauskas, A. A., Vibration of tubes in heat exchangers, in *High Performance Single Phase Heat Exchangers*, Hemisphere, Washington, DC, 1989, pp. 316–348.
14. Pettigrew, M. J., and Taylor, C. E., Fluidelastic instability of heat exchanger tube bundles: Review and design recommendations, *Trans. ASME, J. Pressure Vessel Technol., 113*, 242–255 (1991).
15. Chen, S. S., and Jendrzejczyk, J. A., Stability of tube arrays in crossflow, *Nuclear Eng. Design, 75*(3), 351–374 (1983).
16. Chen, S. S., Some issues concerning fluid elastic instability of a group of circular cylinders in crossflow, *Trans. ASME, J. Pressure Vessel Technol., 111*, 507–518 (1989).
17. Shah, R. K., Flow induced vibration and noise in heat exchangers, *Proc. Seventh National Heat and Mass Conf.*, India, 1981, pp. 89–108.
18. Chenoweth, J. M., and Kistler, R. S., Tube vibration in shell and tube heat exchangers, *AIChE Symp. Ser., Heat Transfer: Research and Application* (1978), pp. 6–14.
19. Standards of the Tubular Exchanger Manufacturers Association, 7th ed., Tubular Exchanger Manufacturers Association, Inc., Tarrytown, New York, 1989.
20. American Society of Mechanical Engineers, Boiler and Pressure Vessel Code, Section III, Appendix N, Nonmandatory Code, New York, 1989.
21. Paidoussis, M. P., and Besancon, P., Dynamics of arrays of cylinders with internal and external axial flow, *J. Sound Vibration, 76*(3), 361–379 (1981).
22. Goyder, H. G. D., The structural dynamics of tube bundle vibration problem, *Int. Conf. Flow Induced Vibrations*, Bowness on Windermere, England, 12–14 May 1987.
23. Gorman, D. J., Experimental study of peripheral problems in heat exchangers and steam generator, Paper V.F4/g., *Proc. Fourth Int. Conf. Structural Mechanics in Reactor Technology*, San Francisco, 1977.
24. Chen, Y. N., and Weber, M., Flow induced vibrations in tube bundle heat exchangers with crossflow and parallel flow, in *Flow Induced Vibrations in Heat Exchangers, Proceedings of a Symposium Sponsored by the ASME*, New York, 1970, pp. 57–77.
25. Chen, Y. N., Flow induced vibration and noise in tube bank heat exchangers due to Von Karmon streets, *Trans. ASME, J. Eng. Ind.*, February, 134–146 (1968).
26. Owen, P. R., Buffeting excitation of boiler tube vibration, *J. Mechanical Eng. Sci.*, (4), 431–439 (1965).
27. Tinker, T., Shellside characteristics of shell and tube heat exchangers—A simplified rating system for commercial heat exchangers, *Trans. ASME*, pp. 36–52 (1958).
28. Bell, K. J., *Delaware Method for Shellside Design in Heat Transfer Equipment Design* (R. K. Shah, E. C. Subbarao, and R. A. Mashelkar, eds.), Hemisphere, Washington, DC, 1988, pp. 145–166.
29. Palen, J. W., and Taborek, J., Solution of shellside flow pressure drop and heat transfer by stream analysis method, *CEP Symposium Ser. Heat Transfer, 92, 65*, Philadelphia, 1969, pp. 53–63.
30. Heat Transfer Research, Inc., Alambhara, CA.
31. Heat Transfer and Fluid Flow Services, Oxon, UK.
32. B-Jac International, Inc., Modlothian, VA.
33. Fitz-Hugh, J. S., Flow induced vibration in heat exchangers, *Int. Symp. Vibration Problems in Industry*, Keswick, UK, 10–12 April 1973.
34. Zukauskas, A., and Katinas, V., Flow induced vibration in heat exchanger tube banks, *Proc. Symp. Practical Experiences with Flow Induced Vibration*, 1980, pp. 188–196.
35. Weaver, D. S., Fitzpatrick, J. A., and El Kashlan, M. L., Strouhal numbers of heat exchanger tube arrays in crossflow, *ASME Symp. Flow Induced Vibration*, Chicago, 1986 (S. S. Chen, J. C. Simonis, and Y. S. Shin, eds.), PVP vol. 104, pp.
36. Pettigrew, M. J., and Gorman, D. J., Vibration of tube bundles in liquid, and two phase crossflow, in *Flow Induced Vibration Guidelines* (P. Y. Chen, ed.), PVP vol. 52 (ASME), New York, 1981.
37. Pettigrew, M. J., and Gorman, D. J., Vibration of heat exchanger components in liquid and two

phase crossflow, presented at *British Nuclear Society International Conference on Vibration in Nuclear Plant*, Keswick, UK, 9–12 May 1978.
38. Rao, M. S. M., Gupta, G. D., Eisinger, F. L., Hibbitt, H. D., and Steininger, D. A., Computer modelling of vibration and wear of multispan tubes with clearances at the supports, presented at *Flow Induced Vibration Conference*, sponsored by BHRA, Bowness-Windermere, England, 12–14 May 1987, pp. 437–448.
39. Weaver, D. S., and Grover, L. K., Crossflow induced vibration in a tube bank—Turbulent buffeting and fluid elastic instability, *J. Sound Vibration*, *59*(2), 277–294 (1978).
40. Soper, B. M. H., The effect of tube layout on the fluid elastic instability of tubes bundle in crossflow, *Trans. ASME, J. Heat Transfer*, *105*, 744–750 (1983).
41. Weaver, D. S., and Schneider W., The effect of flat bar supports on the crossflow induced response of heat exchanger U-tubes, *Trans. ASME, J. Eng. Power*, *105*, 775–781 (1983).
42. Connors, H. J., Jr., Fluid elastic vibration of tube arrays excitation by crossflow, in *Flow Induced Vibration in Heat Exchangers*, (D. D. Reill, ed.), ASME, New York, 1970, pp. 42–56.
43. Lever, J. H., and Weaver, D. S., A theoretical model for fluid elastic instability in heat exchangers tube bundles, *Trans. ASME, J. Pressure Vessel Technol.*, *104*, 147–158 (1982).
44. Lever, J. H., and Weaver, D. S., On the stability of heat exchanger tube bundles: Part 1—Modified theoretical model, *J. Sound Vibration*, *107*(3), 375–392 (1986).
45. Lever, J. H., and Weaver, D. S., On the stability of heat exchanger tube bundles: Part 2—Numerical results and comparison with experiments, *J. Sound Vibration*, *107*(3), 393–411 (1986).
46. Tanaka, H., and Takahara, S., Fluid elastic vibration of a tube array in crossflow, *J. Sound Vibration*, *77*(1), 19–37 (1981).
47. Tanaka, H., and Takahara, S., Unsteady fluid dynamic force on tube bundle and its dynamic effects on vibration, in *Flow Induced Vibration of Power Plant Components* (M. K. Au-Yang, ed.), ASME, New York, 1980, Special Publication No. PVP 141, pp. 77–92.
48. Price, S. J., and Paidoussis, M. P., Fluid elastic instability of a double row of circular cylinders subject to a crossflow, *Trans. ASME, J. Vibration, Acoustics, Stress Reliability Design*, *105*, 59–66 (1983).
49. Price, S. J., and Paidoussis, M. P., An improved mathematical model for the stability of cylinder rows subjected to crossflow, *J. Sound Vibration*, *97*(4), 615–640 (1984).
50. Whiston, G. S., and Thomas, G. D., Whirling instabilities in heat exchanger tube arrays, *J. Sound Vibration*, *81*(1), 1–31 (1982).
51. Chen, S. S., Instability mechanisms and stability criteria of a group of circular cylinders subjected to crossflow, Part I, ASME Paper No. 81-Det 21, ASME, New York.
52. Chen, S. S., Instability mechanisms and stability criteria of a group of circular cylinders subjected to crossflow, Part II: Numerical results and discussions, ASME Paper No. 81-Det 22, ASME, New York.
53. Chen, S. S., Instability mechanism and stability criteria of a group of cylinders subjected to crossflow, Part I: Theory; Part II: Numerical results and discussions, *J. Vibration, Acoustics, Stress Reliability Designs*, 253–260 (1983).
54. Chen, S. S., and Jendrzejczyk, J. A., Experiments and analysis of instability of tube rows subjected to liquid crossflow, *Trans. ASME, J. Appl. Mech.*, *49*, 704–709 (1982).
55. Chen, S. S., and Jendrzejczyk, J. A., Experiments on fluid elastic instability in tube banks subjected to liquid crossflow, *J. Sound Vibration*, *78*, 355–381 (19).
56. Chen, S. S., Flow induced vibration of circular cylindrical structures, Argonne National Laboratory Rep. No. ANL-CT-85-51.
57. Eisinger, F. L., Prevention and cure of flow induced vibration problems in tubular heat exchangers, *Trans. ASME, J. Pressure Vessel Technol.*, *102*, 138–145 (1980).
58. Blevins, R. D., Review of sound induced by vortex shedding from cylinders, *J. Sound Vibration*, *92*(4), 455–470 (1984).
59. Blevins, R. D., Acoustic modes of heat exchanger tube bundles, *J. Sound Vibration*, *109*(1), 19–30 (1986).
60. Blevins, R. D., and Bressler, M. M., Acoustic resonance in heat exchanger tube bundles, Part

I: Physical nature of the phenomenon, *Trans. ASME, J. Pressure Vessel Technol., 109*, 275–281 (1987).

61. Blevins, R. D., and Bressler, M. M., Acoustic resonance in heat exchanger tube bundles—Part II: Prediction and suppression of resonance, *Trans. ASME, J. Pressure Vessel Technol., 109*, 282–288 (1987).
62. Pettigrew, M. J., Taylor, C. E., and Yasuo, A., Vibration damping of heat exchanger tube bundles in two phase cross flow," and Blevins, R. D., Acoustic resonance in heat exchanger tube bundles, Welding Research Bulletin No. 389, Welding Research Council, New York.
63. Barrington, E. A., Experience with acoustic vibration in tubular heat exchangers, *Chem. Eng. Prog.*, 69(7), 62–68 (1973).
64. Parker, R., Acoustic resonance in passages containing bank of heat exchanger tubes, *J. Sound Vibration, 57*, 245–260 (1978).
65. Burton, T. E., Sound speed in a heat exchanger tube bank, *J. Sound Vibration, 71*, 157–160 (1980).
66. Grotz, B. J. and Arnold, F. R., Flow induced vibration in heat exchangers, Department of Mechanical Engineering Tech. Rep. No. 31, 1956, DTIC No. 104568, Stanford University, Stanford, CA.
67. Barrington, E. A., Cure exchanger acoustic vibration, *Hydrocarbon Processing*, 193–198 (1978).
68. Fitzpatrick, J. A., The prediction of flow induced noise in heat exchanger tube arrays, *J. Sound Vibration*, 425–435 (1985).
69. Ziada, S., and Oengoren, A., Flow induced acoustical resonances of in-line tube bundles, *Sulzer Tech. Rev.*, 45–47 (1990).
70. Rae, G. J., and Murray, B. G., Flow induced acoustic resonances in heat exchangers, *Int. Conf. Flow Induced Vibrations*, Bowness-on-Windermere, England, May 1987, pp. 221–231.
71. Fitzpatrick, J. A., and Donaldson, J. A., *Symposium on Flow Induced Vibrations*, (M. P. Paidoussis, ed.), vol. 2, *Effects of Scale on Parameters Associated with Flow Induced Noise in Tube Arrays*, American Society of Mechanical Engineers, New York, 1984, pp. 243–250.
72. Ziada, S., Oengoren, A., and Buhlmann, E. T. *International Symposium on Flow Induced Vibration and Noise* (M. P. Paidoussis et al., eds.), vol. 3, *On Acoustical Resonance in Tube Arrays*, American Society of Mechanical Engineers, New York, 1988, pp. 219–254.
73. Reill, D. D., *Flow Induced Vibration in Heat Exchangers*, ASME, New York, 1970, pp. 2–7.
74. Halle, H., Chenoweth, J. M., and Wambsganss, M. W., Shellside water flow induced tube vibration in heat exchanger configurations with tube pitch to diameter ratio of 1.42, *Trans. ASME, J. Pressure Vessel Technol., 111*, 441–449 (1989).
75. Saunders, E. A. D., Shellside flow induced tube vibration, in *Heat Exchanger: Design, Selection and Construction*, John Wiley and Sons, New York, 19 , Chapter 11, pp. 245–273.
76. Halle, H., Chenoweth, J. M., and Wambsganss, M. W., Flow induced vibration in shell and tube heat exchanger with double segmental baffles, pp. 2763–2768.
77. Gentry, C. C., Young, R. K., and Small, M. W., RODbaffle heat exchanger thermal-hydraulic predictive methods, in *Heat Transfer 1982*, Hemisphere, Washington, DC, 1982, vol. 6, pp. 197–202.
78. Boyer, R. C., and Pase, G. K., The energy saving NESTS concept, *Heat Transfer Eng., 2*(1), 19–27 (1980).
79. Byrne, K. P., The use of porous baffles to control acoustic vibration in cross flow acoustic vibrations in crossflow tubular heat exchangers, *Trans. ASME, J. Heat Transfer, 105*, 751–757 (1983).
80. Walker, E. M., and Reising, G. F. S., Flow induced vibrations in crossflow heat exchangers, *Chem. Process Eng., 49*, 95–103 (1968).
81. Rogers, J. D., and Penterson, C. A., Predicting sonic vibration in crossflow heat exchangers—Experience and model testing, American Society of Mechanical Engineers, New York, paper 77-FE-7, 1977.
82. Zdravkovich, M., and Nuttal, J. A., On elimination of aerodynamic noise in staggered tube bank, *J. Sound Vibration, 34*, 173–177 (1974).
83. Thorngren, J. T., Predict exchanger tube damage, *Hydrocarbon Processing*, April, 129–131 (1970).
84. Blevins, R. D., Fretting wear of heat exchanger tubes, Part I: Experiments, *Trans. ASME, J. Eng. Power, 101*, 625–629 (1979).

85. Blevins, R. D., Fretting wear of heat exchanger tubes, Part II: Models, *Trans. ASME, J. Eng. Power, 101*, 630–633 (1979).
86. Haslinger, K. H., Martin, M. L., and Steininger, D. A., Pressurized water react or steam generator tube wear prediction utilizing experimental techniques, *Proc. Int. Conf. Flow Induced Vibration*, Bowness-on-Winderemere, England, May 1987, pp. 437–448.
87. Ko, P. L., and Basista, H., Correlation of support impact force and fretting wear for heat exchanger tube, *Trans. ASME, J. Pressure Vessel Technol., 106*(1), 69–77 (1984).
88. Cha, J. H., Wambsganss, M. W., and Jendrzejcyk, J. A., Experimental study of impact/fretting wear in heat exchanger tubes, Argonne National Laboratory publication ANL-85-38, 1985.
89. Hofmann, P. J., Schettler, T., and Steininger, D. A., Pressurized water reactor steam generator tube fretting and fatigue wear characteristics, *Proc. ASME Pressure Vessel and Piping Conf.* (ASME 86PVP-2), Chicago, July 1986.
90. Fisher, N. J., Olsen, M., Rogers, R. J., and Ko, P. L., Simulation of tube-to-support dynamic interaction of heat exchange equipment, *Trans. ASME, J. Pressure Vessel Technol., 111*, 378–384 (1989).
91. Eisinger, F. L., Rao, M. S. M., Steininger, D. A., and Haslinger, K. H., Numerical simulation of fluid elastic vibration and comparison with experimental results, reprinted from PVP-Vol. 206, *Flow Induced Vibration and Wear Book*, No. H00632, ASME, New York, 1991, pp. 101–111.
92. Rao, M. S. M., Steininger, D. A., and Eisinger, F. L., Computer simulation of vibration and wear of steam generator and tubular heat exchanger tubes, *Int. Symp. Advanced Computers for Dynamics and Design '89*, Tsuchiura, Japan Mechanical Division, JSME, 6–8 September 1989.
93. Rao, M. S. M., Steininger, D. A., and Eisinger, F. L., Numerical simulation of fluid elastic vibration and wear of multispan tubes with clearances at supports, reprinted from *Flow Induced Vibration in Heat Transfer Equipment*, Vol. 5, book no. G00445 (J. M. Paidoussis, S. S. Chenoweth, J. R. Chen, Stenner, and W. J. Bryan, eds.).
94. Blevins, R. D., Vibration induced wear of heat exchanger tubes, *Trans. ASME, J. Eng. Materials Technol., 107*, 61–67 (1985).
95. Moretti, P. M., and Lowery, R. L., Hydrodynamic inertia coefficients for a tube surrounded by rigid tube, *Trans. ASME, Pressure Vessel Technol., 97* (1976).
96. Timoshenko, S. P., and Young, D. H., *Vibration Problems in Engineering*, Van Nostrand Reinhold Co., Toronto, 1965, Chapter 5.
97. ABAQUS, Version 4-7, Hibbits, Karlsson and Sorensen, Inc.
98. Pettigrew, M. J., Goyder, H. G. D., Qiao, Z. L., and Axisa, F., Damping of multispan heat exchanger tubes, Part 1: In gases, in *Flow Induced Vibration* (S. S. Chen, J. C. Simon, and Y. S. Shin, eds.), PVP vol. 104, ASME, New York, 1986, pp. 81–87.
99. Pettigrew, M. J., Rogers, R. J., and Axisa, F., Damping of multisoan heat exchanger tubes, Part 2: In liquids, in *Flow Induced Vibration*, (1986), PVP vol. 104, ASME, New York, 1986, pp. 89–98.

SUGGESTED READINGS

1. Nguyen, D. C., Lester, T., Good, J. K., Lowery, R. L., and Moretti, P. M., Lowest natural frequencies of multiply supported U-tubes, *106*, p. 414 (1984).
2. Moretti, P. M., Fundamental frequencies of U-tubes in tube bundles, *Vibration in Power Plant Piping and Equipment*, ASME Symposium Volume, Denver, 21–25 June 1981.
3. Moretti, P. M., Fundamental frequencies of U-tubes in tube bundles, *J. Pressure Vessel Technol.*, 107/207 (1985).
4. Gorman, D. J., *Free Vibration Analysis of Beam and Shafts*, John Wiley and Sons, New York, 1975.
5. MacDuff, J. N., and Felgar, R. P., Vibration design charts, *Trans. ASME*, 1459–1474 (1957).
6. Bolleter, U., and Blevins, R. D., Natural frequences of finned heat exchanger tubes, *J. Sound Vibration, 80*, 367–371 (1982).
7. Moretti, P. M., Fundamental frequencies of U-tubes in tube bundles, *Trans. ASME, J. Pressure Vessel Technol, 107*, 207–209 (1985).
8. Naguyen, D. C., Lester, T., Good, J. K., Lowery, R. L., and Moretti, P. M., Lowest natural frequen-

cies of multiply supported U-tubes, *Trans. ASME, J. Pressure Vessel Technol.*, *106*, 414–416 (1984).
9. Sing, K. P., and Soler, A. I., *HEXDES User Manual*, Arcturus, Cherry Hill, NJ, 1984.

APPENDIX

Calculation Procedure for Shell-Side Liquids

Draw a sketch of the exchanger and identify the most probable zone susceptible for FIV. Then follow these steps.

Step 1. Calculate Tube Mass per Unit Length, m

a. Calculate hydrodynamic mass coefficient, C_m by TEMA method (read C_m from Fig. 35):

$C_m =$

or by Blevins method:

$$\frac{De}{D} = \left(1 + 0.5\,\frac{p}{D}\right)\frac{p}{D}$$

$$C_m = \frac{(De/D)^2 + 1}{(De/D)^2 - 1}$$

b. Calculate the tube mass per unit length, $m = \dfrac{\Pi D^2 Cmp_s}{4} + \dfrac{\Pi D_i^2 p_i}{4} + \dfrac{\Pi(D^2 - D_i^2)p}{4}$

Step 2: Calculate Tube Natural Frequency, f_n

For Straight Tube:

a. Calculate the area moment of inertia of the tube cross section, I:

$$I = \frac{\pi}{64}(D^4 - D_i^4)$$

b. Calculate cross section of the tube, A_t:

$A_t = \pi(D^2 - D_i^2)/4$

c. Calculate tube axial longitudinal load, F_a:

$F_a = \sigma_t A_t$ (positive for tensile load and negative for compressive, σ_t tube longitudinal stress calculated as per TEMA RCB-7.23 or by any other method)

d. Identify the span with pinned-pinned condition between two baffles in window zone. Find out the tube span length, L, to calculate f_n and other parameters. L is given by:

$L = L_{BC} + L_{BC}$ (for central window zone)

e. Calculate the buckling load for the tube span:

$$F_{cr} = \frac{\pi^2 EI}{L^2}$$ for pinned–pinned condition

f. Calculate natural frequency multiplier:

$\chi_n = F/_a F_{cr}$

g. From Table 10.4 choose the value of frequency constant λ_n for central window span:

$\lambda_n =$

h. Calculate natural frequency, f_n:

$$f_n = \frac{1}{2\pi}\frac{\chi_B \lambda_n^2}{L_i^2}\left(\frac{EIg_c}{m}\right)^{0.5} \qquad \text{for } L_i = L_{BC} + L_{BC}$$

Note: f_n is calculated for the central baffle window region. If it is suspected that the tube span between the tube sheet and the first baffle in the window zone will be controlling, then calculate f_n with $L = L_{BI} + L_{BC}$ (inlet window zone).

For U-Tube:

a. Draw a sketch of the U-bend section and identify the configuration with TEMA Fig. V-5.3-V-5.3.3.

   Calculate $l_b/r = s/r =$

b. Determine C_u from TEMA charts.
c. Calculate the natural frequency for the first mode.

$$f_{n,u} = 68.06\frac{C_u}{R^2}\left(\frac{EI}{m}\right)^{0.5} \qquad \text{(use TEMA dimensional units)}$$

Note: TEMA dimensional units are E = psi, I = in.^{4}, m = lbm/ft, R = in.

Step 3. Calculate damping parameter δ

TEMA Method.

$$\delta_1 = \frac{3.41D}{mf_n} \quad \text{and} \quad \delta_2 = \frac{0.012D}{m}\left(\frac{\rho_s\mu}{f_n}\right)^{0.5}$$

$$\delta = \max\{\delta_1, \delta_2\}$$

Correlations of Pettigrew, Rogers, and Axisa.

$$\frac{D}{D^*} = (1.7p/D)^{-1} \qquad \text{for triangular array}$$

$$= (1.9p/D)^{-1} \qquad \text{for square array}$$

$$\xi_n = \frac{\Pi}{\sqrt{8}}\frac{1 + (D/D^*)^3}{[1 - (D/D^*)^2]^2}\left(\frac{\rho_s D^2}{m}\right)\left(\frac{2U}{\Pi f_n D^2}\right)^{0.5} + \left(\frac{N-1}{N}\right)\left(\frac{22}{f_n}\right)\left(\frac{\rho_s D^2}{m}\right)\left(\frac{t_b}{L_t}\right)^{0.6}$$

$$\delta = 2\pi\xi_n$$

Note: If δ is less than 0.0377, then assume $\delta = 0.0377$.

Step 4. Calculate the crossflow velocity, U

Calculate U for the shell under consideration by TEMA/Bell/other methods. Otherwise, take the value from the TEMA thermal specification sheet.

Step 5. Check for Vortex Shedding

TEMA Criterion. Not available for liquids; only available for gas flow.

Correlations of Weaver and Fitzpatrick.

a. Calculate Strouhal number, S_u:

$$S_u = \frac{1}{1.73X_t} \quad \text{for 30° layout}$$

$$= \frac{1}{1.16X_t} \quad \text{for 60° layout}$$

$$= \frac{1}{2X_t} \quad \text{90° and 45° layout}$$

b. Calculate vortex shedding frequency, f_v:

$$f_v = \frac{S_u U}{D}$$

c. Check

$0.8f_v < f_n < 1.2f_v$ Resonance

$f_n D/U > 2S_u$ Acceptable

$f_n D/U < 0.2S_u$ Acceptable

Au-Yang et al. Criteria. Calculate the reduced damping C_n:

$$C_n = \frac{4\pi\xi_n m}{\rho_v D^2}$$

a. Both lift and drag direction lock-in are avoided if

$$\frac{U}{f_n D} < 1 \quad \text{Check: OK or not OK}$$

b. For a given vibration mode, if the reduced damping satisfies the following condition, then lock-in will be suppressed in that vibration mode.

$C_n > 64$ Check: OK or not OK

c. For a given vibration mode, if $C_n > 1.2$ and the following condition is satisfied, then lift direction lock-in is avoided and drag direction lock-in is suppressed:

$$\frac{U}{f_n D} < 3.3 \quad \text{Check: OK or not OK}$$

Maximum Deflection Due to Vortex Shedding at Resonance.

a. Determine lift coefficient C_L from Table 2. Interpolation is not recommended. If C_L for the pitch ratio under consideration is not available, assume the conservative value of 0.091.
b. Calculate the maximum response, y_{max}, of the tube span between two baffles.

$$y_{max} = \frac{C_L \rho_s D U^2}{4\xi_n \pi^3 f_n^2 m^2}$$

c. Check: If $y_{max} < 0.02D$, OK.

Step 6. Turbulence-Induced Excitation

a. Determine $C_R(f)$ from Fig. 7.
b. The mean square response for a pinned-pinned span is given by

$$\bar{y}_{max}^2 = \frac{\left[C_R(f)\rho_s U^2 D\right]^2}{128\pi^3 \xi_n f_n^3 m^2}$$

$$y_{rms} = \sqrt{\bar{y}_{max}^2}$$

c. Check: If $y_{rms} < 0.01$ in (0.254 mm), OK.

Step 7: Fluid Elastic Instability
TEMA Criterion.

a. Calculate reduced velocity parameter, χ:

$$\chi = \frac{m\delta}{\rho_s D^2}$$

b. Calculate critical velocity by referring to Table 5.

$U_{cr} =$

c. Check: If $U < U_{cr}$ or $U/U_{cr} < 0.5$, OK.

Au-Yang et al. Criteria. Choose K_{mean} from Table 4, (a) for the particular tube layout pattern and (b) for all arrays.

a. For the particular tube layout pattern:

$$\frac{U_{cr}}{f_n D} = K_{mean}\left(\frac{m\delta}{\rho_s D^2}\right)^{0.5}$$

$U_{cr} =$

Check: If $U < U_{cr}$ or $U/U_{cr} < 0.5$, OK.

b. $K_{mean} = 4.0$ for all arrays:

$$\frac{U_{cr}}{f_n D} = 4.0\left(\frac{m\delta}{\rho_s D^2}\right)^{0.5}$$

$U_{cr} =$

Check: if $U < U_{cr}$ or $U/U_{cr} < 0.5$, OK.

c. Check as per conservative criteria. Assume $\delta = 0.09425$ and $K = 2.1$

$$\frac{U_{cr}}{f_n D} = 2.1 \left(\frac{m\delta}{\rho_s D^2} \right)^{0.5}$$

$U_{cr} =$

Check: If $U < U_{cr}$, certainly FIV will not be a problem.

Pettigrew and Taylor Criterion.

$$\frac{U_{cr}}{f_n D} = 3.0 \left(\frac{m\delta}{\rho_s D^2} \right)^{0.5}$$

Check: If $U < U_{cr}$ or $U/U_{cr} < 0.5$, OK.

Step 8

Fill the preceding parameters into the flow-induced vibration specification sheet–liquids shown in Table 5.

Calculation Procedure for Shell-Side Vapors

Repeat steps 1 to 7 as already described. For gases, the damping parameter is calculated by this correlation:

$$\delta = 3.463 \times 10^{-3} \frac{N-1}{N} t_h \qquad \text{for } t_h < 12.7$$

$$\delta d = 0.314 \frac{N-1}{N} \left(\frac{t_h}{L_t} \right)^{0.5} \qquad \text{for } t_h \geq 12.7$$

and the criterion for amplitude at peak resonance due to turbulent buffeting may be neglected.

Step 9. Check for Acoustic Resonance

Calculate the acoustic vibration frequency, f_a:

TEMA Method (for Cylindrical Volume Only).

$$f_a = \frac{483.2}{L_a} \left(\frac{p_s}{\rho_s} \right)^{0.5} \qquad \text{(use TEMA dimensional units)}$$

Blevins Method.

a. Calculate velocity of sound C through the tube bank.

$$C = \sqrt{g_c Z \gamma R_s T / M_g}$$

b. Calculate tube layout solidity factor, σ:

$$\sigma = 0.9069 \left(\frac{D}{p} \right)^2 \qquad \text{for } \theta = 30^\circ \text{ or } \theta = 60^\circ$$

$$= 0.7853 \left(\frac{D}{p} \right)^2 \qquad \text{for } \theta = 90^\circ$$

$$= 1.5707\left(\frac{D}{p}\right)^2 \qquad \text{for } \theta = 45°$$

c. Calculate effective velocity of sound through the tube bank:

$$C_{\text{eff}} = \frac{C}{\sqrt{(1+\sigma)}} \qquad \text{Parker}$$

$$C_{\text{eff}} = \frac{C}{\sqrt{(1+C_m\sigma)}} \qquad \text{Burton}$$

Note: Choose C_{eff} by Burton method for conservative values.

d. Calculate the acoustic resonance frequency, f_a:

For a cylindrical volume,

$$f_a = \frac{C_{\text{eff}}\lambda_i}{2\pi R}$$

where $\lambda_1 = 1.84$ and $\lambda_2 = 3.054$.

For a rectangular volume

$L_x =$, $L_y =$, and $L_z =$

$$f_a = \frac{C_{\text{eff}}}{2}\left[\left(\frac{i}{L_x}\right)^2 + \left(\frac{j}{L_y}\right)^2 + \left(\frac{k}{L_z}\right)^2\right]^{0.5}$$

where $i = 0$, $j = 1$, and $k = 0$. Note: In heat exchangers of normal size the fundamental or the second mode is the most likely to occur. For large exchangers with shell diameter of the order of 20–30 m the acoustic vibration can be excited up to fifth or sixth mode.

Step 10. Criteria for Occurrence of Acoustic Resonance

Criteria for Vortex Shedding Mechanism. Calculate Strouhal number due to vortex shedding:

$$S_u = \frac{f_v D}{U}$$

a. Chen number and Eisinger criteria: Calculate Reynolds number, Re:

$$\text{Re} = \frac{UD}{\nu}$$

Calculate Chen number, ψ:

$$\psi = \frac{\text{Re}\,(2X_1 - 1)^2}{S_u(4X_1^2X_t)}$$

Check:

$\psi < 2000$	No vibration
$\psi = 2000$–4000	Low likelihood of vibration
$\psi > 4000$	High likelihood of vibration

TEMA condition: Acoustic resonance is possible if $\psi = 2000$.

b. Blevins criteria:
Normal criteria:

Check: If $\frac{0.8S_tU}{D} < f_a < \frac{1.2S_tU}{D}$ resonance will occur

Conservative criteria:

Check: If $\frac{0.6S_tU}{D} < f_a < \frac{1.48S_tU}{E}$ resonance will occur

c. Sound pressure level (SPL) at resonance: Calculate SPL from the following equation or determine from the sound pressure level maps of Blevins, Fig. 16.

$SPL = 20 \log_{10}(p_{rms}/0.00002)$

Check: If SPL < 140 dB, no damage either to the structural components or harmful to the surroundings. Note: Sound level maps are valid for Reynolds numbers up to 95.1×10^3.

d. Resonance will occur if $\frac{U}{f_aD} > 2$

Criteria for Turbulent Buffeting.

a. Owen's criterion for the central dominant frequency when $p/D > 1.25$ is:

$$f_{tb} = \frac{U}{DX_tX_l}\left[3.05\left(1 - \frac{1}{X_t}\right)^2 + 0.28\right]$$

Check: If $0.8f_{tb} < f_a < 1.2f_{tb}$ resonance will occur

b. Criterion of Rae and Murray:

Check: If $\frac{U}{f_aD} < 2(X_l - 0.5)$, OK.

This criterion is included in TEMA.

c. Grotz and Arnold criterion (for in-line arrays): Calculate the slenderness ratio τ.

$$\tau = \frac{L_a}{Dn(X_l - 1)}$$

Check: Resonance will occur for $\tau = 62–80$.

Step 12

Fill the parameters and design criteria into the acoustic resonance specification sheet of Table 6.

11
Mechanical Design of Shell and Tube Heat Exchangers

1 STANDARDS AND CODES

Standards and codes were established primarily to ensure safety against failure. The need for safety standards is obvious in a world growing increasingly aware of the hazards posed to people, property, and the environment by complex technology, which may have the potential for doing immense harm [1a,1b]. The codes and standards give guidance and in some cases govern the design, manufacture, construction, operation, and maintenance of heat exchangers and pressure vessels. These codes and standards are themselves based upon research, development, and experience. The present-day codes have their origin in the rules laid down by the insurance companies in the past for the safe operation of boilers and pressure vessels against explosions or accidents and consequential damage to the human lives and property.

1.1 Standards

A standard can be defined as a set of technical definitions and guidelines, or how-to instructions for designers and manufacturers [2]. Standards are mostly voluntary in nature. They serve as guidelines but do not themselves have a force of law. Standards are universally adopted in manufacturing, procurement, and operation of thousands of devices and products, including raw materials, equipment, etc. Many standards have been adopted as a means of satisfying the regulatory or procurement requirements. Standards help to reduce the cost of products and processes in the following manner:

At the design level, rationalization of design procedure, drawings and specifications takes place. This avoids the repetition of detailed design analysis for either identical or similar jobs.

Standards help in complete interchangeability and uniformity of fundamental design, tools, gages, tool accessories, etc.

The standards can be of the following major four types:

1. Company standards
2. Trade or manufacturers association standards
3. National standards
4. International standards

Company Standards

Company standards are followed by individual companies, subcontractors to the companies, and the licence holders.

Trade or Manufacturers Association Standards

Trade or manufacturers association standards are the rules and the recommendations of various manufacturers of common interest, developed based on experience in design, manufacture, installation, and operation. While making the standards, feedback from users is normally included. Manufacturers association standards that are most famous among heat exchanger manufacturers are TEMA [3], HEI [4–6], and API Standards [7]. There are also EJMA Standards [8] for the design of membrane type expansion joints and ANSI (American National Standards Institute) standards for design of fittings, flanges, valves, piping and piping components.

National Standards

National Standards are followed in the country where the standard has been issued and by subcontractors or licence holders in other countries or complied with when the purchasers have so specified. National standards like BSI (Britain) [9], JIS (Japan) [10], and DIN (Germany) [11] are discussed next.

British Standards (BSI), 1993. BSI's major function is to help British industry compete effectively in world markets. Its work in standards, testing, quality assurance and export guidance is geared to enable British companies to meet the quality needs of buyers at home and abroad. BSI is independent, operating under a Royal Charter. BSI was the first national standards body in the world. There are now more than 80 similar organizations that belong to the International Organization for Standardization (ISO) and the International Electrotechnical Commission (IEC). Over 11,000 British Standard publications are listed in British Standards, 1993. Orders for publications should be directed to BSI Publications at Linford Wood, Milton Keynes, United Kingdom MK14 6LE.

Japanese Industrial Standards (JIS). JIS (Japanese Industrial Standards) are national voluntary standards for industrial and mineral products. Various industrial associations also establish voluntary standards for their specific needs. Many companies have a set of company standards like operation manuals some of them adopted from JIS and/or industrial association standards.

DIN—German Standards. The creation of German standards is the task of DIN, Deutsches Institut fur Normung e.V., a self-governing institution of trade and industry. On the basis of its statutes and of DIN 820, the standard that specifies the principles directing its activities, and by virtue of an agreement concluded with the government in 1975, DIN is the institution that is competent for standardization in the Federal Republic of Germany. As the representative of Germany, it fulfills an equivalent function in the European (CEN/CENELEC) and international standards organizations (ISO), while in the field of electrical engineering such activities are coordinated through the Deutsche Elektrotechnischen Kommission von DIN and VDE (DKE).

International Standards. ISO (International Organization for Standardization) is a worldwide federation of national standards bodies, at present comprising 92 members, one in each country. ISO coordinates the exchange of information on international and national standards, technical regulations, and other standards type documents, through an information network called ISO-NET, which links the ISO Information Centre in Geneva with similar national centers in other countries.

International Standards are followed all over the world. International Standards for quality, NDT, materials, heat exchangers, and others are framed by the ISO, Geneva. Relevant international standards for our studies include ISO 1993 [12] and ISO 9000 Series on Quality. Information on ISO 1993 is given next, whereas the ISO 9000 Quality series is covered in Chapter 14, Quality Control and Quality Assurance, Inspection, and NDT.

ISO 1993. The scope of ISO 1993 [12] covers standardization in all fields except electrical and electronic engineering standards, which are the responsibility of IEC, the International Electrotechnical Commission. Together, ISO and IEC form the specialized system for worldwide standardization—the world's largest nongovernmental system for voluntary industrial and technical collaboration at the international level. The results of ISO technical work are published in the form of International Standards. The 1993 ISO Catalogue lists 8651 published international standards. They are available as single documents, in handbook compilations for specific fields, and, in many countries, on microfilms and microfiches as well as on CD-ROM (compact disk–read-only memory).

1.2 Design Standards Used for the Mechanical Design of Heat Exchangers

Some design standards used for the mechanical design of heat exchangers include these: TEMA-USA, HEI-USA, API-USA, BS 3274-UK, and IS:4503-India.

TEMA Standards

Founded in 1939, the Tubular Exchanger Manufacturers Association, Inc., or TEMA, is a group of leading manufacturers of shell and tube heat exchangers who have pioneered the research and development of heat exchangers for over 50 years. TEMA Standards are followed in most countries of the world for design of shell and tube heat exchangers. Standards such as BS 5500 and API 660 incorporate part or all part of the TEMA Standards by reference.

Scope and General Requirements (Section B-1, RCB-1.1). The TEMA mechanical standards are applicable to unfired shell and tube heat exchangers with inside diameters not exceeding 60 in (1524 mm), a maximum product of nominal diameter (inches) and design pressure (psi) of 60,000 lb/in, or a maximum design pressure of 3,000 psi. The intent of these parameters is to limit the maximum shell wall thickness to approximately 2 in (50.8 mm) and the maximum stud diameter to approximately 3 in (76.2 mm). Criteria contained in these standards can be applied to units constructed with larger diameters. For units outside this scope, refer to TEMA Standards Section 10, Recommended Good Practice.

Scope of TEMA Standards. Table 1 shows the scope of the TEMA Standards.

Contents. The contents of TEMA Standards is given here. Each section is identified by an uppercase letter symbol, which precedes the paragraph numbers of the section and identifies the subject matter. TEMA classes R, C, and B have been combined into one section titled class RCB. The differences in design practices among the classes have been to some extent simplified. Section 5 has mechanical standards that apply to three classes of heat exchangers R, C, and B.

Table 1 Scope of TEMA Standards

Parameter	Limit
Inside diameter	60 in (1524 mm)
Nominal diameter × pressure	60,000 lb/in (10,500 N/mm)
Pressure	3000 psi (20,670 kPa)
Shell wall thickness	2 in (50.8 mm)
Stud diameters (approx.)	3 in (76.2 mm)
Construction code	ASME Section VIII, Div. 1
Pressure source	Indirect (unfired units only)

TEMA Standards Contents

Section	Symbol	Paragraph
1	N	Nomenclature
2	F	Fabrication tolerances
3	G	General fabrication and performance information
4	E	Installation, operation, and maintenance
5	RCB	Mechanical standards TEMA class RCB heat exchangers
6	V	Flow-induced vibration
7	T	Thermal relations
8	P	Physical properties of fluids
9	D	General information
10	RGP	Recommended good practice

Construction Code. According to Section RCB-1.13, the construction of heat exchangers shall comply with the ASME Boiler and Pressure Vessel Code, Section VIII, Div. 1.

Differences Among TEMA Classes R, C, and B. Differences among TEMA classes R, C, and B have been summarized by Taborek et al. [13] and are listed in Chapter 5.

TEMA Engineering Software. The Tubular Exchanger Manufacturers Association (TEMA) has made available user-friendly, state-of-the-art engineering software for the IBM PC and compatibles. This software complements the TEMA Standards, seventh edition, in the areas of

1. Flexible shell elements (expansion joints) analysis
2. Flow-induced vibration analysis
3. Fixed tube-sheet design and analysis

The programs handle the complex calculations of their respective sections of the seventh edition TEMA standards.

When Do the TEMA Standards Supplement or Override the ASME Code Specification? ASME Code provides rules for the design of the pressure boundary components like the shell, front and rear heads, flanges and covers, openings, nozzle, and reinforcements, and rules for construction, manufacturer's inspection, and hydrostatic testing. In the 1992 edition, formulas are also included for tube-sheet design, design of membrane-type expansion joints, and flanged and flued type expansion joints (procedures for determination of spring rate and stress analysis are not given). The rest of the information comes from the TEMA Standards. This includes the minimum thickness of shell and end closures, thickness of the pass partition plates and

baffles, baffle spacing, tube to baffle hole clearance, drill drift, tolerance on ligaments, shell to baffle clearance, dimensional tolerances, standard clearances and tolerances applying to tube sheets, partitions, covers and flanges, impingement protection, tube-sheet design, stress induced in the shell and the tube bundle, tube-to-tube-sheet joints, design criteria for flat cover deflection, fabrication tolerances, standard tolerances on external dimensions, nozzle and support locations, nozzle extension into the shell and angularity, etc. The seventh edition of TEMA Standards includes formulas to determine the minimum thickness of the tube sheet extended as a flange and a section on flow-induced vibration guidelines. In situations where the specifications are provided both by the codes and the TEMA Standards, the latter generally override the former [14]. However the following points warrants comment here: (1) Maximum allowable stresses in the components designed according to TEMA Standards are limited to ASME Code values, and (2) tube sheets shall be designed as per TEMA only, even though separate procedures are included in the nonmandatory section of ASME Code.

Heat Exchange Institute Standards

The Heat Exchange Institute (HEI), Cleveland, Ohio, is an association of manufacturers of heat transfer equipment used in power generation. The association promotes improved designs by developing equipment design standards. It publishes standards for tubular heat exchangers used in power generation. Such exchangers include surface condensers, feedwater heaters, and other power plant heat exchangers. Among these standards are

1. Standards for Surface Condensers [4]
2. Standards for Power Plant Heat Exchangers [5]
3. Standards for Feedwater Heaters [6]

API Standard 660

API Standard 660, Shell and Tube Heat Exchangers for General Refinery Services [7], covers technical sections that exceed or supplement the TEMA Standards R class heat exchangers. This standards is a purchaser's specification intended for removable bundle floating head or U-tube construction. It does not discuss sections concerned with commercial matters. It requires exchangers to meet the requirements of TEMA Standards, Sections 1, 2, 3, 5 (Class R), and 8, and to be constructed as per ASME Code.

EJMA Standards

The Expansion Joint Manufacturers Association Inc. [8], or EJMA, is a group of leading manufacturers of bellows-type expansion joints. This association issues standards on the design of bellows-type expansion joints known as EJMA Standards. The bellows-type expansion joints are employed primarily in piping systems to absorb differential thermal expansion while containing the system under pressure. Other applications include in pressure vessels and heat exchangers. Typical service conditions range from pressures of 25 μm to 1000 psig and –420 to 1800°F (–251 to 982°C).

1.3 Codes

A code is a system of regulations or a systematic book of law often given statutory force by state or legislative bodies [15]. A code becomes a legal document in a state, a province, or a country if the government concerned passes appropriate legislation making it a legal requirement. Among the codes, the ASME Code for construction of boilers and pressure vessels including heat exchangers is the most widely used and referred to code in the world today. Apart from ASME Code, many other codes are issued by various countries. These codes are shown in Table 2. Basically the codes differ in their legal status in their own countries. Range

Table 2 International Design Codes Used for the Mechanical Design of Heat Exchangers

Code name	Country
ASME Code, Section III [21], Section VIII, Divs. 1 & 2	United States
BS 5500	United Kingdom
CODAP, SNCT [22]	France
A. D. Merkblatter	Germany
ANNC [23]	Italy
Stoomwenzen [24]	Dutch
ISO/DIS-2694 [25]	International
IS:2825-1969 [26]	India
GOST	USSR
The Pressure Vessel Code [27][a]	Japan
Regels Voor Toesellen onder Druck [28]	Netherlands

[a]Dai Isshu Atsuryoku Youki Kousou Kikahu.

of applicability varies with regards to the scope of the codes, which includes basis of design and stress analysis, design pressure and temperature, diameter, volume, materials of constructions, fabrication, inspection, etc. There is no specific code available exclusively for construction of heat exchangers in the world. Generally heat exchanger standards quote certain codes to be followed for construction of the heat exchangers. In the following paragraphs, codes like ASME Code [16,17], BS 500 [18], CODAP [19], and A. D. Merkblatter [20] are discussed.

Addresses of important codes outside the United States and Canada are furnished by Yokell [29].

ASME Codes

What Is the ASME Boiler and Pressure Vessel Code? ASME Code establishes minimum rules of safety governing the design, fabrication, inspection, and testing of boilers, pressure vessels, and nuclear power plant components. It covers new construction and rerating the existing equipment. The existence of the code stamp on a pressure vessel, with the indicated pressure and temperature, establishes the design conditions, new and old. The service conditions such as corrosion, erosion, change in operating pressure, and/or temperature may be reasons to rerate the unit, but the original stamping remains valid. Supplemental stamping is a requirement to address rerating [30].

ASME Code—Historical Background. The steady increase in boiler explosions in the 40 years from 1870 to 1910 excited public feeling to make rules and regulations for safe operation of steam boilers. In 1911, ASME formed a Boiler Committee, now called as Boiler and Pressure Vessel Code (BPVC) Committee, to devise a uniform code to protect life, limb, equipment, and property. With the publication of the ASME Code for Construction of Boiler and Pressure Vessels in 1914, serious boiler explosions steadily decreased despite the fact that the number of boilers in use has increased enormously. Primarily as a result of the ASME Boiler Code, boiler explosions and the consequent loss of life and damage to property are a rarity today [31]. To become familiar with the important aspects of ASME Codes, refer to refs. 1, 29, and 30, Nichols [32], and refs. 33a–35. Readers are advised to refer the latest codes and standards

to know the state of the art. Unless otherwise mentioned, the mention of ASME Code throughout this book refers to ASME Code Section VIII, Div. 1, only.

ASME Codes. ASME Codes consist of 11 sections, and Section VIII deals with unfired pressure vessels. The various sections are:

I Power Boilers
II Material Specifications
  Part A—Ferrous Materials
  Part B—Nonferrous Materials
  Part C—Welding Rods, Electrodes, and Filler Metals
  Part D—Material Properties
III Rules for Construction of Nuclear Power Plant Components
  Subsection NCA—General Requirements for Division 1 and Division 2
  Division 1
    Subsection NB—Class 1 components
    Subsection NC—Class 2 components
    Subsection ND—Class 3 components
    Subsection NE—Class MC components
    Subsection NF—Component Supports
    Subsection NG—Core Support Structures
    Appendices
  Division 2—Code for Concrete Reactor Vessels and Containments
IV Heating Boilers
V Nondestructive Examination
VI Recommended Rules for Care and Operation of Heating Boilers limited to the operating ranges of heating boilers (Section IV)
VII Recommended Rules for Care of Power Boilers
VIII Pressure Vessels, Division 1
  Pressure Vessels, Division 2 Alternative Rules
IX Welding and Brazing Qualifications
X Fiberglass-Reinforced Plastic Pressure Vessels
XI Rules for In-Service Inspection of Nuclear Power Plant Components
  Division 1
  Division 2
  Division 3

Addenda
Interpretations
Code Cases Boilers and Pressure Vessels

Publication of the SI (Metric) edition of the ASME Boiler and Pressure Vessel Code was discontinued with the 1986 edition.

Address trade enquiries to:

ANSI/ASME—BOILER AND PRESSURE VESSEL CODES
American National Standards Institute
11 West 42nd Street
New York, NY 10036, USA

Sections relevant for the fabrication of heat exchangers other than nuclear power plant units (i.e., unfired pressure vessels) are Section II, Section V, Section VIII, and Section IX. The ASME Code does not dictate what section of the code to use. The law or regulatory body at the point of installation determines what section to use.

Section VIII—Pressure Vessels. This section has two divisions. Division 1 gives the traditional approach for the design of pressure retaining components, and Division 2 presents alternate rules for pressure vessels which permit higher stress level.

Division 1. In terms of scope and limitations, this division covers the minimum safety requirements applicable to the construction, design, fabrication, and certification of unfired pressure vessels under either internal and/or external pressure for operation to pressures exceeding 15 psig and to vessels having an inside diameter, width, height, or cross-section diagonal exceeding 6 in. The pressure may be obtained from an external source, or by the application of heat from a direct or indirect source, or any combination thereof. This division contains both mandatory and nonmandatory appendices detailing supplementary design criteria, nondestructive examination, and inspection acceptance criteria for the fabrication of vessels. Division 1 does not prohibit the application of the U-stamp on any vessel provided the design and construction satisfies all of the code rules in the section. The code calls attention to the fact that above 3000 psi MAWP, variations in the rules and details may be necessary. Salient features of design rules of Section VIII, Divs. 1 and 2, are reviewed by Farr [36].

Except as permitted by UG-10, UG-11, or a Code Case, materials are limited to those listed in the ASME Code, Section II, and also listed in the tables of allowable stresses given in Subsection C.

Division 2 Alternative Rules. These rules provide an alternative to the minimum construction requirements for the design, fabrication, inspection and certification of pressure vessels within the scope of Div. 1. Div. 2 rules cover only vessels to be installed in a fixed location for a specific service where operation and maintenance control is retained during the useful life of the vessel by the user who prepares or causes to be prepared the design specifications. Rules in Div. 1 are not to be mixed with rules in Div. 2. In comparison to Div. 1, Div. 2 requirements on materials and nondestructive examination are stringent, and higher design stress values are permitted. The basic premise in Section VIII, Div. 2, as well as many other sections of the code, is that when more design analysis is made and when more restrictive requirements for materials, fabrication, inspection, and testing are met, the factor of safety may be lowered [36].

ASME Code Section VIII, Divs. 1 and 2—Design Criteria: A Comparison. Section VIII, Div. 1, is based on "design-by-rule" principles. It utilizes formulas, charts, tables, and graphs for sizing and determining the basic thicknesses of pressure retaining components. It is based on a factor of safety of 4 on the ultimate tensile strength (UTS). On the other hand, Div. 2 is based on a factor of safety 3 on the UTS. Division 2 is based on use of some design charts and formulas; however, the basic method is "design-by-analysis," where stresses are arrived at after detailed stress analysis and compared with allowable stresses. The higher permissible stress levels for service temperature below the creep range will permit thinner vessels in Div. 2 than Div. 1. For detailed comparison of Div. 1 and Div. 2, refer to ref. 37.

When should one consider using Div. 2 rules? Some of the conditions that favor Div. 2 rules are [29]:

1. Service is severe enough to indicate the need for intensive analysis; the costs of the necessary engineering analysis and more rigorous construction requirements are economically justified by the anticipated savings in materials and labor.
2. Pressure exceeds 3000 psi (20,670 kPa).

3. The product of pressure times shell diameter exceeds 60,000 lb/in (1.216 N/m).
4. Fatigue may affect the safety and life of the exchanger.
5. The ratio of shell diameter to thickness is less than 16, or shell thickness calculated by Div. 1 rules exceeds 3 in (76.2 mm).

Addenda. Colored sheet Addenda, which include additions and revisions to individual sections of the code, are published annually and will be sent automatically to the purchasers of the applicable sections up to the publication of the next edition/revision.

Interpretations. The ASME issues written replies to inquiries concerning interpretation of technical aspects of the Code. The interpretations for each individual section will be published separately and will be included as part of the update service to that section. They will be issued semiannually (July and December) up to the next publication of the Code. Interpretations of Sections III, Div. 1 and 2, will be included with the update service to Subsection NCA. Interpretations are not part of the Code or the Addenda.

Code Cases, Boilers and Pressure Vessels. This contains provisions that have been adopted by the Boiler and Pressure Vessel Committee that cover all sections of the Code other than Section III, Divs. 1 and 2, Section XI, to provide, when the need is urgent, rules for materials or constructions not covered by existing Code rules. Case revisions in the form of supplements will be sent automatically to purchasers up to the publication of the 1995 Code. Code Cases may be used in the construction of components to be stamped with the ASME Code symbol beginning with the date of their approval by ASME.

Technical Inquiries. When a user of the code has difficulty in understanding a part of the Code, a technical inquiry may be sent to the ASME Code Committee for an interpretation of the provisions or requirements of the Code. The letter should be addressed to the secretary to the following address:

Secretary
Boiler and Pressure Vessel Code Committee
American Society of Mechanical Engineers
345 East Forty Seventh Street
New York, NY 10017

There are several reasons why an inquiry will not be handled by the Committee, and the inquirer is so informed. The reasons for rejection include [37] (1) basis of Code rules, (2) indefinite question with no reference to Code paragraphs, figures, or rules, (3) semicommercial question with doubt as to whether question is related to Code requirements or is asking approval of design, and (4) approval of specific design.

ASME Code Symbol Stamp and Certificate of Authorization Program. To insure compliance with code requirements, ASME has administered a certificate of authorization as a part of its codes and standards program since 1915, and recently it was expanded to include all types of pressure vessels, including nuclear power plant components.

BS 5500

The main design code for pressure vessels as per British Standards is BS 5500 [18]. It covers pressure vessels manufactured from carbon, ferritic alloy, austenitic steels, and aluminum. BS 5500 replaced the earlier standards: (1) BS 1500 fusion-welded pressure vessels for general purposes, and (2) BS 1515 fusion-welded pressure vessels for use in the chemical, petroleum, and allied industries. Annexure AA Supplement to BS 5500 is the requirements for aluminum and aluminum alloys in the design and construction of unfired fusion-welded pressure vessels. BS 5500 contains rules for both "design-by-analysis" and "design-by-rule." Section 3 of BS

5500 provides design rules for specific well-known and established geometries under design pressure and temperature loading only. Salient features of design rules of BS 5500 are given in Houston [38].

BS 5500 Software Solution. ESDU International markets a software package incorporating BS 5500. For further details contact:

ESDU International
27 Corsham Street
London NI 6UA, United Kingdom

BS 3274. This is the specification for tubular heat exchangers for general purposes, design, construction, and inspection testing of the cylindrical shell and plain tube heat exchangers. Shell diameters are 6–42 in, tube lengths 6–16 ft, tube diameters $\frac{1}{2}$–1.5 in. Type 1 is the fixed tube sheet (nonremovable tube bundle); type 2 is the U-tube (removable tube bundle); and type 3 is the floating head (removable tube bundle).

French Codes and Standards on Boiler and Pressure Vessels

Several construction codes and standards are in application in France for the design and construction of pressure components. Steam generators are covered by a set of AFNOR Standards. Unfired pressure vessels are covered by the CODAP Code. Salient features of design rules of French codes and standards on boiler and pressure vessels are reviewed by Thomas et al. [39].

CODAP Code. CODAP Code is applicable to components subjected to pressure whose internal pressure exceeds 0.5 bar or whose external pressure exceeds 0.1 bar [19]. It is not applicable to piping covered by the SNCT industrial piping code, steam generators covered by the AFNOR Code, or storage tanks covered by the CODRES, among others. CODAP Code is updated each year, but there are no formal interpretation or modification request procedures. Requests are sent to the SNCT Union or to the AFIAP Society. CODAP Code rules are based on a "design-by-rule" approach for all categories of construction. The general structure of the CODAP Code is given in Table 3.

Rules for tube sheets are codified in part C7 of the CODAP Code and in NF E 32.104 standard.

German Boiler and Pressure Vessel Codes and Standards

A. D. Merkblatter is the German boiler and pressure vessel codes and standards [20]. It contains rules in the form of data sheets covering different aspects of vessel design and construction, and is produced by a group of associations. Revisions are made from time to time to keep up with technological advancements. Some aspects of vessel and exchanger design are not covered, and the method is agreed upon by the purchaser, inspecting authority, and designer. Design aspects of German boiler and pressure vessel codes and standards are discussed by Hone [40].

Table 3 General Structure of the CODAP Code

Part G	General provisions
Part M	Material
Part C	Design rules
Part F	Fabrication
Part I	Control and inspection
Part S	Protection against overpressure

2 BASICS OF MECHANICAL DESIGN

The structural integrity of pressure vessels and heat exchangers depends on proper mechanical design arrived at after detailed stress analysis keeping in view all the static, dynamic, steady, and transient loads. Heat transfer efficiency and fabrication costs of a tubular exchanger are directly influenced by proper functional and mechanical design. Therefore, an optimum mechanical design of various components of heat exchangers is of paramount importance. Mechanical design of various pressure-retaining components and some non-pressure-retaining components of heat exchangers is discussed in this section. Also discussed in this section are the fundamentals of mechanical design and stress analysis, classification of stresses and stress category concept, allowable stress, weld joint efficiency and joint category, and various design terms. Important source books on mechanical design of heat exchangers and pressure vessels are Singh and Soler [41] and Escoe [42] and on pressure vessels Moss [43], Brownell and Young [44], Bednar [45], Harvey [46], and Chuse [47], among others.

2.1 Fundamentals of Mechanical Design

Mechanical design involves the design of pressure-retaining and non-pressure-retaining components and equipments to withstand the design loads and the deterioration in service so that the equipment will function satisfactorily and reliably throughout its codal life. Mechanical design is done as per the procedure given in the construction codes and standards. Where no guidance is provided by the codes and standards, the procedure may be arrived at by mutual agreement between the purchaser and the fabricator.

Information for Mechanical Design

For mechanical design of shell and tube heat exchangers, certain minimum information is required [14]. The following listing summarizes the minimum information required:

1. Thermohydraulic design details in the form TEMA or an equivalent specification sheet.
2. TEMA class, type of TEMA shell, channels/heads.
3. Shell-side and tube-side passes.
4. Number, type, size, and layout of tubes.
5. Diameter and length of shell, channel/head, and its configuration.
6. Design temperatures and pressures.
7. External pressure if the equipment is under external pressure or is under internal vacuum.
8. Worst-case coincident conditions of temperature and pressure.
9. Nozzle, wind, and seismic loads, impact loads (including water hammer, if any).
10. Superimposed loads due insulation, piping, stacked units, etc.
11. Corrosion properties of the fluids and the environment in which the unit will be installed and the expected service life. This will help to specify corrosion allowances or better material selection to reduce the material loss due to corrosion.
12. Materials of construction except tube material, which is arrived at the thermal design stage.
13. Fouling characteristics of the streams to be handled by the exchanger. This will determine if closures are required for frequent cleaning of internal parts of the exchanger. Many fixed tube-sheet heat exchangers, if not specified otherwise, may be of welded head and shell construction.
14. Flow rate to size the nozzles and to determine whether impingement protection is required.
15. Special restrictions imposed by the purchaser on available space, piping layout, location of supports, type of material, servicing conditions, etc.

16. Construction code and standard to be followed.
17. Installation—vertical or horizontal.

In addition to these points, plant personnel should consider the following factors that influence mechanical design:

Considerations of startup, operating, shutdown, and upset conditions that decide tubesheet thickness [48].

Handling of lethal or toxic fluids, which demand more stringent welding and NDT requirements.

When high-pressure fluid is routed through the tube side, the effect of tube failure in the low-pressure shell. It is essential to provide overpressure protection on the shell side.

Sequence of Decisions to Be Made During Mechanical Design. In addition to the information required at the mechanical design stage as mentioned already, certain decisions are also to be made at the mechanical design stage. Soler [49] summarizes a typical sequence of decisions that must be made at the mechanical design stage of a heat exchanger design. Some of the points are:

1. What kind of connections (welded, flanged, or packed) should be provided at the front head, tube sheet, and rear head?
2. What style of flanged joint should be used—for example, ring type gasket or full face gasket?
3. What kind of closures (hemispherical, ellipsoidal, torispherical, conical, etc.) should be used?
4. What combination of load will govern the pressure part design? (Typical loads are shell-side pressure, tube-side pressure, differential thermal expansion, self-weight, mechanically transmitted vibration and seismic vibration, etc.)
5. Type and style of openings.
6. Type of nozzle connections, such as self-reinforcing forging stock versus pipe schedule.
7. Details of vent and drain design.
8. Minimum bend radii for U-tubes.
9. Whether an expansion joint is required. If so, what is the best type and style of the expansion joint?
10. Whether installation is horizontal or vertical, to decide the type/style of heat exchanger supports.
11. Evaluation of the ability of the exchanger to withstand operational transients, startup, and pressure testing.

Each of these decisions and evaluation steps requires a proper adjudication among various possibilities; many of these considerations require and/or are amenable to mathematical analysis, while others are derived from past experience or experimental data [49].

Content of Mechanical Design of Shell and Tube Heat Exchangers

Mechanical design of shell and tube heat exchangers involves at a minimum the following components design and the determination of stresses induced in that component:

1. Shell thickness.
2. Shell flange and channel flange design.
3. Dished end calculation.
4. Design of openings and nozzles.
5. Tube-sheet thickness. If the differential expansion between shell and tubes is excessive, then an expansion joint is to be designed and thus final tube-sheet thickness is arrived at.

6. Shell longitudinal stress and bending stress.
7. Tube longitudinal stress, both at the tube bundle inside and at the periphery.
8. Channel longitudinal stress and bending stress.
9. Tube-to-tube-sheet joint load.
10. Flat cover thickness.
11. Design of supports.

B-Jac Program Structure for Mechanical Design. One of the pioneers in developing computer software for thermal and mechanical design of shell and tube heat exchanger is M/s B-Jac International, Inc., Midlothian, VA. An insight into the logic of their mechanical design programs for the design of shell and tube exchangers is discussed next.

TEAMS—Mechanical Design Program. TEAMS is the mechanical design program of B-Jac. TEAMS covers a wide range of construction alternatives, including most types of heads, flanges, nozzles, and expansion joints. It can also be used for horizontal pressure vessels. TEAMS conforms with all provisions of the Standards of the Tubular Exchanger Manufacturers Association (TEMA), and appropriate mechanical engineering codes, including ASME and CODAP. The programs are regularly updated as revisions and addenda are issued by TEMA and Code authorities. The contents of TEAMS output are given in Table 4.

Additionally, the following features are available:

1. Cost estimate summary—Cost of materials, tubing, labor, markup, and selling price.
2. Material and labor summary—Material costs for major components (shell, front head, rear head, bundle), assembly costs, labor hours for parts and assembly, major component weights.
3. Final assembly summary—Material and labor costs for final assembly operations (e.g., x-ray, testing, inspection, painting).
4. Bill of materials—Rough (as purchased) and finished dimensions and quantity of all components, material costs and labor hours, material specification, subcontracted labor.
5. Part labor details—Labor hours required for each operation (layout, saw, shear, burn, bevel, drill, machine, mill, form, roll, weld, grind, ream, groove, chamfer) for each component.
6. Assembly labor details—Labor hours to assemble, weld, and grind for the shell components, front head components, rear head components, and bundle components.

Mechanical Design Procedure

A typical sequence of mechanical design procedures is discussed by Singh [50]. They are:

1. Identify applied loadings.
2. Determine applicable codes and standards.
3. Select materials of construction (except for tube material, which is selected during the thermal design stage).
4. Compute pressure part thickness and reinforcements.
5. Select appropriate welding details.
6. Establish that no thermohydraulic conditions are violated.
7. Design nonpressure parts.
8. Design supports.
9. Select appropriate inspection procedure.

Design Loadings

A list of loadings to be considered in designing a heat exchanger or a pressure vessel part is given in UG-22 of ASME Code Section VIII, Div. 1. They include

Table 4 TEAMS Output

Design conditions	Concise summary of design pressures, temperatures, corrosion allowances, radiography, precise weights (empty, full, bundle)
Cylinder and covers	Diameters, Code calculated thickness, TEMA minimum thickness, external pressure minimum thickness, actual thickness, maximum external pressure, maximum length for external pressure, materials of construction
Nozzles	Diameters, Code calculated thickness, actual thickness, reinforcement pad diameter and thickness, materials of construction
Flanges	Flange outer diameter, bolt circle, bolt diameter, bolt number, gasket outer diameter, gasket width, gasket thickness, Code calculated flange thickness, actual flange thickness, lap joint ring dimensions, hub dimensions, materials of construction
Tube sheets	Diameters (front and rear), TEMA bending thickness, shear thickness, flange extension thickness, effective thickness, recesses, actual thickness, clad thickness, tubing details, outer tube limit, materials of construction
Expansion joints	Number of joints, diameter, flexible element thickness, dimensions, spring rates, cycle life, materials of construction
Supports	Support dimensions, gussets, hole dimensions, wear plate thickness, Zick stress analysis, materials of construction
Maximum allowable working pressures (MAWP)	MAWP for all code components at design and ambient conditions, with controlling components flagged
Fitting locations	Elevations and distances from front tube sheet and from front head nozzle for each nozzle, coupling, support, and expansion joint, plus center of gravity
External loadings on nozzles	Local stresses in cylinders with applied loads, design conditions, coefficients, maximum loads and moments, interaction diagram
Overall dimensions	Lengths for head assemblies, tube sheets and shell, unit overall length
Calculation documentation	Formulas used and intermediate results for verification of Code and TEMA calculations
Tubesheet layout details	Number of tubes per row, distances offset from horizontal and vertical center lines for each row, tie rod locations, pass partition locations, balance of tubes per pass, baffle cut dimensions
Drawings	Setting plan (with or without bill of materials and design conditions), sectional drawing, bundle layout, tube-sheet layout
Bill of materials	Rough (as purchased) and finished dimensions and quantity of all components, specification

Source: Courtesy of M/s B-Jac International, Inc., Midlothian, VA 23112, USA.

1. Internal and/or external design pressure (as defined in UG-21).
2. Weight of vessel and normal contents including the static head of liquid.
3. Local loadings on the shell, such as those due to internals, vessel supports, lugs, etc.
4. Cyclic and dynamic reactions due to pressure or thermal variations, mechanical loadings, etc.
5. Wind, seismic, and snow loadings where required.
6. Impact loadings, such as those due to fluid shock.

Topics Covered in the Next Sections

In the next sections, the following topics are covered:

1. Stress analysis, classes, and categories of stress.
2. Calculation or design of (a) shell thickness, (b) dished end thickness, flat cover thickness, (d) flange thickness, (e) tube-sheet thickness, (f) shell longitudinal stress, (g) tube longitudinal stress, (h) tube-to-tube-sheet joint loads at the periphery of the tube bundle, (i) expansion joint, (j) nozzle openings and reinforcement of nozzle openings, and (k) supports.

2 STRESS ANALYSIS, CLASSES, AND CATEGORIES OF STRESS

2.1 Stress Analysis

Stress analysis is the determination of the relationship between external forces applied to a vessel and the corresponding stress. The stress analysis of heat exchangers and pressure vessels is similar to other structural members in that it involves mathematical operations with unknown forces and displacements. In the evaluation of the stress field in heat exchangers and pressure vessels, the problem is considerably simplified due to these reasons [41]: (1) The pressure-retaining components such as shell, heads, and cones are surfaces of revolution; (2) pressure loading—the primary mechanical loading is spatially uniform; (3) the thickness of a pressure vessel is small compared to its characteristic dimensions; and (4) with little accuracy loss, we can assume that the meridian, tangential, and through thickness directions are principal directions.

2.2 Classes and Categories of Stresses

Classes of stress, categories of stress, and allowable stresses as permitted by Codes are based on the type of loading that produced them and on the hazard they cause to the structure.

Stress Categories

The combined stresses due to a combination of loads acting simultaneously are called stress categories.

Stress Classification

The stresses that are present in pressure vessels are separated into various classes in accordance with the types of loads that produced them and the hazard they pose to the vessel. The reason for classifying stresses into various groups is that not all types of stresses require the same safety factors in protection against failure. Limit analysis theory indicates that some stresses may be permitted to a higher level than other stresses. Before discussing stress classification, membrane stress and primary stress are defined.

Membrane Stress

When the thickness is small in comparison with other dimensions ($R_m/t > 10$), vessels are referred to as membranes and the resulting stresses due to contained pressure are called membrane stresses [43]. The membrane is assumed to offer no resistance to bending. When the wall offers resistance to bending, bending stresses occur in addition to membrane stresses.

Primary Stress

Primary stress is a normal stress or a shear stress developed by the imposed loading that is necessary to satisfy the laws of equilibrium. The basic characteristic of a primary stress is that it is not self-limiting. Primary stresses that exceed the yield strength will result in plastic

deformation, gross distortion, or failure. Thermal stress is not classified as a primary stress. It is classified as a secondary stress only.

Classes of stress and categories of stress are dealt in detail by refs. 41, 43, and 45, among others.

2.3 Stress Classification

In the design codes, stresses are classified into five types. They are:

1. Primary membrane stress, P_m
2. Primary bending stress, P_b
3. Local membrane stress, P_l
4. Secondary stress, Q
5. Peak stress, F

Primary Membrane Stress, P_m

The component of primary stress that is obtained by averaging the stress distribution across the thickness of the pressure vessel is referred to as the primary membrane stress. It is the most significant stress class. An important characteristic of the primary membrane stress is that beyond the yield point, redistribution of stresses in the structure does not take place. It is remote from discontinuities such as head–shell intersections, nozzles, and supports. Design codes limit its value to the allowable stress for the component material. Examples for primary membrane stresses are:

1. Circumferential (hoop) and longitudinal (meridian) stresses due to internal or external pressures
2. Stress due to vessel weight
3. Longitudinal stress due to the bending of the horizontal vessel over the supports
4. Membrane stress in the nozzle wall within the area of reinforcement due to pressure or external loads
5. Stress caused by wind and seismic forces

Primary Bending Stress, P_b

In contrast to a cylindrical shell, certain structural shapes cannot resist external loadings without bending, and the resulting stress is known as primary bending stress. Primary bending stress is capable of causing permanent distortion or collapse of the vessel. Some examples of primary bending stress are

1. Bending stress due to pressure in a flat cover
2. Bending stress in the crown of a torispherical head due to internal pressure
3. Bending stress in the ligaments of closely spaced openings, such as bending stress in the tube sheet averaged across the ligament

Primary general stresses are divided into primary membrane and primary bending stresses, and the reason for such a division so that the calculated value of a primary bending stress may be allowed to go higher than that of a primary membrane stress.

Local Membrane Stress, P_l

Local (primary) membrane stress is produced either by pressure load alone or by other mechanical loads. It has some self-limiting characteristics. Since the loads are localized, once the yield strength of the material is reached, the load is redistributed to stiffer portions of the vessel. Typical examples for local primary membrane stress are stresses at supports and stresses due to internal pressure at structural discontinuities [45].

Secondary Stress

Secondary stress is a normal or shear stress arising because of the constraint of adjacent material or by self-constraint of the structure. These stresses arise solely to satisfy compatibility conditions and are not required to satisfy laws of equilibrium. They are self-limiting in nature. Local yielding can relieve the conditions that lead to the development of these stresses and limit their maximum value. Failure from secondary stress is not to be expected. The concept of primary and secondary stresses is not relevant for brittle materials. Two sources of secondary stresses are (1) temperature and (2) gross structural discontinuity.

Secondary stresses can be subdivided into two major categories: (1) load-actuated secondary stresses and (2) temperature-actuated secondary stresses. Examples for these classes are given next.

Some examples of load actuated secondary stresses are:

1. Bending stress in a shell where it is connected to a head or to a flange
2. Bending stress in a shell or a head due to nozzle loads
3. Bending stress in the knuckle at a head to shell joint

Some examples of temperature-actuated secondary stresses are:

1. Stresses caused by axial temperature variation in a shell.
2. Both membrane and bending stresses due to differential thermal expansion between two adjoining parts of a structure such as nozzle to shell or shell to head.

Moss [43] additionally classifies secondary stresses into two groups: membrane and bending. Examples of secondary membrane stress, Q_m, are:

1. Thermal stresses
2. Membrane stress in the knuckle area of the head

Examples of secondary bending stress, Q_b, are:

1. Bending stress at a gross structural discontinuity due to relenting loads only, such as nozzles and lugs
2. The nonuniform portion of the stress distribution in a thick-walled vessel due to internal pressure

Peak Stress, F

Peak stresses are the additional stresses due to stress concentration in highly localized areas. They are caused by mechanical and thermal loads and they apply to both limiting and self-limiting loads. Peak stresses are added to the primary and secondary stresses to give the total stress at a point. A peak stress does not cause any noticeable distortion. The determination of peak stress is necessary only for fatigue analysis or a source of stress corrosion cracking, or it can be a possible source of brittle fracture [45]. Peak stress applies to membrane, bending, and shear stresses. Examples for peak stresses due to thermal and mechanical loads are given next.

Some examples of peak stresses due to thermal loads are

1. Thermal stress in the cladding or weld overlay of a tube sheet, shell, or vessel head
2. Thermal stresses in a wall caused by a sudden change in the surface temperature (thermal shock)

Some examples of load-actuated peak stresses for specific situations are:

1. Peak stress in a ligament (uniform ligament pattern)
2. Stress at a local structural discontinuity
3. Stress at corner of a discontinuity

4. Stress due to notch effect or stress concentration or small radius fillet, hole, or incomplete penetration [45]
5. Additional stresses developed at the fillet at a nozzle-to-shell junction due to internal pressure or external loads

Discontinuity Stresses

Pressure vessel components and sections usually contain regions of different thickness, material, diameter, and abrupt changes in geometry. The juncture at these locations are known as "discontinuity" areas. Examples include the skirt junction with the shell/vessel and head and shell. The stresses induced in the respective parts at or near discontinuity areas are called discontinuity stresses. Discontinuity stresses are necessary to satisfy compatibility conditions at discontinuity regions. They are not serious under static loads such as internal pressure with ductile materials if they are kept with in limits by the design, but they are important under cyclic loads [45]. The characteristics of discontinuity stresses are [43]:

1. These stresses are local in extent but can be of very high magnitude.
2. Discontinuity stresses are considered as "secondary stresses" and self-limiting, if their extent along the length is limited.
3. In average application, discontinuity stresses will not lead to failure. However, they may be a major consideration for (1) brittle materials and (2) high-pressure applications (>1500 psi).

2.2 Fatigue Analysis

When a vessel is subjected to repeated loading that could cause failure by the development of a progressive fracture, the vessel is said to be in cyclic service.

2.3 Design Methods and Design Criteria

There are two basic design methods used by the codes for the design of heat exchangers and pressure vessels; these are termed, "design-by-rule" and "design-by-analysis." The first is based on experience and does not require a detailed evaluation of all stresses. It gives formulas for sizing the majority of widely used components. The latter is based on criteria requiring detailed stress analysis.

ASME Code Section VIII Design Criteria

In general, pressure vessels conforming to the ASME Code, Section VIII, Div. 1 are designed by "design-by-rules" and do not require a detailed stress analysis. It is recognized that high localized and secondary bending stresses may exist but they are allowed for by use of a higher safety factor. However, as per Code rules, all loadings applied to a vessel or its structural attachments must be considered (UG-22). The Code establishes allowable stresses by stating in Paragraph UG-23 that the maximum primary membrane stress must not exceed the maximum allowable stress value in tension. Further, it states that the maximum primary membrane stress plus primary bending stress may not exceed 1.5 times the allowable stress of the material in tension. It also recognizes that high localized discontinuity stresses may exist, but the design rules have been written to limit such stresses to a safe level consistent with experience.

Design Criteria: Comparison of ASME Code Section VIII Div. 1 Versus Div. 2

Salient features and differences among Code rules between Div. 1 and Div. 2 are discussed in ref. 43 and the differences are given in Table 5.

Table 5 Comparison of Design Criteria of ASME Code Section VIII Divisions 1 and 2

Div. 1	Div. 2
Design is by "design-by-rules" principle and does not require a detailed evaluation of all stresses. It gives formulas for sizing the majority of widely used components.	Design is by "design-by-analysis" and requires a much more rigorous design analysis.
Does not explicitly consider the effects of combined stress and does not give detailed methods on how stresses are combined.	Provides specific guidelines on classes of stresses, stresses categories, and how they are combined.
Stress analysis considers a biaxial state of stress combined in accordance with the maximum principal stress theory.	Considers all stresses in a triaxial state combined in accordance with the maximum shear stress theory.
Does not specifically provide for design of vessels in fatigue.	Criteria for determining when a vessel must be analyzed for fatigue are specified.

2.4 Allowable Stress

Allowable stresses are used in the design of pressure vessels, heat exchangers, structures, machine elements, etc. The Code gives tables for allowable stresses in tension for most structural materials at discrete temperatures. The allowable stresses in compression depend on the slenderness of the pressure components, and are therefore presented in terms of slenderness ratio. The basis of the ASME Code allowable stress values is discussed in ref. 50.

2.5 Combined-Thickness Approach for Clad Plates

In general, the Code does not permit using the clad thickness as additional thickness to resist pressure but rather treats it only as a corrosion allowance. As an exception, for clad material conforming to SA-263, SA-264, and SA-265, the cladding thickness after deducting the corrosion allowance can be used for the thickness calculation purpose. As per Paragraph UCL-23(c), if the nominal thickness of base plate is t_b, then the allowable combined thickness, t_t, that can be used for pressure calculations is given by

$$t_t = t_b + (S_c/S_b)\, t_c$$

where S_c is the maximum allowable stress of cladding at design temperature, S_b the maximum allowable stress of the base material at design temperature, and t_c the nominal thickness of cladding less corrosion allowance. Where S_c is greater than S_b, the multiplier S_c/S_b shall be taken equal to unity.

Example. Given the base plate thickness is 1.0 in, clad plate thickness is 0.25 in, allowable stress for the base plate is 17,500 lb/in^2, and allowable stress for the clad material is 11,200 lb/in^2, what is the allowable combined thickness t_t that can be used for pressure calculations if the corrosion allowance on the cladding is 0.050 in?

$$t_t = 1.0 + (11{,}200/17{,}500)\,(0.25 - 0.05) = 1.128 \text{ in}$$

2.6 Welded Joints

The most common way to fabricate a pressure vessel is by welding. For vessel members with weld joints, all thickness formulas shall contain the weld joint efficiency term E inserted into the equation. The multiplication of the efficiency term E with the code allowable stress, S,

gives the effective allowable stress, SE, for the weld seam. If no E term is contained in the formula, the allowable stress may have to be modified by a quality factor of 80% [36]. Special restrictions prevail at the weld joint for the following cases:

1. The vessel contains a lethal substance.
2. The vessel will operate at a temperature lower than −20°F.
3. The vessel is an unfired steam boiler with design pressure exceeding 50 psi.
4. The vessel is subjected to direct firing.

In these cases, all joints are restricted to butt joints and full penetration welds.

Welded Joint Efficiencies

In industry, radiographic examination (RT) is the most common technique to establish soundness of the weld joints. Depending on the type of weld joint (single or double butt, double full fillet lap, single welded butt joint without backing strip, etc.), and also on the extent of RT used to check the soundness of the joint, most of the pressure vessel codes prescribe a "joint efficiency" E to be used in the thickness formulas. The Code recognizes full radiography, spot radiography, and none. As per ASME Code Table UW-12, for a double-welding butt joint, the corresponding efficiencies would then be: fully radiographed 100%, spot radiographed 85%, and none 70%. The decrease in joint efficiency from 100% to 70% when no spot radiographic examinations are made on the welded joints means that a fabricator must provide more thickness.

Joint Categories

As per Paragraph UW-3 of ASME Code Section VIII, Div. 1, the term "category" is used to define the location of a joint in a vessel, but not the type of the joint. Categories are established for the purpose of specifying special requirements regarding joint type and degree of inspections of certain welded pressure vessels. ASME Code categorizes various joint locations into the following four types: Category A locations, Category B locations, Category C locations, and Category D locations. These locations are schematically shown in Fig. 1. Some examples for Category A, B, C, and D are given next. For complete details, refer to ASME Code Section VIII, Div. 1.

Category A Locations. Category A locations are longitudinal welded joints within a main shell, and welded joints within a sphere, within a formed or flat head, or within the side plates

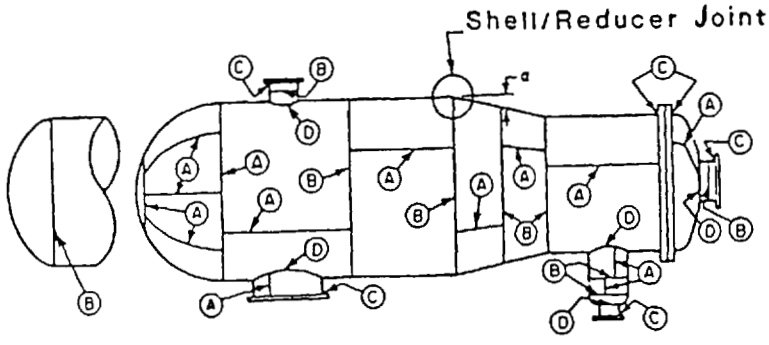


Figure 1 ASME Code joint category designation [16].

of a flat sided vessel; circumferential welded joints connecting hemispherical heads to main shells and several other locations.

Category B Locations. Category B locations are circumferential welded joints within the main shell, and circumferential welded joints connecting formed heads other than hemispherical to main shells, to transitions in diameter, to nozzles, or to communicating chambers, and several other locations.

Category C Locations. Category C locations are welded joints connecting flanges, tube sheets, or flat heads to the main shell, to formed heads, to transitions in diameter, and to nozzles; any welded joints connecting one side plate to another side plate of a flat sided vessel, and several other locations.

Category D Locations. Category D locations are welded joints connecting communicating chambers or nozzles to main shells, to spheres, to heads or to flat sided vessels, those joints connecting nozzles to communicating chambers, and several other locations.

Weld Joint Types

The category of the weld joint determines permissible joint types, weld examination requirements, and associated weld joint efficiencies used in pressure part thickness calculation. The Code defines six weld joint types (UW-2); their definitions are given in Table 6.

2.7 Key Terms in Heat Exchanger Design

Design Pressure

Design pressure for a pressure vessel or a heat exchanger is the gage pressure at the top of the vessel, and together with the coincident design metal temperature, used in the design calculations of a pressure vessel for the purpose of determining the minimum thickness of the various pressure-retaining components of the vessel. Since a heat exchanger is made of two different pressure zones—tube side and shell side—at least two design pressures shall be defined. ASME code encourages (UG-21) that the design pressure be higher than the normal operating pressure with a suitable safe margin to allow for probable pressure surges in the vessel up to the setting of pressure relief valves (UG-134). When vessels are subjected to inside vacuum and external positive pressure on the outside, then the maximum difference between the inside and outside of the vessel shall be taken into account.

Table 6 Weld Joint Types

Type	Description
Joint type 1	Double-welded butt joint, or by other means that produce the same quality of weld on the inside and outside. Welds using metal backing strips that remain in place are excluded.
Joint type 2	Single-welded butt joints with backing strip.
Joint type 3	Single-welded butt joints with backing strip.
Joint type 4	Double full fillet lap joint.
Joint type 5	Single full fillet lap joints with plug welds.
Joint type 6	Single full fillet lap joint without plug welds.

Design Temperature

This is the temperature stamped on the nameplate along with the design pressure. This temperature shall not be less than the mean metal temperature expected across the thickness, under the operating conditions for the parts under consideration (UG-20). Design temperature can be different for the different pressure parts if the operating conditions ensure a defined temperature variation [50]. For example, in a multipass shell and tube heat exchanger in which there is an appreciable temperature drop or rise on the tube side, the inlet headers and outlet headers can have different design temperatures. In no case shall the design temperature exceed the temperature corresponding to the Code allowable stress for the material used in the thickness calculations nor exceed the allowable working temperature for the material specified in the Code.

Maximum Allowable Working Pressure (MAWP)

The maximum allowable working pressure is the gage pressure for a specified operating temperature that is permitted for the vessel in operation, such that, together with any other likely loadings other than pressure, the stresses computed using Code formulas do not exceed the Code allowable stress values. Metal thickness specified as corrosion allowance is not considered for the calculation of thickness. It is the basis for the pressure setting of the pressure-relieving devices that protect the vessel. The MAWP is normally specified for two conditions—new (uncorroded) and old (corroded).

Operating Temperature or Working Temperature

As per ASME Code, this is defined as the temperature that will be maintained in the metal of the part of the vessel being considered for the specified operation of the vessel.

Operating Pressure or Working Pressure

As per ASME Code, this is defined as the pressure at the top of the vessel at which it normally operates. It shall not exceed the maximum allowable working pressure, and it is kept at a suitable level below the setting of the pressure-relieving devices to prevent their frequent opening.

3 TUBE-SHEET DESIGN

3.1 Fundamentals

A tube sheet is an important component of a heat exchanger. It is the principal barrier between the shell-side and tube-side pressures. The cost of drilling and reaming the tube holes as well as the overall cost of the tube sheet of a given dimension will have direct bearing on the heat exchanger cost. Additionally, proper design of a tube sheet is important for safe and reliable operation of the heat exchanger. In this section fundamentals of tube-sheet design such as classification of tube sheets, constructional features, etc., are discussed.

Tube-Sheet Connection with the Shell and Channel

Tube sheets are mostly flat circular plates with uniform pattern of drilled holes. Tube sheets of surface condensers are rectangular in shape. The tube sheet is connected to the shell and the channel either by welding (integral) or bolts (gasketed joints) or a combination thereof. The possible tube-sheet connection with the shell and channel of a fixed tube-sheet exchanger can be categorized into two types:

1. Both sides integral construction (Fig. 2a)
2. Shell-side integral and the tube-side gasketed construction (Fig. 2b)

The possible tube-sheet connection with the shell and channel in the case of fixed tube sheet of floating head and U-tube exchanger can be categorized into these three types:

1. Both sides integral construction (Fig. 3a)
2. One side integral and the other side gasketed construction (Fig. 3b)
3. Both sides gasketed construction (Fig. 3c)

Supported Tube Sheet and Unsupported Tube Sheet

Heat exchanger tubes other than a U-tube heat exchanger may be considered to act as stays that support or contribute to the strength of the tube sheets in which they are attached. In the case of fixed and floating head heat exchangers, the tube bundle behaves like an elastic foundation. However, the floating nature of one of the tube sheets makes the staying action partial. This is especially true for an outside packed floating type heat exchanger. In the case of U-tube heat exchangers, tubes provide only a reactive bending moment to the tube-sheet bending. According to the level of support provided by the tubes, TEMA classifies the tube sheets as (1) supported tube sheet, and (2) unsupported tube sheet; examples are:

1. Unsupported tube sheets, e.g., U-tube tube sheets
2. Supported tube sheets, e.g., fixed tube sheets and floating tube sheets

Tube-Sheet Thickness

Being a plate type structure, the tube sheet resists the lateral pressure by bending and the membrane loads are negligible. Hence the limiting stress is the primary bending stress only. The factors that control the tube-sheet thickness are:

1. Tube pitch and layout pattern, which define the ligament efficiency of perforated tube sheets.
2. The manner in which the deformation of tube sheet is influenced by the support being provided by the tube bundle to the tube sheets. For the same process conditions and tube-

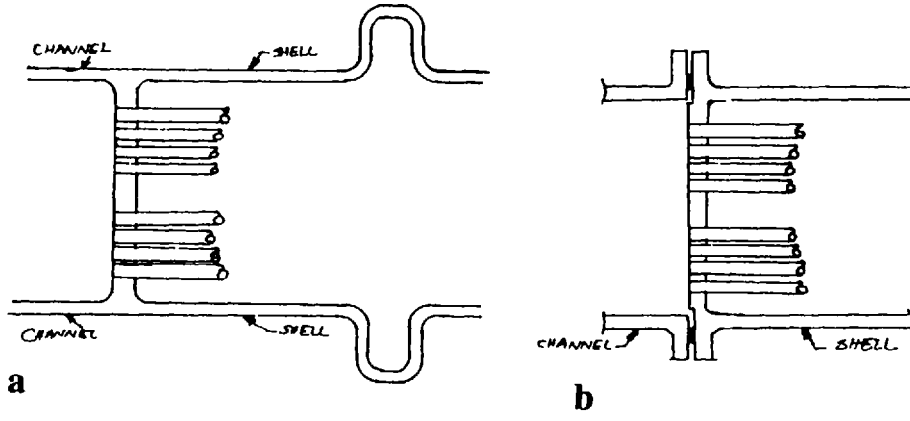


Figure 2 Fixed tubesheet exchanger connection with shell. (a) Both sides integral; and (b) shellside integral and tubeside gasketed.

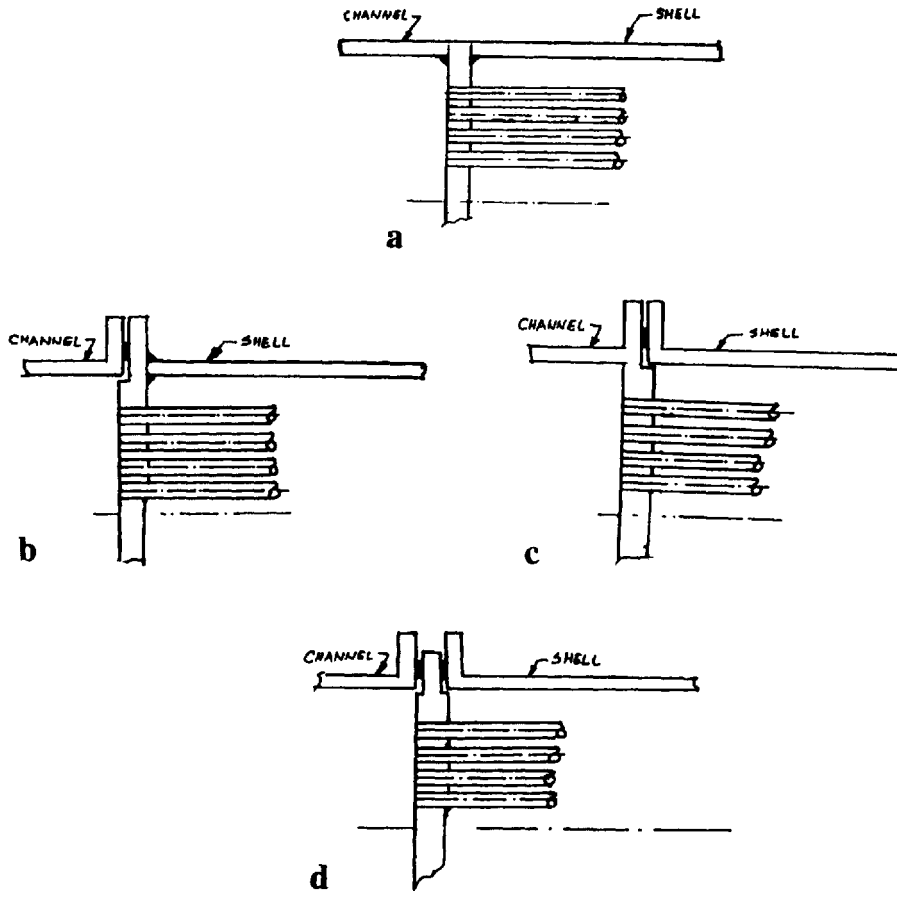


Figure 3 Floating head and U-tube exchanger tubesheet connection with shell. (a) Both sides integral; (b) and (c) one side integral and the other side gasketed; and (d) both sides gasketed.

sheet diameter, tube-sheet thickness decreases in the order of the following exchanger types:

U-tube heat exchanger
Floating head exchanger
Fixed tube-sheet exchanger.

3. Mean metal temperatures of tube sheet, tube, and shell
4. Number of tubes
5. Limits of the tube field and the extent of untubed portion
6. Method of joining the tubes to the tube sheets, e.g., rolled, seal welded, or strength welded
7. Shell and the channel connection with the tube sheets, e.g., gasketed and integral
8. Shell and the channel thickness

Tube-Sheet Design Procedure: Historical Background

TEMA set up rules for the design of U-tube and floating head heat exchangers in 1941. These rules were simple but do not ensure an overall safety for all heat exchangers. Hence many

researchers [51–75] published papers on tube-sheet design and interpreted Code rules from 1948 onward.

The Codes and Standards periodically updated the procedure for tube-sheet design as and when better methods were published. In recent years, new tube-sheet design procedures have been incorporated in TEMA, British Standards 5500, Stoomwezen—Dutch code, ISO/DIS 2694 Pressure Vessels, ASME Section VIII Div. 1, CODAP, and others. BS 5500 and CODAP have adopted Gardner's method [58] as the basis for the design of tube sheets for floating head and U-tube exchangers. Historical background of tube-sheet analysis is covered in ref. 73.

Among the heat exchanger standards and codes, the tube-sheet design procedures of the Standards of the Tubular Exchanger Manufacturers Association (TEMA) have been used successfully for the last 50 years, partly due to simplicity and partly due to satisfactory performance of the heat exchangers designed as per this standards, and during this period TEMA standards have been modified several times. TEMA with its seventh edition (1988) revised its original formula by including a term for mean ligament efficiency η in the tube-sheet bending formula. The required effective tube-sheet thickness for any type of heat exchanger shall be determined for both tube-side and shell-side conditions with or without the thermal load, using whichever thickness is greater. This procedure is followed in BS 5500. However, in CODAP and ASME Code, the simultaneous action of shell-side and tube-side pressures along with thermal load are considered to arrive at the tube-sheet thickness.

Design procedure for tube sheets varies among the code rules and standards and hence designers get different thickness for the same design condition due to reasons such as:

1. Assumptions that tube sheets are either simply supported or clamped or elastically restrained at its edges.
2. Local stresses developed at the shell/tube-sheet and channel/tube-sheet junction are neither calculated nor required to be limited.
3. Failure to consider the effect of untubed annular rim.

With this background knowledge, tube-sheet design procedure is explained next. First, the assumptions made in various tube-sheet design models are discussed, followed by the basis of fixed tube-sheet design procedure. Subsequently, the tube-sheet design procedure for fixed, floating head, and U-tube-sheet procedure included in TEMA, CODAP, BS 5500, and ASME Code Section VIII Div. 1 is dealt with. Finally, the fixed tube-sheet bending formula of TEMA is compared with that of CODAP and BS 5500. While discussing tube-sheet design procedure, emphasis is on TEMA tube-sheet design procedure. Design aspects of double tube sheets, rectangular tube sheets, and curved tube sheets are covered at the end.

Assumptions in Tube-Sheet Analysis

While analyzing the tube sheets, certain assumptions are made in their models by many researchers. The tube sheets are treated as thin plates compared to their radial dimension, both circumferential and radial stresses vary linearly through the thickness of the tube sheets, and shear stresses vary parabolically from zero at one face to zero at the other face with a maximum at the center. Other assumptions include the following:

1. The tube sheet is uniformly perforated over its whole area; the unperforated annular rim is not considered by some standards; For example, TEMA Standards do not consider the unperforated tube-sheet portion for all classifications of tube sheets; CODAP and BS 5500 neglect it for fixed tube-sheet design only. ASME Code Section VIII, Div. 1, considers the unperforated rim for all types of construction.
2. The membrane loads in the tube sheets are negligible as compared to the bending loads [53].

3. No slip occurs at the junction between the tubes and the tube sheet.
4. The tubes are adequately stayed by baffle plates to enable them to stand up to the calculated loads without sagging.
5. The bending moments in the tubes at their attachment with the tube sheet are neglected.
6. The exchanger is axis symmetrical and symmetric about the plane midway between the tube sheets.
7. Modeling of the tube bundle: The tubes are assumed uniformly distributed over the whole tube sheet and in sufficient number (N_t) so as to act as a uniform elastic foundation of modulus K_w. The expression for K_w is

$$K_w = \frac{N_t K_t}{\pi R^2} \tag{1}$$

where K_t represents the axial rigidity of one tube as given by

$$K_t = \frac{\pi E_t t(d - t)}{L} \tag{2}$$

Note: The elastic modulus for a half bundle, k_w, is equal to $2K_w$, and the axial rigidity of one half tube, k_t, is equal to $2K_t$.

8. Modeling of the tube sheet: The perforated tube sheet is replaced by an equivalent solid plate of effective elastic constants E^* and ν^* (the determination of effective elastic constants is discussed separately). The flexural rigidity of the perforated plate D^*, in terms of the flexural rigidity of unperforated plate D and deflection efficiency η is given by

$$\eta = D^*/D \tag{3}$$

where D^* and D are given by

$$D = \frac{ET^3}{12(1 - \nu^2)} \quad \text{and} \quad D^* = \frac{E^*T^3}{12(1 - \nu^{*2})} \tag{4}$$

One of the drawbacks of the work of Gardner [52] and Miller [53] is the assumption that the Poisson ratio of the perforated tube sheet is same as for the unperforated tube sheet; accordingly, a constant value of $\nu^* = 0.3$ was assumed in their treatment.

9. The maximum stress in the perforated plate will be the maximum stress in the homogeneous plate divided by the ligament efficiency, μ.
10. The analysis is based on the optimum design of tube sheets within their elastic behavior of all components attached to the tube sheet. If the temperatures are high enough, creep becomes of primary importance [56].
11. The deflection of the tube sheet is small, and hence the angular distortion of the tube ends due to the bending of the tube sheet can be neglected.
12. The effect of rotational resistance of the tubes is negligible since it is minor in nature.

Boundary Restraint

Tube sheets are weakened due to drilling holes, whereas they are stiffened by the tube bundle and tube-sheet edge restraint offered by the shell and channel connected with the tube sheet by welding. Based on the tube-sheet connection with the shell and the channel, the edge restraint condition is treated as simply supported, clamped, and an intermediate case. However, the complication of the combined effects of discontinuity stresses due to shell-side and tube-side pressures and differential thermal expansion between the shell and the tube bundle, and the tube sheet and the channel head, makes the determination of boundary restraint an uncertain factor in the estimation of the tube-sheet stresses [52]. In view of these factors, Gardner [52]

suggests that the designer be guided by judgment and experience in determining the relative fixity of the tube-sheet periphery as between the simply supported and the clamped. According to Miller [53], the boundary restraints may be treated as (1) a simply supported case, (2) a clamped case, and (3) the intermediate to these two cases. The examples suggested by Miller for these cases are:

1. Simply supported case: a narrow joint face, or trapped ring gasket
2. Clamped case, e.g., full-face gasketed joint

Treatment of Boundary Restraint in TEMA Standards. In the seventh edition of TEMA [3], the weakening effect of the tube hole drilling is taken into account by including the mean ligament efficiency term η in the tube-sheet bending formula. However, the tube-sheet edge restraint offered by the shell and channel connection with the tube sheet is not taken care of adequately. As in the earlier editions, the F factor used to account for the simply supported condition, fixed (clamped) condition, and intermediate condition is retained. Due to this reason, the TEMA formula is not safe for all sizes and all operating pressures [73]. This is especially true for large units with high operating pressures. For certain values of the parameter X (used to represent the relative rigidity of the tube bundle with respect to the tube sheet) the TEMA formula is safe, but for lower values it is not adequate and hence unsafe. The TEMA fixed tube-sheet formula is compared with CODAP by Osweiller [70,73].

Effective Elastic Constants of Perforated Plates

While designing the perforated tube sheets, the weakening effect due to the tube hole perforations has been taken into account by replacing the plate by an equivalent solid plate with new elastic constants known as the effective Young's modulus, E^*, and effective Poisson's ratio, ν^*. The values of E^* and ν^* are such that the equivalent plate has the same deflection as that of the original unperforated plate. This is known as the equivalent solid plate concept. The equivalent solid plate concept has been found to be quite useful in the design and analysis of perforated plates by equating strains in the equivalent solid material to the average strains in the perforated material [76]. These effective elastic constants must be evaluated correctly, especially in fixed tube-sheet heat exchangers [77]. If they are too low, the stresses at the junction with the shell and the head will be lower than in real units. If they are too high, the stress at the center of the plate, which may be a maximum, will be too low.

Determination of Effective Elastic Constants. The effective elastic constants depend on the pattern, size, and pitch of the perforations. During the last two decades many researchers have proposed theoretical and experimental methods to determine the effective elastic constants. However, there are disparities in the values obtained by these methods. Modern pressure vessel codes such as ASME , ISO, BS 5500, CODAP, Stoomweazen, etc. present curves to determine effective elastic constants. TEMA does not determine the effective elastic constants. It assumes a constant value of 0.178 for deflection efficiency. An excellent review of about 60 papers on the elastic constants was done by Osweiller [77]. Osweiller proposed curves for determination of effective elastic constants that have been adopted in CODAP.

Mean Ligament Efficiency

The ligament efficiency is a very useful dimensionless parameter for analysis of perforated plates. The ligament efficiency, defined in terms of the tube layout pattern and pitch ratio in TEMA, is known as mean ligament efficiency, η, and in terms of pitch ratio is known as minimum ligament efficiency in codes such as CODAP (Fig. 4) and BS 5000 and ligament efficiency in ASME Code Section VIII, Div. 1. The general expression for ligament efficiency is:

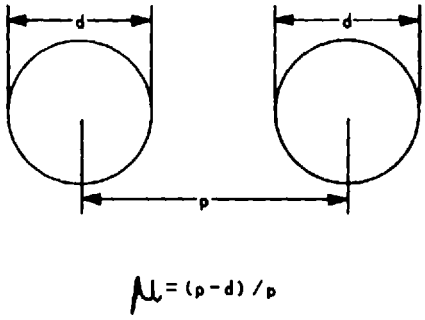


Figure 4 Mean ligament efficiency.

$$\mu = \frac{p - d}{p} \tag{5}$$

where d is the tube outer diameter and p the tube pitch.

A specific expression for ligament efficiency as defined in TEMA, CODAP, and BS 5500 is given while discussing the tube-sheet design as per these standards/codes.

3.2 Basis of Fixed Tube-Sheet Design

Thin Circular Plate on Elastic Foundation

Most tube-sheet design analysis treats the tube sheet as a thin circular plate on an elastic foundation. The elastic foundation is provided by the tube bundle. The basis of tube-sheet design procedure is discussed here. This discussion closely follows the method of Galletly [56], which was further expanded by Osweiller [70,73] for inclusion in CODAP. The heat exchanger is assumed to be of revolution and symmetrical about a plane midway between the tube sheets, so as to analyze a half exchanger as shown in Fig. 5a. Figure 5b shows a circular plate of thickness T resting on an elastic foundation. To minimize the complexity, the untubed tube-sheet portion is neglected and the tube sheet is integral with both the shell and the channel. The tube sheet is disconnected from the remainder of the exchanger, that is, from shell and channel. The plate is elastically restrained against deflection and rotation around its periphery, θ_c by (1) an axial reaction V_E due to the end load acting on the head and to the axial displacement Δ_s of the half shell, and (2) a reactive bending Moment M_E $(-K_\theta\theta_c)$ as shown schematically in Fig. 5c. The plate is subjected to a uniform net effective pressure $q(r)$ given by [73]:

$$q(r) = p_s f_s - p_t f_t - \nu_t \left[\frac{N_t}{R^2} \frac{(p_t - p_s)(d - t)^2}{2} \right] + 2\nu_s p_s Q - k_w \left[w(r) - \frac{\gamma}{2} + \Delta_s \right] \tag{6}$$

In the expression for $q(r)$, the first term takes into account the differential pressure acting on the equivalent plate, which is corrected for the tube hole areas by the shell-side drilling coefficient, f_s, and tube-side drilling coefficient, f_t, respectively; the second and third terms take into account the loads resulting from the axial displacements of tubes and shell by the Poisson effect of shell-side pressure, p_s, and tube-side pressure, p_t, respectively (Q is the ratio of rigidity of tube bundle to the shell); and the fourth term traduces the reactive effect of the elastic foundation. In this, the term $w(r)$ is the deflection of the plate at a distance r from the center axis, and $\gamma/2$ is the differential thermal expansion between the tubes and the shell, which is given for the half exchanger by:

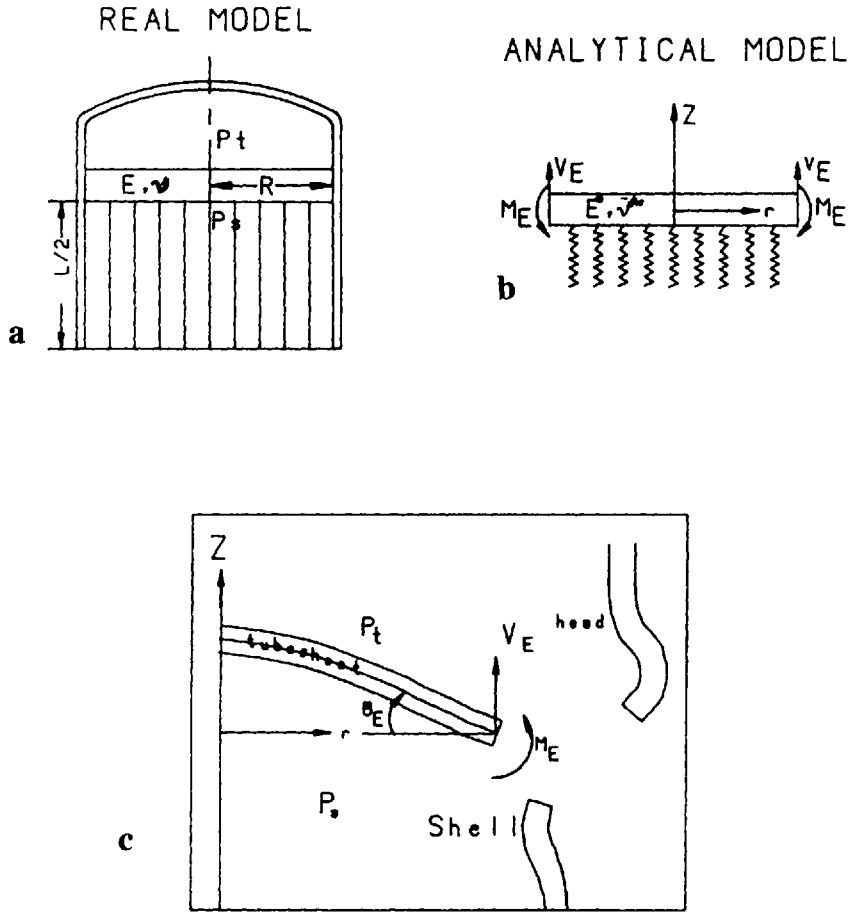


Figure 5 Basis of fixed tube sheet heat exchanger, (a) Half heat exchanger, (b) circular plate on an elastic foundation, and (c) Force and moment at the tubesheet edge. (From Ref. 73.)

$$\frac{\gamma}{2} = [\alpha_t(\theta_t - \theta_{amb}) - \alpha_s(\theta_s - \theta_{amb})]\frac{L}{2} \tag{7}$$

The expressions for f_s, f_t, and Q are:

$$f_s = 1 - \frac{N_t d^2}{4R^2} \tag{8}$$

$$f_t = 1 - \frac{N_t(d - 2t)}{4R^2} \tag{9}$$

$$Q = \frac{N_t K_t}{K_s} \tag{10}$$

$$= \frac{1}{K} \tag{11}$$

where K is the ratio of axial rigidity of the shell (K_s) to the axial rigidity of the tube bundle ($N_t K_t$). The parameter K signifies the ratio of the force required to produce a given strain in the shell to the force necessary to produce the same strain in the tube bundle. It is thus the measure of the ability of the shell to resist movement of the two tube sheets relative to the tube bundle [51]. However, when there is a considerable thermal expansion between the shell and the tube bundle, the high rigidity of the shell may induce very high thermal stresses in the tube bundle and the shell. This ability is reduced by the introduction of an expansion joint into the shell. An externally packed floating head exchanger for purposes of tube-sheet design is considered as a perfect expansion joint, and for exchangers so constructed the value of K is zero. The expression for the axial rigidity of the shell K_s is given by:

$$K_s = \frac{\pi t_s (D_o - t_s)\, E_s}{L} \tag{12}$$

From the expression for K_t(Eq. 2) and K_s(Eq. 12), the resulting expression for K is given by

$$K = \frac{E_s t_s (D_o - t_s)}{E_t N_t t (d - t)} \tag{13}$$

where D_o is the shell outside diameter. The expression for axial rigidity of the half shell, k_s, is equal to $2K_s$, and axial rigidity of the half tube, k_t, is equal to $2K_t$.

Deflection, Slope, and Bending Moment

From classical thin-plate theory, the deflection of a solid circular plate of elastic constants E^*, ν^*, and flexural rigidity D^* resting on elastic foundation k_w, subjected to net effective pressure $q(r)$ and elastically restrained at its periphery, is given by:

$$\frac{d^4w}{dr^4} + \frac{2}{r}\frac{d^3w}{dr^3} - \frac{1}{r^2}\frac{d^2w}{dr^2} + \frac{1}{r^3}\frac{dw}{dr} = \frac{q(r)}{D^*} \tag{14}$$

The solution of this equation is of the form

$$w(r) = A\,\mathrm{Ber}(x) + B\,\mathrm{Bei}(x) + \frac{p^*}{k_w} - \Delta_s + \frac{\gamma}{2} \tag{15}$$

Deflection, slope and bending moment

$$p^* = p_s f_s - p_t f_t - \nu_t \left[\frac{N_t\,(p_t - p_s)\,(d - t)^2}{R^2 \quad 2} \right] + 2\nu_s p_s Q \tag{16}$$

$$x = kr = \sqrt[4]{\frac{k_w}{D^*}}\, r \tag{17}$$

In Eq. 15 $\mathrm{Ber}(x)$ and $\mathrm{Bei}(x)$ are the modified Bessel functions of the first kind, and A and B are unknown constants.

At the periphery of the tube sheet (i.e., $r = R$), x becomes X. It represents the relative rigidity of the tube bundle with respect to the tube sheet. It may vary from 0 (no tube in the bundle) to above 50 for very stiff tube bundle. The expression for X is:

$$X = k\mathrm{R} = \sqrt[4]{\frac{k_w}{D^*}}\, R \tag{18}$$

$$= \sqrt[4]{\frac{\pi N_t E_t t (d - t)}{\pi R^2 L/2} \quad \frac{12(1 - \nu^{*2})}{E^* T^3}}\, R^4 \tag{19}$$

Substituting for $N_t E_t (d - t)$ by $E_s t_s (D_o - t_s)/K$ and for $E^*/(1 - \nu^{*2})$ by $\eta E/(1 - \nu^2)$ and $D_o - t_p \approx 2R$, X becomes

$$X = \sqrt[4]{\frac{24E_s t_s (D_o - t_s)}{KL} \frac{R^2(1 - \nu^2)}{\eta E}} \tag{20a}$$

$$= \sqrt[4]{\frac{6(1 - \nu^2)}{\eta} \frac{E_s t_s}{KLE} \left(\frac{2R}{T}\right)^3} \tag{20b}$$

From $w(r)$, one may determine the shear forces, the bending moment, and the slope at any point in the tube sheet. By employing the Kirchoffs–Kelvin equation, the expression for slope, dw/dr, and bending moment, M, are given by

$$\theta = \frac{dw}{dr} \tag{21}$$

$$M = D^*\left(\frac{d^2w}{dr^2} + \frac{\nu^*}{r}\frac{dw}{dr}\right) \tag{22}$$

The two constants of integration A and B and the axial displacement of the half shell, Δs, are determined by the three boundary conditions:

1. At $r = R$, the deflection $w(r)$ at the edge of the plate due to bending is zero.
2. At $r = R$, the radial bending moment at the edge of the plate equals the moment exerted by the rotational spring, i.e.,

$$D^*\left(\frac{d^2w}{dr^2} + \frac{\nu^*}{r}\frac{dw}{dr}\right)\Big|_{r=R} = -K_\theta \frac{dw}{dr}\Big|_{r=R} \tag{23}$$

   where K_θ is the spring constant for half shell. Its value is the sum of the bending rigidities of the shell and the channel.
3. The vertical force at the edge, V_E, is given by the net effective force acting on the plate in terms of net effective pressure $q(r)$:

$$2\pi \int_0^R q(r)\, dr = 2\pi R V_E \tag{24a}$$

   where

$$V_E = \frac{\pi R^2 p_t - k_s \Delta_s}{2\pi R} \tag{24b}$$

3.3 Tube-Sheet Design as Per TEMA Standards

Tube-Sheet Formula for Bending

As per RCB-7.131, the formula for minimum tube-sheet thickness to resist bending is given by

$$T = \frac{FG}{3}\sqrt{\frac{P}{\eta S}} \tag{25}$$

where F is the parameter used to account for the elastic restraint at the edge of the tube sheet due to shell and channel connection, G the diameter over which the pressure is acting, P the effective design pressure, S the ASME Code allowable stress, and η the mean ligament effi-

ciency, given in terms of tube layout pattern angle θ and pitch ratio p/d whose expression is given by

$$\eta = 1 - \frac{\pi}{4(\sin\theta)(p/d)^2}$$

$$= 1 - \frac{0.785}{(p/d)^2} \quad \text{for } \theta = 90° \text{ and } 45°$$

$$= 1 - \frac{0.907}{(p/d)^2} \quad \text{for } \theta = 60° \text{ and } 30° \tag{26}$$

The values of F, P, and G differ for supported and unsupported tube sheets. For a fixed tube-sheet exchanger, G shall be the shell inside diameter. For other types of exchangers refer to TEMA for the definition of G. For a fixed tube-sheet exchanger, the effective design pressure, P, shall be calculated as per Sections RCB-7.163, RCB-7.164, and RCB-7.165. The definition of F for supported and unsupported tube sheets is discussed next. For all types of tube sheets, the thickness shall be calculated both for uncorroded and corroded conditions.

Parameter F

Supported Tube Sheet.

1. Gasketed both sides, e.g., stationary tube sheet and floating tube sheet and floating head exchanger:

   $F = 1.0$
2. Integral on both sides or a single side, e.g., stationary tube sheet of fixed tubesheet exchanger and floating head exchanger.

When the tube sheet is integral with both sides or a single side (for fixed tube-sheet exchangers the gasketed side refers to the tube side), F is determined by curve H in Fig. RCB-7.132. The curve is presented in terms of the ratio of wall thickness to internal diameter (ID) of the shell or channel, i.e., (t/ID), whichever yields the smaller value of F. For the shell-side integral condition, use the shell ID to find F. The H curve can be represented by:

$$F = 1.0 \quad \text{for } \frac{t}{\text{ID}} \le 0.02$$

$$= \frac{17 - 100\frac{t}{\text{ID}}}{12} \quad \text{for } 0.05 \ge \frac{t}{\text{ID}} > 0.02$$

$$= 0.8 \quad \text{for } \frac{t}{\text{ID}} > 0.05 \tag{27a}$$

As per this condition, the minimum value of F is 0.8 and maximum value is 1.0.

Both the tube sheets of the fixed tube-sheet exchanger are satisfied by this condition, and both the tube sheets shall have the same thickness, unless the provisions of RCB-7.166 are satisfied.

Note: The F value for the tube sheet at the floating head for all configurations is 1.0.

Unsupported Tube Sheet, For Example, U-Tube Sheet.

1. When gasketed at both sides, $F = 1.25$.
2. For tube sheets integral on both sides or a single side, F shall be determined by curve U in Fig. RCB-7.132. The curve is presented in terms of the ratio of wall thickness to internal diameter (ID) of the integral side, i.e., (t/ID). The U curve can be represented by:

$$F = 1.25 \qquad \text{for } \frac{t}{\text{ID}} \le 0.02$$

$$= \frac{17 - 100\frac{t}{\text{ID}}}{15} \qquad \text{for } 0.05 \ge \frac{T}{\text{ID}} > 0.02$$

$$= 1.0 \qquad \text{for } \frac{t}{\text{ID}} > 0.05 \tag{27b}$$

As per this condition, the maximum value of F is 1.25 and the minimum value is 1.0.

The term P is the effective design pressure where $P = p_s + p_b$ or $p_t + p_b$; p_b is defined as equivalent bolting pressure when the tubesheet is extended as a flange. The expression for p_b is given by

$$p_b = \frac{-6.2M^*}{F^2G^3} \tag{28}$$

where M^* is defined in Paragraph RCB-7.1342. Expression for M^* is furnished in the section on 3.6 flanged tubesheet—TEMA design procedure.

Shear Formula RCB-7.133

The effective tube-sheet thickness T to resist shear is given by

$$T = \frac{0.31D_e}{(1 - d/p)}\frac{P}{S} \tag{29}$$

where D_e is the equivalent diameter of the perforated tubesheet ($4A_p/C$), C is the perimeter of the tube layout measured stepwise in increments of one tube pitch from center to center of the outermost tubes (Fig. 6 shows the application to typical triangular and square tube patterns; only a portion is shown), and A_p is the total area enclosed by the perimeter C.

The shear stress formula was derived by limiting the maximum allowable shear stress to

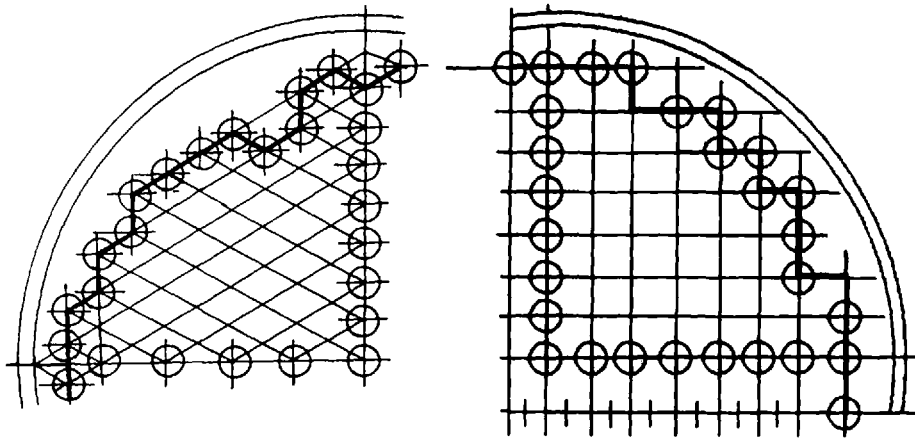


Figure 6 Perimeter of tube layout for shear stress calculation. (a) Triangular layout; and (b) square layout.

0.8 times the Code allowable stress S. The shear formula controls the tube-sheet thickness only in high-pressure and small-diameter cases. Since the quantities C and A_p are available after the tube layout is finalized, TEMA provides a formula to check whether shear stress will be controlling the tube-sheet thickness or not. Shear formula will not control the tube-sheet thickness if

$$\frac{P}{S} < 1.6\left(1 - \frac{d}{p}\right)^2 \tag{30}$$

Stress Category Concept in TEMA Formula

The primary stress in the tube sheet is limited to ASME Code Section VIII, Div. 1, allowable stress S, and the primary stress plus the thermal stress (secondary stress) is limited to $2S$. Accordingly, the expression for effective pressure is halved before being used in the thickness formula.

Determination of Effective Design Pressure, P (RCB-7.16)

The determination of (1) effective shell-side design pressure involves the terms p_s', equivalent differential expansion pressure p_d, and equivalent bolting pressure (p_{bs} and/or p_{bt}), and (2) effective tube-side design pressure involves p_t', p_d, and p_{bs} and/or p_{bt}. The expressions for p_d, equivalent bolting pressure (p_{bs}, p_{bt}), p_s', and p_t' are given next.

Equivalent Differential Expansion Pressure, p_d (*RCB 7.161*). The equivalent differential expansion pressure, p_d, is given by [70]:

$$p_d = \frac{4Jt_sE_s[\alpha_s(\theta_s - \theta_{amb}) - \alpha_t(\theta_t - \theta_{amb})](D_o - t_s)/(D_o - 2t_s)^2}{1 + JKF_q} \tag{31}$$

where D_o is the shell outer diameter, F_q a parameter that is a function of X (G_4 of Miller [53] and H_4 of Galletly [56]),

$$\theta_t = \theta_{t,m} - \theta_{amb}$$

$$\theta_s = \theta_{s,m} - \theta_{amb}$$

and where J is the expansion joint flexibility parameter (=1.0 for shells without expansion joint).

The expressions for J and F_q and the final expression for p_d follow.

1. The expansion joint flexibility parameter J is given by

$$J = \frac{1}{1 + \dfrac{K_s}{S_j}} \tag{32}$$

Substituting the expression for K_s, J is given by

$$J = \frac{S_jL}{S_jL + \pi(D_o - t_s)\,E_st_s} \tag{33}$$

J can be assumed equal to zero for a shell with expansion joints if the following condition is satisfied:

$$S_j < \frac{(D_o - t_s)t_sE_s}{10L} \tag{34}$$

where S_j is the spring rate of the expansion joint.

2. From Osweiller [70], the expression for F_q in terms of X is given by

$$F_q = 0.25 + \alpha X \tag{35}$$

where α is a function of the tube-sheet correction factor F. By substituting the expression for α, the resulting expression for F_q is given by

$$\alpha = (F - 0.6)\frac{\sqrt{2}}{0.8} \tag{36}$$

$$\therefore\ F_q = 0.25 + (F - 0.6)\frac{\sqrt{2}}{0.8}\left[\frac{6(1-\nu^2)}{\eta}\frac{E_s t_s}{KLE}\left(\frac{G}{T}\right)^3\right]^{0.25} \tag{37}$$

By assuming that the tube-sheet deflection efficiency η is 0.178 and ν is 0.3, we get an expression for F_q similar to the TEMA form:

$$F_q = 0.25 + (F - 0.6)\sqrt[4]{\frac{300\,E_s t_s}{KLE}\left(\frac{G}{T}\right)^3} \tag{38}$$

where G is the shell inside diameter ($2R$, where R is the shell inside radius). Note: use the calculated value of F_q or 1.0 whichever is greater. By approximating

$$\frac{D_o - t_s}{(D_o - 2t_s)^2} \approx \frac{1}{(D_o - 3t_s)} \tag{39}$$

and replacing $\alpha_s(\theta_s - \theta_{amb})$ and $\alpha_t(\theta_t - \theta_{amb})$ by $\Delta L/L$, the expression for p_d is given by

$$p_d = \frac{4JE_s t_s\left(\dfrac{\Delta L}{L}\right)}{(D_o - 3t_s)\,(1 + JKF_q)} \tag{40}$$

where ΔL is the differential thermal expansion between the shell and the tube bundle.

Equivalent Bolting Pressure (RCB 7-162). When the tube sheet is extended as a flange for bolting to head or channel with a ring type gasket, the effect of the flange moment acting upon the tube sheet is accounted for in effective design pressure in terms of equivalent tube-side bolting pressure, p_{bt}, and equivalent shell-side bolting pressure, p_{bs}, as given by:

$$p_{bt} = \frac{6.2M_1}{F^2G^3} \tag{41a}$$

$$p_{bs} = \frac{6.2M_2}{F^2G^3} \tag{41b}$$

where M_1 is the bolting moment acting under the operating condition, as defined by the ASME Code as M_o under flange design; M_2 is the bolting moment acting under the gasket seating condition, as defined by the ASME Code as M_o under flange design; and G is the inside diameter of the shell.

Expression for p_s'. The expression for p_s' is given by [70]:

$$p_s' = \frac{p_s\left[JK[2\nu_t + f_s(1 - 2\nu_t)] + 2\nu_s J - \left(\dfrac{1-J}{2}\right)\left(\dfrac{D_j^2}{G^2} - 1\right)\right]}{1 + JKF_q} \tag{42}$$

By substituting $\nu_s = \nu_t = 0.3$, and rearranging the terms, p_s' is given in TEMA form:

$$p_s' = \frac{p_s\left[0.4J[1.5 + K(1.5 + f_s)] - \left(\frac{1 - J}{2}\right)\left(\frac{D_j^2}{G^2} - 1\right)\right]}{1 + JKF_q} \quad \text{for } \nu_s = \nu_t = 0.3 \tag{43}$$

Expression for p_t'. The expression for p_t' is given by [70]:

$$p_t' = \frac{p_t[1 + JK\{f_t + 2\nu_t(1 - f_t)\}]}{1 + JKF_q} \tag{44}$$

$$= \frac{p_t[1 + 0.4\ JK(1.5 + f_t)]}{1 + JKF_q} \quad (\text{for } \nu_t = 0.3) \tag{45}$$

where D_j is the expansion joint diameter, G the inside diameter of the shell, p_{bt} the equivalent bolting pressure when tube-side pressure is acting, p_s the shell-side design pressure, and p_t the tube-side design pressure.

Differential Pressure Design, after Yokell [29]

In differential pressure design, the pressure parts exposed to both fluids are designed for the difference in operating pressures between the two fluids, i.e., simultaneous action of both the shell-side and tube-side pressures. Differential pressure design is seldom used when the simultaneous design pressures are less than 1000 psi (6895 kPa). The operating circumstances that favor differential pressure design are:

1. A common source of supply of the shell-side and tube-side fluids
2. Shell-side and tube-side operating pressures in the range of 1000 psi (6895 kPa) and above, when the pressure in one side is directly controlled by the other
3. High pressure on both sides in which the differential pressure can be measured and controlled

Merits of Differential Pressure Design. Differential pressure design reduces the tube-sheet thickness below what would be required for conventional design. However, this design involves certain safety and protection devices to be incorporated into the system, in the event of failure on one side [29]. To justify this design, the reduction in capital cost due to thin tube sheet and the associated machining cost savings must exceed any operating cost associated with differential pressure design and safety devices to be provided. TEMA and BS 5500 recognize differential pressure design when it is mutually agreed between the purchaser and the seller.

Effective Differential Design Pressure, P (*RCB 7.165*). For differential pressure design, the effective differential design pressure is calculated as per RCB 7.165. For practical use TEMA considers the seven combined design loading cases where pressure acts on the shell side ($p_t = 0$), on the tube side ($p_s = 0$), on both sides, and in each case with and without thermal expansion; the seventh case is obtained for thermal expansion acting alone ($p_s = 0$ and $p_t = 0$).

Longitudinal Stress Induced in the Shell and Tube Bundle

After arriving at the tube-sheet thickness, it is necessary to determine the stresses induced in the shell, channel, and tubes located at the periphery and interior of the tube bundle in the case of fixed and floating tubesheet exchangers. The check for longitudinal stress induced in the shell is calculated as per RCB-7.22. However, there is no procedure in TEMA to calculate the bending stresses induced in the shell and both the longitudinal stress and bending stress in the channel. The check for tube longitudinal stress both in tension and in compression in the tubes

located at the periphery of fixed tube-sheet exchangers are calculated as per RCB-7.23 and RCB-7.24, respectively. This is discussed next.

Shell Longitudinal Stress, $\sigma_{s,l}$ (RCB-7.22). The maximum longitudinal stress induced in the shell, $\sigma_{s,l}$ is given by

$$\sigma_{s,l} = \frac{p_s^* (D_o - t_s) Z_s}{4t_s} \tag{46}$$

Seven loading cases are examined, which lead to seven values of p_s^*. The value of parameter Z_s depends on the stress category concept. Its value is either 0.5 or 1.0; p_s^* is determined as per TEMA definition.

Longitudinal Stress Induced in the Tubes Located at the Periphery of the Tube Bundle, $\sigma_{t,l}$ (RCB-7.23). The maximum longitudinal stress induced on the tubes located at the periphery of tube bundle is given by

$$\sigma_{t,l} = \frac{F_q G^2 p_t^* Z_t}{4N_t t(d - t)} \tag{47}$$

As for the shell longitudinal stress case, seven loading cases are examined, which lead to seven values of p_t^*. The value of parameter Z_t depends on the stress category concept. Its value is either 0.5 or 1.0; p_t^* is determined as per TEMA definition.

Longitudinal Stresses Inside the Tube Bundle. Although the tubes located at the interior of the bundle can become loaded both in tension and compression, longitudinal stresses inside the tube bundle are not calculated in TEMA. Tensile forces are generally not a problem if the requirements of RCB-7.22 are met. However, compressive forces might create unstable conditions for tubes at the interior of the bundle. Typical conditions that can cause this are loading and geometry, as follows:

Loading: Tube-side pressure and/or differential thermal expansion where the shell, if unrestrained, would lengthen more than the tubes (positive P_d per RCB-7.161).

Geometry: Flexible tube-sheet systems. Generally, those that are simply supported at the edge ($F = 1$) and have a value of F_q greater than 2.5.

Methods similar to those provided in the references cited in TEMA, and others such as in refs. 56, 67, 70, and 73 can be used to predict loadings on tubes at the interior of the bundle.

Compressive Stress Induced in the Tubes Located at the Periphery of the Tube Bundle (RCB 7-24). The compressive stress acting on the tubes located at the periphery is limited to the allowable compressive stress S_c based on the Euler critical buckling load for a column as given by

$$\sigma_c = \frac{\pi^2 E_t}{F_s \left(\frac{kl}{r_G} \right)^2} \qquad \text{when} \quad \Lambda \le \frac{kl}{r_G} \tag{48}$$

$$= \frac{S_y}{F_s} \left[1 - \frac{kl/r_G}{2\Lambda} \right] \qquad \text{when} \quad \Lambda > \frac{kl}{r_G} \tag{49}$$

where

$$\Lambda = \sqrt{\frac{2\pi^2 E_t}{S_y}} \tag{50}$$

r_G is the radius of gyration of the tubes,

$$r_G = 0.25\sqrt{d^2 + (d - 2t)^2} \tag{51}$$

and kl the equivalent unsupported buckling length of the tube, k a factor that takes into account the tube span end conditions, l the unsupported tube span between two baffles, and F_s the factor of safety

Tube-to-Tube-Sheet Joint Loads (RCB-7.25)

The maximum effective tube-to-tube-sheet joint load, F_j, acting on the tubes located at the periphery of the tube bundle is given by

$$F_j = \frac{\pi F_q p_t^* G^2}{4N_t} \tag{52}$$

where p_t^* is determined as per TEMA definition. This joint load is to be less than the maximum allowable joint load calculated as per ASME Code Section VIII, Div. 1.

Maximum Allowable Joint Loads. In the design of shell and tube heat exchangers other than U-tube construction, the maximum allowable axial load on tube-to-tube-sheet joints shall be determined in accordance with the code formula. The basis for establishing allowable loads for tube-to-tube-sheet joints loads is given in ASME Code Appendix AA. In ASME Code, various joints types are identified by a, b, c, d, e, f, g, h, i, j, and k. The maximum allowable joint load F_{max} is calculated as follows:

1. For joint types a, b, c, d, e:

$$F_{max} = A_t S_a f_r \tag{53}$$

2. For joint types f, g, h, i, j, k:

$$F_{max} = A_t S_a f_e f_r f_y \tag{54}$$

where A_t is the nominal transverse cross-sectional area of tube wall, S_a the Code allowable stresses in tension of tube material at design temperature, f_e a factor for the percentage of tube expansion length, $f_e = 1.0$ for joints made with expanded tubes in grooved tube holes, d the tube outer diameter, f_r the factor for efficiency of joint, and f_y the ratio of tube-sheet material yield stress to tube material yield stress.

Refer to ASME Code Section VIII, Div. 1, for complete details including joint types on the nomenclature.

TEMA Fixed Tube-Sheet Design with Different Thickness

Fixed tube sheets of different thickness in the same unit are designed as per RCB-7.166. Considerable savings may be realized when a process dictates a high-quality material at only one end of a unit where the temperature is very high.

Tubesheet Design as per ASME Code Section VIII, Div. 1

A "design-by-formula" procedure for the design of fixed tube sheets of shell and tube heat exchangers and the connected components is included in the ASME Code, Section VIII, Div. 1, Appendix AA—Nonmandatory. The method follows the approach of Singh and Soler [41] and extended by Soler et al. [67] to present a unified treatment for all fixed tube-sheet styles.

The procedure is based on classical thin plate and shell theory. It includes the effect of unperforated rim of the tube sheet, differential thermal expansion in the radial direction, arbitrary combinations of material properties and arbitrary joint configurations—three different tubesheet, shell, and head configurations, namely, (1) two sides gasketed type construction, (2) two sides integral type construction, (3) one side gasketed and the other side integral type construction—and heat exchanger styles, and the elastic–plastic method, which takes into account the discontinuity stresses at the tube sheet to shell/channel joint and considers the possibility of plastic hinges at the shell–tube sheet and channel joints. As a part of the calculations procedure, charts are provided to evaluate certain parameters. Kuppan [75] provides alternate charts in place of those presented in ASME CODE, numerical values for certain functions used to derive the charts that will help to do design calculations without referring the charts, and extensions of the existing charts for larger values of tubesheet parameter X.

CODAP

The maximum stress, σ, in the tube sheet due to bending is given by [73]:

$$\sigma = \frac{1}{\mu H_1(X,Z)} \left(\frac{R}{T} \right)^2 p^* \tag{55}$$

Inverting this equation, the expression for tube-sheet thickness to resist bending is given by

$$T = \frac{R}{\sqrt{\mu H_1(X,Z)}} \sqrt{\frac{p^*}{\sigma}} \tag{56}$$

where S_f is the CODAP allowable stress, $H_1(X,Z)$ the tube-sheet coefficient depending on parameters X and Z (its expression is given in the Appendix), p^* the equivalent differential pressure, R the outer tube-sheet radius where shell-side pressure is acting, T the tube-sheet thickness, μ the minimum ligament efficiency, and X and Z the parameters of the heat exchanger (an expression for X was given earlier, and Z is given in the Appendix).

Parameters X, Z, *Ligament Efficiency*, μ, *and* p*. The parameter X represents the relative rigidity of the tube bundle with respect to the tube sheet. It may vary from 0 (no tube in the bundle) to above 50 (very stiff tube bundle). The parameter Z represents the elastic rotational restraint at the periphery of the tube sheet due to channel and shell connection. It may vary from 0 for the simply supported case to infinity for the clamped case. The expression for minimum ligament efficiency μ is given by

$$\mu = \frac{p - d}{p} \tag{57}$$

$$= \frac{p - (d - t)}{d} \tag{58}$$

where d is the tube outer diameter, p the tube pitch, and t the tube wall thickness.

Equation 57a is applicable to tubes welded to the tubesheet, and Eq. 58b is applicable to tubes expanded more than 90% of tube-sheet thickness.

Equivalent Design Pressure, p*. The expression for p^* for simultaneous action of shell-side pressure, tube-side pressure and differential thermal expansion (assuming there is an expansion joint on the shell side) is given by [73]:

$$p^* = \frac{p_s}{1 + JKH_4(X,Z)} \tag{59}$$

$$p_s = p_s\left\{[JK\{f_s + 2\nu_t(1 - f_s)\} + 2\nu_s J] - \left[\frac{D_j^2 - G^2}{G^2}\right]\frac{JK_s}{4S_j}\right\}$$

$$- p_t[JK\{f_t + 2\nu_t(1 - f_t)\} + 1] + \frac{JK\gamma k_w}{2} \tag{60a}$$

$$= p'_s - p'_t + p_d \tag{60b}$$

where p'_s, p'_t, and p_d are the same as in Eq. 42, 44, and 40, respectively.

Stress Category Concept in CODAP Formula. The stress category concept used in CODAP is discussed by Osweiller [70]. The primary membrane stress plus bending stress in the tube sheet is limited to $1.5f$ (f = nominal or allowable design stress in CODAP). When the tube sheet is not extended as a flange, the bending stress due to pressures has been taken up to $2f$. When the tube-sheet rim is extended as a flange, the additional moment at the periphery of the tube sheet is taken into account by limiting the allowable stress to $1.5f$.

Fixed Tube-Sheet Formula as per BS 5500

The fixed tube-sheet design formula of BS 5500 [18] bears certain commonalities with the fixed tube-sheet design procedure of CODAP and TEMA. Similar to CODAP, the fixed tube-sheet formula in BS 5500 takes into account the tube-sheet restraint offered by shell and channel to the tube sheet through the term $H_1(X,Z)$. However, the effective design pressure is calculated like the TEMA procedure. The minimum tube-sheet thickness shall be greater of the values calculated to resist bending and shear given by the following formulas.

Bending:

$$T = \max\left|\frac{G_1}{\sqrt{4H_1(X,Z)}}\sqrt{\frac{p_1}{\Omega\mu S_b}}, \frac{G_2}{\sqrt{4H_1(X,Z)}}\sqrt{\frac{p_2}{\Omega\mu S_b}}\right| \tag{61}$$

Shear:

$$T = \max\left|\frac{0.155D_{otl}p_1}{\lambda\tau}, \frac{0.155D_{otl}p_2}{\lambda\tau}\right| \tag{62}$$

Simultaneous action of both the shell-side and tube-side pressure: If agreed, the design shall be based on the simultaneous action of both the shell-side and tube-side pressure (TEMA specifies this condition as effective differential pressure design; RCB-7.165)

Bending:

$$T = \max\left|\frac{G_1}{\sqrt{4H_1(X,Z)}}\sqrt{\frac{p_d}{\Omega\mu S_b}}, \frac{G_2}{\sqrt{4H_1(X,Z)}}\sqrt{\frac{p_d}{\Omega\mu S_b}}\right| \tag{63}$$

Shear:

$$T = \frac{0.155D_{otl}p_d}{\lambda\tau} \tag{64}$$

where G_1 is the diameter to which shell-side pressure is acting, G_2 the diameter to which tube-side pressure is acting, D_{otl} the diameter of the outer tube limit circle, S_b the allowable stress in BS 5500, p_1 the shell-side effective design pressure, p_2 the tube-side effective design pressure, p_d the effective differential design pressure, Ω the design stress factor (its value is 1.5 for fixed tube sheet and 2 for floating head tube sheet), λ the ligament efficiency of the tube sheet in shear, and μ the ligament efficiency of the tube sheet in bending and allowable shear stress

for tubesheet material. Note: The definition of p_1, p_2, and p_d are the same as the effective shell-side design pressure calculated as per TEMA para RCB-7.163, the effective tube-side design pressure calculated as per TEMA para RCB-7.164 and the effective differential design pressure calculated as per TEMA para RCB-7.165, respectively.

The expression for μ and λ are

$$\mu = \lambda = \frac{p - d_h}{P} \tag{65}$$

$$= \frac{p - (d_h - t)}{p} \tag{66}$$

where d_h is the tubehole diameter. Equation 65 applies to:

1. Tubes not expanded into the full depth of the tube sheet
2. Tubes seal-welded to the tube sheet
3. Tubes having significantly lower elastic modulus than the tube-sheet material

Equation 66 applies to:

1. Tubes fully expanded into the tube sheet
2. Explosion-bonded tubes

The determinations of effective design pressure p_1 (Section 4.9.3.4.1), p_2 (Section 3.9.4.3.2), and p_d (Section 4.9.3.4.3) are similar to TEMA procedures RCB-7.163, RCB-7.164, and RCB-7.165, respectively.

Stress Category Concept in BS 5500 Formula. The stress category concept in BS 5500 is similar to that of TEMA but with an additional design stress factor. This factor allows for the fact that the stress calculated using these requirements is the average bending stress across the ligament at the surface of the tube sheet, and the permissible value is higher than the nominal allowable stress f (in ASME Code the allowable stress is designated by S) by a factor Ω, whose value is 1.5 for fixed tube-sheet exchanger and 2 for floating tube-sheet exchanger.

Determination of Joint Load. Determination of the stress induced in the shell and the tube is similar to the TEMA procedure. The determination of compressive stress in the tube due to buckling differs slightly from the TEMA procedure. The determination of the tube joint load is different in BS 5500. It specifies six typical joints types. The joint load formula involves the determination of parameters such as tube joint reliability factor, expansion factor, and material factor.

Comparison of Fixed Tube-Sheet Thickness Formula of TEMA with CODAP and BS 5500

For comparison purposes, assume that (1) the ASME Code allowable stress $S = S_h$ of BS 5500 and (2) for a fixed tube sheet to resist bending, $\sigma = 2S$. The resulting equations for tube-sheet thickness per TEMA, CODAP, and BS 5500 can be written as

$$T_{\text{TEMA}} = \frac{FG}{3\sqrt{\eta}}\sqrt{\frac{p}{S}} = \frac{F}{1.5\sqrt{\eta}}\frac{G}{2}\sqrt{\frac{p}{S}} \tag{67}$$

$$T_{\text{CODAP}} = \frac{1}{\sqrt{\mu H_1(X, Z)}}\frac{G}{2}\sqrt{\frac{p^*}{2S}} \left(\because R = \frac{G}{2},\ \sigma = 2S\right) \tag{68}$$

$$T_{\text{BS5500}} = \frac{G}{2\sqrt{H_1(X,Z)}}\sqrt{\frac{P}{\Omega\mu S}} \text{ (for } p_1 = p_2 = p_d = p,\ G_1 = G_2 = G,\ S_b = S) \tag{69}$$

It is seen from these equations that TEMA simplified its formula, replacing $1/\sqrt{H_1}$ (X,Z) by F, with an intention to have a simple hand calculations procedure for the tube-sheet design.

Under the assumptions $p = p^* = p'$ and that the tube sheet is not extended as a flange, and separating the common terms, the F factor in the TEMA, CODAP, and BS 5500 formats can be written as

$$F_{\text{TEMA}} = \frac{F}{1.5\sqrt{\eta}} \tag{70a}$$

$$F_{\text{CODAP}} = \frac{1}{\sqrt{2\mu H_1(X,Z)}} \tag{70b}$$

$$F_{\text{BS5500}} = \frac{1}{\sqrt{1.5\mu H_1(X,Z)}} \tag{70c}$$

The F values of TEMA are compared with CODAP by Osweiller [70,73]. As per the comparison, TEMA formula is not safe for the entire range of X values. It is unsafe for lower values and conservative for higher values of X.

Appendix

The expression for Z [56] and $H_1(X,Z)$ and $H_4(X,Z)$ taken from ref. 70 are given by:

$$Z = \frac{K_\theta}{k\, D^*} = \frac{K_\theta}{\sqrt[4]{k_w\, D^{*3}}} \tag{71}$$

where K_θ is the edge moment coefficient. It depends on the bending rigidities of the shell (δ_s) and the channel (δ_c). It represents the degree of elastic restraint of the tube sheet offered to it by the shell and the channel connected to it. Its value varies between the two extreme values: 0, which corresponds to the simply supported case; and ∞, which corresponds to the clamped case.

$$k_\theta = 2[\delta_s + \delta_c]$$

$$K_\theta = 2\left[\frac{E_s t_s^{2.5}}{[12(1-\nu^2)]^{0.75}(D_s + t_s)^{0.5}} + \frac{E_c t_c^{2.5}}{[12(1-\nu^2)]^{0.75}(D_c + t_c)^{0.5}}\right] \tag{72}$$

$$H_1(X,Z) = \frac{kR}{3\Psi(kr)}\left[bei'(kR)\,\frac{g_1(kR)}{g_2(kR)} - ber'(kR)\right] \tag{73}$$

$$H_4(X,Z) = \frac{kR}{2}\,\frac{\left[ber(kR)\,\dfrac{g_1(kR)}{g_2(kR)} + bei(kR)\right]}{\left[bei'(kR)\,\dfrac{g_1(kR)}{g_2(kR)} - ber'(kR)\right]} \tag{74}$$

where

$$\Psi(kr) = f_1(kr) - \frac{g_1(kR)}{g_2(kR)}\, f_2(kr) \tag{75}$$

The expression for $f_1(kr)$ and $f_2(kr)$, $g_1(kr)$, and $g_2(kr)$ are given by

$$f_1(kr) = ber(kr) - \frac{(1 - \nu^*)bei'(kr)}{kr} \tag{76}$$

$$f_2(kr) = bei(kr) + \frac{(1 - \nu^*)ber'(kr)}{kr} \tag{77}$$

$$g_1(kR) = f_1(kR) + Zbei'(kR) \tag{78}$$

$$g_2(kR) = f_2(kR) - Zber'(kR) \tag{79}$$

3.4 Rules for Tube Sheet of Floating Head Exchangers

BS 5500 and CODAP

The floating head heat exchanger tube-sheet design is comparatively simpler than for a fixed tube-sheet exchanger due to the reason that in the floating head exchanger only one tube sheet is fixed to the shell or channel or both sides, either by welding or by bolting. The second tube sheet is free to move inside the shell. The method of Gardner [58] for the design of floating head exchangers is adopted in BS 5500 and CODAP, and this code procedure is discussed by Osweiller [73]. The tube-sheet thickness to resist bending is given by

$$T = (C_o + \Delta C_o)D_p \sqrt{\frac{|p_s - p_t|}{2\mu S_f}} \tag{80}$$

where C_o is a coefficient that depends on two parameters X_o and R_D (these two parameters are defined later), D_p is the diameter of the perforated region, and f is the nominal design stress.

In CODAP, the tube-sheet thickness to resist bending is expressed in terms of a stress-oriented formula as [73]:

$$\sigma = \frac{(C_o + \Delta C_o)^2(p_s - p_t)}{\mu}\left(\frac{D_p}{T}\right)^2 \qquad \text{(where } \sigma \text{ is limited to } 2S\text{)} \tag{81}$$

Parameters X_o *and* R_D.

1. X_o is similar to the coefficient X related to the fixed tube sheets with modifications so as to present a direct formula for calculating T.

$$X_o = \frac{\left[1.5\,(1 - \nu^2)(f_t - f_s)\frac{E_t}{E^*}\frac{D_p}{L}\right]^{1/3}}{\sqrt{\frac{|p_s - p_t|}{2\mu S_f}}} \tag{82}$$

2. $R_D = 2R/D_p$, which accounts for the untubed rim at the periphery of the tubesheet.

Another parameter relevant to the discussion is the mean solidity factor of the tube sheet, f_m, given by

$$f_m = \frac{f_s + f_t}{2} \tag{83}$$

The values of coefficient C_o are given in Fig. 7 for a mean solidity factor of 0.6. The coefficient ΔC_o gives the correction for other values of the solidity factor. It can be seen from Fig. 7 that values for C_o are given only for two limiting cases of tube-sheet edge conditions: (1) simply supported ($Z = 0$), and (2) clamped tube sheet ($Z = \infty$). No credit is given for the other edge

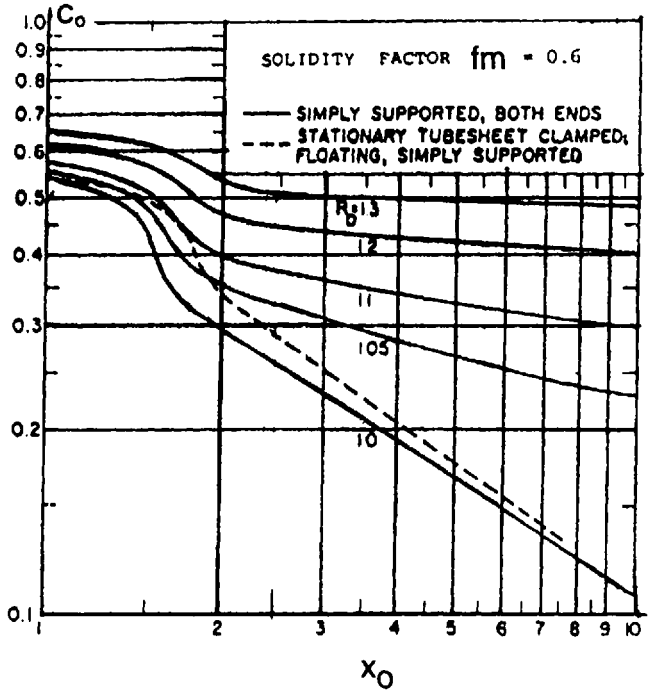


Figure 7 Coefficient C_0 for mean solidity factor $f_m = 0.6$. (From Ref. 58.)

conditions. Therefore for other cases the designer must judge whether the tubesheet is simply supported, clamped or halfway between the extreme cases as defined next [73].

BS 5500.

1. Simply supported condition: tubesheet (either fixed or floating) gasketed at both sides using narrow-faced gaskets.
2. Clamped condition: full-face gaskets on both sides, or full-face gasket on a single side and the tube sheet integral on the other side.

CODAP.

1. Simply supported when bolted on both sides.
2. Halfway between simply supported and clamped in the following cases: gasketed on one side and integral on the other side, or integral on both sides.

Accordingly, the value for C_o for the intermediate case is the average of the simply supported case $C_{o,s}$ and the clamped case $C_{o,c}$ as given by

$$\therefore \quad C_o = \frac{C_{o,s} + C_{o,c}}{2} \tag{84}$$

Maximum Axial Stress in Tubes. The maximum axial stress in the tubes located both at the periphery $\sigma_{t,p}$ of the tube bundle and in interior $\sigma_{t,i}$ is given by [73]:

$$\sigma_{t,p} = \frac{(p_s f_s - p_t f_t) - F_{tp}(p_s - p_t)}{f_t - f_s} \tag{85}$$

$$\sigma_{t,i} = \frac{(p_s f_s - p_t f_t) + F_{ti}(p_s - p_t)}{f_t - f_s} \tag{86}$$

The coefficients F_{tp} and F_{ti} are analogous to coefficient C_o and are given by curves [18,58] that depend on parameters X_o and R_D.

3.5 U-Tube Tube-Sheet Formula

BS 5500

For U-tube exchangers, the design method is simpler since the tubes do not act as an elastic foundation. Hence, the CODAP formula for the floating head exchanger can be used by setting $X_o = 0$ in the tube-sheet formula. This is done in codes/standards such as ISO, BS 5500, and CODAP. The tube-sheet thickness formula to resist bending is given by

$$T = (C_o + \Delta C_o) D_p \sqrt{\frac{|p_s - p_t|}{2\mu S_f}} \tag{87}$$

where $C_o + \Delta C_o$ is given directly as a function of mean solidity factor f_m and ratio $2R/D_p$. The values for C_o and ΔC_o are given in Table 7.

CODAP

The CODAP formula for U-tube exchangers is same as for BS 5500.

ASME Code Section VIII, Div. 1

ASME Code Section VIII, Div. 1, Appendix AA, provides rules for the design of U-tube sheets of (1) simply supported, (2) both sides integral, and (3) integral construction with tube sheet extended as flange.

3.6 Flanged Tube Sheets—TEMA Design Procedure

Formulas are included in the TEMA seventh edition for the calculation of the minimum thickness required on the flanged portion of the tube sheet of fixed, floating, and U-tube exchangers. The calculation procedure is based on the work of Singh et al. [74]. The purpose of this new method is to insure that there is sufficient tubesheet thickness to withstand bending moments transmitted by the adjoining flange.

Table 7 Values for Coefficients C_o and ΔC_o [58]

	Clamped		Simply supported			
				ΔC_o		
R	C_o	ΔC_o	C_o	$f_m = 0.45$	$f_m = 0.60$	$f_m = 0.80$
1.00	0.433	0	0.560	0.000	0	0.000
1.05	0.433	0	0.576	−0.002	0	0.002
1.10	0.433	0	0.592	−0.010	0	0.010
1.20	0.433	0	0.625	−0.025	0	0.025
1.30	0.433	0	0.660	−0.040	0	0.040

Fixed Tube Sheet or Floating Tube Sheet

The thickness of the portion of the tube sheet extended as a flange, t_F, is given by [74]:

$$T_f = 0.98 \left[\frac{M\{r_f^2 - 1 + 3.72 \ln(r_f)\}}{S(D_T - G)(1.0 + 1.86 r_f^2)} \right]^{0.5} \tag{88}$$

where M is the bolting moment due either to gasket seating condition or operating condition, whichever is greater; if a joint is integral (welded connection), then the corresponding edge moment is zero; D_T and G are the tubesheet outer diameter and effective gasket diameter as defined in TEMA RCB-7.132, respectively; and S is the Code allowable stress at the design temperature. The quantity r_f is the ratio of D_T to G:

$$r_f = D_T/G \tag{89}$$

U-Tube Tube Sheet

The minimum thickness of the portion of the tube sheet of thickness T extended as a flange, T_f, is given by [87]:

$$T_f = 1.38 \left[\frac{M^* + M + 0.39\ PG^2\ W}{(D_T - G)\ S} \right]^{0.5} \tag{90}$$

where

$$M^* = \frac{\left(\frac{0.069w}{\eta}\right) F^3 PG^3 \left(\frac{T_f}{T}\right)^3 - MG - 0.39wPG^3}{G + \left(\frac{1.37}{\eta}\right)\left(\frac{T_f}{T}\right)^3 w} \tag{91}$$

where M is the bolting moment either due to gasket seating condition or operating condition whichever is greater (if a joint is integral, such as welded connection, then the corresponding edge moment is zero); G has different values for different styles of construction (for example, G is the inside diameter of the pressure part for the pressure acting on an integral side of a tube sheet; it is the location of the gasket load reaction as defined in the code for the pressure acting on the gasketed side of a tube sheet, TEMA RCB-7.132); $P = p_s$ or p_t or maximum differential pressure or as defined in TEMA; and $w = 0.5\ (D_T - G)$.

For each pressure loading, the calculation procedure is as follows:

1. Compute M^* from Eq. 91, assuming $T_f = T$ (rim and interior tube-sheet thickness equal).
2. Assume $P = p_s$ or p_t or maximum differential pressure, as applicable.
3. Compute the required tube-sheet rim thickness T_f from Eq. 90 If $T > T_f$ and both are set equal to the computed T, then the calculation may be terminated at this point.
4. If it is desired to reduce the rim thickness below T, the value of T_f arrived at in step 3 is used to calculate a new M^* in Eq. 91. Next, the calculation returns to step 2.

3.7 Rectangular Tube-Sheet Design

The rectangular tube sheet of a surface condenser is designed as per HEI Standards [4]. The basis of the rectangular tube-sheet design as per HEI standards is discussed by Bernstein et al. [78].

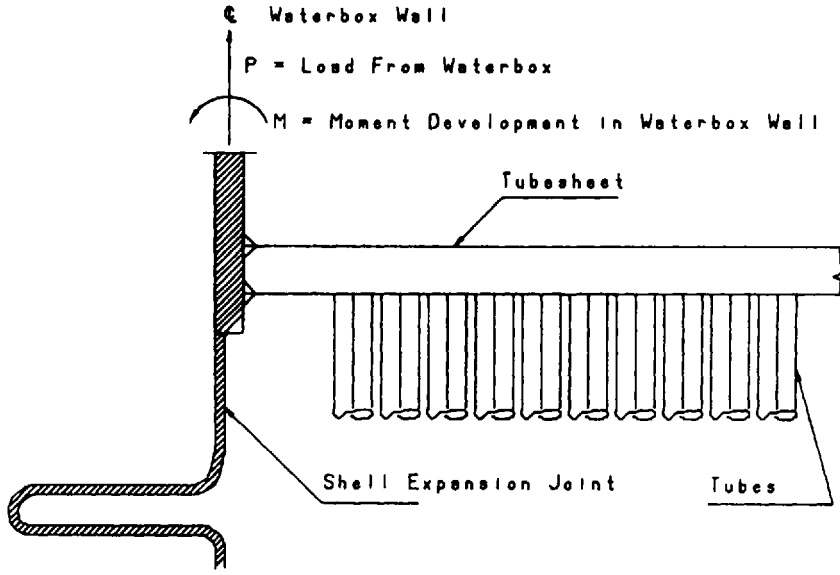


Figure 8 Surface condenser tubesheet connection with waterbox and the shell. (From Ref. 78.)

Methods of Tube-Sheet Analysis

Figure 8 shows the plan section of a surface condenser waterbox and shell end assembly with an expansion joint. Figure 9 shows an idealized representation of the tube sheet and the tube bundle. A condenser tube sheet is seen to be a partially perforated plate on an elastic foundation, with the tubes comprising the foundation. The hydrostatic pull from the water box and surface pressure on the tube sheets are the dominant loads. Irregular tube patterns and variations in edge boundary conditions make solutions of the plate problem difficult. The HEI Standards mention the following four methods by which the structural integrity of the tubesheet and tubes may be demonstrated [78]:

1. Interaction analysis using plate and shell formulas
2. Experimental modeling techniques, or prior services
3. Finite-element analysis (elastic or elastic–plastic)

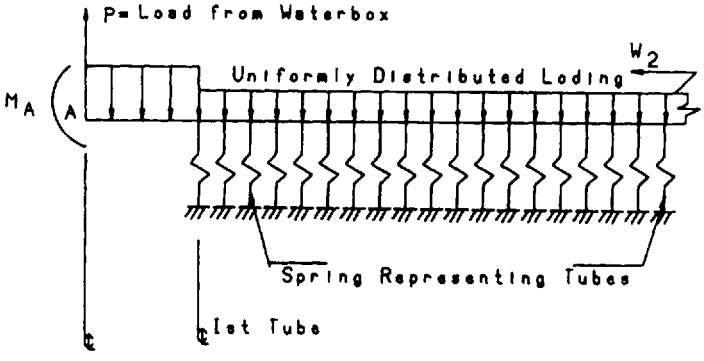


Figure 9 Rectangular tubesheet modelling. (From Ref. 78.)

4. Beam strip on elastic foundation (single or multiple strips)

Of these four methods, the basis of the beam strip method is discussed next.

Beam Strip Method. In the beam strip method, the problem of an elastically restrained perforated rectangular plate on an irregular elastic foundation is replaced by several more readily solved beams on an elastic foundation as shown in Fig. 10. The beams represent narrow strips of tube sheets supported by tubes, loaded by hydrostatic pressure and waterbox pull. The loading on each beam strip must be estimated, taking into account forces and moments acting on the waterbox and the type of end fixity.

The standard explains the steps in the beam strip method, with an example. Briefly, these steps cover the choice of the beam strip models (width, length, reduced stiffness of perforated zones), the loading to be applied, and an estimate of the edge restraint against rotation provided to the beam strip by the water box flange.

The notable features of HEI Standards on tubesheet design include features such as consideration of pressure surges, pump shutoff, head circulating water system characteristics, adequate means for provision of expansion, etc. Allowable stress and loads are to be chosen similar to the design-by-analysis approach of Appendix 4 in the ASME Code, Section VIII, Div. 2.

3.8 Curved Tube Sheets

Traditionally, heat exchangers use thick flat tube sheets. The problem of replacing thick flat tube sheets by thinner curved tube sheets was suggested first by Rachkov and Morozov [79]. They designed a much thinner semi-ellipsoidal curved tube sheet based on membrane theory of shells. The design of shallow spherical curved tube sheets for heat exchangers is discussed by Paliwal et al. [80]. Similar to a flat tube sheet treated as a thin flat plate on an elastic foundation, the curved tube sheet model uses the theory of a thin elastic shallow spherical shell on an elastic foundation, and replaces the curved plate by an equivalent plate having effective elastic constants; the nominal bending and membrane stresses and deflections are determined. A curved tube-sheet exchanger is shown in Fig. 11. So far, no code or standard has included curved tube-sheet design.

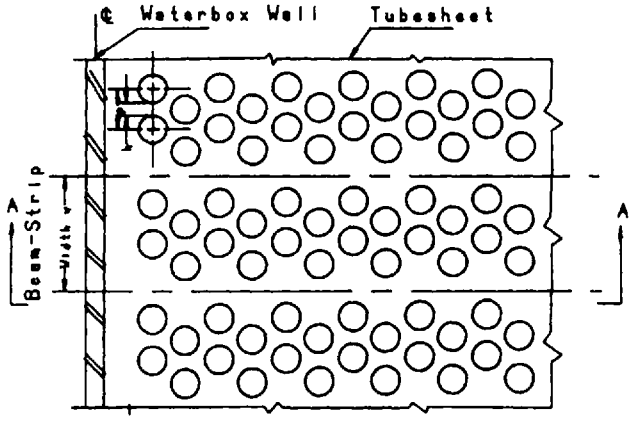


Figure 10 Beam strip for rectangular tubesheet design. (From Ref. 78.)

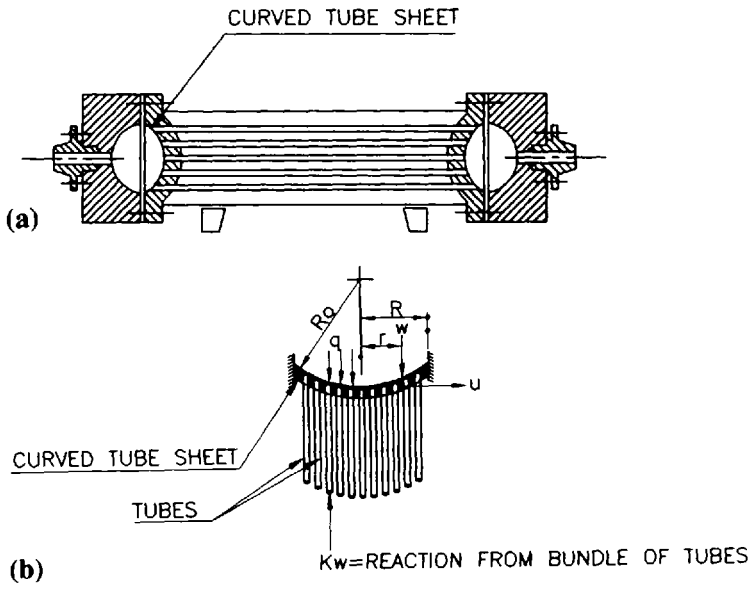


Figure 11 Curved tubesheet exchanger. (From Ref. 80.)

Advantages of Curved Tube Sheets

As compared with thick flat tube sheets, elliptical tube sheets have many advantages [81]:

1. Material savings due to thin tube sheet.
2. Because the sheet is thin, the thermal stresses developed in the tube sheet will be less.
3. Because the elliptical tube sheets are perforated elliptical shells, their stress levels will be far lower than those of flat tube sheets of the same thickness under the same operating conditions.
4. The deformation ability of a thin-wall shell is larger than that of flat plates, so the elliptical tube sheet can compensate for larger thermal deformations produced by temperature differences between the tube side and shell side.

3.9 Conventional Double Tube-Sheet Design (After Singh and Soler [41])

In a conventional double tube-sheet construction as shown in Fig. 12, in addition to the usual thermal loading, a new thermal condition arises due to in-plane differential thermal loading of

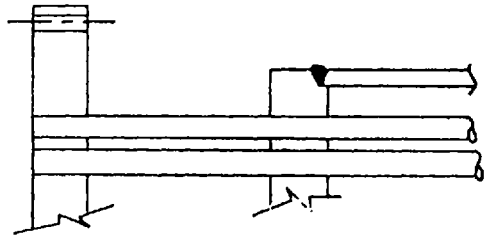


Figure 12 Conventional double tube sheet. (From Ref. 29.)

the two tube sheets. This differential radial expansion of the adjacent tube sheets may be caused by the two tube sheets having different coefficients of thermal expansion and/or differences in mean metal temperatures. The portion of tube bundle between the two tube sheets induces coupling between out-of-plane bending and direct radial expansion of the two tube sheets. Therefore, in contrast to the single tube-sheet analyses, any double tube-sheet analysis must encompass both tube-sheet bending and radial growth. These requirements make the solution procedure amenable to computer analysis only. Design of double tube sheets is discussed by Singh and Soler [41].

4 CYLINDRICAL SHELL, END CLOSURES, AND FORMED HEADS UNDER INTERNAL PRESSURE

The following symbols are used in the formulas required to calculate the minimum thickness of a cylindrical shell and various end closures.

t = minimum required thickness of shell or heads or end closures
P = internal design pressure, psi (see UG-21) (or maximum allowable working pressure, see UG-98)
C = a factor depending upon the method of attachment of head, shell dimensions, and other items as listed in ASME Code
D = inside length of the major axis of an ellipsoidal head; or inside diameter of a torispherical head; or inside diameter of a conical head at the point under consideration measured perpendicular to the longitudinal axis
D_o = outside length of the major axis of an ellipsoidal head; or outside diameter of a conical head at the point under consideration measured perpendicular to the longitudinal axis
d = dimension of the short span for flat heads
G = mean gasket diameter (not the effective gasket diameter as defined in the ASME Code)
h = maximum inside depth of the ellipsoidal head, exclusive of the flange
h_G = gasket moment arm (i.e., radial offset between the circle and bolt circle)
IDD = inside depth of torispherical head
K = factor in the formulas for ellipsoidal heads depending on the head proportion $D/2h$
L = inside spherical radius or crown radius
L_o = outside spherical radius or crown radius
M = factor in the formulas for torispherical heads depending on the head proportion L/r
P = internal design pressure
R = inside radius of the shell course under consideration
R_o = outside radius of the shell course under consideration
r = inside knuckle radius
S = maximum allowable stress value, psi (see UG-23 and the stress limitations specified in UG-24)
E = joint efficiency, or the efficiency of appropriate joint in cylindrical or spherical shells, or the efficiency of ligaments between openings, whichever is less (in decimal form)
W = total bolt load
α = one-half of the included (apex) angle of the cone at the center line of the head

4.1 Cylindrical Shell Under Internal Pressure

Design of cylindrical shell is carried out as per UG-27 or UG-29 of the ASME Code. The design formulas in the code are based on equating the maximum membrane stress to the allowable stress corrected for weld joint efficiency. As per ASME Code procedure, the thick-

Table 8 ASME Code Formulas for Minimum Thickness of Thin Cylindrical Shell to Withstand Internal Pressure [16]

Member	Thickness, t	Maximum internal pressure, P	Limitation
Longitudinal joints	$t = \dfrac{PR}{SE - 0.6P}$	$P = \dfrac{SEt}{R + 0.6t}$	$P \le 0.385SE$ $t \le 0.5R$
Circumferential joints[a]	$t = \dfrac{PR}{2SE + 0.4P}$	$P = \dfrac{2SEt}{R - 0.4t}$	$P \le 1.25SE$ $t \le 0.5R$
In terms of outside radius R_o	$t = \dfrac{PR_o}{SE + 0.4P}$	$P = \dfrac{SEt}{R_o - 0.4t}$	$P \le 0.385SE$ $t \le 0.5R$

[a]Formulas based on stress across circumferential joint will govern only if circumferential joint (Category B) efficiency is less than one-half the longitudinal joint efficiency.

ness of shells under internal pressure shall not be less than that computed by the following formulas. In addition, provision shall be made for any of the other loadings listed in UG-22, when such loadings are expected (see UG-16).

Thin Cylindrical Shells

The minimum thickness or maximum allowable working pressure of cylindrical shell shall be the greater thickness or lesser pressure as given by Eq. 92 and 93.

Circumferential Stress (Longitudinal Joints). When the thickness does not exceed one-half of the inside radius, or P does not exceed $0.385SE$, the following formulas shall apply:

$$t = \frac{PR}{SE - 0.6P} \quad \text{or} \quad P = \frac{SEt}{R + 0.6t} \tag{92}$$

Longitudinal Stress (Circumferential Joints). When the thickness does not exceed one-half of the inside radius, or P does not exceed $1.25SE$, the following formulas shall apply:

$$t = \frac{PR}{2SE + 0.4P} \quad \text{or} \quad P = \frac{2SEt}{R - 0.4t} \tag{93}$$

These formulas are presented in Table 8 along with the formulas based on shell outside dimension; Table 9 gives formulas for thick cylindrical shells.

Design for External Pressure and/or Internal Vacuum

There is no straightforward formula as in the case for the design under internal pressure, because buckling has to be taken into account. The procedure to be followed is given in the ASME Code Section VIII, Div. 1, Paragraph UG-28, and requires the use of various charts given in Appendix 5.

4.2 End Closures and Formed Heads

End closures for heat exchangers and pressure vessels are in the form of either flat covers or formed heads. ASME Code Section VIII, Div. 1, recognizes the following end closures:

1. Flat cover
2. Hemispherical cover
3. Ellipsoidal cover

Table 9 ASME Code Formulas for Minimum Thickness of Thick Cylindrical Shells to Withstand Internal Pressure [16]

Member	Thickness, t	Maximum internal pressure, P	Limitation
Longitudinal joint	$t = R(\sqrt{z} - 1) = R_o \dfrac{(\sqrt{z} - 1)}{\sqrt{z}}$ where $z = \dfrac{SE + P}{SE - P}$	$P = SE \dfrac{(z_1 - 1)}{(z_1 + 1)}$ where $z_1 = \left(\dfrac{R + t}{R}\right)^2 = \dfrac{R_o^2}{(R_o - t)^2}$	$P > 0.385SE$ $t > 0.5R$
Circumferential joint[a]	$t = R(\sqrt{z_2} - 1) = R_o \dfrac{(\sqrt{z_2} - 1)}{\sqrt{z_2}}$ where $z_2 = \left(\dfrac{P}{SE} + 1\right)$	$P = SE(z_1 - 1)$ where z_1 is as defined earlier	$P > 1.25SE$ $t > 0.5R$

[a]Formulas based on stress across circumferential joint will govern only if circumferential joint (Category B) efficiency is less than one-half the longitudinal joint efficiency.

4. Torispherical cover (flanged and dished)
5. Conical/toriconical cover

These end closures are shown schematically in Fig. 13. TEMA designates the front and rear covers by B and M, respectively. Closures other than flat heads are normally formed type; sometimes for low-pressure application cast heads are also used. Closures are designed as per UG-32 or UA-4 of the ASME Code. First a brief description of various end closures is presented, and then the determination of minimum thickness to retain internal pressure is presented.

Flat Cover

Flat covers are easy to fabricate in any thickness from plates or forgings. They are widely used from low to high pressure applications. Since a flat cover resists pressure load only by bending, its thickness is significantly greater than that of the cylindrical section to which these are attached as a closure.

Hemispherical

Hemispherical heads are used for high-pressure service since their thickness is about half that of a cylindrical shell. The degree of forming and accompanying costs are greater than any other heads and the available sizes from single plates are limited [44].

Ellipsoidal

These are widely used for low- to intermediate-pressure services. When the minor-to-major axis ratio is 0.5 (most common), the head thickness is almost the same as that of the cylindrical shell. This simplifies the joining of these two and minimizes the discontinuity stresses at the joint. Another popular ellipsoidal head is with minor axis 25% of D.

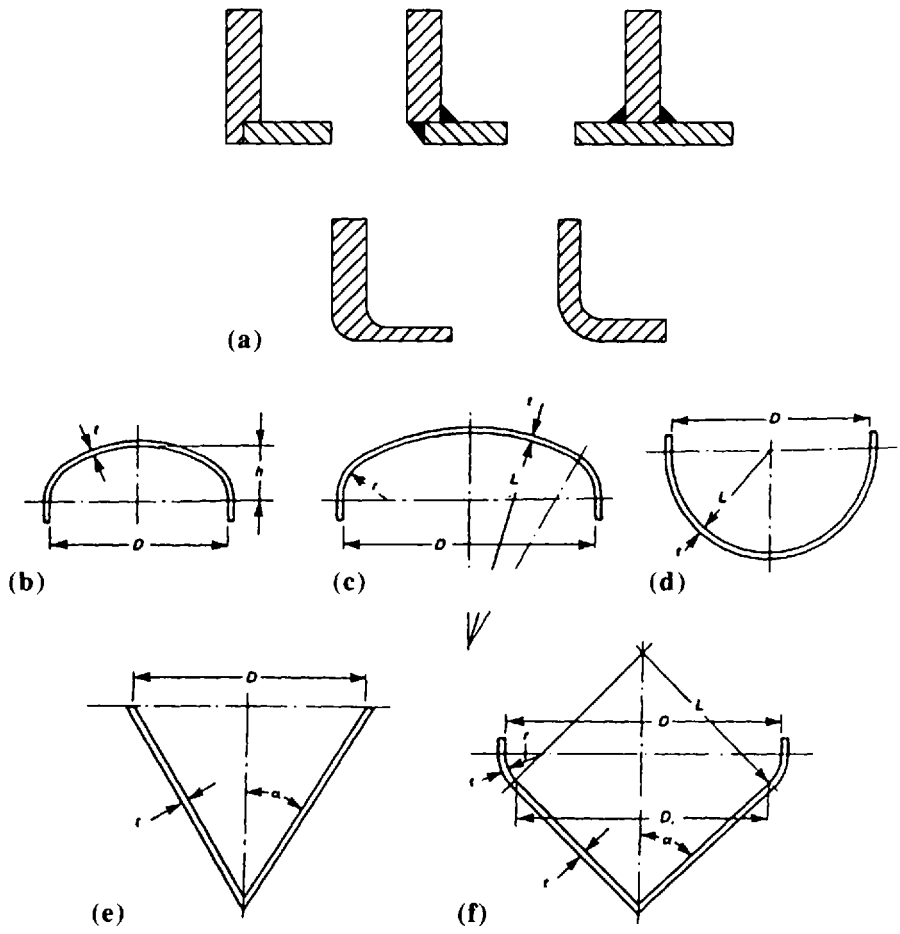


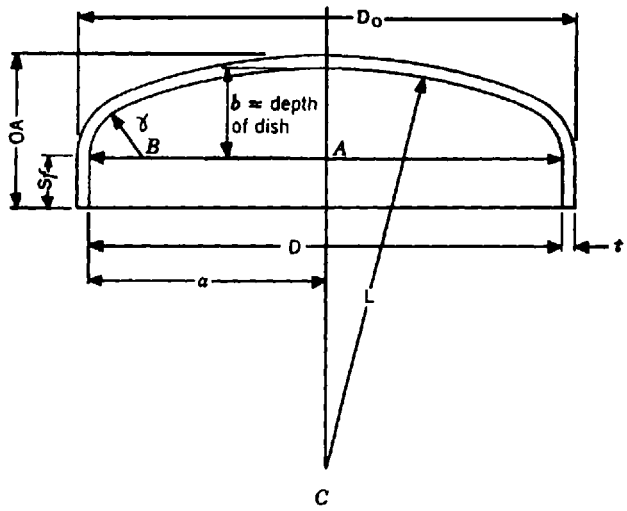
Figure 13 ASME CODE end closures. (a) Flat head (a partial list); (b) ellipsoidal head; (c) torispherical head; (d) hemispherical head; (e) conical head; and (f) toriconical head. (From Ref. 16.)

Torispherical

Among the various types of formed heads, the torispherical head is the most widely used in the industries, particularly for low-pressure service, i.e., up to 200 psi [50]. For pressures over 200 psi gage, ellipsoidal heads are used. The torispherical head is characterized by four geometric parameters: inside head diameter D, crown radius L, knuckle radius r, and head thickness t. Figure 14 shows the details of the torispherical head geometry. In Fig. 14, the depth of dish b is a geometric function of crown radius L and knuckle radius r and the straight cylindrical flange is integral with the dished end. By varying the ratios of L/D and L/r, heads of different shapes can be manufactured. Heads wherein $L \approx D$, $L \approx 16\frac{2}{3}r$, and $r = 0.06D$ are referred to as ASME flanged and dished heads in the pressure vessel industry. Another popular variation is the 80 : 10 head where $L \approx 0.8D$ and $r = 0.1L$.

Conical

These are used for low- and intermediate-pressure service with the half apex angle generally not more than 30°. A knuckle portion is provided to minimize the discontinuity stresses where it joins the shell.



$a = \frac{D}{2}$; $b = L - \sqrt{(BC)^2 - (AB)^2}$; $AB = \frac{D}{2} - \gamma$; $BC = L - \gamma$; $AC = \sqrt{(BC)^2 - (AB)^2}$; and $OA = t + b + S_f$.

Figure 14 Dimensional details of flanged and dished head.

4.3 Minimum Thickness of Heads and Closures

The required thickness at the thinnest point after forming of ellipsoidal, torispherical, hemispherical, conical, and toriconical heads under an internal pressure shall be computed by the appropriate formulas in UG-16 of the ASME Code. In addition, provision shall be made for any of the other loadings given in UG-22. The head design formulas in the code are based on equating the maximum membrane stresses to the allowable stresses corrected for weld joint efficiency.

Flat Cover

1. As per UG-34, the minimum required thickness of flat head, cover, and blind flanges shall be calculated by the formula:

$$t = d\sqrt{\frac{CP}{SE}} \tag{94a}$$

2. The minimum required thickness of flat head, cover, and blind flange attached by bolts causing an edge moment is given by the formula:

$$t = d\left(\frac{CP}{SE} + \frac{1.9Wh_G}{SEd^3}\right)^{0.5} \tag{94b}$$

TEMA Standards. The TEMA Standards have a deflection-based formula that seeks to limit the maximum deflection, d, of the flat cover of a multitube pass unit to 0.030 in (0.762 mm) [50]. The resulting formula for flat cover thickness, t, in inches, is given by [50]:

$$t = \left[\frac{1.425G^4P}{E} + \frac{0.5h_G A_b G \times 10^6}{Ed_b^{1/2}} \right]^{1/3} \tag{95}$$

Ellipsoidal Heads

The thickness or the maximum allowable working pressure of a dished head of semi-ellipsoidal form, in which half the minor axis equals one-fourth of the inside diameter of the head skirt, shall be determined by

$$t = \frac{PD}{2SE - 0.2P} \quad \text{or} \quad P = \frac{2SEt}{D + 0.2t} \tag{96}$$

Torispherical Heads

The required thickness or the maximum allowable working pressure of a torispherical head for the case in which the knuckle radius is 6% of the inside radius and the inside crown radius equals the inside diameter of the skirt (i.e., $L \approx D$, $L_i \approx 16\frac{2}{3}r$, and $r = 0.06D$) shall be determined by

$$t = \frac{0.885PL}{SE - 0.1P} \quad \text{or} \quad P = \frac{SEt}{0.885L + 0.1t} \tag{97}$$

Hemispherical Heads

When the thickness or the maximum allowable working pressure of a hemispherical head does not exceed $0.356L$, or the internal pressure P does not exceed $0.665SE$, the required thickness or the maximum allowable working pressure of a hemispherical head is given by

$$t = \frac{PL}{2SE - 0.2P} \quad \text{or} \quad P = \frac{2SEt}{L + 0.2t} \tag{98}$$

Conical Heads and Sections (without Transition Knuckle)

The required thickness of conical heads or conical shell sections that have a half apex angle α not greater than 30° shall be determined by

$$t = \frac{PD}{2(\cos\alpha)(SE - 0.6P)} \quad \text{or} \quad P = \frac{2SEt(\cos\alpha)}{D + 1.2t(\cos\alpha)} \tag{99}$$

These formulas and formulas for minimum head thickness referred to outside head dimension are given in Table 10.

4.4 Comparison of Various Heads

1. Compared to a flat cover, which resists pressure load only by bending, a formed head resists pressure by developing membrane stress, and hence the thickness of formed heads will be less than the flat cover [50].
2. The formed head has the drawback of thinning out in areas of sharp curvature and thickening in adjacent regions of moderate curvature. Such a variation is more pronounced in spun heads, and more particularly in hot-formed heads than in cold-formed heads.
3. As far as the cost is concerned, the head that is the lowest in cost and meets the code requirements should be designed. The ellipsoidal and hemispherical heads have the least weight per unit volume.
4. Salient features of fabrication of various heads are discussed in Chapter 15, Heat Exchanger Fabrication.

Table 10 ASME Code Formulas for Minimum Thickness of Heads/End Closures to Withstand Internal Pressure [16]

Heads	Minimum thickness, t	Maximum pressure, p
Ellipsoidal	$t = \dfrac{PD}{2SE - 0.2P}$	$P = \dfrac{2SEt}{D + 0.2t}$
	$t = \dfrac{PDK}{2SE - 0.2P}$	$P = \dfrac{2SEt}{KD + 0.2t}$
	$t = \dfrac{PD_oK}{2SE + 2P(K - 0.1)}$	$P = \dfrac{2SEt}{KD_o - 2t(K - 0.1)}$
		where $K = \dfrac{1}{6}\left[2 + \left(\dfrac{D}{2h}\right)^2\right]$
Torispherical	$t = \dfrac{0.885PL}{SE - 0.1P}$	$P = \dfrac{SEt}{0.885L + 0.1t}$
	$t = \dfrac{PLM}{2SE - 0.2P}$	$P = \dfrac{2SEt}{LM + 0.2t}$
	$t = \dfrac{PL_oM}{2SE + P(M - 0.2)}$	$P = \dfrac{2SEt}{ML_o - t(M - 0.2)}$
		where $M = \dfrac{1}{4}\left[3 + \left(\dfrac{L}{r}\right)^{0.5}\right]$
Hemispherical	$t = \dfrac{PL}{2SE - 0.2P}$	$P = \dfrac{2SEt}{L + 0.2t}$
Conical	$t = \dfrac{PD}{2(\cos\alpha)\,(SE - 0.6P)}$	$p = \dfrac{2SEt(\cos\alpha)}{D_o + 1.2t(\cos\alpha)}$
	$t = \dfrac{PD_o}{2(\cos\alpha)(SE + 0.4P)}$	$P = \dfrac{2SEt(\cos\alpha)}{D_o - 0.8t(\cos\alpha)}$

5 BOLTED FLANGED JOINT DESIGN

5.1 Construction and Design

Flanges are often employed to connect two sections by bolting them together so that the sections can be assembled and disassembled easily. In heat exchangers, the flange joints are used to connect together the following components:

1. Channel and channel cover
2. Heads or channels with the shell/tube sheets
3. Inlet and outlet nozzles with the pipes carrying the fluids
4. To close various openings such as manholes, peepholes, and their cover plates

The flanged joints play an important role from the standpoint of integrity and reliability of heat exchangers. Improper design of flanges causes leakage of heat exchanger fluids. Therefore, preventing the liquid or gas leaks is one of the most important considerations while designing flanged joints.

Flanged Joint Types

From a conceptual standpoint, flanged joints may be subdivided into two major categories [41]:

1. Bolted joints
2. Pressure-actuated or self-energizing joints

The bolted joint is by far the most common type. The basic difference between these two joint types lies in the manner by which the pressure load is resisted and leak tightness is achieved. A bolted joint essentially consists of a gasket interposed between two structural members called flanges, which in turn are connected to other structural members like cylindrical shells or pipes, and a set of bolts for joining together the two flanges. To make the joint, the gasket is compressed to a desired value by prestressing the bolts. Pressure-actuated joints exploit the header pressure force to compress and to seal the gasket. Pressure-actuated joints find application in the higher pressure range, typically over 2000 psi [41].

Constructional Details of Bolted Flange Joints

Types of Bolted Flanges. Based on the width of gasket, flange joints are classified as (1) ring type gasket joint and (2) full-face gasket joint. For very-low-pressure applications (100–300 psi), wide gaskets that span the entire flange face may be used. This construction is known as "full-face gasket" design. A design method for flanges utilizing full-face gaskets is presented in ref 41. In general, for high-pressure and medium- to high-pressure applications, only ring type gaskets are used. Sometimes even for low-pressure applications ring type gaskets are used. Based on constructional details, flanged joints are classified as

1. Ring flange
2. Weld neck integral flange or tapered hub flange
3. Lap joint flange
4. Reverse flange

Ring Flange. The ring flange consists of an annular circular plate welded to the end of the cylindrical shell. A number of equidistant bolt holes are drilled on a uniform pitch circle, and the gasket is confined inside the bolt circle. This joint is utilized in low- to moderate-pressure applications. A ring type gasket joint is shown schematically in Fig. 15a.

Weld Neck Integral Flange. The weld neck flange or a tapered hub flange, as shown in Fig. 15b, may be viewed as a structural member consisting of an annular ring and a tapered hub butt welded to the cylindrical shell. This flange has the best characteristics for preventing failure from fatigue and thermal stresses. These flanges have been used at pressures as high as 5000 psi, although the flange becomes massive and heavy as pressure and diameter increase.

Lap Joint Flange. The lap joint flange, shown in Fig. 15c, finds use in low-pressure applications where economy of construction is an important consideration. The backing ring can be made from low-cost but strong structural material (e.g., carbon steel), whereas the "lap ring" may be made from expensive corrosion-resistant material. Furthermore, this flange design facilitates alignment of bolt holes in matching rings in opposing pipe ends. In outside packed floating head heat exchangers, the flange at the rear end is of the lap joint type.

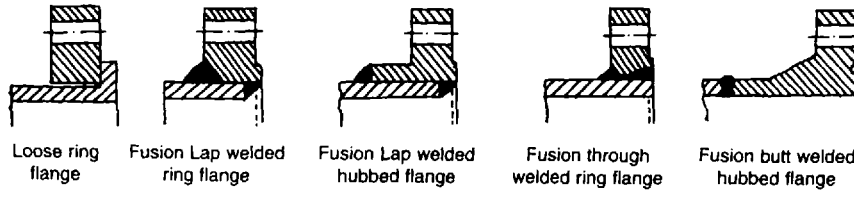


Figure 15 Flange joint construction.

Design of Bolted Flange Joints

The objectives in flange design are to ensure that the residual gasket stress levels and the pressure induced in the flange during bolt preload, as well as under operating conditions, do not exceed allowable stress values in the structural members.

The earliest treatment of the problem of flange design to receive widespread recognition was that of Waters et al. [82], which gave the general basis for the design rules in the ASME Code. Design of flanged joints with ring type gaskets is carried out as per Appendix 2 of ASME Code Section VIII, Div. 1. Appendix S of the Code gives general guidelines for bolting requirements of flanges. The Code method for design of integral type flange and ring flange is briefly described here. Unless otherwise mentioned, the mention of ASME Code throughout this book refers to ASME Code Section VIII, Div. 1 (1992 edition) only [16].

ASME Code Classification of Circular Flanges for Design Purposes. For computation purposes, ASME Code Section VIII, Div. 1, classifies circular flanges with ring type gaskets as

1. Loose type flanges
2. Integral type flanges
3. Optional type flanges
4. Flanges with nut stop
5. Reverse flanges

Salient constructional details, design features, and step-by-step design procedures of various flanged joint types except flanges with nut stop and reverse flanges are described in the following sections.

Loose Type Flanges. This type covers those designs in which the flange has no direct connection to the nozzle neck, vessel, or pipe wall, and designs where the method of attachment is not considered to give the mechanical strength equivalent of integral attachment. Figures 1 to 4a of the ASME Code conform to loose type flanges [16].

Integral Type Flanges. This type covers those designs in which the flange is cast or forged integrally with the nozzle neck, vessel, or pipe wall, butt welded thereto, or attached by other forms of arc or gas welding of such a nature that the flange and nozzle neck and vessel or pipe wall are considered to be the equivalent of an integral structure. Figures 5 to 7 of the ASME Code [16] conform to integral type flanges.

Optional Type Flanges. This type covers those designs in which the attachment of the flange to the nozzle neck, vessel, or pipe wall is considered to act as a unit, which shall be calculated as an integral flange, except that for simplicity the designer may calculate the construction as a loose type flange provided none of the values given in the ASME Code are exceeded. Figures 12 and 12a of the ASME Code [16] conform to optional type flanges.

Design Procedure. The integrity and reliability of a bolted flanged joint depend to a large extent upon the correct choice of materials, dimensions, and loads on the gasket. The flange design procedure can be summarized as three separate elements:

1. Gasket design
2. Bolting design
3. Flange design

To start with, materials of construction of flange, bolting and gasket, and gasket properties are chosen. Flange inner diameter and shell thickness to which the flange is to be welded are also known. A rough guess of the various dimensions of the flange is made, taking into account the permissible hub slope, and minimum hub length in the case of weld neck flange, and bolting dimensional requirements. Suitable gasket outer diameter and width are also chosen,

keeping the minimum width requirements. Flange dimensions shall be such that the calculated stresses in the flange shall not exceed code stress values. In the following paragraphs, the detailed design procedures of the three elements of flange design are described.

Gasket Design.

Gaskets and Their Characteristics. A leak-proof joint with metal-to-metal surfaces without a gasket is difficult to achieve even with use of accurately machined fine finish surfaces. Surface irregularities only a few millionths of an inch will permit the escape of a fluid under pressure [44]. Being a semiplastic material, the gasket deforms under load, which in turn seals the minute surface irregularities and prevents leakage of the fluid.

Selection of Gasket Material. A gasket is essentially an elastoplastic material that is softer than the flange faces. In the gasket seating condition the entire bolt load is borne by the gasket. Hence, the gasket must be strong enough to withstand load due to bolting and operating conditions without crushing or extruding out. Therefore, soft materials like asbestos and organic fibers are precluded for high-pressure applications. Also, the gasket material shall withstand the operating temperature and exhibit corrosion resistance to the fluid contained in the pressure vessel [83].

Gasket Materials. Gaskets are made out of a myriad variety of materials. Good references are available from many gasket manufacturers for the selection of proper gaskets for the intended applications. Table 2-5.1 of the ASME Code gives a list of many commonly used gasket materials (see Table 11). This is a partial list of gasket materials included in Table 2-5.1 of the ASME Code [16]:

Elastomers without fabric or high percentage of asbestos fiber
Asbestos with suitable binder
Elastomers with cotton fabric insertion
Elastomers with asbestos fabric insertion
Spiral-wound asbestos-filled metal
Corrugated metal with asbestos fill
Corrugated metal
Flat metal, jacketed asbestos fill
Grooved metal
Solid flat metal

The choice of the gasket material is often based upon the required gasket width. If the gasket is made too narrow, the unit pressure on it may be excessive, whereas if the gasket is made too wide, the bolt load will be unnecessarily high [44].

Gasket Factors. The basic behavior of the gasket is defined by the gasket factor m and gasket or joint contact surface unit seating load y, which are tabulated in the ASME Code, Section VIII, Div. 1.

Gasket Factor, m. This is the ratio of the residual stress on the gasket under operating pressure to that pressure. In other words, m = (bolt load − hydrostatic end load)/(gasket area × internal pressure).

Gasket or Joint Contact Surface Unit Seating Load, y. This is the stress required to make the gasket surface take up the shape of the flange faces, or the gasket stress required to contain zero internal pressure. The factor y is usually expressed as a unit stress in pounds per square inch and is independent of the pressure in the vessel. Table 2-5.1 of the ASME Code gives suggested design values of gasket factor m and minimum design seating stress y.

Table 11 ASME Code List of Gasket Materials [16]

Gasket Material	Gasket Factor *m*	Min. Design Seating Stress *y*, psi	Sketches	Facing Sketch and Column in Table 2-5.2
Self-energizing types (O rings, metallic, elastomer, other gasket types considered as self-sealing)	0	0	. . .	. . .
Elastomers without fabric or high percent of asbestos fiber:				
Below 75A Shore Durometer	0.50	0		(1a),(1b),(1c),(1d), (4),(5); Column II
75A or higher Shore Durometer	1.00	200		
Asbestos with suitable binder for operating conditions:				
1/8 in. thick	2.00	1600		(1a),(1b),(1c),(1d), (4),(5); Column II
1/16 in. thick	2.75	3700		
1/32 in. thick	3.50	6500		
Elastomers with cotton fabric insertion	1.25	400		(1a),(1b),(1c),(1d), (4),(5); Column II
Elastomers with asbestos fabric insertion (with or without wire reinforcement):				
3-ply	2.25	2200		(1a),(1b),(1c),(1d), (4),(5); Column II
2-ply	2.50	2900		
1-ply	2.75	3700		
Vegetable fiber	1.75	1100		(1a),(1b),(1c),(1d), (4),(5); Column II
Spiral-wound metal, asbestos filled:				
Carbon	2.50	10,000		(1a),(1b); Column II
Stainless, Monel, and nickel-base alloys	3.00	10,000		
Corrugated metal, asbestos inserted, or corrugated metal, jacketed asbestos filled:				
Soft aluminum	2.50	2900		(1a),(1b); Column II
Soft copper or brass	2.75	3700		
Iron or soft steel	3.00	4500		
Monel or 4%–6% chrome	3.25	5500		
Stainless steels and nickel-base alloys	3.50	6500		

(*continued*)

Table 11 Continued

Gasket Material	Gasket Factor *m*	Min. Design Seating Stress *y*, psi	Sketches	Facing Sketch and Column in Table 2-5.2
Corrugated metal:				
Soft aluminum	2.75	3700		(1a),(1b),(1c),(1d); Column II
Soft copper or brass	3.00	4500		
Iron or soft steel	3.25	5500		
Monel or 4%–6% chrome	3.50	6500		
Stainless steels and nickel-base alloys	3.75	7600		
Flat metal, jacketed asbestos filled:				
Soft aluminum	3.25	5500		(1a),(1b),(1c),[2] (1d);[2](2)[2]; Column II
Soft copper or brass	3.50	6500		
Iron or soft steel	3.75	7600		
Monel	3.50	8000		
4–6% chrome	3.75	9000		
Stainless steels and nickel-base alloys	3.75	9000		
Grooved metal:				
Soft aluminum	3.25	5500		(1a),(1b),(1c),(1d), (2),(3); Column II
Soft copper or brass	3.50	6500		
Iron or soft steel	3.75	7600		
Monel or 4%–6% chrome	3.75	9000		
Stainless steels and nickel-base alloys	4.25	10,100		
Solid flat metal:				
Soft aluminum	4.00	8800		(1a),(1b),(1c),(1d), (2),(3),(4),(5); Column I
Soft copper or brass	4.75	13,000		
Iron or soft steel	5.50	18,000		
Monel or 4%–6% chrome	6.00	21,800		
Stainless steels and nickel-base alloys	6.50	26,000		
Ring joint:				
Iron or soft steel	5.50	18,000		(6); Column I
Monel or 4%–6% chrome	6.00	21,800		
Stainless steels and nickel-base alloys	6.50	26,000		

NOTES:
(1) This Table gives a list of many commonly used gasket materials and contact facings with suggested design values of *m* and *y* that have generally proved satisfactory in actual service when using effective gasket seating width *b* given in Table 2-5.2. The design values and other details given in this Table are suggested only and are not mandatory.
(2) The surface of a gasket having a lap should not be against the nubbin.

Gasket Dimensions. A relationship for making a preliminary estimate of the proportions of the gasket may be derived as follows [41]:

Residual gasket force = gasket seating force – hydrostatic pressure force

The residual gasket force cannot be less than that required to prevent leakage of the internal fluid under operating pressure. This condition results in the following expression:

$$\frac{d_o}{d_i} = \sqrt{\frac{y - pm}{y - p(m + 1)}} \tag{100}$$

where d_o is the gasket outside diameter, m is the gasket factor, and y the minimum design seating stress.

The inside diameter of the gasket (in inches) is normally as follows:

$$d_i = B + 0.01$$

where B equals the shell inside diameter for weld neck flange and shell outside diameter for ring flange.

Gasket Width and Diametral Location of Gasket Load Reaction. The steps involved in arriving at the gasket width and diametral location of gasket load reaction are as follows:

1. Calculate the gasket width, N, given by

$$N = (d_o - d_i)/2 \tag{101}$$

2. Select the gasket width such that it is not less than the minimum specified width of the gasket as specified in Table 2-5.2 of the ASME Code and reproduced in Table 12.
3. Calculate the basic gasket width, b_o, given by Table 2-5.2 of the ASME Code.

Bolting Design. With the size and shape of the gasket established, next determine the bolting required. The bolting should be designed to maintain the required compression on the gasket with the internal pressure acting. Various design aspects of bolting are discussed next.

Determination of Bolt Loads. The bolt loads, W, required under the following conditions could be considered:

1. Gasket seating condition in the absence of internal pressure
2. Operating conditions

The thickness of flanges shall be determined as the greater required either by the operating or by the bolting up conditions, and in all cases both conditions shall be calculated in accordance with the following.

Gasket Seating Conditions. The gasket seating conditions are the conditions existing when the gasket or joint contact surface is seated by applying an initial load on the bolts when assembling the joint, at atmospheric pressure and temperature. The minimum initial load considered to be adequate for proper gasket seating is a function of the gasket material and the effective or contact area to be seated. The minimum initial bolt load required for this purpose, W_{m2}, shall be determined using the following formula

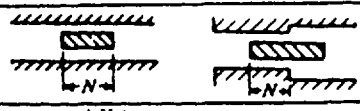
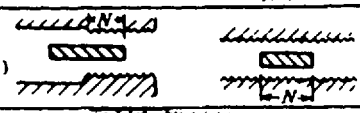
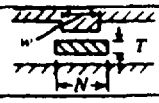
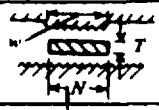
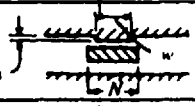
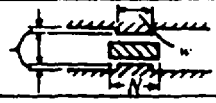
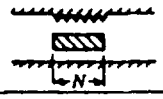
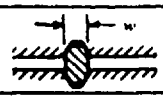
$$W_{m2} = \pi b G y \tag{102}$$

The need for providing sufficient bolt load to seat the gasket or joint contact surfaces in accordance with this formula will prevail on many low-pressure designs and with facings and materials that require a high seating load, and the bolt load calculated for operating conditions is not sufficient to seat the joint. When formula 102 governs, flange dimensions will be a function of the bolting instead of internal pressure.

As per Code formulas, for flange pairs used to contain a tube sheet (both sides gasketed) for a floating head or a U-tube type of heat exchanger, or for any other similar design, and where the flanges and/or gaskets are not the same, W_{m2} shall be the larger of the values obtained from formula 102 as individually calculated for each flange and gasket, and that value shall be used for both flanges.

Operating Conditions. The operating conditions are the conditions required to resist the hydrostatic end force (H) of the design pressure, which tends to part the joint and to maintain on the gasket or joint contact surface sufficient compression force (H_p) to assure a tight joint at all operating conditions. The minimum load is a function of the design pressure, the gasket

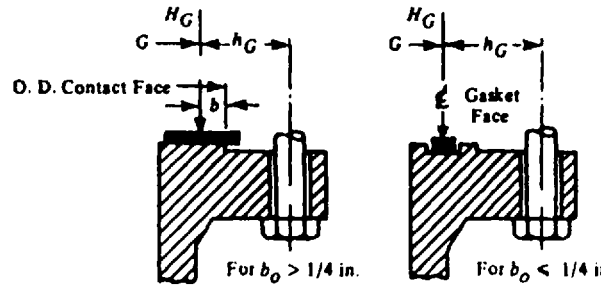
Table 12 Effective Gasket Width

Facing Sketch (Exaggerated)	Basic Gasket Seating Width, b_o Column I	Basic Gasket Seating Width, b_o Column II
(1a) 	$\frac{N}{2}$	$\frac{N}{2}$
(1b) See Note (1) 		
(1c)  $w \le N$	$\frac{w+T}{2}; \left(\frac{w+N}{4}\text{ max.}\right)$	$\frac{w+T}{2}; \left(\frac{w+N}{4}\text{ max.}\right)$
(1d) See Note (1)  $w \le N$		
(2) 1/64 in. Nubbin  $w \le N/2$	$\frac{w+N}{4}$	$\frac{w+3N}{8}$
(3) 1/64 in. Nubbin  $w \le N/2$	$\frac{N}{4}$	$\frac{3N}{8}$
(4) See Note (1) 	$\frac{3N}{8}$	$\frac{7N}{16}$
(5) See Note (1) 	$\frac{N}{4}$	$\frac{3N}{8}$
(6) 	$\frac{w}{8}$	...

Effective Gasket Seating Width, b

$b = b_o$ when $b_o \le \frac{1}{4}$ in.; $b = 0.5\sqrt{b_o}$ when $b_o > \frac{1}{4}$ in.

Location of Gasket Load Reaction



NOTES:

(1) Where serrations do not exceed 1/64 in. depth and 1/32 in. width spacing, sketches (1b) and (1d) shall be used.

(2) The gasket factors listed only apply to flanged joints in which the gasket is contained entirely within the inner edges of the bolt holes.

material, and the effective gasket area or the effective contact area to be kept tight under pressure. The required bolt load W_{m1} for the operating condition is given by

$$W_{m1} = H + H_p = \frac{\pi}{4} G^2 P + 2\pi b G m P \tag{103}$$

Various flange forces are shown schematically in Fig. 16 for the ring flange and weld neck integral flange [84].

Bolt Area at the Root of the Threads. The necessary bolt area at the root of the threads, A_m, required for both the gasket seating and operating conditions is the greater of the values W_{m1}/S_b and W_{m2}/S_a as given by the following expression:

$$A_m = \max | W_{m1}/S_b,\ W_{m2}/S_a | \tag{104}$$

From the required bolt area, determine the minimum number of bolts required (generally in multiples of 4) and observe the minimum sizes as recommended by TEMA, RCB-11. From the number of bolts chosen, find out the actual bolt area, A_b. In no case shall A_b be less than A_m. At this point the designer should sketch a tentative layout showing the desired location and size of gasket or contact surface, hub thickness, and diameter of bolts and bolt circle, and from these set the outside diameter of the flange.

Flange Bolt Load W. The bolt loads used in the flange design shall be the values obtained from these formulas:

1. For the gasket seating condition,

$$W = \frac{(A_m + A_b)\, S_a}{2} \tag{105}$$

2. For the operating condition,

$$W = W_{m1} \tag{106}$$

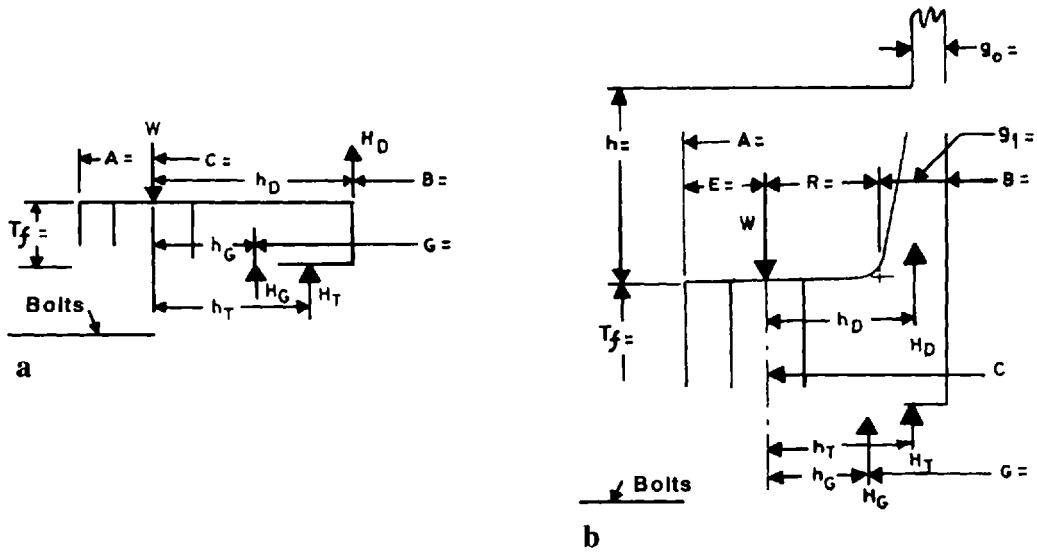


Figure 16 Dimensional data and flange forces. (a) Ring flange; and (b) weld neck flange. (From Ref. 84.)

Pitch Circle Diameter. In general the pitch circle diameter for each particular size of bolt considered should be kept small, to keep the flange bending moment and flange outside diameter small [85].

Minimum Bolt Size. Small bolts should be avoided wherever possible, owing to the case with which they may be over stressed by torsion applied with a wrench. Bolts, studs, nuts, and washers must meet the Code requirements. Appendix 2 of the Code recommends not using bolts and studs smaller than 0.5 in (12.7 mm). If bolts or studs smaller than 0.5 in (12.7 mm), alloy steel bolting material must be used. Precautions must be taken to avoid overstressing small-diameter bolts.

TEMA Standards give guidelines for minimum bolt size in RCB-11. The minimum bolt size is 0.75 in for *R*, 0.5 in for C, and 0.625 in for B class exchangers.

Minimum Recommended Bolt Spacing. Bolts should be spaced far enough apart to permit the clearance necessary for socket wrenches and to insure a uniform compression on the gasket. Likewise, the bolt circle on hubbed or integral flanges should have sufficient diameter to permit a generous fillet between the back of the flange and hub. Waters-Taylor recommends a bolt spacing of at least 2.25 times bolt diameters between centers to avoid high stress concentration.

In the TEMA guidelines, the minimum chordal pitch between adjacent bolts and minimum recommended wrench and nut clearances may be read from TEMA Table D-5.

Maximum Recommended Bolt Spacing. The bolt spacing should not be so great as to result in an appreciable reduction in gasket pressure between bolts. Waters-Taylor recommends a spacing of $3.5d$ (d is the nominal diameter of bolt) between bolt hole centers as a reasonable maximum. An empirical expression given by Taylor Forge and Pipe Works [84] expresses the maximum bolt pitch in the form

$$B_{max} = 2d + \frac{6T_f}{m + 0.5} \tag{107}$$

where B_{max} is the maximum bolt spacing for a tight joint (in), d the nominal bolt diameter (in), T_f the flange thickness (in), and m the gasket factor, which is obtained from ASME Code Table 2-5.1. This is included in TEMA, RCB-11.22.

Load Concentration Factor. As per TEMA RCB-11.23, when the distance between bolt centerlines exceeds the recommended B_{max}, the total flange moment determined shall be multiplied by a load concentration factor equal to [3]:

$$\sqrt{\frac{B}{B_{max}}} \tag{108}$$

where B is the centerline-to-centerline bolt spacing.

Note: To prevent over stressing of bolted flanged connections, the designer should, wherever possible, set the lengths of wrench to be used.

Relaxation of Bolt Stress at Elevated Temperature. A rise in temperature of a flanged joint causes the bolt and flange stresses to diminish, and on maintaining the joint at temperature, further reduction in stresses may occur due to creep as time elapses [85]. A multiphase PVRC elevated temperature program was initiated in 1982 by a task group of the PVRC Subcommittee on Gasket Testing Elevated Temperature Joint Behaviour, and the committee's report is published through WRC Bulletin 391 by Derenne et al. [86].

Flange Design. After the gasket and bolting design, next determine the flange dimensions required to withstand the bolt load without exceeding the allowable stress for the flange material. The outside diameter of the flange must be large enough to seat the bolt with manufactur-

ing tolerance. In addition to bolting data, some more details on flange dimensions can be read from TEMA Table D-5. Since the flange design procedure is iterative in the case of integral weld neck flange and slip-on flange, initially assume a flange thickness. In the case of the ring flange, a closed-form solution for flange thickness is possible. The next step is to determine the moment arm of the various forces and reactions.

Flange Moments. In the calculation of flange stress, the moment of a load acting on the flange is the product of the load and the moment arm.

Various forces acting during the operating condition are the hydrostatic end force on area inside of the flange, H_D, the pressure force on the flange face, H_T, and the gasket load under operating conditions, H_G:

$$H_D = \frac{\pi B^2 P}{4} \tag{109a}$$

$$H_T = H - H_D \tag{109b}$$

$$H_G = W - H \tag{109c}$$

where W is bolt load, W_{m1} or W_{m2}, whichever is greater. For the operating condition, the flange moment M_o is the sum of the three individual moments M_D, M_T, and M_G. Determine the moment arms h_D, h_T, and h_G for flange loads under operating conditions from Table 13 for the three types of flanges. Calculate M_D (moment due to H_D), M_T (moment due to H_T), and M_G (moment due to H_G) as given by

$$M_D = H_D h_D \tag{110a}$$

$$M_T = H_T h_T \tag{110b}$$

$$M_G = H_G h_G \tag{110c}$$

and

$$M_o = M_D + M_T + M_G \tag{111}$$

For the gasket seating condition, the total flange moment M'_o (ASME Code uses the term Mo for moment due to gasket seating condition also), which is opposed only by the gasket load W, is given by

$$M'_o = \frac{W(C - G)}{2} \tag{112}$$

Flange Thickness. For a ring flange, the flange thickness t_f required is the greater of the gasket seating condition or operating condition, given by

$$T_f = \max\left(\sqrt{\frac{M_o Y}{S_{fb} B}}, \sqrt{\frac{M'_o Y}{S_{fa} B}} \right) \tag{113}$$

where Y is the shape constant, defined in Section 5.2, Step 5.

Table 13 Moment Arms for Flange Loads Under Operating Conditions

Type of flange	h_D	h_T	h_G
Integral flange	$R + 0.5g_1$	$0.5(R + g_1 + h_G)$	$0.5(C - G)$
Loose or ring flange	$0.5(C - B)$	$0.5(h_D + h_G)$	$0.5(C - G)$
Lap flange	$0.5(C - B)$	$0.5(C - G)$	$0.5(C - G)$

For the weld neck integral flange, as mentioned earlier, flange thickness is calculated by iterative process until such time as the flange stress falls within allowable stress for the flange material. If not within the limit, increase the flange thickness and continue the steps mentioned earlier. The stresses induced in the flange shall be determined for both the operating condition and gasket seating condition, whichever controls. The procedure to determine flange stresses is listed in the step-by-step procedure given in the Appendix.

Flange Facings. The geometric details of the mating flange surfaces on which the gasket seats are known as flange facings. The ability of a flanged joint to maintain a leak-proof joint depends on a number of parameters, of which the gasket and flange facing details are the most important [41]. Flange facings are prepared to suit the gasket type, the kind of application, and the service conditions. Some of the classifications of the flange facings are:

1. Unconfined and prestressed: flat face and raised face (Fig. 15)
2. Semiconfined and prestressed (male and female joint) (Fig. 17a)

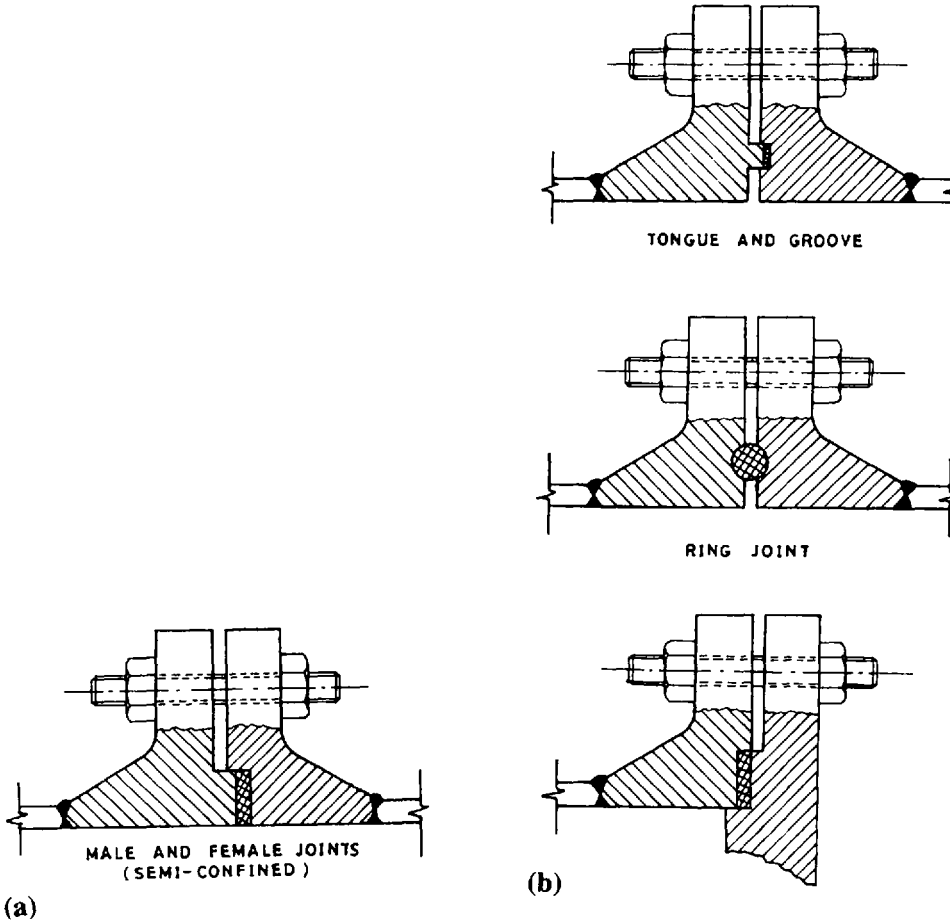


Figure 17 Flange facings. (a) Semiconfined and prestressed; and (b) confined and prestressed. (After Ref. 41.)

3. Confined and prestressed: tongue and groove, double step joint, ring joint (Fig. 17b)
4. Self-energizing: O-rings, metallic, elastomer, etc.

The applicability of various flange facings is discussed in refs. 41 and 44. Flat face and raised face are used for low-pressure applications; the male and female facings have the advantage of confining the gasket, thereby minimizing the possibility of blowout of gaskets. Since the mating flanges are nonidentical, male and female facings are widely used on heat exchangers and not on pipelines. Also, the tongue-and-groove type facings give protection against deforming soft gaskets into the interior of the vessel. Table 2-5.2 of the ASME Code gives a list of many commonly used contact facings.

Flange Facing Finish. The type and texture of surface finish are important for leak tightness of a flanged joint. There are five distinct styles of surface finish that are commonly used in the industry [41]: rounded nose spiral finish, spiral serrated finish, concentric serrated finish, smooth finish, and cold water finish.

Requirements for Flange Materials. The material used for flanges must meet the ASME Code general requirements for materials for pressure retaining parts. Some specific ASME Code Section VIII, Div. 1 (Appendix 2) requirements for flange materials include the following:

1. Flanges made from ferritic steel must be given a normalizing or full annealing heat treatment when the thickness of the flange section exceeds 3 in (76.2 mm).
2. Material on which welding is to be performed must be proved to be of good weldable quality.
3. Welding shall not be performed on steel that has a carbon content higher than 0.35%.
4. All welding on flange connections must comply with the Code requirements for postweld heat treatment.
5. Fabricated hubbed flanges may be machined from a hot-rolled or forged billet or a forged bar.

Rating of Standard Flanges. Standard flanges are rated as 150, 300, 400, 600, 900, 1500, and 2500 lb flanges. TEMA Table D-3 provides dimensions of ANSI standard flanges and bores of welding neck flanges. Lengths of alloy steel stud bolts for various flange ratings are furnished in TEMA Table D-4.

Drawback of the Existing Flange Design Procedure

The flange design methods given in the ASME Code and several others base the design criteria strictly on the flange stress limits [87]. According to Singh [87], the stress-limit-based design methods do not offer any assurance of sealability; they merely protect the flange from gross plastic deformation. A complete analysis of the bolted joint requires evaluation of the gasket residual pressure, flange stress, and bolt stress. These requirements commanded the attention of many committees on bolted joints study.

Bolted Joint Integrity and Intertube Pass leakage in U-Tube Exchangers

An analysis technique to determine the structural behavior of the both sides gasketed U-tube tube-sheet exchanger is studied in ref. 88. The method also provides procedure to compute the magnitude of the interpass leakage between the channel pass partition lanes. Some of the main conclusions of this study with reference to flange stresses are as follows:

1. The flange for the low pressure chamber may be grossly overstressed if sized using the ASME Code.
2. The stresses in the high-pressure side flange are generally higher than those predicted by the ASME Code.

3. Increasing the bolt prestress increases the stresses in the flanged joint elements. It has, however, a minor effect in reducing the leakage area.

Pressure Vessel Research Council Activities on Bolted Flanged Connections

The PVRC Committee on Bolted Flanged Connections (BFC) was established in 1985 to improve the ASME design rules for bolted full-face flanged connections. It is led by Chairman Dr. K. H. Hsu of Babcock & Wilcox Co. In 1990, the committee developed a 5-year plan and the goals have recently been organized into six committee assignments [89]:

1. Implement PVRC gasket constants and test procedure developments.
2. Issue flange design guidelines considering items such as behavior, tightness, transients, relaxation, etc.
3. Flange rating parameters for standard flanges.
4. Design parameters for ASME joints.
5. Gasket testing for temperature behavior data and test method development.
6. Flanged joint assembly and interaction effects.

Task Group on Flange Parameters Studies (Chairman: J. R. Winter, Jr.). This is a task group to study the parameters and tools for the rating of standard flanges and the design of code flanges consistent with the committee's long-range plans. Flange rotation, leak rate, thermal loads, and gasket performance need to be considered. The emergence of new emissions regulations, new and tighter gaskets, tightness-based gasket constants, and improved analytical tools all support such a new effort.

5.2 Step-by-Step Procedure for Integral/Loose/Optional Flanges Design

The ASME Code procedure for bolted flange joints for integral/loose/optional design is given here. The design procedure for reverse flange design is not covered. Certain steps may not be relevant for any one or two of these varieties. The procedure given here is similar to the ASME Code procedure detailed in the Taylor and Forge Company Bulletin on flange design [84]. The flange design procedure for ring flange and weld neck flange is shown in the Working Sheets furnished in Annexures 1 and 2. The essential steps on bolted flange design are as follows:

1. Selection of material for flange, gasket, bolts
2. Calculation of load for gasket seating condition
3. Calculation of load to withstand hydrostatic pressure known as operating condition
4. Bolting design and number of bolts decided
5. Thickness of flange estimation to withstand governing moment
6. Calculation of stress in the flange and to verify that the calculated stresses are within Code allowable stress

Data Required

Design pressure, P
Design temperature, T
Atmospheric temperature, T_a
Material specification for
  Flange
  Bolting
  Gasket
Code allowable bolt stress
  At design temperature, S_b

At atmospheric temperature, S_a
Code allowable flange stress
At design temperature, S_{fo}
At atmospheric temperature, S_{fa}

Step-by-Step Design Procedure
Step 1.

a. Draw a sketch of the flange with dimensional details, including flange forces, and moment arms. It depicts the flange thickness as t.
b. Select gasket material and choose the gasket factors m and y.
c. Determine the gasket dimensions—internal diameter, d_i, and outside diameter, d_o, as follows: The inside diameter of the gasket (in inches) is normally taken as

$$d_i = B + 0.01$$

where B equals the shell inside diameter for a weld neck flange and shell outside diameter for a ring flange. From d_i, calculate d_o using the following formula:

$$\frac{d_o}{d_i} = \sqrt{\frac{y - pm}{y - p(m + 1)}}$$

where m is the gasket factor and y the minimum design seating stress.
d. Gasket width and gasket load reaction diameter:

Calculate the gasket width, N, given by

$$N = (d_o - d_i)/2$$

Calculate the basic gasket width, b_o.
Calculate gasket load reaction diameter, G:

G = mean diameter of gasket face (if $b_o \leq 0.25$ in)
= OD of gasket contact face-2b (if $b_o > 0.25$ in)

Step 2.

a. Calculate bolt load for gasket seating condition W_{m2} and operating condition W_{m1}:

$$W_{m2} = \pi b G y$$
$$W_{m1} = H + H_p$$

where H is total hydrostatic end force and H_p total joint contact surface compression load. They are given by

$$H = \frac{\pi}{4} G^2 P$$

$$H_p = 2\pi b G m P$$

b. Calculate bolt cross-sectional area, A_m, required to resist the bolt load, which is the greater of

$$\frac{W_{m1}}{S_b} \quad \text{or} \quad \frac{W_{m2}}{S_a}$$

c. From A_m determine the number of bolts required (normally in multiples of 4), keeping the minimum bolt size as recommended in TEMA.

Step 3. Calculation of flange forces and their moments:

a. Calculated various flange forces:

$$H_D = \frac{\pi B^2 P}{4}$$

$$H_T = H - H_D$$

For operating condition: $H_G = W - H$
For gasket seating condition: $H_G = W$

b. Determine the moment arms h_D, h_T, and h_G for flange loads under operating conditions from Table 13 for the three types of flanges.

c. Calculate M_D (moment due to H_D), M_T (moment due to H_T), and M_G (moment due to H_G):

$$M_D = H_D h_D \qquad M_T = H_T h_T \qquad M_G = H_g h_G$$

Step 4. Calculate flange moments.

a. For operating conditions, the total flange moment M_o is the sum of the three individual moments M_D, M_T, and M_G:

$$M_o = M_D + M_T + M_G$$

b. For gasket seating M_o' (ASME Code uses the term Mo for moment due to gasket seating condition also) as given by

$$M_o' = \frac{W(C - G)}{2}$$

Step 5. Calculate the parameters E and K, and hub factors T, U, Y, and Z as follows, or they may be read from Fig. 2-7.1 of the ASME Code.

$$E = 0.5(A - C) \qquad \text{(shown in Fig. 16.)}$$

$$K = \frac{A}{B}$$

$$U = \frac{K^2\left(1 + 4.6052\dfrac{1 + \nu}{1 - \nu}\log_{10} K\right) - 1}{1.0472(K^2 - 1)(K - 1)(1 + \nu)}$$

$$T = \frac{(1 - \nu^2)(K^2 - 1)U}{(1 - \nu) + (1 + \nu)K^2}$$

$$Y = (1 - \nu^2)U$$

$$Z = \frac{K^2 + 1}{K^2 - 1}$$

Formulas for factors F, V, F_L, and V_L pertaining to loose flange are given in Table 2-7.1

of the ASME Code. Otherwise, read from ASME Code Figs. 2-7.2, 2-7.3, 2-7.4, and 2-7.5, respectively.

Step 6. Calculate factor h_o:

$$h_o = \sqrt{Bg_o}$$

Step 7. Calculate factors d_1 and e.

$$d_1 \quad \text{(for loose flanges)} = \frac{U h_o g_o^2}{V_L}$$

$$\text{(for integral flanges)} = \frac{U h_o g_o^2}{V}$$

$$e \quad \text{(for loose flanges)} = \frac{F_L}{h_o}$$

$$\text{(for integral flanges)} = \frac{F}{h_o}$$

where g_o is the thickness of the hub at the small end.

Step 8. Determine flange thickness:

a. For weld neck integral flange and loose flange, calculate the flange stresses as detailed in step 10 and check if they are within limit (step 11). If not within the limit, increase the flange thickness and continue from Step 9 onward.
b. For ring flange, flange thickness required is the greater of gasket seating condition or operating condition, given by

$$T_1 = \sqrt{\frac{M_o Y}{S_{fo} B}} \quad \text{or} \quad T_1 = \sqrt{\frac{M'_o Y}{S_{fa} B}}$$

where Y is the ring flange shape factor.

Step 9. Calculate stress formula factors:

$$\alpha = te + 1$$

$$\beta = \frac{4}{3}te + 1$$

$$\delta = \frac{t^3}{d_1}$$

$$\gamma = \frac{\alpha}{T}$$

$$\lambda = \gamma + \delta$$

$$m_o = \frac{M_o}{B}$$

$$m'_o = \frac{M'_o}{B}$$

Step 10. Calculate flange stresses. Flange stresses shall be determined for the governing moment, namely, more severe of the operating or the bolting conditions.

For operating conditions, calculate:

a. Longitudinal hub stress, S_H:

$$S_H = \frac{fm_o}{\lambda g_1^2}$$

b. Radial flange stress, S_R:

$$S_R = \frac{(1.33te + 1)m_o}{\lambda t^2}$$

c. Tangential flange stress, S_T:

$$S_T = \frac{Ym_o}{t^2} - ZS_R$$

For the gasket seating condition, repeat the stress calculations replacing m_o by m'_o.

Step 11. Allowable flange stress: The stresses as calculated earlier are compared with the allowable stresses for the flange material at the design temperature S_{fo} (equation follows), and if required, the thickness can be modified. These stresses shall be calculated separately both for the gasket seating condition and operating condition. For the operating condition, the allowable stresses are given by

$$S_H = 1.5S_{fo}$$
$$S_R = S_{fo}$$
$$S_T = S_{fo}$$
$$S_{fo} = \max|0.5(S_H + S_R),\ 0.5(S_H + S_T)|$$

For the gasket seating condition, the flange stresses are compared with the allowable stresses for the flange material at the atmospheric temperature S_{fa} (equation follows), and if required, the thickness can be modified.

$$S_H = 1.5S_{fa}$$
$$S_R = S_{fa}$$
$$S_T = S_{fa}$$
$$S_{fa} = \max|0.5(S_H + S_R),\ 0.5(S_H + S_T)|$$

6 EXPANSION JOINTS

Expansion joints are promising for accommodating differential thermal expansion of heat exchanger shells, pressure vessels, and pipelines carrying high-temperature fluids. Differences in the axial expansion of the shell and the tube bundle due to high mean metal temperature differentials warrant incorporation of expansion joints in heat exchangers. This is particularly true for fixed tube-sheet exchangers. For fixed tube-sheet exchangers, when the difference between shell and tube mean metal temperatures becomes large (greater than approximately 50°C for carbon steel), the tube-sheet thickness and tube end loads become excessive [34]. Therefore, an expansion joint is incorporated into the shell. Expansion joints also find applications in floating head exchangers, in the pipe between the floating head cover and the shell cover to cushion the thermal expansion between the tube bundle and the shell. Figures 2a and 8 show expansion joints incorporated into a fixed tube-sheet exchanger.

6.1 Flexibility of Expansion Joints

Expansion joints used as an integral part of heat exchangers or other pressure vessels shall be designed to provide flexibility for thermal expansion and also to function as a pressure-retaining structural element. Hence, an expansion joint must compromise between two contradictory loading conditions [90]: (1) pressure-retaining capacity and (2) flexibility to accommodate the differential thermal expansion. In many cases, the design for a particular application will involve a compromise of normally conflicting requirements. For example, to retain a high pressure, usually a thick-walled bellows is required, whereas high flexibility and high fatigue life require a thin-walled bellows.

6.2 Classification of Expansion Joints

Expansion joints are broadly classified into two types:

1. Formed head or flanged and flued head
2. Bellows or formed membrane

Formed Head or Flanged and Flued Head

Formed head expansion joints, also called thick-walled expansion joints, are characterized by higher spring rates (i.e., force required for unit deflection of a bellow) and usually a lower cycle life than thin-walled bellows. Because of the higher wall thickness, this type of expansion joint is rugged and the most durable from the standpoint of abuse, but it has the disadvantage of very limited flexibility. Construction details of formed head expansion joints are discussed in refs. 41 and 50 and by Singh [91].

Formed head expansion joints are made in two halves from flat annular plates. The outside edges of the plates are formed in one direction (flanged), and the inside edges are formed in the other direction (flued). The two halves are welded together and then welded into the heat exchanger shell as shown in Fig. 18. A flanged and flued head expansion joint consists of the following elements:

1. An outer shell or outer tangent
2. Two outer tori
3. Two annular plates
4. Two inner tori
5. Two inner shells or inner tangents butt welded to the main shell on both sides

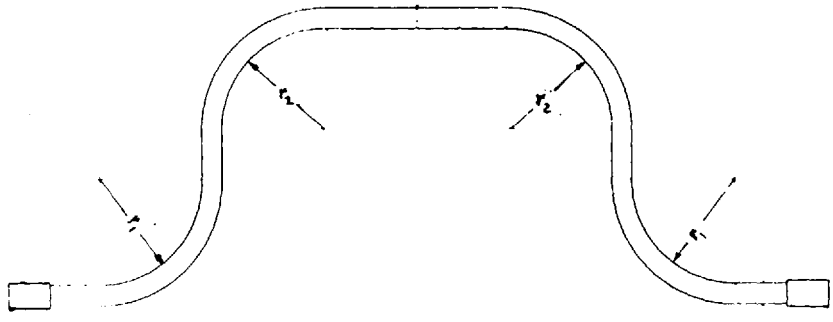


Figure 18 Flanged and flued expansion joint. (After Ref. 41.)

The inner and outer tori serve to mitigate the stress concentration due to geometric discontinuities between the shell and the annular plates. The radii of the tori are seldom less than three times the expansion joint thickness [41]. The annular plate contributes to lower the spring rate of the joint. Where the flexibility requirement is rather feeble, annular plate and the outer shell are eliminated. This type of construction results in the semitorus construction (Fig. 19a) [41,50]. The formed head type, i.e., without the inner tori, will lead to a flanged expansion joint as shown in Fig. 19b.

Bellows or Formed Membrane

According to EJMA Standards [8], a bellows type expansion joint is defined as a device containing one or more bellows used to absorb dimensional changes, such as those caused by thermal expansion or contraction of a pipeline, duct, or vessel. A bellows is defined as a flexible element of an expansion joint, consisting of one or more convolutions and the end tangents, if any. The bellows type expansion joint is also known as a "thin-walled expansion joint." The name "thin-walled expansion joint" is used to mean any form of expansion joint whose thickness is less than the thickness of the heat exchanger shell. A bellows type expansion joint is shown in Fig. 20.

Generally, the thin-walled bellows is formed from a thin plate whose thickness does not exceed $\frac{1}{8}$ in (3.2 mm) of corrosion-resistant material such as austenitic stainless steel or nickel-

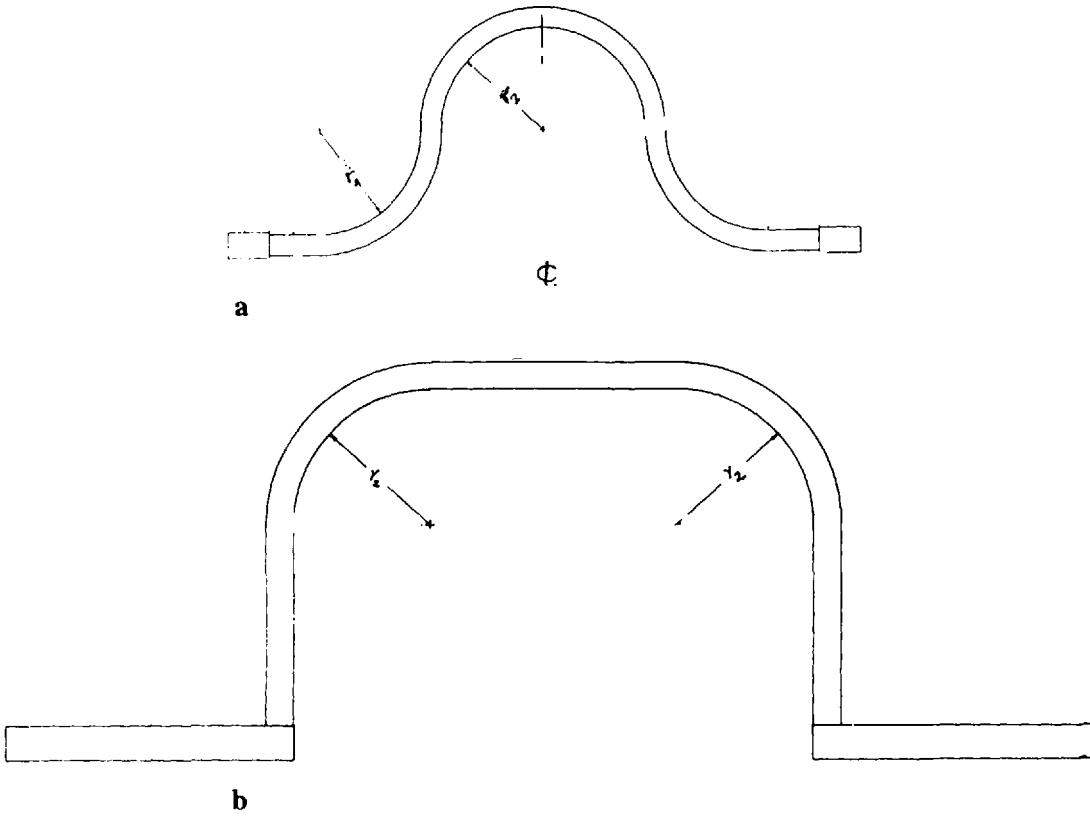


Figure 19 Modified version of flanged and flued expansion joint. (a) Semi-torus expansion joint; and (b) flanged expansion joint. (After Ref. 41.)

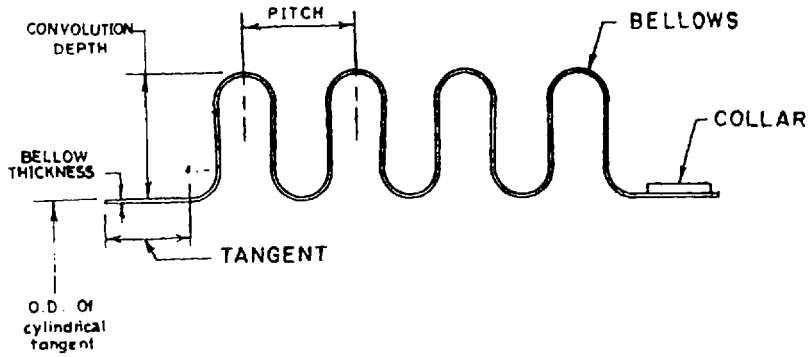


Figure 20 Bellows type expansion joint. (From Ref. 8.)

base alloys or high-alloy material using manufacturing processes like (1) disc or diaphragm forming, (2) elastomeric forming, (3) expansion forming, (4) hydraulic forming, and (5) pneumatic tube forming.

Bellows type expansion joints are made primarily for piping applications. When used in heat exchangers they are costly and delicate [90]. The cost is derived from the fact that such vessels require special sizes and material. They are said to be delicate because a heat exchanger containing a thin-walled joint must be handled and supported carefully in order to avoid damage, puncture, and buckling of the joint.

Deciding Between Thick- and Thin-Walled Expansion Joints

Conditions That Favor Using Thick-Walled Joints. Some of the conditions that favor thick-walled expansion joints are [29]:

1. Shell-side pressure is 300 psi (2070 kPa) or less.
2. Deflections per flexible element are moderate, in the range arbitrarily set at $\frac{1}{8}$ to $\frac{1}{4}$ inch (3.2 to 6.3 mm).
3. Application is noncyclical.
4. The joint must be capable of being vented and drained.

Conditions That Favor Using Thin-Walled Joints. Some of the conditions that favor thin-walled expansion joints are [29]:

1. Shell-side pressure exceeds 300 psi (2070 kPa).
2. Deflections per flexible element are high—arbitrarily greater than $\frac{1}{4}$ in (6.3 mm).
3. Application requires high cyclic life.

6.3 Design of Expansion Joints

Formed Head Expansion Joints

Kopp and Sayre [92] are generally credited for the first comprehensive work to determine analytically the axial stiffness of "flanged only" expansion joints. The method of analysis is based upon replacing the geometric configuration by an equivalent geometry. The outer torus (total length $\pi r/2$) is replaced by an equivalent corner end. One-half of the meridian of the outer torus is assigned to the annular plate and the other half to the outer shell. Figure 21 shows their idealized model. The structural characteristics of the annular plate are modeled by a unit width beam strip, the inner shell (heat exchanger main shell) is modeled using thin-shell

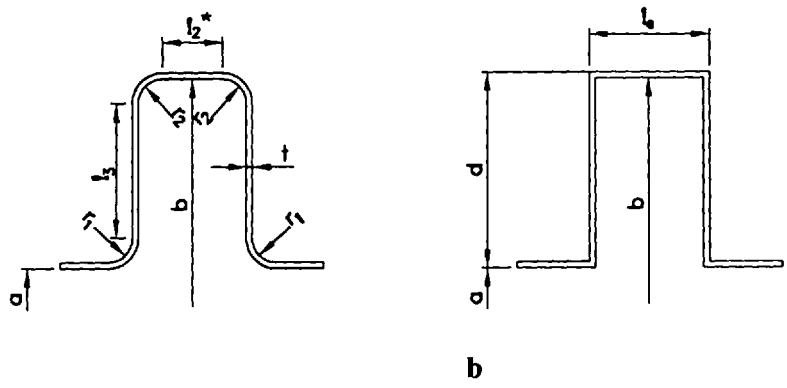


Figure 21 Kopp and Sayre model. (a) Actual model; and (b) idealized model. Note: Dimensions a and b are radii. (From Ref. 91.)

bending equations, and the outer shell is not modeled using classical thin shell equations but instead an approximate relationship is used. Kopp and Sayre also conducted some experimental tests to verify their mathematical model.

Wolf and Mains [90] applied finite-element analysis. The flanged and flued expansion joint is broken into its basic geometric components—a short cylinder, a toroidal segment, a flat annular plate, another toroidal segment, and a semi-infinite cylinder, as shown in Fig. 22. Their method did not attract wide usage, since the acceptance of a purely mathematical method is only a matter of time [41].

Singh and Soler [41] upgraded the Kopp and Sayre solution by using classical plate and shell solutions in place of "beam" solutions. This model suffers from the limitation of considering one standard expansion joint geometry only. In practical applications, myriad variations of the standard flanged and flued configuration are employed. Hence, Singh and Soler [91] present generalized treatment of various forms of flexible shell element (FSE) geometry, while retaining its modeling assumptions, which were directly borrowed from Kopp and Sayre. This model is included in the TEMA seventh edition.

Singh and Soler Model. The basics of the Singh and Soler [91] model are discussed next without the details of stress analysis and determination of spring constant. The most

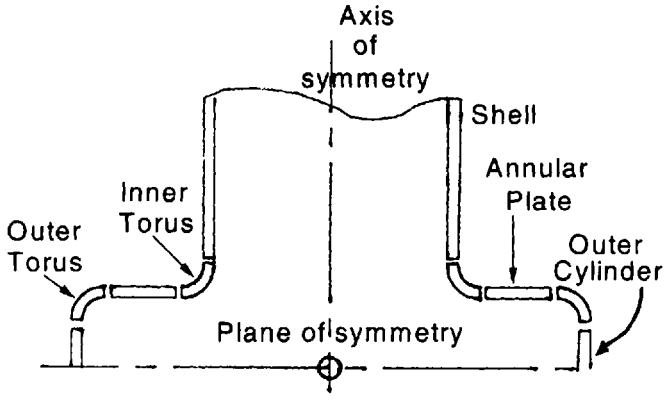


Figure 22 Finite element model for flanged and fluid expansion joint. (From Ref. 90.)

general form of the flexible shell element is shown in Fig. 23. The flexible shell element is one half of a standard expansion joint. Two flexible elements together make a standard expansion joint, such as the one shown in Fig. 18. The first step in the model simplification is to replace the circular segments with straight ones in the manner of Kopp and Sayer. By this step, the composite shells located at radii a and b are replaced by an equivalent shell of thickness t_1 and t_2, respectively, with modified flexural rigidities. Since the chief contribution of the tori lies in reducing in local bending stresses, which are secondary stresses, and since secondary stresses are of less importance, elimination of tori and replacement by sharp corners does not detract from the essence of developing a simple practical solution. The flexible shell element is reduced to two concentric shells of radii a and b connected by an annular plate. The Young's moduli of the three elements can be different. The resulting idealized model has the appearance of Fig. 23b. The three elements of the flexible shell element can be characterized as follows:

1. Inner shell of thickness t_1, equivalent Young's modulus E_1, equivalent length l_1, and radius a.
2. Outer shell of thickness t_2, equivalent Young's modulus E_2, length l_1, and radius b.
3. Annular plate of thickness t_e, with inner and outer radii a and b, respectively.

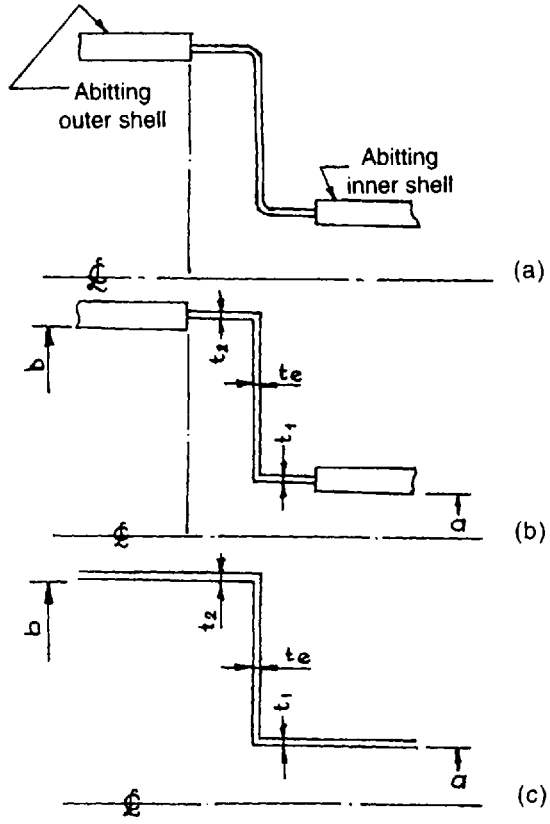


Figure 23 Singh and Soler (final) model for flanged and flued expansion joint. (a) General model; (b) equivalent Kopp and Sayre model; and (c) final idealized model. (From Ref. 91.)

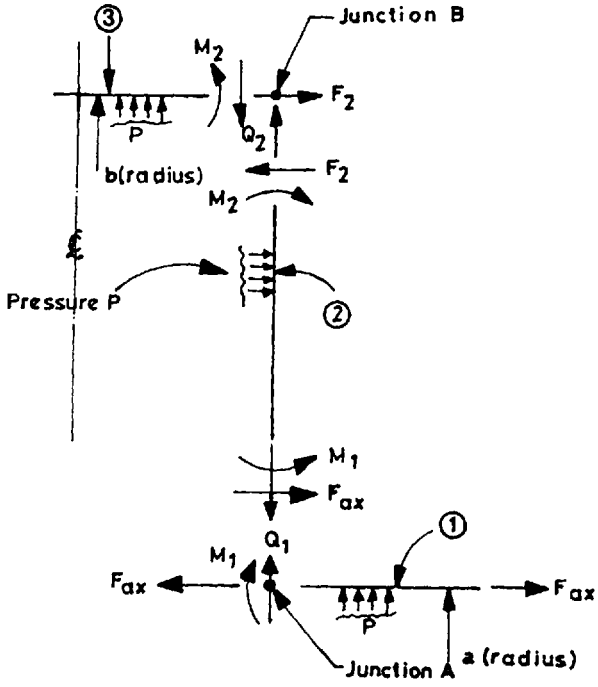


Figure 24 Loading and internal stress resultant acting on the flanged and flued expansion joint. (From Ref. 41.)

The equivalent lengths l_1 and l_2 warrant further comment. For the inner shell l_1 should be taken sufficiently long such that the edge effects (at the annular plate and shell junction) die out. Taking $l_1 = 2.5\ (at)^{0.5}$ will suffice, unless the shell is shorter, in which case the actual length should be used. Similarly, the length l_2 is actually the half-length of the top shell in the expansion joint.

Analysis for Axial Load and Internal Pressure. The resultant loading and internal stress acting on the elements along their inner junction A (the interface between the main shell element and annular plate) and outer junction B (the interface between the annular plate element and the outer shell) are shown in Fig. 24 and listed in Table 14.

Force Due to Internal Shell-Side Pressure. The equilibrium of one-half of the joint, in the axial direction, gives F_2 in terms F_{ax} [41]:

$$2\pi F_2 b = 2\pi F_{ax} a + \pi(b^2 - a^2)p_s \tag{114}$$

Equation 114 can be written as

Table 14 Loading and Internal Stress Resultant Acting on the Expansion Joint [41]

Joint A	Joint B
Moment M_1	Moment M_2
Applied axial load per unit circumference on the exchanger shell, F_{ax}	Applied axial load per unit circumference on the exchanger shell, F_2
Shell edge shear, Q_1	Shell edge shear, Q_2

$$F_2 = F_{a2}\frac{a}{b} + \frac{b^2 - a^2}{2b}p \tag{115}$$

The load deflection relations for short shell and annular plate elements to assemble the stiffness equations are derived in their work. They are not repeated here. Most of the formulas that are part of the TEMA procedure are arrived at after substituting $n = 0.3$ in the formulas of Singh and Soler [41] model.

Procedure for Design of Formed Head Expansion Joints

Rules for designing the formed head expansion joint currently exist in TEMA, ASME Code Section VIII, Div. 1, ANCC VSR1P, and A. D. Merkblatter, among others. HEDH [34] summarizes the salient features of flanged and flued type expansion joint design.

TEMA Procedure. The seventh edition (1988) of the TEMA Standards includes a new section RCB-8 on flexible shell elements (not light-gauge bellows type expansion joints), to be used in conjunction with fixed tube-sheet design. The paragraph encompasses several different shapes, such as flanged and flued heads, flanged only heads, and others. Also included is a method to calculate the maximum stress for cycle life calculations. The shell flexible elements shall be analyzed in both corroded and uncorroded conditions and shall be evaluated for hydrostatic test conditions also.

Minimum Thickness. As per TEMA RCB-8.9, the minimum thickness of the flexible shell elements shall be determined by the method of analysis. However, in no case shall the minimum uncorroded thickness be less than 3.2 mm (0.125 in) for nominal diameters up to 18 in, 4.8 mm (3/16 in) for nominal diameters in the range of 19–30 in (482.6–762 mm), or 6.35 mm (0.25 in) for nominal diameter greater than 30 in (762 mm). The industry practice is to set the FSE thickness one gauge less than the shell thickness [41]. When required, use more than one set of formed heads.

Allowable Stress (TEMA RCB-8.8). The allowable stresses in the flexible element, both in the corroded and uncorroded conditions, shall be as defined in the ASME Code using an appropriate stress concentration factor for the geometry.

Design Procedure as Per ASME Code

ASME Code Section VIII, Div. 1, does not give formulas for sizing the formed head expansion joints. However, rules are given for materials of construction, stress limits, cycle life calculation, fabrication, inspection and pressure test, stamping, and reports. The design of expansion joints shall conform to the requirements of Appendix CC of the ASME Code. Design aspects of multilayer, asymmetric geometries or loadings that differ from the basic concepts of Appendix CC are dealt in Paragraph U-2(g). Details of fabrication and inspection of formed type expansion joints are covered in Chapter 15, Heat Exchanger Fabrication. Stamping details are covered here.

Construction Materials and Minimum Thickness. According to ASME Code Section VIII, Div. 1, the materials for pressure retaining components shall conform to the requirements of UG-4. For thick-wall formed heads type expansion joints, in general, the bellows are of the same material as the shell.

Stamping and Reports. Details of stamping and reports are outlined in Section CC-6. As per this section, the expansion joint manufacturer shall have a valid ASME Code U certification of authorization and shall complete a Form U-2 Manufacturer's Partial Data Report, as required by UG-120(c). The Manufacturer's Partial Data Report shall contain data and information like:

1. Maximum allowable working pressure and temperature
2. Spring rate and axial movement
3. Service conditions
4. Design life in cycles
5. A certification that the expansion joint has been constructed as per the rules of Appendix CC
6. Details of the vessel manufacturer

6.4 Design of Bellows or Formed Membranes

Bellow type expansion joint design shall conform to the requirements of EJMA Standards, the ANSI Piping Codes, and the ASME Codes as applicable. The design of structural attachment shall be in accordance with accepted methods, based on elastic theory. In addition to EJMA Standards, design analysis and rules are also included in Appendix BB, ASME Code Section VIII, Div. 1, for circular type bellows with single-ply reinforced and nonreinforced bellows with thickness less than 3.2 mm (0.125 in).

Shapes and Cross Section

The bellows are available both for circular shells and rectangular shells. Rectangular shapes are used for surface condensers.

Bellows Materials

The bellows material shall be specified and must be compatible with the fluid handled, the external environment, and the operating temperature. Particular consideration shall be given to possible corrosion attack.

Bellows Design—Circular Expansion Joints

The design of bellows type expansion joints involves an evaluation of pressure-retaining capacity, stress due to deflection, spring rate, fatigue life, and instability (squirm). The spring rate is a function of the dimensions of the bellows and the bellows material. The determination of an acceptable design further involves the bellows parameters such as material, diameter, thickness, number of convolutions, pitch, height, number of plies, method of reinforcement, manufacturing technique, and heat treatment.

Limitations and Means to Improve the Operational Capability of Bellows

Single-ply bellows are used for low-pressure applications. They are fragile and hence they are easily damaged; external covers to protect personnel against the hazards of bellows blow-out due to failure are necessary. Drainable varieties are expensive, and external supports may be required to maintain alignment of the shell sections welded to the expansion joint [29]. Additionally, single-ply bellows are susceptible to instability. Since a bellows is a thin shell of revolution with repeated U-shaped convolutions, there exists a large number of natural vibration modes. Basically, these vibration modes are classified into three types: axial accordion modes, lateral bending modes, and shell modes, among which the former two are easily excited [93]. Methods and improved designs to overcome various shortcomings are discussed in the EJMA Standards. The following measures are normally adopted by designers to improve the single-ply expansion joint:

1. Use of external reinforcement
2. Use of multi-ply construction and thicker convolutions
3. Pressure balanced expansion joints

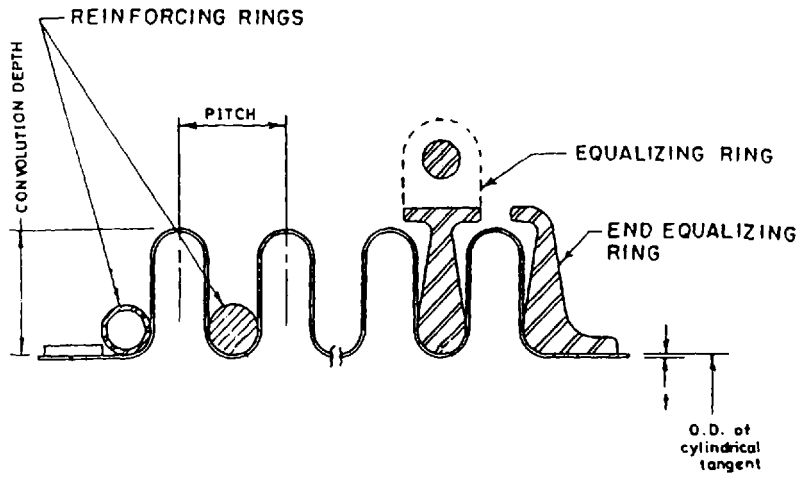


Figure 25 External reinforcement for bellows. (From Ref. 8.)

4. Flow sleeve inside the convolutions

External Reinforcement. A combination of high internal pressure-retaining capacity and large deflection can be achieved by external reinforcement of the U-shaped bellows. The external reinforcement offers circumferential restraint and supports the root radius against collapse from internal pressure loading. Reinforcing rings are also added where instability or squirm of the bellows is a concern. Equalizing and reinforcing ring devices used on some expansion joints fitting snugly in the roots of the convolutions are shown in Fig. 25.

Multi-Ply Construction and Thicker Convolutions. The pressure-retaining capacity of a bellows can be increased by the use of multi-ply construction and by increasing the thickness of the convolutions; however, the latter significantly reduces the bellows flexibility.

Pressure-Balanced Expansion Joints. The pressure balanced expansion joints (Fig. 26) are used for applications where pressure loading upon piping or equipment is considered excessive. The major advantage of the pressure-balanced expansion joint design is its ability to absorb externally imposed axial movement and/or lateral deflection while restraining the pressure thrust by means of tie devices interconnecting the flow bellows with an opposed bellows also subjected to line pressure. Their design should be as per EJMA Standards.

Flow Sleeve Inside the Convolutions. To overcome flow-induced vibration, install a sleeve inside the convolutions as shown in Fig. 27. In this case the bellow is thought to be two coaxial cylinders consisting of the convolutions and the sleeve, and the coupled vibrations through the fluid in the annular region may significantly affect the lateral vibration of the convolutions.

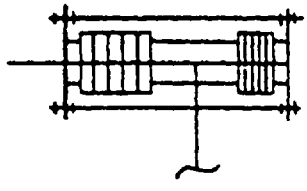


Figure 26 Pressure balanced expansion joint. (From Ref. 8.)

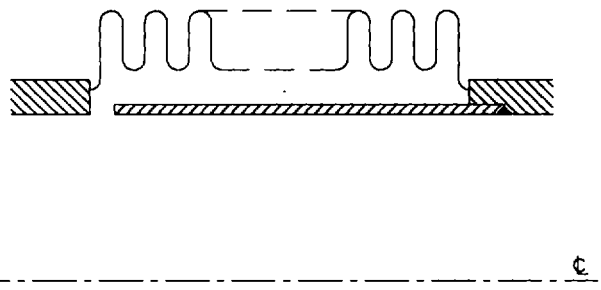


Figure 27 Flow sleeve to overcome FIV of bellow type expansion joint.

Fatigue Life

For a given bellows configuration and material thickness, the fatigue life of the bellows will be proportional to the imposed pressure and deflection. Depending on its material of construction, the suitability of an expansion joint to withstand the required number of cycles shall be determined from equations given in EJMA Standards or Appendix BB of the ASME Code.

7 OPENING AND NOZZLES

7.1 Openings

Openings in pressure vessels and heat exchangers refer to the cuts made in shells, flat covers, channels, and heads for accommodating the nozzles and to provide manholes, peepholes, drains and vents, instrument connections, etc. Openings can be circular, elliptical, or oblong. Whenever an opening is made in the wall of the shell or in the head, the wall is weakened due to the discontinuity in the wall and decrease in cross-sectional area perpendicular to the hoop stress direction. To keep the local stresses within the permissible limits, reinforcements to the openings are made.

Reinforcement Pad

The design of reinforcement is covered in UG-36 to UG-42 of the ASME Code by an area-to-area method. Reinforced pads whenever required as per drawings/codes shall be of the same material or equivalent to the component to which they are welded. Even though a reinforcement pad can be applied on either the outside or inside of the shell, it is the common practice to provide it at the outside due to easiness, and no need to meet the requirement of compatibility of the pad material with the process fluids, except that the pad should be resistant to general corrosion, and of weldable equality. The factors to be kept in mind while considering the reinforcement pad are:

1. The pad should match the contour of the component to which it should be attached.
2. Provide a tell-tale hole to release the entrapped gases during welding and to check the soundness of the welding.

Reinforced Pad and Air–Soap Solution Testing

As per ASME Code UW-15, reinforcing plates and saddles of nozzles attached to the outside vessel shall be provided with at least one tell-tale tapped hole (maximum size NPS 1/4 tap) for compressed air–soap solution test for tightness of welds that seal off the inside of the vessel. Air pressure of 1.25 kg/cm^2 is suggested for these tests. Higher test pressures are not

recommended because the soap bubbles have a chance to blow off. Tell-tale holes in the reinforcing pads may be left open or plugged when the vessel is in service.

7.2 Nozzles

Nozzles are incorporated to convey process fluids into the heat exchanger and out of it. Their sizes are arrived after calculating permissible fluid velocity limited by erosion–corrosion, impingement attack, pressure drop, etc. Minimum wall thickness is arrived using the cylindrical shell formula. Good nozzle design involves better distribution of process fluids, ability to withstand operating load and the other loads, and should provide easy accessibility to connect or disconnect the pipes. A well designed nozzle should have a very low pressure drop. Nozzle openings can be circular, elliptical, and oblong. Nozzles are connected by weldment to the shell by

1. Butt welding
2. Through type
3. Reinforcing pads

In addition to the welded type connections, brazed, threaded, studded, and expanded connections are also employed. Nozzle design is carried out as per Code. Considerations in nozzle design should include the inspectability of the nozzle-to-pipe and nozzle-to-vessel welds inspection [94]. Figure 28 shows some design types with reference to inspectibility.

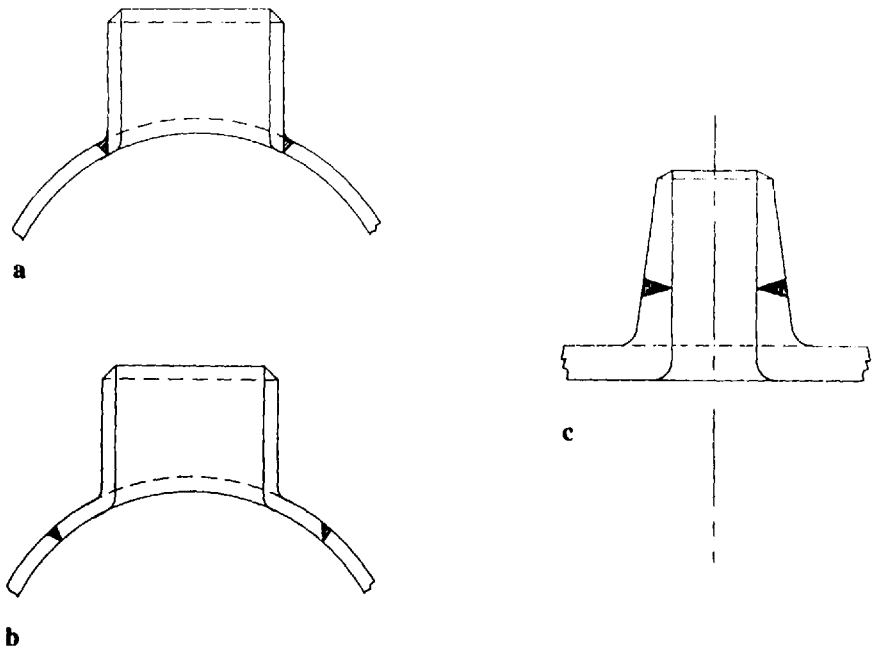


Figure 28 Nozzle design types. (a) Poor inspectiability; (b) better inspectiability; and (c) better than (b), which makes ultrasonic examination easier. (From Ref. 94.)

Reinforcements

Nozzle openings are reinforced by the following means:

1. Using thick forged-blank nozzle (Fig. 29a)
2. Opening compensated by reinforcement pad (Fig. 29b)
3. Welding of thick-walled nozzle pipe (Fig. 29c).

Design aspects of various nozzle reinforcements are discussed by Schoessow et al. [95]. Requirements of reinforcement for openings in shells and formed heads are covered in UG-37 to UG-42, UG-82, and attachment welds in UW-15, and exemption from reinforcement in UG-36. As far as possible, nozzle design should avoid the separate reinforcement plate being welded to the shell, because the weld metal cracks at the interface between the reinforcement pad plate and the shell plate pose additional problems.

7.3 Stacked Units

Stacked units with interconnecting nozzles are a source of many problems for the designer as well as the fabricator. Most of the trouble comes as a result of differential thermal expansion, either radial or longitudinal or both. Several general rules will help avoid trouble [96]:

1. Do not stack one-pass shells more than two deep, without thorough check of differentials.
2. Keep intermediate shell nozzles as near channel nozzles as possible.
3. Avoid ring-type joint intermediate nozzles, if possible.
4. Avoid offset direct interconnecting nozzles.

8 SUPPORTS

All vessels shall be supported and the supporting members shall be attached to the vessel wall. The design of supports shall normally conform to good engineering practice. The supports should be designed to resist internal and external pressure and accommodate the self-weight of the unit and contents, including the flooded weight during hydrostatic test. Based on their installation, the supports differ for horizontal vertical installation. The selection of the type of

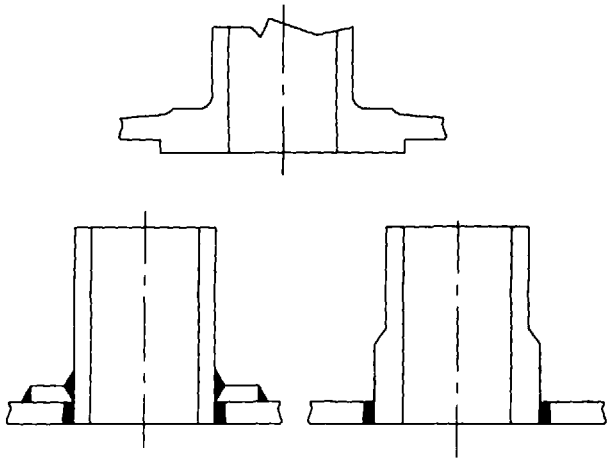


Figure 29 Nozzle opening reinforcement. (a) Thick forged blank nozzle; (b) compensation by reinforcement pad; and (c) thick walled nozzle.

support for a pressure vessel is dependent on parameters such as the elevation of the vessel from the ground level, the materials of construction, and the operating temperature [44].

8.1 Design Loads

While designing the supports of a vessel, care should be taken to include all the external loads likely to be imposed on it. Such external loads include: (1) wind loads, (2) loads due to connected piping, (3) superimposed loads, (4) shock loads due to surging or hydraulic hammer, and (5) seismic vibration. As per TEMA Standards, supports for a removable tube bundle heat exchanger should be designed to withstand a pulling force equal to 1.5 times the weight of the tube bundle, and when additional loads and forces from external nozzle loadings, wind loads, and seismic forces are assumed for the purposes of supports design, the combinations need not be assumed to occur simultaneously. Care should be taken that the thermal stresses in external supports do not exceed those permitted by the code.

8.2 Horizontal Vessel Supports

Horizontal vessels are subject to longitudinal bending moments and local shear forces due to the weight of their contents. They are generally supported by three types of supports: (1) saddle supports, (2) ring supports, and (3) leg supports. Saddle support is used most commonly for heat exchangers. It is shown in Fig. 30. Whenever possible, horizontal vessels shall be supported by two supports only, with holes for anchor bolts. If more than two supports are used, the distribution of the reaction is affected by difference in support level, the straightness and local roundness of the vessel, and the relative stiffness of different parts of the vessel against local deflection [26].

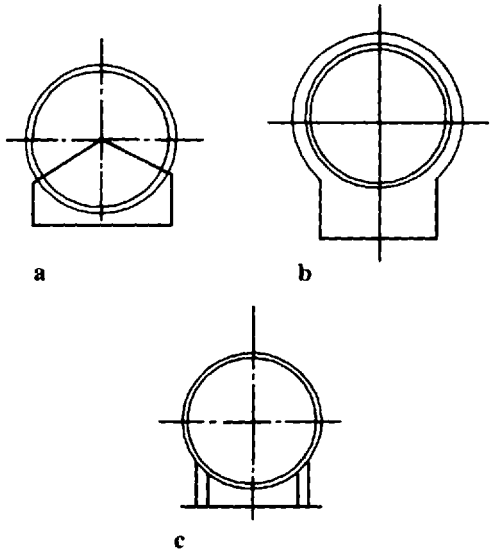
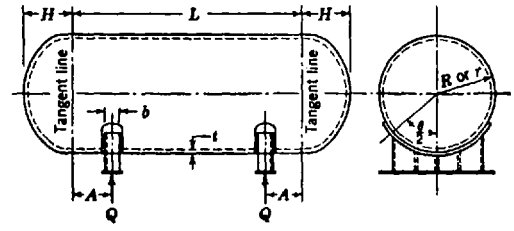


Figure 30 Examples of horizontal supports of pressure vessels. (a) Saddle support; (b) ring support; and (c) lug support.

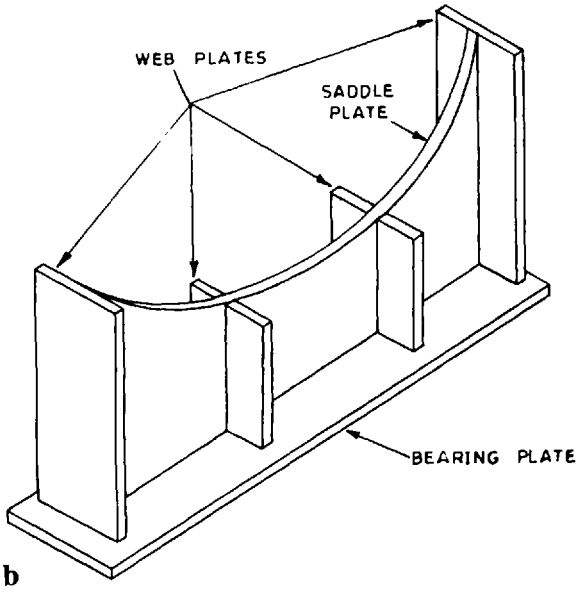
Saddle Supports

Saddle supports may be used for vessels whose wall is not too thin. Horizontal vessels when supported on saddle supports such as in Fig. 31a behave as beams, and with these kinds of supports, the maximum longitudinal bending stresses occur at the supports and at the mid span of the vessel (Fig. 31c). Hence the location of supports from the mid span of the vessel or head tangent is critical to minimize the bending stresses at the supports. Consideration shall be given to ensure that the saddles should be preferably extended over at least 120° of the

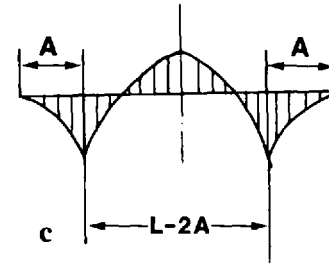


A = distance from tangent line to saddle, feet
L = length of vessel, tangent to tangent, feet
H = depth of head, feet
Q = total load per saddle, pounds
= total weight divided by two
R = radius of vessel, feet
b = width of saddle (or width of concrete for formed concrete saddles, inches
r = radius of vessel, inches
t = shell thickness, inches
θ = total included angle, degrees
w = load per unit length, pounds/ft

a



b



c

Figure 31 A vessel on horizontal saddle support. (a) Schematic; (b) details of the saddle support; and (c) bending stress distribution. (Item (a) is reproduced from Ref. 44.)

circumference of the vessel. The limitation, which is imposed by most codes of practice is an empirical one based on experience with large vessels [26].

Zick Stress. Zick [97] developed a method for analyzing supports for the horizontal cylindrical shells. The analysis gives a detailed derivation of the equations for longitudinal bending stresses at the supports and at the mid span. These stresses are named as Zick stress. Zick's method is discussed in detail in refs. 41, 42, and 45, among others. Zick's method is adopted in codes such as IS:2825–1969 and BS 5500.

Ring Supports

Ring supports as shown in Fig. 30b are preferred to saddle supports for large thin-walled vessels, vacuum vessels, and in the case of saddles located away from the head. Ring supports are also preferred when to support a vessel at more than two cross sections becomes inevitable. The welds attaching ring supports should have a minimum leg length equal to the thickness of the thinner of the two parts being joined together.

Leg Supports

Leg supports as shown in Fig. 30c are usually permitted for small vessels by the usual code practice because of the severe local stresses that can be set up at the connection of the support to the vessel wall.

8.3 Vertical Vessels

Supports for the vertical units may be skirt supports, ring supports, and lugs (columns). Some of these vertical supports are shown in Fig. 32.

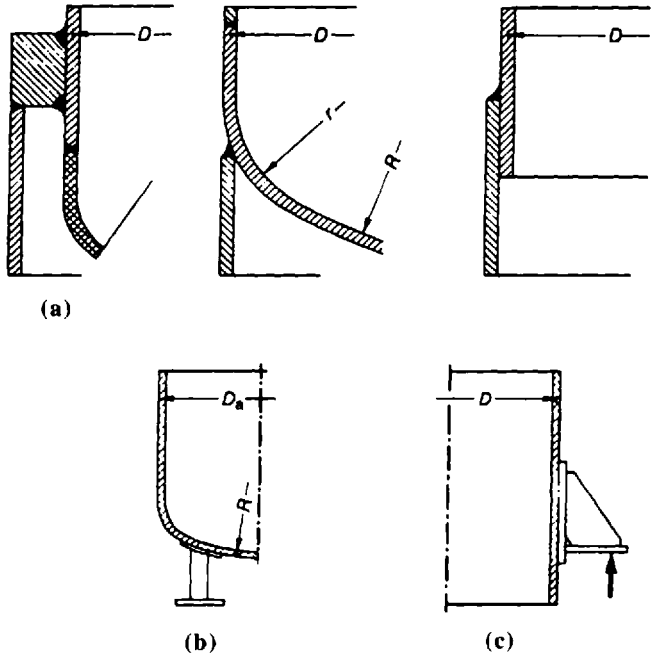


Figure 32 Examples of vertical supports of pressure vessels. (a) Skirt supports, (b) lug support, and (c) ring support. (From Ref. 40.)

Skirt Supports

Skirt supports (Fig. 32a) are recommended for large/tall vertical vessels. Skirt supports are preferred because they do not lead to concentrated local loads on the shell, offer less restraint against differential thermal expansion, and reduce the effect of discontinuity stresses at the junction of the cylindrical shell and the bottom [26]. The skirt supports shall be provided with at least one opening for inspection unless there is a provision to examine the bottom of the vessel accessible from below.

Lug Supports

Vertical vessels may be supported by a number of posts or lugs as shown in Fig. 32b. Lug supports are ideal for thick-walled vessels. For thin-walled vessels, it is not convenient unless proper reinforcements are used or many lugs are welded. Brackets or lugs offer many advantages over other types of vessels [41]: They are inexpensive, can absorb diametrical expansion by sliding over greased or bronze plates, and requirements of welding are minimal.

8.4 Procedure for Support Design

TEMA Rules for Supports Design (G-7.1)

TEMA rules for supports for horizontal units are listed in G-7.11 and for vertical units in G-7.12. For calculating resulting stresses due to the saddle supports, references are suggested under TEMA G-7.13. The "Recommended Good Practice" section of TEMA Standards provides additional information on support design.

ASME Code

ASME Code requirements for supports design are covered in UG-54. Appendix G contains suggested good practices for support design.

8.5 Lifting Devices and Attachments

TEMA rules for the design of lifting devices are given in G-7.2. ASME Code rules for the construction of lifting devices and fitting attachments are covered in UG-82. Some of the TEMA Standards for design of lifting devices are as follows:

1. Channels, bonnets, and covers that weigh more than 60 pounds are to be provided with lifting lugs.
2. Lifting devices are designed to lift the component to which they are directly attached. When lifting lugs are required by the purchaser to lift the complete unit, the device must be adequately designed.
3. The design load shall incorporate an appropriate impact factor.
4. Lifting devices and attachments shall be formed and fitted to conform to the curvature of the component surface to which they are attached.

REFERENCES

1a. Hirschfeld, F., Codes, standards and certificate of authorization program: Part 1—Establishing safety standards, *Mech. Eng.*, January, 33–39 (1979).

1b. Hirschfeld, F., Codes, standards and certificate of authorization program: Part 2—Policies, programs and organization, *Mech. Eng.*, February, 31–37 (1979).

2. Statement of the Council on Codes and Standards of the American Society of Mechanical Engineers on the federal role in international standards, *Trans. ASME, J. Pressure Vessel Technol.*, *112*, 425–426 (1990).

3. Standards of the Tubular Exchanger Manufacturers Association, 7th ed., Tubular Exchanger Manufacturers Association, Inc., Tarrytown, New York, 1989.
4. Standards for Surface Condensers, 8th ed., Heat Exchange Institute, Cleveland, OH, 1984.
5. Standards for Power Plant Heat Exchangers, 1st ed., Heat Exchange Institute, Cleveland, OH, 1984.
6. Standards for Closed Feedwater Heaters, Heat Exchange Institute, Cleveland, OH, 1984.
7. Shell and Tube Exchangers for General Refinery Services, API Standard 660, 4th ed., American Petroleum Institute, Washington, DC, September 1982.
8. Standards of the Expansion Joint Manufacturers Association, 5th ed., Tarrytown, New York, 1980.
9. British Standards (BSI), 1993.
10. Japanese Industrial Standards, 1993.
11. DIN, German Industrial Standards, Beuth, Beuth Verlg GmbH, Berlin.
12. International Organisation for Standardization (ISO), 1993.
13. Taborek, J., and Aurioles, G., Effect of 1988 TEMA standards on mechanical and thermo hydraulic design of shell and tube heat exchangers, *Heat Transfer* (1989).
14. Gupta, J. P., *Fundamentals of Heat Exchanger and Pressure Vessel Technology*, Hemisphere, Washington, DC, 1986.
15. Codes, standards and the ASME: Part 3—Standards, safety standards, *Mech. Eng.*, August, 24–25 (1972).
16. ASME Boiler and Pressure Vessel Code, Section VIII, Division 1, American Society of Mechanical Engineers, New York, 1992.
17. ASME Boiler and Pressure Vessel Code, Section VIII, Division 2, American Society of Mechanical Engineers, New York, 1992.
18. BS 5500, British Standard Specification for Fusion Welded Pressure Vessels, 1991.
19. CODAP, French Code for the Construction of Unfired Pressure Vessels, edited by SNCT, Paris, France, 1985.
20. A. D. Merkblatter, German Pressure Vessel Code, Carl Heymans Verlag KG, Koln, Germany.
21. ASME Boiler and Pressure Vessel Code, Section III, Division 2, American Society of Mechanical Engineers, New York, 1992.
22. SNCT, Syndicat National de la Chaudronnerie-Tolerie, National Association for Pressure Vessels.
23. ANCC Italian Code, Milano, Italy.
24. Stoomwenzen (Dutch Code), Rules for Pressure Vessels, Tryckkarskomissionnen IVA, Stockholm, Sweden.
25. ISO/DIS 2694, Pressure Vessels, 1973.
26. IS:2825-1969, Code for Unfired Pressure Vessels, Bureau of Indian Standards, Manak Bhavan, New Delhi, India.
27. The Pressure Vessel Code (Dai Isshu Atsuryoku Youki Kousou Kikahu), Ministry of Labour, Japan Boiler Association, Tokyo, Japan.
28. Regels Voor Toesellen onder Druck, Ministry of Social Affairs, Dienst voor het Stoomwesen, Government Printing Office, Christoffel, Plantjnstraat, The Hague, The Netherlands.
29. Yokell, S., *A Working Guide to Shell and Tube Heat Exchangers*, McGraw-Hill, New York, 1990.
30. Cepluch, R. J., The ASME Boiler and Pressure Vessel Code Committee—Challenges: Past and future, *Trans. ASME, J. Pressure Vessel Technol., 112*, 319–322 (1990).
31. Blackall, F. S., Jr., ASME Standards save lives and dollars, *Mech. Eng.*, December, 979–871 (19XX).
32. Nichols, R. W., ed., *Pressure Vessel Codes and Standards: Developments in Pressure Vessel Technology–5*, Elsevier, London, 1987.
33a. Codes, standards and the ASME: Part 1—Performance test codes, *Mech. Eng.*, June, 24–25 (1972).
33b. "Codes, Standards and the ASME: Part 2-ASME Boiler and Pressure Vessel Codes," Mechanical Engineering, July 1972, pp. 16–18.
33c. "Codes, Standards and the ASME: Part 4—International Standardization Committee," Mechanical Engineering, September 1972, pp. 20–24.
34. Schlunder, E. U., Editor-in-Chief, "Mechanical Design Codes," Heat Exchanger Design Handbook, in five volumes, Hemisphere, Washington, D.C. (1982). Section 4.1.6, "Expansion Joints."

35. Mase, J. R., and Smolen, A. M., ASME Pressure Vessel Code: Which division to choose, *Chem. Eng.*, January, 133–136 (1982).
36. Farr, J. R., The ASME Boiler and Pressure Vessel Code: Section VIII—Pressure Vessels, in *Pressure Vessel Codes and Standards, Developments in Pressure Vessel Technology–5* (R. W. Nichols, ed.), Elsevier Applied Science, London, 1987, vol. 5, pp. 35–58.
37. Farr, J. R., "The ASME Boiler and Pressure Vessel Code: Overview, in *Pressure Vessel Codes and Standards, Developments in Pressure Vessel Technology–5* (R. W. Nichols, ed.), Elsevier, London, 1987, vol. 5, pp. 1–34.
38. Houston, R., British Standards Institution boiler and pressure vessel design criteria, in *Pressure Vessel Codes and Standards, Developments in Pressure Vessel Technology–5* (R. W. Nichols, ed.), Elsevier, London, 1987, vol. 5, pp. 105–158.
39. Thomas, A., and Grandemange, J. M., French codes and standards on boiler and pressure vessel technology, in *Pressure Vessel Codes and Standards, Developments in Pressure Vessel Technology–5* (R. W. Nichols, ed.), Elsevier, London, 1987, vol. 5, pp. 175–222.
40. Hohne, K. J., German boiler and pressure vessel codes and standards: Design aspects, in *Pressure Vessel Codes and Standards, Developments in Pressure Vessel Technology–5* (R. W. Nichols, ed.), Elsevier, London, 1987, vol. 5, pp. 249–282.
41. Singh, K. P., and Soler, A. I., *Mechanical Design of Heat Exchangers and Pressure Vessel Components*, Arcturus, Cherry Hill, 1984.
42a. Escoe, K. A., *Mechanical Design of Process Systems, Vol. 2—Shell and Tube Heat Exchangers, Rotating Equipment, Bins, Silos, Stacks*, Gulf, Houston, TX, 19XX.
42b. Escoe, K. A., *Mechanical Design of Process Systems, Vol. 1*, Chap. 4, Gulf, Houston, TX, 19XX.
43. Moss, D. R., *Pressure Vessel Design Manual*, Gulf, Houston, TX, 19XX.
44. Brownell, L. E., and Young, E. H., *Process Equipment Design*, John Wiley & Sons, New York, 1968.
45. Bednar, H. H., *Pressure Vessel Design Handbook*, Von Nostrand Reinhold, New York, 1981.
46. Harvey, J. F., *Pressure Component Construction*,Von Nostrand, Reinhold, New York, 1980.
47. Chuse, R., *Pressure Vessels, The ASME Code Simplified*, 6th ed., McGraw-Hill, New York, 1954.
48. Roach, G. H., and Wood, R. M., Shell and tube exchangers having improved design features, *Heat Transfer Eng.*, *7*(1–2), 19–23 (1986).
49. Soler, A. I., *Heat Transfer Eng.*, *8*(3), 84–89 (1987).
50. Singh, K. P., Mechanical design of tubular heat exchangers—An appraisal of the state-of-the-art, in *Heat Transfer Equipment Design* (R. K. Shah, C. Subba Rao, and R. M. Mashelekar, eds.), Hemisphere, Washington, DC, 1988, pp. 71–87.
51. Gardner, K. A., Heat exchanger tubesheet design, *ASME J. Appl. Mech.*, *70*, A-377–385 (1948).
52. Gardner, K. A., Heat exchanger tubesheet design—2—Fixed tubesheets, *Trans. ASME, J. Appl. Mech.*, *74*, 159–166 (1952).
53. Miller, K. A. G., 1952–53, The design of tube plates in heat exchangers, *Proc. Inst. Mech. Eng., Sect. B, Lond.*, *1*, 672–688 (1952–1953).
54. Yu, Y. Y., Rational analysis of heat exchanger tubesheet stresses, *Trans. ASME, J. Appl. Mech.*, *78*, 468–473 (1956).
55. Galletly, G. D., and Garbett, C. R., Pressure vessels—Let the tubes support the tubesheet, *Ind. Eng. Chem.*, *50*(9), 1227–1230 (1958).
56. Galletly, G. D., Optimum design of thin circular plates on an elastic foundation, *Proc. Inst. Mech. Eng., Lond.*, *173*, 689–698 (1959).
57. Gardner, K. A., Heat exchanger tubesheet design—3, U-tube and bayonet tubesheets, *Trans. ASME, J. Appl. Mech., Ser. E*, *82*, 25–33 (1960).
57. Boon, G. B., and Walsh, R. A., Fixed tubesheet heat exchangers, *Trans. ASME, J. Appl. Mech.*, June, 175–180 (1964).
58. Gardner, K. A., Tubesheet design: A basis for standardization, *ASME, Proc. First Int. Conf. Pressure Vessel Technology: Part I, Design and Analysis*, pp. 621–668, 1969.
59. Chiang, C. C., Closed Form Design Solutions for Box Type Heat Exchangers, ASME publication 75-WA/DE, ASME, New York, 1975.

60. Hayashi, K., An analysis procedure for fixed tubesheet exchangers, *Proc. Third Int. Conf. Pressure Vessel Technology: Part 1, Analysis, Design and Inspection*, ASME, New York, pp. 363–373, 1977.
61. Malek, R. G., A new approach to exchanger tubesheet design, *Hydrocarbon Processing*, 165–169 (1977).
62. Singh, K. P., Analysis of vertically mounted through tube heat exchangers, *Trans. ASME, J. Eng. Power, 100*, 380–390 (1978).
63. Soler, A. I., and Soehrens, J. E., Design curves for stress analysis of U-tube heat exchanger tubesheet with integral channel and head, *Trans. ASME, J. Pressure Vessel Technol., 100*, 221–232 (1978).
64. Soehrens, J. E., Tubesheet thicknesses and tube loads for floating head and fixed-tubesheet heat exchangers, *Trans. ASME, J. Pressure Vessel Technol., 106*, 289–299 (1984).
65. Cascales, D. H., and Militello, C., Tubesheet thicknesses and tube loads for fixed tubesheet heat exchangers [letter to the editor], *Trans. ASME, J. Pressure Vessel Technol., 107*, 318–323 (1985).
66. Singh, K. P., and Soler, A. I., An elastic-plastic analysis of the integral tubesheet in U-tube heat exchangers—Towards an ASME Code oriented approach, *Proc. 1985 PVP Conf.*, New Orleans, Vol. 98, Book, No. Hoo 322, pp. 39–51, 1985.
67. Soler, A. I., Caldwell, S. M., and Singh, K. P., Tubesheet analysis—A proposed ASME design procedure, *Proc. ASME, Thermal/Mechanical Heat Exchanger Design—Karl Gardner Memorial Session* (K. P. Singh and S. M. Shenkman, eds.), ASME PVP. Vol. 118, H00343, 1985, pp. 93–101. Reprinted in *Heat Transfer Eng., 8*(3), 40–48 (1987).
68. Soehrens, J. E., Stress analysis of heat exchangers, *ASME Proc. Thermal/Mechanical Heat Exchanger Design—Karl Gardner Memorial Session* (K. P. Singh and S. M. Shenkman, eds.), 1985, pp. 79–91. Reprinted in *Heat Transfer Eng., 8*(3) (1987).
69. Osweiller, F., Methode de calcul des exchangers a deux ictes fixes le CODAP, Etude CETIM, No. 14B031, 1986.
70. Osweiller, F., Analysis of TEMA tubesheet design rules, *Proc. 1986 Pressure Vessel and Piping Conference*, Chicago, 1986.
71. Cascales, D. H., and Militello, C., A model for fixed tubesheet heat exchanger, *Trans. ASME, J. Pressure Vessel Technol., 109*, 289–296, 1987.
72. Paliwal, D. N., Design of fixed tubesheet for heat exchangers, *Trans. ASME, J. Pressure Vessel Technol., 111*, 79–85 (1989).
73. Osweiller, F., Basis of the tubesheet heat exchanger design rules used in the French pressure vessel code, *Trans. ASME, J. Pressure Vessel Technol., 114*, 124–131 (1992).
74. Singh, K. P., and Marks, P., Proposed extension of the TEMA tubesheet design method to determine tubesheet rim thickness, in *Proc. ASME, Thermal/Mechanical Heat Exchanger Design—Karl Gardner Memorial Session* (K. P. Singh and S. M. Shenkman, eds.), ASME PVP. V. 118, H00343, pp. 111–119 (1985). Reprinted in Heat Transfer Engineering, Vol. 8, No. 3, 1977, pp. 50–57.
75. Kuppan, T., Alternate design charts for fixed tubesheet design procedure included in ASME Boiler and Pressure Vessel Code, Section VIII, Div. 1, *Trans. ASME, J. Pressure Vessel Technol., 117*, 189–194 (1995).
76. O'Donnell, W. J., and Langer, B. F., Design of perforated plates, *ASME J. Eng. Ind., 84*, 307–320 (1962).
77. Osweiller, F., Evolution and synthesis of the effective elastic constants concept for the design of tubesheets, *Trans. ASME, J. Pressure Vessel Technol., 111*, 209–217 (1989).
78. Bernstein, M. D., and Soler, A. I., The tubesheet analysis method in the new HEI condenser standards, *Trans. ASME, J. Eng. Power, 100*, 363–368 (1978).
79. Rachkov, V. I., and Morozov, V. H, Designing curved tube plates, *Khim-i-reft. Masb., 7*, 14 (1968).
80. Paliwal, D. N., and Sinha, S. N., Design of shallow spherical curved tubesheet for heat exchangers, *Int. J. Pressure Vessels Piping, 17*, 158–192 (1984).
81. Sang, Z.-F., and Widera, G. E. O., Stress analysis of elliptical tube plates in heat exchangers, *Trans ASME, J. Pressure Vessel Technol., 109*, 310–314 (1987).
82. Waters, E. O., Wesstrom, D. B., and Williams, F. S. G., Design of bolted flanged connections, in

Pressure Vessel and Piping Design, Collected Papers 1927–1959, American Society of Mechanical Engineers, New York, 1960, pp. 58–61. Reprinted from *Mech. Eng.* (1934).
83. Bickford, J. H., Gasketed joints and leaks, in *An Introduction to the Design and Behavior of Bolted Joints*, 2nd Ed., Marcel Dekker, New York, 1990, pp. 495–548.
84. Modern Flange Design, 7th ed., Bulletin 502, Taylor Forge International, Inc.
85. Lake, G. F., and Boyd, G., Design of bolted, flanged joints of pressure vessels.
86. Derrene, M., Marchand, L., Payne, J. R., and Bazergui, A., Elevated Temperature Testing of Gaskets for Bolted Flanged Connections, WRC Bulletin 391.
87. Singh, K. P., Study of bolted joint integrity and inter tube pass leakage in U-tube heat exchangers—Part I: analysis, *Trans. ASME, J. Eng. Power, 101*, 9–15 (1979).
88. Singh, K. P., Study of bolted joint integrity and inter tube pass leakage in U-tube heat exchangers—Part II: Analysis, *Trans. ASME, J. Eng. Power, 101*, 16–22 (1979).
89. PVRC, *Trans. ASME, J. Pressure Vessel Technol., 114*, 385–387 (1992).
90. Wolf, L. J., and Mains, R. M., The stress analysis of heat exchanger expansion joints in the elastic range, *Trans. ASME, J. Eng. Ind.*, 145–150 (1973).
91. Singh, K. P., A rational procedure for analyzing flanged and flued expansion joints, *Trans. ASME, J. Pressure Vessel Technol., 113*, 64–70 (1991).
92. Kopp, S., and Sayre, M. F., Expansion joints for heat exchangers, *ASME Winter Annual Meeting*, New York, 1952.
93. Morishita, M., Ikahata, N., and Kitamura, S., Simplified dynamic analysis methods for metallic bellows expansion joints, *Trans. ASME, J. Pressure Vessel Technol., 113*, 504–510 (1991).
94. Sattler, F. J., Forrer, G. R., and Parker, W. O., Jr., Inservice Inspection of Nuclear Plants, Materials Evaluation, November 1972, pp. 18A–22A and 27A–29A.
95. Schoessow, G. J., and Brooks, E., Analysis of experimental data regarding certain design features of pressure, in *Pressure Vessel and Piping Design, Collected Papers 1927–1959*, American Society of Mechanical Engineers, New York, 1960, pp. 24–34.
96. Spencer, T. C., Mechanical design and fabrication exchangers in the United States, *Heat Transfer Eng., 8*(3), 58–61 (1987).
97. Zick, L. P., Stresses in large horizontal cylindrical pressure vessels on two saddle supports, in *Pressure Vessel and Piping; Design and Analysis*, ASME, New York, 1972.

This page intentionally left blank

12
Corrosion

1 BASICS OF CORROSION

Most common metals and their alloys are attacked by environments such as the atmosphere, soil, water, or aqueous solutions. This destruction of metals and alloys is known as corrosion. It is generally agreed that metals are corroded by an electrochemical mechanism. With practically all commercial processes engineered on a continuous basis of operation, premature failure from corrosion of various types of equipment, including heat exchangers, piping, and others, may mean costly shut downs and expensive maintenance operations. It is especially troublesome in oil refining, chemical industries, and electric power plants on land and sea, as well as in food and liquor processing, paper manufacture, refrigeration, air conditioning, etc. Therefore, an understanding of corrosion principles and corrosion control should be of great interest to industry and the general public.

1.1 Reasons for Corrosion Studies

There are two main reasons for concern about and study of corrosion: (1) economics and (2) conservation of materials. Of these, the economic factors mostly favor study and research into the mechanisms of corrosion and the means of controlling corrosion. Economic reasons for corrosion study include:

1. Loss of efficiency: Corrosion can result in the build up of corrosion products and scale, which can cause a reduction in heat transfer as well as an increase in the power required to pump the fluid through the system.
2. Loss of product due to leakage: High fuel and energy costs as a result of leakage of steam, fuel, water, compressed air, or process fluid that absorbed energy.
3. Possible impact on the environment: If the leaking fluid is corrosive in nature, it will attack its surroundings, and if lethal or poisonous, it will create hazards and environmental problems. Discharge of copper and chromate-treated water is severely regulated to conserve aquatics and biosphere.

4. Lost production as a result of a failure.
5. High maintenance costs.
6. Warranty claims on corroded equipment and the consequent loss of customer confidence, sales, and reputation.
7. Contamination and loss of product quality, which can be detrimental to the product, such as foodstuffs, soap products, discoloration with dyes, etc.
8. Extra working capital to carry out maintenance operations and to stock spares to replace corroded components.
9. Overdesign: In many instances, when the corrosive effect of a system is known, additional thickness to components is provided for in the design. This is known as corrosion allowance and involves additional material cost and extra weight of new units.
10. Highly corrosive fluids may require the use of expensive materials such as titanium, nickel-base alloys, zirconium, tantalum, copper–nickels, etc. The use of these materials contributes to increased capital cost.
11. Damage to adjacent equipment and the system components.

1.2 Corrosion Mechanism

According to electrochemical theory, the combination of anode, cathode, and aqueous solutions constitutes a small galvanic cell (Fig. 1), and the corrosion reaction proceeds with a flow of current in a manner analogous to the way current is generated by chemical action in a primary cell or in a storage battery on discharge. Due to the electrochemical action, the anode is dissolved. For a current to flow, a complete electrical circuit is required. In a basic corroding system as shown in Fig. 1a, the circuit is made up four components:

1. Anode
2. Electrolyte
3. Cathode
4. An external circuit

1. Anode: The anode is the electrode at which oxidation (corrosion) takes place and current in the form of positively charged metal ions enters the electrolyte. At the anode, the metal atom loses an electron, oxidizing to an ion.
2. Electrolyte: The electrolyte is the solution that surrounds, or covers, both the anode and the cathode. The conductivity of the solution is the key to the speed of the corrosion process. A solution with low conductivity produces a slow corrosion reaction, while a solution with high conductivity produces rapid corrosion [1]. In the total absence of an electrolyte little or no corrosion takes place. For example, iron exposed to dry desert air remains bright and shiny since water necessary to the rusting process is not available, and in arctic regions no rusting is observed because ice is a nonconductor [2]. The electrolyte need not be liquid. It can be a solid layer also. For example, at elevated temperatures, corrosion of a metal can occur in the absence of water because a thick metal oxide scale acts as the electrolyte (Fig. 2). The surface metal oxide is the cathode, and the metal oxide and metal interface are the anode [2].
3. Cathode: The cathode is the electrode at which reduction takes place and current enters from the electrolyte.
4. External circuit: If there are two pieces of metal, they must either be in contact or have an external connection in order for the corrosion to take place. The external circuit is a metallic path between the anode and cathode that completes the circuit. Where the anode and cathode are on the metal surface, as shown in Fig. 3, the metal itself acts as the external circuit.

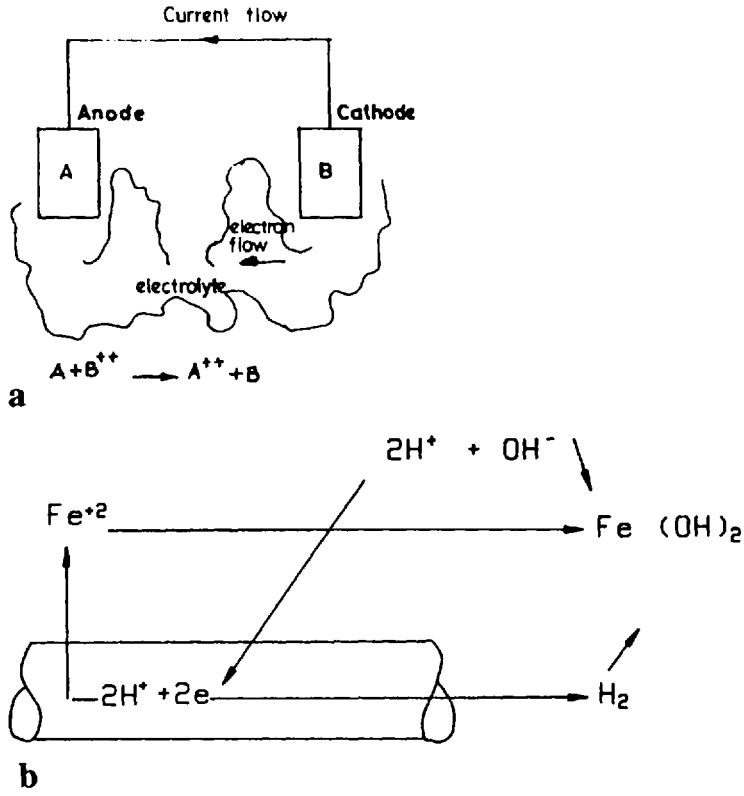


Figure 1 Corroding system. (a) Basic corroding system (From Ref. 6); and (b) corrosion of iron in water (From Ref. 3.)

Basic Corrosion Mechanism of Iron in Aerated Aqueous System

The corrosion principle is explained by the basic corrosion mechanism of iron in an aerated aqueous system (Fig 1b). In its simplest form, this reaction consists of two parts: (1) the dissolution of iron at the anode, and (2) cathodic reaction in the absence of oxygen is or the reduction of oxygen to form hydroxyl ions at the cathode: Hence, the overall theoretical corrosion reaction becomes

$$Fe = Fe^{+2} + 2e^{-} \tag{1}$$

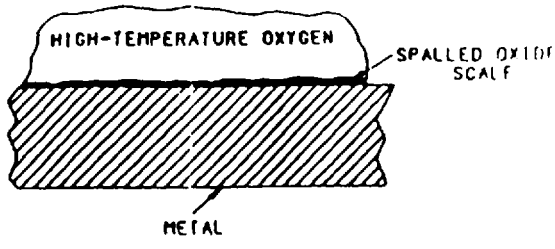


Figure 2 Thick metal oxide scale as the electrolyte. [From Roger Pludek, *Design and Corrosion Control*, The Macmillan Press Ltd., London (1977).]

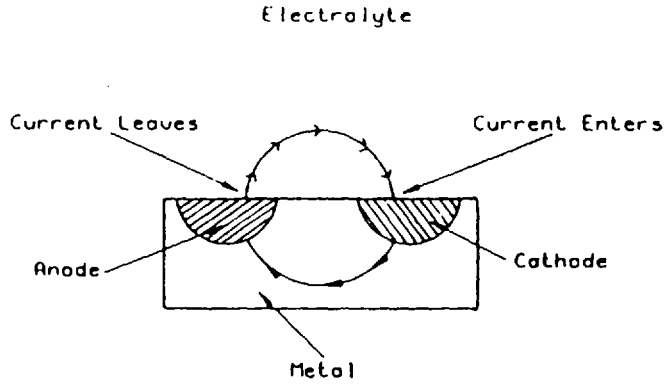


Figure 3 Anode and cathode on the same metal surface. (From Ref. 6.)

$$2H^{+} + 2e^{-} \rightarrow H_2 \tag{2}$$

$$\frac{1}{2}O_2 + H_2O + 2e^{-} = 2OH \tag{3}$$

$$Fe + \frac{1}{2}O_2 + H_2O = Fe^{+2} + 2OH^{-} \tag{4}$$

followed by

$$Fe^{+} + 2OH^{-} \rightarrow Fe(OH)_2 \tag{5}$$

In practice, however, these reactions are much more complex. The rate of corrosion is governed by the rate of either the cathodic reaction or anodic reaction or less frequently by the electrical resistance of the electrolyte [2]. When the anodic reaction is severely limited by films that form on the metal surface, as in the case of stainless steels, the metal is called passive.

1.3 Forms of Electrochemical Corrosion

Various forms of electrochemical corrosion are the (1) bimetallic cell or dissimilar electrode cell, (2) concentration cell, and (3) differential temperature cells.

Bimetallic Cell

In a bimetallic cell, two dissimilar metas are in contact and are immersed in an electrolyte. The farther the two metals are apart in the electromotive series, the more severe is the corrosion. Bimetallic corrosion also takes place when a metal is nonhomogeneous. One part of a metallic structure may be anodic to another part if it is not exactly the same alloy. A bimetallic cell is also known as a dissimilar electrode cell.

Concentration Cell

A concentration cell is produced in an identical electrode, in contact with an electrolyte of differing concentration. The area of metal in contact with the dilute solution will be anodic and it will corrode. It is often called crevice corrosion because a crevice acts as a diffusion barrier and corrosion occurs most often within a crevice. There are mainly two kinds of concentration cell, as shown in Fig. 4: (1) the salt concentration cell, formed due to differences in concentration of the salt in the electrolyte (Fig. 4a), and (2) the differential aeration cell, where the oxygen concentration varies on the electrode surface, with the anodic area being the one

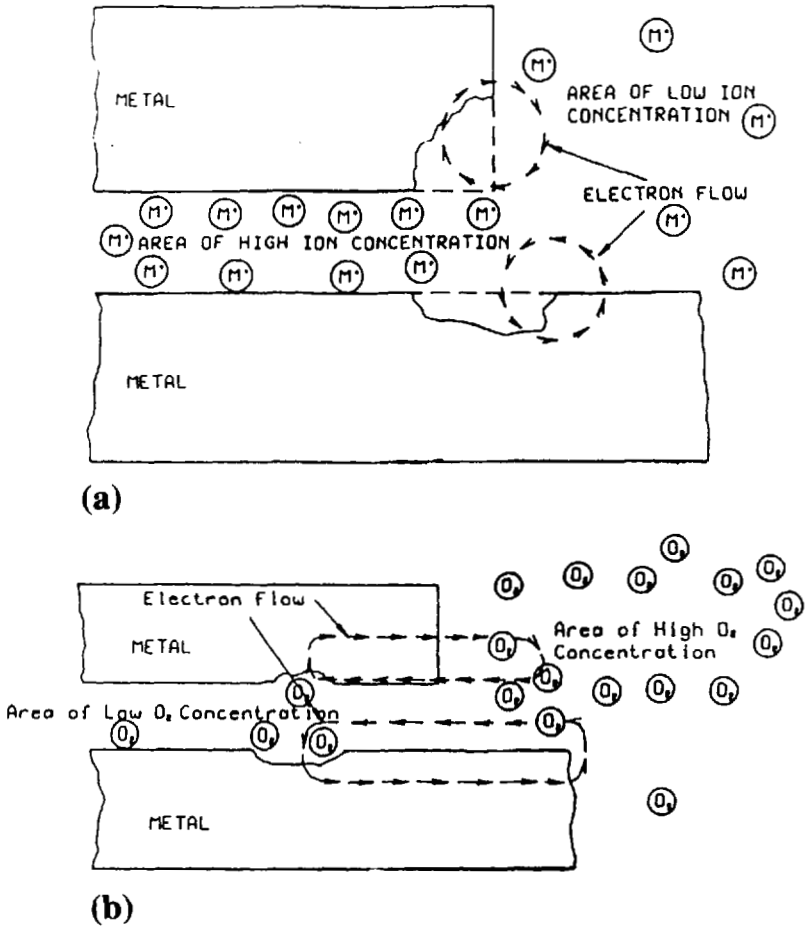


Figure 4 (a) Salt concentration cell; and (b) oxygen concentration cell. (From Ref. 3.)

having lower oxygen concentration (Fig. 4b). Such cells account for localized corrosion of metals at crevices formed by overlapping joints, threaded connections, or by microorganisms growing on metal surfaces [2]. The shielded area tends to be low in dissolved oxygen concentration and hence become anodic to the outside area with higher oxygen concentration.

Differential Temperature Cells

Components of these cells are electrodes of the same metal, each of which is at a different temperature, immersed in an electrolyte of the same initial composition. The surfaces at higher temperatures are generally anodic with respect to cooler ones.

1.4 Corrosion Potential and Corrosion Current

The driving force for current and corrosion is the potential developed between the metals. When no current flows between the anode and cathode, the potential difference between them is at a maximum known as the open circuit potential. The current that flows between the anode and cathode when a metal corrodes in an electrolyte is called the corrosion current, and the net potential of the corroding surface is the corrosion potential.

1.5 Corrosion Kinetics

The preceding discussion deals with the criteria leading to the formation of an electrolytic cell, which is the essential step in the corrosion process. However, the potential difference of the galvanic couple can change with time. As corrosion progresses, corrosion products may accumulate at the anode, cathode, or both. This reduces the speed at which corrosion proceeds. The phenomena affecting the corrosion kinetics are referred to as polarization and passivation. These two phenomena are also extremely important in the preventive measures that can be used for corrosion control.

Polarization Effects

The phenomenon that controls the rate of corrosion reaction is known as polarization, which is the ease with which anodic and cathodic reactions take place. The principle of polarization effects is as follows. As soon as current begins to flow through an electrolytic cell, it produces chemical changes at the electrodes, and these changes tend to set up a new voltaic cell with a voltage in the opposite direction to that of the main cell voltage. This new countervoltage is known as polarization, and it always opposes the main voltage of the cell; it never reinforces it. In simple terms, due to polarization the potentials of the metals in a corrosion cell tend to approach each other. The decrease in anode potential is anodic polarization, and the decrease in cathode potential is cathodic polarization. This reduced voltage can drive less additional current through the cell. It is not always true that both anodic and cathodic polarization will take place to the same extent. In some cases, greater polarization is at the anode and in other cases at the cathode. In the former case, the reaction is said to be anodically controlled. In the latter case, it is said to be cathodically controlled.

Polarization in Iron–Water System. In the iron–water system, the reaction is cathodically controlled because hydrogen ions are available in small quantity. In other words, cathodic polarization limits the rate of reaction [3]. Oxygen is a depolarizer because it decreases the slope of one of the lines, thereby increasing the corrosion current and, in this reaction, the amount of corrosion. A little consideration of this will indicate the importance of polarization in limiting corrosion rate without it reaching an infinite value, which would have been the case in the absence of any polarization. It can take the form of slow ion movement in the electrolyte, slow combination of atoms to form gas molecules, or slow solvation of ions by electrolyte [1].

Factors Affecting Polarization. The degree of polarization is variable; some corrosion reactions proceed rapidly owing to high spontaneity and low polarization, and others proceed very slowly owing to high polarization even though they have a pronounced tendency to corrode as shown by reversible emf of the corrosion cell [4]. Factors affecting polarization include the following [1]:

1. Increasing the reaction area allows the corrosion to take place more readily and hence lowers the rate of polarization.
2. Agitation or electrolyte movement carries away the products of corrosion reaction from the surface and thereby provide a maximum number of ions contacting the electrodes, thus increasing the rate of corrosion and decreasing the polarization. On the other hand, if the cathodic reaction is activation controlled, agitation would have no effect on the corrosion rate.
3. Oxygen effectively depolarizes the electrode or makes the reaction go more rapidly by removing the reaction product atomic hydrogen.
4. Increasing the temperature increases the rate of most reactions, and therefore lowers the polarization rate.

Polarization Diagrams. Plots of anode and cathode potential versus current flow (E_p vs. I) are called polarization diagrams. By plotting current density on a logarithmic scale, the polarization lines will be linear, in accordance with the Tafel equation. These diagrams are also called Evans diagrams, after one of the founders of corrosion science, Ulick Evans. Idealized polarization diagrams are shown in Fig. 5. Figure 5a shows a polarization diagram for a cathodically controlled corrosion cell. A polarization diagram for a passive metal anode is shown schematically in Fig. 5b, and it can be seen from this figure that it does not polarize along a straight line as shown in an idealized diagram, but follows an S-shaped curve. The electrochemical behavior of active–passive transitions is illustrated by such curves. Figure 5c shows a polarization diagram for an anodically controlled corrosion cell. Such diagrams can be used to show the effects of cathodic polarization by hydrogen, and anodic polarization by accumulated metal ions and corrosion products. In actual practice, the polarization curves would not be straight lines. The shapes of these curves will depend on the particular process responsible for the polarization [4].

Polarization Measurement. Polarization measurements on the members of a galvanic couple can provide precise information regarding their behavior, particularly the prediction of local-

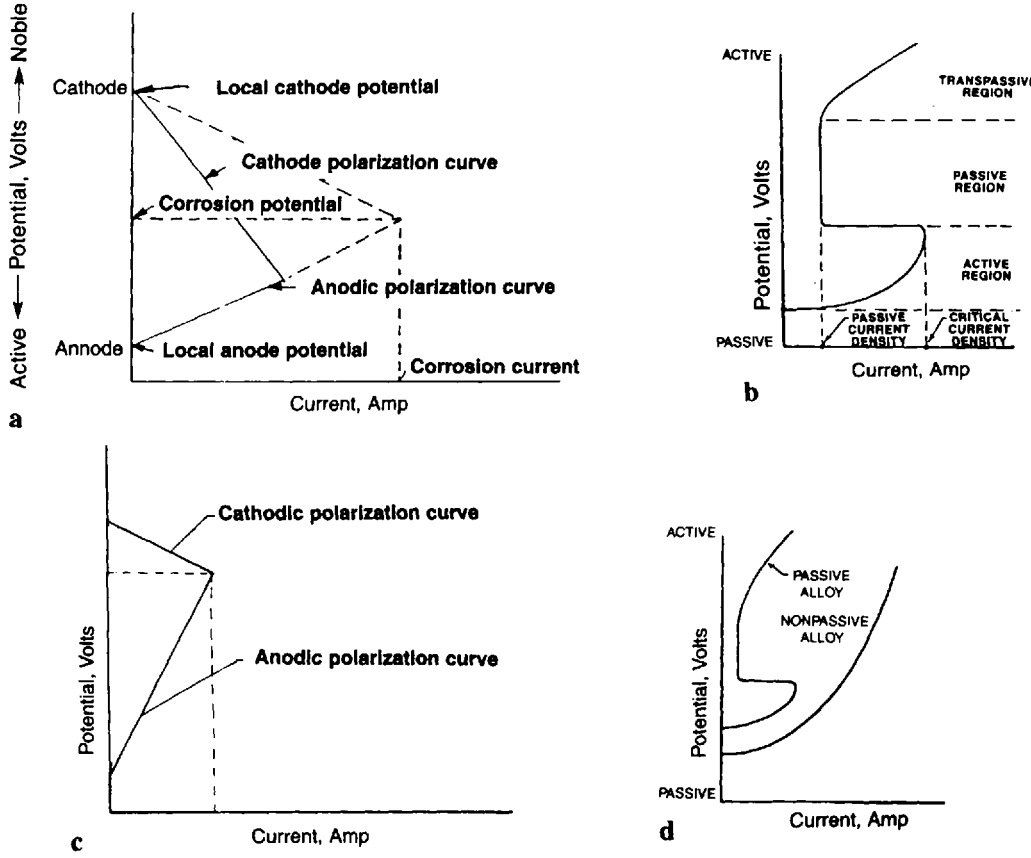


Figure 5 Polarization diagrams. (a) Cathodically controlled corrosion cell; (b) passive metal; (c) anodically controlled corrosion cell; and (d) comparison of anodic polarization curves for passive and nonpassive materials. (Items (b) and (d) are from Ref. 7.)

ized corrosion. Polarization techniques and critical potentials are used to measure the susceptibility to pitting and crevice corrosion of metals and alloys in a chloride solution [5].

Passivation

Sometimes material corrodes, producing an adherent corrosion product that protects it from further corrosion. Such (passivated) material corrodes very little in a specific environment, even though it would otherwise corrode considerably [6]. For example, a look at the galvanic series will indicate that aluminum should corrode at a high rate. In practice, however, it is found that aluminum is highly resistant to attack in most of the media except halides. This phenomenon is known as passivation. Materials such as nickel, titanium, zirconium, chromium, and stainless steel owe their corrosion resistance to natural passivation.

Passivity can be understood through a study of polarization diagrams (schematic) presented by Roser et al. [7]. The anodic polarization curves of passive alloys shown in Fig. 5b are distinctly different from those of nonpassive alloys. Comparison of anodic polarization curves for passive and nonpassive materials is shown in Fig. 5d. Passivation is a result of marked anodic polarization whereby a barrier of thin protective film, either metal oxide or chemisorbed oxygen, is formed between the metal and the environment, preventing further contact with the electrolyte. In the case of iron, when more oxygen reaches the metal surface than can be used in the cathodic reaction, a protective passive film is able to form [3]. Thus, the attainment of passivity is thus most important in avoiding accelerated corrosion. Whether a given alloy will be passive in a given situation depends on both the anodic and cathodic polarization effects.

Passive alloys are widely used as corrosion-resistant materials for the construction of heat exchangers. The corrosion resistance of passive alloys depend on the chromium content, chloride and oxygen content in the environment, and the temperature [7]. Attainment of passivity in a given situation depends on the relative value of all factors rather than on any one of them. For example, high chromium aids passivity, low temperature aids passivity, depassivating ions such as chlorides hinder passivity, and oxygen aids passivity.

Behavior of Passive Alloys. Passive material corrodes very little in a specific environment, even though it would otherwise corrode considerably [6]. Conversely, alloys that commonly exhibit passivity are invariably quite active in the nonpassive state. Some elements break down passive films, causing the metal to corrode where the film is discontinuous. Chlorine ions, for example, destroy the passivity of aluminum, iron, and the stainless steels, causing pitting corrosion. Therefore, the users of passive alloys should be particularly on guard for pitting, stress corrosion cracking, sensitization, and oxygen starvation type corrosion [7].

1.6 Factors Affecting Corrosion of a Material in an Environment

The corrosion process is affected by various parameters:

1. Environment factors such as concentration of chemicals, pH, velocity, impurities and suspended matter, and temperature of the medium.
2. Source of heat, if any. If the environment is heated through the material being selected, the effects of heat transfer and surface temperature may be the controlling factors.
3. Material factors like composition, alloying elements, passivity, tendency for fouling, etc.
4. Design conditions and geometry of the joints, like gasketed surfaces, crevices, stagnant areas, and U-bends.
5. Fabrication techniques: corrosion due to welding, brazing, soldering, and heat treatment.

Factors influencing corrosion is shown schematically in Fig. 6. Only the environmental factors are discussed next. The other factors are discussed while discussing various forms of corrosion.

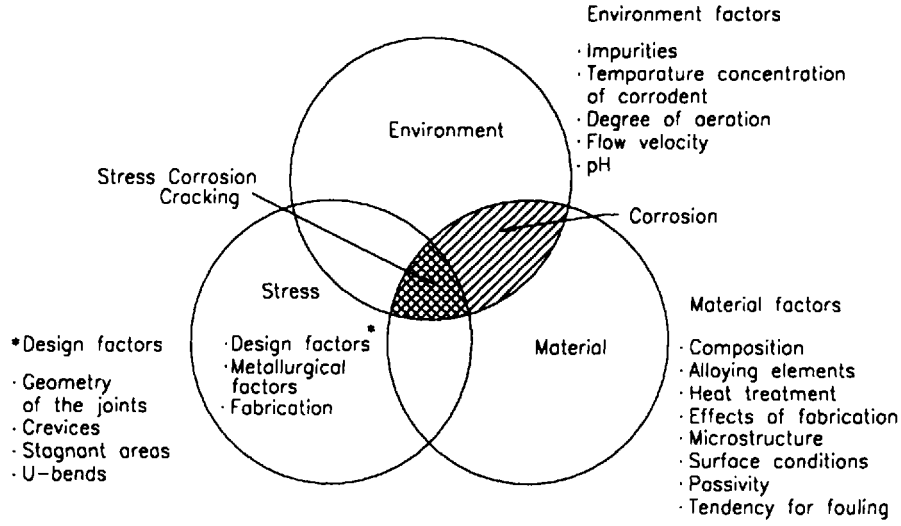


Figure 6 Factors influencing corrosion.

Environmental Factors

Environmental factors that control corrosion of a material in an environment are:

1. The presence of impurities
2. The temperature of the corrodent
3. The degree of aeration
4. Velocity of corrodent
5. Adherent deposits
6. Concentration of corrodent
7. Effects of pH

Presence of Impurities. Impurities or contaminants in the corrosive environment can cause either general corrosion or localized attack within the system, or both. The presence of even minor amounts of impurities can alter the corrosion rate significantly. For example, chlorides above 30 ppm will increase the corrosion rate of austenitic stainless steel drastically.

Temperature of the Corrodent. As a rule, the degree of corrosion increases with increase in temperature, but increasing temperature also tends to drive dissolved gases out of solution so that a reaction that requires dissolved oxygen can often be slowed down by heating [2]. There are numerous cases where metals satisfactory for cold solutions are unsuitable for the same solutions at elevated temperatures. For instance, refrigerant-quality brine can be handled by a plate heat exchanger in 18Cr-12N-2.5Mo (AISI 316) stainless steel, provided the surface temperature does not exceed 10°C (50°F). At higher temperatures, plate failure due to pitting and/or stress corrosion is inevitable.

Degree of Aeration and Oxygen Content. The design of the plant and equipment selection in particular can influence the amount of air introduced into a process stream, which in turn may have an influence on corrosion. Oxygen can behave as a depolarizer and increase the rate of corrosion by speeding up the cathodic reaction. It can also act as a passivator because it promotes the formation of a stable passive film [2]. It also must be understood that the major contributor to the corrosion of all metals in the atmosphere is oxygen.

Velocity of Corrodent. Velocity of the corrodent affects both the type and severity of the corrosion and removal of fouling deposits. Corrosion is favored by too low or too high velocities. Uniform and constant flow of process fluids past heat exchanger favors less fouling and hence less corrosion. High velocity helps to prevent the accumulation and deposition of corrosion products, which might create anodic sites to initiate corrosion, to maintain clean surfaces free from fouling deposits, avoid crevices, and stagnant areas. On the other hand, too high a velocity can destroy the protective surface film and result in erosion–corrosion, especially on metals such as copper and aluminum alloys.

Adherent Deposits. Deposits on the metal surface cause crevices. These act as sites for accelerated corrosion. Adherent deposits cause localized hot spots, which in turn contribute to high-temperature corrosion.

Concentration of Corrodent. In general, the corrosion rate increases with increasing concentration, including the concentration of the aggressive chemical species such as chloride ions. However, there are exceptions also. For example, iron is attacked vigorously in dilute nitric and sulfuric acids, but the corrosion rate is drastically reduced in concentrated acids due to passivation of the metal surfaces when once corrosion has begun.

Effects of pH. Increasing the acidity of a solution can result in a very large increase in general corrosion rate below a critical value or a range for a given alloy and environment. Since the reaction of a metal in an aqueous environment can be expressed as a simple displacement reaction

$$M + H^+ \rightarrow M^+ + H \tag{6}$$

it is evident that where a greater number of hydrogen ions (low pH) is available, the corrosive reaction should occur more rapidly. Corrosion rate versus pH is presented schematically in Fig. 7. The general shape of this curve may be considered as fairly typical for copper-base alloys. Such curves prepared for various metals and alloys could have their minima broadened or shortened, the slopes varied considerable, and the whole curve displaced in any direction, depending upon the characteristics of the alloy and the composition of the solution.

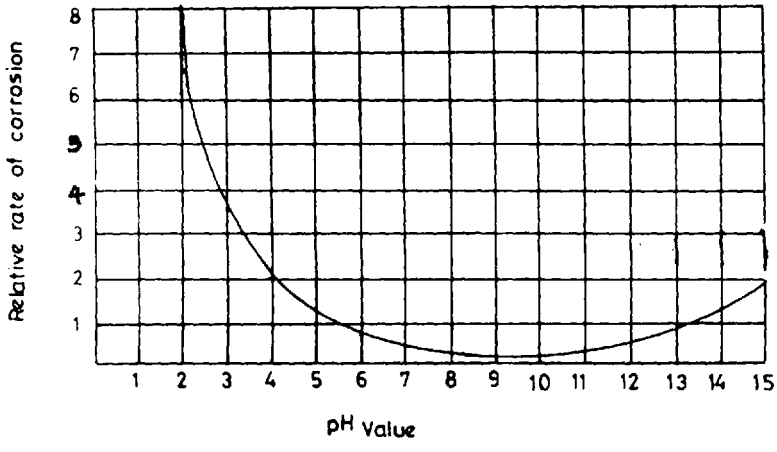


Figure 7 Corrosion rate versus pH.

2 FORMS OF CORROSION

2.1 Uniform Corrosion Versus Localized Corrosion

Corrosion attack on the metal surfaces can be either uniform or localized, where the major part of the surface of the metal remains almost unaffected while certain localized areas are attacked at a very high rate with rapid penetration into the section of the metal. Uniform corrosion occurs during the corrosion of a metal in an acid, alkali, and during the exposure of certain metals to natural environments like air, soil, etc. In general, uniform corrosion takes place when the metal and environment system is homogeneous; that is, the metal is uniform in composition and structure and the nature of the environment (composition, oxygen concentration, acidity/alkalinity), temperature, velocity, etc. are the same at all parts of the metal surface [4]. Conversely, in many metals and environment systems, due to heterogeneities in the metal or variations in the environment or both, corrosive attack may be localized. Various forms of localized corrosion are pitting corrosion, crevice corrosion, intergranular corrosion, dealloying, erosion–corrosion, etc.

2.2 Factors That Favor Localized Attack

For metals and alloys, grain boundaries, intermetallic phases, inclusions, impurities, regions that differ in their mechanical or thermal treatments, discontinuities on metal surface such as cut edges or scratches, discontinuities in oxide or passive films or in applied metallic or nonmetallic coatings, and geometrical factors such as crevices favor localized attack [4]. Localized corrosion of a metal surface due to irregularities in metals is shown in Fig. 8a [8].

2.3 Forms of Corrosion

Over the years, corrosion scientists and engineers have recognized that corrosion manifests itself in forms that have certain similarities and therefore can be categorized into specific groups. The most familiar and often used categorization of corrosion is probably the eight forms presented by Fontana and Greene [9]:

1. Uniform corrosion
2. Galvanic corrosion
3. Pitting corrosion
4. Crevice corrosion
5. Intergranular corrosion
6. Dealloying or selective leaching
7. Erosion–corrosion
8. Stress corrosion cracking

Hydrogen damage, although not a form of corrosion, often occurs indirectly as a result of corrosive attack [9]. This classification of corrosion was based on visual characteristics of the morphology of corrosion attack. Other forms of corrosion classified based on the mechanisms of attack rather than the visual characteristics are as follows:

Fretting corrosion
Corrosion fatigue
Microbiologically influenced corrosion

General corrosion takes place uniformly over a broad area. In galvanic corrosion, two dissimilar metals form a galvanic couple, and the less noble metal in the couple corrodes. Pitting is the localized attack that produces small pits, which may penetrate the metal thickness.

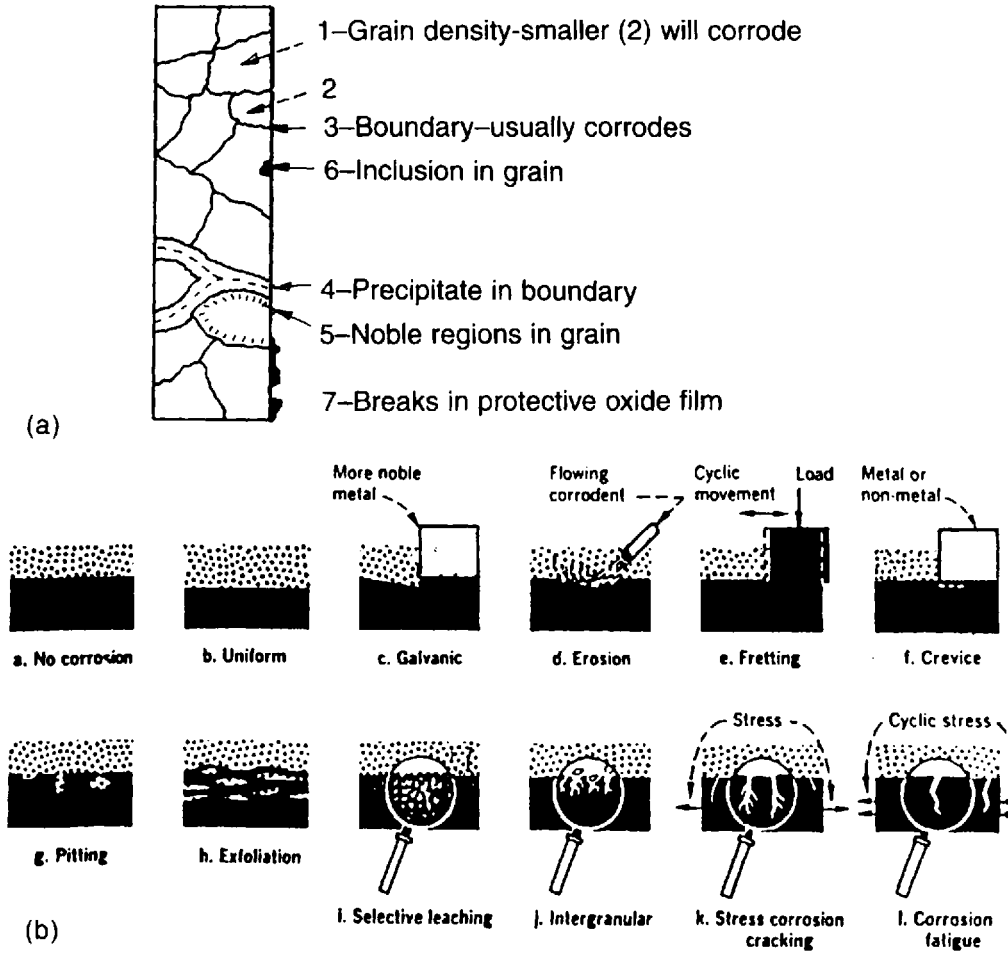


Figure 8 Localized corrosion. (a) Factors influencing localized corrosion of a metal [8]; and (b) forms of localized corrosion [28].

Crevice corrosion is another form of localized corrosion and takes place under crevices or deposits. Intergranular corrosion takes place at grain boundaries in weld metal or in heat-affected zones of sensitized metals. In dealloying, an alloying element is preferentially corroded over others from the parent alloy, leaving behind a weak structure. Erosion–corrosion is a localized corrosion that occurs mostly on the tubeside, in areas where the turbulence intensity at the metal surface is high enough to remove the protective surface film. Stress corrosion cracking results when the corrosive action of a suspectible metal and the tensile stress combine in a particular environment. Corrosion may combine with other forms of attack, such as fatigue, to produce severe damage. Corrosion fatigue is the reduction in the fatigue strength of a metal exposed to a corrosive environment. Various forms of corrosion are discussed in detail in the following sections.

Uniform or General Corrosion

Uniform corrosion is the most common form of corrosive attack on metals and nonmetals. It refers to the corrosion process dominated by uniform thinning and proceeds without apprecia-

ble localized attack. Uniform corrosion is also referred as general corrosion. Uniform corrosion results from prolonged contact with environments such as atmosphere, water, acids, alkalies, soil, etc. It is manifested by a chemical or electrochemical reaction. Uniform corrosion of the metal surface, as in the rusting of iron, results from anodes and cathodes rapidly interchanging sites at random; should the anode become fixed on the surface, a localized pitting corrosion will result instead [2]. Like other forms of corrosion, many factors influence general corrosion. The corrosive media is the most important factor governing corrosion. Environmental factors such as acidity, temperature, concentration, motion relative to metal surface, degree of oxidizing power and aeration, and presence or absence of inhibitors influence general corrosion [3].

Forms of Uniform Corrosion. Most general types of uniform corrosion are atmospheric corrosion and high-temperature (gaseous) corrosion. Although high-temperature attack in gaseous environments may manifest itself as various forms of corrosion, it has been incorporated into the category "general corrosion" because it is often dominated by uniform thinning [10]. Biological corrosion can manifest itself in a general or a localized form. It is covered at the end of this section.

Atmospheric Corrosion. Atmospheric corrosion is defined as the corrosion of a material exposed to the air and its pollutants rather than immersed in a liquid. Many variables influence the atmospheric corrosion. Relative humidity, temperature, contents like sulfur dioxide, hydrogen sulfide, and chloride, amount of rainfall, dust, etc. influence corrosion behavior. Therefore, in an arid atmosphere, free of contaminants, only negligible corrosion would be expected. It also must be understood that the major contributor to the corrosion of all metals in the atmosphere is oxygen.

Types of Corrosive Atmospheres. A common practice is to divide atmospheres into categories such as rural, industrial, marine, and indoor [11]. Most of them are mixed and present no clear lines of demarcation, and the type of atmosphere may vary with the wind pattern, particularly where corrosive pollutants are concentrated. Except for severe marine environments, there is no need to protect against atmospheric corrosion except with protective coatings [12].

Protection Against Atmospheric Corrosion. Important considerations to protect against atmospheric corrosion should involve [12] (1) specific plant environment around the equipment, (2) operating temperature, and (3) protection against ingress of rain water into crevices. Merrick discusses these factors in detail [12].

The specific plant environment around the equipment that involves releases of corrosive gases, such as hydrogen sulfide, sulfur dioxide, or ammonia, from nearby process plant will significantly increase atmospheric corrosion of equipment.

The operating temperature of the pressure vessels and heat exchangers has a significant effect on atmospheric corrosion. Units that operate below the dew point experience more corrosion than those operating at higher temperatures.

For protection against ingress of rain water into crevices, saddles and reinforcing pads for supports should be continuously welded to the vessel. Partial welding or stich welds will act as a crevice. This will permit the ingress of rain water between the saddle and the vessel and can accelerate crevice corrosion.

Control of Uniform Corrosion. Uniform corrosion can be easily predicted and controlled by

Proper material selection
Small alloying additions to the base metal
Cathodic protection using sacrificial anodes
Use of inhibitors
Surface coatings

Adding extra material known as corrosion allowances. Although uniform corrosion is obviously detrimental it is least predictable, and corrosion allowances for losses are frequently made in the design of equipments. For corrosion-resistant materials, in general no corrosion allowance is given.

Rating of Metals Subject to Uniform Corrosion. In contrast to localized forms of corrosion, uniform corrosion is rather predictable. The uniform attack on an entire area exposed to a corrosive environment is usually expressed in terms of an average loss of metal thickness for a given period of time in units of mils (1 mil = 1/1000 in) per year (mpy), inches per month (ipm), or millimeter per year (mm/yr). Rating of various materials against uniform corrosion is given in Table 1.

Determination of General Corrosion. General corrosion is determined by immersion tests conducted according to ASTM G-31. Eight different boiling acid and alkali solutions—20% acetic acid, 45% formic acid, 10% oxalic acid, 20% phosphoric acid, 10% sodium bisulfate, 50% sodium hydroxide, 10% sulfamic acid, 10% sulfuric acid—are used to compare the performance of different alloys in a variety of solutions rather than to simulate a particular process industry environment. Duplicate samples are exposed for five 48-h periods and an average corrosion rate is determined.

Material Selection for General Corrosion. Of the various forms of corrosion, general corrosion is the easiest to evaluate, and hence the material selection is straightforward; if a material shows only a general and uniform attack, a corrosion rate, 0.25 mm/yr (10 mils/yr) or less for low-cost material such as carbon steel, a negligible contamination of the process fluids, and availability, ease of fabrication etc., then that material favors the choice of selection. For more costly materials such as the 300 series austenitic stainless steels and copper-and nickel-base alloys, a maximum corrosion rate of 0.1 mm/yr (4 mils/yr) is generally acceptable [14].

Galvanic Corrosion

When two dissimilar metals or alloys placed at different positions in electromotive series are in contact with each other in a electrolyte, a galvanic couple is formed and results in corrosion of one of the metals, known as the anode of the couple. In other words, galvanic corrosion does not affect the cathode, which is known as a noble metal. This form of corrosive attack is known as galvanic corrosion since the entire system behaves as a galvanic cell. Galvanic corrosion can also take place even within the same group of metals due to local imperfections or hetrogenities on the metal surfaces or due to variation in local solution chemistry. Most often, galvanic corrosion shows up as furrows or troughs on the corroded metal at its point of contact with the more noble metal. For initiation of galvanic corrosion four essential components are required: the anode, the cathode, the electrolyte, and a metallic path between the

Table 1 Rating of Metals Against Uniform Corrosion

Corrosion Rate	Rating	Applications
<5 mpy	Excellent	Very critical
5–20 mpy	Satisfactory	Critical
20–50 mpy	Useful	Noncritical
>50 mpy	Unsatisfactory	None

mpy = mil per year.
Source: Ref. 13.

anode and cathode, which completes the circuit. These four basic components were already discussed.

Heat Exchanger Locations Susceptible to Galvanic Corrosion. Components such as tube sheets, water box, bolts and flanges, and supports made of less noble metals will corrode at the following locations:

Interfaces between the tube and baffle plates
Between the tubes and tube-sheet areas
Welded joints, brazed joints, and soldered joints
Heat exchanger supports with the frame or shell bolts and fasteners if they are less noble than the flange materials

In seawater-cooled condensers, tube materials such as copper-nickels, stainless steels, or titanium are more noble than tube-sheet materials such as Muntz metal, naval brass, or aluminum bronze; consequently, the tube sheets may suffer galvanic attack when fitted with more noble tube materials. This is also true with tubes made of seawater resistant stainless steels like superferritics and superaustenitics used to replace the copper alloy tubes in a Muntz metal tube-sheet. Similarly, a cast iron water box may suffer galvanic attack because all other materials in the condenser are more noble than cast iron. In general, weld metal corrosion can be eliminated by using suitably balanced electrode; the remaining problems are discussed in the section on weld-metal corrosion. Brazed joints are always at risk to galvanic corrosion because the fillers are invariably of different composition than that of the parent metals being joined. Fortunately, these fillers are normally noble than the metals being joined and hence the corrosion problem is not faced. Corrosion of brazed joints and corrosion of soldered joints are discussed in detail in Chapter 15, Heat Exchanger Manufacture, in the second part, Brazing and Soldering.

Galvanic Corrosion Sources. Two important sources of galvanic corrosion are (1) metallurgical sources and (2) environmental sources.

Metallurgical Sources. Metallurgical sources are within the metal and/or in relative contact between dissimilar metals. Such sources include difference in potential of dissimilar materials, distance apart in galvanic series, relative areas of anode and cathode, oxide or mill scales, strained metal (cold work), inclusions in metal, and differences in microstructure, heat affected zone (HAZ), and sensitization [15,16].

Environmental Sources. Environmental sources include conductivity of the fluid, concentration differences in solution, changes in temperature, velocity and direction of fluid flow, aeration, and ambient environment (seasonal changes) [15].

Types of Galvanic Corrosion. Among the various forms of electrochemical corrosion, (1) bimetal corrosion, (2) differential aeration corrosion, (3) differential concentration corrosion, and (4) work area corrosion belong to galvanic corrosion [17]. Items 1–3 have been discussed earlier. Only work area corrosion is defined here.

When a metal is cold worked so that it is denser in one place than another, a corrosion cell with the stressed area as an anode and the remaining area as cathode is set up if these two areas are immersed in an electrolyte [17]. This is called work area corrosion.

Magnitude of Galvanic Effects. The discussion given earlier deals with the criteria leading to the formation of an electrolytic cell, which is the essential step in the corrosion process. However, the extent of corrosion attack taking place is dependent on many factors as follow:

1. The polarization behavior of the metals or alloys
2. Passivation of the alloys

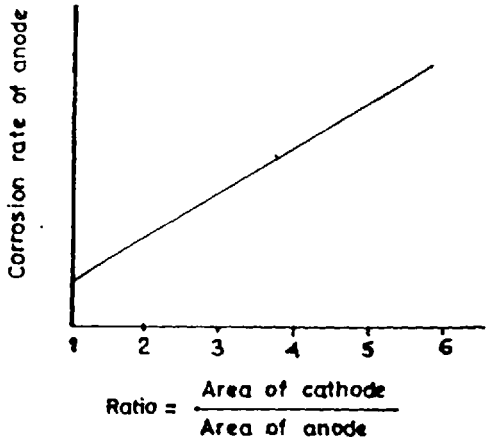


Figure 9 Galvanic corrosion due to area effect.

3. Potential difference between the metals or alloys, that is, the distance effect
4. Area effect, that is, the geometric relationships such as relative surface area

Items 1 and 2 have been discussed earlier and the remaining points are discussed next.

Distance Effect. Enhanced corrosion takes place when the metals in galvanic couple are placed further apart in the galvanic series. This is due to high electrochemical current density. In some cases, the separation between the two metals or alloys in the galvanic series gives an indication of the probable magnitude of the corrosive effect.

Area Effect. Another important factor in galvanic corrosion is the area effect. As the ratio of the cathode to anode area increases, the corrosion rate of the anode metal is rapidly accelerated (Fig. 9). On the other hand, if the area of anode is large compared to the cathode area, the corrosion of the anode is so widely distributed that the amount of metal loss in terms of its thickness may be so small that it may be ignored. These observations suggest the well-established rule in corrosion engineering that when dissimilar metals are coupled, the anode area must be maintained as large as possible compared to cathode area. For example, the nuts and bolts that are critical to the flanged joints must always be noble (cathodic) to the larger area of the flange. The nuts and bolts (Fig. 10) corrode at a rate well below normal at the

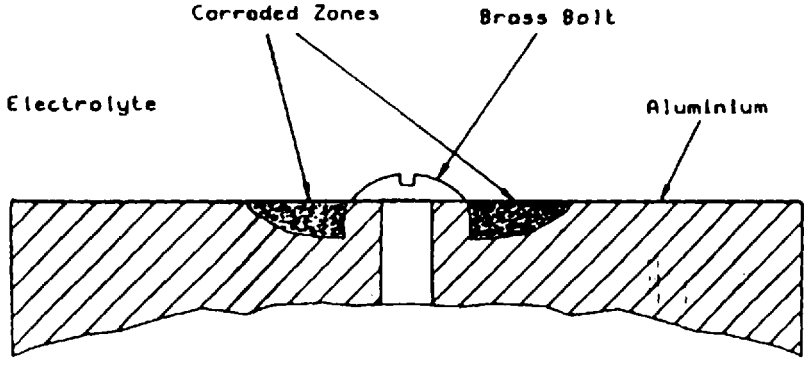


Figure 10 Nuts and bolts (cathodic) in a flanged joint (anodic). (From Ref. 3.)

negligible expense of the flange, which corrodes at only slightly above normal rate over a large area.

Tools to Determine the Degree of Galvanic Corrosion. The degree of galvanic corrosion is normally known from the following two tools. They are the electromotive force (emf) series and the galvanic series.

Electromotive Force (EMF) Series. The electromotive force series is a list of elements arranged according to their standard electrode potentials, with the sign being positive for elements whose potentials are cathodic to hydrogen and negative for those anodic to hydrogen. In this listing, hydrogen is used as an arbitrary reference element, and metals such as gold and platinum have large positive values indicating little tendency for corrosion attack. Since the emf series is of little value to the practical corrosion scientist or technologist, it is necessary to develop some alternate system by which the relative corrodibility of a galvanic couple may be assessed [4]. Such a listing is known as the galvanic series.

Galvanic Series. Whether a given metal or alloy is naturally anodic or cathodic with respect to another metal is judged by the galvanic series, which consists of an arrangement of metals and alloys in accordance with the measured potentials in flowing seawater at velocities ranging from 2.5 to 4 m/s. A typical tabulation is given in Table 2. With certain exceptions,

Table 2 Galvanic Series in Seawater at 25°C (77°F)

Anodic (least noble) end or active end	Cartridge or yellow brass C27000
Magnesium	Admiralty brass C44300, C44400, C44500
Zinc	Aluminum bronze C60800, C61400
Galvanized iron	Red brass C23000
Aluminum alloy 5052H	ETP copper C11000
Aluminum alloy 3004	Silicon bronze C65100, C65500
Aluminum alloy 3003	Copper–nickel, 10%
Aluminum alloy 1100	Copper–nickel, 30%
Aluminum alloy 6053T	Nickel 200 (passive)
Alclad aluminum alloys	Inconel alloy 600 (passive)
Aluminum alloys, 2117	Monel alloy 400
Aluminum alloys, 2017T	Stainless steel type 410 (passive)
Aluminum alloys, 2024T	Stainless steel type 430 (passive)
Low-carbon steel	Stainless steel type 304 (passive)
Low-alloy steel	Stainless steel type 316 (passive)
Cast iron	E-Brite alloy
Stainless steel type 410 (active)	AL-29-4C alloy
Stainless steel type 430 (active)	AL-6XN alloy
50-50 Lead–tin solder	Inconel alloy 825
Stainless steel type 304 (active)	Inconel alloy 625, alloy 276
Stainless steel type 316 (active)	Hastelloy alloy C
Lead	Silver
Tin	Titanium
Muntz metal C28000	Graphite
Manganese bronze A—C67500	Zirconium
Naval brass: C46400, C46500, C46600, C46700,	Tantalum
Nickel 200 (active)	Gold
Inconel alloy 600 (active)	Platinum
Hastelloy alloy B	Cathodic (most noble) end

Source: Adapted from Refs. 3, 13, and 18.

this series is broadly applicable in other natural waters and in uncontaminated atmospheres. The galvanic series allows one to determine which metal or alloy in a galvanic couple is more active. The metals closer to the active end of the series will behave as the anode and will corrode, whereas those closer to the noble end will behave as the cathode and will be protected. The metals and alloys that are next to each other have little tendency to galvanic corrosion when connected together, so it is relatively safe to use such combinations in jointed assemblies.

Galvanic Corrosion Control. Design is a major factor in preventing or minimizing galvanic corrosion. Typical measures to control galvanic corrosion are:

1. Choose the combination of metals as close together as possible in the galvanic series, unless the more noble metal is easily polarized.
2. Avoid the unfavorable area effect, that is, small area of anode and a large cathode area. Otherwise small components such as bolts and fasteners should be of more noble metal.
3. Insulate or break the circuit between the two metals by applying coatings, introducing gaskets, nonmetallic washers, etc., and make sure that metal-to-metal contact is not restored in service.
4. Add corrosion inhibitors to decrease the aggressiveness of the environment or to control the rate of cathodic and/or anodic reaction.
5. Maintain coatings. Coating is the most common method for combatting corrosion.
6. Cathodic protection is one of the recommended methods of protecting the anode. Use a sacrificial anode such as Zn, Al, or Mg that is anodic to both the structural metals. Examples include sacrificial cladding (Alclad) applied in the internal aluminum tube surfaces of radiators to give protection to the tube core alloy, and planting of Zn anode on the water box of condensers to protect both the tubes and the tube-sheet. It is important to note that overprotection of the titanium tube-sheet may result in the hydriding of the titanium tubes.

Pitting Corrosion

Instead of a uniform corrosion in a corrosive environment, a metal very often suffers localized attack resulting in pitting. Pitting usually occurs on metals that are covered with a very thin adherent protective surface film that formed on the metal surface during a surface treatment process or produced by reaction with an environment [19]. Thus, pitting corrosion occurs on aluminum, titanium, stainless steels, nickel, and their alloys, in which surface film develops. Pitting takes place when there is a breakdown of protective surface film. The protective film is an oxide layer in the case of carbon steel and ferritic stainless steel, whereas it is a passive film in the case of austenitic stainless steel. Once pits are initiated, they may continue to grow by a self-sustaining or autocatalytic process; that is, the corrosion process within a pit produces conditions that are both stimulating and self-propagating [9]. Pitting is the most aggressive form of corrosion and leads to premature failure due to perforation of the surfaces. Pitting corrosion is shown schematically in Fig. 11.

Parameters Responsible for Pitting Corrosion. Pitting corrosion is caused by factors such as [20] (1) metallurgical and structural factors, (2) environmental factors, and (3) polarization phenomena. Other causes for pitting are the attachment of microorganisms, presence of corrosion products, deposits, etc. These parameters are explained next.

Metallurgical and Structural Factors. The following metallurgical and structural factors act as nucleation sites for initiation of pitting corrosion:

1. The breakdown of passive film, mill scale [21], or applied coating.
2. Defect structures.
3. A compositional heterogeneity; inhomogeneities in the alloys caused by segregation of alloys or by cold working [7].

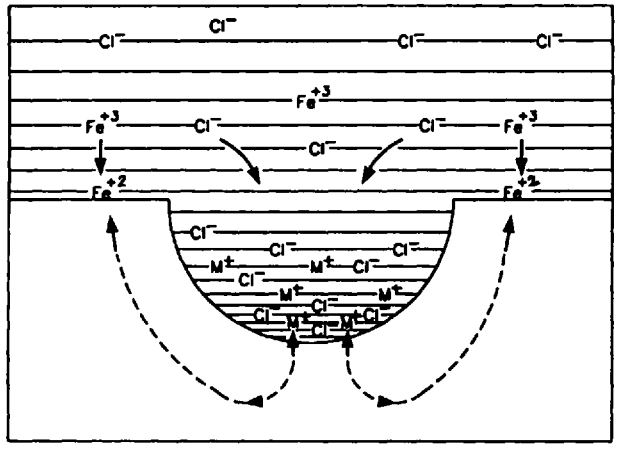


Figure 11 Schematic illustration of a growing pit. (Metal or alloy M is being attacked by a solution of ferric chloride. The dissolution reaction, $M \rightarrow M^{+} + e$ is localized within a pit and cathodic reduction of the ferric ion, $Fe^{+3} + e \rightarrow Fe^{+2}$, occurs on the rest of the exposed metal surface.) (From Ref. 3.)

4. Weld-related parameters [6]: Inclusions, multiple phases, compositional differences within the same phase, sensitization, arc strikes, spatter, and inhomogeneities in the base materials can act as potential pitting sites.

Pits develop if there is a breakdown of passive film, mill scale, or applied coatings due to high turbulence in the flow, chemical attack, or mechanical damage or under deposits. Mill scale is cathodic to steel and is found to be one of the more common causes of pitting. Figure 12 illustrates the pit action due to mill scale. A pit caused by broken mill scale becomes deeper, an oxygen concentration cell is formed by the depletion of oxygen in the pit, and this will accelerate the rate of penetration.

Studies show that the sites for initiation of pits on passive metal surfaces may be generally related to defect structures of the underlying metal such as dislocations, grain boundaries, or nonmetallic inclusions [20].

In terms of compositional heterogeneity, nonmetallic inclusions like sulfide inclusions, particularly manganese sulfides (MnS), are potential nucleation sites in austenitic stainless

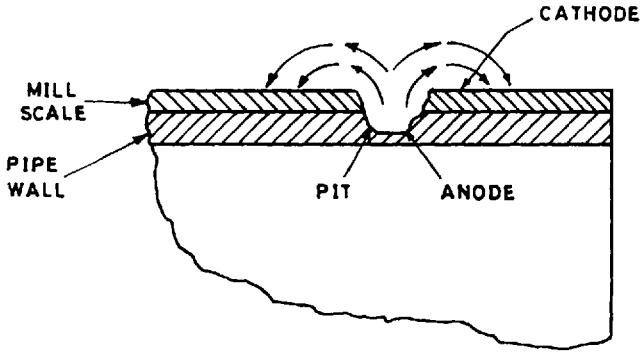


Figure 12 Pit action due to break down of mill scale. (After Ref. 21.)

steels and ferritic stainless steels. Possible ways of eliminating the MnS inclusions in austenitic stainless steels are further explained in Chapter 13, Material Selection, in the section on austenitic stainless steels.

Environmental Factors. Certain chemicals, mainly halide salts and particularly chlorides, are well-known pit producers. The passive metals are particularly susceptible to pitting in chloride environments (Fig. 11). The chloride ions accumulate at anodic areas and either penetrate or dissolve the passive film at these points. Pitting can take place on stainless steel and other alloys exposed to marine life when natural water is left after hydrotesting. In this case, the marine life dies after a period of time. Due to the sulfides produced by the dying or decaying matter, the protective oxide film or passive film on the metal surface is destroyed and pitting is initiated [1].

Influence of Polarization on Passive Alloys, After Roser et al. [7]. Pitting can occur even in a relatively homogeneous alloy due to electrochemical causes. This is explained by polarization curves as shown schematically in Fig. 13. If the cathodic polarization curve crosses the anodic polarization curve in the active region, the alloy will be active; if it crosses in the passive region, it will be passive; and if it passes in the intermediate region, the alloy will be partly active and partly passive. If the active regions are small and passive regions are large, the alloy can pit. Pitting can be avoided by either increasing or decreasing the polarization of the cathode to avoid the pitting region. Changes in alloy composition or structure can also be useful.

Attachment of Microorganisms, Presence of Corrosion Products, and Deposits. Costly pitting failures of austenitic stainless steel components and weldments can take place by attachment of microorganisms. Austenitic stainless steels form small tubercles from microbial action, under which severe pitting occurs. Or, the sulfides produced by the dying microorganisms depassivate stainless steel and pitting takes place underneath the fouling. Figure 14 illustrates the pit action due to the galvanic cell formed between the corrosion deposit and the base metal.

Basic Condition for the Initiation and Propagation of Pitting Corrosion. A basic condition must be fulfilled for the initiation and propagation of pitting corrosion: "Pitting takes place

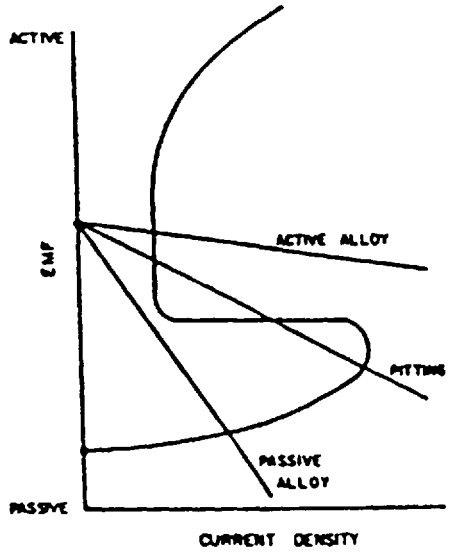


Figure 13 Polarization curves showing pitting. (From Ref. 23.)

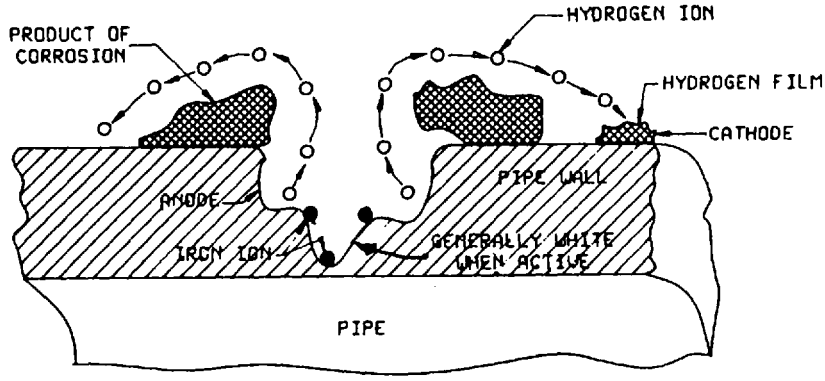


Figure 14 Pitting due to deposit (galvanic cell). (From Ref. 21.)

when the anodic breakdown potential of the metal surface film is equal to or less than the corrosion potential under a given set of conditions."

Mechanisms and Theories of Pitting Corrosion.

Nucleation and Growth. The modern theory of pitting presupposes the formation of a pit at a minute area of a metal surface that suffers a breakdown in passivity [22]. This is known as the pit nucleation stage. The passive film breakdown is followed by formation of an electrolytic cell, which leads to growth and propagation of a pit rather than to spreading along the entire surface. The anode of this cell is a minute area of active metal, and the cathode is a considerable area of passive metal [23]. The large cathode to anode area ratio accounts for the considerable flow of current with rapid corrosion at the anode. Pits once initiated can propagate inside the pits. They stop propagating if the metal is polarized to (or below) the potential of metal inside the pits, which in the extreme is that of the active (nonpassive) state [24].

Growth and Propagation of Pit. A pit develops in stages: original attack, propagation, termination, and reinitiation [19]. Termination will occur with increase in internal resistance of the local cell.

Pitting Potential. For passive metals, pits are initiated at or above a specific potential. The potential at which pit initiation occurs is called the pitting potential. Resistance to pitting increases with the pitting potential. The pitting potential is an important criterion for evaluation of the stability of a passive film in an environment. The value of pitting potential depends on the material and its composition, the environment, and the concentration of aggressive ions, pH of the solutions, temperature, and history of heat treatment operation [24]. The effects of various alloying elements on the polarization behaviour of AL-6 × N (Fe-Cr-Nt-Mo) alloy when exposed to an acid chloride solution like HCl are shown in Fig. 15. Pitting potential can be readily evaluated by lab test.

Determination of Pitting Potential. Pitting potential is determined by electrochemical techniques, which consist of measuring current and potential potentiostatically either stepwise or by applying a constant potential sweep rate in a standard chloride-containing solution. The recorded values of the current and potential are plotted. A theoretical curve obtained by electrochemical method is shown schematically in Fig. 16 [13]. From such a curve the following values are obtained and used to characterize alloys with respect to pitting and crevice corrosion: (1) pitting potential E_p where pits start to grow, (2) repassivation potential E_{rpp} below which

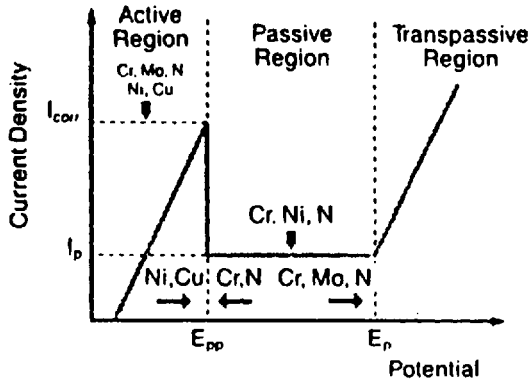


Figure 15 Schematic anodic polarization diagram for an Fe-Cr-Ni-Mo in an acid chloride solution. (From Ref. 13.) (I_p = passive current; I_{corr} = corrosion current; E_p = pitting potential; E_{pp} = repassivation potential.)

already growing pits are repassivated, and (3) critical current densities characterizing the active/passive transition.

Morphology of Pits. While the shapes of pits vary widely, they usually are roughly saucer shaped, conical, or hemispherical. If appreciable attack is confined to a relatively larger area and is not so deep, the pits are called shallow, whereas if the pit is confined in a small area, it is called deep pit. The depth of pitting is sometimes expressed by the term "pitting factor" [25]. This is the ratio of deepest metal penetration to average metal penetration as determined by the weight loss of the specimen. This is shown schematically in Fig. 17.

Detection. Pitting is usually a slow process (taking several months or years to become visible) but still can cause unexpected failures. However, the small size of a pit and the small amount of metal dissolution make its detection difficult in the early stages.

Prevention of Pitting Corrosion. Surface cleanliness and selection of materials known to be resistant to pitting in the given environment are usually the safest ways of avoiding pitting corrosion. Details of these measures are:

1. Reduce the aggressiveness of the environment, which includes the control of acidity, temperature, oxidizing agents, and chloride ions concentration [25].
2. Modify the design to avoid crevices, circulate/stir to eliminate zero velocity regions, and ensure proper drainage.
3. Systematic cleaning and elimination of stagnant areas: Since the presence of microorganisms, corrosion products, deposits, etc., stimulates pitting and, in particular, crevice corrosion in the tubes, keep the tubes clean [26].
4. Upgrade the materials of construction; chromium and nickel reduce pitting tendency very effectively, and these are often given a considerable boost with an alloy addition of molybdenum [6]. The resultant alloys are many superaustenitics highly resistant to pitting. Nitrogen improves the pitting resistance of wrought stainless steels but has the opposite effect in the weld metal, although either way the effect is fairly small compared to molybdenum [27]. Overlay with lining resistant to corrosion. Typical alternative materials that are resistant to pitting are: (a) For aqueous solutions of chlorides, choose molybdenum-containing steels such as AISI 316 or 317, or alloys containing greater amounts of chromium and molybdenum such as Hastelloy G-3, Inconel alloy 625, and Hastelloy C-22 [14], copper–

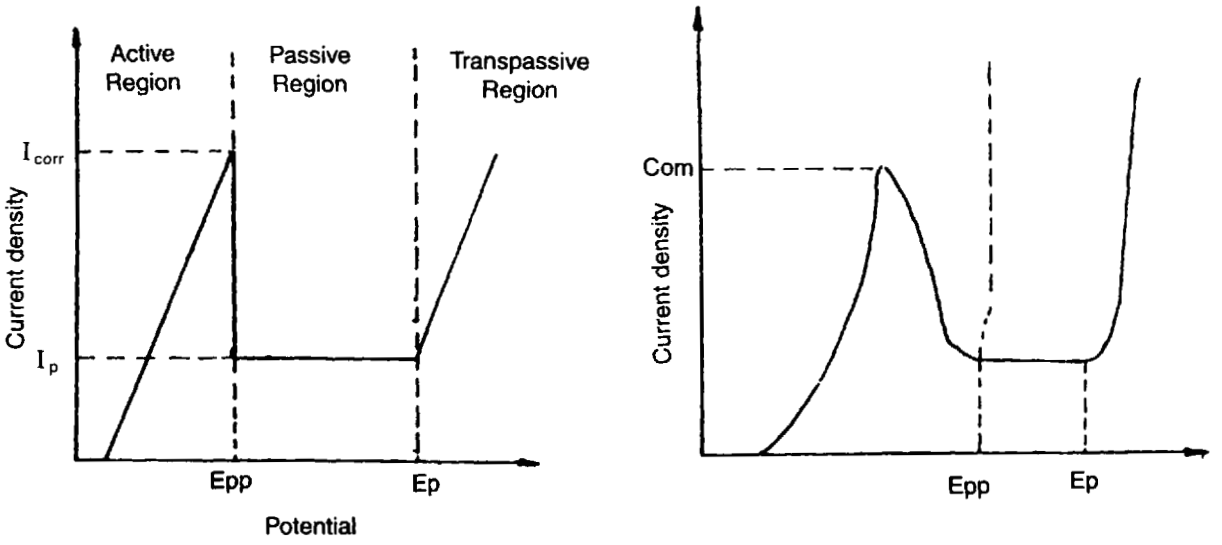


Figure 16 Pitting potential determined by electrochemical method. (a) Theoretical curve; and (b) actual curve.

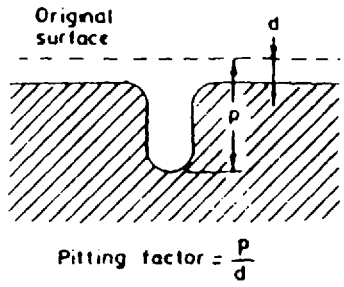


Figure 17 Pitting factor. (From Ref. 25.)

nickel, Monel, or titanium. (b) In seawater and stagnant natural water applications, use materials such as copper–nickel, aluminum bronze, inhibited admiralty brass, titanium, superferritics, and duplex stainless steels. (c) Proven lower cost nonmetallic coatings, linings, or cladding can be helpful. (d) The rating of certain stainless steel materials for pitting corrosion is discussed in Chapter 13, Material Selection, and in the section on stainless steels.

Avoid the metals and corrosive combinations that have the pitting tendencies [14]:

1. Al and Al alloys: electrolytes containing ions of heavy metals such as copper, lead, and mercury.
2. Plain carbon and low-alloy steels: waters containing dissolved O_2 or sulfate-reducing bacteria.
3. Austenitic stainless steel weldment: exposed to stagnant natural waters that are infected with iron and/or manganese bacteria.

How to Gauge Resistance to Pitting. The susceptibility of passive metals to pitting corrosion is usually investigated by experimental techniques: (1) simple immersion tests, (2) electrochemical methods, and (3) using empirical correlation for stainless steels. The methods are described next.

Critical Pitting Corrosion Temperature (CPT). The formation of visible pits in specimens exposed to aqueous chloride containing solutions, at different temperatures, is frequently used as a measure of pitting resistance. The temperature at which the pits begin to form is known as the critical pitting temperature (CPT). This is determined as per ASTM G48.

ASTM G48 is a laboratory test method for determining the resistance of stainless steels and related alloys to pitting and crevice corrosion. The method uses a ferric chloride ($FeCl_3$) solution. The concentration of ferric chloride is usually 6%, but sometimes 10% is used instead and sometimes in an acidic mixture of chlorides and sulfates [4% NaCl + 1% $Fe_2(SO_4)_3$ + 0.01 *M* HCl]. The resulting indices are known as critical pitting corrosion temperature (CPT or CPCT) and critical crevice corrosion temperature (CCT or CCCT). These are the minimum temperatures at which these types of localized attack start in the $FeCl_3$ solution. CCT is determined with crevices.

To determine the CPT, a coupon of stainless steel is exposed for 24 h in the corrosive solution at a fixed temperature and then examined visually for pits on the rolled surface (edge pits are counted). If no pits exists, the temperature is increased by 2.5°C and the coupon is reimmersed. By stepwise increase in temperature of 2.5°C, the pits initiated are to be noted for each step.

Pitting Potential. Another laboratory test that is frequently used for ranking stainless steel is pitting potentials as measured using an electrochemical apparatus in a standard chloride containing solution. The pitting potential indicates the relative susceptibility of an alloy to localized corrosion. Resistance to pitting increases with the pitting potential.

Pitting Index Number (PRE_N). Because the resistance of a stainless steel against pitting and crevice corrosion is primarily determined by the amount of chromium, molybdenum, and nitrogen in it, an index for comparing the resistance to these types of attack is often evaluated in terms of these elements. The index is called the pitting resistance equivalent number (PRE or PRE_N). It is defined, in weight percent, using the following equation:

$$\begin{aligned} PRE_N &= \%Cr + 3.3\%Mo + 16\%N && \text{for austenitic and duplex stainless steel} \\ &= \%Cr + 3.3\%Mo && \text{for ferritic stainless steel} \\ &= \%Cr + 3.3\%Mo + 30\%N && \text{for 6\% Mo superaustenitic stainless steel} \end{aligned}$$

The higher the PRE_N number, the better the performance of an alloy in chloride environments. For example the PRE number for 6% Mo superaustenitic alloys containing nitrogen is 43, Alloy 2205 has 35, while for type 316L it is 24.

Crevice Corrosion

Crevice corrosion, similar to pitting, is a localized form of corrosion that takes place at localized environments/areas that are distinctly different from the bulk environments. Such localized environments include metal-to-metal joints, metal-to-nonmetal joints such as gasketed joints, shielding by corrosion products and fouling deposits (Fig. 18), beneath biological growth, stagnant areas, and sharp corners. At these locations the crevice corrosion is usually attributed to one or more of the following [28]: (1) changes in acidity in the crevice, (2) lack of oxygen in the crevice, (3) buildup of a detrimental ion species, (4) for passive metals, the loss of passivity within the crevices, and (5) depletion of inhibitors. This leads to concentration cells or aeration cells.

Susceptible Alloys. Similar to pitting corrosion, metals or alloys that depend on protective surface film for corrosion resistance are particularly susceptible to crevice corrosion. Typical metals affected by crevice corrosion include aluminum, stainless steels, and titanium. In the

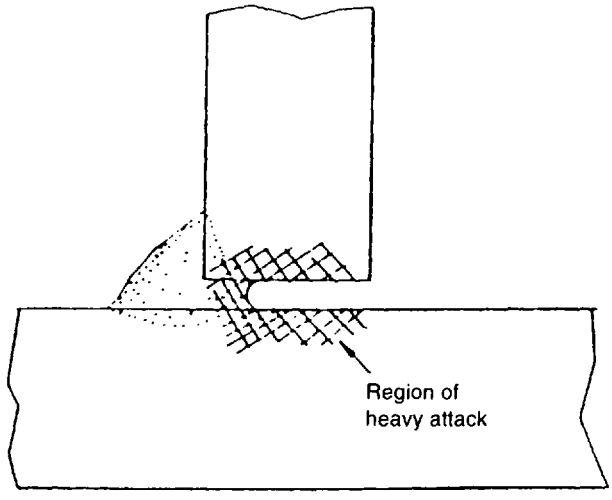


Figure 18 Crevice corrosion of a metal-to-metal welded joint.

case of passive metals like aluminum or the stainless steels, oxygen starvation within the crevice usually destroys the passive film responsible for the corrosion resistance, and forms a passive–active cell. The passive–active cell exhibits a greater potential difference and hence induces higher current than occurs within crevices formed by nonpassive metals like iron and copper [2].

Mechanism of Crevice Corrosion. Crevice corrosion takes place when a small volume of solution gets into a crack or a small opening. It stays there, stagnant, and its composition changes by the corrosion process so that its composition is different from the bulk solution. It may be oxygen depleted (oxygen concentration cell), enriched in metal ions (metal ion concentration cell), or enriched in chloride ions or at a lower pH than the rest of the solution. The corrosion rate increases as the crevice mouth narrows and as the external cathode area is increased. Crevices are particularly detrimental when alternate wetting and drying occurs, because corrosive liquids retained in the crevices are concentrated by evaporation [27,28]. To avoid crevice corrosion, the crevice must be wide open to allow the free movement of electrolyte. It usually occurs in gaps just a few micrometers wide, not in wide gaps or grooves [6].

Heat Exchanger Locations Prone to Crevice Corrosion. Areas prone to crevice corrosion in a shell and tube heat exchanger (STHE) and plate heat exchangers (PHE) are:

Shell and tube heat exchanger: clearance between the rolled tubes and the tube sheet, open welds at tube sheet, beneath deposits, water box gaskets, bolt holes, nuts, washer, disbonded water box linings, etc.

Plate heat exchanger: beneath gaskets, plate contact points, and beneath deposits.

Crevice Corrosion Versus Pitting Corrosion. The mechanism of propagation of pits and crevice corrosion is identical; however, the mechanisms of initiation differ [24]. Crevice corrosion is initiated by differential concentration of oxygen or ions in the electrolyte, whereas pitting is initiated (on plane surfaces) by metallurgical factors and structural factors only [29]. These may include discontinuities in a protective film or coating, or compositional variations such as inclusions. The level of crevice corrosion occurring at crevices such as under deposits or gaskets or at joints between two metals is significantly greater than that of pitting on open surfaces. These two forms of corrosion are compared with reference to austenitic stainless steels in Chapter 13, Material Selection and Fabrication, in the section on austenitic stainless steel.

Crevice Corrosion Control. Like all forms of localized attack, crevice corrosion does not take place in all metal and corrodent combinations. Passive metals are more susceptible to it than others. These materials can be alloyed to improve resistance to crevice corrosion. This approach, together with designing to minimize crevices and maintenance practices to keep surfaces clean, is used to overcome crevice corrosion. Various practices recommended for safeguards against the occurrence of crevice corrosion include the following:

1. Structural designs should avoid any and all crevices. This is especially true for passive metals like aluminum, stainless steels, and various nickel-base alloys. Unavoidable crevices should be filled by weld metal or with nonconducting sealants or cements [2].
2. In a new equipment, specify butt welding joints and emphasize the necessity for complete penetration of the weld metal to guard against even minute crevices.
3. During the design stage avoid sharp corners, stagnant areas, or other sites favorable to the accumulation of precipitates or wherein the solute or O_2 concentration cell takes place. For example, projection of tubes beyond the tube sheet as shown in Fig. 19 can lead to crevice corrosion. Figure 19a shows the original design with protrusion of tubes and rolling-in operation that produced a crowned tube sheet. This created crevices between

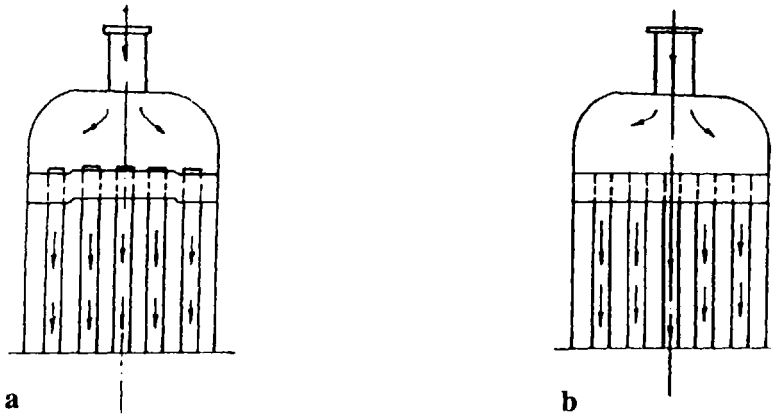


Figure 19 Projection of tubes beyond the tubesheet. (a) Original design with protrusion of tubes and rolling-in operation which produced a crowned tubesheet; and (b) absence of crevices: flat tubesheet as a result of a correct rolling-in operation.

the tubes and the tube sheet, which trapped process fluid and ultimately caused leakage due to crevice corrosion. Figure 19b shows absence of crevices, that is, flat tube sheet as a result of correct rolling-in operation.

4. Modify the design to avoid crevices—for example, rolling-in of tubes into the tube sheets instead of welding.
5. For heat exchanger tubing, a minimum velocity of 5 ft/s is recommended to keep free of deposition. Also, regular cleaning will reduce susceptibility to crevice corrosion, as well as to pitting.
6. During the design stage and operation of tubular heat exchangers, endeavor to provide uniform velocity throughout the exchanger.
7. Upgrade the materials of construction. Use a higher alloy, which offers resistance to a broader range of conditions. Nitrogen combined with molybdenum has a beneficial effect on crevice corrosion resistance in chloride-bearing, oxidizing, and acid solutions. Use materials composed of these elements. High-molybdenum steels, particularly the super-austenitic stainless steels, give good corrosion resistance. Overlaying susceptible alloys with alloy that is resistant to crevice corrosion may also help.
8. Keep the crevices wide open or shallow to allow continued entry of the bulk fluid.
9. Reduce the aggressiveness of the environment, such as acidity, chloride ions concentration, oxidizing agents, or cathodic reactants.
10. Wherever possible use solid nonabsorbent gaskets like Teflon for gasketed metal joints [9]. This prevents the entry of moisture.
11. Crevice corrosion is not initiated at a specific externally applied potential. Its propagation can be avoided by polarizing metal outside the crevice (cathode) to the potential of metal inside the crevice (anode) [24].

Prediction of Crevice Corrosion—Critical Crevice Corrosion Temperature (CCCT). Tests that establish the temperature of a ferric chloride solution at which crevice corrosion is first observed on mill-produced alloy samples with crevices, which is referred to as the critical crevice corrosion temperature (CCCT), are often used to compare the crevice corrosion resistance of various alloys. CCCT is determined as per ASTM Practice G 48 B (6% or 10% $FeCl_3$ for 72 h with crevices).

Intergranular Corrosion

A localized and preferential form of corrosion attack in a narrow region along the grain boundaries or closely adjacent regions without appreciable attack on the grains is called intergranular corrosion. Due to this form of corrosion, the metal looses its strength and metallurgical corrosion. Intergranular corrosion generally takes place because the corrodent preferentially attacks the grain boundary phase or a zone adjacent to it that has lost an element necessary for adequate corrosion resistance. The depletion of a particular alloying element along the grain boundaries is usually caused by improper heat treatment or heat from welding or any other high-temperature operation that causes the precipitation of certain alloying element at the grain boundary. Conversely, alloys that do not form second-phase microconstituents at grain boundaries, or those in which the constituents have corrosion potentials similar to the matrix, are not susceptible to intergranular corrosion. It should be noted that the problem of sensitization seldom occurs in thin sheet metal [27].

Susceptible Alloys. In austenitic stainless steels (18-8) this form of attack is most common. Other susceptible alloys include ferritic, superferritic, and duplex stainless steels. Nonferrous metals such as nickel 200 and nickel-base alloys like Inconel alloys 600 and 601, Incoloy alloys 800 and 800H, and Hastelloys B and C are susceptible to intergranular corrosion [14].

Sensitization of Austenitic Stainless Steels. During heating of austenitic stainless steels between 800 and 1500°F (450 and 815°C) while the metal is subjected to welding, heat treatment, or high-temperature exposure, chromium carbides ($Cr_{23}C_6$) are precipitated along the grain boundaries. This precipitation causes the steel to loose chromium below 11% and makes the zone susceptible to corrosion, and this is known as sensitization. Compared to the rest of the grain, the chromium-depleted region is anodic, and severe attack occurs adjacent to the grain boundary if the metal comes into contact with an electrolyte. In the extreme case, whole grains become detached from the materials, which are considerably weakened.

Intergranular Corrosion Mechanism. Intergranular corrosion is an electrochemical corrosion that takes place as the result of local cell action in the grain boundaries. A galvanic cell is formed due to potential difference between second-phase microconstituents and the depleted solid solution from which the constituents are formed. The carbide precipitate and the grain matrix are cathodic to the locally depleted grain boundary region. The high cathode to anode area ratio results in rapid corrosion of the grain boundary material and the metal disintegrates [27].

Weld Decay. During welding there will be a region of the HAZ at either side of the weld bead, which is inevitably sensitized, and these regions are susceptible to intergranular corrosion. This phenomenon is invariably termed weld decay, which is an unfortunate choice of words since, as discussed earlier, welding alone does not cause sensitization of stainless steels [27].

Control of Intergranular Corrosion in Austenitic Stainless Steel. There are three basic remedies for combating intergranular corrosion of austenic stainless steel:

1. Heat treatment. Employ a suitable high-temperature solution heat treatment, commonly known as quench annealing or solution annealing. This involves heating the steel to 1976°F (1080°C) followed by rapid cooling. High-temperature heating causes decomposition of the $Cr_{23}C_6$ and homogenization of the chromium by diffusion. Rapid cooling is necessary to prevent the reformation of the carbide.
2. Low-carbon steel. Ensure that the steel contains insufficient carbon to form $Cr_{23}C_6$ and resulting alloy depletion. Such steels contain less than 0.03% C and are called extra-low-carbon (ELC) steels, signified by the suffix L (e.g., type 304L and 316L). Type 304L

(0.03%C max), the low-carbon version of type 304, is now used extensively in applications calling for resistance to intergranular attack in the welded condition. In a similar manner, type 316L is the low-carbon version of type 316. Lowering the carbon content bellow 0.03% is normally achieved by argon oxidation process (AOD) and other modern steel melting/refining processes.

3. Stabilization. It is possible to stabilize an austenitic stainless steel, such as the 18Cr–8Ni, by adding a potent carbide-forming element such as niobium (also known as columbium) or niobium plus tantalum or titanium. These elements fix the carbon so that it is unable to form $Cr_{23}C_6$. The added elements are called stabilizers. It is usual to add titanium or niobium at about $5–10 \times$ %C in order to ensure that no chromium carbides are formed. Typical stainless steels produced by adding stabilizers are type 347 (columbium stabilized) and type 321 (titanium stabilized).

Intergranular Corrosion in Ferritic Stainless Steels. Ferritic stainless steels are susceptible to intergranular corrosion after being heated to 1700–1800°F (925–982°C) due to welding or improper heat treatment. It appears that sensitization of ferritic stainless steel occurs under a wider range of conditions than for austenitic steels. This problem is overcome by alloying with titanium and/or columbium to form the carbides of these elements.

Test for Detecting Susceptibility of Austenitic Stainless Steels to Intergranular Corrosion. ASTM A262, Standard Practices for Detecting Susceptibility to Intergranular Attack in Stainless Steels, is followed for evaluating austenitic stainless steel HAZ for sensitization. In this method, if the grain boundaries of the metallographic specimen are not preferentially attacked during etching, the material is said to be "nonsensitized." On the other hand, if a preferentially attacked microstructure is developed, other tests must be performed to confirm sensitization of the microstructure. Detailed test methods for various stainless steel grades are given in Chapter 13, Material Selection and Fabrication.

Dealloying or Selective Leaching

Dealloying or selective leaching (sometimes called parting) is a corrosion process in which an alloying element is preferentially corroded over others from the parent alloy, leaving behind a weak structure. The corrosion is detrimental largely because it leaves a porous metal with poor mechanical properties. Dealloying takes place in specific alloy and environment combinations. Combinations of alloys and environments subject to dealloying and elements preferentially removed are given in Table 3. The most common example is dealloying of zinc in brass

Table 3 Combinations of Alloys and Environments Subject to Dealloying and Elements Preferentially Removed [30]

Alloy	Environment	Element
Brasses	Waters under stagnant conditions	Zinc
Aluminum bronzes	Hydrofluoric acid, acids containing chloride ions	Aluminum
Silicon bronzes	High-temperature steam and acidic species	Silicon
Copper–nickels	High heat flux and low water velocity	Nickel
Monels	Hydrofluoric and other acids	Copper in some acids and nickel in others

(copper–zinc alloys), known as dezincification. Specific categories of the dealloying process normally carry the name of the alloying element that is selectively leached out in their titles, such as dezincification, denickelification, dealuminification, decobaltification, or desiliconification.

Factors Influencing Dealloying. Dealloying is influenced by many critical factors; in general, factors that increase general corrosion will promote dealloying. However specific accelerating factors may be further classified into one of the three categories: (1) metallurgical, (2) environmental, and (3) water chemistry. These factors are explained while discussing dezincification of brasses.

Dealloying of zinc from brass containing more than 15% Zn (e.g., yellow brass 70% Cu: 30% Zn) under conditions of slow-moving water or stagnant water or under deposits is known as dezincification. Alloys susceptible to dezincification include C 23000, C 26000, C 26800, C 27000, C 28000, C 36500, C 44300 (uninhibited), and C 46400.

Dezincification Types. Two major types of dezinification are (1) layer and (2) plug type. The names are taken from the characteristic corrosion product morphologies.

In layer type dezincification, the component surface is converted to corrosion product to roughly uniform depth. The alloying generally increases with increasing temperature, and with increasing chloride content of the cooling water. Since the corrosive wear is normally slight, visual observation is difficult; only microscopic examination will reveal the damage.

When dealloying is generally restricted to localized areas such as beneath deposits, at hot spots, or in stagnant regions, it is called "plug type" dealloying. Plug type dezincification produces small pockets of plugs of almost pure copper.

Factors Influencing Dezincification.

Metallurgical. Metallurgical factors cover the classes of copper alloys like brass, aluminum bronzes, and cupronickel susceptible to dealloying and the alloying elements parted from them. This has been given in Table 3. One important metallurgical factor influencing dezincification is known as beta-phase attack.

For beta-phase attack, in the two-phase (alpha and beta) alloys such as Muntz and naval brasses, dezincification may be concentrated initially on the beta phase and may be sufficient to weaken the metal. If the attack spreads to both alpha and beta phases, complete dezincification may result with the formation of a layer of porous copper [31].

Environment. Stagnant conditions, deposits, high heat flux, crevice condition, and stresses accelerate dealloying. Porous or granular deposits further enhance the attack.

In common with many other types of corrosion and chemical reactions, an increase in temperature accelerates the rate of dezincification of brasses. At lower temperature, the rate of dezincification is low, and this explains the long life obtained from naval brass and Muntz metal piping, tubing, plates, sheets, etc. used in contact with cooling brine [31].

In terms of water chemistry, soft water, high concentration of dissolved carbon dioxide, acidic or high-pH conditions, and high chlorine concentrations promote dezincification.

Waters that deposit magnesium, calcium or iron silicates, or silica scale are protective to the underlying brass. Dense adherent calcium and iron carbonate scales are also effective in reducing or preventing dezincification. But thick scales are objectionable for well-known reasons [31].

Prevention of Dealloying—General. Dealloying is overcome by material substitution, surface cleanliness, and chemical treatment. The most common method of preventing dealloying is to

ensure that the tubes are kept clean and free of deposits by screening methods and cleaning procedures. Stagnant conditions should also be avoided.

Prevention of Dezincification. Though dezincification can be minimized by reducing the aggressiveness of the environment, (e.g., oxygen removal) or by cathodic protection [9], it is mostly overcome by substituting alloys immune to or less susceptible to this form of attack. The resistance of brass is greatly increased by the addition of a little arsenic, antimony, and phosphorus, and the resulting alloy is known as inhibited admiralty brass. As a result, inhibited grades of brasses are routinely used in condensers. Typical alloys resistant to dezincification include:

Admiralty brass, developed by addition of tin

Inhibited admiralty brass, developed by the addition of inhibitors such as phosphorus, antimony, or arsenic

Alternate alloys like aluminum brass (inhibited), cupronickel, and titanium. Among the copper alloys resistant to dealloying, Cu–Ni alloys are considerably more resistant than Cu–Zn alloys.

Erosion–Corrosion

Erosion–corrosion, a form of localized corrosion, takes place due to the movement of a fluid over a material surface. It takes place mostly on the tube side with water flowing through it. The corrosion damage involves both mechanical and chemical factors that allow the corrosion to proceed unhindered. The relative importance of mechanical wear (erosion) and corrosion is often difficult to assess and varies greatly from one situation to the other [28]. The role of erosion is usually attributed to the removal of protective surface film or adherent corrosion products by the fluid shear stress under high turbulence conditions.

Erosion–corrosion is usually accelerated when the fluid is entrained with air or abrasive solid particles, such as sand, but erosion–corrosion can also occur in filtered, bubble-free water [26]. The nature and properties of the protective films that form on some metals or alloys are very important from the standpoint of resistance to erosion–corrosion. A hard, dense, adherent, and continuous film would provide better protection than one that is easily removed by mechanical means or hydraulic force [9]. Erosion–corrosion is normally restricted to copper and certain copper-base alloys and aluminum alloys. In this section, erosion–corrosion is discussed in two different forms: (1) erosion–corrosion, and (2) erosive wear.

Parameters Influencing Erosion–Corrosion. Erosion–corrosion is influenced by two parameters: (1) turbulence and parameters related to process fluids, such as fluid velocity, impingement attack, level of suspended particles, aeration, bubble level, local partial pressure, cavitation, etc., and (2) flow geometry. Turbulence increases with increasing velocity so that higher velocities favor the initiation of erosion–corrosion. Turbulence intensity is higher at tube inlets than downstream, resulting in the phenomenon of inlet-end erosion–corrosion. Similarly, on the shell side, the peripheral tubes located beneath the inlet nozzle without impingement plate protection are most affected by turbulence. Erosion–corrosion also occurs adjacent to a partial blockage in a tube where local velocities through the restricted opening are high or in the turbulent region just downstream of the blockage.

Pattern of Erosion–Corrosion. Erosion–corrosion mostly exhibits a directional property and is characterized by directional grooves, waves, valleys, gullies, holes, etc. [9], or pits in the shape of horseshoes at the site where the protective surface film is damaged [32], or crescent-shaped indentations facing upstream of the water flow that are often influenced by the local flow conditions; consequently, this form of attack has been sometimes referred as

"horseshoe," "star," "crescent," and "slot" attack [26]. A typical pattern of erosion–corrosion is shown in Fig. 8b (item d).

Condenser Tube Failure Due to Erosion–Corrosion. The most common condenser tube failure is due to erosion–corrosion from impingement attack, which develops from a number of causes such as (1) general impingement attack, (2) lodged debris, (3) localized impingement attack due to blocking by iron oxide scale, (4) waterborne debris, and (5) mussel fouling [33]. Probability of impingement attack of various condenser tube materials in sea water is shown in Fig. 20.

Erosive Wear. Four distinct forms of erosive wear have been listed by Paul Crook [34]:

1. Solid particle impingement erosion
2. Slurry erosion
3. Liquid droplet impingement erosion
4. Cavitation erosion.

They have a common mechanism of attack, namely, damage to the surface film by mechanical action followed by localized corrosion.

Solid Particle Impingement Erosion. Solid particle impingement erosion is associated with solid particle and surface interaction in gaseous environments. Relative velocities range from 2 to 500 m/s; particle sizes range in average diameter from 5 to 500 μm [34].

Slurry Erosion. Slurry erosion refers to wear due to particle-laden fluid streams.

Liquid Droplet Impingement Erosion. Impingement attack has been defined as localized erosion–corrosion caused by turbulence or impinging flow. Entrained solids and air bubbles accelerate this action. Liquid droplet impingement erosion or impingement attack takes place in pumps, valves, pipelines, elbows, heat exchanger tubes, and on the shell side underneath the inlet nozzle. The solution to impingement attack is the use of more resistant alloys like cupronickel containing 0.4–1.0% Fe, titanium, and stainless steels [35]. Impingement attack has become one of the most frequently reported failure modes in condenser tubes primarily located beneath the inlet nozzle that receive the direct impact of the exhaust steam. This is discussed next.

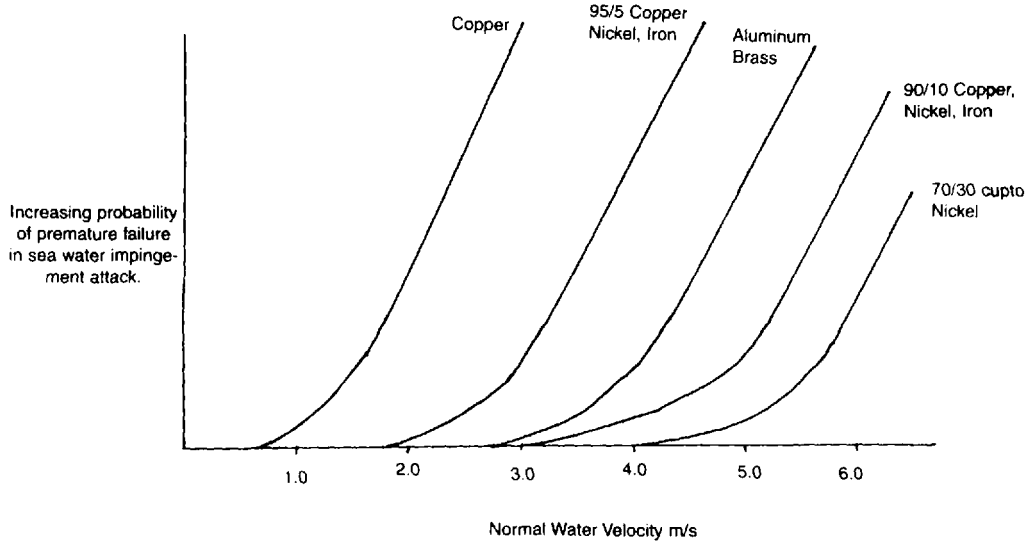


Figure 20 Probability of impingement attack of various tube materials in sea water [33].

Impingement Attack or Steam-Side Erosion of Condenser. Impingement attack, so called steam-side erosion, has been discussed in detail in ref. 26. The problem arises when water droplets entrained in the steam enter the condenser and impact on the tubes at high velocity. While corrosion may play a small part in the overall process, purely mechanical processes are considered more important. To resist impingement attack, stainless steel and titanium tubes are superior to copper alloys. For this reason, it is common practice to install stainless steels or titanium tubes, at least in the peripheral sections of condensers where high erosion resistance is required. When thin-walled titanium tubes are used in the peripheral sections, adequate tube support must be provided to avoid the flow-induced vibration (FIV) problems. Properly designed condenser necks will reduce the collection and development of big droplets, which are especially harmful. Other popular methods of controlling impingement attack are shown Fig. 21. Figure 21a shows the installation of impingement plate protection, and Fig. 21b shows clip-on or angle tube protectors made from a more erosion-resistant material [36].

TEMA [37] Guidelines to Limit Impingement Attack. On the shell side, an impingement plate or other means to protect the tube bundle against impinging fluids shall be provided when entrance line values of ρV^2 exceed the following (where V is the velocity of the fluid in ft/s and ρ is fluid density in lb/ft^3):

1. Noncorrosive, nonabrasive, single-phase fluids, 1500
2. All other liquids, including a liquid at its boiling point, 500

In no case shall the shell or bundle entrance or exit area produce a value of ρV^2 in excess of 4000.

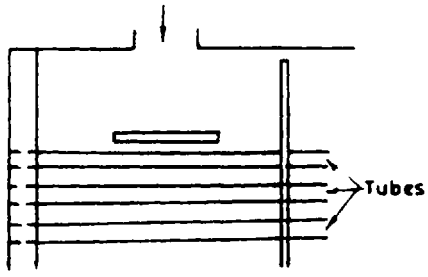
On the tube side, consideration shall be given to the need for special devices to prevent erosion of the tube ends under the following conditions:

1. Use of an axial inlet nozzle.
2. Liquid ρV^2 is in excess of 6000.

Cavitation. Cavitation damage, sometimes referred to as cavitation corrosion or cavitation erosion, is a form of localized corrosion combined with mechanical damage that occurs in turbulent flow or high-velocity fluids. It takes the form of areas or patches of pitted or roughened surface [38]. Cavitation is caused by rapid formation and collapse of vapor bubbles (i.e., voids or cavities), which exert high pressure forces at the metal surface; these high-pressure forces can deform the underlying metal and remove protective surface films and form pits on surfaces. The occurrence of cavitation damage is shown schematically in Fig. 22. The bubbles are created as a result of turbulence or when pressure in liquid falls below its vapor pressure. Collapse is caused by subsequent pressure increase. Among various factors, the surface finish plays an important rule in the formation of bubbles. Smooth surfaces are beneficial since they reduce the number of sites for bubble formation [28].

Control of Cavitation Erosion. Cavitation damage involves both physical as well as electrochemical processes. Cavitation resistance increases as the grain size of a metal becomes smaller. Among the alloys, stainless steels is more resistant to cavitation damage because of its ductility, toughness, high corrosion fatigue limit, homogeneity, fine grain size, and ability to work harden (38). Preventing cavitation damage requires the use of the most resistant alloys and designing the system to avoid turbulence and cavitation.

Control of Erosion–Corrosion. Current engineering practice limits fluid velocities in tubes, pipes, and heat exchangers to some arbitrary value based on empirical tests or field experience [39]. The maximum allowable velocity is known as the threshold velocity or critical velocity. Below the critical velocity, the impingement attack does not occur, and above it, it increases rapidly. For example, the critical velocity for the protective film on aluminum brass and 70Cu–



a

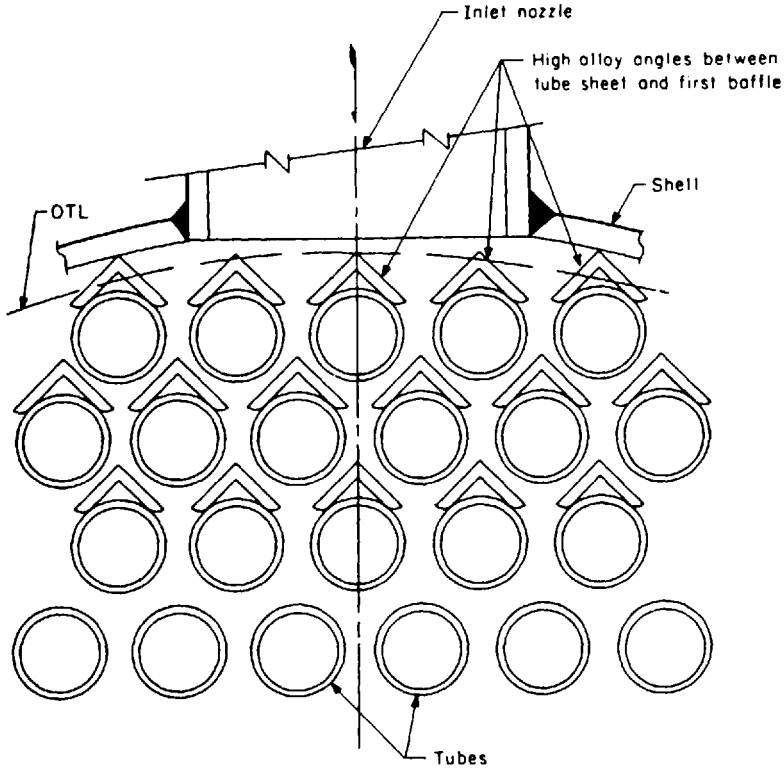


Figure 21 Impingement protection. (a) Plate; and (b) angle tube protectors. (OTL, outer tube limit.) [Ref. 36.]

30Ni copper–nickel are 2.5 m/s and 4 m/s, respectively [33]. However, not only is the fluid hydrodynamics important, but also the corrosiveness of the process stream and the use of inhibitors, if any, to control corrosion affects corrosion; therefore, a simple prediction based on velocity is not always valid [39]. Recent research demonstrates that it is possible to quantify and model flow-enhanced corrosion and erosion–corrosion phenomena in terms of hydrodynamics, electrochemical corrosion kinetics, and film growth/removal phenomena [40]. Erosion–corrosion is mostly overcome by these measures [26]:

Use filtered water.

If susceptibility to erosion–corrosion is unusually high, it may be necessary to avoid the use of copper and certain copper alloys like brasses, and aluminum alloys, and to use titanium

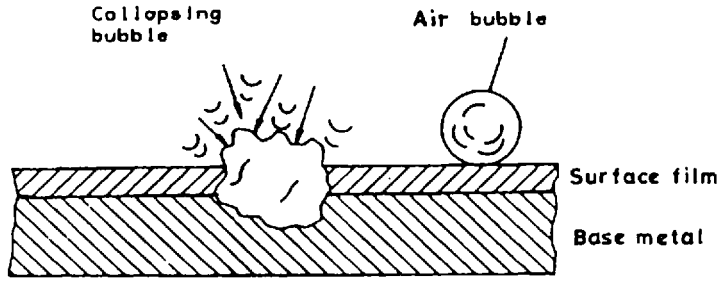


Figure 22 Cavitation damage. [*Source*: Roger Pludek, *Design and Corrosion Control*, The Macmillan Press Ltd., London (1977).]

or stainless steel or aluminum brasses or copper–nickel tubes, since these alloys are essentially immune to erosion–corrosion.

Installation of tube inserts made of wear-resistant materials like stainless steel or plastics at the tubes inlets. This aspect is further discussed in detail later. An alternative to inserts, sprayed-on epoxy coatings, is also preferred.

Inlet-end erosion–corrosion can sometimes be prevented by streamlining the flow, redesigning the water box or inlet nozzle, or installing vanes and diffusers to reduce turbulence in the inlet region or eliminate low-pressure pockets.

An important and even newer application of protective coatings is for the inlet end of tubes to prevent inlet-end erosion–corrosion [32].

Install a cathodic protection system in the water box.

On the shell side, use impingement plate protection beneath the inlet nozzle as shown in Fig. 21a.

Periodic injection of ferrous sulfate into the cooling water has proven to form protective surface film on brass that can be a effective method of controlling erosion–corrosion of power-plant condenser tubes.

It has been shown for several multiphase alloys that if the ratio of surface hardness to abrasive hardness is less than 0.6, wear resistance is low, independent of microstructural conditions [34].

Erosion–corrosion that takes place due to partial blockage of condenser tube ends can be overcome by [41]:

Installing an upstream filtration in the intake point

Introducing an online cleaning methods like sponge rubber ball cleaning to remove the fouling and corrosion deposits

Periodical reversal of the flow

Prevention of biological fouling by injection of biocides or subjecting to thermal shock

Periodical off-line cleaning program

Tube Inserts. To overcome the tube inlet erosion–corrosion, metallic or plastic inserts, also known as sleeves, have been used in many applications. Some sleeves are leak limiting and others are designed to be sealable sleeves that can serve as a new pressure boundary should a through-wall penetration develop in the tube. Inserts are typically 150–300 mm long, but are occasionally longer. They are fabricated from erosion-resistant materials like stainless steel, copper–nickels, plastics, etc. One important area where inserts are used is in steam generators that have caustic intergranular attack of tubing in the tube sheet or sludge pile, primary-side

stress corrosion cracking of tubing in the tube sheet roller expanded region, and pitting attack of tubing in the sludge pile [42]. Tube inserts are available with various trade names. Among the tube inserts, a patented tube insert known as Shield/Seals for inlet-end erosion–corrosion and Pop-A-Plug for plugging a leaking tube are discussed next.

Shield/Seals. CTI Industries, Inc., Stratford, CT, has developed and patented Shield/Seals, which are inserted into the tubes to reduce wear from high-velocity water that causes turbulence near the tube inlet. Shields/Seals are made of various think-walled (0.016–0.020 in, 0.4–0.51 mm) alloys with premium erosion–corrosion resistance. They are expanded to a preset tightness inside the tube inlets by CTI's patented mechanical expansion or hydraulic expansion method.

Seals for Plugging Leaking Tubes. Patented seals known as Pop-A-Plug for plugging leaking tubes can serve as a new pressure boundary should a through-wall penetration develop in the heat exchanger; they have been patented and marketed by M/s. Expando Seal Tools Inc. [43]. The salient features of Pop-A-Plug are discussed next.

The patented Pop-A-Plug System uses a 6600-lb or 17.5-ton hydraulic ram to expand a two-piece, mechanical plug inside a leaking heat exchanger tube. The ram pulls a tapered center pin through an externally serrated ring. As the ring expands, the serrations compress against the tube wall. At a precise, predetermined pressure a breakaway "pops," sealing the tube and separating the plug from the ram. The plugs are available in brass, carbon steel, stainless steel, Monel, copper–nickel, aluminum bronze, and Inconel. Sizes fit tube inner diameters from 0.400 to 1.250 in. Pop-A-Plug is shown schematically in Fig. 23.

Considerations While Using Inserts. While using metallic inserts, care should be exercised to avoid formation of galvanic couple between the tube metal and the insert metal. Also, ensure a smooth transition between the end of the tube insert and the tube surface at the downstream to avoid turbulence, which will further enhance the erosion–corrosion in the downstream.

Stress Corrosion Cracking

Corrosion Involving Stressed Materials. When the combined effects of corrosion and stresses are considered, they are usually divided into two classes [22]:

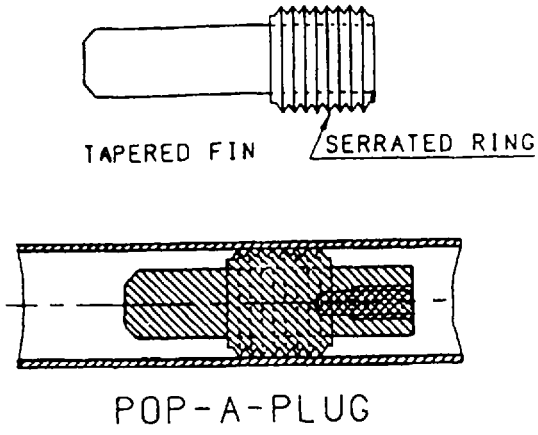


Figure 23 POP-A-PLUG to plug a leaking tube. (Courtesy of Expands Seal Tools Inc., Montgomeryville, PA.)

1. Stress corrosion cracking, involving the effects of static stresses and corrosion
2. Corrosion fatigue, involving variable stresses and corrosion

Cracks resulting from the first phenomenon are predominantly intergranular; those resulting from the latter phenomenon are transgranular.

Environmental Effects on Properties of Materials. Certain environments drastically alter the strength and stability of engineering structures, whereas the same structures performs satisfactorily in air and other environments. For example, a deep drawn brass fails spontaneously by cracking in air containing traces of ammonia, a stressed mild steel may crack when exposed to condensates of gaseous combustion products containing nitrates, and 18-8 stainless steel above room temperature on exposure to moist environment containing traces of chlorides. These are examples of what is called stress corrosion cracking.

Stress Corrosion Cracking. Stress corrosion cracking (SCC) is defined as the corrosion attack on a susceptible alloy due to combined and synergistic interaction of tensile stress and conducive environment. The stress required to cause SCC is normally low and usually below the yield stress, and it can be applied or residual stress, but it is always a tensile stress. In simple terms, SCC requires the simultaneous occurrence of the following three conditions:

1. A susceptible material
2. A corrosive environment
3. Tensile stress

These conditions are shown schematically in Fig. 24.

Time for cracking ranges from few minutes under highly accelerated laboratory conditions to months or even years for resistant materials exposed to a mildly corrosive environment. SCC is much more insidious; the cracks propagate perpendicular to the tensile stress and may be transgranular, common in stainless steels (Fig. 25a), or intergranular (Fig. 25b), as found in many aluminum alloys with little or no evidence of telltale corrosion products. There is little plastic deformation so that the material appears to behave in a brittle fashion. The characteristic appearance of stress corrosion cracking includes the lack of deformation and relatively small amounts of general corrosion [45]. Stress corrosion cracking is the result of the interaction of a number of variables—mechanical, metallurgical, and environmental. The level of the corrosive attack depends on factors like:

1. Stress level and stress state
2. Aggressiveness of the corrosive environment
3. Temperature of the medium
4. Level of cold work and the level of stress relief treatment, grain structure, surface condition, etc.
5. Crack geometry
6. Electrode potential
7. Composition, metallurgical condition

Heat Exchanger Components Susceptible to SCC. The most common places wherein SCC takes place include at (1) tube-to-tube-sheet expanded joints, (2) U-tube bends, (3) bellows type expansion joints, and (4) indented locations by the baffle plates. Items (2) and (4) are shown in Fig. 26.

Tube-to-Tube-Sheet Expanded Joint. All tube expanding methods leave residual stresses in the tube wall. To minimize residual stress, the tube expansion should not exceed certain percentage of the tube wall thickness, which varies from metal to metal (carbon steel 5–8%,

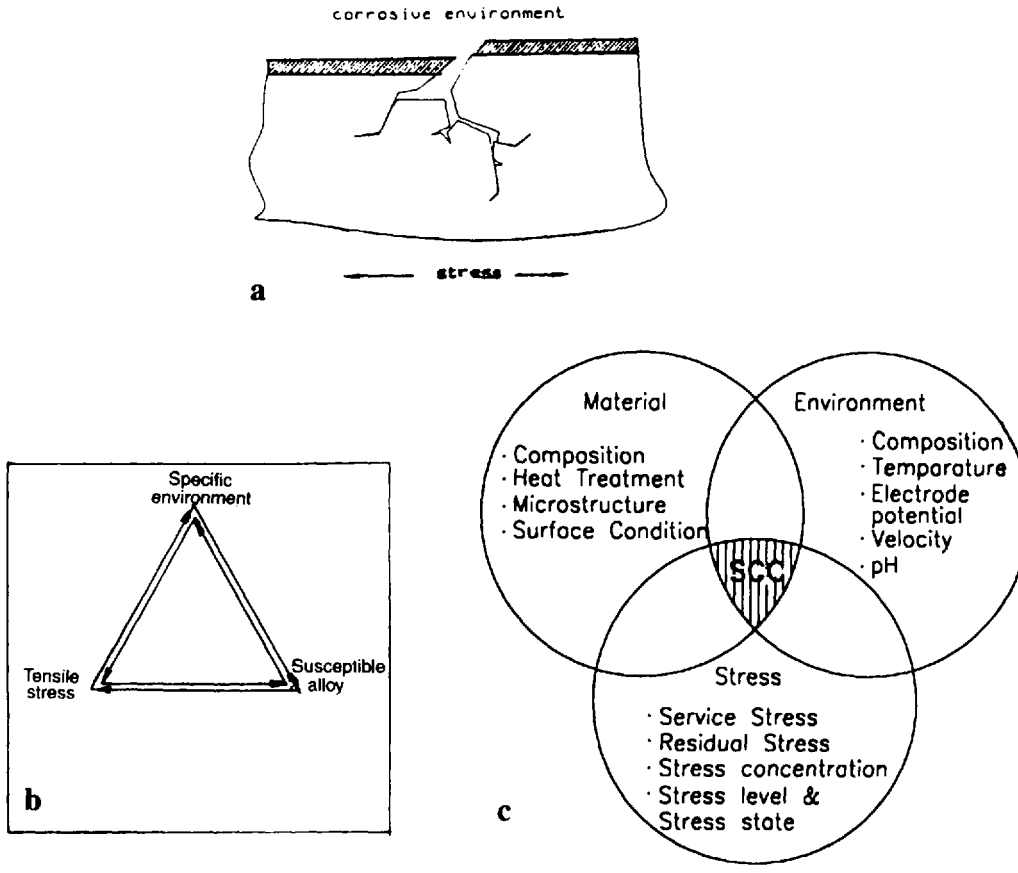


Figure 24 (a) Schematic; (b) stress corrosion triangle; and (c) factors influencing SCC. (From Ref. 44.)

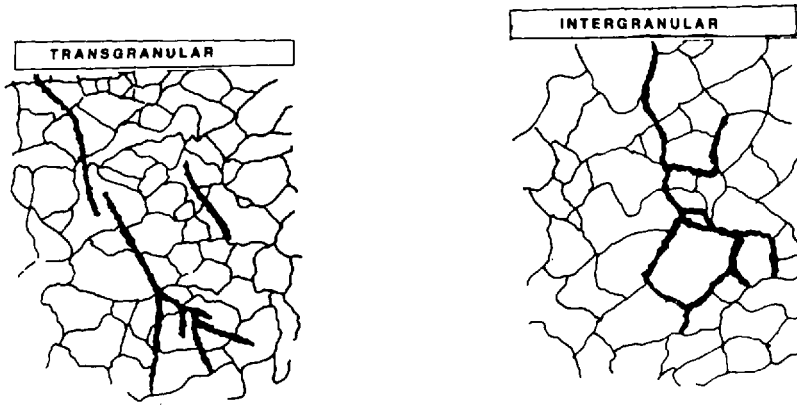


Figure 25 SCC cracking patterns. (a) Transgranular; and (b) intergranular. Reprinted by special permission from *Chemical Engineering*, April 1961, by McGraw-Hill, Inc., New York, pp. 206–210.

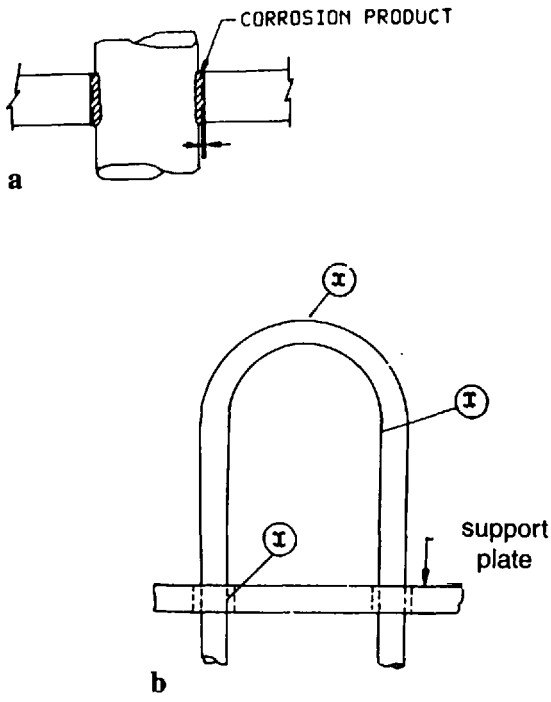


Figure 26 Some components of heat exchanger susceptible to SCC. (a) Tube indented locations by the baffle plate; and (b) regions of U-bend.

stainless steel 3–5%, alloy steel 4–6%). This value is to be controlled during rolling-in operation. The stresses are the higher for these conditions [32]:

Bigger tube hole in relation to the tube diameter
Smaller tube diameter in relation to the bore hole
Higher deformation of the tube after being rolled into the bore hole
Rolling-in extending beyond the tube sheet (Fig. 19)

U-Bend. Cold forming of U-bend tubes induce severe residual tensile stress in the outer portion of the bend, which subsequently fails by stress corrosion cracking. Annealing of the bend tubes will prevent SCC. Other areas prone to SCC are near the U-bend apex for tubes of steam generators where the tube's legs were brought closer together via the denting forces and at nonsmooth transition region of U-bends [42]. Various regions of U-bend tube susceptible to SCC are shown in Fig. 26.

Thin-Walled Expansion Joints. Stress corrosion cracking occurs in thin-walled expansion joint elements made of austenitic stainless steel materials on the bottom of horizontal units that are not drainable.

Classification of Stress Corrosion Cracking Failures. Stress corrosion cracking failures may involve an electrochemical mechanism, attack by a molten phase, hydrogen embrittlement, or some other factors. According to the environment causing cracking of metals and metal alloys, SCC can be categorized as:

Chloride cracking, e.g., austenitic stainless steel, aluminum
Caustic cracking, e.g., carbon steel
Ammonia cracking, e.g., admiralty brass

Polythionic acid cracking, e.g., austenitic stainless steel
Sulfurous acid cracking, e.g., austenitic stainless steel

Discussion of Conditions Responsible for SCC.

Susceptible Alloys and the Environment. Stress corrosion cracking, like most forms of corrosion, is electrochemical and involves metals in contact with an electrolyte. The environments that cause stress corrosion cracking are specific for each metal. Except for ferritic stainless steel, virtually all metals and alloy systems are susceptible to SCC by a specific corrodent under conditions of temperature, stress level, etc. Chloride ions lead to stress corrosion cracking in 304 and 316 stainless steels when oxygen is present. Typical hostile environments for few of the most widely used metals are given in Table 4. Tables of environments and alloy combinations known to result in SCC are published by the National Association of Corrosion Engineers (NACE) [46], the Materials Technology Institute [47], and others for the chemical process.

Stress. Tensile stress at the surface of the metal is an essential factor in stress corrosion cracking. Cracking has never been found in metals under compression. The tensile stresses may be due to internal stress caused by metal deformation near welds and bolts, deformation caused by shrink fit, unequal cooling from high temperature, or volume changes in the material caused by phase change or rearrangement of crystal structure [48], or residual stress from some prior cold work or metal forming operation or caused by an applied stress (i.e., service-induced external load). Residual and applied stresses are additive to evaluate the effect on cracking, and both must be known. Welding often leaves residual stresses that lead to stress corrosion cracking in susceptible environments.

SCC of Welded Joints. Welded joints are particularly prone to SCC for three reasons [27]: (1) The welding operation will leave a residual tensile stress in the weld area unless effective postweld stress relief is carried out, (2) stress concentrations are usually present, and (3) the thermal cycle can produce a susceptible microstructure. SCC is overcome by shot peening after welding to induce compressive stress on the surface, stress-relief heat treatment, and use of alloys resistant to such cracking.

How to Detect SCC. Some cracks may be visible to the naked eye and thus require no special detection means. Others may be seen after surface deposits are removed, particularly under magnification. Sophisticated microanalytical instruments such as the electron beam microprobe analyzer, scanning electron microscope, and mass spectrometer are being increasingly applied

Table 4 Environments That Cause Stress Corrosion Cracking

Metal	Environment
Al and Al-base alloys	NaCl solution, seawater, H_2O_2, chloride solution, and other halide solutions
Cu and Cu-base alloys	Ammonia and ammonium hydroxide, amines, mercury, sulfur dioxide, H_2S, steam
Carbon steel	Sodium hydroxide solutions, ammonia and sodium nitrate solutions, carbonate/bicarbonate
Austenitic stainless steel	Aqueous chlorides, seawater, sulfurous and polythionic acid
Nickel and nickel-base alloys	Caustic above 315°C, fused caustic soda, hydrofluoric acid, polythionic acid
Titanium and titanium alloys	Reducing acids such as chlorides, iodides, fluorides, red fuming nitric acid, nitrogen tetroxide, methanol

to failure analysis of power plant components [49]. Crack detection methods like magnetic particle testing, dye penetrant testing, x-rays, ultrasonics, and eddy current testing can also be used [48].

Theory of SCC. No unified theory for SCC is at present accepted. Theories attributed the failure to mechanical, chemical, fracture mechanics, surface energy, etc. The sequence of events involved in the SCC process is usually divided into three stages [50]:

1. Crack initiation and propagation
2. Steady-state crack propagation
3. Crack propagation or final failure

Metallurgists at the Naval Research Laboratory, Physical Metallurgy Branch, have applied a fracture mechanics theory to SCC [51]. According to this theory, SCC occurs by nucleation and growth at the site of discontinuity in a protective surface oxide or passive film or at the site of preexisting cracks or defects. Under stress or chemical action, pitting initiates at these sites, and pitting continues until the crack extends to its critical length and subsequent fracture. Growth and propagation of SCC are shown schematically in Fig. 27.

Avoiding Stress Corrosion Cracking. Since SCC is due to the interaction of variables associated with (1) mechanical, (2) metallurgical, and (3) environmental factors, adjustment of these variables should minimize cracking [52]. To resist chloride SCC, use higher austenitic nickel-base alloys such as Inconel 600, Incoloy alloys 800 and 825, ferritic and superferritic stainless steels, duplex stainless steels such as ferralium 255, or titanium. Another important measure to prevent SCC is to avoid the metal and environment combinations that are favorable for SCC as shown in Table 4. Other measures involving mechanical, metallurgical and environmental aspects to control SCC are given in Fig. 28 and discussed next.

Mechanical.

1. Exercise control on the level of cold work and grain size. For example, adopt optimum clearance between the tube and tube hole in the tube sheets to avoid excessive cold work.
2. Reduce tensile stress by design change, reduce operating pressure, avoid misalignment of connections, prevent differential thermal expansion, etc. [48,53].
3. Reduce residual stress to a safe level by thermal stress relief, which usually can be applied without significantly decreasing strength; mechanical surface treatment (shot peening to put metal surface in compression).
4. Avoid stress concentrations.

Metallurgical.

1. Replace the susceptible alloy by an alternate alloys which show resistance or immune to SCC; e.g., replace type 304 SS by Inconel and superferritic stainless steels.
2. Use metallic or conversion coating.

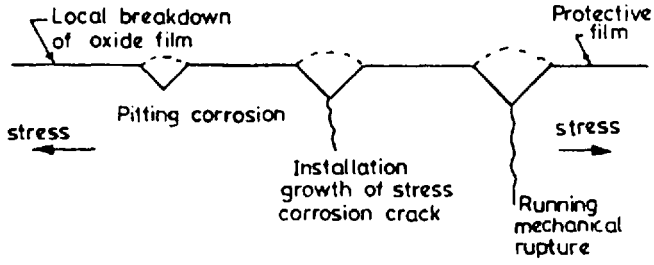


Figure 27 Growth and propagation of SCC. (From Ref. 56.)

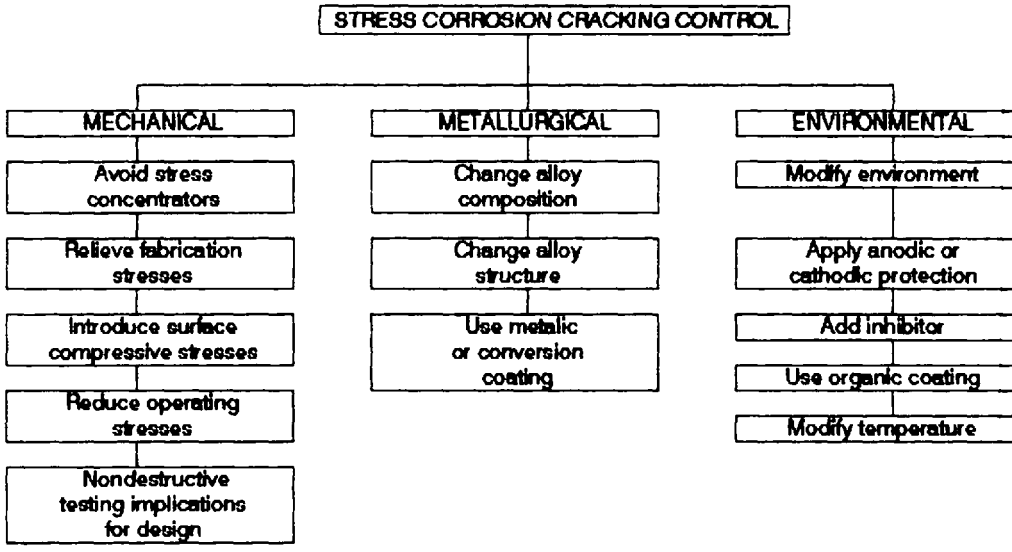


Figure 28 Approaches to stress corrosion control. [From Parkins, R. N., *Mat. Perf.* (Aug. 1985).]

3. Since SCC occurs by nucleation and growth at the site of discontinuity in protective surface oxide or passive film or at the site of preexisting cracks or defects, keep the surface free from these surface defects.

Environmental.

1. Modify environment: If possible reduce the aggressiveness of critical environment by degassification or demineralization or by any other method [9]. For example, elimination of chloride ions from water by an ion-exchange process may permit the use of stainless steels in high-temperature water [48], or it may be possible to lower the concentration less than 30 ppm for safe operation.
2. Exclude corrodents with protective coating,
3. SCC in aqueous solution can be prevented by cathodic protection.
4. Modify the environment by adding a corrosion inhibitor.
5. Modify the temperature.

Test for SCC. The sensitivity of a steel to SCC is determined by boiling a stressed sample in concentrated magnesium chloride or sodium chloride solutions. Stresses may come from a bead-on-plate weld or from plastic deformation of the specimen. The chlorine ions depassivate the steel, and lead to SCC and eventual failure of the stressed specimen. ASTM B 154, Mercurous Nitrate Test, is the standard test method for detecting the SCC of copper and copper alloys.

Hydrogen Damage

Monoatomic hydrogen can diffuse into steel and recombine to molecular hydrogen at voids, laminations, microcracks, or discontinuities around inclusions, generating extremely high pressures. As an interstitial element in the body centered cubic ferritic lattice, hydrogen can cause a number of mechanical problems. It stiffens the metal and impairs its ductility. At higher temperatures, hydrogen diffused in a steel can react with carbon atoms to form methane. The accumulation of methane at certain locations in steels, such as grain boundaries and nonmet-

allic inclusions, causes the irreversible loss of strength and ductility. Elevated temperature exposure in hydrogen sometimes results in surface decarburization, followed by fissuring due to high gas pressure at localized sites. These changes in the steel are called hydrogen attack. The different forms of hydrogen damage are:

1. Hydrogen embrittlement
2. Hydrogen blistering
3. Hydrogen SCC
4. High-temperature attack

The development of hydrogen damage would presumably be hindered by anything present in the steel that would [54]:

1. Decrease the rate of corrosion.
2. Decrease the rate at which the hydrogen produced by corrosion entered the steel instead of escaping into the process stream.
3. Speed up the passage of hydrogen through steel, thus reducing the time available for reaction.
4. Decrease the rate of reaction of hydrogen with carbon in the steel.

Other remedial measures include stress relief, the selection of material that does not harden so readily during the welding cycle, or the inhibition of the hydrogen evolution reaction causing the trouble. Hydrogen damage due to high temperature exposure is discussed in detail in Chapter 13, Material Selection, and hydrogen damage in the sour environment is discussed at the end of this chapter.

Fretting Corrosion

Fretting corrosion is the combined wear and corrosion process that takes place at locations where there is a relative movement between two components and the movement is restricted to very small amplitude. At the mating surfaces, the degree of deterioration increases because of repeated corrosion of the freshly abraded surface and the accumulation of abrasive corrosion products between these surfaces. A typical example is the wear of the heat exchanger tubes at the tube-baffle contacts. Various metallurgical, geometrical, and environmental factors influence the fretting wear of heat exchanger tubes. Factors that affect fretting wear include [55] contact load, amplitude, frequency, number of cycles, and temperature. Fretting wear of heat exchanger tubes has been covered in Chapter 10 on flow induced vibration.

Corrosion Fatigue

Corrosion Fatigue. Corrosion fatigue is the reduction in the fatigue strength of a metal as a result of exposure to a corrosive environment. When a metal is subjected to cyclic stress in a corrosive environment, a marked drop in or elimination of the endurance limit may occur even in a mildly corrosive environment. Surface film protected alloy is especially susceptible to corrosion fatigue [56]. Corrosion fatigue is shown schematically in Fig. 29a and the drop in endurance strength in Fig. 29b. In film-protected alloys, stress reversals cause repeated cracking of the otherwise protective surface film, and this allows access of the corrodent to the unprotected metal, with resultant corrosion. The reduction in fatigue strength has a consequence on the life and reliability of a component. The reduction may be so severe that a detail that has been ignored at the design or inspection stage can lead to catastrophic failure in service [27]. In heat exchangers, corrosion fatigue can occur in any tube material; it is caused by steam buffeting in the case of the condenser or flow-induced vibration in association with inadequate

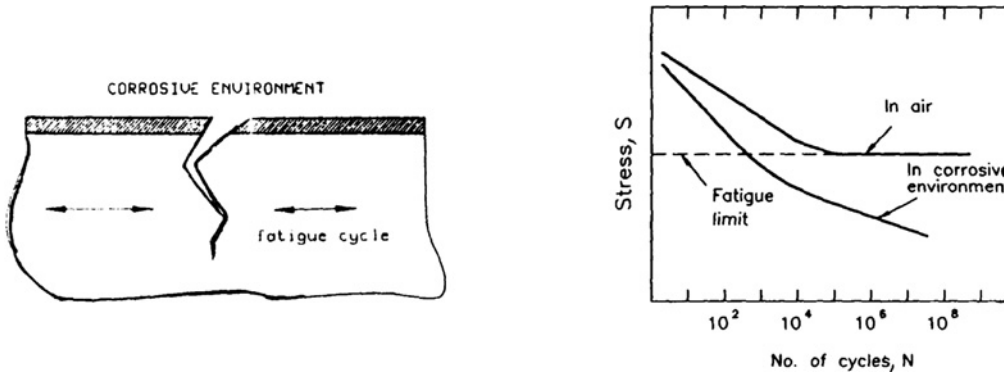


Figure 29 Corrosion fatigue. (a) Diagrammatic representation; and (b) S-N curve for steels subjected to cyclical stress showing drop in endurance strength due to corrosion fatigue.

tube support [33]. Generally, failure occurs at tube mid span due to collision between adjacent tubes above critical velocity.

Factors Influencing Corrosion Fatigue and Crack Growth. Corrosion fatigue occurs in metals as a result of the combined action of a cyclic stress, a corrosive environment, and metallurgical factors. The factors that influence corrosion fatigue include [55] stress intensity range, load frequency, stress state, environment, electrode potential, and metallurgical variables. The environmental factors include pH, concentration of corrosive species, dissolved oxygen content, conductivity, pressure, temperature, and flow conditions. Corrosion fatigue cracks are always initiated at the surface unless there are nearby surface defects that act as stress concentration sites and facilitate subsurface crack initiation.

Intensity of Corrosion Fatigue. At any given time prior to failure, damage due to corrosion fatigue will be greater than the sum of corrosion damage plus fatigue damage [6]. Localized corrosion, such as pitting or intergranular corrosion, has a greater accelerating effect than the uniform corrosion [56]. The reduction in fatigue strength due to corrosion is sometimes expressed in terms of damage ratio, which is the ratio of corrosion fatigue strength in a particular environment divided by the air fatigue strength. The damage ratio for aluminum in seawater is 0.4, stainless steel 0.5, and for mild steel 0.2 [27].

Corrosion Fatigue of Various Metals. The alloys that are generally affected by corrosion fatigue include aluminum alloys exposed to chloride solution, Cu–Zn and Cu–Al alloys exposed to aqueous chloride solutions, and high-strength steel in a hydrogen atmosphere.

Ferrous Alloys. In a corrosive environment, ferrous alloys lose their fatigue limit, and hence the bottom of the standard stress-cycle curve (S-N) dips down from horizontal. As per theory, the drop in fatigue strength takes place as the cyclic stress causes progressive slip within metal grains, constantly producing clean metal surfaces that are anodic in nature and hence dissolve continuously [6].

Aluminum Alloys. Aluminum alloys exposed to aqueous chloride solutions or humid air are subject to corrosion fatigue. Corrosion fatigue cracks originate at sites of pitting or intergranular corrosion, but pitting is not a requisite for crack initiation.

Copper and Copper Alloys. Corrosive environments have little additional effect on the fatigue life of pure copper. Copper–zinc and copper–aluminum alloys exhibit a marked reduction in fatigue strength, particularly in aqueous chloride solutions.

Corrosion Fatigue of Welded Joints. Under normal circumstances, welded joints are likely to be associated with fatigue cracks associated with structural and mechanical discontinuities that are usually present in the welds [27]. The toes of fillet welds provide site for crack initiation, particularly in the presence of undercuts.

Relationship Between Corrosion Fatigue and SCC. Corrosion fatigue is mostly interrelated to environmentally induced corrosive attack forms such as SCC and hydrogen embrittlement [55]. The relationship between corrosion fatigue and two other environmental cracking mechanisms, SCC and hydrogen embrittlement, is shown in Fig. 30.

Prevention of Corrosion Fatigue. Corrosion fatigue can be prevented by several methods such as (1) use of protective coatings, (2) adding inhibitors to the environment, (3) cathodic protection, and (4) introduce residual compressive stresses by methods such as shot peening.

Microbiologically Influenced Corrosion (MIC)

Microbiologically influenced corrosion (MIC) is the deterioration of metal by a corrosion process that occurs directly or indirectly as the result of metabolic activity of microorganisms on heat transfer surfaces. It also implies, however, that the corrosion would not have taken place in the absence of these organisms [57]. MIC is not a new form of corrosion, but some of the conditions created by microbes can lead to electrochemical reactions that make an environment much more corrosive. Certain microbes can metabolize nutrients (e.g., oxygen) and generate corrosive agents (e.g., organic acids) and other chemical compounds (e.g., sulfur and iron) or create a living crevice or active–passive cell due to biofouling [13]. Natural waters may contain several classes of microorganisms. Attack can be caused by sulfate-reducing bacteria, biological slimes, mates, and tubercles by fungi and other microorganisms, including the iron bacterium [58]. Other synonyms for MIC are microbial corrosion, biodeterioration, and biocorrosion. Since the concept of anaerobic MIC was introduced in 1934, scientists and engineers have recognized that MIC can be a significant contributor to component failures.

Susceptible Metals. All but the higher nickel–chromium alloys and titanium have been found to be subject to microbiological corrosion. Common engineering metals and alloys such as carbon steel, lined steel, stainless steels, aluminum alloys, and copper alloys, 6% Mo stainless

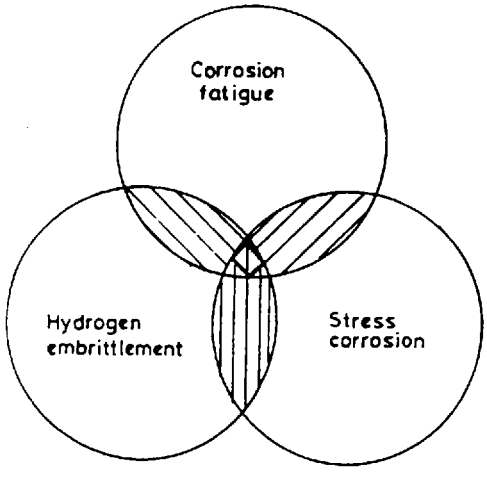


Figure 30 Relationship between corrosion fatigue, SCC and hydrogen embrittlement. (From Ref. 55.)

steels, and high-nickel alloys (Monel 400 and Alloy B-2) have exhibited susceptibility to MIC [59].

Sources of Microorganisms. Microorganisms are widely distributed in nature, being present in streams, rivers, lakes, seawater, and coastal estuaries. Such microorganisms include bacteria, fungi, algae, and yeasts, depending on the sources of water.

Classification of Microbiological Organisms. Microbiological organisms, or microbes, known to cause corrosion of metals may be classified in four general flora groups [60]: (1) bacteria, (2) fungi, (3) algae, and (4) yeasts. According to their metabolic activities, corrosive microbes are classified into six general metabolic groups [60]: (1) acid producers, (2) mold growers, (3) slime formers, (4) sulfate reducers, (5) hydrocarbon feeders, and (6) metal ion concentrators/oxidizers. The three major types of microbes commonly associated with MIC are (1) sulfate-reducing bacteria (SRB), (2) iron and manganese bacteria, and (3) sulfur oxidizing bacteria [13].

Sulfate-Reducing Bacteria (SRB). The sulfate-reducing bacteria seem to be involved in at least some form of MIC of most of the susceptible alloys like iron and mild steels, aluminum alloys, and copper alloys [61]. They reduce sulfates to sulfides and depolarize cathodic sites on metal surfaces by consuming hydrogen.

Iron and Manganese Bacteria. Iron-and manganese-oxidizing bacteria, known as metal ion concentrators/oxidizers, are the most often associated with the corrosion of stainless steels [13]. Such bacteria produce iron and manganese metabolites that form deposits that in turn create concentration cells or harbor other corrosive microbes.

Sulfur-Oxidizing Bacteria or Acid Producer. Some microbes can oxidize sulfur compounds to sulfuric acid; a pH as low as 2 has been recorded where sulfur-oxidizing microbes are active.

Attachment, Growth, and Influence of Microorganisms on Metal Surfaces. On attachment to metal surfaces, microorganisms begin colonizing and produce a biofilm, known as slime or mat. Certain microbes can metabolize nutrients and other chemical compounds (e.g., sulfur and iron) to create corrosive environments or they can directly participate in electrochemical reactions. The metabolic processes of the microorganisms can influence the corrosion behavior of materials by [60,62,63]: (1) destroying protective surface films, (2) producing a localized acid environment, (3) creating corrosive deposits, (4) creating corrosion cells, notably differential aeration and ion concentration cells, and (5) altering anodic and cathodic reactions, depending on the environment and organisms involved. These processes may occur either alone or in combinations. The microorganisms tolerate elevated pressures and a wide temperature range, and oxygen content from 0 to almost 100%. Temperatures greater than 40°F (4°C) but less than 140°F (60°C) tend to promote MIC.

Categories of MIC. MIC can be divided into two categories: aerobic and anaerobic. Aerobic microbes exist in the presence of air. Anaerobic microbes can exist and multiply in the absence of air. Sulfate-reducing bacteria are the most important microorganisms in the anaerobic category, whereas slime-forming bacteria, sulfur bacteria, and iron bacteria are important microorganisms in the aerobic category.

MIC of Industrial Alloys.

Mild Steel. Due to MIC, carbon steels have experienced random pitting, general corrosion, and formation of tubercles on surfaces. MIC of carbon steels can be prevented by chemicals, coatings, or cathodic protection [61].

Austenitic Stainless Steel and Weldments. Pitting failures of austenitic stainless steel components and weldments by MIC commonly results when residual natural water is left in stainless steel equipments after hydrotesting. MIC failures of austenitic stainless steel welds have been reviewed by Pope et al. [61] and in refs. 63 and 64. The conditions/mechanisms responsible for the MIC of austenitic stainless steels include [64]:

1. Austenitic stainless steels form small tubercles from microbial action under which severe pitting occurs.
2. Oxygen concentration cells produce carbonic acid, which is corrosive to stainless steels.
3. Crevices are ideal sites for MIC to occur; perhaps the consumption of oxygen by the biofilm prevents the oxygen in the external environment from reaching the interior of the crevice.
4. Depassivation: Microbes, by forming a slime layer, produce a crevice in which regions of the normally passive film damaged by mechanical means or through halide attack go unrepaired.
5. Weldment surface conditions that are commonly associated with poor corrosion resistance, such as heat tint and conditions that are associated with residual stresses, such as gouges, may produce conditions that are susceptible to MIC.

Measures to overcome MIC in stainless steel include, solution annealing and pickling, and a temporary measure, spraying the heat exchanger tube interior by a quick set epoxy to a distance of 5–6 ft instead of plugging [65].

Copper Alloys. Copper and copper alloys are more resistant to the attachment of biofouling organisms than steel and most of the other common materials of construction. This is due to the inherent characteristic of copper alloys and appears to be associated with copper ion formation within the corrosion product film. Therefore, coupling of steel or less noble materials or cathodic protection, which suppresses copper ion formation, allows biological fouling to occur [66]. However, the belief that copper ions and salts formed by copper alloy corrosion are lethal to most of the microorganisms is now known to be erroneous. For example, *Thiobacillus thiooxidans* can withstand copper concentrations as high as 2% [67]. Copper alloys are particularly sensitive to sulfate-reducing bacteria and ammonia-producing bacteria and have exhibited failures by pitting, plug type dealloying, stress corrosion cracking, and erosion–corrosion [61].

Titanium's Resistance to MIC. Titanium and its alloys exhibit excellent resistance to MIC under both anaerobic and aerobic conditions. More than 30 years of extensive titanium alloy use in biologically active process and raw cooling waters, especially seawater, appears to substantiate titanium's resistance to MIC [68]. Characteristic features of titanium alloys resistance to MIC include the following [68]:

1. Titanium alloys are fully resistant to the reduced chemical species associated with anaerobic activity over the total range of concentrations and temperature as high as 212°F (100°C).
2. Titanium alloys are exceptionally resistant to the oxidizing and acidic conditions and compounds associated with aerobe activity.
3. The surface oxide film remains intact under fully deoxygenated, reducing conditions down to a pH of 2 at 100°C.
4. The surface oxide film exhibits excellent resistance to atomic and diatomic hydrogen absorption, the hydrogen being produced by the metabolism of sulfate-reducing bacteria.
5. Both algae and fungi cannot produce conditions that affect titanium alloy passivity.

Nevertheless, titanium alloys are not biotoxic and permit growth or attachment of any micro or macro biofilm or organism on metal surfaces. However, in no case has localized corrosion ever been observed beneath these biofilms. Periodical cleaning to avoid the buildup of the biofouling is necessary or the water velocity should be sufficiently high.

Control of MIC. Prevention of MIC in most of the metals involves trying to prevent the occurrence, growth, and metabolic activities of MIC causing microbes in the vicinity of the metals. The important means of microbial control are:

1. Untake filtration
2. Systematic cleaning and elimination of stagnant areas
3. Proper use of a biocide
4. Thermal shock treatments.

Uptake Filtration. Intake screens are now available with mesh sizes down to 0.5 mm, small enough to filter out stringy debris and all but the smallest organisms [26].

Systematic Cleaning and Elimination of Stagnant Areas. Since the presence of scales, shellfish, corrosion products, etc. stimulates pitting and, in particular, crevice corrosion in the tubes, keep the tubes clean either continuously by on-line cleaning systems, or intermittently by off-line cleaning methods [26].

Biocides. The most practical and efficient method of controlling microbiological activity in cooling waters is through chemicals known as biocides. These biocides kill the organism or inhibit their growth and reproductive cycles. Biocides used in cooling water system include chlorides, chlorine dioxide, bromine, organo-bromide, methylene bisthiocynate, isothiazolinone, quaternary ammonium salts, organo-tin/quaternary ammonium salts [69], copper salts, chlorine donors (e.g., phenates), thiocynates, and acrolein [70].

Limitations of Biocides.

1. Even though these chemicals can do a good job of killing organisms in the bulk water phase, they are much less effective in penetrating biofilms (slime) and killing the organisms therein.
2. While selecting biocides, consideration should be given for toxicity to plant and animal life exposed to the discharged water.
3. Hard-shelled organisms such as barnacles, mussels, and others possess the ability to tightly close their shells when first sensing a toxic substance such as chlorine in the water, to remain closed until it passes, and then to reopen and resume feeding [66].

Thermal Shock. The thermal shock treatment involves recirculating the cooling water to allow the temperature to increase to 120°F (49°C), a condition that ensures the death of most organisms.

Microbiologically Influenced Corrosion Failure Analyses. MIC can be diagnosed by techniques such as in situ bacterial sampling of residual water, bacterial analysis of corrosion products using analytical chemistry, culture growth, and scanning electron microscopy, as well as nondestructive examination using ultrasonics and radiographic techniques. Metallographic examination can reveal MIC characteristics such as dendritic corrosion attack in weld metal [71]. If special techniques are not followed, they can be misdiagnosed as attack caused by conventional chloride crevice/pitting corrosion attack.

Corrosion of Weldments

Weld Metal Versus Parent Metal. Corrosion of weldments occurs in spite of proper selection of base metal and filler metal, codes and standards followed, and postweld heat treatment (PWHT) carried out. In welded joints, the weld metal is usually of matching composition to the parent material or overmatched, with its choice normally being dictated by the need to

obtain a sound weld of mechanical properties comparable with those of the parent material and resistance to galvanic corrosion [72]. A survey of weld failures, reported at Corrosion 82, a forum on corrosion sponsored by the National Association of Corrosion Engineers, showed that poor welding practices such as poor fitups, misalignments, and incompletely fused root beads have caused many weld failures in process vessels. Incomplete fusion, particularly in root passes, is a common source of notches and crevices [6]. The factors that control the corrosion resistance of the weldments and how to optimize the weld quality are discussed in this section.

Causes of Corrosion of Weldments. In addition to the material composition, the following welding design/process-related features contribute to weld material corrosion [73]:

1. Weldment design
2. Fabrication technique
3. Heat input and welding practice
4. Protection of welding environment; carbon and nitrogen pickup during welding [6].
5. Formation of oxide film and scale
6. Weld slag and spatter
7. Welding defects like, incomplete weld penetration or fusion, porosity, cracks, crevices, HAZ, and high residual stresses
8. Metallurgical factors like microsegregation, precipitation of intermetallic phases, formation of unmixed zones, recrystallization and grain growth in the weld HAZ, volatization of alloying element(s) from the molten weld pool
9. Postweld heat treatment (PWHT)
10. Postweld cleaning

The thermal cycle due to the welding process affects the microstructure and surface composition of welds and adjacent base metal. Often both crevice corrosion (Fig. 31) and pitting corrosion are associated with the weld defects. The presence of secondary phases having different oxidation potential and the attack on the phases of highest potential can be quite common. Weld deposits containing nonmetallic inclusions and porosity can accelerate the corrosion rate. Sometimes the weld metal may be deficient in corrosion resistance compared to the parent metal due to microsegregation of an important alloying elements of the parent metal. This is especially true for welding 6-Mo superaustenitic stainless steel. This situation is overcome by overalloying the filler metal. Weld deposits containing entrapped slag particles or residues from fluxes act as sites for cathodic reaction and can lead to increased weld metal corrosion.

Measures to Improve the Corrosion Resistance of Weld Metal. Corrosion resistance of the weld metal can be improved by:

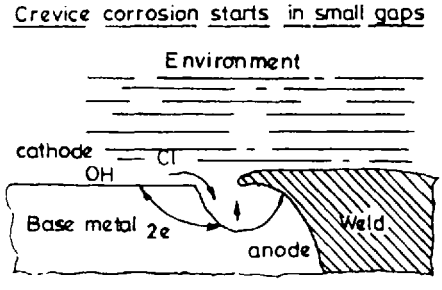


Figure 31 Crevice corrosion due to weld defect. (From Ref. 6.)

1. Shielding the molten and hot metal surfaces from reactive gases in the weld environment, including protection of underside of the root
2. Controlling grain growth in the HAZ
3. Controlling the precipitation of the intermetallic phases during welding/postweld heat treatment.
4. Proper postweld heat treatment
5. Postweld cleaning and passivating the surfaces in the case of stainless steels
6. Subjecting the weldments for thorough nondestructive testing (NDT) for weld defects

4 CORROSION PREVENTION AND CONTROL

The majority of the corrosion control techniques employed center around the ideas of either isolating the corroding metal from the environment, or modification of the environment so that either the anodic or the cathodic reaction is brought under control [27]. Alternately, use corrosion-resistant metals in equipment construction. The last 25 years have seen the development of many specialized methods for improving the corrosion resistance of structural components in corrosive environments. These include coatings and cladding of alloy steels and minor alloy additions to the 300 series stainless steels, chromizing of internal surfaces of 2.25Cr–1Mo [74], and alonizing steel tubes. Corrosion control measures have been mentioned already briefly while discussing various forms of corrosion. However, some generalized procedures are explained in this section.

4.1 Principles of Corrosion Control

Corrosion control can be divided into two principal approaches: (1) corrosion prevention, and (2) corrosion protection. Corrosion prevention is based on the idea of designing equipment so that corrosion cannot occur, whereas corrosion protection aims at minimizing the corrosion attack. Since corrosion of a material takes place due to electrochemical reaction with its environment, in most practical situations this attack cannot be prevented; it can only be controlled so that a useful life is obtained from the equipment. Various techniques for corrosion control are as follows:

1. Use of proper design
2. Changing the characteristics of the corrosive environment
3. Use of corrosion-resistant materials
4. Bimetal concept involving cladding and bimetallic tubes
5. Application of barrier coats, surface treatment
6. Providing electrochemical protection by cathodic or anodic protection
7. Passivation

There are advantages, disadvantages, and areas of the most economical use for each of these methods. No single method is a universal cure for all corrosion problems [1]. Each problem must be individually studied before implementing the corrosion control measure. The technical solution most suitable to these problems should be decided through cost-benefit analysis by the plant user.

4.2 Corrosion Control by Proper Engineering Design

Design is an important aspect in the prevention of corrosion. In fact, in many engineering structures the "weakest spot" is the lack of consideration given to corrosion control during the design stage.

Design Details

The design details of pressure vessels and heat exchangers can have a significant effect on corrosion. Design details to minimize corrosion are discussed in ref. 15. During the design stage, give consideration to crevices, galvanic couples, drainage, and ventilation. Vessels should allow complete drainage. Inclined heat exchanger installation permits a dead space that may allow overheating if very hot gases are allowed on the tube side (Fig. 32). Disturbances to flow can create turbulence and cause impingement attack, and direct impingement should be avoided—introduce deflectors or protection devices. Nonaligned assembly distorts the fastener, which forms crevices. Supports should allow drainage; continuous welding is necessary for horizontal stiffeners and supports.

Preservation of Inbuilt Corrosion Resistance

The design details should preserve the inbuilt corrosion resistance, including the passivity of the materials. For metals like carbon steels, alloy steels, stainless steels, aluminum, titanium, zirconium, etc., corrosion resistance is inbuilt by means of an adherent protective surface film that separates the metal from the surrounding media. The designer must consider potential corrosion problems from fabrication practices and postweld heat treatment.

Design to Avoid Various Forms of Corrosion

Crevice and galvanic corrosion, erosion–corrosion, and stress corrosion cracking can be controlled by proper design. Figure 33 illustrates the insidious nature of crevices occurred in the tubesheet of a vertical condenser handling vapors of formic and acetic acid [75,76]. If there is a dead space (air pocket) at which chlorides are allowed to concentrate by alternate wetting and drying of tubing surfaces, the tubes will be attacked by SCC. This problem is overcome by air venting the dead space or allowing complete flooding of all tubing surfaces.

Weldments, Brazed and Soldered Joints

Corrosion in weldments and brazed and soldered joints is also controlled through proper design, fabrication, and joining techniques. Give attention to joint design, surface continuity, and concentration of stress and complete corrosive flux removal.

Plant Location

Nearby sources of exhaust and atmospheric pollution due to local industries have an important bearing on the materials of construction [76]. Plant structures should be located in the upwind direction. For example, placing stainless steel equipment just downwind of a hydrochloric acid scrubber can make the condenser susceptible to SCC [12,28].

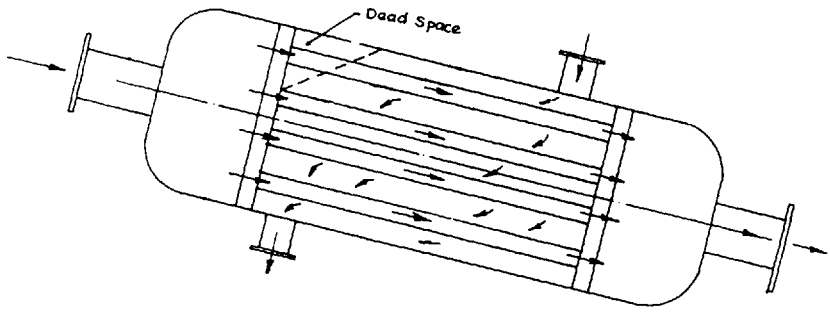


Figure 32 Inclined heat exchanger which permits a dead space at the top of the shell zone.

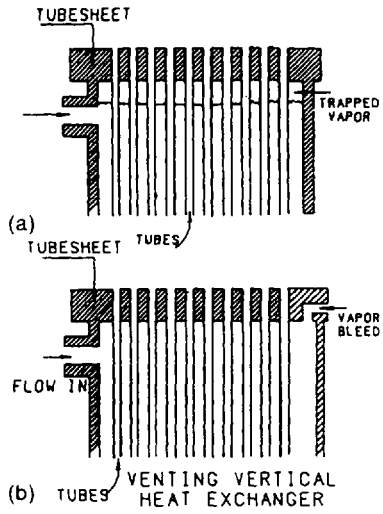


Figure 33 Crevice corrosion due to concentration of vapor phase and remedial measure. (a) Poor design, and (b) correct design.

Startup and Shutdown Problems

The construction materials should withstand not only the requirements at the design conditions but also the process upsets, startups, shutdowns, and standby. During these conditions, corrosion conditions can change significantly. Many corrosion problems do not originate when a plant is onstream. Rather, they can be traced to irregularities during startup or shutdown. Startup problems are often related to high temperature, difference in corrodent concentration, inadequate distribution of inhibitors, or incomplete oxygen removal [28]. Downtime problems are usually caused by residual process fluids or dry residues that result from prolonged shutdown periods or decaying of organic matter during shutdown periods. Residual fluids can promote localized corrosion such as pitting or crevice corrosion of stainless steel. Typical cases for shutdown problems are polythionic acid corrosion of stainless steel vessels in refinery applications, and SCC and sulfide attack of copper alloys due to ammonia liberated from putrefying organisms during shutdown periods.

Overdesign

In many instances, when the corrosive effect of a system is known, additional thickness to various components will be provided for in the design. This is known as a corrosion allowance. Because this thickness is in addition to that required for the design conditions, an extra cost is involved. Highly corrosive fluids may require the use of expensive corrosion-resistant metals such as stainless steel, titanium, nickel base alloys, zirconium, tantalum, and nonmetals such as ceramics, graphite, glass, Teflon, etc. However, with the use of the special materials normally the corrosion allowance is neglected or minimized.

Effect of the Service Environment: Code and Regulatory Requirements. The codes recognize that corrosion can occur and provide rules for including corrosion allowances to be specified by the designer in the calculation of required thickness.

4.3 Corrosion Control by Modification of the Environment (Use of Inhibitors)

Since corrosion is the reaction between a metal and its environment, any modification to the environment that makes it less aggressive will be beneficial in limiting the corrosion attack upon the metal. The corrosivity of a corroding medium can be changed by using various methods such as the following [77]:

1. Use a chemical additive, known as an inhibitor, that will have an effect on the electrochemical reaction to stifle corrosion.
2. Change the corrosivity of the environment by removing the active corrosive constituents. Some examples are removal of oxygen and carbon dioxide from boiler feed water, softening, demineralization of cooling waters, removal of chloride ions from a solution, and deaeration of acid solutions in contact with copper and nickel alloys.

Inhibitors

An inhibitor can be generally defined as a material that, when added to a corrodent (liquid), interferes with or retards the electrochemical reaction. To control corrosion, inhibitors are commonly added in small amounts to acids, cooling waters, steam, and other environments, periodically or continuously [78]. Inhibitors can be roughly classified according to the way in which they retard the electrochemical reaction to stifle corrosion. On this basis, if they inhibit the anodic reaction, they are called anodic inhibitors; those that inhibit the cathodic reaction are cathodic inhibitors; and if they inhibit both the anodic and cathodic reactions, they are called mixed inhibitors. The effect of an inhibitor in most cases is to form a barrier between the metal surface and the environment. Inorganic compounds such as chromates and nitrites interfere with the anodic reaction while the polyphosphates suppress the cathodic reaction. Another classification of inhibitors is single-component inhibitors and multicomponent inhibitors. The underlying principles of anodic and cathodic inhibitors are discussed next.

Anodic Inhibitors. During electrochemical reaction, a metal is dissolved at anodic areas to give metal ions, and electrons that flow to cathodic areas. This may be represented as follows for a divalent metal:

$$M \rightarrow M^{++} + 2e \tag{7}$$

A chemical that prevents or restricts action (in Eq. 7) is called an anodic inhibitor and usually functions by combining with the M^{++} ions emerging from the corresponding area to form an insoluble compound on the metal surface. Typical anodic inhibitors include chromates, nitrites, phosphates, molybates, orthophospates, silicates, and some organic materials.

There are of three general types of anodic inhibitors:

1. Passivators
2. Oxidizing inhibitors
3. Nonoxidizing inhibitors such as orthophosphate

The passivators function by converting an anodic area to cathodic area, usually by means of impermeable oxide films. Oxidizing inhibitors function by increasing the oxidation potential at the anodic surfaces to increase the rate of formation of gamma-iron oxide [79] or are effective in repairing discontinuity in the passive film by quickly oxidizing iron wherever the surface is exposed. Chromate is the best known oxidizing anodic inhibitor in cooling-water systems. Its merits and demerits are discussed next.

Chromate. Chromate is probably the most effective corrosion inhibitor for water systems. Protection is afforded by a film consisting of alpha-ferric oxide and chromic oxide [8]. Chromates are the least expensive for use in water systems and are widely used in the recirculating cooling-water systems of internal combustion engines. However, chromates and heavy metals have recently become ecologically unacceptable in many places. To avoid toxic chemicals and meet regulations on effluent discharge, a large number of substitutes were developed, including zinc, poly-and orthophosphates, phosphonates, and a variety of polymers.

Cathodic Inhibitors. Cathodic inhibitors work by increasing the degree of cathodic polarization, thereby reducing the overall corrosion rate and current density, or they reduce corrosion by interfering with any of the steps of the oxygen reduction reaction. The cathodic reactions that complement the anodic process (Eq. 6) are Eqs. 2 and 3, and these reactions are necessary to absorb the electrons released by the dissolution of the metal at the anode. A compound that restricts reactions by Eq. 2 or 3 is called a cathodic inhibitor. Reaction by Eq. 2 will prevail in acid solutions. Reaction by Eq. 3 will prevail over reaction by Eq. 2 when there is an ample supply of dissolved oxygen and a low concentration of hydrogen ions as in alkaline solutions. By preventing absorption of the electrons released by the anodic reaction, corrosion must stop. Zinc is a well-known cathodic inhibitor [80]. Typical cathodic inhibitors are calcium bicarbonate, polyphosphates, phosphonates, metal cations, and organics. Cathodic inhibitors are often termed "safe" because they do not usually cause localized pitting attack [16]. Cathodic inhibitors are somewhat less effective than anodic inhibitors [81].

Adsorption Inhibitors or Organic (Nonchromate) Corrosion Control Polymers. Some organic compounds are effective as inhibitors because of adsorption mechanisms. Oil inhibitors are effective because of the physical adsorption process [82]. Organic inhibitors used in automotive diesel engine cooling-water systems include amines, benzoates, organic phosphates, mercaptants, triazoles, and polar type oils. Organic inhibitors such as starch quinoline and its derivatives and thiourea and its derivatives are commonly used for inhibition in acid media.

Multicomponent Systems. Single-component inhibitors include chromates, sodium nitrite, silicates, sodium molybdate, and sodium phosphate. Multicomponent systems with many combinations have pronounced synergism in controlling steel corrosion in recirculating cooling-water systems compared with the individual components. Multicomponent systems can be either heavy metal treatments or non-heavy metal treatments (no zinc or chromate). Typical heavy metal multicomponent treatments include zinc chromate, zinc chromate/phosphonate, zinc polyphosphate, and zinc phosphonates. Non-heavy metal multicomponent systems (no zinc or chromium) in current use are [69,81] (1) combination of the phosphates (AMP/HEDP), (2) polyphosphate-phosphonate mixtures, and (3) the polyphosphate-orthophosphate.

Non-heavy metal treatment programs are receiving increased attention because of environmental regulations against discharge.

Passivation Inhibitors. Passivation inhibitors, also known as film formers, work by depositing protective films over the entire surface, which provides a barrier to the dissolution of the metal in the corrosive environment. Typical passivation inhibitors include (1) chemical oxidizing substances, such as chromate and nitrate, and (2) organic substances such as tannin, gelatine, saponin, and beta-diketones, used in alkaline solutions.

Precipitation Inhibitors. Precipitation inhibitors produce insoluble films on the cathode under conditions of locally high pH and isolate the cathode from the environment [69]. Sodium polyphosphate and zinc salts such as zinc sulfate and zinc chloride are examples of precipitation inhibitors.

Copper Inhibitors. Though the previously mentioned ferrous inhibitors exert some control over corrosion of copper base alloys, three specific inhibitors are extensively used on to protect

copper base alloys [69]: (1) mercaptobenzothinzole (MBT), (2) benzotriazole, and (3) polytriazone.

Requirements for Effectiveness of Inhibitors. The key to the success of an inhibitor is the maintenance of clean metal surfaces, which are essential for effective inhibitor film formation [83]. The inhibitors used should be compatible with the process fluids being used. Consideration should be given to avoiding adverse effects such as foaming, decrease in catalytic activity, degradation of another material, and loss of heat transfer [78].

Inhibitor Evaluation. To determine the effectiveness of an inhibitor for use in a specific application, a comparison is made by using any of the corrosion testing techniques to determine the corrosion rate of the medium without inhibitor and the test is repeated with each inhibitor present in the medium. The effectiveness of each inhibitor can be calculated from the following equation:

$$\eta_i = \frac{m_o - m_i}{m_o} \times 100 \tag{8}$$

where η_i is the inhibitor efficiency, m_o the corrosion rate without inhibitor, and m_i the corrosion rate with inhibitor.

Electrochemical techniques such as the galvanostatic pitting potential test can be used to determine the effectiveness of various corrosion inhibitors in the automobile cooling-water system. This method correlates the effectiveness of inhibitors in the prevention of pitting corrosion by measuring the inhibitor's effect on the pitting potential (E_p).

4.4 Corrosion-Resistant Alloys

Corrosion of certain metals is due to impurities in them. By controlling the impurities, the corrosion resistance can be improved markedly. Before the advent of the advanced refining techniques, ferritic stainless steels had relatively high levels of interstitials like carbon and nitrogen, and as a result had serious limitations with respect to fabricability, toughness, and corrosion resistance. The newer ferritics, especially those with high chromium content and very low carbon content, have become possible through argon oxygen decarburization (AOD), vacuum induction melting (VIM), and vacuum oxygen decarburization (VOD) [84]. On the other hand, a small addition of alloying element may have a profound effect on an alloy's resistance to certain types of corrosion. Addition of small amounts of copper to steel increases its atmospheric corrosion reistance; small amounts of phosphorus, antimony, and arsenic added to brasses inhibit dezincification; and small amounts of arsenic added to copper, and iron added to copper–nickel, increase the resistance to impingement attack and erosion–corrosion.

Besides changes in composition, metallurgical variations and mechanical effects may have an effect on reducing corrosion damage. Introduction of compressive stresses on the surface by shot peening will reduce corrosion fatigue or SCC. Annealing to reduce the internal stresses and solution annealing to remove the grain boundary segregation help in eliminating SCC and intergranular attack, respectively.

If corrosion of a metal in an environment is inevitable, use an alternate material, such as borosilicate glass, impervious graphite, zirconium, tantalum, Teflon, etc., that shows chemical inertness to most of the chemicals.

A recent focus to tackle severe corrosion is on three alloy families [85]: (1) duplex stainless steels, which exhibit good corrosion resistance to both pitting and SCC, and have about twice the yield strength of the typical austenitic stainless steel, (2) 6-Mo superaustenitic stainless steels, and (3) high-nickel alloys such as UNS NO 6625, UNS NO 4400, and UNS NO 7716.

4.5 Bimetal Concept

The term bimetal is applicable to any combination of two metals or alloys having nearly matching or widely dissimilar physical and chemical properties and bonded by one of a variety of processes. The bimetal concept is employed in (1) cladding, and (2) duplex or bimetallic tubes.

Cladding

Cladding has been used for many years in pressure vessels, piping systems, and heat exchangers (Fig. 34). Nuclear and petrochemical pressure vessels are weld overlay clad with 300 series stainless steels or high-chromium nickel-base alloys. The severe corrosion problems in various coal combustion and incineration environments have renewed interest in cladding technology for both Code-approved and enhanced-strength developmental alloys [74]. Typical cladding alloys include ferritic (straight chrome) and austenitic stainless steels, nickel-base alloys, titanium, zirconium, and tantalum. Clad steels satisfy severe service conditions at less cost than full-thickness sections of the costly corrosion-resistant material used for the cladding. Various cladding methods are discussed in detail in a separate section in Chapter 13.

Bimetallic or Duplex Tubing

Two dissimilar corrodents in a heat exchanger can cause havoc, with material having a propensity to corrosion to one fluid and virtually immune to the other fluid, or the problem of severe corrosion of different natures that sometimes attacks both sides of a tube can often be solved by treating such a condition as two separate corrosion problems. By selecting the specific kind of metal that is best for each condition, it is possible to combine two such metals into one tube, known as duplex tubing or bimetallic tubing. Duplex tubing is shown schematically in Fi.g 35. Specific information on duplex tubing is given in ref. 86.

The tube manufacturing method, mostly hot coextrusion, ensures close mechanical contact between the two metals without affecting the heat transfer properties. Duplex tubing is made up of various combinations of ferrous and nonferrous materials. Bimetallic tubes are available in a variety of stainless steel–carbon steel, Cu, brass, Al, and other combinations. Duplex tubings have been used in actual service for the past 25 years in oil refining, in production of synthetic rubber, and in process industries, chemical plants, coke by-products plants, refrigeration systems, and other applications. Typical metal combinations of bimetallic tubes used in refinery applications, high-temperature boiler corrosion, and condenser applications are discussed below.

Duplex Tubing for Refinery Applications. For oil refining and in the natural gas industry, duplex tubing with the following combinations is used [31]:

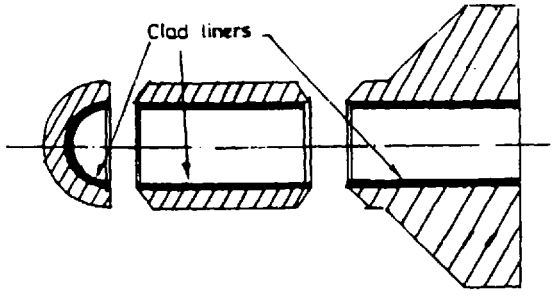


Figure 34 Cladded heat exchanger.

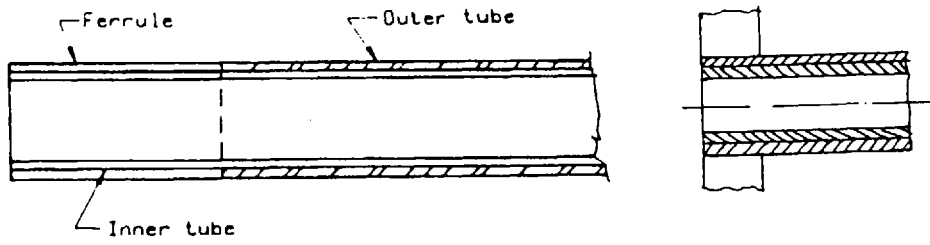


Figure 35 Duplex tubing.

1. Steel outside to resist various corrosive petroleum vapors and copper or copper alloy inside toward the fresh water.
2. Steel outside toward the oil and admiralty, aluminum brass, or cupronickel inside toward circulating saltwater.
3. Other applications in these industries call for the combinations of alloy steels with copper alloys or of aluminum with copper or brass either inside or outside.

Duplex Tubing in High-Temperature Boiler Corrosion. C-Mn or low-alloy steels, clad with a stainless steel or superalloys, are used in parts of the boiler where loss is excessive due to high-temperature corrosion [87].

Duplex Tubing in a Condenser Application. Ina condenser with stainless steel tubing, hot corrosive vapors caused little trouble within the tubes. But brackish cooling water on the shell side caused a problem. This situation was overcome by installing Carpenter bimetallic tubing consisting of type 304 welded stainless on the inside and deoxidized copper tube on the outside. Ferrules at the tube ends facilitated expanding of the tubes into type 304 stainless tube sheets.

4.6 Protective Coatings

Coatings are generally relatively thin films separating the two reactive materials or a metal from an environment. Applying a protective barrier between a corrosive environment and the material to be protected is a fundamental method of corrosion control [88]. It is most widely used for the protection of steel and other metals. Coatings can be metallic, plastic, paints, or organic. Typical metallic coatings include nickel coatings, lead coatings, zinc coatings, cadmium coatings, tin coatings, and aluminum coatings. Mechanisms by which coatings protect can be summarized as follows [89]:

1. They isolate the metal substrate and the environment, as with nickel electroplating.
2. They limit contact between the environment and the substrate, as with most organic coatings.
3. They release substances that are protective or inhibit attack, as with chromate primers.
4. They produce an electrical current that is protective, as with galvanizing.

Plastic Coatings

Plastic coatings often represent the ideal solution to a cooling water problem. Typical plastic materials used for coatings are polyethylene, polyvinyl chloride (PVC), epoxy resins, and polymides. Under certain conditions, they allow a cheap and corrosion-susceptible metal to be covered with a high-grade corrosion-resistant plastic coating. To ensure satisfactory protection, these must be nonporous and sufficient thickness (0.150–0.250 mm) [90].

Effectiveness of Coatings

To be effective, the coating film must be completely continuous. Any breakdown of the coating film leads to corrosion. Resistance to water is the most important requirement of the coating, since all coatings will come in contact with water or moisture in one form or another [88,89].

Surface Treatment

Surface treatment is resorted to on certain metals to improve their corrosion resistance in specific applications. For example, (1) mild steel or low-alloy steel heat exchanger tubes are alonized or aluminized (aluminum vapor diffused) for high-temperature oxidation resistance and protection from sulfide corrosion in refinery applications [91], and (2) titanium tubes are anodized or thermally oxidized to form an inert surface oxide film for its corrosion resistance, especially where hydrogen uptake is of concern.

4.7 Electrochemical Protection (Cathodic and Anodic Protection)

Principle of Cathodic Protection

Cathodic protection is defined as the reduction or elimination of corrosion by making a metal cathode by means of an impressed current or attachment to a more anodic metal (sacrificial anode) than the metal in the galvanic couple. These two methods are discussed next, and both the methods are shown schematically in Fig. 36. Cathodic protection is one of the recommended methods of protecting the tube sheet.

Sacrificial Anode. A cathode is the electrode where practically no corrosion takes place. If follows, then, that if all anodic areas can be converted to cathodic areas, the entire structure will become a cathode, and corrosion will be eliminated. Corrosion control by this principle is known as cathodic protection by sacrificial anode. By coupling the structure with a less noble metal, it is allowed gradually to corrode but is replaced after an interval of time. Zinc is often coupled with iron for this purpose and is termed a sacrificial anode (Fig. 36a). This method is mostly followed in heat exchangers for protecting the end closures.

Galvanic combinations such as zinc or cadmium or magnesium coatings on steel, often used to avoid corrosion, are known as sacrificial anodic coatings, because they corrode in preference to steel and protect the latter from rusting. Galvanizing a steel heat exchanger of a tube bundle did not improve the life expectancy, and galvanizing is not sufficiently effective to be worth even the slight extra cost involved [92].

Impressed Current Method. Because the corrosive action is electrochemical, electric current can be applied to effectively stop the attack of metals exposed to corrosive media. This technique is called cathodic protection by impressed current. In this method, an impressed current from a dc source is passed on to the metal to be protected and coupled to an insoluble anode such as platinum, graphite or ferrosilicon alloy or an expendable anode such as zinc, aluminum, or magnesium, thus forcing the structure that has to be protected to have as a large cathode so that it will not suffer attack. This method is presently employed in practice to protect buried pipelines carrying gas, oil, and water from corrosion by the surrounding soil. The protection of the tube sheet and the end closure when titanium tubes are installed in a exchanger is shown in Fig. 36b [93].

Shortcomings of Cathodic Protection. With a cathodic protection system in seawater and in certain applications, if condenser and heat exchanger tubes happen to be cathodic, they may become covered with an undesirable thermal resistance layer. This may require a decrease in

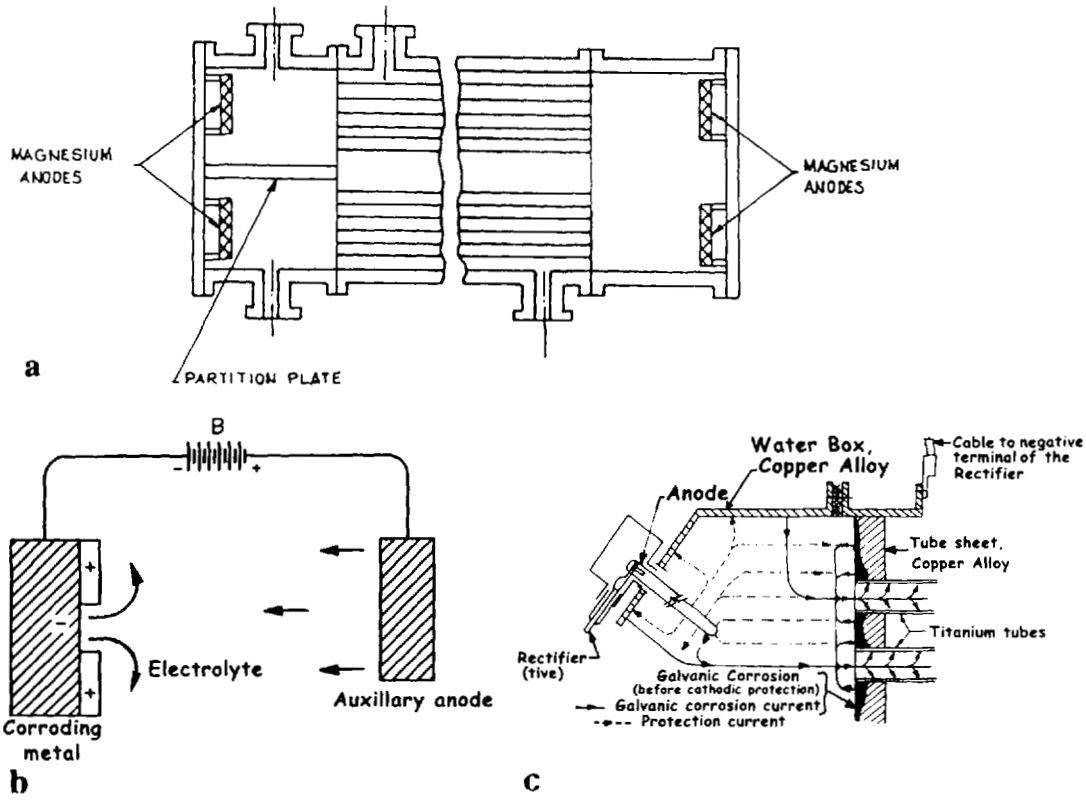


Figure 36 Cathodic protection. (a) Sacrificial anode; (b) impressed current method, and (c) impressed current method. (From Refs. 90 and 93.)

the amount of current flowing in the circuit or a change in the kind of anode, its location, or size [31]. Overprotection of a titanium tube sheet may result in the hydriding of the tube sheet.

Anodic Protection

If the potential of a metal is maintained in the range that leads to passivity, then the corrosion current density may be very low and will be stable. Consequently, the corrosion will be very low. This principle is employed in anodic protection. Anodic protection is an established, cost-effective method for corrosion control that can be applied in almost any electrically conductive solution in which a metal exhibits active–passive behavior [28,94]. The metals protected by anodic protection are iron, nickel, aluminum, titanium, zirconium, etc., and alloys containing major amounts of these metals. Electrolytes can vary from acid to alkaline. The pulp and paper industry was one of the first to investigate the use of anodic protection, particularly for carbon steel vessels containing alkaline solutions.

The advantages of using anodic protection are [28]: (1) low operating costs, (2) applicability to a wide range of severe corrodents, (3) high throwing power (can protect complex structures, needs few auxiliary electrodes), (4) protection current can give an idea of the corrosion rate, and (5) it is often possible to substitute for an expensive alloy in an unprotected plant a cheaper material that is anodically protected. The disadvantages of this method include the following [28]:

1. Anodic protection does not stop corrosion completely, but reduces it to a minimum level.
2. The failure of the electrical supply may be hazardous because of depassivation.
3. High installation costs: requires potentiostat, reference and auxiliary electrodes, and high starting current.
4. The requirement for electrical current makes this measure unsuitable for protection in organic liquid environments, or for components that are not continuously immersed.

4.8 Passivation

"Passivation" is the conditioning of a metal surface to produce a protective surface film that blocks corrosive ions from reaching the metal, thereby retarding corrosion. To change a metal from an active to a passive state, the electrode potential must be raised above the passivation potential. Passivation can be achieved by methods such as the following [95]: (1) applying an external current of sufficient strength or (2) using agents of sufficient oxidizing power to give a mixed potential above the passivation potential of the metal.

5 CORROSION MONITORING

Continuous operation, associated with higher operating efficiency, is putting a heavier burden on heat exchangers operating in various process industries such as oil refining, chemical, electric power plants, food and liquor processing, pulp and paper industries, etc. Changes in process parameters such as temperature, pressure, velocity, and concentration can accelerate corrosion rates. When the process changes occur, it is imperative to monitor their effects on corrosion rates to prevent equipment failure caused by corrosion. Corrosion monitoring can be used to optimize process conditions to achieve the maximum capabilities without sacrificing the integrity of the equipment. Corrosion monitoring has been discussed in detail by Britton et al. [96] and in ref. 97.

5.1 Benefits

Effective corrosion monitoring is justified economically for a large, complex plant at which production continuity is essential. The benefits of a successful corrosion monitoring program include the following [96]:

1. Corrosion problems can be predicted.
2. Plant maintenance and inspection can be scheduled.
3. Unscheduled shutdowns of plants can be avoided.
4. Improvements in reliability of equipments.
5. Better use of construction materials.
6. Detection of changes or abnormalities in the process affecting the corrosion rate.

5.2 Approaches to Corrosion Monitoring

In general there are three approaches for corrosion monitoring [98]: (1) local approach, (2) component approach, and (3) systems approach. The local approach involves investigations of corrosion in terms of local conditions. The component approach involves investigating plant components and their corrosion phenomena that arise due to the complex environmental and operational conditions. The systems approach considers the plant system in its totality. This approach deals with interrelations of phenomena occurring in different components of the system.

5.3 Corrosion Monitoring Techniques

Several techniques are used in corrosion monitoring, and the techniques are generally classified as either online or offline. Various online and offline techniques are described next.

Online Monitoring Techniques

Online corrosion monitoring is conducted to assess the corrosivity of the process stream and for detecting changes that may occur in operation. Online corrosion data are obtained from probes or sensors inserted into the system at accessible points that reproduce the particular area of interest. Various online monitoring techniques include corrosion coupons, electrical resistance principle, pitting potential, linear polarization principle and Tafel plots, hydrogen test probe, galvanic measurements, pH measurements, dimensional changes through online ultrasonic testing, radiography, and acoustic emission technique [96]. Some of these techniques are discussed next.

Corrosion Coupons. The most common online monitoring technique is with corrosion coupons. Corrosion coupons can be made in any size or shape, such that they are retrievable from process equipment without shutting down the unit. Normally, the corrosion coupons are carefully weighed before insertion and weighed after retrieval.

Weight Change. When results of other techniques are in question, they are usually verified with weight loss testing. However, weight loss determination would give misleading information in the case of localized attack such as pitting.

Hydrogen Diffusion. Atomic hydrogen can diffuse into steel and form molecules. If hydrogen diffusion is detected, it shows imminent danger due to hydrogen damage/hydrogen attack. Hydrogen diffusion can be measured using either a hydrogen probe (pressure measurement) or a hydrogen monitoring system (electrochemical).

Electrochemical Techniques. Electrochemical techniques are particularly useful in determining the corrosion rate that is actually happening in a metal at any given time. The three techniques most often used involve (1) electrical resistance principles using zero-resistance ammeters, (2) polarization curves, and (3) linear polarization curves. In the electrical resistance technique, the change in resistance of a thin wire under consideration due to the corrosion process is measured. Polarization curves may be determined galvanostatically, potentiostatically, or potentiodynamically. Anodic polarization measurements (where the electrode potential is changed in the positive direction to show current variations over a wide range of oxidizing potentials) are used primarily to determine critical pitting potentials, or breakdown potentials for localized corrosion. The principle of linear polarization technique, now referred to as the polarization technique, is as follows: The amount of externally applied current needed to change the corrosion potential of a freely corroding specimen by a few millivolts (approximately 10 mV) is measured. This current is related to the corrosion rate of the sample; that is, a linear relationship exists between the applied current and the resulting potential. If the metal is corroding rapidly, a large external current is needed to change its potential, and vice versa. This is the basis for the precise determination of corrosion rate.

Other methods include Tafel extrapolation (where the linear portion of the anodic or cathodic polarization curve is extrapolated back to the corrosion potential to locate the current density associated with corrosion rate at that potential), and current measurements at constant potential (where corrosion rate is monitored for a given oxidizing condition) [99].

Monitoring of Pitting Potential. The potential at which pit initiation occurs is called the pitting potential. Pitting potential is determined by electrochemical techniques, which consist

of measuring current and potential potentiostatically, either stepwise or by applying a constant-potential sweep rate in a standard chloride-containing solution.

Online Monitoring of Water Purity in Thermal Power Stations. Corrosion inhibition in a cooling-water system involves monitoring calcium hardness, alkalinity, total solids, pH, dissolved gases, etc. Automatic analyzers continuously monitor water and steam purities of thermal power stations. These permanent analyzers, whose results appear on a strip chart recorder, give more information than single manual analyses. Typical parameters monitored by online instruments include [100]:

Conductivity, pH (purity and acidity of the water)
Ammonia, hydrazine phosphate (control of conditioning)
Oxygen, hydrogen (dissolved gases)
Sodium, chloride, silica (harmful impurities in the loop)

Offline Monitoring Techniques

Offline monitoring techniques involve various nondestructive examination methods to determine the thickness and integrity of the heat exchanger and pressure vessel components. The various nondestructive testing (NDT) methods employed are:

1. Visual examination with or without optical aids such as borescopes
2. Eddy current testing
3. Magnetic particle examination
4. Liquid penetrant test
5. Ultrasonic examination
6. Radiography
   Thermography

Corrosion Monitoring of Condensers by Systematic Examination of the State of the Tubes

This procedure involves extracting representative tubes and examining them in the laboratory with modern analytical equipment [101]. In a tube investigation procedure one considers the three zones (inlet, center, and outlet) separately, because they are exposed to different conditions. On all samples the following four criteria are checked:

1. Microscopic examination of the condition of the tube surface
2. Residual wall thickness
3. Weight of the surface layer
4. Composition of the surface layer

5.4 Limitations of Corrosion Monitoring

It is important to be aware of the limitations of corrosion monitoring data. Some of the important limitations of corrosion monitoring are [96]:

1. The data are only a qualitative guide to the actual behavior of the plant or process.
2. A confidence factor is established only through experience, and particularly through comparison with other sources of information, notably that provided by NDT.

5.5 Requirements for Success of Corrosion Monitoring Systems

Many factors contribute to the success of a monitoring program. Some of the most important considerations include the following [96]:

1. Use of correct technique.
2. Correct location of monitoring probes.
3. Reliability of the equipment and instrumentation.
4. Data obtained must be straightforward to interpret.

6 COOLING-WATER CORROSION

Water, the most commonly used cooling medium, removes unwanted heat from process fluids. Water is an excellent solvent for numerous substances: It washes the mineral elements out of the earth, it absorbs gases (O_2, CO_2) from the atmosphere, it entrains suspended matter, and it promotes growth of microorganisms. If cooling water is used without treatment, it leads to the twin problems of fouling and corrosion [90]. Corrosion in cooling-water systems is electrochemical in nature and the corrosion products may be either soluble or insoluble. The insoluble material that forms a deposit on the heat transfer surfaces retards heat transfer and promotes corrosion in long run.

6.1 Corrosion Processes in Water Systems

Corrosion of metals in contact with water is electromechanical in nature. A generalized anodic oxidation reaction for ferrous metal has already been presented and for copper and aluminum materials are represented by [69]:

$$M \rightarrow M^{n+} + ne^- \tag{9a}$$

$$Cu \rightarrow Cu^{+} + e^- \tag{9b}$$

$$Al \rightarrow Al^{3} + 3e^- \tag{9c}$$

where M represents the metal that has been oxidized to its ionic form having a valence of n^+ and the release of n electrons. The reactions at the cathodic site on the metal surface are given by ref. [69]:

$$O_2 + 4H^+ + 4e^- \rightarrow 2H_2O \quad \text{(in the presence of oxygen)} \tag{10a}$$

$$O_2 + 2H_2O + 4e^- \rightarrow 4OH^- \quad \text{(in the neutral solution)} \tag{10b}$$

$$2H^+ + 2e^- \rightarrow H_2 \quad \text{(in the absence of oxygen)} \tag{10c}$$

6.2 Causes of Corrosion in Cooling-Water Systems

Depending on the sources of water—river, lake, ocean, or sea—cooling-water corrosion that attacks heat exchangers is due to one or more of the following impurities [8,69,81,90]:

1. Dissolved solids and water hardness
2. Chloride
3. Sulfate
4. Silica
5. Oil
6. Iron and manganese
7. Suspended mater such as turbidity, dirt, clay, silt, sand, etc.
8. Dry residue
9. Dissolved gases such as O_2, carbon dioxide, hydrogen sulfide, ammonia
10. Dissolved organic matter
11. Microbiological organisms

Apart from these factors, water temperature, pH, and flow velocity also influence corrosion. Effects of these factors on the cooling water corrosion are discussed next.

Dissolved Solids and Water Hardness

All waters containing calcium and/or magnesium salts such as calcium carbonate ($CaCO_3$), calcium bicarbonate [$Ca(HCO_3)_2$], magnesium carbonate ($MgCO_3$), and magnesium bicarbonate [$Mg(HCO_3)_2$] in considerable amounts are called "hard." The following classifications for hardness are often applied to fresh water [102]:

Soft: 0–50 ppm
Medium hard: 50–100 ppm
Hard: >100 ppm.

Total dissolved solids is the concentration of dissolved solids that cannot be removed by filtration. Seawater is many times higher in dissolved solids than freshwater.

Total hardness is the amount of calcium and magnesium salts, which may be present as bicarbonates (temporary hardness) or as sulfates, chlorides, nitrates, or carbonates (permanent hardness).

The overall aggressiveness of water is related to its hardness and alkalinity. Soft waters, which are low in calcium, are more corrosive than hard waters [69]. Hard water, high in calcium and magnesium, is less corrosive than soft water because of the tendency of the salts in the hard water to precipitate on the metal surface and form a protective film. However, increasing the dissolved solid contents of the waters increases its conductivity and hence a larger corrosion current can flow resulting in higher corrosion rate. The dissolved constituents can also have a variety of effects including increased scale and deposit formation. Hardness ions (Ca^{2+} and Mg^{2+}) and HCO_3^- ions are inhibitive and will suppress corrosion, but chloride (Cl^-) and sulfate (SO_4^{2-}) ions are deleterious and will increase the rate of some forms of corrosion [69].

Scale Deposition. Water-formed deposits are commonly referred to as scale. This scale increases the resistance for heat transfer and increases pressure drop, and promotes localized hot corrosion spots. Some hardness in the water may be helpful if the pH and alkalinity can be controlled to permit formation of a thin protective scale (termed stabilization of the water). Unfortunately, the buildup of a thick scale on the tube surface seriously interferes with heat transfer. The normal scale-forming compounds commonly found in cooling-water systems are calcium carbonate, calcium sulfate, calcium phosphate, and silicates. Of these compounds, calcium carbonate has very low solubility and perhaps is the principal scale-forming material in cooling waters. Bicarbonate ions react with hydroxyl ions generated at the cathode to produce carbonate, which precipitates with calcium from the water as calcium carbonate. The equation for calcium carbonate scaling is given by:

$$Ca(HCO_3)_2 + OH^- \rightarrow CaCO_3 + HCO_3^- + H_2O \tag{11}$$

Prevention of Calcium Carbonate Scale. Scale-forming tendencies of cooling water can be predicted by determining the Langelier saturation index (LSI), also known as the calcium carbonate saturation index, of the water. Some prefer the Ryznar stability index. The Langelier saturation index is defined as the difference between the actual pH value of the water and the value of pH that the water would have if it was in equilibrium with $CaCO_3$, also known as saturation pH. Accordingly, the LSI is given by

$$LSI = pH - pH_s \tag{12}$$

The LSI is not applicable to seawater because of the high salt content [102].

Determination of LSI. The LSI is calculated from (1) the alkalinity, (2) the calcium hardness, (3) the ionic strength (total solids), (4) the pH value, and (5) the temperature. The index can also be found out by direct determination of the pH of water as such and after saturating it with calcium carbonate. A condition of carbonate equilibrium with the absence of scale can be accomplished by adjusting any of the variables of the Langelier saturation index. The common practice is to lower the alkalinity and pH by adding sulfuric acid to the cooling water [70]. A chart for calculating the saturation index is shown in Fig. 37.

Scaling Control. If the Langelier saturation index is positive, scale will be deposited and will probably stifle corrosion of the metal. If it is negative, the water is unsaturated with $CaCO_3$, and it is likely to be corrosive and may dissolve existing hardness salts or may not be scale forming. Table 5 gives an indication of what may be expected [31]. From Table 5, the main choice appears to be between keeping the LSI low and controlling scale formation, or having a high index and controlling the corrosion. Methods to control scale formation are discussed in Chapter 9, Fouling.

Chloride

Chlorides are the main salts in seawater, around 19,000 ppm [102]. High-chloride waters are usually corrosive. High chloride ion concentrations easily destroy the protective surface films including passive films on a large number of metals [90], or the chloride forms complex ions with dissolved iron, thereby preventing or interfering with the formation of protective corrosion product scales [16]. In the case of austenitic stainless steels, chloride ions will easily destroy the passive film and result in pitting corrosion or when the metal is subjected to simultaneous tensile stress can cause chloride SCC. Aluminum is also easily attacked by chloride.

Sulfates

Sulfates are not as corrosive as chlorides [102]. However, concrete cooling water basins are endangered as soon as the water contains more than 250 ppm of sulfate ions [90].

Silica

Silica will react with magnesium or calcium to form deposits of insoluble magnesium or calcium silicates. Also, it will form siliceous glassy scales. To avoid such deposits, the silica concentration must be limited.

Oil

Oil is one of the most undesirable contaminants of industrial cooling-water systems. Oils usually leak into the system as a result of poor maintenance. They interfere with the action of corrosion inhibitors; by forming a thin film on metal surfaces, oils retard heat transfer; and they become nutrients for biological organisms [8].

Iron and Manganese

Iron oxide is produced either by internal corrosion of steel heat exchanger surfaces and transmission lines or from precipitation of soluble iron brought into the cooling system from the earth by the makeup water. Less than 0.2 ppm of iron and manganese is desirable. With higher contents, sludge-type hydroxides are precipitated in the presence of oxygen [90]. Iron oxide scale, which forms as easily dislodged "plate-like" layers, becomes lodged in the tubes and leads to localized impingement attack. Iron oxide scale is prevented by applying cathodic protection or by protective coatings [33].

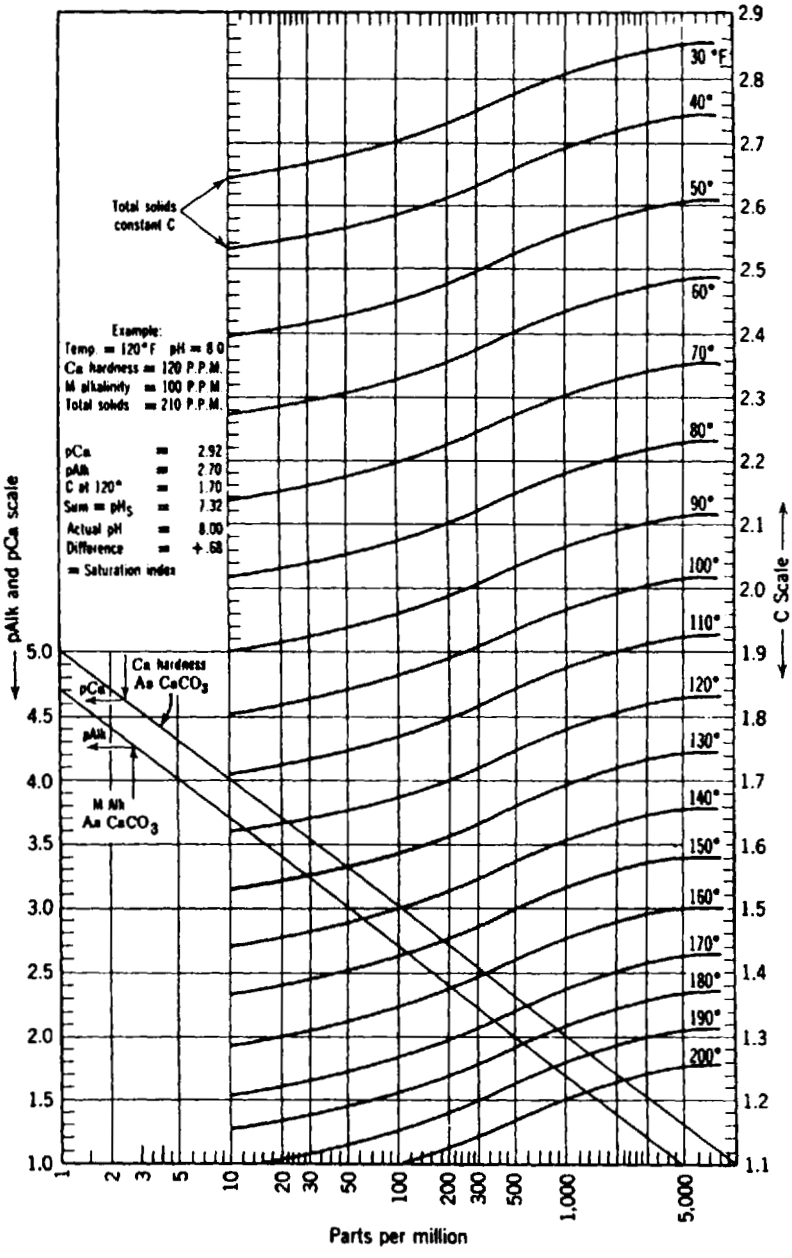


Figure 37 Chart for calculating saturation index. (Ca and alkalinity expressed as ppm $CaCO_3$; temperature in degrees F.) [Reproduced from S. Powell et al., *Ind. Eng. Chem., 37,* 842 (1945).]

Table 5 LSI Versus Probable Nature of Water

Actual pH	Saturation pH	LSI	Probable nature of water
6.5	8.5	−2.0	Corrosive, non-scale-forming
6.5	7.0	−0.5	Slightly corrosive and non-scale-forming
7.5	7.5	0.0	Slightly corrosive
7.5	7.0	+0.5	Slightly corrosive and scale-forming
9.0	7.0	+2.0	Practically noncorrosive and definitely scale-forming

Source: Ref. 31.

Suspended Matter

Suspended matter such as clays, silt, and corrosion products present in once-through or open cooling water system is capable of depositing on metal surfaces in low-velocity areas (<1 m/s), forming a physical barrier. This buildup will contribute to the formation of differential aeration cells and will promote localized corrosion [69].

Dry Residue

Dry residue after evaporation includes all the dissolved substances in the water. If dry residue expressed as salt content is greater than 500 ppm, the conductivity of water when it comes in contact with the dry residue will increase, which in turn will enhance corrosion [90].

Dissolved Gases

The most common dissolved gases are oxygen, carbon dioxide, hydrogen sulfide, and ammonia. Their role in cooling water corrosion is discussed next.

Oxygen. Cooling water saturated with oxygen will lead to increased corrosion. Oxygen can behave as a depolarizer and can increase the rate of corrosion by speeding up the cathodic reaction. It can also act as a passivator because it promotes the formation of a stable passive film. Dissolved oxygen is a major factor contributing to the natural corrosion of steel. Oxygen in traces promotes SCC of brass in the presence of ammonia; oxygen when coexisting with ammonia leads to the highest rate of sulfide attack; and oxygen also promotes condensate corrosion. Nevertheless, a minimum quantity of oxygen is need to form the carbonate-rust protective film. This should amount to about 5–6 ppm at normal ambient temperature [31].

Removal of Oxygen. Control of oxygen corrosion is critical to the reliability of a steam generator system. Mechanical deaeration and oxygen scavenging by chemical means effectively reduce oxygen levels in boiler feedwater systems [103]. Some of the successful devices to reduce the influence of oxygen on cooling water corrosion are mentioned in ref. 31. One of these methods is the mechanical method, which consists of raising the water temperature and lowering the pressure (vacuum) so that the gas is liberated (all gases are less soluble in water with increasing temperature and decreasing pressure). This method is applicable for removing other gases also from water. Another mechanical method consists of passing water over scrap iron, which removes the dissolved oxygen and is applicable to closed systems. There is also the chemical method that consists of adding a slight excess of sodium sulfite. The sodium sulfite reacts rapidly with the dissolved oxygen to form sodium sulfate:

$$2\,Na_2SO_3 + O_2 \rightarrow 2Na_2SO_4 \tag{13}$$

This method has been economically used for years for the removal of the last traces of oxygen from boiler water.

Carbon Dioxide. Natural cooling water always contains free carbon dioxide, in larger or smaller quantities. Dissolved free carbon dioxide makes water acidic. The free carbon dioxide is defined as the quantity that is required to retain the alkaline earth carbonate in accordance with the equation:

$$CaCO_3 + CO_2 + H_2O \leftrightharpoons Ca^{++} + 2HCO_3^- \tag{14}$$

Cooling waters without excess free carbon dioxide lead to the formation of a protective carbonate-rust scale, which represents one of the most important protective surface layers [90]. However, excessive carbon dioxide will cause corrosion. Excess carbon dioxide is removed from cooling water by spraying water over a mass of coke or other inert material exposed to the air. Sometimes by this process the carbon dioxide content can be reduced to 5–10 ppm. The second method involves treating the water with lime [31].

Hydrogen Sulfide. Hydrogen sulfide in cooling waters generally results from the action of bacteria on organic matter, particularly sewage. The presence of even few parts per million may change the corrosivity of water drastically. The presence of hydrogen sulfide in a water has the tendency to reduce inlet-end or impingement corrosion, but increases the probability of pitting corrosion occurring along the entire length of a tube [102]. Additionally, the salts created by this attack (copper sulfide, iron sulfide, etc.) are insoluble and precipitate on the metal surface as loose, noninhibitive deposits that promote galvanic couple and thus promote corrosion [8].

Ammonia. Ammonia is originally derived from the thermal degradation of various nitrogen-containing compounds added to the boiler feedwater to reduce corrosion. Ammonia does not cause excess corrosion on ferrous metals. However, traces of ammonia will cause both rapid general thinning and stress corrosion cracking in brasses. Pure copper and copper–nickel alloys are not susceptible to ammonia SCC, but a higher rate of uniform corrosion will take place with higher ammonia contents [90].

Dissolved Organic Matter. Dissolved organic matter in excess quantity tends to produce sludge-type deposits and fouling. Dissolved organic matter is detected indirectly by determining the potassium permanganate ($KMnO_4$) consumption. If the $KMnO_4$ consumption exceeds about 25 mg/L water, then the water is "dirty," which tends to produce sludge-type deposits and fouling [90].

Microbiological Organisms. Corrosion due to microbiological organisms has been discussed in the section on microbiologically influenced corrosion.

pH Value. The pH of the water can have several specific effects. High pH levels make the formation of heavy calcium carbonate and calcium phosphates scales likely. From Eq. 6, it is evident that where a greater number of hydrogen ions (low pH) is available, the corrosion reaction should occur more rapidly. Natural waters produce more or less neutral solution (pH value about 7). Clean seawater has a pH of about 8. In general the neutral and weakly alkaline waters usually cause no or only very slight corrosion on metallic materials, but weakly to strongly acidic water is always corrosive. Type of water also influences corrosion. The corrosiveness of a natural freshwater with a pH of 7–8 usually is much less than that of seawater with a similar pH. The difference is due to the presence of more mineral salts in seawater. Nevertheless, the pH is not the only determining factor. Water hardness, particularly the carbonate hardness, is of decided importance [90]. An additional factor that decides the water corrosion is the dissolved mineral salts.

Temperature. In general an increasing temperature will increase corrosion rates. Temperature plays a dual role with respect to oxygen corrosion. For an open system, beyond 175°F (80°C)

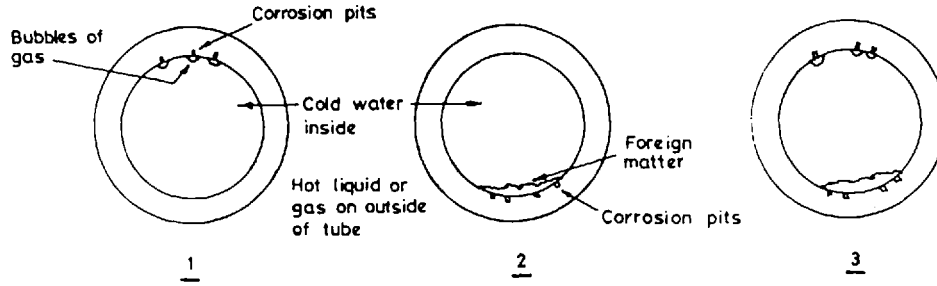


Figure 38 Hot wall effect. (From Ref. 31.)

increasing the temperature will reduce oxygen solubility, whereas for a closed system in which the oxygen cannot escape, corrosion continues to increase linearly with temperature [69]. Another effect of increased temperature is the increase of fermentation of organic materials with formation of sulfides, which promote corrosion [102]. In certain waters the corrosion rate drops off with an increase in temperature because the water deposits a thin scale. Calcium carbonate forms as a result of the decomposition of calcium bicarbonate at elevated temperatures [31]:

$$Ca(HCO_3)_2 \rightleftarrows CaCO_3 + H_2O + CO_2 \tag{15}$$

Hot Wall Effect. Severe local corrosion or pitting can rapidly perforate condenser and heat exchanger tubes on the cooling-water side where bubbles of air or foreign material separate from the water as shown in Fig. 38. Here the metal is hotter and the corrosion proceeds at a correspondingly higher rate. This is known as the hot wall effect.

Flow Velocities. Corrosion is favored by too low or too high cooling-water velocities. High velocity helps to prevent the accumulation and deposition of corrosion products, which might create anodic sites to initiate corrosion, and helps to maintain clean surfaces free from fouling deposits, stagnant areas, and hot wall effect. On the other hand, too high a velocity can destroy the protective surface film and result in erosion–corrosion or impingement corrosion, especially on metals such as copper and aluminum. The velocity, in general, should not be less than about 1 m/s. The following values apply in respect of the maximum admissible flow velocities [90]:

Pure aluminum	1.2 m/s
Pure copper	1.8 m/s
Copper containing arsenic	2.1 m/s
Naval brasses	2.0–2.4 m/s
CuNiFe 90/10	3.0 m/s
CuNiFe 70/30	4.5 m/s
Steel	3.0–6.0 m/s
Nickel alloys	Up to 30.0 m/s
Titanium	Above 30.0 m/s
Plastics	6.0–8.0 m/s

6.3 Cooling Systems

An understanding of the relationship between cooling water and the buildup of deposits and corrosion of heat transfer surfaces requires an awareness of cooling-system characteristics. There are basically three types of cooling systems:

Once-through cooling systems (Fig. 39a)
Open recirculating or closed cycles with cooling towers (Fig. 39b)
Closed recirculating systems (Fig. 39c)

A choice among these depends on quantity and quality of water available, water temperature, type of process plant, heat exchanger size, and means for water disposal.

Once-Through System

In a once-through cooling-water system, the water is pumped from a water source and supplied through the equipment and discharged. This is used where cheap supplies of water in large quantity are available (e.g., river, lake, sea). The water may be hard or soft, may contain dissolved solids, iron and manganese, silica, oil, dissolved gases, chlorides, micro-or macroorganisms, and suspended matter such as turbidity, dirt, clay, silt, etc., either singly or jointly. The major advantage of this system is low initial cost. The possibilities of water treatment of the large quantity of water handled for corrosion control are practically nil due to economic reasons, and environmental regulation on discharges [90]. Only upstream filtration or inoculation with dispersing agents or ferrous sulfate dosing can be considered. Additionally, cathodic protection control may be instituted.

Open Recirculating Systems

Open recirculating systems continuously reuse the water that passes through the heat exchanger. Circulated water can be drawn from spray ponds or cooling tower basins. Open recirculating cooling systems are oxygen saturated and may contain a high level of dissolved solids. This type of system requires large quantities of treated fresh makeup water because of the high

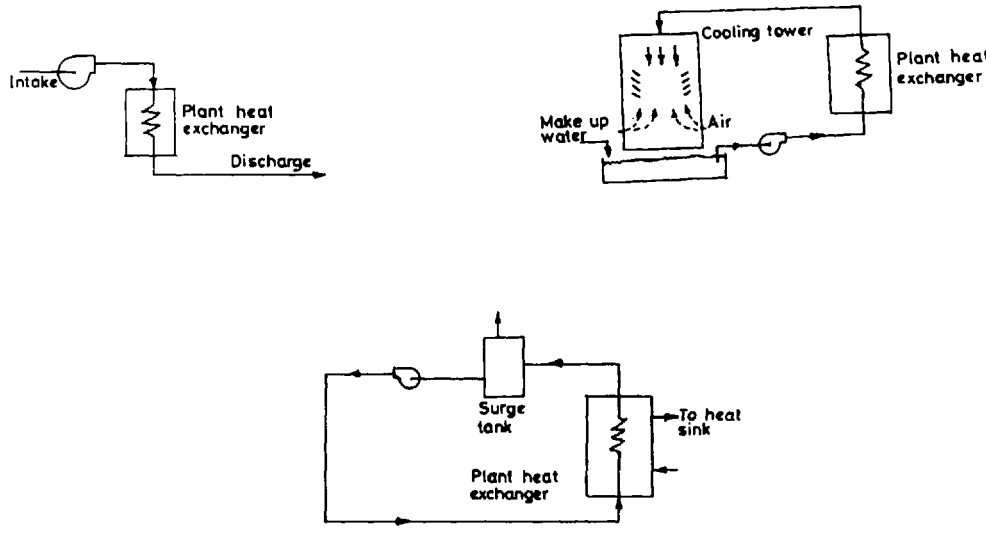


Figure 39 Cooling water system. (a) Once through; (b) open recirculating; and (c) closed circulating. (From Ref. 69.)

evaporation losses. Open recirculating systems are susceptible to corrosion and deposits. The intensive contact between the cooling water and air, as well as the solar radiation, stimulates the growth of algae and microorganisms. The treatment of cooling water of this system calls for the following measures [90]:

Monitoring and control of pH
Adding a corrosion inhibitor
Adding an algae-destroying agent
An additive (stabilizer) to prevent calcium carbonate precipitations
Possible makeup water treatment
Partial filtration

Closed Recirculating Systems

Closed recirculating systems continuously recirculate the same water. This system has little water loss and is free from algal growth. Because there are no evaporation losses, the requirement for makeup water is minimal, and the mineral content remains essentially constant. However, corrosion by-products can fould the heat exchanger. Hence, fouling deposits should be removed periodically by suitable offline cleaning methods. The completely closed cycle represents the ideal possibility for a clean and effective water treatment. Corrosion control by inhibitors is the most important control measure.

6.4 Corrosion Control Methods for Cooling-Water Systems

In principle, damage to cooling systems can be checked in many ways:

1. Proper material selection
2. Cooling water system design
3. Continuous water treatment system
4. Use of inhibitors
5. Ferrous sulfate dosing
6. Protective coatings
7. Cathodic protection
8. Passivation
9. Biological control
10. Scale control
11. Systematic cleaning

Corrosion control measures such as protective coating and cathodic protection, biological control, and various scale control measures have been discussed earlier in this chapter. Additional measures to control scaling as a foulant were discussed in Chapter 9, Fouling.

Material Selection

Corrosion control by means of cooling water design should take into account two possibilities: (1) the water treatment program, and (2) selecting corrosion-resistant material. Proper material selection involves selecting a material that can be exposed to the cooling water without the danger of corrosion. The question of whether corrosion in cooling systems can be checked by means of suitable material selection at the design stage or by instituting a permanent water treatment program when the unit starts functioning must be considered on the basis of corrosion damage and economic considerations [90]. On the material side, cupronickel and titanium are costly compared to carbon steel, aluminum and copper, and certain copper alloys such as brasses. One the water treatment side, continuous online treatment including dosing of chemicals and additives involves money, especially when the quantity of water handled is large, as

in once-through cooling water system. The objectives of such a strategy are to ensure that the operating costs are minimized throughout the life of the plant. This can be established by studying the following technical and economic considerations [33]:

Estimated life of candidate tube materials from trials, manufacturer's literature, and experience
Predicted number of outages and associated costs
Number of retubes required
Capital costs of materials and retubing costs
Heat transfer efficiency and thermal performance effects
Compatibility with other cooling-water system materials

Cooling-Water System Design

In planning a heat exchanger cooled by natural water, the first step is to obtain the following information about the water [32]:

Analysis of water
Water temperature upon entry
Solids content
Content of organic matter including H_2S

Certain guiding principles to be considered at the design stage are as follows [90,92]:

Empty the cooling system completely when in the standstill condition. Many more cases of corrosion have taken place when the cooling system was at a standstill than in operation.
When welding on the cooling-water side, care should be taken to avoid protruding weldments or crevices as a result of unsatisfactory weld penetration.
Design sealing in such a way that seals cannot lift on the water side.
Narrow gaps should be avoided in the design stage. If this is not possible, the gap width should preferably be large (>0.5 mm).
The flow velocities should be neither too low nor too high. Except for coppers and brasses, maintain water velocities as high as practical. Velocities of 3–8 ft/s are the minimum desired.
Beware of galvanic coupling.
Always maintain vents on top tube sheets.
Locate water inlet and outlet nozzles on the shell side as near the tube sheets as possible to reduce "dead pockets."
Place water on the tube side, and the process liquid on the shell side.

Additional guidelines were given by Forchhammer [32]:

In the construction phase, check the integrity of system components for tightness with low-chloride water free from solids.
To form the first oxide layer in the tubes, the unit should run several weeks without interruption.

Water Treatment

By water treatment, we either remove the aggressive components to a great extent or add specific chemicals to the water. In this way, both corrosion and fouling are avoided. Water treatments can be generally subdivided into three main groups:

Chlorination/settling/filtration to remove the turbidity and microorganisms
Water softening to remove water hardness
Partial or full demineralization for the removal of hardness and all dissolved salts

Removal of hardness is effected by (1) the cold lime process, (2) the sodium cation exchange process, (3) demineralization, and (4) the acid process.

Corrosion Inhibitors

The use of corrosion inhibitors is one of the foremost methods of controlling corrosion in a cooling-water system. The main effect that corrosion inhibitors have in aqueous ferrous systems is to reduce the initial corrosion rate sufficiently to allow the gamma-iron oxide passive film to form and, in some cases, to take part directly in film formation. Corrosion control by inhibitors has been discussed in the section on corrosion prevention and control.

Ferrous Sulfate Dosing

It is difficult to form protective films on copper alloys such as aluminum brass while subjected to brackish water and seawater. The addition of ferrous sulfate offers a possibility of building up a protective film and diminishing the danger of erosion–corrosion [104]. Experience has shown that the best results are obtained under the following conditions [32,93]:

Ferrous sulfate dosing, tube cleaning by sponge balls or brushes, and deaeration must start working from the very beginning, as startup after the first corrosion attack has occurred cannot stop corrosion.
Cleaniness of tube surfaces is especially important while commissioning.
A water temperature above 8–10°C.
Association with continuous tube cleaning.
Solution injected at water box inlet.
Chlorination stopped during injection, since investigation shows that a synergistic effect between iron and chlorine can lead to rapid attack and early failure.

The optimum dose to form the protective film depends on the temperature and content of organic matter in seawater. Typical injection values range between 0.5 and 1 ppm of Fe^{2-} 1 h per day or continuous injection of 0.02–0.05 ppm [105]. A graph for ferrous sulphate dosing is given in Fig. 40.

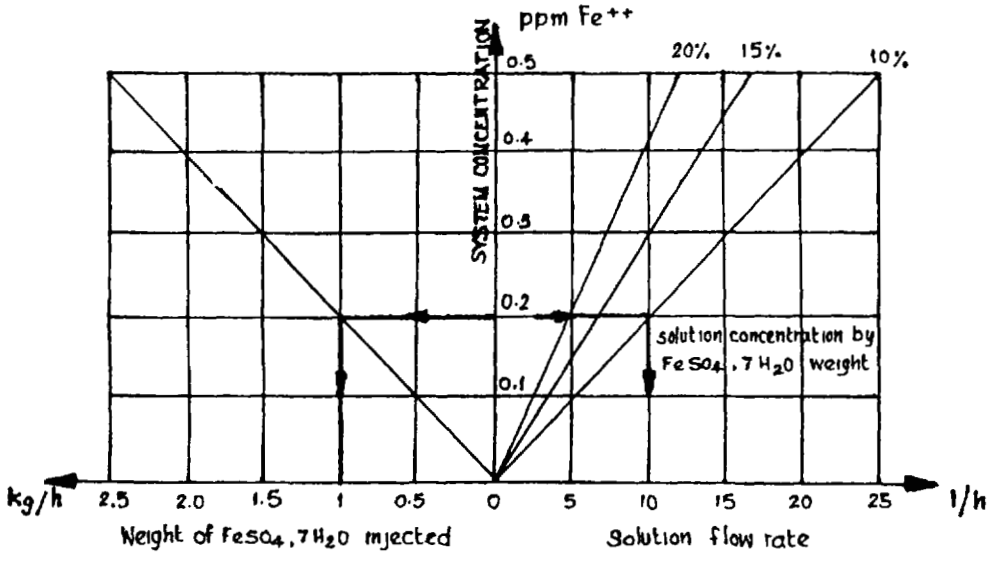


Figure 40 Ferrous sulfate dosing (per 1000 m^3/h of circulating water to be treated). (From Ref. 93.)

Passivation

Donohue et al. [95] discussed passivation of clean metal surfaces in cooling-water system through pretreatment of surfaces by application of a polyphosphates–surfactant combination and prefilming with chromate or nonchromate zinc polyphosphate or polymer polyphosphates. Chromate, nitrite, and orthophosphate (in the presence of oxygen) can promote passivity on clean iron surfaces.

6.5 Influence of Cooling-Water Types on Corrosion

Cooling waters may vary from the purest of distilled or demineralized waters to full-strength seawater. High-conductivity chloride-bearing water, saturated with oxygen, leads to concentration cell corrosion or deposit attack on almost all alloys, ferrous or nonferrous, regardless of their inherent resistance to water.

Fresh Water

In general, if fresh water is involved, no serious corrosion problems are likely to arise. Fresh waters are normally handled with tubes of arsenical copper, inhibited admiralty brass, inhibited aluminum brass, aluminum bronze, red brass, or copper–nickels [102].

Seawater Corrosion

Some of the key findings of 20 years of corrosion research on seawater are as follows [106]:

1. The presence of dissolved oxygen in seawater and desalting brine is the single most important factor in determining the performance of mild steel, low-alloy steels, copper alloys, and, to some extent, stainless steels.
2. For optimum performance of mild steel, low-alloy steel, copper alloys, and stainless steels in seawater and brine, the pH should be as high as possible without promoting calcium carbonate scale or precipitation of magnesium hydroxide.
3. Low-alloy steels can perform well, as much as 30% better than mild steels in typical desalination environments.

In seawater applications, arsenical copper and red brass 85:15 would not be used for tubes in power plant condensers cooled with seawater. Inhibited aluminum brass tubes are most widely used. Aluminum bronze (5%) would be suitable for acid-polluted seawater. Copper–nickels will give better service than other tubes in polluted waters [102].

Brackish Waters

Brackish waters are a mixture of seawater and fresh water. They are generally less corrosive than seawater except where contaminated with industrial wastes and sewage. In general, when contaminants are present, aluminum brass and aluminum bronze prove more satisfactory than other alloys. In the absence of contaminants, arsenical admiralty and the cupronickel alloys are satisfactory. The choice between these two depends upon water velocity [31]. Among ferrous alloys, the ferritic stainless steels, such as type 410 (12% chrome) and type 430 (18% chrome), are unsatisfactory in brackish cooling water due to insufficient alloy content to repair the passive films that are broken down by the deposit attack. Hence, the use of straight chrome stainless steel is to be avoided in brackish cooling water [92].

Boiler Feedwaters

Generally, boiler feedwaters are only slightly corrosive toward copper and its alloys due to deaeration and water treatment. The selection of the proper alloy is generally based on the temperature and pressure requirements. Copper and arsenical admiralty brass are the most commonly used for the low-pressure and low-temperature feedwater heaters, whereas cupron-

ickels are used for the higher pressure and higher temperature heaters because of their higher creep strength [31].

6.6 Corrosion of Individual Metals in Cooling-Water Systems

Aluminum

Waters containing small amounts of the heavy metal ions such as iron, copper, chlorides, and mercury will cause pitting corrosion. Waters that are essentially neutral offer no problem. Pitting of aluminum may be experienced beneath deposits. Use of the Alclad products often makes aluminum usable in cooling-water services like automobile radiators.

Copper and Its Alloys

Copper and its alloys are very important heat exchanger materials because of their generally high resistance to corrosion in waters. However, these alloys too can suffer corrosion under deposits, erosion–corrosion, dezincification of the brasses, and sulfide attack.

Steel

The corrosion of steel in cooling water is governed mainly by the oxygen availability and water composition [92]. Corrosion attack is overcome by addition of inhibitors and cathodic protection.

Austenitic Stainless Steel

The corrosion resistance of chromium–nickel (18-8) stainless steels depends upon a passive surface film. This film is readily penetrated by the chloride ion. For this reason, the stainless steels are subject to pitting and stress corrosion cracking from the chlorides. The pitting rate of the 18-8 alloys is usually quite low in closed-cycle cooling waters and in inhibited water associated with periodic tube cleaning.

Superferritics and Superaustenitics

These steels have been primarily developed for seawater applications.

Titanium

Titanium is an ideal material for seawater applications in the absence of fouling deposits.

6.7 Forms of Corrosion in Cooling Water

A wide spectrum of materials is used on the cooling-water side. These materials are affected by most forms of corrosion discussed earlier. The corrosion prevention and control measures discussed therein are equally applicable to combat cooling-water corrosion also. Various forms of corrosion, susceptible alloys or susceptible components, and remedial measures are mentioned very briefly in the following paragraphs.

Uniform Corrosion

All alloys, especially copper and its alloys, suffer uniform corrosion, which is controlled by pH adjustment, inhibition, and proper material selection.

Galvanic Corrosion

Less noble metals experience galvanic corrosion. Susceptible components are tube sheets, water boxes, bolts, and flanges. Alloys close to one another in the galvanic series should be used. Use insulation to separate the active metal from the noble metal.

Pitting Corrosion

Susceptible materials include aluminum, stainless steels, and copper alloys. Pitting corrosion takes place on the tube sheet and tube wall in the form of pits after local destruction of the protective film by deleterious chemical species such as chlorine or mercury ions. Additionally, at water speeds below about 3 ft/s, suspended solids tend to settle on the tube and may initiate pitting corrosion under the deposits due to differential cell action [104]. Causes for pitting on the tube side include the following [32]:

Nonhomogeneous tube surface
Irregular sludge deposition from the water
Local concentration of salt during standstill
Putrescent products with H_2S
Dry-out of protective layer followed by peeling off
Small metallic inclusions like oxides, and sulfides
Foreign matter, such as sand, oil, barnacles, etc.

Most of these potential causes of pitting corrosion can be avoided by tube cleaning or removing chloride ions and others involving the water chemistry; use steel containing Mo.

Crevice Corrosion

Crevice corrosion takes place in the area between the tube and the tube sheet, at gasketed joints, beneath deposits, and at bolt holes. Proper tube expanding will prevent the circumferential tube crack in tube-to-tube-sheet joints. While pitting and crevice corrosion normally occur fairly uniformly throughout the heat exchanger, the attack may predominate on the bottom of the internal surfaces of the tubes if mud or sediment has collected there and promotes crevice corrosion [26].

Stress Corrosion Cracking

Most common metals and alloys are susceptible to SCC. This form of corrosion takes place at the tube-to-tube-sheet expanded joints, and at U-tube bends.

Corrosion Fatigue and Fretting Wear

All alloys, at the tube and baffle interface, and tubes at midspan due to collision between adjacent tubes are susceptible to corrosion fatigue and fretting wear.

Erosion of Tube Inlet

When the cooling water contains large quantities of suspended abrasive solid particles, any protective film formed is rapidly removed and the tube is liable to thin [104]. The most common tube failures due to erosion–corrosion from impingement attack are discussed in the section on erosion–corrosion. The problem of inlet-end tube erosion (erosion–corrosion) in high-pressure feedheaters with carbon steel tubes and condensers with copper alloy tubes is discussed here. In general, the factors governing erosion–corrosion in feedwater heaters are [107]:

Feedwater velocity (turbulence)
pH value of feedwater (protective layer of FE_3O_4)
O_2 content of feedwater (corrosion)
Feedwater temperature (protective layer)

It has been suggested that at the usual pH values (9–9.5) and O_2 contents (0.002–0.007 ppm) and with water chambers and tube inlets designed to promote uniform water flow, erosion at the tubes and tube inlets can be eliminated, even for high water velocity [107].

Dezincification

Tubes and tube sheets made of brasses are susceptible to dezincification.

Microbiologically Induced Corrosion

All but the higher nickel–chromium alloys and titanium have been found to be subject to microbiological corrosion. This form of failure was discussed earlier.

6.8 Material Selection for Condenser Tubes

The following main physical and chemical parameters revealed by water analysis are used to select the tube materials [105]: total dissolved solids (TDS), total suspended solids, sand content, chloride content, sulfur and NH_3 content, and biochemical oxygen demand. The selection of materials for cooling water applications based on flow velocity and total dissolved solids is shown in Fig. 41.

6.9 Operational Maintenance of Condensers and Feedwater Heaters

Important corrosion control measures for the maintenance of condensers and feedwater heaters include the following [108]:

1. The tubesheets are clad with stainless steel.
2. All water boxes are fitted with sacrificial anodes.
3. Depending on the water quality, ferrous sulfate is dosed.

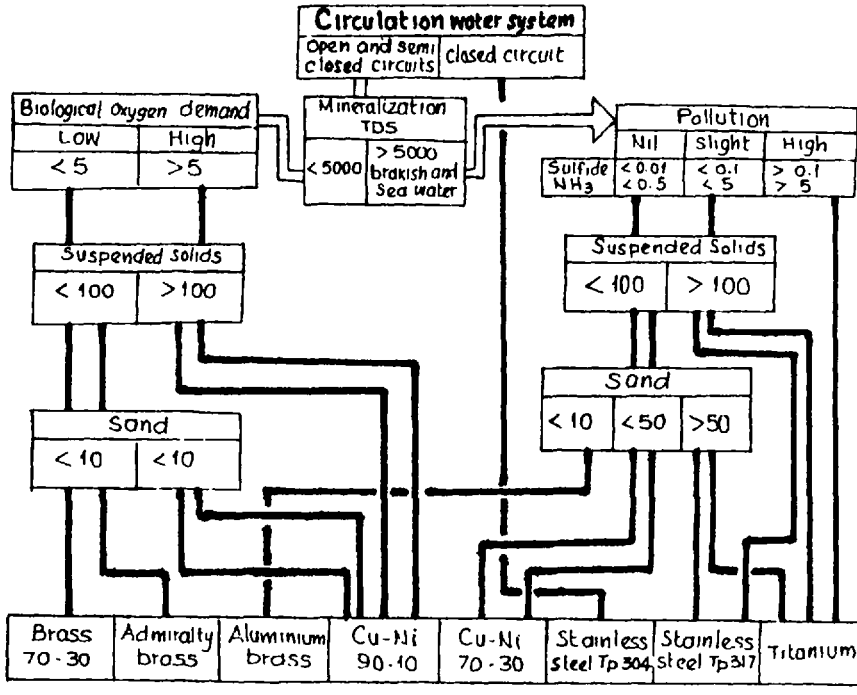


Figure 41 Selection of tube materials for cooling water applications [93].

4. Upstream filtration ensures clean filtered water in association with an online cleaning system using sponge rubber balls to permit continuous cleaning of the tubes.
5. Excessive biological growth is controlled with chlorine.
6. Operation and shutdown based on many years of experience ensure correct treatment of the heat exchangers.

7 MATERIAL SELECTION FOR HYDROGEN SULFIDE ENVIRONMENTS

Degradation of steel by hydrogen sulfide (H_2S) is now recognized as a serious problem in pipelines handling sour crude oil or gas in petroleum refinery equipment. Sour environments are defined as fluids containing water as a liquid and hydrogen sulfide. Hydrogen sulfide resistance steels for pressure vessels or pipelines in sour environments are often required to have both resistance to H_2S cracking and low-temperature toughness. Because iron-base alloys are principal materials of construction, these alloys have been the focus of study for many years. An important reference on hydrogen effects on steels is Warren [109].

7.1 Effects of Hydrogen in Steel

Hydrogen sulfide below dewpoint forms complex sulfides on metallic surfaces. Monoatomic hydrogen can then diffuse into the material and recombine to form molecular hydrogen at voids, laminations, microcracks, or discontinuities around inclusions, generating extremely high pressures [109]. As an interstitial element in the body-centered cubic (bcc) ferrite lattice, hydrogen can cause a number of mechanical problems for steels. It gives rise to blistering and cracking. It stiffens the metal, impairing its ductility. Spontaneous cracking of materials is possible if the material hardness is not limited. The effect of hydrogen absorbed by carbon steels is well known and extensively reported in the literature. The primary effects are:

1. Hydrogen-induced cracking (HIC) producing stepwise cracks to the metal surface.
2. Hydrogen embrittlement (HE) due to loss of ductility under a slow tensile loading.
3. Cracking in high-strength or high-hardness steels, known as hydrogen sulfide stress cracking (HSCC) or sulfide stress corrosion cracking (SSCC).
4. Blister formation originating at nonmetallic inclusions, known as hydrogen blistering.

Figure 42 shows the effects of hydrogen on steel except hydrogen embrittlement. Requirements for the manufacture of pressure vessels for wet H_2S source is discussed in WRC Bulletin 374 [110].

7.2 Sources of Hydrogen in Steel

Hydrogen embrittlement and other phenomena influenced by hydrogen require a susceptible material and a fabrication method or process capable of promoting the entry of hydrogen into the steel. Before hydrogen can enter a metal, it must first adsorb on the metal surface as atomic hydrogen. Nascent or newly created atomic hydrogen can result from various operational processes [109]: initial melting, electroplating, acid pickling, high-pressure hydrogen environment, decomposition of gases (e.g., ammonia), hydrogen pickup during welding, corrosion with cathodic liberation of hydrogen, and hydrogen from cathodic protection. Acid corrosion, particularly in the presence of a "poison" such as sulfide, cyanide, arsenic, selenium, or antimony ions, promotes the entry of the hydrogen into the steel [3]. The nascent atomic hydrogen (H°) charged into the steel as a by-product of the corrosion reaction rather than gas evolution as H_2 is shown by the following equation [109]:

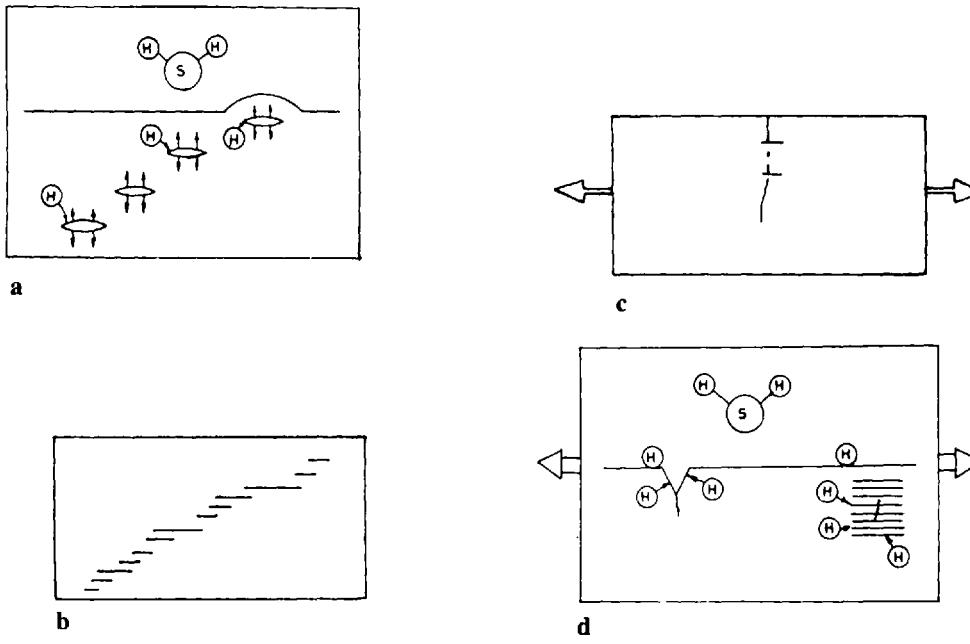


Figure 42 Schematic views of cracks. (a) Blister; (b) HIC; (c) SSCC in low tensile strength steel; and (d) SSCC in high tensile strength steel. (From Refs. 110 and 111.)

$$Fe^0 \rightarrow Fe^+ + +2e \quad (16a)$$

$$2H^+ + 2e \rightarrow 2H^0 \quad (16b)$$

7.3 Hydrogen-Induced Cracking

Some of the atomic hydrogen evolved by the corrosion reaction diffuses into the steel and forms molecular hydrogen, which accumulates at discontinuities, principally inclusion metal interfaces [111]. When the internal pressure due to the molecular hydrogen buildup exceeds a critical level, hydrogen-induced cracking (HIC) is initiated. It is recognized that HIC can occur in sour environments in the absence of external stress. Cracking can proceed along segregated bands containing lower temperature transformation products such as bainite and martensite. Cracking tends to be parallel to the surface but can be straight or stepwise.

Stress-Oriented Hydrogen-Induced Cracking

When the small hydrogen-induced cracks or stepwise cracks coalesce perpendicular to the axis of an applied tensile stress on a relatively low-hardness steel having a ferrite-pearlite microstructure, the phenomenon is known as stress-oriented hydrogen-induced cracking (SOHIC) [112]. It occurs around weldments (Fig. 43) in fabricated steel vessels and process equipment [113]. According to Kane et al. [113], the combination of stress concentration, residual tensile stress, hardness, and microstructure makes these locations prone to SOHIC.

Susceptibility of Steels to HIC

Metallurgy of Steels. The susceptibility of steels to cracking is influenced strongly by inhomogeneities such as the nonmetallic inclusions, their shape and distribution, and segregation

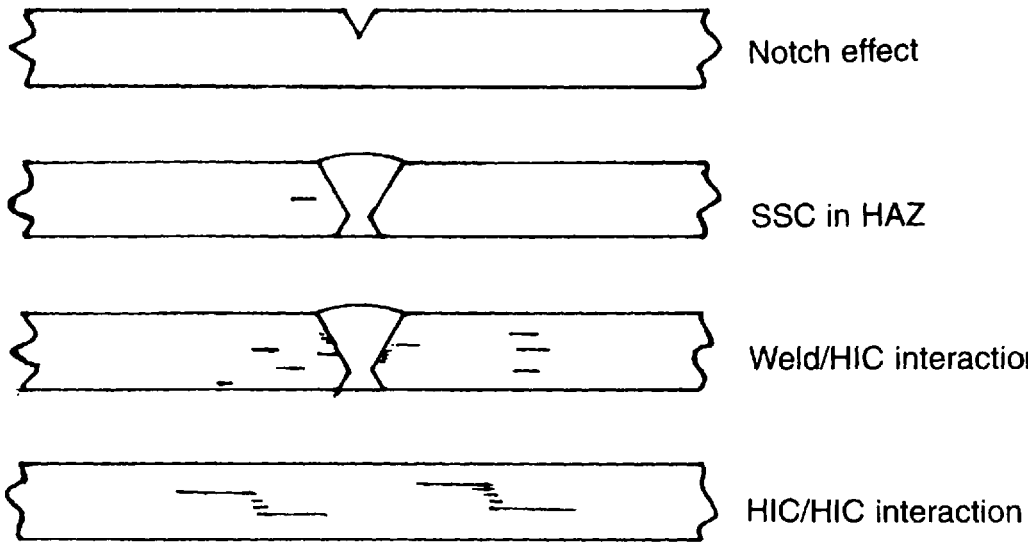


Figure 43 Schematic of SOHIC formation in carbon steel weldment [113].

of alloying elements [111]. Voids, MnS stingers, oxide inclusions, and laminations present in the steels act as nucleation sites for blistering, stepwise cracking, and SOHIC [112].

Environmental Factors. Environmental factors such as H_2S partial pressure, pH of the solutions, and other phenomena relevant to the absorption of hydrogen by the steel influence HIC [111].

Strength and Alloying Elements. The risk of cracking is increased by increasing the strength of steel as well as the partial pressure of H_2S.

Microstructure. In general a nonhomogeneous microstructure such as pearlite banding can give high susceptibility to hydrogen embrittlement.

Prevention of HIC

Steels with resistance to HIC embody the following features:

1. The effects of segregation can be minimized by restricting the levels of elements such as C, S, Mn, and P and controlled rolling of plates, which enables high strengths to be obtained at low carbon levels. For wet H_2S systems, there are recommendations to use low-sulfur steels that have been qualified for HIC and SOHIC resistance using laboratory testing. The sulfur content is generally reduced to below 0.01%.
2. Addition of calcium or rare earth metals to globularize the sulfide inclusions.
3. Low levels of oxide inclusions.
4. Mn is beneficial in improving toughness by refining the ferrite grain size, and therefore a minimum level of Mn must be maintained. Long elongated inclusions such as type II MnS are particularly favorable sites for crack initiation. Spheroidal inclusions are less susceptible to crack initiation except when they are in clusters [111].
5. Freedom from segregation so as to avoid bainitic or martensitic bands.
6. Reduced corrosion effects.
7. Periodic inspection of the wet H_2S refinery equipment even if it is made from HIC-resistant steel, as these steels may not provide total resistance to HIC and SOHIC in actual refinery service [113].

8. Use of stainless steel and stainless steel clad material for severe wet H_2S service as an alternative to reduce inspection and reinspection requirements. Clad products can be used for repair, replacement, or new construction [113].

7.4 Hydrogen Embrittlement

Mechanism of Hydrogen Embrittlement

Hydrogen embrittlement involves two issues: (1) The crack has been formed by hydrogen, and (2) the toughness changes because the material has been embrittled. Atomic hydrogen dissolved in steel can interfere with the normal process of plastic deformation. If a steel of initially limited notch ductility (e.g., a steel hardened to 175,000 psi) is charged with atomic hydrogen and strained at the appropriate rate and temperature, it cannot plastically deform to locally accommodate a notch or stress raiser. Consequently, a crack is initiated and brittle fracture can take place. Severely cold-worked ferritic steels and as welded steels of higher carbon content are similarly vulnerable [109]. Plain carbon or alloy steels heat-treated to tensile strengths greater than 120,000 psi or hardness >Rc 22-23 are susceptible to hydrogen embrittlement. However, the other forms of hydrogen damage such as hydrogen attack or hydrogen blistering are associated with unhardened low-alloy or carbon steel [114]. The susceptibility of steels to hydrogen embrittlement increases with [109]:

1. Increasing strength level (hardness) of the steel
2. Increasing amounts of cold work (plastic deformation)
3. Increasing residual or applied stress

The risk of cracking initiation should be reduced by avoiding notch effects, whether geometrical or "metallurgical." Metallurgical notches include the formation of hard zones in the parent metal and in the weld areas. Crack propagation can be controlled by limiting operating and/or residual stresses and also by postweld heat treatment.

Hydrogen Embrittlement of Steel Weldments

Susceptible Steels. Steels with weldments susceptible to hydrogen embrittlement include pressure vessel quality steels with 0.25–0.35% C, in plate thickness 1–2 in (25.4–50.8 mm), such as ASTM A515 and A516 [109].

Prevention of Hydrogen Embrittlement and Cracking of Welds. Welding-related measures for prevention of hydrogen cracking, such as use of dry electrode, joint surface cleanliness, sufficient preheat, and postweld heat treatment, will be helpful to prevent hydrogen embrittlement of welds. Hardness testing of weldments is a necessary requirement for most typical operating refinery or chemical plant environments. Limiting the weld hardness of carbon and low-alloy steels as indicated in NACE Standard MR-01-75 [115] can generally avoid this problem. Hardness of completed P-1 welds should be 200 BHN or less.

7.5 Hydrogen-Assisted Cracking

Hydrogen-assisted cracking (HAC), also known as hydrogen sulfide stress corrosion cracking (HSCC), is a special case of localized hydrogen embrittlement where the nascent atomic hydrogen is supplied to the steel as a by-product of the corrosion reaction. Acid corrosion of steel in the presence of a "poison" such as sulfide, cyanide, arsenic, antimony, or selenide ions is a prime example [109]. Examples for HSCC include sulfide stress cracking and cyanide stress cracking of hardened steel.

Prevention of HSCC

HSCC can be controlled or prevented by (1) selecting a material that is resistant to process corrosion, and (2) avoiding the formation of hard and brittle microstructures. These two aspects are discussed next.

Material Selection. HSCC can be controlled or prevented by selecting a material that is resistant to process corrosion; that is, if there is no corrosive attack on the material, there can be no cathodic liberation of hydrogen and, hence, no localized hydrogen embrittlement.

Avoiding the Formation of Hard and Brittle Microstructures. HSCC poses problems in weld zones. It can occur especially in heat-affected zones with high hardness [111]. Attention should be given to composition, hardenability, and welding procedures to avoid the formation of hard and brittle microstructures. The occurrence of HSCC observed typically in high-strength steels having yield strength higher than 90,000 psi (620 MPa) is currently mitigated by imposing a restriction of maximum hardness of 22 Rc or 225–235 BHN. Nevertheless, countermeasures similar to those described for the prevention of HIC are necessary to prevent HSCC in HAZ even with relatively low hardness [111].

7.6 Hydrogen Blistering

Hydrogen blistering is a mechanism that involves hydrogen damage of unhardened steels near ambient temperature [114]. The blister originates at nonmetallic inclusion or other internal defects such as voids, laminations, or microcracks. Blistering requires a vulnerable material and a fabrication method or process condition that promotes the entry of atomic hydrogen into the steel as a by-product of the corrosion reaction rather than gas evolution as H_2.

Susceptible Materials

Blistering is usually confined to the lower strength grades of steel, with tensile strength 70,000–80,000 psi, and Rc 22 or less hardness, rimmed or semikilled steels because of laminations, and free machining steels with extensive sulfide or selenide stringers that can serve as blister sites.

Prevention of Blistering

Some of measures suggested by Warren [109] for prevention of blistering include the following:

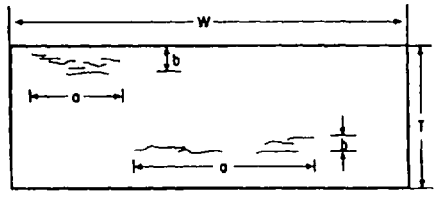


Figure 44 Determining hydrogen induced cracking (HIC) resistance (NACE specification TM-02-96). Test specimen and crack dimensions to be used in calculating: crack sensitivity ratio (CSR) = $\frac{\Sigma (a \times b)}{(W \times T)} \times 100\%$; crack length ratio (CLR) = $\frac{\Sigma a}{W} \times 100\%$; crack thickness ratio (CTR) = $\frac{\Sigma b}{T} \times 100\%$ where a = crack length; b = crack thickness; W = section width; and T = test specimen thickness. Note: in the past CSR has been calculated by some investigators as $(\Sigma a \times \Sigma b)/(W \times T)$, which is simply the product of CLR × CTR (i.e., $\Sigma a/W \times \Sigma b/T$). This does not give the same value as $\Sigma (a \times b)/(W \times T)$.

1. Selection of steel: (a) Where blistering is a concern, calcium-treated and argon-blown steels with 0.010% S maximum offer optimum resistance, (b) steels fully killed by silicon additions are preferable to aluminum-killed steel, (c) avoid susceptible steels such as rimmed, semikilled, and free machining steels, (d) hot-rolled or annealed material is preferable to cold-rolled material, and (e) apply cladding, lining, or protective coating with a more corrosion-resistant material.
2. Quality control and inspection of steel: To minimize blistering at planar defects, such as laminations and inclusion aggregates, steel plate should be ultrasonically inspected as per ASTM standards E114 and A578.
3. Venting of multilayer vessels.

Detection of Blisters in Service

Surface blisters may be detected by (1) visual inspection or by hand touch, (2) wet fluorescent magnetic particle inspection, (3) ultrasonic inspection to detect internal blisters within the steel, and (4) acoustic emission testing for locating active sites of SSC, HIC, and SOHIC [113]. Inspect both internal and external surfaces, including the less obvious items such as repair patch plate and unvented attachments (e.g., lifting lugs and support legs).

Correction of Blistered Condition in Steel Equipment

If blisters have jeopardized the vessel integrity, cut out the blistered areas and replace with ultrasonically inspected plate. Vent the blisters by careful drilling from the outside of the vessel. Avoid ignition of hydrogen within the blister; do not torch cut [109].

7.7 Pressure Vessel Steels for Sour Environments

Plates for Pressure Vessels in sour gas service are normally constructed of low-carbon steel ASME SA 516-70 normalized to ASTM Specification A300.

7.8 HIC Testing Specification

HIC testing is performed according to NACE TM-02-96 [116]. Refer to Fig. 44 for the various parameters evaluated by this test method. Testing frequency by the manufacturer is one plate of each thickness rolled from each heat of steel. Melting practices by Lukens, one of the leading manufacturers of A 516-70, are mentioned here [117]. All "HIC-Tested A 516" steels are produced to the Lukens Fineline Double-O Two or more restrictive requirements, which utilize various maximum sulfur levels and calcium treatment for inclusion shape control. Phosphorus and oxygen level maximums may also be accepted. Two classes of chemistry control and HIC test guarantee levels may be specified for crack length ratio (CLR), crack thickness ratio (CTR), and crack sensitivity ratio (CSR).

REFERENCES

1. Munger, G. C., Corrosion as Related to Coatings, in *Corrosion Prevention by Protective Coatings*, National Association of Corrosion Engineers, Houston, TX, 1984, Chapter 2.
2. Uhlig, H. H., Environmental effects on properties of materials, *Mater. Protect. Perform.*, July, 23–27 (1972).
3. Resistance to Corrosion, Inco Alloys International, WV, 4th ed., 1985.
4. Jarman, R. A., and Shreir, L. L., The basic principles of corrosion, *Welding & Metal Fabrication*, October, 370–379 (1987).
5. Corrosion Tests and Standards—Application and Interpretation, ed., R. Baboian, ASTM, Philadelphia, 1995.

6. Brosilow, R., Can you weld to avoid corrosion, *Welding Design & Fabrication*, September, 67–74 (1982).
7. Roser, W. R., and Rizzo, F. E., The corrosion engineer's look at passive alloys, *Mater. Protect. Perform.*, April, 51–54 (1973).
8. Silverstein, M. R., Cooling, *Chem. Eng.*, August 9, 84–94 (1971).
9. Fontana, M. G., and Greene, N. D., *Corrosion Engineering*, 2nd ed., McGraw-Hill, New York, 1978.
10. Craig, B., Introduction, in *Metals Handbook*, vol. 13, *Corrosion*, 9th ed., American Society for Metals, OH, 19XX, p. 79.
11. Atmospheric corrosion, in *Corrosion Basics—An Introduction*, NACE, Houston, TX, 1984.
12. Merrick, R. D., Design of pressure vessels and tanks to minimize corrosion, *NACE, Materials Performance*, January 1987, pp. 29–37.
13. AL-6XN^{R} Alloy, Allegheny Ludlum Allegheny Ludlum Steel Corporation, Pittsburgh, PA.
14. Kobrin, G., Materials selection, in *Metals Handbook*, Vol. 13, *Corrosion*, 9th ed., American Society for Metals, OH, 19XX, pp. 321–337.
15. Elliott, P., Design details to minimize corrosion, in *Metals Handbook*, Vol. 13, *Corrosion*, 9th ed., American Society for Metals, OH, 19XX, pp. 338–343.
16. Freedman, A. J., and Boies, D. B., Causes and cures for cooling water corrosion problems, *Petroleum Refiner*, April, 157–162 (1961).
17. Stanfield, B. M., Polarization cell: A common cure for corrosion, *Mater. Protect. Perform.*, March, 32–35 (1973).
18. Steven, P. L., General corrosion, in *Metals Handbook*, Vol. 13, *Corrosion*, 9th ed., American Society for Metals, OH, 19XX, pp. 80–103.
19. Open pitting corrosion, in *Corrosion Basics—An Introduction*, NACE, Houston, TX, 1984.
20. *Corrosion in Power Generating Equipment* (M. O. Speidel and A. Atrens, eds.), Plenum Press, New York, 19XX.
21. Lichtenstein, J., Fundamentals of corrosion causes and mitigation, *NACE, Materials Performance*, March, 29–31 (1978).
22. Wilten, H. M., Microscope speeds diagnosis of refinery corrosion, *Hydrocarbon Processing & Petroleum Refiner*, *40*(10), 151–280 (1961).
23. Asphahani, I. A., Corrosion resistance of high performance alloys, *Mater. Perform.*, *19*(12), 33–43 (1980).
24. Uhlig, H. H., Discussion—An essay on pitting, crevice corrosion, and related potentials, *Discussion, Materials Performance*, August 1983, pp. 35–36.
25. Dexter, C. S., Localized corrosion, in *Metals Handbook*, Vol. 13, *Corrosion*, 9th ed., American Society for Metals, OH, 19XX, pp. 104–122.
26. Syrett, B. C., and Coit, R. L., Causes and prevention of power plant condenser tube failures, *NACE, Materials Performance*, February, 44–49 (1983).
27. Jarman, R. A., and Shreir, L. L., Corrosion of jointed structures—Part II, *Welding & Metal Fabrication*, November/December, 445–449 (1987).
28. Henthorne, M., Understanding corrosion, *Chem. Eng.*, Desk Book Issue, December 4, 19–33 (1972).
29. Guide to selecting engineered materials, metals polymers ceramics composites, *Advanced Materials & Processes*, *137*(6), (1990).
30. Stengerwald, R., Metallurgically influenced corrosion, in *Metals Handbook*, Vol. 13, *Corrosion*, 9th ed., American Society for Metals, OH, 19XX, pp. 123–135.
31. *Condenser Tube Handbook*, Bridgeport Brass Company, UK.
32. Forchhammer, P., Results of damage research on corrosion failures in heat exchangers, *Heat Transfer Eng.*, *5*(3–4), 19–32 (1984).
33. Woodward, A. R., Howard, D. L., and Andrews, E. F. C., Condensers, pumps and cooling water plant, in *Modern Power Station Practice*, Vol. C, *Turbines, Generators, and Associated Plant* (D. J. Littler, E. J. Davies, H. E. Johnson, F. Kirkby, P. B. Myerscouh, and W. Wright, eds.), Pergamon Press, New York, 19XX, Chapter 4.

34. Crook, P., Practical guide to wear for corrosion engineers, *Mater. Perform.*, February, 64–66 (1991).
35. Erosion–corrosion, in *Corrosion Basics—An Introduction*, NACE, Houston, TX, 1984.
36. Yokell, S., *A Working Guide to Shell and Tube Heat Exchangers*, McGraw-Hill, New York, 1990.
37. Standards of Tubular Exchanger Manufacturers Association, 7th ed., Tubular Exchanger Manufacturers Association, Inc., Tarrytown, NY, 1988.
38. Cavitation, in *Corrosion Basics—An Introduction*, NACE, Houston, TX, 1984.
39. Dawson, J. L., Shih, C. C., Gearey, D., and Miller, R. G., Flow effects of erosion–corrosion, *Mater. Perform.*, April, 57–60 (1991).
40. Dawson, J. L., and Shigh, Corrosion Under Flowing Conditions—An Overview and Model, *CORROSION/90*, Paper No. 21, Houston, TX, 1990.
41. Syrett, B. C., Corrosion in fossil fuel power plants, in *Metals Handbook*, Vol. 13, *Corrosion*, 9th ed., American Society for Metals, OH, 19XX, pp. 985–1010.
42. Theus, G. J., and Daniel, P. L., Corrosion in steam generating systems, in *Corrosion in Power Generating Equipment* (M. O. Speidel and A. Atrens, eds.), Plenum Press, New York, 19XX, pp. 185–231.
43. M/s. Expando Seal Tools, Inc., Montgomeryville, PA.
44. Irving, B., Stress corrosion cracking: Welding's no. 1 nemesis, *Welding J.*, December, 37–40 (1992).
45. Kedzie, D. P., and Rizzo, F. E., The corrosion engineer's look at stress corrosion, *Mater. Protect. Perform.*, October, 53–56 (1972).
46. Logan, H. L., *The Stress Corrosion Cracking of Metals*, John Wiley, Inc., New York, 19XX.
47. McIntyre, D. R., and Dillon, C. P., Guidelines for Preventing Stress Corrosion Cracking in the Chemical Process Industries, Publication 15, Materials Technology Institute, 1985, pp. 8–14.
48. Berry, W. E., Stress Corrosion Cracking—A Nontechnical Introduction to the Problem, Defense Metals Information Centre, Battell Memorial Institute, Columbus, OH, DMIC Report 144, January 6, 1961.
49. Pement, F. W., Wilson, I. L. W., Reynolds, S. D., and Fletcher, W. D., Microanalytical characterization of stress corrosion cracking in power plant heat exchanger tubing, *Mater. Perform.*, pp. 26–39 (1977).
50. Craig, B., Environmentally induced cracking, in *Metals Handbook*, Vol. 13, *Corrosion*, 9th ed., American Society for Metals, OH, 19XX, pp. 145–149.
51. Brown, B. F., Stress Corrosion Cracking in High Strength Steels and in Titanium and Aluminum Alloys, Naval Research Laboratory, Washington, DC, 1972.
52. Parkins, R. N., and Foroulis, Z. A., Stress corrosion cracking of mild steel in monoethanolamine solutions, *NACE, Materials Performance*, January, 19–29 (1988).
53. Thompson, D. H., How to prevent stress-corrosion cracking of copper alloys, *Chem. Eng.*, February 6, 130–134 (1961).
54. Partridge, E. P., Hydrogen damage in power boilers, *Trans. ASME, J. Eng. Power*, July, 311–320 (1964).
55. Glaser, W., and Wright, I. G., *Mechanically Assisted Degradation*, pp. 136–144.
56. Corrosion fatigue, in *Corrosion Basics—An Introduction*, NACE, Houston, TX, 1984.
57. Tatnall, R. E., MIC: A corrosion engineer's enigma?, *Mater. Perform.*, August, 56 (1988).
58. Pollock, W. I., What is MIC?, *Mater. Perform.*, August, 56 (1988).
59. Scott, P. J. B., Goldie, J., and Davies, M., Ranking alloys for susceptibility to MIC—A preliminary report on high-Mo alloys (1), *NACE, Material Performance*, January, 55–57 (1991).
60. Kobrin, G., Corrosion by microbiological organisms in natural waters, *NACE, Materials Performance*, July, 38–42 (1976).
61. Pope, D. H., Duquette, D. J., Arland, J. H., and Wayner, P. C., Microbiologically influenced corrosion of industrial alloys, *NACE, Materials Performance*,, April, 14–18 (1984).
62. Pope, D. H., Soracco, R. J., and Wilde, E. W., Studies on biologically induced corrosion in heat exchanger system at the Savannah River Plant, Aiken, SC, *NACE, Materials Performance*, July 1982, pp. 43–50.

63. Borenstein, S. W., Microbiologically influenced corrosion of austenitic stainless steel weldments, *Mater. Perform.*, January, 52–54 (1991).
64. Borenstein, S. W., Microbiologically influenced corrosion failures of austenitic stainless steel welds, *Mater. Perform.*, August, 62–66 (1988).
65. Puckorius, P. R., Massive utility condenser failure caused by sulfide producing bacteria, *NACE, Materials Performance*, December, 19–22 (1983).
66. Tuthill, A. H., Guidelines for the use of copper alloys in seawater, *NACE, Materials Peformance*, September, 12–22 (1987).
67. Booth, G. H., and Mercer, S. T., *Nature (Lond.), 199*, 162 (1962).
68. Schutz, R. W., A case for titanium's resistance to microbiologically influenced corrosion (1), *NACE, Material Performance*, January, 58–61 (1991).
69. Boffardi, P., Control of environmental variables in water-recirculating systems, in *Metals Handbook*, Vol. 13, *Corrosion*, 9th ed., American Society for Metals, OH, 19XX, pp. 487–497.
70. Poole, J. S., and Bacon, H. E., Monitoring cooling water systems, *Mater. Protect. Perform.*, March, 16–25 (1972).
71. Borenstien, S. W., and Lindsay, P. B., Microbiologically influenced corrosion failure analyses, *NACE, Materials Performance*, March, 51–54 (1988).
72. Gooch, T. G., Stress corrosion cracking of welded austenitic stainless steel, *Welding in the Word, 22*(3/4) , 64–76 (1984).
73. ASM Committee on Corrosion of Weldments, Corrosion of weldments, in *Metals Handbook*, Vol. 13, *Corrosion*, 9th ed., American Society for Metals, OH, 19XX, pp. 344–368.
74. Swindeman, R. W., and Gold, M., Developments in ferrous alloy technology for high-temperature service, *ASME J. Pressure Vessel Technol., 113*, 133–140 (1991).
75. Collins, J. A., Effect of design, fabrication and installation in the performance of stainless steel equipment, *Corrosion*, January (1955).
76. Landrum, J. R., Designing equipment for corrosion resistance, in *Materials Engineering I: Selecting Materials for Process Equipment* (K. J. McNaughton, ed.), Chemical Engineering Magazine, McGraw-Hill, New York, 19XX, pp. 157–164. Originally published October 12, 1970.
77. Shabin, H. I., Corrosion inhibition in a cooling water system, *Corrosion Prevent. Control*, February, 9–12 (1982).
78. Inhibitors, in *Corrosion Basics—An Introduction*, NACE, Houston, TX, 1984.
79. Freedman, A. J., Cooling water technology in the 1980s, *NACE, Materials Performance*, November, 9–16 (1984).
80. Kaplan, R. I., and Ekis, E. W., Jr., The on-line removal of iron deposits from cooling water systems, *NACE, Materials Performance*, November, 40–44 (1984).
81. Boffardi, B. P., Corrosion control of industrial cooling water systems, *NACE, Materials Performance*, November, 17–24 (1984).
82. Beynon, E., Cooper, N. R., and Haningan, H. J., Cooling System Corrosion in Relation to Design and Materials, Engine Coolant Testing: State of the Art, ASTM STP 705, (W. H. Ailor, ed.), American Society for Testing and Materials, Philadelphia, 1980, pp. 310–326.
83. Hinchcliffe, D., and Town, J., Experience with nonchromate cooling water treatment (case histories), *NACE, Materials Performance*, September, 36–38 (1977).
84. *Source Book on the Ferritic Stainless Steels*, compiled by R. A. Lula, American Society for Metals, Metals Park, OH.
85. Debold, T. A., Select the right stainless steel, *Chem. Eng. Prog.*, November, 38–43 (1991).
86. Saunders, E. A. D., *Heat Exchangers: Selection, Design and Construction*, John Wiley and Sons, New York, 1989.
87. Llewellyn, D. T., *Steels, Metallurgy and Applications*, Butterworth-Heineman, 1992.
88. Munger, C. G., Corrosion prevention by protective coatings, *Mater. Perform.*, April, 57–58 (1987).
89. Coatings and linings, in *Corrosion Basics—An Introduction*, NACE, Houston, TX, 1984.
90. Weber, J., Corrosion and deposits in cooling systems—Their causes and prevention, *Sulzer Tech. Rev.*, 3, 219–232 (1972).

91. McGill, W. A., and Weinbaum, M. J., Aluminum vapor diffused steels resist refinery corrosion, *Mater. Protect. Perform.*, July, 28–32 (1972).
92. Asbaugh, W. G., Corrosion in heat exchangers using brackish water, *Chem. Eng.*, July 5, 146–152 (1965).
94. Singbell, D., and Garner, A., Anodic protection to prevent the stress corrosion cracking of pressure vessel steels in alkaline sulfide solutions, *NACE, Materials Performance*, April, 31–36 (1987).
95. Donohue, J. M., and James, E. W., Passivation and its application in cooling water systems, *NACE, Materials Performance*, October, 34–36 (1977).
96. Britton, C. F., and Tofield, B. C., Effective corrosion monitoring, *NACE, Materials Performance*, April, 41–44 (1988).
97. Schweitzer, P. A., ed., *Corrosion and Corrosion Protection Handbook*, 2nd ed., Marcel Dekker, New York, 19XX.
98. Somm, E., Schlachter, W., and Schwarzenbach, A., Power Generating Equipment, in *Corrosion in Power Generating Equipment* (M. O. Speidel and Andrejs Atrens, eds.), Plenum Press, New York, 19XX, pp. 3–25.
99. Chance, R. L., Walker, M. S., and Rowe, L. C., Evaluation of engine coolants by electrochemical methods, *Engine Coolant Testing: Second Symposium*, ASTM STP 887 (R. E. Beal, ed.), American Society for Testing and Materials, Philadelphia, 1986, pp. 99–122.
100. Bodmer, M., Baden, Ruston, C. A., and Luton, On-line monitoring of water purity in thermal power stations, *Brown Boveri Rev., 8*, 546–554 (1978).
101. Muller, R., and Baden, Improving the resistance of condensers to corrosion by systematic examination of the state of the tubes, *Brown Boveri Rev., 8*, 516–522 (1978).
102. Tracy, A. W., Nole, V. F., and Duffy, E. J., Water analyses and their functions in selecting condenser tube alloys, *ASME J. Eng. Power*, July, 329–332 (1965).
103. Cotton, I. J., Oxygen scavengers—The chemistry of sulfide under hydrothermal conditions, *Mater. Perform.*, March, 41–47 (1987).
104. Lockhart, A. M., Reducing condenser tube corrosion at Kincardine Generating Station with ferrous sulphate, *Proc. Inst. Mech. Eng.*, 1964–1965, pp. 495–512.
105. Paren, J., and Pouzenc, C., Design of power station condensers, *GEC Alsthom Tech. Rev.*, No. 6, 1991, pp. 19–38.
106. Schreiber, C. F., and Coley, F. H., CORROSION/75, paper no. 36, NACE, Houston, TX, 1975.
107. Sonnenmoser, A., Design and operation of large high pressure feedheaters, *Brown Boveri Rev., 7/8*, 352–359 (1973).
108. Sonnenmoser, A., and Wollschlegal, P., The design of extremely watertight condensers, *Brown Boveri Rev., 65*(8), 505–515 (1978).
109. Warren, D., Hydrogen effects on steel, *NACE, Materials Perform.*, January, 38–46 (1987).
110. Sauvage, M., Requirements for the manufacture of pressure vessels for wet H_2S Service, *WRC Bull., 374*, 72–81.
111. Kobrin, G., Materials selection, in *Metals Handbook*, Vol. 13, *Corrosion*, 9th ed., American Society for Metals, OH, 19XX, pp. 321–337.
112. Terasaki, F., Ohtani, H., Ikeda, A., and Nakanishi, M., Steel plates for pressure vessels in sour environment applications, *Proc. Inst. Mech. Eng., 200*(A3), 141–158.
113. Mirabal, E., Bhattacharjee, S., and Pazos, N., Carbonate-type cracking in an FCC wet gass compressor station, *Mater. Perform.*, July, 41–45 (1991).
114. Kane, R. D., and Cayard, Improve corrosion control in refining processes, *Hydrocarbon Processing*, November, 129–142 (1995).
115. Methods and Controls to Prevent In-Service Cracking of Carbon Steel (P-1) Welds in Corrosive Petroleum Refinery Environments, NACE RP-04-72 (1976 rev.), National Association of Corrosion Engineers, 1976.
116. Please supply ref.
117. Technical Services Bulletin No. 778, A516 Steels Including HIC-Tested A516 Steels, rev. November 1992, Lukens Steel Company, Coatesville, PA.

This page intentionally left blank

13
Material Selection and Fabrication

1 MATERIAL SELECTION PRINCIPLES

In engineering practice the selection of materials of construction depends on the equipment being designed and the service requirements imposed on them. Selection of materials involves the thorough understanding of their availability, source, lead time, product forms, and size. In simple terms, the following factors are to be considered while selecting the materials for heat exchanger and pressure vessel components:

1. Compatibility of the materials with the process fluids.
2. Compatibility of the materials with the other component materials.
3. Ease of manufacture and fabrication by using standard methods like machining, rolling, forging, forming, and metal joining methods such as welding, brazing, and soldering.
4. Strength and ability to withstand operating temperature and pressure.
5. Cost.
6. Availability.

While selecting materials one has to balance many requirements; these requirements include the following [1]:

Expected total life of plant or process.
Expected service life of the material.
Reliability (safety, hazard, and economic consequences of failure).
Material costs.
Fabrication costs.
Maintenance and inspection costs.
Availability in required size, shape, thickness, and so on, and delivery time.
Return on investment.

Materials are selected based on past experience, corrosion tests, the literature, and the recommendations of material suppliers. The direct measure of success in materials selection and fabrication is reflected in the behavior of the equipment in service. In order to assure safe, reliable and uninterrupted service with monetary benefits, proper attention must be given to materials selection commencing from the design stage and must continue through fabrication, installation, and maintenance. Once onstream, the equipment should be monitored for specified performance. With this background information, the logical sequence of material selection for the construction of pressure vessels and heat exchangers is discussed next.

1.1 Materials Selection

While selecting materials for the construction of heat exchangers and pressure vessels, the following points may be considered for the desired performance and the life of the equipment [2]:

1. Review of operating process.
2. Review of design.
3. Selection of material.
4. Evaluation of material.
5. Specification.

Finally the material should be cost-effective. Do cost-benefit analysis for an optimum material selection.

1.2 Review of Operating Process

The foremost step in the material selection is the thorough review of the process environment and equipment operating conditions like operating temperature, pressure, and phases of the fluids. The following operating data are required by the design engineer [3]:

1. Environment—nature and composition of fluid handled, water chemistry, steam quality, constituents/concentration of a solution, conductivity, pH, aeration, impurities, and so on.
2. Pressure—average and range, constant or cyclic, internal and external loadings.
3. Temperature—average and range, constant or variable, thermal gradients, and thermal shock.
4. Velocity—flow rate, linear velocity, nominal and range, degree of agitation, turbulence, etc.

In addition to operating temperature and pressure, other factors such as the startups and shutdowns, intermittent operation, transients and pressure surges, and momentary failure of the system must be considered for the satisfactory performance of a material.

1.3 Review of Design

After the review of the operating process, the type or design of the equipment and various assemblies and subassemblies, size, complexity, and criticality in service should be considered. Applicability of various fabrication techniques like forging, machining, welding, soldering, brazing, etc., is considered.

1.4 Selection of Material

The selection of proper materials for wetted and nonwetted parts, pressure and nonpressure parts, and equipment support is an important design step. Material Standards like ASTM, DIN, BS, ISO, and JIS give data on a large number of ferrous and nonferrous materials. Many of

these materials have been adopted in the Pressure Vessel Codes by the country of origin in the Material Standards. Data from these material standards are generally restricted to the physical properties, such as Young's modulus, yield strength, minimum tensile strength, maximum permissible operating temperature, elongation, coefficient of expansion, etc. But codes and standards do not explicitly express the suitability of the materials for the intended service environment, either internal or external. These details must be provided by the corrosion engineer or many sources are to be referred.

ASME Code Material Requirements

Pressure Parts. All materials used for pressure-retaining parts must meet the ASME Code (ASME Boiler and Pressure Vessel Code, Section II—Material Specifications, Part A—Ferrous Materials, Part B—Nonferrous Materials, Part C—Welding Rods, Electrodes, and Filler Metals, and Part D—Material Properties, 1992, American Society of Mechanical Engineers, New York) general requirements for materials. Only code-specified material shall be used in the vessel construction or repair. The manufacturer should deliver the material after thorough inspection, with the chemical composition and metallurgy and properties as stipulated in the relevant specification. The allowable stresses for the different code-permitted materials should not be exceed.

Nonpressure Parts. Materials used for nonpressure parts shall be compatible with the process fluids, ambient environment, and/or shall be of weldable quality.

Functional Requirements of Materials

Function of equipment has frequently been equated with long, trouble-free service [4]. Selected material has certain functional requirements, which ultimately reflect on the function of the equipment. Those functional requirements are given in Table 1. Functional requirements of materials given in Ref. 5 have been enlarged to include additional information and presented in Table 1.

With reference to functional requirements, the following features/parameters are discussed.

Table 1 Functional Requirements of Materials

Characteristics	Functional requirements
Strength	Tensile, torsion, bending, compression, shear, buckling, fatigue, creep, rupture strength, etc.
Physical properties	Design may require certain properties peculiar to the materials (thermal, electrical, acoustic, magnetic, etc.), coefficient of thermal expansion, thermal conductivity, modulus of elasticity, specific gravity (strength to weight ratio).
Temperature resistance	Low temperature: subzero and cryogenic. Intermediate temperature. Elevated temperature.
Geometric stability	Stiffness of the structure, effect of sustained loading, etc.
Toughness	Ability to cope with a sudden load, impact, low-temperature operation, etc.
Fabricability	Ability to be formed, forged, machined, joined, ease of heat treatment, etc.
Corrosion resistance	Compatibility of the materials with the process fluids, with the other component materials in contact; resistance to ambient environment; passivity; hydrogen attack.
Wear and abrasion	Loss of surface oxide film (passive films), which is helpful in corrosion resistance.

1. Strength.
2. Fatigue strength.
3. Brittle fracture.
4. Toughness.
5. Creep.
6. Resistance to temperature.
7. Heat and corrosion.
8. Corrosion resistance.
9. Hydrogen attack.
10. Fabricability.

Strength. While the term strength applies to many mechanical properties, it most commonly refers to tensile strength and yield strength. These strengths are best understood by examining a stress-strain curve. Other related strengths are compression, bending (flexural), shear, and torsional strength. Its is better to use high strength materials to keep the thickness of parts less.

Fatigue Strength. Fatigue is the failure of a metal by fracture when it is subjected to cyclic stress. The usual case involves rapidly fluctuating stresses that may be well below the tensile strength. As stress is increased, the number of cycles required to cause failure decreases. A stress–number of cycles (S–N) curve is conventionally plotted for a metal as shown in Fig. 1. The stress is plotted against the logarithm of the number of cycles. There is usually a stress level below which no failure will occur, for a specified large number of cycles, and this is called the endurance limit. Since the stress limits that are required to prevent distortion and bursting keep the nominal stresses at or below the endurance limit, the possibility of fatigue failure is almost always associated with discontinuities, notches, shocks, residual stresses, etc.

Fatigue failures are most likely to occur at welded joints, which, by virtue of their design, give rise to significant stress concentration effects. Some of the material and design characteristics favorable to fatigue resistance are as follows [6]: increased tensile strength via alloying or heat treatment, minimum workpiece thickness, polished surfaces., low design stress, smaller grain size, absence of metallurgical discontinuities and residual stresses, presence of surface compressive stress, minimize environments conducive to corrosion and fatigue, and avoidance

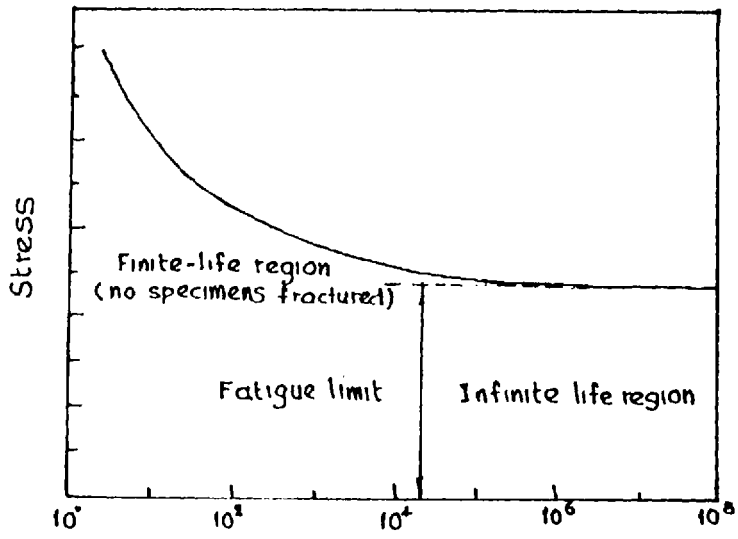


Figure 1 Stress-cycle (S–N) curve.

of metallic coating, such as Cr, Ni, or Cd plating, which can reduce fatigue strength due to microcracks in the plating. For pressure vessels, hydrostatic pressures that exceed the yield strength of the metal can relieve residual stresses and can improve fatigue strength [7].

Brittle Fracture. Brittle fracture is the term given to describe failure by rapid crack propagation at nominal stress below the yield strength. Brittle fracture has been mostly observed in bcc crystal structure metals, notably ferritic steels, in which complete rupture takes place under certain conditions at stress levels not only below the ultimate tensile strength but even lower than yield strength. The conditions associated with brittle fracture of steels include the following [8, 9]:

1. A preexisting defect.
2. The presence of residual and/or applied tensile stress across the defect, which is more serious if triaxial.
3. A sufficiently low temperature.
4. Several metallurgical factors—deoxidation practice, composition, rolling practice, and subsequent heat treatment [8].

The subject of brittle fracture is of interest to the designers of long-life pressure vessels for the following reasons [9]:

1. Even if the vessel is to operate at an elevated temperature, where the brittle fracture is not to be expected, there is a danger of failure of the vessel during the preservice cold hydrostatic test; another case of practical importance is the temper embrittlement of Cr-Mo steels, a condition caused by elevated temperature service after a long time in refinery service.
2. Cyclic variations of load and temperature during long service may enlarge small initial defects to the critical size and result in brittle fracture during startup, shutdown, or cold periodic tests.
3. In the special case of nuclear vessels, neutron bombardment can produce large increase in the transition temperature.

In welded structures, brittle fractures invariably initiate from weld defects. Weldment failure due to brittle fracture is dependent on through-thickness toughness, the critical defect/notch size, residual welding strains, mechanical constraints, grain size, inclusion content, and temperature [10]. It must not be overlooked that a normally ductile material can fail in a brittle manner at locations where complex and triaxial stress fields exist [11].

Measures to Minimize Brittle Fracture. Brittle fracture may be prevented by selecting a notch-tough material, and avoiding notches. The following design practises will help to minimize brittle fracture [12]:

1. Eliminate all defects, which is impracticable.
2. Employ design stress less than required for propagation, but this may not be justified economically.
3. Select materials whose transition temperature is below operating temperature.
4. If the structures are not stress relieved, residual stresses may be superimposed on the applied stress, and will cause local yielding in the vicinity of a defect and thus initiate a brittle crack.

Some simple practices to minimize the chance of nonservice failure have been suggested by Bravenec [13]. These recommendations include [13]:

1. Sheared and torched edges should be conditioned by grinding prior to forming.
2. Warm forming should be used whenever the ambient temperature is less than 75°F.
3. Material selection should meet end use requirements and code requirements; however, it must be recognized that Code stipulates only a minimum standard.

Toughness. A material's toughness is its ability to absorb energy and deform plastically before fracture, and the amount of energy absorbed during both the deformation and fracture is the measure of toughness. Toughness rather than strength is the most important low-temperature mechanical property. Notch toughness is influenced by chemical composition, microstructure, grain size, grain flow pattern, section size, hot and cold working temperature, method of fabrication, and surface conditions like carburization and decarburization [6].

Basic Tests. The most common toughness tests use notched specimens and measure either notch toughness, usually by an impact test, or fracture toughness, which is measured at a relatively low strain rate. Impact tests reveal low-temperature strength, lack of ductility, and brittleness, and these tests are being particularly relevant to ferritic materials, which may show a transition from ductile-to-brittle behavior. Two commonly used methods are the Charpy and Izod tests.

Charpy V-Notch, CVN (ASTM E23). The Charpy V-notch test is considered the most appropriate because a part or structure will generally fail due to a notch or other stress concentration. This test is used to obtain absorbed energy, lateral expansion, and fracture appearance from a 10 mm × 10 mm × 55 mm piece of a material subjected to impact loading. The specimen has a 0.254-mm (0.010-in) radius notch. Test results given in foot-pounds measure the capacity to absorb energy and thus signify the material ability to resist failure at points of local stress concentration.

Precracked Charpy V-Notch. This is a test often used as a correlative measure of fracture toughness.

Nil-Ductility Transition Temperature, NDTT (ASTM E208). This test defines the temperature at which a small flaw will initiate when subjected to yield loads. It is used with a Charpy V-notch test to establish the reference fracture toughness in ASME Code.

Fracture Toughness. The notch toughness approach does not work well with high-strength steels and nonferrous metals because of the gradual transition from ductile to brittle behavior [6]. Also, it is felt that CVN test results alone are not reliable enough to predict whether an existing crack of a certain size will grow slowly, causing leakage before failure, or fail catastrophically under the very slow strain rates likely to be encountered in LNG containment vessels [14]. In these situations, fracture toughness value is used to assess metals toughness, and the approach is known as fracture mechanics approach. Plane-strain fracture toughness, or K_{Ic}, values are used to calculate the critical crack size in a stressed component that can result in an abrupt failure. K_{Ic} values, unlike notch toughness values, are independent of test specimen shape [6].

Fracture Toughness (ASTM E399 and E813). These are the only two tests that yield "ASTM valid" fracture toughness values. E399 is for linear-elastic fracture toughness K_{Ic}; and E813 is for the "J-Integral," which can be converted to K_{Ic}.

Creep. Creep is defined as slow deformation of material with time, with the deformation taking place at elevated temperatures without increase in stress. Creep curve is shown in Fig. 2. At room temperature creep is nonexistant in steel. Many pressure vessel steels have to operate in creep conditions and the general basis of design is based on data from test specimens and involves the definition of stress below which failure will not occur within the expected life of the component. The phenomenon of creep is well understood, the basis of design is

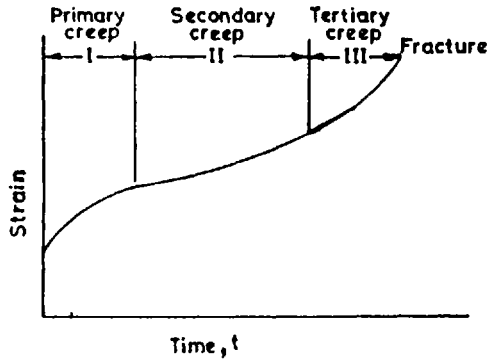


Figure 2 Creep curve.

clear, and no special problems need be encountered. It is worth, however, sounding two notes of warning [15]:

1. If the design is poor so that unforseen high local stresses occur, then the local creep deformation may exceed the creep ductility and lead to premature failure.
2. If the structures are not stress relieved, residual stresses may be superimposed on the applied stress, and again lead to premature creep failure. This may well occur in welds around nozzles. It is thus important to remember that vessels operating under creep conditions should be stress relieved prior to service.

Creep Test. Tests for resistance of a material to elevated temperature generally fall into three classes: short-time tests (tension, compression, bending, shear, torsion, and impact) run at elevated temperature, short-time tests run at room temperature after elevated-temperature exposure for various lengths of time, and long-time tests run at room temperature. Long-time strength tests, in turn, can be classified as constant load (creep, stress-rupture, and many fatigue tests) or constant deflection (stress relaxation and some fatigue tests) tests [6].

The standard test followed to determine creep is ASTM E139, "Standard practice for conducting creep, creep-rupture, and stress-rupture tests of metallic materials." The Larsen–Miller parameter is considered reliable for using data from high-temperature tests to predict creep-rupture time. The Larson–Miller parameter used for predicting stress-rupture data for low alloy steels is given by

$$P = 1.8T(k + \log t) \times 10^{-3}$$

where T is temperature (K), t is hours, and k is a constant (= 20) for low alloy steels. For temperature in °R, eliminate the constant 1.8 in the equation.

Temperature Resistance. Temperature resistance of construction materials is discussed with reference to various temperature of operation, since basic materials behavior is intimately related to operating temperature. Accordingly, the temperature of operation is classified into these four ranges:

1. Subzero and cryogenic operation.
2. Low-temperature operation (up to 200°C).
3. Intermediate-temperature operation (200°C—650°C).
4. High-temperature operation (>650°C).

Subzero and Cryogenic Operation. A major requirement of materials for subzero applications is toughness at the handling temperature. Steels and nonferrous materials are used in cryogenic services for containment, handling, and transportation of liquified gas and liquification of gases. Some metals display a marked loss of ductility in a narrow temperature range below room temperature or nil ductility temperature. This is called the ductile–brittle transition temperature (DBTT). The application of metals below their nil ductility temperature is avoided because of the danger created by brittle crack propagation. Below the nil ductility temperature, very little energy is required for crack propagation [16].

Intermediate-Temperature Operation. The intermediate temperature category includes most of the vessels used in petroleum and petrochemicals services. Here the most important consideration is that materials be used to best advantage. The principal criteria in this respect are design stress values, adequacy of design formulas, and ductility of material.

High-Temperature Operation. In high-temperature service, the materials operate in a pseudo-plastic or fully plastic state, and designs must be based on stresses that will keep the inelastic deformations below limits that would permit failure [12]. High-temperature design stress limits are established on the basis of long-time creep strength, as well as by the metal's scaling resistance [17]. For the use of the high-temperature applications, the selected materials should exhibit certain properties that are given in Table 2 [18]. At temperatures above 800°F (425°C), materials should be heat resistant, and must maintain corrosion resistance, mechanical strength, metallurgical stability, creep resistance, oxidation resistance, stress-rupture strength, toughness and surface stability against combustion gas and chemicals handled [19].

Alloying Elements for Heat-Resistant Material. Heat-resisting materials must contain chromium for oxidation resistance. Cobalt, aluminum, silicon, and rare earths enhance the formation, stability, and tenacity of the oxide surface layer. Nickel provides strength, stability, toughness, and carburization resistance. Tungsten and molybdenum increase high-temperature strength [19].

Material Groups and Their Service Temperature. Approximate operating boundaries for various heat exchanger materials along with ceramic are shown in the chapter on Regenerators. For temperatures above 600°C, the following materials groups are usually considered:

1. Ferritic steels with 17–27% Cr and Mo addition.
2. Austenitic high-temperature, high-strength steels (Cr-Ni-Mo steels having more than 8% Ni) like Type 321, 347, 316, and 310.
3. Cast stainless steel heat resistant alloys: HC, HK, HT, HP, HX.
4. Solution-hardened nickel-base alloys with the addition of Cr and Fe, such as 800H, Incoloy 800HT, and 330.
5. Precipitation-hardened nickel-base alloys with the addition of Cr, such as X-718 and X-750.

Table 2 Mechanical Properties for High-Temperature Operation [18]

Tensile strength or yield strength at room temperature, hardness, toughness.
Tensile strength or yield strength at high temperatures.
Creep and creep rupture strength at high temperatures.
Thermal fatigue characteristics.
Thermal shock characteristics.
Structural stability and changes in mechanical properties after prolonged high temperature service (temper embrittlement).
Metallurgical stability.

6. Cobalt-base alloys: N-155, 188, L605, 25.
7. Advanced ceramics and other highly refractory material (>1200°C).

Items 4–6 are often called the superalloys.

Steels for High-Temperature Applications.

1. Low-alloy steels for high-temperature service. C-Mo alloy steels, chromium-molybdenum alloy steels, and manganese-molybdenum-(nickel) alloy steels are regarded as steels for high-temperature service. When high-temperature strength (creep strength) is the principal consideration, molybdenum content in the steel composition is usually increased, but when high-temperature corrosion resistance is paramount, chromium content is increased. In the case of petroleum refinery equipment, which is subject to hydrogen attack, molybdenum and chromium are added to the steel to resist hydrogen attack [18].
2. Stainless steels for elevated-temperature service. While carbon steels can be conveniently used at temperatures up to about 752°F (400°C) and low-alloy steels up to 1112–1200°F (600–650°C), their reliability ceases beyond these temperatures due to creep. While nickel-base and cobalt-base superalloys can withstand elevated temperatures without much loss of mechanical properties, their economics and availability may not permit their use for general applications such as in fossil fuel power plants operating in the middle temperature range of 1112–1247°F (600–675°C). For this temperature range, austenitic stainless steel is preferred [20]. While selecting stainless steels for high-temperature applications, in addition to creep strength, consider high-temperature corrosion, oxidation, scaling and carburization, and precipitation of secondary phases. Among the ferritics, E-Brite 26-1 (Allegheny Ludlum) appears to fill many gaps associated with the drawbacks of type 316 stainless steel.
3. Developments in ferrous alloy technology for high-temperature service. During the past 25 years, new alloys with improved strength and corrosion resistance were developed for use in nuclear, fossil, and petrochemical industries. Specific groups of alloys include vanadium-modified low-alloy steels, 9Cr-1Mo-V steel, niobium-modified lean stainless steels, and high chromium-nickel-iron alloys [21]. Alloying additions of vanadium, niobium, titanium, and nitrogen have been effective in strengthening both ferritic and austenitic alloys.

Nickel-Base Heat-Resistant Material. INCONEL (nickel-chromium alloys) and INCO nickel-chromium alloys resist oxidation, carburization, and other forms of high-temperature deterioration. Typical heat-resistant alloys include (1) INCONEL ally 600, INCONEL alloy 601, INCONEL alloy 617, INCONEL alloy 625, INCONEL alloy 718, INCONEL alloy X-750, INCO alloy HX; (2) nickel-iron-chromium alloys and INCO nickel-iron-chromium alloys such as INCOLOY alloy 800, INCOLOY alloy 800HT, INCOLOY alloy 825; and (3) other newer alloys such as 253MA, 556, HR-120, HR-160, 45TM 230, and 214. Table 3 shows material groups and their service temperatures.

Tests to Evaluate Steels at High Temperature. Types of tests used to evaluate the mechanical properties of steels at elevated temperature include

Short-term elevated-temperature tests.
Long-term elevated-temperature tests.
Short-term and long-term tests following long-term exposure to elevated temperature.
Fatigue tests (including thermal fatigue and thermal shock tests).
Time-dependent fatigue tests.
Ductility and toughness tests.

Heat and Corrosion. Alloys that have both heat and corrosion resistance are necessary for successful long-term operation of high-temperature processing equipment, particularly where the environment may be contaminated by corrosive constituents [22].

Table 3 Material for High-Temperature Applications

Temperature range	Alloys
Up to 1202°F (650°C)	Carbon steels having <1% Cr, or steels having 1–12% Cr and Mo upto 1%
1202–1472°F (650–800°C)	Carbon steels and low-alloy steels, Cr-Ni-Mo steels that can contain 12–25% Cr and 5–25% Ni, e.g., AISI type 310.
1472–1832°F (800–1000°C)	Steels with 17–27% Cr and Mo addition, or higher Cr-Ni-Mo steels having more than 8% Ni
1832–2192°F (1000–1200°C)	Higher alloyed nickel- or cobalt-base alloys with 18–35% Cr; Al additions to these alloys improve resistance to high-temperature oxidation and cyclic oxidation
>2192°F (1200°C)	Advanced ceramics and other highly refractory material

Note. This table was compiled from Kane et al. [22].

Mechanisms of High-Temperature Corrosion. Most high-temperature corrosion is due to the destruction of protective surface scale. Common impurities that increase the severity of high-temperature corrosion include carbon, nitrogen, halogens, sulfur and ash, and molten salt. High-temperature corrosion mechanisms include [22]: (1) carburization, which results in internal carbide precipitates and embrittlement; (2)nitridization, which results in internal nitride precipitates and embrittlement; (3) formation of volatile metal halides on the surface; (4) deposits of hot ash and formation of molten deposits; and (5) corrosion due to the presence of sulfur in the process fluids, known as sulfidation. Alloy modifications to overcome these high-temperature corrosion problems involve the addition of Cr, Ni, Si, Al, and Mo, either individually or jointly. Various high-temperature corrosion mechanisms, the impurity or contaminant responsible for the corrosion, alloying modification, and process change to overcome the damage are discussed by Kane et al. [22].

Corrosion Resistance. Most common metals and their alloys, and nonmetals including plastic, glass, and graphite are attacked by environments such as the atmosphere, water, or aqueous solutions. This destruction of metals and alloys is known as corrosion. With practically all commercial processes engineered on a continuous basis of operation, failure of equipment, heat exchangers, piping components, or other system components may mean costly shutdowns, expensive maintenance operations, and replacement of components. Therefore, the construction materials for pressure vessels and heat exchangers should have a well-defined corrosion rate in the service environment. Additional concern is corrosion due to surrounding atmosphere. Various forms of corrosion and their prevention and control are discussed in the chapter on corrosion.

Selecting Materials to Resist Corrosive Conditions.

Favored Combinations. In alloys selection, there are several natural metal and environment combinations. These combinations usually represent the maximum corrosion resistance at the lowest cost and should always be considered. A partial list includes the following combinations [3]:

Carbon steels/concentrated sulfuric acid.
Stainless steels/nitric acid.
Aluminum/nonstaining atmospheric exposure.
Copper-nickels/sea and brackish water.
Nickel and nickel alloys/caustic soda.

Monel 400/hydrofluoric acid.
Hastelloys/hot hydrochloric acid.
Titanium/hot strong oxidizing solutions.
Tantalum/most chemicals.

Additionally, consider the combination of superferritics/seawater.

Avoid These Combinations. There are some metal and environment combinations that are readily attacked by corrosion and must be avoided; a partial list is [3]:

Ammonia and ammoniacal solutions/copper and copper alloys except-copper-nickels.
Halogens and halides/austenitic stainless steels.
Mercury/aluminum and aluminum alloys, copper and copper alloys, Monel.
Sulfur and sulfides (at high temperatures)/nickel and nickel alloys.
Caustic soda, other strong alkalies/aluminum.

Sources of Material Data. To know the performance of a given material, the materials engineer must have information on corrosion of materials in various environments. There is a wide spectrum of corrosion data sources available. The following are identified as typical sources of corrosion data [4]:

1. Process licensors.
2. Existing plants, i.e., plant experience.
3. Pilot unit test data and plant corrosion monitoring.
4. Technical publications.
5. Internal databases collected by individual industrial companies (usually materials suppliers), which may become available upon request to these companies—e.g., Inco Alloys, Allegheny Ludlum, Lukens Steels, US Steels, TIMET, RMI, Titanium Company, etc.
6. Publications of the trade.

Other material sources include:

Publications from associations of common technical interest, like the National Association of Corrosion Engineers (NACE), American Society for Testing and Materials (ASTM), American Society for Metals (ASM), Aluminum Association (AA), Copper Development Association (CDA), Society of Automotive Engineers, etc.
Professional associations such as HTRI and HTFS.
Government publications.
Databases and abstract services, and expert systems.
Corrosion Abstracts [23].
Corrosion Data Survey [24].

Corrosion Failures. Even with careful material selection and corrosion prevention methods employed, there will always be a few unexpected failures and we must have procedures for dealing with them. Unexpected corrosion failures result from one or more of the following [1]:

1. Defective material.
2. Improper design.
3. Abnormal operating conditions.
4. Improper fabrication and inadequate inspection.
5. Inadequate maintenance.

Hydrogen Attack. Hydrogen attack is a damage mechanism that is associated with carbon and low-alloy steels exposed to hydrogen containing environments above 430–470°F (220–243°C) [25,26]. At room temperatures, even high-pressure hydrogen can be handled in steel cylinders.

At higher temperatures, hydrogen diffused in a steel can react with carbon atoms to form methane gas:

$$2H_2 + FeC \rightarrow CH_4 + 3Fe$$

At elevated temperature/pressure, hydrogen can react with carbon in interstitial solid solution, resulting in initial decarburization, followed by destabilization of the carbides and the formation of methane bubbles at grain boundaries. Since methane cannot diffuse out of steel, its accumulation causes fissuring and blistering, resulting in loss of ductility, and in ultimate failure. Stable carbide compositions, morphologies, and distributions are required to reduce this problem [27].

Prevention of Hydrogen Attack. The only practical way to prevent hydrogen attack is to use steels that, based on plant experience, have been found to be resistant to this type of deterioration. The following general rules are applicable to hydrogen attack:

1. Carbide-forming alloying elements such as chromium and molybdenum, or carbide-stabilizing elements, such as chromium, titanium, and vanadium, increase the resistance of steel to hydrogen attack [28]. Molybdenum is four times as effective as chromium [29]. Vanadium is known to be a potent strengthener in low-alloy steels and to form a stable VC precipitate that is resistant to hydrogen attack [21].
2. All of the austenitic stainless steels resist high-temperature hydrogen damage because of their high chromium content [25,28]. Hence, as an additional corrosion prevention measures, the inside surfaces of low alloy steel vessels are often lined with stainless steel overlay.
3. Heat-affected zones are more susceptible to hydrogen attack than the base metal or weld metal. Hence, limit the hardness of the HAZ.

Prevention of Hydrogen Attack: Nelson Curves. Hydrogen attack is often an important consideration in the selection of steels for use in petroleum refinery equipment. Hydrogen attack on steel can best be avoided by following the operating limits on temperature, partial pressure of hydrogen, and alloy composition set forth by Nelson curves [30]. The Nelson curves are used throughout the world for the selection of materials for refinery applications. The curves are based on long experience in refinery operations rather than on laboratory studies. The curves are periodically revised by the API Subcommittee on Materials Engineering and Inspection, and the latest edition of API 941 [30] should be consulted.

The Nelson curves are shown schematically in Fig. 3. Carbides of chromium and molybdenum are less reactive with hydrogen than iron carbide; therefore, Cr-Mo steels are more resistant to hydrogen attack than plain carbon steel. Austenitic stainless steels are completely resistant to hydrogen attack at all temperatures and hydrogen pressures.

Fabricability. Fabricability includes ease of forming, machining, welding and other metal joining processes, and the subsequent heat treatment. Not all fabrication shops are technically qualified to handle the more sophisticated materials properly. Therefore, it is essential that a user know the capabilities of his or her fabricator [31]. Furthermore, advanced fabrication techniques require more sophisticated inspection criteria to judge the fabrication.

1.5 Evaluation of Materials

Evaluation of materials involve the testing the properties and metallurgy of the materials, fabricability, including metal joining, and the suitability of the material under lab tests or field tests. Material tests and material evaluation to resist corrosion are discussed further.

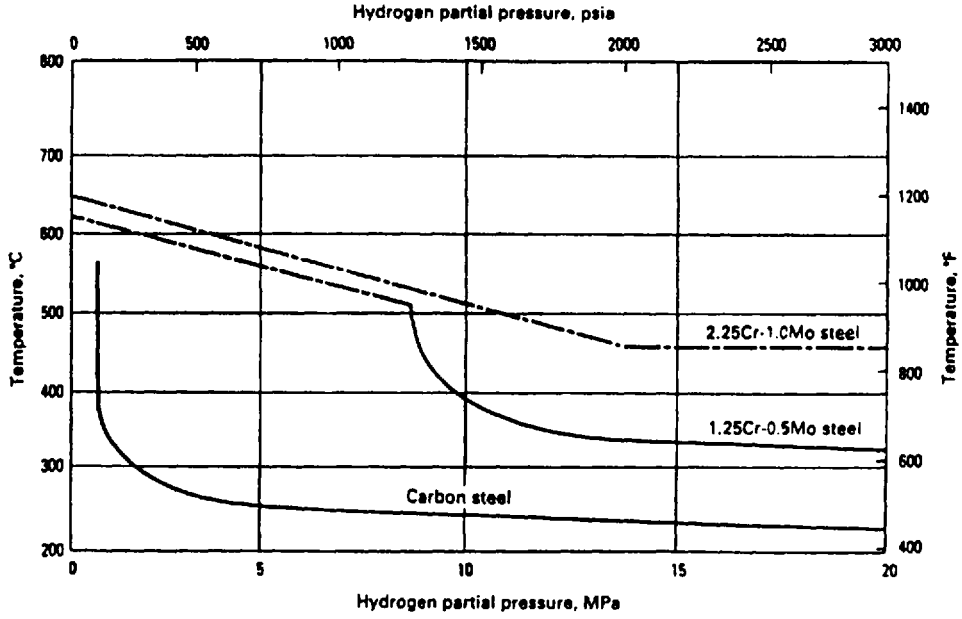


Figure 3 Nelson curve. (From Ref. 30.)

Material Tests

In addition to chemical analysis required to check the material composition, visual examination and mechanical tests of selected samples are usually called for to establish that the materials supplied are as per code requirements. Tests on welded samples are also needed to assess the quality of welds. Various mechanical tests employed for these purposes are the tensile test, bend test, impact test, etc. Metallographic examination of a sectioned specimen of the material provides information on the cleanliness of the material with respect to inclusions as well as metallurgical structure and grain size. In the case of welds, such examination may reveal weld defects such as inclusions, porosity, and cracks, and evidence of unsatisfactory welding techniques, etc. These tests are typically destructive in nature.

Materials Evaluation and Selection to Resist Corrosion

Materials engineers are increasingly using data from simulated environment tests as the basis for materials selection to prevent corrosion including high-temperature corrosion. A partial list includes these [22]: (1) corrosion coupons, (2) thermogravimetric analysis (TGA), (3) dynamic burner studies, (4) thermal cycling, (5) laboratory glassware tests, and (6) field tests.

1.6 Cost

Cost-Effective Material Selection

Two important strategies for selecting materials without paying attention to other factors are (1) minimum cost, i.e., selection of low-cost materials, followed by scheduled periodic replacements or follow corrosion control methods, and (2) minimum corrosion, i.e., selection of the most corrosion resistant material regardless of cost.

Low-Cost Material Versus Expensive Material. The common belief that advanced construction materials are expensive is not entirely true. Manufacturers often deliberately select low-

cost materials for their products, using the philosophy that manufacturing costs will be at a minium and the product is therefore competitively priced. Plate steels with improved properties often cost a little more per unit weight but the total vessel package is often less expensive. Savings are made possible because of these factors [31]:

1. Less material required.
2. Less welding time and less filler material required.
3. Shorter heat treatment cycles.
4. Lower freight charges to destination.
5. Easier handling requirements in the field during shipment and erection.

Currently, the most common starting material is steel. About three-quarters of all pressure vessels are fabricated from carbon steel plate ranging from 0.2 to 0.3% in carbon content to provide easy forming and welding [32]. Although the strength to weight ratio of steel is not as favorable as those of certain aluminum alloys and titanium alloys, when combined with cost, steel often is quite favorable. The factors that favor steel as heat exchanger material are:

Steel is relatively inexpensive.
Available in standard shapes.
Well-established mechanical properties, and these properties can be changed as a function of composition.
Fabricable by a wide variety of methods.
Easily joinable by a wide variety of welding processes, brazing, soldering to itself, and other materials.
Its corrosion performance in most environments has been established and techniques of protecting steel against corrosion in these environments are also widely developed.

1.7 Possible Failure Modes and Damage in Service

Failure may take place in service either as a result of overloading, by the imposition of nominal service stresses that are above the safe stress of the material, or as a result of local deformation at stress concentration. Mostly it is considered that the failure modes are based on the material properties in their final condition. Various possible modes of failure under pressure are [9]:

1. Excessive elastic deformation and elastic instability.
2. Plastic instability, deformation and bursting.
3. Brittle fracture.
4. Fatigue failure.
5. Creep deformation and creep rupture.
6. Environmental damage such as corrosion and hydrogen damage.

The great majority of service failures involve the initiation of cracking at defects situated in regions of stress concentrations. In welded structures, weld defects are quite common. It is therefore necessary not only to design against overload, but also to avoid the possibility of low-stress failures by brittle fracture, fatigue, creep, and corrosion. Excessive elastic deformation and elastic instability are overcome by the choice of material, limiting primary plus secondary stresses; plastic instability by limiting primary plus secondary stresses; and brittle fracture by proper material selection, manufacturing and inspection, verification of notch toughness, and so on. Failure due to general corrosion is a rarity in pressure vessels and heat exchangers since designers are well aware of the possibilities of general corrosion and normally introduce corrosion allowance and/or choose corrosion resistant material. However, in certain environ-

ments, stress corrosion cracking is a possibility, and design and material selection should prevent the possibility of this form of failure occurring.

2 EQUIPMENT DESIGN FEATURES

2.1 Maintenance

To design for maintenance, the particular equipment should be well understood at the design stage. Some typical maintenance-related items that must be considered at the design stage include tube pull space required for retubing/space required for pulling the bundle, material handling facilities, proposed cleaning methods and facilities required for the purpose, ease of component replacement, ability to monitor corrosion and fouling, facility to perform in situ welding operations, and facilities and adoptability for inservice inspection.

2.2 Failsafe Features

The failsafe design concepts employed recognize the limitations in manufacturing but also provide large safety margins for operations. This concept is relevant for fracture mechanics study. In designing the various parts of an equipment to have failsafe features, the following considerations are usually made [33]:

1. Determine points in the structure where fatigue cracks might develop.
2. Define a minimum detectable crack size.
3. Define the maximum detectable crack size, depending upon the maximum damage level and at any load between the minimum detectable crack and the critical crack size.

2.3 Access for Inspection

The design of pressure vessels should provide access for plant personnel to enter the vessel to inspect for corrosion damage. Vessels that have a sufficient diameter for personnel entry should have internal components that can be removed to permit access to all parts of the vessel.

2.4 Safety

Safe operation of pressure vessels and heat exchangers requires conservative design and standard construction practices, and use of those materials permitted by the Codes/Standards. For heat exchangers and pressure vessels, the overriding reasons for safety are to avoid the consequences of failure, which can be catastrophic in human, monetary, and environmental terms. To ensure safety, the equipment should be fabricated properly and adequately inspected to prove compliance with the specifications. The equipment must be operated properly.

2.5 Equipment Life

To realize returns on the investment and for uninterrupted service, the equipment components and the equipment itself should have adequate life [4]. The life of a component is dependent on design, the properties of the construction materials and their interaction with the service environments, effect of fabrication and inspection, operation, maintenance, etc. [34,35]. To get a satisfactory life, the equipment construction materials shall withstand (1) design stress, (2) wear, and (3) corrosion in service [35]. Corrosion problems should be as important during the design stage as other operational conditions and design parameters like pressure, temperature, and velocity. For best service life, the material selection should be based on the corrosion standpoint. Concise and clearly written specifications should be provided to the material sup-

plier to ensure the proper material supply. The design details should preserve the built-in corrosion resistance of the materials.

Component Life

Exchanger shells, channels, and tubesheets should be designed for a minimum of 10 years or the original tube bundle life plus two additional retubings. The initial tubes should be chosen for a minimum of two run lengths or 5 years unless spare exchangers are provided, in which case a shorter expected life may be attractive [4]. However, this may not be relevant for nuclear heat exchangers and pressure vessels.

2.6 Field Trials

A number of accelerated tests are used to build and to increase confidence in heat exchanger design, particularly, radiator design, before large-scale fleet trials. Some of these tests were designed to represent worst field conditions and were later correlated with field service returns. These tests are primarily used to assess the mechanical durability and the internal and external corrosion resistance of aluminum radiators. This aspect is further discussed in detail in the chapter on brazing.

3 RAW MATERIAL FORMS USED IN THE CONSTRUCTION OF HEAT EXCHANGERS

In the construction of heat exchangers, various forms of raw materials are used. The raw material forms include plates, sheets and strips, pipes and tubes, forgings, castings, bars and rods, etc. Major use for sheets and strips are in the construction of compact heat exchangers and plate heat exchangers. Tubes are used both in compact heat exchangers and shell-and-tube heat exchangers. The other forms are used extensively in the fabrication of shell-and-tube heat exchangers.

In this section, various raw material product forms are discussed with specific reference to ASTM specifications [36]. As far as the plates and tubes are concerned, plate steels and ferrous tubings are discussed here. Nonferrous plates and tubes are covered in their respective sections.

3.1 Castings

Castings may be used in the construction of pressure vessels and vessel parts. Cast heads are used for feed water heaters. Codes restrict maximum allowable stress values for acceptable casting materials. These allowable stress values should be multiplied by the applicable casting quality factor for all materials except cast iron.

3.2 Forgings

Forged materials may be used in pressure-vessel and heat-exchanger construction provided the materials have been worked sufficiently to remove the coarse ingot structure. Tubesheets, channel covers, blind flange covers, etc., when made from forgings should be supplied as proof machined forgings. All further machine operations, drilling, etc. should be done by the fabricator. Before machining, the forging is to be examined ultrasonically. Most of the defects in a forging are caused by conditions produced in the ingot stage, such as segregation, piping or nonmetallic inclusions, laps or seam due to subsequent hot or cold forging, and excessive scale leading to surface flaws, etc. For this reason, the acceptance standard for a forging is usually

based on an ultrasonic test [37]. SA 388/ASTM A388/A388M covers standard practices for ultrasonic examination of heavy steel forgings.

Forgings are available in carbon steels, carbon-molybdenum steels, chromium-molybdenum steels, ferritic (straight chromium) stainless steels, austenitic, precipitation hardened, and other high-alloy steels, and nickel steels. According to Section VIII, Div. 1, the heat analysis of steel forgings to be fabricated by welding shall not exceed 0.35% carbon. When welding involves only minor nonpressure attachments or repairs, the carbon content shall not exceed 0.5% by heat analysis. When carbon exceeds 0.5% by heat analysis, no welding is permitted.

Some of ASTM specifications for pressure vessel forging steels are (1) A336—seamless drums, heads, and other components (ferritic steels and austenitic steels), (2) A372—thin-walled pressure vessel steels (carbon and alloy steels), (3) A508—quenched and tempered vacuum-treated carbon steels, (4) A541—quenched and tempered forgings (carbon and alloy steels), and (5) A592—quenched and tempered, high strength, low alloy steel, forged fittings and parts.

3.3 Rods and Bars

Rod and bar stock may be used in pressure vessel construction for pressure parts such as flange rings, stiffening rings, frames for reinforced openings, stays and staybolts, and similar parts. ASTM specification for bars include A453, A479, A666, and A739.

3.4 Bolts and Studs

Bolts and studs may be used for the attachment of removable parts.

Materials for Corrosion-Resistant Fasteners

Corrosion-resistant metallic fasteners are made of stainless steels and nonferrous alloys of copper, nickel, aluminum, and titanium. Fasteners can also be made from exotic materials such as tantalum. Orlando et al. [38] discuss materials for corrosion-resistant fasteners. Standard corrosion-resistant fastener alloys and their ASTM specifications are:

1. F593—Stainless bolts, hexagonal cap screws, and studs.
   F594—Stainless steel nuts conforming to 17-4 PH, types 302, 303, 304, 305, 309, 310, 316, 317, 321, 347, 410, 416, and 430.
2. F468—Nonferrous bolts, external cap screws and studs for general use and F467 nonferrous nuts for general use: (a) Copper and copper alloys: electrolytic tough pitch (ETP) copper, yellow brass, high leaded brass, free cutting brass, naval brass 63.5%, uninhibited naval brass, silicon-bearing aluminum bronze, low-silicon bronze B, high-silicon bronze A. (b) Nickel: Monel 400, 405, K-500, Inconel 600. (c) Aluminum: 1100, 2024, 6061. (d) Titanium: ASTM Grades 1, 2, 3, and 4.

3.5 Handling of Materials

To preserve the quality and finish of the materials and to avoid any rusting and minimize additional cleaning, the following preventive measures should be taken:

1. Material should be kept in original cases or wrappers until fabrication actually begins. Cases or wrappers opened for initial inspection should again be carefully packed after inspection.
2. Store the materials/cases indoors on clean racks, which should be free from corrosive fumes.
3. Fabrication equipments should be cleaned of all residues, dirt, rust, and scales before being employed for a new operation on stainless steels and other materials where surface

contamination can initiate corrosion or embrittlement during fabrication. Paper or other protective covering should be placed on all surfaces.

3.6 Material Selection for Pressure Boundary Components

Material for pressure boundary components such as shell, channel, tubesheet, and tubes should conform to material for pressure retaining components. For item like baffles, corrosion-resistant material compatible with the process fluid should be chosen, whereas for supports, strength and corrosion resistance to the ambient environment shall be considered. Guidelines for selecting material for shell, channel, tubesheet, tubes, and baffles are discussed next. For more information, refer to Danis [39] and Ref. 40.

Shell, Channel, Covers, and Bonnets

Specify the materials with a corrosion allowance adequate for the design life of the exchanger. Often, this means selecting materials that should last for 15 years or more [39]. For corrosive service, consider clad material if it is economical. Materials such as chromium-molybdenum steels, Q&T steels, cryogenic materials, austenitics, duplexes, 6Mo steels, cupronickels, nickels, titanium, etc. should be carefully evaluated from a fabrication standpoint prior to their selection as a pressure boundary material.

Tubes

Specify a material and corrosion allowance for both the shell side and the tube side of the exchanger. Tubes are often designed with a life span significantly shorter than that of the shell or channel, since they can be retubed. The tube material must be compatible with the tubesheet material. To avoid galvanic corrosion due to unfavorable area ratio, the tube must be cathodic to the tubesheet material.

Tubesheet

Most tubesheets are made from rolled plates or forged ingots. Tubesheets of small production line units may be cast. Carbon steel tubesheets less than about 5 in (127 mm) thick are most often burned from plate. Thicker tubesheets are machined from forgings. Nonmetallic materials and composites of thin metals coated with epoxy resins have been used in small air-conditioning units. Commonly used tubesheet metals for corrosive applications are AISI types 304 and 316, aluminum, bronze, mutz metal, copper-nickels 10% and 30%, and titanium.

Specify a material with a corrosion allowance that reflects both shell-side and the tube-side conditions. Cladding may often be required on the shell side, the tube side, or both sides of the tubesheet. Solid alloy construction can be utilized if both sides of the tubesheet require cladding [39]. In general, if austenitic stainless steel or titanium alloy tubing is required, a tubesheet with a matching alloy clad on the corrosive side should be specified. Some of the considerations to choose clad tubesheets are [41]:

1. A metal that is resistant to corrosion by the fluid on one side while it is corrosive to the other side fluid.
2. It is desirable to fusion weld the tubes to the tubesheet, but the tube and tubesheet materials are not compatible.
3. The granular structure of the tubesheet is not uniform, making it unsuitable for fusion welding the tubes to the tubesheet.

Baffles

Specify a material to match the nominal chemistry of the tube material and shell-side fluid. If the shell-side conditions favor galvanic coupling, or if shell-side fluid is not conducive to baffles, corrosion rates would cause the baffles to fail before the tubes.

4 MATERIALS FOR HEAT EXCHANGER CONSTRUCTION

A wide spectrum of materials is used in the construction of heat exchangers. The materials may be metals or nonmetals like glass, graphite, ceramic, and plastics. The principles of selection of heat exchanger materials have been discussed earlier. In this section, the properties of the following common heat exchanger materials that favor them for heat exchanger construction, metallurgy, corrosion resistance, and fabrication including welding are discussed.

1. Cast iron.
2. Carbon steel.
3. Low-alloy steel.
4. Stainless steel: martensitic, austenitic, ferritic, superferritic, duplex, superaustenitic.
5. Aluminum and aluminum alloys.
6. Copper and copper alloys.
7. Nickel and nickel alloys.
8. Titanium and titanium alloys.
9. Zirconium.
10. Tantalum.
11. Graphite.
12. Glass.
13. Teflon.
14. Ceramics.

5 PLATE STEELS

Plates used in the construction of pressure parts of pressure vessels shall conform to one of the specifications in ASME Code Section II, for which allowable stress values are given in the tables referenced in UG-23. Important sources on selection of pressure vessel quality plate steels include Weymuller [42,43], Ref. (18), and Hagel et al. [29], among others.

5.1 Classifications and Designations of Plate Steels—Carbon and Alloy Steels

Regular quality is the common designation for carbon steel plate sold only on the basis of a maximum carbon content of 0.33% by heat analysis. Plate of this quality can vary substantially in chemical composition due to the broad range of carbon content permitted and unspecified chemical composition limits for other elements.

Structural quality plate is intended for application in structures such as bridges, buildings, tanks, railroad cars, mobile equipment, and miscellaneous fabrications. General specifications for structural quality plate steels are covered by ASTM A6.

Pressure vessel quality plate is intended for applications in pressure vessels, heat exchangers, and similar end uses. The manufacturing practices for pressure vessel applications are set up to provide plate with improved quality. Additional testing is required, such as mechanical and nondestructive testing (NDT), including notch toughness tests, radiography, and ultrasonic inspection. General specifications for pressure vessel quality plate steels are covered by ASTM A20.

Forging quality plate is intended for forging, heat treating, or similar purposes or when uniformity of composition and freedom from injurious imperfections are essential.

How Do Plate Steels Gain Their Properties?

The primary function of alloying elements is to improve the mechanical properties, stability at moderately high temperatures and also to increase resistance to specific corrosive environment. Plate steels achieve strength and ductility through these alloying elements [42]:

1. Carbon, manganese, nickel, chromium, boron, and molybdenum raise hardenability and hence increase strength.
2. Silicon and aluminum remove oxygen, ensuring porosity-free microstructures.
3. Aluminum, titanium, columbium, vanadium, and zirconium are used as grain refiners.
4. Copper increases atmospheric corrosion resistance.

One of the principal functions of alloying elements is to increase hardenability, which is the property that determines the depth to which the steel will harden. In addition to alloying elements, heat treatment is used to develop certain desirable properties.

Changes in Steel Properties Due to Heat Treatment

Heat treatments that steel plates undergo at the fabricator's plant vary from fabricator to fabricator. To meet the heat treatment requirements of individual fabricators, plate makers give, under simulated conditions, the same heat treatments that will be used by the fabricator to test specimens taken from each plate ordered [18]. This guarantees the required properties. Therefore, in his purchase order, the fabricator must provide information on the heat treatments likely to be given while processing the plates in shop floor.

ASTM Specifications on Plate Steels Used for Pressure Vessel Fabrications and Heat Exchangers

Material specifications list, in order, topics pertaining to the material—scope of the specification, referenced documents, terminology, ordering information, materials and manufacture, responsibility for quality assurance, heat treatment, chemical requirements, metallurgical structure, mechanical requirements, certification, identification, marking of product, packaging and package marking, mill test report, and supplementary requirements. Each specification is unique to the material; committees add some topics and drop others to fit the material and its expected use. General ASTM specifications for pressure vessel quality plate steels are given in Table 4.

Carbon Steels. ASTM specifications for carbon steels include A285, A299, A442, A455, A515, A516, A537, A562, A612, A662, A724, A738, and A841. Carbon steels lack the alloying elements that are required for heat and corrosion resistance. Carbon steels are mostly used for moderate-temperature applications. ASTM specifications for various carbon steels are given in Table 5.

HSLA Grades. ASTM specifications A734 and A737 cover high-strength, low-alloy (HSLA) steels. A734 covers two steels, both quenched and tempered: Type A, a nickel-chromium-molybdenum steel, retains its properties down to −80°F. Type B finds uses at −20°F and above. Two HSLA steels, designated Grades B and C, are described in A737.

Alloy Steel. Alloy steels for pressure vessels contain three major alloying additions: chromium, nickel, and molybdenum, and other elements such as carbon, manganese, and silicon, found in killed steels. Alloy steels exhibit mechanical properties superior to carbon steel as the result of chromium, nickel, and molybdenum. Various alloy steels are given in Table 6.

Table 4 General ASTM Specifications for Pressure Vessel Quality Plate Steels [42]

ASTM number	Content
A20	Pressure vessel quality steel plates: descriptive terms, ordering instructions, manufacture and quality control, material identification, packaging, and shipment
A370	Mechanical testing: Requirements for tension, bend, hardness, and impact tests.
A435	Standard specifications for ultrasonic examination of steel plates to determine internal discontinuous such as pipes, ruptures, and laminations.
A577 and A578	Ultrasonic testing procedures to locate and size interior defects.
A673	Mechanical testing: sampling procedures for impact (Charpy V-notch) tests of steel products.
A700	Product handling: packaging, marking, and loading of steel products for shipping.
A770	Mechanical testing: procedures and acceptance standards for through-thickness tension tests, which determine propensity to lamellar tearing.

Table 5 ASTM Specifications for Carbon Steel Plate (Pressure Vessel Quality)

Title of specification	ASTM no.
Low and intermediate tensile strength carbon seel plates	A285
Manganese-Silicon carbon steel plates	A299
Improved transition properties carbon steel plates	A442
High strength manganese carbon steel plates	A455
Intermediate and higher temperature service carbon steel plates	A515
Moderate and lower temperature service carbon steel plates	A516
Heat-treated, carbon-manganese-silicon steel plates	A537
Manganese-titanium carbon steel plates for glass or diffused metallic coatings	A562
High strength, for moderate and lower temperature service, carbon steel plates	A612
Carbon-manganese steel plates for moderate and lower temperature service	A662
Carbon steel, quenched and tempered, for welded layered pressure vessels	A724
Heat treated, carbon-manganese-silicon steel plates	A738
Carbon steel plates produced by the thermo-mechanical control process (TMCP)	A841

Subzero and Cryogenic Applications. Steels for subzero and cryogenic applications include, A203, A353, A442, A517, A537, A542, A543, A553, A612, A645, A662, A724, A735, A736, A782, and A844.

Specification for Stainless Steels. Most of the AISI types—austenitic (types 302, 304, 304L, 316, 316L, 317, 317L, 321, 347), duplex, ferritic and martensitic stainless steels, plus some special stainless like superferritic and superaustenitic steels—are included in A240.

Clad Steels and Other Grades. Clad steels are covered by ASTM A263, A264, and A265. The cladding materials specifications A263 and A264, chromium and Cr-Ni cladding, respectively, must conform to ASTM A240. Clad steels listed in A265, nickel- and nickel-base alloys, are covered by a number of ASTM specs and trade designation, such as (1) Nickel 200, Monel 400, Inconel 625, Incoloy 800 and 800H, and Incoloy 825, produced by Inco Alloys International; (2) Hastelloy B and B-2, C4 and C276, and G and G2, produced by Haynes Interna-

Table 6 ASTM Specifications for Alloy Steel Plate (Pressure Vessel Quality)

Title of specification	ASTM no.
Chromium-manganese-silicon alloy steel plates	A202
Nickel alloy steel plates	A203
Molybdenum alloy steel plates	A204
Manganese-vanadium-nickel alloy steel plates	A225
Heat-resisting chromium and chromium-nickel stainless steel plates	A240
Steel plate clad with corrosion resistance chromium alloy	A263
Steel plate clad with corrosion resisting stainless steel (Cr-Ni)	A264
Steel plate clad with corrosion resisting nickel base alloy	A265
Manganese-molybdenum, and manganese-molybdenum-nickel alloy steel plates	A302
9% nickel double normalized and tempered alloy steel plates	A353
Chromium-molybdenum alloy steel plates for elevated temperature services	A387
High tensile strength quenched and tempered (Q&T) alloy steel plates	A517
Quenched and tempered manganese-molybdenum and manganese-molybdenum-nickel alloy plates	A533
Quenched and tempered chromium-molybdenum alloy steel plates	A542
Quenched and tempered nickel-chromium-molybdenum alloy steel plates	A543
Quenched and tempered 8% and 9% nickel alloy steel plates	A553
Quenched and tempered nickel-cobalt-molybdenum-chromium alloy steel plates	A605
Specially heat treated 5% nickel alloy plates	A645
36% nickel plate for low thermal expansion	A658
High strength and low alloy, quenched and tempered, alloy steel plates for crysgenic use	A734
Low carbon manganese-molybdenum-columbium alloy steel for moderate and lower temperature service	A735
Low carbon age hardening nickel-copper-chromium-molybdenum-columbium alloy plates	A736
High-strength low-alloy steel plates	A737
Quenched and tempered, manganese-chromium-molybdenum-silicon-zirconium alloy steel plates	A782
Chromium-molybdenum-vanadium-titanium-boron alloy steel plates	A832
9% nickel alloy steel plates, produced by the direct-quenching process	A844

tional, Inc.; and (3) Carpenter 20 CB-3, produced by Carpenter Technology. Descriptions of these clad steels are given in Table 7. Producers include Lukens Steel and du Pont.

Producers of Steel Plates in USA. Major producers of plate steels include:

Bethleham Steel Corporation.
Gulf States Steel Company.
Inland Steel Industries.

Table 7 ASTM Specification for Clad Steel Plate

Description	ASTM no.
Chromium steel clad plate, sheet, and strip	A263
Chromium-nickel stainless steel clad plate, sheet, and strip	A264
Nickel and nickel base alloy clad steel plate	A265

Oregon Steel Mills.
Lukens Steel Company.
USS Div., USX Corporation.

Major producers of stainless steel include:

Allegheny Ludlum Steel Corporation.
Eastern Stainless Steel Division.
Cyclops Corporation.
Jessop Steel Company.

6 PIPES AND TUBES

ASME code requirements are:

1. Pipes and tubes of seamless or welded construction conforming to one of the specifications given in ASME Code Section II may be used for shells and other parts of pressure vessels. Allowable stress values for the materials used in pipe and tubes are given in the tables referenced in UG-23.
2. Integrally finned tubes may be made from tubes that conform to one of the specifications given in Section II.

6.1 Tubing Requirements

For heat exchanger applications, the tubing must meet four requirements [44]: (1) the tube must withstand the pressures from both the shell side and tube side at the operating temperature, (2) the tube must be corrosion resistant to both shell-side and tube-side fluids, (3) the tube must be capable of being fixed into the tubesheets either by rolling or welding, and (4) the tube must achieve optimum economy.

The tubes may solid drawn, electric resistance welded (ERW), or fusion welded. It is a common practice to prefer solid drawn tube to ERW tube for high-pressure duties. BS 3606, Steel Tubes for Heat Exchangers, identifies the following methods of manufacture [45]:

1. Cold-finished seamless.
2. Electric resistance welded and induction welded.
3. Cold-finished electric resistance welded and induction welded.
4. Longitudinally welded and heat-treated austenitic stainless steel.
5. Longitudinally welded, cold-finished and heat-treated austenitic stainless steel.
6. Longitudinally welded, bead-conditioned and heat-treated austenitic stainless steel.

6.2 Selection of Tubes for Heat Exchangers

In addition to the choice of material for the tubes themselves, consideration must be given to the following factors [46]:

1. The tubesheet material.
2. The method of fixing the tubes into the tubesheet(s), for example, roller expansion, explosive expansion, or fusion welding.
3. Materials for ends/end closures.
4. In the case of water-cooled units, there may be a need for corrosion protection measures such as coatings on water boxes, and cathodic protection to protect the water boxes, tubesheets and tube ends; also, water treatment may be necessary to prevent scaling, fouling, and corrosion.

5. In addition to compatibility with the environments concerned, they must be compatible with one another in any electrolyte involved so that excessive galvanic corrosion is avoided.

6.3 Specificatons for Tubes

At minimum, specifications must require at least one method for leak detection, ductility test, and a check on the dimensional tolerances. Tubing used in corrosive environments may be further evaluated by one or more of the corrosion tests. Inspection and testing should also be carried out after any specified heat treatment or pickling operation. U-tubes usually cannot be inspected by electric test methods. Visual inspection and air-underwater tests should be performed on all U tubes after bending. Tubes should be fully heat-treated condition as received from the mill.

6.4 Defect Detection

Inspection to detect and eliminate defective tubes is the key to tubing reliability. All the defect testing methods can be applied to tubing at the mill. Different defect detection methods applied to tubing are discussed next. These methods detect mechanical-type defects that will produce leaks regardless of the corrosive environment [44]. Typical mechanical defects include through-wall defects, partial through-wall defects, delamination, ductility defects, and dimensional tolerance defects. Even mild and uniform corrosion may open up defects, causing premature leaks.

6.5 Standard Testing for Tubular Products

Standard tests for tubular products are visual examination; the eddy current test; hydrostatic pressure testing including pneumatic air-underwater testing; the magnetic particle test; an ultrasonic test; corrosion tests; mechanical tests, including tensile, flaring, flattening, and reverse flattening; metallographic testing; and dimensional tolerance testing. Hydrostatic pressure tests including pneumatic air-underwater tests, corrosion tests, and dimensional tolerance tests are discussed next.

Hydrostatic Pressure Testing

Hydrostatic testing is the most common test performed on tubing at the mill and is required on ASME Code exchangers. Test pressures are usually 6.9 MPa (1000 psi), but this may be decreased for large-diameter, thin-wall tubing. Most ASTM specifications allow testing at higher pressures as long as the hoop stress does not exceed a certain value; however, equipment limitations usually restrict pressures to about 38 MPa (5500 psi).

According to ASTM Standards, each tube shall withstand a hydrostatic pressure sufficient to subject the material to a fiber stress of 48 MPa (7000 psi) determined by the following equation for thin walled cylinder under internal pressure:

$$P = \frac{2St}{D - 0.8t} \quad or \quad P = \frac{2\ \text{Set}}{D - 0.8t} \qquad \text{(ASME Code procedure)}$$

where P is the hydrostatic pressure (MPa or psi), S the code allowable stress of the tube material (MPa or psi), E is weldjoint efficiency which is equal to 0.85 for welded tube and 1.00 for seamless tube, D the tube outer diameter (mm or in), and t the thickness of the tube wall (mm or in). The tube should not show any evidence of leakage. The tube need not be tested at a hydrostatic pressure more than 6.9 MPa (1000 psi), unless so specified.

Pneumatic Test

The pneumatic air-underwater test is a superior test for detecting through-wall defects that result from tube manufacturing, compared to the hydrostatic test. Air pressure up to 1.0 MPa (150 psi) is applied to the tubing submerged in water, and the tube is observed for leaks for 5 s. This test method is dependent solely on visual observation of leaks and not on pressure drop, which is an indication of leaks during hydrostatic testing. Extremely small through-wall defects may not be detected by air passage.

Corrosion Tests

Corrosion tests are used to evaluate tube material for its corrosion resistance. Usually, only a small section of tubes from a lot or heat is subjected to corrosion testing. Some of the most common corrosion tests include the uniform or general corrosion test, intergranular corrosion test, stress corrosion cracking test, critical pitting corrosion test, critical crevice corrosion test, and exfoliation corrosion test.

Dimensional Tolerance Tests

Dimensional tolerance tests such as outer diameter and inner diameter, wall thickness, weld flash thickness, ovality, length, straightness, and squareness of end cut are checked by use of measuring instruments such as micrometers, ring gages, feeler gages, and others.

6.6 Mill Scale

Most carbon steel, irrespective of form, is manufactured by hot working. The hot-working operations produce a thin but rough film of black magnetic iron oxide (Fe_3O_4) on the surface of the steel. This film is commonly referred to as "mill scale" [47]. Mill scale is anodic to the base metal, and any discontinuity in the mill scale will induce pitting corrosion in a corrosive environment. For this reason, mill scale is regarded as a contaminant, and mostly this is removed prior to installation in a heat exchanger.

6.7 ASTM Specifications for Ferrous Alloys

ASTM specifications for some ferrous alloy tubings are given in Table 8. For nonferrous tubes, the specifications are given while discussing various nonferrous metals.

The ferrous tubing is further specified by A498, the specification for seamless and welded carbon, ferritic, and austenitic alloy steel heat exchanger tubes with integral fins. The finned tubes shall be manufactured from plain tubes that conform to one of the following ASTM specifications: A179, A199, A213, A214, A249, and A334.

7 WELDABILITY PROBLEMS

In the following pages, selection of various metals, the properties that favor them as heat exchanger materials, corrosion resistance, and fabrication by welding are discussed. Before that, certain weldability problems common to some or many metals are discussed in this section.

Weldability is defined as the degree of ease or difficulty of joining two metals to produce a weld that gives the required properties in service. De facto, weldability is the ease or difficulty of making a joint that is free of cracks [48]. Cracking of any nature cannot be allowed in a weld metal. Some important weldability considerations, such as cold cracking, hot cracking, and laboratory tests to determine susceptibility to cracking, are discussed in this section. References 49–57 provide general or specific information on weldability problem. Other im-

Table 8 ASTM Specifications for Some Ferrous Tubing for Heat Exchangers

Description	ASTM no.
Seamless cold-drawn low-carbon steel heat exchanger and condenser tubes	A179
Seamless cold-drawn intermediate alloy (Cr-Mo, and Cr-Mo-Si) steel heat exchanger and condenser tubes	A199
Seamless ferritic and austenitic alloy steel boiler superheater, and heat exchanger tubes	A213
Electric resistance welded carbon steel heat exchanger and condenser tubes	A214
Welded austenitic steel boiler, superheater, heat exchanger, and condenser tubes	A249
Seamless and welded carbon, ferritic and austenitic alloy steel externally finned tubes	A498
Seamless cold drawn carbon steel feedwater heater tubes, includes U-tubes	A556
Electric resistance welded carbon steel tubes (straight and U-tubes) for feedwater applications	A557
Welded austenitic stainless steel feedwater heater tubes, includes U-tubes	A688
Welded ferritic stainless steel feedwater heater tubes, includes U-tubes	A803
High frequency induction welded, unannealed, austenitic steel steam surface condenser tubes	A851

portant sources on weldability considerations include Brosilow [58] and the leading welding research institute publications.

7.1 Cold Cracking

Cold cracking, also known as delayed cracking, occurs at lower temperatures, sometimes long after the weld has cooled to room temperature. These cracks go through the alloy grains.

Some forms of cold cracking of base metal are hydrogen-induced cracking, underbead cracking, lamellar tearing, and fish-eye cracking.

Hydrogen-Induced Cracking

Hydrogen-induced cracking (Fig. 4) is the most common heat-affected zone defect, but may also occur in the weld metal. It occurs after solidification, often showing up as zigzag transgranular fractures. Three conditions present simultaneously make a hydrogen-induced crack:

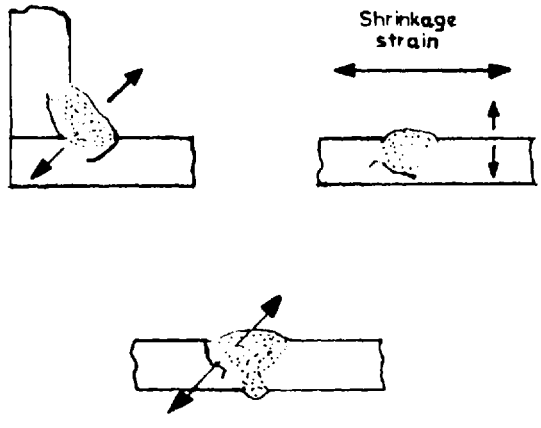


Figure 4 Hydrogen-induced cracking. (From Ref. 15.)

1. The presence of hydrogen in the steel.
2. A susceptible microstructure that is partly or wholly martensitic.
3. A tensile stress of significant magnitude at the sensitive location.

Hydrogen-induced cracking will not take place if one or more of these conditions is not present or is at a low level. Also, this form of cracking is generally not encountered in section thickness less than 0.4 in (10.6 mm). Heavy sections rapidly draw heat from the weld zone and thereby intensify thermal stress.

Susceptible Materials. When other factors such as hydrogen, restraint, and thermal cycle are constant, a steel with higher carbon content and/or alloying elements level has a greater tendency to form a harder microstructure, which is more susceptible to hydrogen-induced cracking. Therefore, hydrogen-induced cracking is usually more prevalent when welding hardenable carbon and alloy steels than when welding plain carbon steels. Steels with 0.15% carbon or less are immune to this problem, especially when thick sections are welded.

Hydrogen Sources. Hydrogen is generally introduced during welding. The source may be the filler metal, moisture in the electrode coating, welding flux, the atmosphere or shielding gas, or a surface contaminant on the filler or base metal.

Stresses. Welding stresses arise from external restraint of the welded sections, unequal thermal expansion and contraction of the base metal and weld metal, volumetric expansion resulting from microstructural changes in the weldmetal, and also from welding practices-related factors like low amperage, high welding speed, low heat input, fast cooling of weld metal, as well as from poor joint design and fit-up, and from no preheating.

Avoiding Hydrogen Cracking. Hydrogen-induced cracking can be controlled using (1) hydrogen-free welding by using low-hydrogen electrodes (5–10 mL/100g), clean wire, a wire brush, and/or a clean surface; (2) use of ductile nonmartensitic structure with low carbon equivalents—the toughest and strongest welds contain acicular ferrite [58]; (3) welding methods incorporating preheating, high amperage, low speed, high weld heat, interpass temperature control, and slow cooling—preheating to reduce cooling rate and maintaining interpass temperature to let hydrogen diffuse out of the weld bead before a subsequent pass covers it, and when preheating is impractical, using austenitic filler metal; (4) use of a low-hydrogen process such as gas metal arc or gas tungsten arc welding; (5) adoption of welding procedures that result in low welding stresses; (6) use of electrodes containing a deoxidizer like aluminum, manganese, or silicon; and (7) adoption of special welding techniques like the temper bead technique (Fig. 5) in multipass welding to soften the final weld pass, and two-layer welding, which uses the second pass to refine the HAZ of the previous pass [58].

Preheating, Interpass Temperature, and Postheating.

Preheating Temperature. Preheating is specified primarily to prevent hydrogen induced cracking. Preheat reduces the cooling rate of the HAZ of each weld bead, which in turn reduces hardness, hydrogen content in the vicinity of the weld, and stresses. Preheating of a joint is commonly done with torches or electrical strip heaters. If the part is small enough, it can be placed in a furnace. The temperature for preheating depends on the welding process, base metal thickness, composition, and properties.

1. Thumb rule. The preheating temperature t_p (°F) is given by the following formula:

   $$t_p = 1000\,(C - 0.1) + 18t$$

   where C is the percent C in the base material and t the thickness of base material (in).
2. An alternate formula to predict the preheating temperature t_p (°F) is given by

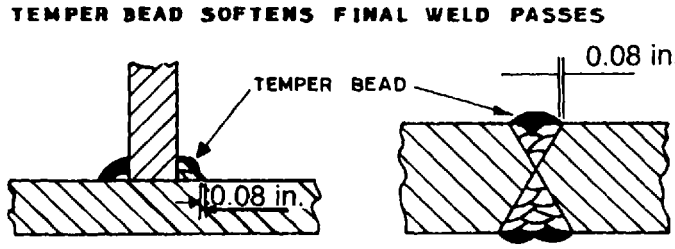


Figure 5 Temper bead technique. (From Ref. 58.)

$$t_p = 350\sqrt{(CE - 0.25)}$$

where CE, the carbon equivalent, is calculated by the following formula:

$$CE = C + \frac{Mn}{6} + \frac{Cr + Mo + V}{5} + \frac{Ni + Cu}{16}$$

3. Yet another formula is recommended as follows [49]:

$$CE = \%C + \frac{\%Mn}{6} + \frac{\%Ni}{15} + \frac{\%Mo}{4} + \frac{\%Cr}{4} + \frac{\%Cu}{13}$$

With this formula,

CE < 0.45% preheat generally not used.
0.45% < CE < 0.60% preheat at 200–400°F (93–204°C).
0.60% < CE preheat at 400–700°F (204–371°C).

Interpass Temperature. A preheat temperature that is maintained between weld beads throughout the welding cycle is known as the interpass temperature. Hydrogen-induced cracking can occur if the interpass temperature becomes too low. An upper limit also must be maintained because too high an interpass temperature may cause excessive grain growth in the HAZ, with a reduction in mechanical properties. Maximum interpass temperatures of about 250°C are usually specified for austenitic steel welds.

Postheating. The situation of heavy welding carried out in a localized area where the stress will be high and causing cracks can be avoided by postheating the weldment for 1 or 2 h immediately after welding. This is essential for high-thickness and low-alloy steel weldments.

Specification for Preheating, Interpass, and Postheating Temperatures. Specification of preheat and postweld heat-treatment conditions should generally follow the relevant code/standard for the particular parent materials.

Carbon Equivalent to Assess Cold Cracking. The tendency to hydrogen-induced cracking in carbon and low-alloy steels seems to correspond roughly to the composition of the steel. Therefore, calculation of the carbon equivalent (CE), an index figure that relates steel composition to cracking, is the usual first step to estimate weldability of the steel. The higher the CE and the thicker the components to be joined, the greater is the risk of hydrogen cracking. Several carbon equivalent formulas have been proposed as parameters indicating a steel's susceptibility to hydrogen-induced cold cracking at the heat-affected zone. These formulas reduce the significant composition variables to a single number, known as the carbon equivalent.

1. IIW formula. Traditionally, the International Institute of Welding (IIW) formula has been used to assess the weldability of carbon steels:

$$CE(IIW) = C + \frac{Mn}{6} + \frac{Cu + Ni}{15} + \frac{Cr + Mo + V}{5}$$

Values of CE(IIW) below 0.42 denote a steel that is easy to weld without cracking; values above 0.5 are difficult. It is reported that CE(IIW) is a more appropriate parameter for evaluating the cold-working susceptibility of steels whose carbon content is more than 0.16%. A more accurate estimate will be obtained if the factor of Si/6 is added to the CE(IIW) formula [59]:

$$CE = C + \frac{Mn + Si}{6} + \frac{Cu + Ni}{15} + \frac{Cr + Mo + V}{15}$$

2. Low-carbon steels. There is a general feeling that the IIW formula is not adequate to define the behavior of modern steels with low carbon contents (0.07 to 0.22% C), and the following relationship by Ito and Bessoy is sometimes preferred [49]:

$$P_{cm} = CE = C + \frac{Si}{30} + \frac{Ni}{60} + \frac{Mn + Cu + Cr}{20} + \frac{Mo}{15} + \frac{V}{10} + 5B$$

CE is in the range 0.35 to 0.45 depending on the plate thickness, and restraint is susceptible to cold cracking. P_{cm} has been shown to be reliable for evaluating the cold-cracking tendency in low-carbon steels.

3. Yurioka et al. formula [60]. This is a general-purpose formula. Due to the reason given in item 2, it is not possible for one simple carbon equivalent formula to describe, overall, the cold-working tendency of steels if their carbon contents range widely [60]. It is with this in mind that Yorioka et al. proposed the following CE formula, which has an accommodation factor A (C) as a function of the CE:

$$CE = C + A(C)\left\{\frac{Si}{24} + \frac{Mn}{6} + \frac{Cu}{15} + \frac{Ni}{20} + \frac{Cr + Mo + Nb + V}{5} + 5B\right\}$$

where $A(C) = 0.75 + 0.25 \tanh\{20(C - 0.12)\}$. A(C) increases with an increase in carbon content. It approaches 0.5 as the carbon content decreases below 0.08% and 1.0 as it increase above 0.18%. As a parameter describing the probability of the occurrence of cold cracking in steel welding, a cracking index (CI) was proposed. It is expressed as

$$CI = CE + 0.15 \log H_{JIS} + 0.30 \log(0.017\, K_t \sigma_w)$$

where H_{JIS} is the hydrogen content in the deposited weld metal determined using JIS glycerin displacement method, $(H_{IIW} - 0.61)/1.3$; K_t is the stress concentration factor at root and toe weld positions where a crack is initiated—K_t is 1.5 for V (root), 4 to 5 for Y (root), and 3.5 for double V (root) (for others refer to Ref. 60); and σ_w is the mean stress acting on the weld metal.

Yurioka et al. proposed the necessary preheating temperatures to avoid cold cracking by the following criterion:

$$t_{100} \geq (t_{100})_{cr}$$

where t_{100} is the cooling time to 100°C (212°F); this is influenced not only by the preheating temperature employed, but also by welding heat input, plate thickness and preheating method. Critical time $(t_{100})_{cr}$ is given as

$$(t_{100})_{cr} = \exp(67.6\ CI^3 - 182.0\ CI^2 + 163.8\ CI - 41.0)$$

4. Stout and Doty formula for CE [48]:

$$CE = \%C + \frac{\%Mn}{6} + \frac{\%Ni}{20} + \frac{\%Cr + \%Mo}{10} + \frac{\%Cu}{40}$$

If CE is <0.40, the steel may be insensitive to hydrogen cracking; over 0.50, cracking is sure, and low hydrogen welding procedures are necessary.

5. Hardenable carbon steels and alloy steels. This formula takes into account the silicon content and equation for CE is given by [56]:

$$CE = \%C + \frac{\%Mn}{6} + \frac{\%Cr + \%Mo + \%V}{5} + \frac{\%Si + \%Ni + \%Cu}{15}$$

Using this formula, steels having carbon equivalents of less than 0.35% usually require no preheating or postheating. Steels with carbon equivalents between 0.35 and 0.55% usually require preheating, and steels with carbon equivalents greater than 0.55% may require both preheating and postheating.

6. Recently, expressions that include fabrication conditions such as heat input, cooling rate, joint design, and restraint conditions have also been proposed. This includes:

$$P_H = P_{cm} + 0.075 \log_{10} H + R_f/40{,}000$$

where P_H is the cracking susceptibility parameter, H is the concentration of hydrogen (ppm), R_f the restraint stress (MPa), and P_{cm} was defined earlier.

Maximum Carbon Equivalent as per ASTM A20. As per ASTM Specification A20, for weldability considerations, the plates shall be specified with a specific maximum carbon equivalent (CE) value based on heat analysis. The CE shall be calculated using the following formula:

$$CE = C + \frac{Mn}{6} + \frac{Cr + Mo + V}{5} + \frac{Ni + Cu}{15}$$

The maximum values of the carbon equivalent for C-steels, including C-Mn, C-Mn-Si, and C-Mn-Si-Al steels, are given in Table 9.

Caution About Using the Carbon Equivalent Formulas to Predict Preheating Temperature. Because the carbon equivalent is calculated from the base metal composition and includes no other variables related to filler metal and welding procedures, it is only an approximate measure of weldability or predicting susceptibility to hydrogen-induced cracking.

Table 9 Maximum Carbon Equivalent of Plate Steels Conforming to ASTM A20 for Weldability

	Maximum CE value	
Specified minimum UTS, ksi (MPa)	Up to 2 in thick	>2 in thick
60 ≤ UTS < 70 (415 ≤ UTS < 485)	0.45	0.46
70 ≤ UTS < 80 (485 ≤ UTS < 550	0.47	0.48
UTS ≥ 80 (UTS ≥ 550)	0.48	...

Note. For applicability of various conditions, refer ASTM Specification A20.

Underbead Cracking

Underbead cracks are cold cracks that are most frequently encountered when welding a hardenable base metal. This is found at the toes of weld deposits and is promoted by these factors [56]: (1) increased base metal hardenability contributed by high carbon and alloying elements content; (2) depositing small welds so that the cooling rates after welding favor the formation of hard, brittle HAZ; (3) weld designs that impose a high degree of mechanical restraint on the weld metal; and (4) the presence of hydrogen. Underbead cracking can be minimized or prevented by using low-hydrogen electrodes or by preheating joints to the range of 250–400°F and avoiding the already mentioned facators that cause underbead cracking.

Lamellar Tearing

Lamellar tearing is a cold-cracking phenomenon that occurs beneath welds, and is principally found in rolled steel plate fabrications. The tearing always lies within the parent plate, often outside the visible heat-affected zone (HAZ). It is characterized by step-like cracking parallel to the rolling plane [15,56,61,62]. Lamellar tearing is due to the presence of planar inclusions lying parallel to the plate surface, and it is shown schematically in Fig. 6.

For a given type of welded joint—T (Fig. 7), L, or cruciform configuration—the occurrence of lamellar tearing will be governed by the drop in strength and ductility of a plate in the through-thickness direction (z direction) as compared with the rolling direction. This anisotropy results in particular from the content and shape of the nonmetallic inclusions such as silicates, sulfides, and alumina, which in turn are influenced by degassing and the rolling technique. Such conditions usually are present in conventionally melted steels. When the ingot

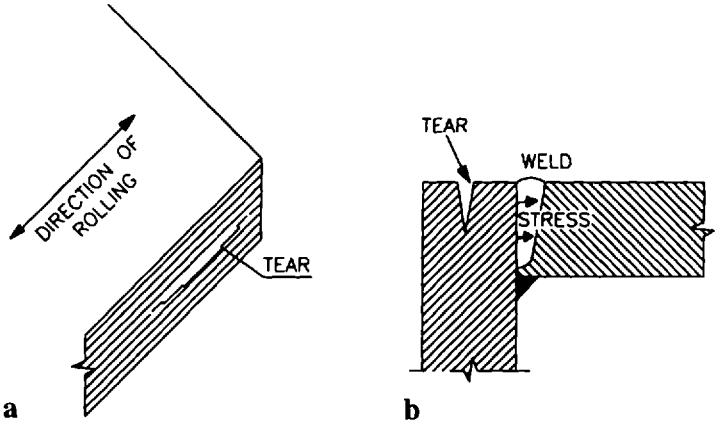


Figure 6 Lamellar tearing due to planar inclusion lying parallel to the surface. (From Ref. 63.)

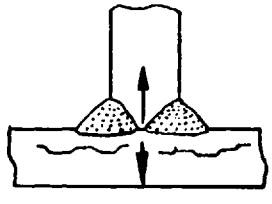


Figure 7 T-Joint susceptible to lamellar tearing.

is rolled to form plates, the inclusions deform into platelets with resultant loss in through thickness direction strength. All conventional steels are susceptible to lamellar tearing to some extent: mild and low-alloy steels whether semikilled or fully killed and including vacuum-degassed steels. For a given inclusion content, lamellar tearing is more likely as the strength of the steel increases. A considerable amount of rectification is usually necessary to repair the defect, and hence this is of considerable concern and trouble to the fabricator should it occur [63]. Because of this, lamellar tearing has attracted increasing interest from both the steel-making industry and the fabrication industry.

Conditions That Promote Lamellar Tearing. For lamellar tearing to occur, these conditions must be satisfied [56,62]:

1. Strains must develop in the short transverse direction of the plate. These strains arise from weld metal shrinkage in the joint but can be greatly increased by strains developed from reaction with other joints in restrained structures.
2. The fusion boundary is roughly parallel to the plate surface.
3. Susceptible base material with a local concentration of inclusions, particularly those extended in planar directions.
4. Section thickness: Lamellar tearing does not normally occur in welds of lighter gage plates because of insufficient constraint. Most reported occurrences of tearing are in plates greater than 25 mm in thickness [62].

Factors affecting weldment cracking due to lamellar tear (subcritical mode) include [10] through-thickness ductility, size, shape, and distribution of inclusions, matrix-inclusion cohesion, residual welding strains, mechanical constraints, and temperature.

Structures/Locations Prone to Lamellar Tearing. Any joint may be subject to lamellar tearing under certain conditions where a restrained weld is laid against a plate surface rather than the edge. From an analysis of fabrication failures, it appears that three major categories of structure type are commonly associated with the problem [62]:

1. Nozzle or penetrator set through a rigid plate (Fig. 8).
2. Stiffeners or end closure plates in cylindrical structures.
3. Shell to tubesheet connection on fixed-tubesheet heat exchangers (Fig. 6b).

Prevention of Lamellar Tearing. The risk of lamellar tearing can be solved by directing attention toward steel quality, appropriate design, and welding and fabrication techniques. These approaches are discussed next.

Melting Practice. The most reliable method of avoiding lamellar tearing involves special melting and solidification technique. Any steel-making technique that reduces the inclusion content of the steel will improve the steel properties in the through-thickness direction (z direction) and reduce the risk of tearing. Examples are deoxidation practices such as (1) low sulfur content accomplished by ladle addition of cerium or calcium, (2) sulfide shape control, i.e., to "ball up" the sulfides into spheres that do not spread out into relatively large platelets during rolling, and (3) use of aluminum or other strong deoxidizers to protect the shape control and prevent silicate formation and improve through thickness ductility; also, (4) slabs may be continuously cast rather than being rolled from ingots, and (5) vacuum melting can reduce oxygen content and incremental rapid solidification to reduce segregation. These techniques are described in detail in Refs. 56, 61, and 62 and by Gross et al. [64].

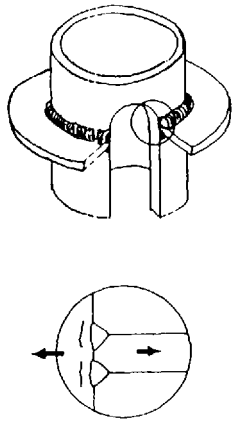


Figure 8 Locations in heat exchanger prone for lamellar tearing; nozzle set through a rigid plate. (From Ref. 62.)

Design Improvements. Many instances of lamellar tearing can be avoided in practice by improvements in design:

Replacement of cruciform joints by offset T configurations.
Replacement of T or L joints by butt joints.
Location of T joints in regions of lower restraint.
Replacement of plates by forgings, castings, or extrusions in critical T and L joints, or to avoid fillet welds.

Design improvements to overcome lamellar tearing are shown in Fig. 9a.

Welding Procedural Factors. The following can be helpful measures:

Buttering or grooving and buttering, and in situ buttering of the plate surface [62].
Selection of sequence of turns to reduce strains in plates susceptible to lamellar tearing.
Balanced welding.
Control of preheating and interpass temperature to minimize tensile strains around the joint.
Following low-hydrogen welding practice.
Shot-peening the weld beads.

Welding procedures such as buttering and balanced welding are shown in Fig. 9b.

Complentary Information Test for Lamellar Tearing. Conventional pulse echo techniques, although useful for detecting laminations in plate, cannot reliably detect small inclusions, which can give rise to lamellar tears [62]. Hence for further assurance, additional testing is conducted at room temperature, known as the through-thickness tensile test. In this test, the strain developed during weld cooling is simulated, and the material parameter associated with lamellar tearing resistance, through-thickness reduction of area (TTRA), is easily measured. A TTRA value of 20% or more is indicative of resistance to lamellar tearing. Steels are processed so as to achieve high TTRA values and thereby provide high resistance to lamellar tearing. ASTM Specification A770 covers procedures and acceptance standards for through-thickness tension tests. The room-temperature through-thickness tensile tests specimens of any one of the following can be used [65]:

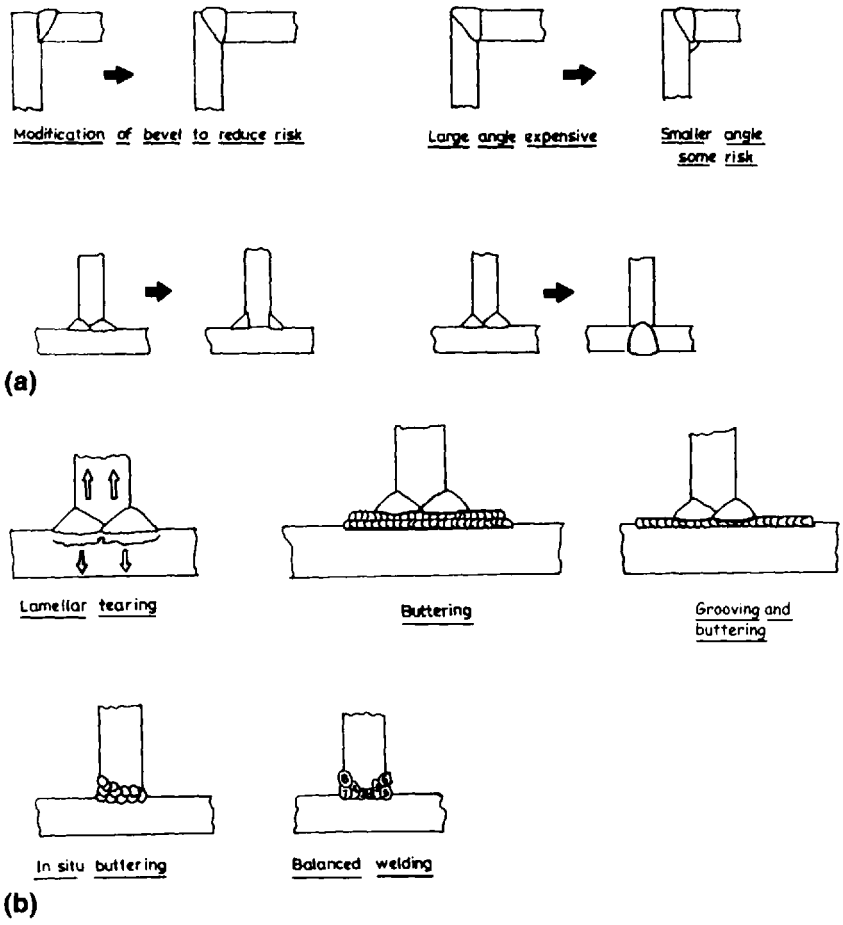
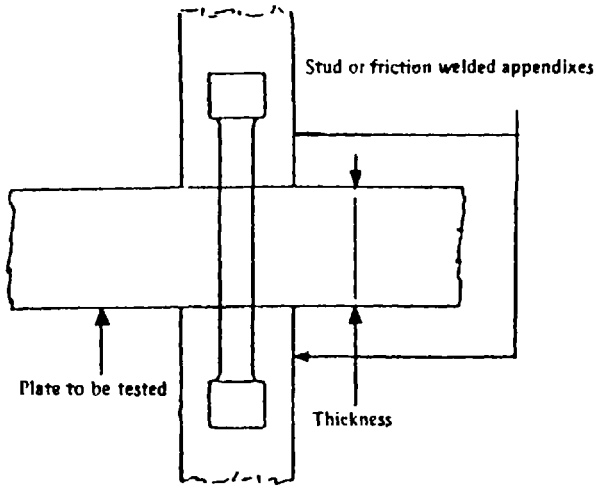


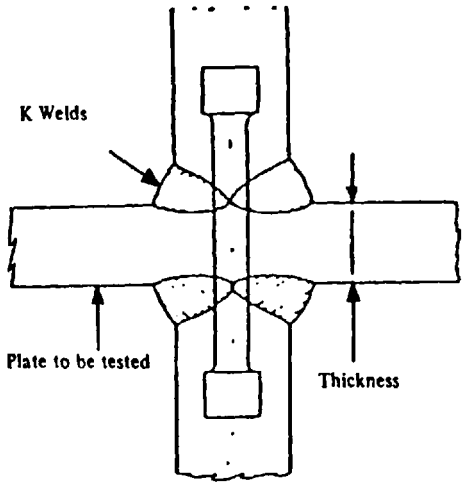
Figure 9 Methods to overcome lamellar tearing. (a) T-Joint original design and improvements and (b) welding techniques. (From Ref. 62.)

1. Type 1. These tests are recommended for all thicknesses and fitted with welded extensions. They may be machined from friction-welded assemblies or stud-welded or fusion-welded extensions. Friction- or stud-welded extensions are recommended in order to test the plates as close to the surface as possible. The Type 1 specimen is shown schematically in Fig. 10a.
2. Type 2. Test pieces of this type are recommended for plates having a thickness over 25 mm. The Type 2 specimen is shown schematically in Fig. 10b.

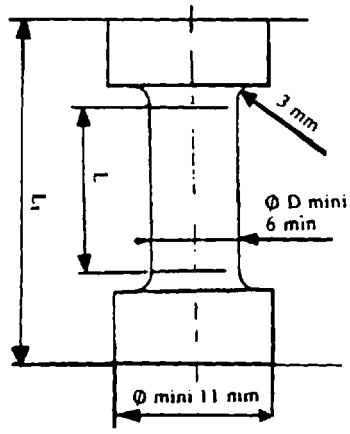
Detection of Lamellar Tearing After Welding. For surface tears, visual, dye penetrant and magnetic particle testing will be satisfactory. For subsurface tears, ultrasonics is probably the most widely used technique, but there may be problems in distinguishing true lamellar tears from inclusion bands and other forms of cracking. Therefore, pay particular attention to the position of the cracking in relation to the plate thickness and weld fusion boundary, to avoid confusion with lack of penetration defects, entrapped slags, etc. [62].



(a)



(b)



(c)

Figure 10 Complementary information test for lamellar tearing. (a) Type 1 specimen; (b) type 2 specimen; and (c) test piece geometry [65].

Fish-Eye Cracking

Fish-eye cracking is a form of hydrogen-induced cracking that occurs in weld metal and appears as small bright spots on the fractured faces of broken specimens of weld metal. These small bright spots are similar to fish eyes, and hence the name fish-eye cracking. The fish-eye usually surrounds some discontinuity in the metal, such as a hydrogen gas pocket or a nonmetallic inclusion, which gives the appearance of a "pupil in an eye." The conditions that lead to fish-eye cracking can be minimized by using dry low-hydrogen electrodes or by heating the weldments for some period in the temperature range of 200–300°F. Longer times are required with lower temperatures.

8 HOT CRACKING

Hot cracking occurs during solidification and cooling of a weld, in the weld metal or in the heat-affected zone. It occurs above solidus temperature of the lowest melting phase present. During the final stages of solidification, narrow solid bridges separating areas of low melting liquid are subject to the maximum proportion of the shrinkage-induced strains. An increase in the amount of low-melting phase or the inherent strain resulting from solidification shrinkage may cause fracture of these solid bridges, thus resulting in hot cracks [66]. Hot cracking is the subject of most fabrication weldability testing, so much so that many fabricators equate the term "weldability" with "hot cracking" and use the terms interchangeably [48].

8.1 Factors Responsible for Hot Cracking

Most mechanisms proposed deal with the metallurgical factors that can lead to hot cracking. Hot cracking will occur due to (1) segregation of low-melting-point elements, (2) sufficient stress applied to a susceptible microstructure, and (3) the mode of solidification.

Segregation of Low-Melting-Point Elements

The segregation of low-melting-point elements, such as phosphorus and sulfur, or the presence of a eutectic can cause hot cracking by extending the temperature range over which liquid is present in the microstructure. By restricting the individual concentrations of sulfur and phosphorus, resistance to solidification cracking may be obtained.

Stress States That Induce Restraint

Stresses are invariably present in a solidifying weldment due to the complex thermomechanical transients that occur during welding. Thermal expansion and contraction, plastic strains, phase transformations involving volumetric changes, etc. contribute to the stress states that induce restraint [67].

Mode of Solidification

In certain cases, as in austenitic stainless steel, the mode of solidification, whether as primary austenite or primary ferrite, strongly influences the sensitivity to hot cracking, presumably due to the differing distribution of minor elements between these two phases.

8.2 Susceptible Alloys

These include (1) copper-base alloys like silicon bronzes, aluminum bronzes, and copper-nickels, (2) aluminum alloys, (3) fully austenitic and superaustenitic stainless steels, and (4) nickel-base alloys.

8.3 Types of Hot Cracking

Various types of hot cracking are:

Solidification cracking.
HAZ liquation cracking, microfissuring.
Reheat cracking.
Ductility dip cracking.
Chevron cracks.
Crater cracks.

Solidification Cracking

Solidification cracking of the weld metal takes place within a few hundred degrees of the nominal liqidus temperature of the weld metal. It is caused by welding stresses and the presence of low melting point constituents that form as a result of segregation during solidification. Solidification cracking is shown schematically in Fig. 11.

Elements Contributing to Solidification Cracking. Increased amounts of carbon, phosphorus, and sulfur enhance the solidification cracking tendency. Resistance to solidification cracking may be obtained if the concentrations of sulfur and phosphorus are restricted. Cracking is less troublesome in carbon steel than in the high-alloy steel. Susceptibility to solidification cracking is given by the following empirical formula [48]:

$$UCS = 230C + 190S + 75P + 45Cb - 12.3Si - 5.4Mn - 1$$

As a rating of 20, a T fillet welds is likely to crack.

Welding Procedure-Related Factors Responsible for Solidification Cracking. These include:

1. Small electrode, excessive travel speed, high thermal stress, small weld, and low weld current.
2. No or low preheat, high restraint, poor joint preparation, poor weld profile, poor fit-up, inadequate jigging or tacking, unbalanced heat input, and poor electrode manipulation.
3. Weld metal used is not chosen correctly to accommodate the impurity level in the plate.

Welding Procedure to Overcome Solidification Cracking. Eliminate or overcome the various welding-related factors responsible for solidification cracking discussed earlier. The degree

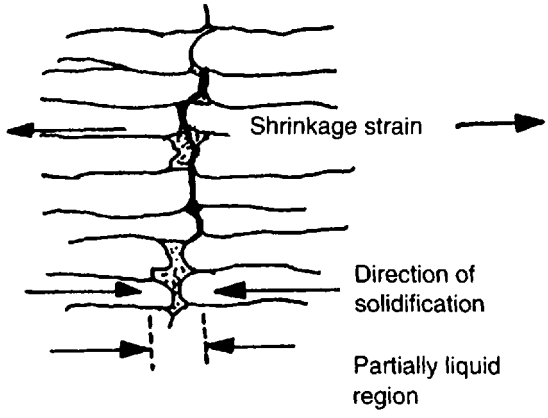


Figure 11 Solidification cracking (schematic). (From Ref. 15.)

of restraint should be reduced, and low-heat-input processes and procedures should be used. Susceptible solidification patterns, such as those with high weld pool depth-to-width ratios and those that include long columnar crystals, should be avoided. Measures such as low travel speed, use of larger electrode, improved joint design and fit-up, improved joint cleanliness, modification of tacking and jigging procedures, and the use of welding procedures tolerant of impurities will minimize hot cracking tendency. For example, basic-coated electrodes are more tolerant of sulfur than rutile-coated electrodes, and manganese-silicon dexoidized CO_2 wires than manganese-silicon-aluminum deoxidized wires [15].

Heat-Affected Zone Liquation Cracking

HAZ liquation cracking is a type of high temperature weld cracking that occurs in the HAZ adjacent to the fusion boundary during welding. In the region adjacent to the fusion boundary, where high peak temperatures are attained during welding, local melting may occur at the grain boundaries in ferritic steels due to the formation of a sulfide eutectic. The phenomenon has been known for many years to occur on steels heated at too high a temperature during processing and is known as "burning" [15].

The metallurgical basis for cracking involves the presence and persistence of liquid films at grain boundaries and the inability of these films to accomodate the thermal and/or mechanical strains experienced during weld cooling [68]. Impurity elements like sulfur and phosphorus promote hot cracking in ferrous alloys. The degree of HAZ liquation cracking will be affected by the welding process used. Heat-affected zone liquated cracking is illustrated schematically in Fig. 12.

This problem can be controlled by restricting the sulfur level in the parent material and increasing the manganese, in sufficient concentrations [66]; usually a 20 : 1 ratio (manganese to sulfur) ties up most of the available sulfur as globular manganese sulfide and leaves no sulfur for the formation of low-melting intergranular sulfide films. Welding processes characterized by a relatively high heat input, such as submerged arc and electroslag welding, are likely to produce a greater degree of HAZ liquation cracking than processes such as the manual metal arc and MIG welding processes [15]. Cleanliness and purity of the base material and welding consumables also lessen the tendency to hot cracking.

HAZ Liquation Cracking Susceptible Alloys. HAZ liquation cracking is often encountered during welding of austenitic stainless steels, nickel- and aluminum-base alloys [68], and super-

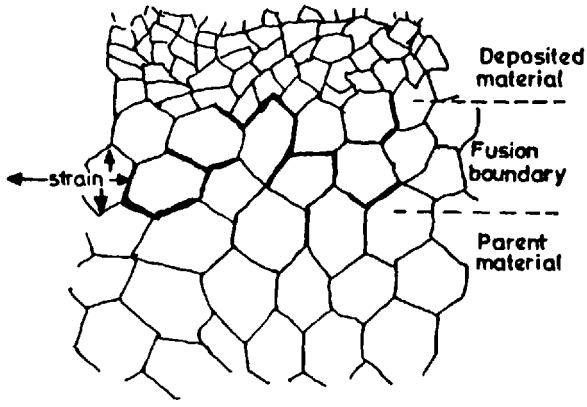


Figure 12 Liquation cracking (schematic). (From Ref. 15.)

austenitic stainless steel and duplex stainless steels. HAZ liquation cracking in austenitic stainless steel is known as microfissuring.

Reheat Cracking or Stress Relief Cracking

Reheat cracking (RC) is defined as intergranular cracking in the heat affected zone, and occasionally in the weld metal of a welded joint, being initiated during heat treatment in the temperature range of 950 to 1200°F or during service at a sufficiently high temperature [69]. The process is driven by the relaxation of residual welding stresses. The extent of cracking during heat treatment depends on composition, the microstructure of the heat-affected zone, heat-treatment temperature, and time at temperature; for some steels, it is greater with slow cooling, as in stress relieving. Reheat cracking (RC), stress relief cracking (SRC), and stress rupture cracking are equivalent forms of cracking.

Causes include poor creep ductility in HAZ coupled with thermal stress, accentuated by severe notches such as preexisting cracks or tear at weld toes, or in the fused root of a partial penetration weld.

Susceptible Alloys. Reheat cracking is reported in low-alloy structural steels, quenched and tempered steels, ferritic creep-resisting steels (Cr-Mo and Cr-Mo-V steels), nickel-base alloys, and austenitic stainless steels. Chromium, molybdenum, and vanadium contribute to this crack susceptibility. The appearance of the cracking and its position will depend on the local factors, such as [15] geometry of the joint, the relative properties of the weld metal and HAZ, and presence or absence of long-range stresses.

Phosphorus was found to enhance the RC susceptibility of Cr-Mo steels, as it segregates to some extent to the austenite grain boundaries during the weld thermal cycle. For a particular alloy, there exists a critical level of P above which embrittlement is apparent. The addition of a small amount of Ti (0.07%) decreases the RC susceptibility [69].

Empirical Check for Reheat Cracking. Nakamura, Naiki, and O'Dabayaski [70] observed that susceptibility to stress rupture cracking (ΔG) in the HAZ of welds is related to composition as follows:

$$\Delta G = \%\text{Cr} + 3.3(\%\text{Mo}) + 8.1(\%\text{V}) - 2$$

According to this equation, cracking is possible if ΔG is greater than zero. However, experience has shown that this relationship does not always give a reliable estimate of crack susceptibility. Furthermore, factors other than chemical composition are known to affect crack susceptibility.

Avoidance of Reheat Cracking. It is possible to weld any steel without the risk of reheat cracking if proper design and welding procedures are followed. Some procedures that may be used to minimize stress relief cracking in the steels include [69]:

1. Welding process changes:

   Proper selection of consumables, joint cleanliness, and proper preheat.
   Use of lower strength weld metal than that of the HAZ.
   Buttering of susceptible alloys.
   Increasing heat input and/or preheat.
   Increasing the amount of grain refinement by overlapping of the HAZ.
   Use of temper beads, i.e., small stringer beads placed over the last pass to refine the grain structure of the HAZ.

2. Complete normalization after welding.
3. Use low PWHT temperatures and high heating rates (provided stresses due to temperature gradients can be avoided).

4. Dress weld to remove discontinuities at weld toes, and minimize stress concentrations in the weld joint.
5. Reduce weld stresses by weld sequencing, back stepping techniques, and interpass PWHT; shot peen each layer of the weld metal to reduce residual tensile stresses at the surface of the weld.
6. Lower the overall level of restraint.
7. Control of sulphur level to avoid liquation cracking will also be beneficial since it has been established that liquation cracks can be potent initiation points for reheat cracking [15].

Underclad Cracking

Reheat cracking taking place under clad surfaces is known as underclad cracking (UCC). Underclad cracking of low-alloy steels is a potential problem associated with the fabrication of internally clad pressure vessels, in particular nuclear reactor vessels [69]. The incidence of underclad cracking has been reduced considerably by measures such as [71]:

1. Avoid liquation and hydrogen-induced cracks.
2. Use low-susceptibility alloys, such as SA508 C13.
3. Use clean steels: restrict impurity levels, minimize residual solidification segregation remaining in the surfaces to be clad.
4. Reduction of carbide and carbide forming elements consistent with the compositional requirements to achieve adequate strength.
5. Adopt cladding procedures that can ensure a fine-grained structure in the entire HAZ.

Ductility Dip Cracking

Ductility dip cracking may occur in either weld metal or the heat-affected zone of austenitic steels, cupronickels, aluminum bronzes, and some nickel-base alloys while the weld cools through a range of temperatures where the ductility of the particular metal is inherently low. Cracking occurs if sufficient restraint is present as the metal cools through the ductility dip temperature range. The ductility dip temperature for austenitic steels is 100–300°C (212–600°F) below the equilibrium solidus, and the cracks formed are generally much less extensive than solidification cracks [66].

Chevron Cracking

Transverse cracking in submerged arc welds has been observed when welding 2.25Cr-1Mo steel for pressure vessels, carbon-manganese-niobium steel, and 1Ni-0.5Cr-0.5Mo steel. This form of cracking lies at 45° to the weld surface in multipass welds in thick-walled plate. Due to the inclination of these cracks, they are called chevron cracks. Chevron cracking is associated with large weld beads resulting from high heat inputs [59], the moisture content in the submerged arc fluxes and when high-basicity (low-oxygen-potential) submerged arc fluxes are used. They are not easily detected by ultrasonic inspection method and usually found only with detailed metallographic examination.

Crater Cracks

These are cracks formed from a circular surface with a depression either in the weld or at the end of a weld. They are cased by a volume contraction of molten metal during solidification, usually the result of abrupt interruption of the welding arc in the root run. Crater cracks are avoided by taking back the electrode and keeping stationary for a moment at the weld pool while stopping the weld.

9 LABORATORY TESTS TO DETERMINING SUSCEPTIBILITY TO CRACKING

9.1 Weldability Tests

Tests are conducted to determine the susceptibility of metals and their alloys to various forms of cracking such as cold cracking, hot cracking, lamellar tearing, etc. They are also carried out by development laboratories for materials development of steel, aluminum, and copper, and by fabricating shops for preliminary welding procedure qualification. The laboratory tests come in a wide range of sophistication. All tests restrain the welding during cooling by some means, then gauge the amount of cracking that occurs. Tests for lamellar tearing have been already discussed. Some tests used to determine hot cracking, cold cracking (delayed cracking), or underbead cracking are:

Spot Varestraint test, for hot cracking.
Longitudinal Varestraint test, for hot cracking.
Sigmajig, for hot cracking.
Hot ductility test, for hot cracking.
Lehigh restraint test, for cold cracking.
Controlled thermal severity test, for cold cracking.
Cruciform cracking test, for cold cracking.
Battelle underbead cracking test, for cold cracking.

The HAZ liquation cracking susceptibilities of several commercial austenitic and duplex stainless steels were evaluated using the spot Varestraint test by Lippold et al. [72]. According to them, low ferrite potential (FP) heats (FP 0–1) of Type 304L were found to be more susceptible to cracking than a Type 304 alloy with FP 8, whereas duplex stainless steels, Ferralium 255 and Alloy 2205, were roughly equivalent to that of the low-FP austenitic stainless steels.

Tigamajig is the original name for the spot Varestraint test. Additional tests are discussed and detailed in Ref. 73. The drawings in Fig. 13 show some common tests for weld cracking [74,75]. Only the Varestraint test is discussed next.

Varestraint (Variable Restraint) Test

This test measures the hot-cracking tendency of a weld as it is being laid down on a specimen plate. The Varestraint is one of the few hot-cracking tests that tests for cracking by imposing an external stress. The strain can be calculated from the geometry of the test setup, and it can be reproduced time and time again, independent of the welding procedure. The applied augmented strain, ε, can be varied by adjusting the radius of the die block, R, using the equation $\varepsilon = t/(2R + t)$, where t is the specimen thickness. In this method, the Varestraint test plate (Fig. 13a) is bent to a preset radius while an autogenous weld bead is being arc-melted past point X.

10 SERVICE-ORIENTED CRACKING

10.1 Temper Embrittlement or Creep Embrittlement

Cr-Mo low-alloy steels are susceptible to temper embrittlement, a condition caused by long-term, elevated-temperature exposure in the 370 to 560°C (700 to 1050°F) range, coupled with the presence of impurity elements such as phosphorus, tin, antimony, and arsenic. The phenomenon results in the progressive reduction of the notch toughness of the material as embrittlement develops. As the material toughness decreases, its resistance to brittle fracture decreases. This phenomenon is discussed further in the section on Cr-Mo steel.

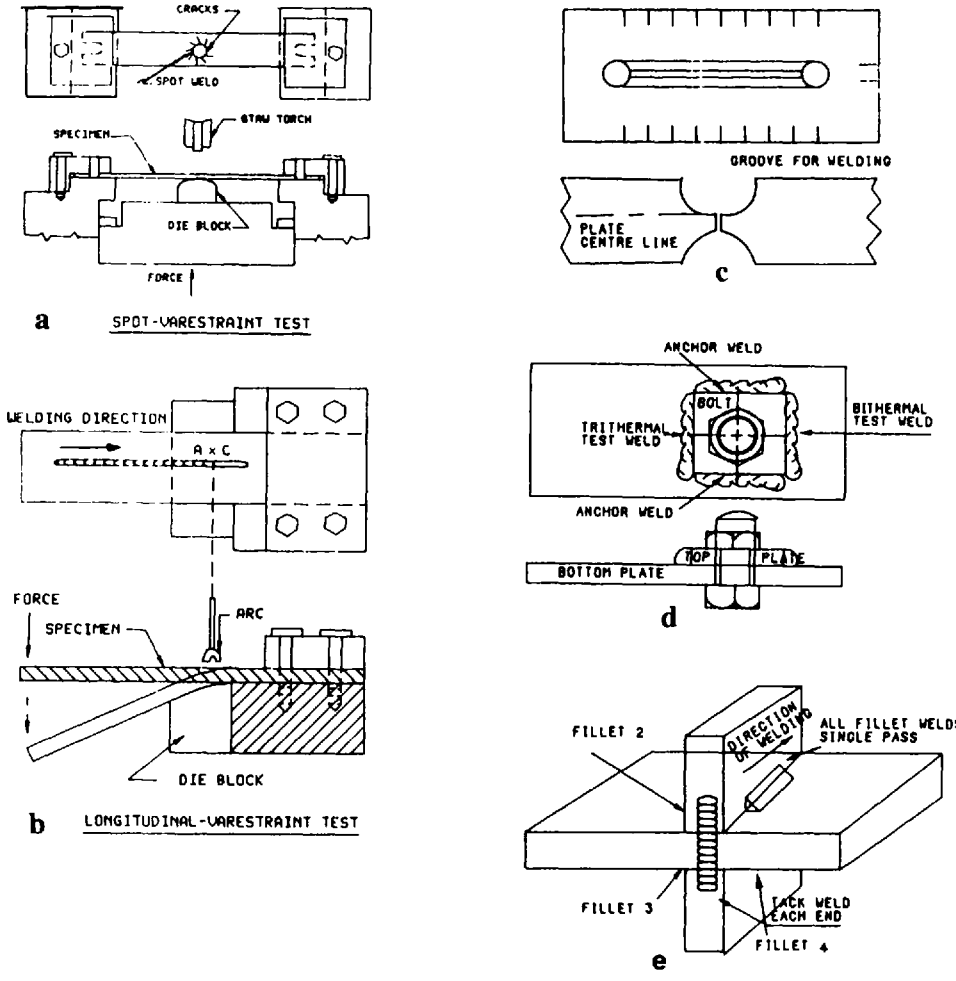


Figure 13 Configuration for testing weld cracking. (a) Spot varestraint test; (b) longitudinal varestraint test; (c) Leigh restraint cracking test; (d) controlled thermal severity test; and (e) cruciform cracking test. (From Ref. 74.)

11 WELDING-RELATED FAILURES

Welding related failures take place (1) during welding, e.g., Lamellar tearing, cold cracking, and hot cracking; (2) during stress relief annealing, e.g., temperature-induced embrittlement, elongation-induced embrittlement, and stress relief cracking; and (3) during operation, e.g., stress-induced corrosion, intergranular corrosion, stress corrosion cracking, crack growth, and creep embrittlement [76]. Inadequate welding techniques often degrade the inherent corrosion resistance of parent metals.

12 SELECTION OF CAST IRON AND CARBON STEELS

12.1 Cast Iron

For low-pressure applications, cast-iron bonnets and covers are used. According to ASME Code, Section VIII, Div. 1, cast-iron vessels shall not be used for the following services:

To contain lethal or flammable substances, either liquid or gases.
For unfired steam boilers.
For direct firing.

The design pressure and temperature limitations for the vessels and the vessel parts constructed of cast iron are listed in ASME Code Section VIII, Div. 1, UCI-3.

12.2 Steels

Grades of steel may vary in chemical composition from almost pure iron to a material of complex composition made up of several elements. Widely dissimilar properties and qualities may be obtained from a carbon steel within specified chemical limits of a given grade by changes in steel making and mill processing. In selection of the proper quality within a given grade, the end use and method of fabrication should be considered. Various practices are employed in all phases of steel production which determine the type and quality of the finished product.

Carbon steel is steel for which no minimum content is specified or required for alloying elements such as, chromium, cobalt, columbium, molybdenum, nickel, titanium, tungsten, vanadium, or zirconium, or any other element added to obtain a desired effect; when the specified minimum for copper does not exceed 0.40%; or when the maximum content specified for any of the following elements does not exceed the percentages noted: manganese 1.65, silicon 0.60, and copper 0.60. Carbon steel depends on carbon and manganese in conjunction with proper processing to improve mechanical properties

High-strength low-alloy (HSLA) steel comprises a group of steels with chemical composition specially developed to impart higher values of mechanical properties—in certain of these steels, greater resistance to atmospheric corrosion than is obtainable from conventional carbon structural steels. It is not considered to be alloy steel, even though an intentionally added alloy would qualify it as such. The minimum yield point and tensile strength requirements most often specified are 42 to 80 ksi (290 to 550 MPa) yield point and 60 to 90 ksi (415 to 620 MPa) tensile strength. These steels achieve high strength, high toughness, good formability, and good weldability.

Low-alloy steels are divided into groups according to their chemical composition, i.e., molybdenum alloy steel, manganese-molybdenum-nickel alloy steel, and chromium-molybdenum alloy steel, and each group is further divided according to strength level. Steels are commercially classified as low-alloy steels when they have:

1. Manganese content exceeding 1.65%,
2. Silicon content exceeding 0.60%.
3. Copper content in excess of 0.60%.
4. A range or a minimum amount of any other alloying element such as nickel, molybdenum, vanadium, chromium, etc. specified or added to obtain any alloying effect.

Alloy steels can utilize a wide variety of alloying elements and heat treatments to develop the most desirable combination of properties.

Process Improvements

Steel making has undergone considerable change in the last 25 years, resulting in various steels with changes in properties of the end product. Improved refining techniques, vacuum induction melting technique (VIM), low-sulfur steel-making methods, refining processes such as argon-oxygen decarburization (AOD), and vacuum oxygen decarburization (VOD), electroslag remelting, ladle metallurgy, vacuum degassing, pressure casting, continuous casting, controlled

rolling, etc. resulted in clean, low-carbon-equivalent steels of high design strengths and improved weldability, increased corrosion resistance, and increased toughness.

Carbon Steels

Carbon steels are alloys of iron and carbon in which carbon does not usually exceed 1%, manganese does not exceed 1.6%, and copper and silicon do not exceed 0.60%. Other alloying elements are normally not present in more than residual amounts. The properties and weldability of carbon steels mainly depend on carbon content. Carbon steel can be classified according to various deoxidation practices, as rimmed, capped, semikilled, or killed steel. Variations in carbon content will influence the mechanical properties. Carbon steels are normally used in the as rolled condition, although some may be in the annealed or normalized condition.

Types of Steel

In steel making, the principal reaction is the combination of carbon and oxygen to form a gas. If the oxygen is not removed, the gaseous product continues to evolve as the steel changes from a liquid to a solid. Silicon and/or aluminum are added to remove the oxygen. Control of the amount of gas evolved during solidification determines the type of steel. If practically no gas is evolved, the steel is completely deoxidized and is termed "killed" because it lies quietly in the molds. Increasing degrees of gas evolution result in semikilled, capped, or rimmed steels [77].

Killed steels are fully deoxidized and are characterized by more uniform chemical composition and mechanical properties as compared with other types. In general, killed steel is specified when homogeneous structure and internal soundness are required. It may be made fine grained or coarse grained. Generally, most carbon specifications require that plate over 1.5 in (38 mm) thick be made from killed steel.

Semikilled steels are characterized by variable degrees of uniformity in composition that are intermediate between those of killed and rimmed steel. They are deoxidized less than killed steels.

Rimmed and capped steels are characterized by marked difference in chemical composition across the section and from top to bottom of the ingot. There is a continuous evolution of gas during solidification resulting in a rim, or case of purer, cleaner solid metal free from blowholes and inclusions. They are, therefore, primarily used for making products requiring a very good surface. Most sheet and strip products are this type of steel. Steels that rim best contain no more than 0.15 percent carbon. Steels containing more than 0.30 percent carbon cannot be made to rim at all. Steels which are completely deoxidized cannot be rimmed [77].

Product Forms

Steels are available in plates, tubes, pipes, forgings, etc.

Carbons Steels for Pressure Vessels

These are specified as A285, Grade A, B, C; A229; A442, Grade 55, 60; A515, Grade 55, 60, 65, 70; A516, Grade 55, 60, 65, 70; A537, Grade 1 (Q&T condition) and Grade 2 normalized and tempered condition. For additional listing refer to Table 2.

Use of Carbon Steels

Due to low cost, carbon steels are most widely used, despite their low corrosion resistance, in large quantities as heat exchanger material in the chemical industries, fossil fuel power plants, petroleum refining operations, etc. Apart from cost, the other properties that favor low carbon steels are (1) easy availability, and (2) ease of fabrication by conventional methods. Features

that favor carbon steels for feedwater applications and refinery applications are discussed next.

Carbon Steel Tubes for Feedwater Applications. In recent years, manufacturers were forced to abandon copper alloy tubes for high-pressure feedwater heater tubing. At the elevated feedwater temperatures used in modern power plant cycles, the corrosion of copper tubes by the feedwater, although very slight, gives rise to the problem of carryover of copper into the steam generator and possible blockage in turbine units [47,78]. Sometimes low-molybdenum alloy steel is also used. The factors that favor plain carbon steel or low-molybdenum alloy steel are better weldability, high strength, and low cost. The slightly lower thermal conductivity of carbon steel than the copper-nickel is of little significance in the small-bore thin-wall tubes used in high-pressure feed heaters. The fundamental deficiency of carbon steel tubing is its low resistance to corrosion. The general corrosion and pitting problems with carbon steel tubes can be minimized with improved handling and fabrication techniques, controlled water conditions, and proper shutdown practices. These materials require corrosion protection when the plant is idle for considerable periods.

Refinery Operations. In refinery operations, carbon steel is a acceptable material for crudes up to 260°C to resist hydrogen attack and sulfide corrosion. At higher temperatures, corrosion rates increases and alloy steels or ferritic or stainless steel may be used.

Corrosion Resistance

The corrosion resistance of carbon steel is somewhat limited, and is dependent on the formation of an oxide film on its surface. Carbon steel should not be used in contact with dilute acids.

Carbon steels are susceptible to SCC by several corrosives including aqueous solutions of amines, carbonates, acidified cyanides, hydroxides, ammonium nitrate, anhydrous ammonia, coal gas liquors [2,79], and sulfide cracking of steels used in sour oil fields containing hydrogen sulfide. The temperature and concentration limits for the susceptibility of carbon steel to SCC in caustic soda are fairly well defined and given in chart form in Fig. 14 [24]. Of all the metallic materials, carbon steel is the most economical for handling solutions of up to 50%

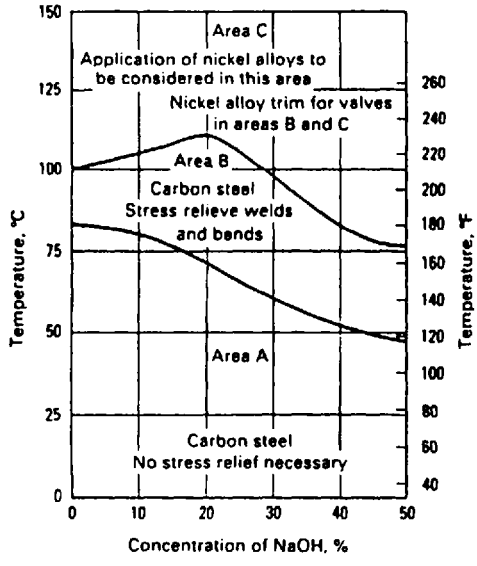


Figure 14 Temperature and concentration limits for SCC susceptibility of carbon steel in caustic soda. (From Ref. 24.)

concentration at temperatures up to 190°F (88°C). If iron contamination is permissible, steel can be used to handle caustic soda up to 75% concentration and up to 100°C (212°F). Stress relieving should be employed to reduce caustic embrittlement.

Brine and seawater corrode steel at a slow rate. Steel is little affected by neutral water and most organic chemicals. In general, the presence of oxygen and/or acidic conditions will promote the corrosion of carbon steel, while alkaline conditions will inhibit the corrosion of carbon steel.

General Aqueous Corrosion. Principal factors governing the overall corrosion of carbon steel include solution pH, dissolved oxygen in the solution, temperature, dissolved salts, and solution. The effects of these factors are well discussed by Kirby [80]. Salient features of carbon steel in aqueous solutions are discussed next [80]:

Effects of pH. Acidic solutions (pH less than 5) are highly corrosive to carbon steel. The work of Berl and VanTaack [81] has been used to relate the relative corrosion of steel over a range of pH values. According to Fig. 15, the protective oxide is soluble at pH values below 5.0 and above 13.0. Corrosion is low over a wide band of pH values.

Effects of dissolved oxygen. At ambient temperatures in near-neutral solutions, the overall corrosion rate is proportional to the oxygen concentration, up to air saturation.

Temperature effects. High temperatures increase the corrosion rate by accelerating the diffusion of oxygen through cathodic layers of hydrated iron oxide.

Effects of dissolved salts. The presence of acid or neutral salts may increase the corrosion rate, whereas the presence of alkaline salts may lower them.

Effects of velocity. In general, increasing the solution velocity steps up corrosion rates, especially if NaCl is present. To prevent failures due to the impingement of natural waters on equipment walls, velocities should be limited to a maximum of 8 ft/s.

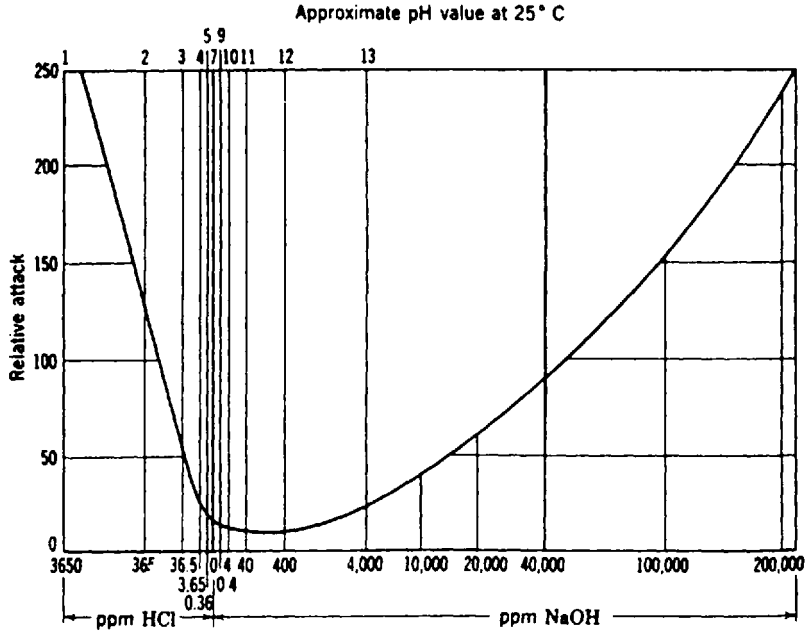


Figure 15 pH–Corrosion diagram for carbon steel [81].

Carbon steels exhibit passivity in alkaline environment and have minimal corrosion rates. This property is exploited in phosphating. Corrosion prevention measures for carbon steels include metallic coatings, painting, cathodic protection, addition of inhibitors, alloying additions, removal of oxygen from environment, elimination of galvanic couples, and organic coatings.

Fabrication

Plate Cutting. Carbon steel plates are to cut to size by flame cutting and/or machining. All plate edges after cutting must be examined for laminations and to ensure that the sheared edges are free from cracks. Dye penetrant and ultrasonic check of edges forming main weld seams is recommended, especially for higher thickness plates when these plates are used for low-temperature or hydrogen service.

Rating of Weldability. The weldability of a steel in terms of its susceptibility to cracking can be roughly estimated by carbon equivalent (CE). The influence of CE on weldability has already been covered in the section on weldability problems.

Weldability Considerations. While welding carbon steel, consider the following factors:

1. Hydrogen-induced cold cracking.
2. Solidification cracking.
3. Lamellar tear.
4. Hardness limitation for refinery service and sour gas service.

These problems are also discussed by Campbell [82]. Factors 1–3 were discussed in the earlier section on weldability problems.

Hardness Limitation for Refinery Service. The prevention of inservice weld cracking is of special concern to the refining industry because carbon steel is widely used for refinery pressure vessels, heat exchangers, tanks, and piping. Three primary factors are believed to be involved in producing inservice cracking of welds: corrosive environment, total stress, and hardness. NACE Standard RP-04-72 establishes a hardness limitation of 200 HB on completed P-1 welds. Hardness limitation is further discussed in Chapter 12.

Welding Processes. Most carbon steels can be welded using covered electrodes and appropriate welding procedures including preheating when required. Welding processes used for carbon steel are GMAW, FCAW, SAW, electroslag and electrogas welding, and oxyacetylene welding.

Arc Welding of Carbon Steels. Selection of welding electrodes is based on compatibility between base metals to be joined and the service requirements of the weldment. The essential factors in the selection of electrodes for the carbon steels are (1) mechanical properties, (2) material composition, (3) welding current, (4) position of welding, and (5) cost. Precautions should be taken to store electrodes in dry places.

The minimum thickness of low-carbon steel that can be welded by SMAW depends on welder's skill, welding position, characteristic of the current, type of joint, fit-up, class and size of electrode, amperage, arc length, and welding speed. Steel as thin as 0.036 in (0.91 mm) has been successfully welded with flux-covered electrodes.

In terms of thick sections, all commercial thicknesses can be welded successfully by SMAW provided that the root of the joint can be reached with the electrode.

Welding Defects

Since carbon steels are used extensively, the welding defects associated with various arc welding methods are given in Table 10.

Table 10 Carbon Steel Welding Defects Associated with Various Arc Welding Methods

SMAW	FCAW	SAW	GMAW and GTAW
Slag inclusion	Due to excessive arc voltage:	Weld porosity:	GMAW
Porosity	Porosity	Contaminants in the flux	Weld-metal cracks
Wormhole porosity	Heavy spatter	Insufficient flux coverage	Porosity
Undercuts	Undercutting	Excessive viscous fluxes	Inclusions
Hot cracking	Due to excessive current:	Arc blow	Incomplete fusion
Cold Cracking	Convex weld beads	Cracking:	Lack of penetration
Center-line cracking	Large droplet	Solidification cracking	Undercutting
Underbead cracks	Due to travel speed:	Hydrogen cracking	Excessive melt-through
Base metal cracks	Slag interferrence	Chevron cracking	Wire feed stoppage
Microfissuring	Convex weld bead	Underbead cracking	Inadequate shielding
Weld craters		Slag inclusions	GTAW
Arc strikes			Contamination of tungsten electrodes
Oxidation			Tungsten inclusion
Gaps from incomplete fusion			Electrode extension
Sink or concavity			
Weld reinforcement			
Overlapping			
Excessive weld spatter			

Note. This table has been compiled from the *Metals Handbook* [83].

13 LOW-ALLOY STEELS

13.1 Selection of Steels for Pressure Vessel Construction

The most important factors to be considered in selection of steels for pressure vessels and heat exchangers are tensile strength, creep strength, notch toughness, weldability, and heat treatment. In general, thinner steel plates are preferred for these reasons [29]: low weight, ease of fabrication, and low foundation cost; ease of welding, heat treatment and stress relief, NDT, erection, higher fatigue strength and resistance to brittle fracture. The inherently poorer properties of thicker sections of carbon steels are well known. For example, increased thickness offers greater internal restraint at a defect and thus increases the likelihood of defect growth by brittle fracture. Therefore, the trend is to use high-strength steels in place of thicker plates.

13.2 Low-Alloy Steels for Pressure Vessel Constructions

Low-alloy steels used in pressure vessel and heat exchanger construction are:

1. Carbon-molybdenum steels.
2. Carbon-manganese steels.
3. Carbon-manganese-molybdenum steels.
4. Manganese-molybdenum-nickel alloy steels.
5. Chromium-molybdenum steels or creep-resistant steels such as Cr-Mo, Cr-Mo-V, and modified Cr-Mo steels.

Items 1–4 are covered here, and chromium-molybdenum steels are covered separately.

Applications of Low-Alloy Steel Plates

Principal applications for low-alloy steel plates include [18]:

1. Boiler drums for thermal power plants.
2. Reactor pressure vessels, steam generators, and pressurizers for nuclear power plants.
3. Various types of reactors, converters, steam drums, separators, pressurizers, heat exchangers, and hydrocrackers for chemical plants

Of all these types of equipment, large nuclear reactors and heavy oil desulfurizers require particularly heavy steel plates, ranging from 150 to 300 mm in thickness and 30 to 50 tons in unit weight.

Carbon-Molybdenum Steels

Carbon-molybdenum steels are similar to carbon steels except they have an addition of approximately 0.5% Mo. The addition of 0.5% Mo and a little boron to carbon steels has a considerable effect on the transformation to lower bainite at normal rates of cooling [84]. This has a relatively high strength, which is retained to a moderately high temperature. These steels include ASTM A204 Grades A, B, and C, A302 Grades A and B, and ASTM A182 Grade F1 forging. Steels with 0.5% Mo find considerable use in the petroleum industry, where they have replaced carbon steel because of their resistance to hydrogen at higher temperatures. The possibility of graphitization limits their use to a maximum temperature of 875°F (470°C) [29]. These steels are produced in the as rolled or normalized condition. The weldments should be given postwelding heat treatment (PWHT).

Carbon-Manganese Steels

These steels find use in pressure vessels, ships, and other large fabrications. Manganese is added to steel for a number of reasons [15,85]:

1. Manganese combines preferentially with sulfur to form manganese-rich sulfide inclusions of high melting point that are not liquid during the hot working of the steel and hence have little effect on the toughness of the resulting product, since they are distributed more uniformly in the steel.
2. Manganese increases the strength of the steel by forming a solid solution with the iron.
3. Manganese retards the transformation of austenite to ferrite and pearlite. This means effectively that in thicker plates and sections, which cool more rapidly at the surface than in the interior, better and more uniform properties can be obtained.

The properties of carbon-manganese steels can be further improved in a number of ways [15,85]:

1. By grain refining: The addition of aluminum to a killed steel refines its grain size to produce greater toughness.
2. By normalizing.
3. By controlled rolling—this leads to relatively high strength and toughness.
4. Quenching and tempering: If carbon-manganese steels are quenched, products with a good combination of strength and toughness can be obtained.

Fabricators have not been able to join these steels by the most productive processes, like electroslag welding and submerged arc welding, because these steels cannot tolerate the high heat input of these processes. As heat input increases, austenite grains in these base metals and in weld heat-affected zones grow large; slow cooling results in a grain-coarsened ferrite

microstructure of low toughness [58]. For continuously cast steels of thickness 2 in and less, titanium treatment involving titanium nitride additions provides inclusion sites for grain refinement, whereas thicker sections (>2 in/50.4 mm) and ingot-cast steels cool too slowly to achieve grain refinement.

To avoid the formation of hard constituents in weld metal susceptible to hydrogen cracking, slow the cooling rate by increasing heat input to the weld; in multipass welding, proper sequencing can reaustenize previous passes to form softer microconstituents and temper hard ones [58].

Application of Carbon-Manganese Steels. Carbon-manganese steels are cheaper and they are relatively easy to produce in large quantities. They include the so-called mild steel boiler quality plate with yield strengths of about 15 tonf/in^2 (230 N/mm^2) and ultimate strengths of about 25 tonf/in^2 (385 N/mm^2). They are extensively used in boilers and high-pressure plants working at up to, say, 350°C (660°F). Above this temperature, however, they lose their strength very rapidly, and in addition they have inadequate corrosion resistance and scaling resistance. The ambient temperature strength can be improved substantially by normalizing, by controlled rolling, and by quenching and tempering [15]. Controlled rolled steels are available with minimum yield strengths exceeding 25 tonf/in^2 (385 N/mm^2) and quenched and tempered steels with even higher strength.

Carbon-Manganese-Molybdenum Steels

The addition of molybdenum to carbon-manganese steel increases the strength at ambient temperature slightly but has a marked effect on the strength at higher temperature. Carbon-manganese steels containing about 0.5% Mo have found extensive use in pressure vessels. However, their creep ductility is rather limited, and for that reason and for their improved resistance to high-temperature corrosion and oxidation, the chromium-molybdenum steels may be preferable in some cases.

14 QUENCHED AND TEMPERED STEELS

An important group of steels is those in which the hardenability is increased by alloy additions so as to produce martensite throughout the plate thickness when the steel is quenched or even air-cooled from the austenite range. The steels are then tempered to give the required properties. The total alloy content of such steels may be relatively high but they have a very attractive combination of strength and toughness. These steels are known as quenched and tempered (Q&T) steels. They are also relatively easy to weld since the carbon content to achieve a given strength can be kept low. The use of the term "quenched and tempered" is a little misleading since it may not always be applied to martensitic steels. Some "normalized and tempered" steels have to be quenched and tempered when used in thick sections to achieve the required rate of cooling and hence the desired properties [15]. Better properties can be obtained by quenching and tempering carbon-manganese steels as well as more highly alloyed steels.

14.1 Compositions and Properties

These steels contain not more than 0.25% carbon and a total content of alloying elements (not including Mn and Si) ranging from 0.85% to about 16%. Quenched and tempered steels are furnished in the heat-treated condition with yield strengths ranging from 50 to 150 ksi depending on chemical composition, thickness, and heat treatment. They have high strength in combination with good ductility. Various combinations of toughness, fatigue strength, and corrosion resistance can be developed to meet the requirements of pressure vessels for use in atmospheric conditions, at elevated temperature, or at cryogenic temperatures. Some Q&T steels fall within

the ASTM carbon steel classification, and others within the alloy steel classification. Typical Q&T plate steels are given in Table 11. A brief description of some of these Q&T steels is given next, and important sources on Q&T steels include Refs. 18, 43, and 86.

1. A517 alloy steel: Fifteen grades, quenched and tempered to yield strengths (minimum) of 90 ksi (more than 2.5 to 6 in) and 100 to 125 ksi (less than 2.5). Amounts of C, Mn, Si, and other minor alloying elements such as Ni, Cr, Mo, B, V, Ti, Zr, and Cu vary with grades.
2. A533 alloy steel: Four types, quenched and tempered to three tensile strength ranges, 80 to 100 ksi, 90 to 115 ksi, and 100 to 125 ksi. Composition: 0.50 Mo (Type A), 0.50 Mo + 0.55 Ni (Type B), 0.85 Ni (Type C), and 0.30 Ni (Type D). This steel, with a somewhat higher carbon content, has the least susceptibility to hot cracking because it has a high manganese to sulfur ratio, usually about 50 : 1. ASTM A533 Grade B steel is used in thick section for nuclear pressure vessels, and at its highest strength level (Class 3) it may be used for thin-walled or layered pressure vessels.
3. ASTM A537 (Class 2) carbon steel is used in pressure vessels where high notch toughness is required.
4. A542 Alloy steel: Five classes, quenched and tempered to tensile strengths (minimum) of 85 ksi, 95 ksi, 105 ksi, and 115 ksi. Two types of 2.25 Cr-1 Mo steels, one type of 3Cr-1Mo-0.25V-Ti-B steel.
5. A543 Alloy steel: Three classes, quenched and tempered to tensile strengths (minimum) of 90 ksi, 105 ksi, and 115 ksi. Two types of Ni-Cr-Mo steels.
6. A553 Alloy steel: Two types, quenched and tempered to 85 ksi yield strength (minimum).
7. ASTM A592 used as forgings where good notch toughness is needed in a steel having a yield strength of 100 ksi.

Table 11 Q&T Steel Plates, ASTM Specification

A203 Grade F	A542 Type A Cl. 1	A553 Type 1 (8% and 9% Ni steel)
	A542 Type A Cl. 2	
A517 (15 Grades)	A542 Type A Cl. 3	
	A542 Type A Cl. 4	A645 5% Ni steel
A533 Type A Cl. 1	A542 Type A Cl. 4a	
A533 Type A Cl. 2	A542 Type B Cl. 1	A724 Grade A
A533 Type A Cl. 3	A542 Type B Cl. 2	A724 Grade B
A533 Type B Cl. 1	A542 Type B Cl. 3	A724 Grade C
A533 Type B Cl. 2	A542 Type B Cl. 4	
A533 Type B Cl. 3	A542 Type B Cl. 4a	A734 HSLA Type A
A533 Type C Cl. 1	A542 Type C Cl. 1	A734 HSLA Type B
A533 Type C Cl. 2	A542 Type C Cl. 2	
A533 Type C Cl. 3	A542 Type C Cl. 3	A738 Grade A
A533 Type D Cl. 1	A542 Type C Cl. 4	A738 Grade B
A533 Type D Cl. 2	A542 Type C Cl. 4a	
A533 Type D Cl. 3		A782 Class 1
	A543 Type B Cl. 1	A782 Class 2
A537 Cl. 2	A543 Type B Cl. 2	A782 Class 3
	A543 Type B Cl. 3	
	A543 Type C Cl. 1	
	A543 Type C Cl. 2	
	A543 Type C Cl. 3	

Note: A543 Grade is: Q&T up to 4 in. A738 Grade A is N or Q&T up to 2.5 in; Q&T over 2-5 in.

14.2 Weldability

The carbon content of Q&T steels generally does not exceed 0.22% for good weldability. The alloying elements are carefully selected to ensure the most economically heat-treated steel with the desired properties and acceptable weldability. The development of good notch toughness in the HAZ of Q&T steels depends on the rapid dissipation of welding heat to permit the formation of martensite and bainite on cooling. This requirement may increase the susceptibility of the Q&T steel to hydrogen-induced cold cracking.

14.3 Joint Design

Appropriate joint design, good workmanship, and adequate inspection are needed to take advantage of the high strength of Q&T steels and to optimize the serviceability of weldments made from these steels. Weld joint design should avoid abrupt changes in sections to reduce stress concentrations, the welds must be located at sites where there is sufficient access for weld inspection, and fillet welds are preferred to butt welds. Joint preparation can usually be done by gas or arc cutting without preheating. Excessive weld reinforcement should be avoided.

14.4 Preheat

Preheat for welding Q&T steels must be used with caution because it reduces the cooling rate of the weld heat-affected zone. If the cooling rate is too slow, the reaustenized zone adjacent to weld metal can transform to ferrite with regions of high-carbon martensite or coarse bainite, with loss of strength and toughness.

14.3 Welding Processes

Welding processes such as SMAW, SAW, GMAW, FCAW, and GTAW can be used to join Q&T steels having minimum yield strength up to 150 ksi and carbon content up to 0.25%. Filler metal should be selected with care. Adopt low-hydrogen welding practices: use properly dried low hydrogen electrodes, clean and dry flux, moisture-free shielding gas, clean low-hydrogen electrode wire, etc.

14.4 Postweld Heat Treatment

The heat treatment for most of these steels consists of austenitizing, quenching, and tempering. A few are given a precipitation hardening (aging) treatment following hot rolling or a hardening treatment. Welded structures fabricated from these steels generally do not need further heat treatment except for a stress relief in special situations. Stress relief is necessary for these circumstances: (1) The steel has inadequate notch toughness after cold forming or welding, (2) to maintain dimensional stability after fabrication, and (3) the weldment with high residual stress is susceptible to stress corrosion cracking.

14.5 Stress Relief Cracking

The weldments of many quenched and low-alloy steels are susceptible to stress relief cracking (SRC), also known as reheat cracking (RC). Chromium, molybdenum, and vanadium contribute to this type of cracking, but other carbide-forming elements also contribute to stress relief cracking. Measures to overcome stress relief cracking have been discussed in the earlier section weldability consideration.

15 CHROMIUM-MOLYBDENUM STEELS

Chromium-molybdenum steels, also referred as creep-resistant low-alloy steels, are used for fabricating pressure vessels to be operated under high temperature and high pressure conditions. These steels contain varying amounts of chromium up to a nominal composition of 9%, and 0.5 or 1% molybdenum. The carbon content is normally less than 0.20% to achieve good weldability, but the alloys have high hardenability. The chromium provides improved oxidation and corrosion resistance and the molybdenum increases strength at elevated temperatures. These steels usually come from the steel manufacturer in the annealed, normalized and tempered, or quenched and tempered condition. The most popular grades of creep-resistant Cr-Mo steels are 0.5Cr-0.5Mo-0.25V, 1Cr-0.5Mo, and 1.25Cr-0.5Mo and 2.25Cr-1Mo (with or without vanadium). 1Cr-0.5Mo (Grade 11) and 2.25Cr-1Mo steel (Grade 22, Class 2) have long been used to fabricate heavy sections of pressure vessel and piping for fossil power, petroleum, and petrochemical applications. 2.25Cr-1Mo steel is frequently used for its superior hot strength; plates are covered by specification SA-387, Grade 22, Class 2, and forgings by specification SA-336, Grade F22. 5Cr-1Mo and 9Cr-1 Mo are widely used in the petrochemical industry for their superior corrosion and oxidation resistance.

15.1 Composition and Properties

ASTM specification A387, Grades 2, 5, 7, 9, 11, 12, 21, 22 and 91, cover plates, and ASTM A182 Grades F2, F5, F7, F9, F11, F12, F21, and F22 deal with forging. The nominal chemical compositions of certain grades of Cr-Mo steels are given in Table 12 and 13. Some alloys may contain small additions of columbium, titanium, or vanadium, or increased amounts of carbon

Table 12 Cr-Mo Steel Nominal Composition

Grade	Cr%	Mo%
2	0.50	0.50
12	1.00	0.50
11	1.25	0.50
22,22L	2.25	1.00
21,21L	3.00	1.00
5	5.00	0.50
7	7.00	0.50
9	9.00	1.00
91	9.00	1.00

Table 13 Composition of ASTM 387 Cr-Mo Steel Plate

Grade	Generic name	Composition (%)				
		C	Mn	Si	Cr	Mo
12	1.00Cr	0.05–0.17	0.40–0.65	0.15–0.40	0.80–1.15	0.45–0.60
11	1.25Cr	0.05–0.17	0.40–0.65	0.50–0.80	1.00–1.50	0.45–0.65
22	2.25Cr	0.05–0.15	0.30–0.60	0.50 max	2.00–2.50	0.90–1.10
5	5.00Cr	0.15 max	0.30–0.60	0.50 max	4.00–6.00	0.45–0.65
91	9.00Cr	0.06–0.15	0.30–0.60	0.50–1.00	8.00–10.00	0.90–1.10

or silicon for specific applications. The structure of the chromium-molybdenum steels is usually a ferrite/bainite. These steels are used in pressure vessels as plates, tubes, pipes, forgings, and castings. ASTM specifications for various product forms are shown in Table 14.

15.2 Applications

Chromium molybdenum steels are primarily used for service at elevated temperatures up to about 1300°F (704°C) in applications such as power plants and petroleum refineries, and in chemical industries for pressure vessels and piping systems. These alloys exhibit excellent resistance to refinery corrosives like sulfur, elevated temperature, and hydrogen attack. For improved corrosion resistance these alloys are often overlayed with stainless steel.

15.3 Creep Strength

The optimum creep strength is developed in chromium-molybdenum steels by tempering following normalizing or quenching. In the more highly alloyed steels, the tempering treatment results in the precipitation of fine particles of alloy carbide, which are very effective in produc-

Table 14 ASTM Specification for Chromium-Molybdenum Steel Product Forms [86]

Type	Forgings	Tubes	Pipe	Castings	Plate
0.5Cr-0.5Mo	A182-F2	A213-T2	A335-P2		A387-Gr2
			A369-FP2		
			A426-CP2		
1Cr-0.5Mo	A182-F12	A213-T12	A335-P12		A387-Gr12
	A336-F12		A369-FP12		
			A426-CP12		
1.25Cr-0.5Mo	A182-F11	A199-T11	A335-P11	A217-WC6	A387-Gr11
	A336-F11/F11A	A200-T11	A369-FP11	A356-Gr6	
	A541-C15	A213-T11	A426-CP11	A389-C23	
2Cr-0.5Mo		A199-T3b	A369-FP3b		
		A200-T3b			
		A213-T3b			
2.25Cr-1Mo	A182-F22/F22A	A199-T22	A335-P22	A217-WC9	A387-Gr22
	A336-F22/F22A	A200-T22	A369-FP22	A356-Gr10	A542
	A541-C16/6A	A213-T22	A426-CP22	A643-GrC	
3Cr-1Mo	A182-F21	A199-T21	A335-P21		A387-Gr21
	A336-F21/F21A	A200-T21	A369-FP21		
		A213-T21	A426-CP21		
5Cr-0.5Mo	A182-F5/F5a	A199-T5	A335-P5	A217-C5	A387-Gr5
	A336-F5/F5A	A200-T5	A369-FP5		
	A473-501/502	A213-T5	A426-CP5		
5Cr-0.5Mo-Si		A213-T5b	A335-P5b		
			A426-CP5b		
5Cr-0.5Mo-Ti		A213-T5c	A335 P5c		
7Cr-0.5Mo	A182-F7	A199-T7	A335-P7		A387-Gr7
	A473-501A	A200-T7	A369-FP7		
		A213-T7	A426CP7		
9Cr-1Mo	A182-F9	A199-T9	A335-P9	A217-C12	A387-Gr9
	A336-F9	A200-T9	A369-FP9		
	A473-501B	A213-T9	A426-CP9		

ing good creep strength. It should be noted, however, that there is usually a corresponding decrease in the fracture toughness. A further increase in creep strength is achieved by the addition of vanadium to give normal compositions such as 1Cr-0.5Mo-0.25V and 0.5Cr-0.5Mo-0.25V. The presence of a fine dispersion of V carbides makes the steels more stable than other chromium and molybdenum carbides. Like other grades, vanadium is added to 2.25Cr-1Mo steel to improve creep strength.

15.4 Welding Metallurgy

Cr-Mo steels are weldable, but they require a higher degree of welding design and control than low-carbon steel. The primary difference is the air hardenability of alloy steels. These steels are susceptible to cracking from inadequate ductility. Such types of cracking include lamellar tearing, hot cracking, and reheat or stress relief cracking. The welding procedures must incorporate low-hydrogen welding practices to prevent hydrogen-induced cracking in the weld metal and in the HAZ. They are welded in various heat-treated conditions: annealed, normalized and tempered, or quenched and tempered. Welded joints are often heat-treated prior to use to improve ductility and toughness and reduce welding stresses.

Joint Design

Joint design should provide adequate room for electrode manipulation to ensure root bead penetration and subsequent ease of slag removal. The joint geometry should minimize any notch conditions that act as stress raisers. Sharp corners and rapid changes in section size are to be avoided.

Joint Preparation

Joint edges can be prepared by shearing, machining, grinding, gas cutting, or arc cutting. Before welding, surface irregularities that act as stress raisers must be ground out. Surface contaminations and other foreign materials must be removed. Tenacious chromium oxides that form during thermal cutting and heating and that melt at higher temperatures than the base metal and scale should also be removed by suitable means.

Preheating

Preheating is extremely important when welding air hardening Cr-Mo steels. Preheating is required to prevent hardening and cracking. Preheating reduces stresses, limit or temper martensitic areas, and reduce the amount of hydrogen retained in the weld. A weld without preheat or even a small arc strike will cause localized hard spots that can initiate solidification or delayed cracking. Holding the joint at a postheat temperature (equal to the preheat temperature) after the weld is completed allows hydrogen to diffuse out of the weld.

Welding Processes

Most fusion welding processes can be applied for joining Cr-Mo steels. Typical welding processes include SMAW, GTAW, PAW, SAW, Electroslag welding, GMAW and FCAW.

Filler Metal

The filler metal composition should be nearly the same as that of the base metal, except for carbon content to obtain uniform strength and resistance to heat and corrosion. The carbon content of the filler metal is usually lower than that of the base metal. A matching carbon content is required when the weldment is to be quenched and tempered or normalized and tempered.

15.5 Temper Embrittlement Susceptibility

Cr-Mo steels, especially 2.25Cr-1Mo steels, are susceptible to temper embrittlement, a condition caused by long-term, elevated-temperature exposure in the 370 to 560°C (700 to 1050°F) range, associated with the presence of impurity elements, such as phosphorous, tin, antimony, and arsenic [88–90]. The phenomenon results in the progressive reduction of the notch toughness of the material as embrittlement develops. In other words, due to embrittlement, steels ductile at room temperature tend to become brittle during service. This phenomenon is shown schematically in Fig. 16a. Temper embrittlement susceptibility of 2.25Cr-1Mo steel is very high among Cr-Mo steels and ranks next to (but almost equal to) that of 3Cr-1Mo steel [91]. It has been established that higher silicon and manganese levels will have an even greater effect on toughness degradation.

Requirements for resistance against temper embrittlement and low-temperature toughness are becoming severer recently, especially for the Cr-Mo steel to be used for fabricating the pressure vessels, particularly in the petroleum industry, since it indicates that the potential for brittle fracture increases with service time in the critical temperature range. The resulting implication is that certain units may become susceptible to brittle failure during startup or shutdown without any warning [92].

Temper embrittlement of all 2.25Cr-1Mo plates, forgings, and weld metal can be minimized by ordering all material to chemical specifications that limit the elements that cause temper embrittlement. All materials can also be subjected to special temper embrittlement testing prior to being used in the vessel. Modern steel-making practices produce steels of sufficiently high purity that temper embrittlement can be virtually eliminated. Temper embrittlement resistance is often specified by various factors which combine the effect of these and other elements. Two of these factors, Watanabe number or J factor and $\bar{X}$ factor, for 2.25Cr-1Mo can be specified [95]:

$$J = (\%Si + \%Mn)(\%P + \%Sn) \times 10^4 \quad \text{(weight\%)}$$

$$\bar{X} = \frac{(10P + 5Sb + 4Sn + As)}{100} \quad \text{(all elements in ppm)}$$

The other known contributors to temper embrittlement, arsenic and antimony, are less effective in 2.5Cr-1Mo steel when they are controlled under 0.020 and 0.004% respectively [91].

Good resistance to temper embrittlement is generally obtained with a J factor below 200

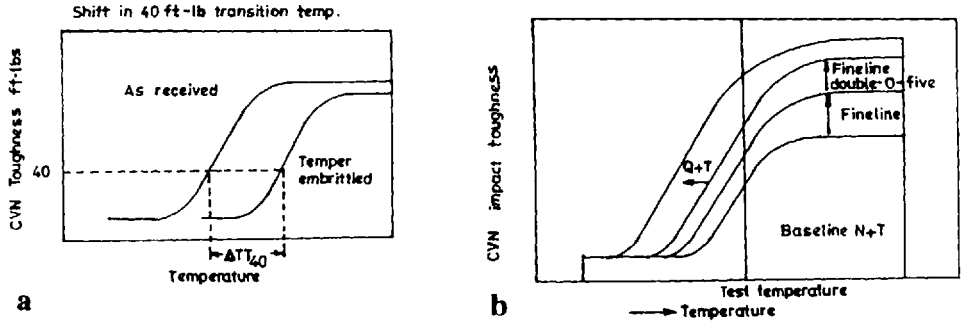


Figure 16 Temper embrittlement susceptibility of Cr–Mo steel. (a) Shift in the DBT curve shows the effect of temper embrittlement on toughness. (b) DBT curves show the effects of various processing techniques on CVN. (From Ref. 95.)

[93], most recent specifications require a J factor less than 150 [88], but there is appreciable scatter in the correlation between the J factor and the shift in the 54-J (40 ft-lb) CVN transition temperature for individual heats [94]. The attainable maximum levels of J and $\bar{X}$ for Grades 12, 11, and 22 are given in Table 15 [95].

Temper embrittlement is measured by testing the notch toughness of the material before and after a slow cooling cycle from 595 to 315°C. The shift in an energy transition temperature usually the 54-J transition is the measure of embrittlement.

Modern ASTM A387 steels are most often fine grain, low silicon, low sulfur, calcium treated for inclusion shape control, and occasionally quenched and tempered to provide the highest possible toughness levels (Fig. 16b). The resulting changes in chemistry over the past 15 years include the general reductions in silicon content from 0.25 to 0.1%, in sulfur from 0.02 to 0.002%, and in phosphorus from 0.015 to 0.005%. The finer grain sizes have allowed a shift in the typical ductile-to-brittle transition (DBT) curve toward lower temperatures [90]. It can be stated with reasonable confidence that quenched and tempered 2.25Cr-1Mo plate should not experience rapid embrittlement in vessels operating at or below 400°C (750°F) [92].

15.6 Step-Cooling Heat Treatment

Some specifications additionally require a step-cooled simulation treatment, which is an accelerated embrittling treatment used to predict temper embrittlement susceptibility in a relatively short test period. Manufacturers will perform this laboratory step-cooling treatment and meet commonly specified shifts in the 40 ft-lb CVN transition temperature (TT).

15.7 CVN Impact Properties

Improved Charpy V-notch properties can be met for A387 steels with Fineline Processing (0.010 % or 0.005 % maximum sulfur, vacuum degassed, with calcium treatment for inclusion shape control). When thick plates are specified with high CVN toughness requirements, a quenching and tempering heat treatment may be required. Multiple austenizations may also be utilized for increased toughness.

15.8 Temper Embrittlement of Weld Metal

Correlation of the J factor with the temper embrittlement of weld metal is poor. This is probably due to significantly different chemical composition and microstructure of weld metal compared to the wrought product. Therefore, the susceptibility of the weld metal to temper embrittlement is frequently determined by a direct measurement of CVN impact toughness using the equation [94]:

$$vTr40 + 1.5\,\Delta vTr40 < 100°F$$

Table 15 Available Maximum Levels for J and X [95]

Grade	J Factor	$\bar{X}$ Factor
12	110	12
11	150–180	12
22	90	14

where vTr40 is the transition temperature for embrittlement weld metal, and ΔvTr40 is the change in transition temperature for weld metal that has been step-cooled to cause temper embrittlement.

Control of Temper Embrittlement of Weld Metal

Control of temper embrittlement in weld metal of 2.25Cr-1Mo is considerably more difficult than with plate and forgings. Higher silicon and manganese contents are necessary to sound weld metal. Basic fluxes generally provide the minimum susceptibility to temper embrittlement consistent with high-temperature strength requirements [88,96]. The other factors that may affect the low temperature toughness and temper embrittlement are discussed next [88,96]:

1 It is well known that reduction of grain size is effective for improving the low-temperature toughness of the weld metal. Addition of nitrogen results in reduction in grain size, which in turn improves low-temperature toughness.
2. It is known that reduction of oxygen content in weld metal leads to improved toughness. C, Si, Mn, and Ti are generally used as the deoxidants. Be cautious because extremely low oxygen content can cause a reduction in toughness.
3. Control of chemical compositions and impurities in the weld metal. The influencing elements are phosphorus, arsenic, antimony, and tin. In the case of manganese, the recommended range for the weld metal is 0.7–1.0% Mn.
4. The best temperature range for the PWHT is 1250–1300°F (677–704°C). The CVN values can be improved by prolonging the time of PWHT.

15.9 Postweld Heat Treatment (Stress Relief)

ASME boiler and pressure vessel code requires postweld heat treatment, or stress relieving, primarily to soften the HAZ, minimizing the presence of hard zones and stabilizing its microstructure. Otherwise, hydrogen attack or creep embrittlement could occur in service. Various stress-relieving requirements are specified by end users and fabricators of A387 grade steels. Some specifications have increased the stress-relieving temperatures and hold times for these steels because of the interest in stabilizing the microstructure of the heat-affected zones after fabrication and accounting for possible weld repairs of the vessels while in service. However, as stress-relieving temperatures and times are increased, the capability of the chemical composition of each grade of steel to achieve the tensile requirements of the specification using a normalized and tempering heat treatment is limited [95]. It is found that there is deleterious influence of extensive stress relief treatments on CVN toughness levels.

Larson–Miller Tempering Parameter

The Larson–Miller parameter is usually employed to obtain some idea of the change in a given property of a material during a heat-treatment process performed at different temperatures and with different holding times [8,96]. It is widely used because of its usefulness in summarizing the heat-treating characteristics of low-alloy steels and in estimating their long-time strengths at given temperatures [18].

Cr-Mo steel has a hardened structure in the as-welded condition. This is given postweld heat treatment for changing it to a softened structure (tempered bainite) before use. By softening the structure, the toughness recovers gradually, but the heat-treatment parameter commonly known as the Larson–Miller parameter $P = T(20 + \log t)$, where T is the absolute temperature in Kelvin (°K) and t is heat-treatment time in hours, becomes large. Excessive increase in this parameter causes reduction in the toughness. Therefore, it is necessary to carefully examine the heat-treatment conditions.

15.10 Reheat Cracking in Cr-Mo and Cr-Mo-V Steels

Phosphorus and sulfur were found to enhance the reheat cracking (RC) susceptibility of Cr-Mo steels. For a particular alloy, there exists a critical phosphorus content below which embrittlement will not take place. Measures such as (1) reduction of P and S, (2) addition of a small quantity of titanium (0.07%), which decreases the RC susceptibility due to phosphorus effects, and (3) the addition of calcium or rare earth metals, in accordance with sulfur, improve resistance to reheat cracking.

15.11 Modified 9Cr-1Mo Steel

Small additions of niobium (0.06–0.10%) and vanadium (0.18–0.25%) to the standard 9Cr-1Mo elevated-temperature steel result in a steel that is stronger and more ductile. This new steel exhibits improved long-term creep properties, lower thermal expansion, higher thermal conductivity, and better resistance to stress corrosion cracking [97]. Proposed applications for the modified 9Cr-1mo steel include boilers, reaction vessels, breeder reactor systems, pressure vessels for coal liquefaction and gasification , oil refining hydrotreating equipment, and geothermal energy systems.

15.12 Advanced 3Cr-Mo-Ni Steels

Advanced 3Cr-Mo-Ni steels have been developed for use in thick-section pressure vessels, specifically for coal liquefaction and gasification, by minor alloy modifications to commercial 2.25Cr-1Mo (ASTM A387, Grade 22, Class 2 steel) [98]. Specifically, the new alloy shows improved hardenability (i.e., fully bainitic microstructures following normalizing of 400-mm plates), enhanced strength, superior hydrogen attack resistance, and better Charpy V-notch impact toughness, with comparable ductility, creep rupture resistance, and temper embrittlement resistance.

16 STAINLESS STEELS

Stainless steels (SS) are those alloy steels that have a normal chromium content of not less than 12%, with or without other alloy additions. Stainless steels are more resistant to rusting and staining than plain carbon steel and low-alloy steels. They have superior corrosion resistance because of relatively high contents of chromium. These metals are available in both wrought and cast forms.

16.1 Classification and Designation of Stainless Steels

Stainless steel (SS) may be classified in five families, according to metallurgical structure:

1. Martensitic SS.
2. Austenitic SS.
3. Ferritic SS.
4. Duplex SS.
5. Precipitation hardening (PH) SS.

The first four groups are characterized by the predominant metallurgical phase present when the stainless steel is placed in service. In iron and steel, the body-centered cubic lattice is called ferrite and the face-centered cubic lattice is austenite, so the steels are described as ferritic or austenitic depending on their major structural constituent. As the name implies, duplex stainless steel consists of both austenite and ferrite phases in 50 : 50 proportion. The

fifth group contains those stainless steels that can be strengthened by an aging heat treatment. This steel is generally not used in heat exchanger applications. Therefore it is not covered here.

Designations

Wrought stainless steels are assigned designations by the American Iron and Steel Institute (AISI) according to composition: the Cr-Ni-Mn austenitic stainless steels as 2xx series, and the Cr-Ni austenitic stainless steels as 3xx series and 4xx series. The precipitation hardening grades are assigned designations based on their Cr and Ni contents.

ASTM Specification for Stainless Steels

Most of the AISI types—austenitic, duplex, ferritic, and martensitic stainless steels, plus some special stainless like superferritic and superaustenitic steels—are included in A240.

Guidance for Stainless Steel Selection

Guidelines for selection of the types of available stainless steels are discussed by Brown [99] and DeBold [100]. According to Brown, the following guidelines will serve to select a proper grade for the service under consideration:

Select the level of corrosion resistance required for the application.
Select the level of strength required.
For special fabrication problems, select one of the basic alloy modifications that provides the best fabrication characteristics.
Do a cost-benefit analysis to include the initial raw material price, cost of installation, and the effective life expectancy of the finished product.
Determine the availability of the raw material at the most economical and practical choice.

DeBold [100] discusses the approach to select stainless steels to meet corrosion resistance and strength.

16.2 Martensitic Stainless Steel

The martensitic stainless steels are on the lower scale of corrosion resistance, because they contain only 11–18% Cr, with carbon content usually less than 0.4%. The lower limit on chromium is governed by corrosion resistance, and the upper limit by the requirement for the alloy to convert fully to austenite on heat treatment [101]. The key feature of this family is that it can be hardened by heat treatment. Its utility as heat exchanger material in aqueous environments is limited. But these steels do exhibit a useful combination of strength, ductility, toughness, and corrosion resistance in mild environments. Resistance to corrosion is obtained only when the material is fully hardened and tempered [102]. AISI 410 is the most widely used of the martensitic grades. It is occasionally used in heat exchangers.

16.3 Austenitic Stainless Steel Properties and Metallurgy

Austenitic stainless steels make up approximately 80–90% of the stainless steels in use today [103]. The common austenitic stainless steels type 300 series are low carbon, iron, and chromium alloys sufficiently alloyed with nickel and sometimes manganese or nitrogen, or combinations of these elements, to have an austenitic structure, most or all of it when the steel is cooled rapidly to room temperature. The chromium content is between 15 and 32%, nickel between 8 and 37%, and carbon is restricted to a maximum of 0.03%. Chromium provides oxidation resistance and resistance to corrosion in certain media. An important source book on stainless steels is Llewellyn [104].

Types of Austenitic Stainless Steel

The conventional types of 3xx stainless steel include types such as 304, 304L, 309, 310, 316, 316L, 321, 347, and 348. The basic alloy Type 304 stainless steel contains 18% chromium and 8% nickel. It has moderate strength, excellent toughness, and moderate corrosion resistance. Additional resistance to chloride pitting was achieved by the addition of Mo, creating Types 316 and 317. Types 316 (18% Cr, 12% Ni, 2.5% Mo) and 317 (18% Cr, 15% Ni, 3.5% Mo) have greater resistance to corrosion in chloride environments than Type 304.

Alloy Development

The 18Cr-8Ni austenitic stainless steels have been successfully used in fresh water and mildly corrosive industrial conditions for more than 50 years. The corrosion resistance, weldability, and strength of the austenitic family of alloys have been constantly improved for more demanding industrial applications by changing the basic chemical composition [105]. Such features include:

1. Molybdenum is added to enhance corrosion resistance in chloride environments, such as, AISI Types 316 and 317. These steels possess a greatly increased resistance to chemical attack as compared to that of the basic Cr-Ni Type 304.
2. Low-carbon steels (Types 304L, 316L, and 317L) are resistant to carbide precipitation in the 800–1600°F range and can thus undergo normal welding without reduction in corrosion resistance. These steels are generally recommended for use below 800°F.
3. Nitrogen is added to compensate for the reduced strength of the low-carbon-grade steels (L grades); it increases strength at all temperatures—cryogenic through elevated—improves localized corrosion resistance in acid chloride solutions, and improves pitting resistance and phase stability. Nitrogen addition also improves passivation characteristics, and enhances the effects of other alloy elements additions, particularly, Cr and Mo, that add corrosion resistance [106]. Nitrogen addition may be of the order of 0.1 to 0.25%. Maximum nitrogen content in austenitic stainless steels is typically restricted to 0.25% by weight to avoid problems such as ingot porosity, hot workability, and nitride precipitation that are associated with excess nitrogen content. Nitrogen addition is denoted by the suffix N.
4. Chromium is increased to enhance pitting and crevice corrosion resistance.
5. Nickel is added to stabilize the austenitic microstructure and to improve resistance to stress corrosion cracking as well as general corrosion in reducing environments. The effect of nickel on SCC of stainless steels is explained by the Copson curve.
6. Stabilized grades: The addition of titanium and niobium forms stable carbides, which prevents chromium depletion by the formation of complex chromium carbides, thereby avoiding sensitization of weldments or heat-treated parts; examples are Type 321 (Ti stabilized) and Type 347 (Nb stabilized).
7. LR stands for low residuals, and in this case the restrictions are on carbon for corrosion resistance. Reducing the carbon also allows the Nb to be reduced and so minimizes the risk of Nb-rich interdendritic films. There is also restriction on Si, S, and P for liquation cracking resistance. Manganese is usually raised to improve resistance to solidification cracking.

Stainless Steel for Heat Exchanger Applications

Austenitic stainless steels are used primarily because of their low cost, corrosion resistance, and good mechanical properties over a broad temperature range from cryogenics to high temperature. They have been applied successfully in a large variety of environments including acids, fresh water, and seawater. On the other hand, the martensitic and ferritic stainless steels

have acquired a more restricted field of application due to low toughness at room temperature. Factors that favor austanitic stainless steels selection as heat exchanger material include the following [107,108]:

High resistance to uniform corrosion, such as erosion corrosion.
Resistance to high-pH solutions.
Resistance to oxidation and sulfidation.
Suitability for intended fabrication techniques.
Can be easily maintained and cleaned to remove fouling deposits by most of the chemical and mechanical means without damage.
Compatible with other materials commonly used for fabrication of heat exchangers.
Stability of properties in service.
Generally compatible with the process fluids.
Toughness at cryogenic temperature and strength at elevated temperatures.
Resistance to galling and seizing.
Moderate thermal conductivity.
Dimensional stability.

Newer Stainless Steels for Heat-Exchanger Service. New steel making technologies like argon-oxygen deoxidation (AOD) and vacuum induction melting (VIM) in the last two decades have introduced a variety of new grades of ferritic, austenitic, and duplex stainless steel with low impurity elements, and a wide range of alloying elements tailored to the requirements of specific applications.

Against these good properties, the following are the demerits of stainless steels [109]:

1. Sensitive to crevice corrosion under deposits.
2. Sensitive to pitting corrosion and stress corrosion cracking in the presence of chloride ions if temperature exceeds 50°C.
3. Sensitization leads to intergranular corrosion.
4. Sensitive to fouling.

Properties of Austenitic Stainless Steels

Stainless steels are known for excellent fabricability, weldability, good mechanical properties (strength, toughness, and ductility) over a broad temperature range, and corrosion resistance in many environments. Other relevant properties are lower melting points, higher electrical resistance, lower thermal conductivity, and higher coefficients of thermal expansion than carbon steels.

Mechanical Properties at Cryogenic Temperature and Elevated Temperature. Although, austenitic stainless steels are used primarily because of their high corrosion resistance, they also possess excellent mechanical properties over a wide range of temperature from cryogenic to elevated temperature.

Cryogenic Applications. Unlike ferritic materials, austenitic stainless steels do not exhibit ductile-to-brittle transition. They maintain a high level of toughness at cryogenic temperatures. Austenitic stainless steels types such as 304, 304L, 316, 316L, and 347 are used in cryogenic applications for liquid gas storage and transportation vessels.

Elevated Temperature Strength. Austenitic stainless steels exhibit good creep rupture strength at temperatures up to 600°C. If still higher creep strength and elevated temperature strength are required, addition of V, Nb, and Ti is necessary. Addition of these elements can lead to an increase in strength, but also a reduction in the low-temperature toughness. Stainless steels also exhibit high-temperature oxidation resistance due to the oxide layer formed on the surface.

Alloying Elements and Microstructure

The microstructures most important in weldable stainless steels are ferrite and austenite. Although chromium and nickel are the principal alloying elements in austenitic stainless steels, other elements are added to meet specific requirements and therefore consideration must be given to their effects on microstructure. Molybdenum, columbium, and titanium promote the formation of delta ferrite in the austenitic matrix and also form carbides similar to that of chromium. These elements are known as ferrite-forming elements. On the other hand, copper, manganese, cobalt, carbon, and nitrogen have a similar effect to nickel and promote the formation of austenite. These elements are known as austenite-forming elements.

Composition of Wrought Alloys. The compositions of typical wrought austenitic stainless steels are given in Table 16. There are several variations for some of those listed.

Alloy Types and Their Applications

The workhorse materials for the process industries are Types 304, 304L, 316, and 347. Stainless steel is used as a heat-exchanger material for condensers, feedwater heaters and other heat exchangers, and has wide use in refineries, chemical process industries, fertilizer industries, pulp and paper industries, food processing industries, etc. The properties and their usage of AISI Types 304, 310, 316, 321, and 347 are discussed next.

Type 304. Type 304 (18Cr-8Ni) is the most popular grade in the series and is used in a wide variety of applications that require a good combination of corrosion resistance and formability. Its homogeneous structure, high ductility, and excellent strength ensure excellent performance in cold forming, deep drawing, and spinning. It is nonmagnetic in the annealed condition. Its excellent toughness at low temperature is utilized for the construction of cryogenic vessels. It is particularly well suited for applications where welded construction is required and where the finished product must resist the more severe forms of corrosion. The lighter sections can be welded with little trouble from carbide precipitation or loss of corrosion resistance. Hence, for this reason, postweld heat treatment is not necessary in most cases.

Type 304 is highly resistant to ordinary rusting and immune to foods, most of the organic chemicals, dyes, and a wide range of inorganic chemicals. It has excellent corrosion resistance in oxidizing solutions. It resists nitric acid very well but sulfuric acid only moderately and halogen acids poorly. For best results it is recommended to passivate this grade of stainless

Table 16 Composition of Typical Wrought Austenitic Stainless Steels

Grade	C (max)	Mn (max)	P (max)	S (max)	Si (max)	Cr	Ni	Mo	Other elements
304	0.08	2.0	0.045	0.03	1.0	18.0–20.0	8.0–12.0	—	
304L	0.03	2.0	0.045	0.03	1.0	18.0–20.0	8.0–12.0		
316	0.08	2.0	0.045	0.03	1.0	16.0–18.0	10.0–14.0	2.0–3.0	
316L	0.03	2.0	0.045	0.03	1.0	16.0–18.0	10.0–14.0	2.0–3.0	
317	0.08	2.0	0.045	0.03	1.0	18.0–20.0	11.0–15.0	3.0–4.0	
317L	0.03	2.0	0.045	0.03	1.0	18.0–20.0	11.0–15.0	3.0–4.0	
321	0.08	2.0	0.045	0.03	1.0	17.0–19.0	9.0–12.0		Ti = 5C min (0.70 max)
347	0.08	2.0	0.045	0.03	1.0	17.0–19.0	9.0–13.0		Nb + Ta = 10C min (1.10 max)
348	0.08	2.0	0.045	0.03	1.0	17.0–19.0	9.0–13.0		Nb + Ta = 10C min (1.10 max)

steel to retain its corrosion resistance. It resists scaling up to 1600°F. For intermittent heating and cooling applications, temperatures should not exceed 1500°F. The maximum temperature for continuous service is 1650°F [110].

Type 310. Type 310 (25Cr-20Ni) represents the most highly alloyed composition in the popular range of austenitic stainless steels and exhibits the greatest resistance to corrosion and oxidation.

Type 316. The addition of molybdenum gives this grade the highest resistance to pitting corrosion of any of the chromium-nickel grades, which makes this grade particularly suitable for applications involving severe chloride corrosion. Therefore, alloys 316 and 316L are "workhorse" materials in both the chemical industries and pulp and paper industries [111]. Type 316 has excellent resistance to sulfates, chlorides, phosphates, and other salts. Nevertheless, the resistance of Types 316 and 316L to pitting and crevice corrosion is often not high enough, particularly in stagnant or slow-moving seawater (<1.5 m/s). for this reason, in the last two decades, several more highly alloyed grades have been developed. They are known as superferritic, duplex, superaustenitic stainless steels.

Type 316 is used for applications requiring high strength and creep resistance at elevated temperatures. Its molybdenum content provides higher creep strength than Type 304. Type 316 has excellent resistance to oxidation and has a low rate of scaling in ordinary atmosphere at temperatures up to 1650°F in continuous service and 1500°F when used intermittently (110). It can be welded without difficulty and usually does not require subsequent heat treatment. This steel is used for applications requiring high strength and creep resistance at the elevated temperatures. Its molybdenum content provides several times the resistance to creep that is available with Type 304. This grade is used for chemical and pulp handling equipment, and photograpic and food processing equipment.

Because of their freedom from chromium carbide precipitation and intergranular attack, Type 321 (18%Cr, 10.5%Ni, Ti), Type 347 (18%Cr, 11% Ni, Nb), and Type 348 (18%Cr, 11% Ni, Nb) are often referred to as stabilized stainless steels.

16.4 Mechanism of Corrosion Resistance

Stainless steels owe their corrosion resistance to a relatively thin passive surface film that provides a physical barrier between the steel and the service environment. This layer, only 20-30 angstroms thick, of hydrated chromium oxide (Cr_2O_3), is extremely adherent and resistant to chemical attack [15]. The passive films are formed on the surface interacting with the environment, essentially containing O_2 or oxidizing conditions. If the passive film is damaged by abrasion or scratching, a healing process or repassivation occurs almost immediately in the presence of oxygen. On the other hand, stainless steel will show rapid corrosion attack in reducing conditions or under crevices or local deposits, which produce an O_2 depleted zone [16].

Another reason for loss in corrosion resistance of stainless steels is the formation of oxide films on the surface due to bad cleaning after heat treatment. The oxide film is different from passive film. Cleaning of heat-treated components should be done in an inert solution to avoid the formation of oxide films, which render the SS susceptible to various forms of corrosion [107].

Sigma Phase. Sigma phase, an intermetallic compound, in stainless steels may significantly reduce their ductility and toughness, and renders stainless steel susceptible to stress corrosion cracking and other forms of corrosion.

The sigma phase is one cause of low ductility creep failure of certain austenitic welds[112]. When cooling a weld metal from 1800 to 1000°F, the rate of cooling must be

relatively rapid to avoid the formation of a sigma phase. Avoidance of prolonged time in this temperature range will usually result in a weld metal containing very small amounts of sigma phase, which is generally harmless. Like sensitization, precipitation of intermetallic phases can be corrected by solution annealing. In newer varieties of austenitic stainless steels, namely, superaustenitics, alloying with nitrogen retards sigma-phase formation and allows for the production of thicker plates [113].

Passive Versus Active Behavior. In most natural environments, stainless steel will remain in a passive state. When exposed to conditions that remove the passive film, stainless steels are subject to the active state. Change to an active state usually occurs when chloride concentrations are high, as in seawaters or in reducing solutions, or when there is oxygen starvation. Oxygen starvation occurs when there is no free access to oxygen, such as in crevices and beneath deposits.

Resistance to Chemicals. Stainless steel alloys have excellent resistance to nitric acid, particularly to all concentrations and temperatures. Type 304 is most widely used in nitric acid plants. To handle sulfuric acid without inhibitors, Type 316 stainless steel has limited application.

Stainless Steel in Seawater. While Type 304 (18Cr-8Ni) alloys have been satisfactorily used in fresh water, the Mo-containing Type 316 is preferred in saltwater. Variable results have been obtained with Type 316 in seawater. In the case of seawater-cooled condenser tubes, satisfactory use was obtained where tubes were cleaned regularly in service to prevent fouling. However, the alloy content of Type 316 was found to be too lean to prevent pitting and crevice corrosion in stagnant seawater. This is because of the breakdown of the passive film by the chloride ions in the seawater under stagnant/low velocity conditions.

Resistance to Various Forms of Corrosion. In general, the corrosion and oxidation resistance of stainless steels increases with chromium content, and the materials are used in a wide range of aggressive media in the chemical and process industries. They are resistant to uniform corrosion, erosion and erosion-corrosion, and high-pH solution [109]. However, under certain conditions, stainless steel are attacked by localized corrosion forms.

Galvanic Corrosion. Consideration should be given to when stainless steel is connected to a more noble metal. However, if the stainless steel is passive in the environment, galvanic corrosion may not take place. The most important aspect for the prevention of galvanic corrosion of stainless steel is to select the weldments and fasteners of adequate corrosion resistance in the bulk of the material and/or possessing larger exposed area.

Localized Forms of Corrosion. Under certain conditions, stainless steels are susceptible to highly localized forms of corrosion. For stainless steels, almost 60% of equipment failures in the chemical process industries are due to (1) pitting corrosion, (2) crevice corrosion, and (3) stress corrosion cracking (SCC) [114]. Additionally, they also fail by intergranular corrosion. Operating parameters and environmental factors such as pH, temperature, and chloride and oxygen levels greatly affect alloy performance. Various forms of SS localized corrosion are discussed next.

Pitting Corrosion. The corrosion resistance of stainless steels relies on the stability and the maintenance of continuity of passive films on the exposed surfaces. The stability of the passive film to resist pitting initiation is controlled mainly by chromium and molybdenum contents in stainless steels. Another element that improves resistance to pitting and crevice corrosion is nitrogen [100,115]. Nitrogen addition is considerably cheaper than molybdenum steels. The breakdown of the passive films takes place due to imperfections in the films, mechanical damages, inhomogeneities in the metal surface such as inclusions or surface scale,

precipitates, second phases, and the presence of chloride ions in the environment [116]. High chloride levels locally break down the passive film, as well as provide a good conductor that promotes corrosion [117]. The severity of attack is related to the chloride content and the acidity, pH, and presence of oxygen and oxidizers [114]. Welding-related factors/defects such as inclusions, secondary phases, compositional differences within the same phase, sensitization, arc strikes, spatter, and local inhomogeneities in the base material act as potential sites where pitting can initiate [118,119]. In terms of microstructure, MnS inclusions are important sites for pit initiation. Other features such as delta ferrite and sigma phase can also promote pitting corrosion.

Pitting Index. The resistance to pitting increases with chromium content, but major benefit is obtained from the addition of molybdenum in stainless steel, such as Type 316 (18% Cr, 12% Ni, 2.5% Mo). The addition of nitrogen is also beneficial, and the combined effects of chromium, nitrogen, plus molybdenum are used as a measure of potential pitting resistance of stainless steels, often expressed in terms of a pitting index number, PRE_N: Pitting index or $PRE_N = Cr\% + 3.3\ Mo\% + 16\ N\%$

Critical Pitting Corrosion Temperature. In addition to the surface condition and the presence of deposits, chloride ions, pitting initiation is also influenced by the environment temperature. For a given grade of stainless steel, there is a single temperature, or a very narrow range of temperature, of an environment at which pitting is first observed, known as the *critical pitting temperature* (CPT). It is therefore possible to select a grade that will not be subject to pitting attack if the environment temperatures do not exceed the critical levels [107]. CPT can be also used to rate the relative performance of various alloys. CPT values have been determined in according to practice ASTM G 48A [120] in ferric chloride (10% $FeCl_3 \cdot 6H_2O$) and in an acidic mixture of chlorides and sulfates [4% NaCl + 1% $Fe_2(SO_4)_3$ + 0.01 *M* HCl]. CPT values have been determined in 10% $FeCl_3 \cdot 6H_2O$ by Garner [121] and in 4% NaCl + 1% $Fe_2(SO_4)_3$ + 0.01 *M* HCl by Bandy et al. [122]. However, laboratory tests on pitting behavior are now more generally based on electrochemical techniques. The ranking of various metals according to pitting resistance number and critical pitting temperature is given in Table 17 [105].

Resistance to pitting corrosion is achieved by steel grades with higher chromium and molybdenum contents, such as austenitic stainless steel in the progression of levels of Types 304, 316, and 317. Otherwise, use alternate materials such as nickel-base alloys (e.g., Inconel alloy 625, Hastealloy and G-3); certain proprietary steels like 317 LM, Jessop 700, and Alloy AL-6X; and titanium, copper-nickel, and nickel-copper alloys.

Table 17 Pitting Resistance Number and Critical Crevice Corrosion Temperature [105]

Alloy	Composition (Wt.%) Cr-Mo-N	PRE_N[a]	CPT,[b] °F (°C)	CPT,[c] °F (°C)
Type 304	18-0-0.6	19.8	—	—
Type 316	16.5-2.1-0.05	24.9	59 (15.0)	
Type 317	18.5-3.1-0.06	30.5	66 (18.9)	77 (25)
904L	20.5-4.5-0.05	36.9	104 (40.0)	113 (45)
AL-6XN	20.5-6.3-0.23	47.9	177 (80.5)	172 (78)

[a] $PRE_N = Cr + 3.3Mo + 30N$.
[b] Based on ASTM G-48A (6% $FeCl_3$ for 72 h).
[c] Test solution: 4% NaCl + 1% $Fe_2(SO_4)_3$ + 0.01*M* HCl.

Crevice Corrosion. Crevices due to metal-to-metal joint, gasket, and fouling deposits, which tend to restrict oxygen access, result in crevice corrosion. For austenitic stainless steels, numerous factors affect both crevice corrosion initiation and propagation and include the following [123]:

1. Geometrical factors: crevice type (metal-to-metal, nonmetal-to-metal), crevice gap and depth, exterior to interior surface area ratio.
2. Environmental factors: oxygen content, pH, chloride level, temperature, agitation, diffusion and convection, crevice solution, biological influences.
3. Electrochemical reactions: metal dissolution, oxygen reduction, hydrogen evolution.
4. Metallurgical factors: alloy composition impurities, passive film characteristics.

Although it is unlikely that one can avoid design crevices, the problem can be minimized by maintaining uniform flow velocity in the bulk of the heat exchanger and using higher chromium and molybdenum grades, which are more resistant to crevice corrosion. Austenitic stainless steel grades with higher Mo contents, like 316L, 904L, and 254 SMO, ferritic grades like 18Cr-2Mo, and duplex steel like 2205 exhibit resistance to crevice attack.

Critical Crevice Corrosion Temperature. For a particular grade of stainless steel, crevice corrosion is also influenced by the temperature of the environment. Above a critical temperature, crevice corrosion will initiate, and below this it will not initiate. It is therefore possible to select a grade that will not be subject to crevice corrosion, if the chemical environment temperature do not exceed the critical levels. Critical crevice corrosion temperature (CCCT) values have been determined according to practice ASTM G-48B in ferric chloride (6% $FeCl_3$ for 72 h with crevices). The critical crevice corrosion temperatures for some industrial alloys are given in Table 18 [105].

Comparison of Pitting and Crevice Corrosion of Stainless Steels. These two forms of corrosion are compared in the chapter on corrosion, in its section on Crevice Corrosion. The mechanism of propagation of pits and crevice corrosion is identical; however, the mechanisms of initiation differ [124]. Crevice corrosion does not require the same aggressive conditions, that is, not as high chloride content, as pitting. A steel that is resistant to pitting in a certain solution can, in the same solution, be attacked by crevice corrosion. Control measures of metallurgical nature that improve the resistance to pitting are also beneficial to crevice corro-

Table 18 Critical Crevice Corrosion Temperature (CCCT) [105]

Alloy	°F	°C
Type 304	<27	<–3
Type 316	27	–3
Alloy 825	27	–3
Type 317	36	2
904L	68	20
2205	68	20
E-Brite®	75	24
Alloy 625	100	38
AL-6XN®	110	43
AL 29-4C®	127	53

Note. Based on ASTM G-48B (6% $FeCl_3$ for 72 h with crevices).

sion. If the manganese sulfides are eliminated, the resistance to both pitting and crevice corrosion will improve [111]. According to Blom et al. [111], the three possible ways of eliminating manganese sulfide inclusions include: (1) decreasing Mn content below the solubility product of MnS, (2) decreasing sulfur content to get below the solubility product of MnS, and (3) adding an element, like Ti, and Zr, that forms a stronger and more beneficial sulfide than MnS.

Stress Corrosion Cracking. It is well known that austenitic stainless steel may be subject to stress corrosion cracking (SCC). A range of environmental conditions are associated with SCC, but these can be rationalized into two types, depending on whether they promote predominantly transgranular or intergranular cracking. Transgranular SCC is found mostly in media containing chloride ions and, less frequently, hydroxyl ions. Intergranular cracking occurs in a range of aqueous environments, but is dependent upon achieving a "sensitized" condition [125]. The important environments that cause SCC of SS are

1. Aqueous chlorides.
2. Caustic (hydroxide) solutions.
3. Polythionic acid.

The stress below which SCC cannot occur is not well defined but must be assumed to be low; weld residual stresses are often significantly high [79].

Chloride SCC of Austenitic Stainless Steel. The usual failure mode of chloride SCC of austenitic stainless steel is transgranular and highly branched. Factors that influence the rate and severity of cracking are chloride content, oxygen level, temperature, stress level, and pH of the aqueous solution. Generally, for stainless steels to suffer chloride SCC, chloride concentrations must be 30 ppm or higher, and 20 ppm is normally noncorrosive. However, when chlorides are present in trace amounts, high concentrations may develop locally that will lead to cracking. Proper design—for example, venting—can often eliminate places where chlorides can concentrate. Most of the SCC failures occur above 170°F (75°C), and 120°F (50°C) is generally considered the threshold limit below which SCC is not a problem [114].

Caustic SCC. Caustic SCC of SS occur at temperatures above 120°C. At higher temperatures, the newer ferrite SS, nickel, and high-nickel alloys are substituted for austenitic SS in caustic evaporators.

Influence of Nickel Content on Stress Corrosion Cracking. The influence of nickel content on SCC of austenitic SS can be studied through the Copson curve [126], which is shown in Fig. 17. Figure 17 shows that the maximum propensity for austenitic stainless steels to SCC

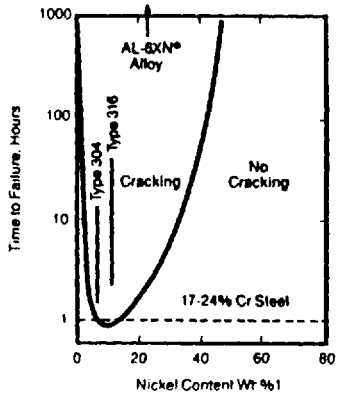


Figure 17 Copson curve. (From Ref. 105.)

is with the nickel content in the 8–12% range, typical of those standard austenitic steels such as Types 302, 304, and 316 [127,128]. A reduction in nickel from these levels leads to an improvement in the SCC behavior, but this is associated with the progressive replacement of austenite by delta ferrite in the microstructure. With increasing nickel content, resistance to SCC improves until about 42–45% nickel, where alloys are virtually immune. This includes Alloy 825, Alloy G, and Alloy 625. Thus, it can be stated as a practical guide that alloys with a nickel content above 22% seldom experience SCC, and this includes Alloy 904, Alloy 28, and Alloy 20 [114]. These materials have performed well in many industrial applications containing chlorides.

SCC of Welded Austenitic Stainless Steels. Austenitic stainless steels that contain surface tensile stresses either locked in during fabrication or externally applied may fail by transgranular cracking in chloride solutions. Welded joints are particularly prone to SCC for three reasons [79]: (1) The welding operation will leave a residual tensile stress in the weld area unless effective postweld stress relief is carried out, (2) stress concentrations are usually present, and (3) the thermal cycle can produce a susceptible microstructure. Postweld stress relief can be of substantial remedy in avoiding intergranular SCC. In this regard, full solution treatment at 1922°F (1050°C) may not be necessary, but a stabilizing anneal at 1598–1742°F (870–950°C) is frequently applied to welded components that find application in the petrochemical industry, to guard against polythionic acid corrosion.

Polythionic Acid Stress Corrosion Cracking (PASCC). Intergranular stress corrosion cracking is specifically caused by the action of polythionic acids on sensitized materials, and such conditions can be present in some types of refinery equipment, particularly during shutdown periods. PASCC requires the presence of sensitized material, oxygen, water, tensile stress, and iron sulfide scale. Polythionic acid can form readily during shutdown as a result of the interaction of the sulfide with moisture and oxygen. Normal grade stainless steels such as Type 304 and Type 316 and Incoloy alloy 800 can be sensitized due to welding; sulfide scales can form during service, and oxygen and water can be introduced during shutdown. Remedial measures to control PASCC include [89]:

Nitrogen purging of components or assemblies exposed to atmosphere.
Neutralizing the acid by ammonia and soda ash washing.
Use of stabilized materials for the construction of heat exchangers. It is reported, that even the stabilized stainless steels (321 or 347) are susceptible to PASCC, unless they have been heat-treated properly [129].

Suitable procedures to overcome this form of corrosion attack are dealt with and well documented in NACE RP-01-70 [130].

Laboratory Tests to Determine SCC. Susceptibility of alloys to chloride SCC is assessed by laboratory corrosion testing as per ASTM 636 or by relating the rate of crack propagation to stress intensification at the crack tip, and polythionic SCC by laboratory corrosion test ASTM G 35.

Evaluation of Sensitization of Austenitic SS to PASCC. The electrochemical potentiokinetic reactivation (EPR) method can be used during inservice periodic inspection for evaluating the degree of sensitization of austenitic stainless steels in high-temperature water [129].

Methods to Prevent Stress Corrosion Cracking of SS. Typical methods to overcome stress corrosion cracking of austenitic stainless steels are discussed in Ref. 107 and by Fontana and Greene [131]. Such measures include:

1. Use of alternative materials that are more resistant to chloride SCC. Typical examples are new ferritics Type 430, superferritics such as E-Brite, Sea-Cure, etc., duplex SS, and titanium or higher nickel austenitic alloys. Ferritics are either immune to SCC or least attacked by SCC. Otherwise, grades such as 304 and 316L, which are susceptible to SCC, may be used when precautions are taken to eliminate one or more of the factors that cause SCC, namely, residual tensile stress, chloride environment, and temperature.
2. Method of safe ending: In vertical heat exchangers, SCC is overcome by a procedure known as *safe ending*. This method consists of butt welding of short lengths of resistant material to austenitic SS tubes at the place of greatest exposure to SCC conditions, i.e., under the top tubesheet.
3. If there is a dead space (air pocket) at which chlorides are allowed to concentrate by alternate wetting and drying of tubing surfaces, the tubes will be attacked by SCC. This problem can be overcome by air venting the dead space or allowing complete flooding of all tubing surfaces (for the schematic representation, refer to Fig. 12.33 of Chapter 12).
4. Bimetallic tubing.

Prevention of SCC in Boiling Water Reactors. Intergranular stress corrosion cracking (IGSCC) adjacent to girth welds in stainless steel piping systems has been a serious problem in boiling water reactor (BWR) plants [132]. The pipe cracking remedies for BWRs and remedies for protection of internals and attachments are [132].

1. Materials-related remedies: The aim of the materials-related remedies is to prevent contact between sensitized material and the BWR coolant, including (a) use of nuclear grade (NG) stainless steels, where the NG suffix signifies tightly controlled requirements for carbon and nitrogen contents to ensure that the materials do not sensitize due to welding; (b) solution heat treatment (SHT), where SHT following welding redissolves grain boundary carbides and restores the grain boundary chromium concentration; and (c) use of corrosion-resistant cladding (CRC). Fractographic observations, which showed the superior IGSCC resistance of duplex weld metals, provided the basis for the CRC remedy, in which the pipe inside surface adjacent to the girth weld is clad with weld metal. The result is enhancement of life by a factor of 6.5.
2. Stress-related remedies: These aim to prevent IGSCC by subjecting the sensitized material at the inside surface of the weld heat-affected zone (HAZ) to large compressive residual stresses.
3. Adopt heat-sink welding (HSW) and last pass heat-sink welding (LPHSW).
4. Adopt induction heating stress improvement (IHSI) and mechanical stress improvement process (MSIP).
5. Environment related.

The remedy called hydrogen water chemistry (HWC) consists of reducing the electrochemical potential (ECP) of stainless steel in the recirculation systems of operating BWRs to values below −230 mV standard hydrogen electrode (SHE) by injecting hydrogen into the feedwater (hence the name "hydrogen water chemistry").

Intergranular Corrosion. Sensitization of stainless steels is covered in Chapter 12, Corrosion. Sensitization of stainless steel with $C \geq 0.05\%$ that takes place in the temperature range 500–900°C when exposed to high-temperature operations like welding (known as weld decay), heat treatment, or brazing. The degree of severity of sensitization depends on welding process variables and plate thickness, since these determine the time in the critical temperature range. The sensitization temperature range is schematically shown in Fig. 18 [119,133], in which the curves show the times required for carbide precipitation in steels with various carbon contents. Carbides precipitate in the areas to the right of the various carbon content lines.

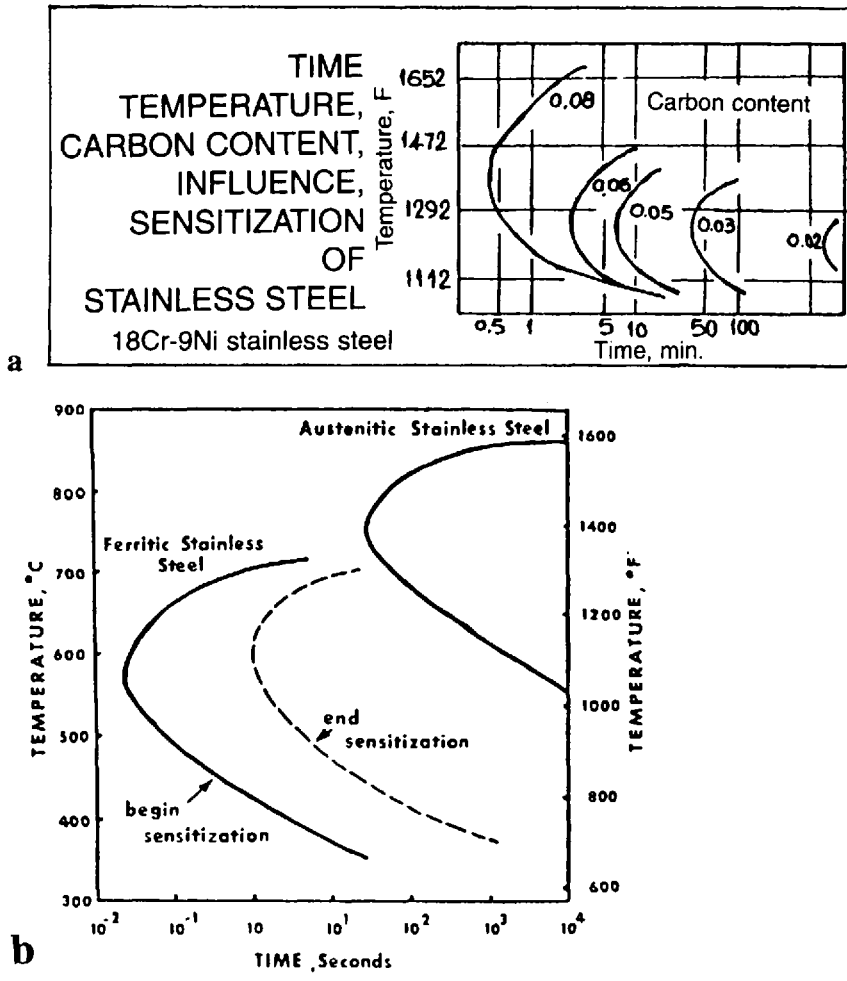


Figure 18 Typical time–temperature sensitization diagram. (a) Austenitic stainless steels and (b) ferritic stainless steels and austenitic stainless steels. (From Refs. 119, 134.)

Factors Influencing Susceptibility to Weld Decay. The main factors that determine the sensitivity of austenitic stainless steels are [134]:

1. Metal composition and microstructure: The main compositional factor that determines the susceptibility to weld decay is the carbon content, with increasing carbon being detrimental; the presence of ferrite is beneficial in resisting weld decay, but a large grain size is deleterious.
2. Thermal history: Sensitization is mainly dependent on the maximum time spent at temperatures between 550 and 850°C.
3. Internal or external stresses arising from prior deformation, welding, or service loads.
4. Environment: Stainless steel will be attacked by intergranular corrosion when a sensitized metal is exposed to a corrosive environment. Not all environments will cause weld decay. Weld decay can arise only in three distinct types of environments [134]: (a) marginally

oxidizing, (b) moderately oxidizing, and (c) highly oxidizing. Risk of weld decay is most commonly encountered in moderately oxidizing conditions.

Measures to Overcome Weld Decay. Measures to overcome weld decay are discussed by Jarman et al. [79]. They are summarized here: (1) To ensure optimum corrosion resistance, especially in welded thick plate, subject the weldment to solution treatment followed by quenching. (2) The problem of sensitization is overcome for lower temperature heat-exchanger materials by selection of extra-low-carbon (ELC) steels or stabilized steels such as Type 321 (Ti stabilized) and Type 347 (Nb stabilized). Ti and Nb have a greater affinity for carbide formation than Cr, thus preventing the precipitation of $Cr_{23}C_6$. The additions made to stainless steels are slightly in excess of those required by stoichiometry for complete precipitation of carbon and nitrogen, namely, [135], Ti = 5(C + N)% and Nb = 8(C + N)%. Another measure is (3) low heat input (<3 kJ/mm) and an interpass temperature maintained below 175°C. (4) Fillers and electrodes should also be stabilized or of ELC. (5) Increase the nickel and chromium contents of the filler to offset losses in the arc transfer. Note that titanium-stabilized fillers should not be used in argon arc welding, as titanium will be vaporized and its effectiveness as a stabilizer is lost.

Even though the problem intergranular corrosion is overcome by the use of low-carbon grades or stabilized grades, these grades have some *drawbacks*:

1. Low-carbon grades have lower strength than stabilized grades.
2. Stabilized grades may be more hot-cracking sensitive and require more careful ferrite control, compared to nonstabilized grades.
3. Stabilized grades are susceptible to localized precipitation of carbides in narrow regions of the HAZ that can lead to intergranular corrosion known as knifeline attack [103,107,135]. Knifeline attack is further discussed next.

Knifeline Attack. While welding stabilized grades such as Types 321 and 347, the heat-affected zone is raised to temperatures above 2102°F (1150°C), and this can result in the partial dissolution of TiC or NbC. Carbon is therefore taken into solution in a narrow region adjacent to the weld and can be available for the formation of chromium carbide on cooling through the sensitization temperature range. The susceptible region, being only a few grains in width, can give rise to a thin line of intergranular attack and hence the name knifeline attack. Nb-stabilized steels appear to be more resistant to knifeline attack than the Ti-stabilized steels. In both types, elevated-temperature solution treatment and quenching cannot adequately restore the original properties [79]. Knifeline attack differs from weld decay in the following ways [131]:

1. Knifeline attack occurs in a narrow band in the parent metal immediately adjacent to the weld, whereas weld decay develops at an appreciable distance from the weld.
2. Knifeline attack occurs in the stabilized steels.
3. The thermal history of the metal is different.

Knifeline attack can be avoided by the proper choice of welding variables and by the use of stabilizing heat treatments [135]. Therefore, the trend is to use low-carbon grades rather than the use of stabilized grades [136].

Prediction of IGC by Laboratory Tests. Two laboratory tests are most widely used to predict intergranular corrosion. They are described next.

1. *Direct exposure testing.* Direct exposure testing is the most satisfactory way of evaluating the risk of weld decay in a given environment [122]. The ASTM test method by direct exposure for detecting susceptibility to intergranular corrosion is given in Table 19. More details on tests for susceptibility to intergranular corrosion of SS are furnished in Ref. 107.

Table 19 ASTM Standard Test for Susceptibility to Intergranular Corrosion in Stainless Steels [107]

ASTM test method	Alloys
A262, Practice A	Types 304, 304L, 316, 316L, 317L, 321, 347, casting alloys
A262, Practice B	Same as Practice A
A262, Practice C	Same as Practice A
A262, Practice D	Austenitic stainless steel (molyodenum bearing)
A262, Practice E	Austenitic stainless steel
A708	Austenitic stainless steel
G28	Hastelloys C-276, and G; 20Cb-3, Inconel alloys 600, 625, 800, and 825
A763, Practice X	Ferritic stainless steel, including Types 430, 446, 26-1, 29-4, 29-4-2
A763, Practice Y	Ferritic stainless steel, including Types 446, XM27, XM33, 29-4, 29-4-2
A763, Practice Z	Ferritic stainless steel, including Types 430, 434, 436, 439, 444

2. *Potentiostatic test method.* This technique involves exposing a polished weld sample to a suitable electrolyte at a constant potential, which can be varied over the entire range of passivity or corrosion. The potentiostatic test method offers advantages over conventional test methods in enabling quantitative assessment of the risk of weld decay, and gives data relevant to a wide range of service conditions [134].

16.5 Austenitic Stainless Steel Fabrication

Austenitic stainless steels may be formed by the usual processes, such as drawing, bending, spinning, pressing, etc. They are extremely ductile and will accept a considerable amount of cold work, work harden rapidly, and with increasing thickness, severe forming operations may need subsequent or even interstage heat treatment [137]. Austenitic steels are difficult to machine because they work harden and gall. Rigid machines, heavy cuts, and high speeds are necessary.

Hot working may be carried out in the temperature range 2012–1652°F (1100–900°C), duly observing the susceptibility to sensitization of unstabilized varieties. When heating for forming, electric furnaces are preferred to minimize scaling. Gas- or oil-fired furnaces are also used in the fabrication industry. Use fuels of low sulfur content, to reduce the possibility of sulfur contamination, which embrittles the material and reduces corrosion resistance. Flame selection is important; a slightly oxidizing flame is preferred, since reducing flames may lead to carbon pickup with loss of corrosion resistance, and highly oxidizing flames result in excessive scaling [137].

Pickling

Hot worked-material will generally need to be descaled, usually by acid pickling. Pickling may be carried out in one of a number of suitable acids, e.g. hydrochloric, sulfuric, nitric, or various mixtures, either hot or cold.

Passivation

Passivation of stainless steel consists of treating stainless steel parts in a solution of HNO_3 and a combination of oxidizing salts. This treatment dissolves the embedded or smeared iron and restores the original corrosion-resistant surface. Passivate austenitic and ferritic grades for 20 to 30 min at 130°F. Rinse in clean hot water. Tests should be made to check on the extent of free iron removal.

Cutting to Shape

Mechanical Cutting Methods. All stainless steels may be cut using friction saws with greater than 3/8 in (9.5 mm) thickness. Heat removal becomes a problem, resulting in rapid deterioration of the saw blade and burning of the material. High-speed abrasive discs can be used for cutting tube and bar to length, although a coolant should be used and this should not be sulfur based. Rubber-bonded discs should also be avoided [137].

Gas Cutting Method. One of the major difficulties in the fabrication of stainless steel is the gas cutting of the material. Stainless steel cannot be cut by the conventional oxyacetylene process because of the highly refractory chromium oxide that is formed on heating [137,138]. The powder cutting technique employed in the past involved the injection of iron powder into an oxyacetylene stream. This method is undesirable, because it gives rise to considerable fumes and the resulting cut is normally of poor quality and contaminated by iron powder, so that it is essential to machine an appreciable amount from a cut edge. Recent introduction of the plasma arc cutting technique has eliminated this difficulty. For thickness up to 15 mm, cold shearing may also be used.

16.6 Austenitic Stainless Steel Welding

Good weldability is an attractive feature of stainless steels, and this contributes to the wider usage and versatility of these materials in the fabrication of pressure vessels, storage tanks, chemical plants, and domestic appliances. Welds in austenitic stainless steels usually have chemical compositions and mechanical properties, and toughnesses comparable to those of the parent metals. They are not prone to cold cracking. Due to a stable structure, there is no need to preheat or postheat the weldment. Normally, there is no heat input limitation and high arc energies can be used without any adverse effects.

Being austenitic, these weldments are virtually nonmagnetic and not subject to arc blow while welding. Compared with plain carbon steels and low-alloy and 400 series stainless steels, the austenitic stainless steels have lower melting points, higher electrical resistance, 30–50% lower thermal conductivity, and 50% higher coefficient of thermal expansion. For these reasons, less heat input (less current) and the heat concentration in a small zone adjacent to the weld arc required for fusion. Even though stainless steels are ductile enough to accommodate a fair amount of shrinkage, welds may be cracked when restrained [139].

Welding Processes

SMAW, SAW, GMAW, GTAW, and PAW are used extensively for joining stainless steels. In general, those steels that contain aluminum or titanium or both can be arc welded only with the gas-shielded processes. For GTAW process, use direct current, straight polarity, employing 2% thoriated tungsten electrodes [140]. SAW is not recommended when the austenitic stainless steel weld deposit must be fully austenitic or low in ferrite content. However, it is suitable when a ferrite content of 4% is permissible in the weld metal. Demands for Fluxcored arc welding (FCAW) of stainless steels have markedly increased recently. This is because of excellent applicability of FCAW in satisfying the requirements for streamlining and productivity improvement in the welding of stainless steel.

Oxyfuel welding of stainless steel is to be avoided since the heat input is high and the gas combustion produces carbon monoxide and carbon dioxide, likely to carburize the weld metal and increase the chances of sensitization [119]. Therefore, oxyacetylene welding is not recommended except for emergency repairs where suitable arc welding equipment is not available. A neutral or a sightly reducing flame is recommended.

Carbon arc welding was never suitable due to the danger of carbon pickup. CO_2 consum-

able electrode welding can be used in applications in which corrosion can be tolerated. When corrosion resistance is a major factor, metal arc welding with covered electrodes or one of the inert gas processes can be used [137].

The welding of stainless steels has been reviewed extensively by Fenn [136], Banks [137], Weymuller [139], Beigay et al. [140,141], and Castro and deCadnet [142], and the topic has been updated more recently by Castner [143]. Various aspects of SS welding are discussed next.

Filler Metal Selection

In order to optimize the properties of stainless welds, careful selection of welding consumables and fabrication procedures is mandatory. AWS A5.4, Specification for Corrosion Resisting Chromium and Chromium-Nickel Steel Covered Welding Electrodes, lists types, compositions, and other data for standard electrodes. AWS ER 3xx filler metals or overmatching 300 series filler metals are used in over 90% of stainless steel welding applications. Such welds exhibit good corrosion resistance, toughness, and excellent strength at both low and high temperatures, and a high degree of toughness in the as-welded condition. A few recommended filler metals and the austenitic steel base metals are given in Table 20.

Shielding Gases

Single gases or mixtures of different gases such as argon, helium, oxygen, carbon dioxide, hydrogen, nitrogen, and nitrogen monoxide (NO) in fairly different proportions can be used in GMAW of SS.

Weld Preparation

Weld preparations for stainless steels are similar to those used for carbon steels and may be obtained by machining, grinding, or plasma cutting.

Joint Design

Weld penetration is generally less in stainless steels than in carbon steels, so weld preparation angles are greater, root faces smaller, and root gaps wider; greater welding skill is required to ensure that adequate penetration is achieved without root defects [137]. A typical joint design for stainless steel is shown in Fig. 19.

Preweld Cleaning

To obtain sound welds free from cracks or embrittlements, the surfaces to be joined require cleaning prior to welding. The area to be cleaned should include the weld groove faces and

Table 20 Filler Metals for Austenitic Stainless Steels

Filler metal	Base metal
AWS E308 or ER308	Types 405, 409, 410, 430, 304
AWS E308L or ER308L	Types 304L, 304, 321, 347
AWS E316 or ER316	Types 304, 317
AWS E316L or ER316L	Types 321, 347
AWS E317 or ER317L	Type 304
AWS E347 or ER347	Types 304, 304L, 321, 347

Note. This table was compiled from Beigay et al. [140].

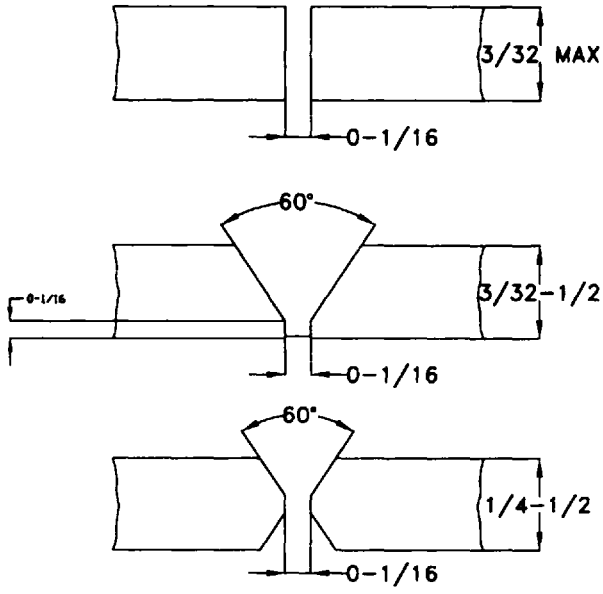


Figure 19 Joint design for austenitic stainless steel welding. (From Ref. 140.)

the adjacent surfaces for at least 0.5 in on each side. The most common form of surface contaminants are iron contamination and organic contamination.

Iron Contamination. On occasion, forming equipment and tools made of carbon steel can cause embedding of iron particles on stainless steel surfaces. Since rust is anodic to the bulk austenitic surface, galvanic corrosion will take place, resulting in pit formation. Hence, it is desired during fabrication to use cardboard or plastic sheets on carbon steel machinery and plants and handling equipment to avoid carbon embedding on stainless steel surfaces. Remove the embedded iron by pickling.

Organic Contamination. During the fabrication stage, organic contamination on the metal surfaces takes place as the result of grease, oil, cutting fluids, crayon markings, paint, and sticky substances. Even small amounts of these contaminants can crack or embrittle welds or heat-affected zones. To avoid this, make sure both the base metal and filler metals are clean. Removal of organic contaminants is best accomplished by degreasing using a nonchlorinated solvent. Oxide films can be removed by mechanical methods or by pickling with 10–20% nitric acid solution. Mechanical cleaning techniques for surface oxide removal include (1) stainless wire brushing where the brushes have not been used for any other purpose, (2) sand or grit blasting, and (3) machining and grinding using chloride-free cutting fluid.

Welding Considerations

There are a number of welding processes and material considerations that are important to the production of sound welds with suitable properties in austenitic stainless steels. Here are some of the most important of those considerations:

1. Microfissuring or liquation cracking is the most frequently encountered problem.
2. Autogenous welds may be subject to variable penetration.
3. Sensitization of HAZ may affect corrosion resistance. Other factors which govern the corrosion resistance of weldment include microstructure in the vicinity of the surface,

inclusions, surface oxides, residual weld stresses, spotter, and contaminations and geometric surface defects and crevices [118].

4. Greater thermal expansion may result in warping or distortion, especially in thin sections, suggesting greater need for jigging to maintain dimensional control.
5. Welding fumes present potential hazards to workers.
6. Several factors must be considered when postweld heat treatment (PWHT) is required.
7. Dissimilar metal weld joints require selection of proper filler metal and procedures.

Microfissuring or Liquation Cracking in Austenitic Stainless Steel Weld. The structures of most importance in the weldable stainless steels are ferrite and austenite. The structure of austenitic stainless steel weld metals varies from fully austenitic in Type 310 to dual-phase austenitic–ferritic in Types 304, 308, 309, 312, and 316. Fully austenitic alloys tend to be hot short, and welds in these materials show fine cracking or microfissuring, also known as liquation cracking, either in the weld metal itself or in the heat-affected zone, while those that solidify with delta ferrite as the primary solidification mode are the least susceptible to hot cracking.

Segregation of low-melting-point impurities like S, Si, and P between the grain boundaries can cause liquation cracking or microfissuring in the weldment, the HAZ, and weld overlays. Shrinkage stresses combined with high restraint (clamping is often used on stainless steel during welding to prevent distortion) may cause these films to rupture prior to complete solidification [144]. Each element exhibits detrimental effects on hot cracking. Phosphorus content above 0.025%, sulfur content above 0.025%, or silicon content above 2.0% may cause the same length of solidification crack. The combined effect of these impurities may be much more disastrous [145].

HAZ Liquation Cracking Susceptible Alloys. Austenitic stainless steels susceptible to HAZ liquation cracking include AISI 304, 304L, and the stabilized grades such as Type 321 and Type 347. HAZ liquation cracking has been reported in both cast and wrought versions of a wide variety of nickel-base alloys such as Incoloy Alloy 800, Alloy 718, and Hastelloy X [72].

Avoiding liquation cracking is the most important issue in fusion welding of austenitic stainless steels. In general, alloys that solidified with ferrite as the primary phase and containing 4–11% by volume of ferrite in the as-welded condition were more resistant to cracking than alloys solidified as austenite. Hence, in order to control microfissuring in stainless welding, the alloying elements are balanced in such a way as to attempt to produce a weld deposit containing ferrite in the order of 4 to 11 FN (ferrite number). The ferrite number is a magnetically determined scale of ferrite measurement. This provides sufficient control in most applications where minimum ferrite content or a ferrite range is specified.

Benefits of Ferrite in Austenitic SS. Major benefits of ferrite to austenitic stainless weld metal are improved resistance to microfissuring and hot cracking, improved resistance to stress corrosion cracking, and good low-temperature impact strength [144].

Optimum Weld Metal Ferrite Content. It is a common practice today to specify a minimum ferrite content about 3 or 4 FN in a nominal austenitic stainless steel weld metal to provide assurance that the weld will be free of hot cracks and microfissures. Following are the minimum recommended levels of weld metal ferrite content (a range of 8 to 10 FN is considered optimum under most conditions) for various types of austenitic stainless steels [144]:

Type 308/308L, 3 FN
Type 309/309L, 5 FN
Type 316/316L, 3 FN
Type 347, 6 FN

However, a ferrite number in excess of 11 can have a detrimental effect in these applications [144,146]:

1. Weldments intended for cryogenic service where ferrite is less tough than austenite.
2. Weldments intended for certain special corrosive environments where ferrite is preferentially attacked, such as in the manufacture of urea.
3. Weldments that must experience postweld heat treatment or service at elevated temperatures where ferrite can transform to embrittling phases such as the sigma phase.
4. Duplex stainless steel weldments with excessive ferrite can result in poor ductility, toughness, and corrosion resistance.

Industrial Use of Ferrite Standards. In practice, standards and industrial measurement of ferrite have three areas of application [146]:

1. Certification and verification of filler metals.
2. Development of qualified welding procedures for particular critical applications, using certified filler metals.
3. Quality assurance examination of production weldments.

Effects of Alloying Elements on Microstructure. The addition of alloying elements to steel affects the stability of the various phases, with some stabilizing the ferrite and others the austenite. The amount of delta ferrite in the weld metal is largely, but not completely, controlled by a balance in the weld metal composition between the ferrite-promoting elements, expressed by chromium equivalent, and the austenite-promoting elements, expressed by nickel equivalent. Many workers have examined these effects, and Anton L. Schaeffler [147a] produced a diagram known as a *constitution diagram*, indicating the phase distribution in weld deposits of various compositions. Schaeffler expressed the empirical expressions for chromium equivalent and nickel equivalent as follows:

$$\text{Chromium equivalent} = \%Cr + \%Mo + 1.5 \times \%Si + 0.5 \times \%Nb$$

$$\text{Nickel equivalent} = \%Ni + 30 \times \%C + 0.5 \times \%Mn$$

The composition of the weld metal required to satisfy the ferrite content requirement is found to be fulfilled when Cr_{Eq}/Ni_{Eq} is above 1.48 [103].

Schaeffler assumed that the level of nitrogen, a strong austenizer, was constant in his diagram. This has been taken into consideration by such workers as De Long and Schneider. De Long developed a diagram that included the effects of nitrogen [147b]. The Welding Research Council (WRC) published modified diagrams in 1988 and 1992 [147c] that allow accurate prediction of the ferrite number. According to the De Long diagram, the chromium and nickel equivalents are expressed by [147c]:

$$\text{Chromium equivalent} = \%Cr + \%Mo + 1.5(\%Si) + 0.5(\%Nb)$$

$$\text{Nickel equivalent} = \%Ni + 30(\%C) + 30(\%N) + 0.5(\%Mn)$$

As per the 1992 WRC constitution diagram for stainless steels, the chromium and nickel equivalents are expressed by [147c]:

$$\text{Chromium equivalent} = \%Cr + \%Mo + 0.7(\%Nb)$$

$$\text{Nickel equivalent} = \%Ni + 35(\%C) + 20(\%N) + 0.25(\%Cu)$$

Prevention of Microfissuring: Influence of Welding Procedure and Welding Parameters on Ferrite Content. The ferrite number of an arc weld made with filler metal is primarily a function of filler metal and base metal composition and base metal dilution, which are con-

trolled by the welding procedure, whereas the ferrite number of an autogenous arc weld is a function of the composition of the base metal and the welding procedure. Microfissuring can be minimized by selecting (1) welding consumables, (2) welding process parameters, and (3) welding procedure variations that ensure solidification as delta ferrite. These three parameters are discussed next.

Welding Consumables. The composition of electrodes and filler wires for welding the fully austenitic steels is normally adjusted to provide 3–5% ferrite in the weld metal deposit to protect against microfissuring. Elements such as nickel, silicon, sulfur, and phosphorus increase the susceptibility to cracking, whereas chromium, nitrogen, and manganese reduce the cracking tendency. Therefore, filler metals can be designed that are completely austenitic and free from microfissuring. Such fillers are low in sulfur, phosphorus, and silicon but often contain 7–10% Mn. The principle of prevention of microfissuring by increasing manganese content is made use of in the "zero ferrite electrode."

Welding Process. High heat input welding procedures, deep and narrow weld beads, high interpass temperatures, and high levels of restraint may result in cracking even with 4 FN ferrite in the completed weld bead [143]. Certain welding process parameters can also help to prevent microfissuring. Such parameters are:

1. A long arc tends to reduce the ferrite content due to chromium loss across the arc [137].
2. Due to dilution, root pass welding generally results in a low ferrite content in the root weld metal. To offset this effect, a filler metal with a higher ferrite number should be used [144]. Hot wire GTAW is particularly good from this standpoint [112].
3. High welding speeds that result in teardrop-shaped weld pools increase the solidification rate at the weld center line and promote primary austenite formation, which makes these welds more likely to crack [143].

Welding Procedure Variations. Any procedure variation that admits nitrogen into the arc will reduce weld FN, and very high welding heat input tends to reduce ferrite content. The influence of nitrogen pickup is further discussed next.

Nitrogen Pickup. Higher than normal nitrogen levels can reduce weld ferrite and cause hot cracking. Excessive nitrogen pickup can result from (1) poor shielding gas coverage for GTAW and GMAW, (2) loss of flux coverage during SAW, and (3) use of excessively long arc lengths during SMAW or self-shielded flux-cored arc welding [143].

Mock-up Test. Prior to production welding where ferrite content is critical, pretesting in a mock-up is necessary to ensure that the combination of process, consumable, technique, and cooling rate will produce the desired ferrite number in the weld [144].

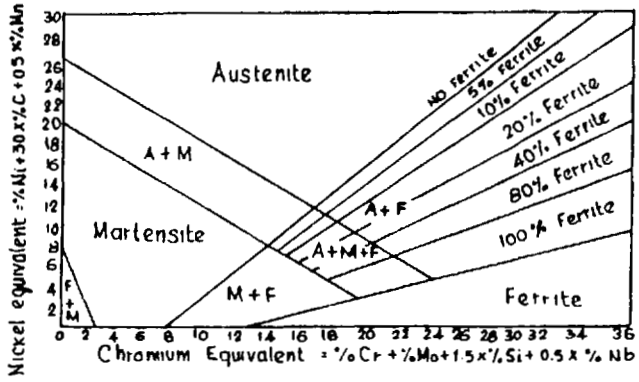
Standards for Ferrite Determination. Determination of ferrite at room temperature has taken four forms over the years. They are (1) metallographic examination, (2) constitution diagrams, (3) magnetic measuring instruments, and (4) X-rays.

1. *Metallographic examination.* In the metallographic method, the ferrite content is determined by microscopic analysis. This method provides a statistical determination of the amount of ferrite. One of the common statistical methods of metallographic examination is by point-count analysis, where evenly spaced points are superimposed on a field on the specimen and the points found on a constituent are counted. A large number of fields are sampled to ensure statistical accuracy. The drawbacks associated with this method include: Examination is destructive in nature, interpretation is subject to error, and due to variations in etching, lab-to-lab reproducibility is sometimes poor [144].

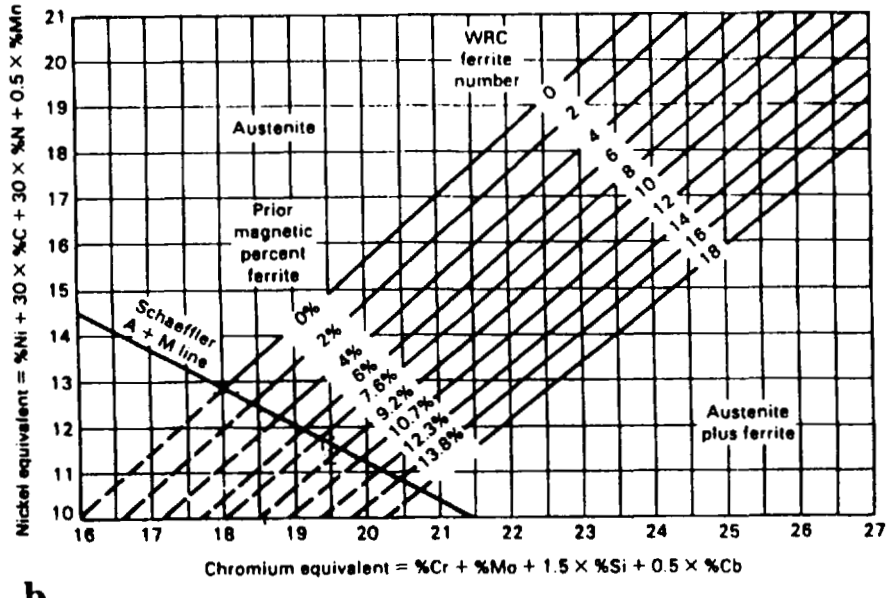
2. *Constitution diagrams.* As an alternative to metallographic examination, constitution diagrams have been developed that permit estimation of weld metal ferrite from deposit composition. The Schaeffler diagram [147a] has been used in purchase specifications for filler metals;

the De Long diagram is not only used in purchase specifications for filler metals but also has become part of standards such as the ASME code [146]. Recently, with the Winter 1994–1995 Addendum to the ASME code, the 1992 WRC diagram [147c] has replaced the De Long diagram [147b] in that code.

The Schaeffler diagram shown in Fig. 20a, the Delong diagram shown in Fig. 20b, and the 1992 WRC diagram shown in Fig. 20c use an x axis of chromium equivalents versus a y axis of nickel equivalents. Carbon contents are 0.03% minimum unless otherwise indicated. The Cr-Ni equivalents of the consumable and base material are plotted on a set of ferrite content lines that have been empirically derived. The dotted line indicates the approximate boundary of the austenite region for wrought alloys. Ferrite contents are determined by calcu-



a



b

Figure 20 Constitution diagram. (a) Schaeffler diagram; (b) De Long diagram; and (c) WRC 1992 diagram. (From Ref. 147.)

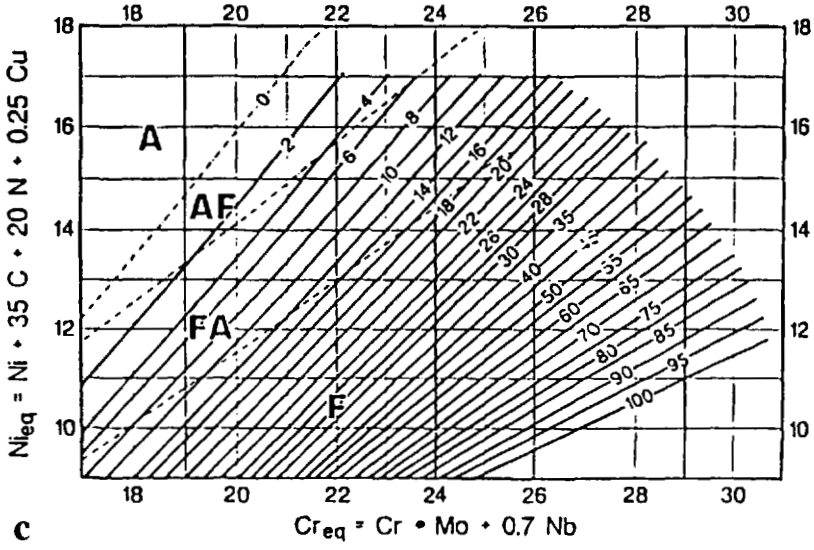


Figure 20 Continued.

lating specific chromium and nickel equivalents from alloy compositions and plotting the respective points on the diagram.

Caution is required in the use of these diagrams [144]:

1. These diagrams may not accurately reflect the effects of welding process, technique, dilution, or cooling rate on ferrite content; they are really applicable to welds made under conditions similar to those used by these researchers.
2. Neither the Schaeffler nor the Delong diagram accounts adequately for the effects of manganese in amounts greater than 2.5% in a weld metal, in which case both the diagrams seriously underestimate ferrite content.

For these reasons, the constitution diagrams just described should be used only as guidance to choosing a particular consumable or for an approximation of ferrite content and never as a final word regarding weld metal ferrite content. Where accurate ferrite measurement is required, magnetic instruments should be used and the consumable manufacturers recommendations followed.

3. *Magnetic Measuring Instruments or Ferrite Gages.* Ferrite is ferromagnetic, while austenite is not; this provides the basis for magnetic determination of ferrite at room temperature. Ferrite determinations by magnetic means using ferrite gages are reproducible, and this is a nondestructive test. Standard methods of ferrite determination by magnetic methods for industrial use are discussed in ANSI/AWS A4.2 and ISO 8249. Portable ferrite gages or indicators are designed for on-site use. Various trade names for magnetic measuring instruments are Magnegauge, Ferritescope, Severn gauge, Foerster gauge, and Elcometer [144].

Secondary Weld Metal Standards. The austenitic stainless steel weld metal standards intended to be used for the calibration and a cross-referencing of instruments for measuring ferrite in weld metal are available from VEW-Bohler in Austria, among others. These samples have been prepared on behalf of Commission II on Arc Welding of the IIW and contain varying amounts of delta ferrite. Ferrite numbers for the eight samples, in the approximate

range 3 to 27 FN, have been determined using the IIW recommended procedure, and are given on an accompanying card.

4. *X-rays.* This method of ferrite determination relies on the fact that all materials consist of different crystal structures. The intensities of diffraction lines of the different phases allow determination and measurement of their presence. This type of analysis is only possible on the surface thickness (approximately 2 mils) and can only measure amounts of ferrite in excess of 3 FN. Equipment of this type is costly, complicated, and not always practical [144].

Ferrite in Duplex Stainless Steels. Heat-affected zones in duplex stainless steels have a tendency to form a high level of ferrite, and this provides a special problem for ferrite measurement. The ferrite content can be kept within acceptance limits by controlling the composition of the base metal and by controlling the heat input, typically 0.5 to 2.5 kJ/mm, with more restrictive limits for higher alloyed "super duplex" stainless steels [146]. In duplex stainless steels, HAZ ferrite content determination using a precisely defined metallographic point counting procedure is recommended. Ferrite content by magnetic means can be determined as per ANSI/AWS A4.2.

Variable Weld Penetration. Variable penetration refers to the marked differences in the depth of penetration observed when steels of nominally the same composition but produced from two different heats were welded under identical conditions. There is a tendency for the weld to deflect to one side of the joint when steels from different casts are welded together, and deviation to one side of the joint sometimes results in a lack of fusion. For this reason, the problem is also known as cast-to-cast or "heat-to-heat" variability [104,143]. Variable penetration is mostly experienced with the introduction of automatic autogenous welding processes, such as orbital TIG for tube-to-tubesheet joining, particularly with stainless steels grades such as AISI 304 and 316 [103].

Factors Responsible for Variable Penetration. It is now generally agreed that variable penetration is associated with the influence of surface-active elements such as S, O, Se Te, and Ce on the fluid flow in the weld pool [148]. In steels containing surface-active elements, the flow is toward the center of the liquid pool, giving downward axial flow and good penetration (Fig. 21a). On the other hand, in high purity steels with surface active elements absent, the penetration is shallow or off center (Fig. 21b,c). Problems are particularly evident for heats containing less than 0.003% sulfur [149]. In high-purity steels such as calcium-treated steels, calcium forms sulfides, thus consuming the sulfur available to assist in producing the convergent flow. In order to achieve good weld penetrations, fabricators may specify a minimum of 0.01% S but with a caution that high sulfur content affects the corrosion resistance of stainless steels.

Measures to Overcome Variable Penetration. Penetration can be achieved by increasing welding current or decreasing travel speed. However, it is difficult to implement these changes for individual heats in automatic welding operations [143]. Process tolerance can be increased by using short arc lengths and sharp-pointed electrodes, but these practices are often already in use when variable penetration is encountered. The following recommendations were given by Castner [143] and others to avoid variable penetration:

1. Avoid calcium- and rare-earth-treated steels; calcium and rare earth elements content should not exceed 10 ppm [103].
2. Avoid steels with sulfur contents of less than 0.006% and steels with aluminum contents greater than 0.01%.
3. Change the shielding gases. Additions of helium and/or hydrogen to argon have been found to be effective in overcoming variable penetration. Argon with 5% hydrogen is very

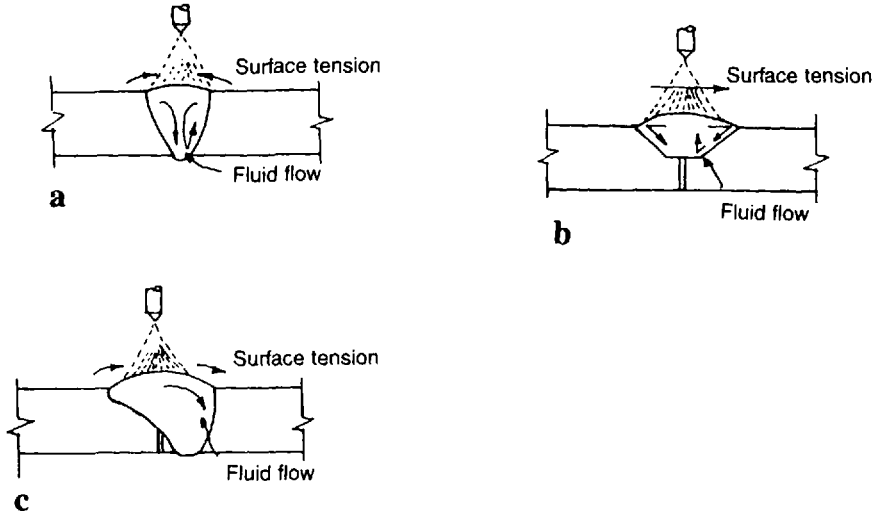


Figure 21 Weld metal penetration: (a) good penetration; (b) variable penetration due to absence of surface active elements, shallow penetration; and (c) off-center penetration. (After Ref. 148.)

effective [143]. The influence of shielding gas on penetration in austenitic stainless steel is shown schematically in Fig. 22.

4. Massive copper alloy heat sinks surrounding the weld joint successfully overcome the problem [148].

Sensitization and Corrosion Resistance. Most widely used methods to prevent sensitization have already been discussed. Even stabilized grades are susceptible to localized precipitation of carbides in narrow regions of the HAZ, which can lead to intergranular corrosion known as knifeline attack. For welding purposes, the niobium-stabilized steel electrodes are preferred because less niobium is lost during transfer across the arc and thus more niobium is retained in the weld metal for carbide-forming purposes [136]. Residual stress from welding can cause SCC. Loss of corrosion resistance in austenitic stainless steels can be minimized by selecting the proper materials and welding procedure.

Control of Distortion. The relatively high coefficient of thermal expansion and the low thermal conductivity of austenitic stainless steels may result in more warping, especially in thin

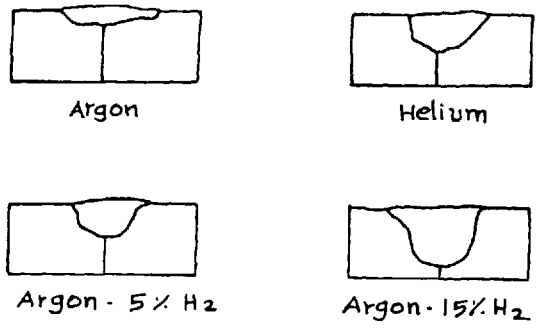


Figure 22 Shielding gas influencing austenitic stainless steel weldment. (From Ref. 143.)

sections, than in other types of stainless steels, carbon steels, and alloy steels [137]. This suggests a greater need for jigging to maintain dimensional control. Measures to control distortion are discussed by Banks [137] and Castner [143]. They are:

1. More frequent tack welds are required to limit shrinkage.
2. Thin sections should be restrained with fixtures and strong backs.
3. Heat sinks can be used to minimize the size of the area affected by the heat of welding.
4. Fabrication of complex structures should employ the minimum permissible weld size and minimum weld heat input.
5. Heavy sections should be welded in as few passes as practical, using stringer beads and welding sequences that limit interpass temperature. Weld passes should be balanced around the neutral axis.

Mild steel jigs, strongbacks, etc. must not be directly attached to stainless steel items that form part of the final fabrication, because this results in reduction in corrosion resistance, dilution effect, or air-hardening compositions susceptible to cracking.

Welding Fumes. Fumes from arc welding processes are a potential hazard to personnel. On-site measurements of fume concentrations are required to determine exposure for a given application. Local exhaust ventilation and/or respiratory protection are recommended to control exposure when welding austenitic stainless steels [143]. It may be possible to minimize fumes by selection of consumables and welding parameters as discussed in Ref. 143.

Welding Practices to Improve the Weld Performance

1. Minimize porosity in welds by using electrodes containing a deoxidizer like silicon or manganese [150].
2. Use lowest possible heat input to minimize the width of HAZ and minimize time at temperature in the range that can cause carbide precipitation. The degree of sensitization caused by welding is mostly related to the heat input processes. An arc welding process carried out at fast travel speeds, GTAW in particular, is better. A high heat input process, like submerged arc welding, is likely to sensitize stainless steel unless travel speed is high and auxiliary cooling is applied [119].

Protection of Weld Metal Against Oxidation and Fluxing to Remove Chromium Oxide. While welding stainless steels, the welding process must protect the molten weld metal from the atmosphere during transfer across the arc and during solidification. Some welding processes require fluxing to remove chromium and other oxides from the surfaces to be joined and from the molten weld metal. The presence of chromium oxide impairs the quality of stainless steel weldments. Fluorides are the most effective agents for removing chromium oxide. Calcium and sodium fluorides are used in covered electrode coatings and submerged arc welding fluxes.

Protecting the Roots of the Welds Against Oxidation.

Gas Shielding. Oxidation of the underside surface of root beads of full-penetration welds can occur if proper shielding is not provided. This oxidation is detrimental in corrosive environments because the oxide layer may reduce the corrosion resistance and facilitate preferential corrosion [118,143]. Therefore, protect the roots of welds from oxidation with argon; nitrogen also can be used as a backup gas. For multipass welds, the gas shield should be maintained during welding of the root pass and a few additional passes.

Root Flux. Root flux is a powder that, when made into paste and applied to the metallic surfaces to be protected, reacts with the heat from welding to form a thin slag that helps to protect the metal surface from oxidation [118]. However, root flux is not a substitute for gas shielding, but an improvement to welding with no root shielding.

Porosity: Beginning-and-End. One of the porosity problems of stainless steel welding is known as "beginning-and end." It takes place at the beginnings and ends of welds (Fig. 23) in stainless steels and nickel alloys due to hydrogen entrapped during solidification [150]. Preheating will help to reduce the amount of porosity in stainless and nickel alloy welds. According to Vackar [150], the probable causes of beginning-and-end defects are

Base metal too cold.
Poor shielding at the start; poor shielding all along would produce porosity along the length of the weld.
Fast cooling at the end.

Once made, grind at least 1/16 in deep and get rid of front and back weld defects.

Underbead Cracking. This can occur in the HAZ of the austenitic stainless steel base metal immediately adjacent to the weld metal, especially in sections more than 0.75 in thick.

Welding Processes Generate Different Weld Defects

The different arc welding processes typically generate different weld defects in SS. Among the gas-shielded arc welding methods MIG process generates spatter and leaves slag residues on the weld affected areas; TIG and plasma arc processes, raise the risk of losing alloying elements from the weld pool, and thereby locally decrease the pitting resistance of the weld metal; and slag shielding methods (SMAW, SAW, and FCAW) leave slag and spatter during the process, and generate inclusions in the vicinity of the weld metal surface [118].

Postweld Heat Treatment

Austenitic stainless steel weldments are normally placed in service in the as-welded condition. However, environments that can cause SCC due to residual stress from welding, or to overcome the susceptibility to intergranular corrosion due to carbide precipitation, or the need to assure dimensional stability, may require a form of PWHT known as solution annealing. Solution annealing puts carbides back into solution and restores normal corrosion resistance. PWHT temperature ranges and heating and cooling rates must be selected to avoid the following potential problems [143]:

1. Heating in the range of 800–1650°F (425–900°C) can result in sensitization.
2. Heating welds between 1000 and 1700°F (540–925°C) can transform ferrite to a hard, brittle sigma phase. Sigma-phase formation while carrying out PWHT can be minimized if the maximum weld metal ferrite number is limited to 10–12 FN.
3. Stabilized stainless steels such as Types 321 and 347 will be susceptible to reheat cracking.

Solution Annealing. PWHT of stainless steels usually involve solution annealing at temperatures of 1950–2050°F (1065–1120°C) followed by rapid cooling or water quenching. Material not stabilized with columbium or titanium should be cooled through the range from 1700 to

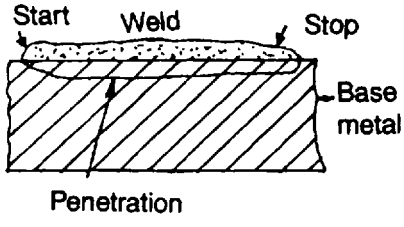


Figure 23 Beginning-and-end defect. (From Ref. 150.)

1000°F (927 to 538°C) in not more than 3 minute. The rapid cooling should be continued to below 800°F (427°C). Since the solution annealing temperature range is very high (1900°F minimum), unless stainless steel is protected from air at these temperatures, it oxidizes rapidly, forming adherent oxide scale; if thin sections are not adequately supported, they may sag or warp.

PWHT Cracking. Stainless steels may suffer cracking in the HAZ during PWHT or during high-temperature use. PWHT cracking is more likely to form in the stabilized grades containing niobium and titanium; it does not occur in molybdenum-bearing grades unless niobium is present, and therefore niobium additions should be avoided in molybdenum-bearing steels that are likely to be used in high-temperature applications [103].

Welding Stainless Steels to Dissimilar Metals

On many occasions, it is necessary to weld austenitic stainless steels to other materials, including carbon, low-alloy steel, martensitic and ferritic stainless steel, copper alloys, and nickel alloys. Welding procedures for dissimilar metal joints must consider differences in strength, chemical composition, corrosion resistance, thermal expansion, and heat-treatment response [143]. Important weldability problems with dissimilar metals welding include (1) solidification cracking, and (2) dilution of the weld metal, which can result in martensitic weld metal that is susceptible to hydrogen-induced cold cracking.

Methods to Overcome Dilution Problems. Dilution problems associated with the mixing of dissimilar metals in weld runs can be solved with reference to a Schaeffler constitutional diagram. This can be particularly helpful in choosing a proper filler metal and welding parameters to give adequate control of the delta ferrite and austenite phase. Methods to overcome dilution problems are [143]:

1. Base metal dilution should be minimized by use of low heat input and stringer bead techniques.
2. When joining stainless steel to mild steel, it is a usual practice to use a more highly alloyed filler metal in order to allow for the dilution on the mild steel side.
3. Buttering the carbon steel base metal prior to completing the joint is an effective technique to minimize dilution.

Filler Metals for Welding SS With Dissimilar Metal. Welding filler metals for joints between carbon or low alloy steels and austenitic stainless steels must be selected to prevent solidification cracking. For dissimilar metal welding, particularly between carbon steels and austenitic stainless steels, Type 309 electrodes and filler metals are probably the most commonly used filler metals. Nickel-alloy filler metals are recommended for critical service conditions and service temperatures above 800°F. To weld one of the extra-low-carbon unstabilized varieties, a correct choice is to use a matching electrode, rather than using a high-carbon stabilized electrode [137].

PWHT. If postweld heat treatment is required, the temperature and heat treatment cycles must be carefully selected to avoid sigma phase formation in the weld, sensitization of austenitic steels, or problems due to differences in thermal expansion.

Postweld Cleaning

Welding-related surface contamination and imperfections such as weld splatter, welding slag, arc strikes, heat tint, oxides, and other surface contaminants can be a source of corrosion initiation. Thorough postweld cleaning is necessary to remove the welding contaminations and to obtain optimum corrosion resistance of the parent metal. The cleaning procedure should avoid the formation of oxide films, which render the SS susceptible to various forms of corrosion. Procedures should allow for repassivation [118].

Welding contamination is best removed by the use of a wire brush not used for other purposes, abrasive disks, flapper wheels, or pickling. Grinding should be avoided, since this procedure tends to overheat the surface, thereby reducing its corrosion resistance. Or subsequently, overheating or "bluing" of the surface must be avoided, or removed perfectly, preferably by acid pickling. Avoid chloride-bearing solvents for cleaning stainless steels. Generally, a nitric acid final wash oxidizes the surface and passivates the metal [119]. ASTM A380 details ways to clean stainless steel.

Corrosion Resistance of Stainless Steel Welds

During all welding processes, the surfaces affected by welding will be subjected to various metallurgical and surface-related phenomenon that locally weaken the passive film and make it susceptible to pitting corrosion. The general rules of good welding practice also apply to welding of stainless steels for corrosion resistance. Pitting corrosion resistance of stainless steel welds depends on the following factors [118]:

1. Microstructure and chemical composition in the vicinity of the weld metal surface.
2. Inclusions.
3. Weld spatter, arc strikes, contaminations from fabrication and shop environment.
4. Residual welding stresses.
5. Geometric surface defects, notches, solidification cracks, and crevices.
6. Surface oxides, inhomogeneous structure, depletion of the alloying element from the underlying parent metal.

Measures for optimization of the pitting corrosion resistance of stainless steel welds are as follows:

1. Careful selection of welding consumables and fabrication procedures.
2. Gas shielding to avoid surface oxide formation.
3. Root fluxes to protect the metallic surfaces from oxidation.
4. Postweld cleaning.

17 FERRITIC STAINLESS STEELS

17.1 Conventional Ferritic Stainless Steels

Ferritic stainless steels are basically Fe-Cr (conventional ferritics) or Fe-Cr-Mo (mostly superferritics) alloys containing approximately 11 to 30% chromium, and when molybdenum is added, resistance to pitting corrosion increases. Conventional ferritic stainless steels are listed in the 400 series. Ferritics are magnetic. Typical conventional ferritic stainless steels are given in Table 21. High-chromium ferritic stainless steels have good resistance to corrosion, including resistance to chloride stress corrosion cracking. Oxidation resistance of the ferritic steels is also very good, especially for the high-chromium grades such as Type 446, or when aluminum and rare earths are added. They cannot be hardened by heat treatment and only moderately by cold working. In spite of equivalent corrosion resistance and low-cost alloying elements, the ferritic steels have been surpassed by the austenitic stainless steels, primarily because of their lower formability and toughness and reduced weldability [151,152]. These drawbacks are minimized in light gages, so the bulk of current use of ferritic steels is in light gage tubular and sheet form. To improve the weld metal ductility, sometimes welding of Types 430 and 446 is done with austenitic filler metals. This solves the ductility problem but can lead to loss of corrosion resistance [119]. These alloys have higher thermal conductivity, lower thermal expansion, and lower cost. Types 430, 443, and 446 have become popular in low-pressure,

Table 21 Composition (%) of Ferritic SS [151]

Gr	Cr	C	Mn	Si	Other
405	13.0	0.06	0.50	0.30	0.25 Al
409	11.0	0.05	0.50	0.30	0.40 Ti
429	15.0	0.05	0.50	0.30	—
430	16.5	0.05	0.50	0.30	—
434	16.5	0.04	0.50	0.30	1.0 Mo
436	16.5	0.04	0.50	0.30	1.0 Mo, 0.4 Cb
442	21.0	0.08	0.50	0.30	—
446	26.0	0.08	0.50	0.30	(N_2 optional)

high-temperature heat exchangers [153]. A new kind of ferritic stainless steel, Type 444 has less carbon than L grades and is stabilized with titanium and columbium to prevent sensitization. This grade shows major improvements in as-welded ductility compared with conventional ferritics.

17.2 "New" and "Old" Ferritic Stainless Steels

When reviewing the various commercial ferritic stainless steels, it is appropriate to distinguish between the "old" and the "new" steels. The newer varieties are called as superferritics. The old ferritic stainless steels are represented by the standard AISI grades as shown in Table 21.

Superferritic Stainless Steels, Superaustenitic Stainless Steels, and Duplex Stainless Steels

Type 316, which is generally considered one of the most corrosion-resistant of the common austenitic stainless steels, has not performed consistently well under conditions of total immersion in seawater. Even though copper-nickels or nickel-base materials or titanium can serve the purpose, these materials are usually expensive than stainless steels. A need was recognized for less costly materials for use in seawater applications, with greater resistance to chloride stress corrosion cracking and crevice corrosion than Type 316. Thus, a new generation of austenitic stainless steels known as superaustenitics and ferritic stainless steels known as superferritics were developed, usually with Mo as an alloying element to stabilize the passive film in the chloride-bearing environment. Since 1980, the high-performance stainless steels have become the first choice for seawater-cooled steam condensers [101]. These steels are discussed in the next section.

17.3 Superferritic Stainless Steel

Superferritics refer to iron-chromium stainless steel alloyed with molybdenum for improved pitting corrosion resistance and titanium or niobium for improved resistance to intergranular corrosion. Their major advantage is very high resistance to chloride stress corrosion cracking. The ferritic structure and low or zero nickel content also provide high resistance to stress corrosion cracking (SCC). They also exhibit better general corrosion resistance.

Before the advent of the advanced steel melting and refining methods, ferritic stainless steels had relatively high levels of interstitials—carbon and nitrogen—and as a result had serious limitations with respect to fabricability, toughness, and corrosion resistance. The newer ferritics, especially those with high chromium content, have become possible through argon-oxygen decarburization (AOD), vacuum induction melting (VIM), and vacuum oxygen decarb-

urization (VOD). All are capable of producing low interstitials content [154]. During the refining stage, care is taken to reduce interstitials to very low levels and/or to "tie up" carbon and nitrogen by stabilizing them with elements such as titanium or niobium.

Alloy Composition

The superferritic grades contain up to 29% Cr (although grade 18Cr-2Mo is sometimes considered a superferritic material), 4% Mo, and in some alloys, 3.5% Ni, and have completely ferritic microstructures. The well-known superferritics include 18-SR (Armco), 18Cr-2Mo, 26-1S, E-Brite 26-1 (Airco, Alleghney Ludlum), and 29Cr-4 Mo (Du Pont), with UNS S44735, 29Cr-4 Mo-2Ni (Du Pont), and Sea-Cure (UNS S44660), containing 26% Cr, 3% Mo, and 1% Ni. They are primarily proprietary grades. Their compositions are given in Table 22 and their product form ASTM/ASME reference in Table 23. For the most part, the workhorses in the superferritics category have been Alloy 29-4 (UNS S44735) and Alloy Sea-Cure (UNS S44660) [115]. Both have titanium and niobium (also known as columbium) added to stabilize their carbon and nitrogen contents. Alloy trade designations for various superferritics, superaustenitics, and duplexes to be discussed in next sections are given in Table 24.

Table 22 Selected Ferritic Stainless Steels

UNS no.	Alloy	C	Cr	Ni	Mo	N_2	Others
S43035	18-SR	0.05	18	0.5	—	0.020	2Al, 0.4Ti, 1Si
S44400	18-2	0.02	18	—	2	0.020	0.4Ti, 0.3Cb
S44625	26-1	0.01	26	0.5	1	0.015	0.5Ti
S44627	E-Brite	0.003	26	—	1	0.008	0.10Cb
S44660	Sea-Cure	0.01	26	2.5	3	0.025	0.4Ti
S44635	Monit	0.025	25	4	4	0.025	Nb + Ti
S44735	29-4C	0.02	29	0.3	4	0.020	0.4Ti, 0.2Cb
S44800	29-4-2	0.01	29	2	4	0.020	—

Note. The ferrite content is not explicitly mentioned.

Table 23 Superferritic Stainless Steel Grades, ASTM/ASME Code References, and Product Shapes [113]

Grade UNS no.	ASTM spec.	Products forms available	ASME, Section VIII, Div. 1
Sea-Cure S44660	A240, A268, A176, A763	Welded tubing, sheet, strip	Code case 1922
Al 29-4-2 S44800	A176, A240, A240, A268, A276, A314, A479, A731	Welded tubing, sheet, strip, plate upto 0.5 in, welding wire	SA240, SA268, SA479, SA731
AL 29-4C S44735	A176, A240, A268, A511	Welded tubing, plate, sheet, strip	Code case 1921
Monit S44635	A176, A240, A268	Welded tubing, sheet, strip, welding wire	Code case 1900
E-Brite (XM-27) S44627	A176, A240, A268, A276, A314, A479, A731	Plate, sheet, strip, seamless and welded tubes	SA176, SA240, SA268, SA276, SA314, SA479, SA731

Table 24 Alloy Trade Designations

Alloy UNS no.	Registered trade name	Producers
S44635	Monit	Uddeholm Steel Corp.
S44627	E-Brite	Allegheny Ludlum Steel Corp.
S44735	AL 29-4C	Allegheny Ludlum Steel Corp.
S44660	Sea-Cure	Trent Tube Div. of Colt Ind., Crucible Steel Co.
S44800	AL 29-4-2C	Allegheny Ludlum Steel Corp.
S31254	254 SMO	Avesta Jarnverks AD
N08904	AL 904L	Allegheny Ludlum Steel Corp.
N08366	AL-6X	Allegheny Ludlum Steel Corp.
N08367	AL-6XN	Allegheny Ludlum Steel Corp.
N08925	1925hMo, 25-6MO	VDM Technologies, Inco-Alloys Internationals
N08026	20Mo-6	Carpenter Technology

Note. This table gives only partial information on various alloy manufactures.

Applications

Superferritics have found extensive applications as tubing for power plant condensers, and heat exchangers handling chloride solutions, seawater, and brine. Types 18Cr-2Mo, E-Brite 26-1, Sea-Cure, and AL 29-4 are used in the petrochemical and chemical industries and in seawater applications. Because of its high chromium content, E-Brite 26-1 offers substantial resistance to oxidation and sulfidation at elevated temperatures. The E-Brite alloy is being used in air preheaters and heat recuperators.

Physical Properties

The ferritic stainless steels offer two physical properties that are of particular importance [154]:

1. Their thermal conductivity is about 50% higher than that of the austenitics, or about half that of carbon steel.
2. Their thermal expansion coefficient is low, roughly equal to that of carbon steel and about 30% less than that of type 304 stainless steel.

Strength. The strength of ferritics is compared with austenitic stainless steels as follows [151]:

1. The room-temperature yield strength in the annealed condition is 20–40% higher than that of the austenitic steels.
2. The rate of work hardening of the ferritic steels is lower.
3. At high temperature, the ferritic steels have lower strength than the austenitics, but their oxidation resistance is very good.

Toughness and Embrittling Phenomena. Toughness of the ferritic stainless steels is influenced by three embrittling mechanisms [151]: (1) "885°F (475°C) embrittlement," (2) sigma phase precipitation, and (3) high-temperature embrittlement. Each of these conditions lowers the ductility and toughness of the ferritic stainless steels at room temperature and hence imposes restriction on the fabricator and user in various operations such as hot forming, brazing, welding, and heat treating in order to minimize high-temperature exposure [155].

"885°F (475°C) Embrittlement." All ferritic stainless steels, with the possible exception of Type 409, are susceptible to this embrittlement phenomenon when exposed in the temperature range of 720–950°F (400–540°C). Peak hardening and embrittlement occur at approximately 885°F as a result of the formation and precipitation of alpha prime, a coherent chro-

mium-rich particle in the iron-rich matrix [151]. Consequently, an increase in hardness and tensile strength is observed, concurrent with substantial decrease in ductility and impact resistance [156]. The phenomenon is observed at chromium levels in excess of about 12%. In order to overcome this form of embrittlement during processing, fast cooling is recommended through the 700–950°F temperature range. Consequently, neither the new nor the old ferritics should be exposed to this temperature range [151,154].

Sigma Phase Precipitation. Sigma phase may form in the higher chromium ferritic steels (15 to 20%) when they are exposed for prolonged periods at 1100 to 1500°F. The precipitation results in room-temperature embrittlement as well as loss of corrosion resistance [151]. Formation of sigma phase may be minimized or prevented by a proper selection of composition, or sigma phase may be transformed into austenite and ferrite by suitable heating, followed by water quenching or rapidly cooling by other means.

High-Temperature Embrittlement. When high-chromium stainless steels of intermediate and high interstitial content are heated normally above about 1000°C and cooled to room temperature, precipitation of carbide and nitride can result in embrittlement as well as susceptibility to intergranular corrosion, especially in alloys containing high interstitial elements [151].

Ductile–Brittle Transition. The superferritic stainless steels with body-centered cubic (bcc) crystal structure exhibit a ductile-to-brittle transition temperature (DBTT) that for many grades is close to room temperature. The interstitial elements carbon and nitrogen have a potential effect on the DBTT; a low interstitial elements content is essential for a low DBTT and hence good toughness at room temperature. For this reason, all the new ferritic stainless steels have very low interstitial elements content, obtained by special melting techniques [151]. The new grades are acceptably tough as both sheet and tubing, and therefore these alloys are typically used in thin sections, such as tubing, light-wall pipe, sheet, and strip. However, VIM-produced superferritics have extremely low carbon and nitrogen levels and thus improved toughness. These materials are usually used in all product forms up to plate thickness of about 0.50 in (12.7 mm) [101].

Corrosion Resistance

Because the chromium content of the ferritic stainless steels ranges from 11 to 29%, the general corrosion resistance can vary from moderate to excellent [151]. An important feature of the ferritic stainless steels is their resistance to chloride stress corrosion cracking. Because the austenitic steels are highly susceptible to SCC, the ferritic steels provide a more economical alternative than the nickel-base alloys for applications requiring resistance to SCC. Superferritic stainless steels offer outstanding resistance to chlorides, alkalies, nitric acid, urea/ammonium carbomate, amines, and organic acids [152]. Additions of molybdenum increase the resistance to pitting corrosion by producing a more stable passive film. The pitting resistance equivalent (PRE) number is calculated using the formula

$$\text{PRE} = \%\text{Cr} + 3.3(\%\text{Mo})$$

Intergranular Corrosion in Ferritic Stainless Steels. A major obstacle to the use of ferritic stainless steels has been their susceptibility to intergranular corrosion [157]. Ferritic stainless steels are sensitized when exposed to a temperature of about 1800°F (982°C) due to welding or improper heat treatment, and this makes them susceptible to intergranular corrosion. The mechanism responsible for intergranular corrosion is generally accepted as being the same as that in austenitic stainless steels [158]. This problem is overcome by alloying with titanium and/or columbium to form the carbides of these elements. Lowering the carbon content below

0.03%, as in austenitic stainless steels, is not effective. Even with 0.01% maximum carbon content, it is necessary to add carbide-stabilizing elements [151].

Fabricability

The ductility and toughness of the ferritic stainless steels are low at room temperature. The sequence of fabrication operations, and often the design, should consider the relatively low toughness and ductility of the material at room temperature. Cold-forming operations must also be commensurate with possibly reduced ductility and toughness [155].

Welding

The two most important factors in making good welds in the superferritics are (1) the maintenance of alloy purity and (2) that ferritic weld metal structure cannot be refined by heat treatment [103]. Superferritic stainless steels tend to retain the problem of conventional ferritic steels in relation to grain growth in HAZ, grain coarsening in the weld metal, and loss of toughness after welding and reduced corrosion resistance due to sensitization and sigma phase precipitation. The problems faced while welding ferritic stainless steels are summarized by Walker [159]:

Grain growth.
Coarse-grained weld metal.
Reduced impact strength.
Reduced corrosion resistance due to sensitization and precipitation of sigma phase.

Being highly magnetic, they are subjected to arc blow during welding. The following measures will help to reduce some of these problems [159]:

TIG welding with good shielding and backing.
Extreme cleanliness of weld preparation.
Autogenous welding or matching filler.
Low heat input to minimize grain growth.

Since the high quality of these steels is based on low carbon and nitrogen contents, it is essential that the pick up of these elements during the welding process should be avoided due to the risk of chromium carbide and nitride formation, resulting in loss of corrosion resistance [103,140]. Avoid the pickup of oxygen and hydrogen also. Careful shielding, front and back, with dry argon or helium is necessary [154]. Cleanliness and extraordinary inert gas shielding are essential for successful welding, particularly when matching filler metal is used.

Low heat input is necessary to limit grain growth. The grain growth problems can also be minimized by using austenitic filler materials, and still there is some grain growth in the HAZ; this can be reduced by keeping preheat temperature below 200°C [137].

The ferritics are less prone to welding defects than the austenitics, but their notch sensitivity makes any defects that are present much more detrimental. Therefore, special care must be taken to avoid undercutting or poor penetration, and thorough inspection of welds is essential [154].

Surface Preparation and Joint Design. Surface preparation and cleaning before and after welding are important for assured weld quality and corrosion resistance. Edge preparation of weld joints includes removal of all contaminated metal by machining or grinding the thermally cut surfaces. Weld joints and filler metal surfaces must be free of surface contaminants. A nonchlorinated, residue-free solvent, such as methyl ethyl ketone (MEK), is useful for this

purpose. Cleaning should immediately precede welding. Optimum corrosion resistance is obtained by mechanically or chemically removing the heat tint after welding.

Good Practices for Welding Ferritic Stainless Steels. Beigay et al. [140] discuss good practices for ferritic stainless steel welding. Some of the good practices include the following:

1. Minimize contamination by running stringer beads. Stringer beads are preferred over a "weaving" technique.
2. Keep ends of filler rods protected in shielding gas. Filler metal must not be pulled in and out of the shielding gas. Once pulled away from the shielding gas, the contaminated tip must be removed before the wire is used again.
3. Welding techniques that minimize contamination must be employed.
4. Allow shielding gas to flow after extinguishing the arc, protecting the weld bead and filler tip until both cool sufficiently to prevent oxidation.
5. To protect weld puddles, shield with pure argon or helium, or by vacuum. Avoid shielding gases containing carbon dioxide, nitrogen, or oxygen. Prefer gas metal arc welding and gas tungsten arc welding, because they shield the welding area well.
6. Brush tack welds with a stainless steel wire brush, then weld to complete the root pass. Finish the weld using the same shielding used for tack welds and root pass.
7. Between passes, remove oxides with brushes having bristles of stainless steel, not ordinary carbon steel. Carbon steel bristles, or grinding wheels containing carbon, will carbonize and crack stainless steel welds [150].

The gas tungsten arc welding (GTAW) process is required to achieve the degree of shielding necessary.

Filler Metals. Although matching filler metals have been used successfully in a few cases, the most satisfactory results are obtained with low-carbon, austenitic stainless steel or nickel-base fillers.

PWHT. This structure cannot be refined by heat treatment; however, the use of low heat inputs during welding will restrict the amount of martensite formation, and following by an annealing heat treatment will be useful.

18 DUPLEX STAINLESS STEELS

As the name implies, duplex stainless steels have a mixed microstructure of ferrite and austenite in the proportion of 50 : 50. For these steels, the chromium content may vary from 22 to 27% and molybdenum 2 to 4%, depending upon corrosion resistance required. Typical newer varieties of duplex stainless steels include Alloy 2205, known as Code Plus Two, 44LN, and Ferralium 255 (S32550), which also contain 2% copper, 7 Mo-PLUS (UNS S32950), Atlas 948, and 253 ME. Of these varieties, Ferralium 225 is regarded as the only seawater duplex stainless steel [101]. 7 Mo-PLUS is being used very successfully in both tube-side and shell-side cooler condensers for nitric acid production [115]. Because of their higher strength and better resistance to stress corrosion cracking than conventional austenitic stainless steels, duplexes are now gaining acceptance.

18.1 Composition of Duplex Stainless Steels

Duplex stainless steels usually contain high chromium (22–27%) and Mo (2–4%). The compositions are carefully controlled to maintain the proper balance of austenites and ferrites. The high chromium content makes duplex alloys exhibit strong resistance to oxidation. The nickel content varies from 4 to 7%. Because of lower nickel content, duplexes costs less. The addition

of 0.15–0.25% nitrogen enhances strength and toughness, and improves pitting and chloride stress corrosion cracking. Their carbon content is low. Material compositions for a selected duplex SS are given in Table 25. The specification for various product forms has been included both in the ASTM and ASME Code Section VIII, Div. 1. A partial list is shown in Table 26.

18.2 Comparision With Austenitic and Ferritic Stainless Steels

Because the duplex stainless steels are balanced with the composition of austenitic and ferritic phases, their physical properties fall between the comparable properties of the austenitic and ferritic stainless steel. Salient features of their properties compared to austenitic and ferritic stainless steels are:

1. Duplexes offer higher strength and toughness, good corrosion resistance, and better resistance to chloride SCC than austenitics and they are relatively low cost material.
2. Duplexes have a higher yield strength than the austenitics; this provides an economic advantage due to use of lighter gauge material compared to austenitic stainless steel. But duplexes are not suitable for cryogenic service.
3. At higher temperatures, there is a change in phase balance, and their use is not recommended for high-temperature applications.
4. The large amount of ferrite phase present in the duplexes makes them magnetic.
5. Because of the segregation of the ferrite and austenite phases, various duplex alloys can show variability in pitting and crevice corrosion resistance.
6. Duplexes have better toughness than ferritic grades. Compared to ferritics, the ductile-to-brittle transition temperature of the duplex alloy is more gradual and occurs at a lower temperature (below room temperature), thus allowing the production of thick plates; this allows manufacture of tubesheets.
7. The thermal conductivity is less than half that of carbon steel, but about 25% more than that of austenitic stainless steel.

Table 25 Selected Duplex Stainless Steels [116]

UNS no.	Alloy	C	Cr	Ni	Mo	N	Others
S31803	2205	0.02	22	5.5	3	0.12	—
S32550	Ferralium 255	0.04	25	5.5	3	0.15	2Cu
S32900	7 Mo	0.052	27	4.22	1.39		0.28Mn, 0.39Si, 0.014S
S31200	44 LN	0.028	25	5.9	1.46	0.19	1.75Mn, 0.53Si, 0.03S
	Ferralium 225	0.02	26.2	5.64	3.20	0.19	0.77Mn, 0.37Si, 0.16Cu

Table 26 ASTM Specification for Duplex Stainless Steels

Product form	ASTM spec.	ASME spec.
Bar	A276	—
Sheet, strip, plate	A240	SA240
Pipe (welded and seamless)	A790	SA790
Tubing (welded and seamless)	A789	SA789

8. The coefficient of thermal expansion is about 40% less than that of austenitic stainless steel, but equal to that of carbon steel.

18.3 Corrosion Resistance of Duplex Stainless Steels

Although their nickel contents (4 to 7.5%) are less than those of austenitic stainless steels, their SCC resistance is much better than would be expected from nickel content alone. Duplex stainless steels have two important advantages over Types 304 and 316 stainless steels [115]: (1) good resistance to chloride stress corrosion cracking, and (2) higher mechanical properties with good ductility. Because the duplexes have a higher yield strength than the austenitics, SCC resistance may usually be maximized with a 50 : 50 microstructure. Because nickel is a factor for providing corrosion resistance in reducing environments, the duplexes show less resistance in these environments than the austenitics.

The high chromium and molybdenum contents of the duplex stainless are particularly important in providing resistance in oxidizing environments and are also responsible for the better pitting and crevice corrosion resistance, particularly in chloride environments. The pitting resistance equivalent (PRE) number is calculated using the formula [116]:

$$PRE = \%Cr + 3.3(\%Mo) + 16(\%N)$$

Duplexes are produced with low carbon contents, usually less than 0.03%, and hence, intergranular corrosion due to sensitization of weld metal as a result of carbide precipitation generally is not a problem.

Laboratory corrosion tests include Critical pitting temperature by ASTM G-48A, ASTM A262-C (Huey Test) for IGC, and ASTM G30 and G36 for SCC.

18.4 Process Applications

The duplex alloys have excellent resistance to oxidizing and reducing acids, sulfuric acid below 25% concentration, organic and acid mixtures, seawater and sour oil and gas wells, and alkali solutions [160]. Duplexes are applied successfully in applications containing corrosive chlorides, like oil and gas plant components, pulp and paper plants, chemical processing as heat exchangers, tanks, pressure vessels, columns, flue gas scrubbers, boiler tubes, digester preheaters, evaporators, etc.

18.5 Welding Methods

Welding methods used for austenitic SS can be used except for the use of pure argon shielding during welding to protect cerium addition. The welding processes most applicable are GTAW, GMAW, PAW, SMAW, and SAW [161].

Weldability

The goal in welding duplex SS is to obtain weld metal and HAZ having the same corrosion resistance, toughness, and absence of intermetallics. The trick in welding the duplex SS is avoiding the formation of excess ferrite. The advantage of corrosion resistance and mechanical properties can be achieved in welded assemblies when the welding practice ensures formation of a 50 : 50 austenitic–ferrite phase both in the weld metal and in the HAZ. The following problems are normally faced while welding duplex stainless steels [159]:

High ferrite phase and hence reduced toughness.
Liquation cracking.
Grain growth in HAZ.

Reduced corrosion resistance due to sigma phase, and carbonitrides precipitates.
Precipitation of chromium nitrides, which reduce corrosion resistance.

To overcome these problems, the following measures will help [159]:

Overalloyed filler metal with higher Ni content and with a guaranteed PRE value of not less than 40 [162].
Controlled heat input.
Controlled interpass temperature (limited to 200°C maximum).

Balancing the Austenite and Ferrite Phases. Balanced phases can only be ensured if the cooling rate is slow enough to allow austenite to reform as the weld cools. If the rate is too slow, embrittling phases may form; on the other hand, if it is too fast intermetallics could form. Autogenous welding will increase the ferrite phase in the weldment and adjacent areas of the base metal. Subsequent annealing will tend to restore the balance of phases in the base metal.

Heat Input. High weld heat inputs, preheat, and interpass temperatures promote coarse-grained weld deposits and HAZ and the tendency to precipitation is enhanced [161]. Welding heat input should be controlled to limit the ferrite level, whereas too low a heat input produces too much ferrite, and it has been suggested that heat inputs above 1.5 kJ/mm must be employed [163].

Liquation Cracking. Duplex SS is susceptible to HAZ liquation cracking due to the formation of low-melting-point films of S and P along the grain boundaries, and the effect is aggravated in the presence of restraint and residual stresses.

Precipitations of Secondary Phases. Duplexes are susceptible to the precipitation of sigma phase due to the higher concentration of ferrite-forming elements. Base metals with low carbon, balanced ferrite–austenite phases, and adequate nitrogen speed the reformation of austenite during cooling, and avoid secondary sigma phase formations.

Precipitation of Chromium Nitrides. Due to the increased amounts of nitrogen that are now used to strengthen the austenite, chromium nitrides (Cr_2N) are usually formed in the weldments intragranularly, along with sigma phase. This causes the formation of secondary austenite in the surrounding material due to reduction in concentration of ferrite-forming elements. This secondary austenite causes the localized loss of corrosion resistance due to its low chromium content [103].

Welding Consumables. When consumables that match the parent plate material compositions are used, the final weld metal microstructure may be low in austenite and high in ferrite, causing a loss in toughness unless a slow cooling rate is ensured. Satisfactory phase balance is obtained by use of consumables that are overmatched in nickel by 2 to 3%.

Welding Practices. Welding practices should ensure cleanliness, provide inert gas shielding, and avoid carbon contamination. Since ferrite is susceptible for hydrogen embrittlement, low-hydrogen welding practices should be followed. It is not necessary to heat-treat these duplexes after welding.

Welding Practices to Retain Corrosion Resistance. Welding practices to retain corrosion resistance include the following [161]:

1. Special attention is need to control weld spatter, slag residues, and oxide formation, since these have adverse effects on resistance to pitting and crevice corrosion.
2. As far as possible, postweld cleaning is to be done; when cleaning is not possible, restrict oxygen to values of 10 ppm and 25 ppm maximum inert backing gases. To promote arc stability and penetration, small additions of CO_2 and O_2 may be made to argon shields when employing GMAW technique.

18.6 Nondestructive Testing (NDT) of Duplex SS

Radiographic and dye penetrant inspection procedures are readily applicable. NDT by conventional ultrasonic techniques with angle beam shear waves can be difficult, owing to the anisotropy of the parent materials and weld deposits, especially the tendency to epitaxial columnar structures in the latter [161]. Improved techniques using angle beam compression wave probes and creep wave probes at diminished frequencies are reported.

19 SUPERAUSTENITIC STAINLESS STEELS WITH Mo + N

Superaustenitic stainless steels are alloys with a face-centered cubic (fcc) structure, highly alloyed, usually containing substantial amounts of chromium, molybdenum, and nitrogen, along with sufficient nickel to stabilize a fully austenitic microstructure. They are classified by their molybdenum content, which is in the range of 4.5–7%. The addition of 0.3 to 0.5% N provides yield strength typically twice that of conventional stainless steels [116]. Relatively high nickel content (18–31%) and high chromium content and Mo content give the alloys excellent resistance to SCC. Copper is intentionally added to some of the alloys and improves resistance to reducing media such as hot phosphoric acid, acetic acid, and dilute sulfuric acid. In this section, superaustenitics are covered under two headings: 4.5% Mo superaustenitic steels, and 6% MO superaustenitic steels.

19.1 4.5% Mo Superaustenitic Steels

The 4.5% Mo austenitic alloys like AL 904L, Ciramet, 254SLX, and JS700 have demonstrated sufficient resistance to corrosion in seawater to perform reasonably well as tubing. They are readily weldable and workable, available in a wide range of product forms such as tubing, sheet, plate, and forgings. Nitrogen content in the range of 0.4 to 0.5% gives good resistance to pitting and crevice corrosion [115]. The high nickel (25%) and molybdenum (4.5%) contents provide good resistance to chloride SCC. They also exhibit resistance to intergranular corrosion. Chlorination to control microbiological fouling is necessary to minimize under-deposit corrosion; flange faces and gasketed surfaces are subject to crevice corrosion in brackish water and seawater [164].

19.2 6% Mo Superaustenitic Stainless Steel

The 6% Mo superaustenitics are now well established in the chemical process industries. They contain about 20% chromium, nickel contents range from 18 to 25%, and they are enhanced with more than 0.10% nitrogen. Nitrogen addition serves to improve strength, stabilize the austenitic structure, and improve pitting corrosion resistance. 6% Mo superaustenitics exhibit excellent toughness and ductility characteristic of the 300 series austenitics. Several 6% Mo superaustenitic stainless steels, their product forms, and ASTM/ASME Code references are listed in Table 27 and their compositions in Table 28 along with Types 304 and 316. Although there are differences in their chemistry to permit three different UNS numbers (UNS S31254, N08367, and N08926) for these 6% Mo superaustenitics, for most applications they have similar corrosion resistance and are used more or less interchangeably [115]. Superaustenitics have an iron content less than 50% and therefore do not fall under the jurisdiction of ASTM Committee A1 on Steel, Stainless Steel, and Related Alloys, except for 254 SMO.

Corrosion Resistance

In general, the high-alloy superaustenitic steels show superior resistance to uniform corrosion, pitting and crevice corrosion, and stress corrosion cracking [165]. The 6% Mo superaustenitics

Table 27 6% Mo Austenitics, with ASTM/ASME References and Product Shapes [167]

Grade UNS no.	ASTM specification	Products forms available	ASME Section VIII, Div. 1
254 SMO S31254	A167, A182, A193, A194, A240, A249, A267, A269, A312, A358, A403, A409, A473, A479	Plate, sheet, strip, bar, billet, wire, pipe, fittings, tube, condenser tube	UHA 23
AL-6X N08366	B675, B676, B688, B690, B691	Condenser tube	UNF-23.3
AL-6XN N08367	B366, B462, B472, B564, B675, B676, B688, B690, B691	Plate, sheet, strip, bar, billet, wire, pipe, fittings, tube, pipe fittings, condenser tube	UNF-23.3
1925hMo N08925	B625, B649, B673, B674, B677	Plate, sheet, strip pipe, tubing, bar, billet	UNF-23.3
25-6MO N08925	B625, B649, B673, B674, B677	Plate	UNF-23.3
20Mo-6 N08026	B463, B464, B468, B474	Plate, sheet, bar, billet, strip, wire, tube, pipe	UNF-23.3

Table 28 Composition of Selected Superaustenitic Stainless Steels Along With Types 304 and 316

UNS No.	Alloy	C	Cr	Ni	Mo	N	Others
S30400	304	0.06	18	8	—	—	—
S31600	316	0.08	17	12	2.5	—	—
S31254	254SMO	0.02	20.0	18	6.2	0.2	0.75Cu
N08367	AL-6XN	0.02	21	24.5	6.5	0.2	0.75Cu, max
	1925hMo,						
N08926	25-6 MO	0.01	20	25	6.5	0.2	1.1Cu
N08366	AL-6X	0.018	21	24.5	6.5		1.39Mn, 0.41Si

resist both localized corrosion and SCC in oxidizing chloride and sulfide/chloride-containing solutions, as well as a broad range of process chemicals. They are widely used in severe seawater applications. The corrosion performance of 6% Mo superaustenitics falls between Types 316 and 317 stainless steels and the nickel-based alloys 625 and C-276 [115]. In order to be resistant to some corrosive environments, some steels also contain additions of copper, which improves its resistance to acids in general. The fully austenitic 6% Mo steels are primarily characterized by a high (Cr + Mo) content, with a pitting resistance equivalent given as [166]:

$$PRE_N = \%Cr + 3.3(\%Mo) + 30(\%N)$$

exceeding 35 in all of the steels.

Applications

In process industries, the 6% Mo superaustenitic stainless steels have replaced common austenitic stainless steels that have failed by pitting, crevice corrosion, and chloride stress corrosion

cracking [167]. They have been used extensively in the offshore and desalination industries, in seawater handling, in chlorine and chlorine dioxide stages and bleach plants in the pulp and paper industries, and in flue gas desulfurization plants. Equipment fabricated of 6% Mo austenitics includes pressure vessels, columns, seawater-cooled condensers, evaporators, heat exchangers, crystallizers, pumps, piping, and components.

Welding

In general, fully austenitic 6% Mo superaustenitic stainless steels exhibit satisfactory weldability. The main concern when using the superaustenitic stainless steels is adequate corrosion resistance in welds. During welding, particular concern has to be paid to the following three phenomena:

1. Hot cracking.
2. Elemental microsegregation.
3. Precipitation of intermetallic phases.

Since the carbon content of the 6% Mo steels is low (<0.03%), the risk of chromium carbide precipitation in the grain boundaries of HAZ and thus the susceptibility to intergranular corrosion is negligible [166].

Hot cracking. Hot cracking occurs either directly during solidification, and is referred to as liquation cracking, or upon reheating of successive weld runs, known as reheat cracking. Both types of cracking are related to the solidification mode of weld deposit and the presence of impurities such as sulfur and phosphorus [165]. Steels that exhibit a primary austenitic solidification mode are more susceptible to hot cracking than those that exhibit ferritic or mixed phases. Susceptibility to hot cracking is overcome by measures such as the use of fillers that deposit weld metals with relatively low levels of trace elements like P, S, and Sn and keep stresses due to restraint during welding to a minimum [166]. Welding should be done with low arc energy.

Molybdenum Microsegregation. 6% Mo steels with high molybdenum levels show large molybdenum microsegregations in autogenous weld metals. The areas depleted in molybdenum have a lower local pitting index and hence they are less resistant to chloride pitting corrosion [165,166]. Therefore, autogenous welds are not recommended for these steels, unless the completed equipment is to receive subsequent homogenization and solution annealing. To overcome the reduction in corrosion resistance, fillers are overalloyed with molybdenum.

Precipitation of Intermetallic Phases. When exposed to high temperature, the relatively high Cr and Mo contents of these steels may stimulate the precipitation of intermetallic phases such as the chi or sigma phases. These intermetallics can reduce the steel's corrosion resistance. To overcome this problem, limit the heat input and interpass temperatures. The heat input should be limited to <15,000 J/cm and the interpass temperature should be restricted to 100°C, with an absolute maximum of 150°C [166].

Arc Welding Filler Metals. If it is practicable to solution anneal and homogenize the weld metal, use a matching filler metal. For applications in severe pitting or crevice corrosion environments, use filler metals that are overalloyed with molybdenum so that the welds are more resistant to corrosion than the base metal [162]. The use of overalloyed filler metals compensates for the lean areas in the deposit caused by microsegregation. The filler metal most frequently used is Alloy 625 with 9% molybdenum, but some fabricators prefer alloy C-276 or C-22 [115]. Welds made with these fillers can be used in the as-welded condition. In addition to proper filler selection, certain measures are to be taken to obtain weld metal of required qualities. They include the following [105,166]:

1. Keep the surface free from contaminations before and after welding. Vapor degreasing or scrubbing with a solvent should be effective in removing all but paint. Alkaline cleaners are required to remove paint.
2. When using nickel-base filler metals, the proper weld preparation is also necessary. Excessive dilution has to be prevented, especially in the root pass area. In order to ensure a sufficiently high proportion of filler metal in the root pass, the root gap should be 2 to 3 mm.
3. To inhibit the formation of oxidation during welding, gas shield the root side.
4. The shielding gas for 6% Mo superaustenitic stainless steels is 90–95% hydrogen and 5–10% pure nitrogen.
5. Cleaning and pickling are necessary.

Welding Processes. The main welding processes employed are SMAW, and manual and automatic GTAW with filler metals. GTAW without filler should only be considered in cases where a subsequent solution anneal heat treatment is to be applied. GMAW, SAW, and automatic plasma arc welding with filler metals are also used.

Postweld Heat Treatment. If the 6% Mo superaustenitics need to be annealed or stress relieved, they must be given a full anneal and water quench. Solution annealing at temperatures of 2102 to 2282°F (1150 to 1250°C) followed by quenching is also commonly used; this helps in better homogenization of the material properties of the weldments. Heat treatments that permit the 6% Mo austenitics to spend time in the 1300 to 1900°F (705 to 1040°C) temperature range make the material susceptible to sigma phase precipitation with loss of corrosion resistance and possibly toughness [167]. Depending on the alloy composition, stress relieving at a temperature up to 1112°F (600°C) for several hours may be used in special cases. In all these cases, the fabricator should follow the material manufacturer's recommendations.

19.3 Corrosion Resistance of Superaustenitic Stainless Welds

The factors that contribute to the loss of corrosion resistance of superaustenitic stainless steel welds and the measures to overcome them are [105]:

1. Microsegregation of molybdenum at localized regions, which most likely takes place when the GTAW process involves autogenous welds, filler metal that has the same composition as the base metal, and high heat input.
2. Unmixed zones. High heat input welding can leave narrow bands of base metal adjacent to the fusion line, which have been melted but not mixed with the overmatched filler metal. This problem is overcome by controlling heat input and avoiding undercutting.
3. Crevices, cracks, and microfissures. Crevice corrosion sites can also occur at the beginning or end of weld passes, between weld passes, or under weld spatter.
4. Sensitization and carbide precipitation. Low carbon content (<0.02%) provides an alloy that is not susceptible to this problem. Molybdenum and nitrogen content increase the level of carbon and/or heat input that can be tolerated.
5. Precipitation of intermetallic phases like sigma and chi phases.
6. Surface contamination by embedded iron, which is removed by acid pickling or abrasive blasting with clean sand or glass beads, and organic contamination, which is removed by suitable solvent.
7. Surface oxide scale or heat tint, which is to be removed by descaling.
8. Shielding gases composition. Adding nitrogen at 3 to 5% by volume to the torch and backing shielding gases enhance corrosion resistance.
9. To impart optimum corrosion resistance to the weld metal, especially for the autogenous

welds, follow these measures: postweld anneal, postweld clean the surfaces, pickle for optimum corrosion resistance, and passivate the surface.

20 ALUMINUM ALLOYS: METALLURGY

Aluminum is a reactive metal. It is known for its higher thermal conductivity, light weight, corrosion resistance, and moderate cost. Its density is about one-third that of steel, which provides a high strength to weight ratio. Untempered, commercially pure aluminum has a tensile strength of 13000 lb/in^2 (89622 kPa) and cold working can double this strength. The low mechanical properties can also be improved by alloying. Typical alloying elements include magnesium, manganese, zinc, copper, and silicon. By taking advantage of cold working, heat treatment, and aging, the strength of aluminum can be raised to 100,000 lb/in^2 (689,476 kPa) [7]. With the addition of copper at 1.9 to 6% (2000 series), the heat-treated properties exceed those of mild steel. Designing in aluminum is much like designing in other metals. Publications from the Aluminum Association, Aluminum Welding Seminar Technical Papers, and others [168] will be of great help.

20.1 Properties of Aluminum

Aluminum alloys have a high resistance to corrosion in most atmospheres, waters, and many chemicals. They are nontoxic, permitting applications with foods, beverages, and pharmaceutical; and they are colorless, permitting applications with chemicals and other materials without discoloration. Their corrosion products are not damaging to the ecology. Aluminum is fabricated and joined readily by most of the metal joining processes. Aluminum is excellent for cryogenic applications; most aluminum alloys have higher ultimate and yield strengths at −350 to −450°F (−212 to −268°C) than they have at room temperature. Other properties of aluminum and its alloys for certain applications are high electrical conductivity, high reflectivity, and nonmagnetic (ensures arc stability).

Aluminum for Heat Exchanger Applications

The unique combinations of properties provided by aluminum and its alloys make aluminum one of the most versatile and economical materials for heat exchanger applications. The properties that favor aluminum for heat exchanger applications are:

1. Light weight and high specific strength. This offers automotive heat exchanger designers the potential for compact low-cost heat exchangers over the more traditional copper and brass materials [169].
2. High thermal conductivity. The thermal conductivity of pure aluminum is about 60% that of pure copper.
3. High resistance to atmospheric corrosion and environments like fresh water, saltwater, and many chemicals and their solutions.
4. Depending on temper, it can be hot or cold formed; it has the ability to be formed into various shapes, tubes, fin patterns, etc.
5. Ability to be joined by welding, brazing, and soldering.
6. Aluminum clad products protect pitting corrosion of the core alloys.
7. They retain toughness and strength, and exhibit high thermal conductivity at subzero temperature. Aluminum maintains excellent strength and ductility to temperatures as low as −321°F (−196°C). It also exhibits high thermal conductivity at cryogenic temperature. For cryogenic services, aluminum alloy 3003 is generally used for the parting sheets, corrugated fins, and edge bars that form the plate fin heat exchangers (PFHE) block. Headers and nozzles are made from aluminum alloys 3003, 5154, 5083, 5086, or 5454.

8. It has hygienic and nontoxic qualities.
9. It is nonmagnetic and nonsparking.
10. There is availability in many product shapes and moderate cost.

Limitations of Aluminum.

1. Aluminum and its alloys rapidly lose strength at temperatures above 100°C; aluminum does not resist fire as well as other materials. It is not generally used for PFHE process temperatures above 150°C, particularly in high-pressure service [170].
2. Aluminum is susceptible to damage by rough handling, excessive vibration, and localized unrelieved stresses.

Wrought Alloys Designations

A system of four-digit numerical designations is used to identify the various wrought aluminum alloys, as shown in Table 29. The first digit indicates the alloy group. The second digit indicates a modification of the original alloy, or the impurity limit in the case of unalloyed aluminum. The third and fourth digits identify the alloy or indicate the aluminum purity.

Classification of Wrought Alloys

Wrought alloys are of two types: not heat-treatable, of the 1xxx, 3xxx, 4xxx, and 5xxx series, and heat-treatable, of the 2xxx, 6xxx, and 7xxx series. In the non-heat-treatable type, strengthening is produced by strain hardening. All non-heat-treatable alloys have a high resistance to general corrosion. Aluminum alloys of the 1xxx series, representing unalloyed aluminum, have a relatively low strength. Alloys of the 3xxx series (Al-Mn, Al-Mn-Mg) have the same desirable characteristics as those of the 1xxx series and somewhat higher strength. Common wrought alloys and their compositions are given in Table 30.

1xxx Series. This grade of aluminum, with minimum 99.00% purity, exhibits excellent corrosion resistance, high thermal and electrical conductivity, excellent formability, but low mechanical properties. They are readily brazed and welded by all methods, and non-heat-treatable. Moderate increase in strength may be obtained by strain hardening. They are used as fin stocks in heat exchangers.

2xxx Series. These alloys are copper based. The copper content is in the range of 1.9 to 6%. These alloys are heat-treatable, and more susceptible to corrosive attack than other groups of

Table 29 Wrought Aluminum Alloy Designations

Designation	Alloying elements	Major alloying elements	Heat treatable
1xxx	99% min. Al	None	No
2xxx	Al-Cu, Al-Cu-Mg-Si (3-6%/Cu)	Copper	Yes
3xxx	Al-Si-Mn	Manganese	No
4xxx	Al-Si-Cu	Silicon	No
5xxx	Al-Si-Cu-Mg Al-Mg (1–2.5% Mg) Al-Mg-Mn (3–6% Mg)	Magnesium	No
6xxx	Al-Mg-Si	Magnesium-silicon	Yes
7xxx	Al-Zn-Mg Al-Zn-Mg-Cu	Zinc	Yes

Table 30 Common Wrought Alloys and Their Compositions [171]

	Composition (%), remainder Al and impurities					
Nominal	Cu	Si	Mn	Mg	Zn	Cr
1050				99.60% minimum aluminum		
1060				99.60% minimum aluminum		
1100				99.00% minimum aluminum		
3003	0.12	0.6	1.2	—	0.1	—
3004	—	—	1.2	1.0	—	—
3005	—	—	1.2	0.4	—	—
5005	—	—	—	0.8	—	—
5050	—	—	—	1.2	—	—
5052	—	—	—	2.5	—	0.20
5154	—	—	0.4	3.5	—	0.25
5454	—	—	0.75	2.7	—	0.12
5456	—	—	0.8	5.2	—	0.1
6061	0.25	0.6	—	1.0	—	0.20
6063	—	0.4	—	0.7	—	—
6151	—	1.0	—	0.6	—	0.25
6951	0.25	0.35	—	0.6	—	—
7005	—	—	0.45	1.4	4.5	0.13
7072	—	—	—	—	1.0	—

wrought aluminum alloys. Heat-treated properties exceed those of mild steel. Fusion welding is not recommended, but resistance welding is recommended.

3xxx Series. The major alloying element is manganese, up to about 1.5%. These alloys are non-heat-treatable. They have moderate strength, good corrosion resistance, and good workability/formability, and are used in pressure vessels and brazed and soldered heat exchangers. These are readily brazed and welded by all methods. Alloys 3003, 3004, and 3105 are widely used as general-purpose alloys for moderate-strength applications requiring good formability and workability. The strength of 3003 is higher than that of 1100 alloy, and 3004 is stronger than 3003. Alloy 3004 is known for fine grain size and general freedom from critical grain growth.

4xxx Series. The major alloying element is silicon. These are non-heat-treatable and are often used for welding and brazing as filler metal with enough silicon to lower the melting point. For example, 4343 containing 7.5% silicon and 4045 containing 10.5% silicon are used as the clad brazing sheet. The core alloy is either 3xxx or 6xxx series.

5xxx Series. Alloys of the 5xxx series (Al-Mg) are the strongest non-heat-treatable aluminum alloys. In most products, they are more economical than alloys of the 1xxx and 3xxx series in terms of strength per unit cost. Alloys of the 5xxx series have high resistance to general corrosion and good resistance in marine atmospheres. The most widely specified weldable grades are alloys 5083, 5052, and 5454. Their applications are numerous in the pressure vessel fields, including cryogenic applications. They are typically available as sheet and plate product forms. These are most fusion welded of any series with a minimum loss of strength. Alloys with more than 3.5% Mg are essentially free from hot cracking. Because of their heavy oxide films, extra care in surface preparation is necessary [172]. These alloys solder and braze poorly.

6xxx Series. These alloys contain both silicon and magnesium, which make the alloys heat-treatable. Compared with other aluminum alloys, these have high resistance to rural atmos-

pheres, and good resistance to industrial and marine atmospheres. They generally possess excellent SCC resistance. These alloys possess good formability, machinablility, and weldability.

The mechanical properties of the heat-treatable 6xxx series alloys are superior to those of the 3xxx series alloys. Compared to 3xxx series, the yield strength of the 6xxx series is about four to five times as high after heat treatment. The higher strength is desirable from the radiator manufacturers' point of view; this helps to minimize tube wall thickness in order to save weight and material cost. But the disadvantages of 6xxx series are their lower melting temperature and higher susceptibility to silicon penetration from the cladding to the core.

The 6xxx series alloys can be soldered, brazed, and resistance spot welded satisfactorily. Alloy 6061 is the most widely specified weldable grade. The most popular temper for 6061 is T6, although the T651, T4, and F tempers are also popular.

The 6xxx series alloys are prone to hot cracking. However, this problem can be overcome by correct choice of filler metal and proper joint design. Care in joint and component design is also needed because of losses in strength in the heat-affected zones. The heat-affected zones strength can be improved, however, through postweld heat treatment [172].

7xxx Series. These alloys contain zinc in the range of 1–8%, and smaller percentage of Mg, Cu, and Cr. They are heat-treatable alloys. 7072 is most widely used as the anodic coating of the tubes and brazing sheet made of 3003, 3003, 5505, 6061, 6951, 7075, and 7178, and as fin stock.

Temper Designation System of Aluminum and Aluminum Alloys

A temper designation system is used to indicate the condition of the product forms. The system is based on the sequences of mechanical or thermal treatments, or both, used to produce the various tempers. The temper designation follows the alloy designation and is separated from it by a hyphen. Aluminum alloys come in four tempers: F, O, H and T. Another, W, is sometimes used to state the unstable condition following solution heat treatment. The digits designate the sequence of basic treatments (e.g., 1100–H14 and 7075–T651). The basic temper designations are shown in Table 31.

Product Forms and Shapes

Aluminum is available in many forms and shapes, which include heat exchanger tubes (plain and integral fin), plates and sheets, bars and rods, and extrusions. Some ASTM specifications for tubes, plates and sheets, pipes, bar, rods, extrusions, and forgings are given in Tables 32 to 34.

Table 31 Basic Temper Designations for Aluminum Alloys

Designation	Conditions
F	As fabricated
O	Annealed, the softest temper
H	Strain hardened
H1	Strain hardened only
H2	Strain hardened and partially annealed
H3	Strain hardened and thermally stabilized
T (T1 to T12)	Heat-treated forms; heat treatment produces needed workability, dimensional stability, and strength
W	Solution heat-treated

Table 32 Heat Exchanger Tubes

ASTM spec.	Description	Alloys UNS no.
B234	Aluminum and aluminum alloy drawn seamless tubes for condensers and heat exchangers	1060, 3003, Alclad 3003, 5052, 5454, 6061, 7072
B404	Aluminum and aluminum alloy drawn seamless condensers and heat exchanger tubes with integral fins	1060, 3003, Alclad 3003, 5052, 5454, 6061, 7072

Table 33 Aluminum Plates and Sheets

ASTM spec.	Description	Alloys UNS no.
B209	Aluminum and aluminum alloy plates and sheets	1060, 1100, 3003, Alclad 3003, 3004, Alclad 3004, 5050, 5052, 5083, 5086, 5154, 5254, 5454, 5456, 5652, 6061, Alclad 6061

Table 34 Pipes, Bars, Rods, Extrusions, and Forgings

ASTM specification	ASME spec.
Aluminum and aluminum alloy drawn seamless tubes	SB210
Aluminum and aluminum alloy bar, rod, and wire	SB211
Aluminum and aluminum alloy extruded bars, rods, wire, shapes, and tubes	SB221
Aluminum and aluminum alloy seamless pipe and seamless extruded tube	SB241
Aluminum and aluminum alloy die forging, hand forging, and rolled ring forging	SB247
Aluminum alloy 6061—T6 standard structural shapes	SB308

20.2 Corrosion Resistance

Surface Oxide Film on Aluminum

Aluminum owes its excellent corrosion resistance to the presence of a thin, compact, adherent aluminum oxide film on its surface. In air, aluminum swiftly acquires a surface film that is self-healing and self-limiting in thickness. The normal surface film thickness in air is about 50 Å [173]. Even if the surface film is damaged, it readily forms on the surface whenever a fresh aluminum surface is created and exposed to either air or moisture/water. Generally the oxide film is stable over the pH range of 4 to 9.0. In strong acids and alkali, the oxide dissolves and hence the metal corrodes rapidly by uniform dissolution, but there are exceptions, such as stability in concentrated nitric acid (pH 1) and concentrated ammonium hydroxide (pH 13).

Chemical Nature of Aluminum: Passivity

Aluminum is an active metal whose resistance to corrosion depends on the passivity exhibited by the protective surface film. In aqueous solutions, the thermodynamic conditions under which the film develops are expressed commonly by the potential–pH diagram (Fig. 24) according to Pourbaix [174]. This diagram shows that aluminum is passive only in the pH range of about

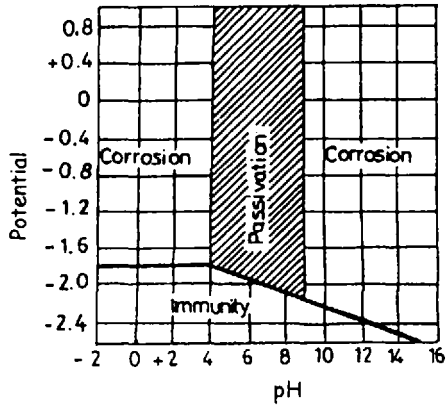


Figure 24 Pourbaix diagram for aluminum. Conditions of corrosion, immunity, and passivation of aluminum at 25°C (77°K) [174].

4–9. Most of the aluminum alloys have good corrosion resistance to natural atmospheres, fresh water, seawater, many oils and chemicals, and most foods. Aluminum tubing is used to handle Freon refrigerants.

Resistance to Waters

Alloys of the 1xxx, 3xxx, and 5xxx, and 6xxx series exhibit corrosion resistance in high-purity water, natural waters, and seawater. A mild reaction takes place when the alloys are first exposed to high-purity water, but it decreases to a low rate within a few days upon formation of a protective oxide film of equilibrium thickness on the alloys.

Natural Waters. Aluminum alloys of the 1xxx, 3xxx, and 5xxx, and 6xxx series have good resistance to most natural fresh waters. If corrosion does occur it takes the form of pitting. The main components of natural water that cause pitting of aluminum are copper ions, bicarbonate, chloride, sulfate, and oxygen. Hard waters have a higher tendency of pitting.

Seawater. Aluminum alloys of the 2xxx and 7xxx series are less resistant and should not be used in seawater unless protected or clad. Among wrought alloys, 1xxx, 5xxx, and 6xxx exhibit good resistance to sea water, and of these alloys, the aluminum-magnesium alloys (5xxx) series has the highest resistance to seawater; hence they are mostly used in seawater applications [175].

Forms of Corrosion

Uniform Corrosion. Most aluminum alloys have excellent resistance to atmospheric corrosion. If surface oxide film is soluble in the environment as in phosphoric acid or sodium hydroxide, aluminum dissolves uniformly and constantly.

Galvanic Corrosion. From its galvanic position, aluminum and its alloys are anodic to most other metals except zinc and magnesium. Contact of aluminum with more cathodic metals should be avoided in any environment in which aluminum by itself is subject to pitting [175]. The most common examples of galvanic corrosion of aluminum alloys in service will take place when they are joined to steel or copper and exposed to a wet saline environment. It is also undesirable to use copper components in aluminum vessels and heat exchangers used in cooling water systems; the presence of a few parts per million of copper in the supply water greatly increases the incidence of pitting attack on the aluminum [176]. Guidelines given to minimize galvanic corrosion in Chapter 12 are applicable for aluminum alloys also. The position of aluminum in galvanic series, which makes the aluminum and aluminum alloys anodic

to most other metals and alloys, is utilized in Alclad products (sacrificial anode) to give cathodic protection to the core alloys.

Pitting Corrosion.

Susceptible Alloys. Of the commercial alloys, 1xxx, 3xxx, and 5xxx have excellent pitting resistance. However, with copper content higher than 0.04%, 3xxx alloys are susceptible to pitting. At 0.15% copper, they pit more extensively, especially in seawater. Alloys of the 2xxx, 6xxx, and 7xxx series are normally clad to protect against pitting.

Factors Responsible for Pitting Corrosion. Pitting corrosion is mostly due to copper, mercury, and halide ions, of which chloride is the most damaging and often encountered in service. Pitting corrosion can be prevented by removal of the reducible species required for a cathodic reaction. In the absence of dissolved oxygen or other cathodic reactant, aluminum will not corrode by pitting since it is not polarized to its pitting potential. Pitting in neutral solutions is caused usually by oxygen.

Pitting Behavior. The rate of pitting corrosion of aluminum depends on its polarization behavior. As with other passive metals, corrosion of aluminum in the passive range, that is, pH range 4–9, may be of pitting corrosion. Pitting of aluminum diminishes beyond this range, and corrosion proceeds uniformly.

Stress Corrosion Cracking. SCC does not occur in commercial-purity alloys (1xxx), aluminum-manganese alloys (3xxx), and aluminum-magnesium alloys containing less than 3% magnesium (5xxx) and strengthened by cold work. On very rare occasions, SCC occurs in the aluminum-magnesium-silicon alloys (6xxx).

Susceptible Alloys. SCC in wrought aluminum alloys is generally limited to those containing appreciable amounts of soluble alloying elements of copper, magnesium, silicon, and zinc [175]. Alloys that can be strengthened by cold work are relatively immune to SCC. The wrought alloys that are susceptible to SCC include the following [175,177]:

The 2xxx series containing copper with smaller amounts of magnesium, manganese, and other elements.

The 7xxx series containing zinc with small amounts of magnesium, manganese, copper, and silicon, if any.

The 5xxx series containing more than 3% magnesium with or without other alloying elements.

Factors Affecting Resistance to SCC. In aluminum alloys, this cracking is characteristically intergranular. Factors that affect SCC of aluminum alloys are given next.

Directional Property of Aluminum. SCC of an aluminum wrought alloy in a susceptible temper is determined by the magnitude and the duration of a tensile stress acting on its surface, and additionally, it is also determined by the direction of stressing. The effect of stressing in different directions is caused by the highly directional grain structure that is typical of many aluminum wrought products [173,175]. Resistance, which is measured by the magnitude of tensile stress required to cause cracking, is highest when the stress is applied in the longitudinal direction, lowest in the short transverse direction, and intermediate in the other direction. Resistance in the short transverse direction usually controls application of products that are of thick section or machined products with sustained tensile stresses in the short transverse direction.

Environment. Water or water vapor is a requisite for the SCC of aluminum, and in its absence, cracking does not occur. Among the species that accelerate cracking further, chlorides have the greatest effect [175].

Mitigation of SCC of Aluminum Alloys. In addition to the usual procedures for preventing SCC of materials, there are several methods specifically applicable to aluminum alloys [173]:

1. Forging and extrusions should be machined to their final dimensions prior to heat treatment.
2. Stressing of extrusions in the short transverse direction of extrusion should be avoided.
3. Cathodic protection in the form of Alclad layers on the surface of high-strength sheet material may be used to prevent general corrosion and SCC.
4. For most commercial alloys, stress-relieved tempers have been developed that provide a high degree of immunity to SCC.

Standard Test Method for Determining Susceptibility to SCC of High-Strength Aluminum Alloys Products: ASTM G47. This is the standard practice for determining the susceptibility to SCC of high-strength 2xxx (with 1.8–7.0% Cu) and 7xxx(with 0.4–2.8% Cu) aluminum alloy products, particularly when stressed in the short transverse direction relative to the grain structure.

Exfoliation Corrosion. Exfoliation is subsurface corrosion that begins on a clean surface but spreads below it. It is well known in aluminum alloys and to a certain extent to copper-nickels. The attack differs from pitting in that the attack has a laminated appearance. It proceeds generally along the grain boundaries, laterally from the sites of initiation along planes parallel to the surface. The corrosion attack causes a leafing or delamination and sometimes a blistered surface. Due to exfoliation, whole layers of material are eaten away. The end of a sample looks like a pack of cards in which several cards have wasted away.

Susceptible Alloys. In certain tempers, wrought products of some aluminum alloys are subject to exfoliation corrosion, which causes a leafing or delamination of the products. This type of corrosion develops in products that have a pronounced directional structure, in which the grains are elongated highly and thin relative to their length and width. Alloys of the 2xxx, the 5xxx series with higher magnesium, and 7xxx series are most prone to exfoliation corrosion. It is rare in wrought alloys of the non-heat-treatable type (1xxx, 3xxx) and heat-treatable type 6xxx. Exfoliation can be overcome by heat treatment and alloying [173,178].

Standard Test Method for Determining Exfoliation Corrosion Susceptibility. ASTM G34 is the immersion test method for determining exfoliation corrosion in 2xxx and 7xxx series aluminum alloys (EXCO test). This test method is applicable to wrought products such as plates, sheets, extrusions, and forgings. ASTM G66 is an immersion test of 5xxx series aluminum alloys for exfoliation corrosion, known as the ASSET test.

Intergranular Corrosion. Aluminum alloys that do not form second-phase microconstituents at grain boundaries, or those in which the constituents have corrosion potentials similar to the matrix, are not susceptible to intergranular corrosion. Aluminum alloys such as 1100, 3003, and 3004, aluminum-magnesium alloys (5xxx) containing less than 3% magnesium, are not affected by intergranular corrosion. The 6xxx series alloys generally resist this type of corrosion [175]. Thermal treatment in 2xxx, 5xxx with more than 3% Mg, and 7xxx series alloys that cause grain boundary precipitation is susceptible to intergranular corrosion. The level of susceptibility to corrosion increases with (1) magnesium content, (2) the amount of cold work, and (3) exposure time at temperature [173]. Resistance to intergranular corrosion is achieved by use of heat treatments that cause precipitation to be more uniform throughout the grain structure or by restricting the alloy element that causes the intergranular corrosion.

Crevice Corrosion. Crevice corrosion of aluminum is negligible in fresh water. In seawater, it takes the form of pitting and the corrosion rate is low.

Erosion-Corrosion, Cavitation, and Impingement Attack. Aluminum and its alloys are susceptible to cavitation, impingement, and erosion-corrosion.

Corrosion Fatigue. Aluminum alloys, like many steels, have relatively low corrosion fatigue strength, about half the fatigue strength in air and about 25% of the original ultimate strength

of material. Corrosion fatigue failures of aluminum alloys are characteristically transgranular and differ from SCC failures, which are usually intergranular. Localized corrosion of the aluminum surface provides stress rises and greatly lowers fatigue strength and hence fatigue life [173].

Corrosion of Aluminum in Diesel Engine Cooling Water System. Uniform corrosion may take place in poorly inhibited or uninhibited glycol/water mixtures. Localized corrosion is initiated with the breakdown of the passive film by chloride ion. Pitting and crevice corrosion may be prevented by the use of inhibitors. Anions commonly used to reduce the effect of corrosion may be classified into two classes: (1) oxidizing, those that form a passive film on the metal surface; and (2) nonoxidizing, those that act as blocking agents by forming insoluble precipitates with aluminum ions [179]. Benzoate, phosphate, and silicate are examples of nonoxidizing inhibitors. Oxidizing inhibitors include nitrates and chromates.

Corrosion Prevention and Control Measures

A number of corrosion preventive measures have already been described. Important methods of preventing corrosion of aluminum include [173,175]: (1) alloy and temper selection, (2) design considerations of equipment, (3) inhibitors, (4) cathodic protection, (5) use of Alclad products, (6) modification of environment, and (7) thickened surface oxide film and organic coating. Some of these methods are discussed next.

Alloy and Temper Selection. In general, aluminum-magnesium alloys 5xxx series have the best corrosion resistance, followed by commercial-purity alloys series 1xxx and 3xxx, and 6xxx in that order. Alloys 2xxx and 7xxx are usually given a protective coating such as cladding. Temper selection gives better resistance to intergranular corrosion and exfoliation corrosion for alloys 5xxx, whereas in alloys 7xxx, improved resistance to SCC is being achieved [173].

Design Aspects. The design aspects that influence corrosion behavior include improper choice of alloy or temper, galvanic couple, failure to provide sealants in the crevices to avoid crevice corrosion, and selection of the joining method and filler metals.

Inhibitors. Phosphates, silicates, nitrates, fluorides, benzoates, etc. have been recommended for use with aluminum in some services. If copper is present in a closed system, use sodium mercaptobenzothiazole to prevent copper corrosion and subsequent depostion corrosion of the aluminum.

Cathodic Protection. In some applications, aluminum alloy parts are protected by cathodic protection, either by sacrificial anode or impressed current method. Since cathodic reaction produces hydroxyl ions, the current on these alloys should not be high enough to make the solution sufficiently alkaline to cause significant corrosion [180].

Alclad Alloys. The use of Alclad products to resist corrosion has been well established. Alclad alloys is a composite product in which a thin surface layer of one aluminum alloy (anodic), usually 5 to 10% of the total thickness, is metallurgically bonded to the main core alloy (cathodic), which was selected to provide the desired strength and the cladding to provide the maximum resistance, mostly to perforation by pitting. The difference in the potential between the core alloy and the cladding alloy provides cathodic protection to the core. The cladding generally used is alloy 7072, which contains 1% zinc and has a solution potential of –0.96V, which is at least 100 mV more anodic than typical core alloys such as 3003 and 6951. Since the claddings are anodic to the core, preferential corrosion of the cladding takes place until the core and cladding interface. After reaching the interface it spreads laterally, avoiding localized corrosion. Alclad products are primarily available in the form of sheets and tubes, coated on one or both sides. For example, Alclad tubes are used in brazed aluminum radiators to avoid

pitting corrosion of tubes on the water side. Typical combinations of Alclad products generally used in heat exchanger applications are given in Table 35.

Modification of the Environment. Such modifications are reducing the corrosivity of an environment, adjustment of pH of a solution, deareation of water to minimize oxygen content and hence to reduce the tendency to pit aluminum, etc.

Thickened Surface Oxide Film and Organic Coating. Coatings by diffusion cladding or thermal spray will act in the same way as the cladding layer and corrode sacrificially to protect the core alloy [175].

Aluminum Diffused Steels in Petroleum Refinery Heat Exchangers. Aluminum vapor diffusion into the surface of iron-base or nickel-base alloys offers one method of protecting steel tubes (the process is known as alonizing) and other components in heat exchangers from the harmful effects of high-temperature oxidation, sulfidation, and carburization [181]. As a result, this process finds broad application for heat exchangers used in chemical plants and petroleum refineries.

20.3 Fabrication

Aluminum alloys can be joined by most fusion and solid-state welding process as well as by brazing and soldering. Fusion welding is commonly done by GMAW, GTAW, FCAW, SMAW, resistance spot, and seam welding. Plasma and electron beam welding are used for special applications. Oxyfuel gas welding may be used for applications where high strength and quality are not essential for the intended service. Flux shielding is unsuitable for aluminum because flux tends to corrode the metal and produce spatter. Fusion welding of aluminum is discussed next. Brazing and soldering are covered in the chapter on heat-exchanger fabrication.

Parameters Affecting Aluminum Welding

The parameters that influence welding aluminum and its alloys include surface oxide film, thermal conductivity, thermal expansion, reflectivity, lack of color change during melting, nonmagnetic, use of backing bars, surface preparation and cleanliness, gas shielding, welding heat on base metal properties, and hot cracking. These parameters are discussed in detail by Lancaster [176] and Young [182]. Salient features of these points are discussed here.

Surface oxide film. The surface oxide film on aluminum and its alloys is insoluble in the weld metal and inhibits wetting by molten filler metals. Additionally, the dielectric nature of the oxide film may prevent a stable starting of the welding arc. Therefore, to permit good wetting and fusion, the surface oxide must be removed from its surface before welding, brazing, and soldering.

Thermal conductivity. The higher thermal conductivity of aluminum (approximately three times that of steel) requires higher heat inputs. Thick sections may require preheating to reduce the heat input.

Table 35 Alclad Alloys

Core alloy	Cladding alloy
3003	7072
3004, 6061	7072 or 7013
6951	7072
7075	7072, 7008, or 7011
7178	7072

Thermal expansion. Higher thermal expansion diminishes the root gap in a butt joint; shrinkage during solidification (about 6%) narrows the root gap, and stresses try to crack the weld metal and warp the weldment. Measures to prevent cracking and distortion include clamping, fixturing, use of chill bars, and changing welding techniques.

Reflectivity. Aluminum sheets and plates reflect about 80% of light and heat rays. When employing arc welding, therefore, the welders must be protected against burns from reflected as well as direct rays. The intensity of burns is maximum when welding curved surfaces, such as the inside of a cylinder.

Lack of color change during melting. Aluminum does not assume a dark red color at 1200°F (649°F) just prior to melting, as does steel, but it appears to collapse suddenly at the melting point. The lack of color change makes it difficult to judge when the metal is approaching the molten state. Hence, practice in welding is required to learn to control the rate of heat input.

Nonmagentic. Aluminum is nonmagnetic, and therefore, arc blow is not encountered when arc welding with direct current.

Backing bars. While welding, some form of backing for the molten pool is necessary. Removable backing bars of steel or cast iron are satisfactory, provided that the welding groove is of adequate depth [176]. Permanent backing bars are rarely used because they introduce undesirable notch effect and welds are subjected to defects that originate at the root of the joint.

Root gaps. Large root gaps cannot be bridged.

Cleanliness. When fabricating aluminum, maintain a high standard of cleanliness. The method of edge prepartion and cleaning determines weld quality.

Gas shielding. In a gas-shielded process, the maintenance of a satisfactory nonturbulent argon cover in the vicinity of arc and weld pool is essential [182]. Failure to observe this leads to weld defects like oxide inclusions, lack of fusion, and porosity. While employing GMAW, puckering and tunneling occur in welding at high currents due to turbulent conditions in the molten pool and entrainment of air in the gas shield. This is overcome by using an auxiliary gas shield or by increasing the primary gas coverage to prevent air being sucked in with argon.

Effect of welding heat on base metal. Welding heat weakens the base metal next to the weld; the weak zone is about an inch either side of the center of the butt or fillet welds. Heat-treatable alloys can be stengthened by heat treatment, but only cold working strengthens non-heat-treatable alloys [7].

Hot Cracking. Aluminum welds are susceptible to hot cracking. Sensitivity to hot cracking is influenced by composition of the filler metal, the degree of dilution by the base metal, and restraint on the weldment. The following meaures help to overcome hot cracking:

1. Avoid weld metal compositions known to be sensitive to cracking. Combining magnesium and copper in an aluminum weld metal is not desirable.
2. Use welding procedures that minimize restraint of the alloy being welded.
3. Select a filler metal of a compostion whose solidus temperature is close to that of the base metal [48].
4. Use a filler metal of higher alloy content than the base metal.

Surface Preparation and Surface Cleanliness. Most porosity in aluminum welds is due to surface contaminants like shop dirt, cutting fluids, oils, grease, and marking crayons. Therefore, to obtain weld metal of desired quality, aluminum surfaces are to be clean. Surface cleaning may be done by these methods [7]:

Solvent degreasing. Wiping, spraying or dipping, and vapor degreasing remove oil, grease, dirt, and loose particles.

Mechanical cleaning. This is oxide removal by stainless steel wire brushing, filing, milling, rubbing with steel wool, sanding, rotary planing.

Chemical cleaning. Use immersion in 5% sodium hydroxide (caustic soda) solution at 160°F (70°C) for 10–60 s, followed by rinse in commercial desmuting solution at room temperature for 10–30 s, followed by a hot-water rinse and air-dry.

Plate Cutting and Forming. Cut aluminum to size and shape and prepare its edges with most metal-working tools and methods. However, oxygas cutting won't work with aluminum. Care has to be taken while bending aluminum and its alloys with regard to scoring and mechanical damage because of their softness. It is essential to avoid iron and other foreign metallic embedments or inclusions into aluminum surfaces. To ensure this, cover the plates with plastic or sheets of paper and pasting paper over the rolls or by inserting a sheet of hardboard between the plate and the rolls. Lift large sheets or plates with vacuum lifters.

Joint Design. Joint design is important in selecting the joining method. If butt joints are required, the choice is limited preferably to an inert gas or vacuum-shielded fusion welding process or a solid-state welding process.

Joint Geometry. In general, the recommended joint geometries for arc welding aluminum are similar to those for steel. However, smaller root openings and larger groove angles are generally used because aluminum is more fluid and welding gun nozzles are larger. Joint geometry for aluminum welding is shown in Fig. 25.

Preheating. Preheating is usually avoided, because the properties and metallurgy of aluminum almost always suffer from high heat. If preheating is unavoidable, heat aluminum for a short while without exceeding 300°F (149°C).

Corrosion Resistance: Welded, Brazed, and Soldered Joints

Most aluminum base metal and filler metal combinations are satisfactory for service under normal conditions. For best performance in specific corrosive environments, the filler metal composition should nearly match the composition of the base metal. Some environments or chemicals may require the use of high-purity filler metals or tight limits on composition. For example, for some saltwater applications, weld 1100 plate with 1100 filler weld.

Welding Filler Metals

Aluminum welding rods and bare electrodes are generally used with the gas tungsten arc, gas metal arc, and oxyfuel gas welding processes. While selecting aluminum filler metal, consider these factors: (1) ease of welding, (2) corrosion resistance, (3) resistance to high temperatures, (4) response to anodic treatments, (5) enhanced strength or ductility, and (6) minimized chances for hot cracking. Choose a filler with higher alloy content than the base metal. To obtain the desired weld metal properties, the filler metals should be free from gas and nonmetallic inclusions and surface contamination. Keep the welding wire covered and store it in a dry area at even temperatures. Do not open a new box of wire until ready to use it. Filler metals for the most widely specified weldable grade alloys 5052, 5083, 5454, and 6061 are given in Table 36.

Welding Methods

Gas-Shielded Arc Welding. Gas metal arc welding (GMAW) and gas tungsten arc welding (GTAW) have almost entirely replaced other arc welding processes for aluminum alloys. The workhorse welding process is GTAW, argon shielded for root passes, followed by GMAW fill

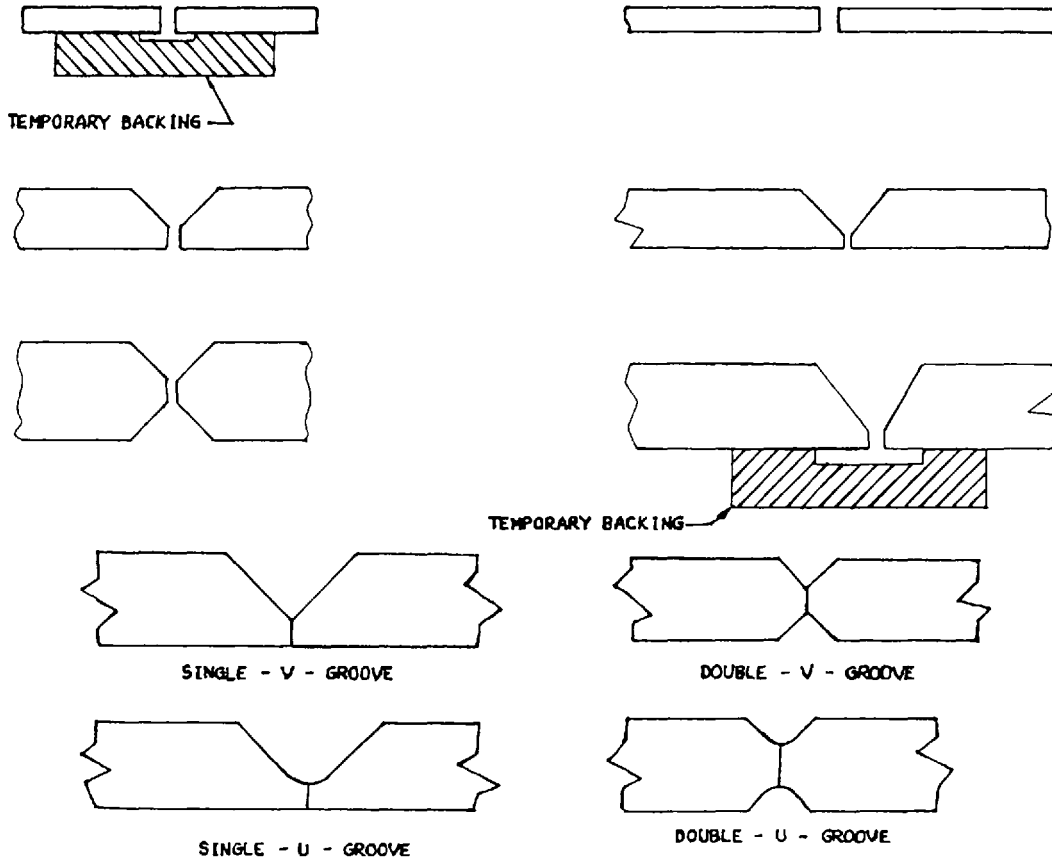


Figure 25 Typical joint design for arc welding of aluminum.

Table 36 A Guide to Aluminum Welding Filler Metal Selection [172]

Base metal	Filler metal
5052	5183, 5356, 5556
5083	5183, 5356, 5556
5454	5183, 5556
6061	5183, 5556, 4043

passes and in some cases a GTAW cover pass to dress the weld surface. Edge preparation is typically a 45 to 73° opening with a 1/16-in low.

Gas Tungsten Arc Welding Process. The GTAW process solved the two problems associated with aluminum, namely, high heat conductivity and aluminum oxide surface film, by concentrating large amounts of heat to remove the refractory oxide, then melting the base metal rapidly. The GTAW process uses a consumable aluminum filler rod, and inert gas shielding (usually argon, which protects the electrode, filler, and weld metal from oxidation). An alternat-

ing current (ac) is most often used, because it not only provides heat input to the base metal but also removes the oxide surface film. Fluxes are not required. Welders usually restrict ac operation to thickness less than 0.25 in (6.35 mm), handling heavier gages by dcsp GTAW or GMAW.

GTAW by Direct Current. GTAW is performed with direct current straight polarity (dcsp) or reverse polarity (dcrp). With straight polarity welding, current flows (electron) from the electrode to the work, and the oxide film is not removed. To remove the oxide film, electrons must flow from the joint, and this is achieved with reverse polarity (dcrp).

Gas Metal Arc Welding. GMAW is probably the most popular method for welding aluminum in heavier gages other than GTAW. It is capable of much higher production rates than GTAW. Higher current density, coupled with efficient heat transfer in the arc, give deep penetration, high welding speeds, minimum distortion of base metal, and good mechanical strength. Weld metal transfer modes include spray (the most desirable), globular, short-circuit, and pulsed spray. In GMAW, direct current reverse polarity is used to establish arc between the consumable electrode and the work piece in a shield of inert gas (argon or helium).

Merits of Gas-Shielded Arc Welding Processes. GMAW and GTAW processes result in optimum weld quality and minimum distortion, and they require no flux. Since there is no flux is used, (1) difficult-to-reach places and completely inaccessible interiors are left without the danger of corrosion from residual corrosive flux, (2) welding can be done in all positions, because there is no slag to be removed out of the weld by gravity or by puddling, and (3) visibility is good because the gas envelope around the arc is transparent and the weld pool is clean.

21 COPPER

Metallurgy and Physical Properties. Copper is a noble metal. It has excellent electrical and thermal conductivity; it is malleable and machinable. Being a noble metal, it resists many corrosive environments. Other useful properties include ductility, formability, easy joinability by most conventional methods, nonmagnetic, availability in many products, proven service performance, and moderate cost. However, it has low mechanical properties and must be cold worked or alloyed to obtain strength. Typical alloying elements include zinc, aluminum, nickel, silicon, tin, iron, and so on. There are hundreds of copper alloys. Copper combines with zinc, tin, silicon, aluminum, and nickel to create the major copper alloy families. Copper is completely soluble in nickel and vice versa. Small additions of alloying elements ensure specific purposes—for example, silver provides resistance to softening; beryllium, hardenability; lead, machinability; phosphorus deoxidizes; phosphorus, antimony, arsenic, and tin give resistance to dezincification; iron adds strength and resistance to erosion-corrosion; and nickel adds high strength and resistance to various corrosion types [183,184].

21.1 Copper Alloy Designation

To bring order and to identify the many alloys, the Copper Development Association [185], together with the American Society of Testing and Materials and the Society of Automotive Engineers, developed a five-digit system. This system is part of the Unified Numbering System (UNS) for metals and alloys. In this system, the numbers C10000 through C79999 denote the wrought alloys; cast copper and copper alloys are numbered from C80000 through C99999. Wrought copper alloys are divided in the UNS system in the following groups.

Copper and high-copper alloys	C1xxxx
Zinc brasses (Cu-Zn)	C2xxxx
Zinc-lead brasses	C3xxxx
Zinc-tin brasses	C4xxxx
Tin bronzes	C5xxxx
Aluminum, manganese, silicon bronzes	C6xxxx
Copper-nickel alloys	C7xxxx

For selecting copper cast products, refer to Peters et al. [186].

Wrought Alloys

In Table 37, the major alloy groupings used for pressure vessels and heat exchangers, the UNS number ranges, and the major alloying elements are given.

21.2 Heat-Exchanger Applications

Heat-exchanger materials require good thermal conductivity, strength, corrosion resistance, ease of formability into various shapes like tubes, tubesheets, and fins by processes like drawing, roll forming, bending, blanking, shearing, machining, etc., and joinability. Copper and copper alloys offer good combinations of these properties. In addition, copper alloys have a biostatic action, which gives tube surface antifouling properties. The three major areas of applications of copper and copper alloys are in (1) steam condenser tubings, (2) automotive heat exchangers such as charge air coolers, radiators, and oil coolers, and (3) condensers and evaporators of refrigerators and air conditioners.

21.3 Copper in Steam Generation

Copper alloys such as admiralty brass, cupronickels, aluminum bronze, and the nickel-base alloy Monel have found wide use in feedwater heaters. Their subsequent corrosion by the feedwater, although minor, gives rise to the problem of carryover of copper into the steam generator and possible blockage in turbine units. With the advent of the high-pressure supercritical units, the use of carbon steel tubes in feedwater heaters became common practice in order to eliminate the main source of copper carryover into the steam generator [47,78].

21.4 Wrought Copper Alloys: Properties and Applications

In this section, wrought copper and copper alloys that are used for the construction of heat exchangers and pressure vessels are discussed.

Coppers

High-purity coppers such as C10100, C10200, C10400, C10500, C10700, C10800, C11000, C11300, C11400, C11500, and C11600 are included in this category. They contain at minimum

Table 37 Alloy Groupings and UNS Number Ranges

Coppers	C10100–C15760	>99% Cu
High-copper alloys	C16200–C19600	>96% Cu
Brasses	C20500–C28580	Cu-Zn
Leaded brasses	C31200–C38590	Cu-Zn-Pb
Tin brasses	C40400–C49080	Cu-Zn-Sn-Pb
Aluminum bronzes	C60600–C64400	Cu-Al-Ni-Fe-Si-Sn
Silicon bronzes	C64700–C66100	Cu-Si-Sn
Copper-nickels	C70000–C79900	Cu-Ni-Fe

99.3% copper. The elements like silver, arsenic, antimony, sulfur, phosphorus, lead, nickel, cadmium, zirconium, magnesium, boron, and bismuth may be present singly or in combination. These commercially available in various types (oxygen-bearing, oxygen-free, and deoxidized). Due to their high thermal conductivity, these metals are entirely used for fins and tubes for charge air cooler, intercooler, oil cooler, soldered radiator, and condenser and evaporator of air conditioner, refrigerator, and heater coils. They have good resistance to atmospheric corrosion and galvanic corrosion.

Oxyen-Free Coppers. The oxygen-free coppers have mechanical properties similar to those of the oxygen-bearing coppers, but their microstructures are more uniform. They have excellent ductility and resistance to fatigue, and can be joined readily by welding, brazing, and soldering. Silver is sometimes added to oxygen-free copper to increase the strength at elevated temperature.

Phosphorus-Deoxidized Copper (C12000 to C12300). C12000 (DLP), C12200 (DHP), and C12300 (DHP) belong to this category. Due to good thermal conductivities, they are extensively used as tubes in charge air coolers, condensers, and evaporators in sugar and fertilizer industries, refrigerators, and air conditioners. Deoxidized copper is popular in the construction of process equipment because it can be oxyacetylene welded, silver brazed, and soldered. Deoxidized coppers suffer embrittlement when heated in a reducing atmosphere at 370°C or above.

Fire-Refined Copper. C12500, C12700, C12800, C12900, and C13000 are used for radiator manufacture.

High-Copper Alloys

The wrought high-copper alloys C19200 and C19400 contain a minimum of 96% copper. C19400 is essentially, copper with the addition of about 2.4% iron. Iron addition enhances strength and corrosion resistance. These alloys are known for good formability, excellent soldering, brazing, and shielded arc welding, and good oxyacetylene welding. They are resistant to SCC. The alloys are primarily used as seam-welded condenser tubing in desalting service.

Brasses (Copper-Zinc Alloys)

Brasses contain zinc as their principal alloying element. C23000, C24000, C26000, C26800, C27000, and C28000 belong to this category. Other major alloying elements are lead, tin, and aluminum. The addition of zinc to copper decreases the melting point, density, thermal conductivity, and modulus of elasticity, among others. It increases the strength, hardness, ductility, and coefficient of thermal expansion. These alloys are suspectable to dezincification and SCC. Lead is added to improve machinability. The addition of tin, nominally about 1%, increases strength and resistance to dezincification. Aluminum is added to stabilize the protective surface film.

Muntz Metal (60Cu-40Zn), C28000. This has generally better resistance to sulfur-bearing compounds than higher copper alloys. It shows poor cold-working but excellent hot-working properties, and is the strongest of Cu-Zn alloys.

Leaded Brasses (Cu-Zn-Pb), C31200–C38590

Leaded Muntz metal or leaded brasses such as C36500, C36600, C36700, and C36800 belong to this series, with good resistance to corrosion in both fresh and saltwater. C36500 is an uninhibited alloy and susceptible to dezincification. Others, C36600, C36700, and C36800, are inhibited alloys containing As, Sb, or P as an inhibitor element (0.02–0.1%), which imparts high resistance to dezincification.

Tin Brasses (Cu-Zn-Sn-Pb), C40400–C49080

Admiralty brass, C44300, is extensively used in water-cooled condensers and coolers of petroleum refining and petrochemical operations. It is attacked by pitting, and ammonia SCC and dezincification in environments containing high concentrations of ammonia and hydrogen sulfide. Cracking of admiralty brass tubes has been a recurring problem in a number of refinery heat exchangers during shutdown when ammonia-containing deposits on the tube surfaces are exposed to air. This problem can be overcome by spraying the tube bundle with a very dilute solution of sulfuric acid, immediately after the tube bundle is withdrawn from the shell. Small amounts (0.02–0.11%) of P, As, or Sb increase resistance to dezincification.

Inhibited Admiralty Brass. C44300, C44400, and C44500 exhibit resistance to dezincification and good corrosion resistance in various service environments such as fresh water, seawater, brackish water, steam and steam condensates, and sulfur compounds encountered in refinery operation. However, they may fail in service due to high impingement velocity and ammonia SCC.

Naval Brass—C46400, C46500, C46600, C46700. Addition of 0.75% tin to Muntz metal (60Cu-40Zn) results into naval brass. Naval brass exhibits good resistance to industrial, rural, and marine atmosphere, petroleum products, alcohols, dry gases, and seawater. It has fairly good resistance to weak bases, but generally poor resistance to solutions of cyanides and ammonium compounds. It resists dezincification and offers good resistance to both fresh and saltwater. Addition of inhibitor elements P, As, or Sb in small amounts (0.02–0.11%) to C46400 results in inhibited naval brasses—C46500, C46600, and C46700—which resist dezincification.

Aluminum Bronzes (Cu-Al-Ni-Fe-Si-Sn), C60600–C64400

Aluminum bronze contains typically 5–17% aluminum with or without iron, nickel, manganese, and silicon. Typical wrought copper-aluminum alloys are C60800, C61000, C61300, C61400, C61500, C61800, C62300, C63000, and C63200. Alloys range from single-phase composition containing up to about 7% aluminum to complex two-phase alloys containing up to 11% aluminum with additions of iron, nickel, and manganese. They are available in cast and wrought forms. They are generally suitable for service in alkalies, neutral salts, nonoxidizing acid salts, and many organic acids and compounds. They resist corrosion of water—potable, brackish, or seawater. Aluminum bronze and copper-nickel alloys represent the two most important copper alloy groups for seawater applications. Salient characteristic features of aluminum bronzes are:

1. Aluminum bronzes resist oxidation and scaling at elevated temperatures due to the formation of aluminum oxide on the surface.
2. Aluminum bronzes offer outstanding strength and resistance to erosion-corrosion.
3. They can be joined by welding and brazing.
4. Susceptible to SCC in moist ammonia and mercurous solution.
5. Resist dealloying but to different degrees depending on alloy composition.
6. The corrosion characteristics are affected by the microstructure of the alloy. A small amount of tin added to C61300 will inhibit intergranular stress corrosion.

Aluminum bronze tubesheets and wrought tubes are extensively used in condensers using seawater. Tubesheets of these alloys are compatible with most condenser tube alloys like C70600, C71500, C68700, and titanium. The cast from (C95400, C95500, C95800) is used as heat exchanger tubesheets and water box.

Silicon Bronzes (Cu-Si-Ag), C64700–C66100

C65100 silicon bronze B (98.5Cu-1.5Si) and C65500 silicon bronze A (97Cu-3Si) are notable in this group. These alloys contain about 3% silicon and manganese at about 1%. They are known for excellent mechanical properties, workability (both cold working and hot forming), good joinability, and corrosion resistance, particularly corrosion fatigue.

Aluminum Brass

Aluminum brass owes its resistance to impingement attack in high-velocity seawater and brackish water to a strong tenacious oxide film on its surfaces. It is prone to dezincification; however, this is overcome by inhibiting with arsenic (0.02–1%). The inhibited arsenical aluminum brass (C68700) finds extensive use in fossil power plant condensers, boiler feedwater heaters, and shipboard condensers. It is an alternative to inhibited admiralty brass, where cooling-water velocity is high.

Copper-Nickels (Cu-Ni-Fe), C70000–C79900

Copper-nickels or cupronickels, C70400, C70600, C71000, C71500, and C72200, are single-phase solid solution alloys, with nickel as the principal alloying element. Alloys containing 10 and 30% nickel are important from the heat-exchanger construction point of view. They are resistant to fresh, brackish, and seawater. Copper-nickel alloys with the addition of iron and sometimes manganese are resistant to erosion-corrosion and SCC. Iron enhances the resistance to impingement attack of these alloys, if it is in solid solution. The presence of iron in small microprecipitates can be detrimental to corrosion resistance. Copper-nickels are an alternative to inhibited admiralty metal tubes where cooling-water velocity is high. General corrosion rates for C70600 and C71500 in seawater are about 1 mpy. Maximum design velocities for condenser tubes are 3.6 m/s (12 ft/s) for C70600 and 4.6 m/s (15 ft/s) for C71500.

At elevated temperatures, the creep strength of cupronickels is greater than that of copper and brasses. Therefore, they find use in high-temperature and high-pressure feedwater heaters and heat exchangers [187]. The cupronickels are highly resistant to SCC. Of all the copper alloys, they are the most resistant to SCC in ammonia environments. Therefore, they are sometimes installed in the air removal sections (Fig. 26) of large-surface condensers.

They are prone to nonuniform and pitting corrosion, if sulfide is present, for instance, during intermittent service [109]. Dealloying has rarely been seen in the cupronickels.

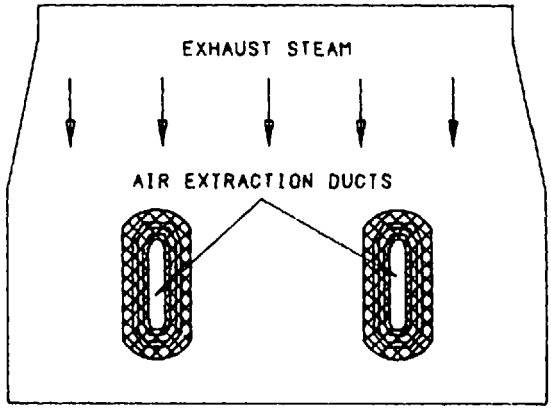


Figure 26 Air removal section in a surface condenser [196].

The 10% copper-nickel (90Cu-10Ni), C70600, finds applications in heat exchangers and condensers in seawater applications, feedwater heaters, and refinery heat exchangers.

The 30% copper-nickel (70Cu-30Ni), C71500, is also known as chromium copper-nickel (67.2Cu-30Ni-2.8Cr). Among all the copper alloys, this alloy exhibits excellent resistance to impingement attack, SCC, and corrosion of most acids and waters and steam condensates. It is used in applications involving severe corrosion problems such as power-plant condensers, feedwater heaters, shipboard heat exchangers and condensers, refinery heat exchangers like overhead condensers and coolers, and aftercoolers. Because of its lower thermal conductivity than brass, some designers provide 5–10% more heat-transfer area [187].

21.5 Designation of Copper and Copper Alloys Used as Heat-Exchanger Materials

A detailed list of copper and its alloys and the nominal compositions used in various types of heat exchangers is given in Table 38.

21.6 Product Forms

Copper alloys are available in shapes like plates, sheet and strip, heat exchanger tubes (bare and integral fin), and ferrule stock. ASTM designations for heat exchanger tubes are shown in Table 39, and for plates, sheets, and strips in Table 40.

22 COPPER CORROSION

22.1 Corrosion Resistance

Copper is classed as a noble metal, and therefore copper is corrosion resistant. The formation of a thin protective layer on the surface is the reason for the corrosion resistance of the copper alloys, such as brass, copper-nickel, and bronze. The presence of oxygen or other oxidizing agent is essential for corrosion to take place. Copper alloys are resistant to neutral and slightly alkaline solutions with the exception of those containing ammonia, which causes SCC [131]. They are resistant to urban, marine, and industrial atmospheres. Copper and most of the copper alloys are sensitive to velocity effects. They are resistant to water and find use in domestic and industrial systems and in seawater applications. They are attacked by oxidizing acids, NH_4OH plus O_2 can cause SCC, and hydrogen sulfide, sulfur, and its other compounds attack [189]. Important sources on corrosion of copper are Ref. 183 and Cieslewicz et al. [190].

22.2 Galvanic Corrosion

Copper and copper alloys occupy a mid position in the galvanic series. Copper is cathodic to aluminum and stainless steel, yet anodic to passive stainless steel, high-nickel alloys, and titanium. In seawater applications, tubes made of cupronickels, stainless steel, and titanium are more noble than tubesheets made of Muntz and aluminum bronze. Therefore, there will be a galvanic corrosion of tubesheets made of the latter alloys when the tubes are made of the former materials. Galvanic corrosion will also take place between tube inserts and tubes when the stainless steel inserts are fitted into copper tubes to overcome erosion-corrosion.

22.3 Pitting Corrosion

The main drawback of copper alloys is their susceptibility to pitting corrosion in water containing the combination of oxygen and sulfide. Hence, copper is not suitable for coastal water

Table 38 Copper and Its Alloys Used in Heat Exchangers

UNS no.	Common name	Composition
C10100 (OFE)	Oxygen-free electrolytic (electronic) copper	99.99% Cu min
C10200 (OF)	Oxygen-free copper without residual deoxidants	99.95% Cu min
C10300	Oxygen-free extra-low-phosphorus copper	99.95% Cu min
C10400	Oxygen-free copper with silver	99.95% Cu min
C10500		
C10700		
C10800	Oxygen-free low-phosphorus copper	99.95% Cu min
C11000	Electrolytic tough-pitch copper	99.95% Cu min
C11300	Silver-bearing tough-pitch copper	99.95% Cu min
C11400		
C11500		
C11600		
C12000 (DLP)	Phosphorus-deoxidized copper (low-residual copper)	99.9% Cu min
C12200 (DHP)	Phosphorus-deoxidized copper (high-residual copper)	99.9% Cu min
C12300 (DHP)	Phosphorus-deoxidized copper (high-residual copper)	99.9% Cu min
C12500	Fire-refined copper	99.88% Cu min, remainder Ag, As, Sb, and others
C12700		
C12800		
C12900		
C13000		
C14200	Phosphorized, arsenical copper	99.94% Cu min, 0.1–0.5% As, 0.015–0.04% P
C19200	Phosphorized copper with 1% iron	98.97% Cu, 1.0% Fe, 0.03% P
C19400	High-strength modified copper	97.4% Cu, 2.4% Fe, 0.13% Zn, 0.04% P
C23000	Red brass	84–86% Cu, remainder Zn
C26000	Cartridge brass	70% Cu, 30% Zn
C26800	Yellow brass	65% Cu, 35% Zn
C27000		
C28000	Muntz metal	60% Cu, 40% Zn
C36500	Leaded Muntz metal, uninhibited	58–61% Cu, 0.4–0.9% Pb, 0.25% Sn max, remainder Zn
C36600	Arsenical inhibited leaded Muntz metal	58–61% Cu, 0.4–0.9% Pb, 0.25% Sn
C36700	Antimonial inhibited	max, remainder Zn
C36800	Phosphorus inhibited	
C44300	Admiralty brass	70–73% Cu, 0.9–1.2% Sn, remainder
C44300	Arsenical inhibited admiralty brass	Zn
C44400	Antimonial inhibited admiralty brass	
C44500	Phosphor inhibited admiralty brass	
C46400	Uninhibited naval brass	59–62% Cu, 0.5–1.0% Sn, remainder
C46500	Arsenical inhibited naval brass	Zn
C46600	Antimonial inhibited	
C46700	Phosphorus inhibited	
C60800	Aluminum bronze	95% Cu, 5% Al

Table 38 Continued

UNS no.	Common name	Composition
C61300	Aluminum bronze, 7%	90% Cu, 6–7.5% Al, 0.15% Ni, 2–3% Fe
C61400	Aluminum bronze D	91% Cu, 7% Al, 2% Fe
C63000	10% Aluminum-nickel bronze	82% Cu, 10% Al, 5% Ni, 3% Fe
C63200	9% Aluminum-nickel bronze	82% Cu, 9% Al, 5% Ni, 4% Fe
C65100	Low-Si bronze B	98.5% Cu, 1.5–2.0% Si, 0.7% max Mn
C65500	High-Si bronze A	97% Cu, 3% Si
C68700	Aluminum brass D, arsenical inhibited	77.5% Cu, 20.5% Zn, 2% Al
C70400	Copper-nickel, 5%	95% Cu, 5% Ni
C70600	Copper-nickel, 10%	90% Cu, 10% Ni
C71000	Copper-nickel, 20%	80% Cu, 20% Ni
C71500	Copper-nickel, 30%	70% Cu, 30% Ni
C71640	Copper-nickel-iron-manganese	29–32% Ni, 1.7–2.3% Fe, 1.5–2.5% Mn
C71900	Chromium copper-nickel	67.2% Cu, 30% Ni, 2.8% Cr
C72200	Chromium copper-nickel	83% Cu, 16.5% Ni, 0.5% Cr

Note. This table has been compiled from the ASM Metals Handbook [188].

Table 39 ASTM Specifications for Copper Alloy Heat Exchanger Tubes

ASTM spec.	Description	Alloys UNS no.
B111	Copper and copper alloy seamless condenser tubes and ferrule stock	C10100, C10200, C10300, C10800, C12000, C12200, C14200, C19200, C23000, C28000, C44300, C44400, C44500, C60800, C61300, C61400, C68700, C70400, C70600, C71000, C71500, C71640, C72200
B359	Copper and copper alloy seamless condenser and heat exchanger tubes with integral fins	C10100, C10200, C10300, C10800, C12000, C12200, C14200, C19200, C23000, C44300, C44400, C44500, C60800, C68700, C70400, C70600, C71000, C71500, C72200
B395	U-bend seamless copper and copper alloy heat exchanger and condenser tubes	C10200, C10300, C10800, C12000, C12200, C14200, C19200, C23000, C44300, C44400, C44500, C60800, C68700, C70400, C70600, C71000, C71500, C72200
B543	Welded copper and copper alloy heat exchanger tube	C10800, C12200, C19400, C23000, C44300, C44400, C44500, C68700, C70400, C70600, C71000, C71500, C71640, C72200
B552	Seamless and welded copper-nickel tubes for water desalting plants	C70600, C71500, C71640, C72200

Table 40 Copper Alloy Plates, Sheets, and Strips

ASTM spec.	Description	Alloys UNS no.
B171	Copper alloy plate and sheet for pressure vessels, condensers, and heat exchangers	C36500, C36600, C36700, C36800, C44300, C44400, C44500, C46600, C46700, C61300, C61400, C63000, C63200, C70600, C71500, C72200
B569	Brass strip in narrow widths and light gage for heat-exchanger tubing	C26000
B96	Copper-silicon alloy plate, sheet, strip, and rolled bar for general purposes and pressure vessels	C65100, C65400, C65500, C65800

applications. However, alloys C70600 and C71500 display excellent resistance to pitting in seawater.

22.4 Intergranular Corrosion

The most susceptible alloys for this form of corrosion are Muntz metal, admiralty metal, aluminum brasses, and silicon bronzes.

22.5 Dealloying (Dezincification)

Various forms of dealloying, including dezincification, have been covered in the chapter on corrosion. Dealloying of copper-base materials is briefly discussed here. Brasses containing more than 15% Zn, such as leaded Muntz metal, admiralty brass, and naval brass, are susceptible to dealloying when subjected to prolonged contact with slow-moving water or mildly acidic water. Trends of dezincification, stress corrosion cracking, and impingement attack with increasing zinc content in copper-zinc alloys are shown in Fig. 27. A few methods to control dezincification are:

1. Copper alloys with copper contents more than 85% resist dezincification.
2. Small amounts (0.02–0.11%) of As, Sb, or P added to admiralty brass (C44300) impart high resistance to dezincification, and the inhibited alloys are called arsenical admiralty brass, antimonial admiralty brass, and phosphorous admiralty brass. Similarly, the addition of As, Sb, or P tends to inhibit dezincification in leaded Muntz metal C36500, and in naval brass (C46400). The uninhibited alloys and the corresponding inhibited alloys are given in Table 41.

Dealuminification

Dealuminification in the 5 to 8% aluminum bronzes is occasionally reported, but it is not a significant problem until aluminum reaches the 9 to 11% range [191]. The microstructure is particularly important in the dealloying resistance of the alloys. Dealloying is rarely seen in all alpha, single-phase alloys such as aluminum bronzes C60800, C61300, and C61400, and when seen, conditions of low pH and high temperatures are usually present. But duplex structures are more prone to dealloying. Proper heat treatment can control dealloying in the duplex alloys.

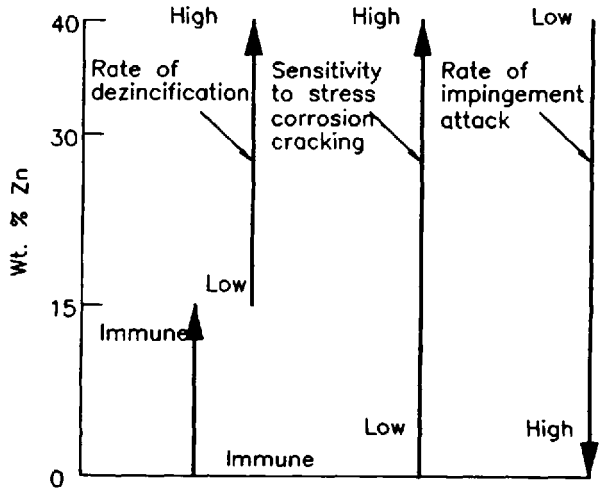


Figure 27 Trends of dezincification, stress corrosion cracking, and impingement attack with increasing zinc content in copper–zinc alloys (brasses). [From Ref. 81.]

Table 41 Inhibited Alloys

Uninhibited alloys	Inhibited alloys
C36500 Leaded Muntz metal	C36600, C36700, C36800—As, Sb, P inhibited leaded Muntz metal, respectively
C44300 Uninhibited admiralty brass	C44300, C44400, C44500—As, Sb, P inhibited admiralty brass, respectively
C46400 Uninhibited naval brass	C46500, C46600, C46700—As, Sb, P inhibited naval brass, respectively

Denickelification

Denickelification is occasionally reported in the higher nickel copper-nickel alloys, 70Cu-30Ni (C71500), in feedwater pressure tubes at temperatures over 212°F (100°C), in low-flow conditions, and in high local heat flux [135], and in refinery overhead condensers, where hydrocarbon streams condense at temperatures above 300°F (149°C) [191]. According to Tuthill [191], denickelification problem appears to be associated with hot sports that develop in the tubing as a result of fouling and thermogalvanic differences that arise.

22.6 Erosion-Corrosion

Erosion-corrosion is the common tube-side phenomenon in copper and some copper alloys with water on the tube side as the result of excessively high velocity and turbulence. To improve resistance to erosion-corrosion, copper is alloyed with iron, chromium, and titanium [109]. Aluminum brass and copper-nickels are highly resistant to erosion-corrosion. Remedial measures to overcome erosion-corrosion include (1) proper design and sizing of the system so that maximum velocity is kept about 4–5 ft/s, (2) redesigning the waterbox or install vanes and diffusers to reduce turbulence in the inlet region, (3) installing cathodic protection system

in the waterbox, (4) installing tube inserts made of stainless steel or plastics, and (5) using chromium modified copper-nickel alloys or copper-nickel-iron alloys.

22.7 Stress Corrosion Cracking

Pure copper is immune to SCC, but the higher zinc content brasses with Zn content in the range of 20–40% are subject to stress corrosion cracking. Susceptibility increases as zinc content increases from 20 to 40%. Prominent copper alloys susceptible to SCC include C23000, C26000, C26800, C27000, C28000, C36500, C44300 (uninhibited), and C46400. Copper-nickels and pure copper are more resistant.

The combined action of at least three substances usually is necessary to produce stress corrosion cracking in stressed copper-base alloys [191]: (1) ammonia or ammonia-producing material (organic and inorganic substances containing nitrogen), (2) moisture (or water), and (3) oxygen. It is rarely encountered in feedwater heaters and condensers because of their low oxygen content. To keep the oxygen level to the lowest amount, air in-leakage during downtime periods should be minimized. Environments like sulfates, nitrites, and nitrates under certain circumstances also cause SCC of copper alloys. SCC in copper alloys is usually intergranular, whereas admiralty and aluminum brass almost invariably crack transgranularly and so does brass [192]. Cracks can be detected by eddy current inspection. Relative resistance of the various copper alloys to SCC is as follows [190,192].

Low resistance
  Brass containing over 20% zinc.
  Brass containing over 20% zinc and small amounts of lead, tin, or aluminum such as leaded high brass, naval brass, admiralty and aluminum brass.
Medium resistance
  Brasses containing less than 20% zinc, such as red brass.
  Aluminum bronze.
  Phosphorus bronze.
High resistance
  Silicon bronze.
  Phosphorized copper.
Very high resistance
  Cupronickel.
  Tough-pitch copper.
  Commercially pure copper.

SCC can be controlled by

1. SCC can be controlled, and sometimes prevented, by selecting copper alloys with less than 15% Zn. Brasses containing less than 15% Zn are resistant SCC. DHP copper and tough-pitch copper are generally immune to SCC.
2. Reduce the stress to a safe level by stress relieving or annealing.
3. Controlling the aggressiveness of the environment by addition of inhibitors.
4. Since the water-side SCC is often associated with surface deposits, it is important to keep the tubes free from deposits by proper tube cleaning.

Steam-Side Stress Corrosion Cracking

Among the copper alloys typically used for condenser tubes, the brasses (copper-zinc) are the most susceptible to SCC in environments containing ammonia. Other susceptible materials include arsenical aluminum brass and admiralty brass. The environmental conditions leading

to SCC on the steam side of copper alloy condenser tubes are ammoniacal solutions containing dissolved oxygen. The ammonia is derived from the water treatment compounds used for boiler feedwater, which decompose due to thermal effects in the boiler [193–195]. The ammonia concentration is particularly high in the air removal section, and this location suffers SCC most often. The high ammonia concentrations develop because the baffles locally shield the tubes and prevent the condensate in this area from being continually washed away by condensate falling from above. The other necessary ingredient for SCC to occur, oxygen, comes from the air drawn into the condenser through leaking joints, valve packing glands, etc. In addition to usual methods, some methods of controlling SCC in condenser tubes include the following [193]:

1. Use alloys resistant to SCC. Brass tubes may be replaced by cupronickel, stainless steel, or titanium tubes, particularly in the air removal section where steam-side environments can be quite aggressive.
2. Reduce or minimize the addition of ammonia and ammonia-producing additives to the boiler feedwater.
3. Ammonia concentrations in the air removal section can be reduced by modifying the design to eliminate horizontal baffles or by installing a water showering system to dilute the ammoniacal condensates.
4. If SCC is due to ammonia liberated from putrefying organisms during shutdown periods, flush the system with fresh water for a short period every day.
5. Eliminate oxygen from the system. All potential sources of air leakages should be attended and rectified.

Test for SCC—ASTM B154. ASTM B154, mercurous nitrate test, is a standard test method for detecting SCC of copper and copper alloys. This test method is an accelerated test for detecting the presence of residual (internal) stress that might result in SCC of individual parts in storage or in service.

22.8 Condensate Corrosion

Copper alloy tubes, particularly brass, can withstand the action of steam condensate in a very satisfactory manner except where the steam condensate contains high concentrations of ammonia and oxygen [194]. Condensate corrosion, also known as "ammonia attack," on the steam side of condensers, generally takes place in the air removal section where ammonia and oxygen concentrations are particularly high. Many of the methods of preventing ammonia SCC are also helpful to prevent condensate attack.

22.9 Deposit Attack

Deposit attack on condenser tubes occurs under conditions of stagnant or low water velocities, generally less than 3.1 ft/s (1 m/s). Deposition of waterborne particles on tube surfaces leads to differential aeration and anodic dissolution of the tube material [196]. Deposit attack is overcome by these measures [194]:

1. Maintain tube-side water velocity above 1 m/s and avoid stagnant conditions in aggressive media by flushing with treated water during shutdown.
2. Use more resistant materials like 70/30 and 90/10 copper-nickels and titanium.

22.10 Hot-Spot Corrosion

Hot-spot corrosion is a localized form of pitting corrosion that takes place at "hot spots" on the condenser tube wall due to low water velocity and/or high heat flux [196]. These conditions

can be caused by poor steam distribution or the absence of water on the cooling-water side of the tube. This form of corrosion rarely takes place in main steam condensers.

22.11 Snake Skin

Snake skin is as the result of deposition of copper corrosion product carried from low-pressure feedwaters employing admiralty brass tubes or high-pressure feedwater heater tubes made of Monel 400 or 70Cu-30Ni. The deposition results in thin flaky skin formation similar in appearance to skin shed by snake. This snake skin falls from the tubes when dried [194].

22.12 Corrosion Fatigue

Copper and copper alloys such as beryllium copper, cupronickels, phosphorus bronzes, and aluminum bronzes exhibit resistance to corrosion fatigue in many environments involving corrosiveness and applied stress.

22.13 Biofouling

Copper and copper alloys including copper-nickel exhibit excellent resistance to marine biofouling such as barnacles, mussels, and marine invertebrates.

22.14 Cooling-Water Applications

The principal constituents of water that affect the performance of copper alloys are dissolved oxygen, nutrients, bacteria, organisms, biofouling, sediment, and residual chlorine from the cholorination practice [191]. Inhibited admiralty brass, aluminum brass, and cupronickels exhibit excellent resistance in seawater, and show erosion-corrosion and biofouling resistance. Hence, these alloys are now extensively used in fossil power-plant heat exchangers.

22.15 Resistance to Seawater Corrosion

Corrosion resistance of copper and copper alloys in seawater is determined by the nature of the naturally occurring and protective corrosion product film [191]. The main drawback of copper alloys is their susceptibility to pitting corrosion in sulfide-bearing seawater in the presence of oxygen. This is especially true with polluted coastal water. Sulfide attack is further discussed next.

22.16 Sulfide Attack

Sulfide attack is accelerated corrosion of copper alloys that occurs when the cooling water, most often brackish water or seawater, is polluted with sulfides, polysulfides, or elemental sulfur, and no copper alloy is resistant to sulfide attack [194]. Various sources of sulfides include (1) the natural sulfates present in sea water and (2) the putrification of organic sulfur compounds from decaying plant and animal matter during periods of extended shutdown [193]. The major effect of the sulfide is to destroy the existing protective surface oxide film, if any. It can greatly increase general corrosion, and it can induce or accelerate dealloying, pitting, and erosion-corrosion [194]. The corrosion attack is enhanced in the presence of oxygen. The following remedial measures will overcome sulfide attack [193].

1. If sulfide forms during periods of extended shutdown due to the putrification of organic sulfur compounds, it can be removed daily by flushing the system using fresh water.
2. Precondition the copper alloy surfaces by ferrous sulfate dosing to make them more corrosion resistant.

3. Use alternative materials such as stainless steel and titanium tubes in place of copper.

22.17 Exfoliation

Copper-nickel alloy feedwater heater tubes are subjected to exfoliation [189,197]. Exfoliation is due to pronounced schistous oxidation of the materials, and the resulting loss in strength of the feedheater tubes, which is no longer sufficient to withstand the water pressure and hence burst. The factors that cause exfoliation are (1) cyclic and peak loads, i.e., where the plant was frequently started up and shut down, and (2) the presence of oxygen, water vapor, and water. Among the copper-nickels, 70 : 30 copper-nickel was the most susceptible, but 80 : 20 and 90 : 10 are better. Monel alloy 400, Inconel alloy 600 and titanium retain their "as-installed" appearance under test conditions [197].

22.18 Copper and Aquatic Life

Copper is declared poisonous to aquatic life. Hence its discharge into the source of cooling water is prohibited by laws and environmental regulations.

23 COPPER WELDING

Copper and its alloys are welded by shielded metal arc welding (SMAW), gas tungsten arc welding (GTAW), plasma arc welding (PAW), submerged arc welding (SAW), and oxyacetylene welding (OAW). Of these, GTAW and GMAW are the most popular, with argon, helium, or nitrogen gas shielding. The primary criteria for choosing between GMAW and GTAW are thickness of the metal to be welded and amount of welding to be performed. GMAW is generally preferred for thicknesses greater than about 1/4 in (6.4 mm). The GMAW process provides intense heat generated by the arc, high deposition, dense deposits, low preheat and interpass temperatures, good properties, and minimum distortion [184]. GTAW is used for thickness less than about 0.08 in (2 mm). Generally, welding is carried out using dcsp with a 3 : 1 mix of helium and argon. For thickness between 2 and 6 mm, both processes can be used. Other joining methods include resistance welding and induction welding, brazing, and soldering. Welding of copper and its alloys are discussed in detail by Gaffoglio [184], in Ref. 198, by Dawson [199–201], by Callcut et al. [202], and in Ref. 203.

23.1 Weldability

In all welding processes, the dominant factor in establishing weldability is thermal conductivity of the base metal. When welding copper, allowances are necessary for the chilling of the welds because of the very high thermal conductivity of the metal. Preheating is often required. Considerable distortion is possible in coppers because of the higher thermal expansion than other commercial metals. These characteristics pose difficulties that must be overcome for satisfactory welding.

Factors Affecting Weldability

Other than the elements that comprise a specific alloy, the principal factors that influence weldability are (1) thermal conductivity, (2) preheating, (3) thermal expansion, (4) alloying elements, (5) surface cleanliness and surface oxide, (6) shielding gas, (7) joint design, (8) welding position, (9) consideration for precipitation hardenable copper alloys, (10) hot cracking, and (11) porosity.

Thermal Conductivity. The high thermal conductivities of copper and certain high-copper alloys such as aluminum bronze, commercial bronze (90%), and red brass (85%) pose problems

for satisfactory welds. Unless adequate measures are taken to counteract the rapid heat-sink effect, it is not possible to establish the fully fluid weld pool necessary for good fusion, adequate joint penetration, and deoxidation [184,203]. Therefore, the type of current and the shielding gas must be selected for maximum heat input to counteract the rapid heat dissipation from the weld region. Make all joint preparation with wide root gaps, and tack frequently.

Preheating. The relatively high thermal conductivities of copper and most copper alloys result in the rapid conduction of heat from the weld joint to the surrounding base metal. Preheating copper is generally necessary for thicknesses above about 1/8 in (3 mm) when using argon shielding [203]. Preheating of these alloys will reduce welding heat requirements for fusion. Recommended preheat temperature varies from 302 to 1292°F (150 to 700°C) depending on the thickness, shielding gas, welding current, and process used. To reduce the preheat requirement, substitute helium for argon in the shielding, and make heavy root passes in all multipass welds to insure deoxidation and to prevent cracking [184]. The interpass temperature should be the same that for preheating.

Thermal Expansion. The high thermal expansion causes root gaps to close as welding proceeds, and due allowance must be made when fixturing the assembly for welding. The effect of high contraction stresses on the weld metal during solidification must also be taken into account and may require reduction of cooling rate by some means to give sufficient time for these stresses to be accommodated.

Effects of Alloying Elements on Welding. Alloying elements have pronounced effects on the welding behavior of copper alloys. Small amounts of volatile, toxic alloying elements are often present in copper and its alloys, and, as a result, the use of an effective ventilation system to protect the welder or welding machine operator is necessary.

Precleaning and Surface Preparation. The joint faces and adjacent surfaces should be clean. Oil, grease, dirt, paint, oxides, and mill scale should be removed by degreasing followed by suitable chemical or mechanical cleaning.

Surface Oxides. Surface oxides must be removed from the work surfaces before welding. Surface oxide can cause a serious problem of nonwetting of filler metal during welding, brazing, and soldering. The oxides on beryllium copper, chromium copper, aluminum bronze, and silicon bronze are difficult to remove. Wire brushing is not effective for copper alloys that develop a tenacious surface oxide. These alloys should be cleaned by appropriate chemical or abrasive methods. Mill scale on copper-nickels must be removed by grinding or pickling, since wire brushing is ineffective.

Shielding Gas. Argon or a mixture of argon and helium at 25 to 70% is normally used for welding.

Joint Design. Joint design and fixturing should minimize restraint and residual stresses, and provide allowance for the high coefficient of thermal expansion to prevent hot cracking. Backing strips are extensively used on the highly fluid coppers and high-copper alloys. Joint design for copper and copper alloy is shown in Fig. 28.

Welding Position. Because of high fluidity of copper and copper alloys, the flat horizontal position is used whenever possible.

Problems With Precipitation-Hardenable Alloys. For precipitation-hardenable copper alloys with Be, Cr, Bo, Ni, Si, and Zr, take care to avoid oxidation and incomplete fusion. Weld in the annealed condition, and the weldment should be given a precipitation-hardening heat treatment.

Hot Cracking. Copper alloys with wide liquidus to solidus temperature ranges, such as copper-tin and copper-nickel, are susceptible to hot cracking. Low-melting interdendritic liquid

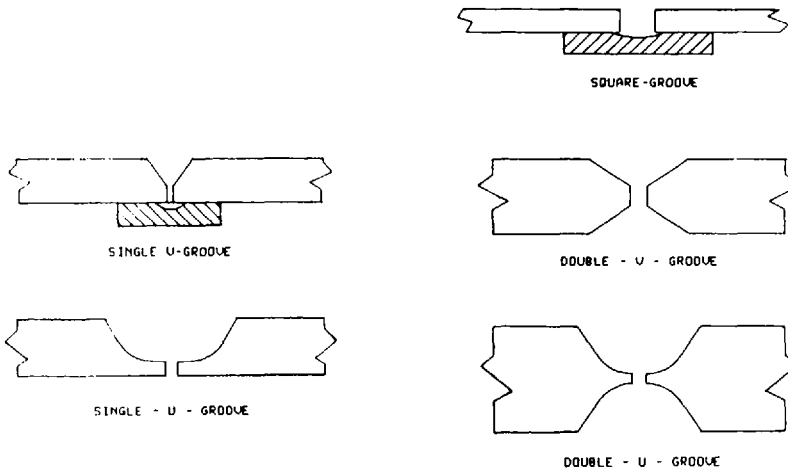


Figure 28 Typical joint design for copper and copper alloys.

solidifies at a temperature lower than the bulk dendrite. Shrinkage stresses produce interdendritic cracking during solidification. Hot cracking can be minimized by reducing restraint on the weldment, preheating to slow the cooling rate, reducing the magnitude of the welding stresses, reducing the root opening, and increasing the size of the root pass.

Porosity. Elements such as zinc, lead, cadmium, and phosphorus have low boiling points. Vaporization of these elements during welding will result in porosity. Porosity can be minimized by fast weld speeds and use of filler metal low in these elements.

23.2 Alloy Classification From Weldability Considerations

Copper and its alloys are considered from the welding viewpoint under the following general headings:

1. Copper with small additions: copper-cadmium and precipitation-hardenable alloys (copper-beryllium, copper-chromium, copper-zirconium); oxygen-free copper, tough-pitch copper, phosphorus-deoxidized copper.
2. High-alloy copper.
3. Copper alloys:
   a. Brasses—admiralty brass, naval brass, aluminum brass.
   b. Silicon bronzes.
   c. Tin bronzes.
   d. Aluminum bronzes.
   e. Copper-nickels.

Copper

Oxygen-Free and Tough-Pitch Coppers For welding oxygen-free copper (C10200) or electrolytic tough-pitch copper (C11000) in thickness to about 1/2 in (12.7 mm), gas tungsten arc welding is preferred to GMAW, or other processes generating less localized heat input.

Deoxidized Copper. Up to about 1.5 in (38 mm), heavy-walled components made from phosphorus-deoxidized copper are normally welded by GMAW. To ensure high heat input, welding current and preheat temperatures are usually high.

High-Copper Alloys

Because these alloys have lower thermal conductivities than pure copper, they require lower preheats and welding current. Generally, except for beryllium coppers, the welding procedures are similar to deoxidized copper.

Copper Alloys

The most notable feature distinguishing the welding of most copper alloys from the welding of pure copper is the reduction of heat input and preheating requirements due to low thermal conductivities of the copper alloys compared to the pure metal. Copper alloys commonly welded, notably brasses, aluminum bronzes, and cupronickels, are readily weldable by all gas-shielded arc welding processes. Metallurgical and welding features that may require particular attention are discussed under the individual alloys.

Brasses. Alloying elements lower conductivity. The alloys most commonly welded are naval brass, admiralty brass, and aluminum brass. Compared to the coppers, brasses require much less preheat and less current to weld. Copper's problems with hydrogen and oxygen reactions are absent when welding brasses, because brasses have low hydrogen solubility limits and zinc deoxidizes [184]. Lead contributes to hot cracking. Evolution of zinc fume causes suffocation to the welder and obstructs the view of the welding. Zinc fume makes welds porous and unacceptable, particularly in autogenous welding [200]. The gas-shielded arc processes provide a means of reducing problems associated with zinc volatilization to a minimum, and due consideration should be given to the possibility of using a nonmatching filler metal like silicon bronze or aluminum bronze, which will reduce the evolution of zinc fumes by forming a surface film on the weld pool [200,203]. When using argon-shielded TIG welding, alternating current is essential, and for direct current working helium is preferred [203].

Silicon Bronzes. Silicon bronzes are the most weldable of the copper alloys. Adding as little as 1.5% silicon reduces conductivity to 15% of that of copper. As a result, preheating is not essential and little heat input is required so that welding speeds can be high [184]. Silicon bronzes are fluid when molten, but fluxes are needed to penetrate the viscous silica that covers weld metal pool. Both TIG and MIG processes are suited to silicon bronzes. TIG welding is used on thin to moderately thick nonleaded silicon bronzes. With TIG welding, employ dcsp with argon or helium shielding. Sometimes, alternating current with argon is preferred because it facilitates the removal of the tenacious oxide surface film, but at the cost of arc stability [203]. For thickness above 1/2 in (12.7 mm), MIG is often preferred due to higher deposition, though TIG is also suitable.

Silicon bronze is hot short in the temperature range of 1472–1742°F (800–950°C), and cooling through this critical temperature range should be as rapid as possible, especially when the welded structure is restrained. This is particularly faced when using the MIG welding process, known for high welding speeds and high deposition rates. However, with rapid cooling there is a possibility of forming brittle, nonequilibrium phases in the weld metal, which, under conditions of restraint, can cause weldment cracking [200].

Copper-Aluminum Alloys (Aluminum Bronzes). Due to relatively high thermal conductivity and the ease with which refractory oxide films form on its surface, aluminum bronzes require a highly concentrated heat source with full shielding of the weld pool [204]. The high gas solubility and affinity of oxygen for molten aluminum bronze, its higher thermal expansion and contraction, and its susceptibility for hot shortness, particularly single-phase aluminum bronzes that contain less than 7% Al, should be considered. Clean welding conditions, a proper weld design and joint preparation, and a welding procedure to accommodate thermal stresses and reduce the tendency for weld metal cracking are suggested [204].

Single-phase aluminum bronzes that contain less than 7% Al are difficult to weld, whereas single-phase alloys with more than 7% Al and two-phase alloys are weldable by GTAW or GMAW techniques, using procedures designed to avoid hot cracking [184]. GTAW produces high-quality welds. When welding, use argon and alternating current to remove tenacious aluminum oxide surface films. For greater success, use dcrp in helium [203]. Porosity is minimized by the presence of iron, manganese, or nickel in the filler metal or base metal, or in both. Preheating should be avoided whenever possible and interpass temperatures kept to a minimum to avoid a buildup of temperature in the structure, which may give rise to loss of ductility and associated cracking problems. Oxyacetylene welding is not recommended due to the problem with fluxing of aluminum oxide from the weld metal.

Copper-Nickel or Cupronickel Alloys. Thermal and electrical conductivities approximate those of carbon steels. These properties facilitate welding without preheating, and the interpass temperature during welding should not exceed 150°F (66°C). The chief problems faced in the welding of copper-nickels are:

1. Since resistance to erosion-corrosion requires that the iron be in solid solution, welding of the alloy must be done in a manner that does not cause precipitation of iron compounds.
2. Like nickel base alloys, the copper-nickel alloys are susceptible to lead, phosphorus or sulfur embrittlement. Restrict the phosphorus to 0.01% and the sulfur level to a maximum of 0.02%. Maintain surface cleanliness and avoid surface contamination by any of them [184].
3. Copper-nickels have high affinity for the absorption of oxygen, hydrogen, or nitrogen into the molten weld metal, which gives rise to porosity. This problem is overcome by using filler metals containing suitable deoxidants. Titanium, together with manganese, is at present the major deoxidant in the standard filler alloys for the cupronickels. For this reason, the autogenous welding of copper-nickel alloys will leave porous welds.
4. Protection of the weld metal and the underside of the weld by inert gas shielding may be desirable to avoid contamination from oxygen, hydrogen, etc. [203].
5. Both TIG and MIG techniques are used with filler metals containing suitable deoxidants. Welding speeds should never be high enough to cause breakdown of the gas shielding and subsequent oxygen and hydrogen pickup by weld metal, leading to porosity problems.

Cupronickels can be joined by gas metal arc welding, gas shielded arc welding, and oxyacetylene welding. Copper-nickel filler metal of 70Cu-30Ni composition is normally used for welding all of the cupronickel alloys. Filler metals of matching composition may be used in special cases. Mostly, argon is preferred for shielding because it gives easy arc control and uniform weld appearance. Helium is preferred for welding thicker sections, because it gives improved welding conditions. A direct-current, electrode-negative arc is used for GTAW with helium and argon gas shielding. Since the lower copper-nickel alloys are higher in conductivity, they require higher current. A short arc is generally recommended [184]. Use slow welding speeds for GMAW, laying beads with slight weaves, shield with argon, or argon plus helium.

23.3 PWHT

Copper alloys are not frequently postweld heat-treated, but they may require controlled cooling to minimize residual stress and hot shortness. After welding, the heat-affected zone will be softer and weaker than the adjacent base metal. For copper-zinc alloys, postweld stress relief heat treatment at 482–572°F (250–300°C) is advisable from stress corrosion cracking point of view [203].

23.4 Dissimilar Metal Welding

The requirement to join copper and copper alloys to other copper alloys or to other nonferrous or ferrous alloys is frequently encountered. A few examples for these combinations are given next.

Copper to Steel

Copper materials may fulfill the design function of corrosion resistance or conductivity, whereas ferrous materials may give structural strength on an economical basis.

Copper to Aluminum Bronze

Frequently the main shell of the assembly is of copper, and the welding of the aluminum bronze branches and various fittings to the shell must be accomplished.

Aluminum Bronze to Cupronickel

Heat exchanger shells made of cupronickel alloys, both 90 : 10 and 70 : 30, may involve welds with aluminum bronze castings for branches and tubesheets.

Cupronickels to Steel

Cupronickels of 90 : 10 and 70 : 30 are increasingly being used for heat exchanger shells. Mild steel supports and flanges are attached by welding. Cupronickel tubes are commonly welded into steel tubesheets.

Factors Influencing the Dissimilar Metal Weld

Important factors to be considered when welding dissimilar metals include the following [201]: interalloying, electrochemical corrosion, differential expansion, and weld metal dilution.

1. *Interalloying:* Where the materials to be joined are metallurgically incompatible, the binary phase diagram gives some indication as to the ultimate weld metal composition and structure.
2. *Galvanic or electrochemical corrosion.* In a dissimilar joint, the possibility of electrochemical corrosion of the weld metal can be prevented by ensuring that it is cathodic to the base metals.
3. *Differential thermal expansion.* In a welded joint between dissimilar metals, additional stresses are set up due to differential thermal expansion and contraction. Joint design and fixturing must allow for the effect of expansion, which will tend to close the root gap and generally distort the structure as welding proceeds. Problems due to differential thermal expansion are overcome by the following means [201]: (1) select a filler alloy having expansion characteristics midway between the two parent metals, and (2) accommodate the metallurgical stresses by the structure as a whole by preheating or post heating the joint area to reduce the cooling rate sufficiently. This is particularly important with inert-gas arc welding where heating is often localized and cooling rates are very high.
4. *Weld metal dilution.* Another important consideration when welding copper to steel is to minimize dilution of iron in the weld metal and the penetration of copper into the steel. Standard techniques to overcome weld metal dilution include the following [201]:
   a. Buttering, by laying down an overlay of copper filler alloy on to the steel joint face.
   b. Select a filler metal compatible with both parent metals.
   c. In dissimilar metal joints with copper, use the cupronickel rather than the copper filler alloys to minimize the risk of porosity.
   d. While joining copper-nickel to steel, dilution is controlled by attaining low penetration using globular transfer, which occurs at subthreshold welding currents, for the initial overlay on the steel face area.

Filler Alloys Selection

Filler metal standards are usually specified by codes and standards, but if not specified, alloys of parent metal composition are generally used [203].

24 NICKEL AND NICKEL-BASE ALLOYS: METALLURGY AND PROPERTIES

Nickel is a hard, tough and malleable white metal. Nickel exhibits unique properties of high-temperature strength, toughness, wear resistance, and resistence to corrosion and oxidation. Nickel alloys were developed to withstand corrosives found in the chemical, petrochemical power, marine, and pulp and paper industries. Nickel readily forms alloys with ferrous and nonferrous metals like Fe, Cr, Cu, and Co. The properties that favor the nickel and nickel-base alloys for construction of process equipment include the following:

1. Ability to withstand a wide variety of severe operating conditions involving high temperature, high stresses, corrosive environments, and a combination of these factors.
2. Nickel-base superalloys exhibit good resistance to corrosion, creep-rupture, fatigue, thermal fatigue, thermal shock, and impact.
3. Resistance to elevated-temperature oxidation, sulfidation, and carburization.
4. Used as an alternative material in place of austenitic stainless steel to combat SCC. For all practical purposes, nickel alloys containing more than 30% nickel are immune to SCC.
5. Ability to be formed by conventional methods and to be joined by most conventional welding process such as GTAW, GMAW, and SMAW using coated electrodes.
6. Purity and nontoxic character are exploited in food processing and fine chemical industries.
7. *Low-temperature applications:* Nickel is a face-centered cubic (fcc) metal that retains good ductility and toughness at subzero temperatures. Among the nickel alloys, Monel K-450, Hastelloy B, Hastelloy C, Inconel alloy 600, Inconel alloy 706, Inconel alloy 718, Invar-36, and Inconel X-700 exhibit excellent combinations of strength, ductility, and toughness up to −263°C [205].

24.1 Classificaton of Nickel Alloys

Nickel alloys are in general classified into the following groups:

1. Commercially pure nickel.
2. Nickel-copper alloys and copper-nickel alloys
3. Nickel-chromium alloys
4. Nickel-iron-chromium alloys.

Information on material properties of various nickel, nickel-copper, INCONEL, and INCOLOY alloys has been taken from the Product Handbook (Publication No. IAI-38) [206].

Commercially Pure Nickel

Alloys 200 and 201 are the major examples of this class. Because of its corrosion resistance, nickel is used to maintain product purity in the processing of foods and synthetic fibers. Nickel is highly resistant to various reducing chemicals and is unexcelled in resistance to caustic alkalies. A major area for use of alloys 200 and 201 is in caustic evaporators because of their outstanding resistance to hot alkalies. Thermal conductivity of nickel is relatively high. In reducing environments, such as dilute sulfuric acid, nickel is more corrosion resistant than iron but not as resistant as copper or nickel-copper alloys. Annealed nickel has a low hardness and good ductility and malleability. These attributes, combined with good weldability, make the

metal highly fabricable. The nominal composition of commercial pure nickel is given in Table 42.

Nickel 200 (UNS No. 02200) is a commercially pure (99.6%) wrought nickel with good mechanical properties and resistance to a range of corrosive media. It is especially useful in handling caustic alkalies and has good thermal, electrical, and magnetostrictive properties. It is used for a variety of processing equipment, particularly to maintain product purity in handling foods, synthetic fibers, and alkalies.

Nickel 201 (UNS No. 02201) is the low-carbon version of alloy 200. The low carbon content prevents embrittlement by intergranular carbon at temperatures over 600°F (315°C). Lower carbon content also reduces hardness, making Nickel 201 particularly suitable for cold forming.

Nickel-Copper Alloys and Copper-Nickel Alloys

Nickel and copper are completely soluble in each other so that a series of alloys has been available. Nickel-copper alloys are known as Monel alloys. Monel alloy 400, Monel alloy R-405, Monel alloy 450, and Monel alloy K-500 offer somewhat higher strength than unalloyed nickel without loss of ductility. Monel alloys resist corrosion in a broader range of environments. Monels exceed nickel in resistance to sulfuric acid, hydrofluoric acid, brines, and water. The thermal conductivity of Monel alloys, although lower than that of nickel, is significantly higher than that of nickel alloys containing substantial amounts of chromium or iron. Monel alloys have essentially the same high level of formability and weldability as nickel. The nominal composition of nickel-copper alloy is given in Table 42.

Monel 400 (UNS 04400). Alloying of 30 to 32% copper with nickel produces Monel alloy 400, which shares many of the characteristics of commercially pure nickel but improves on others. It has high strength and excellent corrosion resistance in seawater, hydrofluoric acid, sulfuric acid, and alkalies. Water handling, including brackish and seawaters, is the major area of application. It gives excellent service under high velocity conditions, as in condenser and feedwater heater tubes. Addition of iron improves resistance to cavitation and erosion-corrosion. Monel 400, like some other high-nickel alloys, is susceptible to stress corrosion cracking in moist aerated hydrofluoric acid. Cracking may not take place if the metal is completely immersed in the acid. Monel 400 also exhibits stress corrosion cracking in high-temperature, concentrated caustic, and in mercury. It is used for marine engineering, chemical, and hydrocarbon processing equipment.

MONEL alloy R-405 (UNS 04405) is similar to MONEL alloy 400. controlled sulfur is added for improved machining characteristics. Other characteristics are essentially same as those of MONEL alloy 400.

MONEL alloy 450 (UNS C71500) is a copper-nickel alloy of the 70-30 type having supe-

Table 42 Nominal Composition of Major Alloying Elements of Pure Nickel and Nickel-Copper Alloys [207]

Alloy name	Ni	Cu	Fe	Others
Nickel 200	99.6	—	—	C 0.15 max
Nickel 201	99.6	—	—	C 0.02 max
MONEL alloy 400	66.5	31.5	1.2	Mn 2.0 max
MONEL alloy R-405	66.5	31.5	1.2	S 0.04
MONEL alloy 450	31.0	68.0	0.7	—
MONEL alloy K-500	66.5	29.5	1.0	Al 2.7

rior weldability. It is resistant to corrosion and biofouling in seawater, has good fatigue strength, and has relatively high thermal conductivity. It is used for seawater condensers, condenser tubesheets, distiller tubes, evaporator and heat exchanger tubes, and saltwater piping.

MONEL alloy K-500 (UNS 05500) is a precipitation-hardenable nickel-cooper alloy that combines the corrosion resistance of MONEL alloy 400 with greater strength and hardness.

INCONEL

INCONEL includes nickel-chromium alloys and INCO nickel-chromium alloys. The combination of nickel and chromium in the alloys provides resistance to both reducing and oxidizing corrosive solutions. The nickel-chromium alloys resist oxidation, carburization, and other forms of high-temperature deterioration. The alloys do not become brittle at cryogenic temperatures, have good tensile and fatigue strengths at moderate temperatures, and display excellent creep-rupture properties at high temperatures.

In most of the INCONEL and INCO alloys, the valuable basic characteristics of the nickel-chromium system are augmented by the addition of other elements. Some of the alloys are strengthened by aluminum, titanium, and niobium (columbium). Others contain cobalt, copper, molybdenum, or tungsten to enhance specific strength or corrosion resistance attributes. The alloys also contain iron in amounts ranging from about 1% to over 20%. In most cases, however, elements other than iron have dominant effects on properties. Nominal compositions of major alloying elements of INCONEL are given in Table 43.

INCONEL alloy 600 (UNS 06600) is a nickel-chromium alloy with good oxidation resistance at high temperatures and resistance to chloride stress corrosion cracking, corrosion by high-purity water, and caustic corrosion. Alloy 600 is almost entirely resistant to attack by solutions of ammonia over the complete range of temperatures and concentrations. The absence of molybdenum in the alloy restricts its use in applications for which pitting corrosion is the primary concern. Alloy 600 is subject to stress corrosion cracking in high temperature and high-concentration alkalies. Hence, the alloy should be stress relieved before use and the operating stresses kept at a minimum.

INCONEL alloy 601 (UNS 06601) is a nickel-chromium alloy with an addition of alumi-

Table 43 Nominal Composition (%) of Major Alloying Elements of INCONEL and INCO Alloys [208]

Alloy name	Ni	Cr	Fe	Cu and others
INCONEL alloy 600	76.0	15.5	8.0	—
Inconel alloy 601	60.5	22.0	14.1	Al 1.4
Inconel alloy 617	53.0	22.0	1.5	Mo 9.0, Co 12.5, Al 1.2
Inconel alloy 625	61.0	21.5	2.5	Mo 9.0, Cb & Ta 3.6
INCO alloy C-276	55.0	16.0	6.0	Mo 16.0, Ti 4.0
INCONEL alloy 718	52.5	19.0	18.5	Mo 3, Al 0.5, Ti 0.9, Cb & Ta 5.1
INCONEL alloy X-750	73.0	15.5	7.0	Ti 2.5, Al 0.7, Cb & Ta 0.95
INCO alloy G	44.0	22.0	19.5	Mo 6.5, Cu 2.0, Cb & Ta 2.1
INCO alloy G-3	44.0	22.2	19.5	Mo 7, Cu 2.0
INCO alloy HX	48.0	21.8	18.5	Mo 9.0, Co 1.5, Ti 0.6
Incoloy alloy 800	32.5	21.0	46.0	C 0.05
Incoloy alloy 800HT	32.5	21.0	46.0	C 0.08, Al + Ti 1.0
Incoloy alloy 825	42.0	21.5	30.0	Mo 3.0, Cu 2.2
Inco alloy 330	35.5	18.5	44.0	Si 1.2
Inco alloy 020	34.0	20.0	38.0	Cu 3.5, Mg 1.0, Mo 2.5, Cb & Ta 0.5

num for high resistance to oxidation and other forms of high-temperature corrosion. It also has high mechanical properties at elevated temperatures. It resists oxidation up to 2300°F, and has good resistance to sulfidizing atmospheres.

INCONEL alloy 617 (UNS 06617), a nickel-chromium-cobalt-molybdenum alloy, exhibits an exceptional combination of metallurgical stability, strength, and oxidation resistance and carburization resistance at high temperatures. Resistance to oxidation is enhanced by aluminum addition. This alloy resists a wide range of corrosive aqueous environments.

INCONEL alloy 625 (UNS 06625) is a nickel-chromium-molybdenum alloy with an addition of niobium that acts with the molybdenum to stiffen the alloy's matrix and thereby provide high strength without a stengthening heat treatment. Its high strength allows the use of more thin-walled vessels and tubing than is possible with many other materials, thereby saving weight and improving heat transfer. Exhibit strength and toughness from cryogenic temperatures to 1800°F (980°C). It exhibits good oxidation resistance, fatigue strength, and corrosion resistance. The alloy resists a wide range of severe corrosive environments and is especially resistant to pitting and crevice corrosion.

INCONEL alloy 718 (UNS 07718) is a precipitation-hardenable nickel-chromium alloy containing significant amounts of iron, niobium, and molybdenum along with lesser amounts of aluminum and titanium. It combines corrosion resistance and high strength with outstanding weldability including resistance to postweld cracking. The alloy has excellent strength from −423 to 1300°F (−253 to 705°C). Oxidation resistance up to 1800°F (980°C).

INCONEL alloy X-750 (UNS 07750) is a nickel-chromium alloy similar to INCONEL alloy 600 but made precipitation hardenable by additions of aluminum and titanium. The alloy has good resistance to corrosion and oxidation along with high tensile and creep-rupture properties at temperatures to about 1300°F (700°C).

INCO alloy G-3 (UNS 06985) is a nickel-chromium-iron alloy with additions of molybdenum and copper. It has good weldability and resistance to intergranular corrosion in the welded condition. The low carbon content helps prevent sensitization and subsequent intergranular corrosion of the weld heat-affected zones. It is used for flue gas scrubbers and for handling phosphoric and sulfuric acids.

INCO alloy C-276 (UNS 10276) is a nickel-molybdenum-chromium alloy with an addition of tungsten, having excellent corrosion resistance in a wide range of severe environments. The high molybdenum content makes this alloy especially resistant to pitting and crevice corrosion. The low carbon content minimizes carbide precipitation during welding to maintain corrosion resistance in as-welded conditions. It is used in pollution control, chemical processing, pulp and paper production, and waste treatment.

INCO alloy HX (UNS 06002) is a nickel-chromium-iron-molybdenum alloy with outstanding strength and oxidation resistance at temperatures to 2200°F (1200°C). Matrix stiffening provided by the molybdenum content results in high strength in a solid-solution alloy having good fabrication characteristics.

Nickel-Iron-Chromium Alloys and INCO Nickel-Iron-Chromium Alloys for High-Temperature Applications

The INCOLOY alloys are based predominantly on the nickel-iron-chromium ternary system. Some alloys contain molybdenum and copper for enhanced corrosion resistance, and aluminum, titanium, or niobium for strengthening by heat treatment. The INCOLOY alloys are characterized by good corrosion resistance in aqueous environments and by excellent strength and oxidation resistance to high-temperature atmospheres. At high temperatures, the substantial chromium content provides resistance to oxidizing environments, and the combination of nickel, iron, and chromium results in good creep-rupture strength. The high nickel content

makes the alloys superior to stainless steels in resisting corrosion, especially chloride stress corrosion cracking. Nominal compositions of major elements of INCO alloys for high-temperature applications are given in Table 43.

INCOLOY alloy 800 (UNS 08800) is a nickel-iron-chromium alloy known for its strength, and its excellent resistance to oxidation and carburization in high-temperature applications. The alloy maintains a stable, austenitic structure during prolonged exposure to high temperatures. It is particularly useful for high-temperature equipment in the petrochemical industry because the alloy does not form the embrittling sigma phase after long exposures at 1200 to 1600°F (649 to 871°C). It is used for process piping, heat exchangers, and nuclear steam generator tubing. High creep and rupture strengths are other factors that contributes to its performance in many applications.

INCOLOY alloy 800HT (UNS 08811) is a nickel-iron-chromium alloy having the same basic composition as INCOLOY alloy 800 but with significantly higher creep-rupture strength in the 1100–1800°F (595–980°C) range. The higher strength results from close control of the carbon, aluminum, and titanium contents in conjunction with a high-temperature anneal. It is used in chemical and petrochemical processing, and in power plants for superheater and reheater tubing.

INCOLOY alloy 825 (UNS 08825) is a nickel-iron-chromium alloy with additions of molybdenum and copper and stabilized with titanium. It has excellent resistance to both reducing and oxidizing acids and seawater. It exhibits good resistance to stress corrosion cracking and intergranular corrosion. The alloy is especially resistant to sulfuric, nitric, and phosphoric acids. It is used in evaporators, heat-treating and chemical-handling equipment and propeller shafts, and for chemical processing, pollution control equipment, nuclear fuel reprocessing, acid production, and pickling equipments.

24.2 Product Forms

Nickel and its alloys are available as rounds, flats, pipe, tube, plate, sheet, forging stock, strip, and wire. Alloy description, product forms, and ASTM/ASME Code references are given in Table 44. The ASTM specifications for nickel-base tubular products are given in Table 45.

24.3 Magnetic Properties and Differentiation of Nickels

Nickel, like steel, is strongly magnetic at room temperature. When the Curie temperature (i.e., the temperature at which the metal loses its magnetic properties) is known, a simple magnetic test can be used to differentiate the nickel alloys. For nickel, the Curie temperature is about 680°F (360°C); nickel-copper alloy is slightly magnetic at room temperature and has a Curie temperature of 110 to 140°F (43 to 61.7°C); nickel-chromium alloy is nonmagnetic at room temperature and has a Curie temperature of −40°F (−40°C).

25 NICKEL AND NICKEL-BASE ALLOYS: CORROSION RESISTANCE

Nickel and nickel-base alloys exhibits resistance to general corrosion in aqueous solution, localized attack, SCC, and erosion-corrosion.

Table 44 Nickel Alloy Product Forms and Specifications [206,207]

Alloy	Standard product forms	Spec. ASTM(B)/ASME(SB)
Nickel 200	Round, flats, pipe, tube, plate, sheet, forging stock, strip, and wire	160–163, 366, B725, B730
MONEL alloy 400	Round, hexagon, flats, forging stock, pipe, tube, plate, sheet, strip, and wire	127, 163–165, 564
MONEL alloy R-405	Round, hexagon, flats, and wire	164, B165
Monel alloy 450	Round, hexagon flats, forging stock, pipe, tube, plate, sheet, and wire	111, 171, 359, 395, 466, 467, 543
Monel alloy K-500	Round, hexagon, flats, forging stock, pipe, tube, plate, sheet, strip, and wire	Code Cases 1192, N-119
INCONEL alloy 600	Round, hexagon, extruded section, flats, forging stock, pipe, tube, plate, sheet, strip, and wire	163, 166–168, 516, 517, 564, Code cases 1827, N-20
INCONEL alloy 601	Round, flats, forging stock, pipe, tube, plate, sheet, strip, and wire	B166–B168, Code Case 1500
INCONEL alloy 617	Round, forging stock, extruded section, plate sheet, strip, pipe, tube, and wire	166
INCONEL alloy 625	Round, flats, forging stock, extruded section, pipe, tube, plate, sheet, strip, and wire	443, 444, 446, 564, B704, B705, B751, Code Cases 1409, N-188
INCO alloy C-276	Round, forging stock, tube, pipe, plate, sheet, strip, and wire	574, 575, 619, 622, 626
INCONEL alloy 718	Round, flats, extruded section, pipe, tube, forging stock, plate, sheet, strip, and wire	637, 670, Code Cases N-62, N-47, N-119
INCONEL alloy X-750	Round, flats, extruded section, forging stock, plate, sheet, strip, pipe, tube, and wire	637, Code Cases N-62, N-60, N-119
INCO alloy G-3	Round, plate, sheet, strip, pipe, tube, and wire	581, 582, 619, 622, 626
INCO alloy HX	Round, extruded section, flats, forging stock, plate, sheet, strip, and wire	435, 572, 619, 622, 626
INCOLOY alloy 800	Round, flats, forging stock, pipe, tube, plate, sheet, strip, and wire	163, 407–409, 514, 515, 564, 751, Code Cases 1325
INCOLOY alloy 800 HT	Round, flats, forging stock, pipe, tube, plate, sheet, strip, and wire	163, 407, 408, 409, 514, 515, 564, Code Cases 1987
INCOLOY alloy 825	Round, flats, forging stock, pipe, tube, plate, sheet, strip, and wire	163, 423–425, 424, 425, B704, B705
INCO alloy 020	Round, flats, forging stock, pipe, tube, plate, sheet, strip, and wire	462–464, 468
INCO alloy 330	Round, flats, forging stock, pipe, tube, plate, sheet, strip, and wire	511, B512, 536, 535, B546, 710

Table 45 ASTM Specification for Nickel Alloy Tubular Products

ASTM spec.	Description	UNS No.
B751	General requirements for nickel and nickel alloy seamless and welded tubes	—
B163	Specification for seamless nickel and nickel alloy condenser and heat exchanger tubes	N02200, N02201, N04400, N06600, N06690, N08800, N08810, N08825
B468	Welded chromium-nickel-iron-molybdenum-copper, columbium-stabilized alloy tubes	N08028, N08024, N08026
B515	Welded nickel-iron-chromium alloy tubes for general corrosion resisting and low- or high-temperature service	N08800, N08810
B516	Welded nickel-iron-chromium alloy tubes for general corrosive service and heat-resisting applications	N06600
B626	Welded nickel and nickel cobalt alloy tube	N10001, N10665, N10276, N06455, N06007, N06975, N08320, N06985, N06002, N06022, N06030, N06059, N08031, N30556, N06230
B720	Seamless cold-worked tubes of nickel alloy for use in condenser and heat-exchanger service	N08310

25.1 Galvanic Corrosion

The element nickel (passive) is nobler than iron and copper in the electrochemical series.

25.2 Intergranular Corrosion

Nickel-chromium alloys with carbon content above 0.2% exposed to temperatures between 1100 and 1500°F (593 to 816°C) will be sensitized, resulting in chromium carbide precipitation in grain boundaries. This leaves areas adjacent to the boundaries low in chromium and susceptible to intergranular corrosion. Such corrosion can be counteracted in three ways [209]:

1. Select low-carbon alloy and consumables.
2. Select titanium- and columbium-alloyed base metal and welding consumables.
3. Solution anneal the weldment at 2000–2200°F (1093–1204°C) to dissolve precipitated carbides.

25.3 Stress Corrosion Cracking

There is a possibility that welded joints in nickel-rich alloys will suffer SCC if in contact with strong caustic soda, fluorosilicates, and certain mercury salts [79]. Nevertheless, nickel alloys have very good resistance to SCC in alkalies and solutions containing chloride ions, definitely much better than the austenitic stainless steels. Important information on SCC of nickel and nickel-base alloys includes [177]: (1) low-carbon nickel (0.02% C max) is recommended for use in contact with caustics if the service temperature is above 850°F (455°C), (2) nickel-iron alloys and nickel-chromium-iron alloys containing upto 40% nickel can fail by SCC on exposure to hot chloride solutions, (3) sensitized Ni-Cr-Fe alloys containing higher amounts of nickel may be subjected to polythionic acid SCC at ambient temperature, (4) aqueous solutions

of mercury salts are found to produce cracking in highly stressed Ni-Cu alloys, (5) high-nickel alloys are susceptible to SCC in aerated hydrofluoric acid vapors and in hydroflurosilicic acid, and (6) in addition to normal measures, complete annealing of nickel welds and annealing Monel 400 at 1100 to 1200°F (595 to 650°C) are recommended as a means of eliminating residual stresses that could cause SCC. In hydrofluoric acid service, stressed alloy 400 should not be exposed to aerated acid vapors.

26 NICKEL AND NICKEL-BASE ALLOYS: WELDING

The solid-solution-strengthened (non-age-hardenable) wrought nickel and its alloys can be arc welded under conditions similar to those used in the arc welding of austenitic stainless steels.

The precipitation-hardenable (PH) alloys like Monel K-500, Inconel 700, Alloy 718, and Inconel X-750 require special welding procedures because of their susceptibility to cracking. Residual welding stress and stress induced by precipitation cause cracking in the base metal or heat-affected zone on aging or in service, at temperatures above the aging temperature. If precipitation-hardenable alloys undergo any operation that introduces high residual stresses, welding should be done after annealing.

26.1 Considerations While Welding Nickel

While welding nickel and nickel-base alloys, greater care such as precleaning and cleanliness are required to prevent contamination-induced cracking or porosity, or embrittlement due to sulfur and lead [209,210]. As nickel content increases, the weld puddle viscosity increases; the coefficient of expansion decreases, as does weld penetration [209]. Additional considerations should include effect of minor elements on weldability, susceptibility to cracking in the weld bead caused by high heat input or excessive welding speeds, and SCC of certain welded structures in service. These welding considerations are discussed next.

Effects of Minor Elements on Weldability

Calcium and cerium are used as deoxidizers. Small additions of aluminum and titanium also serve as deoxidizers. These elements tend to contribute to the formation of oxide films, and slag spots on the weld surface. In multipass welding, such tenacious slag films should be removed between passes to avoid weld defects.

Precleaning and Surface Preparation

Cleanliness is the single most important requirement for successful joining of nickel alloys [210]. Welding, brazing, soldering, and any postheating must be performed only on base metal that is clean and completely free of surface contaminations. Surface contaminations due to manufacturing processes, like grease, oil, paint or lacquers, cutting fluids, machine lubricants, marking crayons and inks, and shop dirt, must be removed completely either by chemical or by vapor degreasing. Vapor degreasing or swabbing with perchloroethylene or other suitable solvents can remove oil- or grease-base shop dirt. Paint and other materials not soluble in degreasing solvents may be removed by methylene chloride, or alkaline cleaners. Alkaline cleaners that contain sodium sesquisilicate or sodium carbonate must be removed prior to welding. Wire brushing will not remove the residue completely. The best method is spraying or scrubbing with hot water.

Surface Oxide Removal

Nickel oxide melts at a higher temperature than the base metal. Therefore, oxides should be thoroughly removed from the surfaces to be welded because they can inhibit wetting and result

in lack of fusion. Oxides are normally removed by grinding with an aluminum oxide or silicon carbide wheel or a carbide burr, machining, abrasive blasting, or pickling. Any cleaning tools, including wire brushes and carbide burrs, should be clean and free from metals that may be transferred to the base metal. Wire brushes used for cleaning should be made of austenitic stainless steel. However, they will not remove tenacious surface oxides from welds. It merely polishes the oxide.

Weld Metal Porosity

Surface contaminations, poor welding techniques, improper shielding, and the presence of hydrogen, carbon dioxide, nitrogen, and oxygen gases often cause porosity in nickel weldments. To overcome this problem, electrodes/filler metals containing deoxidizers are a necessity. The deoxidizers combine chemically in the molten weld with inorganic compounds, which then float on the surface.

Joint Designs

Molten nickel-alloy weld metals do not flow and wet the base metal as readily as do carbon-steel and stainless-steel weld metals. The operator must place the metal at the proper location in the joint. Therefore, the joint must be sufficiently open to permit proper manipulation of the electrode, and deposition of the weld beads. Suggested joint designs for butt joints in nickel alloys (except submerged arc welding) are shown in Fig. 29.

Preheat and Interpass Temperatures

Guidelines on preheat and interpass temperatures are:

1. In general, preheat is not required for welding nickel base alloys. However, the area to be welded should not be below about 60°F (16°C) to avoid moisture condensate that could produce weld metal porosity.
2. The interpass temperature may be limited to 200°F (93°C). Cooling mediums used to reduce interpass temperature should not introduce contaminants that will cause weld discontinuities. Examples are traces of oil in compressed air and mineral deposits from the water spray.

Heat Input

High heat input during welding may result in constitutional liquation, carbide precipitation, or other metallurgical phenomena. Some degree of annealing and grain growth can take place in the heat affected zone. These, in turn, may cause cracking or loss of corrosion resistance, or both.

Hot Cracking

Weldments of nickel base alloys are susceptible to liquation cracking or hot cracking. This takes place particularly when welding conditions of high restraint are present, as in circumferential welds that are self-restraining. Therefore, all weld bead surfaces should be slightly convex. Convex beads are virtually immune to center-line cracking; flat and concave beads are particularly susceptible to center-line cracking. Excessive width to depth or depth to width ratio can also result in cracking. Measures to overcome hot cracking include (1) limit heat input during welding, (2) obtain fairly small grain sizes in the microstructures, and (3) minimize the amount of deleterious minor elements such as sulfur and phosphorus that are known to cause hot cracking.

Sulfur Embrittlement

Nickel combines with sulfur at elevated temperature to form a brittle sulfide. This phenomenon takes place preferentially at the grain boundaries, and is exhibited when the material is stressed

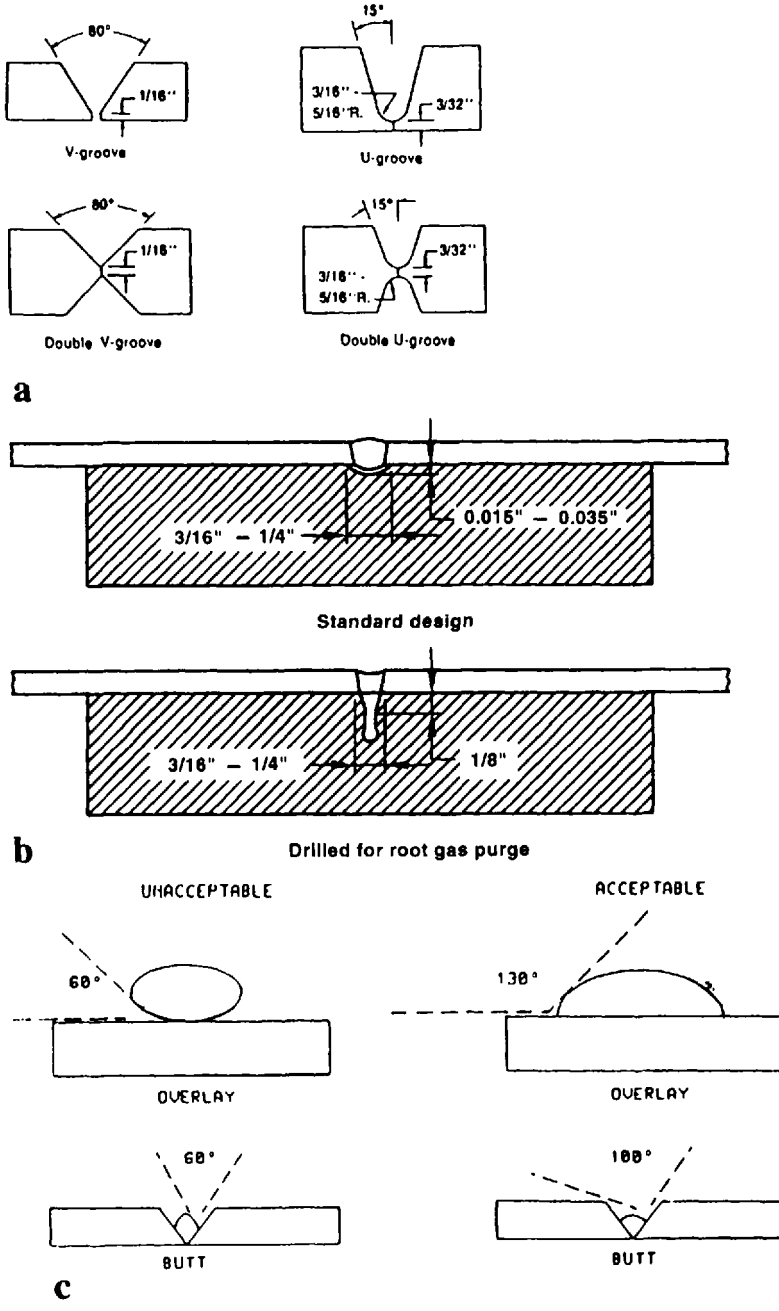


Figure 29 Nickel welding: (a) joint design except SAW; (b) groove in backup bar; and (c) acceptable bead profile shape. (From Refs. 209 and 210.)

or bent. Nickel is the most affected, nickel-copper less, and nickel-chromium-iron the least. Prior to carrying out any operation involving high-temperature operations such as welding, brazing, hot forming, PWHT, etc., the surfaces should be cleaned throughly and should be free from sulfur-bearing substances. For more details refer to ASME Code Section VIII, Div. 1, NF-14.

Lead Embrittlement

Lead causes embrittlement in all nickel-base alloys in much the same manner as sulfur. Therefore lead-containing fluids or lubricants should be removed from the surfaces.

Design for Penetration

Nickel alloys give lower weld penetration than ferrous materials. Increasing amperage beyond the recommended range will not significantly increase the penetration of the arc, but it will cause harm. The harmful effects due to over amperages are [210]: (1) overheating of the electrode and the resulting flux flaking off as heat breaks down the binder, and (2) puddling of the molten weld metal and resultant loss of deoxidizers, leading to porous welds.

Welding Fixtures

Proper fixturing and clamping is required to hold the workpieces firmly in place, minimize buckling, maintain alignment, and, when needed, provide compressive stress in the weld metal. A backing bar or any portion of a fixture that might be contacted by the arc should be made of copper. Since copper has high thermal conductivity, an inadvertent arc touch on the copper will not result in fusion of the bar to the weldment. A groove in the backup or chill bar (Fig. 29b) allows weld metal penetration and avoids entrapment of gas or flux at the weld root [210].

Good Bead Shape

Increased puddle viscosity can cause poor wetting and lack of fusion along bead edges. With low penetration in materials of high nickel content, the angle between the base metal and weld bead edge should be greater than 100° to facilitate good tie-ins with subsequent beads [209]. Nickel alloy beads should be slightly convex. Avoid flat and concave beads. Susceptibility to center-line cracking during solidification increases as flat or concave beads become stressed in root passes [210]. Acceptable bead profile shape is shown in Fig. 29c.

Carbide Precipitation

Like some austenitic stainless steels, nickel-chromium and nickel-iron-chromium alloys with carbon content above 0.2% exposed to temperatures between 1100 and 1500°F (593 to 816°C) will be sensitized due to carbide precipitation in the weld HAZ. Such sensitization does not result in accelerated attack in most environment. In general, carbide precipitation is overcome by these measures [209]:

1. Use low-carbon base alloy and consumables.
2. Select titanium- or columbium-stabilized alloy base metal and consumable.
3. Solution anneal the weldment at 2000–2200°F (1093–1204°C) to dissolve carbide precipitate.

Pitting Corrosion of Weldments

To resist pitting and crevice corrosion, weldments must have smooth surfaces and be chemically homogeneous on a microscopic level. Molybdenum imparts pitting resistance to nickel-chromium alloys. Use filler metal with sufficient molybdenum; even in the event of iron dilution, enough molybdenum will impart greater resistance to weld metal than that of base metal.

For this reason, many base metals with 4% or 6% Mo have been welded with filler metal such as Inconel 112 (60% Ni) electrode and Inconel 625 filler metal, both containing 9% Mo [209].

Strain Age Cracking

Most of the precipitation-hardenable alloys are susceptible to strain age cracking. Alloys containing columbium have a better resistance to cracking because of the slower hardening response of the columbium precipitate than the aluminum or titanium precipitate.

26.2 Welding Methods

Typical arc welding processes employed for welding nickel and nickel base alloys are gas tungsten arc welding (GTAW), gas metal arc welding (GMAW), and shielded metal arc welding (SMAW). Submerged arc welding (SAW) and plasma arc welding (PAW) have limited applicability. The GTAW process is preferred for welding the precipitation-hardenable alloys, although GMAW and SMAW can also be used. Reference 211 details the welding of nickel and nickel-base alloys.

Gas Tungsten Arc Welding

GTAW is widely used for joining thin sections of nickel alloys, for the root pass of pipe welds, and where flux residues are harmful. This process is the principal welding method for precipitation hardenable alloys. Argon, helium or a mixture of the two are the recommended shielding gases. Since presence of oxygen, carbon dioxide or nitrogen cause porosity in the weld metal, they should be avoided. GTAW usually requires shielding of the weld root. If a complete penetration weld is made in the open, the weld metal exposed on the underside of the bead will be oxidized. Various shielding methods employed to protect the rootside include, grooved backup bars, inert gas backup shielding, and a backing flux.

Shielded Metal Arc Welding

SMAW is primarily used for welding commercially pure nickel and solution-strengthened nickel alloys 1/16 in (1.6 mm) thick and over. The precipitation-hardenable alloys are seldom welded with SMAW process, because the alloying elements that contribute to precipitation hardening are difficult to transfer across the arc.

Gas Metal Arc Welding

GMAW is used to weld the solution-strengthened nickel alloys except high-silicon casting alloys. Many precipitation-hardenable alloys may also be welded. Spray, pulsed spray, globular, or short-circuiting filler metal transfer may be used. The protective shielding gas is usually argon or argon mixed with helium. Use dcrp for all methods of metal transfer with GMAW.

Submerged Arc Welding

Submerged arc welding (SAW) can be used for joining solid-solution-strengthened nickel alloys. Monel 400 is mostly welded by this process. It is especially useful for welding thick sections. SAW uses dc with sp or rp. SAW process cannot be used for welding the precipitation-hardenable alloys.

Oxyacetylene Welding

The oxyacetylene flame is the only gas flame that burns hot enough, 5000–6300°F (2760–3482°C), to join nickel alloys. Oxyacetylene welding gives good results in all welding positions. It is a cheap process. To weld nickel-base alloys, use a slightly reducing flame. A strongly reducing flame is not recommended when welding nickel alloys containing chromium, to avoid carbon pickup in the weld. Oxidizing flame is not recommended to weld (1) nickel-

copper alloys, because, the oxidizing flame forms cuprous oxide, which dissolves in the molten metal, which causes weld brittleness and reduces corrosion resistance, and (2) high-chromium alloys, because an oxidizing flame produces chromium oxide that is not readily soluble in the flux [211].

26.3 Postweld Heat Treatment

Nickel and nickel-base alloys generally do not experience any metallurgical changes, either in the weld metal or in the heat-affected zone, that affect normal corrosion resistance. Hence, no postweld heat treatment is normally required. However, heat treatment may be necessary in circumstances such as (1) to meet specification requirements, or (2) for stress relief of a welded structure to avoid age hardening or SCC of the weldment used to contain hydrofluoric acid vapor or caustic soda. If welding induces moderate to high residual stresses, the precipitation-hardenable alloys require a stress-relief anneal after welding and before aging.

27 TITANIUM: PROPERTIES AND METALLURGY

Titanium is a reactive, nontoxic, and low-density metal. Titanium and its alloys are used in major applications for which their inherent properties justify their selection: (1) for corrosion resistance, and (2) where specific strength is of major advantage. Titanium "bridges the design gap" between aluminum and steel, and offers a combination of many of the most desirable properties of each. Its light weight with specific gravity lying between aluminum and steel (approx. 60% of steel) gives a high strength-to-weight ratio. For example, the strength-to-weight ratio for annealed Ti-6Al-4V (grade 5) is about 7.81 (density is 0.160 lb/in^3 and yield strength is 125 ksi), whereas it is about 1.25 for annealed stainless steels. Increases in strength, as with other materials, are achieved by the addition of alloying elements such as Al, Cu, Mo, Si, V and Zr. It is known for its excellent corrosion resistance due to a stable, tenacious oxide film formed on its surface. Corrosion failures with titanium are rare and usually associated with weld defects. All titanium alloys contain minute amount of interstitial elements such as carbon, oxygen, nitrogen, and hydrogen.

27.1 Properties that Favor Heat-Exchanger Applications

The combination of high strength, stiffness, good toughness at cryogenic temperature, immunity to corrosion in wet chlorine, excellent corrosion resistance to many chemicals, and erosion resistance allows widespread use of titanium and titanium alloys from cryogenic (–423°F) to moderately high temperature (1000°F). Titanium is used as heat-exchanger material in chemical industries, refinery, absorption refrigeration and air conditioning, refinery heat exchangers, brine heat exchangers, desalination plants, power-plant surface condensers, and auxiliary exchangers. Titanium finds its widest use in chemical process industries as process equipment, wet scrubbers, heat exchangers, valves, pumps, and piping systems. Almost all nuclear stations the world over have standardized on the use of titanium as tube material. It is available in various product forms including sheets, plates, cladded plates, pipes, tubes, including U-bend, and enhanced tubes (integral fin tube, applied fin tube, and corrugated and rope tube).

The arguments against titanium are its high price, high quality standards, sensitivity to fouling, corrosion fatigue, and possibility of hydrogen embrittlement if cathodic protection in excess is applied [109]. For fixed-baffle spacing, titanium tube heat exchangers are susceptible to flow-induced vibration due to its low modulus of elasticity and the use of thin-walled sections for cost considerations. However, this can be overcome by reducing the baffle spacing.

27.2 Alloy Specification

Titanium specification and grades include Grade 1, Grade 2, Grade 3, Grade 4, Grade 5, Grade 6, Grade 7, Grade 9, Grade 11, and Grade 12. Grades 1, 2, 3, and 4 apply to commercially pure titanium (98.5 to 99.5%) and differ in the amounts of interstitials like oxygen, nitrogen, carbon, and iron. By varying these interstitials elements, the unalloyed titanium grades can be strengthened. The higher the grade, the greater is the amount of oxygen and the greater is the metal's strength. Grades 5, 7, 11, and 12 are titanium alloys. Various ASTM grades, alloy designations, compositions, and metallurgical phases present are given in Table 46; characteristics and applications areas are given in Table 47. An important source book on titanium is the *Titanium Handbook* [212]; also see Schutz et al. [213].

27.3 Titanium Grades and Alloys

Unalloyed Grades

Pure titanium has low tensile strength and is extremely ductile. Dissolved oxygen and nitrogen markedly strengthen the metal, and carbon and iron to a lesser extent. Grade 1 is purer and therefore more ductile, and finds use where severe forming is required; Unalloyed titanium mill products of Grade 2, most widely used and more ductile, find use where severe forming is required; this grade has outstanding resistance to general and other forms of corrosion in many environments, but it is not resistant to crevice corrosion [105]. Grade 3 provides slightly higher strength due to its higher percentage of interstitial elements [215].

Alloy Grades

1. Titanium is not as widely used in the alloyed form in chemical process industries, the exception being titanium-0.2% palladium alloy (Grade 7) to enhance corrosion resistance in mildly reducing solutions and high-temperature chloride solutions. Typical applications extend to hydrochloric, phosphoric, and sulfuric acid solutions and areas of service where the operating conditions vary between oxidizing and mildly reducing conditions [114, 216]. The presence of palladium has no other significant effect on the physical or mechanical properties of titanium and it makes titanium costlier.

Table 46 Titanium Grades, Composition, and Structure

Grade	UNS no.	Description	Phase
Grade 1	R 50250	Unalloyed titanium	α
Grade 2	R 50400	Unalloyed titanium	α
Grade 3	R 50550	Unalloyed titanium	α
Grade 4	R 50700	Unalloyed titanium	α
Grade 5	R 56400	Ti-6Al-4V	α-β
Grade 5	R 56401	Ti-6Al-4V ELI[a]	α-β
Grade 6	R 54520	Ti-5Al-2.5Sn	α
Grade 6	R 54521	Ti-5Al-2.5Sn ELI[a]	α
Grade 7	R 52400	Ti-0.20 Pd	α
Grade 9	R 56320	Ti-3Al-2.5 V	Near α
Grade 11	R 52250	Ti-0.20 Pd	α
Grade 12	R 53400	Ti-0.3Mo-0.8Ni	Near α

[a]Extra-low interstitials grade. R 52550 and R 52700 are titanium alloy castings.

Table 47 General Characteristics of Titanium Alloys, and Applications [214]

Alloy	General characteristics	Applications
Grade 1	Highest purity, lowest strength and high ductility, cold formability, good corrosion resistance among the four ASTM unalloyed grades due to low interstitials.	Used in continuous service up to 425°C (800°F) and for plate heat exchangers (PHE).
Grade 2	Workhorse for industrial applications requiring good ductility and corrosion resistance. Minimum yield strength of 275MPa, which is comparable to those of annealed austenitic stainless steels.	Continuous service up to 425°C (800°F) and in intermittent service up to 540°C (1004°F). Piping, tubular heat exchangers, values, tanks, vessels.
Grade 3	Lower iron limits than Grade 4. Improved strength with reasonable ductility, good corrosion resistance.	Same as Grade 2. Higher strength than Grade 2. Tubesheets and valves.
Grade 4	Highest strength of the unalloyed ASTM grades. Moderate formability, outstanding corrosion and fatigue resistance in saltwater.	Often used interchangeably with Grade 3. The strength-to-weight ratio is higher than 301 stainless steels up to 315°C (600°F). Tubular heat exchangers, piping, vessels.
Grades, 7 and 11	Better resistance to crevice corrosion at low pH and high temperature than corresponding unalloyed Grades 1 and 2.	Special corrosion application. Tubular heat exchangers, vessels, valves, gasketed plate heat exchangers.
Grade 12	Stronger and more resistant to crevice corrosion at higher temperatures than unalloyed Ti grades. Less expensive than Grades 7 and 11, but it does not offer the same crevice corrosion resistance at low pH (pH 3). In near neutral brines, crevice corrosion resistance are similar to Grades 7 and 11.	Application requiring moderate strength and enhanced corrosion resistance such as heat exchangers, pressure vessels, chlorine cells, and salt evaporators.
Grade 9	Excellent cold formability and 20 to 50% higher strength than unalloyed Ti.	Used in tubular forms.
Grade 6	A medium-strength alloy with excellent weldability. It has good oxidation resistance and intermediate strength at service temperatures up to 480°C (896°F).	The primary use is for cryogenic applications, in which the ELI grade has good strength and toughness for low temperature. It has been replaced by Grade 5 (Ti-6Al-4V) in other applications.
Grade 5	It is the most widely used Ti alloy. The alloy is most commonly used in the annealed condition. It is hardenable in sections up to 25.4 mm (1 in) with yield strengths as high as 1140 MPa (165 ksi).	Aeorspace industry, medical prostheses.

2. To overcome the cost disadvantage of Grade 7, a new alloy designated Grade 12 with 0.8% Ni and 0.3% Mo has been developed for increased corrosion resistance in specific media [217].
3. Lower alloy Grade 9 (3% Al and 2.5% V) is used for pressure-vessel applications.
4. For cryogenic applications the basic titanium alloy Ti-6Al-4V or Ti-5Al-2.5Sn-ELI is used.

ASTM and ASME Specifications for Mill Product Forms

ASTM and ASME specifications that govern unalloyed titanium and alloyed titanium in various mill product forms such as strip, sheet and plate, seamless and welded pipe, seamless and welded tube for condensers and heat exchangers, bars and billets, and forgings in various grades are given in Table 48. For these alloys the design temperatures should be less than approximately 806°F (430°C) to avoid excessive oxidation and oxygen embrittlement in continuous service.

Industry uses titanium in sheet and plate form in addition to tubes and plate used in heat exchangers. Construction can be solid titanium, titanium-clad steel, or with titanium linings. Solid titanium construction is generally more cost-effective than clad construction when vessel wall thickness is below approximately 1–1.5 in (25.4–38.1 mm).

28 TITANIUM CORROSION RESISTANCE

28.1 Surface Oxide Film

Titanium exhibits excellent corrosion resistance to general corrosion, pitting, erosion-corrosion, and galvanic corrosion. The superior corrosion resistance of titanium alloys is derived from the formation of a highly stable, tenacious, protective oxide film on its surface. This film, typically 50 to 200 Å thick, is primarily titanium dioxide (TiO_2) in rutile (highly crystalline) and/or anatase (somewhat amorphous) form [218]. Even if the oxide film is damaged, being a reactive metal and with a high affinity for oxygen, the protective oxide films form spontaneously and instantaneously whenever fresh metal surfaces are exposed to traces of oxygen or moisture [213]. Film growth is also accelerated under strongly oxidizing conditions such as in HNO_3 and CrO_3 media [219]. Another desirable feature is that at low temperatures, this surface oxide film provides a barrier for penetration of hydrogen into titanium surfaces. Conversely, titanium is severely corroded in a reducing environment wherein it is not readily repassivated. Once the brakedown of the passive film occurs, the corrosion process is unhindered. Loss of oxide film could occur due to abrasion, chemical reduction of the oxide, or surface contamination, notably by iron oxide [220].

28.2 General Corrosion

The oxide film on titanium is attacked only by a few media, including hot concentrated reducing acids, most notably hydrofluoric acid. Anhydrous conditions in the absence of oxygen

Table 48 Titanium Product Shapes, Grades, and ASTM/ASME Specifications

Product description	Grades	ASTM/ASME
Strip, sheet, and plate	Grades 1, 2, 3, 4, 5, 7, 9, 11, 12	B265/SB265
Seamless and welded pipe	Grades 1, 2, 3, 4, 7, 9, 11, 12	B337/SB337
Seamless and welded tube for condensers and heat exchangers	Grades 1, 2, 3, 4, 6, 7, 9, 11, 12	B338/SB338
Bars and billets	Grades 1, 2, 3, 4, 5, 6, 7, 11, 12	B348/SB348
Forgings	Grades 1, 2, 3, 4, 5, 6, 7, 11, 12	B381/SB381

should be avoided since the protective film may not be regenerated if damaged. General methods to improve corrosion resistance of titanium in a reducing environment are suggested by Schutz et al. [213]. Such measures include the following:

Alloying with metals such as palladium, nickel, and/or molybdenum.

Addition of inhibitor to the environment, such as oxidizing metal cations, oxidizing anions, precious metal ions, oxidizing organic compounds; adding oxidizing species (inhibitors) to the reducing environment is to permit oxide film stabilization; additions of minute amounts of water to certain anhydrous environments is to maintain passivity.

Precious metal surface treatments; this includes precious metals such as platinum and palladium that have been ion implanted, ion plated, or diffused thermally.

Anodizing and thermal oxidation: As stated earlier, titanium relies on the presence of an inert surface oxide film for its corrosion resistance, especially where hydrogen uptake is of concern. Therefore, surface treatment processes such as anodizing and thermal oxide treatment are practised to thicken and toughen the oxide film, which in turn will improve the metal's corrosion resistance.

Anodic protection by impressed current or galvanic coupling with a more noble metal in order to maintain the surface oxide film.

Surface pickling in HNO_3-HF solution to remove smeared surface iron.

Metallic coatings.

Noble alloy contact or by the applications of their oxides such as Ni, Cu, Fe, and Mo on titanium alloy surfaces, which is effective for crevice corrosion.

28.3 Resistance to Chemicals and Solutions

Titanium resists corrosion in seawater, brines, aqueous chlorides, organic and oxidizing acids, and neutral and inhibited reducing conditions better than other metals. Titanium is unique in its resistance to chlorides. Titanium, being immune to corrosion in wet chlorine, would face little maintenance problems. Since the heat transfer rates of titanium are so much better than glass, the titanium coolers require only about 12–15% the space to do the same job as glass exchangers for chlorine applications. High corrosion resistance to oxidizing and chloride solution led to widespread use in marine, chemical process industries, power plants, and petrochemical industries.

Titanium alloys are attacked severally by red fuming nitric acid or nitrogen tetroxide. Titanium and its alloys are sensitive to reducing acids, and the breakdown of the surface oxide films can take place when the temperature and/or concentration of pure acid exceeds certain values. Typical reducing acids includes hydrochloric, hydrobromic, hydroiodic, hydrofluoric, phosphoric, sulfuric, and sulfamic acids. In some acids that do attack titanium, the addition of small amounts of an oxidizing acid such as nitric or salts (such as copper sulfate) inhibits attack.

Resistance to Waters

Titanium exhibits good corrosion resistance to fresh water, industrial cooling waters including raw seawater, brackish estuary water, and polluted water. Titanium (like many other metals) is subject to the formation of mineral scales when water temperatures are excessive [220]. It resists all forms of corrosive attack by fresh water and steam to temperatures as high as 600°F (316°C) and corrosion by seawater to temperatures as high as 500°F (260°C) [219]. The presence of sulfides in seawater does not affect the corrosion resistance.

Forms of Corrosion

Galvanic Corrosion. From its position in the galvanic series, Titanium is highly immune to galvanic corrosion but tends to accelerate the corrosion of the other metal of the galvanic couple. The exception is in highly reducing acid environments where titanium may not passivate. Under these conditions, it has a potential similar to aluminum and will undergo accelerated corrosion when coupled to other more noble metals [219]. While using titanium tubes, extreme care should be taken to avoid galvanic corrosion of tubesheets and water boxes of a condenser, which have different corrosion potential. Solid titanium or titanium-clad tubesheets are preferred in order to eliminate galvanic corrosion of a tubesheet of an anodic material, such as a copper alloy or carbon steel. Water boxes should be coated for protection. If a titanium-clad tubesheet is used (a minimum of 3/16 in or 4.5 mm thick cladding is required), the tube-to-tubesheet joints should be welded, but if a solid tubesheet is used, roller expansion can be performed.

Hydrogen Embrittlement. In a galvanic couple, if titanium is the cathodic member, hydrogen may be evolved on its surface. Normally the surface oxide film on titanium acts as an effective barrier to penetration by hydrogen. By specification, hydrogen is limited to 150 ppm maximum in all the common tube metal grades [220]. Within the range of pH 3 to 12, the oxide film is stable and presents a good barrier to penetration by hydrogen [219]. Under certain conditions, titanium can absorb hydrogen and become embrittled:

1. Dry, nonoxidizing hydrocarbon or hydrogen stream—the oxide films breaks down since there is no mechanism for replacing oxygen lost to the process stream.
2. Disruption of the oxide film allows easy penetration by hydrogen.
3. If the temperature is above 176°F (80°C), hydrogen may diffuse into the metal and cause hydrogen embrittlement.

Even the risk of failure due to hydrogen embrittlement can be greatly reduced if care is taken to maintain the potential of the tubes/tubesheets in the range –0.5 to –0.07 V on the saturated calomel electrode (SCE) scale [193]. TIMET's recommendation for the limiting temperature for titanium usage in hydrogen environments is 71°C (160°F) [219]. This temperature is based on the barrier effect or near-zero diffusion rate of hydrogen at that temperature [220].

Crevice Corrosion. Titanium alloy as well as commercially pure titanium will be subjected to localized attack in tight crevices exposed to hot (>158°F/70°C) aqueous solutions, or chloride, bromide, iodide, or fluoride solutions. Crevice corrosion of unalloyed titanium may occur in seawater at temperatures above the boiling point. One major exception is the alloys containing 0.2% palladium [221]. Titanium alloy Grade 12 and Ti-Pd (Grades 7 and 11) offer resistance to crevice corrosion in seawater at temperatures up to 500°F (260°C) [219]. Both alloys also provide improved resistance to reducing acid conditions, and Grade 12 offers increased strength particularly as the temperature is increased. The projected immunity of titanium and its palladium alloy from pitting corrosion, as would occur in crevices, is shown in Fig. 30 as a function of chloride concentration and temperature. Where corrosion of titanium is a problem under deposits, molybdenum-bearing titanium grade, Grade 12, R53400 (Ti-0.3Mo-0.8Ni), should be used.

Erosion-Corrosion. An important property of titanium is its excellent resistance to erosion-corrosion and its various forms such as cavitation and impingement attack. Titanium is considered one of the best cavitation-resistant materials available for seawater service. Titanium has the ability to resist erosion due to high-velocity seawater up to 30 m/s [218].

Stress Corrosion Cracking. SCC of commercial titanium and titanium alloys may occur in red fuming nitric acid at room temperatures. The possibilities of SCC in natural seawater can

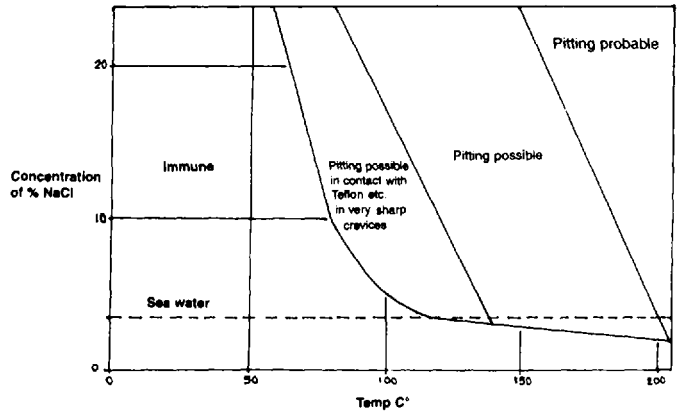


Figure 30 Crevice corrosion of titanium; crevice corrosion in titanium is a function of temperature and chloride concentration. [From Ref. 196.]

be reduced by alloy selection and heat treatment. The presence of defects combined with an unfavorable stress condition can account for almost instantaneous failure of welded structures in contact with trichloroethylene [79].

Corrosion Fatigue. Titanium, unlike many other materials, does not suffer a significant loss of fatigue properties in seawater. In fatigue-limited applications, ASME Code Criteria or actual in situ fatigue should be considered.

MIC. Titanium is highly resistant to MIC. More than 30 years of extensive Titanium alloy use in biologically active process and raw cooling waters, especially seawater, appears to substantiate titanium's resistance to MIC [218].

28.4 Thermal Performance

With its low fouling resistance values in combination with thinner tube walls, the overall heat-transfer coefficient has been more than adequate in all installations. Titanium's resistance to erosion-corrosion permits high flow velocity (up to 120 ft/s if pressure drop considerations permit). High velocity means higher heat-transfer rates and lower fouling factors. Experience has shown that titanium exchangers handling seawater can be designed with a fouling factor as low as 0.0005 h · ft^2 · °F/BTU [219].

28.5 Fouling

As titanium is perfectly passivated, its surface has no biostatic action and would be fouled biologically. Fouling, mussels, and barnacles are a problem in a power station installed on the seashore. Therefore, tubes must be kept clean by an online tube cleaning system such as a sponge rubber ball system, or by a correct system cooling water velocity, or by chlorination treatment.

28.6 Applications

Titanium Tubing for Surface Condensers

Titanium tubing in steam condensers has proven to be the most reliable of all tubing materials. It is immune to corrosion from chlorides. It returns no harmful metal ions to the environment

or to the condensate feedwater stream. Titanium overcomes the problems of random tube failure caused by erosion-corrosion at tube inlets due to turbulence or partial blockage by shells, mussels, debris, and ammonia condensate, and is highly resistant to erosion attack by steam impingement. In addition to fresh tubing, titanium tubings are used for retubing the leaky tubes. When retubing an existing condenser that has been designed for use with tubes other than titanium, there are six areas to consider [219]. They are: (1) Titanium tube heat exchangers require shorter baffle spacings to accommodate thinner tubes and low Young's modulus to overcome FIV problems; (2) tubesheet material for a possible galvanic couple with titanium as cathodic material (titanium can essentially be welded only to titanium, so that the tubesheets must also be made of titanium or be overlaid with titanium if a welded joint is desired); (3) effect of reduced weight due to use of thin-walled tubes and low density; (4) effect of reduced water velocity since the inner diameter has increased due to thin-walled tubes; (5) fouling; and (6) if there is already a cathodic protection system in operation, make it compatible with titanium; such measures/cautions include that hydriding can take place at potentials greater than –0.75 V (SCE)—do not exceed –0.90 V (SCE)—that the system must have an automatic potential control, and that sacrificial anodes should not be placed closer than 30 in from the tubesheet.

Refinery and Chemical Processing: Service Experience

The primary reason for titanium's expanded application in the refinery industries, particularly in the condenser service, is due to its superior resistance to handle refinery process streams containing hydrogen sulfide, chlorides, dilute hydrochloric acid, ammonia, and hydrogen [220,222]. Titanium Grade 2 tubes are used in overhead coolers and condensers. Titanium for refinery services is limited to operating temperature of 260°C. If hydrogen is present, temperature should not exceed 175°C (350°F) to prevent hydrogen embrittlement.

Chemical Processing

The primary basis for titanium's expanded application in the chemical processing industries has been its superior resistance to the aggressive, mildly reducing, oxidizing, and/or chloride-containing process streams.

PHE

Due to its inherent corrosion resistance, titanium is used as a plate heat exchanger material in corrosive applications.

29 TITANIUM FABRICATION

29.1 Welding Titanium

Unalloyed titanium and all alpha titanium alloys are weldable. Alpha-beta alloys, alloy Ti-6Al-4V, and weakly beta-stabilized alloys are also weldable. Beta-phase alloys and strongly stabilized alpha-beta-phase alloys are difficult to weld and they will embrittle.

Welding Methods

Commercially pure titanium and weldable alloys can be arc welded successfully by the manual gas tungsten arc, plasma arc, and gas metal arc processes. If economically justified by thickness, run length, or repetitive work, automatic hot wire TIG with special trailing shields is used. Procedures and equipment are generally similar to those used for welding austenitic stainless steel or aluminum, with two important exceptions [215]: (1) Titanium requires greater cleanliness and (2) it requires auxiliary gas shielding. In general, fluxes are not used due to the high-temperature reactivity of titanium.

Weldability Considerations

When heated in air, titanium oxidizes rapidly and, at temperatures near its melting point (3272°F), (1) molten titanium reacts with most materials, which embrittles the weldment and reduce the corrosion resistance, and (2) it dissolves its own oxide, leaving inclusions in welds. In its solid state, titanium above 1200°F absorbs oxygen, nitrogen, and hydrogen from the atmosphere. Even small amounts of these elements can cause embrittlement in the weld and loss of corrosion resistance [223]. Hydrogen in concentrations exceeding 150 ppm can embrittle the pure metal and also the various commercial alloys available [224]. Consequently, to assure a successful titanium weld, air must be excluded from both the face and back of the weld metal and a secondary inert-gas shield must protect the weld area until it cools to 600–800°F (315–425°C).

Shielding Gases. In arc welding, this is accomplished by replacing the air surrounding the weld area by argon or helium with argon. No other gases can be used.

When titanium parts are heated to more than 500°F (260°C), contact with adhesive tapes, papers, marking crayons, etc. containing more than 50 ppm chlorine or other halogen compounds should be avoided [225].

Welding of Titanium to Dissimilar Metals. Satisfactory fusion welding of titanium to dissimilar metals, except with vanadium and silver, is not possible because of the formation of brittle intermetallic compounds. Therefore, interconnections between dissimilar metals are made by mechanical means such as by bolting. Lining vessels with titanium cannot be accomplished directly by fusion welding. In some instances silver filler metal is used for seal welds [217].

Manufacturing Facilities. While it is not always possible to fabricate large titanium assemblies in a closed clean room as demanded for a clean environment, designating areas of the heavy workshop area to be screened off, paying great attention to preventing weld contamination with shop dirts/dust by screening, and stringent solvent cleaning of weld preparations and filler wire before welding are necessary to achieve the proper weld metal characteristics and corrosion resistance.

Edge Preparation

Prepare joints by sawing, machining, or grinding. Joint surfaces should be smooth and free of crevices, roughness, and overlaps that can trap dirt and cleaning solution. If burrs should occur, remove them with a clean, sharp hand file or rotary file. Dirty shearing equipment is likely to contaminate sheared or slit edges and ultimately cause weld metal porosity.

Joint Design

Joint designs for titanium welding are essentially the same as those found in the inert-gas arc welding of other metals. The joint design should allow for full shielding of both sides or permit the exclusion of air from parts of the joint reaching temperatures of 1000°F (538°C) or greater [226]. For example, argon purge holes are provided in vessel shell nozzle reinforcing plates and tubular stiffeners. Special configurations are necessary on titanium-clad tubesheet joints to give adequate back shielding.

Precleaning and Surface Preparation

A good titanium weld begins with cleanliness, both in the immediate weld area and in the shop floor. Foreign matters that contaminate the weld lead to porosity and low mechanical properties. Consequently, surface residues such as scale, oxide, grease, dust, grinding wheel grit, etc.

must be removed before welding. The surface oxide and scale resulting from normal hot-forming operations can be removed mechanically or chemically.

Cleaning Titanium. Titanium can be cleaned by steam cleaning, alkaline cleaning, vapor degreasing, and solvent cleaning methods. Cleaning solutions for titanium must maintain passivity and avoid possible hydrogen uptake by the titanium. Titanium cleaning is discussed by Chevalier [225], and ASTM Specification B600 details procedure for descaling and cleaning titanium and its alloys.

Degreasing. Titanium parts that are free of scale or oxide require only degreasing. Light or medium contamination is degreased by immersion in hot alkaline solutions or by spraying. Heavy contamination is degreased by cleaning in alkaline solution in two stages, preferably after degreasing. Use nonchlorinated degreasing solvents, reagent methanol, acetone, or methyl ethyl ketone to degrease or remove machining oil. Avoid using chlorinated solvents such as trichloroethylene vapor, alcohols, and methanol in particular [226]. Deposits remaining from solvents of this type may cause cracking in high-strength alloys if the metal is subsequently heated in stress relief or actual service.

Descaling or Oxide Removal. Light oxides may be removed by brushing with a stainless steel wire brush, sand blasting, or draw filing. Steel wool or abrasives should never be used because of the danger of contamination. If grinding is required, the use of silicon carbide is preferred. Heavy oxide scales may be removed by grinding, machining, liquid abrasive blasting, salt-bath descaling, or alkaline cleaning. To remove oxide scale formed at temperatures below 1150°F, a pickling solution is used that consists of 25–30% nitric acid and 2–3% hydrofluoric acid by weight mixed with water. To remove oxide scale formed at temperatures above 1150°F, sandblasting or solutions of sodium hydride, Virgo, Kolene, or similar salt baths followed by acid pickling are required [226]. Proper inhibition is most critical when reducing acids, such as HCl, H_2SO_4, sulfamic, or oxalic acids, are used to remove scaling. Since rapid titanium attack may occur, hydrofluoric acid cleaning solutions are not to be used for scale removal.

Rinsing. Water rinsing after degreasing or acid pickling must be carried out with deionized water having a resistivity of more than 50,000 ohm/cc when intending to do an operation such as heat treatment, welding, etc. above 500°F (260°C) [225].

Handling of Cleaned Components. Handling of cleaned components before being welded must be with clean gloves to avoid fingerprints; during waiting periods the parts must be stored in a packed condition and protected from external contamination.

Fitup

Uniform fitup avoids burn-through, controls underbead contour, and simplifies backup shielding or purging.

Preheating

Titanium welding does not normally require preheating [215]. For very low ambient temperature and low humidity conditions, preheating to 100–150°F (37–65°C) helps moisture removal.

Filler Metal

Thirteen titanium and titanium alloy filler metal (or electrode) classifications are given in AWS A5.16-90. A partial list is shown in Table 49. Maximums are set on carbon, oxygen, hydrogen, and nitrogen contents. Filler metal composition is usually matched to the grade of titanium being welded. ERTi-2 and ERTi-0.2Pd are good overall choices. ERTi-2 can be used on grades 1, 2, and 3 base metal [215]. Recommended filler wire grades and the base-metal grades are given in Table 50.

Table 49 AWS A5.16 Classifications of Titanium Filler Metal

AWS classifications	Composition
ERTi-1	Ti-0.50O
ERTi-2	Ti-0.05O
ERTi-3	Ti-0.13O
ERTi-4	Ti-0.20O
ERTi-5	Ti-6Al-4V
ERTi-5ELI	Ti-6Al-4V
ERTi-6	Ti-5Al-2.5Sn
ERTi-6ELI	Ti-5Al-2.5Sn
ERTi-7	Ti-0.05O-0.2Pd
ERTi-9	Ti-3Al-2.5V
ERTi-9ELI	Ti-3Al-2.5V
ERTi-12	Ti-0.3Mo-0.8Ni

Table 50 Recommended Titanium Filler Metals [215]

Filler grade	Base metal grade
ERTi-1	1
ERTi-2	1
ERTi-3	2
ERTi-4	3
ERTI-7	7
ERTi-12	12

Welding Procedures

Gas Tungsten Arc Welding. Due to the inert-gas shielding characteristics and the high degree of arc control, GTAW is ideally suited for titanium. Use a drooping-characteristic power supply and dcsp. Titanium can be successfully welded with GTAW in thickness ranging from several thousandths of an inch to more than several inches. Use the same techniques as for welding of stainless steel. To avoid contamination, weld joint and wire must be clean, and the shielding gas, usually argon, must be free from moisture and impurities. A facility to ignite the arc is required that prevents contamination of the titanium with tungsten inclusions from the electrode. AWS D10.6, Gas Tungsten Arc Welding of Titanium Piping and Tubing, covers various aspects of GTAW of titanium.

Shielding. Inert-gas shielding (either by argon or helium) of the weld area is accomplished by several methods:

1. A vacuum chamber or special inert-gas-filled chamber, which eliminates the need for elaborate jigs and other fixtures that normally would be required to adequately shield complex assemblies in air; it is generally considered that the highest weld quality is obtained by employing vacuum or argon purged chamber welding.
2. A backup gas shielding with trailing shield by welding in open air.

A section of AWS D10.6 on gas shielding offers several alternatives for shielding, including work-mounted trailing shields and torch-mounted trailing shields.

Welding Titanium in an Open-Air Environment With Three Shielding Gases Techniques. Although historically titanium has been welded in chambers that are either vacuum or argon purged, increased usage of open-atmosphere welding is taking place in the chemical industries and marine sectors with proper shielding techniques. The shielding for welding titanium in an open atmosphere can be accomplished by using a combination of three shielding gases techniques. They are as follows [227]:

1. The primary shielding is provided by the welding torch.
2. The primary shielding is supplemented by a trailing shield, which is known as the secondary shielding; the trailing shield permits cooling of the weld deposit and the adjacent HAZ under a blanket of argon gas.
3. The back shielding protects the backside of the weld and its adjacent heat-affected zone.

Typical gas shielding for tube-to-tubesheet welding is shown in Fig. 31.

Narrow-Groove Welding of Titanium Using the Hot Wire Gas Tungsten Arc Process. Though narrow-groove welding has been dominated by the submerged arc and the gas metal arc welding processes, the use of narrow-groove joint designs with the automatic GTAW process is promising for welding of titanium. The automatic hot wire GTAW process with narrow-groove joint designs combines the advantages of automatic hot wire GTAW (high deposition rates, excellent shielding characteristics) with narrow-groove welding (high groove fill rate, reduced weld distortion) [227]. As is true with all of the narrow-groove welding processes, a problem that must be addressed is inadequate control of face fusion.

MIG Welding. The MIG process employs a direct current supply and reverse polarity. The power supply generally consists of a constant-potential rectifier, although a power supply with a drooping load characteristic is also applicable.

29.2 In-Process Quality Control and Weld Tests

Method to Evaluate the Shielding

Since titanium readily reacts with air at elevated temperatures to form oxides that exhibit specific colors, the oxide color of the weld surface can be used as an effective method to

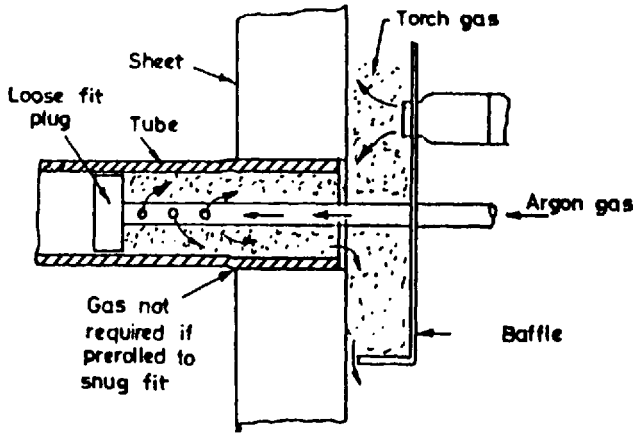


Figure 31 Gas shielding for titanium tube-to-tube sheet welding. (From Ref. 215.)

evaluate the inert-gas shielding. Welds made with proper shielding will exhibit a bright, metallic, shiny silvery weld color; the change in color represents increasing amounts of weld contamination, which usually takes place due to faulty or inadequate trailing shielding [227]. Table 51 differentiates the acceptance criteria and required disposition for each oxide colour category.

Hardness

A clean weld should not be more than 30 points BHN higher than the base metal. A greater increase indicates contamination [215].

Bend Test

Make a simple test by butt welding two narrow strips of titanium together and bending the piece over a mandrel with a radius of about three to four times the thickness of the sheet held in a vice. Welds with satisfactory ductility will bend over the following radii without cracking [215]:

Grades 1, 2, 7, and 12 4T
Grade 3 5T

Weld Defects

1. Titanium and its alloys are not prone to solidification cracking. However, under conditions of severe restraint, solidification cracking has been observed sometimes [229].
2. Weld metal porosity is probably the most frequently encountered weld defect in titanium weld metals [228]. Porosity is generally caused by hydrogen, which may originate from gas entrapment, filler metal, or base metal. Careful shielding of the weld metal and cleaning of the surfaces will help to reduce the weld metal porosity. Welding at low speeds gives extra time for gas escape, and quality of cut edges also affects the incidence of porosity.
3. Contamination cracking will occur when substantial pickup of interstitial elements occurs. This problem can be solved by careful cleaning of the surfaces and the weld joint area, and proper shielding.

29.3 Heat Treatment

Annealing

Titanium and its alloys are annealed to improve ductility, dimensional or thermal stability, fracture toughness, and creep resistance. Since improvement in one or more properties is usually obtained at the expense of some other property, the material producer should be consulted for heat-treatment considerations.

Table 51 Weld Colors and Their Meanings (Visual Colour Acceptance Criteria) [219,227,228]

Color of weld zone	Interpretation
Silver	Correct shielding, noncontaminated weld, satisfactory
Light straw	Slight contamination, but acceptable
Dark straw	Slight contamination, but acceptable
Dark blue	Heavier contamination, may be acceptable depending on service
Light blue	Heavier contamination, unlikely to be acceptable
Grey blue, grey, white powdery (loose deposit)	Very heavy contamination, unacceptable; remove by grinding, repair, then weld again

Stress Relief

Welding generally increases strength and reduces ductility. PWHT can be helpful to improve mechanical properties and to reduce residual welding stress, and the stabilization of the microstructure for elevated-temperature applications [228]. Ordinarily, low-strength alloys require no stress relief. It is often required in high-strength alloys, especially when constructing elaborate titanium welds. Alpha alloys, which include the commercially pure grades of titanium, can be stress relieved at 1000°F (540°C), 1 h per inch of thickness, in 1/2 to 4 h. Alpha-beta alloys welded in the annealed condition but not subsequently heat-treated can be stress relieved in the same manner [225,226].

29.4 Forming of Titanium-Clad Steel Plate

Titanium reacts with iron at elevated temperatures to form a brittle compound. This alloying may take place when the clad material is subjected to high temperatures while rolling, hot forming, stress relieving, welding, and the like. If the bond deteriorates to a great enough degree, the titanium layer may actually fall off the backing plate.

30 ZIRCONIUM

30.1 Properties and Metallurgy

Zirconium is a nontoxic, reactive metal. It is very similar in characteristics to titanium except that its density (6.45 gm/cm^3 or 0.235 lb/in^3) is about 50% higher. The mechanical properties of zirconium are intermediate to those of aluminum and mild steel. It is inert to many chemicals and it has very low corrosion rates in many corrosive environments. The metal has good ductility and strength and hence can be fabricated in most forms common to other metals. It can be welded comparatively easily and can be used as a structural material in corrosive applications. References 230–234 provide either specific or general information on zirconium.

Alloy Classification

Zirconium and its alloys are available in two general categories: (1) commercial-grade zirconium, containing hafnium as an impurity—this includes R60702 (unalloyed zirconium), R60703, R60704 (zirconium-tin alloy), R60705 (zirconium-niobium alloy), and R60706; and (2) alloys of zirconium essentially free of hafnium, for nuclear application, commonly called Zircaloys. These include R60001, R60802 (Zircaloy-2), R60804 (Zircaloy-4), and R60901 (Zr-2.5Nb). The purpose of alloying in zirconium is to improve elevated-temperature strength and corrosion resistance while maintaining low neutron absorption.

Product Forms. Zirconium and its alloys are available in plate, sheet, bar, rod, and tubing to a variety of material specifications. ASTM B550 covers four commercial grades of zirconium ingots: R60702, R60704, R60705, and R60706. ASTM B523 covers three grades of zirconium and zirconium alloy (R60702, R60704, R60705) seamless and welded tubes for condensers and heat exchangers.

Applications. Zirconium finds its applications in the nuclear industry and chemical process industries. The properties which favour its use as a structural material in nuclear reactors include its remarkably low thermal neutron absorption cross section, a high melting point, fair strength, and good corrosion resistance in water and liquid metals [231]. Because of its inertness, it is an excellent material for equipment used in food processing and pharmaceutical preparations. In chemical industries, it is used in process equipment, heat exchangers, piping,

reactor vessels, etc. Zirconium-cladded components are used in heat exchangers exposed to seawater.

Resistance to Chemicals. Zirconium resists corrosion in almost all alkalies, either fused or in solution. Its resistance to alkalies is better than that of tantalum, titanium, and 18 : 8 stainless steel [232]. It has an excellent resistance to HCl, boiling H_2SO_4 up to 70%, boiling HNO_3 up to 90%, most organics, and all alkaline solutions to boiling temperature, but is attacked by HF. Zirconium is corroded severely in wet chlorine, brine, dilute hydrochloric acid, and seawater that contains chlorine. Zirconium, while resistant to most chloride solutions, is not resistant to ferric and cupric chlorides above 1% [235]. Among the organic acids, trichloroacetic acid appears to be the only one corrosive to zirconium. In sulfuric acid at concentrations from zero to 70% at boiling temperatures and above, corrosion resistance of zirconium compares favorably with that of tantalum, glass, and graphite. Consequently, zirconium has replaced these materials in many applications as the cost of tantalum is higher, and glass and graphite are subject to failure from thermal and/or mechanical shock [233].

Limitations of Zirconium. The design of zirconium alloys for elevated-temperature applications is hindered by two factors: (1) the transformation of zirconium from the hexagonal close-packed (hcp) structure to a body-centered (bcc) structure at approximately 1585°F (863°C), and (2) the problem of low corrosion resistance in contact with high-temperature steam.

Corrosion Resistance

Zirconium is a reactive metal. It has a high affinity for oxygen. Its surface is covered with a protective oxide film, which is self-healing in nature. This surface film protects the base metal from corrosion attack. Whenever any fresh zirconium surface is exposed to an oxygen-bearing environment, an adherent, protective oxide film forms on its surface instantaneously.

Forms of Corrosion.

Galvanic Corrosion. Zirconium is treated as a noble metal. Therefore, galvanic corrosion of a less noble metal is possible when it is in contact with zirconium.

Pitting. Zirconium has a susceptibility to pitting in all halide solutions except fluoride.

Crevice Corrosion. Of all the corrosion-resistant metals, zirconium and tantalum are the most resistant to crevice corrosion. In low pH chloride solutions or chlorine gas, zirconium is not subjected to crevice attack.

Stress Corrosion Cracking. Zirconium service failures resulting from stress corrosion cracking (SCC) are few in chemical applications. The environments known to cause SCC include $FeCl_3$, and $CuCl_2$ solutions, concentrated HNO_3, mixtures of methanol and HCl, and liquid mercury. Apart from the standard practices known for control of SCC, the following additional methods can prevent SCC in zirconium alloys:

1. Maintaining a high-quality surface film; the film should be low in impurities, free from defects, and mechanical damage,
2. Using electrochemical protection techniques.

Methods to Improve Corrosion Resistance. The corrosion resistance of zirconium is further improved by corrosion protection methods like oxide film formation, anodizing, autoclave film formation, film formation in air, and electrochemical protection.

Fabrication

Zirconium and its alloys are ductile and workable. In fabrication of zirconium, there are some general considerations that must be taken into account [231]: (1) the purity or composition of the zirconium being fabricated, and (2) its tendency to gale under sliding contact with other metals—hence, while machining zirconium, tools must be kept sharp, and avoid light and

interrupted cuttings. Zirconium is extremely stable in contact with most common gases at room temperature, but at temperatures of a few hundred degrees centigrade, it reacts readily with oxygen, nitrogen, and hydrogen, resulting in embrittlement. Therefore, welding and brazing zirconium requires high-purity inert-gas shielding of weld puddle and hot bead from air.

Welding Method. Zirconium and zirconium alloys are most commonly welded using the gas tungsten arc welding (GTAW) process. Other arc welding processes are not used because most zirconium alloys are used in applications that require very high weld metal purity and integrity. Electron beam welding can be used for welding thick sections. As the most promising commercial property of zirconium is its high resistance to corrosion, it is essential that the welding should not reduce corrosion resistance [234]. Zirconium has a low coefficient of thermal expansion, which contributes to a low distortion during welding.

Weld Metal Shielding. At high temperatures, zirconium is extremely reactive. Therefore, the weld metal and the surrounding area must be carefully shielded from air to avoid reaction of weld metal with atmospheric gases and the resulting embrittlement. Shielding by a standard tungsten arc torch is insufficient to provide adequate protection. Critical nuclear welds are made in controlled atmosphere boxes or chambers. For industrial applications, trailing shield torches and gas backup should be adequate along with a temporary purge chamber or box. The shielding gas should be highly pure argon, helium, or a mixture of these two gases. Moisture, oxygen, hydrogen, nitrogen, or carbon dioxide in the shielding gas will be absorbed by the molten metal and will result in weld embrittlement.

Weld Preparation. The edges to be joined should be draw filed or wire brushed with a stainless steel brush immediately before welding. This should be followed by a thorough cleaning with alcohol or acetone to ensure a clean area for welding; avoid chlorinated solvents.

Surface Cleaning. ASTM Specification B614, Standard Practice for Descaling and Cleaning Zirconium and Zirconium Alloy Surfaces, covers the cleaning and descaling procedure of zirconium and zirconium alloys for the removal of shop dirts, oxides, and scales resulting from heat-treatment operations and surface contaminants, by employing one of these methods or a combination of them: (1) alkaline or emulsion soak type cleaners, (2) ultrasonic cleaning, (3) acetone or trichloroethylene solvent washing or vapor degreasing, and (4) electrolytic alkaline cleaning system.

Filler Metals. Zirconium and zirconium alloys electrodes are covered under AWS A5.24-79.

Weld Inspection. As for titanium, a clean, bright weld is obtained through the use of a proper shielding system. White deposits or a black color in the weld area is not acceptable. A bend test is probably the best test to determine weld acceptability.

Welding of Dissimilar Metals. Zirconium cannot be welded directly to most other structural metals; the exceptions are titanium, vanadium, and niobium. Hence, it is necessary to line/butter the compatible metals with a zirconium coat.

31 TANTALUM

Tantalum is a high-density (16.6 gm/cm^3), inherently soft, fabricable metal. It has a high melting point 5432°F (3000°C). It is categorized as a refractory metal. Tantalum and its alloys (Ta-2.5W and Ta-10W) resist the broadest range of environments, making it a preferred corrosion-resistant material. The outstanding corrosion resistance of tantalum in aqueous media is attributed to the spontaneous formation of a thin, amorphous, passive oxide film on the surface of the metal. The passive film forms in almost all environments, even in ones of extremely low oxidizing tendency, except for fluorides including HF, strong caustic, and oleum [235]. Tantalum often competes with zirconium, niobium, and titanium, whose corrosion resistance also

depends upon an amorphous oxide film. It is inert to practically all organic and inorganic compounds at temperatures under 302°F (150°C). The only exceptions to this are hydrofluoric acid and fuming sulfuric acid. Equipment made of tantalum includes heat exchangers, condensers, spiral coils, U-tubes, side-arm reboilers, and distillation columns. References 235–242 provide either specific or general information on tantalum.

31.1 Corrosion Resistance

Tantalum exhibits excellent resistance to most forms of corrosion. Its general corrosion rate is extremely low. The passive oxide film virtually prevents pitting, crevice and intergranular corrosion, and stress corrosion cracking. Tantalum is cathodic in a galvanic cell with all construction metals and liberates hydrogen. Hydrogen is rapidly absorbed by tantalum with resulting embrittlement. Hydrogen embrittlement is the single most important cause of failure of tantalum [235]. Therefore, it is of utmost importance to avoid applications in which there may be a cathodic reaction [242]. Hydrogen embrittlement of tantalum is discussed next in detail.

31.2 Hydrogen Embrittlement

Even though tantalum does not react with molecular hydrogen below 662°F (350°C), it can absorb atomic hydrogen under persistently aggressive conditions, causing embrittlement and failure even when the corrosion rate is low. To protect equipment from exposure to atomic hydrogen, tantalum should be electrically insulated from all other metals. General practice to prevent hydrogen embrittlement is to attach a small amount of platinum (1 : 1000) to tantalum by spot welding, electroplating, or rubbing with platinum wool. Platinum is effective because it is cathodic to tantalum [238].

31.3 Resistance to Chemicals

Tantalum has excellent corrosion resistance to a wide variety of acids, alcohols, chlorides, sulfates, and other chemicals. Tantalum should be used for equipment handling hot concentrated hydrochloric, sulfuric, or phosphoric acid. The metal oxidizes in air above about 570°F (299°C), and it is attacked by hydrofluoric, phosphoric, and sulfuric acids, and by chlorine and fluorine gases above 300°F.

31.4 Product Forms and Cost

Tantalum and its alloys are available in all common product forms, including foil, strip, sheet, plate, wire, rod, bar, ingot tubes and welded tubes, and clad plates.

The initial material cost is higher than for glass, graphite, fluorocarbons, or other metals. However, when lifetime cost is considered, tantalum is economical, primarily due to its longer life, maintenance-free performance, and considerably reduced downtime. Primarily due to its high initial cost, tantalum is used most often only where other materials fail or will not perform at all or where very high product purity is to be maintained, as in processing of pharmaceuticals and the preparation of cosmetics, soaps, perfumes, etc. [235].

31.5 Performance Versus Other Materials

Tantalum is often compared to glass in regard to corrosion resistance. Of all the metals, tantalum is considered most like glass in corrosion resistance, and due to this property it is used in glass and glass-lined equipment [242]. However, unlike glass, tantalum has good resistance to brittle fracture and failure due to vibration and shock. Its strength and rigidity are similar to that of steel, while its machinability and formability are similar to copper.

31.6 Heat Transfer

Tantalum and its alloys are ideal for heat exchangers because of their high thermal conductivity (thermal conductivity of tantalum is higher than Zr, titanium, 304/316 SS, alloys 600 and 625, and Hastelloys C-276 and B-2), their ability to be used in thin-walled tubes, and nonfouling characteristics. The wall thickness of tantalum tubes, typically 0.015 to 0.20 in (0.381 to 0.508 mm), had become an engineering standard. This compares with 0.035 in (0.889 mm) for titanium and zirconium, since allowances have to be made for corrosion [235]. The heat-transfer rate of tantalum does not change with time, due to the absence of corrosion and deposits.

31.7 Welding

Similar to titanium and zirconium, tantalum readily reacts with carbon, hydrogen, oxygen, and nitrogen at temperatures above 600°F (315°C). When dissolved interstitially in tantalum, these elements increase the strength properties, but reduce the ductility. Therefore, any fusion welding must be performed in air-free atmosphere. This is achieved either by vacuum or by inert-gas shielding.

32 GRAPHITE, GLASS, TEFLON, AND CERAMICS

To solve the corrosion problem, users are turning in increasing numbers from heat exchangers of metal, to graphite, glass, and Teflon fluorocarbon resins. Ceramics are preferred for high-temperature applications, particularly for waste heat recovery. All these nonmetals are characterized by inertness to chemical attack and nonductile nature. Cost and chemical inertness are usually the primary factors in a decision to use a brittle materials instead of a metal [243]. Salient features that favor these material for heat-exchanger construction are discussed next.

32.1 Graphite

Graphite is a unique material; it has a most valuable combination of properties. It has properties common to both metals and nonmetals. Impervious graphite is used as a heat-exchanger material. It is made by impregnating graphite with a phenolic or furfuryl alcohol resin. Graphite is an allotropic form of carbon. It is used as a heat-exchanger material due to the following valuable properties:

1. High thermal conductivity.
2. Resistance to corrosive fluids.
3. Stable over wide range of temperature.
4. Ability to withstand thermal shock.
5. Low coefficient of friction.
6. Ability to be fabricated to the desired (a) strength, (b) porosity, (c) density and compactness, (d) grain structure and fineness, and (e) surface finish.
7. Good machining characteristics and possibility to machine it into desired shapes.
8. Due to smooth surface finish, the fouling is minimum and hence there is less deterioration in thermal performance.
9. Ordered crystal structure.

References 243–246 provide either specific or general information on graphite.

Applications of Impervious Graphite Heat Exchangers

Impervious graphite resists a wide variety of inorganic and organic chemicals. But strong oxidizing acids such as nitric acid, concentrated sulfuric acid, and wet chlorine cannot be

handled [245]. Heat exchangers with improved resistance to oxidizing agents are being developed. Unlike the ceramic, graphite can handle hydrofluoric acid up to 60% and hot caustics [243]. Graphite heat exchangers are employed as boilers and condensers in the distillation by evaporation of hydrochloric acid and in the concentration of weak sulfuric acid and of rare earth chloride solutions.

32.2 Drawbacks Associated with Graphite

Drawbacks associated with graphite are:

1. The principal limitation in the application of graphite lies in the synthetic resins used for both impregnation and laminate. The resins undergo decomposition at temperatures above 356°F (180°C) and hence graphite heat exchangers are limited to this temperature [245].
2. Porosity and permeability poses problems for liquids and gases, and the other problem is poor tensile strength. However, the porosity problem is overcome by impregnation with synthetic resin.
3. Brittleness (poor impact strength), poor abrasion resistance, and low tensile strength are problems; the poor tensile strength is overcome by modifying the design and fabrication.
4. Not recommended for fine chemical industries like pharmaceutical, brewing, and food processing industries.

Forms of Graphite Heat Exchangers

The principle forms of graphite heat exchangers are:

1. Shell-and-tube heat exchanger.
2. Cubic or rectangular block heat exchanger.
3. Modular-block cylindrical exchanger.
4. Plate heat exchanger.

Graphite heat exchangers construction details are discussed by Hills [244,247] and Schley [246].

Shell-and-Tube Heat Exchanger. The shell-and-tube design consists of graphite tubes and tubesheets to exploit its noncorrosive property on the tube side. The tube bank is enclosed in a shell made of steel, cast iron, copper, aluminum, or lead, with or without corrosion-resistant linings. The baffles may be of soft metal or plastic (PTFE). Due to poor strength of graphite, the operating temperature and pressure are limited to 356°F (180°C) and 5 bar, respectively. The graphite shell-and-tube heat exchanger occupies a very large space, and hence these units are not suitable to handle large throughput of chemicals like fertilizers, synthetic fibers, and heavy chemicals [244].

Cubic Heat Exchanger. The cubic heat exchanger is similar to the compact cross-flow heat exchanger, consisting of drilled holes in two perpendicular planes. Cubic heat exchangers are suitable when both the process streams are corrosive. With a cubic exchanger, a multipassing arrangement is possible. It is manufactured by assembling of accurately machined and drilled graphite plates bonded together by synthetic resins, oven cured and sintered. Gasketed headers with nozzles are assembled on both sides to the block to form a block heat exchanger and are clamped together.

Modular-Block Cylindrical Exchanger. In this arrangement, solid impervious graphite blocks have holes drilled in them. These blocks can be multistacked in a cylindrical steel shell that

has gland fittings. The process holes are axial and the service holes are transverse. The units are designed as evaporators and reboilers.

Graphite Plate Exchanger. The Diabon F graphite plate heat exchanger is a heat exchanger with graphite plates developed for use with media normally too corrosive for exotic metals and alloys. For details on this type of heat exchanger, refer to the chapter on plate heat exchangers.

32.3 Glass

Low coefficient of thermal expansion, light weight, inertness to many chemicals, and high compressive strength are the important factors that favor the use of glass. Glass heat-transfer equipment finds excellent applications whenever one or more of the following are required:

1. Corrosion resistance.
2. Product purity.
3. Visibility.
4. Low maintenance.

References 247–251 provide either specific or general information on glass.

Applications

Because of its excellent corrosion resistance and visibility, glass heat transfer equipment proves very desirable in pilot-plant applications in all industries. Its transparency permits fast and accurate troubleshooting if a flow problem arises [243]. The industries that employ glass heat-transfer equipments include [247]:

1. Chemical and petrochemical (corrosion resistance).
2. Pharmaceutical (corrosion resistance and product purity).
3. Food and beverage (product purity and inertness).
4. Dyestuff (visibility and smooth surface).

Composition of Glass

Of the various types of glass available, the type used in heat exchangers is borosilicate glass. The composition of borosilicate glass supplied to the chemical processing industry is given in Table 52.

Mechanical Properties and Resistance to Chemicals

Borosilicate glass has a relatively low coefficient of thermal expansion compared to other glasses. It is subject to thermal shock and is weak in impact strength, although this is improved by thermal tempering [243]. Glass heat-transfer equipment can operate at temperatures to 392°F (200°C). This temperature is limited by the gasket material employed and not by the glass material. The permissible internal operating pressure is a function of diameter. As diame-

Table 52 Composition of Borosilicate Glass [247]

Silica (SiO_2)	80.5%
Sodium monoxide (Na_2O)	4.0%
Potassium oxide (K_2O)	0.5%
Boric oxide (Br_2O_3)	13.0%
Aluminum oxide (Al_2O_3)	2.0%
Total	100.0%

ter increases, permissible operating pressure decreases. The permissible operating pressure may be about 4 bar.

The chemical stability and catalytic inertness of borosilicate glass are more comprehensive than for any other known material of construction. Only hydrofluoric acid, concentrated phosphoric acid, and strong alkalies at high temperatures can appreciably attack the glass surface.

Construction Types

There are three types of glass heat exchangers used today. They are [247]:

1. Shell-and-tube heat exchangers.
2. Coil heat exchangers.
3. Hybrid heat exchangers.

Shell-and-Tube Heat Exchangers. The tubes are individually sealed in a PTFE tubesheet with pliable PTFE packing and a PTFE packing grommet. The shell is constructed from standard glass pipe sections and fittings. Shell-and-tube units are available from 2.5 m^2 to 25.0 m^2 of heat-transfer area; nominal shell diameters range from 6 to 12 in (152.4 to 304.8 mm).

Coil Heat Exchangers. Glass coil exchangers have a coil fused to the shell to make a one-piece unit. This prevents leakage between the coil and shell-side fluids. The units are manufactured to eliminate any stress concentration at the point of fusion. Maximum operating pressure in the coil is 3 bar, while it is a function of diameter in the shell. Heat-transfer areas range from 0.3 m^2 to 15.0 m^2 in these units.

Hybrid Heat Exchangers. Hybrid exchangers utilizing glass and some other material of construction have been developed. These include [247]:

1. Glass shells with metal bayonet, basket, or immersion coil heaters.
2. Glass tubes and end caps with shells fabricated from fiberglass, steel, stainless steel, or other alloys.

These units are used when higher pressures or other factors prohibit the use of an all glass unit.

Glass-lined Steel

Process equipment made of glass lined steel offers the corrosion resistance of glass and the structural strength of steel.

Drawbacks of Glass Material

The parameters that restrict the use of glass as a heat exchanger material are:

1. Glass is sensitive to mechanical shock, thermal shock, thermal stresses, abrasion, and overstressing of nozzles [251].
2. Corrosion: Glass is not completely inert; acids, alkalies, and even water can corrode glass in varying forms and degrees, but very slowly.

32.4 Teflon

With the introduction of Teflon in 1965, E. I. du Pont de Niemours & Co. Inc. made a significant technical contribution with the design and production of heat exchangers with flexible and noncorroding tubes of Teflon fluorocarbon. Teflon (polytetrafluoroethylene, or PTFE), a highly chemically inert, noncorroding material, is well suited for the corrosive applications that have long been a problem in industry. The nonsticking, smooth surface of Teflon tubes resists fouling and scale buildup. Exchangers made of Teflon have replaced many exchangers in corrosive services that use construction materials such as stainless steel, impervious graphite,

glass, zirconium, titanium, Hastelloy, and tantalum [252]. Shell-and-tube heat exchangers and immersion coils made of Teflon are used successfully for corrosion-free heating, cooling, and condensing of many corrosive fluids found in chemical processing, steel, and plating industries. Part of the information on Teflon has been drawn from Ref. 253.

Teflon as Heat-Exchanger Material

The reasons that favor Teflon as a candidate heat exchanger material are [253]:

Noncorrosive: Inert to essentially all industrial chemicals, Teflon is an ideal material for handling corrosives.

Resistant to fouling: The well-known nonstick properties of Teflon help to keep the heat-exchanger tubes clean, minimizing the fouling and scaling, and thus limit downtime and maintenance costs.

Resistant to shock: Heat exchangers of Teflon are less subject to damage from thermal or mechanical shock than those of glass or graphite.

Noncontaminating: Since it is chemically inert, Teflon will not produce corrosion products that can contaminate process solutions. Unlike graphite, it contains no binders that can leach out in corrosive solutions. Heat exchangers of Teflon are being used to replace metal and graphite exchangers to achieve increased product purity.

Low maintenance: Inherent resistance to corrosion and fouling minimizes downtime for unscheduled maintenance. Units are easily cleaned with chemical solutions that could damage metal and graphite exchangers.

Size reduction: The compact flexible tube bundle requires less space than a comparable metal exchanger.

Temperature and pressure resistance: Heat exchangers of Teflon can handle corrosives upto 400°F (204°C), and pressures upto 125 psig (862 kPag), depending on temperature.

Good electrical resistance: The electrical resistance of Teflon enhances applications in the plating industry.

Heat Exchangers of Teflon in the Chemical Processing Industry. Two different types of heat transfer equipment are being produced. They are shell-and-tube units and exposed tube bundles.

Shell-and-Tube Heat Exchanger. Shell-and-tube units with tubing of Teflon are used for heating, cooling, or condensing chemically aggressive process streams. These include sulfuric, hydrofluoric, nitric, hydrochloric, and other acids, caustic and other alkalies, halogenated compounds, salt solutions, and organic compounds [253]. The units are single-pass exchangers containing flexible tubes of Teflon fused at both ends into an integrated honeycomb structure. All surfaces exposed to the corrosive process stream are made of Teflon. Units are available with Teflon-lined shells for heat exchange between two corrosive streams.

Design Considerations. Teflon tubing exhibits relatively low thermal conductivity, that is, 0.11 BTU/h · ft^2 · °F, and this shortcoming is overcome by increasing the heat transfer area and decreasing the wall thickness of the tubing. With small-bore tubing, a large surface area is obtained for a given volume. Practical and economic optimization led to the establishment of 0.1-in outer diameter tubing as the smallest standard product for coils [252].

Size/Construction. For shell and tube units, shell diameters range from 3 to 10 in (76.2 to 254 mm) for standard units. Nominal tube length is 24 to 288 in (610 to 7315 mm), and shells are made of carbon or stainless steel, fiberglass, or other materials. Tubing sizes range from 0.10 to 0.375 in (2.54 to 9.4 mm) for either FEP or Q-series. The heat transfer area is 5.1 to 1104 ft^2 (0.5 to 103 m^2) in standard units [253].

Heat-Exchanger Fabrication Technology. In a unique honeycomb process, the ends of individual tubes of Teflon are fused into an integrated tubesheet. This construction provides the user with an extremely large heat-transfer area in a relatively compact unit at a low cost.

Reactor Coils. Reactor coils are designed for immersion into agitated vessels or storage tanks to heat or cool corrosive fluids.

Fluoropolymer Resin Development

Exchangers based on Teflon FEP can be used to 30 psig (207 kPa) at 300°F (149°C), maximum, and these limits have been extended to 50 psig (9345 kPa) at 400°F (204°C) in exchangers made with Q-series fluoropolymer tubes [253]. Substantially higher pressure capabilities are available at lower than maximum temperatures.

32.5 Ceramics

For high-temperature heat exchangers, material temperature limits are a major constraining factor. For metallic materials in use above 649°C (1200°F), the choice is essentially limited to stainless steels, nickel- and cobalt-base superalloys, and heat-resistant cast alloys. Structural ceramics are used to provide mechanical strength at elevated temperatures, usually in the range of 600 to 1600°C (1110 to 2910°F) [254]. Ceramic materials such as silicon carbide and silicon nitride exhibit excellent high-temperature mechanical strength and are used for high-temperature heat-exchanger applications. Advanced-technology materials such as carbon-bonded carbon-filament composites have adequate elevated-temperature mechanical properties, but their applications are limited because they are not usable in the presence of oxygen [255].

Suitability of Ceramics for Heat-Exchanger Construction

Because of their high temperature capability and oxidation resistance, ceramics are obvious materials for high-temperature heat exchangers, particularly in energy and resource conservation. The following are the important factors that favor the ceramics as heat-exchanger material [255]:

1. Resistance to high-temperature corrosion and oxidation.
2. Stability at elevated temperature.
3. Good thermal shock resistance.
4. Low cost compared to heat-resistant superalloys.
5. Low coefficient of thermal expansion.
6. Commercial availability.
7. Ability to be fabricated in practical geometries.
8. Chemical durability.
9. Low porosity.

The drawbacks of ceramics for high temperature applications are

1. Brittleness.
2. Permeability.
3. Unsuitable for fabrication by joining techniques.
4. Irrepairability.

Classification of Engineering Ceramics

There are three major classifications of engineering ceramics [255]:

1. Ceramic oxides such as alumina, beryllia, and zirconia.
2. Glass ceramics.
3. Ceramic carbides and ceramic nitrites.

Types of Ceramic Heat-Exchanger Construction

Tubular Construction. Applications for tubular ceramic units include [255]:

1. Waste heat recovery in metals industries.
2. Chemical plant waste heat recovery.
3. Incinerators.
4. Closed-cycle gas turbine heat-source exchangers.
5. Open-cycle gas turbines (exhaust-heated cycle).
6. Fluidized-bed heat exchangers.
7. Gas-to-gas heat recovery units.
8. Nuclear process heat intermediate heat exchangers.

Plate Fin Construction. Applications for ceramic plate fin units include [255]:

1. Vehicular gas turbine recuperators.
2. Industrial gas turbine recuperators.
3. Stirling engine heat exchangers.
4. High-temperature gas-to-gas heat exchangers.
5. Rotary generators.
6. Applications requiring very compact, small-volume heat exchangers.

33 ALLOYS FOR SUBZERO TEMPERATURES

Steels and nonferrous materials are used for containment, handling, and transporting of liquefied gas and liquification of gases. Other applications include stationary structures and mobile equipment exposed to adverse climates or operating conditions or both. Temperatures below −150°C (−238°F) often are identified as cryogenic temperatures. The motive for utilizing low-temperature technology is that at cryogenic temperatures liquid gases occupy much less volume than their pressurized gaseous state. Therefore, the containment vessels for liquid gases may be smaller, thinner (because of lower pressure), and less costly [256].

33.1 Ductile–Brittle Transition Temperature (DBTT)

Some metals display a marked loss of ductility in a narrow temperature range below room temperature. This is called the ductile–brittle transition temperature (DBTT). The application of steels below their nil ductility temperature (NDT) is avoided because of the danger created by brittle crack propagation which could lead to the catastrophic failure of a component or entire system [16]. Below the nil ductility temperature, very little energy is required for crack propagation [114]. The following factors can improve the toughness of steels [17]: (1) ASTM grain size has a strong effect on a given steel's NDT. As the grain size number increases (i.e., the grains become smaller), the NDT drops. Therefore, fine-grained steels usually are used for low-temperature applications. (2) Proper heat treatment can be very effective in increasing a steel's fracture toughness. Quenching and tempering is an effective heat treatment for improving toughness. (3) Among alloying elements, nickel, titanium, and manganese tend to increase steel's toughness. (4) Another variable that affects DBTT is thickness.

33.2 Crystal Structure Determines Low-Temperature Behavior

Below ambient temperatures, a metal's behavior is characterized somewhat by crystal structure [256]:

1. The yield and tensile strength of body-centered cubic (bcc) structure metals depend greatly on temperature and generally display a marked loss of ductility in a narrow temperature range below room temperature (e.g., iron and molybdenum).
2. Face-centered cubic (fcc) structure metals such as aluminum, copper, nickel, and austenitic stainless steel often increase in ductility as temperatures decrease, and their tensile strength is more temperature dependent than their yield strength.
3. The tensile and yield strengths of hexagonal close-packed (hcp) structure metals are more temperature dependent, and they usually suffer a severe loss of ductility at subzero temperatures (e.g., zinc, titanium, some alpha-titanium alloys); however, they have good ductility down to cryogenic temperatures.
4. Plastic deformation and cryogenic temperature can cause a normally ductile and tough stainless steel such as 301, 302, 304, and 321 to partially transform to a bcc structure, thus affecting ductility and toughness.
5. Minor variations in composition can affect ductility in certain materials. For example, an increase in oxygen from 0.10 to 0.20% in a ductile titanium alloy can lower ductility at −423°F (−253°F) from 15 to almost 0%.

33.3 Requirements of Materials for Low-Temperature Applications

A major requirement of materials for liquefaction equipment and for containment and transport of liquefied gases is toughness at the handling temperatures of the liquid. Additional requirements include minimum weight, weldability characteristics to resist hot cracking, cold cracking, and embrittlement of heat-affected zones, high strength and toughness of the welded joints, and corrosion resistance, low thermal expansion to minimize dimensional changes due to temperature difference between the ambient and service temperature, relatively low specific heats, low thermal conductivity to minimize thermal conduction, etc. Carbon steels have only limited corrosion resistance and must be replaced with corrosion-resistant alloys when metal loss becomes severe.

33.4 Notch Toughness

Notch toughness is defined as the ability to resist brittle fracture at high stresses, such as can be caused by impact loading. Notch toughness is measured by various means. The favored method recommended by the American Petroleum Institute as well as the ASTM and ASME is the Charpy V-notch test. It is considered the most appropriate because a part or structure will generally fail due to a notch or other stress concentration [257] or a defect such as a gouge, weld crack, arc strike, or a sharp discontinuity [258]. Using the Charpy V-notch test, one can determine the transition temperature at which a material becomes brittle. This information helps the designer to choose a steel that will remain ductile through the range of temperatures or stresses it will be subjected to in service.

Notch Toughness—ASME Code Requirements

The ASME Code should be consulted for allowable stress at low temperatures and for the testing required of the material to ascertain that it is suitable for low-temperature service. The ASME Code stress tables designate −20°F as the beginning of low temperature.

33.5 Selection of Material for Low-Temperature Applications

Selecting materials for low-temperature and cryogenic applications calls for thorough understanding of the application and knowledge of the mechanical properties that each grade of metal provides. Since various low-temperature materials are available, the designer must con-

sider the merits of each material according to the application. Some factors suggested by Marshall [257] include cost by strength ratio, welding, and fabricating costs, and where extra high strength and good impact properties to below −75°F (−59.4°C) are called for, an alloy steel should be chosen.

33.6 Materials for Low-Temperature and Cryogenic Applications

Aluminum, copper, Titanium, nickel-base alloys, ferritic steels including 9% Ni steels, and stainless steels offer designers a wide choice and have been used successfully for liquefaction, containment, and transport of liquefied gases. The selection of aluminum, copper, nickel- and cobalt-base alloys, titanium, low-alloy ferritic steels including 9% Ni steels, and stainless steels is discussed next. Table 53 shows a list of materials for low-temperature application along with the minimum temperature applicability.

Aluminum for Cryogenic Applications

Aluminum and aluminum alloys have fcc crystal structures and retain good ductility at subzero temperatures. Aluminum can be strengthened by alloying and heat treatment while still retaining good ductility along with adequate toughness at subzero temperatures. Among the aluminum and aluminum alloys, 1100, 2014 to 2024, 2219-T87, 3003, 5052, 5083-O, 5086 and 5456, 6061-Tb, and 7005, 7075, 7079, and 7178 are recommended for cryogenic applications.

Table 53 Materials for Low-Temperature Application

Alloy designation	Specification	Approximate lowest temperature
Low-carbon steel	A 442, A 516	−50°F (−46°C)
	A 537	−75°F (−59°C)
	A 662, A 724	—
Alloy steel	A517	−75°F (−59°C)
	A203, Gr. A and B, 2.25% Ni	−90°F (−68°C)
	A203, Gr. D, E, and F, 3.50% Ni	−150°F (−101°C)
	A645, 5.0% Ni	−320°F (−196°C)
	A353	−320°F (−196°C)
	A553, Type II 8% Ni	−275°F (−170°C)
	A553, Type I, 9% Ni	−320°F (−196°C)
	A543	−180°F (−118°C)
	A736	−50°F (−46°C)
	A844 (9% Ni)	−320°F (−196°C)
Stainless steel	304, 304L, 316, 316L, 347	−452°F (−269°C)
Aluminum	1100, 2014 to 2024, 2219-T87, 3003, 5083-0, 5456, 6061-Tb, 7005	−452°F (−269°C)
Copper	C10200, C12200 (DHP), C17200, C22000, C26000, C51000, C70600, C71500	−325°F (−198°C)
Nickel	Monel-K, Hastelloy B, Hastelloy C, Inconel alloy 600, 706, Inconel alloy 718, Invar-36, Inconel alloy X-700	−452°F (−269°C) −441°F (−263°C)
Titanium	Ti-5Al-2.5Sn, Ti-6Al-4V (ELI)	−320°F (−196°C)
	Ti-5Al-2.5Sn (ELI)	−423°F (−253°C)

Note: Refer to code for applicable lowest temperature.

The salient features of these alloys are discussed next. Before that, the factors that favor aluminum use in cryogenics are listed [259]:

1. Unlike other metals, aluminum has no ductile-to-brittle (DBT) transition regardless of the direction of stress.
2. Inertness to cryogenics like methane, ethylene, argon, helium, neon, O_2, N_2, H_2.
3. Absence of corrosion at cryogenic temperatures; protective coatings are rarely necessary, but the designer should be cautious of galvanic couple.
4. The tensile strength increases proportionately more than yield strength in the cryogenics, so heavily stressed tanks can warp more at cold than at room temperature without failing.
5. Tear resistance, another measure of toughness, is the energy needed to propagate a crack. Tear resistance of 5083-O and its welds is as high at −196°C as it is at room temperature.
6. Emissivity and reflectivity: aluminum's low emissivity improves the effectiveness of insulation systems [260].
7. Weldable and provide excellent mechanical properties in the as-welded condition.

3000 series: Aluminum alloy 3003 is used in fabrication of brazed plate fin heat exchangers and other equipment in gas liquefaction plants. It is available as tubing (including finned tubing), pipe, sheet, and plate. It is readily joined by brazing or welding. 3003 meets the requirements of the ASME Boiler and Pressure Vessel Code for working temperatures upto −321°F (−196°C).

5000 series: Alloys such as 5052, 5083, 5086, and 5456 exhibit a combination of properties that make them popular for most applications. Their moderate strength, good toughness, and good weldability have resulted in their selection for oceangoing tankers for carrying oxygen, LNG, and other cryogenic gases, and for tank trailers, stationary storage containers, and processing equipment. For plate fin heat exchangers, 5083-O is used.

6000 series: Alloy 6061 offers the advantage listed for 5000 series alloys except that in the as-welded condition its strength is low.

7000 series: Alloys such as 7075, 7079, and 7178 display the highest strength of all aluminum alloys. But they lose toughness below −320°F (−196°C). They are generally nonweldable and found only in limited application. Two newer alloys, 7039 and X7007, show promise for cryogenic service because they are readily welded and retain adequate toughness at all temperatures [256].

Copper and Copper Alloys

Copper and copper alloys have fcc crystal structures similar to those of aluminum and retain a high degree of ductility and toughness at subzero temperatures, down to −423°F (−253°C). Copper alloys that might be considered for use at subzero temperatures are C10200 oxygen-free copper, C12200 (DHP), C17200, C22000, C26000, C51000, C70600, and C71500 [205]. The development of light-weight brazed aluminum heat exchangers for cryogenic applications caused copper to be replaced by aluminum for many of these components.

Titanium and Titanium Alloys

Commercially pure titanium may be used for tubing and small-scale cryogenic applications that involve only low stresses in service. For temperatures down to −320°F (−196°C), the normal interstitial (NI) grade alloys Ti-5Al-2.5Sn and Ti-6Al-4V are suitable. Interstitial impurities such as iron, oxygen, carbon, nitrogen, and hydrogen reduce the toughness of these alloys at both room and subzero temperatures. For temperatures below −196°C, extra low interstitial (ELI) grades of Ti-5Al-2.5Sn and Ti-6Al-4V are used [205]. The lower strength, all-alpha Ti-5Al-2.5Sn ELI is used down to −423°F (−253°C), the temperature of liquid hydrogen. Titanium

and titanium alloys are not recommended for containment or other use with either liquid or gaseous oxygen in cryogenic service, because any fresh surface caused due to abrasion or impact exposed to oxygen will cause ignition and hence possible explosion.

Nickel and High-Nickel Alloys

Nickel is an fcc metal that retains good ductility and toughness at subzero temperatures. Unalloyed nickel is low in strength and has only limited applications at subzero temperatures. However, several nickel-base alloys, including some superalloys, exhibit excellent combinations of strength, ductility, and toughness up to −441°F (−263°C). Typical nickel-base alloys for cryogenic applications include Monel K-450, Hastelloy B, Hastelloy C, Inconel alloy 600, Inconel alloy 706, Inconel alloy 718, Inconel X-700, and Invar-36 (36% Ni-iron) [205].

Carbon Steels and Alloy Plate Steels

ASTM specifications A203, A353, A442, A516, A517, A537, A553, A612, A645, A662, and A724 describe steel plates with minimum Charpy V-notch energy or lateral expansion requirements at testing temperatures from −15 to −320°F (−26 to −196°C).

Carbon Steels. Carbon steels provide service to −75°F. Less costly than alloy steels, they combine better weldability with low coefficients of thermal expansion and thermal conductivity. In carbon steels, the principal means of improving notch toughness is through changes in composition of C, Mn, Si, and Al contents. Carbon lowers toughness, whereas Mn increases it. Si and Al are added as deoxidizers. Silicon-killed steel has slightly better notch toughness than semikilled steel, and silicon-aluminum-killed steel has still higher toughness [258].

ASTM A516. The major advantage of A516 steels is their low initial cost. But they feature the lowest ASME stresses, 13,750 to 17,500 psi. Thus, a given design strength requires heavier gages than are needed with high-strength steels. A516 steel is used widely in air liquefaction plants, refrigerating plants, transport equipment, and containment vessels operating down to −50°F (−46°C) [257]. For these applications, the steel is normally made to meet impact test requirements of ASTM A300 Class 1 specification, which calls for plates to be normalized and to meet a Charpy keyhole minimum of 15 ft-lb at −50°F.

A517. Of the low-temperature alloy steels, A517 Grade F has the highest allowable stresses. At −50°F its impact strength (Charpy V-notch) is 40 ft-lb, and its notch and crack resistance are sufficient to encourage wide usage.

ASTM A537 Grades. Higher strength with good notch toughness is available in carbon steels such as the two classes listed in ASTM A537 grades, normalized (Class A) or quenched and tempered (Class B), which provides 60,000 min psi yield strength plus 15 ft-lb of impact strength (Charpy V-notch) at −75°F.

2.25% Nickel Steels. ASTM specification A203 Grades A and B are used in service down to −90°F (−68°C). The low-temperature requirements are given in ASTM specification A300.

3.5% Nickel Steels. ASTM specification A203 Grades D and E are used in service down to −148°F (−100°C). Forgings and bolting materials are also covered in ASTM specifications. The low-temperature requirements are given in ASTM specification A300.

5% Nickel Steel. This is used as a wrought material for service down to approximately −185°F (−120°C), for the fabrication of welded vessels for handling and storage of liquid ethylene in land based plant and marine tankers. Quenched, temperized, and reversion annealed, ASTM A645 specifies 5% nickel steel designed for LNG service. Armco Cryonic 5 is covered by ASTM A645.

ASTM A353 Alloy Steel. This is one grade 9% Ni steel, normalized and tempered for subzero use. Yield strength is 75 ksi; specification for longitudinal and transverse impact (Charpy V-notch) energy is 20 ft-lb minimum at −320°F (−196°C).

ASTM A553 steels contain 8% or 9% nickel and are essentially quenched and tempered to 85 ksi yield strength (minimum). Impact energy minimum is 25 ft-lb (longitudinal) and 20 ft-lb (transverse) at −196°C (−320°F) for Type I, 9% Ni, or −170°C (−275°F) for 8% Ni steel (Type II). The welding considerations are the same for both types of steel regardless of heat treatment. The 9% nickel steels have long been used for ethylene, methane, LNG, oxygen, and nitrogen applications. One of the benefits of nickel steels in design of LNG vessels is volume and weight savings due to their relatively high strengths. Selection criteria and fabrication aspect of 9% nickel steel are discussed in detail later.

36% Ni-Iron Alloy. Low expansion 36% nickel-iron alloy is marketed under various trade names, including Invar 36, Nilo 36, and Dilavar. It is used principally for sea transportation and land-based storage of liquefied gases. It is also used at service temperatures down to that of liquid helium −269°C (−452°F). The nickel-iron alloy plate for pressure vessels is covered in ASTM A658.

Products Other Than Plate

A partial list of ASTM specifications for other than plate steel products for subzero service is:

A333 Seamless and welded steel pipe.
A334 Seamless and welded carbon and alloy steel tubes.
A350 Forged or rolled carbon and alloy steel flanges, fittings, and valves.
A352 Ferritic steel castings.
A420 Piping and fittings of wrought carbon steel and alloy steel.
A522 Forged or rolled 8% and 9% nickel steel flanges, fittings and valves.
A671 Electric fusion welded steel pipe.
A757 Carbon and alloy steel castings.

In addition to the steels listed, a number of proprietary ferritic steels have been developed by several steel producers to meet certain requirements for service at subzero temperatures.

Austenitic Stainless Steel

In the last decade, there has been a considerable increase in the use of austenitic stainless steels for cryogenic services at temperatures between −240 and −452°F (−151 and −268.9°C). They play an important role in LNG ships for containment tanks, storage tanks, cargo piping systems, and a variety of ancillary equipment.

The AISI 300 type steels such as 304, 304L, 310S, 316, 316L, 321, and 347 offer a fine combination of toughness and weldability for service down to −452°F (−269°C). Among these alloys, Types 304 and 304L are the most commonly used alloys. Consequently, they have the largest service experience and coverage in design codes. These grades have moderate strength and excellent toughness, and they are selected for their formability, fabricability, and ready availability in a variety of product forms [14,261].

Among the modified varieties, nitrogen-containing, high-proof-strength stainless (e.g., Types 304N, 316L + N) is used for cryogenic processing plants and in liquid oxygen and nitrogen storage and transportation applications. The addition of 0.2% N raises the proof strength by about 40% and moderately increases the tensile strength without sacrificing ductility or fracture toughness [14].

33.7 Fabrication of Cryogenic Vessels and Heat Exchangers

Most of the cryogenic materials are formable and weldable. Most of the units are welded. Brazing is limited to manufacture of PFHE [256]. Important considerations for fabrication of cryogenic plants are discussed in detail in Ref. 262. Some of the considerations are:

1. All raw materials and consumables should undergo rigorous quality and specification tests.
2. Edge preparation is considered to be of the utmost importance for all types of welding, and clear specifications should be laid down and strictly adhered to for all joints.
3. Welding plants should be checked for proper functioning.
4. It is essential that the weld metal and heat-affected zone achieve a fracture toughness greater than or equal to that of the base metal. The weldment should resist hot and cold cracking and embrittlement of the heat-affected zone.

33.8 9% Nickel Steel

Low-carbon 9% nickel steel was developed in the United States by the International Nickel Company, Inc. The fundamental mechanical properties of 9% Ni steel must meet the minimum requirements of ASTM 353 or ASTM 553 Type I specifications. The steel is used for vessels and plant for processing, transportation, and storage of liquefied gases down to −196°C. The excellent low-temperature toughness of this steel results from the alloying addition of approximately 9% nickel and the presence of stable retained austenite at cryogenic temperature. Nickel also suppresses the formation of ferrite/pearlite high-temperature transformation products; thus, a microstructure is produced that is higher in strength and notch toughness [263].

Merits of 9% Nickel Steel

Materials previously used, such as copper and austenitic corrosion-resistant steels, presented no particular difficulties in construction but the cost of these materials was high [264]. The use of 9% nickel steel has increased because it is a cheaper material than those materials previously used for operation down to −321°F (−196°C). The higher strength of this steel compared with aluminum, copper, or even austenitic steels makes possible the use of higher design stresses and hence offers high strength-to-weight ratio. The major factors that favor 9% nickel steel include [14]:

1. High design stress coupled with good fracture toughness characteristics.
2. Relatively low thermal expansion compared with austenitic stainless steel and aluminum alloys.
3. Good weldability by a variety of processes, including shielded metal arc, gas metal arc, and submerged arc welding.
4. High melting point and retention of strength at elevated temperatures; this property is important for the structural integrity under shipboard fire conditions.
5. Chemically resistant to liquid oxygen and nitrogen, producing no corrosion products that would hamper the operation of valves and meters or cause unsafe conditions [265].
6. Low thermal conductivity.
7. Good weldability [266].

Forming of 9% Nickel Steel

The material is readily machinable and may be hot or cold formed. After hot forming, however, the steel must be heat-treated by double normalizing and tempering unless the hot-forming temperature approximates the first normalizing temperature, when the first normalizing treatment can be omitted.

Surface Preparation and Scale Removal for Welding

Prior to the welding operation, all extraneous material and surface oxides should be removed from the weld joint area by wire brushing. Grinding is a more effective procedure. Residual scale can cause porosity in succeeding layers of weld metal. As an alternative to grinding, it

has been found possible to remove the scale from 9% nickel steel by flame cleaning, using conventional oxyacetylene equipment [267].

Edge Preparation

The edges should preferably be machined or cut by employing flame cutting. The shape should be such as to afford easily full penetration. Normally the V bevel with open root or an asymmetrical double V bevel is used [268]. If the edge is prepared by flame cutting, it will be necessary to grind it, to remove the surface oxide formed and to eliminate the underlying layer where the carbon content has become higher.

Welding Procedures

The welding procedures most widely used are manual metal arc welding with covered electrodes, automatic or semiautomatic submerged arc welding with continuous wire, MIG welding, cored wire welding, and for the root pass TIG welding and plasma arc welding. Employ MIG welding with a spray mode of metal transfer to overcome lack of fusion problems, to obtain clean welds while keeping the heat input to relatively low levels [269].

Electrodes

The electrodes that have been used for 9% nickel steel can be considered in three classes [270]:

1. Nickel-based electrodes of the Inconel or Hastelloy type; the trade names are Inco weld A, Inconel 192, and Inconel 182.
2. Chromium-nickel stainless steel electrodes to a very limited extent.
3. Low-alloy ferritic electrodes.

Guidelines for Welding of 9% Ni Steel

As is well known, 9% Ni steel derives its properties through double normalizing and tempering or quenching and tempering. The welding processes and the weld metal must be such as not to alter, beyond acceptable limits, the structural characteristics of the parent metal in the heat-affected zone. To ensure tensile strength and toughness in the fusion zone, and to avoid welding flaws, a few practical rules are suggested by Pozzolini et al. [268]:

1. Use low-hydrogen electrodes with a diameter less than 4 mm and wires with a diameter less than 3.2 mm.
2. Lay narrow beads in a number of passes rather than large beads partially overlapping.
3. Preferably weld in the horizontal position; avoid the vertical position.
4. Do not preheat unless absolutely necessary.
5. Use relatively low heat inputs (9–16 kJ/cm, according to the welding process) and current settings to keep the dilution to a minimum.
6. Use welding processes with high cooling rates, and avoid keeping the material at temperatures exceeding the lowest critical point of transformation.
7. Avoid any stress-relief heat treatment. If really necessary, it should be carried out at temperatures below the lowest critical point of transformation.
8. All the welding materials should be dried prior to welding and the shielding gases should be of controlled purity.

Suggestions for welding 9% nickel steel are also given by Thorneycroft [267] and include the following:

9. For thicknesses less than 1 in (25.4 mm), a single-vee included joint angle of 75–80° is recommended. This practice should also be followed for double-vee joints in heavier plate.
10. The use of chill bars as backup plates is not recommended. The underside of the root run should be cooled in air.

11. It is recommended that the root run size be larger than normal.
12. The welding gun should be inclined so as to lead the welding arc in the welding direction in order properly to shield the molten deposited weld metal from the atmosphere.
13. Use electrodes with lime-fluorspar coatings, properly dried to ensure low hydrogen contents in the weld zone.

Welding Problems With 9% Ni Steel

Conventionally, welding of 9% Ni steel is made using high-nickel alloy of the austenitic type. This process presents some critical problems [271]:

1. The yield strength of the weld metal is low compared with that of the base metal.
2. During welding there is a high susceptibility to various forms of hot cracking such as longitudinal bead cracking, and crater cracking of the weld metal.
3. The high-alloy filler material is relatively expensive and results in higher construction cost.

Postweld Heat Treatment (PWHT)

Since the 9% nickel steel retains its toughness after welding, there is no need for postweld stress-relieving treatment. In October 1960 (see *Operation Cryogenics*), a number of welded pressure vessels in 9% nickel steel were tested to destruction in the United States in the as-welded condition to illustrate that the 9% steel would behave in a tough and ductile manner at −196°C without stress relief [272]. ASME Code Case 1308-S allows use of the steel in the as welded condition in thicknesses up to 2 in (50.8 mm). Fabricators of vessels for some chemical applications may for sections above a certain thickness, typically above 50 mm, wish to apply a stress-relieving operation at a temperature of 1050°F. Further, in some instances it may be necessary to produce large components by welding the plate required size followed by hot forming; in such work a double-normalizing and tempering treatment will normally be required on the welded and formed material [273]. Temperatures for PWHT should be kept below the plate tempering temperature to prevent the formation of excessive amounts of austenite, which would affect the toughness, and very slow cooling rates should not be used; ASME Code specifies cooling rates in excess of 166°C/min down to 320°C to minimize the possibility of "temper embrittlement" [266].

33.9 Welding of Austenitic Stainless Steels for Cryogenic Application

The austenitic stainless steels with or without nitrogen strengthening are readily welded by all of the common welding processes, provided appropriate procedures and consumables are used. The welding processes include SMAW, SAW, TIG, and MIG welding processes. Guidelines on welding of stainless steels for cryogenic applications are discussed in Ref. 261. "Guide to the Welding and Weldability of Cryogenic Steels" (IIS/IIW-844-87), issued by the IIW, is principally devoted to the consideration of welding of fine-grain aluminum-killed steels and nickel-alloyed ferritic steels up to 9% nickel.

Charpy V-Notch Impact Properties

Due to service conditions, the selection of welding consumables is guided by the mechanical property requirements for the weld metal. The most important mechanical property is Charpy V-notch impact at −450°F (−268°C); the minimum energy absorption is 20 ft-lb and lateral expansion is 0.015 in minimum.

Problems in Welding

Four main factors affect the strength and toughness of the as deposited weld metal and take on added significance at cryogenic temperatures [274]:

1. Sensitization.
2. Ferrite content.
3. Nitrogen pickup.
4. Oxide inclusions.

These four phenomena are discussed in detail in Ref. 261. The following discussion is based on that reference.

Sensitization. The grain boundary precipitation of chromium carbides reduces weld metal toughness at low temperatures. Weld metal toughness can be improved by using very low carbon fillers such as 308L (0.04% C max.) and 316L (0.03% C max.). For stainless steels with carbon content higher than 0.03%, annealing of the welds at temperatures greater than 950°C, followed by rapid cooling, dissolves the carbides and improves the toughness.

Ferrite Content. To avoid microfissuring, for a wide range of stainless steel, the weld metal is usually balanced to provide 4–8 FN. However, for cryogenic service, higher ferrite reduces toughness at −196°C and lower temperature. To obtain a good combination of strength and toughness of the weld, ferrite content should be maintained in the range of 0–2 FN [275].

Nitrogen Pickup. Nitrogen increases the yield strength and decreases the toughness of stainless steel weld metals [275,276]. When GTAW and GMAW processes are followed, careful gas coverage should be provided to avoid nitrogen pickup in the weld metal. While employing SMAW, lime coatings of the electrode, generally give better coverage and less nitrogen pickup than titanium coatings.

Oxide Inclusion Content. Oxide inclusions form sites for the initiation of microvoids. The toughness at cryogenic temperatures increases with decreasing inclusion contents [276]. To reduce inclusions, use basic-coated electrodes, since they generally provide better toughness than rutile ones, due to lower oxygen content and oxide inclusions than the rutile coatings [277].

34 CLADDING

Many applications require resistance to corrosive media. It is well known that various grades of austenitic stainless steels of Types 304, 304L, 308, 316, and 347, nickel, Monel, Inconel, cupronickel, aluminum, zirconium, and titanium exhibit excellent corrosion resistance in many corrosive environments. However, the construction of large assemblies such as pressure vessels and heat exchangers in corrosion-resistant metal involves costs. Consequently, increasing use is being made of clad materials to achieve the optimum balance of strength and surface properties to overcome corrosion by an economical means. The potential for severe corrosion in various coal combustion and incineration environments has renewed interest in cladding technology for both Code-approved and enhanced strength developmental alloys [21]. Apart from cladding, the other methods of protecting the base metals are lining, which refers to sheet or strip attached internally to the component by mechanical or intermittent fusion techniques, and sheathing by external attachment.

34.1 Cladding

A clad plate is a composite plate consisting of a base metal and a cladding of corrosion-resistant or heat-resistant metal or a plastic (polyvinyl chloride plastic-clad steel plate is a

newly announced development by Lukens Steel Co., USA) on one or both sides. In effect, the joint obtained represents the welding or bonding of a different metal over a large surface area. Often the base material is being selected for economic reasons and strength purposes and the cladding layer for one or a combination of the following: corrosion and erosion resistance. Cryogenic properties, elevated-temperature properties, and wear-resistance properties. The base plate is generally carbon steel, and the cladding metal may consist of a corrosion-resistant material as mentioned earlier.

34.2 Cladding Thickness

The thickness of the clad layer required is usually small relative to that of the base material, because the latter is designed to take the majority of the load. The thickness of the clad material may vary from 10 to 50% of the base plate thickness, but normally it is held in the range of 10 to 20%. The clad steels are available in the form of sheet, plate, strip, etc.

34.3 Methods of Cladding

The term *cladding* covers a wide range of processes including the following:

1. Loose lining.
2. Resistance cladding.
3. Lining using plug welding.
4. Thermal spray cladding.
5. Hot roll bonding.
6. Weld overlay cladding.
7. Explosive bonding.
8. Centricast pipe.
9. Coextruded pipe or duplex tubing.
10. Hot isostatic process.
11. Explosive cladding plus roll cladding [278].

Loose linings improve either new or existing structures. Cladding by weld overlay and thermal spraying works for new and existing components. Hot roll bonding and explosive bonding offer corrosion resistance to new construction. Centricast pipe involves centrifugal casting of cladding on the base metal. Duplex tubings are coextruded. All cladding methods have some limitation, either economic or practical. These cladding processes, except hot isostatic process, are discussed next. Duplex tubing has been explained in the chapter on corrosion.

Loose Lining

Loose lining refers to the installation of a thin corrosion resistance lining inside a process vessel. The cladding liner is about 0.3–2.0 mm thickness. Early titanium cladding attempts were based on loose lining. Use of thin titanium layers loose clad to steel is limited to process systems where [279]:

1. Heat transfer between the shell and process medium is not critical.
2. Loss of pressure or vacuum will not collapse the liner.
3. Temperatures are low.
4. There is no problem in suspending vessel internals on the lining.

If these four factors are not critical, a loose-clad vessel may be economically practical.

Resistance Cladding

In this process, resistance spot welding is employed with proprietary intermediate materials to bond thin-gauge corrosion-resistant material to the base metal. Resistance cladding provides a means of applying a lining to a base metal regardless of whether or not the base metal and the liner material are metallurgically compatible. The Inco method involves intermittently spot welding a thin (0.6–2.0 mm) copper-nickel lining with an MIG torch and wire feed.

Lining Using Plug Welding

A variation of resistance cladding is lining using plug welding. Plug welding involves the attachment of relatively thin corrosion-resistant sheet to steel surfaces at predetermined locations by fusion welding. For example, two techniques are considered for the attachment of copper alloy sheet to steel, and both are inert-gas processes, MIG and TIG welding [280]. In the MIG technique (intermitting spot welding) shown in Fig. 32a, by triggering the gun as for normal welding operations, the filler wire moves forward and arcs on the clad layer, producing penetration of the clad layer and the base metal to a predetermined depth, then retracting continuously while filling molten metal into the cavity created by arcing until a solid plug weld is completed. Two types of plate preparation suitable for use with TIG plug welding are shown in Fig. 32b.

Thermal Spraying

Thermal spraying is accomplished by heating the cladding metal to a molten state and spraying it on the prepared surface of the base metal. The thickness normally ranges from 0.2 to 2.5 mm. One of the advantages of this process is that the temperature of the base metal normally does not exceed 302–392°F (150–200°C), which normally does not affect the base metal.

Weld Overlaying or Weld Surfacing

For fabrications that involve large clad surfaces or the use of plate material exceeding 3 to 4 in (76.2 to 101.6 mm) thickness, the only practicable method of cladding is by weld deposition. The process consists of application of corrosion-resistant thin sheets or deposition of weld metal by various arc welding process, as opposed to making a joint. The surface to be overlaid must be cleaned of oxide and dirt. Weld overlaying by a fusion process may be applied only when the base metal and the weld metal deposit are compatible. While weld surfacing, an important consideration is weld dilution, which is discussed next.

Weld Dilution. To ensure an overlay of specified composition for the intended purpose, the filler metal must be enriched sufficiently to compensate for dilution. For any given filler metal composition, changes in welding procedures such as maintaining approximately 50% bead

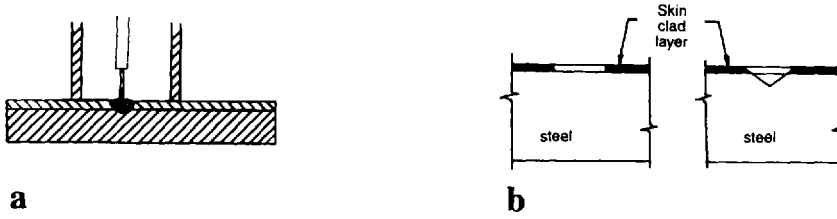


Figure 32 Lining using plug welding: (a) MIG technique; and (b) plate preparation for TIG plug welding. (From Ref. 280.)

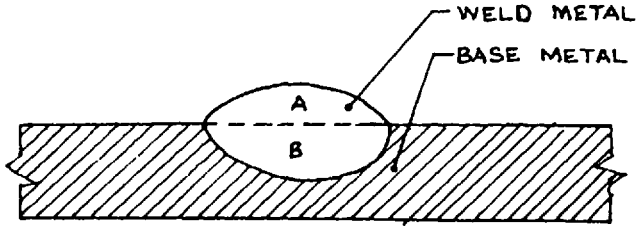
overlap, use of small-diameter electrodes, low heat input, and directing the arc onto the previously deposited bead minimize dilution. The welding procedure specification should contain the acceptable limits of chemical composition of the deposit. Methods of calculating weld dilution and the approximate weld metal content of any element are shown in Fig. 33.

Weld Overlay Cladding Methods. Various methods are employed for overlay cladding. Some of the methods include the following:

GMAW.
FCAW spray transfer.
Manual TIG.
TIG hot wire.
TIG cold wire (mechanized).
Plasma hot wire.
SMAW.
Electroslag strip welding.
Submerged arc—single or multiple wire.
Submerged arc strip cladding.

Of these, (1) manual metal arc process, (2) GMAW or MIG spot welding, (3) strip cladding process, (4) electroslag strip cladding process, and (5) submerged strip cladding process are discusses next. AWS specification for various of corrosion resistant weld surfacing alloys are covered by, for stainless steel, AWS A5.4, A5.9, and A5.22; for copper base, A5.6 and A5.7; for nickel-base surfacing alloys, AWS A5.11 and A5.14; and for cobalt base, AWS A5.13.

Manual Metal Arc Process. The manual metal arc process represents the most flexible means of weld overlaying. This process is economical for small areas and uneconomical for large areas. Submerged arc and electroslag welding is proven economical method for large areas.



$$X_{WM} = \frac{X_{BM} \times B}{A+B} + \frac{X_{FM} \times A}{A+B}$$

where

X_{WM} = Weld metal content of element X.
X_{BM} = Base metal content of element X.
X_{FM} = Filler metal content of element X.

$$\% \text{ DILUTION} = \frac{B}{A+B} \times 100$$

Figure 33 Weldmetal dilution (schematic). (From Ref. 74.)

GMAW or MIG Spot Welding. GMAW process with spray transfer, pulse transfer or spot welding is normally used. The Inco method involves intermittently spot welding a thin (0.6–2.0 mm) copper-nickel lining to the head with a MIG torch and a wire fed, Firth et al. [281].

Strip Cladding Process. In the strip cladding process, a strip is substituted for a solid wire. Advantages claimed for the process are relatively high deposition rates, low dilution and flexibility, 100% bonding and good surface finishing, Bush et al. [282]. Several variations of the strip cladding process exist, mainly subdivided into single and double strip techniques.

Submerged Strip Cladding Methods. The high deposition rates achieved by submerged arc welding (SAW) is well suited to large area surfacing applications. Both single and multiple electrode SAW methods are used for surfacing. The productivity of this process can be improved further by the use of higher welding currents and wider strips. The associated problems are arc blow, increased penetration and poor bead characteristics and dilution. Magnetic steering reduces penetration, and hence, dilution and arc blow control, Mallya et al. [283].

Electroslag Strip Cladding Process. Electroslag surfacing (ESS) with strip electrodes is a highly cost effective cladding process that has been used extensively in industry. Compared to conventional cladding processes, such as pulsed gas metal arc welding (GMAW-P) and strip submerged arc surfacing, the ESS process is known to provide both high deposition rate and low dilution, Devletian et al. [284].

Stainless Steel Strip Cladding.

Consideration for Stainless Steel Strip Cladding. When it is required to clad a thick-walled carbon steel vessel with an austenitic steel by the strip cladding process, three factors must be considered [282,285]. These are:

1. Dilution: In general, the effects of dilution have been overcome either by depositing more than one layer or by using a dual strip process. The dual strip process incorporates a cold noncurrent carrying strip as a "barrier layer" on the parent metal surface.
2. A guaranteed minimum thickness of cladding.
3. Suitable deposit microstructure and mechanical properties (e.g., 4–10% free ferrite in an austenitic matrix and sufficient ductility at the clad metal interface to satisfy a 3T side bend test).

Metal Powder Additions to Control Ferrite. A serious problem when strip cladding stainless steel on carbon steel base metal is the absence of ferrite in the cladding near the interface between the cladding and base metal. The absence of the ferrite content in this transition zone decreases the resistance to hot cracking. Ferrite-stabilizing metal powders are used to control the ferrite content of the cladding and transition zone [286]. Metal powder additions have already been used to enhance deposition rates in many conventional welding processes. According to Oh et al. [286], the other benefits of metal powder additions include good control over weld penetration, heat-affected zone size, and improved fracture toughness of the weld.

Procedure and Welder Qualification. The general requirements for the qualification of cladding are in accordance with the ASME Code, Section IX. Both procedure and welder qualifications are described simultaneously under the outline for corrosion-resistant overlays as recommended in Section IX.

Heat-Treatment Considerations. Stress relieving of clad vessels is fairly common to relieve fabrication stresses, which under a given combination of conditions might lead to stress corro-

sion cracking. While heat treating, one might consider the base metal properties, which may be adversely affected due to heat treatment.

Inspection of Overlays. Soundness of cladding is usually tested by these methods [282]: (1) liquid penetrant to reveal any pinhole porosity; (2) ultrasonic inspection for lack of fusion and to detect large slag inclusions; (2) soundness of bond and ductility by side bend tests—excessive iron dilution or irregular penetration patterns usually fail bend tests; (4) corrosion test for resistance to corrosion; (5) chemical analysis to assure the specified composition; (6) metallography for studying the microstructure; and (7) hardness profile across the overlays. For stainless steel, additional tests include the measurement of delta ferrite in the weld metal.

Inspection of Stainless Steel Cladding. Clad qualities are evaluated by the following tests [283]:

1. Corrosion test according to ASTM A262.
2. Side bend test (ASTM E 190) for the ductility of clad metal and for fusion between clad and base metal.
3. Ferrite content test to ensure resistance to hot cracking or microfissuring.
4. Microprobe analysis to determine the distribution of Cr and Ni across the depth of cladding.
5. Microstructure examination.

Nickel Alloy Cladding. Submerged arc process, GMAW spray transfer, and SMAW are the preferred processes. Nickel alloy weld metals are readily applied as overlays on carbon and low-alloy seels and other materials. Inconel or Monel cladding can be applied to the tubesheet with inert-gas metal arc (MIG) process. These overlays provide excellent chemical and mechanical properties, and ductility to the tube-to-tubesheet joint. In overlaying, avoid excessive dilution with iron and irregular penetration. Large surfaces can be lined by the Inco method. The Inco method involves intermittently spot welding a thin (0.6–2.0 mm) copper-nickel lining with an MIG torch and wire feed.

Roll Cladding

Roll cladding (Fig. 34) involves metallurgically fusing and rolling of corrosion-resistant thin plate to the base metal at the rolling mill. The bond formed is part mechanical and part metallurgical; consequently, metallurgically incompatible materials normally cannot be produced. In the roll cladding process, a rectangular plate pack of compatible base and cladding metals is assembled. The plate pack (Fig. 34a) consists, in this order, of (1) base metal, (2) a layer of cladding metal, (3) a parting compound, (4) a layer of cladding metal, and (5) base metal. The facing surfaces of cladding and base metal are precleaned and surface oxides are removed. The edges of the pack are welded together to maintain the relative positions of the assembly and it is rolled. As the thickness of the entire pack is reduced, the cladding metal forge welds to the base metal (Fig. 34b). When the amount of reduction is appropriate, the plate pack is parted,

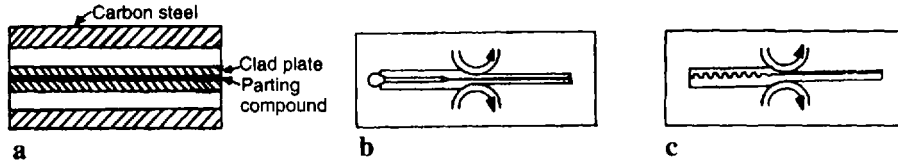


Figure 34 Roll cladding: (a) plate pack; (b) rolling; and (c) rolling of explosively formed clad plate. (Adopted from Ref. 278.)

the surfaces are conditioned, and the clad plates are heat treated and cleaned. Sometimes explosive clad plates are rolled to improve the bonding integrity and to straighten the plates (Fig. 34c).

Explosive Cladding

The explosive cladding process utilizes explosive energy to create a metallurgical bond and to produce clad plate of both conventional and unique metal combinations. In this process, the cladding plate is accelerated by means of an explosive charge to a high velocity of the order of 1000 ft/s (322 m/s), before impacting the base plate. This process makes available a range of metal combinations and many materials that are normally considered incompatible and hence cannot be produced by conventional methods. For example, titanium can be bonded to mild steel, copper to stainless steel, stainless steel to brass, and many other combinations. Explosive welding is principally associated with the fabrication of large clad plates, shells, tubes, nozzles, the fabrication of tube-to-tubesheet joints, and the plugging of defective tube joints of shell-and-tube heat exchangers. Most of the clad tubesheet applications have consisted of nickel and nickel alloys, copper and copper alloys, and stainless steel (SS) clad on SA 516–70 [288]. Table 54 presents a list of alloys commonly supplied as explosion clad [287].

Welding Geometries. Explosive welding geometries are mostly (1) parallel cladding and (2) angular cladding. Large-area clad plates for fabrication of plates are made using the parallel arrangements. Figure 35 illustrates the principles of parallel explosion cladding.

Angular Geometry. In angular geometry arrangement (Fig. 36) the two surfaces to be welded are at an angle to each other, and explosive is sited on the reverse side of one of the compo-

Table 54 List of Alloys Commonly Supplied as Explosion Clad [287]

Cladding metals	Base metals
300 Series SS	Plates—carbon steel A516 and alloy steel A387
400 Series SS	Forgings—carbon steel A266, A350, and alloy steel A182,
Copper alloys	300 Series SS plate and forgings
Nickel alloys	
Titanium	
Zirconium	
Tantalum	

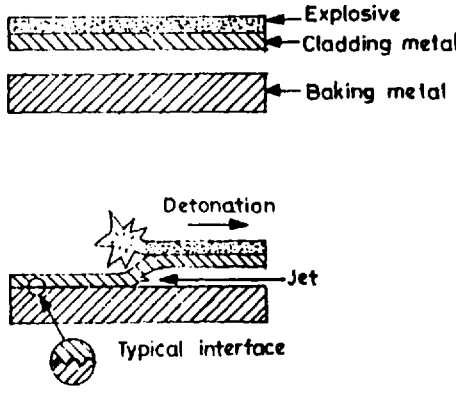


Figure 35 Explosion cladding with parallel geometry.

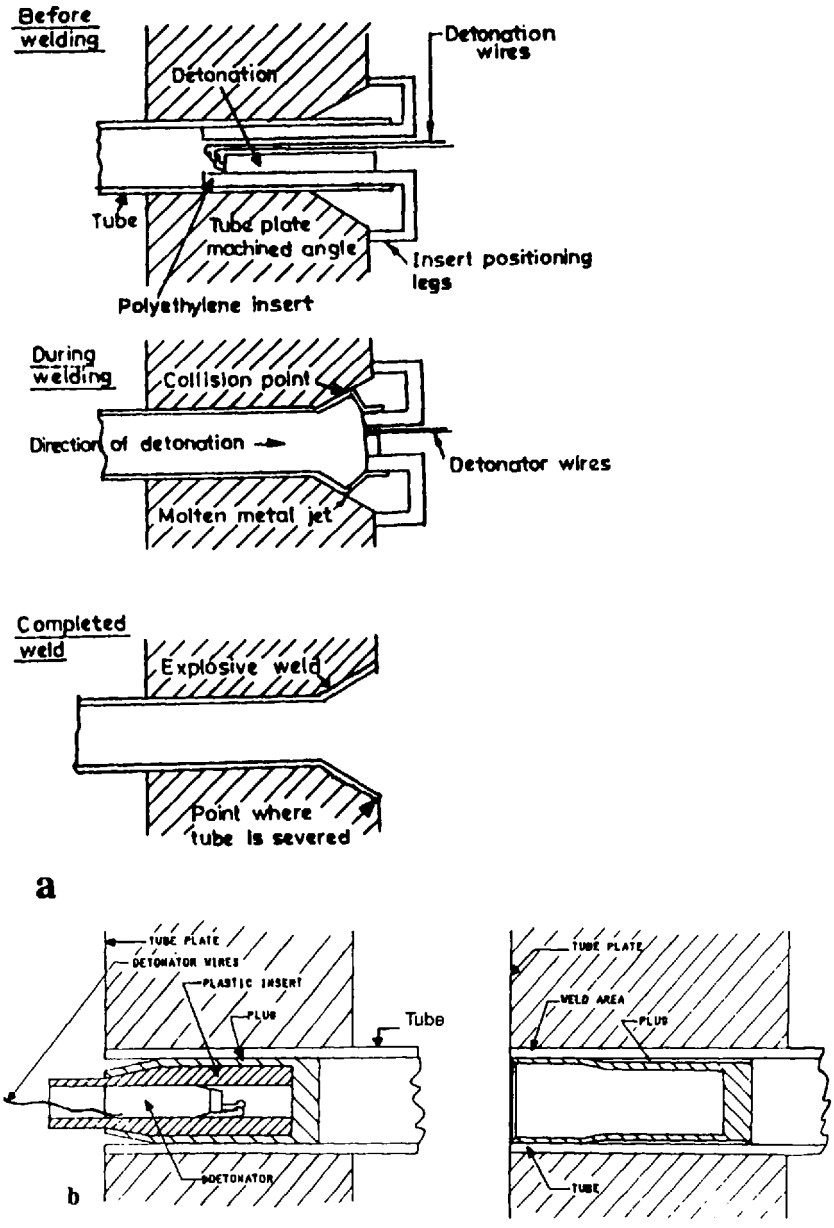


Figure 36 Angular geometry explosion cladding: (a) tube-to-tube sheet expansion (from Ref. 289) and (b) plugging of leaking tube—Dynafusion® explosively welded plug.

nents. On initiation of the explosion the two plates are forced together, colliding intimately to form a junction. Small-area cladding such as tube-to-tubesheet joint expansion (Fig. 36a) and plugging of leaking tubes (Fig. 36b) are made using the angular arrangements. This setup is appropriate in view of the short bond lengths of approximately 1 in that are normally required [289]. Metal combinations that are welded commercially include carbon steel to carbon steel,

titanium to stainless steel, and 90-30 copper-nickels. The principle of geometry applied for tube-to-tubesheet joint expansion and plugging of leaking tubes is explained next.

Tube-to-Tubesheet Welding. In most instances, the weld is located near the front of the tubesheet and has a length of approximately 0.5 in (12.7 mm) or three to five times the tube wall thickness [290]. Most applications of explosion welding in tube-to-tubesheet joints involve tube diameters of 0.5 to 1.5 in (12.7 to 38.1 mm). The angular disposition of the component surfaces is achieved in this instance by machining a countersink at the outer end of the tubesheet hole. The countersink depth is usually 0.5 to 0.6 in at an included angle between 10 and 20° [291]. The detonator is placed in the bore of a polyethylene insert to form a composite cartridge, which is placed within the tube hole. On ignition, the shock waves emanating from the detonator are transmitted by the polyethylene insert to the tube, thus imparting to it the required radial velocity. Tubes may be welded individually or in groups. While determining the choice of explosive welding for tube-to-tubesheet joining, one should consider (1) the thickness of the tubesheet, (2) ligament width, and (3) tube diameter and wall thickness [290].

End Effect. Because of energy losses at the end of the tube, the velocity at the tube extremity is lower than elsewhere in the system, thereby producing an end effect [289]. This area may well have a velocity below that required for welding. The tube is therefore initially positioned with its end projecting some short distance from the face of the tubesheet. The end effect area thus lies outside the tubesheet and a reasonably uniform tube velocity is thereby achieved over the intended weld zone along the machined angle, as shown in Fig. 36a.

Plug Welding. Explosive welding of plugs in leaking tubes is an effective technique for conventional heat exchangers and nuclear heat exchangers where there is a problem of nuclear radiation [292]. These areas may be inaccessible due to hotness, corrosiveness, radiation, etc. Plug welding, being a maintenance operation, is usually carried out on site. The only operation that remains to be carried out within the confines of the exchanger tubesheet is machining of a countersink, similar to tube-to-tubesheet explosion welding.

Inspection of Joint Quality. The usual methods of testing explosive welds are discussed in Refs. 290 and 291. Typical inspection methods in addition to visual inspection include the following: (1) pulse-echo ultrasonic technique (ASTM A578) to asses the bond integrity—an ultrasonic frequency in the range of 2.5 to 10 MHz usually is adequate; (2) radiography applicable to welds between metals with significant density variation and an interface with a large wavy pattern; (3) metallographic examination of the weld interface on a plane parallel to the detonation front and normal to the surface—a well-formed wave pattern without porosity generally is indicative of a good joint; and (4) the bond strength by various destructive tests like chisel test, tension-shear test, and tension test. For critical applications, checking the integrity of tube-to-tubesheet joints, helium leak testing can be applied to the fusion zone of an explosive weld.

34.4 Processing of Clad Plates

Clad plates usually are distorted somewhat during explosion cladding. This requires straightening to meet standard flatness requirements. Also, it is customary to supply explosion-clad plate in the as-cladded condition because the hardening that occurs immediately adjacent to the interface usually does not significantly affect the bulk properties of the base plate. If some service requirements demand postweld heat treatment, this requirement may be complied with. Clad steels are always flame cut from the backing side. While hot forming, extreme care should be taken to ensure there is no danger of sulfur pickup from furnace atmosphere. To overcome this problem, an electric furnace is preferred.

Forming of Clad Steel Plates

Pressure-vessel heads, shells, tubesheets and other components can be made from explosion-clad plates by conventional hot- or cold-forming techniques. A differently stressed condition exists at the bond interface, and this governs the thicknesses and diameters that can be successfully bent [293].

Hot forming, welding, or heat treatment must take into account the metallurgical properties of the materials, grain growth, and the possibility of undesirable diffusion that may occur at the interface [290,291]. Hot forming of compatible materials of stainless clad steel plates does not produce any intermetallic compound at the interface, whereas the incompatible clad plate with base metal, like titanium clad to stainless steel, should be hot formed at not more than 1400°F (760°C) to prevent undesirable formation of intermetallic compounds. Cold forming of clad plates poses little difficulty, provided that the largest possible radius is used to avoid excessive work hardening of the cladding. To retain the corrosion resistance property, forming tools should be free from iron oxide scale and surface contaminants. Use of lubricant is not recommended because of the possibility of sulfur and carbon pickup during subsequent hot working or thermal cycles. Various precautions to be taken while fabricating clad plates are discussed by Eillis [294].

Welding of Stainless Steel Clad Steels. When welding clad steels, the dilution effects should be given consideration. The backing steel should be welded first; however, if the welding does not present any great difficulty, the clad layer can be welded first with a suitable electrode (i.e., a high-alloy electrode), back chipped, and the base plate then welded [290,294]. Joint preparation for clad steels is shown in Fig. 37. A typical welding procedure for stainless steel clad plate is shown in Fig. 38. Joining clad steel to unclad steel sections normally requires making the butt weld and restoring the clad section in a fashion similar to joining two clad plates. Other considerations for welding stainless steels clads are carbide precipitation, sigma phase precipitation, and delta ferrite content.

Selection of Filler Metals. Stainless-steel-clad carbon or low-alloy steel plates are sometimes welded with stainless steel filler metal throughout the whole plate thickness. But it is enough to use carbon or low-alloy steel filler metal on the unclad side, followed by removal of a portion of the cladding and completion of the joint with stainless filler metal. For the clad side, Type 309L filler metal could be used for base metal such as Types 405, 410, 430, 304, and 304L; Type 309 Cb for 321 or 347; and 309 Mo for 316. The user should consider the manufacturer's recommendations in choosing filler metals. Datasheets 37a and 37b [295] give guidance for selection of filler metals for welding clad metals of austenitic stainless steels, ferritic stainless steel, nickel alloys, and copper alloys, and guidance for the butt joint designs for welding clad steels from both sides, respectively.

PWHT. If stress-relief annealing is required, use either stabilized of low-carbon stainless steels to avoid carbide precipitation. Care should be taken to ensure absence of sigma phase precipitation. Differential thermal expansion between mild steel backing and stainless steel cladding will induce stresses in the cladding.

Welding of Plain Chromium or Ferritic Stainless Steel Clad Steels. In welding of plain chromium clad steels of the order of 12–16% Cr and 0.80% C, precautions must be taken to prevent: (1) embrittlement above 1150°C, (2) 475°C embrittlement; (3) brittleness due to sigma phase, and (4) notch sensitivity pronounced at room temperature [294].

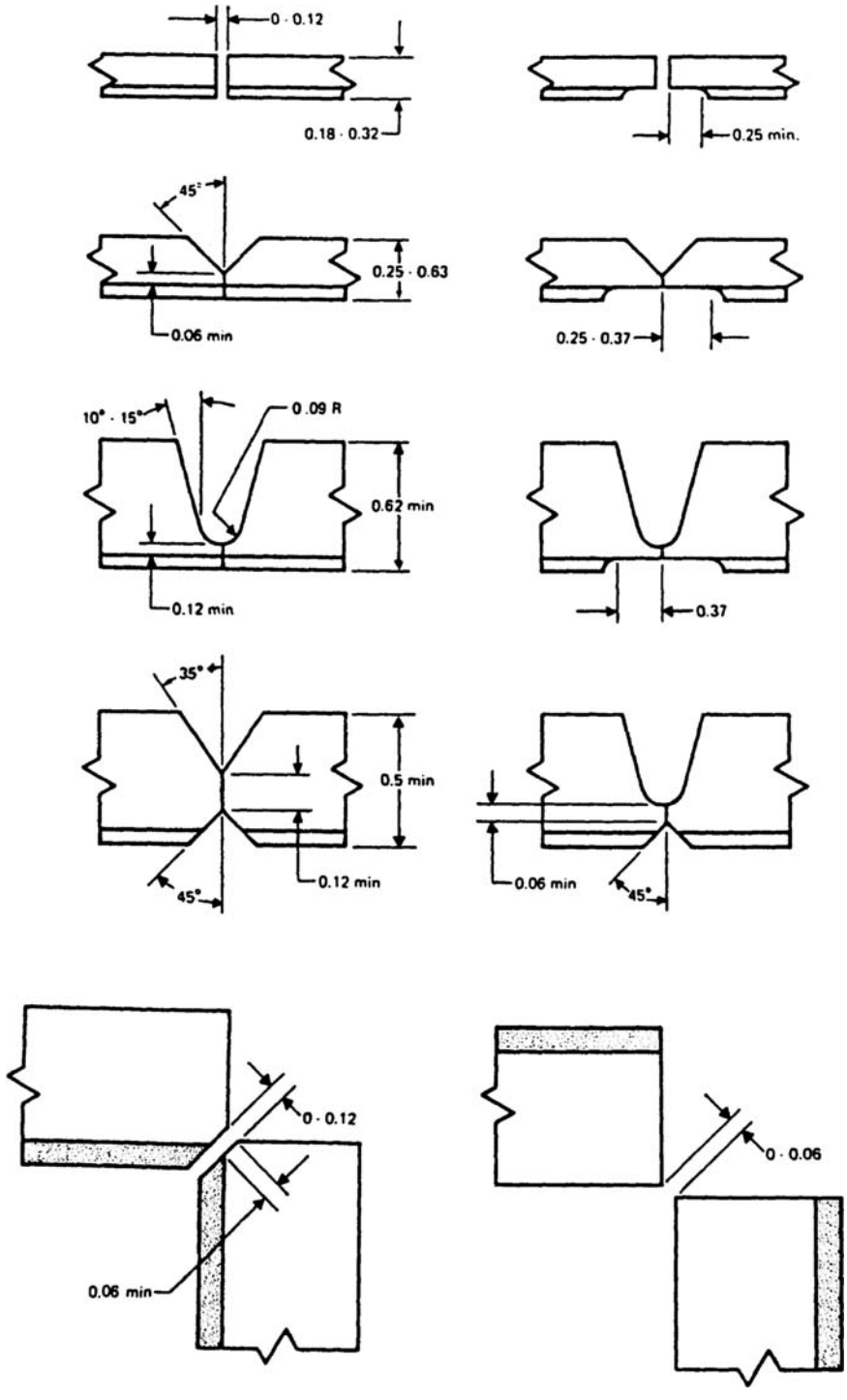


Figure 37 Joint design for welding of clad steel. (From Ref. 295.)

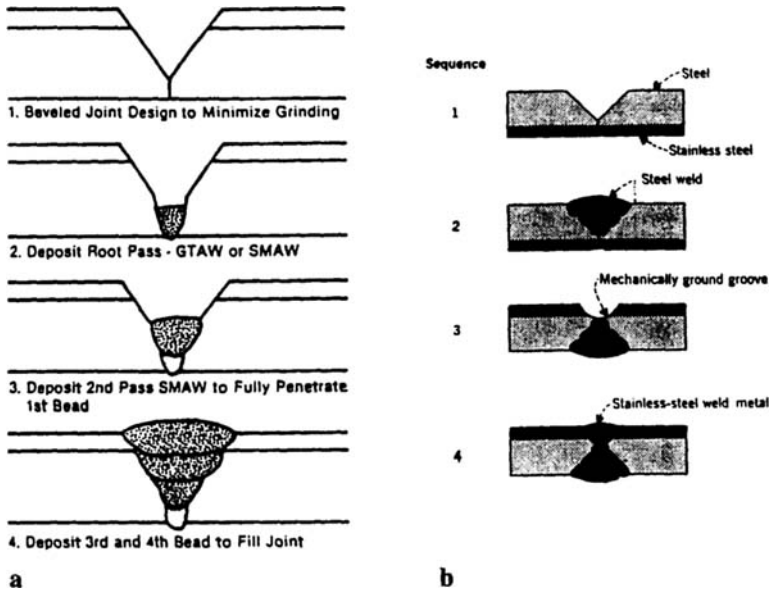


Figure 38 Two typical procedures for the welding of clad plate. [From Refs. 74; 1.]

Welding of Nickel-Clad Steels. Iron dilution is a major problem. This problem is overcome by proper choice of electrode and welding techniques. Remove the top surface of the previous run before further welding and adopt a stringer bead technique. Carbon content of the nickel used for clad steels should be less than 0.05% to avoid the intergranular precipitate of graphite that forms at about 1202°F (650°C) [294].

Welding of Monel-Clad Steels. Iron dilution is a major problem. Iron diluton is overcome by using a root run (from the clad side) of a nickel electrode, and using a low-carbon Monel electrode. If an 80-20 nickel-chromium electrode is used, dilution problems are negligible.

34.5 Failure of Clad Material

Failure of clad material can occur due to cracks in the clad metal or in the welds in the clad plate, or due to a bulged-out clad plate that has separated from the base material.

34.6 ASME Code Requirements in Using Clad Material

ASME Code Section VIII, Div. 1, places the responsibility on the owners and users for determining cladding material that will be suitable for the intended service. Salient features of code rules for clad materials are:

Bond strength. The bond strength between the cladding and the backing plate must meet shear strength requirements of the code to prevent separation of the cladding from the backing plate. This shear strength must be a minimum of 20,000 lb/in^2.

Spot radiography. All welds on clad vessels using the combined-thickness approach per code rules must have at least spot radiography examinations.

Suitability for service. Suitability for service includes adequate corrosion resistance and the retention of expected mechanical properties for the planned service life.

Telltale hole for detecting corrosion. Telltale holes are required on cladded pressure vessels in

order to warn the user when the corrosion-resistant cladding has been penetrated. Telltale holes shall not be provided in vessels that are to contain lethal substances, except as permitted by ULW-76 for vent holes in layered construction.

Welding requirement. Welds that are used on cladding material must have a corrosion resistance at least equal to that of the cladding.

35 POSTWELD HEAT TREATMENT OF WELDED JOINTS IN STEEL PRESSURE VESSELS AND HEAT EXCHANGERS

Though many welded structures and components perform satisfactorily without postweld heat treatment (PWHT), there are certain well-established conditions where application of PWHT is either mandatory or traditional [296]. For example:

1. Heavy thickness metals and alloy steels as specified in applicable fabrication code and customer requirement.
2. Postweld heat treatment of pressure vessel and heat exchanger are mandatory for certain applications (e.g., lethal service).
3. With some welding processes like electroslag and electrogas, PWHT is required. The high heat input and the long thermal cycle inherent in the electroslag welding process produce a large heat-affected zone, which is subject to grain coarsening and a loss of fracture toughness. The coarse-grained weld metal should be refined by a normalizing heat treatment to develop required properties [297]. Normalizing removes nearly all traces of the cast structure of the weld metal and nearly equalizes the properties of the weld metal and the base metal.
4. It is important to note that vessels operating under creep conditions should be stress relieved before being put into service. If the vessels are not stress relieved, residual stresses may be superimposed on the applied stress, and this may lead to premature creep failure.

35.1 Objectives of Heat Treatment

PWHT is intended to relieve the residual stresses generated by thermal contraction after welding and thereby to minimize the risk of subsequent distortion or cracking or to produce improvements in metallurgical structure or properties of the weld metal. PWHT provides the following features in the welded structure:

1. Relieving of residual stresses.
2. Reduction of the risk of failure by brittle fracture.
3. More ductility in the weld metal and a lowering of hardness.
4. Improved resistance to stress corrosion cracking.
5. Improved dimensional stability.
6. Improved machinability.
7. Improved fatigue performance.

35.2 Types of Heat Treatment

Annealing is normally applied to material before cold working or before welding (air-hardenable materials). Annealing consists of heating the steel either in or near its critical temperature range, followed by an extended slow furnace cooling. A full anneal is said to be done when the steel is heated above its critical temperature range, which for carbon and alloy steels is in the range of 1550 to 1675°F, depending on the type of steel, and the steel is slowly cooled to

1200°F for carbon steel and 1000°F for low-alloy steels. The resulting structure will give a very soft material.

Normalizing is used to restore the original microstructure after hot forming and severe cold working. It provides uniform grain structure and improves toughness, which is important in machining and roll forming or bending. In normalizing, the material is air cooled after heating to temperatures above the upper critical temperature or A_3 temperature. The normalizing temperature for carbon and alloy steels is in the range of 1600 to 1800°F, depending on the type of steel.

Quench and temper. Steel is rapidly cooled from above its upper critical temperature or A_3 temperature to a temperature far below this range. Water or oil is used to accelerate the cooling. In the as-quenched condition, the product is not suitable for most commercial applications because of its lower ductility and high hardness. Therefore, steel must be tempered in order to soften to improve its ductility and toughness and relieve internal stresses. Tempering is a reheating treatment done at lower temperatures, usually in the range between 400°F and 1300°F.

Solution heat treatment or quench annealing. This is normally adopted for sensitized austenitic stainless steel. Sensitization causes precipitation of chromium carbide in the HAZ. This precipitation causes the steel to loose chromium below 11% and makes the zone susceptible to corrosion. Also during cold work, stainless steel work hardens to a very high degree. In order to dissolve the carbides in case of welding and to bring down the hardness in cold working, austenitic steels are heated above 1050°C and quenched in water. Solution heat treatment or quench annealing is also employed to heat treat 6Mo superaustenitics.

Stress relieving is a heat treatment designed to relieve residual stresses in the metal structure. The residual stresses may result from cold-working operations, from machining, or from welding. The treatment consists of slowly heating the part to about 1150 to 1350°F and, after holding at this temperature for a period of time, slowly cooling the steel in the furnace or still air. With ferritic steels the treatment preferably consists of heating the complete unit in a furnace to a temperature of 600–700°C. This heat treatment is sometimes called process anneal, subcritical anneal, or post heat treatment after welding [299]. Stress relieving of welded assemblies may be necessary for one or more of the following reasons [300]:

1. To prevent distortion or cracking when externally applied stresses are added to the residual stresses.
2. To reduce the risk of brittle fracture. The brittle fracture may be initiated at weld defects by residual stresses combined with service stresses.
3. To reduce the risk of fatigue failure. The safe range of fatigue stress may be reduced by the presence of residual stresses.
4. To reduce the risk of service-oriented problems such as stress corrosion cracking and corrosion fatigue.
5. To reduce the risk of cracking under creep conditions.

35.3 Effects of Changes in Steel Quality and PWHT

IIW experience [296] shows that steels that are microalloyed with any element (or combination) of Al, Ti, Nb, or V, and that have a carbon equivalent (CE) value ≤0.41% and carbon content value ≤0.15% are susceptible both to heat-affected zones and to degradation of the weld zone by plastic strains, and hence can better accommodate the presence of residual stresses induced in the weld zone.

Under certain conditions, use of a suitable filler metal and proper welding procedures can result in satisfactory weld joints without the application of PWHT, provided there is no manda-

tory code requirement for PWHT. If stress-relief treatment is still required, it may be possible to achieve this with mechanical stress relief or with lower stress relief temperatures than are usually required.

The carbon content in steel should be lowered to meet the HAZ hardness requirements, if PWHT is not employed [301].

35.4 ASME Code Requirements for PWHT

The requirements for PWHT are dictated by most of the codes as a function of base metal composition and thickness. The ASME Code requires specific heating rates, holding times, temperatures, and cooling rates. ASME Code requirements for PWHT of shell sections, heads, and other pressure parts were made of carbon and low-alloy steel fabricated by cold forming are listed in Table 55. For complete information refer ASME Code Section VIII, Div. 1, UCS-79 [302].

Charts for Heat Treatment as per ASME Code

As an aid to determining requirements for PWHT in accordance with the ASME Code, Section VIII, Divisions 1 and 2, Carpenter [303] developed charts in the form of decision trees. One

Table 55 PWHT of Carbon and Low-Alloy Steels Vessels ASME UCS-79

1 Contains lethal substance.

2 Least nominal thickness of butt welds in shell and head exceeds 1.5 in.

3 Material over 1.25 through 1.50 in nominal thickness when preheat is not applied at a minimum temperature of 200°F during welding (Table UCS-56).

4 Material requires impact testing (UCS-66).

5 Carbon and alloy steel fabricated by cold-forming (UCS-56) when the resulting extreme fiber elongation is more than 5% from the as rolled condition and any one of the following condition exists:

a. Thickness of the part before cold forming exceeds 0.625 in.

b. The reduction by cold forming from the as rolled shell or head thickness is more than 10%.

c. Temperature of the material during forming is in the range of 250°F to 900°F.

For P. No. 1 Groups 1 and 2 materials the extreme fiber elongation may be as great as 40% when none of the conditions as 1, 4, and 5 exist.

d. Computation of extreme fiber elongation:

i. Double curvature (for example, head):

$$\text{Percent extreme fiber elongation} = \frac{75t}{R_f}\left(1 - \frac{R_f}{R_o}\right)$$

ii. For single curvature (for example, cylinder);

$$\text{Percent extreme fiber elongation} = \frac{50t}{R_f}\left(1 - \frac{R_f}{R_o}\right)$$

where t is the thickness of plate (in), R_f the final center-line radius (in), and R_o the original center-line radius (infinity for flat plates).

Conclusion;

a. As per code PWHT Reqd/Not Reqd.

b. As per customer's requirement Reqd/Not Reqd.

Note. Refer to code section for more details and special conditions.

case is shown in Fig 39. The proper use of these charts should remove most of the decision-making problems that arise when using the tables in the ASME Code. These charts should be used only as an aid in determining PWHT requirements. They do not contain all requirements.

35.5 PWHT Cycle

When a postweld heat treatment is specified, the operations should be monitored and documented by an inspector. Items of importance in heat treatment may include the following:

1. Area to be heated.
2. Heating and cooling rates.
3. Holding temperature and time.
4. Temperature measurements and distribution.
5. Equipment calibration.

A typical heat treatment chart is shown in Fig. 40. Alloy steels in general require more severe heat treatment than mild steel, but temperature is usually kept below the critical range, that is, below about 700°C, unless normalizing at a temperature around 900°C is adopted [300].

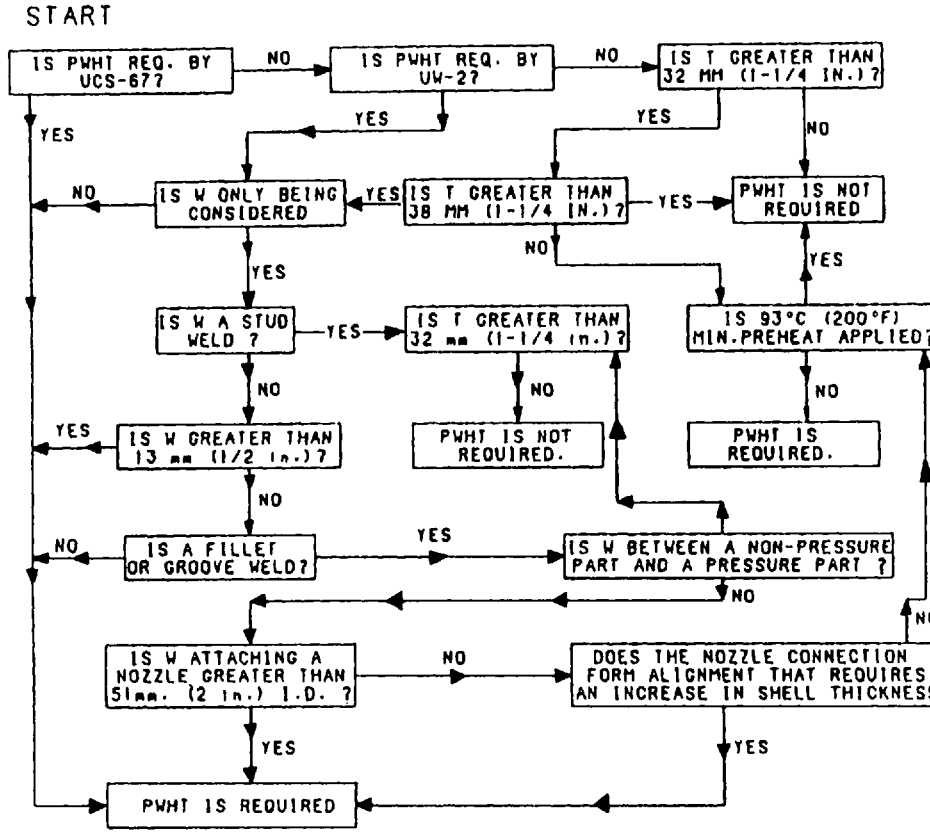


Figure 39 Heat treatment chart as per ASME Code, Section VIII, Div. 1 for P. No. 1, Group No., 1, 2 and 3 materials. (T indicates pressure part thickness; W indicates a fillet weld, a groove weld, a stud weld, or a circumferential butt weld in pipe or tube.) (From Ref. 303.)

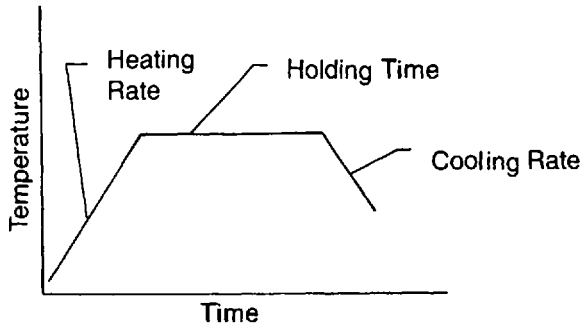


Figure 40 Heat-treatment chart.

The rate of heating varies with the quality, specification, geometry, and size of jobs and will be as low as 100°C/h/in for the case of high-alloy steel and 220°C/h/in for the case of medium carbon steel. Soaking temperature, soaking time, and rate of cooling depend upon the grade and specifications of materials. Refer to UCS 56 tables of ASME Section VIII, Div. 1.

35.6 Quality Control During Heat Treatment

Heat treatment schedules should be based on the code, welding procedures specification, and material specification requirements. The heat treatment must be carried out in accordance with the approved procedures. Such heat-treatment procedures should indicate:

1. Rate of heating.
2. Soaking time and temperature.
3. Rate of cooling.
4. Location of thermocouple.
5. For local heat treatment, the heating band width.

For every heat treatment cycle, a coupon test plate should be made. While heat treating, metals temperature must be measured and recorded. Thermocouple location and number of thermocouples are to be provided as per fabrication code and approved procedure. The time–temperature cycle for heat treatment is recorded on a continuous recorder, which is made available to the authorized inspector for verification. The time–temperature chart and heating diagram are the records of the heat-treatment operation. All thermocouple and temperature measuring and recording instruments are calibrated periodically. For all instruments and gauges, a serial number is allotted. Maintain records giving the following particulars.

1. Type of instrument/gauge.
2. Method of calibration.
3. Last date of calibration.
4. Frequency of calibration/due date for recalibration.
5. Initial date of acceptance.
6. Standard/specification to which the acceptance is made.
7. Place at which calibration has been done.

The details of the heat treatment, such as postweld heat treatment or heat treatment after cold forming, local heat treatments, and annealing on a job site or part/partial annealing—but not the heat treatment of purchased parts (materials, dished heads)—for the equipment or its parts should be prepared as given in Table 56.

Table 56 Heat Treatment Details

Part	Heat treatment	Temp.	Holding time	Holding rate	Cooling rate	Remarks

35.7 Methods of PWHT

The methods of PWHT include furnace heating, in situ heating, and local heating. If the whole assembly is to be heat treated, this is usually carried out in a gas-fired or oil-fired furnace. While heat treating in a furnace, care has to be taken to ensure that the entire exchanger is brought uniformly to the holding temperature to avoid introducing unnecessary thermal stresses. This is ensured by the use of thermocouples on the vessel interior as well as the exterior to verify adequate through-wall heating [39]. When local heat treatment is carried out, electric resistance heating with resistance elements or braided heaters or induction heating or gas burners may be used.

35.8 Effectiveness of Heat Treatment

The level of residual stress after PWHT depends on the material composition, stress-relieving temperature and duration, and stress level before heat treatment. The efficiency of stress relieving can be determined by [300]:

1. Bent bar tests.
2. Tests of creep relaxation type.
3. Determination of stresses in welds.

35.9 Defects Due to Heat Treatment

1. Overheating, which will cause scaling and surface reaction.
2. Distortion due to poor PWHT cycle temperature program.
3. Sagging of the tube bundle or the shell due to inadequate support or because the existing supports are widely spaced.
4. For weld overlays on steel plates, prolonged overheating will cause carbon diffusion from the base metal into the overly and will weaken the base metal, and this may cause intergranular corrosion in corrosive environments. Carbide-forming elements like Mo, V, and Cr slow down diffusion. Other effects include sensitization and sigma phase precipitation if the heat-treatment temperature is high.

35.10 Possible Welding-Related Failures

These are possible welding-related failures during stress relief annealing [76]:

1. Temperature-induced embrittlement.
2. Elongation-induced embrittlement.
3. Stress relief cracking or reheat cracking.

35.11 NDT After PWHT

Certain materials are prone to cracking during PWHT. This is known as reheat cracking or stress relief cracking. Heat-affected zones of welds of such materials are to be subjected to NDT after PWHT. The materials susceptible to reheat cracking and susceptible materials were discussed with weldability problems in the section on material selection and the section on weldability problems.

This page intentionally left blank

14
Quality Control and Quality Assurance, Inspection, and Nondestructive Testing

Part 1: Quality Control and Quality Assurance

Quality, the compliance of a product with the customer's specifications and requirements, has become the buzz word of industry in many parts of the world during the last two decades. Buyers want it; manufacturers claim to strive for it. Competitiveness in the market, safety and the consequences of product failure, and the developing legislation related to product liability known as consumer protection acts have become important factors in the pursuit of high quality. For heat exchangers and pressure vessels, the overriding reasons are to avoid the consequences of failure, which can be catastrophic in human, monetary, and environmental terms.

1 QUALITY MANAGEMENT IN INDUSTRY

It has often been said that quality cannot be inspected into a component; it must be built into it. This is certainly true in heat exchanger fabrication also [1,2]. In the past, quality control (QC) processes relied on separate quality control staff to undertake inspection of the finished products, accepting those that conformed to the specification and rejecting the others. Under this method, higher quality is equated with higher cost. This method is also known for the high rejection of finished products, since control was not exercised at all vital stages of the manufacturing process. Because of this, management faced a conflict between improving quality of the product and reducing product cost. Therefore, a new concept of addressing a more total control of quality of a product/process became known as quality assurance programs (QAP) and provided systems that could cover all aspects, from raw material to finished product, including design, planning, material selection, purchasing, fabrication, and despatch. With the introduction of QAP, the traditional "final inspection and test" approach, particularly that involving third-party inspection, has shifted toward total quality assurance (QA); in which responsibility for quality is placed firmly with the fabricator [2].

2 QUALITY AND QUALITY CONTROL

The term *quality* can be defined as conformance of a material or finished product to specifications and drawings. The definition for quality from ISO 8402-1994 is "The totality of characteristics of an entity (product or service) that bear on its ability to safisfy stated and implied needs."

Some of the definitions of *quality control* (QC) are:

1. The process of inspection to ensure that the material or finished product meets the specifications and drawings.
2. The definition for quality control from ISO 8402-1994 is Operational techniques and activities that are used to fulfil the requirements for quality.
3. The official definition for quality control, provided by the European Organization for Quality Control, is "a management system for programming and coordinating the quality maintenance improvement efforts of the various groups in the design and/or manufacturing organization so as to enable products at the most economic levels which allow for full customer satisfaction."
4. The quality control of a product is the degree to which it meets the requirements of the customer. With manufactured products, it is a combination of both quality of design and quality of manufacture [3].

2.1 Aim of Quality Control

The aim of quality control is to provide quality that is satisfactory, adequate, reliable, and economical. The overall quality system involves integrating the quality aspects of several related steps, including the proper specification, fabrication, and inspection [4]. In order to achieve the quality, a planned and systematic quality assurance program has been established.

3 QUALITY ASSURANCE (QA)

Quality assurance is the establishment of a quality control system to guarantee the desired quality level of a product from design raw materials through fabrication, final assembly and despatch. Quality assurance comprises two aspects [5]: (1) quality control and (2) quality administration. The term quality control was defined already. Rao [5] defines *quality administration* as the systematic organizational effort to effectively implement the quality standards by trained and qualified personnel and to establish documents as proof of quality achieved.

3.1 Need for QA

It is accepted that inspection and nondestructive testing (NDT) applied at appropriate stages during manufacture constitutes an integral and vital part of quality control. There are a number of disadvantages in using inspection to control quality. 1) It is costly; 2) it is operator dependent; 3) it is too late; and 4) it only concentrates on the product, and not the processes. However, there is a growing recognition that quality characteristics and reliability cannot be guaranteed by inspection and tests alone. Such features must be "designed into" and then "built into" the products [2]. Quality assurance techniques have been developed to ensure that critical activities such as material procurement, design, and manufacturing activities such as welding and heat treatment are properly controlled.

3.2 Essential Elements of Quality Assurance Program

A good quality assurance program consists of five basic elements [6]: (1) prevention, (2) control, (3) assurance, (4) corrective action, and (5) quality audit.

QA is based on systematic planning, testing, analysis and documentation in all phases during the manufacture of a product. It begins with the formulation of the specifications and extends through planning, design, development, production, review, testing, commissioning, after sales service and evaluation of the product's performance [7].

In a well-organized company with established QA system, each manager in the organization knows his or her responsibility and has the required competence.

3.3 Requirements of QA Programs for Success

To be effective, QA programs should be sufficiently flexible to cater not only for "high quality" products but also to avoid the unnecessary imposition of high quality standards on "low quality" products. This will enhance the quality cost. Without such flexibility, a company cannot remain competitive [2].

3.4 Quality Assurance in Fabrication of Heat Exchangers and Pressure Vessels

Much of the QA literature is concerned with high-volume mass production industries with emphasis on statistical quality control, quality circles, total quality management (TQM), automation, etc., aimed principally at reducing the rejection, scrap, and rework, and hence at minimizing the product cost [8]. As pressure vessels, boilers, and heat exchangers are usually manufactured for a specific purpose on a "one-off" basis, statistical methods of quality control are not usual, although this applied where justified. Most of the QA literature on fabrication of pressure vessels and heat exchangers lies in standards, codes, and the technical literature of the individual industry.

3.5 Contents of QAP for Pressure Vessels and Heat Exchangers

The quality assurance in fabrication of pressure vessels is comprised of certain activities to be carried out by the pressure vessel manufacturer to assure the quality of design and construction for the safety and reliability of the pressure vessel. The activities that form the quality assurance program for pressure vessels and heat exchangers are discussed in Refs. 2 and 4.

1. Codes and interpretation
2. Approval of designs by the client/third party/consultant
3. Material control, both procurement and receipt
4. Calibration of testing and inspection equipments
5. Qualification of welding procedures and welder performance
6. Qualification of welding inspectors and nondestructive testing (NDT) personnel
7. Production methods and production control
8. Quality control during forming and shaping of components
9. Quality control during assembly of parts
10. Quality control during production welding
11. Nondestructive testing of welds
12. Directing and expediting nonconformance reports (NCR)
13. Quality control during postweld heat treatment (PWHT)
14. Nondestructive testing after PWHT
15. Leak testing of pressure vessels
16. Hydraulic testing or proof testing of pressure vessels
17. Documentation

18. Auditing
19. Periodic preparation of budget reports on inspection costs

4 QUALITY SYSTEM

To assure that the manufacturer has the ability and integrity to build pressure vessels and heat exchangers that meet the code requirement, it should have and demonstrate a quality control system [10]. This system must include a written description, known as a *quality manual*. To be effective, the quality control system must have managerial direction, technical support, and resources are made available for its implementation. Basics of quality control system for pressure vessel manufacture is discussed in detail by Chsu [10]. Chsu lists 15 elements of the quality control system as given below. ASME Code Section VIII, Div. 1 [9a] lists 14 features as part of a quality control system, and they are listed in Section 4.1 of this chapter. The elements of ISO 9000 Series are listed in Section 10.6 of this chapter. The salient features of quality control system for pressure vessel/heat exchanger manufacture are explained next.

1. *Authority and responsibility*. The authority and responsibility of the quality control manager shall be clearly established through management's statement of authority, signed by competent authority in the top management. The quality control manager shall have sufficient and well-defined responsibility, authority, and organizational freedom to identify quality control and quality assurance problems and provide solutions to these problems.
2. *Organization*. An organization chart showing the relationship between management, engineering, purchasing, manufacturing, quality control, and inspection shall be presented. Define responsibilities, authorities, lines of communication to perform and verify activities that affect quality, and for verification of quality; ensure personnel have sufficient freedom from pressure of production. Because a quality control program often crosses departmental boundaries within an organization, a company must fix responsibility for the program [11].
3. *Design specifications, drawings, design calculations*. This system provides for the preparation, issue, maintenance, and subsequent revision of drawings, material specifications to meet code requirements, and procedures for design assessment, verification and review.
4. *Material procurement control*. This system covers material requirements, indenting, and purchasing. Only code-permitted materials shall be indented. Materials such as plate, tubing, pipes, castings, forgings and consumables, including NDT consumables, are to be procured only from vendors approved by the QA department. Concise and clearly written specifications should be provided to the material supplier to ensure the proper material supply. For parts like pipe fittings bought from the trade, the purchase order shall meet code requirements. The manufacturer is responsible for surveying and qualifying vendor quality system, and control of material at source. This is to ensure that only code-permitted material including welding consumable is used and that it is free of defects, and the material is of the proper dimensions, correct composition, and is properly processed for fabrication.
5. *Material control*. This system covers material receipt, inspection and identification of materials, storage, and issue, including welding consumables and vendor evaluation. Procedures shall be established for examination of incoming materials like plates, pipes, forgings, etc.
6. *Process control, examination, and inspection*. This system ensures that the various stages of fabrication are carried out under controlled conditions, and defines work instructions, include criteria for workmanship, requirements for equipment, and inspection after each

work operation affecting quality. Establish written procedures for controlling fabrication and testing, welding, hot forming, NDT, leak testing, postweld heat treatment, hydrostatic testing, etc. At appropriate manufacturing stages, hold points are established so that inspections can be made on the material before commencing the next operation. Quality control personnel are involved in inspection at hold points, including nondestructive tests and interpretation of these tests.

7. *Correction of nonconformities.* This system covers control and disposal of nonconforming materials and components (i.e., items not conforming to code requirements), and ensures conditions adverse to quality are identified and corrected. When a nonconformity is noticed, the component or subassembly shall be segregated by a quarantine tag or sticker and a nonconformity report (NCR) prepared. For repair or rework to be carried out, a supplementary quality control plan, process sheet, and checklist with relevant procedures or reference to rework procedures shall be prepared. These shall be referenced in the main process sheet.
8. *Welding quality assurance.* This system covers quality of welding of components with specific reference to welding process parameters design, like precleaning and surface preparation, joint design, edge preparation and fit-up, base metal preheat, maintenance of interpass temperature and postheating, gas shielding, filler metal selection and preheating welding electrodes, welding procedures, and qualification of welders and welding machine operators. Specify methods to monitor welding before, during, and after welding. Welds must conform to Section IX of the ASME code [9b]. Welding consumables must be stored as per Section II, Part C of the Code [9c]. Documents must cover issue and return of consumable. Proper choice of materials, welding process, qualified personnel, etc., is necessary to ensure building the quality in the product.
9. *Nondestructive examination.* This system covers nondestructive examination and inspection carried out in all stages of manufacture, written procedures for various NDT techniques as per Code [9d] requirements, qualification of personnel, and provides documentary evidence that all code requirements are met.
10. *Heat treatment.* This system covers the requirements of heat treatment and calibration of temperature measuring and recording instruments. The quality control system on heat treatment of components, heat exchangers and vessels shall cover the following:

    a. Specify when preheating is required, and explain procedures for preheating, control of interpass temperature, postheating, and postweld heat treatment.
    b. Preheating and postweld heat treatment means/devices like use of gas burners, electrical heating elements, or furnace.
    c. Describe how furnace is loaded, placement and location of thermocouples, recording system for time and temperature.
    d. Methods of heating and cooling, and how temperature is controlled to achieve uniform temperature.
    e. Support of vessel and components during heating to avoid distortion.
    f . Methods to control scaling and oxidation of metal surfaces.

11. *Maintenance and calibration of measuring instruments.* This system ensures that inspection and test equipment and gages are calibrated and maintained properly. Maintain records documenting the accuracy, calibration methods, and history of equipment and standards used for final acceptance. Establish calibration standards and frequency of calibration.
12. *Documentation.* An extensive system of documentation is required to provide quality

control data records. Send written procedures that define responsibility and assign specific responsibilities to the management, supervisors, and quality control staff. Keep records showing that each has done his or her work for follow-up when necessary [11].

13. *Authorized inspector.* Authorized inspectors, or third-party inspection agencies are involved in design approval, materials selection, followed by inspection and testing during various stages of fabrication.
14. *Retention of records.* This system covers the preservation and retention of records of the product manufactured to meet the code requirement. Such records include mill test reports, NDT reports, radiographs, impact test results, heat treatment charts, etc.
15. *Audits.* An audit is an independent examination of quality to provide information; it is carried out by an independent organization called an audit team [12]. The aim of the audit is to establish that the procedures of the company's quality manual are being followed. Management should establish a schedule for audits and adjust it on a basis of previous results.

4.1 ASME Code: Quality Control System

Comprehensive quality assurance requirements were included in the first issue of ASME Section III in 1970. Mandatory "quality control system" requirements are stated in Appendix 10 of ASME Code Section VIII, Div. 1 [9a]. As per ASME Code, the manufacturer or assembler shall have and maintain a quality control system that will establish that all Code requirements, including those for material, design, fabrication, examination of vessels and vessel parts, and inspection, will be met. The quality control system shall cover these features: (1) authority and responsibility, (2) organization, (3) drawings, design calculations, and specification control, (4) material control, (5) examination and inspection program, (6) correction of nonconformities, (7) welding, (8) NDT, (9) heat treatment, (10) calibration of measuring and test equipment, (11) records retention, (12) sample forms, (13) inspection of vessels and vessel parts, and (14) inspection of pressure relief valves.

5 QUALITY MANUAL

To meet requirements of the codes and standards, the manufacturers develop a quality system and quality assurance program, which is spelt out in the company's quality manual or QA manual. It states the company's quality policy and details the quality systems, organization, and the responsibilities of the interrelated functions to meet the objectives of the QA program. The quality manual will form the basis for the documentation systems developed for quality control. It will be reviewed by the inspection agency, and the manual will serve as the basis for continuous auditing of the quality system. It contains all the sample documents (forms and formats) used in the quality management systems and procedures.

5.1 Details of QA Manuals

The quality assurance manual gives the following details [13]:

The company's quality policy
Organizational charts
Duties of QA personnel, supervisors, and technicians
Disposition of drawings, documents, and facsimile record-keeping forms
Material Control
Testing, inspection, and quality control procedures
Qualification of welding procedures, and qualification of welding personnel
Training and qualification of NDT personnel
Marking of nonconforming products
Heat treatment procedures
Calibration of measuring and testing equipment
Documentation
Possession and use of the code stamp

6 MAIN DOCUMENTS OF THE QUALITY SYSTEM

The main documents used to control the fabrication, examination; and inspection are the quality control plan, process sheet, and checklist. These documents are discussed next.

6.1 Quality Control Plan (QCP)

Based on approved drawings and material registration issued by the client, a quality control plan (QCP) will be prepared that shall indicate

Stages of manufacture at which examination and inspection are to be carried out
Details of examination to be carried out
Reference documents and acceptance standards
Witness/Hold points for Client/Third party
Records to be maintained

Before the commencement of manufacture, the quality control plan shall be made available to the authorized inspector, who shall review the same and indicate the approval. A typical QCP format is shown in Table 1.

6.2 Operation Process Sheet

Based upon the quality control plan, approved drawings, and the hold points indicated by the authorized inspector, the production engineering department in consultation with the quality assurance section shall prepare the operation process sheet for various operations. The operation process sheet will:

1. Describe the stages of manufacture and list them sequentially.
2. Indicate procedures such as WPS (welding procedure specification), heat treatment, etc. to be used for that operation at appropriate columns, and contain special instructions to the operator wherever required.
3. Provide space to record and make reference to reports such as NDT, NCR, etc.
4. Provide space for signature by the quality control inspector after carrying out necessary examination.
5. Provide space for indicating the hold points and witness points as specified on the quality control plan.

Operation process sheets for various operations are given below.

Operations List for Shell Preparation and Forming

Sl. No.	Operation	Ref. Doc.	Inspection			
			QC Dept.	IA	NDT	H/W
1.	Attestation VT/PT/MT/UT					
2.	Cutting					
3.	Edge preparation, PT/MT	Drg.				
4.	Forming—cold	QCP/				
	Forming—hot	Code				
5.	Examination after forming VT/PT/MT/ UT/Dimension					
6.	Heat treatment—Normal/SR/tempering					
7.	CTP testing					
8.	Final clearance					

Note: IA, authorized inspector; H/W, Hold/Witness point; CTP, coupon test plate; PTP, production test plate.

Operations list for longitudinal seams/circular seams welding. Prepare a format as in table above with inspection agency indicated.

1. Tack weld the joint [with PTP] WPS:
   a. Welder T.No.
2. Set up clearance
3. First side welding [note (1)] WPS:
   a. Welder T.No.
4. Second side grooving, PT/MT.
5. Second side welding. WPS:
   a. Welder T.No.
6. Clearance for NDT.
7. RT/UT/PT/MT clearance.
8. PTP testing [Note (2)].
9. Clearance for further processing.

Note: 1. Check PT on root run.
2. PTP testing if no post weld heat treatment is involved.
3. Preserve PTP up to final post weld heat treatment.

Operations list for nozzles on shell/dish welding. Prepare a format as in table above with inspection agency indicated.

1. Hole marking and clearance.
2. Hole cutting. VT/PT/MT/UT
3. Edge preparation. VT/PT/MT
4. Tack weld nozzle on shell/dish WPS:
   a. Welder T.No.
5. Set up clearance

6. First side welding—Note (1) WPS:
   a. Welder T.No. Rev:
7. Second side gouging, PT/MT
8. Second side welding WPS:
   a. Welder T.No. Rev:
9. Dress up of weldment
10. Visual examination
11. UT/PT/MT/Marking clearance
12. Air Leak test of reinforcement pads
    (Pressure . . . Kg/Sq.cm.)
13. Clearance for further process

Note: 1. Check PT on root run.

Operation list for drilling of tubesheets. Prepare a format as in table above with inspection agency indicated.

1. Holes marking
2. Drilling
   Pilot I dia.
   Pilot II dia.
   Pilot III dia.
   Finish reamer
3. Expansion annular rings grooving, and chamfering (if applicable)
4. Pass partition grooving
5. Drilling and tapping for tie rods, pulling eyes, and lugs
6. Obtain clearance

Operation list for fixed tubesheet heat exchanger assembly. Prepare a format as in table above with inspection agency indicated.

1. Set one tubesheet on the fixture.
2. Assemble the baffles, tie rods and spacer tubes or sealing strips.
3. Insert the tubes.
4. Tighten the nuts, lock nuts, and weld.
5. Set and weld the impingement plate.
   Welder T.No.
6. Set and weld the sliding/sealing strips, if any.
   Welder T.No.
7. Check tube bundle with ring gauge.
8. Check shell inside with push through gauge.
9. Obtain clearance for tube bundle insertion.
10. Insert the tube bundle into shell.
11. Set the second tube sheet and draw the tubes through
12. Weld the second tubesheet with shell.
13. Level the tubesheet side and obtain clearance.
14. Complete the tube-to-tubesheet root run welding and inspect by PT.
    Welder T.No.
15. Complete light/strength expansion and obtain clearance.
16. Trim the excess portion in tubes and obtain clearance.
17. Machine the gasket seating surface, if distortion is noticed.

M/s. ABC Engineering Company, Chennai, India.	QUALITY CONTROL PLAN	
Prepared By	Reviewed By	Issued By

SL. No.	COMPONENT / OPERATION	CHARACTERISTICS	TYPE OF CHECK	REFERENCE DOCUMENT	ACCEPTANCE NORM	FORMAT OF RECORD	EXAMINATION BY	INSPECTION BY AUTHORISED INSPECTOR / INSPECTING AUTHORITY		DEPARTMENT
								HOLD POINT	WITNESS POINT	
1.0	Review of drawings	-	-	Drgs., A-VIII, CS & T	A-VIII & T	Drgs.	*			Technical
2.0	Review of QCP	-	-	-do-	-do-	QCP	QA&C, PED			QA&C
3.0	Review of WPS, PQR & WPQR	-	-	A-IX	A-IX	WPS, PQR & WPQR	Welding Engg. & QA&C			Welding Engg.
4.0	Material Receipt Inspection (including bought outs)	As per Technical Delivery Condition and Material Specification	TC verification & C2	Drgs. & TDC	M, Drgs. & TDC	Test Certificates	-do-			Material, Technical, Welding Engg.
5.0	Examination of marking of materials	Dimensions	C2	Drgs.	Drgs.	Material Issue Advise	QA&C			Prodn.
6.0	Material Attestation	Verification of Transferred identification	C2	-do-	-do-	Material Attestation Form	-do-			QA&C

6.3 Checklist

Based upon the quality control plan with the hold and witness points indicated by the authorized inspector, approved drawing, and process sheet, prepare a checklist detailing the examination and inspection to be carried out during the various operations. Provision shall be made for the signature of the authorized inspector. Hold and witness points indicated in the quality control plan shall be transferred to the checklist and submitted to the authorized inspector for verification.

7 ECONOMICS OF QUALITY ASSURANCE

Quality cost may at first seem high due to NDT equipment, measuring instruments, supplies, training, and qualified personnel/labor. Reduced quality may result in low reliability, rework, rejections, down time, which may give rise to complaints, failures, losses, and hazards to human beings and the environment [7,14]. On the other hand, if the requirements for quality, reliability, safety, and availability are too high, product costs will be unnecessarily high. One of the basic management duties is to strike an optimum balance between the various costs of quality assurance. Elements of quality cost and quality cost model are shown in Fig. 1. The quality costs model shown in Fig. 1b is adapted from Ref. 15. Production costs rise disproportionately as designers tighten tolerances. One way to decide where tolerances should be tight is to make a Pareto analysis of the dimensions and tolerances of the work [11]. This method classifies the elements of a total unit in the order of their importance to the performance of that unit. Such a classification of dimensions includes functionally critical, significant, and significant only for good appearance and for good workmanship. Veith [11] cites the Pareto analysis of 5000 dimensions of a pressure vessel, which showed that only 5% of the dimensions are critical, 18% are significant, and the remaining 77% dimensions require only good workmanship and acceptable appearance. Keeping in mind that under a quality control system, every out-of-tolerance dimension is considered nonconforming, decide just exactly which dimensions are critical to the vessel operation and be more selective in assigning tolerances.

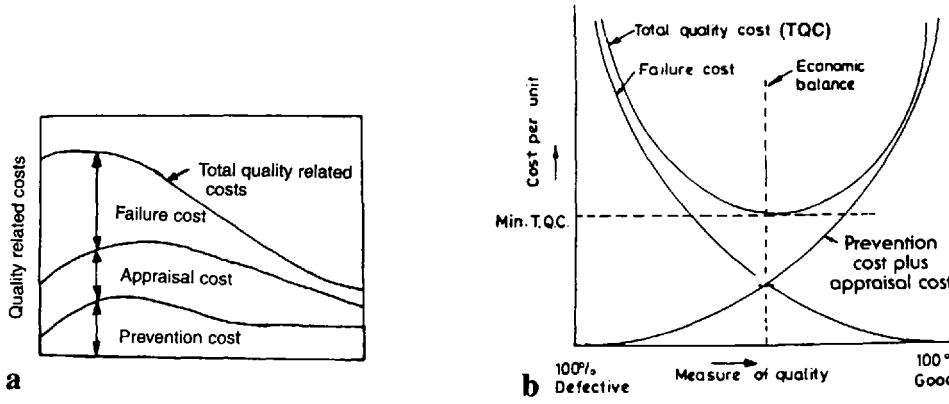


Figure 1 Quality cost. (a) Elements of quality related cost, and (b) total quality cost. (Adopted from Ref. 15.)

8 REVIEW AND EVALUATION PROCEDURES

Review is an important activity in a quality system to ensure that compliance with a set of procedures and agreed standards takes place all the time at all stages of the production process. Reviews must be methodical, and depending on the nature of the organization, they may take the form of (1) management audits, (2) system audits, or (3) project or product audits. Reviews are carried out periodically.

8.1 Auditing

Audits should be conducted at specified intervals in accordance with written procedures and a checklist, to verify by investigation that applicable elements of the quality system and quality assurance programs have been effectively implemented and documented.

8.2 Auditng Procedure

There are four major steps in conducting an internal audit. These same steps apply to audits of all types of activities: engineering, purchasing, manufacturing, and marketing. Only the avenues of inquiry and the specific questions used are different for the various audits. The four steps in conducting audit are [16]: (1) planning and preparation, (2) performing the audit, (3) reporting the results, and (4) follow-up and close-out.

8.3 Contents of an Audit Plan

To carry out an audit adequately, proper planning is essential and auditing procedures be prepared. The audit structure will take the formal pattern: arrangement, meeting, audit, review, report, and reaudit. The auditing procedure will define the following points [12]:

Scope of the audit
Names of audit team members and their organizational affiliation
Name of the group to be audited
Listing of areas or activities to be audited
List of applicable documents
Equipment to be used
Auditing method
Report
Acceptance criteria

9 DOCUMENTATION

The quality system requires extensive and minute documentation of every procedure related to the manufacture of a product. The documentation serves as a proof of the activities carried out and the quality achieved by the manufacturer. The following certificates and records should be documented where applicable, and a copy of these should be sent to the customer:

1. Customer's order
2. Vessel detail drawing together with a materials list
3. Material certificates of chemical and physical properties
4. Welding procedure specification and procedure qualification records
5. Welder qualification records
6. Records of welding consumables used
7. Certificate of radiography and other nondestructive testing operations

8. Reports of nonconformities
9. Heat-treatment charts
10. Leak test report
11. Hydrostatic test report
12. Reproduction of vessel markings and stamping
13. Manufacturer's data report and associated partial data report, if any

10 ISO 9000

Discussion on QC and QA will not be complete unless the ISO 9000 Quality Series is mentioned. In the present decade, ISO 9000 is steering a quality revolution all around the world; it is the key to business survival. ISO is the International Standards Organisation, headquartered at Geneva, Switzerland. One of its purposes is to develop and to promote worldwide quality standards.

10.1 What Is the ISO 9000 Series?

The ISO 9000 series of quality standards defines the basic management systems that a manufacturer should have to ensure that the end product consistently conforms to the order requirements. ISO 9000 places great emphasis on documentation of all the elements/features of quality systems (in manuals and procedures), implemented, audited, and reviewed.

10.2 Principles of ISO 9000

ISO 9000 is a quality system applicable to any industry and describes what to do, but not how to do. The guiding principles are document, establish, implement, and maintain. In simple terms:

1. Say what you do—procedures and documents.
2. Do what you say—implementation.
3. Demonstrate that you do what you say—documents and record keeping.

10.3 Why ISO 9000?

Most of the organizations applying for registration under the ISO 9000 standards are doing so to comply with customer and third-party requirements, and to achieve a climate of competitiveness. Over the years, countries with focus on international trade as diverse as the United States, Japan, European Community countries, Russia, Australia, Canada, New Zealand, India, and Mexico have accepted ISO 9000. Various countries have established national schemes to audit and accredit the certification organizations that audit companies to ISO 9000. More countries are basing their quality systems on the ISO 9000 series.

10.4 Benefits of ISO 9000

The main improvement in the quality system since implementation of ISO 9000 is the continuous improvement of quality, customer confidence in a company's quality system, and efforts targeted towards corrective actions to ensure that the same problems are not repeated. Major benefits of ISO 9000 are:

It introduces a systems concept.
It brings about changes that are organizational, procedural, and operational.
It focuses on prevention of nonconformities.

It improves communication in the system.
It satisfies quality levels, and facilitates improvements.

10.5 Listing of Selected ISO 9000 Quality Standards

ISO 9000—Guidelines for selection and use of quality management and quality assurance system models according to ISO 9001, 9002, or 9003.
ISO 9001—Model for quality assurance system in design, development, production, installation, and servicing.
ISO 9002—Model for quality assurance system in production, installation, and servicing.
ISO 9003—Model for quality assurance in final inspection and test.
ISO 9004—Guidelines for selection and use of various quality management and quality system elements for developing a suitable model.
ISO 10011-1, 2, 3—Guidelines for auditing quality systems.
ISO 10012-1—Quality assurance requirements for measuring equipment; part 1, management of measuring equipment.

10.6 Total Quality Management (TQM)

Total quality management (TQM) is often defined as the establishment of a customer–supplier chain. The ISO 9000 standard is an important tool that can be used to develop links with suppliers and establish long-term partnerships.

10.7 Contents of ISO 9001 Quality Systems

This is a model for quality assurance in design, development, production, installation and servicing. Listed below are the principal clauses of ISO 9001.

4. Quality system requirements
4.1 Management responsibility
4.1.1 Quality policy
4.1.2 Organization
4.1.2.1 Responsibility and authority
4.1.2.2 Resources
4.1.2.3 Management representative
4.1.3 Management review
4.2 Quality system
4.2.1 General
4.2.2 Quality system procedures
4.2.3 Quality planning
4.3 Contract review
4.3.1 General
4.3.2 Review
4.3.3 Amendment to a contract
4.3.4 Records
4.4 Design control
4.4.1 General
4.4.2 Design and development planning
4.4.3 Organizational and technical interfaces
4.4.4 Design input
4.4.5 Design output

4.4.6 Design review
4.4.7 Design verification
4.4.8 Design validation
4.4.9 Design changes
4.5 Document and data control
4.5.1 General
4.5.2 Document and data approval and issue
4.5.3 Document and data changes
4.6 Purchasing
4.6.1 General
4.6.2 Evaluation of subcontractors
4.6.3 Purchasing data
4.6.4 Verification of purchased product
4.6.4.1 Supplier verification at subcontractor's premises
4.6.4.2 Customer verification of subcontracted product
4.7 Control of customer-supplied product
4.8 Product identification and traceability
4.9 Process control
4.10 Inspection and testing
4.10.1 General
4.10.2 Receiving inspection and testing
4.10.3 In-process inspection and testing
4.10.4 Final inspection and testing
4.10.5 Inspection and testing records
4.11 Control of inspection, measuring, and test equipment
4.11.1 General
4.11.2 Control procedure
4.12 Inspection and test status
4.13 Control of nonconforming product
4.13.1 General
4.13.2 Review and disposition of nonconforming product
4.14 Corrective and preventive action
4.14.1 General
4.14.2 Corrective action
4.14.3 Preventive action
4.15 Handling, storage, packing, preservation, and delivery
4.15.1 General
4.15.2 Handling
4.15.3 Storage
4.15.4 Packaging
4.15.5 Preservation
4.15.6 Delivery
4.16 Control of quality records
4.17 Internal quality audits
4.18 Training
4.19 Servicing
4.20 Statistical techniques
4.20.1 Identification of need
4.20.2 Procedures

Part 2: Inspection

1 DEFINITIONS

The term *inspection* can be defined as the process of examination of a material or a finished product using sensory organs, tools, equipments, instruments and gauges to assess the quality of a product.

The term *inspection*, as far as ASME Code Section V [9d] and other referencing Code sections are concerned, applies to the functions performed by the Authorized Inspector, whereas the term *examination* applies to the quality control functions performed as stipulated in the quality manual by quality control staff of the company or the manufacturer.

2 OBJECTIVES OF INSPECTION

During manufacture, inspection has three principal objectives [17]:

1. To provide assurance that there are no defects, indicating manufacturing was above the standard required in the specification.
2. To provide assurance that no defects are present that could impede subsequent processing inspections.
3. To provide assurance that no defects are present in the completed component that will pose safety problem.

3 DESIGN AND INSPECTION

In the preliminary design stage, performance criteria and material selection should be made compatible with NDT, and the aim should be to provide maximum accessibility for inspection both during fabrication and in service. The design should include inspection in critical areas where the fabrication process is likely to introduce defects or where service conditions will impose critical stresses (6).

4 INSPECTION GUIDELINES

Some general rules for organization of inspection are:

1. Prepare inspection briefs in clear and concise formats. Assemble and incorporate into the inspection brief the setting plan, assembly drawings, tools, and instruments required for inspection [18].
2. Collect the required documents.
3. Define the techniques of inspection.
4. Establish the sequence of inspections.
5. Specify inspection of materials and components as soon as possible.
6. Establish safety regulations for inspections.

5 SCOPE OF INSPECTION OF HEAT EXCHANGERS

During the various stages of production process, inspectors examine work and document their observations. The scope of inspection of heat exchangers is briefly listed:

Raw material identification and inspection.
Approve welding procedures by test plates as required.
Approve welders to be employed.
Edge preparation for welding, including visual check penetrant test for laminations.
Inspect weld preparations and setup for welding.
Inspection of back-gouged welded joints such as set-in nozzles, which are not readily radiographed following welding.
Inspection of cladding by dye penetrant examination; verify chemistry following completion of the cladding; measure ferrite content.
Alignment of longitudinal and circumferential seams.
Tolerances on individual shell section.
Alignment of sections and components.
Root pass clearance before welding.
Examine soundness and general contour of welds.
Inspect prefabricated parts/trade items.
Check radiographic or other weld inspection technique.
Thinning of formed heads after forming.
Checking of tube sheet and baffle holes after drilling.
Tube sheet to shell setup prior to welding operation.
Check dimensions after postweld heat treatment.
Witnessing of leak testing or hydrostatic test.
Dimensional examination after hydrostatic test.
Stamping of the vessel and issue of certificates.
Packing and despatch.

A typical stagewise inspection chart is shown in Table 1. Various stages of inspection should be selected to avoid heavy reworks at a later stage. But it should not lead to too many stages of inspection, which only lead to delays and rushing by workmanship to compensate for such delays; resulting in poor quality.

5.1 Material Control and Raw Material Inspection

One of the important duties of inspectors is to inspect the raw materials like plates, forgings and tubes, and certify that they are as per purchase order and free from defects. The code requires goods to be accompanied by documents that detail the mill test reports and certifications. A designated receiver should have the receiving procedure, the purchase order, and a checklist covering component dimensions, and examine for laminations, surface defects, transhipment damage, identification and verification of heat numbers, and test records supplied by vendors [11]. A sound quality control program will rely on more than just a review of the mill test reports that accompany the incoming material. Such a program should include chemistry verification by spot NDT or destructive testing techniques. This may involve in situ x-ray examination, or laboratory wet-chemical or energy-dispersive evaluation [1]. An easy way to avoid using the wrong materials in parts is to check composition using a portable spectroscope, which quickly identifies all major elements [19]. The receiver signs in acceptable material for storage, and tags and segregates nonconforming materials, followed by identification, which includes a job number, serial number, and heat number, if relevant. Throughout production, identification follows the material or component, assuring traceability. All this work is carried out according to the QC procedures laid down in the quality manual [13].

For all high-pressure applications, ultrasonic testing must be carried out to check for lami-

Table 1

STAGEWISE INSPECTION CHART

REF. :
SHEET 1 OF 2

REYNOLDS ENGINEERING CORPORATION

REGD. OFFICE : MEHTA ESTATE, NEAR GERMAN REMEDIES, ANDHERI–KURLA ROAD, ANDHERI (EAST), MUMBAI–400 093. TEL : 837 78 63 (4 LINES). FAX NO. : 441381

FACTORY : PLOT NOS. N–14 & N–17, UDYOGBAGH, KHANAPUR ROAD, BELGAUM–590 008. TEL: 441161, 441018, 441143 & 440388 FAX NO.: 441381

CLIENT :	SIZE	SHELL SIDE	TUBE SIDE
PROJECT :	DESIGN PRESSURE Kg/Cm²/ WORKING PRESSURE Kg/Cm²		
P.O. NO. :	DESIGN TEMPERATURE °C/ WORKING TEMPERATURE °C		
ITEM NO. :	HYDROSTATIC TEST PRESSURE Kg/Cm²		
W.O. NO. :	RADIOGRAPHY		
DRG. NO. :	HEAT TREATMENT		
DESIGN CODE :			
INSPECTION AGENCY :			

SR. NO.	LONG SEAM/ LENGTH	REQUIRED O/D IN mm.	OBSERVED O/D IN mm.	REQUIRED CIRCU. IN mm.	OBSERVED CIRCU. IN mm.	ACCEPTED	H.C. & DP TEST	RADIOGRAPHY	SIGN. & DATE
1									
2									
3									
4									
5									
6									
7									
8									
9									
10									

SR. NO.	CIRCU. SEAM	WELD JOINT	ACCEPTED	SIGN. & DATE	H.C. & DP TEST	ACCEPTED	SIGN. & DATE	RADIOGRAPHY	SIGN. & DATE
1									
2									
3									
4									
5									
6									
7									
8									
9									
10									

TUBE TO TUBESHEET JOINT			REQUIRED		OBSERVED	WELDING			TUBE D/P TEST		
MARK	N. FLANGE TO N. PIPE SETUP	H.C. & DP. TEST	MARK	BEND & REDU. SETUP	H.C. & DP. TEST	MARK	NOZZLE TO VESSEL SETUP	H.C. & DP TEST	MARK	SOCKET SETUP	H.C. & DP. TEST

BAFFLE ASSEMBLY			TESTING REPORT		OTHER REQUIREMENT	
	REQUIRED	OBSERVED				
BAFFLE O/D			SHELL HYDRO.		SHELL GASKING	
BAFFLE PITCH			TUBE HYDRO.		SHELL INTERNAL	
BAFFLE CUT			BUNDLE HYDRO		CHANNEL INTERNAL	
1st. BAFFLE DIST.			PAD TEST SHELL		SHELL COVER INTERNAL	
BAFFLE ARRY. LG.			PAD TEST TUBE		SHELL/CHANNEL SURFACE FINISH	
ORIENTATION			PNEUMATIC TEST		D.P. TEST	
REMARK			TUBE PNEUMATIC TEST		OVERALL DIMENSIONS	
			TUBE D.P. TEST		NDT	
					PWHT	
					MOCK UP	
					U–TUBE SAMPLE	

REMARK : 1) ALL PRESSURE PART COMPONENTS FOR ABOVE UNIT IS IDENTIFIED, STAMPED & CLEANED FOR FURTHER OPERATION.
2) SHEET 2 OF 2 : TUBESHEET INSPECTION REPORT NO.

SURVEYOR STAMP
RELEASED FOR DESPATCH

INSPECTION AGENCY/AUTHORITY

SAMPLE

nation and nonmetallic inclusion. Plate edges are to be examined by magnetic or dye penetrant examination. Similarly, thicker forging must be ultrasonically examined.

6 DETAILED CHECKLIST FOR COMPONENTS

Before conducting the inspection, prepare a checklist of what to inspect, how, and when to inspect. Instruct the inspector to record deviations and their resolutions in an inspector's log [18]. Checklists detail steps in inspection of shell, channel, tube sheet, flanges, expansion joint, tube bundles, final assemblies, etc. A typical checklist for tubesheet, taken from a manufacturer's work, is given next.

6.1 Checklist for Tube Sheet

Outer diameter of the tube sheet
Diameter of the raised face shell side
Depth of the raised face shell side
Diameter of the raised face channel side
Depth of the raised face channel side
Thickness of the tube sheet
Width of the pass partition groove
Depth of the pass partition groove
Number and orientation of pass partitions
Size of the tube holes
Number and layout of tube holes
Outermost tube periphery diameter
Ligament
- (a) Nominal ligament
- (b) Number of holes below nominal ligament [4% of holes can be lower than TEMA minimum ligament]

Minimum ligament near pass partition
Depth of the welding groove
Expansion groove
- (a) Width
- (b) Depth
- (c) Location

Number of pulling eyes and sizes
Number of tie rods and sizing
Number of bolt holes and sizes
Neutral line marking

7 TEMA INSPECTION PHILOSOPHY

TEMA [20] inspection policy is specified in paragraph G-2. G.2.1 specifies manufacturer's inspection, and G-2.2 specifies the purchaser's inspection.

8 MASTER TRAVELER

During fabrication, a traveler that accompanies the part or component is sometimes the easiest way to carry out QC procedure. A drawing with all the welds numbered and marked with the

points to be examined is a convenient and careful way to handle QC of welds. This document is known as a master traveler [11, 21]. The traveler tabulates operations for manufacture of any part or component. The traveler can continue to cover the complete vessel. From a production standpoint, however, it is often better to divide a complex vessel into components, with a traveler for every component and a separate sheet for the final assembly.

9 SCOPE OF THIRD-PARTY INSPECTION

Third-party inspection agencies such as Lloyd's Register and Bureau Varitas Quality International, among others, normally stipulate an involvement starting with approval of design, materials, fabrication, followed by inspection and testing. In general, the scope of third-party inspection includes the following:

1. Approval of design and fabrication drawings to ensure that materials and fabrication details meet code requirements.
2. Material clearance for pressure parts.
3. Verification of WPS/PQR and welder performance qualification tests and heat treatment.
4. Inspection during various stages of fabrication, principally by check points/hold points/witness points, indicated by (R) Review of record of inspection by third party; (H) Hold further process till review of record of inspection by third party; and (W) Witness of process by third party to ensure compliance with code requirements.
5. Examination of radiographs, and auditing of other nondestructive tests and heat-treatment procedures as required by the code.
6. Dimensional examination of the completed vessel.
7. Witnessing of leak test, hydrostatic, or any other special test as required by the code.
8. Stamping of the vessel and issue of certificates.

Lloyd's approach to quality assurance of welded structures is discussed by Frew [22]. The approach is briefly described here. Appraisal at the design stage includes the calculation of thickness and an assessment of materials to be used, together with manufacturing and welding processes to be employed, the effect of fabrication, and welding and heat treatment processes on the materials used. Service conditions are taken into consideration. The efficacy of the fabricator's quality system is evaluated and suitable NDT methods are considered in relation to the joint geometries involved. Approval of fabrication takes into consideration the welding quality design, welder procedure qualification and production tests, postweld heat treatment (PWHT), etc.

9.1 Hold Points and Witness Points

Consideration should be given to the establishment of hold points and witness points, where an examination is to occur prior to the accomplishment of any further fabrication steps [23]. This is of vital importance for fabrication of pressure vessels and heat exchangers as per Code and/or Standard. Through hold points and witness points, authorized code inspectors exercise control over the activities such as design calculations, drawings, receipt of materials and welding consumables, qualification of welding procedures and welders, joint design, work preparation before welding, examination during welding and after welding, NDT, nonconformance report (NCR), PWHT, hydrostatic tests, etc. A typical scheme for hold points/witness points and verification points is given in Table 2.

Table 2 Hold and Witness Points

Number	Stages of manufacture	H	W
1.	Drawing and design calculations approved	X	—
2.	Raw material for pressure parts clearance	X	—
3.	WPS/POR/welder qualifications	X	—
4.	Forming dimensions for shell and dished ends	X	—
5.	U-bends, qualification report	—	X
6.	Heat treatment chart for forming (if applicable)	—	X
7.	Fit up of pr. welds incl. attachments on pr. parts	X	—
8.	Air test for RF pads	—	X
9.	Shell ID check by template	—	X
11.	Radiography for pressure part welds	X	—
12.	MT/PT of nozzle and pressure parts attachment welds	—	X
13.	PWHT (if applicable) clearance for pressure part assly.	X	—
14.	Review of heat treatment charts	—	X
15.	NDT after heat treatment if applicable	X	—
16.	Destructive testing of production test plate	X	—
17.	Tube-sheet and baffle inspection after drilling	—	X
18.	Tube bundle skeleton before tubing	—	X
19.	Tube-to-tube-sheet joints, NDT/LT	—	X
20.	Pneumatic and hydro test for tube-to-tube-sheet joints	—	X
21.	Shell-side and tube-side hydrostatic test	X	—
22.	NCR clearance	X	—
23.	Painting of unit satisfactory	X	—
24.	Stamping and document folder clearance	X	—

Note: H, hold and witness; W, verification of records; X, applicable.

Part 3: Welding Design

1 PARAMETERS AFFECTING WELDING QUALITY

Three important parameters (Fig. 2) that contribute to quality of a welded product are [17]:

1. Material—composition, product form, and mechanical properties.
2. Welding—procedures, welders, equipment, and supervision.
3. Inspection—stage inspection and NDT.

Elements of welding design for building quality into the product are discussed in this part.

2 WELDING QUALITY DESIGN

The highest standards of weld quality demand quality control or NDT or both. Not all welds can be inspected by common NDT methods. The achievement of consistent high-quality welds made by manual or automated welding processes require the following [11, 17]:

1. Well-established and qualified welding procedures.
2. Strict implementation of all the weld procedures.
3. Trained and qualified welders, and welding machine operators.

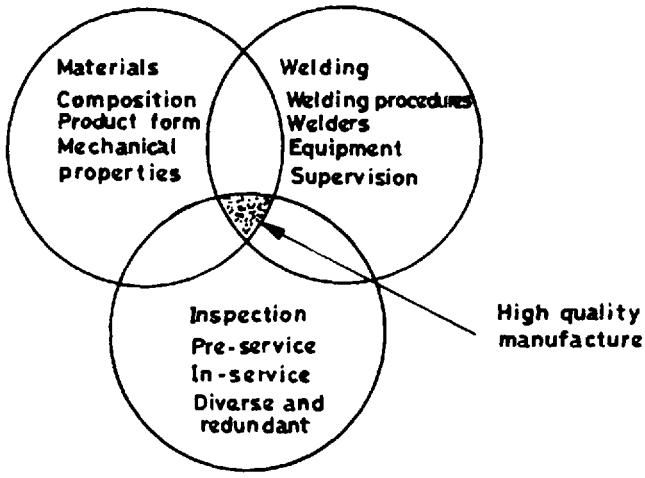


Figure 2 Components of fabrication assessment. (From Ref. 17.)

4. Well-maintained and calibrated equipments, instruments, and gauges.
5. Proper supervision and control of welding operations.
6. Recording of all information and measurements during welding.
7. Detailed NDT.
8. Welding consumables must be stored as per Section II, Part C, of the Code or as per quality manual.
9. Documents must cover issue and return of consumables.

In addition to these, more attention must be paid to the already proven techniques of quality control and particularly in the following areas [3]:

Component design—eliminate sites for fatigue or brittle fracture, improve access for welding and inspection.
Weld detail design—use butt welds, rather than fillets or seal welds.
Material selection—weldability considerations.
Operator selection—test the ability of the welder or welding machine.
Supervision and production control—adequate supervision or monitoring in the case of machines.

For better control of weld quality of major and critical joints, tabulate the various welding parameters as shown in Table 3.

2.1 Variables Affecting Welding Quality

A wide range of welding variables affect the weld quality. They include [17]: welding process, weld preparation, weld bead sequence, parent material compositions, weld metal composition, fluxes, electrodes and filler wires, preheat and interpass temperature, welding speed, heat input, cleaning between passes, PWHT, postweld cleaning, and surface treatment.

3 SCHEME OF SYMBOLS FOR WELDING

Symbols described in any standard provide the means of placing on drawings information such as the type, size, positions, etc. of the welds in the welded joints. To avoid confusion and

Table 3 Welding Parameters for Better Control of Weld Quality

Joint no.	Fig. no.	Base materials	Thickness (mm)	Welding process	No. weld runs	Filler material	Shld. gas/ flux	Preheating (°C)	PQR No.	WPS No.	PTP

Note: If necessary, several tables of this form may be used, having the same revision number. A blank space below the table may be left for notes such as weld details and for numbered sketches of the joint.

misunderstanding, it is essential that only standard symbols are used by all designers and fabricators. However, all information required for welding cannot be conveyed by the symbols alone. AWS welding symbols are used in many countries. Typical AWS welding symbols are given in Fig. 3. For more details on welding symbols, refer to Standard Symbols for Welding, Brazing and Nondestructive Examination, ANSI/AWS A2.4-93.

4 STANDARD FOR WELDING AND WELDING DESIGN

Welding and welding design shall be as per ASME Code Section IX [9b]. The scope of Section IX is given here.

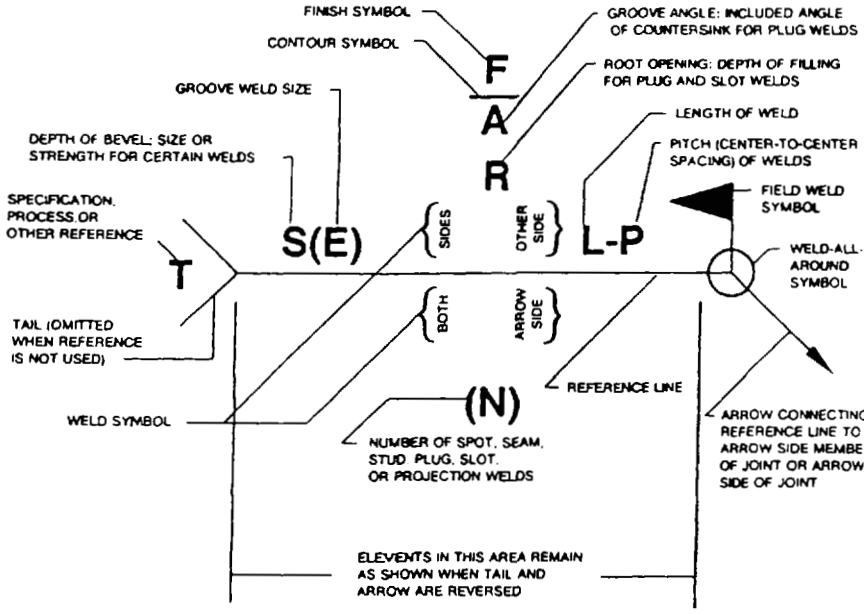


Figure 3 AWS welding symbol and location of elements.

4.1 ASME Code Section IX

Section IX of the ASME code specifies the rules for all manual and machine welding processes and rules for the preparation of welding procedure specifications, and the qualification of welding procedures, welders, and welding operators. There are, in addition, tables of P-numbers that have been assigned to each material specification, so that the various examinations can be classified together. Similarly, F-numbers are assigned to electrodes and welding rods to utilize coverage of several different electrodes or welding rods within one qualification test. This section also includes tables for each process listing essential, supplemental essential, and nonessential variables, welding factors that can be altered.

5 SELECTION OF CONSUMABLES

While selecting the consumables, the requirements for hydrogen control must be satisfied to avoid hydrogen-induced cold cracking. Electrodes and fluxes must be heated before use to ensure low hydrogen contents.

6 P NUMBERS

All materials used for pressure vessel manufacture have been grouped under different P numbers. The P number grouping of materials is based essentially on comparable metal characteristics such as composition, weldability, and mechanical properties. The object of grouping the base materials is to reduce the number of qualifications required. Thus a single qualification may be adequate for several material specifications. The P number groupings are given in Table 3.

7 FILLER METALS

The filler metals are grouped under both F numbers and A numbers.

7.1 F Numbers

All the electrodes and fillers are grouped under different F numbers. The F number grouping is based essentially on their usability characteristics, and the object of the grouping is to reduce the number of welding procedures and performance qualifications. The F number grouping is givin in Table 4.

7.2 A Numbers

As well as classifying the filler metals under F numbers, they are classified under A numbers. The A number classifications of the filler metals are based on the weld metal composition, whereas the F number classifications are based on the usability characteristics.

Table 4 P Number and F Number Groupings

Ferrous metals	P1 to P11	F1 to 6
Aluminum and its alloys	P21 to P25	F21 to 24
Copper and copper alloys	P31 to P35	F31 to 36
Nickel and nickel alloys	P41 to P45	F41 to 44
Unalloyed titanium	P51 to P52	F51

8 WELDING PROCEDURE QUALIFICATION: WELDING PROCEDURE SPECIFICATION AND PROCEDURE QUALIFICATION RECORD

The Code says that all the details of the welding procedure should be listed in a document known as the welding procedure specification (WPS). Each of the welding procedure specifications shall be qualified by the welding of the test coupons and the testing of specimens as required by the Code. The type and number of tests are selected to provide sufficient information on strength, ductility, toughness, or other properties of the joint. The welding data for the test coupons and the results of the tests shall be recorded in a document called procedure qualification record (PQR). A WPS may require the support of one or more PQR, whereas one PQR may support a number of WPS. A WPS will be applicable equally for plate, pipe, and tube joints.

The welding procedure specification (WPS) and the procedure qualification record (PQR) are required to prove that the weldment has desired properties, and not to prove the skill of the welder or the welding machine operator. The welder or operator performance qualification is to prove the ability of the welder to deposit good weld metal; the welding operator performance qualification is to show if the operator can operate the welding equipment.

8.1 Welding Procedure Specification

Welding Variables

Depending on their influence on obtaining a desired weldment, the welding parameters are classified and listed. Some of them are listed as *essential variables*, some of them as *Supplementary Essential variables*, and the others as *nonessential variables.*

Essential variables when changed beyond the allowable limits alter the weld properties and requalification is required. Still, there are a number of variables that are declared essential in case a procedure qualification is applied, for example, a weldment meant for high notch toughness applications. These are called supplementary essential variables.

Nonessential variables when changed (within logical limits) during welding do not alter the desired weld properties and they are entered in the PQR without qualifying the same. Production welds with such altered variables could be continued without any need for requalification of the welding procedure.

Contents of Welding Procedure Specification (WPS)

A WPS shall describe all of the essential/nonessential and supplementary essential variables (when required) for each process used. It will contain information regarding joint details, joint preparation, base metals, type and size of filler metal, welding position, electrical characteristics (type of current, range of current, and voltage), welding techniques, shielding gas, preheat, post weld heat treatment, interpass temperature, not preparation prior to welding from second side, welding speed, etc.

Qualification of a Welding Procedure

The basic steps in the qualification of a welding procedure are as follows:

1. Prepare a preliminary WPS.
2. Prepare a test piece and carry out welding using parameters givin in the WPS.
3. Conduct the required tests.
4. Evaluate the results of the tests.
5. Document results on PQR.

6. If results are not satisfactory, after the variables in the WPS.
7. Repeat steps 2 to 6, until test results are satisfactory.
8. Issue approved PQR.
9. Issue approved WPS.

8.2 Procedure Qualification Record (PQR)

A PQR is a record of the range of welding parameters used to qualify a weling procedure.

Contents of the PQR

The completed PQR shall contain all essential and supplementary essential variables (when required) for each welding process used for welding the test coupon and the test results in compliance with code requirements.

8.3 Welder's Performance Qualification

The object of the welder's performance qualification is to determine the ability of the welders to make sound welds. The welders may be qualified based on the results of the mechanical tests or by radiographic examination of the test coupon. For qualifying welders, only the essential variables (as applicable to welders' skill) are considered. Any change in those variables requires requalifying the welder. In the case of welding machine operator qualifications, ability to operate the welding machine is tested. A welding machine operator is usually qualified along with a procedure test.

8.4 Welder Requalification

Some of the welding parameters that will require welder requalification whenever a change is made in WPS are:

1. If a welder had qualified for a WPS with a backing strip and if the backing is removed then the welder has to requalify. However, if a welder had qualified for a WPS without backing, then that welder is qualified for a WPS with backing also.
2. If the range of thickness has to be increased or there is a change of base metal from one P number to another P number, a new WPS should be prepared and specified by a PQR.
3. A change in F number or A number shall require a new WPS and PQR; a change in the diameter of the electrode also requires a new WPS but need not be qualified by a test.
4. Any change in temperature and duration of the postweld heat treatment shall require requalification.

8.5 Welding Positions and Qualifications

ASME Code has classified five welding positions for qualifications: flat, horizontal, vertical, overhead, and horizontal fixed. Some positions are shown in Fig. 4 with designated notations for groove and fillet welds.

9 WELD DEFECTS AND INSPECTION OF WELD QUALITY

9.1 Weld Defects (Discontinuities)

In the correct sense of the word defect is a rejectable discontinuity or a flaw of rejectable nature. A defect is definitely a discontinuity, but a discontinuity need not necessarily be a defect. Technically, discontinuities are not defects unless they exceed the limits set by the

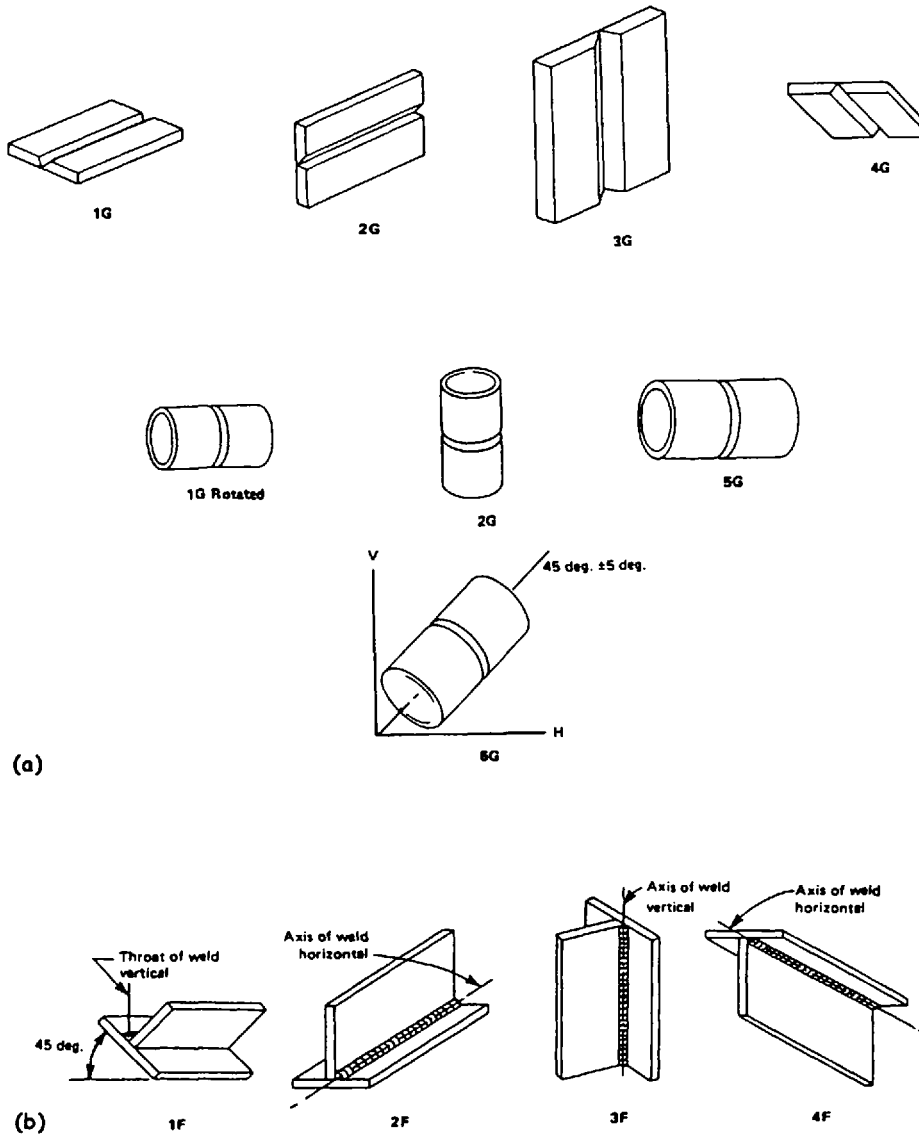


Figure 4 Welding positions for qualification. (a) Groove welds in pipe, and (b) fillet welds in plate. (Reproduced from Ref. 9.)

codes or standards have specified [24]. Discontinuities may be found in weld metal, heat-affected zones, and base metal.

9.2 Causes of Discontinuities

Defects are caused due to inferior design, poor workmanship, wrong welding procedure, poor weldability of the materials, etc.

9.3 General Types of Defects and Their Significance

Defects in weldments in general can be classified as follows:

1. *Welding process defect*: lack of fusion, incomplete penetration, porosity, slag, etc.
2. *Foreign inclusions*: slag, copper, oxide films, tungsten, etc.
3. *Geometric defects*: overlap, undercut, excessive reinforcement, burn through or excessive penetration, distortion, improper weld profile, etc.
4. *Metallurgical defects*: cracks, gas porosity, embrittlement, structural notches, hydrogen induced cold cracking, liquation cracking, solidification cracking, ductility-dip cracking, stress relief cracking, lamellar tearing, low-delta ferrite, etc.

Planar defects, that is, two-dimensional defects, like cracks, lack of fusion, lack of penetration, severe undercut, etc., are critical in nature, involve lack of bonding, and are not tolerated. Three-dimensional defects, like slag inclusion, cavities, and pores, are tolerated to a certain extent, depending on the length of the inclusion and product class. Notches are not allowed for low-temperature and cryogenic applications. Sharp notches, which act as stress raisers, are smoothed out wherever accessible to avoid stress concentration. Some weld defects are schematically shown in Fig. 5. Faults in fusion welds, causes, and detection are given below.

Faults in fusion welds in constructional steels

1. Cracks. Solidification cracking, hydrogen induced HAZ cracking, lamellar tearing, and reheat cracking; longitudinal, transverse, threat, crater, toe, and roof cracks.

2. Porosities. Porosities include uniformly scattered porosity, cluster porosity, linear porosity, elongated porosity, or piping porosity, and worm hole porosity.

1. **Worm holes** result from the entrapment of gas between solidifying dendrites of weld metal.
   Causes. Gas may arise from contamination of surface to be welded or prevented from beneath weld by joints.
2. **Uniformly distributed porosity** results from the entrapment of gas in solidified weld metal. Other forms of porosity are restart porosity and surface porosity.
3. **Surface porosity** is caused by excessive contamination from grease, dampness, or atmosphere entrainment. It is occasionally caused by excessive sulphur in consumables or parent metal.
4. **Crater pipes** result from shrinkage at the end of weld run where the source of heat is removed. They are caused by incorrect manipulative technique or current decay to allow for crater shrinkage.

3. Solid inclusions. Solid inclusions include, linear slag inclusions, and isolated slag inclusions; tungston inclusions or infused filler metal.

4. Lack of fusion and penetration. This type of defect tends to the subsurface and is therefore detectable only by ultrasonic or X-ray methods. Lack of side wall diffusion, which penetrate the surfaces, could be detected using magnetic particle or dye/fluorescent penetrant inspection.

5. Imperfect shape. Detection: All shape defects are detectable by visual examination. Some of the forms of imperfect shape are

1. **Linear misalignment** is caused by the incorrect assembly and/or distortion during fabrication.
2. **Excessive penetration** is caused by the incorrect edge preparation providing insufficient support at the weld root incorrect weld conditions. The provisions of backing strip can alleviate this problem in defective circumstances.

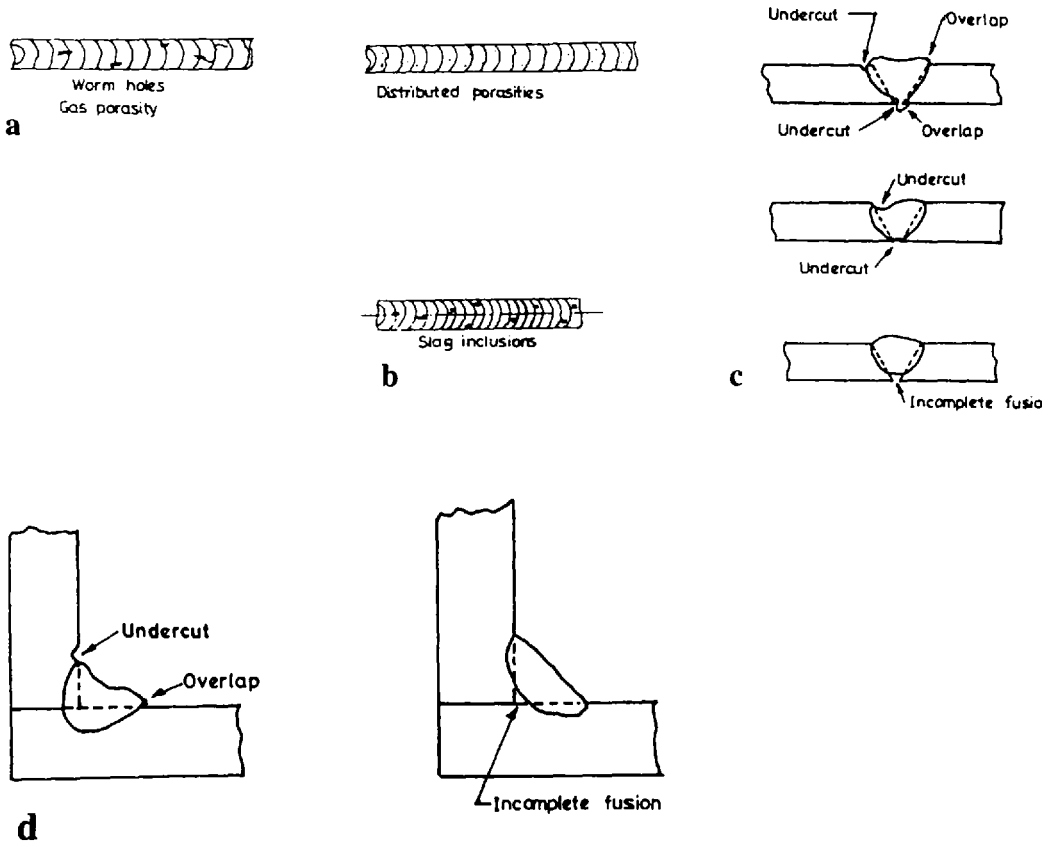


Figure 5 Weld defects. (From Ref. 28.)

6. Arc strike. Accidental contact of electrode or weld torch with plate surface remote from weld. These usually result in simulated hard spots just beneath the surface, which tend to corrode and thus should be avoided.
7. Miscellaneous faults.

1. **Spatter** is caused by the incorrect weld conditions or contaminated consumable or preparations to explosive conditions. Globules of molten metal are thrown out from the weld pool and adhere to the parent metal.
2. **Copper pickup** is the melting of copper duct tube in the MIG weld due to incorrect conditions. In general, detection is only possible by X-ray or ultrasonic techniques.

9.4 Approach to Weld Defect Acceptance Levels

Two quality levels are proposed for weld defect acceptance [25]:

1. One, the fitness-for-purpose level, is such that larger defects might cause failure of the structure and they must, therefore, be repaired. Suitable fitness-for-purpose analyzes the true significance of the defects in place of the old acceptance levels. Fracture mechanics assessment can be used to demonstrate that many defects are not significant in terms of service conditions and that continued safe operation can be assured [26].

2. The second is a quality control level. Repairs are not attended out where welds fall below this, but the cause of the loss of quality is examined so that it may be maintained well above the fitness for purpose level.

Part 4: Nondestructive Testing Methods

Nondestructive testing (NDT), also referred as nondestructive evaluation (NDE), is an integral and the most important constituent of the quality assurance (QA) program of any industry. Nondestructive testing measures and evaluates the effectiveness of procedure, materials, before, during, and after fabrication, and the overall integrity of assemblies and subassemblies. Material identification and composition, quality characteristics of castings, forgings, and welding defects such as cracks, inclusions, porosities, lack of penetration, lack of fusion, lack of bond, undercut, etc. can be evaluated by NDT methods. Without effective means of NDT, it would probably be impossible to build many of the major high-integrity structures [26].

The most commonly used nondestructive testing methods are visual examination (VT), dye penetrant testing (PT), magnetic particle testing (MT), radiography testing (RT), ultrasonic testing (UT), acoustic emission testing (AET), eddy current testing (ET), and leak tests (LT). Besides these, there are other NDT methods, such as radioscopy, thermal imaging, computer tomography, and holography, that are employed for special applications.

1 SELECTION OF NDT METHODS

There are five main parameters to be considered when selecting an inspection method: (1) capabilities and limitations of the inspection method, (2) acceptance standards, (3) cost, (4) personnel, and (5) equipment.

1.1 Capabilities and Limitations of Nondestructive Testing Methods

In fabrication of heat exchangers and pressure vessels, NDT is commonly used for detection of flaws in welds, forgings, castings, plates, tubes, etc. Each NDT method has its own flaw detection characteristics, and therefore no individual NDT method can replace another one. No single test or series of tests will give 100% assurance of quality. To use NDT technique effectively, one must be aware of the limitations of the different methods. NDT selection, applications, advantages, and limitations are tabulated in Refs. 6 and 27–30, among others and a typical example is given in Table 5.

1.2 Acceptance Criteria

For each NDT technique, acceptance criteria are an integral part of most codes and standards. Acceptance criteria define different types of discontinuities and whether particular types of discontinuities are acceptable. Discontinuities are rejected if they exceed specification requirements. Acceptance or rejection of flaws is based on different factors, and a vital few are: (1) accessibility for repair and cost of repair, (2) safety, with hazards and consequences of failure, (3) desired life, (4) type of materials used, (5) material thickness, (6) design stress, and (7) nature of service environment (corrosive or noncorrosive).

Table 5 Common Nondestructive Evaluation Methods

Method	Principle	Applications	Advantages	Limitations
Liquid Penetrant	Liquid penetrant is drawn into surface defects by capillary action. Visible or fluorescent dye reveals flaws.	Surface cracks, laps, porosity, shrinkage areas, laminations, etc that are open to surface.	Inexpensive, portable. Very sensitive. Independent of magnetic and electrical properties of material.	Defects must be open to surface. Porous and rough surfaces excluded. Penetrant must wet surface.
Magnetic Particle	Discontinuities distort applied magnetic field, causing leakage fields that attract iron powder on surface.	Cracks, inclusions, and other discontinuities on or near surface of ferromagnetic materials.	Low cost. Suitable for large, immovable objects.	Sensitivity strongly affected by depth of flaw and presence of coatings. Tests in several directions often required. Experience required to interpret results.
Ultrasonic	Flaws reflect sound waves traveling through material; elapsed time before echo is received determines location of flaw.	Cracks, laminations, bonding faults, etc with principal plane perpendicular to sound source.	Detects flaws deep in part. Inspect from one side. No radiation hazard. Immediate results. Computerized equipment can produce images of flaws (C-scan)	Trained inspectors required. Flaws parallel to sound source are undetectable. Reference standards required.
Radiographic	Metals absorb X-rays and gamma rays. Flaws and thin sections absorb less, so that more radiation strikes film. Flaws appear as dark shadows.	Castings and welds with thick flaws and cracks with principal plane parallel to radiation beam.	Permanent record including evidence of proper test procedures. Detects flaws at any depth.	Requires technicians trained in test methods and radiation hazards. Surrounding areas must be shielded from radiation. Thickness limited by strength of radiation source. High equipment and operating costs. Cracks perpendicular to radiation beam may be undetectable.
Neutron Radiography	Similar to X-ray radiography. Attenuation is greatest in lighter elements and specific isotopes that absorb neutrons.	Inspection of metal-jacketed explosives. Adhesive-bonded metals. Boron-fiber-reinforced metal-matrix composites. Radioactive material inspection.	Detects lightweight substances within metals. Can be made insensitive to other radioactivity.	Requires nuclear reactor or neutron accelerator on site. Trained physicists required.
Eddy Current	Coil induces currents in metal. Same coil detects currents, which are sensitive to electrical properties of part.	Conductive materials with constant cross section; especially pipe inspection. Detects variations in metal type and microstructure as well as flaws.	Very sensitive. No contact with part. Fast enough for continuous on-line inspection. Metal need not be ferromagnetic.	Often too sensitive to unimportant parameters or minor dimensional fluctuations.
Optical Holography	Multiple-exposure holograms of parts in various stages of loading show interference lines where stress is concentrated.	Debonding in honeycomb, composites, and other bonded structures. Hollow turbine blades. Stress corrosion cracking in metals.	Materials need not possess special properties (conductivity, ferromagnetism, etc.) Permanent record of entire surface. Modern techniques have eliminated need for careful positioning.	Less sensitive than ultrasonics. Apparatus must be isolated from vibration.
Acoustical Holography	Ripples in liquid surface caused by interference between two ultrasonic beams create image of flaws in part placed in path of one beam.	Continuous inspection of steel sheet. Porosity and lack of bonding in welds.	No contact. Immediate results. Detects flaws at any depth. Image can be recorded with camera.	Limited resolution. Inspection area no larger than transducer. Parts must be immersed.
Acoustic Emission	Materials emit acoustic energy during crack growth and plastic deformation. Sensor detects noises during loading.	Pressure vessels. Aircraft structures. Welds. Stress corrosion cracking.	Tests parts during structural loading. Pressurized-vessel flaws are detected before failure. All loaded areas are tested, regardless of sensor location.	Plastic deformation during test is irreversible; test is therefore unrepeatable. Test cannot pinpoint source of emission.

Reproduced from Ref. 30.

1.3 Cost

Different NDT methods have different costs in any particular situation. Two basic cost factors that should be considered in the selection of a NDT method are the initial equipment cost and the cost of performing the inspection [28]. The cost of performing NDT tests includes the labor cost, training cost, and cost of consumables such as radiographic film, dyes, magnetic particles, etc. Visual examination (VT) is almost always the least expensive, however, this may not be true sometimes while using the latest optical devices such as borescopes, videoprobes, etc., used to aid the VT. In general, the costs of radiographic, ultrasonic, and eddy current inspections are greater than those of visual, magnetic particle, and liquid penetrant techniques.

1.4 Personnel

Nondestructive testing tends to be rather dependent for its effectiveness on the capabilities of the persons performing it. The first requirement for good NDT is properly trained and experienced personnel. NDT personnel must be able to evaluate and record test results with accuracy and consistency. Poorly run tests or incorrect interpretation of the results leads to rejection of

good parts and acceptance of defective parts [31]. Other requirements for personnel involved in NDT examinations include the following: good eyesight, well developed powers of observation and concentration, high personal integrity, good judgment, and familiarity with codes and standards being practiced.

NDT Personnel Qualifications

In order to promote uniformity in performing and interpreting NDT tests, the American Society for Nondestructive Testing has drawn up some minimum qualification requirements for personnel, who are graded as Level I, Level II, and Level III. An NDT Level I person must have experience or training in the performance of the required inspections and tests, and he or she shall receive the necessary instruction or supervision from a certified NDT Level II or III person. Level II shall be able to prepare written instructions, and to organize and report the results on NDT tests. A Level III person should be capable of planning and supervising inspections and tests, reviewing and approving procedures, and organizing and reporting results and certifying their validity. This person is also authorized for training, qualifying, and certifying NDT personnel.

Personnel involved in the performance, evaluation, or supervision of NDT examinations, including RT, UT, PT, MT, and ET methods, must meet the Level III qualification requirements, and for gas leak test methods must meet Level II qualification requirements as specified in SNT-TC-1A of American Society for Nondestructive Testing.

Training of NDT Personnel

The manufacturer may conduct a training program to meet the requirements of SNT-TC-1A through a designated employee who meets Level III requirements. Qualification and training of NDT personnel are discussed in detail in Ref. 9.

2 INSPECTION EQUIPMENT

Only high-performance flaw-detecting equipment should be used. NDT equipment is to be handled properly in order to assure continued accuracy of examination. The measuring instruments, tools, and gauges are to be calibrated periodically with reference standards.

3 REFERENCE CODES AND STANDARDS

ASME Code, Section V [9d] is the most widely used Code for NDT throughout the world. The basic coverage of ASME Code Section V on nondestructive examination is given here.

3.1 ASME Code Section V—Nondestructive Examination

This section contains requirements and methods for nondestructive examination, which are referenced and required by other code sections. Also included are manufacturer's examination responsibilities, duties of authorized inspectors, and requirements for qualification of personnel, inspection, and examination. Methods of making the nondestructive examinations are given for:

1. Radiographic examination (RT)
2. Ultrasonic examination (UT)
3. Liquid penetrant examination (PT)
4. Magnetic particle examination (MP)
5. Eddy current examination (ET) for tubular products

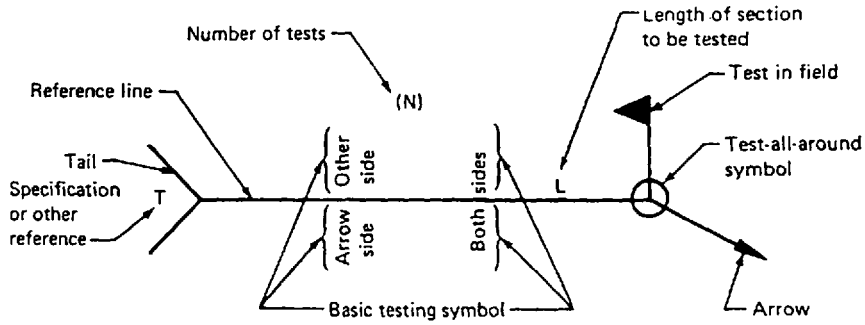


Figure 6 AWS symbols for NDT examination and standard location of elements.

6. Visual examination (VT)
7. Leak testing (LT)

4 NDT SYMBOLS

Figure 6 depicts the AWS symbols for NDT examination.

5 WRITTEN PROCEDURES

NDT should be carried out in accordance with written procedures to achieve consistency and accuracy. Without a written procedure, there is no guarantee as to the effectiveness or repeatability of the test. Detailed NDT procedures/instructions are essential for several reasons [2]: (1) they demonstrate that a fabricator fully understands code and standard, and contractual requirements, (2) they provide comprehensive instructions at the place of test and mitigate against difficulties arising from different operator/inspection authority interpretation, and (3) facilitate surveillance and constitute a record of how testing was carried out. The procedure should state the qualifications of personnel operating the equipment and interpreting the results. In general, the procedure must be approved by the buyer or third-party inspection agency. When written procedures are not available, inspectors are asked to work as per codes and specifications.

5.1 Content of NDT Procedures

NDT should be carried out in accordance with written procedures irrespective of whether or not it is a code requirement [2]. A procedure usually specifies items given in Table 6 [32].

Table 6 Content of NDT Procedures [32]

1. Scope	6. Test method
2. Applicable documents	7. Evaluation and reporting levels
3. Personnel	8. Acceptance criteria
4. Equipment—calibration and reference standards	9. Status marking
5. Surface condition	10. Report

5.2 General Details of Requirements in the NDT Procedure Document

NDT procedures should not be allowed to become lengthy "training manuals" for inexperienced personnel or "educational texts" for the benefit of the customer [2]. However, they must contain sufficient detail to ensure effective examination of the material or component under consideration. The general details of requirements of NDT procedure are listed and discussed by Hamlett et al. [32] and they are summarized here:

1. The procedure should be on company-headed paper so as to clearly demonstrate its origin.
2. The procedure should specify applicable code and standard.
3. The procedure should be approved and signed by a competent authority.
4. The procedure should have a formal specific title.
5. Each page of the procedure should be numbered and should carry the unique procedure code number.
6. Each section should be numbered and each paragraph should be given a subsection number.
7. The first page of the procedure should be an amendment sheet explaining the latest additions or amendments since the original procedure was issued.

5.3 Deficiencies in NDT Procedures

The most common deficiencies in NDT procedures fall into three main categories [2]:

1. They lack detail and simply state "refer to" BS Specifications, ASME Code, and so on in relation to calibration standards, acceptance standards, etc. They fail to identify which of the options contained in the specifications or codes apply to the component under inspection.
2. The method is identified correctly but the techniques and test parameters specified are not specifically tailored to the actual part to be examined.
3. They omit technical requirements specific to the particular procedure.

Typical NDT procedure deficiencies in RT, UT, MT and PT are discussed in Ref. 2, and they are listed in the discussion of these NDT techniques.

6 VISUAL EXAMINATION (VT)

Visual examination is the primary evaluative method of inspection and it is the oldest method of NDT. Visual methods are of necessity restricted to surface examination, but they may sometimes be useful for a detailed examination of an imperfection after other methods have determined its position [33]. In addition to locating surface defects, and raw material identification, visual examination can be an excellent process control technique during various stages of fabrication and can identify subsequent problems revealed during PWHT and hydrostatic testing/leak testing.

6.1 Principle of VT

The basic principle used in visual NDT is to illuminate the specimen with light, usually in the visible region. The specimen is then examined with the eye under adequate illumination, either naturally or by light-sensitive devices such as photocells and phototubes. The visual examination is classified as direct vision technique and remote visual examination.

Direct Vision Examination

Direct vision technique is applicable when access is sufficient to place the eye within 24 in (609.6 mm) of the surface to be examined and at an angle not less than 30° to the surface to be examined. Mirrors as well as aids such as magnifying lens may be used to assist examination.

Remote Visual Examination

Remote visual examination is conducted with aids such as mirrors, telescopes, borescopes, fiber optics, cameras, and other suitable equipment. These optical aids supplement direct vision.

6.2 Merits of Visual Examination

Visual examination is easily applied, quick, and often requires no special equipment other than good eyesight and some relatively simple and inexpensive equipment.

6.3 VT Written Procedure

Written procedure for VT is detailed in ASME Code Section V. The written procedure should contain at a minimum the following:

1. How visual examination is to be performed.
2. Surface condition and criteria for surface cleaning.
3. Surface cleaning procedures.
4. Method or tool for surface preparation, if any.
5. Whether direct or remote viewing is used.
6. Special illumination or optical devices to be used, if any.
7. Sequence of performing examination when applicable.
8. Data to be tabulated, if any.
9. Reports or general statements to be completed.

6.4 Reference Document

Codes and standards or the purchaser's specification is needed. An important document for visual inspectors is the *AWS Guidebook on Visual Examination* [23].

6.5 Visual Examination: Prerequisites

As with any other nondestructive inspection method, there are various prerequisites that should be considered to perform visual examination. Some of the more common attributes to consider are [23]:

1. The visual examiner should have sufficient visual acuity to perform an adequate inspection.
2. Visual inspectors should have sufficient knowledge on welding procedures and safety practices. There are many potential safety hazards present.

Additionally, the inspector should have adequate illumination, either natural or artificial.

6.6 Visual Examination Equipment

Certain tools are some times necessary for some aspects of visual weld inspection. These tools are specified in Refs. 23 and 34. Some of the tools and gages most frequently used in visual welding inspection are:

1. Ammeters to measure current during welding or inspection by MT.
2. Temperature-sensitive crayons for surface markings.
3. Surface contact thermometers and pyrometers.
4. Weld gages, measuring scales, fillet gages and devices.
5. Multipurpose gages capable of performing many measurements such as measuring convex and concave fillet welds, weld reinforcement, and root opening.
6. Taper gage to measure root opening (gap).
7. Hi-lo gage, also known as a mismatch gage, to measure the internal alignment of a pipe joint.
8. Fiber-optic devices such as borescopes, fibrescopes, etc., and video probes.
9. Ferrite gages.

6.7 NDT of Raw Materials

Visual examination of the base materials, such as plates, tubes, pipes, forging, and castings, prior to fabrication can detect scabs, seams, loose rusts, scale, or other harmful surface conditions that tend to cause weld defects. Plate laminations may be observed on cut edges. Dimensions should be confirmed by measurements. Base metal should be identified by type, grade, and heat number. Even though plates and forged pressure parts are ultrasonically tested by material suppliers, these products for critical applications warrant ultrasonic inspection in the manufacturer's premises.

6.8 Visual Examination During Various Stages of Fabrication by Welding

The effectiveness of visual inspections is improved when a quality control system is instituted that provides for coverage at all phases of the welding process—before, during, and after welding. Visual inspection used before, during, and after welding finds 90% of defects that would be detected later using more costly methods such as ultrasonic testing or radiography [35]. The items to be checked by visual inspection prior to welding, during welding, and after welding are detailed in Refs. 23 and 28. Some of the important points are given next.

Visual Examination Before Welding

1. Review drawing and specifications.
2. Check machine settings.
3. Qualification of welding procedures and personnel.
4. Joint preparations, dimensions, cleanliness, and surface preparation.
5. Review welding process and consumables to be used.
6. Establish check points.
7. Check fit and alignment of weld joints: groove angle, root openings, joint alignment, etc.

Visual Examination During Welding

1. Treatment of tack welds.
2. Quality of the root pass and the succeeding weld layers.
3. Joint root preparation prior to welding the second side.
4. Preheat and interpass temperatures.
5. Sequences of weld passes.
6. Interpass cleaning.
7. Checking the welding procedure parameters, i.e., voltage, amperage, speed.

8. Parameters pertaining to shielding gases.
9. Distortion.

Visual Examination after Welding

This covers final weld inspection like (1) weld size, appearance, color, contour, and surface roughness, (2) extent of welding, (3) dimensions, (4) distortion, and (5) visible external weld defects such as cracks, undercut, overlap, exposed porosity and slag inclusions, unacceptable weld profile, arc strike, weld spatter, reinforcement, concavity, and burnthrough.

6.9 Developments in Visual Examination Optical Instruments

Many optical aids are currently available that supplement direct vision. Skill and experience are necessary to handle such optical aids. Recent developments in the optical field include the use of television and also of fiber optics to inspect remote and inaccessible areas. Special TV cameras are available that can be inserted into openings as small as 1.5 in (38.1 mm) diameter [36], and a closed-circuit transmission system can then be arranged to give an image of the internal surface of butt welds in pipelines and bores (33). The three basic remote visual examination aids are borescopes, fibrescopes, and video borescopes. The following information on visual inspection optical aids is based on Ref. [37].

Borescopes

As the name implies, a borescope is an optical instrument designed to enable an observer to inspect the inaccessible areas such as inside of a narrow tube, bore, or a chamber. One can insert them into very small openings, extending the vision to welds far inside the darkest recess in process piping, heat exchangers, pressure vessels, and other equipment. Illuminating the weld, and magnifying it 3× or 4×, borescopes are easy to use, relatively inexpensive, and extremely effective [38].

Basics of Borescopes. The optical train for a borescope is shown in Fig. 7. These instruments use thin glass fibers to transmit light to illuminate the test area and to permit viewing or recording. The brightest images are obtained with borescopes of large diameters and short length. As the length of the borescope is increased, the image becomes less brilliant because of light losses. Likewise, the closer the viewing lens is to the weld, the larger the image.

Flexible Fiberscopes. Flexible fiberscopes, in contrast to the stiff borescope, can be inserted into curved pipes and cavities. The light in the fiberscopes is transmitted via a bunch of ultrathin optical fibers with a diameter as small as 7 μm (0.007 mm).

Stiff Borescopes. The stiff borescope can be compared to a periscope, where the objective is placed quite near the object under examination, while the ocular is placed at the desired distance from the objective. The objective and the ocular are connected by means of one or more removable extension tubes. The borescope's length can thus be varied as required. Where straight-line access is available, rigid borescope offer many advantages over fiberscopes, most notably in resolution, image brightness, design flexibility, and price.

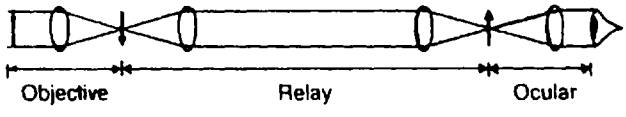


Figure 7 Optical system of a borescope [37].

Videoimagescopes

Videoimagescopes employ video technology for remote visual inspection. At the tip of the flexible videoimagescope probe is a miniature charge-coupled device (CCD) sensor (like a tiny video camera), which sends high-resolution images in full, natural color to be displayed on a TV monitor. Diameters of probes are as small as 8 mm; lengths range from 1.5 m to 22 m.

Video Microscopes

Handheld or fixtured video microscopes sees where traditional microscopes cannot. They feature high-resolution CCD image sensors, fiber-optic self-illumination, special objective lenses or HI-Mag borescopic lenses, shutter speeds to 1/10,000 s, freeze frame, and memory, with multiwindow display of 4, 9, 16, or 25 images simultaneously. They can overlay images for comparison or even measurement. Nominal magnifications are from 20× to 1000×.

Combining Computers and Visual Inspection

Combining visual inspection with computer analysis eases job tracking and planning by storing information and radiographs in databases. Computers that collect and analyze data, update standards, and expand certification programs enable the visual inspector to concentrate on data collection, leaving tedious calculations to the computer [35].

7 LIQUID PENETRANT INSPECTION

7.1 Principle

Liquid penetrant inspection (PT) is a means to find discontinuities that are open to the surfaces by bleedout of liquid penetrant medium that is applied over the test surface. The penetrant enters the discontinuities under the influence of capillary action. If the discontinuity is significant, penetrant will be held in the cavity when the excess is removed from the surface. Upon application of a developer, blotter action draws the penetrant from the discontinuity to provide a contrasting indication on the surface, indicating the presence and location of discontinuities. The indications are examined either in natural daylight or adequate artificial illumination or ultraviolet light, depending on colored or fluorescent penetrant particles used. Various stages of the penetrant examination process are depicted in Fig. 8.

7.2 Applications

Liquid penetrant inspection can be effectively used to detect surface discontinuities such as cracks, porosity, seams, laps, cold shuts, laminations, or lack of bond on nonporous metallic materials, both ferrous and nonferrous, and on nonporous nonmetallic materials such as plastics and glass. The method is particularly useful on nonmagnetic materials, since magnetic particle inspection cannot be applied to test them.

7.3 Merits of PT

Its simplicity and low cost make it a popular test. If properly used, it readily detects minute surface openings. The basic steps involved in the application of the test method are relatively simple. Except for visual examination, it is perhaps the most commonly used nondestructive test for surface examination. Penetrant inspection is reasonably fast. The method is easy to learn and can be applied properly.

7.4 Limitations

The success of penetrant inspection, like most other inspection methods, depends on the visual acuity of the inspector [28]. The parts must be thoroughly cleaned to allow the penetrant to

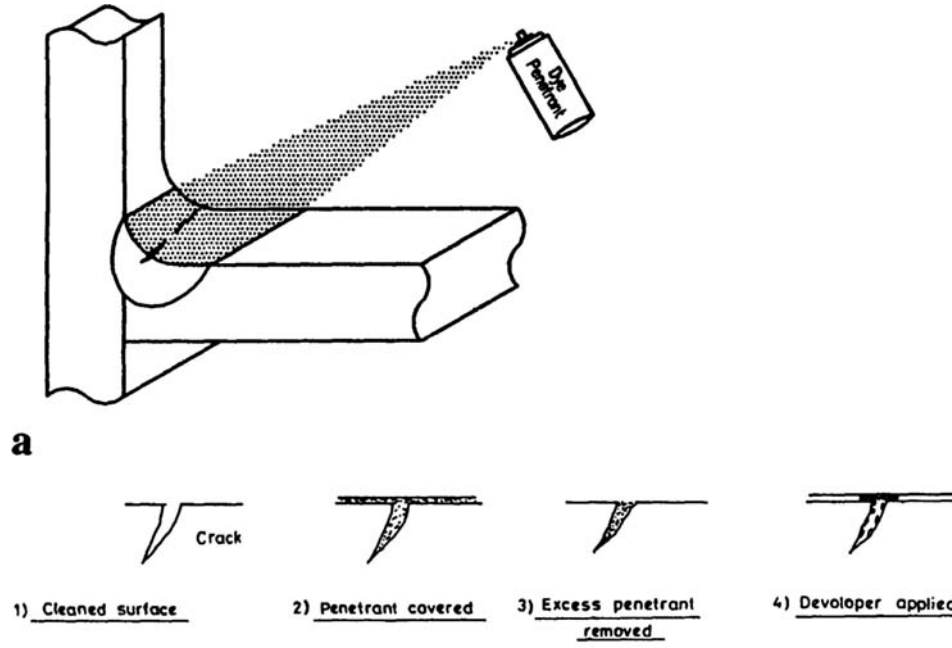


Figure 8 Penetrant examination. (a) Schematic; and (b) stages of penetrant examination. (From Refs. 29, 39.)

enter flaw openings, and flaws must be open to the surface [39]. Experience has shown that very slight variations in performing the penetrant process and subsequent inspection can invalidate the findings by failing to indicate all flaws. Therefore, it has become accepted practice that all penetrant inspections be carried out exclusively by trained and certified personnel. It is not suitable for inspecting porous materials.

7.5 Written Procedure

A written procedure for PT examination is given in Table 7.

Liquid Penetrant Examination Procedure Deficiencies

Incorrect penetrant material selection, excessive penetrant removal, and incorrect developer application [2].

7.6 Standards

ASTM E 165—Recommended practice for PT.
ASTM E 270—Definition of terms relating to PT.

Table 7 PT Written Procedure

1.0 Scope: materials, shapes and sizes to be examined	7.1 Penetrant application, dwell time, and the testing of the surface and penetrant during the examination if outside is 60°F to 125°F
2.0 Reference document	7.2 Excess penetrant removal
3.0 Extent of examination	7.3 Developer application
4.0 Approved method and material: type of penetrant, penetrant removal, emulsifier, and developer	7.4 Examination
5.0 Surface preparation	8.0 Acceptance criteria
6.0 Test environment and lighting condition	9.0 Personnel certification
7.0 Procedure	10.0 List of approved penetrant materials

ASTM E433—Reference photographs for PT.
ASME Sec. V, Articles 6 and 24 ASME Sec. VIII, 1 Div., Appendix 8.

7.7 Test Procedure

Six basic steps make up the liquid penetrant inspection procedure. They are [41]:

1. Precleaning the part to be inspected with a solvent and drying.
2. Application of the penetrant to the part to form a film over the surface and allowing sufficient time for it to enter into the opening.
3. Removal of excess penetrant with water wash, solvent, or emulsifier and drying.
4. Application of a thin coating of developer over the surface under observation.
5. Visual examination under adequate light and interpretation of indications.
6. Postinspection cleaning.

7.8 Penetrants

The penetrants are mixtures of organic solvents, which are characterized by their ability to wet materials, spread rapidly, and penetrate into minute defects and dissolve dyes, so that the indications produce a definite red color as contrasted to the white background of the developer.

Types of Penetrants

Depending upon the type of dye used, penetrants are divided into *visible penetrants*, which are usually red in color to provide a contrast against the white background from the developer under white light, and *fluorescent penetrants*, which provide a greenish yellow indication against a dark background when viewed under a black light (ultraviolet). The fluorescent penetrants are most generally for the detection of fine cracks, but these are not recommended for use on rough surfaces because of the difficulty in removing the excess penetrant.

According to the manner in which the excess penetrants are removed from the surface, i.e., the rinse process, they are classified into three classes: (1) water washable, (2) solvent removable, and (3) postemulsifiable, which are not in themselves water washable, but are made so by applying an emulsifier after the penetration is completed.

7.9 Method

There are two varieties of penetrant method, both using a similar principle: the visible dye method and the fluorescent dye method.

7.10 Selection of Developer

The developer is applied to get the penetrant in the discontinuities back to the surface so that it can form an indication of the discontinuity. The penetrant is drawn out by the capillary action but in the reverse direction. It also serves as a color contrast background for dye material.

7.11 Penetrant Application

The penetrant should be applied by brushing or spraying. The surface temperature of the part should be between 60°F and 125°F (16°C and 52°C).

Penetration Time or Dwell Time

The period of time during which the penetrant is permitted to remain on the specimen is a vital part of the test. The minimum time required for the penetrant to enter into the discontinuity is called the *dwell time*. The recommended dwell times are:

For carbon steel	10 to 20 min
For alloy and stainless steel	15 to 20 min

During the dwell time, the penetrant shall not be allowed to dry up, and fresh penetrant shall be applied as often as required.

Approved Material

Penetrant must be odorless, nontoxic, nonflammable, and stable in storage. The developer should be wet and nonaqueous. The penetrant and developer must be compatible with each other and should be procured from the same manufacturer. For the examination of nickel-based alloys, sulfur content in the penetrant shall not exceed 1% of the residue by weight, whereas for the examination of the austenitic stainless steels or titanium, the chlorides shall not exceed 1% of the residue by weight.

7.12 Surface Preparation

The surface to be inspected shall be clean and free from oil, grease, sand, rust or scale, welding flux and spatter, etc. The presence of surface contaminants prevents spreading of the penetrant and affects penetrability mechanical operations such as shot peening, machining, buffing and sand blasting are strictly prohibited prior to the examination to avoid closing of discontinuities. Weld surface shall be ground free of ripples that might mask the indications of unacceptable discontinuities. Sufficient air circulation is necessary during testing.

7.13 Excess Penetrant Removal

Excess solvent-removable penetrants shall be removed by wiping with a cloth or absorbent paper, repeating the operation until most traces of penetrant have been removed. The remaining traces shall be removed by lightly wiping the surface with cloth or absorbent paper moistened with solvent. To minimize removal of penetrant from discontinuities, care shall be taken to avoid the use of excess solvent.

7.14 Standardization of Light Levels for Penetrant and Magnetic Inspection

Proper illumination of indications from penetrant testing and magnetic particle inspection is essential if an acceptable level of probability of detection is to be achieved with either test method. In order to control the illumination for inspection of workpieces, four separate types of measurement must be specified precisely [42]. These are

1. White light illumination for color contrast processes.
2. Ultraviolet illumination for fluorescent processes.
3. Ambient visible light in darkened inspection rooms.
4. Visible light from ultraviolet sources.

The fluorescent light is more sensitive, due to the fact that the human eye can more easily discern a fluorescent indication.

7.15 Evaluation of Indications

Prior to the evaluation of test results, it is necessary to interpret the indications. Identifying indications requires much practice. Indications can be classified as: (1) false indications, (2) nonrelevant indications, and (3) true or relevant indications. False indications are due to improper cleaning, rough surfaces, contaminations due to penetrants on the hands of operator, etc. Nonrelevant indications are caused by surface irregularities. All nonrelevant indications shall be regarded as a defect until the indication either is eliminated by surface conditioning or is evaluated by other NDT methods and proved to be nonrelevant. True indications are those caused by discontinuities in the specimen. Only those indications are to be studied while evaluating the results of the examination.

7.16 Acceptance Standards

For welds and materials as per ASME Section VIII Div. 1, Appendix 8, all surfaces to be examined shall be free of (1) relevant linear indications, (2) relevant rounded indications greater than $\frac{3}{16}$ in (4.8 mm), and (3) four or more relevant rounded indications in a line separated by $\frac{1}{16}$ in (1.6 mm) or less edge to edge.

7.17 Postcleaning

Penetrants are difficult to remove completely from discontinuities, and if they are corrosive to the material, or otherwise not compatible with the product application, they should be avoided.

7.18 Recent Developments in PT

PT accessories are available from Magnaflux, a Division of ITW, Inc., USA. They include Ni–Cr test panels (Japanese) and TAM panels. Ni–Cr test panels are used for evaluating penetrant system performance and sensitivity; they are available in four types of flaw depths, 10, 20, 30, or 50 μm. A TAM panel is a fast and reliable means of monitoring the proper functioning of a liquid penetrant system. A stainless-steel panel with five star-shaped flaws of decreasing size is on one half, with a rough sand-blasted surface on other half, for checking sensitivity and removability of penetrants.

8 MAGNETIC PARTICLE INSPECTION (MT)

Magnetic particle inspection is a nondestructive testing technique to locate surface and subsurface discontinuities such as cracks, inclusions, pores, shrinkages, laps, folds, seams, etc., arising out of manufacturing operations and service constraints in ferromagnetic materials. Ferromagnetic materials include most of the iron, nickel, and cobalt alloys. Nonmagnetic metals such as aluminum alloys, copper and copper alloys, titanium and its alloys, and austenitic stainless steels and cladding of these metals cannot be inspected by this method.

8.1 Principle

Magnetic particle inspection is based on the principle that if a ferromagnetic object is magnetized, the surface or subsurface discontinuities lying at an angle to the magnetic lines of force cause an abrupt change in the path of magnetic flux flowing through the object. This results in local flux leakage at the surface over the discontinuity (Fig. 9). When finely divided ferromagnetic particles are applied over the surface, some of the particles will be attracted to the regions of leakage field and will pile up and bridge the discontinuity. The piling up of magnetic particles along the discontinuity indicates its location, shape, and extent. While using this method, it should be seen that the magnetic field must be in a direction that will intercept the principal plane of the discontinuity.

8.2 Applications

Magnetic particle inspection is used for testing of weld preparations, weld cutbacks on double-sided welds, roots of welds made from one side only, stub, branch, and nozzle welds and attachment welds to shell, load-carrying nonpressure parts like supports and lifting lugs, and areas where temporary attachments have been removed. The latter areas are particularly vulnerable to cracking [43].

8.3 Reference Documents

ASTM Specifications

E 109—Dry powder magnetic particle inspection
E 138—Wet powder magnetic particle inspection
E 125—MT inspection of ferrous castings
E 269—Definitions of terms related to MT
E 275—MT inspection of steel forgings
E 340—Definition of terms, symbols, and conversion factors relating to MT

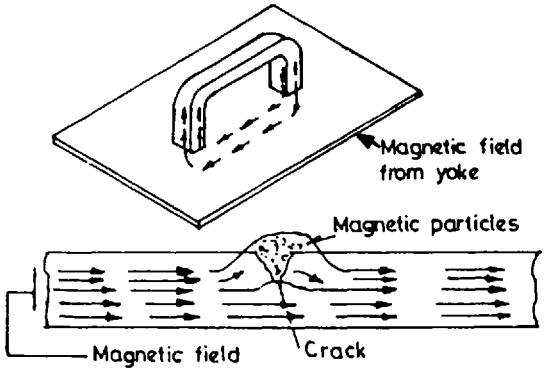


Figure 9 Magnetic particle testing principle—local flux leakage at the surface over discontinuity.

ASME Section V, Article 7, and ASME Section VIII, Div. 1, Appendix 6 and 7 (for steel castings) are also used.

8.4 Test Procedure

There are several basic steps in applying magnetic particle testing:

1. Surface preparation
2. Magnetization of the test object under evaluation
3. Application of magnetic particles
4. Interpretations of the patterns formed
5. If required, demagnetization of the items being tested.

8.5 Factors Affecting the Formation and Appearance of the Magnetic Particles Pattern

There are many factors that can affect the formation and appearance of the magnetic particles on the surface of the component being tested. The most common include [41,44]: (1) discontinuity size, shape, distance below the surface, and its orientation, (2) direction and strength of the magnetic field, (3) method of magnetization employed, (4) intensity of current used, (5) size, shape and mobility of the magnetic particle and the method of application, and (6) shape of the component.

8.6 Merits of Magnetic Particle Inspection

For detection of surface defects, liquid penetrant testing and magnetic particle examination are being very widely used. In the case of ferromagnetic materials, magnetic particle technique will also detect subsurface flaws that are not open to surface. Important advantages of the MT method are [41]: (1) it is rapid and simple to operate, (2) indications are produced directly on the surface of the component, and (3) a skilled operator can make a reasonable estimate of crack depth with suitable magnetic powders and proper technique.

8.7 Limitations of the Method

Magnetic particle testing has certain limitations, like (1) the method is not applicable for non-magnetic metal, (2) the sensitivity to detect subsurface flaw decreases exponentially with distance below the surface, (3) exceedingly heavy currents are required at times to examine very large units, and (4) current imparted by electrodes to induce magnetic fields can cause arc burns, which must be avoided because they can be a source of corrosion attack.

8.8 Written Procedure

The written procedure should contain as minimum requirement the items given in Table 8.

Magnetic Particle Examination Procedure Deficiencies

Deficiencies may include (1) incorrect method; e.g., coil method specified for specimens having L/D ratios less than 2, (2) incorrect magnetizing currents, (3) failure to perform examination at more than one current on complex sections, and (4) incorrect sequence of examination or failure to demagnetize when the second operation produces a lower flux density than the first [2].

Table 8 Written Procedure for MT

1.0 Scope: materials, shapes, and sizes to be examined	7.0 Magnetization current (type and amperage)
2.0 Reference document	7.1 Magnetizing field adequacy
3.0 Magnetizing technique	8.0 Application of examination medium
4.0 Examination equipment	9.0 Evaluation of indication
5.0 Surface preparation	10.0 Acceptance criteria
6.0 Examination medium: type of ferromagnetic particles to be used, manufacturer, color, wet or dry powder, etc.	11.0 Demagnetization
	12.0 Reports
	13.0 Records

8.9 Magnetizing Current

For the purpose of magnetizing parts for magnetic particle inspection, either alternating current (which has relatively little penetrating power and hence is good for surface flaw detection) or direct current (good for the detection of subsurface discontinuities) or half-wave rectified alternating current, which has the merits of DC and AC, is widely used. Since it is difficult to correlate the results obtained with AC with the result obtained using DC, it is important to specify in the specifications or drawings whether AC or DC is to be used. In the event that this is not specified, DC shall be used.

8.10 Equipment for Magnetic Particle Inspection

The magnetic particle test equipment essentially consists of (1) a means to magnetize the component, (2) a device for application of magnetic particles, and (3) demagnetization of components (if required) after inspection.

8.11 Magnetizing Technique

There are numerous methods of magnetization. Some of the methods include (1) coil magnetization (Fig. 10a), (2) prod magnetization (Fig. 10b), and (3) yoke magnetization (Fig. 10c).

Prod Magnetization

Prod magnetization produces a circular magnetic field. This will detect defects that are lengthwise in the test piece. Prods are portable current-carrying copper conductors, which are used to magnetize localized areas as shown in Fig. 10b. Magnetization is accomplished by pressing the prods against the surface area to be examined. When current flows through the prods, a circular magnetic field is created in the test part. The magnetic flux is perpendicular to the line joining the two prods, and the flux density is greatest along this line. During prod magnetization the prods are spaced 150 to 200 mm apart and in line with the suspected discontinuities. AC, DC, or half-wave DC (HWDC) can be used to suit the job requirement. Mostly HWDC magnetization is used for prod magnetization. Normally 100 to 120 A current per inch of prod spacing would be required. Care must be taken to avoid burning of the part under the contact points. To avoid arcing, a remote control switch is built into the prod handles to permit the current to be turned on after the prods have been properly positioned.

Direction of Magnetization

At least two separate examinations shall be performed on each area. During the second examination, the lines of magnetic flux shall be approximately perpendicular to those used during the first examination. Examination shall be done by the continuous method.

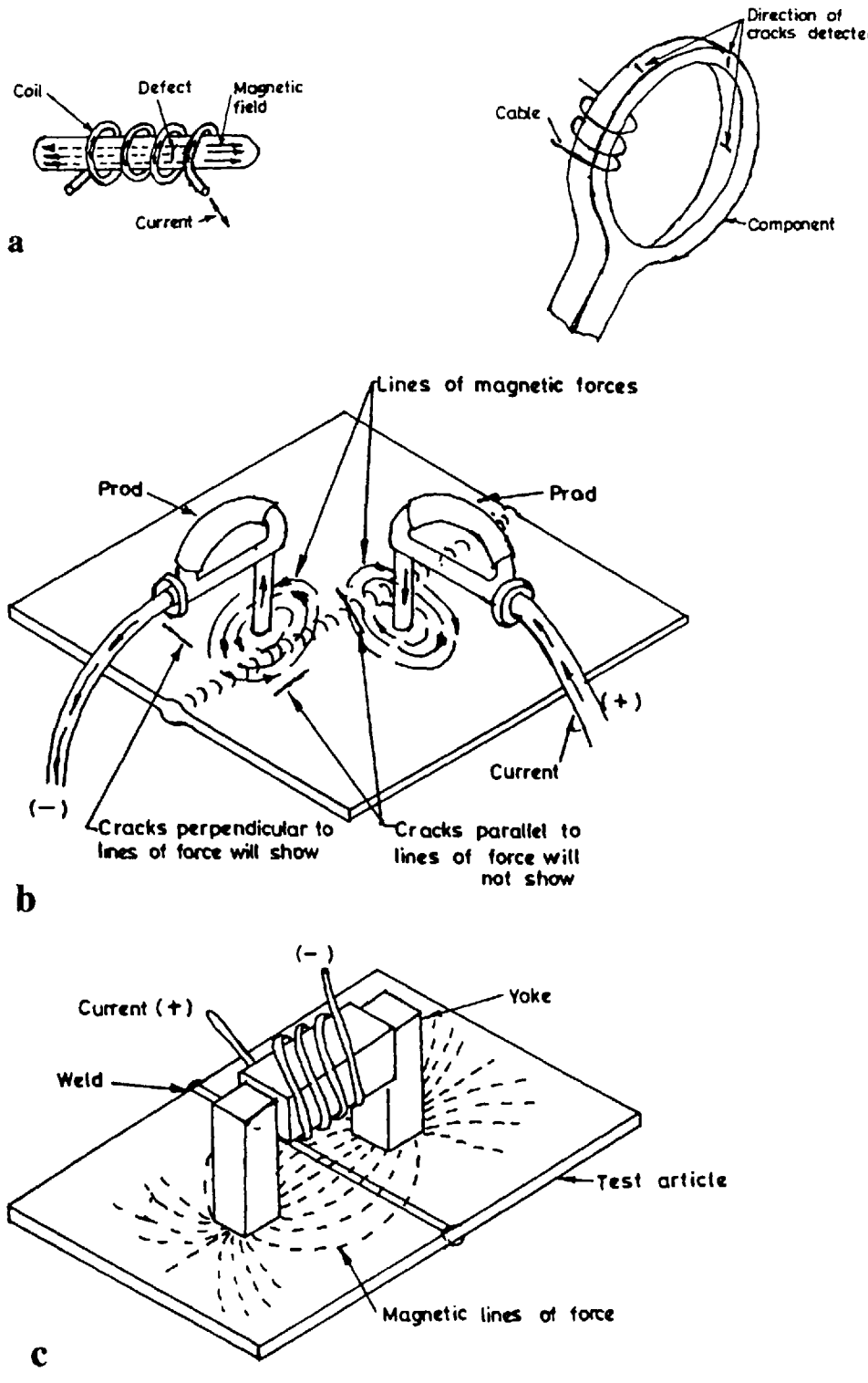


Figure 10 Magnetising techniques. (a) Coil magnetization; (b) prod magnetization; and (c) yoke magnetization. (Courtesy American Welding Society.)

Prod Spacing

Prod spacing should not exceed 8 in (203.2 mm). Shorter spacing may be used to accommodate the geometric limitations of the area being examined or to increase the sensitivity, but not less than 3 in (76.2 mm).

Yoke Magnetization

Yoke magnetization introduces a longitudinal field to show up defects perpendicular to the flaw, or across the surface of the part. Both permanent and electromagnetic yokes are used. Permanent magnetic yokes have magnetic strength limitations but are most useful for spot inspection of welds. They can be used when electricity is not available. Electromagnetic yokes are U-shaped with a coil to carry current as illustrated in Fig. 10c. Longitudinal magnetic fields are set up in the test specimen when the coil is energized either by AC or DC current. Alternating current electromagnetic yokes should have a lifting power of at least 10 lb at the maximum pole spacing. Directions of magnetization should be same as for the prod technique. Pole spacing should be limited to 2 to 8 in (50.4 mm to 203.2 mm).

Examination Coverage

All the examinations should be conducted with sufficient overlap to ensure 100% coverage at the required sensitivity.

8.12 Inspection Medium (Magnetic Particles)

The inspection medium shall consist of finely divided ferromagnetic particles. They must have good mobility, very fine size and shape, high permeability, and low retentivity. The particles may be in dry powder form (for the dry method) or suspended in a suitable liquid medium such as water or kerosene (for the wet method). The size of the dry particles is about 60 μm and a blend of elongated and spherical particles is used to attain good sensitivity and mobility. The wet particle size is about 40 to 60 μm.

Application of Examination Medium

The magnetic particles should be applied in such a manner that a thin uniform dust-like coating settles upon the surface of the test part while the part is being magnetized. Specially designed powder blowers are used for this purpose.

8.13 Inspection Method

According to the condition of the magnetic particles used for inspection, the inspection techniques are known as the dry method and the wet method.

Dry Method

In the dry method, dry magnetic particles are used for examination. The dry powder method is preferred for surface and subsurface defects [44]. The powders are available in colors that will contrast with the background of the part being examined. For example, black or red powders are for use with light-colored surfaces, grey on dark, and yellow on either. The magnetic particles are sprinkled over the surface by using a powder blower operated by a low-pressure air supply. The particles line up along the discontinuities as they reach the surface. When using dry particles, test sensitivity depends to a large extent on how the excess particles are removed. In the field, a small syringe or powder blower is used to push excess particles off the test area under a light burst of air without disturbing the lightly held powder particles along the discontinuities. Inspection by the dry method is carried out with portable magnetizing equipment.

Wet Method

In the wet method, the magnetic particles are suspended in a liquid base of oil or water. The magnetic particles used in this method are finer than those used for the dry method, which makes the wet method more sensitive to detection of fine surface defects. Two types of wet magnetic particles are used. They are (1) visible magnetic particles, either reddish or black, observed under normal white light, and (2) fluorescent magnetic particles, which fluoresce when exposed to near-ultraviolet (black) light. The inspection bath is mostly flowed, sprayed, or brushed over the specimen surface. Most magnetic particle inspection by the wet method is done with stationary-type equipment, although portable equipment may be used.

Comparison of Dry Method and Wet Method

The dry powder method is more sensitive than the wet powder method for the detection of near-surface discontinuities but not as sensitive as wet method in detecting fine discontinuities. The dry method is convenient to use in conjunction with portable equipment for the inspection of large components or for field inspection, whereas the wet method is used with stationary-type equipment.

8.14 Surface Preparation

Surfaces to be inspected shall be clear and free from oil, grease, sand, loose rust, scale, ripples, welding spatters, or any other surface contaminants that could interfere with the interpretation of the magnetic particles indications. Surface preparation by grinding or machining may be necessary where surface irregularities could mask indications due to discontinuities. Magnetic particle test shall not be performed if the surface temperature of the part exceeds 600°F.

8.15 Evaluation of Indications

The types of indications obtained by magnetic particle inspection due to "piling up" of the magnetic particles at the lines of flaws are as follows:

1. Relevant indications are those that result from mechanical discontinuities.
2. Linear indications are those indications in which the length is greater than three times the width.
3. Rounded indications are circular or elliptical with the length equal to or less than three times the width.
4. Nonrelevant indications may arise due to metallurgical discontinuities and magnetic permeability variations. These nonrelevant indications shall be reexamined by other suitable NDT methods such as PT and ET.

8.16 Demagnetization

When the residual magnetism in the part could interfere with subsequent processing or usage, the part shall be demagnetized after completion of the test.

8.17 Record of Test Data

The information such as material, method used (dry or wet), type of magnetization, type of current, amount of current, and nature of defects should be recorded at the time of each test for future reference.

8.18 Interpretation

1. Surface defects appear sharp and distinct.
2. Subsurface flaws appear rough and fuzzy.
3. Width of surface flaw indication varies with depth.

8.19 Acceptance Standards

For pressure vessels, heat exchangers, fittings, and components manufactured to ASME Section VIII Div. 1, as per Appendix 6, all surfaces to be examined shall be free of (1) relevant linear indications, (2) relevant rounded indications greater than $\frac{3}{16}$ in (4.8 mm), and (3) four or more relevant rounded indications in a line separated by $\frac{1}{16}$ inch (1.6 mm) or less edge to edge.

8.20 MT Accessories

Various MT accessories are marketed by M/s Magnaflux, a Division of ITW, Inc., USA, and by others. They include residual field indicators, ASME field indicators, quantitative quality indicators, centrifuge tube and stand for ascertaining bath concentration, easy-to-use puffer bulb for applying dry method powders, copper braided pads to prevent burning by ensuring good electrical contact between test part and contact plates, test bar with artificial surface and subsurface discontinuities for testing with yoke method, and test block with subsurface discontinuities for testing with the prod method and coil method. For testing the magnetic particles, a Betz ring is used. The Betz ring has holes drilled at different depths. As a magnetic field is induced in the Betz ring, magnetic particles are sprinkled to the surface. The number of visible line indications determines the sensitivity of the particles. Typically, specifications require visual detection of the fifth hole, which produces a broad indication [39].

9 RADIOGRAPHIC TESTING (RT)

The term *radiography* usually implies a radiographic process that produces a permanent image on a film. Radiographic testing (RT) technique using x-rays and gamma rays is one of the important methods of NDT, and has developed, as it is applied today, into a very reliable technique. The technique utilizes electromagnetic radiation to penetrate an object to reveal information about its internal conditions, particularly internal flaws and surface flaws/discontinuities.

9.1 Principle of Radiography

When a radiation beam passes through a specimen, some of the radiation energy is absorbed and the intensity of the beam is reduced. To make a radiographic examination of the object, the intensities of the radiation that pass through the specimen must be recorded and compared. Variations in beam intensity are seen as difference in shading that are typical of the types and sizes of the flaw present. The recording is being achieved either by letting the rays strike a photographic film (Fig. 11) or by letting the rays fall on a fluorescent screen that absorbs some of the radiation and converts it to visible light, thus producing a visible image known as fluoroscopy.

9.2 Application

Surface flaws that are detectable by radiography include undercuts, concavity at the weld root, incomplete filling of the grooves, excessive reinforcements, overlaps and electrode spatter,

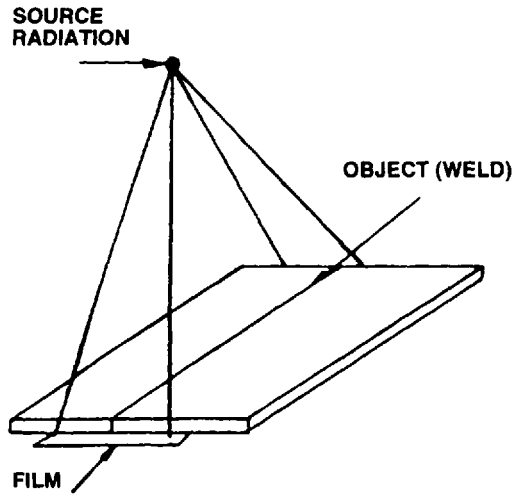


Figure 11 Radiographic testing principle.

and internal flaws such as blow holes, gas inclusions, porosity, piping, slag inclusion, cracks, incomplete penetration, incomplete fusion; and tungsten inclusions. More information on flaw-detecting capabilities is discussed later in this section.

9.3 Radiation Sources (X-Rays and Gamma Rays)

Two types of radiation sources are commonly used in weld inspection. They are x-ray machines and radioactive isotopes. X-rays are produced by machines that range from portable, low-energy units in the range of 50–400 kV used for inspection of relatively thin objects, say, metal thickness up to 7.5 cm steel equivalents, to betatrons and linear accelerators up to 30 meV, capable of radiography of thick objects up to 20 in (508 mm) of steel.

Gamma-ray radiation is emitted by radioisotopes, the two most common being cobalt-60 and iridium-192. Cobalt-60 will effectively penetrate a thickness up to approximately 8 in (203 mm) of steel, whereas iridium-192 is effectively limited to a steel thickness of about 3 in (76.2 mm). The minimum thickness of steel on which x-rays may be normally used is up to and including 19.05 mm, and gamma-ray sources may normally be used for thicknesses greater than 19.05 mm.

Comparison of X-Ray and Gamma-Ray Radiography

Most industrial radiography is performed with x-rays. It is highly effective and versatile, and with modern techniques, it is very accurate. The principal advantage of gamma-ray radiography is lower cost, the source can be very small so that transportability is easy, and it is economical for low-volume test pieces. However, gamma rays are not as sensitive to small defects as are x-rays in thickness less than 1 in (25.4 mm), cracks are the most difficult to detect and generally require a longer exposure time than with x-rays, and they do not provide as sharp a definition [43].

9.4 Merits and Limitations

Merits. Radiography has been the standard for volumetric inspection of weldments for decades. In spite of high cost, hazards, and the time-consuming nature of the process, radiography

stands out as the NDT method that gives a permanent record of test results. Among other advantages, it has surface and subsurface inspection capability, and radiographic images aid in characterizing (identifying type) discontinuities [28].

Limitations. A significant limitation of radiography is that discontinuities must be favorably aligned with the radiation beam. This is usually not a problem for discontinuities round in cross section, such as slag inclusions and porosity [28,33]. On the other hand, cracks and planar defects that diverge considerably from the direction of the radiation beam would nearly miss detection, and therefore ultrasonics is sometimes employed in addition to radiography when very critical examination of a weld is required [33]. Angular notch-type discontinuities such as lack of fusion, incomplete penetration, and cracks must be oriented to the radiation beam so as to show up on the x-rays film [45]. Coarse grain structure, especially in large-pass welding, can cause problem due to diffraction mottling effects [46].

9.5 Radiographic Test Written Procedure

The radiographic test written procedure is given in Table 9.

Radiographic Examination Procedures Deficiencies

These may include incorrect exposure geometry, film placement, source selection, penetrameter selection, incomplete film identification, and failure to submit a technique sheet with sketch [2].

9.6 Requirements of Radiography

Essential requirements for producing a radiograph are [28]:

1. A source of radiation
2. X-ray film
3. A trained person for operating the equipment
4. A means of processing the exposed film
5. A trained person capable of interpreting the radiographic images

Table 9 Radiographic Test Written Procedure

1.0 Scope	11.0 Density
2.0 Techniques	12.0 Sensitivity
3.0 Surface preparation	13.0 Processing of films
4.0 Identification system	14.0 Processing technique
5.0 Location markers	15.0 Personnel certification
6.0 Radiation sources	16.0 Evaluation of radiographs
7.0 Film	17.0 Reporting
8.0 Screens	18.0 Retention of radiographs
9.0 Focus to film or source to film distance.	
10.0 Penetrameter	
10.2 Number of penetrameters	
10.3 Placement of penetrameter	

9.7 General Procedure in Radiography

The steps of performing a radiographic examination are as follows:

1. Surface preparation
2. Selection of radiation source, depending upon the thickness of the part and location of the component/assembly
3. Selection of film and exposure parameters for desired quality (i.e., sensitivity, density), and selection of intensifying screens
4. Processing of exposed films
5. Interpretation of radiographs
6. Record keeping and perservation of radiographs

9.8 Reference Documents

Radiography is one of the most widely established methods for the detection of internal as well as surface defects, and has been written into many national codes and standards. ASTM standards E94, E142, E155, E272, E390, E592, E586, and E747 cover radiographic examination. ASME Code Section V and VIII, Div. 1, Appendix 4, covers RT.

9.9 Safety

One of the most important considerations in x-ray or gamma-ray work is the exercise of adequate safeguards for personnel.

9.10 Identification Marks

The identification marks such as pressure vessel number, job number, seam number, segment number, or spot number, date, and manufacturer's symbol should appear in each film as radiographic images.

9.11 Location Markers

Location markers should appear as radiographic images and should be placed on the part, and their locations shall be hard stamped or engraved on the surface of the part being radiographed. Lead marker accessories containing sets of alphabets and numbers including arrow and oblique are available in the market.

9.12 Processing of X-Ray Films

All the radiographs should be free from fogging and processing defects. While processing, radiograph details should not be lost due to scratches, finger marks, etc. The Welding Engineer Data Sheet provides guidance for troubleshooting radiographs [47].

9.13 Surface Preparation

Weld surfaces should be ground free of ripples so that the resulting radiographic image cannot mask or be confused with the image of discontinuities. Prior dressing of the weld surface ensures interpretation of films with a minimum amount of referring back to the welds themselves. In the case of submerged arc welding, no surface preparation is required provided the weld bead is smooth and free from valleys or ridges.

9.14 Radiographic Techniques for Weldments of Pressure Vessels

The common techniques used for the radiography of welds in cylindrical shapes are (1) single-wall, single-image (unidirectional) (Fig. 12a), (2) single-wall, single-image (panoramic) (Fig. 12b), (3) double-wall, single-image for pipe welds greater than 88.9 mm (Fig. 12c), and (4) double-wall, double-image for pipe welds with OD less than or equal to 88.9 mm (Fig. 12d). Whenever possible, single-wall technique is preferred. This technique is employed for plates, shell welds, and castings of larger sizes. Common techniques for various fillet welds are shown in Fig. 13. A diagrammatic representation of the film and source is shown in Fig. 14.

Panoramic Radiography with Isotopes

One of the important advantages using isotopes is that by a single exposure, the entire circumference of a weld can be radiographed, provided there is accessibility to keep the source at the center of the pipe. Panoramic radiography (Fig. 15) shows the radiation source inserted in the center through an adjacent hole [48].

Gamma-Ray Technique

A gamma-ray technique for branch welds is shown in Fig. 16.

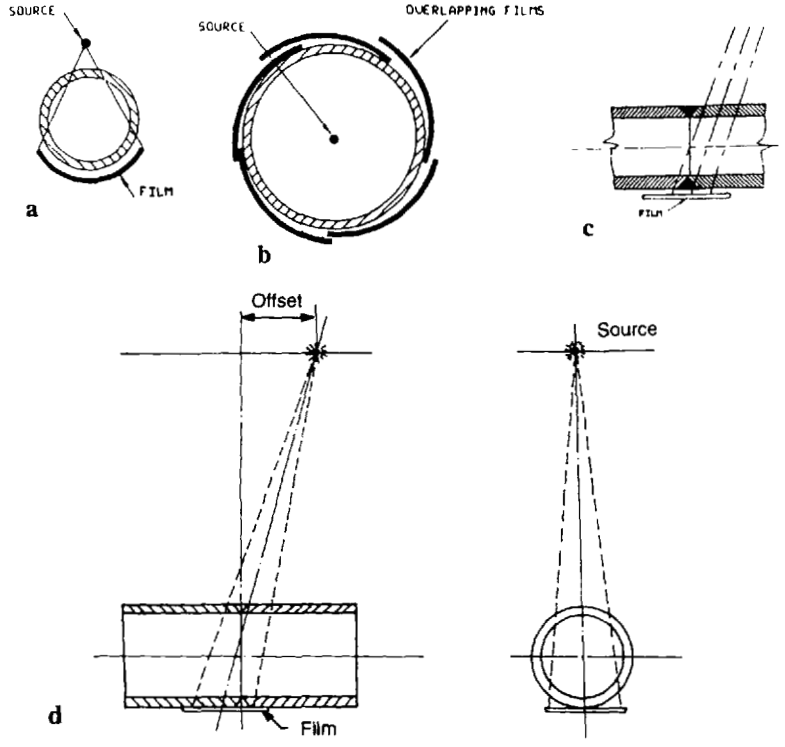


Figure 12 Radiographic techniques for cylindrical shape testing. (a) Single wall, single image (unidirectional); (b) single wall-single image (panoramic); (c) double wall, single image; and (d) double wall, double image (From Ref. 33.)

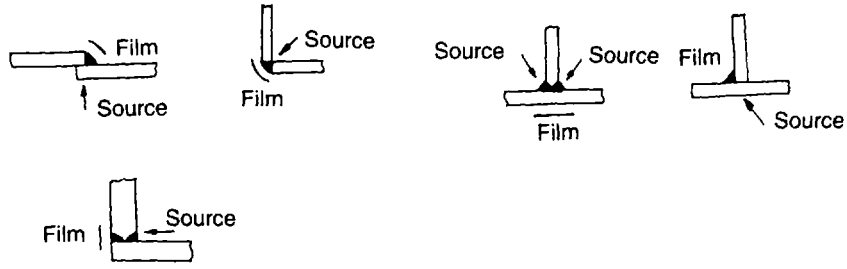


Figure 13 Common RT techniques for corner fillet welds.

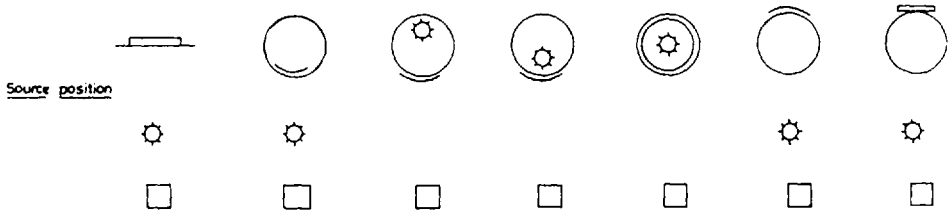


Figure 14 Diagrammatic representation of the film and source.

9.15 Full Radiography

ASME Code Section VIII, Div. 1, UW-11 lists the conditions for which the full RT for the welded joint is mandatory. Some of these conditions are:

1. All butt welds in the shell and heads of vessels used to contain lethal substances
2. All butt welds in vessels in which the least nominal thickness at the welded joint exceeds 1.5 in (38.1 mm).
3. All butt welds in the shell and heads of unfired steam boilers having design pressures exceeding 50 psi.

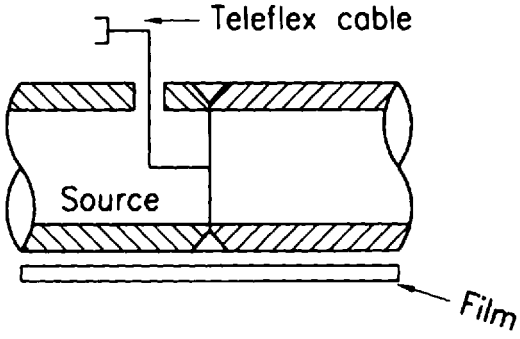


Figure 15 Panoramic radiography.

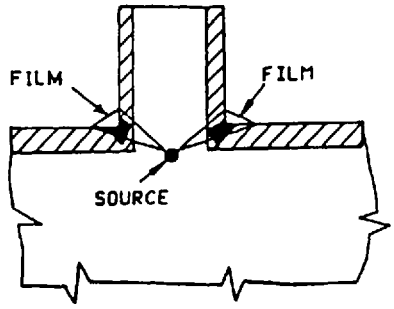


Figure 16 Gamma rays technique for branch welds. (From ref. 48.)

4. All butt welds in nozzles, communicating chambers, etc., attached to vessel sections or heads that are required to be fully radiographed under parts 1 or 3.

Spot Radiography

Spot radiography should be in accordance with ASME Code Sec. VIII, Div. 1, UW-52. Spot radiography means that one spot is examined on each vessel for each 50-ft increment of the weld or part thereof for which a joint efficiency from column (b) of Table UW-12 is selected. For vessels with less than 50 ft of weld, 50-ft increments of weld may be represented by one spot examination. Length of each radiography shall be at least 6 in (152.4 mm). Further, all T joints must be radiographed and at least one shot must be taken on each longitudinal and circumferential seam (Fig. 17).

9.16 Radiographic Quality

The quality of the radiographs that decides the efficiency of flaw detection is determined by two factors: sensitivity and density.

Radiographic Sensitivity

The effectiveness of a radiographic technique to bring out the smallest details in a given thickness of an object is referred to as *radiographic sensitivity*. The more the exactness, the better is the sensitivity. Radiographic sensitivity is affected by two factors: (1) contrast—the magnitude of change in density produced on the film because the defect and sound material absorb different amounts of radiation—and (2) definition—the amount of blurring of the projected shape of the defect produced on the film. The terms and definitions that best represent

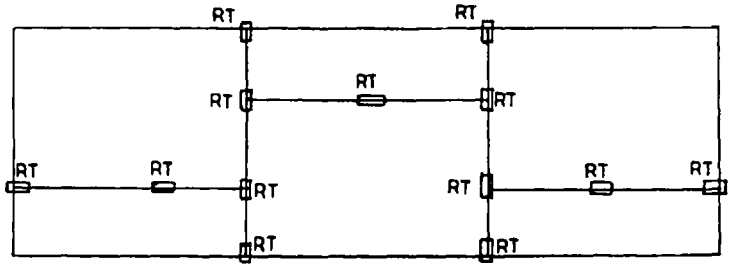


Figure 17 Spot radiography.

(1) and (2) are thickness sensitivity and unsharpness, respectively [49]. In quantitative terms, sensitivity is expressed as a percentage ratio of the smallest size of an artificially produced defect shown on the radiograph to the thickness of the object under examination. The smaller the numerical value of sensitivity, the better is the radiographic sensitivity. The artificial defect in the form of a hole, step, or wire of various dimensions is called as image quality indicator (IQI) or *penetrameter.*

Density of Radiographs

The *density* of a radiograph refers to its darkness. Areas exposed to relatively large amounts of radiation are known as areas of high density and areas exposed to less radiation are known as areas of light density. The density of the radiograph should be minimum of 1.8 for x-rays and 2.0 for gamma rays. When the density of the radiation varies by more than −15% or +30% from the density through the body of the penetrameter, additional penetrameters should be placed in the exceptional areas.

Image Quality Indicators (IQI)

An image quality indicator (IQI), also called a penetrameter (or penny), is a simple geometric form used to judge the quality of a radiograph. It is made of the same material as or a similar material to the component being examined. The dimensions of the IQI bear some numerical relation to the thickness of the part being examined. They are placed on the test piece during setup and are radiographed at the same time as the test piece. IQIs are preferably located in regions of maximum test piece thickness and greatest test piece to film distance, and near the outer edge of the central beam of radiation. The degree to which the image of the IQI is visible in the developed image is a measure of the quality of that image.

IQI Designs. A number of IQI designs are used by different authorities. There are American standards, British standards, and French and German standards. Three basic types of IQI are available. They are the wire type, step-wedge type, and strip–hole type.

The most widely used *wire-type* IQI is of the DIN type (German), conforming to DIN 54109 Fe, Cu, and Al. It specifies a set of three parameters, each containing seven equidistant wires. The diameter of the wires varies in geometric progression. Each diameter is represented by a whole number. The three sets are 1–7, 6–12, and 10–16. The ASTM standard for wire-type IQI is E747 Fe, Cu, and Al. Wire-type IQI is shown in Fig. 18a.

The *step-wedge type* is the simplest IQI. This type of penetrameter is commonly used in UK-BS 3971, and in France-AFNOR Code. It consists of small steps, whose thickness (0.5 to 5% of specimen thickness) increase in geometric progression. Step-wedge type IQI is shown in Fig. 18b. Step-hole type is step-wedge type with holes.

For the *strip–hole type* IQI, the most common and widely used version is the ASTM or ASME penny. Strip–hole IQI is also known as plaque-type IQI, whose thickness is about 2% of the specimen thickness. This consists of a small rectangular piece of metal with appropriate material with three holes. The diameters of the holes are multiples of thickness: 1T, 2T, and 4T, where T is the thickness of IQI. Plaque type IQI are described in ASTM E 142/ASME SE 142 Fe, Cu, Al, Monel, and Ti. Strip–hole type IQI is shown in Fig. 18c.

Number of IQIs

One IQI should be used for each radiograph, generally. In case of radiography using a panoramic exposure, three IQIs placed at 120° apart is accepted.

How to Calculate IQI Sensitivity

An IQI is used to indicate the quality of radiographic technique and not to measure the size of a defect that is shown.

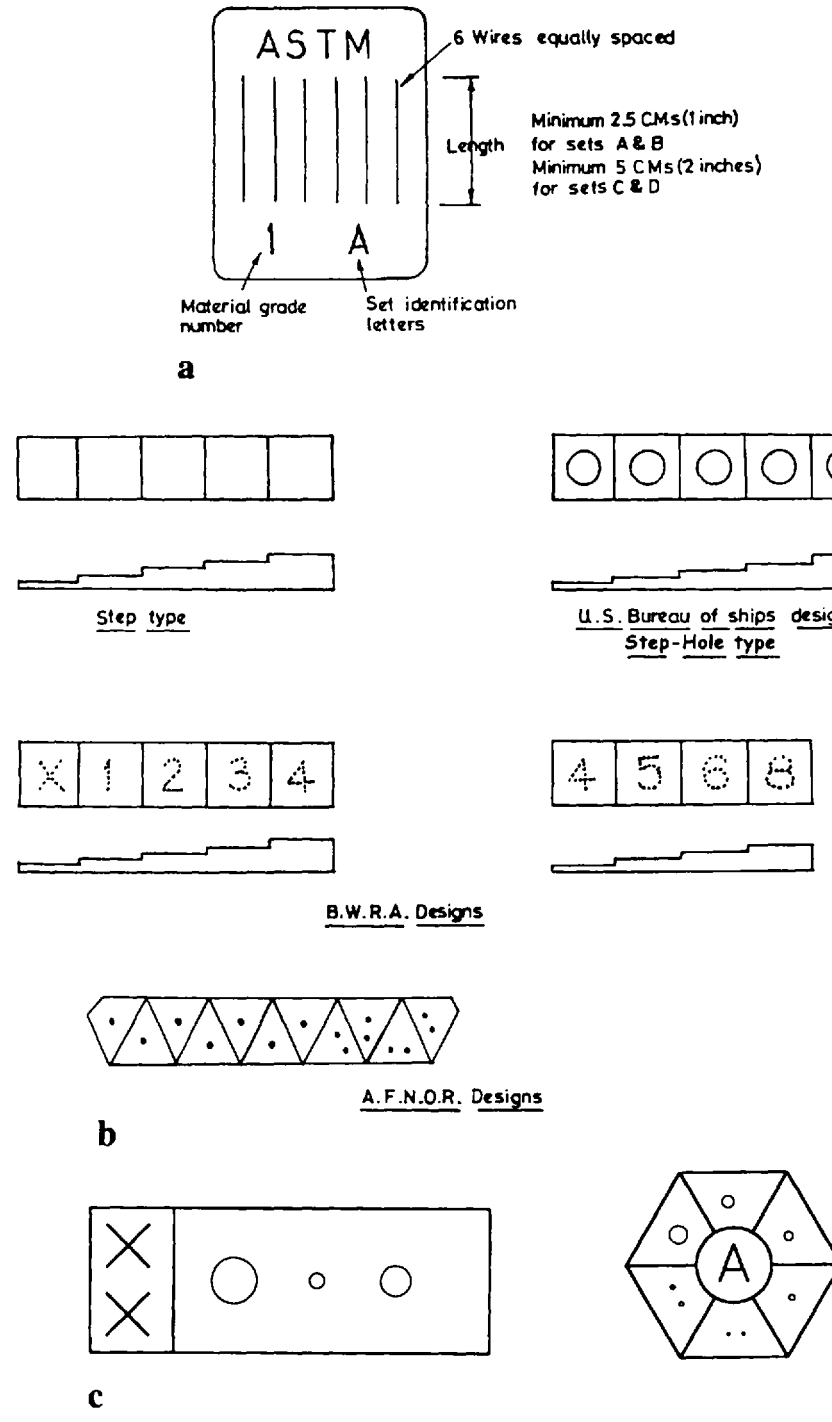


Figure 18 IQI types. (a) Wire; (b) step wedge; and (c) strip hole.

Sensitivity for wire-type IQI is based on the smallest size of wire diameter visible, and for strip–hole type IQI it is based on diameter of the smallest hole:

$$\text{Percent of sensitivity} = \frac{\text{smallest size of penny visible}}{\text{thickness of the object}} \times 100$$

For the strip–hole type or plaque-type IQIs, the IQI image and the specified hole are the essential indications of sensitivity. The thickness of the IQI and the hole diameter to be seen are generally specified in the code. The following are the different sensitivity levels of inspection with strip–hole type pennies:

1—1T	2—1T	4—1T
1—2T	2—2T	4—2T
1—4T	2—4T	4—4T

Normally the image of 2-2T hole should be visible in the radiograph. Critical components require a level of 1-2T or 1-1T, and less critical components may need only a quality level of 2-4T or 4-4T.

Examination of Radiographs

The examination of radiographs of welds should be made on the original films using a viewing device of suitable illuminating power. The standard of acceptance shall be made with respect to the reference chart of x-rays given in ASME Code Section VIII, Div. 1, Appendix 4.

X-Ray Clues to Welding Discontinuities

When interpreting radiographs of weldments, one must look for different types of discontinuities (undercut, porosity, lack of fusion, etc.). All discontinuities, however, must be considered before deciding to accept or reject and to correct welding practices. Some of the common weld defects and their typical radiographic appearances are given in Table 10.

Acceptance Criteria

For porosity, radiographs are often compared with charts showing arbitrary arrays of pores. The charts are intended to limit the porosity to a certain percentage of the area on the radiograph. Slag inclusions are usually accepted on the basis of length (the only dimension readily

Table 10 Weld Defects and Radiographic Appearances [6, 50]

Defect	Image
Crack	Appears as a fine, dark, zig-zag irregular line, may be branched.
Lack of fusion	Very narrow, straight dark line, parallel to the weld image.
Lack of penetration	Continuous or intermittent dark straight line at the center of the weld seam.
Tungsten inclusions	Since tungsten has a higher atomic number than the parent metal, namely iron, the radiographic indications are white distinct marks.
Void	Looks rounded and black, and readily recognized with well defined outlines.
Slag inclusions	Look less distinct than voids. Dark indications and irregular shapes. May appear singly or be linearly distributed or scattered throughout the weldment.
Porosity or gas inclusion or blow hole	Comes in clusters, or in random fashion. The image will be normally round dark spots with smooth edges.

measured by radiographs). Planar defects (cracks, lack of fusion etc.) are normally not permitted [49]. An interpretation is complete and a better conclusion is arrived at only after a thorough visual examination of the part.

For acceptance criteria regarding image density, relevant indications, maximum size of rounded indications, aligned rounded indications, spacing, clustered indications, etc., refer to ASME Code Section VIII, Div. 1, Appendix 4, and Section V, or the IIW collection of reference radiographs.

Documentation

When reporting and documenting the results of radiographic film interpretation, complete and accurate information must accompany the radiographs. This is required for subsequent customer review, and possibly regulatory agency review. As per ASME Code Section V, the films shall be retained up to 5 years, by the manufacturers.

9.17 Recent Developments in Radiography

Over the last few years, several new radiographic techniques have been developed. Important developments in the field of radiography are discussed in Ref. 27 and Hellier [51]. Some of the developments follow.

Tomography

Computer tomography in radiography is a three-dimensional (3D) inspection technique that can be applied for various kinds of objects and materials. This method was adapted from the medical computerized axial tomography (CAT) scanner. The method involves the repeated scanning of a specimen with a narrow beam of radiation in a series of steps around the specimen. The radiation impinges on a linear array of detectors whose output is digitized and provides a reconstruction of an image or slice, which allows a view of the specimen perpendicular to the direction of the radiation [52].

Neutron Radiography

This refers to radiographic inspection using neutrons rather than electromagnetic radiation. Neutrons bring out information that is not revealed by x-rays or gamma rays, because the absorption mechanism of neutrons is different from that of x-rays and gamma rays.

Radioscopy

Radioscopy is similar to radiography; the only difference is that an image receptor replaces the radiographic film. The receptor is an image intensifier coupled to a low-light-level camera. The image shows up on a high-resolution monitor. An operator views the image when it appears on the screen; no film processing is involved. This feature provides on-line examination of longitudinal and circumferential pipe and shell welds. Radioscopy is nearly 10 times as fast as film radiography, considering time to develop film and interpret radiographs, and the image can be recorded on videotape [53]. Radioscopy is included in ASME Code Section V.

Fluoroscopy

X-ray images can be made visible instantaneously by use of a fluorescent screen instead of a photographic film. Thus, this provides a process of real time image viewing. For permanent records, fluoroscopy images can be photographed (fluorography).

Gammascopy

Gammascopy systems with image processing facility are now commercially available for inspection of thick structural parts with iridium-192 or cobalt-60 sources. The sensitivity and resolution obtainable in the gammascopy are inferior to those of film radiography.

Digitization of Radiographs and Laser Scanner System

Although radiographic film remains the main image capture medium in many applications, it has disadvantages in long-term storage of images because of the possibility of image quality loss over time, difficulty of access and retrieval, and strict storage environment requirements [51]. NDT Scan, a recent development of DuPont NDT Systems, converts high-quality film radiographs from analog to digitized form, which offers the prospects of image storage in a digital format on optical media, analysis, recall, and simultaneously providing solutions to the problems associated with film.

Imaging Plate

This is a high-sensitivity imaging plate that essentially replaces conventional radiographic film while utilizing standard radiographic equipment. It is estimated that the imaging plate can be reused about 40,000 times [51].

High-Energy Radiography

Radiation sources such as synchrotrons and betatrons are available.

Gamma Radiography

The development of modern gamma cameras permits safe and reliable remote operations. Apart from the commonly used isotopes, a number of other sources as europium, ytterbium, etc. are finding increasing applications [27].

Microfocus X-Rays Source

The microfocus x-rays source can produce extremely sharp radiographs at exceedingly short film-to-focus distances. An outstanding application is the radiography of bore-side tube-to-tube-sheet weld of steam generators as shown in Fig. 19 [27].

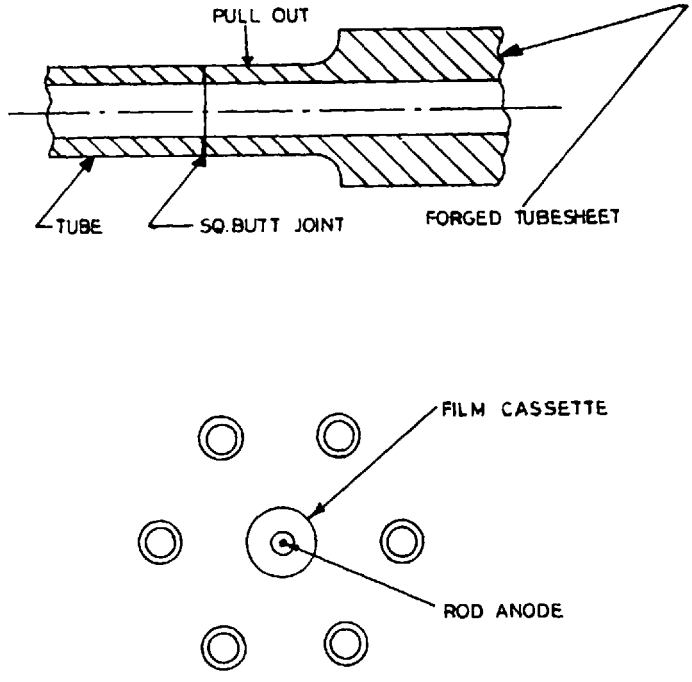


Figure 19 Microfocus X-rays source for bore side tube-to-tubesheet welding. (From Ref. 27.)

10 ULTRASONIC TESTING (UT)

Ultrasonic testing (UT) is one of the most widely used methods of nondestructive inspection. This method uses sound waves having frequencies in the megahertz range. In UT technique, high-frequency sound waves are transmitted through the material being inspected. The sound waves travel through the material with some loss of energy (attenuation) and are reflected at interfaces or discontinuities such as cracks, flaws, inclusions, and seams, as illustrated in Fig. 20 [29,54]. The reflected sound beam from the flaws or interface is detected and analyzed to define the presence and location of discontinuities or the thickness of the material. It is also especially suited for determining characteristics of engineering materials such as elastic moduli, study of metallurgical structure, grain size, and density variation.

10.1 Test Method

The primary ultrasonic testing techniques and their applications are [55]:

1. Pulse echo: most effective for cracks, inclusions and thickness measurements.
2. Through transmission: most effective for porosity, grain size and density measurements.
3. Resonance: most effective for detection of thickness and laminar discontinuities.

There are three modes of ultrasonic vibrations that are frequently used in ultrasonic testing of materials. These are (1) longitudinal waves (Fig. 21a), (2) transverse waves (Fig. 21b), and (3) surface or Rayleigh waves (Fig. 21c).

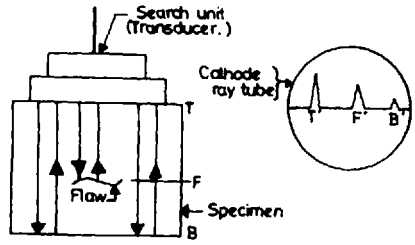
Most ultrasonic weld testing is done manually by an operator manipulating an ultrasonic probe over the test object and visually monitoring the screen of an oscilloscope. The pulse-echo method with A-scan data presentation is most commonly used for inspecting welds. This system utilizes a cathode ray tube (CRT) screen to display the test information. The schematics of A-scan instrument is shown in Fig. 20c.

10.2 Application of Ultrasonic Technique in Pressure Vessel Industry

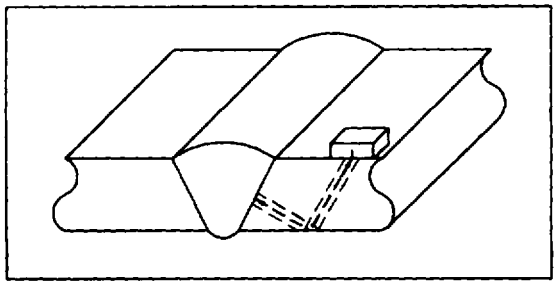
This technique's primary application is the detection and characterization of internal discontinuities [28]. It is also used to determine effectiveness of weld overlay bonding/cladding, and to measure thickness [33]. The information possible to obtain from the UT data includes defect location, orientation, size, and type. Only ultrasonics and radiography can substantially reveal subsurface flaws.

Ultrasonic Plate Tester. Ultrasonic plate testers (Fig. 22) are available to perform edge-to-edge testing before cutting or welding operations in order to check quickly the presence of laminations, gross internal discontinuities such as pipes, ruptures, or slag inclusions. Shell plate areas on which the branches are to be welded are checked ultrasonically to ensure that the steel is free from cluster inclusions. This is to avoid any likelihood of lamellar tearing due to stress introduced by welding [43].

Ultrasonic Examination of Nozzle Welds. Ultrasonics is of prime importance for examining the attachment welds of nozzles and branches where the wall thickness involved is in the order of 25 mm or greater [43]. Various automated and semiautomated equipment has been developed for double-fillet type through nozzles. The branch weld is normally subject to 100% examination before and after weld heat treatment. The equipment almost invariably employs a longitudinal wave probe operated from the bore of the nozzle. Figure 23 shows the UT examination of a defect in double-fillet nozzle welding.

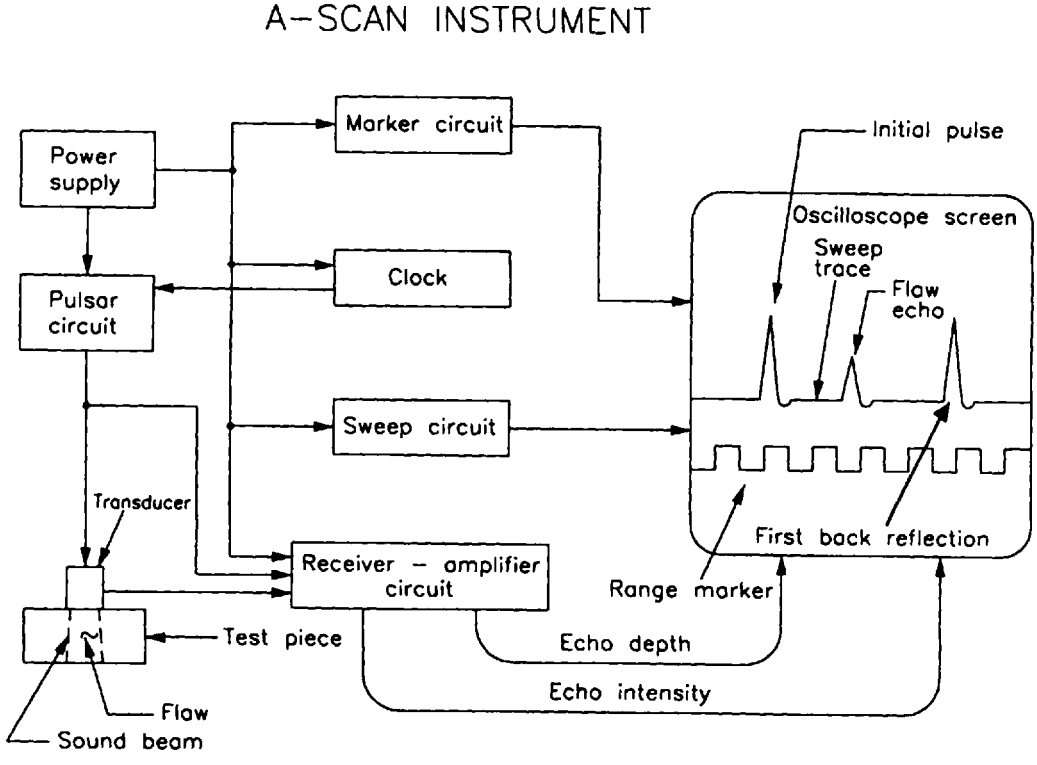


a



Ultrasonic inspection detects discontinuities both on and below the weld surface.Compact, portable equipment makes it easy to use in the field.

b



c

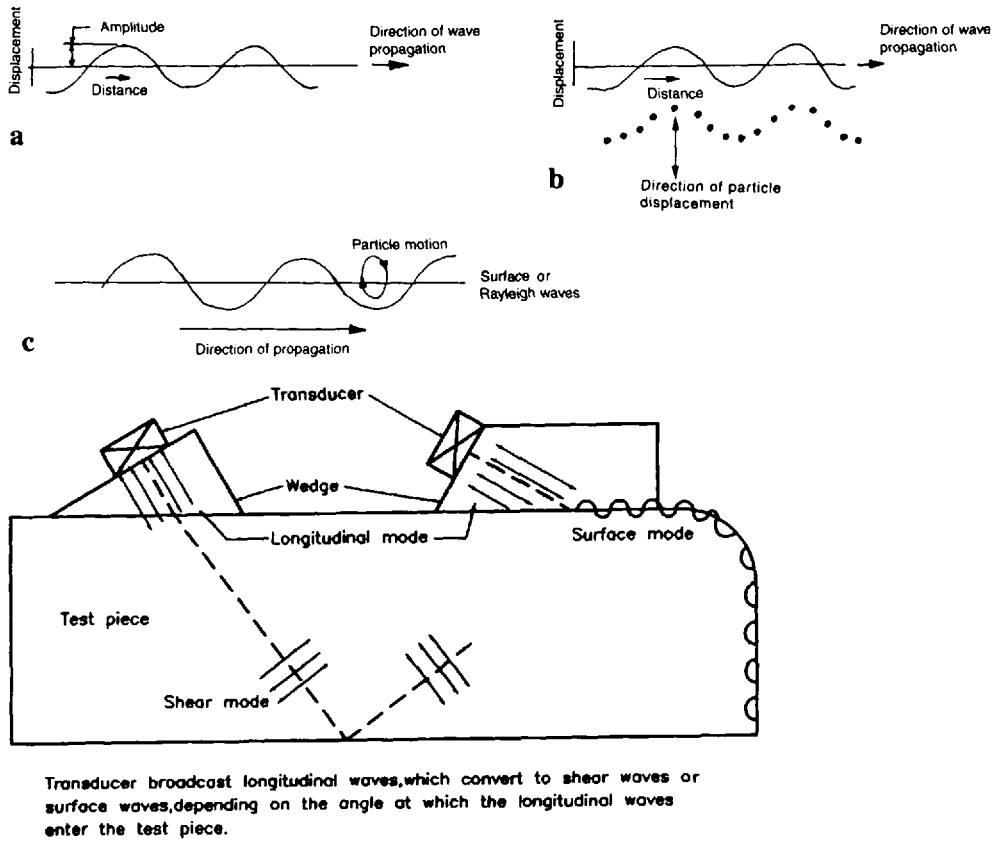


Figure 21 Ultrasonic wave forms. (a) Longitudinal waves; (b) transverse waves; and (c) surface waves, and (d) wave propagation in a test piece. (From Ref. 29.)

10.3 Written Procedure

Minimum information required for written procedure for UT is detailed in ASME Code Section V. A partial list of information to be contained in a UT written procedure is given here:

1. Scope: materials and product form (casting, forging, plate, etc.), weld types, thickness, etc.
2. Surface preparation
3. Couplant
4. Technique (straight beam or angle beam, contact or immersion)
5. Angles and mode(s) of wave propagation in the material
6. Search unit details
7. Ultrasonic instrument details like frequency, screen height, amplitude control linearity.

Figure 20 Ultrasonic testing. (a) Principle; (b) inspection of a weld (schematic); and (c) A-scan signal instrument [29, 54].

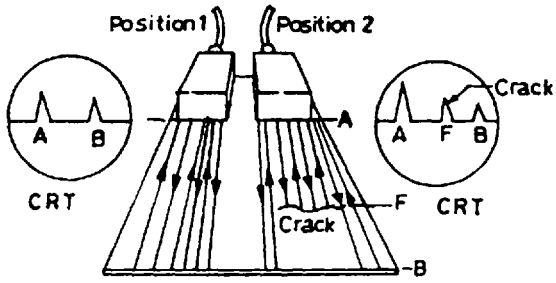


Figure 22 Ultrasonic plate tester.

8. Calibration and reference blocks
9. Extent of scanning, maximum scan speed, and scanning pattern
10. Description of the demonstration or qualification of the procedure used to detect and size flaws
11. Evaluation
12. Acceptance criteria
13. Post cleaning
14. Reporting

Ultrasonic Examination Procedure Deficiencies

These may include insufficient examination, incorrect scanning sensitivity versus calibration sensitivity, failure to describe recalibration, recording, and failure to verify instrument linearity [2].

10.4 Code Coverage

ASME Code Section V/ASTM Specifications are:

(a) SA 388/ASTM, A 388/A 388 M, (b) SA 435/SA 435 M, identical to ASTM A 435/A 435 M, (c) SA 577/SA 577 M, identical to ASTM A577/A 577 M, (d) SA 578/SA 578 M, identical to ASTM A 578/A 578 M, and (e) SA 609, identical to ASTM A 609/A 609 M except for some deletions.

ASME Code Section VIII, Div. 1, Appendix 12.

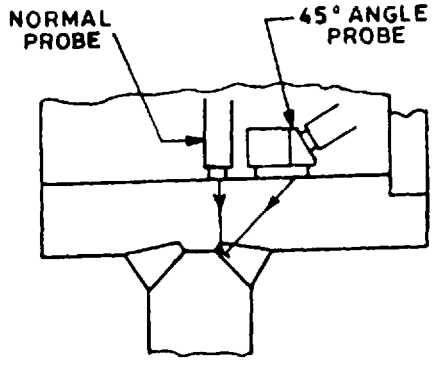


Figure 23 Ultrasonic examination of a defect in a double fillet nozzle welding. (From Ref. 33.)

10.5 Advantages of Ultrasonic Inspection

The conventional ultrasonic flaw detector is well known for its portability, simplicity of operation, superior penetrating power, and high sensitivity, and allows testing from one surface. The method provides almost instantaneous indications of discontinuities. Ultrasonic method is particularly sensitive for the detection of two-dimensional defects such as fine cracks and laminar-type defects, which are not easily found by other methods including radiography [33,56]. UT is sometimes employed in addition to radiography when critical examination of a weld is required [33]. The greater ability of UT techniques to describe the shape and size of a flaw is basic for fracture mechanics analysis, which has led to a growing need for UT inspection in pressure vessel industries [21]. With some electronic systems, a permanent record of inspection results can be made for future reference. By combining angulation, amplitude, signal character, signal movement, signal shape, and frequency analysis, it is possible to accurately determine the discontinuity type [45]. UT presents no health hazards such as radiation or chemical hazard.

10.6 Limitations of Ultrasonic Inspection

Some important limitations of this method include:

1. Accuracy and reproducibility of this method depends largely on the skill of the operator to interpret results since perceptible image is not seen, whereas radiography readily gives the image of the discontinuity.
2. All results are based on subjective evaluation and objective records are not possible to obtain. However, recently various ultrasonic instruments have been developed that automatically scan the weld, and also give permanent record on defect indications, thus eliminating one of the main criticisms of manual UT examination, that no permanent record is available [33].
3. Discontinuities that are present in a shallow layer immediately beneath the surface may not be detectable.
4. Misleading signals due to grain size. For example, the columnar grain structure of stainless-steel welds generally makes ultrasonic testing impracticable, although ultrasonic testing of stainless steel plate presents no problems [43].
5. The ultrasonic signal background that arises from the clad/metal interface of a clad plate can make it difficult to detect defects up to 10 mm deep just below the clad surface and therefore for critical applications machine clad faces [21].
6. Unfavourable joint geometry and backing bars sometimes create false or nonrelevant indications that can be confused with a defective weld.
7. Weld root conditions pose problems; e.g., weldment containing internal concavity and an improperly located counterbore, improper weld capping, sharp reentrant angles, and high–low conditions of vertical fusion zones can cause radiation diffraction and diametrical shrinkage [57].
8. Reference standards made from a similar material as that being tested are required for calibration.
9. UT is less suitable than RT for determining porosity in welds, because round gas pores respond to ultrasonic tests as a series of single-point reflectors [29].

According to Watson [57], simple modifications to the welding procedures and techniques can reduce problems associated with UT and radiographic examination. UT detects more angularly oriented discontinuities and misses some rounded, globular-shaped discontinuities [45]. For more details on UT limitations consult Refs. 21, 43, 45, and 57.

10.7 Examination Procedure

Pulse-Echo Technique

This system is the most versatile and the most employed for inspection. In pulse-echo technique, flaws are detected by measuring the amplitude of signals reflected from a flaw and also the time required for these signals to travel between specific surface and the flaw. It is necessary that an internal flaw reflect at least part of the sound energy onto the receiving transducer for such depth measurements to be made. Depending on test piece shape and inspection objectives, pulse-echo technique can be accomplished with longitudinal, shear, or surface waves, and with straight beam or angle beam techniques. Since it is important to intercept the discontinuity at or near 90°, it is common for more than one angle search unit to be used to inspect a particular weld [28]. Data can be analyzed in terms of type, size, location, and orientation of defects, or any combination of these factors. The basic components of an UT instrument include:

1. An electronic signal generator or pulser
2. An electronic clock
3. A transmitting transducer or search unit
4. Couplant to transfer acoustic energy to specimen and back to the receiver
5. A receiving transducer
6. An echo signal amplifier
7. A display device

Techniques

Two different techniques are employed in UT inspection: (1) contact technique and (2) immersion technique. In the contact technique the probe is in direct contact with the test object with a thin layer of couplant, whereas in the immersion technique the sound waves are generally passed through water and are transmitted to the test object. Contact technique is further divided according to the mode of transmission—normal probe technique, angle beam technique, and surface wave technique. The contact method is most commonly used and readily accepted to field testing, and the immersion method is generally limited to the laboratory.

Angle Beam Technique. In normal probe technique (Fig. 20a), the beam is transmitted at a right angle to the surface, and if there is any crack parallel to the sound beam, it cannot be detected. This problem is overcome by using angle beam technique. The angle beam technique is shown schematically in Fig. 24. In angle beam technique, the sound beam enters the test material at an acute angle and travels with zig-zag reflections from the specimen boundaries. Angle beam technique uses shear waves.

Surface Wave Technique. To detect defects that are very close to the surface, surface waves are used. For its effectiveness, the surface condition should be good.

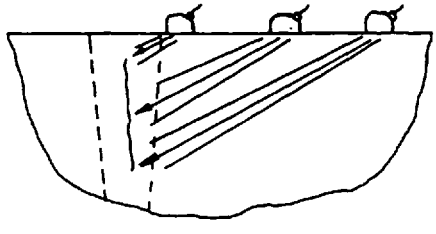


Figure 24 Angle beam technique.

Presentation

A-Scan. Mostly A-Scan presentation is used in NDT for detecting discontinuities. In the A-scan presentation (Fig. 20c), the horizontal baseline on the CRT indicates elapsed time (from left to right) and the vertical deflection shows response amplitude of the reflected waves. The signal amplitude represents the intensities of transmitted or reflected beams. This may be related to flaw size, sample attenuation, or other factors.

B-Scan. The B-Scan representation generally applies to the medical applications and is not used in NDT.

C-Scan. This presentation offers a plane view of the defect in the part. A good estimate of the size and shape of the flaw is obtained, but only a poor estimate of flaw depth. A combination of the B-Scan and C-Scan will give a three-dimensional image of the defect.

10.8 Surface Preparation

The material surfaces to be used for the ultrasonic scanning must be smooth to allow the free movement of the probes and provide satisfactory conditions for the transmission of the ultrasonic waves. The surface should be free, on each side of the weld for a minimum of one skip distance, from weld spatter, loose rust and scale, grinding particles, dirt, paint, or other foreign matter. It may also be necessary to remove gross weld surface irregularities, undercut, sharp ridges, or valleys that will interfere with the interpretation of the test.

10.9 Probes

Generation and detection of ultrasonic waves for inspection are accomplished by means of a transducer element, which is contained within a device known as a search unit or a probe. The active element in a search unit is a piezoelectric crystal.

10.10 Couplant

Where the probes are in direct contact with the sample, a thin layer of viscous medium is used as a couplant between the sample and the probe. Couplants are needed to provide for effective transfer of ultrasonics between search units and parts being inspected. It may be a viscous material, liquid, semiliquid, or paste. Couplant having good wetting characteristics, such as SAE 30, machine oil, grease, or water, should be used. The couplant should be noncorrosive and nontoxic. Couplants may not be comparable to one another, and the same couplant should be used for calibration and examination.

10.11 Ultrasonic Testing of Welds

Procedure for Defect Detection in Butt Welds

To detect all possible defects, the weld is to be examined over its entire cross section and along the length specified. In fixed position, the ultrasonic beam is directed at only a part of the weld; to examine the entire weld the probe is moved over the scanning zone (Fig. 25) in the following ways:

1. Lateral motion
2. Traversing motion

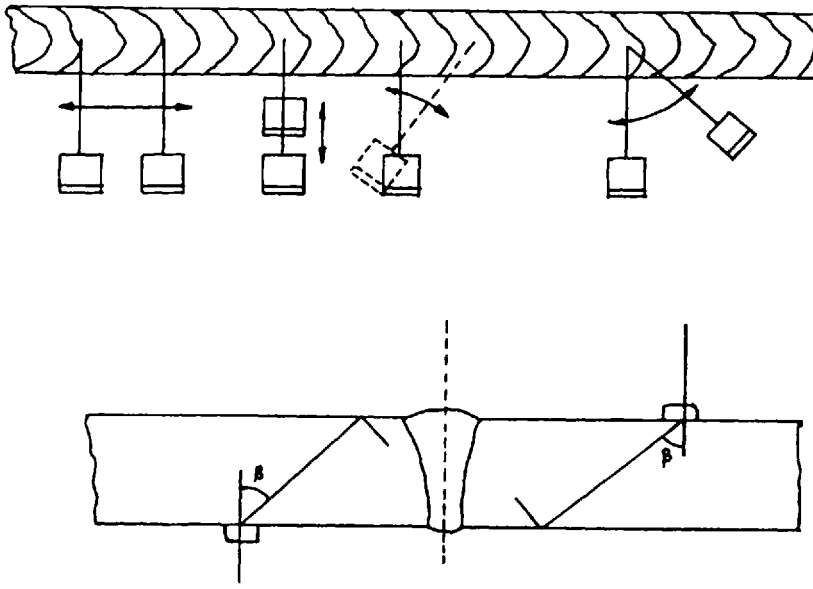


Figure 25 Ultrasonic examination and scanning pattern.

3. Swiveling motion
4. Orbital motion

Use frequencies of at least 2 MHz. Some ultrasonic testing schemes are shown in Fig. 26 [58].

Plate Thickness and Angle of Probe Recommended

The angles of probe recommended for different plate thickness are:

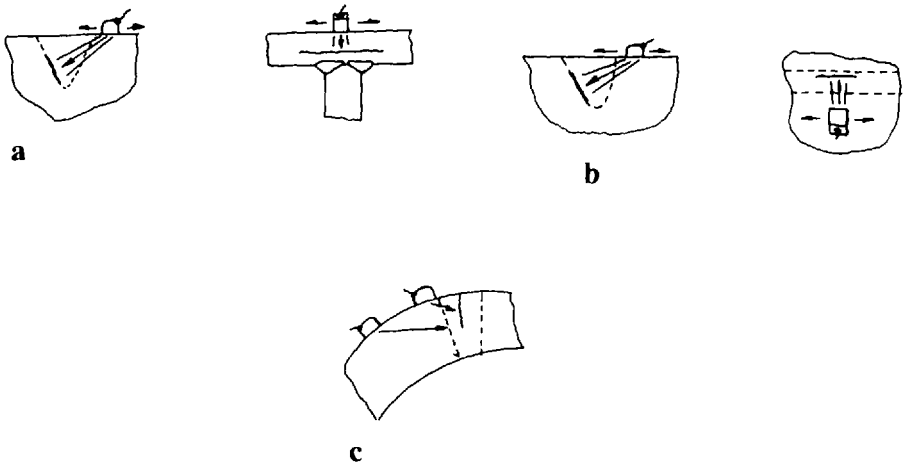


Figure 26 UT techniques for some defects. (Adapted from Ref. 58.)

Plate thickness	Angle of probe recommended
5–15 mm	80°
15–30 mm	70°
30–60 mm	60°
Greater than 60 mm	45°

Thickness over 100 mm When using a single-probe technique, the path length for a full skip distance in thickness over 100 mm (approx. 4 in) becomes too great to examine the entire cross section of the weld from one surface. In this case, the weld should be scanned from four sides, that is, from both sides of the weld on each surface of the plate.

Applications to Butt-Welded Curved Surfaces. While inspecting the curved surface, the probe may be suitably adopted to match the curved surface so as to comply with this requirement. The examination should be carried out with shear wave probes at a frequency of 2 MHz. At least two different probe angles (45° and 60° or 70°) should be used. Tandem technique scan should be made with 45° probes from the four sides of the weld. Figure 27 shows the arrangement of transmitter–receiver probes for detection of longitudinally and transversely oriented defects in welds of butt-welded curved surfaces.

Defect Location

The accurate determination of the position of a defect in a welded joint is important to carry out repairs or from fracture mechanics point of view. The distance and the depth can be easily calculated from the path length, probe angle, and thickness.

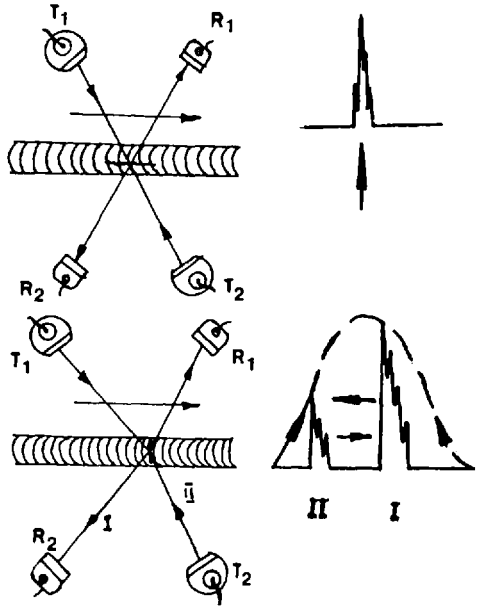


Figure 27 Position of probes for inspection of butt welded curved surfaces-Tandom technique. (After Ref. 27.)

Sensitivity and Resolution

Defect detectability is dependent on the sensitivity, resolution, and noise discrimination of the equipment. Sensitivity is the ability of the equipment to detect the minute amount of sound energy reflected from a defect. Resolution measures the ability to separate the indication resulting from multiple defects that are close together.

10.12 Examination Coverage

The test object shall be examined by moving the search unit over the examination surface so as to scan the entire examination volume. As a minimum, each pass of the search unit shall overlap a minimum of 10% of the transducer dimension perpendicular to the direction of the scan.

10.13 UT Calculators

To determine locations of subsurface indications, inspectors rely on ultrasonic calculators. Calculators come in models for common inspection angles, 45°, 60°, and 70°, used to determine sound path, depth, or surface distance when one variable is known.

10.14 Acceptance Criteria

According to ASME Code Section VIII, Div. 1, Appendix 12, imperfections that produce a response greater than 20% of the reference level shall be investigated and evaluated in terms of the acceptance standards. Indications characterized as cracks, lack of fusion, or incomplete penetration are unacceptable regardless of length. For additional acceptance criteria, consult the referencing code section.

10.15 Reference Blocks

Reference blocks are needed for calibrating the UT equipment. The standard reference flaws in calibration blocks serve as a base of comparison for real flaws. The standard flaws are cylindrical holes, flat-bottom holes, grooves, or edges [59]. The most widely used reference blocks are International Institute of Welding (IIW) reference block and the distance sensitivity calibration (DSC) block (Fig. 28a)., There are other types of reference blocks, like the ASME block (Fig. 28b), BWRA block, Dutch block, Sulzer's block, ASTM block, miniature angle beam block, etc.

10.16 Calibration

The calibration of the instrument is done to check parameters such as time base, linearity, resolution, sensitivity, beam spread, beam angle, probe index, etc. The ultrasonic probes must be calibrated accurately for angle of propagation, probe index, and beam form.

10.17 Fracture Mechanics

The basic premise of fracture mechanics is that every structural component, including pressure vessels, contains defects or discontinuities. Three major factors influence the performance of a fabricated product: stress, material, and defects [60]. The interrelation between these factors is illustrated in Fig. 29. Design of the product takes into account the stresses and specifies the material, so that these two factors are fairly known and controllable to some extent. Modern design theories make use of the concept that welds with defects can be accepted if sufficient

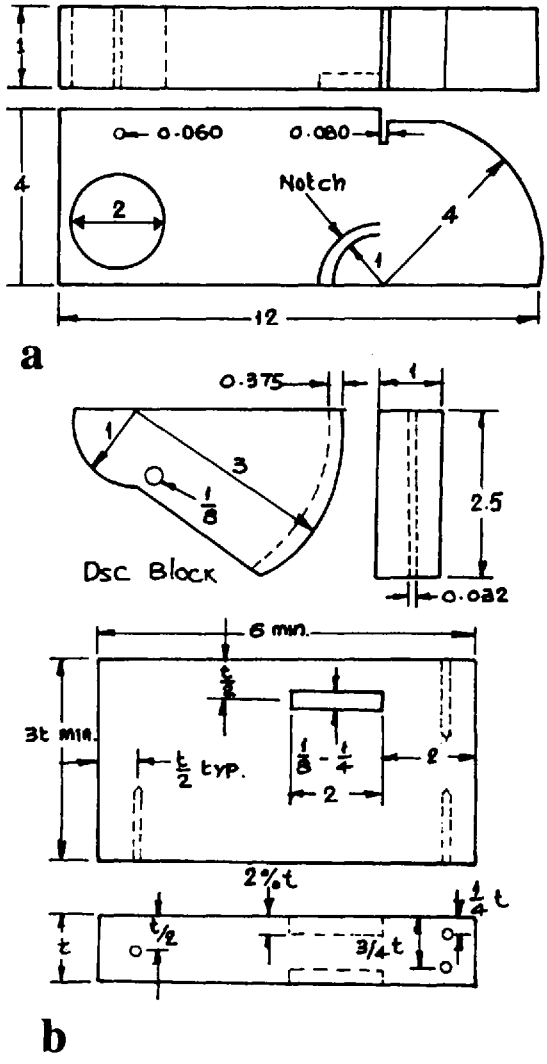


Figure 28 UT reference block. (a) DSC block; and (b) ASME block. (From Ref. 50.)

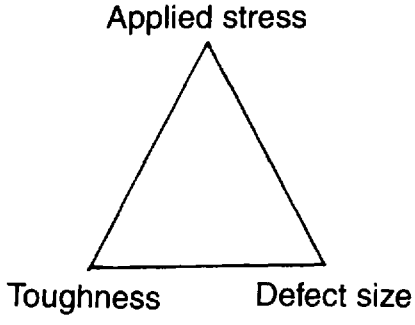


Figure 29 Factors influencing performance of a fabricated product. (From Ref. 60.)

and accurate data are available about the detail of the defects and residual stresses present [49]. Fracture mechanics allows calculation of the critical defect size, i.e., the limiting size between failure and no failure of the product. If the defect is larger than the critical defect size, then the failure is likely to occur. If the defect is smaller than the critical defect size, then the risk of failure is small. Before attempting any remedial action, particularly with thick welds, it is essential that the depth of any imperfection be determined so as to assess its importance and to assist in its removal should that be considered necessary [33].

Crack Evaluation

Fracture mechanics analysis requires a knowledge of both the length and extent in depth of a crack, with the latter being the more important factor. Radiography cannot easily indicate crack depth, since this requires continuous density measurement (with a light beam of the order of 10^{-2} mm wide) across the crack image [49]. However, the well-established radiographic tube shift method may be used for depth location [33]. The UT technique provides actual defect size and position, which are then treated mathematically to determine under what service conditions failure may occur or the discontinuities need to be repaired. Alternately, acoustic emission testing can provide the location of the defect and UT can be used to determine its size. However, fracture mechanics and acoustic emission testing have limits to their uses, especially for tough, low-strength steels.

10.18 What's New in UT?

Some important developments in the field of UT examination in the recent years are:

1. An ultrasonic probe, installed and left in place or attached to a moving fixture, provides a continuous scan of a test part.
2. Automated ultrasonic inspection of weld defects. Computer based ultrasonic imaging system and automatic scanners for automated inspection of defects give permanent record, post processing of signal for detailed analysis, online imaging and 3-D imaging of defects, display of defects in plan, side, end and isometric views, compares the test with previous tests and, where differences are noted, reinspects the area and operator independent evaluation.
3. Ultrasonic plus eddy current. Southwest Research Institute, San Antonio, TX, has successfully combined UT and eddy current in order to simultaneously inspect the surface of a reactor vessel. It is capable of precise location of small cracks [51].
4. Weld scan probes. Several new weld scan probes were developed whose benefits include instant results, that couplant is not necessary, the effects of probe lift-off, that permeability variations and natural conductivity variations are minimized, and that whether welds have reinforcement, flush ground, or are of dissimilar metal, there is a probe type for the application [51].
5. Portable UT equipment is available with digital operation and microprocessor controls. They can be introfaced with computers and can provide hardcopy printouts on video monitoring and recording.

11 ACOUSTICAL HOLOGRAPHY

Acoustical holography is an NDT technique that uses ultrasound to evaluate the interior integrity of a weld or a test object. Holography is basically a two-step process for creating a whole image. In the first step, the amplitude and phase of any type of coherent waves reflected from the object are recorded in a suitable medium by using the principle of interferometry. This record is called a *sound hologram*. In the second step, the wave motion is reconstructed from

the hologram by a coherent laser beam, by using the principle of diffraction, which results in the regeneration of a three-dimensional image of the interior of the test object. Ehlman [61] describes the principle and applications of acoustical holography. Acoustical holography is mainly used for thick materials used for pressure vessels, castings, forging, etc., and inspection of welds in thick and thin materials, contouring of the surfaces, and inspection of nozzle welds. At present, two types of acoustical hologram systems are available: the liquid surface type and the scanning type. Scanning-type equipment is mostly used.

11.1 Merits and Comparison of Acoustical Holography with Radiography and Ultrasonic Testing

In conventional ultrasonic testing, it is difficult to obtain exact information concerning the location, shape, and size of the flaws. Using acoustical holography, a single scanning operation provides top, side, and three-dimensional images that completely characterize weld defects [61]. Ehlman [61] lists the following advantages of acoustical holography over radiography/UT:

1. Standard radiography and UT have limited resolution capability for inspection of thick material due to the widening effect of x-rays and of the ultrasonic beam. Acoustical holography uses focused-beam transducers, which offer good resolution, even on thick material.
2. Acoustical imaging can show a thin horizontal crack that radiography may miss. It is less sensitive to defect orientation than radiography.

11.2 Holographic and Speckle Interferometry

Advanced NDT techniques such as laser holography interferometry (HI) and speckle interferometry (SI) have demonstrated their usefulness for inspecting nuclear pressure vessels and piping. The techniques are suited to measuring deformation resulting from residual stresses or mechanical behavior of materials or fatigue.

12 ACOUSTIC EMISSION TESTING

Acoustic emission testing (AET) offers a new method for analyzing various physical phenomena and behavior of materials, and for performing nondestructive testing of materials, manufacturing processes, and structural components [62]. As an NDT technique, it is used to detect when a flaw or crack occurs and sometimes where it occurs in a wide variety of structures and materials, such as metals, wood, plastic, fiberglass, and concrete. However, the determination of the kind of flaw is normally left to the other methods.

12.1 Principle of Acoustic Emission

Acoustic emission (AE) is the phenomenon of transient elastic wave generation due to a rapid release of strain energy caused by a structural alteration in a solid material. The release of acoustic emission is illustrated in Fig. 30. When a discontinuity approaches a critical size, the acoustic emission count rate increases markedly, warning of impending instability and failure. The emission of transient elastic waves or sound waves can be detected by placing a sensor on the surface of the material. The amplitude of an acoustic emission is proportional to local strain in the base material at the AE site. A time–amplitude noise signature generated during the crack growth can be used to indicate the failure process likely to emanate from the site.

Source of Acoustic Emission

Generally, the structural alterations are the results of either internally generated or externally applied load or due to various physical or failure modes. Physical phenomena and failure modes that can release AE are described in Refs. 62 and 63 and are given in Table 11.

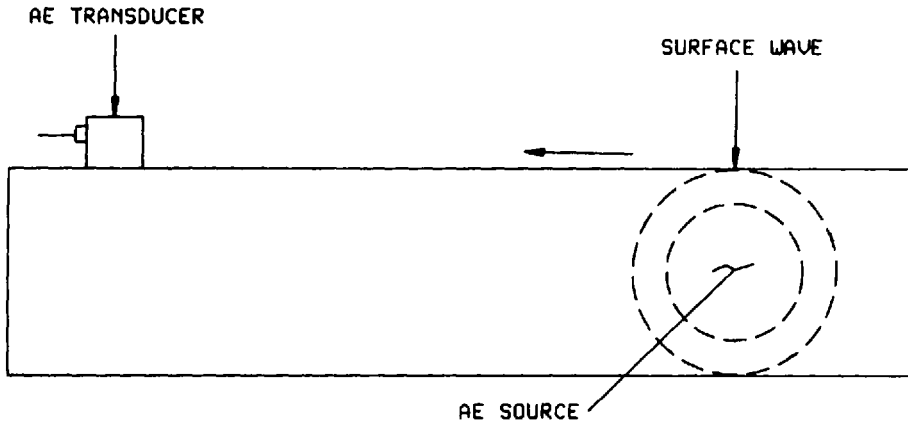


Figure 30 Release and propagation of acoustic emission in a material and the principle of acoustic emission testing. (From Ref. 62.)

Figure 31a shows a body under stress with an initial flaw, and Fig. 31b shows the development of this defect either due to plastic deformation or microcrack initiation. Since acoustic emission reveals its existence during its growth, this leads to one of the advantages of the method: real-time monitoring.

12.2 Emission Types and Characteristics

Basically the AE signals have been classified into two different types [64]: burst type and continuous type. These wave forms are shown schematically in Fig. 32. The characteristics of these wave forms are discussed by Baldev Raj et al. [65]. Both the emission types are generated by discrete processes. The difference between these two types is in the average repetition rate. Some of the differences of these two emission types are as follows [63]: (1) Small releases of strain energy cause burst emissions. The superposition of many repetitive bursts gives the appearance of continuous emission. (2) The amplitude and frequency of continuous emission are usually lower than those of burst emission. (3) In metals and alloys, continuous emission is thought to be associated with the dislocation movements, whereas burst-type emissions are generated by twinning, microfolding, excessive porosity, inclusions, and the development of microcracks.

12.3 Kaiser Effect

An important feature of acoustic emission is its irreversibility. If a material is loaded to a given stress level and then unloaded, usually no acoustic emission will be released upon immediate

Table 11 Physical Phenomena and Failure Modes that Can Release AE

Plastic deformation (dislocation movement, grain boundary slip, twinning, etc.)	Crack growth
Creep, stress rupture	Corrosion, including stress corrosion cracking, corrosion fatigue, and hydrogen embrittlement
Ductile/brittle transition temperature	Metallurgical changes like yielding and crystal dislocations
Phase transformations	Fiber breakage and delamination in composites and overlays
Seismic activity in geological materials	
Leakage of a fluid from a pressure component	

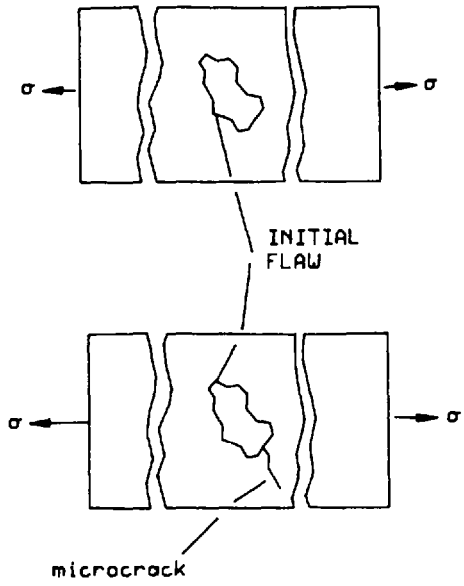


Figure 31 Body under stress with (a) initial flaw, and (b) flaw growth. (From Ref. 62.)

reloading until the previous load has been exceeded. This is known as the *Kaiser effect*. This property has an important practical implication because it can be used in the detection of subcritical growth of flaws, such as stress corrosion cracking, fatigue crack growth, and hydrogen embrittlement.

12.4 Reference Code

ASME Code Section V covers AE examination of metal vessels and fiber-reinforced vessels. Section VIII, Division 1 does not include AE for inspection vessels made as per this section.

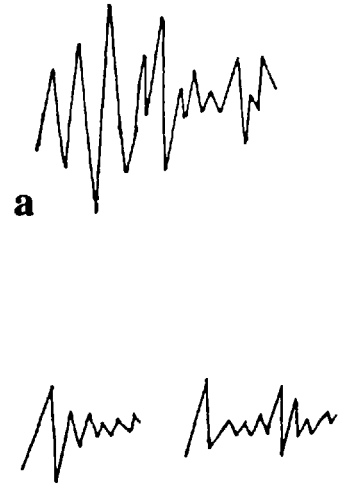


Figure 32 Acoustic emission types. (a) Continuous; and (b) burst.

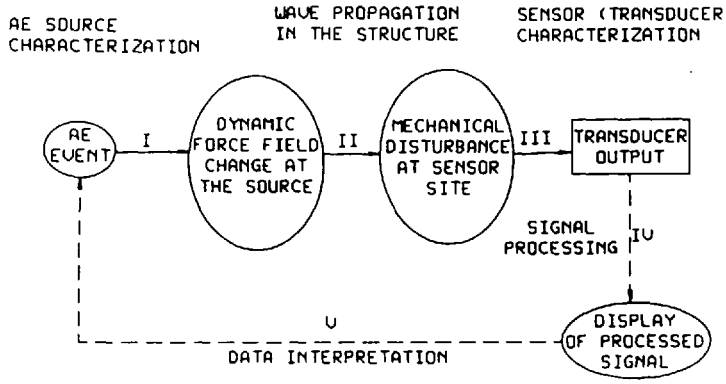


Figure 33 Acoustic emission events. (From Ref. 65.)

12.5 Written Procedure

The written procedure to be applied during an acoustic emission examination usually specifies [63]: (1) the equipment to be used, (2) the placement of acoustic emission sensors, (3) the process for stressing the component, (4) the data to be recorded and reported, and (5) the qualifications of the personnel operating the equipment and interpreting the results.

12.6 AE Testing

A block diagram of the chain of AE events [65] is shown schematically in Fig. 33, and a block diagram of typical acoustic emission instrumentation is given in Fig. 34. The important items of the instrumentation are as follows: (1) a sensor (piezoelectric crystal device) with frequency response between 20 and 600 kHz, (2) a preamplifier to convert signals from 10 μV to 1–10 V DC, (3) high-pass or bandpass filters to eliminate mechanical and electromagnetic noises, (4) an amplifier, (5) a threshold detector, and (6) a counter.

12.7 Signal Analysis

To use AE monitoring, the noise generated by the flaw growth should be picked and the extraneous background noise should be suppressed. One can sort out sound by three characteristics: frequency, amplitude, and rate of occurrence [66]. There are several ways to process the

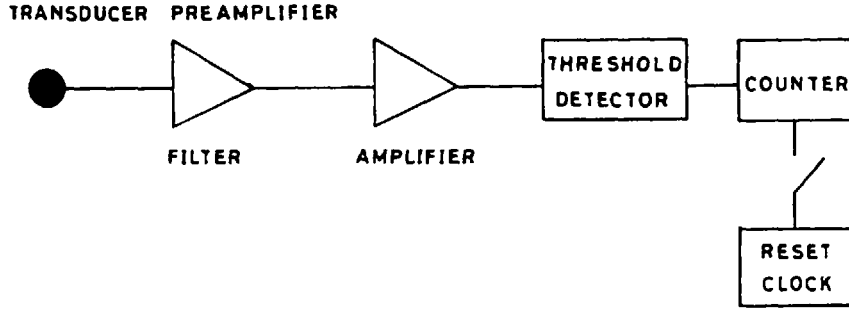


Figure 34 Acoustic emission testing instrumentation for ring down counting method. (From Ref. 62.)

AE signal. The following are the more common ways by which signals are processed: ring-down counting analysis, energy analysis, amplitude distribution analysis, and frequency analysis [62]. However, the most widely used method for the analysis of acoustic emission signals is ring-down counting, which involves the counting of the number of threshold crossings, called counts. Ring-down counting has the major advantages of simplicity and practical effectiveness. Figure 35 shows a representation of an acoustic emission signal, and different parameters characterize the acoustic emission events, like [62] (1) A, peak amplitude; (2) D, signal duration; (3) N, number of counts per event; (4) R, rise time; and (5) U, energy.

12.8 Factors Influencing AE Data

The factors that influence AE data include [65] source characteristics, structural characteristics of the medium, frequency passband, and gain of amplifiers and threshold level.

12.9 Applications—Role of AE in Inspection and Quality Control of Pressure Vessels and Heat Exchangers

Acoustic emission techniques can be successfully used for the following applications [63]:

1. Nondestructive testing of pressure vessels
2. On-line monitoring of pressure vessels
3. Monitoring of welds
4. Detecting of environmental cracking and environmental degradation
5. Monitoring of thermal shock
6. Monitoring of weld overlays
7. Detection of creep failures at welds [67]
8. Leak testing of pressure vessels [34,68]

Proof Testing of Pressure Vessels and Heat Exchangers. Pressure vessel testing has been one of the most successful areas of application of acoustic emission technique. This method is used

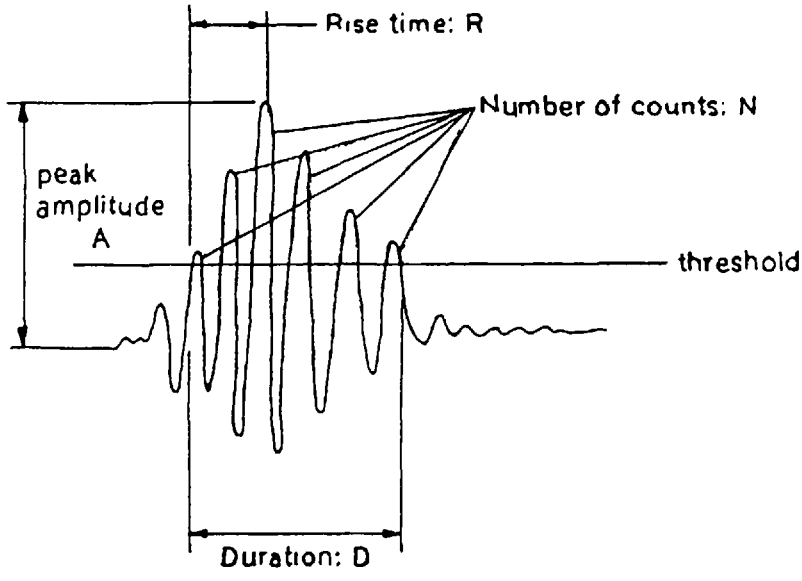


Figure 35 Acoustic emission signal parameters. (From Ref. 62.)

extensively for preservice proof testing, periodic requalification testing, and in continuous on-line monitoring of pressure vessels [63]. When discontinuity approaches critical size, the acoustic emission count rate increases markedly, warning of impending instability and failure.

Online Monitoring. AE is produced when the component undergoes a dynamic change such as deformation, crack growth, phase change, or leakage of a fluid from a pressurized compartment. Hence, continuous on-line monitoring is possible [68].

Monitoring of Welds. AE can monitor and detect failure modes that generate acoustic emission, such as phase transformations, lack of fusion, lack of penetration, voids and porosity, inclusions and contamination, and cracking. The technique offers great promise for preliminary weld screening prior to NDT and for welder training [66].

Environmental Cracking. AE is used for detecting environmental cracking phenomena such as corrosion fatigue, hydrogen embrittlement, and stress corrosion cracking.

Thermal Shock. Frequently, vessels subject to thermal stress cycles are monitored during temperature cycling, during startup, or during shutdown.

Weld Overlays. AE can monitor separation and delamination of weld overlays.

Detection of Creep Failure at Welds. Acoustic emission has been used to study reheat cracking, a form of brittle creep rupture that occurs in the heat-affected zones of welds during stress relief [67].

Leak Detection. Leak detection by AE testing method provides rapid quantitative information. The method is as follows: In the absence of any leak, the AE activity will only be a minimum, caused by the background noise. In the presence of a leak, pressure release from inside the vessel results in the generation of AE that can be detected by the sensor.

12.10 Merits of Acoustic Emission Testing

The advantages of AET are discussed in Ref. 63. Some of the advantages are:

1. In AE monitoring, there is no input energy to the structural system/material as in the case of ultrasonic testing or radiography.
2. AE has the capacity to locate and evaluate discontinuities in the entire structure at one time, rather than selectively testing localized regions.
3. AET may be used as a means for confirming the location and concentration of discontinuities determined by techniques such as radiography and ultrasonic examination.
4. The use of AET with fracture mechanics and ultrasonic examination may allow the complete characterization of a pressure vessel and its life can be predicted.
5. It requires only limited access and downtime for the requalification of in-service structures.
6. AE monitoring on production lines is faster than ultrasonics because its sensors need not be moved over the entire surface being inspected.

13 EDDY CURRENT TESTING

Eddy current testing (ET) is widely used for the nondestructive testing of tubular products. The basis of eddy current testing is the detection of quality problems by observation of the interaction between electromagnetic fields and metals. In this method, a small electric current, known as an eddy current, is induced in a material, and any changes in the flow of this current due to a flaw or inhomogeneities in the material are detected by a nearby coil and subsequently processed electronically. Basically, any discontinuity that appreciably alters the normal flow of eddy current can be detected by eddy current inspection. In heat exchanger and pressure vessel applications, the areas of applications of ET are

1. Production-line inspection of tubular products during manufacture to detect seams, laps, cracks, voids, inclusions, etc., on conductive metal surfaces.
2. In-service inspection of tubes for service-induced defects such as loss of tube wall thickness due to corrosion, fretting and wear, and growth of manufacturing defects.
3. For surface, and in some cases subsurface, inspection of welds for discontinuities.

13.1 Principles of Eddy Current Testing

In eddy current testing, an alternating current is made to flow in a coil (probe), which, when brought into close proximity of the conducting surface of the material to be inspected, induces an eddy current flow in the material. The presence of a defect, a discontinuity, or a metallic object other than the specimen under test disturbs the eddy current flow. These eddy currents in turn generate an alternating magnetic field, which will cut the windings of the coil and try to produce a reverse current. This reverse current may be detected either as a voltage across a secondary coil or by the perturbation of the impedance of the original coil. This impedance change can be measured and correlated with the presence and extent of the defect, discontinuity, or metallic object. The test coil is placed in a unit called a measuring probe. The process lends itself to automated production-line testing. The eddy current testing principle explained in this section is based on Granville [69] and Ref. 70.

13.2 Written Procedure

ASME Code Section V furnishes the minimum information necessary in the written procedure. A partial list includes the following:

1. Scope of examination: for tubing examination, tube material, diameter, and wall thickness.
2. Size and type of probes.
3. Examination frequencies.
4. Eddy current equipment model and manufacturer.
5. Scanning direction and speed during examination.
6. Inspection technique, e.g., hand probe, mechanized probe, remote-control fixtures.
7. Calibration procedure and standards.
8. Description of data-recording equipment and procedure.
9. Signal processing and acceptance criteria.
10. Reporting results.

13.3 ASTM Specifications

E 426 for electromagnetic (eddy current) testing of seamless and welded tubular products of austenitic stainless steel and similar alloys
E 215 for testing of aluminum alloy tubes
E 309 for steel tubular products with magnetic saturation
E 243 for seamless copper and copper alloy tubes

13.4 Probes

Probes can be classified into four categories [34,71]:

1. Surface probes, which are used for crack detection and corrosion measurements.
2. Encircling probes, which are used primarily for production control of wire or tubular products (Fig. 36a).

3. Internal bobbin probes, which are used to check tubings (Fig. 36b).
4. A new development is the rotating probe (Fig. 36c), also known as ID surface riding "pancake coil" (RPC); it can locate very small defects and determine their exact location on the circumference.

Probe Configuration

Two basic probe coil configurations are used for tube inspection. They are (1) the absolute probe configuration which consists of a single coil as shown in Fig. 37a, and (2) differential probe configuration, which consists of two coils connected in opposition as shown in Fig. 37b. The absolute probe is sensitive to gradual changes in tube dimensions such as gradual tube thinning, but relatively poor sensitive for small, sharp defects such as pitting. In differential probes configuration, the net induced voltage is canceled out when the coils experience identical conditions. Because of this, differential probes are highly sensitive to sharp defects such as pitting, but not sensitive to defects such as gradual tube thinning [69].

13.5 Eddy Current Test Equipment

Eddy current test equipment covers a range from simple units to fully automatic systems. In general, the eddy current equipments will incorporate these elements:

1. A source to provide an alternating current of required frequency to excite the test coil.
2. A modulating device consisting of a test coil and test object combination, which brings out desired information in the form of an electrical signal.
3. Signal processing.
4. Signal display.

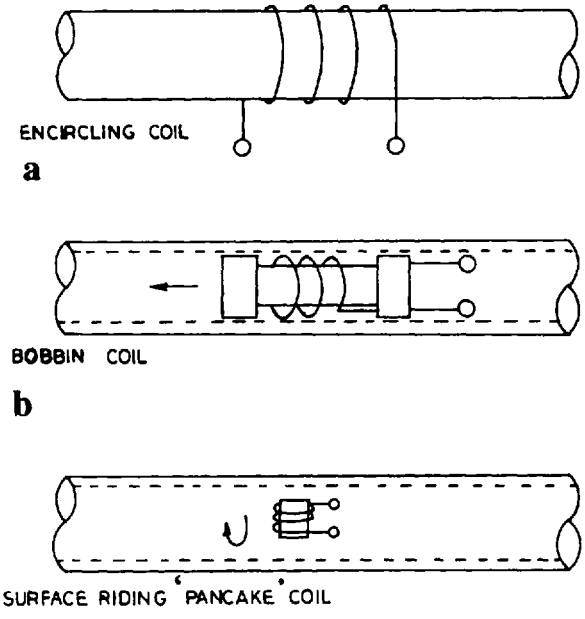
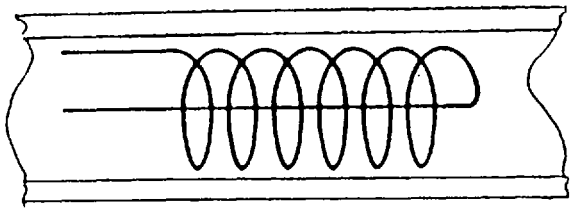
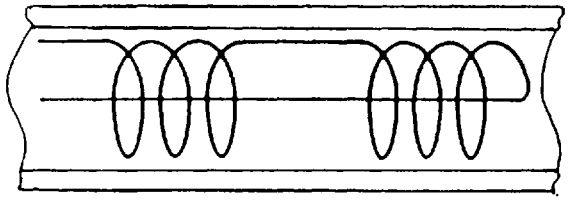


Figure 36 Eddy current testing probes. (a) Encircling probes; (b) internal bobbin probes; and (c) rotating probes. (From Ref. 71.)



a



b

Figure 37 Eddy current probe configuration. (a) Absolute probe; and (b) differential probe. (From Ref. 69.)

13.6 Signal Processing

Eddy current signals are vector quantities and have both amplitude and direction (phase). The amplitude and phase of the signals can be displayed on a cathode-ray oscilloscope. In the case of tube inspection, the phase of the signal can give information regarding the depth and defect origin [69].

13.7 Inspection or Test Frequency and Its Effect on Flaw Detectability

Generally, test frequencies used in eddy current inspection range from 200 Hz to 6 MHz or more. Frequency has a direct bearing on the ability to penetrate the component wall thickness. At lower frequencies, penetration is greater, but the sensitivity to flaw detection decreases, whereas at high frequencies, the depth of penetration is lower, and small flaws remain undetected as the depth increases. An optimum frequency should be selected so that the penetration is sufficient to reach any subsurface flaw. When detecting flaws at some considerable depth below the surface, i.e., a thicker part, very low frequencies must be used and sensitivity is sacrificed [70].

13.8 Operating Variables

The principal operating variables associated with eddy current inspection include coil impedance, electrical conductivity, magnetic permeability, liftoff and fill factors, edge effect, and skin effect. Fill factor, edge effect, skin effect, depth of penetration, and frequency are discussed next.

Depth of Penetration and Frequency

The depth of penetration of eddy current is a critical factor. For example, in the case of tube inspection, if the eddy currents do not penetrate the wall thickness, then it will miss the defects. The depth of penetration of eddy current is given by the following equation [69]:

$$\tau = \frac{500}{\sqrt{\sigma \mu f}}$$

where τ is the standard depth of penetration (mm), σ the conductivity ($m/\Omega \cdot mm^2$), μ the magnetic permeability, f the test frequency (Hz), and μ is the magnetic permeability (1 for nonmagnetic materials), and f is the test frequency (Hz).

The standard depth of penetration is generally taken to be that depth at which the eddy current field intensity drops to 37% of the intensity at the conductor surface. For tube inspection, the test frequency is often the frequency at which the depth of penetration is equal to the tube wall thickness. This is given by the equation [69]:

$$f = \frac{250}{\sigma t^2} \text{ kHz}$$

where t is the tube wall thickness (mm).

When phase analysis is being applied, the f_{90} frequency, that is, the frequency at which there is a 90° phase difference between signals from the inside wall of the tube and signals from the outside wall, will be used. The f_{90} frequency is given by the equation [69]:

$$f_{90} = \frac{3\rho}{t^2} \text{ kHz}$$

where ρ is the resistivity ($\mu ohm \cdot cm$).

Fill Factor and Probe Size Requirements

The probe size requirements for eddy current tube testing are determined by the "fill factor," given by the expression [69]:

$$\text{Fill factor} = \left[\frac{d_1}{d_2}\right]^2$$

where d_1 is the diameter of the probe and d_2 the inside diameter of the tube.

For an internal or bobbin type coil, the fill factor indicates how well the inspection coil fills the inside of the tube being inspected. Ideally the fill factor should be close to 1.0. A fill factor of 1.0 will not allow smooth travel of the probe inside the tube. Therefore, as a thumb rule, the optimum fill factor for tube testing can be about 0.70 [69]. This allows reasonable sensitivity to be achieved while still maintaining adequate clearance when dirt or dents may be present in the tube.

Edge Effect

When an inspection coil approaches the end or edge of a part being inspected, the eddy currents are distorted, because they are unable to flow beyond the edge of the part. The distortion of eddy current results in an indication known as "Edge effect". In general, it is not advisable to inspect any closer than ⅛ in (3.2 mm) from the edge of a part [70].

Skin Effect

Eddy currents are not uniformly distributed throughout a part being inspected. They are densest at the surface immediately beneath the coil and become progressively less dense with increas-

ing distance below the surface. This phenomenon is known as "skin effect." At some distance below the surface of a thick wall there will be essentially no current flowing.

13.8 Inspection Method for Tube Interior

The probe, usually an internal bobbin type, is introduced into the tube under test and passed along the length of the tube to the far end, usually by means of compressed air, but also by other means. It is then withdrawn from the tube at a constant speed, typically in the range of 0.5 to 1.0 m/s, using a winch unit [34,69]. During the probe withdrawal, the eddy current signals are recorded on a chart and analyzed further. The tube inspection method is shown schematically in Fig. 38.

Inspection of Ferromagnetic Tubes

The highly ferromagnetic nature of carbon steel and ferritic stainless steels severely limits the application of standard eddy current technique. Nonferromagnetic materials have a relative permeability of approximately 1, whereas ferromagnetic materials have typical relative permeabilities of 500–2000. Since the higher the permeability is, the lower is the depth of penetration, eddy currents in ferromagnetic materials are concentrated at the surface, and hence buried or back-wall defects remain undetected. Also, small variations in permeability give rise to relatively high noise levels [69]. This limitation is overcome by saturating the ferromagnetic tubes magnetically with a direct current, so that the material reacts as nonmagnetic material when inspecting [34], or by remote field slit eddy current (RFEC) technique. The drawbacks of these two methods are discussed by Bergander [72]. Such drawbacks are as follows: (1) Since magnetic saturation uses high amperage current for saturation, there is a need for probe cooling, the possibility of false indications due to variations in permeability, difficulty in detecting gradual tube thinning, and complicated probe design. (2) To make the RFEC technique sensitive to gradual wall thinning, the probes has to be complex. To overcome these difficulties, Bergander [72] suggests using a magnetic flux leakage method to examine ferritic tubes. The principle of flux leakage as applied to ferrous heat exchanger tubing is illustrated in Fig. 39.

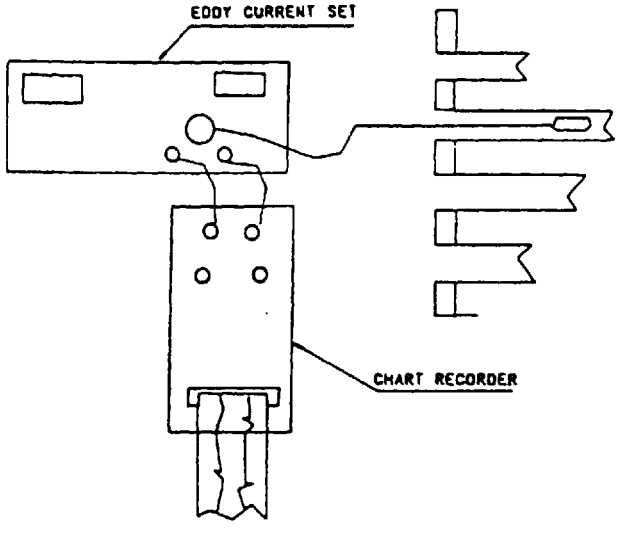


Figure 38 Tube inspection by eddy current testing method. (From Ref. 69.)

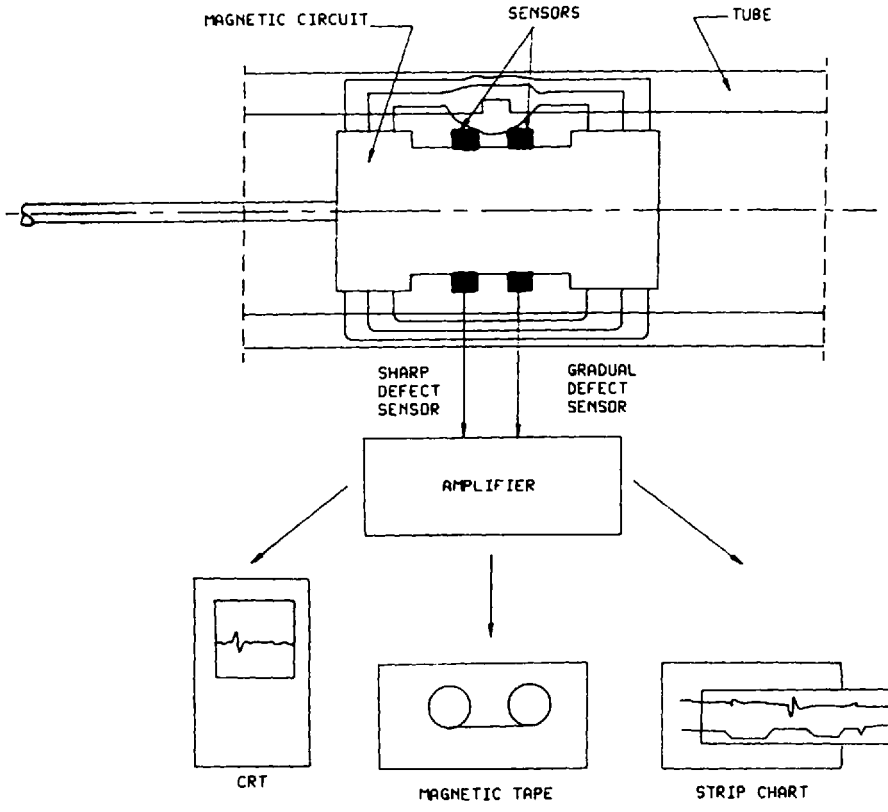


Figure 39 Principle of flux leakage inspection of ferrous tubes. (From Ref. 62.)

13.9 Testing of Weldments

Because of the circumferential orientation of eddy currents flow, this method is effective in detecting most types of longitudinal weld discontinuities such as open welds, and weld cracks. On the other hand, difficulty arises for the detection of a thin planar discontinuity that is oriented substantially perpendicular to the axis of the cylinder.

13.10 Calibration

In order to provide accurate and repeatable results, artificial defects of known size are introduced into a specimen piece of tube of the same material and dimensions as the tubes to be inspected. Reference defects can be of various types. The most commonly used reference standard consists of a number of through holes in a tube as shown in Fig. 40, along with their signal pattern [73].

13.11 Remote Field Slit Eddy Current Testing

The remote field slit eddy current (RFEC) inspection technique is similar to the ET method, which uses low-frequency alternating current and through-wall transmission to inspect pipes and tubes from the inside. The method is most preferred to apply to ferromagnetic materials

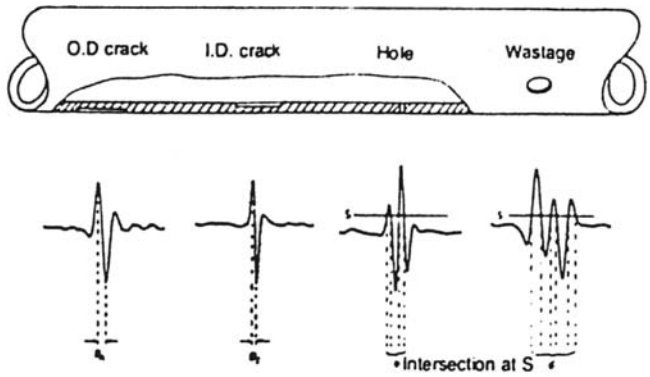


Figure 40 Reference standard for eddy current testing. (From Ref. 73.)

because conventional eddy current testing techniques are not suitable for detecting opposite-wall defects in such materials unless the material is saturated [74].

Principle. The principle of RFEC is explained in Ref. 74 and by Atherton et al. [75]. A typical RFEC probe, shown schematically in Fig. 41, uses a relatively large internal exciter coil, which is driven with a low-frequency alternating current. A detector coil is placed near the inside of the pipe wall, but axially displaced from the exciter coil by about two pipe diameters. Two distinct coupling paths exist between the exciter and the detector coils: (1) the direct path inside the tube, which is attenuated rapidly by circumferential eddy currents induced in the tube wall, and (2) the indirect coupling path that originates in fields that diffuse outward through the pipe wall in the vicinity of the exciter. Anomalies anywhere in this indirect path cause changes in the magnitude and phase of the received signal, and can therefore be used to indicate defects. This method has been used primarily for inspecting well casing, small-diameter boiler tubes, and heat exchanger tubes.

Merits and Demerits. An important advantage of this method is that the method has higher sensitivity to axially and circumferentially oriented flaws in ferromagnetic materials. This allows detecting corrosion damage due to erosion–corrosion, tube wall thinning, pitting, and

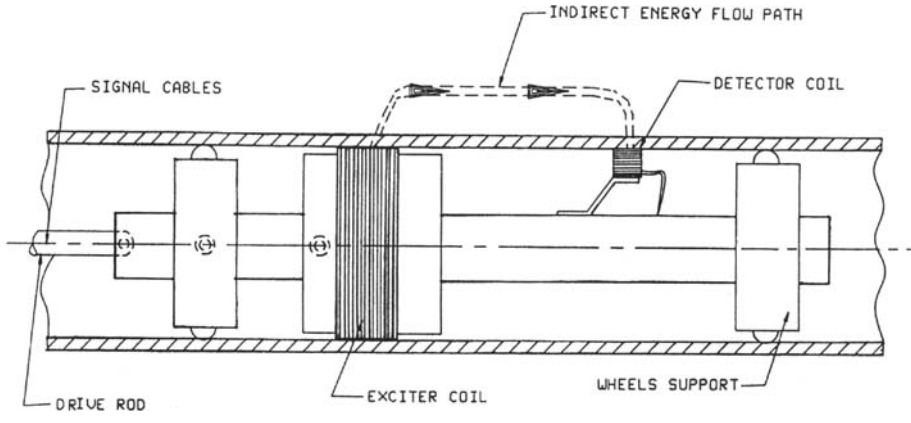


Figure 41 Remote field eddy current inspection technique. (From Ref. 75.)

stress corrosion cracking [74]. The major disadvantage is that when applied to nonferromagnetic material, it is not generally as sensitive or accurate as conventional eddy current testing method.

13.12 Merits of ET and Comparison with Other Methods

ET is attractive because it offers both very high sensitivity and relatively high scanning speeds. Direct contact with the test material is not required and a coupling medium is not necessary; the process is repeatable, the test method is relatively fast, and it can be easily automated.

13.13 Limitations of Eddy Current Testing

The major limitations of eddy current testing are:

1. Skin effects usually restrict the depth of inspection. It is generally limited to 0.25 in (6.4 mm) for nonferromagnetic materials and 0.010 in (0.25 mm) for ferromagnetic materials [28]. The limitation due to high permeabilities of ferromagnetic materials may be significantly overcome by magnetic saturation of the area being inspected or by flux leakage method.
2. Since many variables, namely, permeability, conductivity, probe position, and weld contour, can affect an eddy current signal, an accurate measurement of one property requires the ability to eliminate or at least considerably reduce interference from other properties [76]. Multifrequency techniques are used in practice to increase the information content of signals [73]. A classical solution, due to recent developments in ET, which can reduce but not eliminate this problem, is the application of different ET probes [71].

Other limitations include [69]:

3. The signal is more closely related to volume of material lost than to wall thickness lost.
4. Defects at the tube sheet, and at the tube and baffle plate interface, can be difficult to detect.
5. For critical applications, results may need to be verified by an alternative technique.

13.14 Recent Advances in Eddy Current Testing

The development of computer interfacing for data collection, analysis, and display has led to multiple-frequency testing, eddy current imaging, multiple-element eddy current probes, and automated data interpretation systems that significantly enhance both the capabilities and reliability of the eddy current inspection [71].

13.15 Tube-Sheet Diagram for Windows

The tube-sheet diagram for Windows (TSD) is computer software intended for use by inspection groups in the oil, gas, and power industries to inspect tubes periodically in heat exchangers, boilers, steam generators, chillers, air conditioners, and similar multitube equipment and to award a classification based on user-defined criteria such as corrosion severity, material type, defect position, etc. [77]. TSD is shown in Fig. 42.

Automated Tube Inspection System (ATIS)

ATIS is a software package that carries out automated analysis of the data from eddy current and electromagnetic in-service tube inspection systems in real time [78]. The system discriminates between baffle support plate signals and defect signals and can be utilized on a wide variety of tube materials. The results are classified in terms of defect severity and stored in a

hard disk, from which they can be retrieved and summarized at any time. TSD can accept manual input from the keyboard or the mouse and can also import results from the silver-wing ATIS (automatic tube inspection system) data files. Presently the system is compatible with both standard eddy current instruments and the CENTEST 91 ferrous tube inspection flaw detector.

14 LEAK TESTING (LT)

Leak testing (LT) is a nondestructive testing technique used for the detection and location of leaks and for the measurement of fluid leakage in either pressurized or evacuated vessels and components [79]. A leak may be a crack, fissure, hole, or passage that admits any fluid or lets fluid escape. The operational reliability and serviceability of many devices under pressure or vacuum is greatly reduced if sufficiently large leaks exist. Leak testing is performed for three basic purposes:

1. To prevent material leakage loss.
2. To prevent environmental contamination or hazards, particularly ones that involve handling of radioactive or lethal fluids.
3. To detect unreliable components.

For pressure vessels and heat exchangers, leak testing is used to ensure the leak-tightness of various welded joints, flanged joints, tube-to-tube-sheet joints, mechanical joints, enclosures, etc.

14.1 Written Procedure

Leak testing procedures should encompass one or a combination of the following [80]:

Locating leaks
Determining the leakage rate
Monitoring for leakage

ASME Code Section V specifies the minimum information to be provided for the LT procedure, which include the following:

1. Scope and extent of the examination.
2. Type of equipment to be used for detecting leaks or measuring rate of leakage.
3. Surface cleanliness and surface preparation.
4. Leak test method.
5. Temperature, pressure, gas and percentage concentration to be used.

14.2 Methods of Leak Testing

The basic principle of leak testing involves identification and location of the leaks or the measure of the flow of fluid or the testing medium quantitatively through the leak. This could be the actual flow rate, drop in pressure or vacuum level, etc. Various leak testing methods are detailed in Refs. 79 and 80, ASME Code Section V, and Yokell [18]. The following are the different leak testing methods available, arranged in a rough order of increasing sensitivity.

1. Ultrasonic detection
2. Bubble test—direct pressure technique or immersion technique, or vacuum box method
3. Gas leak lake testing
4. Pressure change test

5. Halogen diode detector probe test
6. Helium mass spectrometer detector (sniffer) probe technique
7. Helium mass spectrometer tracer probe technique
8. Helium mass spectrometer hood method.

Tests for gross leaks involve direct visual inspection for signs of tracers or leakage products, or scanning of leaking systems with an ultrasonic leak detector to locate the sources of hissing sounds. Small leaks can be detected by sophisticated leak testing methods utilizing tracer gases such as halogen vapors and helium with detectors such as the heated anode halogen detector and the helium mass spectrometer, respectively. Leak testing methods listed in items 1 to 8 are discussed next. Yet another method of leak testing is acoustic emission testing, and this method is explained in the section on acoustic emission.

Ultrasonic Leak Detection

The leakage of a gas through small openings, even for small pressure differences, generates noise in the ultrasonic range. Therefore, it is possible to detect the leaks by listening for them using an ultrasonic listening device, which can record low noise levels produced in the high frequencies (40–50 kHz) that occur due to turbulent flow [34].

Bubble Testing

Bubble testing can be performed by the direct pressure technique or vacuum-box technique. The direct pressure technique using bubble solution is the more common one.

Bubble Testing, Direct Pressure Technique. The objective of the direct pressure technique is to locate leaks in a pressurized component by application of a solution or by immersion in liquid that will form bubbles as the leakage gas passes through it. To perform this test, pressurize the shell with inert gas or air; the required pressure differential can be from 1 kg/cm^2 to 1.25 times the design pressure of the vessel but less than 20 kg/cm^2. After sufficient pressure soak time, apply a soap solution over the joints. Generally the surfaces must be in the temperature range of 40–125°F (4.5–52°C). This method can detect leaks of the order of 10^{-5} pascal m^3/sec when the test objects are immersed in detection liquids.

Bubble Testing, Vacuum Box Technique. The objective of the vacuum box technique is to locate leaks in a pressure boundary that cannot be directly pressurized. In this method, on one side of the test joint after application of soap solution, vacuum is created and if there are any through leaks, atmospheric air from the other side will come out to the vacuum side and will be observed as the formation of a bubble.

Gas Leak Lake Testing

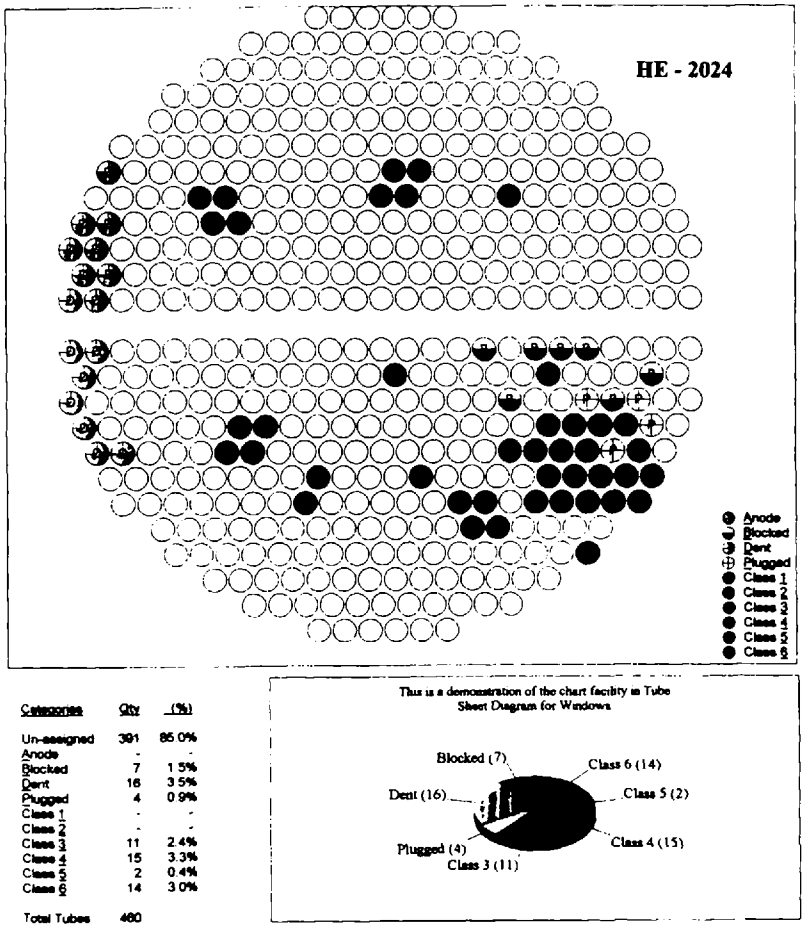
For this method, pressurize the shell side of the heat exchanger with air or nitrogen to the maximum allowable working pressure (MAWP) at room temperature, set the unit vertically. With a ring of about 2 in height (50.8 mm), make a dam on the tubesheet face. Fill the tube side with water to the level of the dam, and observe for bubbles.

Pressure Change Test

This test method describes the technique for detecting the leakage rate of the boundaries of a closed compartment or the vessel at a specific pressure or vacuum by indicating pressure or vacuum change over the given time period.

Halogen Diode Detector Testing

Principle. A detector or a sniffer sucks a mixture of air and leaking tracer gas through a tubular probe into an instrument that is sensitive to small amounts of tracer gas. The tracer gas can be a halide gas (Refrigerant 12) to a maximum of 25% of the design pressure. A heated



Categories	Qty	(%)
Un-assigned	391	85.0%
Anode	-	-
Blocked	7	1.5%
Dent	16	3.5%
Plugged	4	0.9%
Class 1	-	-
Class 2	-	-
Class 3	11	2.4%
Class 4	15	3.3%
Class 5	2	0.4%
Class 6	14	3.0%
Total Tubes	460	

Figure 42 Tubesheet diagram for Windows.

Suitable for use in...
- Power Generation Plant
- Oil and Gas Refining
- Petro-Chemical Plant
- Air Conditioning Plant
- Engineering and Contracting
- Plant Maintenance
- Onshore and Offshore Utilities
- Inspection Departments
- Service Inspection Companies

Use the Report Generator to create a complete report...
- add or delete frames to meet individual preferences,
- drag and drop frames anywhere on the page,
- resize diagrams, chart, or text for ease of viewing,
- use text only to create title pages and written reports,
- report on any Windows compatible printer (colour or b/w),
- print in A3, A4, US Letter, US Legal, etc.,
- use portrait or landscape orientation.

Some of the TSD features include...
- User defined templates with up to 200 x 200 tubes,
- Up to 48 user defined tube classifications per template,
- Up to 12 tube shapes to aid recognition,
- Unlimited number of data Layers per template
- Unlimited colours for tube fills, and tube borders
- Automatic generation of Charts and Tables

TSD can report and analyse the results of almost any tube inspection method including eddy currents, ultrasonics, CCTV, material types, mechanical properties, etc.

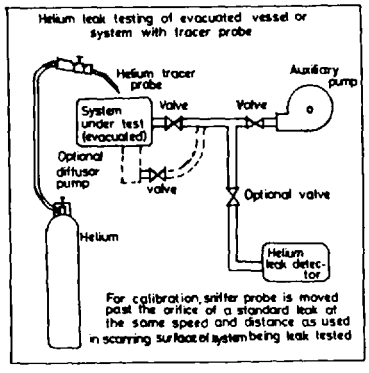
TSD is fully compatible with Silver Wing 'ATIS' data files

platinum element (anode) in the detector ionizes the halogen vapor, and the ions are collected on a cathode plate. A current proportional to the rate of ion formation is measured.

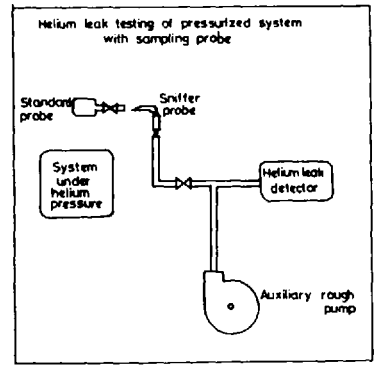
Leak Testing Method. Traverse the tube ends with a probe at a distance of about ⅛ in (3.2 mm) and at a predetermined scanning rate using a standard leak. Also, insert the probe into the tube ends for about ¼ in (6.35 mm). Check for cracked tube ends by inserting the probe into each tube end to a minimum depth of ¾ in (19 mm) and holding it there for about 3 sec. If the tubes are welded to the tube sheet, check the welds by encapsulating each tube end with a funnel connected to the probe [11]. When the tubes are too small to allow the probe to enter and too close to each other for effective scanning, use the halogen sniffer in a bag test system. The halogen diode detector leak test method is a semiquantitative method to detect and locate leakages and should not be considered quantitative. The sensitivity of this method is 10^{-6} Pa·m^3/sec.

Helium Leak Detection Methods

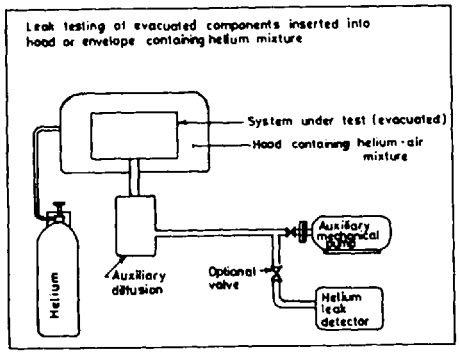
Principle. For the manufacture of nuclear components, leak testing using helium as a tracer gas is one of the mandatory code and customer requirements. Helium leak detection can be done either by pressurizing the vessel with helium and sniffing (detector) the welds or joints



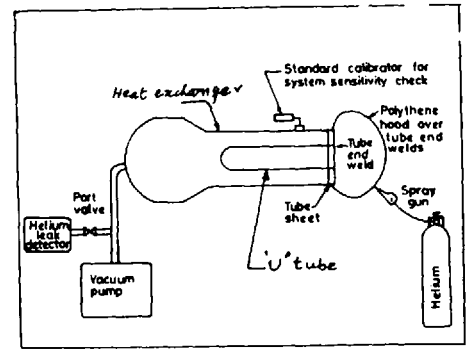
a



b



c



d

Figure 43 Helium mass spectrometer testing. (a) Tracer probe technique; (b) detector probe technique; (c) vacuum technique or hood method; and (d) typical test set-up. (a-c from Ref. 79.)

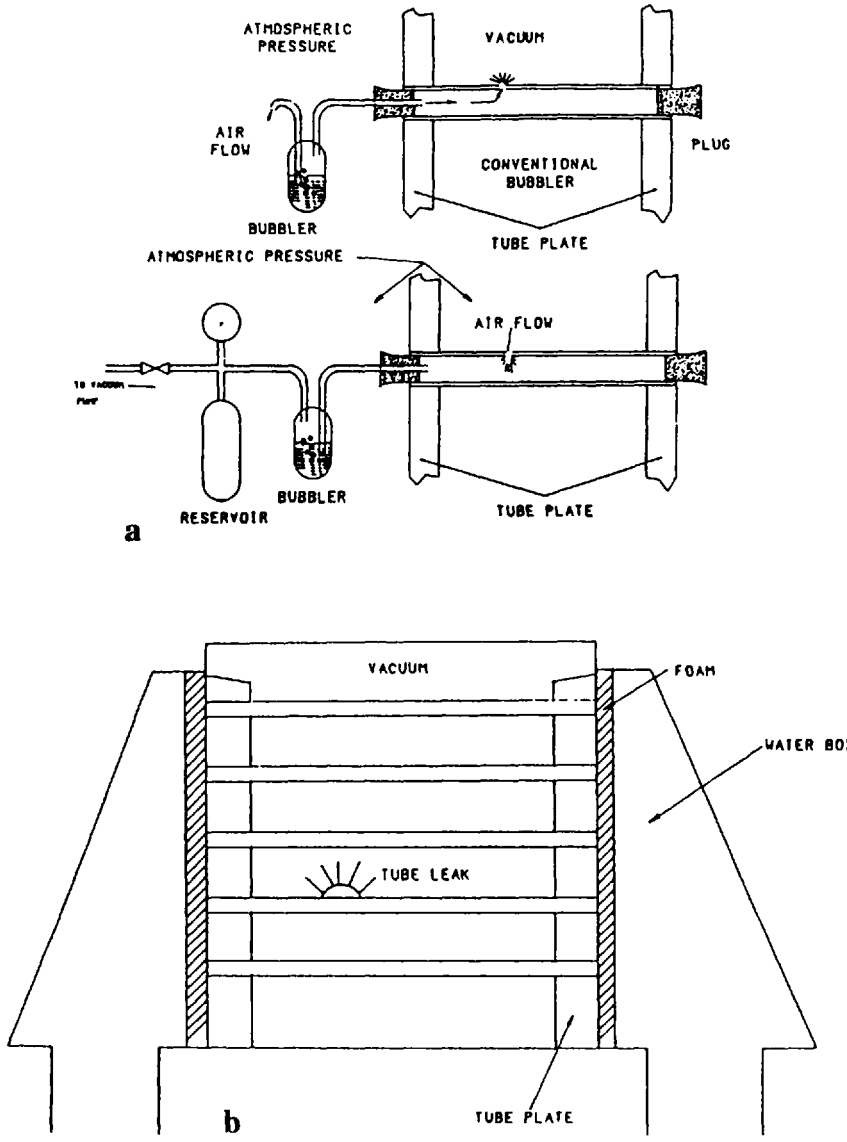


Figure 44 Inservice examination of leaks using. (a) Bubbler; and (b) soap foam. (From Ref. 43.)

from outside or by evacuating the vessel and spraying helium on the welds from outside by a tracer probe or enclosed in a vacuum mask. In each case, the helium atoms passing through a leak are collected to a mass spectrometer, where they are ionized. The current proportional to the quantum of ions is amplified and measured as the leak rate.

Helium Mass Spectrometer Test. The basic methods of helium leak detection include [79]:

1. Detector probe technique
2. Tracer probe method
3. Vacuum technique or hood method

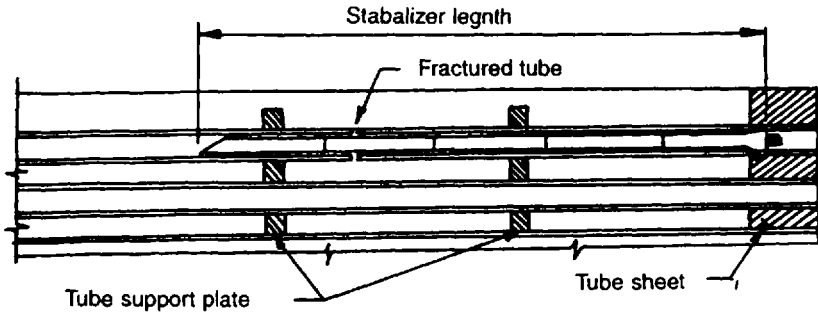


Figure 45 Plugging fractured tube using tube stabilizer. (Courtesy of M/S Expando Seal Tools.)

Detector Probe Technique. The detector probe technique, as shown schematically in Fig. 43a, involves pressurizing the vessel to be leak tested with certain percentage of pure helium and sensing the leaking helium using the detector probe, which is moved at a definite speed over all the joints to be tested. Any leakage from the pressurized system is detected by the mass spectrometer leak detector. The detector probe is a semiquantitative technique to detect and locate leakages and should not be considered quantitative. The sensitivity of this method is of the order of 10^{-7} Pa·m^3/sec.

Tracer Probe Method. In the helium tracer probe method as shown in Fig. 43b, the mass spectrometer leak detector is connected to the internal volume of an evacuated vessel or heat exchanger while helium is sprayed from the probe at each joint and is moved over the external surface to detect the specific locations of leaks. Any leakage into the vacuum side is detected by the mass spectrometer leak detector. The tracer probe is a semiquantitative technique to detect and locate leakages and should not be considered quantitative.

Vacuum Technique or Hood Method. The vacuum technique or hood method involves evacuating the vessel to be tested and filling with almost 100% helium or air–helium mixture in the enclosing mask and detecting the inflow of helium to the vessel under vacuum through leaks if any, using the instrumentation as shown schematically in Fig. 43c. This is a quantitative measurement technique. The high sensitivity of the hood technique makes possible the detection and measurement of total helium gas flow from the high pressure side. The sensitivity of this method ranges from 10^{-7} to 10^{-11} Pa·m^3/sec. ASME Code Section V accepts only the helium hood method (vacuum technique) as quantitative.

In-Service Examination of Heat Exchangers for Detection of Leaks

In-service examination of leaks, either using pressurized air or vacuum technique or bubbler, is shown schematically in Fig. 44. Fractured tubes at the interior section can be plugged using tube stabilizers (Fig. 45), marketed by M/s Expando Seal Tools [81].

15
Heat Exchanger Fabrication

1 INTRODUCTION TO FABRICATION OF THE SHELL AND TUBE HEAT EXCHANGER

With advances in material and welding technology, fabrication processes today call for high standards of understanding and workmanship. Equipment made with materials of correct choice and quality and adequate design may fail in service if the workmanship is sacrificed during fabrication [1]. It is needless to say that failure of any heat exchanger in service due to bad manufacturing practices, apart from causing loss of production, may cause accidents and damage to the equipment and property. Therefore, in industries where heat exchangers are to be made as per code, it is essential that the product quality be controlled at all stages of its manufacture. This section details standard shop floor practices for fabrication of heat exchangers.

The detailed methods of shop floor practices are left to the discretion of the manufacturer in conformity with TEMA Standards [2]. The applicable construction code is ASME Code Section VIII, Div. 1 [3]. The manufacturer shall submit for purchaser's approval three prints of an outline drawing showing overall dimensions, nozzle sizes and locations, supports, and weight. The purchaser's approval of drawings does not relieve the manufacturer of responsibility for compliance with TEMA Standard and applicable code.

2 DETAILS OF MANUFACTURING DRAWING

Manufacturing drawings for heat exchanger fabrication should contain some additional details than any other engineering drawing. Such additional details for the fabrication of heat exchangers are listed by Rao [4]. Some of the details pertaining to welding and testing plan are [4]:

1. Name plate location and details
2. Weld line orientations and locations, weld profiles and sizes
3. Testing plan indicating the tests to be conducted on welds, and assemblies such as NDT test, destructive tests, hydrotest/pneumatic test, etc.

4. Welding plan to show WPS reference to each weld
5. Technical delivery conditions of materials
6. Edge preparation and method employed
7. Electrodes with equivalent AWS specifications
8. Welding methods to be employed
9. Code certification and stamping requirements as indicated in the purchase order
10. Maximum allowable working pressure
11. Design pressure
12. Hydrotest pressure
13. Operating temperature
14. Design temperature
15. Minimum design metal temperature

2.1 Additional Necessary Entries

Rao [4] recommends the following additional entries in the drawing:

Code requirements
Volume of pressure chambers
Special loadings
Corrosion allowance
Joint efficiency
Joining method other than welding (e.g., brazing, adhesive bonding, rolling-in of tubes)
Surface treatment (e.g., painting, pickling, coating, lining)
Inspection authority
Instructions for the jobsite (e.g., assembly weld)

3 STAGES OF HEAT EXCHANGER FABRICATION

The main stages of heat exchanger manufacture are as follows [1]:

1. Identification of materials
2. Edge preparation and rolling of shell sections, tack welding, and alignment for welding of longitudinal seams
3. Welding of shells, checking the dimensions and subject to radiography
4. Checking the circularity and the assembly fit ups, including nozzles
5. Tube sheets and baffles drilling
6. Tube bundle assembly and insertion of the assembly into the shell
7. Tube-sheet to shell welding
8. Tube expansion
9. Tube-to-tube-sheet joint welding
10. Heat treatment
11. Assembly of channel with shell assembly
12. Hydrostatic testing and stamping
13. Preparation for shipment
14. Preparation of data folder

A flow chart for the manufacture of fixed tubesheet heat exchanger is shown in Figure 1.

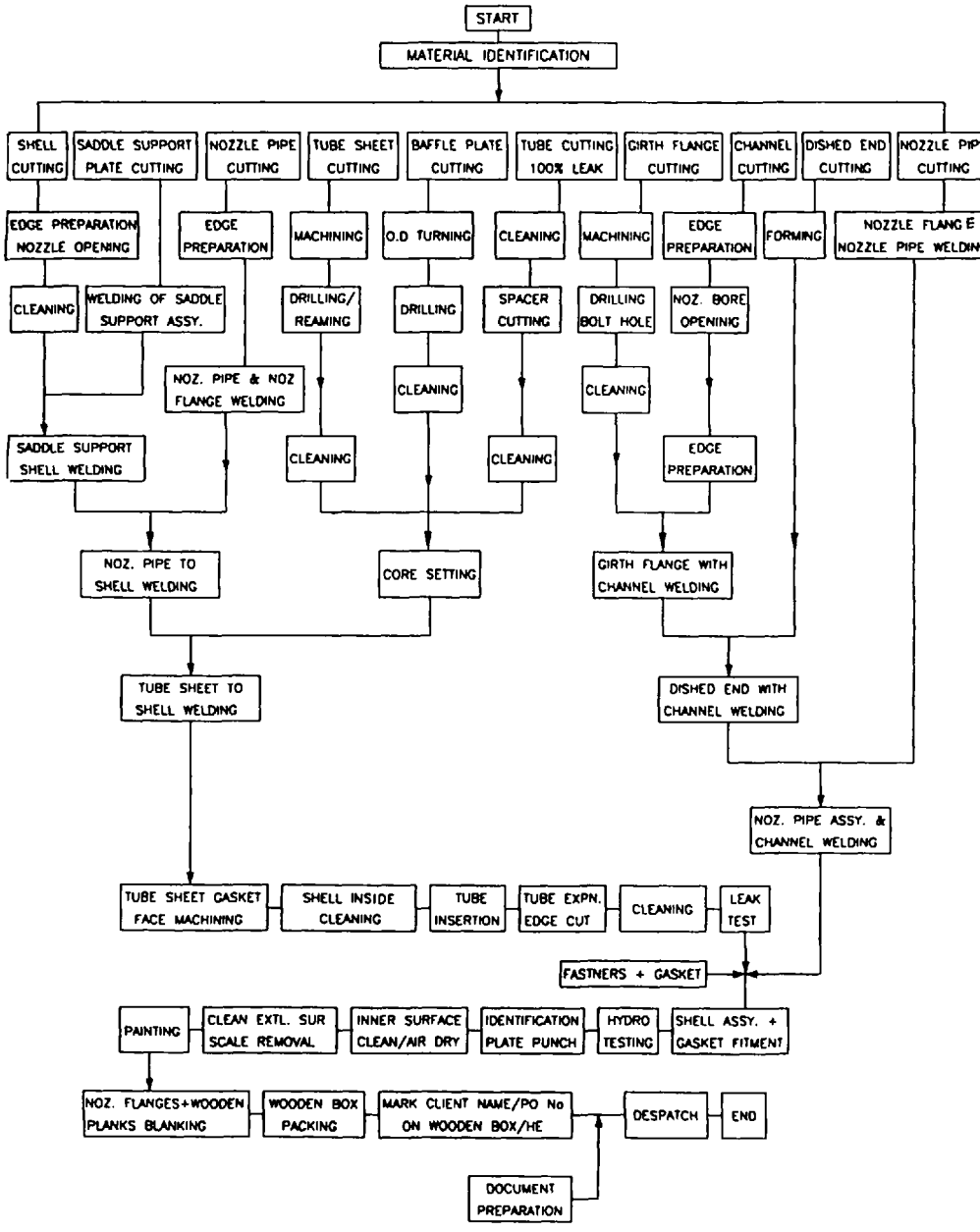


Figure 1 Flow chart for manufacture of fixed tube sheet shell and tube heat exchanger. (Courtesy of Universal Heat Exchangers Ltd., Coimbatore, India.).

3.1 Identification of Materials

Identification includes a job number, serial number, and heat number, if relevant. Throughout production, identification follows the material or component, assuring traceability [5]. The certified plates fall into two categories. One type certifies the physical and chemical properties, while the other type, in addition to chemical and physical properties, also certifies soundness

of material by ultrasonic tests. Ultrasonic tests are used to detect defects like lamination, porosity, and slag inclusions.

3.2 Edge Preparation and Rolling of Shell Sections, Tack Welding, and Alignment for Welding of Longitudinal Seams

General Discussion on Forming of Plates

In general, the forming of plates in the pressure vessel industry covers the bending of plates into shell courses/belts and spinning and pressing of circular plates to form vessel heads. The most critical factors governing the cold forming of a shell course in a given material are (1) the plate thickness and (2) the final diameter of the finished cylinder. Therefore, the radius of bending is limited to a maximum percentage strain in the outer fiber in the range of 3 to 4.5% without an intermediate annealing or stress relief [6]. According to Peacock [6], since local straining during cold bending may cause higher values of strain in localized areas, in practice, a factor of safety is adopted to limit the strain in the outer fibers to 2 to 2.25%. The strain ε on the outer fibers of the shell has been calculated by Carpenter and Floyd [7] as follows:

$$\varepsilon = \frac{R_1 R_2 - 0.5 R_1 t}{R_1 R_2 - 0.5 R_2 t} - 1 \tag{1}$$

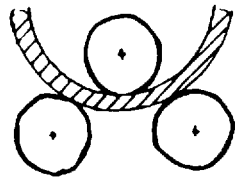
where R_1 is the final radius, R_2 the initial radius (for a flat plate use a value of 1000 in), and t the thickness of plate.

After forming the shell/dished ends, the manufacturer should examine them to make certain that they conform to the prescribed shape/contour and meet the thickness requirements after forming.

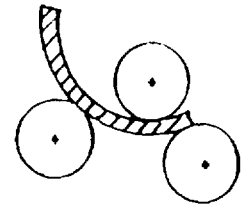
Fabrication of Shell

As per TEMA section RCB-3, the heat exchanger shell should be fabricated from either commercially available seamless or welded wrought pipe or from plate rolled (bending roll position is shown in Fig. 2a) into a longitudinally fusion-welded cylinder. In the case of rolled shells, the certified plates are put into inspection after marking the sizes as per drawing requirements. The inspector will stamp the plates with a monogram and allow for cutting.

The cutting process includes machining or gas cut or plasma arc cut. Aluminum alloy plates are mechanically cut, using midsaw bandsaws, portable handsaws, or guillotines; stainless steel is either sawn, guillotined, or cut by the plasma cutting process. Gas-cut plate edges are then machined for weld preparation. After cutting the plates to size and edge preparation, the edges of plates should be examined for defects like cracks and lamination. The plates are then rolled to the required dimensions. Edge preparation is a critical factor in the production



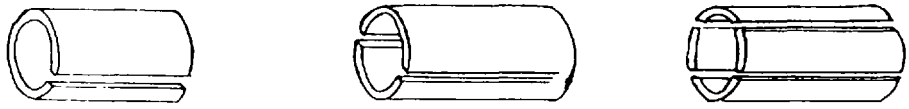
Symmetric roll position



Asymmetric roll position

(a)

Figure 2 (a) Rolled shell.



1 Plate round 2 Plates round 3 Multiple plates round

(b)

Figure 2 (b) Shell fabricated from several longitudinal seam welds [9].

of high-quality joints and in the making of sound welds. Inadequate preparation, resulting in irregular plate edges or rough Vs, prevents close fit, which is essential for quality joints and makes the task of the welder more difficult [8].

Rolling of plates should be in the longitudinal direction of the plates. The direction should be marked on the plates. For longitudinal seam welding, the rolled section is held in position by tack welding. The width, length, and thickness of the tack welds are critical. Too thin tack has an effect similar to arc strike and this local position will reveal cracks from high-carbon martensite due to rapid cooling [1]. Therefore, tacks should have sufficient metal deposition. For satisfactory welding, cleanliness of the edges to be welded is essential. Rolling machines and supporting facilities such as rotators and PWHT of rolled shells are discussed in Annexure 1.

3.3 Welding of Shells, Checking the Dimensions, and Subjecting Pieces to Radiography

After tack welding, the shell section is ready for longitudinal seam welding. During shell welding spiders are tacked internally to avoid distortion of the shell. The welding is first done from one side. The other side is back chipped or gouged and offered for inspection. The inspector examines the area for the weld metal penetration, oxidized metal removal, and the weld free from weld defects. In very large or thick-walled vessels, the shell course may be fabricated from two or more curved plates and joined by several longitudinal seam welds (Fig. 2b) [9]. Before assembly of circumferential joints, each shell course should be checked for shell thickness, inside diameter, and circularity, and shell sections may be rerolled if necessary. If any rerolling is required, it should be done before radiography, and all longitudinal seams should be dye penetrant tested after rerolling. Check the curvature using a sweep board. Circumferential welding is carried out by providing for the components to be rotated on the roller manipulator. While welding two shell sections circumferentially, the longitudinal seams of the adjacent shell courses should not be aligned. After welding the various shell courses (Fig. 3), the circumferential seams are subjected to radiography. If any portion of the weld is found defective, it should be repaired and inspected.

3.4 Checking the Circularity of the Shell and the Assembly Fit, Including Nozzles and Expansion Joints

The ovality of the shell should be kept as low as possible and the shell should be free from flat spots and projections from weld seams and nozzles. Check the positions of connections, supports, expansion joints, and all appurtenances relative to the working points [10]. The clearance between the baffles and the shell shall be as specified in the drawings. Excessive clearances would decrease the heat-transfer efficiency of the exchanger; inadequate clearance will pose a problem when inserting tube bundle. Measure the shell length at the quarter points and

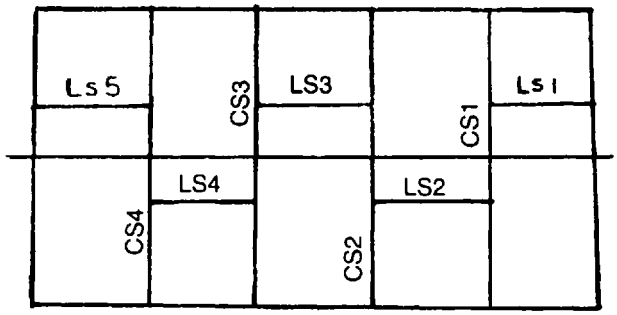


Figure 3 Welded shell courses ((CS), circumferential seam; (LS), longitudinal seam).

the nozzle and support base distances to the shell centerline. To avoid difficulty in insertion of the bundle, a pull-through gauge as shown in Fig. 4 is passed through the shell [11].

Certain advance preparation is necessary while fabricating the shell. For correcting the ovality and weld distortion, and for baffle gage checking, suitable fixtures, spiders, and innovative devices for specific type of exchanger are to be developed and kept in advance to avoid unnecessary hammering, heating, and grinding, which reduce the quality of material and weldment. In a big company manufacturing large numbers of exchangers and pressure vessels, standardization of components like elbows, flanges, nozzles, reinforcement (RF) pad designs, and edge preparation is required. This leads to smooth flow of material.

Welding of Nozzles

After completion of the shell, mark the shell for the nozzle locations, cut open, prepare edges, fit the reinforcement pad and the nozzle, weld and subject the welds of RF pad for leak test, and examine by penetrant/magnetic particle test. Inspection of back-gouged welded joints by magnetic particle or liquid penetrant examination techniques is especially important for joints of set-in nozzles, which are not readily radiographed following welding. Most shops use a special-purpose submerged arc welding machine. The welding is through the entire thickness of the shell plate. If the component to which nozzles are attached is subsequently stress relieved, it is the fabricator's responsibility to maintain true gasket faces by machining or otherwise.

Attachment of Expansion Joints

Fabrication, inspection and pressure test, stamping, and reports for flanged and flued or flanged expansion joints shall conform to the requirements of Part UG and those of (a) through (g) of

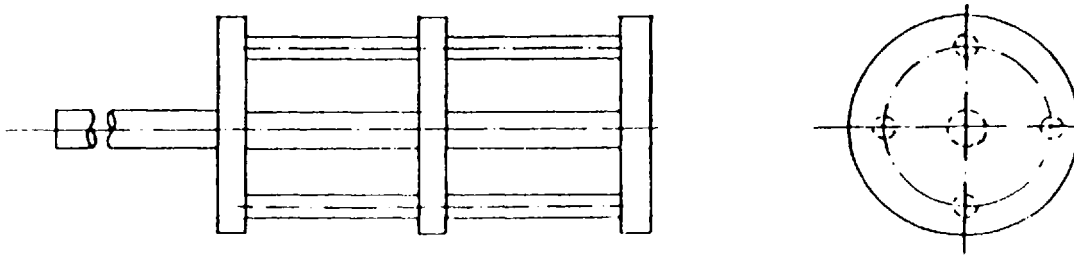


Figure 4 Pull through gauge. (From Ref. 11.)

Appendix CC of ASME Code Section VIII, Div. 1. Some of the ASME Code requirements for the attachment of expansion joint are:

1. Flexible elements shall be attached by full-penetration circumferential welds.
2. Attachments such as nozzles and backing strips shall not be located in highly stressed areas such as inner and outer torus, and annular plate of the expansion joint, unless the welds are ground flush and fully radiographed.
3. The circumferential attachment welds between the expansion joint and shell shall be examined 100% on both sides by penetrant/magnetic particle test.

3.5 Tube Sheet and Baffle Drilling

Tube Sheet Drilling

One of the major time-consuming factors in fabrication of heat exchanger lies in the marking out, drilling, reaming, and counterboring the holes in the tube sheets [12]. Most of the fabricators still use radial drilling machines for drilling of tube sheets and baffles. To avoid delays in this process and to achieve better tolerances on hole sizes and ligaments, use of numerical control (NC) drilling machine is recommended. Lubricating the holes is sometimes not allowed because the lubricant contaminates the tube-to-tube-sheet joint. Holes must be reamed to get smooth finish. After reaming, examine the tube sheets for the tube count, pitch, and the tube layout pattern, which should match the drawings. Tube hole diameters and tolerances shall conform to TEMA Table RCB-7.41. Permissible tube-sheet ligaments, drill drift, for the heaviest tube wall thicknesses shall conform to TEMA Table RCB-7-42.

Tube Hole Finish

The TEMA standard (RCB-7.43) and other manufacturers' standards specify a "workmanlike" finish for the inside surface of tube-sheet holes. In general, tube hole finish ranges from somewhat smoother than 32 rms to the roughest permissible finish. The range of commercially supplied feedwater heater, heat exchanger, and condenser tubing surface finishes is usually 60 to 100 rms [10]. Inspect the holes using a high-intensity light and a magnifying lens. The surfaces of the holes should be uniform throughout and free of scores, longitudinal scratches, spiral, annular, or axial tool marks. The inside edges of tube holes should be free from burrs to prevent cutting of tubes.

Drilling of Baffles

The complete set of baffles is bundled and the bunch is held tightly with the help of clamps or by other suitable means. The holes in baffles are drilled as per TEMA Standards, i.e., 0.8 mm over outer diameter of tube for maximum unsupported length of 900 mm or less. Tube holes are drilled 0.4 mm over outer diameter of tubes for unsupported lengths more than 900 mm. After drilling the baffles, examine baffle holes carefully for burrs and projections on the back face created by the penetration of the drill. These must be removed. It is very important to note that no undersized holes are permitted, since retubing will be very difficult. Reject baffles in which more than 2% of the holes exceed the size limits of the standard [10]. Oversized holes can enhance fretting and wear due to flow-induced vibration and can also reduce the thermal performance. Make sure that the cuts match the drawing dimensions and are free from burrs.

3.6 Tube Bundle Assembly

Tube bundle assembly consists of tubes, baffles, spacers, and tie rods. Before insertion, the ends of the tubes must be fine sand blasted to remove all traces of oxide and scale. Tube ends

are trued by cutting and deburring of the excess length. The tubes must be degreased by a strong solvent for a distance of 1.5 times the thickness of the tube sheet [13]. For a fixed-tube-sheet exchanger, the tube bundle assembly is carried out by two means: (1) assembly of tube bundle outside the exchanger shell, and (2) assembly of tube bundle inside the shell. These methods are discussed next.

Assembly of Tube Bundle Outside the Exchanger Shell

The sequences of operations are discussed in Chapter 14 with quality control, inspection, and NDT. This method has better control on tie rod and baffles set up, and it is easy to insert the tubes. The drawback of this method is that tubes in the bundle are likely to be damaged while lifting and inserting. If the tube bundle is heavy, about 10% of the tubes are inserted on the periphery of the tube sheet to make the baffle assembly true vertical and the partially assembled tube bundle is inserted in the shell. Remaining tubes are inserted after welding the tube sheet to the shell. Guide bullets in the leading end of the tube greatly assists the tubing operation [10,14].

Assembly of Tube Bundle Inside the Shell

To avoid the risk of tubes getting damaged in the case of the bundle assembled outside, some fabricators prefer to assemble tubes inside the shell. Normally, this method is possible when the shell inside diameter is sufficiently large for a person to go inside and arrange tie rods with tube sheet and baffles. The assembly procedure is shown schematically in Fig. 5, and the sequence of operations is [11]:

1. The operator will go inside the shell and arrange the baffle assembly by fixing the tie rods with the tube sheet. Insert a few tubes on the periphery to true up the baffle assembly.
2. Inspect the assembly and tack the nuts wherever required.
3. Insert more tubes on the periphery of the baffles to make these true vertical and insert remaining tubes by starting from bottom to top. Use pilots initially to guide the tubes.
4. After insertion of all tubes, the other tube sheet is fixed in its position. Push a few tubes out at the center and at the peripheral ends of the tube sheet and check the projection of the tubes before tacking and welding of the tube sheet with shell.

Tube Nest Assembly of Large Steam Condensers

Clean conditions are established within the condenser shell prior to commencement of tubing. Tubing is usually started at the bottom rows, working progressively upward. This allows personnel to exit easily.

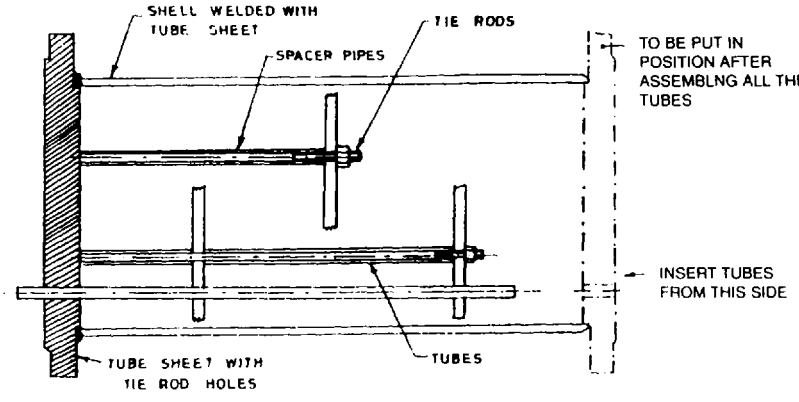


Figure 5 Scheme for assembly of tube bundle inside the shell. (From Ref. 11.)

Cautions to Exercise While Inserting Tubes

Install the tubes carefully such that the tubes do not suffer any damage. When tubes are at their upper size tolerance and tube-sheet holes are at their lower size tolerance, it is difficult to insert tubes. Misalignment of baffles and supports increases the difficulty. It is most important to set as a hold point the beginning of the tube loading and to witness this operation [10].

Assembly of U-Tube Bundle

Assembly of a U-tube bundle is always done outside the shell. The following procedure is normally adopted.

1. Insert the innermost row of the tubes through the baffle and tie rod assembly with the tube sheet.
2. After getting the inner row inspected, tubes are tacked or slightly expanded into the tube-sheet or tightly held into position by any other means.
3. Insert tubes from the center toward the outside, and get each row inspected before proceeding to the next row.
4. After all tubes are inserted, the bundle is carefully lifted with cradles and inserted inside the shell.

3.7 Tube Sheet to Shell Welding

Tube sheets are welded to the shell by various methods [10,15,16]. Some configurations of tubesheet to shell welding are shown in Fig. 6. Welding of tube sheet to shell causes distortion of the tube sheet. The distortion will increase the distance between two tube sheets at some places and reduce at some other places. This will buckle the tubes, and the effect is more prominent in stainless steel material because of its higher thermal expansion coefficient and poor thermal conductivity. Additionally, the distortion will not give a true gasket seating surface, thus causing

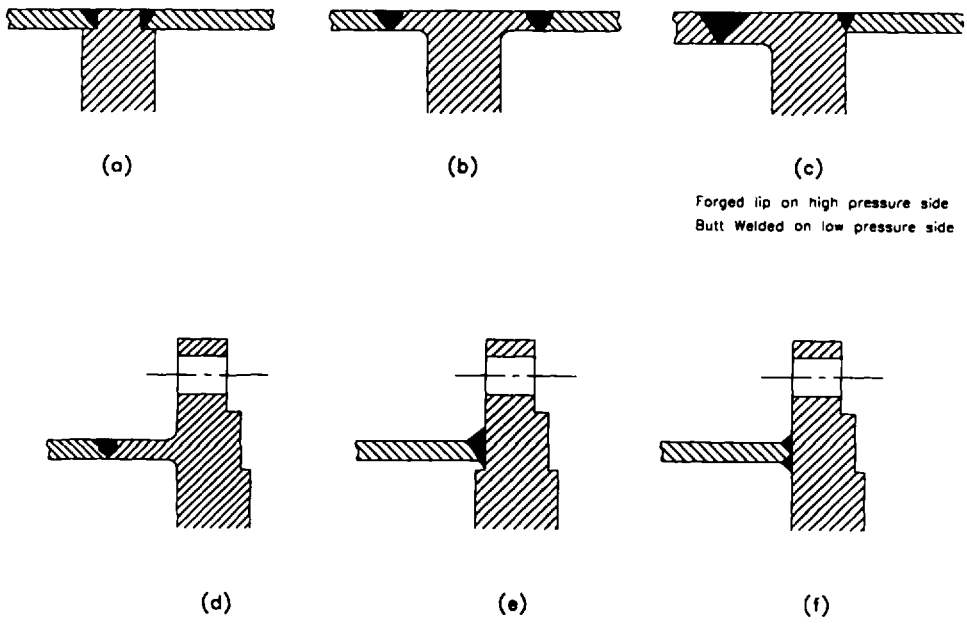


Figure 6 Configurations of tubesheet to shell welding.

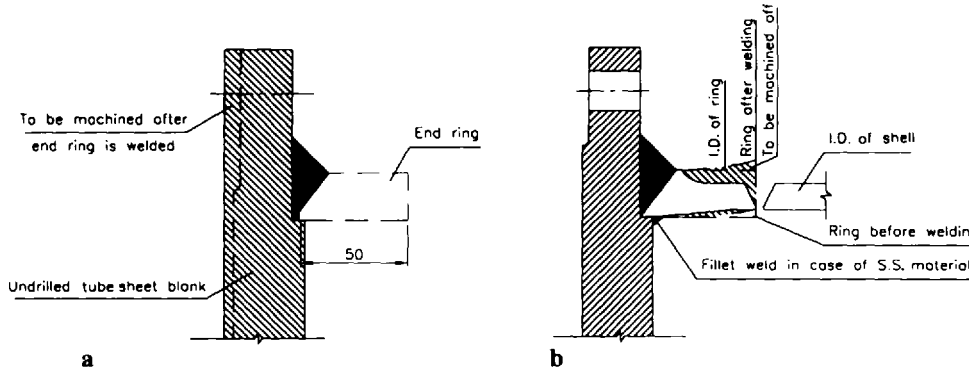


Figure 7 Tubesheet with end ring welded. (a) Before; and (b) after machining. (From Ref. 11.)

the joint to leak unless the surface is machined for its trueness. Also, the pass partition plate has to be machined as per the bow to get proper seating [10]. If the tube sheet is to be machined to suit pass partition, the effective thickness of the tube sheet will be reduced by the amount of the bow. A number of methods are used to control distortion of tubesheets:

1. Put a few long tie rods through the tubes and hold the tubesheets at various positions.
2. Put a thick plate at the face of tubesheet and tighten it. Weld this joint well with a trained and qualified welder.
3. Weld the tube sheet with shell while keeping the exchanger vertical. The tube sheet is clamped to the bed plate on which exchanger is resting.
4. Use of hubbed tube sheets with a method of joining is known as lip welding Fig. 6d.
5. Bolt, with a channel or closure to be assembled with it.
6. Use an end ring.

The end ring method is explained next.

Use of End Ring. In this method, an end ring of about 50 mm width is welded on the tube-sheet step. Suitable restraint is applied to reduce welding distortion on the tube sheet. Whatever distortion appears on the tube sheet and on the end ring will be machined prior to drilling operation. Figure 7 shows the tube sheet with end ring welded, before machining and after machining.

Caution While Welding Shell to the Tube Sheet. Before putting the welder on the actual job, some mock-up test piece should be welded and root fusion should be checked by macroetching. It is a common practice of good fabricators to give a root run by the TIG process as shown in Fig. 8 after purging the exchanger with argon gas [17]. The TIG process gives better root fusion and penetration.

In all cases, after welding the tube sheet with the shell, the joint is inspected for welding defects by RT/UT.

3.8 Tube Expansion

Expanded Tube-to-Tube-Sheet Joints

The reliability of a shell and tube heat exchanger depends upon the integrity of all tube-to-tube-sheet joints, each of which must be virtually free from defects. An effective tube-to-tube-sheet joint must be leak tight under the operating conditions of expansion and contraction,

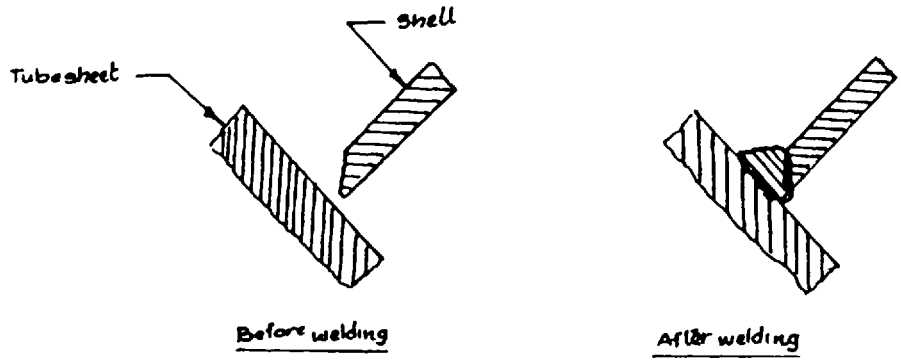


Figure 8 Root run by TIG welding. (After Ref. 17.)

pressure or vacuum, and corrosion attack. The tubes of most tubular exchangers are connected to the tube sheets by expanding only or by welding and expanding. There are several techniques for expanding tubes into the tube sheets. Three main techniques used for tube expansion are (1) rolling in, (2) explosive joining, and (3) hydraulic expansion.

Requirements for Expanded Tube-to-Tube-Sheet Joints

The connection of the tubes to the tubesheets is a critical operation. The requirements for creating the desired interfacial pressure at the tube-to-tubesheet joints are as follows [18]: (1) the tube deformation must be fully plastic; (2) the surrounding tube sheet must deflect under the pressure that the tube applies; and (3) upon pressure release, tube-sheet recovery must be greater than tube recovery. Expanding pressure beyond that required for the tube to hole contact must be applied to meet these conditions.

Tube-to-Tube-Sheet Joining Methods

Explosive Joining. Explosive joining has been successfully used to expand tubes into tubesheets by detonating a carefully sized explosive charge inside each tube hole, causing it to impact with the tubesheet and make a metal-to-metal joint with the tube sheet. Details of explosive joining have been covered in Chapter 13 with material selection and in the section on Cladding.

Hydraulic Expansion. Hydraulic forming is a relatively new method for tube-to-tube-sheet joints in heat exchangers. Hydraulic expansion of tubes into tube sheets can be done by either the bladder or the O-ring technique (also known as direct hydraulic expanding technique) [19]. In the bladder technique (Canadian Patent 1152876), a bladder is inserted into the tube and then pressurized hydraulically to expand the tube. In the O-ring technique, a mandrel with two O-rings at appropriate locations is inserted into the tube. Hydraulic pressure applied between the O-rings causes the tube in that region to expand. Compared to rolled joints, hydraulically expanded joints are weaker than rolled joints, and they are further weakened by thermal cycling [19].

Rolling-In Process. Rolling is by far the most commonly used technique. Tube expanding, known also as tube rolling or "rolling" of tubes, is the art of cold working (plastic deformation) the ends of tubes into intimate contact with the walls of tube-sheet holes. Properly executed, rolling in process produces pressure-tight joints to ensure strength and stability. Tube rolling in has been explained in detail by Sharma [1], Syal [11], Yokell [18], Fisher et al. [20], Sonnenmoser [21], Dudley [22], and in Ref. 23.

Rolling Equipment

A range of electric, electronic, pneumatic or hydraulically driven torque controlled tube expanding machines are used for the expansion of heat exchanger tubes. There are several standard types of expanders, as well as expanders built for specific purpose, each of which may be of different size and roller length. However, all work on the same principle and all have three essential parts, namely, a tapered central mandrel or pin, 3, 4, or 5 rollers of suitable length spaced equally around the mandrel, and a cylindrical roller cage that constrains the loosely held rollers in their respective positions. Most expanders are self feeding type. The roller cage may be fitted with a collar mounted on a ball bearing to prevent it from being drawn into the tube.

Basic Rolling Process

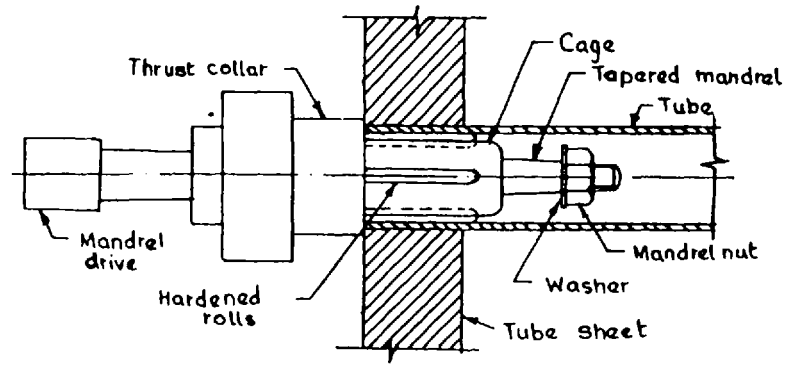
When rolling tubes, an expander as shown in Fig. 9a is inserted into the tube end and the tapered mandrel is rotated. Feeding the mandrel inward causes the expander rollers to be forced apart; by rolling over the inside tube surface, cold work the tube metal. When the tube hole is enlarged and contacts the tube-sheet hole surface, the tube sheet acts as a restraint barrier, and further expanding deforms the tube metal and forces it into more intimate contact with the tubesheet metal (Fig. 10). Since not all displaced tube metal can escape radially, it flows from the center to each end of the rolled joint. The tube-sheet metal is also affected and the hole is slightly enlarged [20]. The net result of the expanding operation is a joint condition similar to shrink-fitted shaft coupling.

Optimum Degree of Expansion

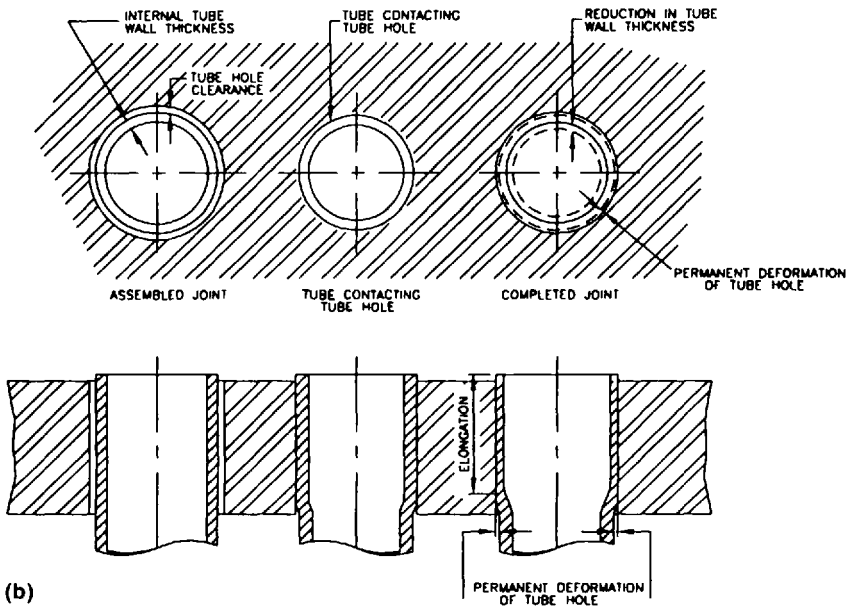
The most important task on any tube rolling job is to determine the optimum degree of expanding for a particular tube and tube sheet material combination. With the introduction of new materials and higher pressures and temperatures, the need for a control method for the rolling-in of the tubes becomes more apparent [22]. The technique used for expanding the tubes should be one that, to the greatest possible degree, avoids both under- and overrolling [23]. Underrolling results in inadequate plastic flow at the tube–tube sheet interface. This will result in leaks, and require rerolling. On the other hand, overrolling will distort the tube sheet, leading to unseating of adjacent tubes and excessive tube sheet radial expansion and/or over hardening of tubes. Therefore, it is important to roll every joint uniformly to the optimum degree. To achieve this, the rolling technique must be one that utilizes automatic control of the tube expansion rather than depending on the skill of the operator.

Methods to Gauge the Degree of Expanding

The methods employed for attaining the desired degree of expanding may be treated under two groups [20]. One is based on measuring the changes in tube dimensions like reduction in tube wall thickness, or methods that limit or measure the mandrel travel. In order to avoid the undesirable features inherent in rolling methods that employ empirical formulas or that measure changes induced by the tube rolling process, many designers prefer methods that measure the torque applied to the expander mandrel. Various rolling methods based on measure of torque employ methods like the manual "feel" method, mechanical feel method, controlled feel rolling methods, elongation or extrusion measurement, etc. Rolling by "feel" may be the most practical method of retubing, since there will generally be considerable variation in the existing tube holes [24].



(a)



(b)

Figure 9 (a) Rolling process by roller expander. (b) Permanent deformation of tube hole.

Criterion for Rolling-in Adequacy

There are many tools designed to actuate the expanding equipment, most with torque controlled by feed and speed limits and some with infinite variable controls. Optimum tube rolls may be predetermined by calculation on the basis of tube wall reduction.

Wall Reduction as the Criterion of Rolling Adequacy

The amount of wall reduction is estimated by measuring hole and tube dimensions before rolling and tube internal diameter after rolling. The following equation may be used for calculating the percent wall reduction [10]:

$$\text{Percent} = \frac{[d_t' - (d_t + \text{clearance})]\ 100}{2(\text{measured unrolled tube wall thickness, } t)} \tag{2}$$

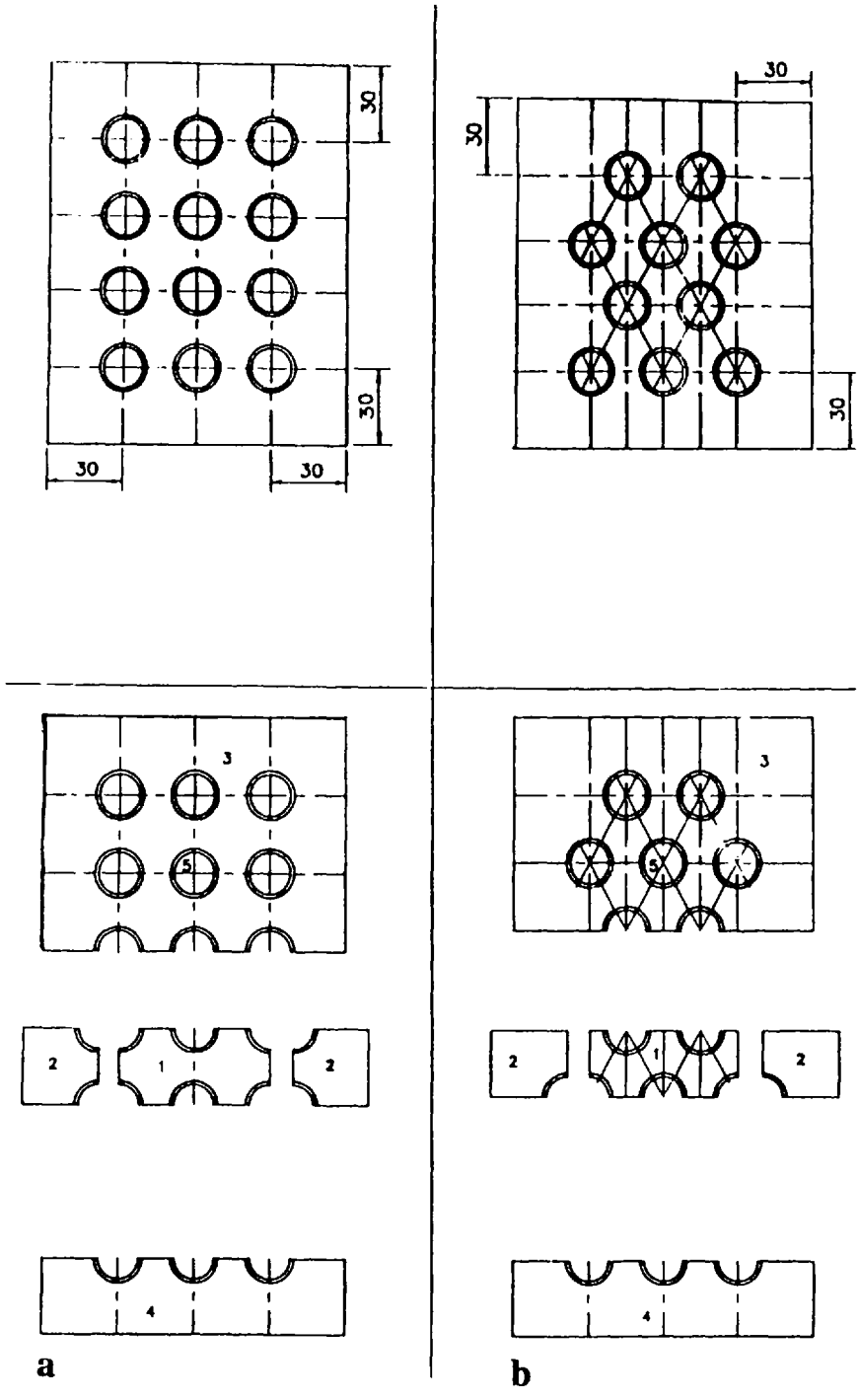


Figure 10 Mock-up model for tube-to-tubesheet expansion.

where d_i' is the tube internal diameter after rolling, d_i the tube internal diameter before rolling, d the measured tube outside diameter, and clearance the measured tubesheet hole diameter D minus d.

From Eq. (2), the desired tube inside diameter after rolling is given by:

$$d_i' = D - 2t(1 - x) \tag{3}$$

where d_i' is the tube inside diameter after rolling, D the diameter of the hole in the tube sheet, t the unrolled tube wall thickness, and x the percent of tube wall thinning.

A go and no-go gauge is made to ascertain that the tubes are properly expanded. While calculating tube dimensions after expansion, tolerances on tube outer diameter and tubesheet hole diameter and tube wall thickness must be taken into account.

Amount of Thinning of Tubes

The amount of thinning of the tubes for full expansion after metal to metal contact depends upon the tube and tube sheet material. Percentages of thinning for a few common tube materials are:

Carbon steel	5–8%
Stainless steel	3–5%
Alloy steel	4–6%
Titanium	10%
Copper alloy	4–8%

The setting of the torque control unit is established on a mock-up model.

Mock-Up Test

Before undertaking the actual tube expansion work, a mock-up model as shown in Fig. 10, is made and tested for the reliability of the tube-to-tube-sheet joints. The test specimens are full-size tube and a test block that models the tube sheets. The test measures tube-to-tube-sheet joint strength, i.e., pull-out or push-out (shear load) strength and leak tightness, and anchorage for grooved tubesheets. Pull-out strength is the axial force required to break the "bond" between the tube and tubesheet. The shear load test subjects the specimens to axial loads until either the tube or the joint fails. Control unit settings of the expanding unit, which show the amount of torque applied, are noted for individual cases. The best possible torque giving the leak tightness of the joints is then used on actual exchanger.

Length of Tube Expansion

According to TEMA, for R and B classless, tubes may be expanded into the tube sheets for a length not less than 2 in (50.8 mm) or the tube-sheet thickness minus ⅛ in (3.2 mm), whichever is smaller, and for C class, the length not less than 2 tube diameters or 2 in (50.8 mm) or the tube-sheet thickness minus ⅛ in (3.2 mm), whichever is smallest.

Full Depth Rolling

Full depth rolling on thicker tube sheets may be desirable to close the clearance between the tube and tube-sheet hole; however, in some cases this may tend to weaken the joint due to differential thermal expansion. For most stringent conditions, welding and rolling may be desirable. When this is considered necessary, the holes should be grooved near the weld face to minimize differential thermal expansion effects [24].

Joint Cleanliness

Cleanliness is one of the basic requirements for making good joints. Both tube holes and tube ends should be well cleaned from scale, rust, and dirt before assembly, and care should be taken to keep oil, soap, and other lubricants out of the unrolled joint.

Phenomenon of Tube End Growth During Rolling and the Sequence of Tube Expansion

While rolling, the rolls are always pushing a wave of metal ahead of them. As with the uniform pressure model, any pressure greater than $(2/\sqrt{3})\ \sigma_t$, where σ_t is the tube yield strength at the manufacturing temperature will cause tube end extrusion. This is the reason for the well-known phenomenon of "tube end growth during rolling" [18]. The length of elongation of the rolled tubes is of the order of a few thousandths of an inch to 1/16 in (3.2 mm) or more, depending on the size, material, and tube wall thickness, as well as the length of the joint to be rolled [20].

Tube End Growth of Fixed-Tube-Sheet Exchanger. When rolling U-tubes or tubes having sufficient flexibility to absorb the elongation, no difficulty will be experienced when rolling the second or closing end of the tubes. They should, however, be rolled uniformly in order to maintain the proper tube alignment. However, this is not true for rolling the second end of the tubes that connect second tube sheet of a fixed-tube-sheet exchanger. If the tubes are expanded sequentially, the tube extrusion can cause a tube sheet to bow and tilt out of perpendicularity. This problem in the fixed-tube-sheet exchanger is overcome by judiciously spacing and rolling in a sufficient number of so-called "tack tubes" consisting of a few tubes at six or eight equally spaced at the peripheral locations and at the center as shown in Fig. 11 [22,23]. On a finished bundle, bowed and dished tube sheets may indicate faulty tube expanding.

Figure 12, taken from Fisher et al. [20], depicts in a somewhat exaggerated form the effects of elongation created by various rolling sequences. Figure 12a shows the effect without tack tubes or other restraining means when rolling operations are carried on successively across the tubesheet. Figure 12b and c illustrate the stress conditions created by the rolling sequenced as enumerated. Figure 12d depicts the behavior of slender tubes when rolled into two fixed tube sheets. The bow shown, to a certain extent, relieves the load on the tube sheets.

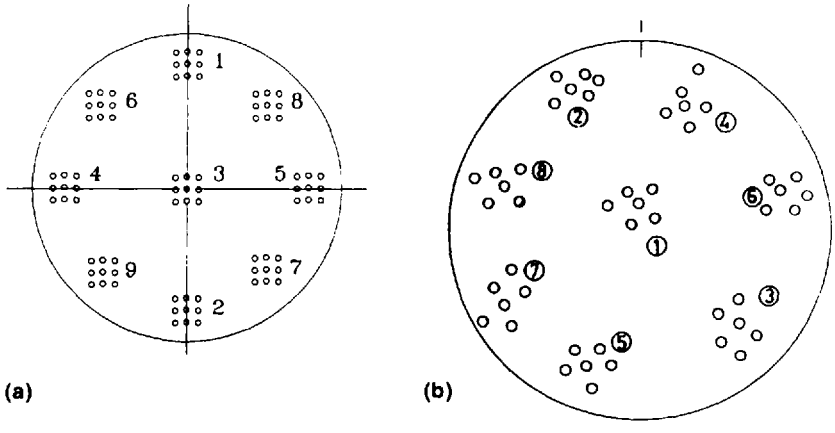


Figure 11 Tack tubes: (a) pattern I; (b) Pattern II. (From Refs. 22,23.)

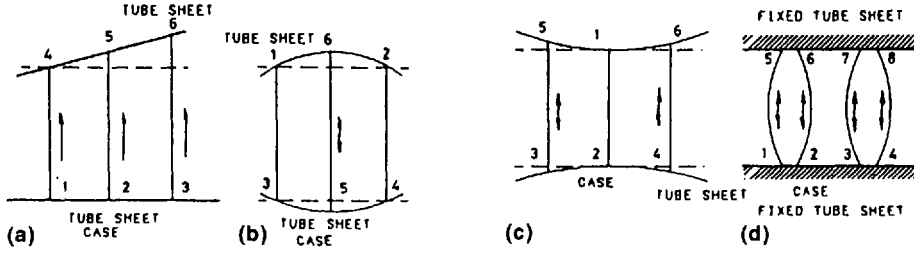


Figure 12 Effects of rolling sequence on tubesheet and tubes. (From Ref. 22.)

Size of Tube Holes

The clearance between tube and tube hole has a definite influence on the tube-expanding operation. Excess clearance lengthens the expanding operation considerably, and increase the plastic deformation and work hardening of the tube material, although the actual joint forming time remains the same [20,21]. Minimum play before rolling is to advantage. Tube hole diameters and tolerances are specified in TEMA standard paragraph RCB-7.4.

Factors Affecting Rolling Process

The factors that affect the quality of the rolling process are discussed in detail by Fisher et al. [20]. Some of the important factors are

1. Cleanliness of the tube, tube sheet, and rollers
2. Conditions of the cage, rollers, and mandrel
3. Lubrication and cooling
4. Tube and hole dimensions
5. Torque cutoff control monitoring and maintenance
6. Rolling technique, roller rotation speed, number of rolls, angle of rolls relative to the tube axis, shape of the rolls
7. Worker fatigue

It is best to avoid the use of any lubricant during the roller expansion. But if, because of undue wear or heating of the rolls, lubrication is thought necessary, then it must be applied with discretion [25]. On completion of assembly and expansion, the localized areas around the tube-to-tube-sheet joint should be cleaned again with the solvent so as to remove the final traces of lubricant.

Strength and Leak Tightness of Rolled Joints

In general, the joint strength and leak tightness of tubes expanded into bare holes, i.e., without grooves, are functions of the surface area in contact between the tube and hole, residual interfacial pressure at the tube-to-tube-sheet interface produced by the expansion process, static coefficient of friction, and Poisson's ratio [20]. Individual factors that affect the joint strength are discussed next.

Expanders Condition. Well-made/maintained expanders having hardened and ground mandrels and rollers are essential for making good rolled joints [24]. Expanders having rollers with sharp or improperly shaped entrance ends are believed responsible for many joint failures [20].

Feed and Speed. In general, faster machine rolling produces better results but with a tendency to greater tube hole deformation, while slower rolling tends to increase tube wall thinning [24].

Length of Tube Expansion. The strength of a rolled joint increases with an increase (not proportional) in length and an increase in the tube wall thickness [20]. Excessive joint length

is more expensive and may cause premature failure, if the tube and tube-sheet materials have a high difference in coefficients of thermal expansion, as, for example, copper tubes and steel tube sheets. Short joint lengths in thick tube sheets have an advantage; that is, in case of joint failure or leaks, the unrolled portion of the joint may be utilized.

Tube and Tube Sheet Materials. Ideally, the tube sheet material should match the mechanical properties of the tubes. As the ratio of elastic limits of tube and tube sheet materials rises, the strength of the joint decreases. Therefore, the elastic limit of the tube material should be relatively low [21]. A tube and tube sheet combination consisting of steel tube and steel tube sheet produces joints having a high holding strength, whereas a steel tube rolled into a copper tube sheet would have low strength. Experience has shown that for the best overall results, the hardness of the tube should be less than that of the tubesheet material. A reversed condition usually results in distorted or greatly enlarged tube holes [20]. For materials with limited ductility, like ferritic stainless steel tubes, rolling should be done carefully.

Friction. Expanded joints are primarily friction joints. Thus, all other factors being equal, increase in friction or resistance to sliding will tend to increase the strength of a rolled joint.

Wall Reduction. Rolled joint pull-out strength increases approximately linearly with wall reduction, but rolling must not proceed to the point at which adjacent holes are distorted and tubes dislodged.

Factors That Decide the Optimum Tube Wall Reduction. Factors that decide the optimum tube wall reduction for an expanded tube-to-tube-sheet joint are specified in TEMA section RGP-RCB-7.5.

Joint Leak Tightness

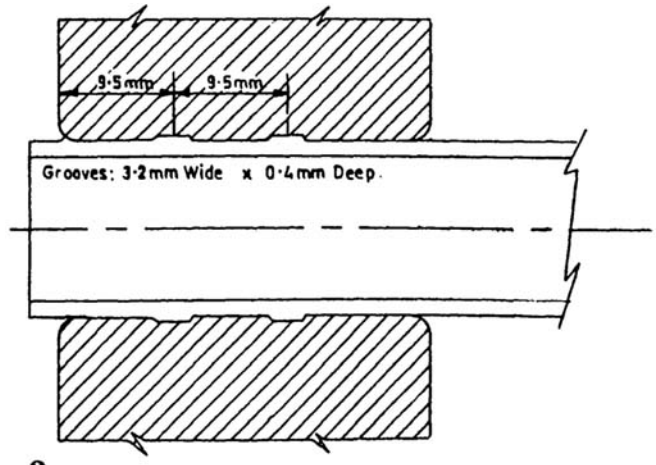
Joint leak tightness depends on factors such as quality of tube, tube ends and tube hole condition in tubesheets, tube wall thickness, and joint reinforcements by tube hole annular grooves.

Quality of Tube Holes (Tube Hole Ovality and Finish). It must always be remembered that strength of joint alone is not enough to guarantee a good joint. Consideration must be given to joint leak tightness, which is influenced greatly by the degree of roughness of the joint interfaces [20] and tube hole ovality [21]. In general, a leak-tight joint can be made much more easily if the contacting surfaces of tube and tube-sheet hole are smooth, but such a joint has, because of this smoothness, a lower joint strength whereas rough tube holes make strong joints. For tubes whose hardness is roughly equal to that of the tube-sheet material, as in boiler and refinery heat exchangers, the conventional "drill and ream" tube hole finish is in order [20]. Spiral machining marks and lateral grooves have a detrimental effect on the quality of the joint. This can be avoided by paying proper attention while drilling/reaming the bore [21]. The effect of tube hole finish on the mechanical strength and leak tightness of an expanded tube-to-tube-sheet joint is discussed in TEMA section RGP-RCB-7.43.

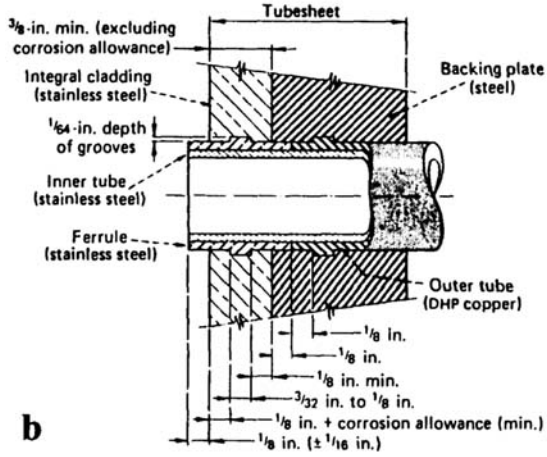
Baffles, Tube Ends, and Tube Hole Condition. Preparation of baffle holes and tube-sheet holes and assembly of the bundle should be performed to avoid longitudinal scratches on tube ends, one of the main causes for leaky expanded joints. Should such scratches or tool marks occur, they should be removed completely by grinding. All tube holes should be truly circular and of cylindrical shape.

Tube Wall Thickness. The thicker the tube wall, the better is the seal, because of the increase in the difference in mean tangential plastic strain. It is shown that within certain limits, thick-walled tubes are more readily sealed by expansion [21].

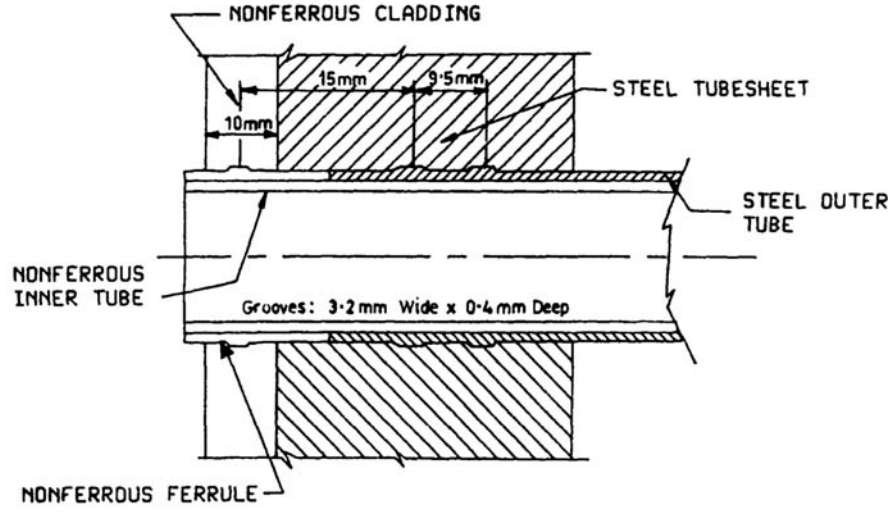
Joint Reinforcements by Tube Hole Annular Grooves. In order to meet the demands of higher pressures, most tube joints are strengthened by the machining of suitably shaped circumferential grooves into the walls of the tube-sheet hole (Fig. 13). During the rolling-in process, a



a



b



c

Figure 13 Joint reinforcements by annular grooves. (a) Plain tube; (b) duplex tube; and (c) clad tubesheet and bimetalic tubes. (From Ref. 26.)

portion of the tube metal is extruded into these grooves. In this manner additional anchorage and shear strength are provided for the rolled joint, hence increasing the pull-out strength. Rectangular grooves are commonly used for reinforcement purposes, and they increase the holding strength and stability of rolled joints by more than 40–50% [23].

Discussion of Tube Hole Annular Grooves Provision in TEMA. TEMA RB Class, require at least two grooves, each approximately 1/8 in wide by 1/64 in deep (3.2 mm wide × 0.4 mm deep). TEMA C class requires grooving for 5/8 in (15.875 mm) and larger diameter tubes for design pressures over 300 psi (2068 kPa) and/or temperatures in excess of 350°F (176.7°C). When integrally clad or applied tube-sheet facings are used, all grooves should be in the base material unless otherwise specified by the purchaser.

When an exchanger is built with small-diameter tubes and with grooving in the tube sheet, the designer should consider [10] (1) the percentage of ligament width removed by the grooving and (2) the percentage of tubesheet thickness that the grooves occupy. For such tubes, better results might be achieved by using a coarse tube hole finish in the range of 250 rms or grooves similar to those desired for thin, high-strength tubes.

More Than Two Annular Grooves. The two 1/8 in wide × 1/64 in deep (3.2 mm wide × 0.4 mm deep) grooves of the TEMA are adequate for most rolled joints. However, for thin-walled, high-strength tubes, a series of smaller, shallower grooves of the same total width is also followed.

Step Rolling

In general, the maximum length of tube that can be roller expanded in one rolling tool application is about 2 in (50.8 mm). For larger joint lengths, rolling is done in steps with overlapped rolled lengths. If the step-rolled lengths do not overlap, there is a series of transitions between the rolled and unrolled lengths [20].

Roller Expander for Tube Extending Beyond the Tube Sheet

For tubes that extend beyond the open face of the tube-sheet, a thrust collar that fits over the tube must be used. The thrust collar positioned against the tube-sheet face will accurately locate the expanding rolls within the tube-sheet hole.

Expanding in Double Tube Sheets

The recommended sequence of expanding for the double-tube-sheet exchangers can be adopted, starting with number 1 as shown in Fig. 14. Tube expansion is carried out at the inlet end inner tube sheet first. Particular care is taken in setting up the expanders to ensure that expansion beyond the edge of the tube sheet does not occur.

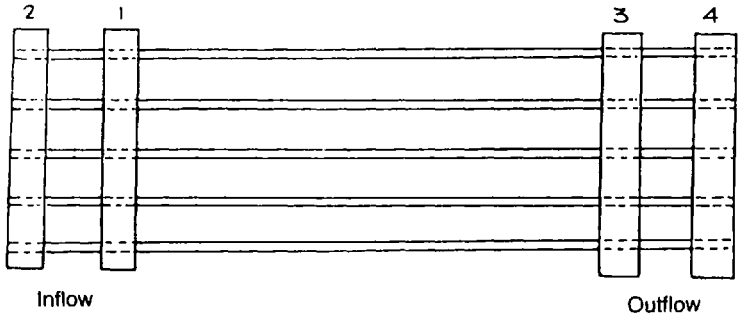


Figure 14 Recommended sequence of expanding for the double tubesheets exchanger. (From Ref. 22.)

Leak Testing

This is discussed in a later section.

Residual Stresses in Tube-to-Tube-Sheet Joints

All tube expanding methods leave residual stresses in the tube wall. If these stresses are tensile and above 100 MPa, the tube is susceptible to stress corrosion cracking. Some steam generator manufacturers do a thermal stress relief after expansion to reduce these residual tensile stresses. However in some situations this is impractical if not impossible [19].

3.9 Tube-to-Tube-Sheet Joint Welding

Expanded joints are adequate for many applications and are still used extensively where pressure differences are not high enough to cause leakage. However, higher temperature and pressure requirements on heat exchangers make expanded joints inadequate, and for certain services the mixing of the shell-side and tube-side fluids is prohibited. For these conditions, welding of tube-to-tube-sheet joints must be carried out. At high operating temperatures the expanded joint undergoes stress relief. The interfacial joint stresses, which give the joint its strength, are relaxed, the tube wall contracts, and leakage develops [27]. Weld joints have no such limits at high temperatures. According to Brosilow [27], tube-to-tube-sheet welding is preferred for the following circumstances:

Tube pitch is too small to permit an expanded joint.
Thermal cycling is severe and operating temperatures are relatively high.
In critical applications where the danger of corrosion is high. The expanded joint is not continuous, since crevices between tube wall and tubesheet lead to crevice corrosion.
When access for maintenance is limited, as in nuclear and in some chemical process exchangers.

If welding is used, either it serves as a seal (known as a seal-welded joint) or the weld is used as the principal means of load-bearing connection (known as a strength-welded joint, though there is no clear demarcation between them).

Various Methods of Tube-to-Tube-Sheet Joint Welding

The following means of tube-to-tube-sheet welded joints are generally followed, depending on the service involved:

1. Expand in plain holes and seal welding.
2. Expand in grooved holes with seal welding.
3. Expand in plain holes and strength welding.

All compatible weldable materials, namely, tubes, tube-sheet, and weld filler metal, may be joined at tube-to-tube-sheet joints with conventional arc welding methods and gas tungsten arc (TIG) welding.

Tube-to-Tube-Sheet Joint Configuration

In general the tube-to-tube-sheet connections have been made by passing the tubes through the tube sheet and fillet welding on the face side using one of the joint geometries shown in Fig. 15.

1. Flush tube weld: The joint in Fig. 15a is suitable for applications in which the tubes are of sufficient size and wall thickness to permit the addition of filler metal.
2. Figure 15b shows a configuration suitable for seal welds and employs simple fusion of the tube and tube sheet.

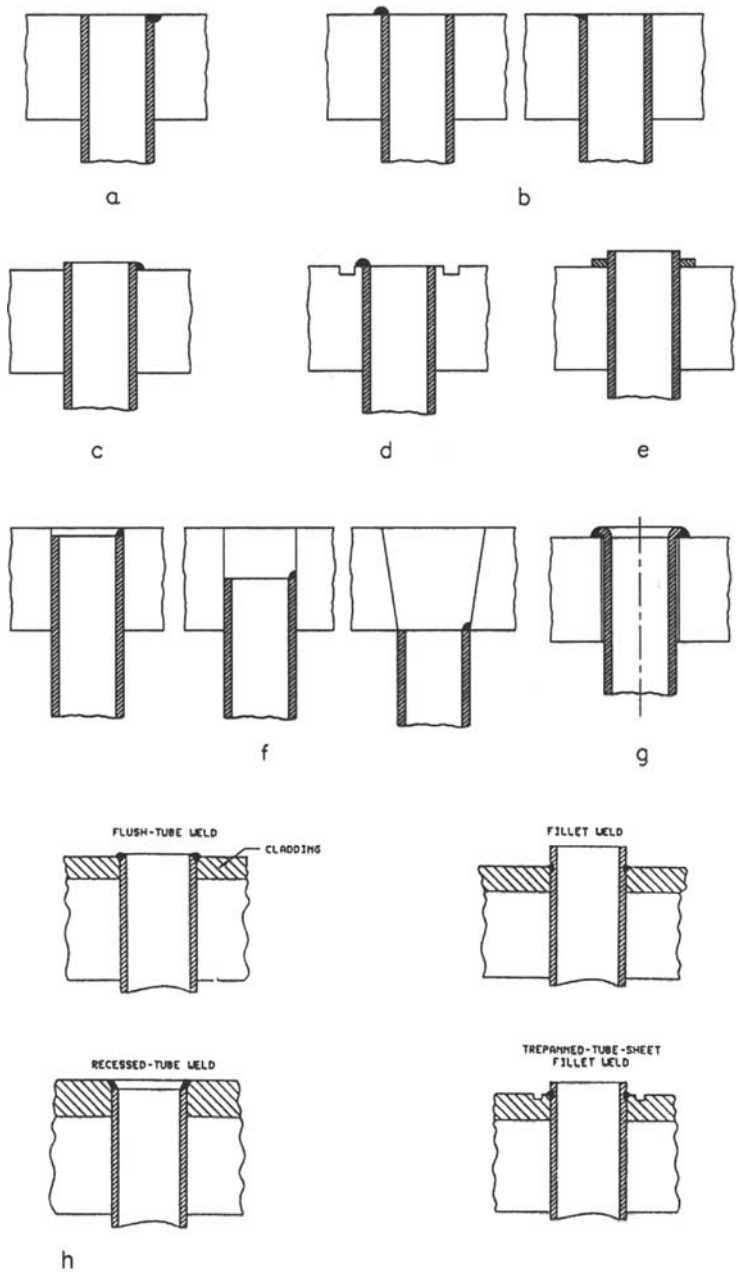


Figure 15 Tube-to-tubesheet welded joints. (a) Flush tube weld; (b) seal welds employing fusion of the tube and tubesheet; (c) projection welding without filler metal; (d) trepanned tubesheet; (e) added ring weld type; (f) recessed tube weld; (g) bell mouthed and fused welding; and (h) welding of clad tubesheet. (From Ref. 31.)

3. In Fig. 15c, projection of 1 mm is preferred because it allows better welding and is suitable for welding without filler metal.
4. A modification of Fig. 15a is shown in Fig. 15d, incorporating a trepan in the tube sheet. It is used for materials in which the welds may be subjected to cracking when made under conditions of restraint. A trepanned joint is more expensive to machine, and the ligament length between tubes is a governing factor in use of such a joint [28].
5. Added ring weld type: Figure 15e shows fillet welds of the tube-to-tube-sheet joint with a ring of special alloy placed on the protruding end and melted by an argon arc process.
6. In Figure 15f, a recessed welded type is employed for avoiding stagnation of the fluid on the tube sheet and to reduce turbulence on the tube side.
7. Figure 15g shows tube end bell-mouthed and fused.
8. Figure 15h shows various forms of tube-to-tube-sheet welding of clad tube sheet.

Internal Bore Welding. Face-side welding techniques shown in Figs. 15a–16e are economical and generally reliable, but they produce a weld that is difficult to inspect by radiography and it introduces a long crevice between the tube and tube sheet [28]. Localized corrosion may start in this crevice. Even if the width of the crevice is made as small as possible by expansion of the tube, inside hole cracks or corrosion still poses a danger. These problems are overcome by internal bore welding methods. In the internal weld joint shown in Fig. 16a, the tube does not pass through the tube sheet. It is welded to a short stub machined on the tube side of the tube sheet. This joint has the important advantages of easy inspectability by radiography and eliminating the crevice. However, it is much more difficult to weld than the face-side design because of the proximity of the tubes. There is not room for an orbiting arc welding head on the outside of the tube. The weld in an internal bore weld is made by welding from the bore side of the tube. An additional internal bore welding method suggested by Franklin et al. [29] is shown in Fig. 16b and c, and the Fosterwheeler method [30] is shown in Fig. 16d.

Recessed Tube Cladding Fusion. The recessed tube cladding fusion technique makes possible mechanical cleaning of all surfaces to be fused (Fig. 15h). This technique requires no addition of filler metal because the cladding provides the filler and it melts only the corner of the clad hole and fuses only to the top of the tube [31].

Welding Process

GTAW of Tube-to-Tube-Sheet Welding. The TIG welding process is used extensively for the welding of nonferrous and austenitic tubes and to a limited extent for carbon steel tubes. This process is particularly useful in the welding of small-diameter tubes where the small ligaments are not suited to the metal arc process [25]. The joint is either autogenous or made with wire feed. Much of the joining of tube to tube sheet is done manually, especially on small units, and automatic equipment has been developed for use in large heat exchangers where thousands of tubes are used.

Manual TIG Welding. Manual welding requires accurate control over torch movement, especially when the tubes used for weldments have thin walls and small diameters. Although the welds are acceptable, they may lack uniformity and production rate is low; weld size and contour depend largely on the skill of the operator in rotating the torch at a constant speed for proper fusion of the filler wire.

Automatic TIG Welding. Using fully automatic equipment, it is possible to obtain uniform high-quality welds with good reproducibility, and production rate is high. Defects that require rework are few. The automatic GTAW equipment consists of orbital welding set up, in which the welding head is automatically rotated. These orbital welding machines often use a mandrel for self alignment on the tube to be welded. Once locked into position, a GTAW torch rotates

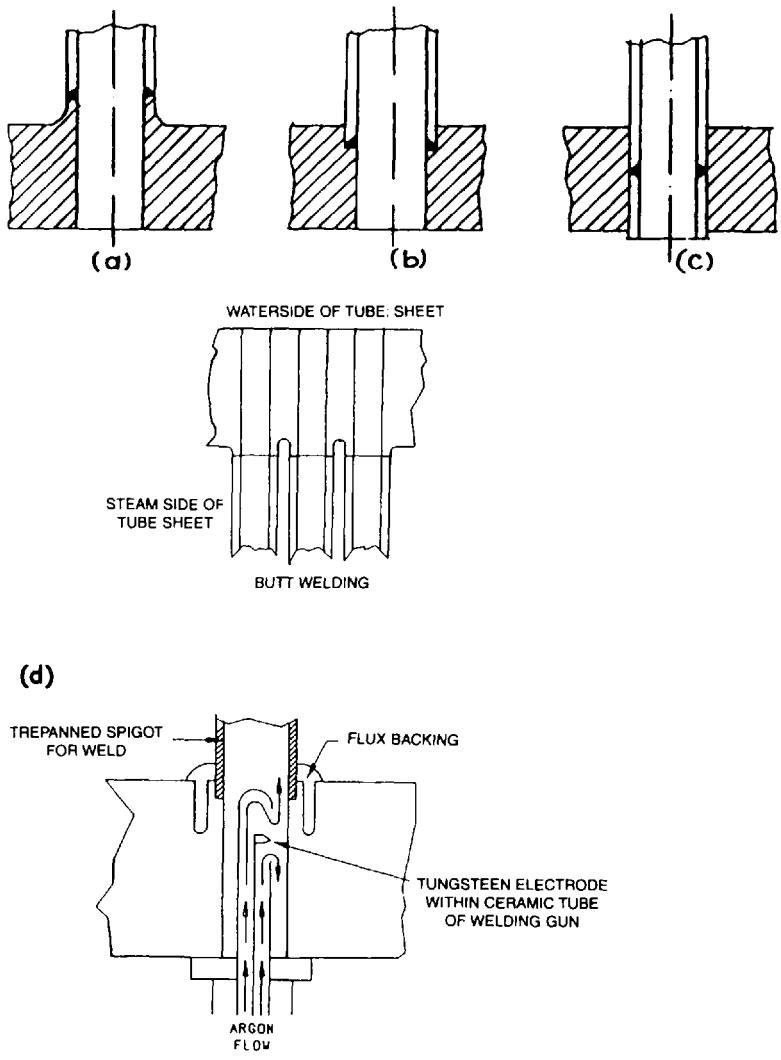


Figure 16 Forms of internal bore welding. (From Ref. 29,30.)

around the face of the tube and joins it to the tube sheet, frequently without the addition of supplemental filler material. In a cold wire method, a cold filler wire is fed to the arc from a spool, through a wire feed drive and an adjustable wire guide tip, all of which rotate with the welding head. Argon shielding gas is automatically fed to the orbiting head. In the actual welding sequence, welding at each end of the tube is staggered to ensure that gas leak rate and pressure are not affected by both ends of the tubes being sealed simultaneously [32].

If TIG welding is to be used, the tube wall should be expanded to intimate contact with the tube hole. This may be done by roller expanding or pinning with a tapered pin; however, the tapered pin method is preferred for two reasons [24]: (1) The tube will be exposed to a minimum chance of contamination, and (2) there will be only a line contact around the periphery of the tube to tube hole. This allows the gases generated during welding to escape behind the weld puddle, reducing weld porosity and the incidence of blow holes as joints are completed.

If preheating and postweld heat treating are required, gas heating can be used or modern equipment is available to carry out the operation in situ. The equipment consist of a computer-controlled temperature monitor and clamp-on cartridge heating elements [32]. Good-quality welds between tube and tube sheet require a high degree of operator skill and concentration. Cleanliness at the joint is always desirable.

Welding of Sections of Unequal Thickness

In SMAW, as in other welding processes, special techniques are required while welding a thick member to a very thin member due to large difference in heat-dissipating capacities. An application involving components of unequal section thicknesses, namely, the welding of heat exchanger tubes having 0.093 in (3 mm) wall thickness to a tube sheet as thick as 10 in (254 mm), is discussed in Ref. 33. In this situation, the welding current needed to obtain good penetration into the thick tube sheet is sometimes very high for the thin tube wall and results in under cutting of the tube and a poor weld. If an adequate amount of current for the tube is used, the heat is not sufficient to provide adequate fusion in the thick tube sheet, and again results in a poor weld. Industrial practices to minimize heat-sink differential are [33]:

1. The usual method of avoiding difficulty is to cut a 0.25 in (6.35 mm) deep circular groove in the upper surface of the tube sheet around the tube hole (Fig. 17a); the groove restricts heat transfer.
2. To place a copper backing block against the thin member during welding. The block serves as a chill, or heat sink, for the thin member.

Yet another method is to preheat the thick member. Normally 150°C is preferred for carbon steel tube sheets; for stainless steel it is not required since the thermal conductivity is very much lower.

Aluminum Tube-Sheet-to-Tube Welding. For good heat balance, trepan a grove in the tube sheet, making a welding lip of the same thickness as the tube wall; then edge weld the lip and wall. Better still, extend the tube one wall thickness beyond the lip to improve melting and fusing [34].

Seal-Welded and Strength-Welded Joints

Tube welds at the tubesheet front face are classified as either seal welding or strength welding.

Seal Welds. Seal welds are used to prevent fluid leakage between the shell side and tube side. Although seal welds confer additional strength on the weld joint, the incremental capacity

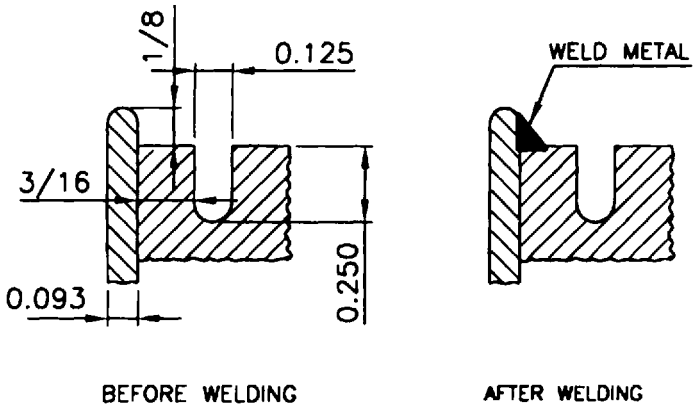


Figure 17 Welding patterns to minimize heat sink differential-grooved tubesheet. (From Ref. 33.)

of the joints to withstand pressure and temperature imposed by loads is neglected in calculating the load-carrying capacity of the joint [18]. Nevertheless, the Code requires a qualified welding procedure to be used. Seal-welded joints are normally used for service pressure up to 80 kg/cm^2(g) and temperature up to 350°C. It is recommended to expand tubes in grooved holes for better holding strength for higher service pressures.

Strength-Welded Joints. Strength-welded joints in lieu of full expansion and seal welding are adopted for higher temperatures and pressures, as expanded joints lose their leak tightness at higher temperatures. Tube-to-tube-sheet strength welds are used to transfer all longitudinal mechanical and/or thermal loads from the tubes to the tubesheet. The suggested definition of strength weld leads to the following considerations [18]: (1) Using the joint efficiencies specified in the Paragraph UW-15 (c) of ASME Code Section VIII, Div. 1, the total weld cross-sectional area times the joint efficiency must equal the tube cross-sectional area; (2) weld strength must be based upon the lower of the tube or tube-sheet allowable stress; and (3) differential thermal expansion between the tube, tube sheet, and weld metal must be considered. Almost all such strength welds are fillet welds, either at the front face of the tube sheet or within the hole; or, in a very few cases, the tube holes may be drilled to match the tube inside diameter and the tubes butt welded to the tube-sheet secondary face (Fig. 16a and d), known as internal bore welding. Some typical strength-welded joints are given in Fig. 18.

Joint Strength. ASME Code procedure to determine joint strength is discussed in Chapter 11 with mechanical design of shell and tube heat exchangers.

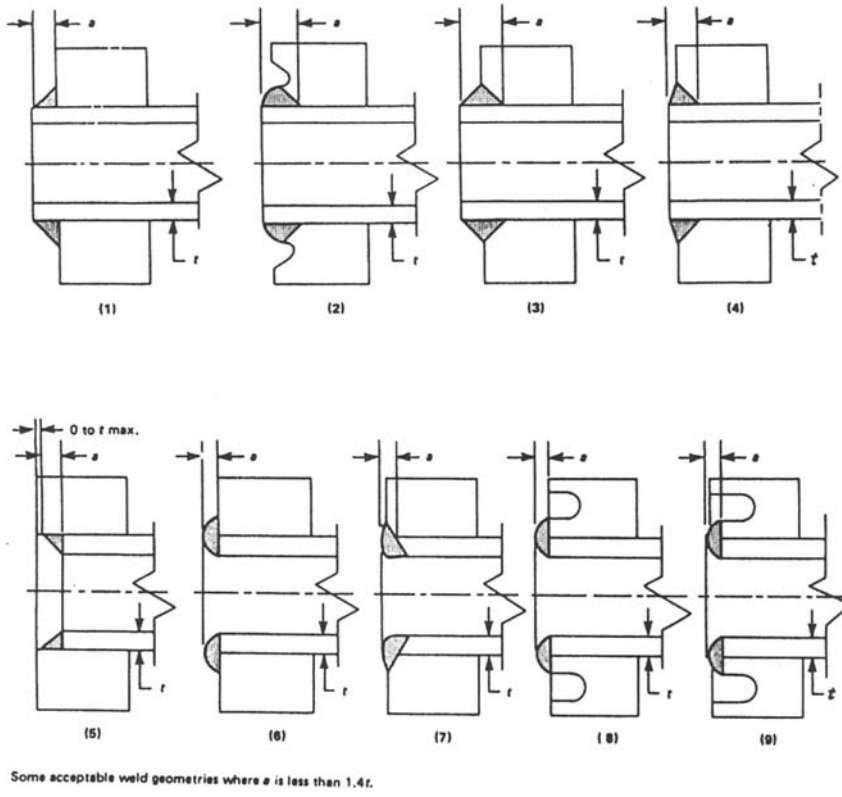


Figure 18 Some acceptable weld geometries where a is less than $1.4t$. (Reproduced from Ref. 3.)

Considerations in Tube-to-Tube-Sheet Welding

There are certain factors to be considered when planning a tube-to-tube-sheet joint [35]:

1. Is the tube-sheet an air-hardening material that will require PWHT?
2. Are the tube ends and the tube-sheet holes clean?
3. Welding before expanding or expanding before welding?

Other factors to be considered include these [18]:

4. Granular structure.
5. The coefficient of thermal expansion of the tubes and tube sheet materials must be close enough.

These factors are discussed next.

Is the Tube Sheet an Air-Hardening Material That Will Require PWHT? While PWHT is possible under shop conditions, it is often difficult to accomplish under field maintenance conditions. This difficulty is overcome by these measures: (1) Frequently, a non-air-hardening austenitic or Inconel overlay (Fig. 19) can be specified for the tube sheet [31], thus eliminating the need for PWHT. (2) If an austenitic overlay is not possible due to corrosion problems, the tube sheet can often be overlaid with a low-carbon filler metal of the same nominal composition as the tubesheet. While PWHT would likely be required after overlaying to decrease the HAZ hardness, the lower carbon content of the overlay would not harden as readily during tube-to-tube-sheet welding, often eliminating the need for a subsequent PWHT [35]. This aspect is discussed with reference to a feedwater heater with carbon steel tubes welded to carbon steel forging tube sheet in Ref. 31.

Are the Tube Ends and the Tube-Sheet Holes Clean? To achieve an absolute seal with good mechanical properties, the welded joint must be free of voids. The tubes, holes, and weld rings should be carefully cleaned to eliminate the danger of voids forming due to evaporation of surface contaminants such as grease, oil, cutting fluids, etc. It may be necessary to solvent clean the tube ends, the tube sheet should be thoroughly degreased, and the tube-sheet holes should be steam cleaned or sand blasted to remove any scale or dirt that could interfere with the tube-to-tube-sheet joints. Titanium tube holes and tube sheets should be cleaned with a solvent such as acetone or methyl ethyl ketone. Methanol or chlorinated solvents such as trichloroethylene should not be used [36]. After cleaning, both the tube ends and tube-sheet holes should be visually examined for longitudinal scratches, which could create a leakage path.

Welding Before Expanding or Expanding Before Welding? A third consideration for achieving successful tube-to-tube-sheet joints is the proper application of rolling. To this day there is ongoing controversy about whether to expand first or weld first [18]. Basically three different sequences are possible for making tube-to-tubesheet joint. They are

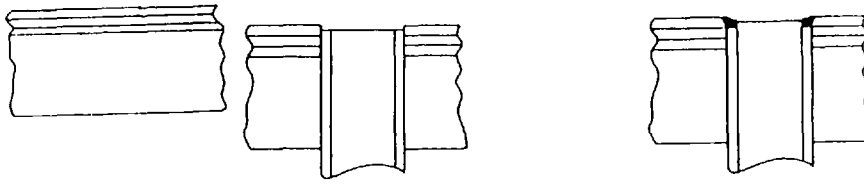


Figure 19 Non air hardening overlay on tubesheet. (From Ref. 31.)

1. Expansion of the tubes followed by welding of tubes.
2. Welding of the tube ends followed by expansion.
3. Light expansion followed by seal welding and followed by full expansion.

The sequence for making a tube-to-tube-sheet joint is determined by the following factors [18]: (1) the requirement that the surfaces be very clean; (2) the need for a path of escape of welding generated gases—otherwise the gases will cause porosity in the weld; (3) the maximum desirable root gap for the material being welded; and (4) the need to repair welds that have failed in service.

If significant rolling is performed prior to welding, a sealed annular space between the tube and the tubesheet is formed (Fig. 20a). The air in this annular region will expand due to welding heat. Since the gas cannot escape, it expands into the tube-to-tube-sheet weld, creating pinhole porosity. Except for joining thin-walled titanium tubes to titanium tube sheets, these requirements indicate that tubes should be welded to the tube sheets prior to expanding [18]. For titanium, the expansion is required to keep air from the back face from contaminating the weld and to prevent vibration of the tube, which could result in weld cracking.

Experience has shown that the best welding results are obtained when tubes are only anchored into the tubesheet prior to welding by these means [18,35]: (1) center punching, (2) a tapered drift pin, and (3) a light expansion (presumably to create tube/hole contact that is not hydraulically tight). Another method, suggested by Yokell [18], is to use one of the commercially available expanders that compresses a polymer in the tube end to produce radial pressure. These can be set to lock the tube in place without creating a hydraulically tight seal.

While performing rolling operation, lubricant should not be used, to avoid contamination. However, without lubricant, there is a possibility that heat due to friction will cause some of the hardened roller and cage material to flake off [18].

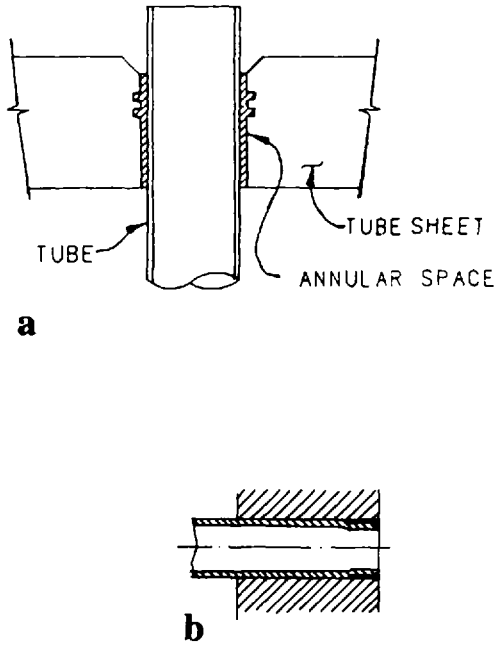


Figure 20 (a) Annular space between tube and tubesheet; (b) rolling technique following welding. (From Ref. 35.)

Proper rolling techniques following welding are required. Some fabricators have found it necessary to start rolling at least 12.5 mm (0.5 in) away from the weld, proceeding toward the shell side of the tube sheet [35]. This is shown in Fig. 20b. Such a procedure minimizes the amount of mechanical loading on the weld. As indicated by TEMA, rolling should not progress closer than 3.2 mm (⅛ in) to the shell side of the tubesheet.

Merits of Sequence of Completion of Expanded and Welded Joints. Merits and demerits of these methods are as follows.

First Expansion Followed by Welding. *Merits*:

1. Welds are free from strains induced by rolling operation.
2. The integrity of the tube expansion can be tested.

Demerits:

1. Welds may contain porosity due to the presence of lubricants used during expansion, if cleaning is not done properly.
2. Expansion may get loosened under the influence of heat during welding. Such tubes would require rerolling.

First Welding Followed by Expansion. *Merits*:

1. Welds are free from porosity due to the absence of lubricants.
2. If the tube-to-tubesheet joint requires PWHT, there is no point in expanding first. The heat treatment will relax the tubes.
3. Tube projection for welding is uniform.

Demerits:

1. Welds may be damaged due to strain caused by expansion.
2. There is no foolproof check for the leak tightness of the expansion carried out, as the seal welds may help in shadowing the underexpansion of the tubes.
3. Weld shrinkage may reduce the tube inner diameter so that it is difficult to insert expanders. This problem is overcome by reaming.

Light expansion followed by seal welding and followed by full expansion is most preferred, since it has the merits of the two sequences just discussed.

Granular Structure. Tube sheets must have a granular structure fine enough to permit consistently uniform weld metal deposits. Carbon steel tube sheets should always be grain refined [18].

Coefficient of Thermal Expansion of the Tubes and Tube-Sheet Materials. Consider, for example, an austenitic stainless steel tube, TIG welded to a carbon steel tubesheet with high-alloy filler metal. The coefficient of thermal expansion of the austenitic stainless steels is about 50% greater than that of the carbon steel. The fusion temperature is in the range of 2800°F (1730°C). As the welds solidify rapidly, the difference in the rates of expansion engenders high levels of thermal stress [18]. Stresses due to operating pressure superimposed on the thermal stresses may cause premature failures.

Full-Depth, Full-Strength Expanding After Welding

When the welds are at or near the tube-sheet front face, it is desirable to full strength expand the tubes for approximately the whole tube-sheet thickness for the following reasons [18]:

1. Expanding the tubes into the holes isolates the welds from the effects of tube vibration.
2. Contact between the tube and hole permits heat to flow between the tube and tube sheet.
3. For full-strength expanded tubes, the ligament efficiency is much greater than when there

is no contact as given by the formulas. For example, the expression for minimum ligament efficiency μ is given by CODAP [37]:

$$\mu = \frac{p-d}{p} \quad \text{for tubes welded to the tube sheet}$$

$$\mu = \frac{p-(d-t)}{d} \quad \text{for tubes expanded more than 90\% of the tube-sheet thickness} \qquad (4)$$

where d is the tube outer diameter, p the tube pitch, and t the tube wall thickness.

Ductility of Welded Joint in Feedwater Heaters

For applications such as feedwater heaters, the tube sheets are subjected mainly to bending stresses due to high feedwater pressure, which may be as high as 5000 psi in modern plant cycles. The tube-to-tube-sheet joints must remain impervious to water under this high pressure while sustaining the cyclic stresses due to tube-sheet flexure, and temperature variations between the tube and tube sheet caused by such operating conditions as startup, load shedding, shutdown, and possible abnormal transient operations [31]. According to Lohmeir et al. [31], due to these reasons, the flexural and thermal stresses can be sufficiently large, even exceeding the elastic limit, to propagate leakage paths from weld metal flaws. In order to cope with such high stresses without suffering damage, the welds must have consistent mechanical properties and high ductility. The main factors to be controlled to ensure the ductility of the joints are [38]:

Combination of tube and tube-sheet materials
Welding parameters
Heat treatment
The carbon content of the basic material and welding alloy (less significant factor)

The following factors ensure welded joints of even quality and high ductility [38]:

1. Tubes and tube sheets are always of the same material, with a maximum carbon content of 0.20%. The filler is of a special alloy whose main feature is an extremely low percentage of carbon.
2. All joints and the electrode are preheated before welding.
3. When all welding is completed the entire tube sheet is stress relieved.

Welded Mockups

To determine correct welding parameters, use mockups to scrutinize tube-to-tube-sheet weldments. Welded mockups are sectioned and prepared for review of the root area and dimension checks of the weld. Examinations of welded mockups are discussed in detail by Syal [11]. An expanded and welded tube-to-tube-sheet mockup is examined by the following methods:

1. Radiography examination: The weld shall be free from porosity, cracks, or other defects that would result in leakage in service.
2. Micro and macro examination: to detect defects, metal flow in the annular grooves (if grooves are present in the tube sheet), fusion, penetration, etc.
3. Minimum leak path: For strength-welded joints, the minimum leak path shall be the tube-sheet thickness, and for seal-welded joints 0.7 times the tube-sheet thickness.
4. Hardness examination: tube sheet, tube, weld, and HAZ; normal hardness limits are for carbon steel 220 HV, low-alloy steel 260 HV, and stainless steels 250 HV or as specified in the specification [11].
5. Tear test for strength welded joint.
6. Pulling test: Tubes shall be pulled on a tensile testing machine with a pulling load not less

than $0.1 \times L \times d \times 3000$ (kgf) for expanded tubes without seal welding, where L is the length of expansion joint (cm) and d tube outer diameter (cm) [11].

7. Pressure test as shown in Fig. 21.

Leak Testing of Welded Tube-to-Tube-Sheet Joints

Leak testing of exchangers will allow one to determine if tubes have been adequately rolled or welded into the exchanger tube sheets. Such testing can be accomplished by pressurizing the shell side with air to a pressure of 1.0 to 1.25 ksc (gauge) and "soaping" the face of the tube sheet and looking for bubbles, or by filling the shell with water, pressurizing the channel with air, and looking for bubbles through the shell-side nozzle. Various leak testing methods are discussed in Chapter 14 on quality control, inspection, and NDT.

TEMA Standards on Testing of Tube-to-Tube-Sheet Joints. As per paragraph RGP-RCB-7.6, tube-to-tube-sheet welds are to be tested using the manufacturer's standard method. Any special testing using halogens or helium will be performed by agreement between manufacturer and purchaser.

Radiographic Inspection of Tube-to-Tube-Sheet Joint Welds

For very critical applications, the acceptance standards for tube-to-tube-sheet welds like the seal, spigot, and butt/fillet weld are generally based on high-definition panoramic radiography. The small size of the welds and their shape necessitate a very short source to film distance [39]. This requires the development of highly specialized equipment such as the microfocus rod anode x-rays set and miniature low-energy gamma sources a unique film cassette for use on small diameter welds to implement radiography on these welds [39,40]. Figure 23 illustrates the principles of the radiographic technique to test tube-to-tube-sheet weld.

Welded Tube-to-Tube-Sheet Joint Quality Control by Hydraulic Testing of Feedwater Heaters

The integrity of tube-to-tube-sheet joints is judged by hydrostatic tests and leak testing techniques. The basic limitations in these tests are that they reveal only those defects that provide, at the time of testing, a flow path completely through the weld. Experience with carbon steel tube-sheet welds has shown that the leaks that can occur after service operation give no indication of leakage during shop floor leak testing or hydrostatic testing [31]. One method that has been successful in detecting subsurface defects involves cycling the heat exchanger to hydro-

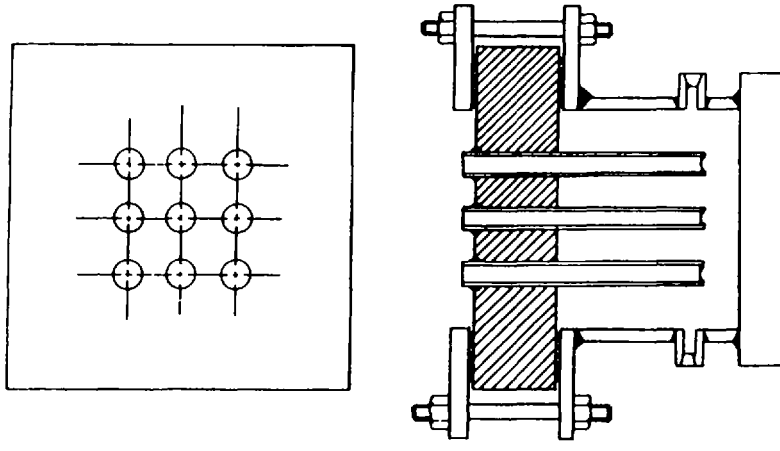


Figure 21 Welded tube-to-tubesheet pressure test model.

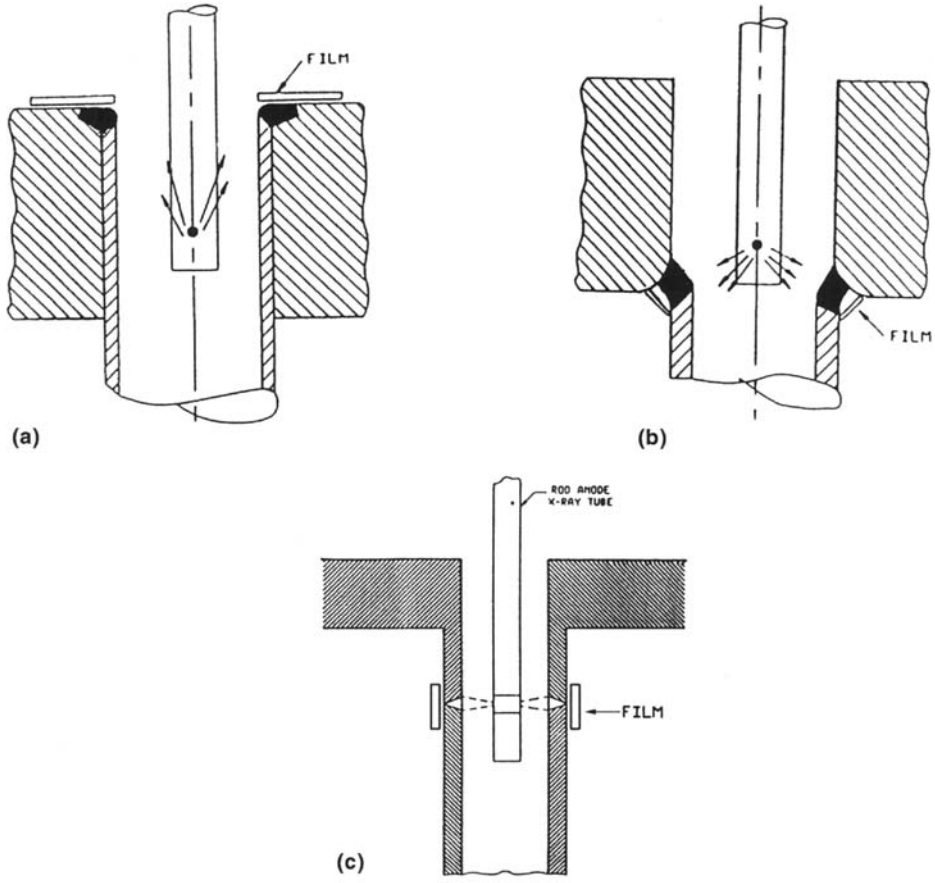


Figure 22 Radiographic inspection of tube-to-tubesheet joint welds. (a) Panoramic radiographic technique, (b) position of the radiation source and film relative to the butt fillet weld, (c) microfocus rod anode x-rays set. (From Ref. 39.)

static test pressure a number of times, and providing a thermal shock to the tube-sheet weld surface in the shop floor. The high tube-to-tube-sheet joint stresses due to pressure cycling have been particularly successful in completing the potential leakage paths that require a short propagation distance.

Brazing

Brazing is used for tube-to-tube-sheet joints that are free from stress concentration and crevice corrosion problems. For the fabrication of heat exchangers three methods of brazing are in common use: torch brazing, furnace brazing, and dip brazing. ASME Code Section VIII, Div. 1 prohibits brazed joints for lethal service and for unfired steam boilers.

3.10 Heat Treatment

Heat treatment of fixed-tube-sheet exchangers may be done by either of these methods:

1. With tubes welded in one tube sheet and left free in the holes of other tube sheet
2. Both ends of the tubes welded with tube sheets

Salient features of these methods are discussed next.

With Tubes Welded in One Tube Sheet and Left Free in the Other Tube Sheet

The procedure adopted is as follows:

1. After welding the tubes on one tube sheet, stress relieve the joints by leaving the tubes free in the second tube sheet.
2. Weld the tubes to the second tube sheet and stress relieve the second tube sheet by placing only part of the exchanger in the furnace: however, this stress relieving may be waived if proper welding procedure with suitable preheating can control the hardness of the weld metal and HAZ within acceptable limit, provided that PWHT is not a mandatory requirement [11].

Both Ends of the Tubes Welded with Tube Sheets

During heat treatment, the rate of heating and cooling should not exceed 30°C per hour. The temperature gradient between the outer skin of the shell and the innermost tube should be narrowed down to an acceptable limit by soaking the exchanger during the heating stages.

Heat Treatment: General Requirements

Prior to PWHT, the exchanger should be thoroughly examined by visual inspection and NDT methods to avoid welding repair after completion of heat treatment. Consider the following points while heat treating heat exchangers:

1. The complete exchanger should be thoroughly cleaned before charging into the furnace. Any scale formation on the tube sheet and tubes, when tubes are kept free on one side, is avoided by the circulation of nitrogen. Alternately, tube ends may be plugged with ceramic fiber plugs, which will not permit the hot gases from entering the tubes, thereby preventing oxidation.
2. Exchangers must be heat treated in a furnace that is heated electrically or by gas burners. The furnace must be of such a design as to prevent direct impingement of flame on the exchanger. Flame selection, i.e., oxidizing, reducing, slightly oxidizing, etc., is important to avoid excessive scaling and oxidation.
3. Sufficient numbers of thermocouples should be provided on the exchanger to verify uniform heating; their locations are also important.
4. Rate of heating, holding temperature, and rate of cooling are generally governed by material used and the construction code. PWHT requirements for welds between dissimilar metals shall conform to the requirements of the material having the more stringent requirements.
5. Ensure that the tubes are adequately supported to prevent sagging of the tube bundle. Similarly, during PWHT of the exchanger, it may be necessary to support the shell, if its supports are widely spaced and sagging is likely.
6. Heat treatment should always be done before hydrostatic test. If for any reason tube end welding, however small, is carried out after heat treatment, it is recommended to repeat the heat treatment when PWHT has been specified as requirement.
7. After heat treatment, the tube sheet and tubes shall be examined to ensure that its surfaces are free from scale, oxidation, and decarburization, fine cracks, distortion, dimensional accuracy, etc.

Details on quality control during PWHT of welded components are discussed in Chapter 13 on material selection and fabrication.

3.11 Assembly of Channels/End Closures

Where a fully pressed end is required, the end closure is purchased from the trade as a pressing or can be fabricated from a series of petals on the shop floor. (Forming of various types of heads discussed in Annexure 2.) Assemble the channels/end closures with the shell assembly and measure the flatness. Measure tube-sheet flatness across the diameter of the gasket ring for conformity with the specifications. Inspect fixed tube sheets extended as flanges for deformation due to weld shrinkage.

Bolt Tightening

After the heat exchanger assembly, tighten the bolts in a controlled sequence crisscross pattern similar to that shown in Fig. 23a [35] or Fig. 23b, as illustrated in TEMA Figure E-3.25, except for special high-pressure closures when the instructions of the manufacturer should be followed. It is important that all the flange bolts carry approximately equal load. For exchangers in critical services where it is essential to avoid leakage, use the ultrasonic bolt tensioning devices to ensure that the bolts are tightened uniformly [35].

3.12 Hydrostatic Testing

The hydrostatic test shall be carried out after PWHT and complete assembly and all NDT performed, prior to applying painting, insulation, coating, and packing, under the supervision of a quality control (QC) engineer and/or third-party inspection, by observing the state and local pressure vessel code. Care has to be taken for safe supporting and complete venting of the pressure vessel. Welded joints are to be cleaned prior to testing the exchanger to permit proper inspection during the test.

The shell side and the tube side are to be tested separately in such a manner that leaks at the tube-to-tube-sheet joints can be detected from one side. When the tube-side design pressure is higher than the shell-side pressure, the tube bundle shall be tested outside of the shell only if specified by the purchaser and the construction permits. In case of stacked assembly these tests will be done in the stacked condition.

Hydrostatic Testing Procedure

The minimum hydrostatic test pressure at room temperature should be 1.5 times the MAWP, corrected for temperature, except where other code requirements govern. Air lock plays a very

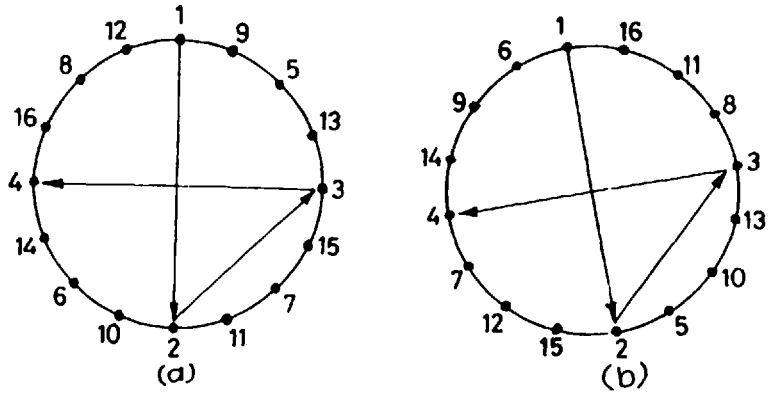


Figure 23 Bolt tightening sequence. (a) Danis [Ref. 35] recommendation; and (b) TEMA recommendation [2].

important role. Make sure that air is removed completely before conducting the hydrostatic test, and the overflow is witnessed by the inspector before closing the nozzle. The pressure has to be measured with two calibrated pressure gauges, connected independently of each other. The indication range must not exceed 150% of the test pressure. Keep a watch on the pressure gauge dial to spot drop in pressure that indicate leaks. The test pressure shall be held for at least 30 min while looking for water oozing from welds, gaskets, and other potential sources for leaks. For the pressure test, in addition to inspecting the expansion joint for leaks, the expansion joints shall be inspected before, during, or after the pressure test for visible permanent distortion.

Hydrostatic Test Fluid

The hydrostatic pressure test is in general carried out with drinking-quality water free from any corrosive and suspended substances, especially, chlorides and microorganisms. In the case of bad water quality, temperatures higher than 30°C combined with longer holding time may cause corrosion. If required, suitable corrosion inhibitors may be used. Do not test austenitic stainless steel exchangers with water that has a chloride ion concentration high enough to cause stress corrosion cracking. Because most potable water supplies are chlorinated, it is necessary to check the chloride levels. The chloride level in testing water is limited to 25 ppm for austenitic stainless steel types 304, 310, and 321, Incoloy 800, and for aluminum, and 100 ppm for Cr-Ni-Mo austenitic steels types 316 and 317. Alternatively, use conditioned demineralized or distilled water for hydrostatic testing.

Use of Fluorescent or Visible Tracer Dyes in Hydrostatic Test Fluids

Fluorescing dye indicators can be added to the water used in hydrostatic pressure tests for improving the visibility for locating leaks.

Pneumatic Tests

As per ASME Code paragraph UG-100, vessels that cannot be filled with water or cannot be readily dried and where traces of water are not tolerated can be tested pneumatically at 1.25 times the MAWP to be stamped on the vessel multiplied by the ratio of the stress values of the test temperature of the vessel to the stress value s of the design temperature, except where other code requirements govern.

Stamping

The vessel shall be stamped as follows:

Shell side Design Pr side.	Tube side Design Pr.
Shell side Design Temp.	Tube side Design Temp.
Shell side Hydrotest Pr.	Tube side Hydro Test Pr.
Serial No.	Inspection By.
Hydrotested On	

3.13 Preparation of Heat Exchangers for Shipment

During plant manufacture, storage, transport to site, and site erection, special precautions are to be taken to ensure that all the components remain clean and reasonably protected:

1. Internal and external surfaces are to be free from loose scale and other foreign matter that is readily removable.
2. Oil, water, or other liquids used for cleaning and hydrostatic testing should be drained before shipment. The shell side may be dried out by vacuum pump and the tube side by blowing through with hot air.

3. All exposed machined contact surfaces shall be coated with a removable rust preventive and protected by suitable cover against damage. Rust-preventive compounds must be regarded as contaminants to be removed before the heat exchanger is put into service [41].
4. All threaded connections are to be suitably plugged.
5. The exchanger and any spare parts are to be suitably protected to prevent damage during shipment.
6. All tell-tale holes shall be packed with hard grease. In the event of alloy material, the grease shall be low lead and should not contaminate the material.

General guidelines for preparation of heat exchangers for shipment are discussed in TEMA, paragraph G-6.

Painting

External surfaces shall be painted as per drawings/specifications. Use paint that will withstand the surface temperature while in operation. Stainless steels do not require painting.

Nitrogen Filling

If desired by the purchaser, the heat exchanger internals may be filled with dry nitrogen to protect the internal parts against corrosion.

3.14 Making Up Certificates

The following documents may be enclosed in a folder along with the heat exchanger:

1. Vessel detail drawing together with a materials list
2. Material certificates of chemical and physical properties for each vessel item
3. Welding procedure specification and procedure qualification records
4. Welder qualification records
5. Records of welding consumables used and their properties
6. Certificate of radiography and other nondestructive testing methods
7. Heat treatment charts
8. Hydrostatic test report
9. Job inspection report
10. Stagewise inspection chart
11. Final inspection report
12. Guarantee certificate

ANNEXURE 1 PLATE BENDING MACHINES, PWHT, AND MANIPULATIVE EQUIPMENT

A Roll Bending Machine

Mechanical and hydraulic three-roll plate bending machines are appropriate for the hot rolling of heavy plate. A four-roll bending machine offers production advantages, although it is not particularly suited to hot work [42].

B Vertical Plate Bending Machine

The vertical plate bending machine can be used for all ASME Code pressure vessel work, and results are claimed to be as good as or better than those obtained with horizontal plate bending rolls. Some of the advantages claimed for vertical roll bending include these [42]: (1) absence of camber in the rolled shell, (2) higher capacity and hence thicker plates can be rolled, (3)

less power consumption, (4) the weight of the plate has very little effect on the bending accuracy, and (5) the mill scale experienced on many plates drops clear during the bending operation, whereas in horizontal machines it tends to get rolled into the plate surface.

C PWHT of Shells

Use spider bracing for adequate support during the stress relieving operation, and thermocouples are fastened to the vessel internally and externally. Temperatures are closely monitored and controlled during the period of temperature raising, soaking, and relaxing. Test plates inserted both inside and outside the vessel during stress relieving are later tested to ensure that the plate has been returned to its proper ductility and tensile strength [43].

D Manipulative Equipment

In the fabrication of heat exchangers, rotator sets or turning rolls are utilized to manipulate the shell for various welding positions. They ensure smoother welds. Circumferential welding is carried out by providing for the components to be rotated on the roller manipulator on the support bed. Basically these comprise two types [44]: (1) self-aligning rotators and (2) conventional rotators. Self-aligning rotators consist of rubber-tired wheels that automatically align themselves to the change from one diameter of vessel to another. In the case of conventional rotators the rolls have to be manually positioned across the frames to suit the diameter of the vessel.

ANNEXURE 2 FORMING OF HEADS AND CLOSURES

A Forming Methods

For thin plates, the cheapest method is by cold spinning, and hot spinning of greater thickness. For still greater thickness a forming press is used. Where the dimension of the head are such that a single forming operation is not possible, several plates are pressed to the required contour and then welded together to a cap. This is known as the crown-and-segment technique.

Blank diameter, D, for the pressure vessel heads shown in Fig. 24 can be determined from the Welding Engineer Data Sheet Nomograph [45] or from the formula given therein:

$$D = 2\sqrt{RH + 1.33R^2} \tag{5}$$

B Spinning

Spinning of ends is applied to a wide range of materials. The forming is done by either hot or cold spinning. With cold spinning there can be substantial savings in production time, particularly in handling time, over conventional hot spinning or dishing and flanging on two separate

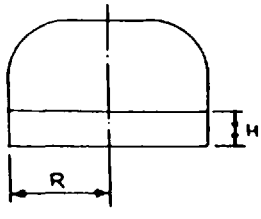


Figure 24 Pressure vessel head formed using Eq. 5 from blank diameter D. (From Ref. 45.)

machines [46]. Salient features of spinning of various materials are discussed by Peacock [4] and include the following:

1. Mild steel ends up to ⅛ in (3.2 mm) thick are cold spun with intermediate anneals, and ends greater than this thickness are hot spun at 1150°C.
2. Low-alloy steels are successfully hot spun.
3. For stainless steels with ends up to ⅝ in (15.9 mm) thickness, cold spinning with intermediate annealing at 1050°C is preferred. Ends greater than this above thickness are satisfactorily hot spun in the temperature range 900–1200°C; due care is to be taken to avoid carbide precipitation.
4. Ends can be made from explosion-clad plates by conventional hot or cold forming techniques. For more details on forming of clad plates, refer to the section on cladding in Chapter 13 on material selection and fabrication.

The spun heads will have a constant thickness in the hoop direction but will vary in the meridional direction. The thickness will be a maximum at the crown and a minimum in the knuckle region. The amount of thinning in the knuckle can be as high as 20–30%. Under internal pressure, the direct hoop stresses are compressive and hence the heads are susceptible to buckling [47].

C Pressing

Pressing, either hot or cold, is usually employed for the smaller diameter ends and is not as flexible in operation as spinning, because slight changes in end dimension require an alteration to the ring and pressing die. The majority of ends are hot pressed for two main reasons [6]: (1) The metal to be pressed undergoes less work hardening and is less prone to cracking, and (2) the load needed to press the material to the required dimensions is less.

For forming of heads by pressing, two major kinds of equipment are required. They are (1) the cold forming and dishing press and (2) the flanging and knuckling machine [48]. Initially the plate is manipulated into position beneath the ram and progressively rotated and tilted as successive ram strokes form the required shape. After dishing, the formed head is transferred to the knuckling machine for forming the edge to a more accurate radius.

D Crown and Segment (C and S) Technique

Large hemispherical heads and torispherical heads are fabricated by the crown-and-segment (C and S) technique. Hemispherical vessel heads are fabricated from a series of hemispherical orange-peel sections and one dish-shaped section to form a hemisphere, whereas the torisphere is fabricated by welding a spherical cap to a toroidal portion made of several segments (or gores) that have been welded together, as shown in Fig. 25. Two methods are followed for making the petals [48]. In one method, the required form is marked around the template on the flat plate; the petal is flame cut and then hot formed. In the more common method, the plate is rolled to the required petal shape and a template made to the form of the finished petal is used to mark out the lines to be cut. Then flame cutting is carried out manually and the edges are beveled and examined. All the plates are assembled on a supporting structure and welded. Caps for the hemispheres/torispheres are welded into position using fully automatic submerged arc welding. At the various welds, there may be local variations in geometry, although these will be reduced in magnitude by hammering and spinning after the welding operation. The thickness in the C and S heads will be essentially the same as that of the base plate material [47].

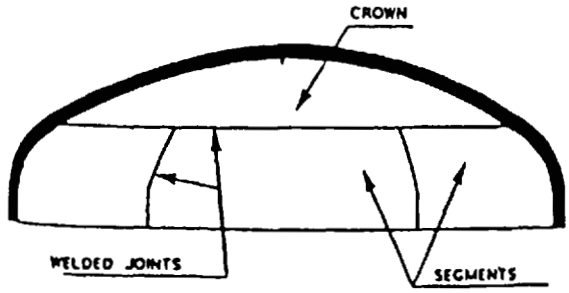


Figure 25 Crown (C) and segment (S) technique of welding pressure vessel head. (From Ref. 6.)

E Purchased End Closures

Purchased end closures should be accompanied by the following certificates.

Mill certificates of raw material and test coupons.
Process of manufacture.
Raw material plate thickness used for pressing.
Minimum thickness achieved after pressing.
Type of heat treatment carried out.
Stress-relieving/normalizing chart (time and temperature chart).
As-built dimensions of dished end.
Mechanical test results on test coupons.
NDT reports.

Important details of a manufactured dished head are shown in Fig. 26.

F Calibration of Heads

Heads distorted during the operations after pressing out have to be checked for reduction or enlargement of diameter, ovality, and increase of height [49].

G PWHT of Dished Ends

Dished ends shall be stress relieved if cold formed, and normalized if hot formed. A stress-relieving/normalizing chart duly certified by an inspection agency shall be furnished. For hot-formed dished ends, mechanical properties shall be proved on a test coupon after subjecting

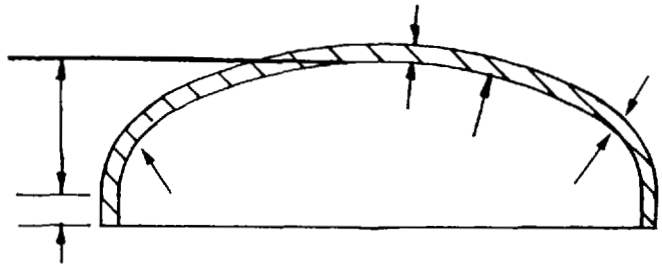


Figure 26 Details of a dished head.

the coupon to the same heat treatment as of the dished end, including the final normalizing. Problems faced during heat treatment of heads include [49]: (1) When the head is quenched, reasonable escaping of gases and steam should be provided to avoid origination of a steam cushion hindering uniform cooling, and (2) the heat treatment is associated with the risk of distortion.

4 DEFINITION AND GENERAL DESCRIPTION OF BRAZING

One of the more important processes of fabrication for complex assemblies is brazing. Most of the plate-fin heat exchangers (PFHE), some tube-fin exchangers, especially automobile radiators, and some highly compact metal rotary regenerators are brazed. Brazing joins two similar or dissimilar metals/nonmetals by heating them in the presence of a filler metal having a liquidus temperature above 840°F (450°C) but below the solidus temperature of the base materials. Heating may be provided by a variety of processes. The molten filler metal distributes itself between the closely fitted surfaces of the joint by capillary action. Brazing differs from soldering in that soldering filler metals have a liquidus temperature below 840°F (450°C).

4.1 Brazing Advantages

Brazing has the advantages of greater flexibility and scope. Strong, uniform, leak-proof joints are made rapidly, inexpensively, and even several joints simultaneously. It is unrivaled for assembling thin or delicate components or assemblies that are being produced in large quantities with the facility to produce many joints simultaneously [50,51]. Precise joining is comparatively easy without application of intense local heat to small areas. There is no heat-affected zone in brazing. Brazing requires little operator skill. Since the base materials do not melt at the brazing temperature, practically any two materials can be joined together in spite of a difference in composition, melting point, or thermal expansion. This includes similar and dissimilar metals. However, not all combinations of dissimilar metals can be brazed.

4.2 Disadvantages of Brazing

The brazing process is often considered an art today [52]. According to Shah, brazing requires considerable expenditure and capital cost, as well as development time, before ideal brazed joints can be manufactured, particularly for complicated assemblies. If there is any change in any one of the brazing process variables, such as flux, filler metals, temperature, brazing atmosphere including vacuum, or equipment and fixture, in general one needs to redefine the brazing process to obtain ideal joints.

The objective of this section is to provide comprehensive details on the fundamentals of brazing, brazing processes, and brazing of important heat exchanger materials including aluminum, stainless steel, and nickel. References 50–59 provide general and specific information on brazing.

5 ELEMENTS OF BRAZING

The proper use of brazing for a given application requires that due consideration be given to several factors:

1. Joint design
2. Filler metal selection
3. Precleaning and surface preparation

4. Fluxing
5. Fixturing
6. Heating method
7. Postbraze treatment and removing flux residues

These factors are discussed in detail next.

5.1 Joint Design

Joint design should consider the following factors:

1. Joint clearance: Joint clearance determines capillary force. The capillary force draws the molten filler metal deeply into every joint clearance. The joint clearance must be within specified limits. Suggested joint clearances as per joint width for various brazing processes are tabulated in Ref. 50.
2. Avoid flux entrapment: Entrapped flux may make the brazed joints susceptible to in-service corrosion. Too tight joint clearance restricts filler metal flow, whereas too wide joint clearance allows filler metal flow around flux. Flux trapped in the joint may also falsify leak test indications.
3. When joining different metals, their differing coefficients of thermal expansion become vitally important.
4. When brazing foil is used, the mating surfaces should be held in contact. The foil thickness will then determine the joint clearance.
5. The brazing symbol on the engineering drawing designates the location, class, and configuration of the brazed joint. Such symbols shall be as per ANSI/AWS A2.4, Standard Symbols for Welding, Brazing, and Nondestructive Examination.

Joint Types

In common with all forms of brazing, lap joints should be used in preference to butt joints. Joint types can be butt, lap, and T.

5.2 Brazing Filler Metals

Brazing filler is a nonferrous metal or alloy that melts at a temperature lower than that of the melting point of the base metal. Most filler metals are alloys, so they melt through a range of temperatures. When molten, the filler metal must wet the base metals, flow, and spread into joints to form brazed joints. The desired characteristics of molten filler metal are a low contact angle (Fig. 27), high liquid surface tension, and low viscosity.

Composition of Filler Metals

The American Welding Society lists in AWS 5.8-81 the specifications for brazing filler metal. Conventional fillers that find use in brazing of heat exchangers are in general based on aluminum, copper, nickel, cobalt, silver, and gold. Vacuum-grade fillers are silver-based, gold–pal-

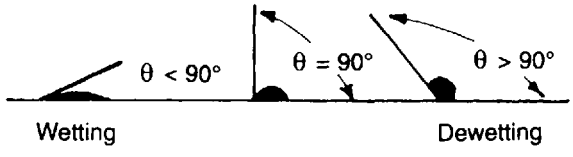


Figure 27 Molten filler metal contact angle.

ladium, aluminum–silicon, and copper-based alloys. The selection of filler metals is discussed by Weymuller [60] and Birchfield [61].

Aluminum Filler Metals

Aluminum filler metals (BA1Si series) are used for brazing aluminum. To reduce the possibility of galvanic corrosion, brazing filler metals are aluminum alloys rather than dissimilar metals [62]. Most of the brazing alloys are based in the aluminum–silicon eutectic system, containing between 7 and 12% silicon with a melting point of 1070°F (577°C). Occasionally other elements are added. They are available as filler metal or as clad brazing sheet. They are used to joint the wrought grades such as 1100, 3003, 3004, 3005, 5005, 5050, 5052, 6053, 6061, 6062, 6063, 6951, and 7005 [54,60]. Figure 28a shows a comparison of brazing temperature ranges of aluminum alloy base metals and aluminum filler metals. Figure 28b shows maximum permissible brazing temperatures for various aluminum alloys [50].

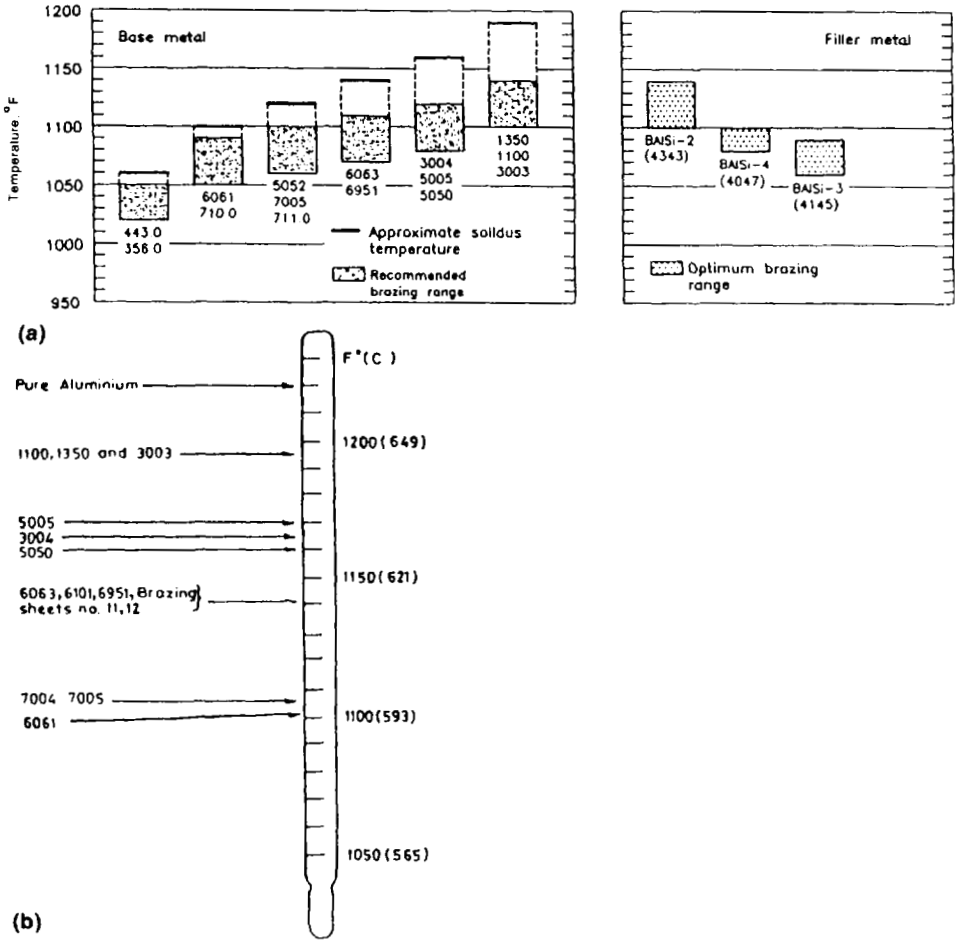


Figure 28 (a) Brazing temperature ranges for aluminum filler metals [59]. (b) Maximum permissible brazing temperatures for various aluminum alloys [50].

Copper Fillers

Copper filler (BCu) metal is used to braze ferrous and nickel base alloys.

Copper–phosphorus fillers (BCuP series) apply mostly for joining copper and its alloys and stainless steel. Avoid using these fillers on ferrous alloys, nickel-based alloys, and copper alloys containing more than 10% nickel [54,60]. These fillers are relatively low in cost, since they lack silver or gold. Copper-based filler alloys are not compatible with sulfur-bearing fuels [60,63].

Copper–zinc fillers (BCuZn series) are used to braze steels, stainless steels, copper and its alloys, and nickel-based alloys.

Nickel-Based Filler Metals

Nickel-based filler (BNi series) metals are used primarily to braze heat- and corrosion-resistant alloys, most commonly nickel- and cobalt-based alloys and the AISI 300 and 400 series stainless steels. These filler metals provide joints that have excellent corrosion resistance and high-temperature strength [64]. Since they require relatively high melting temperature, their use is generally restricted to furnace brazing in a controlled atmosphere including vacuum. Also, nickel fillers tend to be sluggish in the fluid state; therefore, joint design, filler metal selection, and brazing temperature should be carefully considered [54].

Silver-Based Filler Metals

Silver-based brazing alloys (BAg series) find a multitude of uses, because they cover a wide range of brazing temperatures, 1145°F to 1900°F. They are used to join ferrous and nonferrous metals and alloys, except low-melting metals such as aluminum, magnesium, and their alloys [60]. Their advantages are free flow, relatively low brazing temperature, and that they make ductile and smooth joints [54].

Gold-Based Fillers

Gold-based fillers (BAu series) are preferred for specialized applications such as aerospace heat exchangers to braze stainless steel, nickel, and cobalt-based alloys that require oxidation and corrosion resistant at elevated temperatures, and compatibility with sulfur-bearing fuel. These fillers are primarily used in furnace brazing applications. Because gold interacts little with base metals, gold-based fillers will not alter properties of the base metal [60]. Various filler metals and their applications are give in Table 1, and brazing temperature ranges for aluminum, copper, silver, nickel, and gold alloy filler metals are shown in Fig. 29.

Table 1 Typical Filler Metal Applications

Primary metal in filler	Base materials
Aluminum	Aluminum-based alloys
Copper	Copper-based alloys, ferrous metals, nickel-based alloys
Copper–phosphorus	Copper-based alloys; avoid using on ferrous alloys, nickel-based alloys, and copper alloys containing more than 10% nickel
Copper–zinc	Steels, stainless steels, copper and its alloys, and nickel-based alloys
Nickel	SS types 300 and 400, nickel-based and cobalt-based alloys
Silver	Ferrous; nonferrous except aluminum and magnesium and their alloys, which melt at low temperatures
Gold	Thin sections of SS, nickel-based, or cobalt-based alloys requiring high corrosion and oxidation resistance

Forms of Filler Metal

To control the amount of filler metal requirement, the filler metals are available in predetermined amounts and shapes known as preforms. Various preforms are wire, strip, sheet, rod, powder, and shapes that fit specific joints. Preforms suit well with automatic brazing. Aluminum brazing sheet is a standard, commercial product. The constructional features and metallurgy of aluminum brazing sheets are explained next.

Placement of Filler Metal

Placement of filler metal is an important design factor. Usually, the filler material is preplaced near the joints to be brazed. Either the braze metal is metallurgically clad to a thin flat structural member known as a brazing sheet, sandwiched between the parts to be joined, or base metal is coated with a slurry of braze alloy powder and binder.

ASME Code Specification for Filler Metals

Pressure vessel braze metals conform to ASME Section II, Part C. Tables in Part C identify filler metal specifications that are identical to AWS filler metal specifications. The code addresses fluxes or brazing atmospheres indirectly through its requirements to successfully qualify a brazing procedure.

5.3 Precleaning and Surface Preparation

Precleaning

Clean, oxide-free surfaces are essential to ensure sound brazed joints. Grease, oil, dirt, marking crayons, and oxides prevent the wetting, uniform flow and bonding of the brazing filler metal, and they impair fluxing action, resulting in voids and inclusions. Precleaning of components

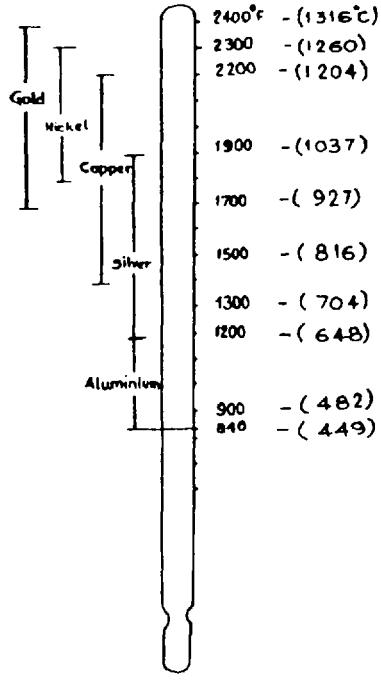


Figure 29 Brazing temperature ranges for filler metals. (From Ref. 54.)

may be accomplished by degreasing with organic solvents or vapors or by a mild chemical etch, such as dilute caustic soda solution [50]. Cleaning should always be carried out before assembly. Otherwise, if an assembled component is immersed in a chemical cleaner, residues will inevitably be trapped in the joints [65].

Scale and Oxide Removal

Good performance, which characterizes the soundness (leak tightness, joint strength, and fillet shape) and integrity of the brazed joint, is possible only when the surface oxide film on the metal surface is dispersed sufficiently for wetting and flow of filler metal to occur.

Chemical Cleaning. Scale and oxide removal can be accomplished mechanically or chemically. Descaling can be done with any of the following solutions [54]:

1. Acid cleaning
2. Acid pickling—sulfuric, nitric, and hydrochloric acid
3. Salt bath pickling

Prior to descaling, degreasing is recommended.

Mechanical Cleaning. Mechanical cleaning is usually confined to those metals with heavy tenacious oxide films. Mechanical methods include abrasive grinding, grit blasting, filing, or wire brushing using stainless steel bristles. Grit blasting should be done with clean blasting material such as silica sand or alumina sand. Care must be taken that the mechanical cleaning materials are not embedded in the metals to be brazed. After mechanical cleaning, air blasting or ultrasonic cleaning should be used to remove all traces of loosened oxides or blasting medium.

Protection of Precleaned Parts

After cleaning, the cleaned parts should be assembled and brazed without delay to avoid oxidation and build up of contamination. The cleaned surfaces should not be hand touched after cleaning. They should be stored and transported to the braze preparation areas in dry, clean containers, such as plastic bags.

5.4 Fluxing

Conventional brazing processes performed in air or other oxygen-bearing atmosphere require fluxing. In other words, vacuum brazing does not require flux, and furnace brazing performed in inert or strongly reducing atmosphere usually does not require flux. Fluxes are necessary to displace the oxide layers at the bonding sites and to allow the wetting by the molten filler metal. Without flux, molten filler forms a ball even though the surface it contacts is clean and the temperature is high. Additionally, the flux protects the bonding sites against reoxidation of the cleaned surface during brazing. However, fluxes are not intended to perform the primary function of removal of oxides, scales, coatings and surface contaminants. Fluxes come as paste, powder, slurry or liquid.

Selection of a Flux

Flux selection is influenced by these factors [54,64]: base material, filler metal, brazing process, joint configurations, and flux dispensing methods such as brush, dip, syringe, spray, etc., which determine flux forms and ease of cleaning.

Composition of the Flux

Fluxes contain one or more heavy metal chlorides in addition to active fluoride salts along with other chemicals. Fluxes are generally mixed with water to form a thick slurry, which is applied to the precleaned parts to be brazed.

Demerits of Brazing Using Corrosive Fluxes

Though several advantages can be claimed for the brazing techniques using fluxes [66], brazing fluxes are chemically active, and their residues are highly corrosive, especially in the presence of moisture. Therefore, after brazing, flux residuals must be removed by a cleaning process to avoid both corrosion and contamination problems. Other problems associated with fluxes include [62]: (1) Postbraze cleaning is costly; (2) for complex structures with closed tortuous passage ways, the elimination of flux residuals can require long cleaning cycles; and (3) disposal of spent cleaning solutions can become costly with ever tighter control of plant effluent.

5.5 Fixturing

As far as possible, components to be brazed should be self-fixturing. Fixtures, being in contact with the part, extend the heating time to bring the components up to the brazing temperature. Slow heating due to attachment of fixturing will change the characteristics of the filler metal [65]. Examples of self-fixturing construction include aluminum screws, rivets, resistance welds, argon arc tack welds, piercing, and tagging. For external fixtures, austenitic stainless steels or heat-resisting nickel alloys is recommended. Mild steel can also be used for low-volume production. Use clean and dry fixtures to avoid pumpdown delays.

5.6 Brazing Methods

Brazing processes are classified according to the sources or methods of heating. There are numerous brazing methods, including:

1. Torch brazing
2. Dip brazing
3. Furnace brazing
4. Vacuum and controlled-atmosphere brazing
5. Induction brazing
6. Resistance brazing
7. Infrared brazing

All these brazing methods include the same brazing procedures. The prime difference lies in the way the parts are heated and the way flux and filler metals are applied. Except for vacuum and controlled-atmosphere brazing, all methods require flux. In this section, the first four brazing methods are discussed.

To braze, surfaces must be cleaned, freed of excess oxide, coated with flux, and spaced a few thousandths of an inch apart. Brazing filler is placed in or near the joint to be formed, assembled, and fixtured. When heat is applied, the flux displaces oxide and shields the metal from air. As the filler flows, it displaces flux and wets the base metal, adapting to submicroscopic irregularities and dissolving the small high points it encounters.

Torch Brazing

Any joint that can be reached by a torch and brought to brazing temperature can be readily brazed by this technique. Torch brazing can be either hand-held or automatic. Hand-held manual torch brazing is most frequently used for repairs, one-of-a-kind brazing jobs, short production runs, and as an alternative to gas or arc welding. For example, repairs or low-production copper-to-copper joints in return bends of an evaporator or a condenser of a airconditioner are preformed by torch brazing. Most commercial torch brazing is carried out by use of oxyacetylene flame in which the torch is adjusted to produce slightly reducing flame for most applica-

tion. In automatic torch brazing, the assembly is moved automatically in relation to the torch, or vice versa. It is used for mass production.

Dip Brazing

In the dip brazing process, often referred to as salt-bath brazing, the part or assembly being joined is held together and immersed in a bath of molten salt, which flows into the joints when the parts reach a temperature approaching that of the bath. The molten flux, at a temperature slightly above the liquidus of the filler metal, serves as a heat source and partially supports the submerged metal parts. In addition to providing the heat for brazing, many of the salts have fluxing properties. Dip brazing has been extensively used in industry for daily production of aluminum and other alloy parts. It has the unique advantages that [52] (1) the time required for heating is about one-fourth that required for furnace brazing, (2) distortion due to self weight is less due to buoyancy, and (3) the parts reach the brazing temperature uniformly.

Choice of Flux. Commercial dip-brazing fluxes are generally similar to fluxes used with other brazing methods. Their main ingredients include the combinations of sodium chloride, potassium chloride, aluminum fluoride, and lithium chloride. Dip brazing requires water-free flux to avoid spattering of moisture from the bath.

Dip Bath Heating Means. Heating may be by gas for lower temperature systems or by one of the two forms of electrical heating: either resistance elements mounted around the pot, or electrodes immersed in the molten salt bath.

Flux Pot. Flux pots comprise steel-reinforced vessels lined with high-alumina, acid-proof fire brick. Pot covers are well insulated. Large covers may be mounted on rollers and power operated.

Preheating the Assemblies. Dip brazing generally requires preheating. This helps in a flux preplaced joint, dries the flux, and vaporizes moisture from the assembly before being immersed into the salt bath and thereby prevents accidents from steam explosions. It also can reduce brazing time, minimize the salt residue that forms on the part, and reduce distortion, as well as reduce bath size [54]. Preheating is achieved either by the flue gases or by electrical heating in a suitable furnace to a temperature 50°F to 100°F (30°C to 60°C) below the solidus temperature of the brazing filler metal until the entire assembly has attained this temperature. For aluminum brazing, the assembly is preheated to approximately 1000°F (538°C).

Dip Brazing Procedure. The dip brazing steps (along with furnace-brazing steps) are given in Table 2.

Immersion Time. The time needed to form the joints depends on the mass of the assembly and its temperature at the moment it enters the molten salt bath. Dip time varies from as little as a few seconds to as long as 10 or 20 min. There is no formula to arrive at the immersion time, but it is arrived by trial-and-error practice [50].

Maintaining the Flux Bath. A properly maintained flux bath will produce a work piece that is bright and shiny, with fillets well formed and complete [54]. To achieve these properties, the bath should be relatively free of sludge and surface film, slightly acidic with a pH between 6.4 and 7.0 (for aluminum a pH between 5.3 and 6.9), and relatively constant chemical composition. The bath is periodically checked for moisture, acidity, chemical composition, temperature, and other physical characteristics by the laboratory and corrective action made as required.

Scum and Sludge Removal. Contaminants in and on top of the hot flux interfere with quality of brazing. Contaminants that float to the surface are called scum, and they are readily removed by skimming the bath's surface with a sheet of aluminum. There are a number of commercial preparations that, when added to the bath, cause the particles to coagulate, making their re-

Table 2 Dip and Furnace Brazing Steps

Dip brazing	Furnace brazing
Precleaning and surface preparation	Precleaning and surface preparation
Preparation of flux bath	Flux preparation and application[a]
Assembly and fixturing	Assembly and fixturing
Preheating	
Brazing in flux bath	Brazing in furnace
Cooling or quenching	Cooling or quenching
Hot water washing	Hot water washing[a]
Flux removal	Flux removal[a]
Finishing and inspection	Finishing and inspection

[a]Not applicable for vacuum brazing.

moval easier [50]. Contaminants that sink to the bottom of the pot are called sludge. The sludge is removed periodically by ladling with a perforated tool.

Ventilation. Salt-bath dip brazing can emit toxic or noxious gas, fumes, and dust. Ventilation to remove air emissions from the above the bath is a must.

Limitations of Dip Brazing. Some of the limitations of dip brazing are:

1. Dip brazing generally requires preheating to prevent accidents from steam explosions.
2. The shape of the part must be designed to avoid trapping air or salt and to be drained completely.
3. Maintenance problem due to power shutdown for internally electric heated salt bath.
4. A different salt will probably be required for the next application if either the parent metals or the brazing alloy has been changed; frequent changing is not economical.

Furnace Brazing

The term *furnace brazing* can be applied to any brazing process where a furnace is used as the heat source to raise the parts to be joined to their brazing temperature. Furnace brazing is extensively used in industry for brazing heat exchangers and joining complex parts. It offers uniform heating, and hence accurate temperature control is possible. The finished product has excellent quality. The process is economically attractive for brazing heavy assemblies in which multiple brazed joints are to be formed simultaneously or many assemblies are to be joined simultaneously.

Furnace Heating. The furnaces may be heated by gas, oil, or electricity, and provided with temperature controls. Fluxes or specially controlled atmosphere that perform fluxing functions must be provided. Filler metal must be preplaced in the form of sheet, wire, rings, powder, or other suitable forms.

Atmospheres. Furnace brazing takes place in a vacuum or in a controlled atmosphere of high-purity inert or reducing gas. Both reduce the amount of flux needed or in some cases eliminate the need for flux completely, and prevent oxidation and scaling during heating. There are, however, examples of this type of furnace being used with an atmosphere of normal air or ultradry air in association with flux. These aspects are discussed later. The brazing atmosphere, whether gaseous or vacuum, should be free from harmful constituents such as sulfur, oxygen, and water vapor. When brazing in a gaseous atmosphere, it is a common practice to monitor the water vapor content of the atmosphere as a function of dewpoint. In general, a furnace atmosphere having a dewpoint less than about −60°C (−75°F) produces better quality.

Brazing Furnaces. In general, brazing furnaces are classified as (1) batch furnace, (2) semicontinuous or locked furnace, or (3) continuous furnace. Single-chambered, batch-type units are used for low-volume production, while multichambered semicontinuous or continuous furnaces are employed for high-volume production applications. Selection of a particular type production furnace depends on the size and geometry of the parts to be brazed, as well as production rates required.

Classification of Batch Furnaces. Batch furnaces are classified as follows [54,67]:

1. Direct-combustion furnaces
2. Muffle furnaces or hot-wall furnaces
3. Retort-bell type combustion furnaces
4. Vacuum brazing furnaces: single pumped retort furnaces, double pumped retort furnace, batch-type vacuum furnace (hot or cold wall design)

These furnace types are briefly discussed next. For more details see Refs. 54 and 67.

Direct Combustion Furnace. The simplest and least expensive furnaces are the direct-combustion type, in which combustion products pass through the brazing zone and hence come into contact with the workpiece. As moisture is always a by-product of combustion and as moisture is a hindrance to good brazing, the direct-combustion furnace will not offer optimum quality joints.

Muffle Furnace or Hot-Wall Furnaces. A gas-fired muffle furnace will normally incorporate a refractory chamber so that the flames pass around the outside of the chamber, which ensures that the products of combustion do not come into contact with the workpiece. Because of this, this furnace offers optimum quality joints. For still better quality, employ electric-resistance or radiant-tube furnaces, or furnaces that combine resistance and combustion heating.

Retort-Bell Type Combustion Furnaces. The retort-bell type combustion furnaces have been developed for high-temperature brazing applications. For brazing in a purified hydrogen atmosphere, there is an inner container of a heat-resistant alloy sealed from outside air and the products of combustion. The workpiece is placed into this container; the container is purged with dry hydrogen and then lowered into a pit-type furnace. Hydrogen flows through the container during preheating, brazing, and cooling.

Vacuum Brazing Furnaces. Vacuum brazing can be of these types: (1) single pumped retort, (2) double pumped retort, (3) batch-type furnace, and (4) continuous furnace.

The *single pumped retort* is loaded with the brazement, evacuated and heated externally by a resistance or by gas or by oil combustion.

The *double pumped retort* is for higher temperature brazing. Manufacturers can employ a double-wall retort; the work load sits in a high vacuum (10^{-2} torr or lower) container that is placed in a rough vacuum (1 to 10 torr) chamber.

The *batch-type vacuum furnace* consists of a chamber with doors at one or both ends and is typically equipped with mechanical roughing and oil vapor diffusion pumps. Batch-type vacuum furnaces can be hot- or cold-walled design; cold-wall furnaces are more popular. The term *cold wall* design refers to the fact that the chamber walls are water cooled and that conventional refractory insulation is not present between the hot zone and chamber walls. A typical batch vacuum furnace is shown schematically in Fig. 30. Depending on the geometry of the workpiece and the desired production rate, the hot zone size can be in the range of 1–600 ft^3 (0.028–17 m^3). The hot zone can be rectangular or cylindrical in shape. Batch furnace cycle times can vary few minutes to longer than a day. Large components such as cryogenic heat exchanger cores have cycle times of many hours.

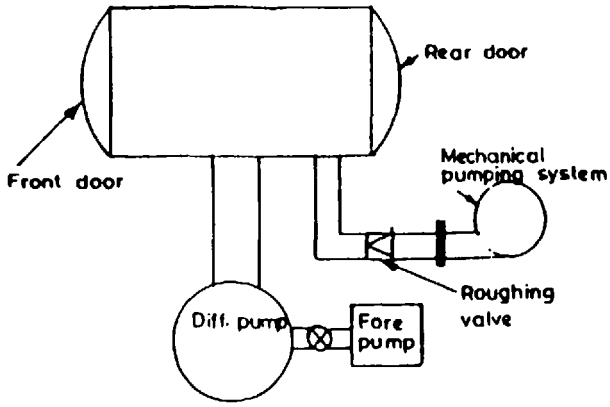


Figure 30 Vacuum type batch furnace. (From Ref. 69.)

In a *semicontinuous vacuum furnace*, the brazing chamber is divided into two or more heating stations so that part movement from station to station brings about the braze. The number of hot zones is determined by the parts to be brazed and the desired production rate. For example, in a three-zone brazing chamber, the braze is completed in three stages, and three carriers of parts, each at a different heating station, are contained in the brazing chamber environment at all times. Cycle times for a three-zone chamber are approximately one-third that for the batch process [68]. A semicontinuous or locked furnace is shown schematically in Fig. 31. It is developed to avoid contamination while loading or unloading work [69]. The entrance vestibule is generally used to preheat and outgas the parts prior to transfer into the brazing zone. The exit vestibule is used for the initial phase of cooling and filler metal solidification under an inert or dry air environment [68]. For more details on batch type and continuous type vacuum furnaces see Ref. 69.

Procedure. Furnace brazing steps are listed in Table 2.

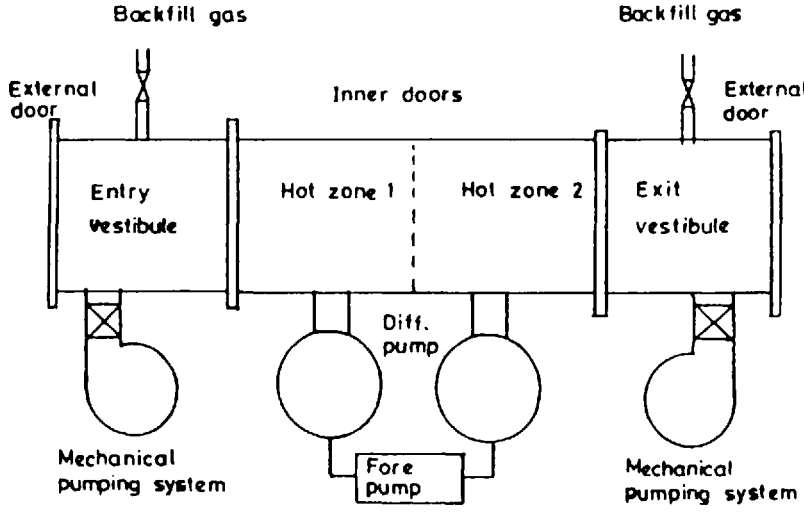


Figure 31 Semicontinuous or locked furnace. (From Ref. 69.)

Brazing Processes Without Corrosive Flux. Various processes have been developed for reducing or eliminating corrosive flux in the brazing of heat exchangers. Three industrial processes are followed to overcome the requirement of corrosive flux. They are

1. Controlled-atmosphere brazing
2. Use of noncorrosive flux under the trade name NOCOLOCK
3. Vacuum brazing

All three methods are commercially used for the manufacture of heat exchangers and high-volume automotive heat exchangers, such as radiators, air conditioning evaporators, heater cores, and turbo air coolers. In general, the fluxless processes require furnace atmosphere having a dew point less than about –60°C (–75°F) to produce better quality.

Controlled-Atmosphere Brazing. In controlled-atmosphere brazing (excluding a vacuum atmosphere), a continuous flow of a certain gas is maintained in the work zone to avoid contamination from outgassing of the metal parts and dissociation of oxides. Controlled atmospheres for furnace brazing include combusted fuel gas, dissociated ammonia, cryogenic or purified $N_2 + H_2$, deoxygenated and dried hydrogen, purified inert gas, etc., as specified by AWS designations. The controlled atmosphere such as pure dry hydrogen or inert gases inhibits the oxidation and scaling of the surfaces. Inert gases, such as helium and argon, do not form compounds with metals and inhibit vaporization of volatile elements. A dry-nitrogen atmosphere is excellent for production volume brazing with a fluoride flux. With controlled-atmosphere brazing, the need for a flux is eliminated or the flux requirement is considerably reduced.

The merits of controlled-atmosphere brazing include: (1) The need for a flux is eliminated or the flux requirement is considerably reduced; (2) there is more rapid and uniform heating than brazing under vacuum, due to convective heating of the component by the circulated gas; and (3) it prevents oxide and scale formation on the parts being brazed and reduces evaporation of volatile elements. Due to these reasons, the assembled components remain clean and bright after brazing, postbraze cleaning is generally not necessary, and there are lower maintenance requirements related to buildup of volatile alloying elements [70]. However, controlled atmospheres are not intended to perform the primary cleaning operation and surface oxide removal.

Use of Noncorrosive Flux Under the Trade Name NOCOLOCK. Use of noncorrosive flux under the Trade name NOCOLOCK pertains to aluminum brazing. Therefore, it is covered in the next part, while discussing aluminum brazing.

Vacuum Brazing

Vacuum brazing is a form of furnace brazing process for brazing assemblies in a vacuum environment without the use of flux. Vacuum brazing is being used commercially to produce automotive and aircraft heat exchangers. Large prototype industrial heat exchangers and massive cryogenic heat exchangers have been successfully vacuum brazed. Commercial vacuum brazing generally is done at pressure varying from 10^{-5} to 10^{-1} torr, depending on the materials brazed and the filler metals being used.

Parent Metals Brazed. Vacuum brazing is most suitable to brazing aluminum alloys, stainless steels, superalloys, titanium alloys, zirconium, or other reactive elements with particularly stable oxides.

Merits of Vacuum Brazing. Merits of vacuum brazing are:

1. The method eliminates the need for fluxes and postbraze cleaning.
2. It is nonpolluting and possesses high braze performance capabilities.
3. Vacuum prevents oxidation of metals by removing air from around the assembly and also removes volatile impurities and gases from the metals.

4. The method imparts a high standard of cleanliness to the work that could not be achieved by any other method.
5. The overall production time is minimized since there is no fluxing action and subsequent postbraze cleaning.

5.7 Postbraze Cleaning

Brazing fluxes are chemically active, and their residues are highly corrosive, especially in the presence of moisture. Therefore, after brazing, flux residuals must be removed to avoid both corrosion and contamination problems. Use boiling water, which usually removes chloride type flux residue, or a strong acid such as nitric, followed by water rinsing. Oxidized areas adjacent to the brazed joint can be cleaned by pickling, wire brushing, or blast cleaning.

Braze Stopoffs

When filler metal flow must be restricted to definite areas, "stopoffs" are employed to outline the areas that are not to be brazed. Braze stopoff materials, if used, must be compatible with base metal, filler metal, fluxes, and furnace atmosphere [71]. Stopoff residue must be removed from the joint after brazing. Wire brush, air blast, or water flush will remove the stopoff residue.

6 FUNDAMENTALS OF BRAZING PROCESS CONTROL

It is generally accepted that the most important variables involved in the brazing process include the brazing temperature, time at temperature, brazing atmosphere, and the rate and mode of heating. Some of the these factors are discussed next.

6.1 Heating Rate

Geometry and the distribution of mass within the part, heating element configuration relative to part location, and vacuum environment characteristics will determine the heating rates needed to realize a good braze.

6.2 Brazing Temperature

Brazing temperature is mostly governed by the base metal characteristics and the type of filler metal. In general, the filler metals with the higher melting points correlate with higher strength joints. Various base metals with their melting and brazing temperatures are shown in Table 3.

6.3 Brazing Time

Brazing time will depend somewhat on the mass/thickness of the parts and the amount of fixturing necessary to hold them. It has become industry practice to minimize the holding time

Table 3 Base Metals and Their Melting Temperatures and Brazing Temperatures

Base metal	Melting temperature	Brazing temperature
Aluminum and aluminum alloys	588–657°C (1090–1215°F)	571–621°C (1060–1150°F)
Stainless steels	1370–1532°C (2500–2790°F)	618–1232°C (1145–2250°F)

at brazing temperatures to minimize excessive filler metal flow and/or erosion, evaporation, and oxidation. Brazing times in the order of less than a minute are common.

6.4 Temperature Uniformity

Producing consistent braze joint quality throughout the part/furnace load/temperature uniformity in all of the workpieces depends on the configuration of the work, its placement, how it interrelates with the hot zone, etc.

6.5 Control of Distortion During the Furnace Cycle

Control of distortion is vitally important for successful furnace brazing, particularly complex parts. Distortion can result from fast heating, fast cooling, stresses that develop during heating, residual stresses in a workpiece, phase transformation, and properties of dissimilar base materials [72]. According to Tennenhouse [72], distortion can be minimized or eliminated by measures like uniform heating and cooling of the part, reduced and controlled heating rates, use of dummy weights, heat shields and lightened fixtures, and adequate supports to the parts.

7 BRAZING OF ALUMINUM

Brazed aluminum assemblies are all aluminum with excellent corrosion resistance when properly cleaned of any residual corrosive flux. Brazed aluminum assemblies conduct heat uniformly. Therefore, brazed aluminum heat exchangers are long-lasting and highly efficient.

Techniques for brazing aluminum are similar to those used for brazing other metals. Commercially the same equipment is often used. But there are some important differences between aluminum and other brazeable metals that affect the standard brazing techniques. These differences stem from the refractory nature of the surface oxide film on aluminum, from the oxide that forms on aluminum having a high melting point (3722°F), and from the low melting point of aluminum [62]. Other characteristic features of aluminum relevant for brazing include: It conducts heat quickly, surface oxides form rapidly, thermal expansion is greater than many other common metals, and it doesn't change color as its temperature changes [50].

7.1 Need for Closer Temperature Control

Aluminum alloys are brazed with aluminum filler metals that are similar to the base metals. Filler metals have liquidus temperatures closer to the solidus temperature of the parent metals, and hence close temperature control is very important [51]. This can be easily understood from the Table 3. The brazing atmosphere should be approximately 70°F (39°C) below the solidus temperature of the base metal, but if temperature is accurately controlled and the brazing cycle is short, the difference can be as close as 10°F (5.5°C) [59].

7.2 Aluminum Alloys That Can Be Brazed

A majority of the non-heat-treatable aluminum alloys like 1100, 3003, 3004, and 5005 and many of the heat-treatable alloys like 6053, 6061, 6063, 6951, 7005, and 7072 can be brazed. Aluminum alloys containing more than 2.5% magnesium are difficult to braze. Common brazeable wrought alloys, their composition, and approximate melting range are shown in Table 4. Approximate brazing temperatures for common aluminum alloys are shown in Fig. 32. In addition to these aluminum can be brazed to many dissimilar metals and alloys. A partial list includes the ferrous alloys, nickel, titanium, Monel, and Inconel [50].

Table 4 Common Brazeable Wrought Alloys With Their Compositions and Approximate Melting Ranges [50]

	Nominal composition (%), remainder Al and impurities							Melting range	
Alloy	Cu	Si	Mn	Mg	Zi	Ni	Cr	°C	°F
1100			99.00% minimum aluminum					643–657	1190–1215
3003	0.12	0.6	1.2	—	—	—	—	643–654	1190–1210
3004	—	—	1.2	1.0	—	—	—	629–652	1165–1205
3005	—	—	1.2	0.4	—	—	—	638–657	1180–1215
5005	—	—	—	0.8	—	—	—	627–652	1160–1205
5050	—	—	—	1.2	—	—	—	627–652	1160–1205
5052	—	—	—	2.5	—	—	0.25	593–649	1100–1200
6061	0.25	0.6	—	1.0	—	—	0.25	616–652	1140–1205
6063	—	0.4	—	0.7	—	—	—	616–652	1140–1205
6151	–	1.0	—	0.6	—	—	0.25	588–649	1090–1200
6951	0.25	0.35	—	0.6	—	—	—	616–654	1140–1210
7004	—	—	0.45	1.5	4.2	—	0.13	604–646	1120–1195
7005	—	—	0.45	1.4	4.5	—	0.13	607–646	1125–1195
7072	—	—	—	—	1.0	—	—	646–657	1195–1215

7.3 Elements of Aluminum Brazing

Joint Clearance

The joint clearances established for aluminum brazing are furnished in Ref. 50.

Precleaning

Brazing aluminum requires that the metal be free from surface contaminants and its oxide layer thin enough to be displaced by the brazing flux. Surface contaminants such as greases, oil, fatty acids, and marking crayons can be removed by vapor degreasing using inhibited trichloroethylene or ultrasonic degreasing.

Surface Oxide Removal

As highly reactive material, aluminum and its alloys are covered with an oxide. This oxide can be an important hinderant in brazing process, where the oxide film acts as a barrier to the wetting and flow of filler metal [68]. Hence, oxide barrier dispersal is a prerequisite for suc-

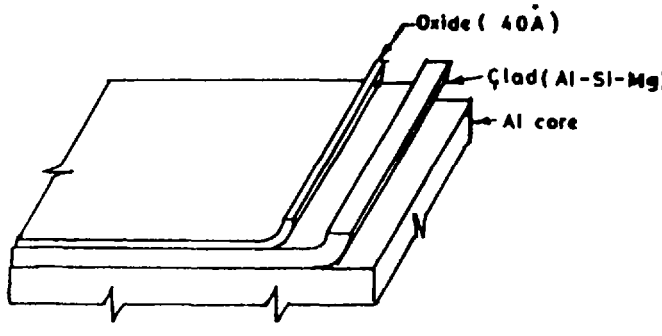


Figure 32 Clad aluminum brazing sheet. (From Ref. 74.)

cessful brazing. For non-heat-treatable aluminum alloys, vapor degreasing or ultrasonic degreasing is adequate [65]. Overly thick oxide layers on heat-treatable alloys can be reduced by either mechanical means or chemical means [50]. Chemical means will consist of a degreasing either in trichloroethylene or a chemical cleaner followed by an acid or alkaline etch. The parts will normally need desmuting in nitric acid, after which they are washed in clean water and dried [65]. Chemical cleaning is not recommended for fluxless vacuum brazing [59].

Aluminum Filler Metals

In the case of aluminum, the major elements in the filler metal are the same as the base metal except for some additional melting-point depressants. Complex parts can be formed and assembled using clad brazing sheet to eliminate the need for separate filler wire or shim. Various flux brazing filler alloys, vacuum brazing filler alloys, and clad aluminum flux brazing sheet are dealt with in Ref. 50.

Aluminum Brazing Sheet. Aluminum brazing sheet consists of a base metal core (typically 3003 or 6951 alloy) and a filler metal, typically either Al-7.5Si (4343) or Al-10Si (4045), clad roll bonded to either to one or both sides as illustrated in Fig. 32. The core provides structural integrity, while the clad plays the role of filler metal. An oxide surface layer is depicted to emphasize the importance of this barrier to the wetting and flow of the filler metal and the requirement that the barrier be dispersed for a successful braze [74].

Fluxing

Except for vacuum brazing or controlled-atmosphere (without oxygen) brazing, or salt-bath brazing processes where the salt bath itself consists of flux, all surfaces must be fluxed to break down the oxide film on the surface of the work and to promote wetting, and the filler itself must be fluxed. Fluxes for aluminum brazing contain fluorides and chlorides of the alkali metals. To the base are added "activators" such as fluorides, lithium compounds, and sometimes zinc chloride [62].

7.4 Brazing Methods

The main processes used commercially to braze aluminum heat exchangers are

1. Torch brazing
2. Furnace brazing: controlled-gas atmosphere brazing and vacuum brazing
3. Flux dip brazing

Torch brazing and dip brazing employ a flux to break down the oxide film on the surface of the work and promote wetting. Furnace brazing with controlled-gas atmosphere requires less flux or no flux, whereas vacuum brazing does not require a flux and the mechanism of oxide breakdown is quite different.

Aluminum Dip Brazing

Aluminum dip brazing has been practiced commercially for many years. The molten salt bath contains chemically active salts that promote brazing. These help to displace the adherent oxide film on aluminum surfaces so that the molten filler metal wets the surfaces and forms the brazed joints. Because of the stability of surface oxide film, and because of low brazing temperatures that have to be used, a highly active flux is required for brazing aluminum. Important parameters pertaining to dip brazing aluminum are given in Table 5. Manufacturing procedure for dip brazing of PFHE is shown in Figure 33.

Table 5 Aluminum Dip Brazing Parameters [54]

Bath composition	Bath melting point	Preheating temperature	Brazing temperature
AlF, NaCl, KCl, or LiCl	900–1000°F (482–538°C)	1100°F (538°C)	1030–1190°F (555–643°C)

Furnace Brazing

Furnace brazing is the second most popular method of brazing aluminum in use today. Furnace brazing's popularity derives from the comparatively low cost of equipment, from the ease with which the existing furnaces can be adapted to aluminum brazing, and from the minimal fixturing required [50].

Inert-Gas or Controlled-Atmosphere Brazing of Aluminum. For inert-gas brazing of aluminum, the process variables that affect moisture and oxygen levels in the brazing chamber must be controlled. This requires that the workpiece along with the fixture and the carrier be adequately outgassed to remove adsorbed moisture and oxygen prior to entering the inert-gas chamber. This is achieved by either repeated heating and evacuations, or a vacuum heating of aluminum with magnesium brazing filler metal clad to getter the contaminants.

Controlled Dry Air Brazing. The amount of moisture in the brazing atmosphere influences the amount of flux required for successful brazing. When the moisture is not controlled, thick flux slurries, about 50 to 75% by weight, are required. Only a small amount of flux serves the intended purpose, and much of it becomes ineffective because it is hydrolyzed by reaction with moisture present in the air, before the brazing alloy melts [75]. In a dry-air atmosphere of −40°F (−40°C) dewpoint or lower, thin slurries containing 20–25% flux will serve the purpose. This brazing process also eases the postbrazing cleaning requirements.

Furnace Brazing of Aluminum with a NonCorrosive Flux—NOCOLOCK Flux (NOCOLOK Owned by Alcan Aluminum Ltd.). It was discovered that a brazing method using a nonhydroscopic, noncorrosive, potassium fluo-aluminate flux material offered the benefits of flux brazing without a requisite postbraze cleaning. When used in an inert-gas atmosphere, it has a significant tolerance to impurities in the furnace atmosphere [76]. The flux is active only at or near the brazing temperature, and is completely inactive at lower temperatures, which allows the flux residue to be left on the work without any danger of subsequent corrosion. The trade name for the noncorrosive flux is known as NOCOLOCK. Heat exchangers such as automotive radiators, heater cores, condensers, evaporators, oil coolers, and charge air coolers are being mass produced using the NOCOLOK flux brazing process [77]. The flux is a fine white powder mixture of potassium fluo-aluminates. It is mixed with water to form a dilute slurry, applied by spray or other methods to cleaned aluminum assemblies, and dried. Parts are normally brazed in a nitrogen atmosphere tunnel furnace. Brazing temperatures of 590°–620°C (1095–1150°F) are suitable.

Postbraze Treatments. Generally speaking, no postbraze treatments are required. The flux residue is noncorrosive, strongly adherent to the aluminum surface, and provides good corrosion protection. However, in recent years, there continues to be a demand for air-oxidized or blackened-surface radiators and condensers [77]. These are based on the controlled introduction of dry air for surface oxidation or carbon dioxide for surface blackening into an inert atmosphere brazing furnace soon after the completion of the braze. These after-treatments are required to improve corrosion resistance of aluminum heat exchangers.

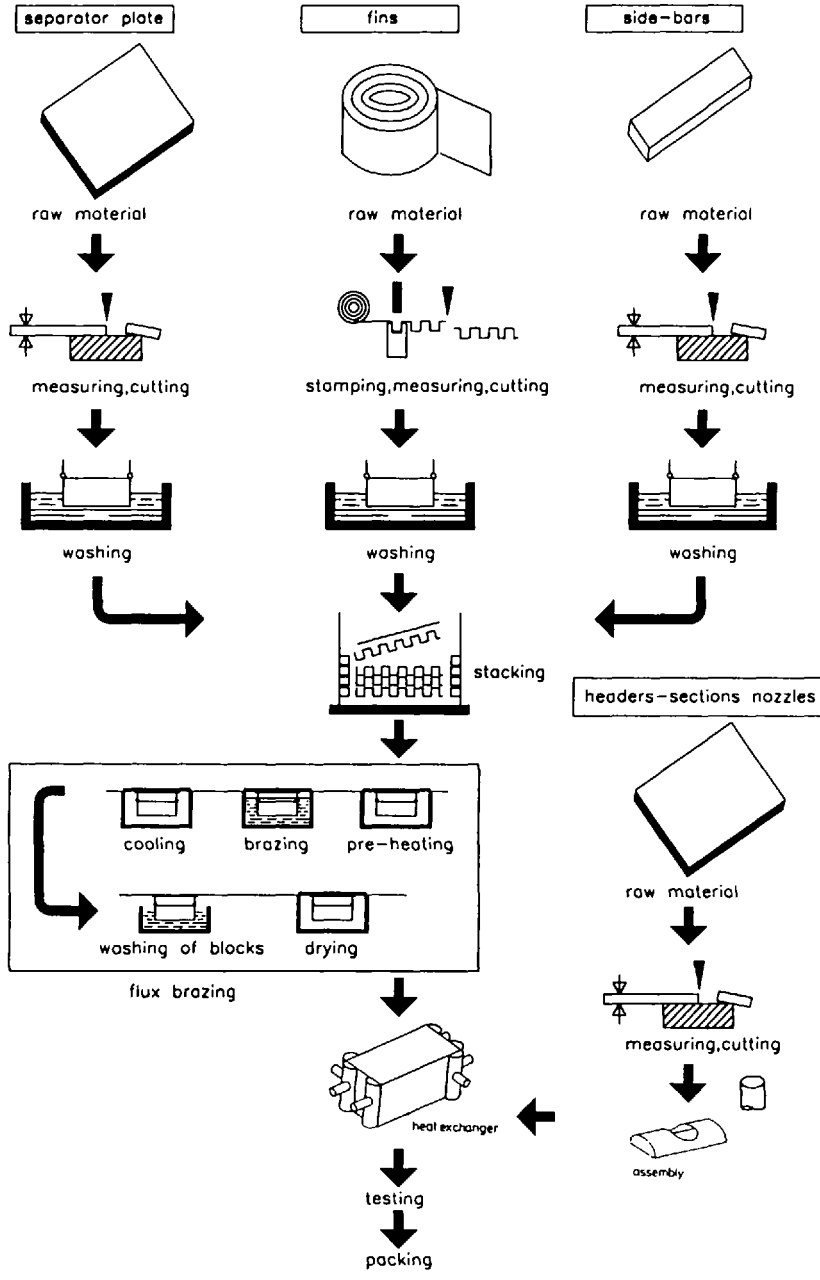


Figure 33 Manufacturing procedure of dip brazing with flux. (From Ref. 58.)

Vacuum Brazing of Aluminum

In vacuum brazing, aluminum assemblies are heated in a vacuum environment by radiation. The principal differences between vacuum brazing and furnace brazing are that (1) the brazing is done in a vacuum of the order of 10^{-4} to 10^{-6} torr, (2) no flux is used, (3) clad brazing sheet and other forms of filler materials usually contain 0.1 to 2.0% magnesium as braze promoter, and (4) heating is by radiation rather than convection.

Typical Procedures for Vacuum Brazing Aluminum Heat Exchanger. These include:

1. Precleaning of components.
2. Assembly and fixturing.
3. Heat/braze in vacuum.
4. Back-fill the furnace: Dry nitrogen is often used, although dry air can be used under some circumstances.
5. Remove the brazed assemblies, which should be air quenched with a fan or allowed to stand until cool.

Typical manufacturing procedure for vacuum brazing of PFHE is shown in Fig. 34.

Important Parameters for Vacuum Brazing Aluminum. Important process variables that control brazing and braze quality are (1) vacuum environment, (2) brazing assembly temperature and temperature uniformity, (3) oxide dispersion and wetting, (4) special vacuum brazing filler and brazing sheet alloy, and (5) vacuum brazing furnace parameters control. Some or all of these parameters are discussed in Refs. 68, 69, and 74.

Vacuum Environment. The most important and difficult to control parameter is the vacuum itself. Pressure is generally monitored for most brazing processes, with the total pressure being the sum of the partial pressure of all the gases present. It is particularly important to monitor and control the partial pressure of contaminants such as oxygen and water vapor [69]. Typical commercial furnaces designed for vacuum brazing operate in the 10^{-4} to 10^{-6} torr pressure range. Mechanical roughing and oil diffusion pumps are used to achieve the vacuum.

Temperature Control. The brazing assembly temperature and temperature uniformity are important processing factors in brazing under vacuum. In designing the temperature programming for the brazing process, several objectives must be borne in mind [68]: minimization of (1) the time for reaction with vapor-phase contaminants, (2) the temperature gradients within the brazed assembly, and (3) the time at brazing temperature, to reduce erosion and other unwanted core and cladding interactions in the brazing sheet. Braze performance is degraded when the interactions causes a reduction in the available filler metal and/or erosion of the core. Vaporization losses of volatile solute from the molten clad can cause similar problems [74]. The most important transport processes are indicated schematically in Fig. 35. The adverse effects of silicon diffusion from core alloy to the braze alloy and vaporization of zinc from base metal on corrosion performance of braze are discussed later.

Oxide Dispersion and Wetting. It is well known that oxygen and water vapor are the important process contaminants. In fluxless vacuum brazing, the presence of a promoter, either a metal or reactive gas, is needed to getter oxygen and water vapor from the furnace and to suppress reoxidation of the aluminum at the joints, once the oxide film is removed. The fluxless processes use either elemental magnesium, magnesium containing filler metal, or magnesium bearing base metals to getter oxygen [71]. Alternatively, brazing also can be achieved in a high vacuum by prolonged exposure at elevated temperatures without using metal activators [75].

Magnesium as a Braze Promoter. Many metals can fulfil the function of a braze promoter, but magnesium is the best, because, magnesium has the highest vapor pressure of the metals that promote vacuum brazing [75], ease of alloying with aluminum, and low cost [69].

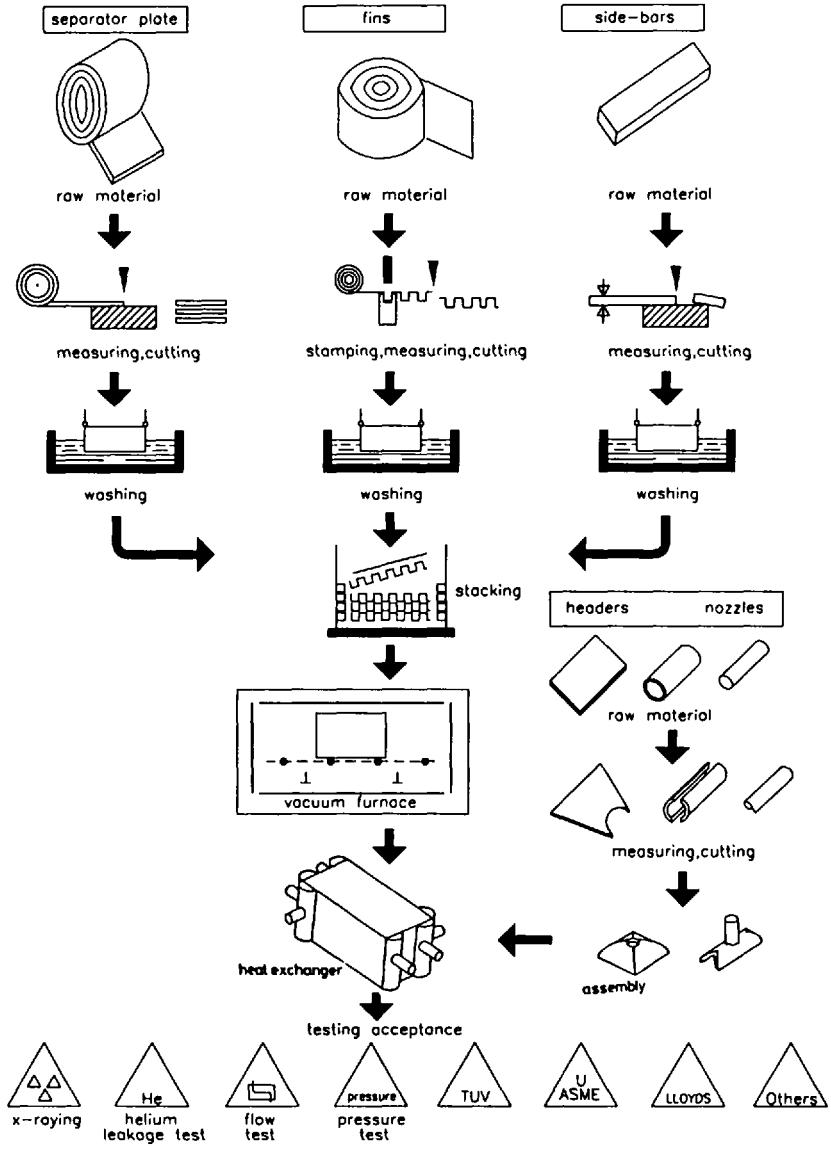


Figure 34 Manufacturing procedure of flux-free brazing in a vacuum. (From Ref. 58.)

Vacuum Brazing Filler Metals. Generally, vacuum brazing filler metals and brazing sheets are aluminum alloys containing 7.5 to 12% silicon and up to 1.5 to 2.5% magnesium [60]. Since gravity adversely affects vertical capillary filler metal flow in vacuum brazing, preplace filler metal in vertical joints or use a brazing sheet. Alloys of the 1xxx, 3xxx, 5xxx, 6xxx, and 7xxx series can be vacuum brazed using No. 7, 8, 13, and 14 brazing sheets, whose compositions are shown in Table 6.

Vacuum Brazing Furnaces. Vacuum furnaces capable of reaching at least $1200 \pm 5°F$ ($650 \pm 3°C$) temperature uniformity in the normal brazing range of 1080–1140°F (582–616°F) are suitable for brazing aluminum [69]. Systems for vacuum brazing of aluminum are discussed

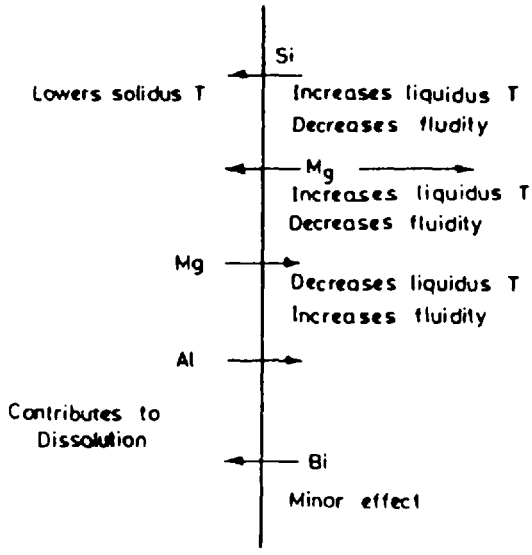


Figure 35 Transport process during brazing. (From Ref. 74.)

in detail in Ref. 68 and Ashburn [78]. Vacuum furnaces are invariably heated by electricity, in any one of a number of forms. A typical electric-heated vacuum furnace has the heating system surrounded by radiation shields and mounted within a water-cooled steel shell, which is known as cold-wall design. Vacuum furnaces for brazing aluminum are equipped with mechanical roughing and oil vapor diffusion pumps to achieve the required 10^{-4} to 10^{-6} torr vacuum.

Nonuniform Mass and Temperature Uniformity. Plate-fin heat exchangers are relatively uniform in mass and usually present no particular problems in heating to brazing temperature in a furnace atmosphere. However, tube-fin exchangers such as the automotive radiator, with different thicknesses of parts like fins, tubes, header sheet, and side supports, require special consideration due to their nonuniform mass distribution. This type of radiator can be heated uniformly using one of these two methods [69]: (1) use of heat shields to slow heating of the core area and (2) orienting the radiator in the furnace with heavier sections facing the heating

Table 6 Composition and Brazing Range of Clad Aluminum Vacuum Brazing Sheet [50]

Brazing sheet designation no.	Number of sides clad	Core alloy	Cladding alloy	Brazing range	
				°F	°C
7	1	3003	4004	1090–1120	588–604
8	2	3003	4004	1090–1120	588–604
13	1	6951	4004	1080–1110	582–599
14	2	6951	4004	1080–1110	582–599

elements. While both methods provide ±5°F temperature uniformity, the latter method is more amenable to production use.

Postbraze Cleaning and Finishing. The brazed aluminum alloys should be free from residual flux to avoid corrosion during service. The postbraze cleaning methods include ultrasonic means or using chemical solutions, or using one of the chemical brighteners.

Cleaning of a Chloride Type Flux.

1. The most rapid and efficient method of removing the chloride type flux is by hot water cleaning, i.e., by the immersion of the still hot part into boiling water. A chloride flux is highly soluble, and boiling water will quickly remove most of it.
2. Ultrasonic cleaning with proprietary cleaning solutions.
3. Chemical cleaning.

Cleaning of a Fluoride Type Flux. Even though residual fluoride flux is noncorrosive, for aesthetic reasons and for surface coating, the fluoride flux is cleaned using a caustic etch or chemical brighteners, since fluoride fluxes are not water washable [50].

Finishing. When a brazing fillet has been properly formed, no finishing is required except flux removal by postbraze cleaning. If necessary, the fillet, like the brazed metal, may be ground, filed, or polished. Caution: The brazed assembly should not be cleaned in caustic solution.

8 BRAZING OF HEAT-RESISTANT ALLOYS AND STAINLESS STEEL

Heat-resistant superalloys are either nickel-based or cobalt-based alloys, with the alloying elements chromium, iron, tungsten, and molybdenum. These alloys exhibit strength, oxidation resistance, and resistance to corrosion at elevated temperatures (1200–2200°F). Some of the nickel-based wrought alloys used as heat exchanger materials are Hastelloy X, Inconel 625, and Inconel 718, and cobalt-based alloy Haynes 188 [52]. Elements of brazing of nickel-based and cobalt-based alloys are discussed in this section.

8.1 Brazing of Nickel-Based Alloys

Requirements for Brazing of Nickel-Based Alloys

The success of brazing of nickel-based alloys depends on the careful consideration of the following parameters [79]:

1. Physical metallurgy of the alloys
2. Surface preparation
3. Thermal cycles
4. Brazing atmosphere

Physical Metallurgy of the Alloys. The surfaces of precipitation-hardenable alloys containing more than 1% Al and Ti are covered with hard, tenacious oxide films. These surface films hinder the wetting of molten filler metal, and the films are in general impossible to reduce, either in a controlled atmosphere or in a vacuum brazing atmosphere. However, these difficulties are not normally encountered with solid-solution-strengthened alloys.

Surface Preparation. Successful brazing requires removal of surface oxide films. To improve the wettability by filler metals, additional surface treatment followed by precleaning may be

required. The surface treatment consists of electroplating of nickel on the surfaces, known as nickel flashing.

Thermal Cycles. The effect of high-temperature thermal cycles are [79]: (1) Brazing temperature above their hardening temperatures of 1100 to 1500°F may alter the alloy properties; (2) at the high brazing temperature of 1850°F, the precipitation-hardenable alloys may be subjected to grain growth and decrease in stress rupture properties, which cannot be recovered by subsequent heat treatment; and (3) the liquid metal is subjected to embrittlement when the molten metal is under the influence of tensile stress. Hence, the residual or applied tensile stress should be relieved before brazing.

Brazing Atmospheres. For successful brazing of nickel-based alloys, either a dry, oxygen-free reducing atmosphere or a vacuum is preferred. The effects of various controlled atmospheres have been covered earlier. Vacuum brazing in the range of 10^{-4} torr has proved adequate for brazing most of the nickel-based alloys. The brazing atmosphere, whether gaseous or vacuum, should be free from harmful constituents such as sulfur, oxygen, and water vapor. In general, a gaseous atmosphere having a dewpoint less than about −60°C (−75°F) will produce better quality.

Brazing Filler Metals

Generally, nickel-based alloys are brazed with nickel-based alloys containing boron and/or silicon, which serve as melting-point depressants. Phosphorous is another effective melting-point depressant, and it also aids good flow in applications of low stress, there temperatures do not exceed 1400°F (760°C). Sometimes chromium is present to provide oxidation and corrosion resistance. Other filler metals include copper and silver brazing alloys for low-temperature applications, and proprietary filler metals for service temperature above 1800°F (982°C).

8.2 Brazing of Cobalt-Based Alloys

Brazing of cobalt-based alloys can be accomplished by adopting the same techniques used for brazing of nickel-based alloys but with less stringent brazing requirements [79]. This is due to the absence of appreciable amounts of aluminum and titanium in the base metals. The filler metals are usually cobalt based, nickel based, or gold–palladium compositions. Most cobalt-based filler metals contain boron and/or silicon as melting-point depressants and Cr, Ni, and W for improved strength, corrosion, and oxidation resistance.

8.3 Brazing of Stainless Steel

In recent years, there has been a demand, particularly from the aircraft and nuclear energy industries, for complex heat exchangers that operate under arduous conditions of temperature and pressure and adverse environments. To meet these requirements, heat exchangers have been fabricated from stainless steel, usually the 18 : 8 type stabilized with titanium. Other wrought stainless steels such as of AISI types 316, 316L, 347, and 430 are also extensively used as heat exchanger materials for high-temperature applications. Many aircraft heat exchangers are of modular construction [80]. Typical brazed forms of stainless steel heat exchangers include plate-fin heat exchangers, shell and tube heat exchangers, and regenerators. To save weight in aircraft and for greater efficiency in heat transfer, the heat exchangers have been made from thin sheet and thin-wall tubing; typical sizes are sheet 0.005 in thick and tubing of 0.006 in wall thickness. One of the problems in fabricating structures from these thin materials has been to make completely sound joints without any distortion in the heat exchanger matrix.

Brazeability of Stainless Steel

Brazing of stainless steels is carried out at high temperatures (see Table 4). Among the various factors, the quality of stainless steel brazing depends on the following [63]:

1. Ability to create a proper brazing atmosphere to eliminate oxidation, scaling, and surface reaction that forms sulfides and nitrides on its surface. Brazing either in a controlled atmosphere or in vacuum eliminates the oxidation of the base metal, is effective in reducing the oxides, and promotes the flow of filler metal.
2. Ability to arrest the sensitization of austenitic stainless steel during brazing, or proper solution treatment of sensitized steels to restore their corrosion resistance.

Brazing Process. Stainless steel can be brazed by all conventional brazing processes including torch, furnace, dip, and induction brazing. Stainless steel heat exchangers are mostly furnace brazed, either in a controlled reducing atmosphere such as dry hydrogen, dissociated ammonia, or argon, or in vacuum.

Furnace Brazing in Dry Hydrogen. Dry hydrogen is the most preferred for brazing of stainless steel since it eliminates the oxidation of the base metal and is effective in reducing the oxides. The principal disadvantages are high cost; difficulty in getting hydrogen in dry condition, free from oxygen and other oxidants; and handling and storage problems [65].

Furnace Brazing in Dry Dissociated Ammonia. Stainless steels are brazed in a dry dissociated ammonia, i.e., with the composition of H_2 and N_2. Even small traces of NH_3 will nitride stainless steel and dissolve in water if traces of moisture are present.

Vacuum Brazing. For high-temperature service applications, vacuum brazing can offer excellent heat and corrosion resistance. A vacuum of 10^{-2} torr of mercury is sufficient to braze most stainless steels. Many structures that could not be brazed in hydrogen have been brazed successfully in vacuum furnaces [65].

Filler Metals. In addition to brazeability, for most applications filler metals are selected for mechanical properties, corrosion resistance, service temperature, and compatibility with process fluids. Filler metals for brazing stainless steels include copper alloys, silver alloys, gold and gold–palladium alloys, and nickel alloys. Nickel-based filler metals alloy with stainless steel and form secondary phases with two undesirable characteristics [79]: (1) low ductility and hence susceptibility to hot cracking, and (2) higher melting point than the base metal and hence likely to freeze and retard the filler metal flow. To achieve flow in deep joints, diametral clearances of as much as 0.004 to 0.008 in (0.1 to 0.2 mm) are necessary. Selection of brazing filler metals for brazing stainless steels is also discussed by Amato et al. [81]. For guidance on selection of brazing filler metals for stainless steels brazing, Welding Engineer Data Sheet No. 493 [82] is useful.

Fluxes. Brazing of stainless steel in a controlled atmosphere or in vacuum does not require flux. In some furnace brazing applications, flux is necessary. But flux is required for torch brazing, dip brazing, or for any other conventional brazing process carried out in an uncontrolled atmosphere.

9 QUALITY CONTROL, INSPECTION, AND NDT OF BRAZED HEAT EXCHANGERS

The principles of quality control, quality assurance, inspection and NDT techniques have been dealt with in Chapter 14. Even though the focus in that chapter was shell and tube heat exchangers, the underlying principle is relevant for any type of heat exchanger and for any manufacturing process. With this in mind, quality control and inspection pertaining to brazing are discussed here. Quality assurance for aluminum brazing is discussed in ANSI/AWS C3.7-93,

Specification for Aluminum Brazing [71]. Salient features of quality systems for brazing are:

1. Data cards. An essential part of the quality system is the use of data cards for each job to record brazing parameters. The data cards contain such information as materials used, joint configuration, brazing alloy, thermal cycle, furnace load configuration, and inspection and NDT requirements.
2. Responsibility for inspection. Unless otherwise specified in the contract or purchase order, the manufacturer is responsible for the performance of all inspections during various stages of brazing operation.
3. Sequence of inspection and manufacturing operations. Brazed joints may be inspected at the assembly or subassembly stage, and after postbraze heat treatment. Flux residue testing shall be performed after completion of all operations of the brazed joint.
4. Temperature measuring devices. All furnaces and molten salt baths used in the brazing shall have automatic temperature controlling and recording devices in proper working order. Periodically calibrate temperature measuring devices, furnace atmosphere controlling instruments, and vacuum measuring devices.
5. Integrity of vacuum furnaces: A critical step for vacuum furnace is to ensure a sound furnace atmosphere through regular, scheduled leak testing.
6. Elements of quality control for dip brazing: Quality control aspects should cover maintenance of flux composition, temperature, pH, removal of scum and sludge, preheating the assembly, etc., as discussed earlier in the section on the dip brazing process.
7. Flux removal test: All components brazed using corrosive flux shall be tested for the presence of residual flux after postbrazing cleaning. The silver nitrate test is popular for determining the presence of flux either in the wash water or remaining on the workpiece after it has been washed and dried. Evidence of any precipitate or cloudy appearance indicates incomplete cleaning, and the piece should be cleaned further or may be rejected. Other test methods may be used as alternates with the written approval of the buyer.

9.1 Quality of the Brazed Joints

The quality of brazed joint shall be such that the brazed assemblies are suitable for the intended purpose and that surfaces are free of excess braze filler material. Quality problems of brazed joints of aluminum heat exchangers are discussed by Shah [52]. Some of these problems may also be common to other metals. Quality of a good brazed joint is shown schematically in Fig. 36. A good brazed joint, as shown in Fig. 36a, has large smooth fillets, absence of discontinuities and voids, and the width of the joint is sufficient. Imperfect brazed joints include the following [52]:

1. Poor fillets: a braze joint with narrow-width fillets, due to insufficient time at the braze temperature.
2. Partial joint (underbrazing): due to low brazing temperature, low amount of melting-point temperature depressant elements in filler metal, or improper heating rate (Fig. 36b).
3. Overbrazing: a braze joint that is a result of too high brazing temperature or the brazing time; filler metal may dissolve the base metal and reduce its strength (Fig. 36c).

Discontinuities

Discontinuities result in all brazing processes. Some may be process specific. Discontinuities may be associated with structural discontinuities or associated with the braze metal or the brazed joint. Typical discontinuities include [50,53,54]: (1) lack of fill, (2) flux entrapment, (3) intermittent bond, (4) noncontinuous fillets, (5) voids, (6) porosity, (7) cracks, (8) base metal erosion, (9) unsatisfactory surface appearance, (10) discoloration, and (11) distortion.

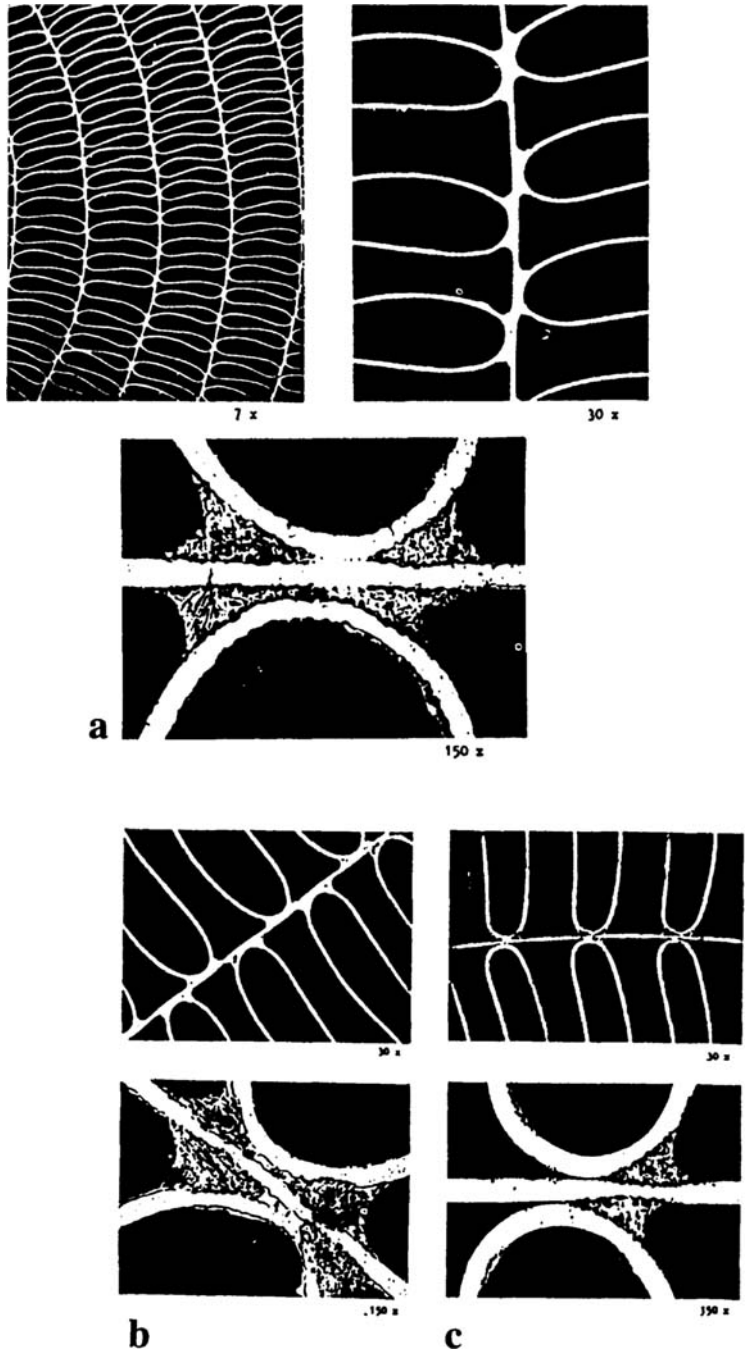


Figure 36 Quality of brazed joint. (a) Good joint; (b) underbrazing; and (c) overbrazing.

All discontinuities reduce joint strength. Acceptance limits for discontinuities must identify shape, orientation, location in the brazement, and relationship to other discontinuities.

9.2 Inspection

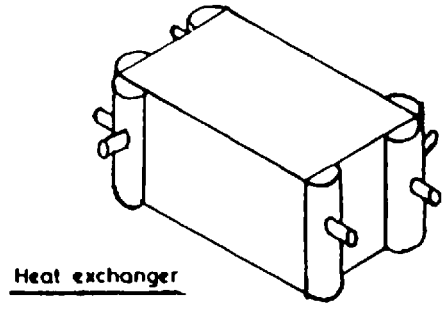
Inspection of brazed joints may be conducted on test specimens or by tests of the finished brazed assembly. The tests may be nondestructive or destructive methods, such as peel tests, tension or shear tests, fatigue test, impact tests, torsion tests, and metallographic examination or proof testing. Various NDT methods include PT, RT, and UT. The scheme of NDT techniques is shown in Fig. 37.

Visual Examination

Visual examination is the most commonly used means for rapidly assessing brazed joint quality, dimensions, and distortion, if any. If the fillet is fully formed and smoothly curvilinear, the joint may be accepted as being reasonably sound pending further, more detailed examination [50]. Visual inspection is unsuitable for the detection of flux entrapment.

Leak Testing

To make certain no leaks exist, heat exchangers are leak tested. The choice of pressure medium will depend to some extent upon the maximum acceptable leak aperture. Thin oil such as kerosene, heated oil, water, air, or Freon may be used. For critical services, where it is necessary to identify the presence of very minute leaks, helium mass spectrometer leak detection technique may be employed.



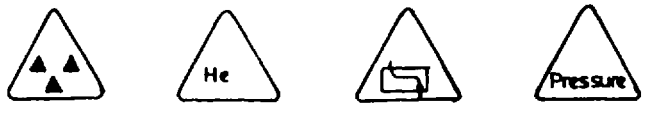


Figure 37 Scheme of NDT techniques for brazing. (From Ref. 58.)

9.3 Brazing Codes and Standards

AWS Brazing and Soldering Documents

B R H	Brazing Hand Book
S M	Soldering Manual
A 2.4	Standard symbols for welding, brazing, and nondestructive testing
A 5.8	Specification for filler metals for brazing, A5.01, filler metal procurement guidelines
B 2.2	Standard for brazing procedures and performance qualification
C 3.2	Standard method for evaluating the strength of brazed joints in shear
C 3.3	Recommended practice for design manufacture and inspection of critical brazed components
C 3.4	Specification for torch brazing
C 3.5	Specification for induction brazing
C 3.6	Specification for furnace brazing
C 3.7	Specification for aluminum brazing
C 3.8	Recommended practices for ultrasonic inspection
	ASME Code Section II, Part C

10 SOLDERING OF HEAT EXCHANGERS

Soldering is defined as a process of joining two similar or dissimilar metals with a filler metal in molten state. Soldering joins materials by heating them in the presence of a filler metal having a liquidus temperature below 840°F (450°C). The filler metal is called *solder*. Heating may be provided by a variety of processes. The filler metal distributes itself between the closely fitted surfaces of the joint.

10.1 Elements of Soldering

Most of the elements of soldering, such as joint design, solder selection, fluxing, precleaning and surface treatment, cleaning after soldering, and inspection, have lot of similarities with brazing process. Therefore, without going deep into these aspects, only salient features of certain elements relevant to radiator design are described here. Subsequently, two versions of the soldering process are described. One involves the conventional soldering of automobile or locomotive radiators, and the other involves the fluxless ultrasonic soldering of all-aluminum core for room air conditioners.

Joint Design

Soldered radiator joints are required to perform in a severe environment. They are subjected to fluctuating temperatures, mechanical vibration, immersion under a water-based fluid, and contact with dissimilar metals. Added to that the frequent neglect of the quantity and quality of coolant solution [83].

Tube Joints

Conventionally, brass flat plates are solder coated and formed into tubes, lock-seam jointed in a soldering machine. Recently tubes with a butt-welded joint have been used for the construction of tubes. This type of radiator tube is stronger and more leak proof than the conventional roll-formed brass lock-seam product, and provides a material savings of about 25% through elimination of the lock seam [84].

Tube-to-Header Solder Joints

Solder alloys generally have lower strength properties than the base materials. Joints between the tubes and header plates are essentially shear loaded in both directions as the radiator is heated, pressurized, and subsequently cooled [85]. Failure of the tube-to-header solder joint occurs because of a variety of problems [86]: weak solder joints due to poor mechanical assembly and fit-up problems, brittle fracture, creep and fatigue, and external or internal corrosion. Possible approaches for increasing the durability of the tube-header solder joints are discussed by Webb et al. [86].

Solders

Solders generally have melting points or melting ranges generally below 800°F (425°C). There is a wide range of commercially available solders designed to work with most industrial metals and alloys. Tin–lead solders, improved tin–lead solders, and zinc–aluminum solders are discussed in the following section and their composition is shown in Table 7. More details on solder selection can be found in Ref. 53.

Lead-Based Solders. Tin–lead solders are most widely used in the joining of metals, particularly conventional automotive radiators. Most commercial fluxes, cleaning methods, and soldering processes may be used with tin–lead solders.

Mechanical Properties. The requirements of a lead-based solder for tube-to-header radiator joints include the following [83]:

1. It must have a minimum amount of tin so that sufficient tin oxide film is formed to passivate the surface.
2. It must have excellent mechanical properties, particularly with regard to creep resistance, to minimize damage to the protective film.
3. It must have good solderability properties.
4. It must be cost-competitive with alternate joining materials.

All lead–based solders have a very low yield point. Under almost any load, they are subjected to some plastic deformation. These alloys are particularly sensitive to creep deformation.

Improved Lead-Tin Solder Alloy. For years, the standard radiator solder had been 70 : 30 lead/tin. The 70 : 30 solder is relatively brittle, and prone to stress cracking as a result of vibrational stresses built up in the radiators. This led to solder-joint failures. This solder has been replaced almost entirely by high-lead solders containing up to 97% lead [87]. This solder, called soft solder, could better withstand engine vibration; it has the following approximate composition: 97% lead, 1.5–2.5% tin, and 0.5–1.5% silver. The tin content was reduced both

Table 7 Solder Compositions

Sn–Pb		Sn–Pb–Ag			Zn–Al–Cu		
Sn	Pb	Sn	Pb	Ag	Zn	Al	Cu
5	95	5.5	94.0	0.5	95	5	—
10	90	5.0	94.5	0.5	89	7	4
15	85	3.8	95.0	1.2			
20	80	2.5	95.0	1.2			
25	75	1.0	97.5	1.5			
30	70						

to save money and to improve mechanical properties. Solders containing less tin will form less eutectic, which will improve the solder's high-temperature mechanical properties [83]. At the same time, a certain concentration of tin in the solder is necessary. If sufficient tin is present in the solder a tenacious and stable oxide film forms over the solder, which improves the corrosion resistance of the solder joint. Hence, it is necessary that the solder contain a minimum of 5% tin. In high-lead solders, where mechanical strength is considered very important, e.g., for tube-to-header joints, silver is added. Typical of these high-lead solders are 95Pb–5Sn and 97.0Pb–0.5Ag–2.5Sn (Modine).

Zinc-Based Solders. Zinc–aluminum solder, the most standard grade 95Zn-5Al is specifically used for ultrasonic soldering of aluminum. It develops joints with high strength and good corrosion resistance.

Cleaning and Descaling

An unclean surface prevents the solder from flowing and makes soldering difficult or impossible. Solvent or alkaline degreasing is recommended for cleaning oily or greasy surfaces. For removing rust or scale, pickling or mechanical cleaning may be used.

Soldering Fluxes

With flux soldering, the flux helps to break up the tenacious oxide layer on the base metal, by reacting with or otherwise loosening that film from the base metal surface. Without the action of the flux, the molten solder cannot wet the surface. Soldering fluxes are divided into three main groups based on their residues [85]: corrosive, intermediate, and noncorrosive. Whenever possible, use the least corrosive flux to eliminate the potential postsoldering corrosion problems stemming from the residual flux. Various compositions of fluxes for copper/brass radiator manufacture include the following:

Zinc chloride, ammonium chloride, and water to make
Zinc chloride, sodium chloride, ammonium chloride, hydrochloric acid, and water to make
Zinc chloride, ammonium chloride, petroleum jelly, and water to make

Soldering Processes

Soldering processes or the heating methods available for heat exchanger manufacture are:

Flame or torch soldering: Hand-held manual torch soldering is most frequently used for repairs to tube-to-tube-plate joints.

Furnace or oven soldering: Furnace soldering is considered when an entire assembly (e.g., radiator) is to be brought to the soldering temperature and when the assembly is complicated in nature, making other heating methods impractical.

Dip soldering: The dip soldering method uses a molten bath of solder to supply both the heat and the solder necessary to join the work pieces. Tube-to-header joints of radiators are made by this process.

Ultrasonic soldering: Ultrasonic soldering can be considered a form of dip soldering, in which the workpiece is immersed in a tank of molten solder. Ultrasonic soldering is discussed separately.

Infrared soldering: This involves focusing infrared light (radiant energy) by means of an optical system. Typical applications include soldering pretinned interference fit return bends by Reynolds interference fit.

Various Stages of Radiator Manufacture by Conventional Soldering Process. In the soldered design, a radiator core is formed by soldering the plain fins or corrugated fins to flattened heat exchanger tubes and the core is connected to the upper and the lower tanks via a pair of header plates. Radiator tubes are normally made by fabricating a lock seam and joining this seam

continuously in a soldering machine. Then the core is formed in a fixture, wherein the fins are stacked and inserted with flat tubes. To insert tubes into the fins stack, a piercing tool is used. The header plates are inserted and pressed onto tubes for making tube-to-header joints. These stages are listed in detail:

1. Tube forming (lock seam), fluxing, solder coating, and cutting to size
2. Burr removal at the tube ends
3. Fin rolling
4. Fin assembly in a fixture
5. Insertion of tubes
6. Fitment of header plates
7. Precleaning
8. Backing in a furnace
9. Squaring of the core assembly and straightening of the blunt fins in the hot condition
10. Expanding the tube ends using a chisel or a blunt formed tool
11. Dip soldering of header plate with tubes
12. Blowing off with air to clear blockages
13. Hot water cleaning and rinsing
14. Leakage test with a dummy water tank
15. Fitment of the metal water tanks and soldering with a tube plate or fitment of plastic/metal water tank and crimping with the tube plate; soldering of inlet, outlet, drain connections, etc.
16. Fitment/soldering of side mounting/side sheet assembly
17. Checking the overall dimensions of the assembly
18. Leak testing
19. Drying and painting
20. Packing and despatch

Flux Residue Removal

Zinc chloride–based flux residue is best removed by hot water washing containing 2% of concentrated hydrochloric acid, followed by hot water rinse. The silver nitrate test can be used to determine whether all of the salts have been removed [53]. Additional tests are discussed later.

10.2 Ultrasonic Soldering of Aluminum Heat Exchangers

All-aluminum coils for the air conditioning industry have been fabricated by flux soldering for many years. Use of flux requires flux cleaning equipment and wastewater treatment facilities. Potential problems from incomplete flux removal and new environmental legislation necessitated development of a fluxless joining process [88], which uses ultrasonic waves to agitate the soldering bath. As ultrasonic waves produce cavitation in the molten bath, they cause a scrubbing action that removes the surface oxide film, thus permitting the solder to wet the aluminum surfaces [89]. Being a fluxless process, ultrasonic soldering is becoming more widely used for the fabrication of all aluminum coils for the air conditioning industry. Various stages of coil joining process both by flux soldering and fluxless soldering are shown in Fig. 38. Excellent, more detailed discussions on the subject can be found in Refs. 88–90.

Material That Can Be Ultrasonically Soldered

By this method, hard-to-wet metals can be successfully soldered in a very few seconds. Aluminum combined with various other materials, stainless steel, and even ceramic materials have

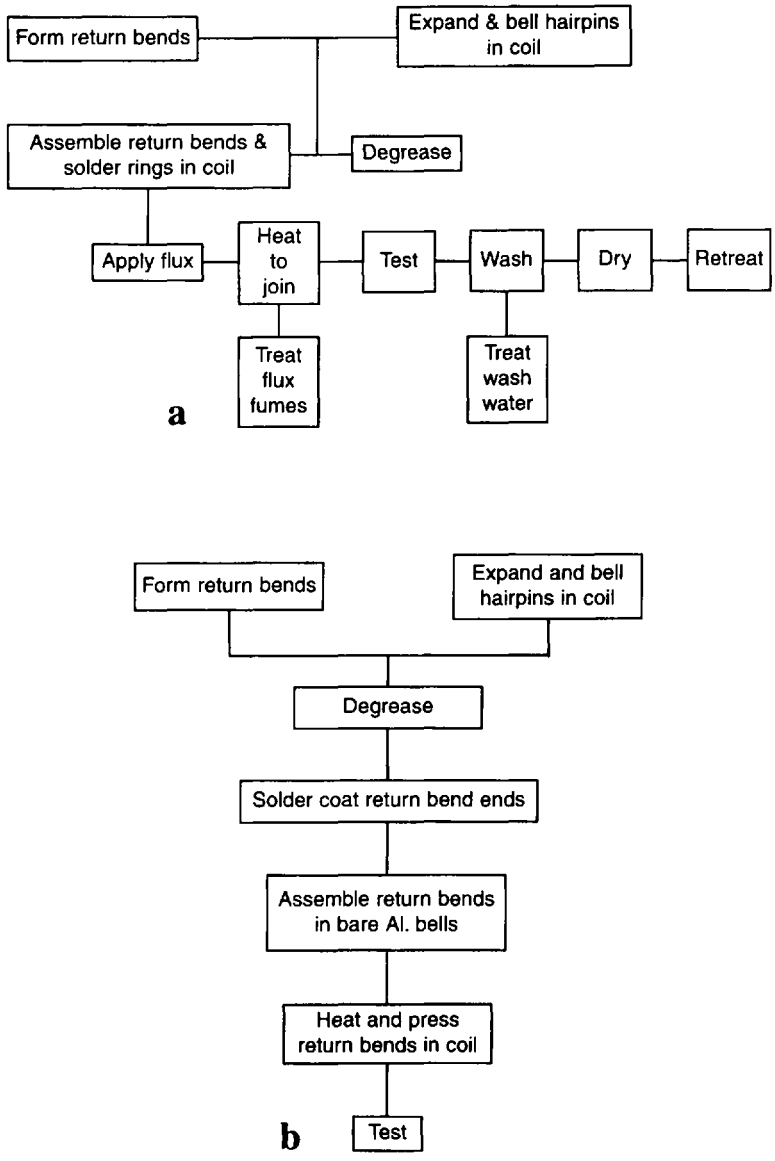


Figure 38 Coil joint sequence. (a) Flux soldered coil; and (b) fluxless soldered coil. (From Ref. 93.)

been wetted rapidly and successfully [91]. The ultrasonic soldering process has been used for joining 1100, 1200, 3003, 6061, 6063, Alclad 7072/3003, and some 2xxx aluminum alloys.

Basic Processes for Soldering All-Aluminum Coils

Two basic processes that make use of ultrasonic soldering are (1) the "dip" or Alcoa 571 process and (2) the Reynolds interference fit process. Of the two, the Alcoa process is widely used, while the Reynolds method shows promise [92].

Alcoa 571 Process. The Alcoa 571 process is a fluxless ultrasonic soldering process specifically developed for the tubular joints in all-aluminum tube-fin air conditioner coils. In simplest

terms, the process requires (1) a heated solder, (2) immersion of the part to be soldered, and (3) cavitation of the solder by ultrasonics. The requirements are met by the following four main components of the ultrasonic equipment [92]: (1) an ultrasonic power supply, (2) a set of transducers, (3) a heated vessel, and (4) a heat control console. More details on Alcoa 571 process are furnished by Denslow [92].

Soldering Procedure. The operations for fabrication and soldering of a coil can be divided into four general areas [90]: (1) coil preparation, (2) coil transport, (3) coil preheat, and (4) coil soldering. The coil preparation includes precleaning the return bends and the tube ends, preferably by ultrasonic vapor degreasing.

The coils or core is made by assembling U-tubes and fins and expanding the tubes in the conventional fashion. The ends of the U-tubes are flared to a prescribed socket geometry to provide a joint and a friction fit for the inserted return bends [90]. After vapor degreasing the return bends and core tubes ends, the return bends are simply tapped into position. The joints are preheated to soldering temperature in the inverted position by hot air or gas flame. The coil is then quickly transferred and lowered into a molten bath of 95% Zn–5% Al solder and exposed for a few seconds to ultrasonic cavitation. The actual soldering of a coil requires only a few seconds of ultrasonic exposure. The sequence of operations is depicted in Fig. 39.

Solder Composition and Maintenance of Soldering Bath. The solder composition recommended is 95Zn–5Al, which is maintained at a temperature of 780–800°F. Since each coil processed through the soldering bath takes out some solder with it, the bath should be replenished with fresh solder to maintain its depth. During the tinning process, some aluminum will be eroded off the parts [93]. Therefore, the replenisher is slightly lean in aluminum, typically 98Zn–2Al, to keep the bath at 5% Al [89].

Process Control. There are four factors that have significant effects on the joint quality [90]: (1) ultrasonic solder pot design, (2) socket design, (3) preheat, and (4) depth of immersion. Another important factor is the soldering time.

Ultrasonic Soldering Pot. The heart of the Alcoa 571 process is the ultrasonic soldering pot, which is the container for the molten zinc-based solder [91]. Generally, the pot is made from AISI 304 type stainless steel. These pots come in rectangular (flat bottom), circular, or contoured shape. Bottoms of rectangular pots usually have one or two rows of transducers. Circular and contoured pots are better for soldering large coils because they have room for more transducers [89]. Figure 40 shows a sketch of the ultrasonic pot. In general, rectangular tanks have not performed satisfactorily when compared to round tanks [92].

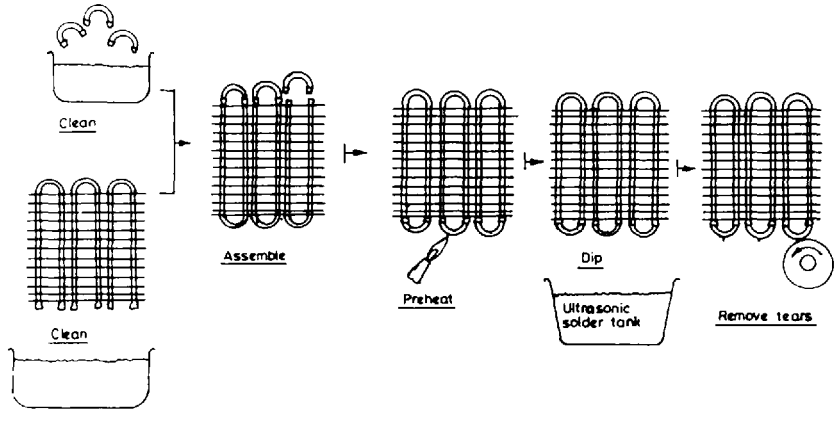


Figure 39 Fluxless ultrasonic soldering by the Alcoa 571 process. (From Ref. 93.)

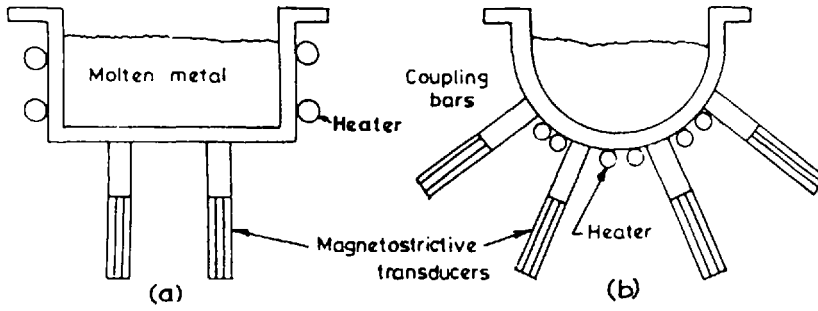


Figure 40 Ultrasonic pot. (a) Rectangular bottom; and (b) round bottom. (After Ref. 91.)

Socket Design. Joints of tube sockets are designed for strength and resistance to corrosion. The ends of the U-tubes are flared to a prescribed socket geometry (Fig. 41) to provide a joint area and a friction fit for the inserted return bends. Solder penetrates the annular space between the return bend and the socket, wets the surfaces, and completes the joint.

Preheat Temperature. The assembled coil must be preheated before it is dipped in the molten solder, to drive out all the moisture. Preheating reduces the pot size and the soldering time. The preheating should be uniform to ensure that all sockets are above the solder temperature. Preheating time should be minimum to reduce the amount of oxidation. Excessive oxide formation due to longer preheating time makes it difficult for the cavitating solder to break up the oxide film [88,89]. At the same time, the preheating temperature must be high enough to keep the solder from solidifying on parts entering the ultrasonic bath. Preheating sockets at 840 to 950°F (450 to 510°C) ensures that all are above the soldering temperature of 780°F (415°C) without being overheated. For preheating, oscillating spear flame burners are used on nearly every production.

Depth of Immersion. In an ultrasonic soldering process, the most important factor is the depth to which the joint is submerged [90], which is shown schematically in Fig. 41. Soldering does not take place until the joint goes deep enough for its interior surfaces to become wet, even though its outer surfaces may start to wet at shallower depths. From the laws of acoustic physics, it is known that the bath develops a gradient of cavitation intensity, reaching a maximum of 1.5 to 2 in (38.50 to 50.8 mm) beneath the bath surface [89].

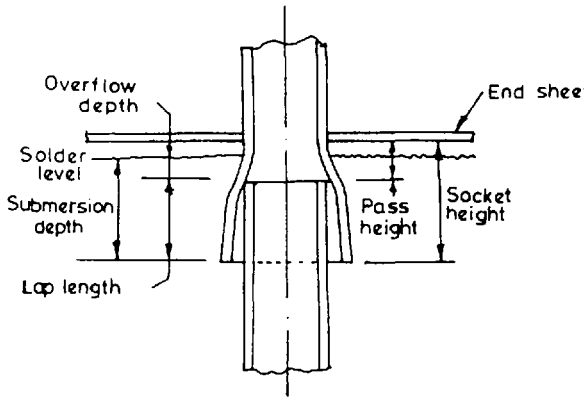


Figure 41 Socket geometry. (From Ref. 90.)

Soldering Time. Aluminum parts to be tinned are preheated to 800°F, inserted in the solder pot, and the ultrasonics are activated for approximately 3–6 sec, depending on the solder temperature, coil complexity, and solder pot characteristics [89]. At least 3 sec is usually required for good joints. For copper and steel the time should be increased to 5–8 sec. Longer duration of soldering time lengthens the joint length, but causes erosion of return bends.

Reynolds Process. The Reynolds Metals Company process (U.S. Patent 3,633,266) or interference process comprises four basic steps [93]:

1. Ultrasonic tinning: Pretinning of the ends of return bends by immersion in a molten solder bath, which is agitated by ultrasonic energy.
2. Assembly of the bare and pretinned tubular components.
3. Heating of the preassembled tubular components to melt the solder film.
4. Final assembly by the mechanical pressing of the "cork-fit" tube joints together to disrupt the oxide on the bare member and thereby provide a metallurgically bonded leak-free joint.

The sequence of the Reynolds process is depicted in Fig. 42.

Merits of the Reynolds Process. Because only the return bend ends need tinning, large ultrasonic pots are not required and the ultrasonic equipment cost is also very much less. Depth of insertion of parts to be tinned in the pot is not critical [93].

10.3 Quality Control, Inspection, and Testing

In this section, quality control, inspection, and testing of soldered heat exchangers are discussed. Some or most of the part of the discussion may not be relevant for ultrasonically soldered heat exchangers. Quality control during various stages of flux-soldered radiator manufacture should consider at a minimum the following points:

1. Fin and tube dimensions, thickness of solder coating
2. Solder bath temperature and composition
3. Tube washing tank temperature and pH
4. Soldering furnace temperature
5. Core washing tanks pH

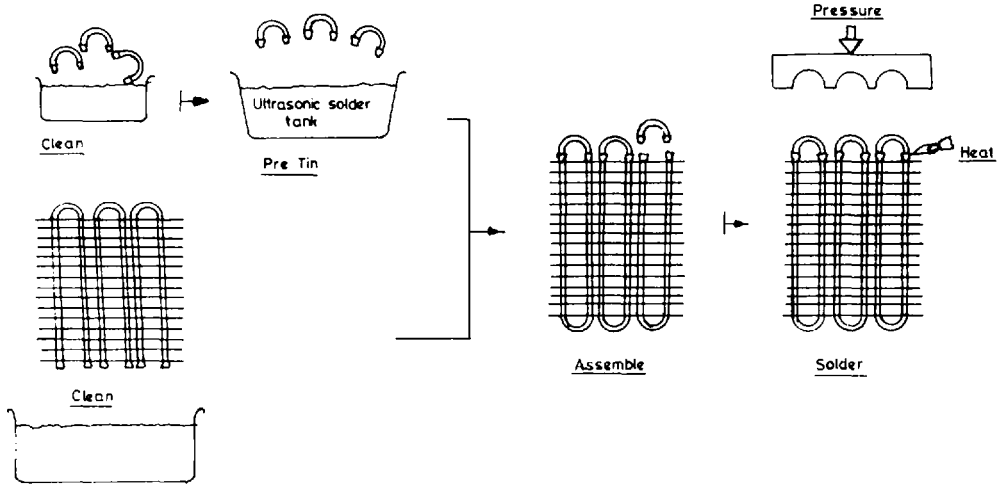


Figure 42 Sequence of Reynolds process. (From Ref. 93.)

6. Leak testing and recording the number of leakages in tank, pipe, plate, tube, and others
7. Core dimensions

10.4 Nondestructive Testing

Visual Inspection

Nearly all soldered joints are visually inspected for defects. A soldered joint surface should be shiny, smooth, and free from cracks, porosity, or holes. Ordinarily, no flux residues should remain.

Discontinuities

Some types of discontinuities common for soldering are dewetting, nonwetting, and dull or rough solder.

Removal of Residual Flux

Corrosivity of residual flux deposits is important. A water extract method of measuring corrosivity through conductivity has been developed. Extracts from flux residues can also be evaluated. The three basic methods of flux residue detection are radioactive tracers, standard chemical analysis, and fluorescent dye evaluation [85]. Minute amounts of dye in the remaining flux readily fluoresce under ultraviolet light.

Pressure and Leak Testing

Pressure testing and leak testing can be used to check the integrity of the soldered joints.

Destructive Testing

Destructive testing involves sectioning of soldered joints for determining the quality of joints in the interior. Normal destructive testing techniques include mechanical tests, corrosion evaluation, and metallographic examination.

11 CORROSION OF BRAZED AND SOLDERED JOINTS

Brazing involves joining of two similar or dissimilar metal pieces by a filler metal with composition different from the base metals or same as the base metals. Therefore, galvanic corrosion is a possibility. In addition to galvanic corrosion, corrosion attack is possible due to entrapment of residual corrosive flux. Similar to soldered radiators, brazed radiator joints are required to perform in a severe environment. They are subjected to fluctuating temperatures, mechanical vibration, immersion under engine cooling water, and in contact with dissimilar metals, engine exhaust gases, etc. Added to that the frequent neglect of the quantity and quality of coolant solution [83].

11.1 Factors Affecting Corrosion of Brazed Joints

All forms of corrosion can take place in brazed joints. Parameters that contribute to the corrosion of brazed joints are:

1. Galvanic couple between the base metal and the filler metal
2. Joint design
3. Brazing method and brazing environment
4. Brazing filler metal
5. Flux material

6. Postbraze cleaning
7. Thermal stresses induced during brazing

In this section, the corrosion of aluminum brazed joints related to galvanic couple, filler metal, and brazing process and solder bloom corrosion of a copper/brass radiator are discussed. The influence of corrosive flux and the importance of postbraze cleaning were discussed earlier.

11.2 Corrosion of the Aluminum Brazed Joint

Galvanic Corrosion Resistance

The corrosion resistance of a brazed aluminum joint, completely free of corrosive flux, is directly related to the solution potential difference that may exist between the alloys in contact. The lower the potential difference, the lower is the rate of corrosion. Potential differences of less than 0.013 V are usually considered insignificant [50,59]. Since the aluminum brazing fillers are aluminum alloys rather than dissimilar metals, they have very slight potential differences. Therefore, the possibility of galvanic corrosion is low. This is explained by referring to the solution potential of certain aluminum alloys given in Table 8.

The common filler alloys 4343, 4045, and 4047 produce a solution potential of −0.82 V in the standard test solution and commonly brazed alloys 1100, 3003, 6061, and 6063 show −0.83 V. The difference in solution potential between these two groups of alloy is 0.01 V, which is insignificant, and this is responsible for the excellent corrosion resistance of the brazed joint.

Brazing Process

It was proposed by Kazuhide et al. [94] that the furnace-brazed radiator was superior to the vacuum-brazed radiator, as far as corrosion resistance is concerned, since the former incorporated a zinc diffusion layer in its surface, which afforded the sacrificial corrosion. This aspect is further discussed next, and suggestions are given to overcome the problem.

Zinc Retention: Pitting Corrosion Property of Vacuum-Brazed 7072 Clad Aluminum Alloy. To attain high pitting corrosion resistance, aluminum heat exchanger tubes in cooling water system are made of 7072 clad aluminum alloy, which contains a nominal concentration of 1% zinc. The 7072 clad is designed to preferentially corrode and thereby delay or prevent pitting attack on the core metal [70]. In the vacuum brazing process, the 7072 clad tube loses its alloying element zinc by vaporization and diffusion [95]. As a result, pitting resistance properties may be changed following vacuum brazing. This is especially true for lighter gauges, 0.02 in (0.5 mm) or less. However, for heavier gauges, 0.05 in (1.3 mm), there is sufficient retained zinc in the postbraze composite [96]. In inert-gas brazing, the evaporation of the zinc is minimized [70]. Four factors influence the degree of zinc loss in the vacuum brazing process [97]:

Table 8 Solution Potential of Certain Aluminum Alloys [50]

Cathodic	−0.73 V	4145 (rapidly corroded)
	−0.82 V	4045, 4047, 4343
	−0.83 V	1100, 3003, 6061, 6063, 6951
	−0.84 V	3004, 5050
	−0.93 V	7005
Anodic	−0.96 V	7072, Alclad 6061, Alclad 3003

1. Initial zinc content in the cladding
2. Cladding thickness
3. Furnace thermal cycles and vacuum
4. Part geometry

The loss of zinc due to evaporation is overcome by the following measures [97]:

1. The zinc content of the cladding may be increased to 2–3% from the 1% level in 7072 to achieve a higher net zinc content in the cladding, after brazing.
2. Clad thickness may be increased, as the zinc must diffuse through a greater distance to the surface, where it is lost.
3. In the brazing operation, shorter furnace cycle times and a "softer" vacuum will retard the loss of zinc, but adjustment of these factors is severely constrained by the primary necessity of producing sound brazed joints.
4. Development of K805: Kaiser Aluminum Co. developed a new cladding alloy, one in which the active alloying element would be nonvolatile in the vacuum brazing process. This cladding alloy has been designated K805.

A Multilayer-Clad Aluminum Material with Improved Brazing Properties [98]. Radiator parts are manufactured from clad braze materials with 3003 or 6063 as the core alloy and 4004 as the cladding. At brazing temperature, silicon from the cladding will to some extent diffuse into the core material. With a non-heat-treatable core of the 3000 series, which has low silicon content and a high and narrow melting range, the penetration is reduced and causes no problem. However, using a heat-treatable core alloy of the 6000 series, the silicon diffusion is more pronounced due to higher silicon content in the core and lower and wider melting range. As silicon diffusion takes place preferentially at the grain boundaries, there are apprehensions that corrosion resistance and strength can be adversely influenced, reducing the amount of filler metal available for flow. To improve the brazing and reliability of the heat-treatable alloys, a multilayer-clad aluminum material known as Multiclad was developed. Multiclad consists of a normal heat-treatable core alloy of the 6000 type clad with commonly used braze cladding of the 4000 type. As an intermediate layer between the core and the braze cladding is an alloy of either pure aluminum or aluminum–manganese such as 3003, as shown schematically in Fig. 43. This intermediate layer acts as a diffusion barrier and significantly reduces silicon penetration into the core during brazing, with reduced risk of intergranular corrosion. The melting range of the interlayer is higher than that of the core material.

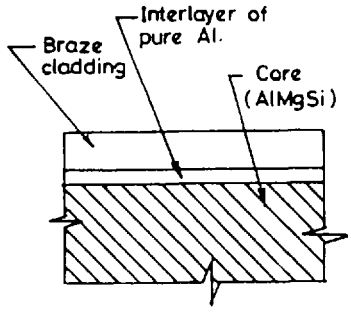


Figure 43 Multilayer clad aluminum brazing sheet. (From Ref. 98.)

11.3 Corrosion of Soldered Joints

The basic corrosion mechanism on high lead solder in a radiator is galvanic. With a galvanic attack, solder is the more active metal and hence corrodes, whereas the more noble metal, the brass, acts as the cathode. Corrosion resistance of various solders in automobile coolant systems is compared by Falke et al. [99].

Solder Bloom Corrosion

Solder bloom corrosion (SBC) can be defined as a corrosion mode of the copper/brass automotive radiator's internal solder joints [100]. Park [100] uses the term *bloom* to describe the flowering appearance of corrosion by products. Solder bloom corrosion, in general leads to the blockage of radiator tube passages when the internal surface is solder coated or of tube openings when the tube outer surfaces are solder coated. Two different field repair methods are employed to clean the blocked tubes. They are (1) roding by utilizing small-size ice picks and thin steel rods, and (2) caustic rinse. Roding involves removal of corrosion products.

Manufacturing Procedures to Control Solder Bloom Corrosion

To reduce the solder bloom corrosion potential of copper/brass radiators, the radiator materials and manufacturing process can be adjusted as recommended [100]:

Introduce air blow-off operation immediately after solder dip to minimize the solder buildup at the opening and inside surfaces of the tube ends.
Change the header dip process to the air-side soldering process to minimize the solder coating inside the tube surface.
Use low-lead solders (Pb below 90%), in place of high-lead solders like 97/2.5/0.5 (Pb/Sn/Ag), 94/5.5/0.5 (Pb/Sn/Ag).
Avoid solder coating inside tube surface.
Use a properly inhibited coolant.
Use an appropriate radiator rinse cleaning system.

12 EVALUATION OF DESIGN AND MATERIALS OF AUTOMOTIVE RADIATORS

In general, mechanically assembled aluminum radiators (MAAR), vacuum-brazed aluminum radiators (VBAR), and copper/brass radiators are evaluated by a number of accelerated tests designed to build confidence in design before large scale fleet trials. Some of these tests are designed to represent worst field conditions [101]. These tests are primarily used to assess (1) the mechanical durability and (2) the internal and external corrosion resistance, inhibitors evaluation, etc. The mechanical durability tests and corrosion evaluation tests carried out for the development and field service history of Ford automotive aluminum radiators are discussed by Barkely et al. [101]. Some of these tests are briefly discussed here.

12.1 Mechanical Durability Tests

Some of the tests developed to evaluate the mechanical durability of the aluminum radiator are given here:

1. Combined pressure cycle and vibration test: Radiators were subjected to higher than normal system pressure pulsating at 145 kPa (21 psi) versus 110 kPa (16 psi) while being vibrated at common engine frequencies.
2. Vibration test: Radiator assemblies were mounted on a simulated vehicle front end, filled with coolant, pressurized, and vibrated at their resonant frequencies to failure.

3. Coolant fill test: Radiator assemblies were subjected to several evacuation and coolant fill cycles, similar to those encountered in auto assembly plants.
4. Thermal shock test: Radiator assemblies were subjected to thermal shocks while mounted to a simulated vehicle front end in an environmental chamber.
5. Vehicle durability test: This test involves the vehicle operation with pressure surges, vibrations, thermally induced loading, and severe vehicle front end torsion and bending.

12.2 Tests for Corrosion Resistance

External Corrosion Tests

The aluminum radiator is susceptible to two major types of external corrosion: galvanic, and localized pitting. In general, uniform corrosion is not an important durability problem for the aluminum radiator, since it results from exposure to very high or very low pH solutions in the absence of inhibitors [101]. Some of the laboratory tests for evaluating external corrosion resistance are:

1. Salt spray (fog) test—ASTM Salt Spray (fog) Testing B-117: This involves internally pressurizing the radiators to 145 kPa (21 psig) and then subjecting them to 1000 hr of salt spray testing.
2. Humidity test: Several thousand hours of testing in a noncondensing humidity chamber, maintained at 38°C (100°F) and approximately 95% relative humidity.
3. SWAAT test: This is a severe acidifided seawater fog corrosion test designed to induce rapid attack.

Internal Corrosion Tests

The major internal corrosion concerns are the possibility of intergranular corrosion, erosion-corrosion, crevice corrosion, and pitting attack. Internal corrosion tests used to evaluate materials and coolants are:

1. Laboratory glassware corrosion tests like static pitting tests and polarization diagrams.
2. Simulated service circulation test.

This page intentionally left blank

References

CHAPTER 1

1. Shah, R. K., Classification of heat exchangers, in *Heat Exchangers: Thermal-Hydraulic Fundamentals and Design*, (S. Kakac, A. E. Bergles, and F. Mayinger, eds.), Hemisphere, Washington, D.C., 1981, pp. 9–46.
2. Shah, R. K., Classification of Heat Exchangers, Lecture Notes, December 1990, pp. 1–66.
3. Gupta, J. P., *Fundamentals of Heat Exchanger and Pressure Vessel Technology*, Hemisphere, Washington, D.C., 1986.
4. Graham Walker, *Cryocoolers, Part 2: Applications*, Plenum Press, New York.

5a. Larowski, A., and Taylor, M. A., Systematic Procedures for Selection of Heat Exchangers, C58/82, Institution of Mechanical Engineers, London, 1982, pp. 32–56.

5b. Larowski, A., and Taylor, M. A., Systematic procedure for selection of heat exchangers, *Proc. Instn. Mech. Eng., 197A*, 51–69 (1983).

6. Kern, D. Q., *Process Heat Transfer*, McGraw-Hill, New York, 1950.
7. Chisholm, D. (ed.), *Developments in Heat Exchanger Technology—1*, Applied Science Publishers, London, England, 1980.
8. Minton, P., Process heat transfer, *Proc. 9th Int. Heat Transfer Conf.*, Heat Transfer 1990–Jerusalem, Paper No. KN-22, *1*, 355–362.
9. Timmerhaus, K. D., and Flynn, T. M., *Cryogenic Progress Engineering*, Plenum Press, New York.
10. Muoio, J. M., Glass as a material of construction for heat transfer equipment, *Industrial Heat Exchangers Conference Proceedings*, (A. J. Hayes, W. W. Liang, S. L. Richlen, and E. S. Tabb, eds.), American Society for Metals, Metals Park, Ohio, 1985, pp. 385–390.
11. Salim Yilmaz, and Samuelson, B., Vertical thermosyphon boiling in spiral plate heat exchangers, *Heat Transfer—1983*, Seattle, Chemical Engineering Progress Symposium Series, No. 225, *79*, 47–53.
12. Markovitz, R. E., Picking the best vessel jacket, *Chemical Engineering*, 1971, pp. 156–162.
13. Usher, J. D., and Cattell, G. S., Compact heat exchangers, in *Developments in Heat Exchanger Technology—1* (D. Chisholm, ed.), Applied Science Publishers Ltd., London, 1980, pp. 127–152.
14. Reay, D. A., Heat exchangers for waste heat recovery, International Research and Development

Co., Ltd., New Castle upon Tyne, UK., in *Developments in Heat Exchanger Technology—1* (D. Chisholm, ed.), Applied Science Publishers Ltd., London, 1980, pp. 233–256.
15. Butterworth, D., and Mascone, C. F., Heat transfer heads into the 21 century, *Chemical Engineering Progress*, September, 30–37 (1991).
16. Taylor, M. A., ed., *Plate-Fin Heat Exchangers, Guide to Their Specification and Use*, HTFS (Harwell Laboratory), Oxon, UK, 1980.
17. *Shell and Tube Exchangers for General Refinery Services*, API Standard 660, 4th ed., American Petroleum Institute, Washington, D.C.
18. Gollin, M., Heat exchanger design and rating, Chapter 2, Part 7, in *Handbook of Applied Thermal Design* (E. C. Guyer, ed.), McGraw-Hill, New York, 1984, pp. 7-24–7-36.
19. Caciula, L., and Rudy, T. M., Prediction of plate heat exchanger performance, *D Symp. Ser., Heat Transfer—1983*, Seattle, pp. 76–89.
20. Fraas, A. P., and Ozisik, M. N., *Heat Exchanger Design*, John Wiley & Sons, New York, 1965.

Suggested Readings

1. Shah, R. K., Classification of heat exchangers, in *Low Reynolds Number Flow Heat Exchangers* (S. Kakac, R. K. Shah, and A. E. Bergles, eds.), Hemisphere, Washington, D.C., 1983, pp. 9–19.
2. Sukhatme, S. P., Devotta, S., Classification of heat transfer equipment, in *Heat Transfer Equipment Design* (R. K. Shah, E. C. Subbarao, and R. A. Mashelikar, eds.), Hemisphere, Washington, D.C., 1988, pp. 7–16.
3. Shah, R. K., What's new in heat exchanger design, ASME, *Mech. Eng.*, *106*, 50–59 (1984).
4. Scaccia, C. and Theoclitus, G., Types, performance and applications, in *The Chemical Engineering Guide to Heat Transfer*, Volume I: *Plant Principles*, (K. J. McNaughton and the Staff of Chemical Engineering, eds.), Hemisphere/McGraw-Hill, New York, 1986, pp. 3–14.

Bibliography

1. Walker, G., *Industrial Heat Exchangers—A Basic Guide*, Hemisphere/McGraw-Hill, New York, 1982.
2. Apblett, W. R., ed., *Shell and Tube Heat Exchangers*, American Society for Metals, Metals Park, Ohio, 1982.
3. Hryniszak, W., *Heat Exchangers: Application to Gas Turbines*, Butterworth Scientific Publications, London, 1958.
4. McNaughton, K. J., and the Staff of Chemical Engineering, eds., *The Chemical Engineering Guide to Heat Transfer:* Vol. I: *Plant Principles*, Vol. II: *Equipment*, Hemisphere/McGraw-Hill, New York, 1986.
5. Afgan, N. H., and Schlunder, E. U., eds., *Heat Exchangers: Design and Theory Sourcebook*, McGraw-Hill, New York, 1974.
6. Shah, R. K., and London, A. L., *Laminar Flow Forced Convection in Ducts*, Supplement I to Advances in Heat Transfer Series, Academic Press, New York, 1978.
7. Reay, D. A., *Heat Recovery Systems*, E. and F. N. Spon Ltd., London, 1979.
8. Schmidt, F. W., and Willmott, A. J., *Thermal Energy Storage and Regeneration*, Hemisphere/McGraw-Hill, Washington, D.C., 1981.
9. Bhatia, M. V., and Cheremisinoff, N. P., *Heat Transfer Equipment*, Process Equipment Series, Vol. 2, Technomic, Westport, Conn., 1980.
10. Somerscales, E. F. C., and Knudsen, J. G., eds., *Fouling of Heat Transfer Equipment*, Hemisphere/McGraw-Hill, Washington, D.C., 1981.
11. Kakac, S., Bergles, A. E., and Mayinger, F., eds., *Heat Exchangers: Thermal-Hydraulic Fundamentals and Design*, Hemisphere/McGraw-Hill, Washington, D.C., 1981.
12a. Schlunder, E. U., editor-in-Chief, *Heat Exchanger Design Handbook*, in five volumes (Vol. 1—*Heat Exchanger Theory*, Vol. 2—*Fluid Mechanics and Heat Transfer*, Vol. 3—*Thermal and Hydraulic Design of Heat Exchangers*, Vol. 4—*Mechanical Design of Heat Exchangers*, and Vol. 5—*Physical Properties*), Hemisphere, Washington, D.C., 1983.

12b. *Hemisphere Handbook of Heat Exchanger Design*, G. F. Hewitt, Coordinating Editor, Hemisphere, New York, 1990.
13. Kern, D. Q., and Kraus, A. D., *Extended Surface Heat Transfer*, McGraw-Hill, New York, 1972, pp. 439–641.
14. Hussain, H., *Heat Transfer in Counterflow, Parallel Flow and CrossFlow*, McGraw-Hill, New York, 1982.
15. Ganapathy, V., *Applied Heat Transfer*, PennWell Publishing Co., Tulsa, OK.
16. Kraus, A. D., *Analysis and Evaluation of Extended Surface Thermal Systems*, Hemisphere, Washington, D.C., 1982.
17. Taborek, J., Hewitt, G. F., and Afgan, N., eds., *Heat Exchangers: Theory and Practice*, Hemisphere/McGraw-Hill, Washington, D.C., 1983.
18. Kakac, S., Shah, R. K., and Bergles, A. E., eds., *Low Reynolds Number Flow Heat Exchangers*, Hemisphere, Washington, D.C., 1983.
19. Bryers, R. W., ed., *Fouling of Heat Exchanger Surfaces*, Engineering Foundation, New York, 1983.
20. Singh, K. P., and Soler, A. I., *Mechanical Design of Heat Exchangers and Pressure Vessel Components*, Arcturus Publishers, Cherry Hill, NJ, 1984.
21. Kays, W. M., and London, A. L., *Compact Heat Exchangers*, third edition, McGraw-Hill, New York, 1984.
22. Manzoor, M., *Heat Flow Through Extended Surface Heat Exchangers*, Springer-Verlag, Berlin, 1984.
23. Rohsenow, W. M., Hartnett, J. P., and Ganic, E. N., eds., *Handbook of Heat Transfer Applications*, McGraw-Hill, New York, 1985.
24. Garrett-Price, B. A., Smith, S. A., Watts, R. L., Knudsen, J. C., Marner, W. J., and Suitor, J. W., *Fouling of Heat Exchangers*, Noyes, Park Ridge, NJ, 1985.
25. Hayes, A. J., Liang, W. W., Richlen, S. L., and Tabb, E. S., eds., *Industrial Heat Exchangers Conference Proceedings*, American Society for Metals, Metals Park, Ohio, 1985.
26. Cheremisinoff, N., ed., *Handbook of Heat and Mass Transfer*, Vol. 1—*Heat Transfer Operation* & Vol. 2—*Mass Transfer and Reactor Design*, Gulf Publishing Company, Houston, pp. 767–805.
27. Foster, B. D., and Patton, J. B., Editors, *Ceramic Heat Exchangers*, American Ceramic Society, Columbus, Ohio, 1985.
28. Mori, Y., Sheindlin, A. E., and Afgan, N. H., eds., *High Temperature Heat Exchangers*, Hemisphere, Washington, D.C., 1986.
29. Jakob, M., *Heat Transfer*, John Wiley & Sons, New York, 1957.
30. Palen, J. W., ed., *Heat Exchanger Sourcebook*, Hemisphere, Washington, D.C., 1987.
31. Chen, S. S., *Flow Induced Vibration of Circular Cylindrical Structures*, Hemisphere, Washington, D.C., 1987.
32. Stasiulevicius, J., and Skrinska, A., *Heat Transfer of Finned Tube Bundles in Crossflow*, Hemisphere, Washington, D.C., 1987.
32. Kakac, S., Shah, R. K., and Aung, W., eds., *Handbook of Single Phase Convective Heat Transfer*, John Wiley & Sons, New York, 1987.
33. Shah, R. K., Subbarao, E. C., and Mashelkar, R. A., eds., *Heat Transfer Equipment Design*, Hemisphere, Washington, D.C., 1988.
34. Zukauskas, A., and Ulinskas, R., *Heat Transfer in Tube Banks in Crossflow*, Hemisphere, Washington, D.C., 1988.
35. Kakac, S., Bergles, A. E., and Fernandes, E. O., eds., *Two-Phase Flow Heat Exchangers: Thermal Hydraulic Fundamentals and Design*, Kluwer Academic Publishers, Dordrecht, 1988.
36. Melo, L. F., Bott, T. R., and Bernardo, C. A., eds., *Advances in Fouling Science and Technology*, Kluwer Academic Publishers, Dordrecht, 1988.
37. Chisholm, D., ed., *Heat Exchanger Technology*, Elsevier Applied Science, New York, 1988.
38. Mahajan, K. K., *Design of Process Equipments*, Pressure Vessel Handbook Publishing Company, Tulsa, Okla., 1985.
39. Shah, R. K., and Mueller, A. C., Heat exchanger, in *Ullmann's Encyclopedia of Industrial Chemistry*, Unit Operations II, Vol. B3, VCH Publishers, Weinheim, Germany, 1989, Chapter 2.

40. Zukauskas, A. A., *High Performance Single-Phase Heat Exchangers*, Hemisphere, Washington, D.C., 1989. J. Karni, English edition editor.
41. Fraas, A. P., *Heat Exchanger Design*, second edition, John Wiley & Sons, New York, 1989.
42. Hewitt, G. F., and Whalley, P. B., *Handbook of Heat Exchanger Calculations*, Hemishpere, Washington, D.C., 1989.
43. Saunders, E. A. D., *Heat Exchangers: Selection, Design and Construction*, Addison Wesley Longman, Reading, MA, 1989.
44. Yokell, S., *A Working Guide to Shell and Tube Heat Exchangers*, McGraw-Hill, New York, 1990.
45. Shah, R. K., Kraus, A. D., and Metzger, D., eds., *Compact Heat Exchangers-A Festschrift for A. L. London*, Hemisphere, Washington, D.C., 1990, pp. 31–90.
46. Mondt, J. R., Regenerative heat exchangers: The elements of their design, selection and use, Research Publication GMR-3396, General Motors Research Laboratories, Warren, Mich., 1980.
47. Cheremisinoff, N. P., *Heat Transfer Pocket Handbook*, Gulf Publishing Company, Books Division, Houston, 19xx.
48. Perry, R. H., and Chilton, C. H., eds., *Chemical Engineers' Handbook*, 5th ed., McGraw-Hill, New York, 1973.
49. Levenspiel, O., *Engineering Flow and Heat Exchange*, Plenum Press, New York, 1984.
50. Sheindlin, A. E., ed., *High Temperature Equipment*, Hemisphere, Washington, D.C., 1986.
51. Hewitt, G. F., Shires, G. L., and Bott, T. R., *Process Heat Transfer*, CRC Press, Boca Raton, Fla., 1994.
52. Martin, H., *Heat Exchangers*, Hemisphere, Washington, D.C., 1992

CHAPTER 2

1. Shah, R. K., and Mueller, A. C., Heat exchanger basic thermal design methods, in *Handbook of Heat Transfer Applications*, second edition (W. M. Rohsenow, J. P. Hartnett, and E. N. Ganic, eds.), McGraw-Hill, New York, 1985, pp. 4-1–4-77.
2. Shah, R. K., Heat exchanger basic design methods, in *Low Reynolds Number Flow Heat Exchangers* (S. Kakac, R. K. Shah, and A. E. Bergles, eds.), Hemisphere, Washington, D.C., 1983, pp. 21–71.
3. Baclic, B. S., ε-NTU analysis of complicated flow arrangements, in *Compact Heat Exchangers—A Festschrift for A. L. London* (R. K. Shah, A. D. Kraus, and D. Metzger, eds.), Hemisphere, Washington, D.C., 1990, pp. 31–90.
4. London, A. L., and Seban, R. A., A Generalization of the Methods of Heat Exchanger Analysis, Mechanical Engineerig Department, Stanford University, Stanford, Calif.
5. *Standards of Tubular Exchanger Manufacturers Association*, seventh edition, Tubular Exchanger Manufacturers Association, Tarrytown, NY, 1988.
6. Fraas, A. P., and Ozisik, M. N., *Heat Exchanger Design*, John Wiley & Sons, New York, 1965.
7. Smith, D. M., Mean temperature difference in crossflow, *Engineering*, *138*, 479–481; *138*, 606–607 (1934).
8. Mueller, A. C., *Handbook of Heat Transfer*, (W. H. Rohsenow and J. P. Hartnett, eds.), McGraw-Hill, New York, 1973.
9. Singh, K. P., Some fundamental relationships for tubular heat exchanger thermal performance, *Trans. ASME, J. Heat Transfer*, *103*, 573–578 (1981).
10. Turton, R., Ferguson, C. D., and Levenspiel, O., Performance and design charts for heat exchangers, *Trans. ASME, J. Heat Transfer*, *106*, 893–895 (1984).
11. Bowman, R. A., Mueller, A. C., and Nagle, W. M., Mean temperature difference, *Trans. ASME*, *62*, 283–294 (1940).
12. Underwood, A. J. V., The calculation of the mean temperature difference in multipass heat exchangers, *J. Inst. Petroleum Technol.*, *20*, 145–158 (1934).
13. Ten Broeck, H., Multipass heat exchanger calculations, *Ind. Eng. Chem.*, *30*, 1041–1042 (1938).
14. Kays, W. M., and London, A. L., *Compact Heat Exchangers*, 2nd edition, McGraw-Hill, New York, 1964.

15. TEMA, *Standards of Tubular Exchanger Manufacturers Association*, 6th edition, TEMA, New York, 1978.
16. Schlinder, E. V., editor-in-chief, *Heat Exchanger Design Handbook*, Vol. 1, Hemisphere, Washington, D.C., 1983.
17. Pignotti, A., Flow reversibility of heat exchangers, *Trans. ASME, J. Heat Transfer, 106*, 361–368 (1984).
18. Pignotti, A., Relation between the thermal effectiveness of overall parallel and counterflow heat exchangers, *Trans. ASME, J. Heat Transfer, 111*, 294–299 (1989).
19. Shah, R. K., Personal Communication, dt. 3.1.1998. Senior Staff Research Scientist, Heat Exchanger Development, DELPHI Harrison Thermal Systems, Lockport, NY.
20. Nusselt, W., A new formula for heat transfer in crossflow [in German], *Tech. Mech. Thermodynam., 1*, 417–422 (1930).
21. Mason, J. L., Heat transfer in crossflow, *Proceedings of the Second U.S. National Congress of Applied Mechanics*, ASME, New York, 1955, pp. 801–803.
22. Baclic, B. S., A simplified formula for crossflow heat exchanger effectiveness, *Trans. ASME, J. Heat Transfer, 100*, 746–747 (1978).
23. Eckert, E. R. G., *Heat Transfer*, 2nd edition, McGraw-Hill, New York, 1959, p. 483.
24. Taborek, J., F and θ charts for crossflow arrangements, in *Heat Exchanger Design Handbook*, Vol. 1, Section 1.5.3 (E. V. Schlunder, editor-in-chief), Hemisphere, Washington, D.C., 1983, pp. 1.5.3-1–1.5.3-15.
25a. Pignotti, A., and Cordero, G. O., Mean temperature difference in multipass crossflow, *Trans. ASME, J. Heat Transfer, 105*, 584–591 (1983).
25b. Pignotti, A., and Cordero, G. O., Mean temperature difference charts for air coolers, *Trans. ASME, J. Heat Transfer, 105*, 592–597 (1983).
26a. Pignotti, A., Analytical techniques for basic thermal design of complex heat exchanger configurations, *Heat Transfer, Eighth International Conference*, San Francisco, 1986.
26b. Pignotti, A., Matrix formalism for complex heat exchangers, *Trans. ASME, J. Heat Transfer, 106*, 352–360 (1984).
27. Schedwill, H., Thermische Auslegung von Kreuzstromwarmeaustauschern, Fortschr-Ber. VDI-Z Reihe 6 Nr. 19, VDI-Verlag, Dusseldorf, 1968.
28. Nicole, F. J. L., Council for Scientific and Industrial Research, Rep. Chem. 223, Pretoria, South Africa, 1972.
29. Stevens, R. A., Fernandez, J., and Woolf, J. R., Mean temperature difference in one, two, three-pass crossflow heat exchangers, *Trans. ASME*, 287–297 (1957).
30. Nagle, W. M., Mean temperature difference in multipass heat exchanger, *Ind. Eng. Chem., 25*, 604–609 (1933).
31. Baclic, B. S., 1-2N shell and tube exchanger effectiveness: A simplified Kraus-Kern equation, *Trans. ASME, J. Heat Transfer*, 181–182 (1989).
32. Pignotti, A., and Tamborenea, P. I., Thermal effectiveness of multiple shell and tube pass TEMA E heat exchangers, *Trans. ASME, J. Heat Transfer, 111*, 54–59 (1988).
33. Whistler, A. M., Correction for heat conduction through longitudinal baffle of heat exchanger, *Trans. ASME*, 683–685 (1947).
34. Rozenmann, T., and Taborek, J., The effect of leakage through the longitudinal baffle on the performance of two pass shell exchangers, *Heat Transfer–Tulsa, 1972*, AIChE Symposium Series No. 118, Vol. *68*, 12–20 (1972).
35. Taborek, J., F and θ charts for shell and tube exchangers, in *Heat Exchanger Design Handbook*, Vol. 1, Section 1.5.2 (E. V. Schlunder, editor-in-chief), Hemisphere, Washington, D.C., 1983, pp. 1.5.2-1–1.5.2-15.
36. Schlinder, D. L., and Bates, H. T., True temperature difference in a 1-2 divided flow heat exchanger, *Heat Transfer—Storrs, Chem. Eng. Prog. Symp. Ser., 56*, 203–206 (1960).
37. Murty, K. N., Heat transfer characteristics of one- and two-pass split flow heat exchangers, *Heat Transfer Eng., 4*, (3–4), 26–34 (1983).

38. Singh, K. P., and Holtz, M. J., Generalization of the split flow heat exchanger geometry for enhanced heat transfer, *Heat Transfer—San Diego, AIChE Symp. Ser.*, *75*, 219–226 (1979).
39. Ishihara, K., and Palen, J. W., Mean temperature difference correction factor for the TEMA H shell, *Proceedings of the Eigth International Heat Transfer Conference, 1986, San Francisco, California* (C. L. Tien, V. P. Carey, and J. K. Ferrel, eds.), Hemisphere, Washington, D.C., pp. 2709–2714.
40. Shah, R. K., and Pignotti, A., Heat Exchanger Basic Design Theory and Resuls, A Report Prepared Under NSF Grant No. INT-8513531, Buffalo, N.Y., 1989. TEMA G_{1-1} exchanger results are also derived in this report by the chain rule methodology.
41. Jaw, L., Temperature relations in shell and tube exchangers having one pass splitflow shells, *Trans. ASME, J. Heat Transfer*, 408–416 (1964).
42a. Gardner, K. A., *Ind. Eng. Chem.*, *33*, 1495 (1941).
42b. Gardner, K. A., *Ind. Eng. Chem.*, *33*, 1215 (1941).
43. Pignotti, A., Effectiveness of series assemblies of divided-flow heat exchanger, *Trans. ASME, J. Heat Transfer*, *108*, 141–146 (1986).
44. Domingos, J. D., Analysis of complex assemblies of heat exchangers, *Int. J. Heat Mass Transfer*, *12*, 537–548 (1969).
45. Baclic, B. S., and Gvozdenac, D. D., Exact explicit equations for some two- and three-pass crossflow heat exchanger effectiveness, in *Heat Exchangers: Thermal-Hydraulic Fundamentals and Design* (S. Kakac, A. E. Bergles, and F. Mayinger, eds.), Hemisphere, Washington, D.C., 1981, pp. 481–494.
46. Baclic, B. S., and Gvozdenac, D. D., NTU relationships for inverted order flow arrangements of two-pass crossflow heat exchangers, in *Regenerative and Recuperative Heat Exchangers* (R. K. Shah and D. E. Metzger, eds.), ASME, New York, 1981, Vol. 21, pp. 27–41.

Bibliography

1. Cho, S. M., Basic thermal design methods for heat exchangers, in *Heat Transfer Equipment Design* (R. K. Shah, E. C. Subbarao, and R. A. Mashelikar, eds.), Hemisphere, Washington, D.C., 1988, pp. 23–38.
2. Effectiveness-Ntu Relationships for Design and Performance Evaluation of Two-Stream Heat Exchangers, Engineering Sciences Data Unit Item No. 86018, July 1986, ESDU International Ltd., McLean, Va.
3. Effectiveness-Ntu Relationships for the Design and Performance Evaluation of Multi-Pass Crossflow Heat Exchangers, Engineering Sciences Data Unit Item No. 87020, October 1987, ESDU International Ltd., McLean, Va.
4. Kays, W. M., and London, A. L., *Compact Heat Exchangers*, third edition, McGraw-Hill, New York, 1984.
5. Gardner, K. A., and Taborek, J., Mean temperature difference: A reappraisal, *AIChE J.*, *23*, 777–786 (1977).

CHAPTER 3

1. Shah, R. K., Heat exchanger design methodology, in *Heat Transfer Equipment Design* (R. K. Shah, E. C. Subbarao, and R. A. Mashelikar, eds.), Hemisphere, Washington, D.C., 1988, pp. 17–22.
2. Kays, W. M., and London, A. L., *Compact Heat Exchangers*, third edition, McGraw-Hill, New York, 1984.
3. Shah, R. K., and Bhatti, M. S., Assessment of correlations for single-phase heat exchangers, in *Two-Phase Flow Heat Exchangers—Thermal-Hydraulic Fundamentals and Design* (S. Kakac, A. E. Bergles, and F. E. Oliveira, eds.), Kluwer Academic Publishers, London, 1988, pp. 81–122.
4. Gollin, M., Heat exchanger design and rating, in *Handbook of Applied Thermal Design* (E. C. Guyer, ed.), McGraw-Hill, New York, 1984, pp. 7-24–7-36.
5. Shah, R. K., Compact heat exchanger design procedures, in *Heat Exchangers: Thermal Hydraulic*

Fundamentals and Design (S. Kakac, A. E. Bergles, and F. Mayinger, eds.), Hemisphere, Washington, D.C., 1981, pp. 495–536.

6. Bell, K. J., Delaware method for shellside design, in *Heat Transfer Equipment Design* (R. K. Shah, E. C. Subbarao, and R. A. Mashelkar, eds.), Hemisphere, Washington, D.C., 1988, pp. 145–166.
7. Cardwell, Optimum tube size for shell and tube type heat exchangers, *Trans. of the ASME*, *72*, November 1950, pp. 1061–1065.
8. Shah, R. K., Afimiwala, K. A., Mayne, R. W., Heat exchanger optimization, in *Heat Transfer*, Vol. 4, Hemisphere, Washington, D.C., 1978, pp. 185–191.
9. Shah, R. K., and Mueller, A. C., Heat exchanger basic thermal design methods, in *Handbook of Heat Transfer Applications*, second edition (W. M. Rohsenow, J. P. Hartnett, and E. N. Ganic, eds.), McGraw-Hill, New York, 1985, pp. 4-1–4-77.
10. Shah, R. K., Heat exchanger basic design methods, in *Low Reynolds Number Flow Heat Exchangers* (S. Kakac, R. K. Shah, and A. E. Bergles, eds.), Hemisphere, Washington, D.C., 1983, pp. 21–71.
11. Chenoweth, J. M., and Kistler, R. S., Computer Program as a Tool for Heat Exchanger Rating and Design, ASME Paper No. 76-WA/HT-4, 1976.
12. Taborek, J., Evolution of heat exchanger design techniques, *Heat Transfer Eng.*, *1*, 15–29 (1979).
13. Shah, R. K., Compact heat exchanger surface selection, optimization, and computer aided thermal design, in *Low Reynolds Number Flow Heat Exchangers* (S. Kakac, R. K., Shah, and A. E. Bergles, eds.), Hemisphere, Washington, D.C., 1983, pp. 983–998.
14. Kays, W. M., Loss coefficients for abrupt changes in flow cross section with low Reynolds number flow in single and multiple tube system, *Trans. ASME*, 1067–1074 (1950).
15. Shah, R. K., Personal Communication, dt. 3.1.1998. Senior Staff Research Scientist, Heat Exchanger Development, DELPHI Harrison Thermal Systems, Lockport, NY.
16. Kays, W. K., and Perkins, H. C., Forces convection, internal flow in ducts, in *Handbook of Heat Transfer* (W. M. Rohsenow and J. P., Hartnett, eds.), McGraw-Hill, New York, 1973.
17. Sleicher, C. A., and Rouse, M. W., A convenient correlation for heat transfer to constant and variable property fluids in turbulent pipe flow, *Int. J. Heat Mass Transfer*, *18*, 677–683 (1975).
18. Kays, W. M., and Crawford, M. E., *Convective Heat and Mass Transfer*, second edition, McGraw-Hill, New York, 1980.
19. Deissler, R. G., Analytical Investigation of Fully Developed Laminar Flow in Tubes with Heat Transfer with Fluid Properties Variable Along the Radius, NACA TN 2410, 1951.
20. Shannon, R. L., and Depew, C. A., Forced laminar flow convection in a horizontal tube with variable viscosity and free convection effects, *Trans. ASME J. Heat Transfer*, *91*, 251–258 (1969).
21. Petukhov, B. S., Heat transfer and friction in turbulent pipe flow with variable physical properties, in *Advances in Heat Transfer*, Vol. 6, 1970, pp. 503–564.
22. Shah, R. K., Compact heat exchangers, in *Handbook of Heat Transfer Applications* (W. M. Rohsenow, J. P. Harnett, and E. N. Ganic, eds.), McGraw-Hill, New York, 1985, pp. 4-174–4-312.
23. Minton, P. E., Process heat transfer, *Proc. 9th Int. Heat Transfer Conf.*, Heat Transfer 1990–Jerusalem, Paper No. KN-22, *1*, 355–362 (1990).
24. Al-Zakir, A. S., and Bell, K. J., Estimating performance when uncertainties exist, *Chem. Eng. Prog.*, *77*, 39–49 (1981).
25. Cho, S. M., Uncertainty analysis of heat exchanger thermal hydraulic design, *Proceedings of the Thermal/Mechanical Heat Exchanger Design—Karl Gardner Memorial Session*, (K. P. Singh and S. M. Shenkman, eds.), *64*, 33–41 (1985).
26. Mahbub Uddin, A. K. M., and Bell, K. J., Effect of uncertainties on the design and operation of systems of heat exchangers, in *Heat Transfer Equipment Design* (R. K. Shah, E. C. Subbarao, and R. A. Mashelikar, eds.), Hemisphere, Washington, D.C., 1988, pp. 39–47.
27. Haseler, L. E., Owen, R. G., and Sardesai, R. G., The sensitivity of heat exchanger calculations to uncertainties in the physical properties of the process fluids, in *Practical Application of Heat Transfer*, IMechE Conference Publications, 1982–84, C56/82, IMechE, London, pp. 11–20.
28. Chiou, J. P., The Effect of Flow Nonuniformity on the Sizing of the Engine Radiator, 800035 SAE, 1981, pp. 222–230.

29. Mueller, A. C., An inquiry of selected topics on heat exchanger design, *Chem. Eng. Prog. Symp. Ser., 73*, 273–287 (1976).
30. London, A. L., Laminar flow gas turbine regenerators—the influence of manufacturing tolerances, *Trans. ASME, J. Eng. Power, Ser. A, 92*, 46–56 (1970).
31. Shah, R. K., and London, A. L., Effect of nonuniform passages on compact heat exchanger performance, *Trans. ASME, J. Eng. Power, 102*, 653–659 (1980).
32. Mondt, J. R., Effects of nonuniform passages on deepfold heat exchanger performance, *Trans. ASME, J. Eng. Power, 99*, 657–663 (1977).
33. Digiovanni, M. A., and Webb, R. L., Uncertainty in effectiveness for crossflow heat exchangers, *Heat Transfer Eng., 10*, 61–69 (1989).
34. Shah, R. K., Nonuniform heat transfer coefficient for heat exchanger thermal design, in *Aerospace Heat Exchanger Technology* (R. K. Shah and A. Hashemi, eds.), Elsevier Science Publishers, Amsterdam, 1993, pp. 417–445.
35. Colburn, A. P., Mean temperature difference and heat transfer coefficient in liquid heat exchangers, *Ind. Eng. Chem., 25*, 873–877 (1933).
36. Butterworth, D., Condensers: Thermal-hydraulic design, in *Heat Exchangers: Thermal-Hydraulic Fundamentals and Design* (S. Kakac, A. E. Bergles, and F. Mayinger, eds.), Hemisphere/McGraw-Hill, Washington, D.C., 1981, pp. 647–679.
37. Sieder, E. N., and Tate, G. E., Heat transfer and pressure drop of liquids in tubes, *Ind. Eng. Chem., 28*, 1429–1435 (1936).
38. Roetzel, W., Heat exchanger design with variable transfer coefficient for crossflow and mixed flow arrangements, *Int. J. Heat Mass Transfer, 17*, 1037–1049 (1974).
39. Bowman, R. A., Muller, A. C., and Nagle, W. M., Mean temperature difference, *Trans. ASME, 62*, 283–294 (1940).
40. Larowski, A., and Taylor, M. A., Systematic Procedures for Selection of Heat Exchangers, C58/82, Institution of Mechanical Engineers, London, 1982, pp. 32–56.
41. Buckley, P. S., Statistical methods in process design, *Chem. Eng.*, September, 112–114 (1950).

Bibliography

1. Breber, G., Computer programs for design of heat exchangers, in *Heat Transfer Equipment Design* (R. K. Shah, E. C. Subbarao, and R. A. Mashelikar, eds.), Hemisphere, Washington, D.C., 1988, pp. 167–178.
2. Cho, S. M., Basic thermal design methods for heat exchangers, in *Heat transfer equipment design* (R. K. Shah, E. C. Subbarao, and R. A. Mashelikar, eds.), Hemisphere, Washington, D.C., 1988, pp. 23–38.
3. Palen, J. W., Design of process heat exchanger by computers—A short history, *Heat Transfer, Eighth International Conference—San Francisco*, 1986, pp. 239–248.
4. Pase, G. K., Computer programs for heat exchanger design, *Chem. Eng. Prog., 70*, 53–56 (1986).
5. Bell, K. J., Overall design methodology for shell and tube exchangers, in *Heat Transfer Equipment Design* (R. K. Shah, E. C. Subbarao, and R. A. Mashelkar, eds.), Hemisphere, Washington, D.C., 1988, pp. 131–144.
6. Lord, R. C., Minton, P. E., and Sulusser, R. P., Guide to trouble free heat exchangers, in *Process Heat Exchange, Chemical Engineering Magazine* (V. Cavaseno, ed.), McGraw-Hill, New York, 1979, pp. 60–67.

CHAPTER 4

1. Shah, R. K., Compact heat exchangers for the process industry, in *Energy Efficiency in Process Technology*, (P. A. Pilavachi, ed.), Elsevier Applied Science, London, pp. 565–580.
2. Shah, R. K., Compact heat exchanger technology, and applications, in *Heat Exchange Engineering*, Vol. 2, *Compact Heat Exchangers: Techniques of Size Reduction* (E. A. Foumeny and P. J. Heggs, eds.), Ellis Horwood, New York, 1991, pp. 1–29.

3. Shah, R. K., Classification of heat exchangers, in *Low Reynolds Number Flow Heat Exchangers* (S. Kakac, R. K., Shah, and A. E. Bergles, eds.), Hemisphere, Washington, D.C., 1983, pp. 9–14.
4. Shah, R. K., Classification of heat exchangers, in *Heat Exchangers: Thermal-Hydraulic Fundamentals and Design* (S. Kakac, A. E. Bergles, and F. Mayinger, eds.), Hemisphere, Washington, D.C., 1981, pp. 9–46.
5. Webb, R. L., Enhancement of single phase heat transfer, In: *Handbook of Single Phase Convective Heat Transfer*, Editors, S. Kakac, R. K. Shah, and W. Aung, Chapter 17, John Wiley & Sons, Inc., New York, 1987, pp. 17.1–17.62.
6. Yang, W.-J., High performance heat transfer surfaces: Single phase flows, *Heat Transfer in Energy Problems*, pp. 109–116.
7. Rabas, T. J., and Taborek, J., Survey of turbulent forced convection heat transfer and pressure drop characteristics of low finned tube banks in crossflow, *Heat Transfer Eng., 8*, 49–61 (1987).
8. Webb, R. L., Enhancement for extended surface geometries used in air cooled heat exchangers, in *Low Reynolds Number Flow Heat Exchangers* (S. Kakac, R. K., Shah, and A. E. Bergles, eds.), Hemisphere, Washington, D.C., 1983, pp. 721–734.
9. Fraas, A. P., and Ozisik, M. N., *Heat Exchanger Design*, John Wiley & Sons, New York, 1965.
10. Webb, R. L., and Farrell, P. A., Improved Thermal and Mechanical Design of Copper/Brass Radiators, SAE, 900724, pp. 737–748.
11. Shah, R. K., Compact heat exchanger surface selection methods, in Heat Transfer, Vol. 4, Hemisphere, Washington, D.C., 1978, pp. 193–199.
12. Bergles, A. E., Blumenkrantz, A. R., and Taborek, J., Performance evaluation criteria for enhanced heat transfer surfaces, in *Heat Transfer*, Vol. II, JSME, 1974, pp. 239–243.
13. Taylor, M. A., ed., *Plate-fin heat exchangers, guide to their specification and use*, HTFS (Harwell Laboratory), Oxon, UK, 1980.
14. Shah, R. K., Compact heat exchanger surface selection, optimization, and computer aided thermal design, in *Low Reynolds Number Flow Heat Exchangers* (S. Kakac, R. K. Shah, and A. E. Bergles, eds.), Hemisphere, Washington, D.C., 1983, pp. 983–998.

15a. Shah, R. K., Perforated Heat Exchanger Surfaces Part 1—Flow Phenomena, Noise and Vibration Characteristics, ASME Paper No. 75-WA/HT-8, 1975.

15a. Shah, R. K., Perforated Heat Exchanger Surfaces. Part 2-Heat Transfer and Flow Friction Characteristics, ASME Paper No. 75-WA/HT-9, 1975.

16. Joshi, H. M., and Webb, R. L., Heat transfer and friction in the offset strip-fin heat exchanger, *Int. J. Heat Mass Transfer, 30*, 69–84 (1987).
17. Kays, W. M., and London, A. L., *Compact Heat Exchangers*, third edition, McGraw-Hill, New York, 1984.
18. Cowell, T. A., Heikal, M. R., and Achaichia, A., Flow and heat transfer in compact louvred fin surfaces, in *Aerospace Heat Exchanger Technology* (R. K. Shah and A. Hashemi, eds.), Elsevier Science Publishers, Amsterdam, 1993, pp. 549–560.
19. Davenport, C. J., Correlations for heat transfer and flow friction characteristics of louvred fin, *Heat Transfer—Seattle, AIChE Symposium Series*, No. 225, *79*, 19–27 (1983).
20. Shah, R. K., Surface Geometrical Properties—Tube-Fin Heat Exchangers, class notes for course no. MEA 522, Spring 1993, pp. 413–418.
21. Shah, R. K., Compact heat exchangers, in *Handbook of Heat Transfer Applications* (W. M. Rohsenow, J. P. Harnett, and E. N. Ganic, eds.), McGraw-Hill, New York, 1985, pp. 4-176–4-312.

22a. Idem, S. A., Jung, C., Gonzalez, and Goldschmidt, V. W., Performance of air-to-water copper finned tube heat exchangers at moderately low airside Reynolds numbers, including the effects of baffles, *Int. J. Heat Mass Transf, 30*, 1733–1741 (1987).

22b. Idem, S. A., Jacobi, A. M., and Goldschmidt, V. W., Heat transfer characterization of a finned tube heat exchanger (with and without condensation), *Trans. ASME, J. Heat Transfer, 112*, 64–70 (1990).

22c. Hedderich, P. C., Kelleher, M. D., and Vanderplasts, G. N., Design and optimization of air cooled heat exchangers, *Trans. ASME, J. Heat Transfer, 104*, 683–690 (1982).

23. Kays, W. M., and London, A. L., Heat transfer and flow friction characteristics of some compact

heat exchanger surfaces, Part 2—Design data for thirteen surfaces, *Trans. ASME*, 1087–1097 (1950).
24. Shah, R. K., Compact heat exchanger design procedures, in *Heat Exchangers: Thermal-Hydraulic Fundamentals and Design* (S. Kakac, A. E. Bergles, and F. Mayinger, eds.), Hemisphere, Washington, D.C., 1981, pp. 495–536.
25. Johnson, B. M., The performance of extended surface heat exchangers, in *Handbook of Heat and Mass Transfer*, Vol. 1, *Heat Transfer Operation* (N. P. Cheremisinoff, ed.), Gulf Publishing Company, Houston, pp. 767–805.
26. Monheit, M., and Freim, J., Experimental performance of staggered equilateral and equivelocity tube layouts in air cooled heat exchangers, *Industrial Heat Exchangers Conference Proceedings* (A. J. Hayes, W. W. Liang, S. L. Richlen, and E. S. Tabb, eds.), American Society for Metals, Metals Park, Ohio, 1985, pp. 181–190.
27. Brauer, H., *Kaltetchnik*, 13 Jehrgang, Heft 8, 1961, pp. 274–279.
28. LaHaye, P. G., Neugebuer, F. J., and Sakhuja, R. K., A generalized prediction of heat transfer surfaces, *Trans. ASME, J. Heat Transfer*, 511–517 (1974).
29. Fletcher, L. S., Recent developments in contact conductance heat transfer, *Trans. of the ASME, Jl. of Heat Transfer, Vol. 110*, 1988, pp. 1059–1070.
30. Nho, K. M., and Yovanovich, M. M., Effect of oxide layers on measured and theoretical contact conductances in finned tube heat exchangers, in *Compact Heat Exchangers* (R. K. Shah, A. D. Kraus, and D. Metzger, eds.), Hemisphere, Washington, D.C., 1990, pp. 397–419.
31. Paikert, P., Air cooled heat exchangers, in *Heat Exchanger Design Handbook* Vol. 3 (E. U. Schlunder, editor-in-chief), Hemisphere, Washington, D.C., 1983, Section 3.8.
32. Giedt, W. H., *Principles of Engineering Heat Transfer*, Van Nostrand, New York, 1957.
33. Engineering Sciences Data Unit Convective Heat Transfer During Crossflow of Fluid Over Plain Tube Banks, ESDU, Item Number 73031, 1973.
34. Grimmison, E. D., Correlation and utilization of new data on flow resistance and heat transfer for cross flow of gases over tube banks, *Trans. ASME, 59*, 583–594 (1937).
35. Shah, R. K., and Bhatti, M. S., Assessment of correlations for single-phase heat exchangers, in *Two-Phase Flow Heat Exchangers—Thermal-Hydraulic Fundamentals and Design* (S. Kakac, A. E., Bergles, and F. E. Oliveira) Kluwer Acadeic Publishers, London, 1988, pp. 81–122.
36. Kays, W. M., London, A. L., and Shah, R. K., Heat transfer and friction characteristics of gas flow normal to tube banks—Use of a transient test technique, *Trans. ASME*, 387–396 (1954).
37. Gram, A. J., Mackey, C. O., and Monroe, E. S., Convection heat transfer and pressure drop of air flowing across inline tube banks II—Correlation of data for ten row deep tube banks, *Trans. ASME*, 25–35 (1958).
38. London, A. L., Kays, W. M., and Johnson, D. W., Heat transfer and flow-friction characteristics of some compact heat exchanger surfaces, *Trans. ASME*, 1167–1178 (1952).
39. Briggs, D. E., and Young, E. H., Convection heat transfer and pressure drop of air flowing across triangular pitch banks of finned tubes, *Chem. Eng. Prog. Symp. Ser., 59*, 1–10 (1963).
40. Robinson, K. K., and Briggs, D. E., Pressure drop of air flowing across triangular pitch banks of finned tubes, *Chem. Eng. Prog. Symp. Ser., 62*, 177–184 (1966).
41. Rabas, T. J., Eckels, P. W., and Sabatino, R. A., The effect of fin density on the heat transfer and pressure drop performance of low finned tube banks, *Chem. Eng. Commun., 10*, 127–147 (1981).
42. Weierman, C., *Chem. Eng. Prog.*, 69–72 (1977).
43. Ganguli, A., and Yilmaz, S. B., New heat transfer and pressure drop correlations for cross flow over low finned tube banks, *AIChE Symp. Ser. Heat Transfer—Pittsburg, 83*, 9–19 (1987).
44. Elmahdy, A. H., and Biggs, R. C., Finned Tube Heat Exchanger: Correlation of Dry Surface Heat Transfer Data, ASHRAE, No. 2544, 1978, pp. 262–273.
45. Gray, D. L., and Webb, R. L., Heat transfer and friction correlations for plate fin and tube heat exchangers having plain fins, *Heat Transfer 1986, Proc. Eighth Int. Heat Transfer Conference*, 6, 2745–2750 (1986).
46. Rich, D. G., The effect of fin spacing on the heat transfer and friction performance of multirow, smooth plate fin tube heat exchanger, *ASHRAE Trans., 79*, 137–145.

47. Zukauskas, A. A., *High Performance Single-Phase Heat Exchangers*, Hemisphere, Washington, D.C., 1989, J. Karni, English edition editor.
48a. McQuiston, F. C., Finned tube heat exchangers—State of the art for the air side, *Trans. ASHRAE*, 1077–1085 (1981).
48b. McQuiston, F. C., Heat, mass and momentum transfer data for five plate fin tube heat transfer surfaces, *Trans. ASHRAE, 84*, 266–281 (1978).
49. Maltson, J. D., Wilcock, D., and Davenport, C. J., Comparative performance of rippled fin plate fin and tube heat exchangers, *Trans. ASME, J. Heat Transfer, 111*, 21–28 (1989).
50. Kroger, D. G., Radiator characterisation and optimization, SAE 840380, 1985, pp. 2.984–2.990.
51. Weiting, A. R., Empirical correlations for heat transfer and flow friction characteristics of rectangular offset-fin plate-fin heat exchangers, *Trans. ASME, J. Heat Transfer* 488–490 (1975).
52. Manglik, and Bergles, A. E., The thermal hydraulic design of the rectangular offset strip-fin compact heat exchanger, in *Compact Heat Exchangers—A Festschrift for A. L. London* (R. K. Shah, A. D. Kraus, and D. Metzger, eds.), Hemisphere, Washington, D.C., 1990, pp. 123–149.
53. Kays, W. M., Pin-fin heat exchanger surfaces, *Trans. ASME*, May, 471–483 (1955).
54. Norris, R. H., and Spofford, W. A., *Trans. ASME, 64*, 489 (1942).
55. Kanzaka, M., Iwabuchi, M., Aoki, Y., and Ueda, S., Study on heat transfer characteristics of pin finned plate type heat exchangers, *Heat Transfer—Philadelphia, 85*, 306–311 (1989).
56. Gardner, K. A., Efficiency of extended surface, *Trans. ASME, 67*, 621–632 (1945).
57. Kern, D. Q., and Kraus, A. D., *Extended Surface Heat Transfer*, McGraw-Hill, New York, 1972.
58. Scott, T. C., and Goldschmidt, I., Accurate, simple expressions for the fin efficiency of single and composite extended surfaces, in *Advances in Enhanced Heat Transfer, ASME Symp., 100122*, 79–85 (1979).
59. Schmidt, T. E., Heat transfer calculations for extended surfaces, *J. ASHRAE*, April, 351–357 (1949).
60. Zabronsky, H., *J. Appl. Mech., 22*, 119 (1955).
61. Sparrow, E. M., and Lin, S. H., Shorter communication, *Int. J. Heat Mass Transfer, 7*, 951–953 (1964).
62. Shah, R. K., Temperature effectiveness of multiple sandwich rectangular plate-fin srufaces, *Trans. ASME, J. Heat Transfer, 91*, 471–473 (1971).
63. Shah R. K., Plate-fin and tube-fin heat exchanger design procedures, in *Heat Transfer Equipment Design* (R. K. Shah, D. C. Subbarao, and R. M. Mashelekar, eds.), Hemisphere, 1988, pp. 255–266.
64. Hesselgraves, J. E., Optimizing size and weight of plate fin heat exchangers, in *Aerospace Heat Exchanger Technology* (R. K. Shah, and A. Hashemi, eds.), Elsevier Science Publishers, Amsterdam, 1993, pp. 391–399.
65. Shah, R. K., and Mueller, A. C., Heat exchanger basic thermal design methods, in *Handbook of Heat Transfer Applications*, second edition (W. M. Rohsenow, J. P. Hartnett, and E. N. Ganic, eds.), McGraw-Hill, New York, 1985, pp. 4-1–4-77.
66. Chiou, J. P., The advancement of compact heat exchanger theory considering the effects of longitudinal heat conduction and flow nonuniformity, in *Symposium on Compact Heat Exchanges—History, Technological Advancement and Mechanical Design Problems* (R. K. Shah, C. F. McDonald, and C. P. Howard, eds.), Vol. 10, ASME, New York, 1980, pp. 101–121.
67. Kroger, D. G., Experimental heat transfer, fluid mechanics and thermodynamics in the development of large air cooled heat exchangers, in *Experimental Heat Transfer, Fluid Mechanics and Thermodynamics* M. D. Kelleher et al., eds., Elservier Science Publishers, Amsterdam, 1993, pp. 135–141.
68. Ganapathy, V., Design of aircooled exchangers—Process design criteria, in *Process Heat Exchange, Chemical Engineering Magazine*, (V. Cavaseno, ed.), McGraw-Hill, New York, 1979, pp. 418–425.
69. North, C. D. R., Air coolers, in *Developments in Heat Exchanger Technology-1* (D. Chisholm, ed.), Applied Science Publishers, London, 1980, pp. 155–177.
70. API Standard 661, Air Cooled Heat Exchangers for General Refinery Service, 7th edition, American Petroleum Institute, Washington, D.C., 1978.
71. ASME Boiler and Pressure Vessel Code, Section VIII, Division 1—Pressure Vessels, 1992, American Society of Mechanical Engineers, New York.

72. Baker, W. J., Selecting and specifying air cooled heat exchangers, *Hydrocarbon Processing*, 173–177 (1980).
73. Shipes, K. V., Air cooled exchangers in cold climates, *Chem. Eng. Prog.*, *70*, 53–58 (1974).
74. Brown, R., Design of aircooled exchangers—A procedure for preliminary estimates, in *Process Heat Exchange, Chemical Engineering Magazine* (V. Cavaseno, ed.), McGraw-Hill, New York, 1979, pp. 414–417.
75. Saunders, E. A. D., Air cooled heat exchangers, in *Heat Exchangers: Selection Design and Construction*, Addison Wesley Longman, Reading, MA, 1989.
76. Larowski, A., and Taylor, M. A., Systematic Procedures for Selection of Heat Exchangers, C58/82, Institution of Mechanical Engineers, London, 1982, pp. 32–56.
77. Mukherjee, R., Avoid operating problems in air cooled heat exchangers, *Hydro. Proc.*, March 1997, pp. 69–76.
78. Larowski, A., and Taylor, M. A., Systematic procedures for selection of heat exchangers, C58/82, *Inst. of Mech. Eng.*, London, 1982, pp. 32–56.
79. Brown, J. W., and Benkley, G. J., Heat exchangers in cold service—A contractor's view, *Chem. Eng. Prog.*, *70*, 59–62 (1974).

Bibliography

1. Webb, R. L., Compact heat exchangers, in *Heat Exchanger Design Handbook*, Vol. 3 (E. U. Schlunder, editor-in-chief), Hemisphere, Washington, D.C., 1983, Section 3.9.
2. Ward, D. J., and Young, E. H., Heat transfer and pressure drop of air in forced convection across triangular pitch banks of finned tubes, *Chem. Eng. Prog. Symp. Ser.*, *55*, 37 (1959).
3. Zukauskas, A., Heat transfer from tubes in cross flow, in *Advances in Heat Transfer* (J. P. Hartnett and T. Irvine, Jr., eds.), Vol. 8, Academic Press, New York, 1972, pp. 93–160.
4. Ganguli, A., Tung, S. S., and Taborek, J., Parametric study of air cooled heat exchanger finned tube geometry, *Heat Transfer—Denver*, *81*, 122–128 (1985).
5. Ward, D. J., and Young, E. H., Heat transfer and pressure drop of air in forced convection across triangular pitch banks of finned tubes, *Chem. Eng. Prog. Symp. Ser. 59*, 37–44 (1963).
6. London, A. L., and Shah, R. L., Offset rectangular plate-fin surfaces—Heat transfer and flow friction characteristics, *Trans. ASME, J. Heat Transfer*, 218–228 (1968).
7. Nir, A., Heat transfer and friction factor correlations for crossflow over staggered finned tube banks, *Heat Transfer Eng.*, *12*, 43–58 (1991).
8. Agarwal, R. S., Ramaswamy, M., and Srivastava, V. K., Simulation of air-cooled condensers, *J. Energy, Heat Mass Transfer (India)*, *13*, 145–164 (1991).
9. Huang, L. J., and Shah, R. K., Assessment of calculation methods for efficiency of straight fins of rectangular profile, *Int. J. Heat Fluid Flow*, *13*, 282–293 (1992).
10. Shah, R. K., and Webb, R. L., Compact and extended heat exchangers, in *Heat Exchangers: Theory and Practice* (J. Taborek, G. F. Hewitt, and N. Afgan, eds.), Hemisphere/McGraw-Hill, Washington, D.C., 1983, pp. 425–468.
11. London, A. L., and Shah, R. K., Offset rectangular plate-fin surfaces—Heat transfer and flow friction characteristics, *Trans. ASME, J. Eng. Power*, *90A*, 218–228 (1968).
12. Shah, R. K., and London, A. L., Influence of Brazing on Very Compact Heat Exchanger Surfaces, ASME Paper No. 71-HT-29, 1971.
13. Bell, K. J., Application of plate-fin heat exchangers in the process industries, in *Compact Heat Exchangers* (R. K. Shah, A. D., Kraus, and D. Metzger, eds.), Hemisphere, Washington, D.C., 1990, pp. 591–602.
14. Kern, M. J., and Wallner, R., Water Cooled Charge Air Coolers for Heavy Diesel Engines, C116/86, 1986, IMechE, London, pp. 261–268.
15. Webb, R. L., Air side heat transfer in finned tube heat exchangers, *Heat Transfer Eng.*, *1*, 33–49 (1980).
16. McQuiston, F. C., Heat transfer and flow friction data for fin-tube surfaces, *Trans. ASME, J. Heat Transfer*, *93C*, 249–250 (1971).

17. McQuiston, F. C., and Tree, D. R., Optimum space envelopes of the finned tube heat transfer surface, *ASHRAE*, 144–152 (1972).
18. Rich, D. G., The efficiency and thermal resistance of annular and rectangular fins, *Proc. 3rd Int. Heat Transfer Conf., 111*, 281–289 (1966).
19. Glass, J., Design of aircooled exchangers—Specifying and rating fans, in *Process Heat Exchange, Chemical Engineering Magazine* (V. Cavaseno, ed.), McGraw-Hill, New York, 1979, pp. 426–430.
20. Taborek, J., Bond resistance and design temperatures for high finned tubes—A reappraisal, *Proceedings of the ASME, Thermal/Mechanical Heat Exchanger Design, Karl Gardner Memorial Session* (K. P. Singh and S. M. Shenkman, eds.), *118*, 49–57 (1985).
21. Mueller, A. C., Air cooled heat exchangers, in *Heat Transfer Equipment Design* (R. K. Shah, E. C. Subbarao, and R. A. Mashelikar, eds.), Hemisphere, Washington, D.C., 1988, pp. 179–190.
22. *Gas Processors Suppliers Association Engineering Data Book*, Vol. 1, 10th edition, 1987.
23. Fletcher, L. S., Experimental techniques for thermal contact resistance measurements, in *Experimental Heat Transfer, Fluid Mechanics and Thermodynamics* (M. D. Kelleher et al., eds.), Elsevier Science Publishers, Amsterdam, 1993, pp. 195–206
24. Sunden, B., and Svantesson, J., Thermal hydraulic performance of new multilouvered fins, *Heat Transfer—Jerusalem*, 1990, Paper No. 14-HX-16, pp. 91–96.
25. Soland, J. G., Mack, W. M. Jr., and Rohsenow, W. M., Performance ranking of plate-fin heat exchanger surfaces, *Trans. ASME, J. Heat Transfer, 100*, 514–519 (1978).

CHAPTER 5

1. Minton, P. E., Process heat transfer, *Proc. 9th Int. Heat Transfer Conf., Heat Transfer 1990—Jerusalem*, Paper No. KN-22, *1*, 355–362 (1990).
2. Shah, R. K., Classification of Heat Exchangers, Lecture Notes, December 1990, pp. 1–68.
3. *Standards of Tubular Exchanger Manufacturers Associaton*, seventh edition, Tubular Exchanger Manufacturers Association, Tarrytown, NY, 1988.
4. Drake, C. E., and Carp, J. R., Shell and tube heat exchangers, *Chem. Eng.*, 165–170 (1960).
5. Lord, R. C., Minton, P. E., and Sulusser, R. P., Design of Exchangers, *Chem. Eng.*, January, 96–118 (1970).
6. Saunders, E. A. D., Features relating to thermal design, in *Heat Exchanger Design Handbook*, (E. U. Schlunder, editor-in-chief), Vol. 4, Hemisphere, Washington, D.C., 1983, Section 4.2.5.

7a. Larowski, A., and Taylor, M. A., Systematic Procedures for Selection of Heat Exchangers, C58/82, Institution of Mechanical Engineers, London, 1982, pp. 32–56.

7b. Larowski, A., and Taylor, M. A., Systematic Procedure for Selection of Heat Exchangers, IMechE, *Proc. Inst. Mech. Eng., 197A*, 51–69 (1983).

8. Phadke, P. S., Determining tube counts for shell and tube exchangers, *Chem. Eng.*, 65–68 (1984).
9. Whitly, D. L., and Ludwig, E. E., Rate exchangers this computer way, *Petroleum Refiner* 147–156 (1961).
10. Fraas, A. P., and Ozisik, M. N., *Heat Exchanger Design*, John Wiley & Sons, New York, 1965.
11. Saunders, E. A. D., *Heat Exchangers: Selection, Design and Construction*, Addison Wesley Longman, Reading, MA, 1989.
12. Escoe, K. A., *Mechanical Design of Process Systems*, Vol. 2, *Shell and Tube Heat Exchangers, Rotating Equipment, Bins, Silos, Stacks*, Gulf Publishing Company, Houston.
13. Palen, J. W., and Taborek, J., Solution of shellside flow, pressure drop and heat transfer by stream analysis method, *Chem. Eng., Symp. Ser.*, No. 92, *Heat Transfer—Philadelphia, 65*, 53–63 (1969).
14. Fanaritis, J. P., and Bevevino, J. W., How to select the optimum shell and heat exchanger, in *Process Heat Exchange, Chemical Engineering Magazine* (V. Cavaseno, ed.), McGraw-Hill, New York, 1979, pp. 5–13.
15. Taborek, J., Shell and tube heat exchanger design—Extension of the method to other shell, baffle, and tube bundle geometries, in *Heat Exchanger Design Handbook*, (E. U. Schlunder, editor-in-chief), Vol. 3, Hemisphere, Washington, D.C., 1983, Section 3.3.11.

16. Gupta, J. P., *Fundamentals of Heat Exchanger and Pressure Vessel Technology*, Hemisphere, Washington, D.C., 1986.
17. Singh, K. P., Mechanical design of tubular heat exchangers—An appraisal of the state-of-the-art, in *Heat Transfer Equipment Design* (R. K. Shah, C. Subbarao, and R. M. Mashelekar, eds.), Hemisphere, Washington, D.C., 1988, pp. 71–87.
18. Boyer, R. C., and Pase, G. K., The energy saving NESTS concept, *Heat Transfer Eng.*, *2*, 19–27 (1980).
19. Butterworth, D., New twists in heat exchange, *Chem. Eng.*, September, 23–28 (1992).
20. Yokell, S., Heat exchanger tube-to-tubesheet connections, *The Chemical Engineering Guide to Heat Transfer*, Vol. I, *Plant Principles* (K. J. McNaughton, ed.), Hemisphere, New York, 1986 pp. 76–92.
21. Yokell, S., *A Working Guide to Shell and Tube Heat Exchangers*, McGraw-Hill, New York, 1990.
22. Yokell, S., Double tubesheet heat exchanger design stops shell-tube leakage, *Chem. Eng.*, May, 133–136 (1973).
23. Woodward, A. R., Howard, D. L., and Andrews, E. F. C., Condensers, pumps and cooling water plant, in *Modern Power Station Practice*, Vol. C, *Turbines, Generators, and Associated Plant*, (D. J. Littler, E. J. Davies, H. E. Johnson, F. Kirkby, P. B. Myerscouh, and W. Wright, eds.), Pergamon Press, New York.
24. Spencer, T. C., Mechanical design and fabrication of exchangers in the United States, *Heat Transfer Eng.*, *8*, 58–61 (1987).
25. Gollin, M., Heat exchanger design and rating, in *Handbook of Applied Thermal Design* (E. C. Guyer, ed.), McGraw-Hill, 1984, pp. 7-24–7-36.
26. Taborek, J., Design procedures for segmentally baffled heat exchangers, in *Heat Exchanger Design Handbook* (E. U. Schlunder, editor-in-chief), Vol. 3, Hemisphere, Washington, D.C., 1983, pp. 3.3.10-1–3.3.10-8.
27. Mueller, A. C., Process heat exchangers, in *Handbook of Heat Transfer Applications*, second edition (W. M. Rohsenow, J. P. Hartnett, and E. N. Ganic, eds.), McGraw-Hill, New York, 1985, pp. 4-78–4-173.
28. Gutterman, G., Specify the right heat exchanger, *Hydrocarbon Processing*, April, 161–163 (1980).
29. Schlunder, E. U., editor-in-chief, Mechanical design codes, in *Heat Exchanger Design Handbook*, Vol. 4, *Expansion Joints*, Hemisphere, Washington, D.C., 1983, Section 4.1.6.
30. Taborek, J., and Aurioles, G., Effect of 1988 TEMA standards on mechanical and thermo hydraulic design of shell and tube heat exchangers, *Heat Transfer*, Philadelphia, 1989.
31. Singh, K. P., and Soler, A. I., *Mechanical design of heat exchangers and pressure vessel components*, Arcturus Publishers, Cherry Hill, N.J., 1984.
32. Jaw, L., Temperature relations in shell and tube exchangers having one pass splitflow shells, *Trans. ASME, J. Heat Transfer*, 408–416 (1964).
33. Grant, I. D. R., Shell and tube exchangers for single phase applications, in *Developments in Heat Exchanger Technology—1* (D. Chisholm, ed.), Applied Science Publishers, London, 1980, pp. 11–40.
34. Martin, D. J., Haseler, L. E., Hollingsworth, M. A., and Mathew, Y. R., The use of sealing strips to block bypassing flow in a rectangular tube bundle, *Heat Transfer—Jerusalem*, 1990, Paper No. 14-HX-23, pp. 33–138.
35. Taylor, C. E., and Currie, I. G., Sealing strips in tubular heat exchangers, *Trans. ASME, J. Heat Transfer*, *109*, 569–573 (1987).
36. Tinker, T., Shellside characteristics of shell and tube heat exchangers—General discussion on heat transfer, *Inst. Mech. Eng., London*, 97–116 (1951).
37. Tinker, T., Shellside characteristics of shell and tube heat exchangers—A simplified rating system for commercial heat exchangers, *Trans. ASME*, 36–52 (1958).
38. Bell, K. J., Final Report of the Cooperative Research Program on Shell and Tube Heat Exchangers, Bull. No. 5, University of Delaware Engineering Experiment Station, New York, June 1963.
39. Bell, K. J. Delaware method for shellside design, in *Heat Exchangers—Thermal Hydraulic Funda-*

mentals and Desgin (S. Kakac, A. E. Bergles, and F. Mayinger, eds.), Hemisphere/McGraw-Hill, Washington, D.C., 1981, pp. 581–618.
40. Bell, K. J., Delaware method for shellside design, in *Heat Transfer Equipment Design* (R. K. Shah, E. C. Subbarao, and R. A. Mashelkar, eds.), Hemisphere, Washington, D.C., 1988, pp. 145–166.
41. Taborek, J., Shell and tube heat exchanger design, in *Heat Exchanger Design Handbook*, Vol. 3 (E. U. Schlunder, editor-in-chief), Hemisphere, Washington, D.C., 1983, Section 3.3.
42. B-JAC International, Inc., Modlothian, Va.
43. Kern, D. Q., *Process Heat Transfer*, McGraw-Hill, New York, 1950.
44. Donohue, D. A., Heat exchanger design, *Petroleum Refiner*: Part 1, Types and arrangements, *34*, 94–100; Part 2, Heat transfer, *34*, 9–18; Part 3, Fluid flow and thermal design, *34*, 175–184 (1955); Part 4, Mechanical design, *35*, 155–160 (1956).
45. Devore, A., Try this simplified method for rating baffled heat exchangers, *Hydrocarbon Processing & Petroleum Refining*, *40*, 221–233 (1961).
46. Bell, K. J., Approximate sizing of shell and tube heat exchangers, in *Heat Exchanger Design Handbook* (E. U. Schlunder, editor-in-chief), Vol. 3, Hemisphere, Washington, D.C., 1983, Section 3.1.4.
47. McAdams, W. H., *Heat Transmission*, third edition, McGraw-Hill, New York, 1954, p. 229.
48. Taborek, J., Ideal tube bank correlations for heat transfer and pressure drop, in *Heat Exchanger Design Handbook*, Vol. 3 (E. U. Schlunder, editor-in-chief), Hemisphere, Washington, D.C., 1983, Section 3.3.7.
49. Kays, W. M., and London, A. L., *Compact Heat Exchangers*, third edition, McGraw-Hill, New York, 1984.
50. Briggs, D. E., and Young, E. H., Convection heat transfer and pressure drop of air flowing across triangular pitch bank of finned tubes, *Chem. Eng. Prog. Symp. Ser.*, No. 41, *Heat Transfer—Houston*, *59*, 1–10 (1963).
51. Briggs, D. E., Katz, D. L., and Young, E. H., How to design finned tube heat exchangers, *Chem. Eng. Prog.*, *59*, 49–59 (1963).
52. Short, B. E., Heat Transfer and Pressure Drop in Heat Exchangers, Publication No. 4324, University of Texas, 1943, pp. 1–55.
53. Donohue, D. A., Heat transfer and pressure drop in heat exchangers, *Ind. Eng. Chem.*, *41*, 2499–2511 (1969).
54. Slipcevic, B., Designing heat exchangers with disk and ring baffles, *Sulzer Tech. Rev.*, *3*, 114–120 (1976).
55. Slipcevic, B., Shellside pressure drop in shell and tube heat exchangers with disk and ring baffles, *Sulzer Tech. Rev.*, *60*, 28–30 (1978).
56. Goyal, K. P., and Gupta, B. K., An experimental performance evaluation of a disk and doughnut type heat exchanger, *Trans. ASME, J. Heat Transfer*, *106*, 759–765 (1984).
57. Ratnasamy, K., Exchanger design using disc and donut baffles, *Hydrocarbon Processing*, April, 63–65 (1987).
58. Hausen, H., *Warmeubertrangung im Gegenstrom und Kreuzstrom*, Springer-Verlag, Berlin, 1950.
59. Gentry, C. C., RODbaffle heat exchanger technolgy, *Chem. Eng. Prog.*, July 48–57 (1990).
60. Gentry, C. C., RODbaffle heat exchanger design methods, *Sixth International Symposium on Transport Phenomena in Thermal Engineering*, Seoul, Korea, May 9–13, 1993, pp. 301–306.
61. Gentry, C. C., Young, R. K., and Small, W. M., RODbaffle heat exchanger thermal and hydraulic predictive methods, *Proc. 7th Int. Heat Transfer Conference—Munich*, Vol. 6, Hemisphere, Washington, D.C., 1982, pp. 197–202.
62. Gentry, C. C., Young, R. K., and Small, W. M., RODbaffle heat exchanger thermal and hydraulic predictive methods for bare and low finned tubes, *Proc. 22nd National Heat Transfer Conference, Heat Transfer—Niagara Falls*, 1984, *AIChE Symp. Ser.*, *80*, 104–109 (1984).
63. Gentry, C. C., Young, R. K., and Small, W. M., A conceptual RODbaffle nuclear steam generator design, *1982 ASME Joint Power Generation Conference, Nuclear Heat Exchanger Sessions*, Denver, Colo., October 17–21, 1982.
64. Hesselgraeaves, J. E., *Proc. 2nd UK National Conference, Heat Transfer*, Vol. 1, Institution of Mechanical Engineers, London, 1988, pp. 787–800.

65. Taborek, J., Longitudinal flow in tube bundles with grid baffles, *Heat Transfer—Philadelphia*, 1989, pp. 72–78.
66. Soler, A. I., Expert system for design integration—Application to the total design of shell and tube heat exchangers, *Proceedings of the ASME, Thermal/Mechanical Heat Exchanger Design, Karl Gardner Memorial Session* (K. P. Singh and S. M. Shenkman, eds.), ASME PVP, Vol. 118, 1985, pp. 135–138.

Suggested Readings

1. Taborek, J., Heat exchanger design, in *Heat Transfer, 4*, 269–285 (1978).
2. Bell, K. J., Overall design methodology for shell and tube exchangers, in *Heat Transfer Equipment Design* (R. K. Shah, E. C. Subbarao, and R. A. Mashelkar, eds.), Hemisphere, Washington, D.C., 1988, pp. 131–144.
3. McNaughton, K. J., ed., *The Chemical Engineering Guide to Heat Transfer*, Vol. I. *Plant Principles*, Hemisphere/McGraw-Hill, New York, 1986.
4. Mehra, D. K., Shell and tube exchangers, in *The Chemical Engineering Guide to Heat Transfer*, Vol. I, *Plant Principles* (K. J. McNaughton and the staff of *Chemical Engineering*, eds.), Hemisphere/McGraw-Hill, New York, 1986, pp. 43–52.

CHAPTER 6

1. Denniston, D. W., Waste recovery in the glass industry, in *Industrial Heat Exchangers Conference Proceedings* (A. J. Hayes, W. W. Liang, S. L. Richlen, and E. S. Tabb, eds.), American Society for Metals, Metals Park, Ohio, 1985, pp. 13–20.
2. Mondt, J. R., Regenerative Heat Exchangers: The Elements of Their Design, Selection and Use, Research Publication GMR-3396, 1980, General Motors Research Laboratories, Warren, Mich.
3. Shah, R. K., Classification of Heat Exchangers, Lecture Notes, December 1990, pp. 1–68.
4. Liang, W. W., and Tabb, E. S., CRI's advanced heat transfer systems program, in *Industrial Heat Exchangers Conference Proceedings* (A. J. Hayes, W. W. Liang, S. L. Richlen, and E. S. Tabb, eds.), American Society for Metals, Metals Park, Ohio, 1985, pp. 29–36.
5. Coombs, M. G., Strumpf, H. J., and Kotchick, D. M., A ceramic finned plate recuperator for industrial applications, in *Industrial Heat Exchangers Conference Proceedings* (A. J. Hayes, W. W. Liang, S. L. Richlen, and E. S. Tabb, eds.), American Society for Metals, Metals Park, Ohio, 1985, pp. 63–68.
6. Newby, J. N., The Regen regenerative burner—Principles, properties and practice, in *Industrial Heat Exchangers Conference Proceedings* (A. J. Hayes, W. W. Liang, S. L. Richlen, and E. S. Tabb, eds.), American Society for Metals, Metals Park, Ohio, 1985, pp. 143–152.
7. Walker, G., *Cryocoolers*, Part 2: *Applications*, Plenum Press, New York, p. 44.
8. Bugyis, E. J., and Taylor, H. L., Heat exchange in the steel industry, in *Industrial Heat Exchangers Conference Proceedings* (A. J. Hayes, W. W. Liang, S. L. Richlen, and E. S. Tabb, eds.), American Society for Metals, Metals Park, Ohio, 1985, pp. 3–12.
9. Hoffman, L. C., and Williams, H. W., Fluid bed waste recovery performance in a hostile environment, in *Industrial Heat Exchangers Conference Proceedings* (A. J. Hayes, W. W. Liang, S. L. Richlen, and E. S. Tabb, eds.), American Society for Metals, Metals Park, Ohio, 1985, pp. 87–94.
10. Hayes, A. J., and Richlen, S. L., The Department of Energy's advanced heat exchangers program, in *Industrial Heat Exchangers Conference Proceedings* (A. J. Hayes, W. W. Liang, S. L. Richlen, and E. S. Tabb, eds.), American Society for Metals, Metals Park, Ohio, 1985, pp. 21–28.
11. McDonald, C. F., The role of the ceramic heat exchanger in energy and resource conservation, *Trans. ASME, J. Eng. Power, 102*, 303–315 (1980).
12. Kleiner, R. N., and Coubrough, L. E., Advanced high performance ceramic heat exchanger designs for industrial heat recovery applications, in *Industrial Heat Exchangers Conference Proceedings* (A. J. Hayes, W. W. Liang, S. L. Richlen, and E. S. Tabb, eds.), American Society for Metals, Metals Park, Ohio, 1985, pp. 51–56.

13. McNallan, M. J., Liang, W. W., and Rothman, M. F., An investigation of the hot-corrosion of metallic and ceramic heat exchanger materials in chlorine contaminated environments, in *Industrial Heat Exchangers Conference Proceedings* (A. J. Hayes, W. W. Liang, S. L. Richlen, and E. S. Tabb, eds.), American Society for Metals, Metals Park, Ohio, 1985, pp. 293–298.
14. Shah, R. K., Counterflow rotary regenerator thermal design procedures, in *Heat Transfer Equipment Design* (R. K. Shah, E. C. Subbarao, and R. M. Mashelikar, eds.), Hemisphere, Washington, D.C., 1988, pp. 267–296.
15. Kays, W. M., and London, A. L., *Compact Heat Exchangers*, third edition, McGraw-Hill, New York, 1984.
16. London, A. L., Young, M. B. O., and Stang, J. H., Glass-ceramic surfaces, straight triangular passages—Heat transfer and flow friction characteristics, *Trans. ASME, J. Eng. Power, 92A*, 381–389 (1970).
17. Baclic, B. S., The application of the Galerkin method to the solution of the symmetric and balanced counterflow regenerator problem, *Trans. ASME, J. Heat Transfer, 107*, 214–221 (1985).
18. Nusselt, W., Die Theorie des Winderhitzers [Theory of the Air Heater], *Z. Ver. Dt. Ing., 71*, 85–91 (1927).
19. Hausen, H., Uber die Theorie des Warmeaustausches in Regeneratoren, *Z. Angew. Math. Mech., 9*, 173–200 (1929). Also, in Vervollstandigte Berechnung des Warmeaustausches in Regeneratoren, *Z. Ver. Dtsch. Ing., 2* (1942).
20. Coppage, J. E., and London, A. L., The periodic-flow regenerator—A summary of design theory, *Trans. ASME, 75*, 779–787 (1953).
21. Lambertson, T. J., Performance factors of a periodic flow heat exchanger, *Trans. ASME, 80*, 586–592 (1958).
22. Bahnke, G. D., and Howard, C. P., The effect of longitudinal heat conduction on periodic flow heat exchanger performance, *Trans. ASME, J. Eng. Power*, 105–120 (1964).
23. Mondt, J. R., Vehicular gas turbine periodic flow heat exchanger solid and fluid temperature distributions, *Trans. ASME, J. Eng. Power*, 121–126 (1964).
24. Li, C.-H., A numerical finite difference method for performance evaluation of a periodic flow heat exchanger, *Trans. ASME, J. Heat Transfer, 105*, 611–617 (1983).
25. Nahavandi, A. H., and Weinstein, A. S., A solution to the periodic flow regenerative heat exchanger problem, *Appl. Sci. Res., 10*, 335–348 (1961).
26. Willmott, A. J., and Duggan, R. C., Refined closed methods for the contra-flow thermal regenerator problem, *Int. J. Heat Mass Transfer, 23*, 655–662 (1980).
27. Baclic, B. S., and Dragutinovic, G. D., Asymmetric-unbalanced counterflow thermal regenerator problem: Solution by the Galerkin method and meaning of dimensionless parameters, *Int. J. Heat Mass Transfer, 34*, 483–498 (1991).
28. Romie, F. E., and Baclic, B. S., Methods for rapid calculation of the operation of asymmetric counterflow regenerator, *Trans. ASME, J. Heat Transfer, 110*, 785–788 (1988).
29. Shah, R. K., Thermal design theory for regenerators, in *Heat Exchangers: Thermal-Hydraulic Fundamentals and Design* (S. Kakac, A. E. Bergles, and F. Mayinger, eds.), Hemisphere/McGraw-Hill, New York, 1981, pp. 721–763.
30. Heggs, P. J., Calculation of high temperature regenerative heat exchangers, in *High Temperature Equipment* (A. E. Sheindlin, ed.), Hemisphere, Washington, D.C., 1986, pp. 115–149.
31. Romie, F. E., A table of regenerator effectiveness, *Trans. ASME, J. Heat Transfer, 112*, 497–499.
32a. Hill, A., and Willmott, A. J., A robust method for regenerative heat exchanger calculations, *Int. J. Heat Mass Transfer, 30*, 241–249 (1987).
32b. Hill, A., and Willmott, A. J., Accurate and rapid thermal regenerator calculations, *Int. J. Heat Mass Transfer, 32*, 465–476 (1989).
33. Razelos, P., An analytical solution to the electric analog simulation of the regenerative heat exchanger with time varying fluid inlet temperatures, *Warme Stoffubertrag, 12*, 59–71 (1979).
34. Romie, F. E., Treatment of transverse and longitudinal heat conduction in regenerators, *Trans. ASME, J. Heat Transfer, 113*, 247–249 (1991).
35. Hahnemann, H. N., Approximate Calculations of Thermal Ratios in Heat Exchangers Including

Conduction in the Direction of Flow, National Gas Turbine Establishment Memorandum No. M36, TPA3/TIB, Ministry of Supply, Millbank, London, 1948.
36. Shah, R. K., A correlation for longitudinal heat conduction effects in periodic-flow heat exchangers, *Trans. ASME, J. Eng. Power, 97A*, 453–454 (1975).
37. Shah, R. K., Compact heat exchangers, in *Handbook of Heat Transfer Applications*, 2nd edition (W. M. Rohsenow, J. P. Hartnett, and E. N. Ganic, eds.), McGraw-Hill, New York, 1985, pp. 4-174–4-311.
38. London, A. L., and Ferguson, C. K., Test results of high performance heat exchanger surfaces used in aircraft intercoolers and their significance for gas turbine regenerator design, *Trans. ASME*, 17–26 (1949).
39. Bowden, A. T., and Hryniszak, W., The rotary regenerative air preheater for gas turbines, *Trans. ASME*, 769–777 (1953).
40. Shepherd, D. G., *Introduction to the Gas Turbines*, 2nd edition, Constable and Company, London, 1960.
41. Bathe, W. W., *Fundamentals of Gas Turbines*, John Wiley & Sons, New York, 1984.
42. Harper, D. B., Seal leakage in the rotary regenerator and its effect on rotary regenerator design for gas turbines, *Trans. ASME, 79*, 233–245 (1957).
43. Vincent, E. J., *The Theory and Design of Gas Turbines and Jet Engines*, McGraw-Hill, New York, 1956.
44. *Industrial Heat Exchangers Conference Proceedings* (A. J. Hayes, W. W. Liang, S. L. Richlen, and E. S. Tabb, eds.), American Society of Metals, Metals Park, Ohio, 1985.
45. Schadt, H. F., High-efficiency fluid-bed heat exchanger recovers heat from combustion gases, in *Industrial Heat Exchangers Conference Proceedings* (A. J. Hayes, W. W. Liang, S. L. Richlen, and E. S. Tabb, eds.), American Society for Metals, Metals Park, Ohio, 1985, pp. 71–80.
46. Williams, H. W., Fluid bed waste heat recovery operating experience on aluminum melting furnace, in *Industrial Heat Exchangers Conference Proceedings* (A. J. Hayes, W. W. Liang, S. L. Richlen, and E. S. Tabb, eds.), American Society for Metals, Metals Park, Ohio, 1985, pp. 241–248.
47. Rodgers, R. J., Vortex flow direct contact heat exchanger conceptual design and performance, in *Industrial Heat Exchangers Conference Proceedings* (A. J. Hayes, W. W. Liang, S. L. Richlen, and E. S. Tabb, eds.), American Society for Metals, Metals Park, Ohio, 1985, pp. 101–108.
48. Godbole, S. S., Gilbert, M. L., and Snyder, J. E., Design verification of the DOE/B&W HTBDR control system using interactive simulation, in *Industrial Heat Exchangers Conference Proceedings* (A. J. Hayes, W. W. Liang, S. L. Richlen, and E. S. Tabb, eds.), American Society for Metals, Metals Park, Ohio, 1985, pp. 45–50.
49. Luu, M., and Grant, K. W., Thermal and fluid design of a ceramic bayonet tube heat exchanger for high temperature waste heat recovery, in *Industrial Heat Exchangers Conference Proceedings* (A. J. Hayes, W. W. Liang, S. L. Richlen, and E. S. Tabb, eds.), American Society for Metals, Metals Park, Ohio, 1985, pp. 159–174.
50. Hackler, C. L., and Dinulescu, M., Porcelain enamelled flat plate heat exchangers—Engineering and application, in *Industrial Heat Exchangers Conference Proceedings* (A. J. Hayes, W. W. Liang, S. L. Richlen, and E. S. Tabb, eds.), American Society for Metals, Metals Park, Ohio, 1985, pp. 381–384.
51. Seehausen, J. W., Thermal-hydraulic performance of radiation recuperators, in *Industrial Heat Exchangers Conference Proceedings* (A. J. Hayes, W. W. Liang, S. L. Richlen, and E. S. Tabb, eds.), American Society for Metals, Metals Park, Ohio, 1985, pp. 175–180.
52. Reay, D. A., Heat exchangers for waste heat recovery, International Research and Development Co., Ltd., New Castle upon Tyne, UK, in *Developments in Heat Exchanger Technology—1* (D. Chisholm, ed.), Applied Science Publishers, London, pp. 233–256, (1980).

Bibliography

1. Atthey, D. R., and Chew, P. E., Calculation of high temperature regenerative heat exchangers, in *High Temperature Equipment* (A. E. Sheindlin, ed.), Hemisphere, Washington, D.C., 1986, pp. 73–113.

2. Schmidt, F. W., and Willmott, A. J., *Thermal Energy Storage and Regeneration*, McGraw-Hill, New York, 1981.
3. Romie, F. E., Periodic thermal storage: The regenerator, *Trans. ASME, J. Heat Transfer, 101*, 726–731 (1979).
4. London, A. L., and Kays, K. M., The liquid-coupled indirect-transfer regenerator for gas-turbine plants, *Trans. ASME*, 529–542 (1951).
5. Shah, R. K., Compact heat exchanger technology and applications, Key Note Lecture, *Eleventh Heat and Mass Transfer Conference*, Madras, India, Indian Society for Heat and Mass Transfer, 1992, pp. 1–25.
6. Jakob, M., *Heat Transfer*, Vol. II, John Wiley & Sons, New York, 1957.
7. Iliffe, C. E., Thermal analysis of the contra-flow regenerative heat exchanger, *Proceedings, Institution of Mechanical Engineers, 159*, 363–371 (1948).
8. Hausen, H., *Heat Transfer in Counterflow, Parallel Flow and Cross Flow*, 2nd edition, McGraw-Hill, New York, 1983.
9. Shah, R. K., Compact heat exchanger design procedures, in *Heat Exchangers: Thermal-Hydraulic Fundamentals and Design* (S. Kakac, A. E. Bergles, and F. Mayinger, eds.), Hemisphere, Washington, D.C., 1981, pp. 495–536.
10. Romie, F. E., Transient response of rotary regenerators, *Trans. ASME, J. Heat Transfer, 110*, 836–840 (1988).
11. Johnson, J. E., Regenerator Heat Exchangers for Gas Turbines, R. A. E. Report Aero. 2266 S.D. 27, 1948, pp. 1–72.
12. Willmott, A. J., The regenerative heat exchanger computer representation, *Int. J. Heat Mass Transfer*, 997–1014 (1969).
13. Kroger, P. G., Performance deterioration in high effectiveness heat exchangers due to axial heat conduction effects, *Adv. Cryogen. Eng., 12*, 363–372 (1967).

CHAPTER 7

1. Focke, W. W., Plate Heat Exchangers: Review of Transport Phenomena and Design Procedures, CSIR Report CENG 445, CSIR, Pretoria, South Africa, 1983.
2. Cooper, A., and Usher, J. D., Plate heat exchangers, in *Heat Exchanger Design Handbook* (E. U. Schlunder, editor-in-chief), Vol. 3, Hemisphere, Washington, D.C., 1983, Section 3.7.
3. Raju, K. S. N., and Bansal, J. C., Plate heat exchangers and their performance, in *Low Reynolds Number Flow Heat Exchangers* (S. Kakac, R. K. Shah, and A. E. Bergles, eds.), Hemisphere, Washington, D.C., 1983, pp. 899–912.
4. Raju, K. S. N., and Bansal, J. C., Design of plate heat exchangers, in *Low Reynolds Number Flow Heat Exchangers* (S. Kakac, R. K. Shah, and A. E. Bergles, eds.), Hemisphere, Washington, D.C., 1983, pp. 913–932.
5. Shah, R. K., and Focke, W. W., Plate heat exchangers and their design theory, in *Heat Transfer Equipment Design* (R. K. Shah, D. C. Subbarao, and R. M. Mashelekar, eds.), Hemisphere, Washington, D.C., 1988, pp. 227–255.
6. Alpha-Laval Product Literature, M/s, Alpha-Laval (India) Limited, Pune, India.
7. Mueller Accu-Therm Plate Heat Exchangers, AT-1601-4, Paul Muller Company, Springfield, Mo.
8. Marriott, J., Where and how to use plate heat exchangers, in *Process Heat Exchange, Chemical Engineering Magazine* (V. Cavaseno, ed.), McGraw-Hill, New York, 1979, pp. 156–162.
9. Saunders, E. A. D., Gasketed plate heat exchangers, in *Heat Exchangers: Selection, Design and Construction*, Addison Wesley Longman, Reading, MA, 1989, Chapter 16.
10. Trom, L., Heat Exchangers: Is it time for a change?, *Chem. Eng.*, February, 70–73 (1996).
11. Caciula, L., and Rudy, T. M., Prediction of plate heat exchanger performance, in *AIChE Symp. Ser., Heat Transfer—Seattle*, 1983, pp. 76–89.
12. Buonopane, R. A., and Troupe, R. A., A study of the effects of internal rib and channel geometry in rectangular channels, Part I: Pressure drop & Part II: Heat transfer, *AIChE J.*, July, 585–596 (1969).

13. *Heat Transfer Handbook, Design and Application of Paraflow Heat Exchangers*, APV Co., Tonowanda, N.Y.
14. Usher, J. D., Evaluating plate heat exchangers, in *Process Heat Exchange, Chemical Engineering Magazine* (V. Cavaseno, ed.), McGraw-Hill, New York, 1979, pp. 145–149.
15. Jenson, S., Assessment of heat transfer data, *Chem. Eng. Prog. Symp. Ser., Heat Transfer—1960*, *56*, 195–201 (1960).
16. Buonopane, R. A., Troupe, R. A., and Morgan, J. C., Heat transfer design method for plate heat exchangers, *Chem. Eng. Prog.*, *59*, 57–61 (1963).
17. Jackson, B. W., and Troupe, R. A., Plate exchanger design by ε-NTU method, *Heat Transfer Los Angeles, Chem. Eng. Prog. Symp. Ser.*, *62*, 185–190 (1966).
18. *Standards of the Tubular Exchanger Manufacturers Association*, 7th edition, Tubular Exchanger Manufacturers Association, Tarrytown, N.Y., 1989.
19. Minton, P. E., Designing spiral plate heat exchangers, *Chem. Eng.*, *77*, 103–112 (1970).
20. Chowdhury, K., Linkmeyer, H., Bassiouny, M. K., and Martin, H., Analytical studies on the temperature distribution in spiral plate heat exchangers, *Chem. Eng. Prog.*, *19*, 183–190 (1985).

Bibliography

1. Cowan, C. T., Choosing materials of construction for plate heat exchangers—I, in *Process Heat Exchange, Chemical Engineering Magazine* (V. Cavaseno, ed.), McGraw-Hill, New York, 1979, pp. 165–167.
2. Cowan, C. T., Choosing materials of construction for plate heat exchangers—II, in *Process Heat Exchange, Chemical Engineering Magazine* (V. Cavaseno, ed.), McGraw-Hill, New York, 1979, pp. 168–169.
3. Cross, P. H., Preventing fouling in plate heat exchangers, in *Process Heat Exchange, Chemical Engineering Magazine* (V. Cavaseno, ed.), McGraw-Hill, New York, 1979, pp. 211–214.
4. Shah, R. K., and Kandlikar, S. G., The influence of the number of thermal plates on plates heat exchanger performance, in *Current Researches in Heat and Mass Transfer, A Compendium and a Festschrift for Professor Arcot Ramachandran*, Hemisphere, Washington, D.C., 1986, pp. 267–288.
5. Edwards, M. F., Heat transfer in plate heat exchangers at low Reynolds numbers, in *Low Reynolds Number Flow Heat Exchangers* (S. Kakac, R. K. Shah, and A. E. Bergles, eds.), Hemisphere, Washington, D.C., 1983, pp. 933–947.
6. Marriott, J., Where and how to use plate heat exchangers, *Chem. Eng.*, *78*, 127–133 (1971).
7. Bond, M. P., Plate heat exchangers for effective heat transfer, *Chemical Engineer*, *367*, 162–166 (1981).
8. Saunders, E. A. D., Thermal appraisal: Gasketed plate heat exchangers, in *Heat Exchangers: Selection, Design and Construction*, Addison Wesley Longman, Reading, MA, 1989, Chapter 16.

CHAPTER 8

1. Bergles, A. E., Some perspective on enhanced heat transfer—Second generation heat transfer technology, *Trans. ASME, J. Heat Transfer*, *110*, 1082–1096 (1988).
2. Webb, R. L., and Bergles, A. E., Heat transfer enhancement: Second generation technology, *Mech. Eng.*, June, 60–67 (1983).
3. Marner, W. J., Bergles, A. E., and Chenoweth, J. M., On the presentation of performance data for enhanced tubes used in shell and tube heat exchangers, *Trans. ASME, J. Heat Transfer*, *105*, 358–365 (1983).
4. Bergles, A. E., Techniques to augment heat transfer, in *Handbook of Heat Transfer Applications* (W. M. Rohsenow, J. P. Hartnett, and E. N. Ganic, eds.), McGraw-Hill, New York, 1985, pp. 3-1–3-79.
5. Webb, R. L., Special surface geometries for heat transfer augmentation, in *Developments in Heat Exchanger Technology—1* (D. Chisholm, ed.), Applied Science Publishers, London, 1980, pp. 179–215.

6. Kohler, J. A., and Staner, K. E., High performance heat transfer surfaces, in *Handbook of Applied Thermal Design* (E. C. Guyer, ed.), McGraw-Hill, New York, 1984, pp. 7-37–7-49.
7. Yang, W.-J., High performance heat transfer surfaces: Single phase flows, *Heat Transfer in Energy Problems*, 109–116.
8. Webb, R. L., Enhancement of single phase heat transfer, in *Handbook of Single Phase Convective Heat Transfer* (S. Kakac, R. K. Shah, and W. Aung, eds.), John Wiley & Sons, New York, 1987, pp. 17.1–17.62.
9. Ravigururajan, T. S., and Rabas, T. J., Turbulent flow in integrally enhanced tubes, Part 1: Comprehensive review and database development, *Heat Transfer Eng.*, *17*, 19–29 (1996).
10. Pate, M. B., Ayub, Z. H., and Kohler, J., Heat exchangers for the airconditioning and refrigeration industry, in *Compact Heat Exchangers—A Festschrift for A. L. London* (R. K. Shah, A. D. Kraus, and D. Metzger, eds.), Hemisphere, Washington, D.C., 1990, pp. 567–590.
11. Khanpara, J. C., Bergles, A. E., and Pate, M. B., Augmentation of R-113 intube evaporation with microfin tubes, *ASHRAE Trans.*, *92*, 506–524 (19xx).
12. Gupta, J. P., *Fundamentals of Heat Exchanger and Pressure Vessel Technology*, Hemisphere, Washington, D.C., 1986.
13. Minton, P. E., Process heat transfer, *Proc. 9th Int. Heat Transfer Conf., Heat Transfer 1990—Jerusalem*, Paper No. KN-22, *1*, 355–362 (1990).
14. Ravigururajan, T. S., and Bergles, A. E., General correlations for pressure drop heat transfer for single phase turbulent flow in internally ribbed tubes, *Conf. Proc. Augmentation of Heat Transfer in Energy Systems*, ASME, Miami Beach, 1985.
15. Webb, R. L., Toward a common understanding of the performance and selection of roughness for forced convection, in *A Festschrift for E. R. G. Eckert* (J. P. Hartnett, T. F. Irvine, Jr., E. Pfender, and E. M. Sparrow, eds.), Hemisphere, Washington, D.C., 1979.
16. Chiou, J. P., Experimental investigation of the augmentation of forced convection heat transfer in a circular tube using spiral spring inserts, *Trans. ASME, J. Heat Transfer*, *109*, 300–307 (1987).
17. Bergles, A. E., and Joshi, S. D., Augmentation techniques for low Reynolds number in-tube flow, in *Low Reynolds Number Flow Heat Exchangers* (S. Kakac, R. K. Shah, and A. E. Bergles, eds.), Hemisphere, Washington, D.C., 1982, pp. 695–720.
18. Ravigururajan, T. S., and Rabas, T. J., Turbulent flow in integrally enhanced tubes, Part 2: Analysis and performance comparison, *Heat Transfer Eng.*, *17*, 30–40 (1996).
19. Sethumadhavan, R., and Rao, R., Turbulent flow friction and heat transfer characteristics of single and multistart spirally enhanced tubes, *Trans. ASME, J. Heat Transfer*, *108*, 55–61 (1986).
20. Junkhan, G. H., Bergles, A. E., Nirmalan, V., and Ravigururajan, T., Investigation of turbulators for fire tube boilers, *Trans. ASME, J. Heat Transfer*, *107*, 354–360 (1985).
21. Bergles, A. E., Webb, R. L., Junkhan, G. H., and Jensen, M. K., *Bibliography on Augmentation of Convective Heat and Mass Transfer*, Engineering Research Institute, Iowa State University, Ames, Iowa, May 1979.
22. Shah, R. K., Compact heat exchanger surface selection methods, in *Heat Transfer*, Vol. IV, Hemisphere, Washington, D.C., 1978, pp. 193–199.
22. Shah, R. K., Compact heat exchanger surface selection methods, in *Heat Transfer*, Vol. 4, Hemisphere, Washington, D.C., 1978, pp. 279–284.
23. Webb, R. L., Performance evaluation criteria for use of enhanced heat transfer surfaces in heat exchanger design, *Int. J. Heat Mass Transfer*, *24*, 715–726 (1981).
24. Maltson, J. D., Wilcock, D., and Davenport, C. J., Comparative performance of rippled fin plate fin and tube heat exchangers, *Trans. ASME, J. Heat Transfer*, *111*, 21–28 (1989).
25. London, A. L., Compact heat exchangers, Part 2: Surface geometry, *Mech. Eng.*, *86*, 31–34 (19xx).
26. London, A. L., and Ferguson, C. K., Test results of high performance heat exchanger surfaces used in aircraft intercoolers and their significance for gas turbine regenerator design, *Trans. ASME*, 17–26 (1949).
27. Bergles, A. E., Blumenkrantz, A. R., and Taborek, J., Performance evaluation criteria for enhanced heat transfer surfaces, in *Heat Transfer*, Vol. II, JSME, 1974, pp. 239–243.

28. K. Takahashi, W. Nakayama, T. Senshu, and H. Yoshida, Heat transfer analysis of shell-and-tube condensers with shell-side enhancement, *ASHRAE Trans. 90* (Part IB), 60 (1984).
29. R. L. Webb, Heat transfer surface having a high boiling heat transfer coefficient, U.S. Patent 3,696,861, October 10, 1972.
30. K. Fujie, W. Nakayama, H. Kuwahara, and K. Kakizaki, Heat transfer wall for boiling liquids, U.S. Patent 4,060,125, November 29, 1977.
31. J. Arshad and J. R. Thome, Enhanced boiling surfaces—heat transfer mechanism and mixture boiling, *ASME/JSME Joint Thermal Eng. Conf. Proc.*, Honolulu, Vol. 1, March 1983, pp. 191–197.

Bibliography

1. J. R. Thome, *Enhanced Boiling Heat Transfer*, Hemisphere, Washington, D.C., 1990.
2. Carnavos, T. C., Some recent developments in augmented heat exchange elements, in *Heat Exchangers: Design and Theory Source Book*, Scripta, Washington, D.C., 1974, pp. 441–489.
3. Bergles, A. E., Enhancement of heat transfer, in *Heat Transfer—1978*, Vol. VI, Hemisphere, Washington, D.C., 1978, pp. 89–108.
4. Bergles, A. E., Junkhan, G. H., and Webb, R. L., Energy conservation via heat transfer enhancement, Paper No. EGY205, *1978 Midwest Energy Conference*, Chicago, 19–21 November 1978, pp. 10–21.
5. Webb, R. L., and Bergles, A. E., Performance evaluation criteria for selection of heat transfer surface geometries used in low Reynolds number heat exchangers, in *Low Reynolds Number Flow Heat Exchangers* (S. Kakac, R. K. Shah, and A. E. Bergles, eds.), Hemisphere, Washington, D.C., 1982 pp. 735–752.
6. Webb, R. L., Enhancement for extended surface geometries used in air cooled heat exchangers, in *Low Reynolds Number Flow Heat Exchangers* (S. Kakac, R. K. Shah, and A. E. Bergles, eds.), Hemisphere, Washington, D.C., 1983, pp 721–734.
7. Song-Jiu Deng et al., Heat transfer enhancement and energy conservation, Hemisphere Publishing Corporation, New York.

CHAPTER 9

1. Collier, J. G., Heat exchanger fouling and corrosion, in *Heat Exchangers: Thermal-Hydraulic Fundamentals and Design* (S. Kakac, A. E. Bergles, and F. Mayinger, eds.), Hemisphere, Washington, D.C., 1981, pp. 999–1011.
2. Zelver, N., Roe, F. L., and Characklis, W. G., Monitoring of fouling deposits in heat transfer tubes: Case studies, in *Industrial Heat Exchangers Conference Proceedings* (A. J. Hayes, W. W. Liang, S. L. Richlen, and E. S. Tabb, eds.), American Society for Metals, Metals Park, Ohio, 1985, pp. 1985, 201–208.
3. Bott, T. R., *Fouling Notebook*, Institution of Chemical Engineers, London, 1990.
4. Chenoweth, J. M., Final Report of the HTRI/TEMA Joint Committee to Review the Fouling Section of the TEMA Standards, Heat Transfer Research, Inc., Alhambra, Calif., 1988.
5. Puckorius, P. R., Contolling deposits in cooling water systems, *Mater. Protect. Perform.*, November, 19–22 (1972).
6. Mukherjee, R., Conquer heat exchanger fouling, *Hydrocarbon Processing*, January, 121–127 (1996).
7. Silvestrini, R., Waste heat recovery: Heat exchanger fouling and corrosion, *Chem. Eng. Prog.*, December, 29–35 (1979).
8. Epstein, N., Fundamentals of heat transfer surface fouling: With special emphasis on laminar flow, in *Low Reynolds Number Flow Heat Exchangers* (S. Kakac, R. K. Shah, and A. E. Bergles, eds.), Hemisphere, Washington, D.C., 1982, pp. 951–964.
9. O'Callaghan, M., Fouling of heat transfer equipment: Summary review, in *Heat Exchangers: Thermal-Hydraulic Fundamentals and Design* (S. Kakac, A. E. Bergles, and F. Mayinger, eds.), Hemisphere, Washington, D.C., 1981, pp. 1037–1047.

10. Kern, D. Q., and Seaton, R. E., A theoretical analysis of thermal surface fouling, *Br. Chem. Eng.*, *4*, 258–262 (1959).
11. Epstein, N., Fouling in heat exchangers, in *Proceedings of the Sixth International Heat Transfer Conference*, Toronto, Canada, August, Vol. 4, Hemisphere, Washington, D.C., 1978, pp. 279–284.
12. Hasson, D., Precipitation fouling, in *Fouling of Heat Transfer Equipment* (E. F. C. Somerscales and J. G. Knudson, eds.), Proceedings of the International Conference on the Fouling of Heat Transfer Equipment, 1979, Hemisphere, Washington, D.C., 1981, pp. 569–586.
13. Pritchard, A. M., Fouling—Science or art? An investigation of fouling and antifouling measures in the British Isles, in *Fouling of Heat Transfer Equipment* (E. F. C. Somerscales, and J. G. Knudson, eds.), Proceedings of the International Conference on the Fouling of Heat Transfer Equipment, 1979, Hemisphere, Washington, D.C., 1981, pp. 513–527.
14. Knudsen, J. G., Apparatus and techniques for measurement of fouling of heat transfer surface, in *Fouling of Heat Transfer Equipment* (E. F. C. Somerscales and J. G. Knudson, eds.), Proceedings of the International Conference on the Fouling of Heat Transfer Equipment, 1979, Hemisphere, Washington, D.C., 1981, pp. 57–81.
15. Marner, W. J., and Henslee, S. P., A survey of gas side fouling measuring devices, in *Industrial Heat Exchangers Conference Proceedings* (A. J. Hayes, W. W. Liang, S. L. Richlen, and E. S. Tabb, eds.), American Society for Metals, Metals Park, OH, 1985, pp. 209–226.
16. Butterworth, D., and Mascone, C. F., Heat transfer heads into 21st century, *Chem. Eng. Prog.*, September, 30–37 (1991).
17. *Standards of Tubular Exchanger Manufacturers Association*, seventh edition, Tubular Exchanger Manufacturers Association, Inc., Tarrytown, N.Y., 1988.
18. Feltzin, A. E., Garcia, H., and Alberto, I. L., Fouling and corrosion in open recirculating cooling water systems: The expert system approach, *Mater. Perform.*, June, 57–61 (1988).
19. Kundsen, J. G., Conquer cooling-water fouling, *Chem. Eng. Prog.*, April, 42–48 (1991).
20. Epstein, N., On minimizing fouling of heat transfer surfaces, in *Low Reynolds Number Flow Heat Exchangers* (S. Kakac, R. K. Shah, and A. E. Bergles, eds.), Hemisphere, Washington, D.C., 1982, pp. 973–979.
21. Deghan, T. F., Corrosion in the chemical processing industry, in *Metals Handbook*, Vol. 13, *Corrosion*, 9th edition, American Society for Metals, Metals Park, Ohio, pp. 1134–1185.
22. Lester, G. D., and Walton, R., Cleaning of heat exchangers, in *Practical Application of Heat Transfer*, C55/82, IMechE, London, 1982, pp. 1–10.
23. Woodward, A. R., Howard, D. L., and Andrews, E. F. C., Condensers, pumps and cooling water plant, in *Modern Power Station Practice*, Vol. C, *Turbines, Generators, and Associated Plant* (D. J. Littler, E. J. Davies, H. E. Johnson, F. Kirkby, P. B. Myerscouh, and W. Wright, eds.), Pergamon Press, New York.
24. Stegelman, A. F., and Renfftlen, R., On line mechanical cleaning of heat exchangers, *Hydrocarbon Processing*, 95–97 (1983).
25. Klaren, D. G., Fluid bed heat exchangers—A new approach in severe fouling heat transfer, *Resources and Conservation*, 301–314 (1981).
26. Boffardi, P., Control of environmental variables in water-recirculating systems, in *Metals Handbook*, Vol. 13, *Corrosion*, 9th edition, American Society for Metals, Metals Park, Ohio, pp. 487–497.
27. Freedman, A. J., Cooling water technology in the 1980s, *NACE, Mater. Perform.*, November, 9–16 (1984).
28. *Condenser Tube Handbook*, Bridgeport Brass Company, U.K.
29. Kaplan, R. I., and Ekis, E. W., Jr., The on-line removal of iron deposits from cooling water systems, *NACE, Mater. Perform.*, November, 40–44 (1984).

Bibliography

1. Somerscales, E. F. C., Introduction and summary, in *Fouling of Heat Transfer Equipment* (E. F. C. Somerscales and J. G. Knudson, eds.), Proceedings of the International Conference on the Fouling of Heat Transfer Equipment, 1979, Hemisphere, Washington, D.C., 1981, pp. 1–30.

2. Characklis, W. G., Microbial fouling: A process analysis, in *Fouling of Heat Transfer Equipment* (E. F. C. Somerscales and J. G. Knudson, eds.), Proceedings of the International Conference on the Fouling of Heat Transfer Equipment, 1979, Hemisphere, Washington, D.C., 1981, pp. 251–292.
3. Gudmundsson, J. S., Particulate fouling, *Fouling of Heat Transfer Equipment* (E. F. C. Somerscales and J. G. Knudson, eds.), Proceedings of the International Conference on the Fouling of Heat Transfer Equipment, 1979, Hemisphere, Washington, D.C., 1981, pp. 357–388.
4. de Deus, J., and Pinheiro, R. S., Fouling of heat transfer surfaces, in *Heat Exchangers: Thermal-Hydraulic Fundamentals and Design* (S. Kakac, A. E. Bergles, and F. Mayinger, eds.), Hemisphere, Washington, D.C., 1981, pp. 1013–1035.
5. Suitor, J. W., Precipitation fouling, in *Fouling of Heat Transfer Equipment* (E. F. C. Somerscales and J. G. Knudson, eds.), Proceedings of the International Conference on the Fouling of Heat Transfer Equipment, 1979, Hemisphere, Washington, D.C., 1981.
6. Smith, S. A., and Dirks, J. A., Costs of heat exchanger fouling in the U.S. industrial sector, in *Industrial Heat Exchangers Conference Proceedings* (A. J. Hayes, W. W. Liang, S. L. Richlen, and E. S. Tabb, eds.), American Society for Metals, Metals Park, OH, 1985, pp. 339–344.
7. Fassbender, L. L., Industrial fouling data base development, in *Industrial Heat Exchangers Conference Proceedings* (A. J. Hayes, W. W. Liang, S. L. Richlen, and E. S. Tabb, eds.), American Society for Metals, Metals Park, OH, 1985, pp. 227–238.
8. Sheikholeslami, R., and Watkinson, A. P., Scaling of plain and externally finned heat exchanger tubes, *Trans. ASME, J. Heat Transfer, 108*, 147–152 (1986).
9. Epstein, N., Fouling models: Laminar flow, in *Low Reynolds Number Flow Heat Exchangers* (S. Kakac, R. K. Shah, and A. E. Bergles, eds.), Hemisphere, Washington, D.C., 1982, pp. 965–971.
10. Branch, C. A., and Muller-Steinhagen, H. M., Influence of scaling on the performance of shell and tube heat exchangers, *Heat Transfer Eng., 12*, 37–45 (1991).
11. Taborek, J., and Aurioles, G., Effect of 1988 TEMA standards on mechanical and thermohydraulic design of shell and tube heat exchangers, *Heat Transfer—Philadelphia*, 1989.
12. Marner, W. J., Progress in gas-side fouling of heat transfer surfaces, in *Compact Heat Exchangers—A Festschrift for A. L. London* (R. K. Shah, A. D. Kraus, and D. Metzger, eds.), Hemisphere, Washington, D.C., 1990, pp. 421–490.

CHAPTER 10

1. Wambsganss, M. W., Tube vibration and flow distributon in shell and tube heat exchangers, *Heat Transfer Eng., 8*, 62–71 (1987).
2. Paidoussis, M. P., Flow induced vibrations in nuclear reactors and heat exchangers: Practical experiences and state of knowledge, in *Practical Experiences with Flow Induced Vibration* (Nandascher and D. Rockwell, eds.), Springer-Verlag, Berlin, 1980, pp. 1–18.
3. Paidoussis, M. P., Fluid elastic vibration of cylinder arrays in axial and crossflow: State of art, *J. Sound Vibration, 76*, 329–359 (1981).
4. Au-Yang, M. K., Blevins, R. D., and Mulcahy, T. M., Flow induced vibration analysis of tube bundles—A proposed Section III Appendix N nonmadatory code, *Trans. ASME, J. Pressure Vessel Technol., 113*, 257–267 (1991).
5. Chen, S. S., Guidelines for the instability flow velocity tube arrays in crossflow, *J. Sound Vibration, 93*(3), 439–455 (1984).
6. Weaver, D. S., and Fitzpatrick, J. A., A review of flow induced vibration in heat exchangers, in *International Conference on Flow Induced Vibration*, sponsored by BHRA, Bowness-on-Windermere, England, 12–14 May, 1987, pp. 1–17.
7. Au-Yang, M. K., Flow induced vibration: Guidelines for design, diagnosis and troubleshooting of common power plant components, *Trans. ASME, J. Pressure Vessel Technol., 107*, November, 326–334 (1985).
8. Blevins, R. D., *Flow Induced Vibration*, second edition, Van Nostrand Reinhold, New York, 1990.
9. Sandifer, J. B., Guidelines for Flow Induced Vibration Prevention in Heat Exchangers, Welding Research Council Bulletin 372, Welding Research Council, New York, May 1992.

10. Chen, S. S., *Flow Induced Vibration of Circular Cylindrical Structures*, Hemisphere, New York, 1987.
11. Singh, K. P., and Soler, S. I., *Mechanical Design of Heat Exchangers and Pressure Vessel Components*, Arcturus, Cherry Hill, N.J., 1984.
12. Gupta, J. P., *Fundamentals of Heat Exchanger and Pressure Vessel Technology*, Hemisphere, Washington, D.C., 1984.
13. Zukauskas, A. A., Vibration of tubes in heat exchangers, in *High Performance Single Phase Heat Exchangers*, Hemisphere, Washington, D.C., 1989, pp. 316–348.
14. Pettigrew, M. J., and Taylor, C. E., Fluidelastic instability of heat exchanger tube bundles: Review and design recommendations, *Trans. ASME, J. Pressure Vessel Technol., 113*, 242–255 (1991).
15. Chen, S. S., and Jendrzejczyk, J. A., Stability of tube arrays in crossflow, *Nuclear Eng. Design, 75*(3), 351–374 (1983).
16. Chen, S. S., Some issues concerning fluid elastic instability of a group of circular cylinders in crossflow, *Trans. ASME, J. Pressure Vessel Technol., 111*, 507–518 (1989).
17. Shah, R. K., Flow induced vibration and noise in heat exchangers, *Proceedings of Seventh National Heat and Mass Conference*, 1983, India, pp. 89–108.
18. Chenoweth, J. M., and Kistler, R. S., Tube vibration in shell and tube heat exchangers, *AIChE Symp. Ser.*, No. 174, *Heat Transfer: Research and Application, 74*, 6–14 (1978).
19. *Standards of the Tubular Exchanger Manufacturers Association*, 7th edition, Tubular Exchanger Manufacturers Association, Inc., Tarrytown, N.Y., 1989.
20. *Boiler and Pressure Vessel Code*, Section III, Appendix N, Nonmandatory Code, American Society of Mechanical Engineers, New York, 1989.
21. Paidoussis, M. P., and Besancon, P., Dynamics of arrays of cylinders with internal and external axial flow, *J. Sound Vibration, 76*(3), 361–379 (1981).
22. Goyder, H. G. D., The structural dynamics of tube bundle vibration problem, in *International Conference on Flow Induced Vibrations*, Bowness on Windermere, England, 12–14 May, 1987.
23. Gorman, D. J., Experimental study of peripheral problems in heat exchangers and steam generator, Paper V.F4/g, *Proceedings of the Fourth International Conference on Structural Mechanics in Reactor Technology*, San Francisco, 1977.
24. Chen, Y. N., and Weber, M., Flow induced vibrations in tube bundle heat exchangers with crossflow and parallel flow, in *Flow Induced Vibrations in Heat Exchangers*, Proceedings of a Symposium Sponsored by the ASME, New York, 1970, pp. 57–77.
25. Chen, Y. N., Flow induced vibration and noise in tube bank heat exchangers due to Von Karmon streets, *Trans. ASME, J. Eng. Industry*, February, 134–146 (1968).
26. Owen, P. R., Buffeting excitation of boiler tube vibration, *J. Mech. Eng. Sci., 4*, 431–439 (1965).
27. Tinker, T., Shellside characteristics of shell and tube heat exchangers—A simplified rating system for commercial heat exchangers, *Trans. ASME*, 36–52 (1958).
28. Bell, K. J., Delaware method for shellside design, in *Heat Transfer Equipment Design* (R. K. Shah, E. C. Subbarao, and R. A. Mashelkar, eds.), Hemisphere, Washington, D.C., 1988, pp. 145–166.
29. Palen, J. W., and Taborek, J., Solution of shellside flow pressure drop and heat transfer by stream analysis method, *Chem. Eng. Prog. Symp. Ser.*, No. 92, *Heat Transfer—Philadelphia, 65*, 53–63 (1969).
30. Heat Transfer Research, Inc., Alhambra, Calif.
31. Heat Transfer and Fluid Flow Services, Oxon, UK.
32. B-JAC International, Inc., Modlothian, Va.
33. Fitz-Hugh, J. S., Flow induced vibration in heat exchangers, in *International Symposium on Vibration Problems in Industry*, Keswick, UK, 10–12 April, 1973.
34. Zukauskas, A., and Katinas, V., Flow induced vibration in heat exchanger tube banks, in *Proceedings of Symposium of Practical Experiences with Flow Induced Vibration*, 1980, pp. 188–196.
35. Weaver, D. S., Fitzpatrick, J. A., and El Kashlan, M. L., Strouhal numbers of heat exchanger tube arrays in crossflow, in *ASME Symposium on Flow Induced Vibration*, Chicago (S. S. Chen, J. C. Simonis, and Y. S. Shin, eds.), *104* (1986).
36. Pettigrew, M. J., and Gorman, D. J., Vibration of heat exchanger tube bundles in liquid and two

phase crossflow, *Flow Induced Vibration Guidelines* (P. Y. Chen, ed.), PVP Vol. 52, ASME, New York, 1981.

37. Pettigrew, M. J., and Gorman, D. J., Vibration of heat exchanger components in liquid and two phase crossflow, presented at *British Nuclear Society International Conference on Vibration in Nuclear Plant*, Keswick, UK, 9–12 May 1978.
38. Rao, M. S. M., Gupta, G. D., Eisinger, F. L., Hibbitt, H. D., and Steininger, D. A., Computer modelling of vibration and wear of multispan tubes with clearances at the supports, presented at *Flow Induced Vibration Conference*, sponsored by BHRA, Bowness-Windermere, England, 12–14 May 1987, pp. 437–448.
39. Weaver, D. S., and Grover, L. K., Crossflow induced vibration in a tube bank—Turbulent buffeting and fluid elastic instability, *J. Sound Vibration*, *59*(2), 277–294 (1978).
40. Soper, B. M. H., The effect of tube layout on the fluid elastic instability of tubes bundle in crossflow, *Trans. ASME, J. Heat Transfer*, *105*, 744–750 (1983).
41. Weaver, D. S., and Schneider, W., The effect of flat bar supports on the crossflow induced response of heat exchanger U-tubes, *Trans. ASME, J. Eng. Power*, *105* October, 775–781 (1983).
42. Connors, H. J. Jr., Fluid elastic vibration of tube arrays excitation by crossflow, in *Flow Induced Vibration in Heat Exchangers* (D. D. Reill, ed.), ASME, New York, 1970, pp. 42–56.
43. Lever, J. H., and Weaver, D. S., A theoretical model for fluid elastic instability in heat exchangers tube bundles, *Trans. ASME, J. Pressure Vessel Technol.*, *104*, 147–158 (1982).
44. Lever, J. H., and Weaver, D. S., On the stability of heat exchanger tube bundles: Part 1—Modified theoretical model, *J. Sound Vibration*, *107*(3), 375–392 (1986).
45. Lever, J. H., and Weaver, D. S., On the stability of heat exchanger tube bundles: Part 2—Numerical results and comparison with experiments, *J. Sound Vibration*, *107*(3), 393–411 (1986).
46. Tanaka, H., and Takahara, S., Fluid elastic vibration of a tube array in crossflow, *J. Sound Vibration*, *77*, 19–37 (1981).
47. Tanaka, H., and Takahara, S., Unsteady fluid dynamic force on tube bundle and its dynamic effects on vibration, in *Flow Induced Vibration of Power Plant Components*, ASME Special Publication No. PVP 141 (M. K. Au-Yang, ed.), ASME, New York, 1980, pp. 77–92.
48. Price, S. J., and Paidoussis, M. P., Fluid elastic instability of a double row of circular cylinders subject to a crossflow, *Trans. ASME, J. Vibration Acoustics Stress Reliability Design*, *105*, 59–66 (1983).
49. Price, S. J., and Paidoussis, M. P., An improved mathematical model for the stability of cylinder rows subjected to crossflow, *J. Sound Vibration*, *97*(4), 615–640 (1984).
50. Whiston, G. S., and Thomas, G. D., Whirling instabilities in heat exchanger tube arrays, *J. Sound Vibration*, *81*(1), 1–31 (1982).
51. Chen, S. S., Instability Mechanisms and Stability Criteria of a Group of Circular Cylinders Subjected to Crossflow, Part I, ASME Paper No. 81-Det 21, ASME, New York.
52. Chen, S. S., Instability Mechanisms and Stability Criteria of Group of Circular Cylinders Subjected to Crossflow, Part II: Numerical Results and Discussions, ASME Paper No. 81-Det 22, New York.
53. Chen, S. S., Instability mechanism and stability criteria of a group of cylinders subjected to crossflow, Part I: Theory; Part II: Numerical results and discussions, *J. Vibration Acoustics Stress Reliability Designs*, 253–260 (1983).
54. Chen, S. S., and Jendrzejczyk, J. A., Experiments and analysis of instability of tube rows subjected to liquid crossflow, *Trans. ASME, J. Appl. Mech.*, *49*, 704–709 (1982).
55. Chen, S. S., and Jendrzejczyk, J. A., Experiments on fluid elastic instability in tube banks subjected to liquid crossflow, *J. Sound Vibration*, *78*, 355–381.
56. Chen, S. S., Flow Induced Vibration of Circular Cylindrical Structures, Argonne National Laboratory, Report No. ANL-CT-85-51.
57. Eisinger, F. L., Prevention and cure of flow induced vibration problems in tubular heat exchangers, *Trans. ASME, J. Pressure Vessel Technol.*, *102*, 138–145 (1980).
58. Blevins, R. D., Review of sound induced by vortex shedding from cylinders, *J. Sound Vibration*, *92*(4), 455–470 (1984).

59. Blevins, R. D., Acoustic modes of heat exchanger tube bundles, *J. Sound Vibration*, *109*(1), 19–30 (1986).
60. Blevins, R. D., and Bressler, M. M., Acoustic resonance in heat exchanger tube bundles, Part I: Physical nature of the phenomenon, *Trans. ASME, J. Pressure Vessel Technol.*, *109*, 275–281 (1987).
61. Blevins, R. D., and Bressler, M. M., Acoustic resonance in heat exchanger tube bundles—Part II: Prediction and suppression of resonance, *Trans. ASME, J. Pressure Vessel Technol.*, *109*, 282–288 (1987).
62. Blevins, R. D., Acoustic Resonance in Heat Exchanger Tube Bundles, Welding Research Bulletin No. 389, Welding Research Council, New York, 1994.
63. Barrington, E. A., Experience with acoustic vibration in tubular heat exchangers, *Chem. Eng. Prog.*, *69*(7), 62–68 (1973).
64. Parker, R., Acoustic resonance in passages containing bank of heat exchanger tubes, *J. Sound Vibration*, *57*, 245–260 (1978).
65. Burton, T. E., Sound speed in a heat exchanger tube bank, *J. Sound Vibration* , *71*, 157–160 (1980).
66. Grotz, B. J., and Arnold, F. R., Flow Induced Vibration in Heat Exchangers, Department of Mechanical Engineering Tech. Rep. No. 31, DTIC No. 104568, Stanford University, Stanford, Calif., 1956.
67. Barrington, E. A., Cure exchanger acoustic vibration, *Hydrocarbon Processing*, 193–198 (1978).
68. Fitzpatrick, J. A., The prediction of flow induced noise in heat exchanger tube arrays, *J. Sound Vibration*, *99*, 425–435 (1985).
69. Ziada, S., and Oengoren, A., Flow induced acoustical resonances of in-line tube bundles, *Sulzer Tech. Rev.*, 45–47 (1990).
70. Rae, G. J., and Murray, B. G., Flow induced acoustic resonances in heat exchangers, *International Conference on Flow Induced Vibrations*, Bowness-on-Windermere, England, 12–14 May 1987, pp. 221–231.
71. Fitzpatrick, J. A., and Donaldson, J. A., Effects of scale on parameters associated with flow induced noise in tube arrays, in *Symposium on Flow Induced Vibrations* (M. P. Paidoussis, ed.), American Society of Mechanical Engineers, New York, pp. 243–250.
72. Ziada, S., Oengoren, A., and Buhlmann, E. T., Acoustical resonance in tube arrays, in *International Symposium on Flow Induced Vibration and Noise* (M. P. Paidoussis et al., eds.), American Society of Mechanical Engineers, New York, 1988, pp. 219–254.
73. Kerner Smith, H., Vibration in nuclear reactor heat exchangers—One manufacturers viewpoint, in *Flow Induced Vibration in Heat Exchangers* (D. D. Reill, ed.), *Proc. ASME*, pp. 1–7.
74. Halle, H., Chenoweth, J. M., and Wambsganss, M. W., Shellside water flow induced tube vibration in heat exchanger configurations with tube pitch to diameter ratio of 1.42, *Trans. ASME, J. Pressure Vessel Technol.*, *111*, 441–449 (1989).
75. Saunders, E. A. D., Shellside flow induced tube vibration, in *Heat Exchangers: Design, Selection and Construction*, Addison Wesley Longman, Reading, MA, pp. 245–273.
76. Halle, H., Chenoweth, J. M., and Wambsganss, M. W., Flow induced vibration in shell and tube heat exchanger with double segmental baffles, in *Heat Transfer 1986, Proc. Eighth Int. Heat Transfer Conference*, 6, 2763–2768 (1986).
77. Gentry, C. C., Young, R. K., and Small, M. W., RODbaffle heat exchanger thermal-hydraulic predictive methods, in *Heat Transfer 1982*, Vol. 6, Hemisphere, Washington, D.C., 1982, pp. 197–202.
78. Boyer, R. C., and Pase, G. K., The energy saving NESTS concept, *Heat Transfer Eng.*, *2*, 19–27 (1980).
79. Byrne, K. P., The use of porous baffles to control acoustic vibration in crossflow tubular heat exchangers, *Trans. ASME, J. Heat Transfer*, *105*, 751–757 (1983).
80. Walker, E. M., and Reising, G. F. S., Flow induced vibrations in crossflow heat exchangers, *Chem. Process Eng.*, *49*, 95–103 (1968).
81. Rogers, J. D., and Penterson, C. A., Predicting Sonic Vibration in Crossflow Heat Exchangers—Ex-

perience and Model Testing, American Society of Mechanical Engineers, New York, Paper 77-FE-7, 1977.
82. Zdravkovich, M., and Nuttal, J. A., On elimination of aerodynamic noise in staggered tube bank, *J. Sound Vibration, 34*, 173–177 (1974).
83. Thorngren, J. T., Predict exchanger tube damage, *Hydrocarbon Processing*, April, 129–131 (1970).
84. Blevins, R. D., Fretting wear of heat exchanger tubes, Part I: Experiments, *Trans. ASME, J. Eng. Power, 101*, 625–629 (1979).
85. Blevins, R. D., Fretting wear of heat exchanger tubes, Part II: Models, *Trans. ASME, J. Eng. Power, 101*, 630–633 (1979).
86. Haslinger, K. H., Martin, M. L., and Steininger, D. A., Pressurized water reactor steam generator tube wear prediction utilizing experimental techniques, in *Proceedings of the International Conference on Flow Induced Vibration*, Bowness-on-Winderemere, England, 12–14 May 1987, pp. 437–448.
87. Ko, P. L., and Basista, H., Correlation of support impact force and fretting wear for heat exchanger tube, *Trans. ASME, J. Pressure Vessel Technol., 106*, 69–77 (1984).
88. Cha, J. H., Wambsganss, M. W., and Jendrzejcyk, J. A., Experimental Study of Impact/Fretting Wear in Heat Exchanger Tubes, Argonne National Laboratory Publication ANL-85-38, 1985.
89. Hofmann, P. J., Schettler, T., and Steininger, D. A., Pressurized water reactor steam generator tube fretting and fatigue wear characteristics, in *Proceedings of the ASME Pressure Vessel and Piping Conference*, ASME 86PVP-2, Chicago, July 1986.
90. Fisher, N. J., Olsen, M., Rogers, R. J., and Ko, P. L., Simulation of tube-to-support dynamic interaction of heat exchange equipment, *Trans. ASME, J. Pressure Vessel Technol., 111*, 378–384 (1989).
91. Eisinger, F. L., Rao, M. S. M., Steininger, D. A., and Haslinger, K. H., Numerical simulation of fluid elastic vibration and comparison with experimental results, in *Flow Induced Vibration and Wear Book* No. H00632, 1991, pp. 101–111. Reprinted from PVP Vol. 206.
92. Rao, M. S. M., Steininger, D. A., Eisinger, F. L., Computer simulation of vibration and wear of steam generator and tubular heat exchanger tubes, in *International Symposium on Advanced Computers for Dynamics and Design '89*, Tsuchiura, Japan, Mechanical Division, JSME. 6–8 September 1989.
93. Rao, M. S. M., Steininger, D. A., and Eisinger, F. L., Numerical simulation of fluid elastic vibration and wear of multispan tubes with clearances at supports, in *Flow Induced Vibration in Heat Transfer Equipment*, Vol. 5, Book No. G00445 (J. M. Paidoussis, S. S. Chenoweth, J. R. Chen, Stenner, and Bryan, W. J., eds.).
94. Blevins, R. D., Vibration induced wear of heat exchanger tubes, *Trans. ASME, J. Eng. Mater. Technol., 107*, 61–67 (1985).
95. Moretti, P. M., and Lowery, R. L., Hydrodynamic inertia coefficients for a tube surrounded by rigid tube, *Trans. ASME, J. Pressure Vessel Technol.*, 190–193 (1976).
96. Timoshenko, S. P., and Young, D. H., Vibration problems in engineering, in *Vibration of Elastic Bodies*, Van Nostrand Reinhold, Toronto, 1965, Chapter 5.
97. ABAQUS, Version 4-7, Hibbits, Karlsson and Sorensen, Inc.
98. Pettigrew, M. J., Goyder, H. G. D., Qiao, Z. L., and Axisa, F., Damping of multispan heat exchanger tubes, Part 1: In gases, in *Flow Induced Vibration 1986* (S. S. Chen, J. C. Simon, and Y. S. Shin, eds.), ASME PVP Vol. 104, ASME, New York, 1986, pp. 81–87.
99. Pettigrew, M. J., Rogers, R. J., and Axisa, F., Damping of multispan heat exchanger tubes, Part 2: In liquids, in *Flow Induced Vibration 1986* (S. S. Chen, J. C. Simon, and Y. S. Shin, eds.), ASME, New York, PVP Vol. 104, pp. 89–98.

Suggested Readings

1. Lowery, R. L., and Moretti, P. M., Natural frequencies and damping of tubes on multiple supports, *AIChE Symp. Ser.*, No. 174, *Heat Transfer: Research and Application, 74*, 1–5 (1978).
2. Gorman, D. J., *Free Vibration Analysis of Beam and Shafts*, John Wiley & Sons, New York, 1975.
3. MacDuff, J. N., and Felgar, R. P., Vibration design charts, *Trans. ASME*, 1459–1474 (1957).

4. Bolleter, U., and Blevins, R. D., Natural frequencies of finned heat exchanger tubes, *J. Sound Vibration, 80*, 367–371 (1982).
5. Moretti, P. M., Fundamental frequencies of U-tubes in tube bundles, *Trans. ASME, J. Pressure Vessel Technol., 107*, 207–209 (1985).
6. Naguyen, D. C., Lester, T., Good, J. K., Lowery, R. L., and Moretti, P. M., Lowest natural frequencies of multiply supported U-tubes, *Trans. ASME, J. Pressure Vessel Technol., 106*, 414–416 (1984).
7. Sing, K. P., and Soler, A. I., *HEXDES User Manual*, Arcturus, Cherry Hill, N.J., 1984.
8. Chenoweth, J. M., Flow induced vibration phenomena, in *Heat Exchanger Design Handbook* (E. U. Schlunder, editor-in-chief), Vol. 4, Hemisphere, Washington, D.C., 1983, Section 4.6.4.

CHAPTER 11

1a. Hirschfeld, F., Codes, standards and certificate of authorization program: Part 1—Establishing safety standards, *Mech. Eng.*, January, 33–39 (1979).
1b. Hirschfeld, F., Codes, standards and certificate of authorization program: Part 2—Policies, programs and organization, *Mech. Eng.*, February, 31–37 (1979).
2. Statement of the Council on Codes and Standards of the American Society of Mechanical Engineers on the Federal Role in International Standards, *Trans. ASME, J. Pressure Vessel Technol., 112*, 425–426 (1990).
3. *Standards of the Tubular Exchanger Manufacturers Association*, 7th edition, Tubular Exchanger Manufacturers Association, Inc., Tarrytown, N.Y., 1988.
4. *Standards for Surface Condensers*, eighth edition, Heat Exchange Institute, Cleveland, Ohio, 1984.
5. *Standards for Power Plant Heat Exchangers*, Heat Exchange Institute, Cleveland, Ohio, 1984.
6. *Standards for Closed Feedwater Heaters*, Heat Exchange Institute, Cleveland, Ohio, 1984.
7. *Shell and Tube Exchangers for General Refinery Services, API Standard 660*, 4th edition, American Petroleum Institute, Washington, D.C., September 1982.
8. *Standards of the Expansion Joint Manufacturers Association*, fifth edition, 1980, Tarrytown, N.Y.
9. *British Standards (BSI)*, BSI Publications at Linford Wood, Milton Keynes, UK, 1993.
10. *Japanese Industrial Standards*, 1993.
11. *DIN, German Industrial Standards*, Beuth, Beuth Verlg GmbH, Berlin.
12. *International Organisation for Standardization* (ISO), 1993.
13. Taborek, J., and Aurioles, G., Effect of 1988 TEMA standards on mechanical and thermohydraulic design of shell and tube heat exchangers, in *Heat Transfer—Philadelphia*, 1989.
14. Gupta, J. P., *Fundamentals of Heat Exchanger and Pressure Vessel Technology*, Hemisphere, Washington, D.C., 1986.
15. Codes, standards and the ASME: Part 3—Standards, safety standards, *Mech. Eng.*, August, 24–25 (1972).
16. *ASME Boiler and Pressure Vessel Code, Section VIII, Division 1—Pressure Vessels*, American Society of Mechanical Engineers, New York, 1992.
17. *ASME Boiler and Pressure Vessel Code, Section VIII, Division 2, Pressure Vessels—Alternative Rules*, American Society of Mechanical Engineers, New York, 1992.
18. *British Standard Specification for Fusion Welded Pressure Vessels*, BS 5500, 1991.
19. *CODAP, French Code for the Construction of Unfired Pressure Vessels*, edited by SNCT, Paris, France, 1985.
20. Merkblatter, A. D., *German Pressure Vessel Code*, Carl Heymans Verlag KG, Koln, Germany.
21. *ASME Boiler and Pressure Vessel Code, Section III, Div. 1 & 2, Rules for Construction of Nuclear Power Plant Components*, American Society of Mechanical Engineers, New York, 1992.
22. SNCT, Syndicat National de la Chaudronnerie-Tolerie, National Association for Pressure Vessels.
23. *ANCC Italian Code*, Milan, Italy.
24. *Stoomwenzen (Dutch Code), Rules for Pressure Vessels*, Tryckkarskomissionnen IVA, Stockholm, Sweden.
25. *ISO/DIS 2694, Pressure Vessels*, 1973.

26. *IS: 2825–1969, Code for Unfired Pressure Vessels*, Bureau of Indian Standards, Manak Bhavan, New Delhi, India.
26. *The Pressure Vessel Code (Dai Isshu Atsuryoku Youki Kousou Kikahu)*, Ministry of Labour, Japan Boiler Association, Tokyo.
28. *Regels Voor Toesellen onder Druck*, Ministry of Social Affairs, Dienst voor het Stoomwesen, Government Printing Office, The Hague, The Netherlands.
29. Yokell, S., *A Working Guide to Shell and Tube Heat Exchangers*, McGraw-Hill, New York, 1990.
30. Cepluch, R. J., The ASME Boiler and Pressure Vessel Code Committee—Challenges: Past and future, *Trans. ASME, J. Pressure Vessel Technol., 112*, 319–322 (1990).
31. Blackall, F. S., Jr., ASME standards save lives and dollars, *Mech. Eng.*, December, 979–981 (1953).
32. Nichols, R. W., ed., *Pressure Vessel Codes and Standards: Developments in Pressure Vessel Technology—5*, Elsevier Applied Science, London, 1987.

33a. Codes, standards and the ASME: Part 1—Codes, *Mech. Eng.*, June, 24–25 (1972).
33b. Codes, standards and the ASME: Part 2—ASME boiler and pressure vessel codes, *Mech. Eng.*, July, 16–18 (1972).
33c. Codes, standards and the ASME: Part 4—International Standardization Committee, *Mech. Eng.*, September, 20–24 (1972).

34. Schlunder, E. U., editor-in-chief, Mechanical design codes, in *Heat Exchanger Design Handbook*, Vol. 4, Hemisphere, Washington, D.C., 1983, Section 4.1.6.
35. Mase, J. R., and Smolen, A. M., ASME pressure vessel code: Which division to choose, *Chem. Eng.*, January, 133–136 (1982).
36. Farr, J. R., The ASME boiler and pressure vessel code: Section VIII—Pressure vessels, in *Pressure Vessel Codes and Standards, Developments in Pressure Vessel Technology—5* (R. W. Nichols, ed.), Elsevier Applied Science, London, 1987, pp. 35–58.
37. Farr, J. R., The ASME boiler and pressure vessel code: Overview, in *Pressure Vessel Codes and Standards, Developments in Pressure Vessel Technology—5* (R. W. Nichols, ed.), Elsevier Applied Science, 1987, London, pp. 1–34.
38. Houston, R., British Standards Institution boiler and pressure vessel design criteria, in *Pressure Vessel Codes and Standards, Developments in Pressure Vessel Technology—5* (R. W. Nichols, ed.), Elsevier Applied Science, London, 1987, pp. 105–158.
39. Thomas, A., and Grandemange, J. M., French codes and standards on boiler and pressure vessel technology, in *Pressure Vessel Codes and Standards, Developments in Pressure Vessel Technology—5* (R. W. Nichols, ed.), Elsevier Applied Science, London, 1987, pp. 175–222.
40. Hohne, K. J., German boiler and pressure vessel codes and standards: Design aspects, in *Pressure Vessel Codes and Standards, Developments in Pressure Vessel Technology—5* (R. W. Nichols, ed.), Elsevier Applied Science, London, 1987, pp. 249–282.
41. Singh, K. P., and Soler, A. I., *Mechanical Design of Heat Exchangers and Pressure Vessel Components*, Arcturus, Cherry Hill, N.J., 1984.

42a. Escoe, K. A., *Mechanical Design of Process Systems*, Vol. 2—*Shell and Tube Heat Exchangers, Rotating Equipment, Bins, Silos, Stacks*, Gulf Publishing Company, Book Division, Houston.
42b. Escoe, K. A., *Mechanical Design of Process Systems*, Vol. 1, *The Engineering Mechanics of Pressure Vessels*, Gulf Publishing Company, Book Division, Houston, 19xx, Chapter 4.

43. Moss, D. R., *Pressure Vessel Design Manual*, Gulf Publishing Company, Book Division, Houston.
44. Brownell, L. E., and Young, E. H., *Process Equipment Design*, John Wiley & Sons, New York, 1968.
45. Bednar, H. H., *Pressure Vessel Design Handbook*, Von Nostrand Reinhold, New York, 1981.
46. Harvey, J. F., *Pressure Component Construction*, Von Nostrand Reinhold, 1980, New York.
47. Chuse, R., *Pressure Vessels—The ASME Code Simplified*, sixth edition, McGraw-Hill, New York, 1984.
48. Roach, G. H., Wood, R. M., Shell and tube exchangers having improved design features, *Heat Transfer Eng., 7*, 19–23 (1986).
49. Soler, A. I., Expert system for design integration—Application to the total design of shell and tube heat exchangers, in *Proceedings of the ASME, Thermal/Mechanical Heat Exchanger Design, Karl*

Gardner Memorial Session (K. P. Singh and S. M. Shenkman, eds.), ASME PVP. Vol. 118, 1985, pp. 135–138.

50. Singh, K. P., Mechanical design of tubular heat exchangers—An appraisal of the state-of-the-art, in *Heat Transfer Equipment Design* (R. K. Shah, C. Subbarao, and R. M. Mashelekar, eds.), Hemisphere, Washington, D.C., 1988, pp. 71–87.
51. Gardner, K. A., Heat exchanger tubesheet design, *Trans. ASME, J. Appl. Mech., 70A*, 377–385 (1948).

52a. Gardner, K. A., Heat exchanger tubesheet design—2, Fixed tubesheets, *Trans. ASME, J. Appl. Mech., 74*, 159–166 (1952).

52b. Gardner, K. A., Heat exchanger tubesheet design—3, U-tube and bayonet tubesheets, *Trans. ASME, J. Appl. Mech., Ser. E., 82*, 25–33 (1960).

53. Miller, K. A. G., The design of tube plates in heat exchangers, *Proceedings of Institution of Mechanical Engineers, Sect. B, 1*, 672–688 (1952–1953).
54. Yu, Y. Y., Rational analysis of heat exchanger tubesheet stresses, *Trans. ASME, J. Appl. Mech., 78*, 468–473 (1956).
55. Galletly, G. D., and Garbett, C. R., Pressure vessels—Let the tubes support the tubesheet, *Ind. Eng. Chem., 50*, 1227–1230 (1958).
56. Galletly, G. D., Optimum design of thin circular plates on an elastic foundation, in *Proceedings of the Institution of the Mechanical Engineers*, IMechE, London, 173, 1959, pp. 689–698.
57. Boon, G. B., and Walsh, R. A., Fixed tubesheet heat exchangers, *Trans. ASME, J. Appl. Mech.*, 175–180 (1964).
58. Gardner, K. A., Tubesheet design: A basis for standardization, in *Proceedings of the First International Conference on Pressure Vessel Technology: Part I, Design and Analysis*, 1969, pp. 621–668.
59. Chiang, C. C., Closed Form Design Solutions for Box Type Heat Exchangers, ASME publication 75-WA/DE, 1975.
60. Hayashi, K., An analysis procedure for fixed tubesheet exchangers, in *Proceedings of the Third International Conference on Pressure Vessel Technology: Part I, Analysis, Design and Inspection*, 1977, pp. 363–373.
61. Malek, R. G., A new approach to exchanger tubesheet design, *Hydrocarbon Processing*, 165–169 (1977).
62. Singh, K. P., Analysis of vertically mounted through tube heat exchangers, *Trans. ASME, J. Eng. Power, 100*, 380–390 (1978).
63. Soler, A. I., and Soehrens, J. E. Design curves for stress analysis of U-tube heat exchanger tubesheet with integral channel and head, *Trans. ASME, J. Pressure Vessel Technol., 100*, 221–232 (1978).
64. Soehrens, J. E., Tubesheet thicknesses and tube loads for floating head and fixed-tubesheet heat exchangers, *ASME J. Pressure Vessel Technol., 106*, 289–299 (1984).
65. Cascales, D. H., and Militello, C., Tubesheet thicknesses and tube loads for fixed tubesheet heat exchangers [Letter to the editor], *Trans. ASME, J. Pressure Vessel Technol., 107*, 318–323 (1985).
66. Singh, K. P., and Soler, A. I., An elastic-plastic analysis of the integral tubesheet in U-tube heat exchangers—Towards an ASME code oriented approach, *ASME Proc. of the 1985 PVP Conference*, New Orleans, *98*, 39–51 (1985).
67. Soler, A. I., Caldwell, S. M., and Singh, K. P., Tubesheet analysis—A proposed ASME design procedure, in *Proceedings of the ASME, Thermal/Mechanical Heat Exchanger Design—Karl Gardner Memorial Session* (K. P. Singh and S. M. Shenkman, eds.), ASME PVP. Vol. 118, ASME, New York, 1985, pp. 93–101.
68. Soehrens, J. E., Stress analysis of heat exchangers, in *Proceedings of the ASME, PVP Vol. 118, Thermal/Mechanical Heat Exchanger Design—Karl Gardner Memorial Session* (K. P. Singh and S. M. Shenkman, eds.), ASME PVP Vol. 118, New York, 1985, pp. 79–91.
69. Osweiller, F., *Methode de calcul des exchangers a deux ictes fixés le CODAP*, Etude CETIM, No. 14B031, 1986.
70. Osweiller, F., Analysis of TEMA tubesheet design rules—Comparison with up to date code methods, in *Proceedings of the 1986 Pressure Vessel and Piping Conference*, Chicago, *107* (1986).

71. Cascales, D. H., and Militello, C., A model for fixed tubesheet heat exchanger, *Trans. ASME, J. Pressure Vessel Technology, 109*, 289–296 (1987).
72 Paliwal, D. N., Design of fixed tubesheet for heat exchangers, *Trans. ASME, J. Pressure Vessel Technol., 111*, 79–85 (1989).
73. Osweiller, F., Basis of the tubesheet heat exchanger design rules used in the French pressure vessel code, *Trans. ASME, J. Pressure Vessel Technol., 114*, 124–131 (1992).
74. Singh, K. P., and Marks, P., Proposed extension of the TEMA tubesheet design method to determine tubesheet rim thickness, in *Proceedings of the ASME, Thermal/Mechanical Heat Exchanger Design—Karl Gardner Memorial Session* (K. P. Singh and S. M. Shenkman, eds.), ASME PVP. Vol. 118, ASME, New York, 1985, pp. 111–119.
75. Kuppan, T., Alternate design charts for fixed tubesheet design procedure included in ASME boiler and pressure vessel code, Section VIII, Div. 1, *Trans. ASME, J. Pressure Vessel Technol., 117*, 189–194 (1995).
76. O'Donnell, W. J., and Langer, B. F., Design of perforated plates, *ASME J. Eng. Ind., 84*, 307–320 (1962).
77. Osweiller, F., Evolution and synthesis of the effective elastic constants concept for the design of tubesheets, *Trans. ASME, J. Pressure Vessel Technol., 111*, 209–217 (1989).
78. Bernstein, M. D., and Soler, A. I., The tubesheet analysis method in the new HEI condenser standards, *Trans. ASME, J. Eng. Power, 100*, 363–368 (1978).
79. Rachkov, V. I., and Morozov, V. H., Designing curved tube plates, *Khim-i-reft. Masb*, 7 14 (1968).
80. Paliwal, D. N., and Sinha, S. N., Design of shallow spherical curved tubesheet for heat exchangers, *Int. J. Pressure Vessels Piping, 17*, 185–192 (1984).
81. Sang, Z.-F., and Widera, G. E. O., Stress analysis of elliptical tube plates in heat exchangers, *Trans. ASME, J. Pressure Vessel Technol., 109*, 310–314 (1987).
82. Waters, E. O., Wesstrom, D. B., and Williams, F. S. G., Design of bolted flanged connections, in *Pressure Vessel and Piping Design, Collected Papers 1927–1959*, American Society of Mechanical Engineers, New York, 1960, pp. 58–61.
83. Bickford, J. H., Gasketed joints and leaks, in *An Introduction to the Design and Behavior of Bolted Joints*, second edition, Marcel Dekker, New York, 1990, pp. 495–548.
84. *Modern Flange Design*, 7th edition, Bull. 502, Taylor Forge International, Chicago.
85. Lake, G. F., and Boyd, G., Design of bolted, flanged joints of pressure vessels, in *Proceedings of Institution of Mechanical Engineers, 171*, 843–858 (1957).
86. Derenne, M., Marchand, L., Payne, J. R., and Bazergui, A., Elevated Temperature Testing of Gaskets for Bolted Flanged Connections, WRC Bull. 391.
87. Singh, K. P., Study of bolted joint integrity and inter-tube pass leakage in U-tube heat exchangers—Part I: analysis, *Trans. ASME, J. Eng. Power, 101*, 9–15 (1979).
88. Singh, K. P., Study of bolted joint integrity and inter-tube pass leakage in U-tube heat exchangers—Part II: Analysis, *Trans. ASME, J. Eng. Power, 101*, 16–22 (1979).
89. PVRC News, *Trans. ASME, J. Pressure Vessel Technol., 114*, 385–387 (1992).
90. Wolf, L. J., and Mains, R. M., The stress analysis of heat exchanger expansion joints in the elastic range, *Trans. ASME, J. Eng. Ind.*, 145–150 (1973).
91. Singh, K. P., A rational procedure for analyzing flanged and flued expansion joints, *Trans. ASME, J. Pressure Vessel Technol., 113*, 64–70 (1991).
92. Kopp, S., and Sayre, M. F., Expansion joints for heat exchangers, in *ASME Winter Annual Meeting*, New York, 1952.
93. Morishita, M., Ikahata, N., and Kitamura, S., Simplified dynamic analysis methods for metallic bellows expansion joints, *Trans. ASME, J. Pressure Vessel Technol., 113*, 504–510 (1991).
94. Sattler, F. J., Forrer, G. R., and Parker, W. O., Jr., Inservice inspection of nuclear plants, *Mater. Eval.*, November, 18A–22A, 27A–29A (1972).
95. Schoessow, G. J., and Brooks, E., Analysis of experimental data regarding certain design features of pressure, in *Pressure Vessel and Piping Design, Collected Papers 1927–1959*, American Society of Mechanical Engineers, New York, 1960, pp. 24–34.

96. Spencer, T. C., Mechanical design and fabrication of exchangers in the United States, *Heat Transfer Eng.*, *8*, 58–61 (1987).
97. Zick, L. P., Stresses in large horizontal cylindrical pressure vessels on two saddle supports, in *Pressure Vessel and Piping: Design and Analysis*, ASME, New York, 1972.

CHAPTER 12

1. Munger, G. C., Corrosion as related to coatings, in *Corrosion Prevention by Protective Coatings*, National Association of Corrosion Engineers, Houston, 1984, pp. 19–46.
2. Uhlig, H. H., Environmental effects on properties of materials, *Mater. Protect. Perform.*, July, 23–27 (1972).
3. *Resistance to Corrosion*, 4th edition, Inco Alloys International, W. Va., 1985.
4. Jarman, R. A., and Shreir, L. L., The basic principles of corrosion, in *Welding & Metal Fabrication*, October, 370–379 (1987).
5. *Corrosion Tests and Standards—Application and Interpretation* (R. Baboian, ed.), ASTM, New York, 1995.
6. Brosilow, R., Can you weld to avoid corrosion, *Welding Design & Fabrication*, September, 67–74 (1982).
7. Roser, W. R., and Rizzo, F. E., The corrosion engineer's look at passive alloys, *Mater. Protect. Perform.*, April, 51–54 (1973).
8. Silverstein, M. R., Cooling water, *Chem. Eng.*, August, 84–94 (1971).
9. Fontana, M. G., and Greene, N. D., *Corrosion Engineering*, 2nd edition, McGraw-Hill, New York, 1978.
10. Uhlig, H. H., *Corrosion and Corrosion Control*, John Wiley & Son, Inc., New York, 1963.
11. Atmospheric corrosion, in *Corrosion Basics—An Introduction*, NACE, Houston, 1984, pp. 221–222.
12. Merrick, R. D., Design of pressure vessels and tanks to minimize corrosion, *Mater. Perform.*, January, 29–37 (1987).
13. *AL-6XN® Alloy*, Allegheny Ludlum Allegheny Ludlum Steel Corporation, Pittsburgh, Pa.
14. Kobrin, G., Materials selection, in *Metals Handbook*, Vol. 13, *Corrosion*, 9th edition, American Society for Metals, Metals Park, Ohio, 1987, pp. 321–337.
15. Elliott, P., Design details to minimize corrosion, in *Metals Handbook*, Vol. 13, *Corrosion*, 9th edition, American Society for Metals, Metals Park, Ohio, 1987, pp. 338–343.
16. Freedman, A. J., and Boies, D. B., Causes and cures for cooling water corrosion problems, *Petroleum Refiner*, April, 157–162 (1961).
17. Stanfield, B. M., Polarization cell: A common cure for corrosion, *Mater. Protect. Perform.*, March, 32–35 (1973).
18. Steven, P. L., General corrosion, in *Metals Handbook*, Vol. 13, *Corrosion*, 9th edition, American Society for Metals, Metals Park, Ohio, 1987, pp. 80–103.
19. Open pitting corrosion, in *Corrosion Basics—An Introduction*, NACE, Houston, 1984, p. 95.
20. *Brown Bowri Symposium on Corrosion in Power Generating Equipment* (M. O. Speidel and A. Atrens, eds.), Plenum Press, New York, 1983.
21. Lichtenstein, J., Fundamentals of corrosion causes and mitigation, *Mater. Perform.*, March, 29–31 (1978).
22. Wilten, H. M., Microscope speeds diagnosis of refinery corrosion, *Hydrocarbon Processing & Petroleum Refiner*, *40*, 151–280 (1961).
23. Asphahani, I. A., Corrosion resistance of high performance alloys, *Mater. Perform.*, *19*, 33–43 (1980).
24. Uhlig, H. H., Discussion—An essay on pitting, crevice corrosion, and related potentials, *Mater. Perform.*, August, 35–36 (1983).
25. Dexter, C. S., Localized corrosion, in *Metals Handbook*, Vol. 13, *Corrosion*, 9th edition, American Society for Metals, Metals Park, Ohio, 1987, pp. 104–122.

26. Syrett, B. C., and Coit, R. L., Causes and prevention of power plant condenser tube failures, *Mater. Perform.*, February, 44–49 (1983).
27. Jarman, R. A., and Shreir, L. L., Corrosion of jointed structures—Part II, *Welding & Metal Fabrication*, 445–449 (1987).
28. Henthorne, M., Understanding corrosion, *Chem. Eng.*, Desk Book Issue, 4 December, 19–33 (1972).
29. Guide to selecting engineered materials, metals, polymers, ceramics, composites, *Adv. Mater. Processes*, *137*(6), (1990).
30. Stengerwald, R., Metallurgically influenced corrosion, in *Metals Handbook*, Vol. 13, *Corrosion*, 9th edition, American Society for Metals, Metals Park, Ohio, 1987, pp. 123–135.
31. *Condenser Tube Handbook*, Bridgeport Brass Company, UK.
32. Forchhammer, P., Results of damage research on corrosion failures in heat exchangers, *Heat Transfer Eng.*, *5*, 19–32 (1984).
33. Woodward, A. R., Howard, D. L., and Andrews, E. F. C., Condensers, pumps and cooling water plant, in *Modern Power Station Practice*, Vol. C, *Turbines, Generators, and Associated Plant* (D. J. Littler, E. J. Davies, H. E. Johnson, F. Kirkby, P. B. Myerscouh, and W. Wright, eds.), Pergamon Press, New York.
34. Crook, P., Practical guide to wear for corrosion engineers, *Mater. Perform.*, February, 64–66 (1991).
35. Erosion-corrosion, in *Corrosion Basics—An Introduction*, NACE, Houston, 1984.
36. Yokell, S., *A Working Guide to Shell and Tube Heat Exchangers*, McGraw-Hill, New York, 1990.
37. *Standards of Tubular Exchanger Manufacturers Association*, seventh edition, Tubular Exchanger Manufacturers Association, Inc., Tarrytown, N.Y., 1988.
38. Cavitation, in *Corrosion Basics—An Introduction*, NACE, Houston, 1984.
39. Dawson, J. L., Shih, C. C., Gearey, D., and Miller, R. G., Flow effects on erosion-corrosion, *Mater. Perform.*, April, 57–60 (1991).
40. Dawson, J. L., and Shih, C. C., Corrosion under flowing conditions–An overview and model, *CORROSION/90*, Paper No. 21, Houston, 1990.
41. Syrett, B. C., Corrosion in fossil fuel power plants, in *Metals Handbook*, Vol. 13, *Corrosion*, 9th edition, American Society for Metals, Metals Park, Ohio, 1987, pp. 985–1010.
42. Theus, G. J., and Daniel, P. L., Corrosion in steam generating systems, in *Brown Bowri Symposium on Corrosion in Power Generating Equipment* (M. O. Speidel and A. Atrens, eds.), Plenum Press, New York, 1983, pp. 185–231.
43. Product Literature, M/s, Expando Seal Tools, Inc., Montgomeryville, Pa.
44. Irving, B., Stress corrosion cracking: Welding's no. 1 nemesis, *Welding J.* December, 37–40 (1992).
45. Kedzie, D. P., and Rizzo, F. E. , The corrosion engineer's look at stress corrosion, *Mater. Protect. Perform.*, October, 53–56 (1972).
46. Logan, H. L., *The Stress Corrosion Cracking of Metals*, John Wiley & Sons, New York, 1966.
47. McIntyre, D. R., and Dillon, C. P., Guidelines for Preventing Stress Corrosion Cracking in the Chemical Process Industries, Publication 15, Materials Technology Institute, 1985, pp. 8–14.
48. Berry, W. E., Stress Corrosion Cracking—A Nontechnical Introduction to the Problem, Defence Metals Information Centre, Battelle Memorial Institute, Columbus, Ohio, DMIC Report 144, 6 January, 1961.
49. Pement, F. W., Wilson, I. L. W., Reynolds, S. D., and Fletcher, W. D., Microanalytical characterization of stress corrosion cracking in power plant heat exchanger tubing, *Mater. Perform.*, 26–39 (1977).
50. Craig, B., Environmentally induced cracking, in *Metals Handbook*, Vol. 13, *Corrosion*, 9th edition, American Society for Metals, Metals Park, Ohio, 1987, pp. 145–149.
51. Brown, B. F., Stress Corrosion Cracking in High Strength Steels and in Titanium and Aluminum Alloys, Naval Research Laboratory, Washington, D.C., 1972.
52. Parkins, R. N., An overview: prevention and control of stress corrosion cracking, *Materials Performance*, *NACE*, August 1985, pp. 9–20.

53. McIntyre, D. R., How to prevent stress corrosion cracking in stainless steels—Part I, in *The Chemical Engineering Guide to Corrosion Control in the Process Industries*, (Edr.) R. W. Greene, McGraw-Hill Publications Co., New York, 1986, pp. 4–7.
54. Partridge, E. P., Hydrogen damage in power boilers, *Trans. ASME, J. Eng. Power*, July, 311–320 (1964).
55. Glaser, W., and Wright, I. G., Forms of corrosion—Mechanically assisted degradation, in *Metals Handbook*, Vol. 13, *Corrosion*, 9th edition, American Society for Metals, Metals Park, Ohio, 1987, pp. 136–144.
56. Corrosion fatigue, in *Corrosion Basics—An Introduction*, NACE, Houston, 1984.
57. Tatnall, R. E., MIC: A corrosion engineer's enigma?, *Mater. Perform.*, August, 56 (1988).
58. Pollock, W. I., What is MIC?, *Mater. Perform.*, August, 56, (1988).
59. Scott, P. J., B., Goldie, J., and Davies, M., Ranking alloys for susceptibility to MIC—A preliminary report on high-Mo alloys, *Mater. Perform.*, January, 55–57 (1991).
60. Kobrin, G., Corrosion by microbiological organisms in natural waters, *Mater. Perform*, July, 38–42 (1976).
61. Pope, D. H., Duquette, D. J., Arland, J. H., and Wayner, P. C., Microbiologically influenced corrosion of industrial alloys, *Mater. Perform.*, April, 14–18 (1984).
62. Pope, D. H., Soracco, R. J., and Wilde, E. W., Studies on biologically induced corrosion in heat exchanger system at the Savannah River Plant, Aiken, SC., *Mater. Perform.*, July, 43–50 (1982).
63. Borenstein, S. W., Microbiologically influenced corrosion of austenitic stainless steel weldments, *Mater. Perform.*, January, 52–54 (1991).
64. Borenstein, S. W., Microbiologically influenced corrosion failures of austenitic stainless steel welds, *Mater. Perform.*, August, 62–66 (1988).
65. Puckorius, P. R., Massive utility condenser failure caused by sulfide producing bacteria, *Mater. Perform.*, December, 19–22 (1983).
66. Tuthill, A. H., Guidelines for the use of copper alloys in seawater, *Mater. Perform.*, September, 12–22 (1987).
67. Booth, G. H., and Mercer, S. T., *Nature (Lond.)*, *199*, 162 (1962).
68. Schutz, R. W., A case for titanium's resistance to microbiologically influenced corrosion, *Mater. Perform.*, January, 58–61 (1991).
69. Boffardi, P., Control of environmental variables in water-recirculating systems, *Metals Handbook*, Vol. 13, *Corrosion*, 9th edition, American Society for Metals, Metals Park, Ohio, 1987, pp. 487–497.
70. Poole, J. S., and Bacon, H. E., Monitoring cooling water systems, *Mater. Protect. Perform.*, March, 16–25 (1972).
71. Borenstien, S. W., and Lindsay, P. B., Microbiologically influenced corrosion failure analyses, *Mater. Perform.*, March, 51–54 (1988).
72. Gooch, T. G., Stress corrosion cracking of welded austenitic stainless steel, *Welding in the Word*, *22*, 64–76 (1984).
73. Corrosion of weldments, in *Metals Handbook*, Vol. 13, *Corrosion*, 9th edition, American Society for Metals, Metals Park, Ohio, 1987, pp. 344–368.
74. Swindeman, R. W., and Gold, M., Developments in ferrous alloy technology for high-temperature service, *Trans. ASME, J. Pressure Vessel Technol.*, *113*, 133–140 (1991).
75. Collins, J. A., Effect of design, fabrication and installation in the performance of stainless steel equipment, *Corrosion*, January (1955).
76. Landrum, J. R., Designing equipment for corrosion resistance, in *Materials Engineering, Part I: Selecting Materials for Process Equipment* (K. J. McNaughton, ed.), McGraw-Hill, New York, 1980, pp. 157–164.
77. Shabin, H. I., Corrosion inhibition in a cooling water system, *Corrosion Prevent. Control*, February, 9–12 (1982).
78. Inhibitors, in *Corrosion Basics—An Introduction*, NACE, Houston, 1984, p. 127.
79. Freedman, A. J., Cooling water technology in the 1980s, *Mater. Perform.*, November, 9–16 (1984).

80. Kaplan, R. I., and Ekis, E. W., Jr., The on-line removal of iron deposits from cooling water systems, *Mater. Perform.*, November, 40–44 (1984).
81. Boffardi, B. P., Corrosion control of industrial cooling water systems, *Mater. Perform.*, November, 17–24 (1984).
82. Beynon, E., Cooper, N. R., and Haningan, H. J., Cooling system corrosion in relation to design and materials, in *Engine Coolant Testing: State of the Art, ASTM STP 705* (W. H. Ailor, ed.), American Society for Testing and Materials, Philadelphia, 1980, pp. 310–326.
83. Hinchcliffe, D., and Town, J., Experience with nonchromate cooling water treatment (case histories), *Mater. Perform.*, September, 36–38 (1977).
84. Lula, R. A., compiler, *Source Book on the Ferritic Stainless Steels*, American Society for Metals, Metals Park, Ohio.
85. Debold, T. A., Select the right stainless steel, *Chem. Eng. Prog.*, November, 38–43 (1991).
86. Saunders, E. A. D., *Heat Exchangers: Selection, Design and Construction*, Addison Wesley Longman, Reading, MA, 1989.
87. Llewellyn, D. T., *Steels, Metallurgy and Applications*, Butterworth-Heineman, 1992.
88. Munger, C. G., Corrosion prevention by protective coatings, *Mater. Perform.*, April, 57–58 (1987).
89. Coatings and linings, in *Corrosion Basics—An Introduction*, NACE, Houston, 1984, pp. 47–48.
90. Weber, J., Corrosion and deposits in cooling systems—Their causes and prevention, *Sulzer Tech. Rev.*, *3*, 219–232 (1972).
91. McGill, W. A., and Weinbaum, M. J., Aluminum vapor diffused steels resist refinery corrosion, *Mater. Protect. Perform.*, July, 28–32 (1972).
92. Asbaugh, W. G., Corrosion in heat exchangers using brackish water, *Chem. Eng.*, 5 July, 146–152 (1965).
93. Paren, J., and Pouzenc, C., Design of power station condensers, *GEC Alsthom Tech. Rev.*, *6*, 19–38 (1991).
94. Singbell, D., and Garner, A., Anodic protection to prevent the stress corrosion cracking of pressure vessel steels in alkaline sulfide solutions, *Mater. Perform.*, April, 31–36 (1987).
95. Donohue, J. M., and James, E. W., Passivation and Its application in cooling water systems, *Mater. Perform.*, October, 34–36 (1977).
96. Britton, C. F., and Tofield, B. C., Effective corrosion monitoring, *Mater. Perform.*, April, 41–44 (1988).
97. Schweitzer, P. A., ed., *Corrosion and Corrosion Protection Handbook*, second edition, Marcel Dekker, New York, 1983.
98. Somm, E., Schlachter, W., and Schwarzenbach, A., Power generating equipment, in *Brown Bowri Symposium on Corrosion in Power Generating Equipment*, (M. O. Speidel and A. Atrens, eds.), Plenum Press, New York, 1983, pp. 3–25.
99. Chance, R. L., Walker, M. S., and Rowe, L. C., Evaluation of engine coolants by electrochemical methods, in *Engine Coolant Testing: Second Symposium, ASTM STP 887* (R. E. Beal, ed.), American Society for Testing and Materials, Philadelphia, 1986, pp. 99–122.
100. Bodmer, M., Baden, Rushton, C. A., and Luton, On-line monitoring of water purity in thermal power stations, *Brown Boveri Rev.*, *8–78*, 546–554 (19xx).
101. Muller, R., Improving the resistance of condensers to corrosion by systematic examination of the state of the tubes, *Brown Boveri Rev.*, *8–78*, 516–522 (19xx).
102. Tracy, A. W., Nole, V. F., and Duffy, E. J., Water analyses and their functions in selecting condenser tube alloys, *Trans. ASME, J. Eng. Power*, July, 329–332 (1965).
103. Cotton, I. J., Oxygen scavengers—The chemistry of sulfide under hydrothermal conditions, *Mater. Perform.*, March, 41–47 (1987).
104. Lockhart, A. M., Reducing condenser tube corrosion at Kincardine Generating Station with ferrous sulphate, *Proc. Inst. Mech. Eng.*, 495–512 (1964–1965).
105. Sato, S., Nagata, K., Yamauchi, S., Evaluation of Various Preventive Measures Against Corrosion of Copper Alloy Condenser Tubes by Sea Water, NACE National Conf., Unpublished Paper No. 195, 1981.
106. Schreiber, C. F., and Coley, F. H., *CORROSION/75*, Paper No. 36, NACE, Houston, 1975.

107. Sonnenmoser, A., Design and operation of large high pressure feedheaters, *Brown Boveri Rev.*, 7/8–73, 352–359.
108. Sonnenmoser, A., and Wollschlegal, P., The design of extremely watertight condensers, *Brown Boveri Rev.*, *65*, 505–515 (1978).
109. Warren, D., Hydrogen effects on steel, *Mater. Perform.*, January, 38–46 (1987).
110. Sauvage, M., Requirements for the Manufacture of Pressure Vessels for Wet H_2S Service, WRC Bulletin 374, pp. 72–81.
111. Terasaki, F., Ohtani, H., Ikeda, A., and Nakanishi, M., Steel plates for pressure vessels in sour environment applications, *Proc. Inst. Mech. Eng.*, *200*, 141–158.
112. Mirabal, E., Bhattacharjee, S., and Pazos, N., Carbonate-type cracking in an FCC wet gas compressor station, *Mater. Perform.*, July, 41–45 (1991).
113. Kane, R. D., and Cayard, Improve corrosion control in refining processes, *Hydrocarbon Processing*, November, 129–142 (1995).
114. Kobrin, G., Materials selection, in *Metals Handbook*, Vol. 13, *Corrosion*, 9th edition, American Society for Metals, Metals Park, Ohio, 1987, pp. 321–337.
115. Methods and Controls to Prevent In-Service Cracking of Carbon Steel (P-1) Welds in Corrosive Petroleum Refinery Environments, NACE RP-04-72 (1976 Rev.), National Association of Corrosion Engineers, Houston, 1976.
116. NACE Standard TM-02-84, Evaluation of Pipeline and Pressure Vessel Steels for Resistance to Hydrogen Induced Cracking, NACE International, Houston.
117. Tech. Services Bull. No. 778: A516 Steels Including HIC-Tested A516 Steels, Rev. November 1992, Lukens Steel Company, Coatesville, Pa., 1992.

Bibliography

1. *Corrosion Source Book* (S. K. Coburn, ed.), American Society for Metals, Metals Park, and National Association of Corrosion Engineers, Houston, 1984.
2. *The Chemical Engineering Guide to Corrosion* (R. W. Greene, ed.), McGraw-Hill, New York, 1986.
3. Craig, B., Forms of corrosion: Introduction, in *Metals Handbook*, Vol. 13, *Corrosion*, 9th edition, American Society for Metals, Metals Park, Ohio, 1987, p. 79.
4. *Materials Engineering, Part I: Selecting Materials for Process Equipment; Part II: Controlling Corrosion in Process Equipment* (K. J. McNaughton, ed.), McGraw-Hill, New York, 1980.
5. Pludek, R. V., *Design and Corrosion Control*, Macmillan, London, 1977.
6. *Cooling Towers, Chemical Engineering Progress*, AIChE, New York, 1972.
7. Brittalan, O. J., Declerks, D. H., and Urhis, F. H., Linings, *Chem. Eng., Deskbook Issue*, 12 October, 127–135 (1972).
8. McDonald, M. M., Corrosion of brazed joints, in *Metals Handbook*, Vol. 13, *Corrosion*, 9th edition, American Society for Metals, Metals Park, Ohio, 1987, pp. 876–886.
9. Bostwick, T. W., Reducing corrosion of power plant condenser tubing, *Corrosion*, August (1961).

CHAPTER 13

1. Henthorne, M., Understanding corrosion, *Chem. Eng.*, Deskbook Issue, 4 December, 19–33 (1972).
2. Kobrin, G., Materials selection, in *Metals Handbook*, Vol. 13, *Corrosion*, 9th edition, American Society for Metals, Metals Park, Ohio, 1987, pp. 321–337.
3. Moore, R. E., Selecting Materials to Meet Environmental Conditions, in *Materials Engineering I: Selecting Materials for Process Equipment* (K. J. McNaughton, ed.), McGraw-Hill, New York, 1980, pp. 31–33.
4. Hildebrand, E. L., Materials selection for petroleum refineries and petrochemical plants, *Mater. Protect. Perform.*, July, 19–22 (1972).
5. Elliott, P., Design details to minimize corrosion, in *Metals Handbook*, Vol. 13, *Corrosion*, 9th edition, American Society for Metals, Metals Park, Ohio, 1987, pp. 338–343.

6. Guide to selecting engineered materials, metals, polymers ceramics, composites, *Adv. Mater. Processes, 137*(6) (1990).
7. Designing and fabricating aluminum weldments, *Welding Design & Fabrication*, February, 53–62 (1977).
8. Daemen, R., Welding heavy gauge high tensile steels, *Brown Boveri Rev., 52*, 512–524 (1965).
9. Langer, B. F., and Harding, W. L., Material requirements for long life pressure vessels, *Trans. ASME, J. Eng. Power*, October, 403–410 (1964).
10. Hattangadi, A. D., and Seth, B. B., Lamellar tearing in fillet weldments of pressure vessel fabrication, *Welding J.*, April, 89-s–96-s (1983).
11. Frew, J. A., Lloyd's approach to quality assurance of welded structures, *Welding and Metal Fabrication*, July–August, 256–260 (1974).
12. Clarke, J. S., and Northup, M. S., Design of vessels for petroleum refining and petrochemicals service, *ASME J. Eng. Power*, October, 411–418 (1964).
13. Bravenec, E. V., Why steel fracture, *Chem. Eng.*, 10 July, 100–108 (1972).
14. Swales, G. L., and Haynes, G. A., Nickel Steels in LNG Tankers, in *Source Book on Materials Selection*, Vol. 1, (R. B. Guina, compiler), ASM, Metals Park, OH, 1977, pp. 469–474.
15. Guide to the Choice and Fabrication of Pressure Vessel Steel, Climax Molybdenum Co. Ltd. (an affiliate of AMAX American Metal Climax, Inc.), London.
16. Schillmoller, C. M., and Craig, B. D., Nickel steels in Arctic service, *Mater. Perform.*, October, 46–49 (1987).
17. Benzer, W. C., Trends in materials application: Steels, *Chem. Eng.*, Deskbook Issue, 12 October, 101–110 (1970).
18. Low Alloy Steel Plates for High Temperature Service, Nippon Steel Corporation, Cat. No. EXE 396, April 1976.
19. Schade, J. P., and Ross, R. W., Control corrosion with nickel base alloys, *Adv. Mater. Processes, 7*, 37–40 (1994).
20. Jana, S. R., and Honavar, D. S., A study in designing of weld metals for high austenitic stainless steels, in *Stainless Steels—Processing and Metallurgy, Proceedings of the International Conf. on Stainless Steels* (P. Krishna Rao, M. K. Asundi, N. B. Ballal, and H. S. Gadiyar, eds.), INCOSS-89, Bombay, Omega Scientific Publishers, New Delhi, 1989, pp. 149–158.
21. Swindeman, R. W., and Gold, M. Developments in ferrous alloy technology for high-temperature service, *ASME J. Pressure Vessel Technol., 113*, 133–140 (1991).
22. Kane, R. D., and Cayard, Improve corrosion control in refining processes, *Hydrocarbon Processing*, November, 129–142 (1995).
23. *Corrosion Abstracts*, National Association of Corrosion Engineers, Houston, Tex.
24. *Corrosion Data Survey—Metals Section*, 6th edition, 1985, and *Corrosion Data Survey—Nonmetals Section*, 1975; National Association of Corrosion Engineers, Houston, Tex.
25. Warren, D., Hydrogen effects on steel, *Mater. Perform.*, January, 38–46 (1987).
26. Richardson, H. T., Application of welding requirements and standards for oil refinery equipment, *Welding and Metal Fabrication*, October, 367–374 (1968).
27. Kar, R. J., and Todd, J. A. Alloy modification of thick section 2.25Cr-1Mo steel, in *Application of 2.25Cr-1Mo Steel for Thick Wall Pressure Vessels, ASTM STP 755* (G. S. Sangdahl and M. Semchyshen, eds.), American Society for Testing and Materials, Philadelphia, 1982, pp. 228–252.
28. Wilten, H. M., Microscope speeds diagnosis of refinery corrosion, *Hydrocarbon Processing & Petroleum Refiner, 40*, 151–280 (1961).
29. Hagel, W. C., and Miska, K. H., How to select alloy steels for pressure vessels—I, *Chem. Eng.*, 28 July, 89–91 (1980).
30. Steels for Hydrogen Service at Elevated Temperatures and Pressures in Petroleum Refineries and Petrochemical Plants, API Publication 941, 1997.
31. Kirchner, W. L., Innovations in Vessel Fabrication, *Mater. Protect. Perform.*, December, 20–22 (1972).
32. Hoffman, H. C., Pressure vessel primer, *Machine Design*, 9 October, 168–171 (1980).

33. Sattler, F. J., Forrer, G. R., and Parker, W. O., Jr., Inservice Inspection of Nuclear Plants, *Mater. Eval.*, November, 18A–22A, 27A–29A (1972).
34. Landrum, R. J., Designing equipment for corrosion resistance, *Chem. Eng.*, Deskbook Issue, 12 October, 75–82 (1970).
35. Equipment Service Life Factors, *Mater. Perform.*, September, 79 (1988). Adapted from R. J. Landrum, *Fundamentals of Designing for Corrosion Control*, National Association of Corrosion Engineers, Houston, Texas.
36. *Annual Book of ASTM Standards for Metal Products, Test Methods and Analytical Procedures. Section 1—Iron and Steel Products; Section 2—Nonferrous Metal Products; Section 3—Metal Test Methods and Analytical Procedures*, ASTM, Philadelphia.

36a. *Annual Book of ASTM Standards, Section 1—Iron and Steel, Steel-Piping, Tubing, and Fittings*, Vol. 01.01, ASTM, Philadelphia, 1992.

36b. *Annual Book of ASTM Standards, Section 1—Iron and Steel: Plate, Sheet, Strip, and Wire*, Vol. 01.03, ASTM, Philadelphia, 1992.

36c. *Annual Book of ASTM Standards, Section 1—Iron and Steel: Bars, Forging, Bearing, Chain, and Springs*, Vol. 01.04, ASTM, Philadelphia, 1992.

36d. *Annual Book of ASTM Standards, Section 1—Iron and Steel: Structural, Reinforcing, Pressure Vessel, Railway*, Vol. 01.05, ASTM, Philadelphia, 1992.

36e. *Annual Book of ASTM Standards, Section 2—Copper and Copper Alloys: Plate/Sheet/Strip Rolled Brass (Cu-Si Alloy) for General Purpose/Pressure Vessels*, Vol. 02.01, ASTM, Philadelphia, 1992.

36f. *Annual Book of ASTM Standards, Section 2—Aluminum and Magnesium Alloys, and Diecast Metals*, Vol. 02.02, ASTM, Philadelphia, 1992.

36g. *Annual Book of ASTM Standards, Section 2—Nonferros Metals: Nickel, Lead, Tin, Zinc, Cadmium Alloys, Precious, Primary, and Reactive Metals*, Vol. 02.04, ASTM, Philadelphia, 1992.

37. Hudgell, R. J., and Tickle, H., Current practices for ultrasonic and radiographic examination of tubes, tubeplates and tubeplate welds of tube bundles in heat exchangers, in *Developments in Pressure Vessel Technology—2, Inspection and Testing*, Applied Science Publishers, UK, 1979, pp. 77–100.
38. Orlando, J. S., and Ballantine, W., Materials for corrosion resistant fasteners, in *Metals Handbook*, desk edition, American Society for Metals, Metals Park, Ohio, 1985, pp. 15.29–15.30.
39. Danis, J. I., Material selection, fabrication and inspection of refinery heat exchangers, *Welding J.*, June, 25–30 (1986).
40. Schlunder, E. U., Editor-in-chief, Mechanical design codes: Expansion joints, in *Heat Exchanger Design Handbook*, Hemisphere, Washington, D.C., 1983, Section 4.16.
41. Yokell, S., *A Working Guide to Shell and Tube Heat Exchangers*, McGraw-Hill, New York, 1990.
42. Weymueller, C. R., ASTM specs guide users of plate steels I—Structural Steels, *Welding Design & Fabrication*, February, 42–48 (1992).
43. Weymueller, C. R., ASTM specs guide users of plate steels II—Pressure vessel steels, *Welding Design & Fabrication*, March, 47–52 (1992).
44. Smallwood, R. E., Heat exchanger tubing reliability, *Mater. Perform.*, February, 27–32 (1977).
45. Specification for Steel Tubes for Heat Exchanger, BS 3606:1978, British Standards Institution, pp. 1–14.
46. Foxall, D. H., and Gilbert, P. T., Selecting tubes for CPI heat exchangers—III, in *Materials Engineering I: Selecting Materials for Process Equipment* (K. J. McNaughton, ed.), McGraw-Hill, New York, 1980, pp. 172–174.
47. Engle, J. P., Chemical cleaning of feedwater heaters, *Mater. Perform.*, July, 30–33 (1974).
48. Brosilow, R., Weldability—What it means to fabricators, *Welding Design & Fabrication*, June, 74–80 (1978).
49. Principles of joining metallurgy, in *Metals Handbook*, Vol. 6, *Welding, Brazing, and Soldering*, 9th edition (E. F. Nippes, ed.), American Society for Metals, Metals Park, Ohio, 1983, pp. 21–49.
50. Arc welding of carbon steels: Shielded metal arc welding, in *Metals Handbook*, Vol. 6, *Welding, Brazing, and Soldering*, 9th edition (E. F. Nippes, ed.), American Society for Metals, Metals Park, Ohio, 1983, pp. 75–95.

51. Arc welding of carbon steels: Submerged arc welding, in *Metals Handbook*, Vol. 6, *Welding, Brazing, and Soldering*, 9th edition (E. F. Nippes, ed.), American Society for Metals, Metals Park, Ohio, 1983, pp. 114–151.
52. Gas metal arc welding (MIG welding), in *Metals Handbook*, Vol. 6, *Welding, Brazing, and Soldering*, 9th edition (E. F. Nippes, ed.), American Society for Metals, Metals Park, Ohio, 1983, pp. 152–213.
53. Plasma arc welding, in *Metals Handbook*, Vol. 6, *Welding, Brazing, and Soldering*, 9th edition (E. F. Nippes, ed.), American Society for Metals, Metals Park, Ohio, 1983, pp. 214–224.
54. Electroslag welding, in *Metals Handbook*, Vol. 6, *Welding, Brazing, and Soldering*, 9th edition (E. F. Nippes, ed.), American Society for Metals, Metals Park, Ohio, 1983, pp. 225–237.
55. Electrogas welding, in *Metals Handbook*, Vol. 6, *Welding, Brazing, and Soldering*, 9th edition (E. F. Nippes, ed.), American Society for Metals, Metals Park, Ohio, 1983, pp. 238–244.
56. Arc welding of low alloy steels and other ferrous metals, in *Metals Handbook*, Vol. 6, *Welding, Brazing, and Soldering*, 9th edition (E. F. Nippes, ed.), American Society for Metals, Metals Park, Ohio, 1983, pp. 245–370.
57. Weld discontinuities, in *Metals Handbook*, Vol. 6, *Welding, Brazing, and Soldering*, 9th edition (E. F. Nippes, ed.), American Society for Metals, Metals Park, Ohio, 1983, pp. 829–855.
58. Brosilow, R., How can fabricators control weld properties?, *Welding Design & Fabrication*, March, 46–50 (1985).
59. Bailey, N., The establishment of safe welding procedures for four low alloy steels, *Welding Journal, 51*, 1972, Welding Research Supplement, pp. 169s–177s.
60. Yurioka, N., Suzuki, H., Ohshita, S., and Saito, S., Determination of necessary preheating temperature in steel welding, *Welding J.*, June, 147-s–153-s (1983).
61. Gross, J. H., Pressure vessel steels: Promise and problems, in *Source Book on Materials Selection*, Vol. 1 (R. B. Guina, compiler), American Society for Metals, Metals Park, OH, 1977, pp. 271–276.
62. Farrar, J. C. M., and Dolby, R. E., Lamellar Tearing in Welded Steel Fabrication, Welding Institute, Abington Hall, Abington, Cambridge, UK, 1972.
63. Wormington, H., Lamellar tearing in silicon-killed boiler plate, *Welding and Metal Fabrication*, September, 370–373 (1967).
64. Gross-Wordemann, J., and Dittrich, S., Prevention of temper embrittlement in 2.25Cr-1Mo weld metal by metallurgical actions, *Welding J.*, May, 123-s–128-s (1983).
65. Complementary information test for lamellar tearing, *Welding in the World, 19*, 47–53 (1981).
66. Lippold, J. C., and Savage, W. F., Solidification of austenitic stainless steel weldments: Part III—The effect of solidification behaviour on hot cracking susceptibility, *Welding J.*, December, 388-s–396-s (1982).
67. Goodwin, G. M., Hot cracking, measurement, mechanisms and modelling, *Welding J.*, February, 26–31 (1990).
68. Lin, W., Lippolod, J. C., and Baseslack, W. A., III, An evaluation of heat affected zone liquation cracking susceptibility, Part I: Development of a method for quantification, *Welding J.*, April, 135-s–153-s (1993).
69. Dhooge, A., and Vinckier, A., Reheat cracking—Review of recent studies (1984–1990), *Welding in the World, 30*, 44–71 (1992).
70. Nakamua, H., Naiki, T., and Okahayaski, H., Fracture in the process of stress relaxation under constant strain, in *Proceedings of the First International Conference on Fracture*, Vol. 2., Sendai, Japan, 12–17 September, pp. 863–878, and Stress Relief Cracking in HAZ, IIW-IX-648-69 and IIW-X-531-69.
71. Onodera, S., Improved quality of heavy steels and their welds as related to the integrity of reactor pressure components, *Nuclear Energy Design, 85*, (1985).
72. Lippold, J. C., Baeslack, W. A. III, and Varol, I., Heat affected zone liquation cracking in austenitic and duplex stainless steels, *Welding J.*, January, 1-s–5-s (1992).
73. Lin, S., and Indacochea, J. E., Weldability of steels, in *Metals Handbook*, Vol. 1, *Properties and*

Selection: Iron, Steels, and High Performance Alloys, 10th edtion, American Society for Metals, Metals Park, Ohio, 1990, pp. 603–613.
74. Connor, L. P., ed., *Welding Hand Book*, Vol. 1, *Welding Technology*, eighth edition, 1987, pp. 102–121.
75. Datasheet No. 111b, Weldability testing—Weld cracking tests, *Welding J.*, February, 73 (1990).
76. Kautz, H. R., and Herbert, E. D., Modern welding techniques and component performance, *Welding in the World, 30*, 337–341 (1992).
77. U. S. Steel Handbook of Plate Products, U. S. Steel Group, Pittsburgh, Pa.
78. Lohmeier, A., and Reynolds, S. D., Jr., Carbon steel tube-to-tubesheet joints for high pressure feedwater heaters, *Westinghouse Engineer*, September, 138–143 (1966).
79. Jarman, R. A., and Shreir, L. L., Corrosion of jointed structures—Part II, *Welding & Metal Fabrication*, November/December, 445–449 (1987).
80. Kirby, G. N., Corrosion performance of carbon steel, in *Materials Engineering I: Selecting Materials for Process, Chemical Engineering*, 12 March 1979, pp. 72–84.
81. Uhlig, H. H., *Corrosion and Corrosion Control*, John Wiley & Son, Inc., New York, 1963.
82. Campbell, H. C., The ABCs of welding metallurgy for plain carbon steels, *Welding J.*, August, 55–57 (1994).
83. *Metals Handbook*, Vol. 6, *Welding, Brazing, and Soldering*, 9th edition (E. F. Nippes, ed.), American Society for Metals, Metals Park, Ohio, 1983, pp. 238—244.
84. Bargett, W. E., and Reeve, L., High strength weldable steel, *Iron and Steel*, Oct./Nov. (1954).
85. Irvine, K. J., The development of high strength structural steels, in *Proc. ISI/BISR, Joint Conference*, ISI Publication 104, ISI, London, 1967.
86. Carbon and low-alloy steels, in *Welding Handbook*, Vol. 4, *Metals and Their Weldability*, seventh edition (Kearns, ed.), American Welding Society, 1982, pp. 2–74.
87. Gutzeit, T., Corrosion in petroleum refining and petrochemical operations, in *Metals Handbook*, Vol. 13, *Corrosion*, 9th edition, American Society for Metals, Metals Park, Ohio, 1987, pp. 1262–1287.
88. Wordemann, G. J., and Dittrich, S., Prevention of temper embrittlement in 2.25Cr-1Mo weld metal by metallurgical actions, *Welding J.*, May, 123-s–128-s (1983).
89. Craig, W. R., Refineries test their metals, *Welding Design & Fabrication*, April, 81–85 (1977).
90. Wilson, A. D., Tougher steels improve pressure vessel performance, *Adv. Mater. Processes, 4*, 39–42 (1993).
91. Murakami, Y., Nomura, T., and Watnabe, J., Heavy section 2¼Cr–1Mo steel for hydrogenation reactors, in *Application of 2.25Cr-1Mo Steel for Thick Wall Pressure Vessels, ASTM STP 755* (G. S. Sangdahl and M. Semchyshen, eds.), American Society for Testing and Materials, Philadelphia, 1982, pp. 383–417.
92. Baumert, K. L., and Polk, C. J., Temper embrittlement studies on 2.25Cr-1Mo steel, *Mater. Perform.*, September, 39–45 (1976).
93. Swift, R. A., Effects of composition and heat treatment on the mechanical properties of 300 mm gage 2.25Cr-1Mo steel plate, in *Application of 2.25Cr-1Mo Steel for Thick Wall Pressure Vessels, ASTM STP 755* (G. S. Sangdahl and M. Semchyshen, eds.), American Society for Testing and Materials, Philadelphia, 1982, pp. 166–188.
94. Imgram, A. G., and Swift, R. A., Pressure vessel, piping and welding needs for coal conversion systems, *J. Mater. Energy Systems*, December, 212–221 (1985).
95. *Lukens Plate Steel Specification Guide*, 1993, Lukens Steel Company, Coatesville, Pa.
96. Yamamoto, S., and Natsume, S., Improvement of toughness of Cr-Mo steel weld metal at low temperature, *Welding and Metal Fabrication*, April, 110–115 (1986).
97. Modified 9 Cr-1 Mo steel for power plants, *Molybdenum Mosaic, 6*, 17, (1982). Climax Molybdenum Company of Michigan.
98. Ritche, R. O., Parker, E. R., Spencer, P. N., and Todd, J. A., A new series of advanced 3Cr-Mo-Ni steels for thick section pressure vessels in high temperature and pressure hydrogen service, *J. Mater. Energy Systems*, December, 151–162 (1964).
99. Brown, R. S., How to select the right stainless steel, *Adv. Mater. Processes, 4*, 20–24 (1994).

100. Debold, T. A., Select the right stainless steel, *Chem. Eng. Prog.*, November, 38–43 (1991).
101. Redmond, J. D., and Miska, K. H., The basics of stainless steels, *Chem. Eng.*, October (1982).
102. Linstroth, R. L., Check for atmospheric corrosion when using stainless steels, *Chem. Eng. Prog.*, July, 49–51 (1991).
103. Metallurgy of fusion welding, Pt 3: Stainless steels, *Welding & Metal Fabrication*, October, 376–378 (1994).
104. Llewellyn, D. T., *Steels, Metallurgy and Applications*, Butterworth-Heineman, 1992.
105. AL-6XN^{R} Alloy, Allegheny Ludlum Steel Corporation, Pittsburgh, Pa.
106. Kearns, J. R., and Deverell, H. R., The use of nitrogen to improve the corrosion resistance of FeCrNiMo alloys for the chemical process industries, *Mater. Perform.*, June, 18–28 (1987).
107. Davison, R. M., Corrosion of stainless steel, in *Metals Handbook*, Vol. 13, *Corrosion*, 9th edition, American Society for Metals, Metals Park, Ohio, 1987, pp. 546–575.
108. Davison, R. M., Rahoi, D. W., and Gemmel, G., Stainless steels for heat exchanger service, in *Industrial Heat Exchangers Conference Proceedings* (A. J. Hayes, W. W. Liang, S. L. Richlen, and E. S. Tabb, eds.), American Society for Metals, Metals Park, OH, 1985, pp. 371–380.
109. Forchhammer, P., Results of damage research on corrosion failures in heat exchangers, *Heat Transfer Eng.*, *5*, 19–32 (1984).
110. Product Literature, Mueller Accu-Therm Plate Heat Exchangers, Paul Mueller Company, Springfield, MO.
111. Blom, K. J., and Degerbeck, J., Low manganese austenitic stainless steels has improved resistance to pitting and crevice corrosion, *Mater. Perform.*, July, 52–54 (1983).
112. Slaughter, G. M., Franco-Ferreira, E. A., and Patriarca, P., Welding and brazing of high temperature radiators and heat exchangers, *Welding J.*, January, 15–22 (1968).
113. Redmond, D. J., and Miska, K. H., High performance stainless steels for high chloride service—Part I, *Chem. Eng.*, 25 July, 93–96 (1983).
114. Schillmoller, C. M., and Althoff, J. H., How to avoid failures of stainless steels, *Chem. Eng.*, May, 119–122 (1984).
115. Pollock, W. I., What's hot in metal alloys, *Chem. Eng.*, October, 78–88 (1992).
116. Kane, R. D., Super stainless steels resist hostile envirnoments, *Adv. Mater. Process*, *7*, 16–20 (1993).
117. Borenstein, S. W., Microbiologically influenced corrosion failures of austenitic stainless steel welds, *Mater. Perform.*, August, 62–66 (1988).
118. Odegard, L., Welding of stainless steels, corrosion in welds, effect of oxides, slag and weld defects on the pitting resistance, *Welding in the World*, *36*, 153–160 (1995).
119. Brosilow, R., Can you weld to avoid corrosion, *Welding Design & Fabrication*, September, 67–74 (1982).
120. Standard Recommended Practice for Examination and Evaluation of Pitting Corrosion, G 46, *Annual Book of ASTM Standards*, American Society Testing and Materials, Philadelphia.
121. Garner, A., Materials selection, for bleached pulp washers, *Pulp & Paper Canada*, *82*, 1 (1981).
122. Bandy, R., Lu, Y. C., Newman, R. C., and Clayton, C. R., Roles of nitrogen in improving the resistance to localised corrosion in austenitic stainless steels, in *Equilibrium Diagrams and Localised Corrosion*, Electrochemical Society, New Orleans, La., 1984, p. 471.
123. Dexter, C. S., Localized corrosion, in *Metals Handbook*, Vol. 13, *Corrosion*, 9th edition, American Society for Metals, Metals Park, Ohio, 1987, pp. 104–122.
124. Uhlig, H. H., Environmental effects on properties of materials, *Mater. Protect. Perform.*, July, 23–27 (1972).
125. Gooch, T. G. Stress corrosion cracking of welded austenitic stainless steel, *Welding in the World*, *22*, 64–76 (1984).
126. Copson, H. R., Effects of composition on stress corrosion cracking of some alloys containing nickel, in *Physical Metallurgy of Stress Corrosion Fracture*, Interscience, New York, 1959, p. 247.
127. Pitcher, J. H., Trends in CPI materials—Steels, *Chem. Eng.*, Deskbook Issue, 4 December, 39–42 (1972).

128. Espy, R. H., Coping with stress corrosion in stainless steel welds, *Welding Design & Fabrication*, October, 82–84 (1977).
129. Nishida, H., Nakamura, K., and Takahashi, H., Intergranular stress corrosion cracking of sensitized 321 SS tube exposed to polythionic acid, *Mater. Perform.*, April, 38–41 (1984).
130. Protection of Austenitic Stainless Steels in Refineries Against Stress Corrosion Cracking by Use of Neutralizing Solutions During Shutdown, NACE RP-01-70, National Association of Corrosion Engineers, Houston, Tex.
131. Fontana, M. G., and Greene, N. D., *Corrosion Engineering*, 2nd edition, McGraw-Hill, New York, 1978.
132. Bangs, S., Gas turbine regenerator uses TIG, laser beam, *Welding Design & Fabrication*, March, 81–88 (1981).
133. Jones, R. L., Prevention of stress corrosion cracking in boiling water reactors, *Mater. Perform.*, February, 70–75 (1991).
134. Gooch, T. G., and Willingham, D. C., Weld decay in austenitic stainless steels, Welding Institute, Abington Hall, Abington, Cambridge, UK.
135. Steigerwald, R., Metallurgically influenced corrosion, in *Metals Handbook*, Vol. 13, *Corrosion*, 9th edition, American Society for Metals, Metals Park, Ohio, 1987, pp. 123–135.
136. Fenn, R., Welding metallurgy of stainless steel, *Welding and Metal Fabrication*, October, 382–386 (1987).
137. Banks, B., Process selection and filler materials for welding stainless steels, *Welding and Metal Fabrication*, March, pp. 107–110 (1969).
138. Allen, J. S., Fabrication of heat exchangers and specialised vessels, *Welding and Metal Fabrication*, July, 240–245 (1968).
139. Weymueller, C. R., Welding the austenitic steels, *Welding Design & Fabrication*, June, 82–87 (1978).
140. Beigay, J. M., and Lovejoy, P. T., How to arc weld the stainless steels, *Welding Design & Fabrication*, August, 57–63 (1981).
141. Dulieu, D., Practical welding aspects of welding stainless steel, *Welding & Metal Fabrication*, July, 277–280 (1995).
142. Castro, R., and DeCadenet, J. J., *Welding Metallurgy of Stainless and Heat Resisting Steels*, Cambridge University Press, London, 1975.
143. Castner, H. R., What you should know about austenitic stainless steels, *Welding J.*, April, 53–59 (1993).
144. Smith, D. V., A practical approach to ferrite in stainless steel weld metal, *Welding J.*, May, 57–60 (1989).
145. Lundin, C. D., Lee, C. H., Menon, R., and Osorio, Weldability evaluation of modern 316 and 347 austenitic stainless steels: Part I—Preliminary results, *Welding J.* 35-s–46-s (1988).
146. Kotecki, D. J., Standards and industrial methods for ferrite measurement, *Welding in the World*, *36*, 161–169 (1995).
147a. Kotecki, D. J., and Siewet, T. A., WRC-1992 constitution diagram for stainless steel weld metals: A modification of the WRC-1988 diagram, *Welding J.*, May, 171-s–178-s (1992).
147b. Schaeffler, A. L., Constitution diagram for stainless steel weld metal, *Metal Prog.*, *56*(11), 68 (1949).
147c. DeLong, W. T., Ferrite in austenitic stainless steel weld metal, *Welding J.*, *53*(7), 273-s–286-s (1974).
148. Datasheet no. 82a, Effects of residual, impurity, and microalloying elements on weldability and weld properties, *Welding J.*, December, 53–54 (1986). Excerpted from Effects of Residual, Impurity, and Microalloying Elements on Weldability and Weld Properties, The Welding Institute, 1985; adapted by Hallock C. Campbell.
149. Polland, B., The effects of minor elements on the welding characteristics of stainless steel, *Welding J*, *67*(9), pp. 202-s–213-s (1988).
150. Vackar, B. K., Satisfying the codes, clean dry materials, good techniques & right chemistry, *Welding Design & Fabrication*, June, 86–87 (1977).

151. Lula, R. A., Introduction, in *Source Book on the Ferritic Stainless Steels* (R. A. Lula, compiler), American Society for Metals, Metals Park, Ohio, 1982, pp. ix–xii.
152. Nichol, T. J., Franson, I. A., and Moller, G. E., Applications of new high chromium ferritic stainless steels in the chemical process industries, in *Corrosion/81*, Paper No. 117, NACE, 1981, pp. 357–401.
153. Wock, W. C., Selecting steel tubing for high temperature service, in *Materials Engineering I: Selecting Materials for Process Equipment* (K. J. McNaughton, ed.), McGraw-Hill, New York, 1980, pp. 252–255.
154. Davison, R. M., and Steigerwald, R. F., The new ferritic stainless steels, *Metal Prog.*, *116*(6) 40–46 (1979).
155. Kaltenhauser, R. H., Improving the engineering properties of ferritic stainless steels, *American Society for Metals, Metals Eng. Q.*, *11*(2), 41–47 (1971).
156. Demo, J. J., *Structure, Constitution, and General Characteristics of Wrought Ferritic Stainless Steels*, ASTM STP 619, McGraw-Hill, New York, 1977.
157. Paul Bond, A., Mechanisms of intergranular corrosion in ferritic stainless steels, *Trans. Metallurgical Society of AIME*, *245*(8), 2127–2134 (1969).
158. Nichol, T. J., and Davis, J. A., Intergranular Corrosion Testing and Sensitization of Two High Chromium Ferritic Stainless Steels, ASTM STP 656, American Society for Testing and Materials, Philadelphia, 1978, pp. 179–196.
159. Walker, R., Duplex and high alloy stainless steels—Corrosion resistance and weldability, *Mater. Sci. Technol.*, *4*, 78–84 (1988).
160. Rayner, R. E., Better metallurgy for process equipment, *Hydrocarbon Processing*, January, 53–60 (1994).
161. Stephenson, N., Welding status of duplex stainless steels for offshore application—Part I & II, *Welding and Metal Fabrication*, June, 159–164, and July, 235–238 (1987).
162. Farrar, J. C. M., Developments in stainless steel welding consumables, *Welding & Metal Fabrication*, January, 27–32 (1990).
163. Faucher, D., and Gilbert, D., in *Proc. of International Conference on Duplex Stainless Steels '86*, October 1986, Netherlands Institute voor lastechniek, The Hague, Netherlands.
164. Tuthill, A. H., Usage and performance of nickel-containing stainless steels in both saline and natural waters and brines, *Mater. Perform.*, July, 47–50 (1988).
165. Mats, L., Development of superaustenitic stainless steels, *Welding in the World*, *36*, 55–63 (1995).
166. Rabensteiner, G., The welding of fully austenitic stainless steels with high molybdenum contents, *Welding in the World*, *27*, 2–13 (1989).
167. Davison, R. M., and Redmond, J. D., Practical guide to using 6 Mo austenitic stainless steels, *Mater. Perform.*, December, 39–43 (1988).
168a. Cary, H. B., Modern welding technology, in *Welding the Nonferrous Metals*, Prentice-Hall, Englewood Cliffs, N.J., 1979, pp. 431–460.
168b. *Welding Kaiser Aluminum*, Kaiser Aluminum and Chemical Sales, Inc., Kaiser Center, Oakland, Calif., 1967.
168c. *Welding Alcoa Aluminum*, Aluminum Company of America, Pittsburgh, Pa.
168e. *Welding Aluminum*, Reynolds Metals Company, Richmond, Va.
169. Swaney, W., Trace, D. E., and Winterbottom, W. L., Brazing aluminum automotive heat exchangers in vacuum: Process and materials, *Welding J.*, May, 49–57 (1986).
170. Taylor, M. A., ed., *Plate-Fin Heat Exchangers, Guide to Their Specification and Use*, HTFS (Harwell Laboratory), Oxon, UK, 1980.
171. *Aluminum Brazing Handbook*, 4th edition, Aluminum Association, Washington, D.C., 1990.
172. Irving, B., Welding the four most popular aluminum alloys, *Welding J.*, February, 51–55 (1994).
173. Corrosion behaviour, in *Aluminum: Properties and Physical Metallurgy* (J. E. Hatch, ed.), ASM, Metals Park, Ohio, 1984, pp. 242–319.
174. Pourbaix, M., *Atlas of Electrochemical Equilibria in Aqueous Solution*, National Association of Corrosion Engineers, Houston, 1974.

175. Corrosion of aluminum and aluminum alloys, in *Metals Handbook*, Vol. 13, *Corrosion*, 9th edition, American Society for Metals, Metals Park, Ohio, 1987, pp. 583–609.
176. Lancaster, J. F., Fabrication of aluminum pressure vessels, *Welding and Metal Fabrication*, December, 455–459 (1958).
177. Logan, H. L., *The Stress Corrosion Cracking of Metals*, John Wiley & Sons, New York, 1966.
178. Henthorne, M., Metals selection for corrosion control, *Chem. Eng.*, 6 March, 113–118 (1972).
179. Darden, J. W., Triebel, C. A., Maes, J. P., and VanNeste, W., Monoacid/Diacid Combination as Corrosion Inhibitors in Antifreeze Formulations, SAE 900804, pp. 135–139.
180. Schwerdtfeger, W. J., Effects of Cathodic protection on the corrosion of an aluminum alloy, *J. Res. Nat. Bureau Standards*, *68C*, 283 (1964).
181. McGill, W. A., and Weinbaum, M. J., Aluminum vapour diffused steels resist refinery corrosion, *Mater. Protect. Perform.*, July, 28–32 (1972).
182. Young, J. G., Quality control in aluminum welding, *Welding and Metal Fabrication*, January, 10–14, 62–67 (1964).
183. Corrosion of copper and copper alloys, in *Metals Handbook*, Vol. 13, *Corrosion*, 9th edition, American Society for Metals, Metals Park, Ohio, 1987, pp. 610–640.
184. Gaffoglio, C. J., Copper takes a lot of heat, *Welding Design & Fabrication*, October, 90–99 (1979).
185. *Standards Handbook*, Wrought Products, Alloy Data/2, Copper Development Association, Inc., Greenwich, Conn., 1985.
186. Peters, D. T., and Kundig, K. J. A., Selecting copper and copper alloys—Part I: Wrought products & Part II: Cast products, *Adv. Mater. Processes*, *2*, 26–32, and *6*, 20–26 (1994).
187. *Condenser Tube Handbook*, Bridgeport Brass Company, UK.
188. Copper in *Metals Handbook*, Vol. 2, *Nonferrous Metals*, 9th edition, American Society for Metals, Metals Park, Ohio, 1979.
189. Baumann, G., Materials for tubes used in the manufacture of high pressure feed heaters, *Brown Boveri Rev.*, *54*, 700–702 (1967).
190. Cieslewicz, J. M., and Schweitzer, P. A., Copper and copper and copper alloys, in *Corrosion and Corrosion Protection Handbook*, second edition (P. A. Schweitzer, ed.), Marcel Dekker, New York, 1983, pp. 125–152.
191. Tuthill, A. H., Guidelines for the use of copper alloys in seawater, *Mater. Perform.*, September, 12–22 (1987).
192. Thompson, D. H., How to prevent stress-corrosion cracking of copper alloys, *Chem. Eng.*, February, 130–134 (1961).
193. Syrett, B. C., and Coit, R. L., Causes and prevention of power plant condenser tube failures, *Mater. Perform.*, February, 44–49 (1983).
194. Syrret, B. C., et al., Corrosion in fossil fuel power plants, in *Metals Handbook*, Vol. 13, *Corrosion*, 9th edition, American Society for Metals, Metals Park, Ohio, 1987, pp. 985–1010.
195. Spencer, E., The effect of material choice on heat transfer in steam surface condensers, *Mater. Perform.*, March, 29–32 (1979).
196. Woodward, A. R., Howard, D. L., and Andrews, E. F. C., Condensers, pumps and cooling water plant, in *Modern Power Station Practice*, Vol. C, *Turbines, Generators, and Associated Plant* (D. J. Littler, E. J. Davies, H. E. Johnson, F. Kirkby, P. B. Myerscouh, and W. Wright, eds.), Pergamon Press, New York.
197. Hopkinson, B. E. Copper-Nickel Alloys for Feedwater Heater Service, ASME Publication No. 62-WA.294, ASME, New York.
198. Copper alloys, in *Welding Handbook*, Vol. 4, *Metals and Their Weldability*, seventh edition (Kearns, ed.), American Welding Society, 1982, pp. 270–316.
199. Dawson, R. J. C., Inert gas shielded arc welding of copper and copper alloy—Dissimilar metal joint, *Welding and Metal Fabrication*, February, 60–66 (1968).
200. Dawson, R. J. C., Inert gas shielded arc welding of copper and copper alloys, Part 2, *Welding and Metal Fabrication*, February, 59–63 (1967).

201. Dawson, R. J. C., *Fusion Welding and Brazing of Copper and Copper Alloys*, Newness-Butterworths, London, 1973.
202. McDonald Scketly, L., Arc welding of copper and copper alloys, in *Metals Handbook*, Vol. 6, *Welding, Brazing, and Soldering*, 9th edition (E. F. Nippes, ed.), American Society for Metals, Metals Park, Ohio, 1983, pp. 400–426.
203. Callcut, V., and Brown, L., Joining copper and copper alloys, *Welding & Metal Fabrication*, June, 232–236 (1996).
204. Modern methods for vessel fabrication—Developments at the Works of Daniel Adamson, *Welding and Metal Fabrication*, January, 4–15 (1963).
205. Campbell, E. J., Alloys for structural applications at subzero temperatures, in *Metals Handbook*, Vol. 3, *Properties and Selection: Stainless Steels, Tool Materials and Special Purpose Metals*, 9th edition, American Society for Metals, Metals Park, Ohio, 1980.
206. *Product Handbook*, Publication No. IAI-38, fourth edition, Inco Alloys International, Inc., Huntington, W. Va., 1988.
207. *Quick Reference Guide to Nickel and High Nickel Alloys*, Inco Alloys International, Inc., Huntington, W. Va.
208. *High Performance Alloys for Thermal Processing*, Publication No. IAI-48-1, fourth edition, Inco Alloys International, Inc., Huntington, W. Va., 1988.
209. Kiser, S. D., Sound welds in nickel alloys, *Welding Design & Fabrication*, October, 86–88 (1988).
210. Conaway, H. R., Welding the nickel alloys, Part 1: Cleaning and joint design, *Welding Design & Fabrication*, February, 73–75 (1977).
211. Conaway, H. R., Welding the nickel alloys, Part 2: SMAW and GMAW, Part 3: GTAW, SAW and OAW, Part 4: Plasma welding, nickel overlays, *Welding Design & Fabrication*, March, 75–79; April, 106–109; May, 70–73 (1977).
212. *Material Properties Handbook: Titanium Alloys*, ASM International, Materials Park, Ohio.
213. Schutz, R. W., and Thomas, E. D., Corrosion of titanium and titanium alloys, in *Metals Handbook*, Vol. 13, *Corrosion*, 9th edition, American Society for Metals, Metals Park, Ohio, 1987, pp. 669–706.
214. Data sheet, summary table of titanium alloys, *Adv. Mater. Processes*, 6, 123–126 (1994).
215. Inskeep, J., Mcmaster, J. A., and Trumbell, C. A., Move over for titanium, *Welding Design & Fabrication*, April, 88–94 (1977).
216. Seagle, S. R., and Bruce, B. P. Titanium: Its properties and uses, *Chem. Eng.*, 8 March, 111–113 (1982).
217. *Titanium Fabricators Ltd.—A Profile*, *Welding and Metal Fabrication*, October 1988, pp. 346–349.
218. Schutz, R. W., A case for titanium's resistance to microbiologically influenced corrosion, *Mater. Perform.*, January, 58–61 (1991).
219. *TIMET CodeWeld® Titanium Tubing*, TIMET, Denver, Colo.
220. Jacobs, R. L., and McMaster, J. A., Titanium tubing: Economical solution to heat exchanger corrosion, *Mater. Protect. Perform.*, July, 33–38 (1972).
221. Gleekman, L. W., Trends in CPI materials: Nonferrous metals—II, *Chem. Eng.*, Deskbook Issue, 4 December, 47–49 (1972).
222. McMaster, J. A., Selection of titanium for petroleum refinery components. *Mater. Perform.*, April, 28–33 (1979).
223. Cooley, J., How to weld titanium without a trailing shield, *Welding Design & Fabrication*, March, 65–66 (1982).
224. Hull, W. G., Fusion welding of titanium and its alloys, *Welding and Metal Fabrication*, January, 24–28 (1961).
225. Chevalier, R., General methods for cleaning titanium, *Welding and Metal Fabrication*, April, 134 (1974).
226. *Facts About Welding Titanium*, RMI Titanium Company, Niles, Ohio.
227. Crement, D. J., Narrow groove welding of titanium using the hot-wire gas tungsten arc process, *Welding J.*, April, 71–76 (1993).

228. Ellis, M. B. D., and Gittos, M. F., Tungsten inert gas welding of titanium and its alloy, *Welding & Metal Fabrication*, January, 9–12 (1995).
229. Baeslack, W. A., and Decker, D. W., Substructural characteristics in titanium alloy weldments, *Metal Trans., 11A*, 605–612 (1980).
230. Yau, T.-L., Zirconium, in *Corrosion and Corrosion Protection Handbook*, second edition (P. A. Schweitzer, ed.), Marcel Dekker, New York, 1983, pp. 231–282.
231. Lacy, C. E., and Keeler, J. H., Zirconium—Fabrication techniques and alloys development, *Mech. Eng.*, October, 875–878 (1955).
232. Cox, F. G., Zirconium, *Welding and Metal Fabrication*, October, 358–365 (1958).
233. Webster, R. T., and Yau, T.-L., Zirconium in sulfuric acid applications, *Mater. Perform.*, February, 21–25 (1986).
234. Rollason, E. C., Weldiing of zirconium, *Welding and Metal Fabrication*, July, 230–234 (1956).
235. Burns, R. H., and Prabhat, K., Conquer corrosion in harsh environments with tantalum, *Chem. Eng. Prog.*, March, 32–35 (1996).
236. Schweitzer, P. A., Tantalum, in *Corrosion and Corrosion Protection Handbook*, second edition (P. A. Schweitzer, ed.), Marcel Dekker, New York, 1983, pp. 213–230.
237. Keeler, J. H., Four refractory metals—W, Ta, Cb and Mo, *Mech. Eng.*, November, 41–45 (1965).
238. Bishop, C. R., and Stern, M., Hydrogen embrittlement of tantalum in aqueous media, *Corrosion, 17*, 379–385 (1961).
239. Schussier, M., Tantalum—Its properties and applications for the chemical industry, *Refractory and Hard Metals*, June (1983).
240. Hampel, C. A., Corrosion resistance of titanium, zirconium and tantalum used for chemical equipment, *Corrosion, 17*, 9–17 (1961).
241. Yan, T.-L., and Bird, K. W., Know which reactive and refractory metals work for you, *Chem. Eng. Prog., 88*(2), 65–69 (1992).
242. Gleekman, L. W., Trends in CPI materials: Nonferrous metals—I, *Chem. Eng.*, Deskbook Issue, 12 October, 111–118 (1970).
243. Sayers, J. A., Trends in CPI materials: Brittle materials, *Chem. Eng.*, Deskbook Issue, 4 December, 51–56 (1972).
244. Hills, D. E. G., Graphite heat exchangers—I, *Chem. Eng.*, 23 December, 80–83 (1974).
245. Hills, D. E. G., Graphite heat exchangers—II, *Chem. Eng.*, 20 January, 116–119 (1975).
246. Schley, J. R., Impervious graphite for process equipment, *Chem. Eng.*, 18 February, 144–150 (1974).
247. Muoio, J. M., Glass as a material of construction for heat transfer equipment, in *Industrial Heat Exchangers Conference Proceedings* (A. J. Hayes, W. W. Liang, S. L. Richlen, and E. S. Tabb, eds.), American Society for Metals, Metals Park, Ohio, 1985, pp. 385–390.
248. Perry, R. H., and Chilton, C. H., *Chemical Engineering Handbook*, fifth edition, McGraw-Hill, New York, 1973.
249. Mejzak, G. J., An introduction of glass for the chemical process industries, in *ASME National Congress on Pressure Vessel and Piping Technology*, 1983.
250. O-I/Schott Process Systems, Heat Exchanger Bulletin OIS-HE-1182, 1984.
251. Lederman, S., Types and prevention of glass lined equipment failures, *Mater. Perform.*, March, 34–41 (1983).
252. Wenner, C. W., Jr., Corrosion-free heating and cooling using Teflon heat exchangers, *Mater. Perform.*, September, 55–58 (1988).
253. Ametek Heat Exchangers of Teflon, M/s. Ametek, Haveg Division, USA.
254. Lehman, R. L., Premier on engineering ceramics, *Adv. Mater. Processes*, June, 31–41 (1992).
255. McDonald, C. F., The role of the ceramic heat exchanger in energy and resource conservation, *Trans. ASME, J. Eng. Power, 102*, 303–315 (1980).
256. Schwartzberg, R. F., Selecting structural materials for cryogenic service, in *Source Book on Materials Selection*, Vol. 1 (R. B. Guina, compiler), ASM, Metals Park, Ohio, 1977, pp. 25–30.
257. Marshall, E. G., Steels for low temperature service, in *Source Book on Materials Selection*, Vol. 1 (R. B. Guina, compiler), ASM, Metals Park, Ohio, 1977, pp. 216–220.

258. Vanderbeck, R. W., Special carbon steels—Tough ductile at subzero temperature, *Chem. Eng.*, May, 103–106 (1960).
259. Aluminum in hot pursuit of cryogenics, *Welding Design & Fabrication*, September, 45–49 (1974).
260. Johnson, E. W., Aluminum alloys, *Chem. Eng.*, 8 August, 133–135 (1960).
261. Welding of stainless steels for cryogenic application, *Welding in the World*, *30*, 100–107 (1992).
262. Fabrication of cryogenic plant, *Welding and Metal Fabrication*, March, 84–89 (1969).
263. Nippes, E. F., and Balaguer, J. P., A study of weld heat affected zone toughness of 9% nickel steel, *Welding J.*, September, 237-s–243-s (1986).
264. Fieldhouse, A. B., New electrode for welding 9% nickel steel, *Welding and Metal Fabrication*, April, 149–150 (1964).
265. Johnson, R. J., Nickel steel alloys for liquids at 320°F, *Chem. Eng.*, July, 115–118 (1960).
266. Tharby, R. H., Welding consumables for 9% nickel steel, *Welding and Metal Fabrication*, February, 51–61 (1973).
267. Thorneycroft, D. R., and Heath, D. J., Further aspects of the welding of 9% nickel steel, *Welding and Metal Fabrication*, February, 59–70 (1963).
268. Pozzolini, P. F., The role of 9% nickel steel in the transport of LNG, *Welding and Metal Fabrication*, February, 40–46 (1973).
269. Coulson, K. J., Shop manufacturing experience with 9% nickel steel, *Welding and Metal Fabrication*, February, 47–50 (1973).
270. Machin, R., Welding aspects of 9% nickel steel, *Welding and Metal Fabrication*, July, 266–269 (1966).
271. Watanabe, M., Tanaka, J., and Watanabe, I., Ferritic filter for gas shielded metal arc welding 9% nickel steel, *Welding and Metal Fabrication*, May, 167–176 (1973).
272. *Operation Cryogenics*, International Nickel Co., Inc., Chicago Bridge & Iron Co., and United Steels Corp, Publication AUDCO A-61.
273. Jordan, D. E., High strength filler material for welding 9% nickel steel, *Welding and Metal Fabrication*, August, 335–339 (1967).
274. McHenry, H. T., The properties of austenitic stainless steels at cryogenic temperatures, in *Austenitic Steels at Low Temperature*, Plenum Press, New York, 1983.
275. Ogawa, T., and Koseki, T., Weldability of newly developed austenitic alloys for cryogenic service: Part II. High nitrogen stainless steel weld metal, *Welding J.*, *67*, 8-s–17-s (1988).
276. Ogawa, T., and Koseki, T., Weldability of newly developed austenitic alloys for cryogenic service: Part I. Up-to-date overview of welding technology, *Welding J.*, *66*, 332-s–341-s (1987).
277. Lancaster, J. F., *The Metallurgy of Welding, Brazing and Soldering*, American Elsevier, New York, 1965.
278. Charles, J., Gagnepain, J. C., Dupoiron, F., Jobard D., and Soulignac, P., Austenitic-Ferritic Stainless Steels and Clad Plates: Properties and Applications to Pressure Vessels, WRC Bull. 374, pp. 25–37.
279. Gleekman, L. W., Trends in CPI materials: Nonferrous metals—II, in *Materials Engineering 1: Selecting Materials for Process Equipment* (K. J. McNaughton, ed.), McGraw-Hill, New York, 1980, pp. 92–94.
280. Newcombe, G., The bimetal concept, *Welding and Metal Fabrication*, November, 379–406 (1974).
281. Firth, K., and Heath, D. J., Nickel alloys provide protective lining and overlays, *Welding and Metal Fabrication*, April, 195–203 (1980).
282. Bush, A. F., and Cohin, P., The successful application of the strip cladding process with austenitic strips, *Welding and Metal Fabrication*, June, 234–241 (1969).
283. Mallya, U. D., and Srinivas, H. S., Effect of magnetic steering of the arc on clad quality in submerged arc strip cladding, *Welding J.*, July, 289-s–293-s (1993).
284. Devletian, J. H., Koch, A., and Buckley, E. N., Unique application introduces electroslag cladding to US industry, *Welding J.*, January, 57–60 (1992).
285. Marshall, A. B., Jordan, M. F., and Aston, J. L., Stainless steel strip cladding, *Welding and Metal Fabrication*, August, 292–293 (1973).

286. Oh, Y. K., and Devletian, J. H., Electroslag strip cladding of stainless steel with metal powder additions, *Welding Journal*, January, 37–44 (1992).
287. Banker, J. G., Try explosion clad steel for corrosion protection, *Chem. Eng. Prog.*, July, 40–44 (1996).
288. Hix Hugh, B., Explosion bonded metals offer diversification in vessel design, *Mater. Protect. Perform.*, December, 28–31 (1972).
289. Hardwick, R., Methods for fabricating and plugging of tube to tubesheet joint by explosion welding, *Welding, J.*, April, 238–244 (1975).
290. Linse, V. D., and Temple, P. I., Explosion welding, in *Welding Hand Book*, Vol. 2, eighth edition, 1991, pp. 766–781.
291. Explosion welding, in *Metals Handbook*, Vol. 6, *Welding, Brazing, and Soldering*, 9th edition (E. F. Nippes, ed.), American Society for Metals, Metals Park, Ohio, 1983, pp. 705–718.
292. Johnson, W. R., Explosive welding: Plugs into heat exchanger tubes, *Welding J.*, January, 22–32 (1971).
293. Peacock, G. A., Fabrication of thick plates, *Welding and Metal Fabrication*, June, 242–252 (1963).
294. Ellis, D., Fabrication in clad steels, *Welding and Metal Fabrication*, September, 359–365 (1967).
295. *Welding Handbook*, Vol. 4, *Metals and Their Weldability*, seventh edition (W. H. Kearns, ed.), AWS, Miami, Fla., 1982, Chapter 12.
296. Recommendation of PWHT of welded joints in steel pressure vessels and other heavy duty structures, by Joint Working Group, IIW Commissions IX and X, *Welding in the World, 29*, 341–362 (1991).
297. Ellis, D. J., and Gifford, A. F., Application of electroslag and consumable guide welding, *Welding and Metal Fabrication*, April, 112–119 (1973).
298. Ricci, W. S., and Eagar, T. W., A parametric study of the electroslag welding process, *Welding J.*, December, 397-s–405-s (1982).
299. Carpenter, O. R., and Floyd, C., Heat treatment of carbon and low alloy pressure vessel steel, *Welding J.* (1957).
300. Watson, S. J., Post weld treatment of welded units for the relief of stress, *Welding and Metal Fabrication*, September, 318–327 (1958).
301. Ohshita, S., Yurioka, N., Mori, N., and Kimura, T., Prevention of solidification cracking in very low carbon steel welds, *Welding J.*, June, 129-s–136-s (1983).
302. ASME Boiler and Pressure Vessel Code, Section VIII, Division 1, Pressure Vessels, The American Society of Mechanical Engineers, New York, 1992.
303. Carpenter, D. D., A guide for determining post weld heat treatment requirements for ASME Code Section VIII pressure vessels, *Trans. ASME, J. Pressure Vessel Technol., 106*, 115–123 (1984).

Bibliography

1. *Materials Engineering, Part I: Selecting Materials for Process Equipment; Part II: Controlling Corrosion in Process Equipment* (K. J. McNaughton, ed.), McGraw-Hill, New York, 1980.
2. Corrosion of nickelbase alloys, in *Metals Handbook*, Vol. 13, *Corrosion*, 9th edition, American Society for Metals, Metals Park, 1987, Ohio, pp. 641–657.
3. *Welding Handbook*, Vol. 1, *Welding Technology*, Vol. 2, *Welding Processes*, Vol. 3, *Materials and Application*, eighth edition (L. P. Connor, ed.), American Welding Society, Miami, Fla., 1987.
4. Weldments, brazed assemblies, and soldered joints, in *Metals Handbook*, Vol. 17, *Nondestructive Evaluation and Quality Control*, ninth edition, American Society for Metals, Metals Park, Ohio, 1989, pp. 582–609.
5. *Metals Handbook*, Vol. 1, *Properties and Selection: Iron, Steels, and High Performance Alloys*, 10th edition, American Society for Metals, Metals Park, Ohio, 1990.
6. *Metals Handbook*, Vol. 2, *Properties and Selection: Nonferrous Alloys, and Special Purpose Materials*, 10th edition, American Society for Metals, Metals Park, Ohio, 1992.
7. Cary, H. B., *Modern Welding Technology*, Prentice Hall, Englewood Cliffs, N.J., 1979.

CHAPTER 14

1. Danis, J. I., Material selection, fabrication and inspection of refinery heat exchangers, *Welding J.*, June, 25–30 (1986).
2. Nicholson, S., The role of NDT within Q. A. programmes applied to pressure vessels and other process plant, *Br. J. NDT*, May, 121–127 (1982).
3. Burgess, N. T., Quality control—What's it all about?, *Welding and Metal Fabrication*, December, 464–468 (1966).
4. Silk, M. G., Developments in ultrasonics for sizing and flaw characterisation, in *Developments in Pressure Vessel Technology—2, Inspection and Testing* (R. W. Nichols, ed.), Applied Science Publishers, UK, 1979, pp. 101–139.
5. Rao, B. S. C., Quality assurance in fabrication of pressure vessels, in *Welding Engineering Handbook*—Vol. I (S. Sundarrajan, S. Vijaya Bhaskar, and G. C. Amarnath Kumar, eds.), Welding Research Group, Radiant Publications, Secunderabad, India.
6. Bryant, L. E., and Mcintire, P., eds., *Nondestructive Testing Handbook*, 2nd edition, Vol. 3, *Radiography and Radiographic Testing*, American Society for Nondestructive Testing, Columbus, Ohio.
7. Blatter, H., and Frey, H., System effectiveness and quality assurance of electronic systems. *Brown Boveri Rev., 11–78*, 739–743.
8. Dale, B. G., and Plunkett, J. J., A study of audits, inspection and quality costs in the pressure vessel fabrication sector of the process plant industry, *Proc. Inst. Mech Eng., 198B*, 49–54.

9a. ASME Boiler and Pressure Vessel Code, Section VIII, Division 1, Pressure Vessels, American Society of Mechanical Engineers, New York, 1992.

9b. ASME Boiler and Pressure Vessel Code, Section IX. Welding and Brazing Qualifications, American Society of Mechanical Engineers, New York, 1992.

9c. ASME Boiler and Pressure Vessel Code, Section II, Material Specifications, Part A—Ferrous Materials. Part—B Nonferrous Materials, Part—C Welding Rods, Electrodes and Filler Metals, Part—D Material Properties, American Society of Mechanical Engineers, New York, 1992.

9d. ASME Boiler and Pressure Vessel Code, Section V. Nondestructive Examination, American Society of Mechanical Engineers, New York, 1992.

10. Chuse, R., *Pressure Vessels, the ASME Code Simplified*, McGraw-Hill, New York, 1984.
11. Veith, C. J., Developing a quality control program, *Welding Design & Fabrication*, September, 71–73 (1975).
12. Lavender, D. H., and Lavender, J. D., An NDT audit—What to expect, *Br. J. NDT*, July, 264–265 (1987).
13. Weymueller, C. R., NDT builds safety into a nuclear plant, *Welding Design & Fabrication*, September, 54–57 (1982).
14. NDT feature-testing triggers big savings, *Welding Design & Fabrication*, February, 31–39 (1975).
15. British Standards Institution: BS 6143:1983—Guide to the Determination and Use of Quality Related Costs.
16. Zairi, M., *Total Quality Management for Engineers*, Aditya Books, New Delhi, India, 1992.
17. Nicholson, R. D., and Hemsworth, B., Assessment of nuclear reactor fabrication: A regulatory view, *Welding in the World, 30*, 126–129 (1992).
18. Yokell, S., *A Working Guide to Shell-and-Tube Heat Exchangers*, McGraw-Hill, New York, 1990.
19. Craig, W. R., Refineries test their metals, *Welding Design & Fabrication*, April, 81–85 (1977).
20. *Standard of TEMA*, seventh edition, Tubular Exchanger Manufacturers Assocation, New York, 1988.
21. Nichols, R. W., Golden rules for nondestructive examination, *Metal Construction, 12*, May (1980).
22. Frew, J. A., Lloyd's approach to quality assurance of welded structures, *Welding and Metal Fabrication*, August, 256–260 (1974).
23. Guide for the Visual Inspection of Welds, ANSI/AWS B1.11-88, American Welding Society, Miami, Fla., 1988.
24. Vackar, B. K., Satisfying Codes, *Welding Design & Fabrication*, June, 86–87 (1977).

25. Harrison, J. D., and Young, J. G., A rational approach to weld defect acceptance levels and quality control, *Welding and Metal Fabrication*, October, 367–371 (1973).
26. Mercer, W. L., NDT—A vital force in engineering, *Br. J. NDT*, January, 11–14 (1987).
27. Raj, B., and Subramanian, C. V., Nondestructive testing—Welding industry, in *Welding Engineering Handbook*, Vol. I (S. Sundarrajan, S. Vijaya Bhaskar, and G. C. Amarnath Kumar, eds.), Welding Research Group, Radiant Publications, Secunderabad, India.
28. Guide for the Nondestructive Inspection of Welds, ANSI/AWS B1.10-86, American Welding Society, Miami, Fla., 1985.
29. Hayes, C., The ABC's of nondestructive weld examination, *Welding Journal*, May 1997, pp. 46–51.
30. *Materials Engineering*, December 1992.
31. Dunn, F. W., Magnetic particle inspection fundamentals, *Mater. Eval.*, December, 42–47 (1977).
32. Hamlet, R. A., and Lavender, D. H., Standardisation within the writing of the NDT procedure, *Br. J. NDT*, 359–360 (1986).
33. Litting, B. G., N.D.T. methods and assessment of weld defects, *Welding and Metal Fabrication*, 435–440 (1967).
34. *NDE Handbook, Nondestructive Examination Methods for Condition Monitoring* (K. G. Boving, ed.), Butterworths, London.
35. Bauer, L., Visual inspection: Looking ahead, *Welding Design & Fabrication*, September, 31–32 (1991).
36. Miller, J. S., Inspect tubes and pipes with mini-TV cameras, *Welding Design & Fabrication*, October, 84–86 (1979).
37. Product Literature, Olumpus America, Inc., Industrial Fibre Optics Division, Lake Success, N.Y.
38. Lang, W. J., Eyeballing welds with a borescope, *Welding J.*, June, 61–62 (1990).
39. Selner, R., Dye penetrant and magnetic particle inspection, *Welding J.*, February, 28–31 (1982).
40a. Kevin Waker, Guide to liquid penetrant testing, *Welding Journal, Supplement*, Nondestructive Examination, October 1997, pp. 21–23.
40b. Lebowitz, C. A., A primer on nondestructive examination methods for weld inspection, *Welding Journal, Supplement*, Nondestructive Examination, October 1997, pp. 29–31.
41. Heine, H. J., Liquid penetrant and magnetic particle inspection, *Foundry Manage. Technol.*, July, 36–39 (1991).
42. Lovejoy, D. J., Standardisation of light levels for magnetic and penetrant inspection, *Br. J. NDT, 36*, 8–9 (1994).
43. Brown, F., and Howes, I., NDT methods and equipment for the quality fabrication shop, *Welding and Metal Fabrication*, 611–618 (1977).
44. Jefferson, T. B., Welder certification: What does it mean?, *Welding Design & Fabrication*, June, 66–68 (1981).
45. Hellier, C. J., What's new in nondestructive testing of welds and heat affected zones?, *Welding J.*, March, 39–43 (1993).
46. Banks, B., Problems of quality control in the manufacture of pressure vessels, *Welding and Metal Fabrication*, July, 241–246 (1972).
47. Welding Engineer Data Sheet, No. 468—Troubleshooting guide for radiographs, *Welding Design & Fabrication*, September, 79 (1979).
48. Litting, B. G., Quality control of welded components, *Welding and Metal Fabrication*, July, 294–297 (1967).
49. Carson, H. L., and Feaver, M. J., An improved means for the measurement of weld radiograph image quality, *Welding and Metal Fabrication*, January, 29–36 (1973).
50. Garrett, W. R., Reading radiographs takes time and patience, *Welding Design & Fabrication*, September, 77–79 (1979).
51. Hellier, C., Weld inspection—Today and tomorrow, *Welding Design & Fabrication*, September, 78–81 (1977).
52. Murray, S. H., Computed tomography used in weld inspections at NASA, *Welding J.*, February, 33–36 (1990).

53. Whritnour, R., Radioscopy speeds inspection, *Welding Design & Fabrication*, September, 24–25 (1992).
54. Carl, R. Weymueller, Ultrasonic testing for the fabricator, *Welding Design & Fabrication*, October 1994, pp. 25–33.
55. Anjard, R. P., Fundamentals of ultrasonic testing, *Heat Treating*, April, 34–38 (1978).
56. Fortunko, C. M., and Schramm, R. E., Ultrasonic nondestructive evaluations of butt welds using electromagnetic-acoustic transducers, *Welding J.*, February, 39–46 (1982).
57. Watson P. D., Design for welding examination, *Welding J.*, February, 32–35 (1982).
58. Ultrasonic signals, document no. 11S/11W-850-86, *The Welding Institute*, Abington, Cambridge.
59. Meyer, H.-J., Estimating flaw size in pressure vessel welds, *Welding Design & Fabrication*, November, 78–81 (1977).
60. Hansen, B., A rational approach to NDT of welds, *Welding Design & Fabrication*, May, 64–67 (1977).
61. Ehlman, W. G., Acoustical holography looks through welds, *Welding Design & Fabrication*, February, 68–70 (1977).
62. Lenain, J.-C., General principles of acoustic emission, *Mater. Eval.*, October, 1000–1002 (1981).
63. *Nondestructive Testing Handbook*, Vol. 5, *Acoustic Emission Testing*, second edition (R. K. Miller and P. McIntire, eds.), American Society for Nondestructive Testing, Columbus, Ohio, 1987.
64. Debel, C. P., *Proc. Fifth Riso International Symposium on Metallurgy and Material Science*, Riso National Laboratory Roskilde, Denmark, 1984, p. 19.
65. Raj, B., and Jha, B. B., Fundamentals of acoustic emission, *Br. J. NDT*, *36*, 16–23 (1994).
66. Prine, D. W., Inspect as you go with acoustic emission, *Welding Design & Fabrication*, January, 74–77 (1977).
67. Clark, J. N., The detection of creep failure at welds by acoustic emission, Part 1: Brittle creep rupture, *Br. J. NDT*, January, 9–21 (1982).
68. Kalyansundaram, P., Raj, B., Kasiviswanathan, K. V., Jayakumar, T., and Murthy, C. R. L., Leak detection in pressure tubes of a pressurised heavy water reactor by acoustic emission technique, *Br. J. NDT*, 539–544 (19).
69. Granville, R. K., In-service eddy current examination of nonferrous industrial heat exchanger tubing, *Br. J. NDT*, *33*, 403–409 (1991).
70. Eddy current inspection, in *Metals Handbook*, Vol. 17, *Nondestructive Evaluation and Quality Control*, ninth edition, ASM, Metals Park, Ohio, 1989, pp. 164–194.
71. Clark, W. G., Multiple-element eddy current probes for enhanced inspection, *Mater. Eval.*, July, 794–802 (1993).
72. Bergander, M. J., Flux leakage examination of ferrous heat exchanger tubing, *Mater. Eval.*, June, 811–812 (1986).
73. Neumaier, P., Testing heat exchanger tubes using eddy current techniques with computerised signal analysis, *Br. J. NDT*, September, 233–237 (1983).
74. Fisher, J. L., Remote field eddy current inspection, in *Metals Handbook*, Vol. 17, *Nondestructive Evaluation and Quality Control*, ninth edition, American Society for Metals, Metals Park, Ohio, 1989, pp. 195–201.
75. Atherton, D. L., Frey, P., and Guo, X., Remote field slit defect responses, *Br. J. NDT*, *36*, 4–7 (1994).
76. Stepinski, T., and Maszi, N., Conjugate spectrum filters for eddy current signal processing, *Mater. Eval.*, July, 839–844 (1993).
77. Product Literature, Inspection Software Limited, Swansea, UK.
78. Product Literature, Silver Wing Limited, Swansea, UK.
79. McMaster, R. C., ed., *Nondestructive Testing Handbook*, Vol. 1, *Leak Testing*, 2nd edition, American Society for Nondestructive Testing and American Society for Metals, Columbus, Ohio.
80. Anderson, G. L., Leak testing, in *Metal Handbook*, Vol. 17, *Nondestructive Evaluation and Quality Control*, ninth edition, American Society for Metals, Metals Park, Ohio, 1989, pp. 57–70.
81. Product Literature, M/s. Expando Seal Tools, Inc., Montgomeryville, Pa.

Bibliography

1. Mikulak, J., Viewpoints on quality, codes, conversions, and pipelines, *Welding Design & Fabrication*, March, 70–73 (1977).
2. Connor, L. P., ed., *Welding Handbook*, Vol. 1, *Welding Technology*, eigth edition, Chapter 11, Weld Quality, Chapter 12, Testing for Evaluation of Welded Joints, Chapter 13, Codes and Standards, American Welding Society, Miami, Fla., 1987.
3. Hingwe, A. K., compiler, *Quality Control Source Book—Application of QC to Ferrous Metalworking*, American Society for Metals, Metals Park, Ohio.
4. Betz, C. E., *Principles of Penetrants*, Magnaflux Corp. Chicago, and *Principles of Magnetic Particle Testing*, Magnaflux Corp, Chicago.
5. Krautkramer, J., and Krautkramer, H., *Ultrasonic Testing of Materials*, Springer-Verlag, New York.
6. Libby, H. L., *Introduction to Electromagnetic Nondestructive Test Methods*, Wiley-Interscience, New York.
7. McGonnagle, W. J., *Nondestructive Testing*, McGraw-Hill, New York.
8. *Radiography in Modern Industry*, 4th edition, Eastman Kodak Co., Rochester, N.Y.
9. Richardson, H. D., *Industrial Radiography Manual*, Government Printing Office, Washington, D.C., 1968. Reprinted in 1979 by the American Society for Nondestructive Testing.
10. Erickson, K. D., Defining the role of a certified visual inspector, *Welding J., Suppl., Nondestructive Examination*, October, 17–19 (1997).
11. Waker, K., Guide to liquid penetrant testing, *Welding J., Suppl., Nondestructive Examination*, October, 21–23 (1997).
12. Lebowitz, C. A., A primer on nondestructive examination methods for weld inspection, *Welding J., Suppl., Nondestructive Examination*, October, 29–31 (1997).
13. Emerson, W. F., Technology reinvents visual inspection. *Welding Design & Fabrication*, May, 31–32 (1995).
14. *Foundry Manage. Technol.*, Testing and Inspection of Castings Series Staff Reports Part 1—Visual and Dimensional Inspection, April 1991, p. 35; Part 2—Ultrasonic and Eddy Current Inspection, May 1991, p. 42; Part 3—Radiographic Nondestructive Testing, June 1991, p. 40; Part 4—Liquid Penetrant and Magnetic Particle Inspection, July 1991, p. 36.
15. *BSI Handbook 22: 1983 Quality Assurance*, British Standards Institution. UK.
16. Jackson, D., ISO 9000: Key to Europe's door, *Welding Design & Fabrication*, April, 59–60 (1992).
17. Kirwillian, A., The true cost of quality, *Welding and Metal Fabrication*, January/February, 5–8 (1987).
18. Welding Engineer Data Sheet No. 414—Effectiveness of nondestructive testing methods. *Welding Design & Fabrication*, February, 41 (1975).
18. Hayes, C., The ABC's of nondestructive weld examination, *Welding J.*, May, 46–51 (1997).
19. Weymueller, C. R., Ultrasonic testing for the fabricator, *Welding Design & Fabrication*, October, 25–33 (1994).
20. Weldments, brazed assemblies, and soldered joints, in *Metals Handbook*, Vol. 17, *Nondestructive Evaluation and Quality Control*, ninth edition, American Society for Metals, Metals Park, Ohio, 1989, pp. 582–609.
21. Ultrasonic inspection, in *Metals Handbook*, Vol. 17, *Nondestructive Evaluation and Quality Control*, ninth edition, American Society for Metals, Metals Park, Ohio, 1989, pp. 231–277.

CHAPTER 15

1. Sharma, D. D., Heat Exchanger Fabrication Techniques, Lecture Notes of Course No. 490-SPL, Energy Efficient Heat Exchangers Design, Continuing Education Department, University of Roorke, Roorke, India.
2. *Standards of Tubular Exchanger Manufacturers Association*, seventh edition, Tubular Exchanger Manufacturers Association, Inc., Tarrytown, N.Y., 1988.

3. *ASME Boiler and Pressure Vessel Code*, Section VIII, Division 1, Pressure Vessels, American Society of Mechanical Engineers, New York, 1992.
4. Rao, B. S. C., Quality assurance in fabrication of pressure vessels, in *Welding Engineering Handbook—Vol. 1* (S. Sundarrajan, S. Vijaya Bhaskar, and G. C. Amarnath Kumar, eds.), Welding Research Group, Radiant Publications, Secunderabad, India.
5. Weymueller, C. R., NDT builds safety into a nuclear plant, *Welding Design & Fabrication*, September, 54–57 (1982).
6. Peacock, G. A., Fabrication of thick plates, *Welding and Metal Fabrication*, June, 242–252 (1963).
7. Carpenter, O. R., and Floyd, C., Heat treatment of carbon and low alloy pressure vessel steel, *Welding Journal*, Research Suppl. (1957).
8. Davies, S., Equipment for boiler fabrication, *Welding and Metal Fabrication*, August, 306–309 (1969).
9. Ellis, D. J., and Gifford, A. F., Application of electroslag and consumable guide welding, *Welding and Metal Fabrication*, April, 112–119 (1973).
10. Yokell, S., *A Working Guide to Shell and Tube Heat Exchangers*, McGraw-Hill, New York, 1990.
11. Syal, P. K., *Fabrication of Heat Exchangers*, Specialised Publication, Cooperative Industries, Mumbai, India.
12. Allen, J. S., Fabrication of heat exchangers and specialised vessels, *Welding and Metal Fabrication*, July, 240–245 (1968).
13. Luthy, A., The role of welding in the fabrication of machines and equipment, *Brown Boveri Rev.*, *52*, 495–511 (1965).
14. Woodward, A. R., Howard, D. L., and Andrews, E. F. C., Condensers, pumps and cooling water plant, in *Modern Power Station Practice*, Vol. C, *Turbines, Generators, and Associated Plant* (D. J. Littler, E. J. Davies, H. E. Johnson, F. Kirkby, P. B. Myerscouh, and W. Wright, eds.), Pergamon Press, New York.
15. Singh, K. P., and Soler, A. I., *Mechanical Design of Heat Exchangers and Pressure Vessel Components*, Arcturus, Cherry Hill, N.J., 1984.
16. Bevevino, J. W., Tube to tubesheet welding techniques, *Chem. Eng. Prog.*, *70*, 71–73 (1974).
17. Committee on Submerged Arc Welding, Submerged arc welding, in *Metals Handbook*, Vol. 6, *Welding, Brazing, and Soldering*, ninth edition (E. F. Nippes, ed.), American Society for Metals, Metals Park, Ohio, 1983, pp. 114–151.
18. Yokell, S., Expanded, and welded-and-expanded tube-to-tubesheet joints, *Trans. ASME, J. Pressure Vessel Technol.*, *114*, 157–165 (1992).
19. Scott, D. A., Wolgemuth, G. A., and Aikin, J. A., Hydraulically expanded tube-to-tubesheet joints, *Trans. ASME, J. Pressure Vessel Technology*, *106*, 104–109 (1984).
20. Fisher, F. F., and Brown, G. J., Tube expanding and related subjects, *Trans. ASME*, 565–575 (1954).
21. Sonnenmoser, A., Expanded joints for austenitic steel tubes in feedheaters for BWR nuclear power station, *Brown Boveri Rev.*, *7/8–73*, 360–370 (19).
22. Dudley, F. E., Electronic control method for the precision expanding of tubes, *Trans. ASME*, 577–584, (1954).
23. Yokell, S., Heat exchanger tube-to-tubesheet connections, *The Chemical Engineering Guide to Heat Transfer, Volume I: Plant Principles*, Edited by Kenneth J. McNaughton, Hemisphere Publishing Corporation, McGraw-Hill Publications Co., New York, 1986, pp. 76–92.
24. Spencer, T. C., Mechanical design and fabrication exchangers in the United States, *Heat Transfer Eng.*, *8*, 58–61 (1987).
25. Cotton, H., Seal welding of heat exchanger tubulars by the metal arc process, *Br. Welding J.*, May, 250–257 (1963).
26. McIntyre, D. R., How to prevent stress corrosion cracking in stainless steels—Part I, in *The Chemical Engineering Guide to Corrosion Control in the Process Industries*, (Edr.) R. W. Greene, McGraw-Hill Publications Co., New York, 1986, pp. 4–7.
27. Brosilow, R., Making the most of tube-tubesheet joints, *Welding Design & Fabrication*, May, 54–56 (1976).

28. Slaughter, G. M. *Welding and Brazing of Nuclear Reactor Components*, AEC Monograph, Rowman and Littlefield, New York, 1964.
29. Franklin, H. N., Roper, D. R., and Thomas, D. R., Internal bore welding method repairs condenser leaks, *Welding J.*, December, 49–51 (1986).
30. Douglass, M., Feedwater heating systems, *Modern Power Station Practice*, Vol. C, *Turbines, Generators, and Associated Plant* (D. J. Littler, E. J. Davies, H. E. Johnson, F. Kirkby, P. B. Myerscouh, and W. Wright, eds.), Pergamon Press, New York, Chapter 3.
31. Lohmeier, A., and Reynolds, S. D., Jr., Carbon steel tube-to-tubesheet joints for high pressure feedwater heaters, *Westinghouse Engineer*, September, 138–143 (1966).
32. Viri, D. P., and Iceland, W. F., Clinch River modular steam generator tube-to-tubesheet and shell closure welding, *Welding J.*, July, 18–21 (1984).
33. ASM Committee on Shielded Metal Arc Welding, Arc welding of carbon steels: Shielded metal arc welding, in , *Metals Handbook*, Vol. 6, *Welding, Brazing, and Soldering*, ninth edition (E. F. Nippes, ed.), American Society for Metals, Metals Park, Ohio, 1983, pp. 73–244.
34. Designing and fabricating aluminum weldments, *Welding Design & Fabrication*, February, 53–62 (1977).
35. Danis, J. I., Material selection, fabrication and inspection of refinery heat exchangers, *Welding J.*, June, 25–30 (1986).
36. TIMET CodeWeld^{R} Titanium Tubing, TIMET, Denver, Colo.
37. *CODAP: French Code for the Construction of Pressure Vessels*, A SNCT, 1985.
38. Sonnenmoser, A., Design and operation of large high pressure feedheaters, *Brown Boveri Rev., 7/8–73*, 352–359.
39. Hudgell, R. J., and Tickle, H., Current practices for ultrasonic and radiographic examination of tubes, tubeplates, and tubeplate welds of tube bundles in heat exchangers, in *Developments in Pressure Vessel Technology—2, Inspection and Testing* (R. W. Nichols, ed.), Applied Science Publishers, UK, 1979, pp. 77–100.
40. Foster, B. E., and McClung, R. W., Study of x-ray and isotopic techniques for boreside radiography of tube-to-tubesheet welds, *Materials Evaluation*, July 1977, American Society for Nondestructive Testing, pp. 43–51.
41. Engle, J. P., Chemical cleaning of feedwater heaters, *Mater. Perform.*, July, 30–33 (1974).
42. Aldridge, M., Plate bending and forming, the choice between 3-roll and 4-roll bending rolls, *Welding and Metal Fabrication*, November, 555–566 (1977).
43. Trawsfynydd Power Station, Part 1: Heat exchanger fabrication, *Welding and Metal Fabrication*, September, 350–361 (1961).
44. Bode, C. F., Manipulators and positioners for welding, *Welding and Metal Fabrication*, January/February, 26–30 (1987).
45. Ganapathy, Welding engineer data sheet, *Welding Design & Fabrication*, October, 104–105 (1979).
46. Cold spinning dished ends, *Welding and Metal Fabrication*, January, 30–32 (1969).
47. Galletly, G. D., Plastic buckling of torispherical and ellipsoidal shells subjected to internal pressure, *Proc. Inst. Mech Eng., 195*, 329–345 (1981).
48. Vessel fabrication at Old Park, *Welding and Metal Fabrication*, November, 392–397 (1991).
49. Jilek, L., Technology of pressing large heads, *Welding and Metal Fabrication*, March, 50–53 (1987).
50. *Aluminum Brazing Handbook*, 4th edition, Aluminum Association, Washington, D. C., 1990.
51. Jones, N. H., Brazing: Its contribution to modern industry, *Welding and Metal Fabrication*, January, 4–9 (1964).
52. Shah, R. K., Brazing of compact heat exchangers, in *Compact Heat Exchangers—A Festschrift for A. L. London* (R. K. Shah, A. D. Kraus, and D. Metzger, eds.), Hemisphere, Washington, D.C., 1990, pp. 491–529.
53. Brazing, in *Welding Hand Book*, Vol. 2, eighth edition, American Welding Society, Miami, Fla., 1991, pp. 279–422.
54. Brazing, *Welding Design & Fabrication*, June (1993).

55. Schwartz, M. M., *Brazing*, ASM International, Metals Park, Ohio, 1987.
56. Shah, R. K., The art of brazing, in *Thermophysical Aspects of Manufacturing and Materials Processing*, Eds. R. K. Shah et al., Hemisphere Publishing Corporation, Washington, D.C., 1992, pp. 193–213.
57. Brooker, H. R., and Beatson, E. V., *Industrial Brazing*, Newnes-Butterworths, London, 1975.
58. Taylor, M. A., editor, *Plate-Fin Heat Exchangers, Guide to Their Specification and Use*, HTFS (Harwell Laboratory), Oxon, UK, 1980.
59. Brazing of aluminum alloys, in *Metals Handbook*, Vol. 6, *Welding, Brazing, and Soldering*, ninth edition (E. F. Nippes, ed.), American Society for Metals, Metals Park, Ohio, 1983, pp. 1022–1032.
60. Weymuller, C. R., How to choose filler metals, *Welding Design & Fabrication*, July, 33–39 (1984).
61. Birchfield, J. R., Paste fillers, automation take pain out of brazing, *Welding Design & Fabrication*, June, 78–80 (1980).
62. Singleton, O. R., A look at the brazing of aluminum—Particularly fluxless brazing, *Welding J.*, November, 843–849 (1970).
63. Brazing of stainless steels, in *Metals Handbook*, Vol. 6, *Welding, Brazing, and Soldering*, ninth edition (E. F. Nippes, ed.), American Society for Metals, Metals Park, Ohio, 1983, pp. 1001–1013.
64. Miller, F. M., How to choose nickel base filler metals for vacuum brazing, *Welding Design & Fabrication*, October, 87–88 (1977).
65. Harvey, J., The brazing of aluminum: Part 1, *Welding and Metal Fabrication*, September, 454–457 (1977).
66. Schultze, W., and Schoer, H., Fluxless brazing of aluminum using protective gas, *Welding J.*, October, 644–651 (1973).
67a. Boughton, J. D., and Roberts, P. M., Furnace brazing, a survey of modern processes and plant, *Welding and Metal Fabrication*, March, 85–92 (1973).
67b. Boughton, J. D., and Roberts, P. M., Furnace brazing—2, A survey of modern process and plant, *Welding and Metal Fabrication*, April, 121–138 (1973).
68. Winterbottom W. L., Process control criteria for brazing aluminum under vacuum, *Welding J.*, October, 33–39 (1984).
69. Patrick, E. P., Vacuum brazing of aluminum, *Welding J.*, October, 159–162 (1983).
70. Schmatz, D. J., and Winterbottom, W. L., A fluxless process for brazing aluminum heat exchangers in inert gas, *Welding J.*, October, 31–38 (1983).
71. ANSI/AWS C3.7-93, Specification for Aluminum Brazing, American Welding Society, Miami, Fla.
72. Tennenshouse, C. C., Control of distortion during the furnace cycle, *Welding J.*, October, 701–704 (1971).
73. Hatch, J. E., Properties of Commercial Wrought Alloys, in *Aluminum: Properties and Physical Metallurgy*, American Society for Metals, Metals Park, OH, 1984, pp. 354–355.
74. Swaney, W., Trace, D. E., and Winterbottom, W. L., Brazing aluminum automotive heat exchangers in vacuum: Process and materials, *Welding J.*, May, 49–57 (1986).
75. Terrill, J. R., Cochran, C. N., Stokes, J. J., and Haupin, W. E., Understanding the mechanisms of aluminum brazing, *Welding J.*, December, 833–839 (1971).
76. Cooke, W. E., Wright, T. E., and Hirschfield, J. A., Furnace brazing of aluminum with a noncorrosive flux, *Welding J.*, December, 23–28 (1978).
77. McCubbin and Lemay, R., A modification of the NOCOLOK™ Flux Brazing Process to Produce Superior Corrosion Resistance or Black Surfaces, SAE-900408, pp. 416–425.
78. Ashburn, L. L., Furnace design considerations for aluminum brazing under vacuum, *Welding J.*, October, 45–54 (1983).
79. Brazing of heat resistant alloys, in *Metals Handbook*, Vol. 6, *Welding, Brazing, and Soldering*, ninth edition (E. F. Nippes, ed.), American Society for Metals, Metals Park, Ohio, 1983, pp. 1014–1021.
80. Lindsay, L. B., and Wireman, D. F., Continuous hydrogen furnace brazing of aircraft heat exchangers, *Welding J.*, October, 737–739 (1975).

81. Amato, I., Cappelli, P. G., and Fenoglio, G., Brazing of stainless steel heat exchangers for gas turbine applications, *Welding J.*, October, 338-s–343-s (1975).
82. Welding Engineer Data Sheet No. 493—Selection guide for brazing filler metals, *Welding Design & Fabrication*, March, 82 (1982).
83. Lane, J. W., and Brennan, D. T., Improved solder alloy enhances auto radiators, *Welding J.*, October, 41–45 (1984).
84. Mill welds thin wall aluminum radiator tubes at 600 fpm, *Welding J.*, October, 52 (1982).
85. Soldering, in *Metals Handbook*, Vol. 6, *Welding, Brazing, and Soldering*, ninth edition (E. F. Nippes, ed.), American Society for Metals, Metals Park, Ohio, 1983, pp. 1071–1101.
86. Webb, R. L., and Farrell, P. A., Improved Thermal and Mechanical Design of Copper/Brass Radiators, SAE-900724, pp. 737–748.
87. Mitchell, W. A., Statistical treatment of laboratory data for ASTM D 1384-70, using soft solder, in *Engine Coolant Testing: State of the Art, ASTM STP 705* (W. H. Ailor, ed.), American Society for Testing and Materials, Philadelphia, 1980; pp. 220–232.
88. Haddon, R. C., Ultrasonics dispenses with need for soldering flux, *Welding and Metal Fabrication*, January/February, 50–54 (1979).
89. Gunkel, R. W., Solder aluminum joints ultrasonically, *Welding Design & Fabrication*, September, 90–95 (1979).
90. Schuster, J. L., and Chilko, R. J., Ultrasonic soldering of aluminum heat exchangers, *Welding J.*, October, 711–717 (1975).
91. Hunicke, R. L., Ultrasonic soldering pots for fluxless production soldering, *Welding J.*, March, 191–194 (1976).
92. Denslow, C. A., Ultrasonic soldering equipment for aluminum heat exchangers, *Welding J.*, February, 101–107 (1976).
93. Jenkins, W. B., Fluxless soldering of aluminum heat exchangers, *Welding J.*, January, 28–35 (1976).
94. Naruki, K., and Hasegawa, Y., Corrosion testing of furnace and vacuum brazed aluminum radiators, in *Engine Coolant Testing: State of the Art, ASTM STP 705* (W. H. Ailor, ed.) American Society for Testing and Materials, Philadelphia, 1980, pp. 109–132.
95. Hattori, T., and Sakamoto, A., Pitting corrosion property of vacuum brazed 7072 clad aluminum alloy, *Welding J.*, October, 339-s–342-s (1982).
96. McNamara, P., and Singleton, O. R., Zinc distribution in vacuum brazed Alclad brazing sheet, *Welding J.*, January, 7-s–11-s (1979).
97. Scott, C. A., A new cladding alloy for coolantside corrosion protection of vacuum brazed aluminum radiators, in *Engine Coolant Testing: Second Symposium, ASTM STP 887* (R. E. Beal, ed.), American Society for Testing and Materials, Philadelphia, 1986, pp. 27–43.
98. Engstrom, H., and Gullman, L. O., A multilayer clad aluminum material with improved brazing properties, *Welding J.*, October, 222-s–226-s (1988).
99. Falke, W. L., Schwaneke, A. E., and Lee, A. Y., Corrosion of solders in automobile coolant systems, *Welding J.*, October, 460-s–465-s (1973).
100. Park, K. H., Solder bloom corrosion analysis based on field survey data, potential causes, and resolution, in *Engine Coolant Testing: Second Symposium, ASTM STP 887* (R. E. Beal, ed.), American Society for Testing and Materials, Philadelphia, 1986, pp. 123–143.
101. Barkley, J. M., Wiggle, R. R., and Winterbottom, W. L., The development and field service history of Ford automotive aluminum radiators, in *Engine Coolant Testing: Second Symposium, ASTM STP 887* (R. E. Beal, ed.), American Society for Testing and Materials, Philadelphia, 1986, pp. 11–26.

Suggested Reading

1. Illingworth, A., Testing and inspection, in *Heat Exchanger Design Handbook*, (E. U. Schlunder, editor-in-chief), Vol. 4, Hemisphere, Washington, D. C., 1983 Section 4.7.
2. McGill, W. A., and Weinbaum, M. J., Alonized heat exchanger tubes give good high temperature service, *Mater. Perform.*, January, 16, 18–20 (1978).

3. Haslinger, K. H., and Hewitt, E. D., Leak Tight, High Strength Joints for Corrosion Resistant Condenser Tubing, ASME Paper No. 83-JPGC-Pwr39, ASME, New York.
4. Moorehead, A. J., and Red, R. W., Internal bore welding of 2.25Cr-1Mo steel tube-to-tubesheet joints, *Welding J.*, January, 26–36 (1980).
5. Dawson, R. J., Silver brazing copper and its alloys, *Welding and Metal Fabrication*, February, 54–59 (1971).

Index

18Cr-2Mo, 754
18-SR, 754
1925hMo, 845
20Mo-6, 755
254 Smo, 755
25-6Mo, 755
26-1S, 754
29Cr-4 Mo, 754
29Cr-4 Mo-2Ni, 754
3.5% nickel steels, 837
36% Ni-Fe alloy, 837
4.5% Mo superaustenitic steels, 792
5% nickel steel, 837
8% nickel steel, 837
Accumulation of methane, 623
Accuracy of the Bell-Delaware method, 289
Acid cleaning of fouling, 412
Acid dosing, 416
Acoustic emission
  emission types and characteristics, 935–936
  Kaiser effect, 936
  sources, 934–935
  factors influencing, 937
Acoustic emission testing (AET), 936–937
  applications, 938–939
  for leak detection, 939
  merits, 939
  principle, 934
  reference code, 936
[Acoustic emission testing (AET)]
  signal analysis, 937
    ring-down counting method, 937
  testing instrumentation, 936–937
  written procedure, 936
Acoustic resonance
  acceptance criteria,
    sound pressure level (SPL), 448
    turbulent buffeting, 448
    vortex shedding, 446–448
  acoustical Strouhal number, 447
  description, 441–443
  tube solidity effect on sound velocity, 443–444
  excitation mechanisms, 446
  frequency, 444–445
  standing waves, 443–444
Acoustical holography, 933
Added mass, 433, 462
Added mass co-efficient, 433, 462, 463
Advantages of compact heat exchangers, 12
Air bumping, 403, 413
Air coolers, 217
Air cooled heat exchangers (ACHE)
  air cooler data sheet, 226
  airside pressure losses, 223
  air velocity, 223
  air vs. water cooling, 217–218
  API Standard 671, 219, 220
  capital vs. running cost, 223

[Air cooled heat exchangers (ACHE)]
design aspects, 221
design procedure,
sizing, 224–226
fan design, 222
as per API 671, 219
fin material, 218
forced draft vs. induced draft, 220–221
header boxes, 218, 219
in low temperature environments, 220
temperature control, 220
orientation of tube bundle, 219
recirculation, 221
tube bundle construction, 218–219
tube bundle-fin geometry, 218
AL-6X, 755
AL-6XN, 755
AL904L, 755
Alclad (*see* aluminium clad alloys)
Alkali dosing, 416
Alloys for subzero temperatures (*see also* 9% nickel steel)
ASME code requirements, 834
aluminum, 834–835
austenitic stainless steel, 837–838
welding considerations, 840–841
carbon steels and alloy steels, 836
9% nickel steel, 838–840
copper and copper alloys, 836
crystal structure, 833
ductile-brittle-transition-temperature (DBTT), 832–833
fabrication of cryogenic vessels, 838
nickel and high-nickel alloys, 836
notch toughness, 833–834
titanium and titanium alloys, 836
Aluminum brazing
alloys, 1014
filler metals, 1015
fluxing, 1015–1016
methods, 1016
precleaning, 1014
principle, 1013
sheet, 1015
surface oxide removal, 1014
temperature control, 1013
Aluminium for low temperature applications, 835
Allowable stress, 503
Alonized, 635
Alonizing, 775
Aluminum and aluminum alloys,
alclad alloys, 774
alloy and temper selection, 774
[Aluminum and aluminum alloys]
diffused steels, 775
classification of wrought alloys, 767–769
for heat exchanger applications, 766
heat exchanger tubes, 770
limitations, 767
pipes, bar, rods, extrusions, and forgings, 770
plates and sheets, 770
product forms and shapes, 769
properties, 766–767
temper designation, 769
wrought alloy designations, 767
Aluminum alloy designation
1xxx series, 767
2xxx series, 767–768
3xxx series, 768
4xxx series, 768
5xxx series, 768
6xxx series, 768–769
7xxx series, 769
Aluminum clad alloys, 774
Aluminium, corrosion of,
chemical nature of aluminum: passivity, 770
in cooling water system, 774
corrosion prevention and control measures, 774–775
in diesel engine cooling water system, 774
forms of corrosion, 771–774
resistance to waters, 771
surface oxide film, 770
Aluminium welding
corrosion resistance of welded joints, 777
filler metals, 777
hot cracking, 776
joint design, 777
joint geometry, 777
parameters affecting welding, 775–776
plate cutting and forming, 777
preheating, 777
surface preparation, 776
welding methods, 777–779
Aluminized (*see* Alonized)
Aluminum bronzes (*see* Copper-Aluminum alloys)
Aluminum dip brazing, 1016
Ammonia cracking, 617
Ammonia in cooling water, 644
Angle tube protectors, 610
Anode, 580
Anodic polarization, 584
Anti-oxidation additives, 402
Antiscalants, 416
API 913

Argon-oxygen decarburization (AOD), 709, 754
Arrhenius law, 402
ASME Code, Section II, 670, 1004
ASME Code, Section III, 10, 11, 13, 14, 15, 424, 427, 428, 430, 435
ASME Code, Section V, 919, 921, 929, 932, 937, 940
ASME Code, Section VIII, 81, 482, 484, 494, 496, 497, 498, 501, 514, 525, 526, 527, 528, 529, 533, 534, 540, 541, 542, 554, 555, 557, 558, 559, 699, 702, 864, 865, 870, 882, 885, 894, 896, 929, 932, 940, 941, 945, 958, 987, 1024
ASME Code, Section IX, 867, 884–885, 888, 901, 924
ASME Code, weld joint types, 505
Assembly of channel/end closures, 993–994
ASSET test, 773
ASTM A 353 alloy steel, 837
ASTM A 357 steel, 836–837
ASTM A 553 steel, 837
ASTM grain size, 833
ASTM salt spray Test B-117, 1038
ASTM Test A262 C, 760
ASTM Test B154, 620, 790
ASTM Test E208, 672
ASTM Test E399, 672
ASTM Test E813, 672
ASTM Test G30, 760
ASTM Test G 34, 773
ASTM Test G36, 760
ASTM Test G 47, 773
ASTM Test G 48A, 760
ASTM Test G 66, 773
Atmospheric corrosion, 590
Attachment of expansion joint to shell, 966
Attachment of microorganisms, 403
Austenitic stainless steel,
  alloy types, 728
  alloy development, 726
  alloying elements, 728
  composition, 728
  cryogenic applications, 727
  elevated temperature strength, 727–728
  in heat exchanger applications, 727
  mechanical properties, 727
  properties, 727
  type 304 stainless steel, 728–729
  type 310 stainless steel, 729
  type 316 stainless steel, 729, 753
  type 321 stainless steel, 729
  type 347 stainless steel, 729
  types of, 726
Austenitic stainless steel
  corrosion resistance of,
  forms, 730–738
  mechanism of, 729
  passive vs. active behavior, 730
  resistance to chemicals, 730
  sigma phase, 730
  stainless steel in sea water, 730
  stress corrosion cracking in boiling water reactors, 735
  welding,
  benefits of ferrite in weld metal, 743
  chromium equivalent, 743
  considerations, 742
  constitution diagram, 743
  control of distortion, 748–749
  corrosion resistance of welds, 752
  decay, 736, 737
  De Long diagram, 744, 745
  dissimilar metals welding, 751–752
  ferrite determination, 745–747
  fumes, 749
  microfissuring, 742–743
  mock-up test, 745
  nickel equivalent, 743
  porosity, beginning and end, 750
  postweld cleaning, 752
  postweld heat treatment, 750–751
  practices to improve weld performance, 749–750
  procedure variation, 744
  roof fluxing, 750
  Schaeffler diagram, 743, 745
  sensitization, 748, 841
  underbead cracking, 750
  variable weld penetration, 747–748
  WRC 1992 constitution diagram, 744, 745
Authority and responsibility, 866
Automotive radiators,
  durability tests, 1037–1038
  tests for corrosion resistance, 1038
AWS Brazing and Soldering documents, 1026
Axial rigidity of the shell, 514
Axial rigidity of the tube bundle, 514

B-Jac program
  for air cooled exchanger (AEROTRAN), 134
  for mechanical design (TEAMS), 489
  for shell and tube exchanger (HETRAN), 133
Bacteria concentration, 403
Baffles
  classification, 234–235
  disk and doughnut baffle, 238
  EGG-CRATE-GRID™ support, 242

[Baffles]
Grimmas baffle, 242
longitudinal baffles, 240–241
NESTS™ baffles, 242
NTIW, 238–240
orifice baffle, 238
RODbaffles, 241
transverse
baffle spacing, 235–236
baffle thickness, 236
double segmental baffles, 236–237
orientation of baffles, 236
segmental baffles, 235
triple segmental baffles, 237
window baffles, 238
Baffle type damage, 460
Baffles drilling, 967
Baking on effect, 396
Balanced exchanger, 14
Bei(x), modified Bessel function of the first kind, 514
Bellows, 557
design,
bellow materials, 563
limitations, 563–565
shapes, 563
Bell-Delaware method (for shellside design)
auxiliary calculations, 277–280
central baffle spacing, 276–277
crossflow velocity, 280
evaluation of geometric parameters, 275
input data, 276
heat transfer coefficient, 283–284
heat transfer correction factors, 277–283
pressure drop, 284–287
correction factors, 277–283
shellside parameters, 276
Ber(x), modified Bessel function of the first kind, 514
Beta phase attack, 608
Bimetallic cell, 582
Bimetallic corrosion (*see* Galvanic corrosion)
Biocide, 403, 417, 418, 419, 625–626
Blast cleaning of fouling, 410
Block heat exchanger, 828
Bolted flanged joint design,
construction of bolted flange joints, 540
design procedure,
bolting design, 543–545
flange design, 545–554
gasket design, 541–543
flanged joint types, 539–540
Borescope, 898
Boundary layer disturbances, 189
Braze stopoffs, 1012
Brazing,
advantages, 1000–1001
of aluminum, 1013–1020
of cobalt base alloys, 1020
codes and standards, 1026
control of distortion during, 1013
definition and description, 1000
disadvantages, 1001
filler metals, 1002–1004
fixturing, 1006
fluxing, 1005–1006
heating rate, 1012
of heat resistant superalloys, 1020
inspection of brazed joint, 1025
leak testing, 1025
methods, 1005–1012
of nickel base alloys, 1020
post braze cleaning, 1012
precleaning, 1004
process control, 1012–1013
quality of the brazed joints, 1023
quality system in brazing, 1022–1023
scale and oxide removal, 1005
of stainless steel, 1021
temperature, 1012
time, 1012
Brazing filler metals, 1002–1003
Brazing furnaces, 1009–1010
Brazing methods
controlled atmosphere brazing, 1011
dip brazing, 1007–1008
furnace brazing, 1008–1010
torch brazing, 1006–1007
vacuum brazing, 1011–1012
Brush and cage system, 414
Bypass lanes, 261–265

C and S technique (*see* Crown and segment technique)
Calibration of measuring instruments, 868
Capacity rate ratio, 14
Carbide precipitation in nickel welding, 808
Carbon dioxide in cooling water, 644
Carbon-manganese steels, 714–715
Carbon-manganese-molybdenum steels, 714, 715
Carbon steels
corrosion resistance, 710–711
fabrication, 711–713
hardness limitation for refinery service, 712
in feedwater applications, 710
in refinery operations, 710
killed steels, 709
for pressure vessels, 710
product forms, 710

[Carbon steels]
rimmed and capped steels, 709
semi-killed steels, 709
weldability considerations, 712
welding defects, 713
welding electrodes, 712–713
welding processes, 712
Carryover leakage, 336
Cast iron, 708
Cathode, 580
Cathodic polarization, 584
Caustic cracking, 617
Caustic scrubbing, 402
Cell density of regenerator matrix, 317
Ceramics
drawbacks, 832
engineering ceramics, 832
favourable properties, 831–832
heat exchangers, 832
Ceramic bayonet tube heat exchanger, 340
Ceramic heat exchanger, 316–317
Ceramic-metallic hybrid recuperator, 317
Characteristic flow length, 189
Characteristics of instability, 437
Chemical brighteners, 1019
Chemical cleaning of scales, 420–421
Chemical reactants, 416
Chen's Strouhal map, 430, 431
Chloride cracking, 617
Chromate inhibitor, 631
Chromium carbides precipitates, 606
Chromium-molybdenum steel, 718–724
Chromium-molybdenum steels,
advanced 3Cr-Mo-Ni steels, 724
applications, 720
composition and properties, 718
creep strength, 720
filler metal, 721
joint design, 720
joint preparation, 720
Larson-Miller tempering parameter, 723–724
modified 9Cr-1Mo Steel, 724
post weld heat treatment, 724
preheat, 720
reheat cracking, 724
temper embrittlement susceptibility
CVN impact properties, 722
step cooling heat treatment, 722
temper embrittlement of weld metal, 723
welding metallurgy, 720
welding processes, 721
Circulation to clean fouling, 412
Cladding (*see also* Explosive cladding; Stainless steel strip cladding),
advantages, 842
ASME code requirements in using clad material, 852–853
cladding thickness, 842
failure of clad material, 852
inspection of overlays, 846
methods of cladding,
explosive cladding, 844, 847–848
loose lining, 842–843
resistance cladding, 843
roll cladding, 846–847
thermal spraying, 843
using plug welding, 843
weld dilution, 844
weld overlaying, 745, 843
purpose, 842
Clad bond strength, 852
Classification of shell and tube heat exchanger
design features, 251
differences between TEMA classes R, C and B, 255–256
fixed tubesheet exchangers, 252–253
floating head exchangers, 253–255
selection, 255
TEMA classification, 255
U-tube exchangers, 253
Clip-on protectors, 610
Cobalt 60, 911
Codes
A.D. Merkblatter, 494
ASME Code, 490–493
Div. 1 vs div. 2, 492–493
Section VIII, div. 1, 492
Section VIII, div. 2, 492
BS 5500, 595–596
CODAP Code, 494
definition, 489
Coil inserts, 374
Coiled tube heat exchanger, 2–4
Colburn j factor, 192
Cold blow, 306
Cold cracking,
defined, 691
fisheye cracking, 700
hydrogen induced cracking, 692–693
lamellar tearing, 696–700
underbead cracking, 696
weldability tests, 706
Collision type damage, 460
Collocation method for Regenerator design, 320

Combined-thickness approach for clad plates, 503
Compact heat exchangers (*see also* Air cooled heat exchangers; Fin efficiency; j and f correlation; Plate-fin heat exchanger; Radiators, rating of; Sizing; Tube-fin heat exchanger),
advantages, 12
characteristics, 159–160
constructional types, 160
plate-fin, 169–177
regenerators, 160
tube-fin, 160–169
j and f factor correlation, 192–201
Complexing agents, 416
Concentration cell, 582
Condensers, 19, 165
Contact resistance, 189–192
Contained fluid mass, 433
Coolant fill test, 1038
Cooling inclusions, 597, 655
Cooling tower, 11
Cooling water corrosion,
causes of corrosion in, 640–646
cooling water systems
once-through, 646–647
open recirculating, 647
closed recirculating, 647
vs. corrosion, 649–650
corrosion control methods, 648–649
corrosion processes, 642
forms, 651–652
of individual metals,
aluminum, 650
austenitic stainless steel, 651
copper and its Alloys, 650
steel, 651
superferritic, 651
superaustenitic, 651
titanium, 651
Langelier saturation index (LSI), 642
materials for condenser tubes, 652
prevention of scale, 642
scale deposition, 641
scaling control, 642
Cooling water fouling,
biological fouling, 417
cleaning of scales, 420–421
in closed recirculating systems, 418
control of scale formation, 419–420
influence of surface temperature on, 418
iron oxide removal, 421
in once through system, 418
online chemical control of foulants, 418–419
[Cooling water fouling]
in open recirculating system, 418
particulate fouling, 418
scaling, 417
Cooperative research programs
HTFS, 158–159, 269, 430
HTRI, 158, 269, 430
Copper alloys, corrosion of,
ammonia attack, 800
biofouling, 801
condensate corrosion, 800
in cooling water, 791
copper and aquatic life, 792
corrosion resistance, 784
dealuminification, 788
denickelification, 788
deposit attack, 790
dezincification, 787–788
exfoliation, 791–792
forms of corrosion, 784–790
hot spot corrosion, 790
inhibited alloys, 788
relative resistance, to stress corrosion, 789
resistance to sea water, 791
snake skin, 790
steamside stress corrosion, 789–790
sulfide attack, 791
Copper and copper alloys designation
admiralty brass, 781–782
aluminum brass, 782–783
aluminum bronzes, 782
brasses, 781
copper-nickels, 782–784
fire refined copper, 781
high copper alloys, 781
high purity coppers, 780
inhibited admiralty brass, 782
leaded brasses, 781
Muntz metal, 781
naval brass, 782
oxygen-free coppers, 781
phosphorous deoxidised copper, 781
silicon bronzes, 782
tin brasses, 781
Copper alloys physical properties
designation of copper alloys, 779–784
copper casting alloys, 780
in heat exchanger applications, 780
product forms, 784
in steam generation, 780
wrought alloys, 780–784

Copper alloys welding
dissimilar metal welding, 796–797
buttering, 797
interalloying, 797
factors affecting weldability, 792–793
of copper alloys, 794–796
of high copper alloys, 794
PWHT, 796
Copper Development Association, 779
Copper-nickel, 10%, 783
Copper-nickel, 30%, 783–784
Copson curve, 733
Core mass velocity equation, 212–213
Correction of nonconformities, 867
Corrosion (*see also* Cooling Water; Corrosion fatigue; Corrosion resistance of individual metals; Crevice; Dealloying; Dezincifiction; Erosion-corrosion; Fretting; Hydrogen damage; Intergranular; Inhibitors; Material selection; Microbiologically influenced; Pitting; Stress corrosion cracking; Uniform).
behavior of passive alloys, 586
brazed joint, 1034–1036
corrosion kinetics, 584
electrochemical, 581–583
factors affecting, 586–588
factors that favor localized attack, 589
forms of corrosion, 589
of iron in aerated aqueous system, 581–582
mechanism, 580–582
passivation, 586
polarization, 584–586
reasons for corrosion studies, 579–580
soldered joint, 1037
uniform corrosion vs. localized corrosion, 579
Corrosion allowances, 146–147, 367, 592, 630
Corrosion coupons, 638
Corrosion fatigue
of aluminum, 622, 773–774
of copper, 622, 791
definition, 621
of ferrous alloys, 622
influencing factors, 621–622
intensity, 622
prevention, 622
relationship with stress corrosion, 622
of titanium, 815
of various metals, 622
of welded joints, 622
Corrosion inhibitors, 649
Corrosion monitoring
approaches, 638
benefits, 637–638
[Corrosion monitoring]
limitations, 640
offline techniques, 639
online techniques, 638–639
requirements for success of, 640
techniques, 638
Corrosion prevention and control
principles of, 627–628
by proper design, 628–630
modification of environment, 630
use of inhibitors (*see* Inhibitors)
use of corrosion resistant alloys, 630–633
bimetal concept
cladding, 633
duplex tubing, 634
protective coatings, 634–635
surface treatment, 635
electrochemical protection, 635–637
cathodic protection, 635–636
sacrificial anode, 635
impressed current method, 636
anodic protection, 637
passivation, 637
in cooling water system, 647–649
Corrosion resistance
of aluminum, 771–775
of carbon steel, 710–711
of copper, 784–792
of duplex stainless steel, 760
of austenitic stainless steels, 729–738
of nickel, 802–804
of superferritic stainless steel, 756–757
of superaustenitic stainless steel, 763
of titanium, 814–817
of zirconium, 823
Corrosion tests of tubes, 690
Corrosion of weldments, 626–627
Corrugated surfaces, 381
Counterflow exchanger, 14
Creep embrittlement (*see* Temper embrittlement)
Creep resistant steels (*see* Chromium-molybdenum steels)
Crevice corrosion
of aluminum, 773
control, 604–605
in cooling water, 652
critical crevice corrosion temperature, 605
description, 603
locations prone for, 603–604
mechanism, 603
vs. pitting corrosion, 604
prediction, 605
of stainless steels, 732–733

[Crevice corrosion]
susceptible alloys, 603
of titanium, 815
of zirconium, 823
Critical crevice corrosion temperature (CCCT), 602, 605, 732
Critical damping ratio, 433, 467, 468
Critical pitting corrosion temperature (CPT), 731
Critical velocity, 437 (*see also* Threshold velocity)
Cross contamination, 352
Crossflow exchanger, 14–16
Crossflow velocity, 449, 453–455
determination of, 290–291
Crown and segment (C and S) technique, 999
Cryogenic gas liquefaction system, 18
Cryogenic separation processes, 304
Crystallization fouling (*see* Precipitation Fouling)
Cupronickel alloys (*see* Copper-nickels)
Curie temperature for nickel, 802
CVN test, 672
Cylindrical shell under internal pressure, 533–534, 535

Damping, determination of, 466
for gases, 467, 468
for liquids, 467, 468
Dealloying,
of copper, 787
description, 607, 787
influencing factors, 607
prevention, 608
Debris filter (*see* Upstream filtration)
Deflection equation for tubesheet, 514
Delaware method (*see* Bell-Delaware method)
Delayed cracking (*see* cold cracking)
Deposit analysis, 408
Depressants, 417
Desalting, 402
Design methods, 502–503
Design criteria, 503
Design problem (*see* sizing)
Design specifications, drawings, design calculations, 866
Design temperature, 22, 506
Design-by-analysis, 503
Design-by-rule, 503
Detuning effect, 454
of tubes, 454
Dezincification (*see also* Dealloying),
in cooling water, 652
influencing factors, 608
prevention of, 608
types, 607
Differential aeration cell, 582
Differential temperature cells, 582–583
Digitization of radiographs, 920
Dimensional tolerance tests of tubes, 690
Dip brazing
brazing procedure, 1007
choice of flux, 1007
flux bath, 1007–1008
flux pot, 1007
heating means, 1007
immersion time, 1007
limitations, 1008
preheating the assemblies, 1007
quality control, 1023
scum and sludge removal, 1008
ventilation, 1008
Direct contact type heat exchanger, 11
Directional property of aluminium, 772
Discontinuities
in brazed joint, 1023–1025
in soldered joint, 1034
Discontinuity stresses, 502
Disk and doughnut heat exchanger design, 291–296
Disk type rotary regenerator, 310
Dispersants, 403, 417, 419
Displacement leakage (*see* Carryover leakage)
Dissolved gases in cooling water, 643
Distortion agents, 403, 416
Divided-flow shell (*see* TEMA G Shell)
Documentation, 868
Double pipe heat exchanger, 2
Double segmental baffles, 454
Double wall single image technique, 913
Doubly enhanced surfaces, 381
Drag force, 429
Drains and vents, 249
Drilling and roding of tubes, 409
Drum type rotary regenerator, 310
Dummying of tubes, 453
Dummy tubes, 265
Duplex stainless steels
composition, 758–759
corrosion resistance, 760
corrosion tests, 760
NDT of welds, 762
process applications, 760
weldability problems, 760–761
balancing the phases, 761
heat input, 761
liquidation cracking, 761
welding methods, 760
welding practices, 761

E-Brite 26-1, 754
Economic benefits of regeneration, 314
Eddy current testing,
  application, 939
  ASTM specification for, 940
  automated tube inspection system (ATIS), 947-948
  calibration, 945
  inspection of ferromagnetic tubes
    magnetic flux saturation method, 944-945
    remote field slit eddy current testing, 945-947
  inspection of tube interior, 944-945
  limitations, 947
  operating variables, 942-944
  principle, 940
    probes, 940-941, 943
  configuration, 941
  recent advances in, 947
  signal processing, 941-942
  test equipment, 941
  test frequency, 942-943
  testing of weldments, 945
  tubesheet diagram for windows, 947-948
  written procedure, 940
Edge effect, 943
Effect of minor elements on nickel welding, 805
Effects of pH,
  on corrosion, 588
  on cooling water corrosion, 645
Effective tube mass, 433
Electrolyte, 580
Electrostatic scale controller cum preventer, 419-420
Elements of brazing,
  brazing methods, 1006-1012
  filler metal selection, 1002-1004
  fixturing, 1006
  fluxing, 1005-1006
  joint design, 1001-1002
  post braze treatment, 1012
  precleaning, 1005
  surface preparation, 1005
Embossed-panel (*see* Panelcoil heat exchanger)
End closures and formed heads design,
  conical/toriconical cover, 536, 538
  ellipsoidal cover, 535, 537
  flat cover, 535, 537
  hemispherical cover, 535, 538
  torispherical cover, 535-536, 538
End ring to weld tubesheet to shell, 970
Enhanced surface cavities, 389
Equivalent bolting pressure, 519
Equivalent design pressure, 523
Erosion-corrosion,
  of aluminum, 773
  cavitation, 611-612
  in cooling water, 652
  condenser tube failure, 609
  control, 612-614
  of copper, 788
  description, 608
  erosive wear, 609
  influencing parameters, 609
  impingement Attack, 610-611
  pattern, 609
  seals for plugging leaking tubes, 613
  TEMA guidelines, 610-611
  of titanium, 815
  tube inserts, 613
Ethylene diaminetetra acetic acid (EDTA), 418
Evans diagram, 585
Evaporators, 164
EverFin-40 (Furukawa Electric) fins, 390
Exchangers for air conditioning and refrigeration, 164-165
EXCO test, 773
Exfoliation corrosion
  of aluminum, 773
  of copper, 791-792
Expansion joints
  classification of, 555-557
    bellows, 556-557
    formed head, 555-556
  design
    bellows, 563-565
    formed head, 557-563
  fatigue life, 564
  flexibility, 555
Expert system, 300
Explosive bonding (*see* Explosive cladding)
Explosive cladding
  angular cladding, 847
  inspection of joint quality, 848-849
  parallel cladding, 847
  processing of clad steel plates, 849-852
    forming, 850
    welding, 850-852
  tube-to-tubesheet welding, 847-848
    end effect, 848
    plug welding, 848
  welding geometries, 847
Extended surface heat exchanger, 10, 159, 376-378
Extension to other shells and geometry, 289-290
External circuit, 580
External lowfin tubes, 378

F, parameter for elastic restraint of the tubesheet, 515, 516
Fabrication of shell and tube exchanger (*see also* Rolling-in process; Tube bundle assembly; Tube-to-tubesheet joining methods; Tube-to-tubesheet joint welding)
details of manufacturing drawing, 959–970
hydrostatic testing, 995–996
making of certificates, 997
nitrogen filling, 996
preparation for shipment, 996
shop floor practice, 959
stages of fabrication, 960–997
flow chart, 961
stamping of vessel, 996
Fatigue analysis, 494
Ferritic stainless steels,
conventional types 752–753
new and old types, 753
Ferrite, in duplex stainless steels, 747
Ferrite gauges, 745
Ferrous sulphate dosing, 649
Fill and soak cleaning of fouling, 412
Final inspection and test approach, 891
Fin efficiency, 201–206
Fill factor, 943
Fin-fans (*see* Air coolers)
Fin length, 201
Finned tubes with surface modifications, 189
Fired systems, 19
FIV (flow induced vibration), 423
Fixed bed regenerators (*see also* Regenerators)
checkers, 308
merits, 309
settings, 308
shape, 307
size, 308
surface geometries, 309
Fixed matrix, 10
Flame soldering (*see* Torch soldering)
Flange moments, 546
Flange thickness, 546
Flexible fibrescopes, 898
Floating head
with backing device, 254
externally sealed, 254
outside packed, 254
pull through, 254
Flocculating agent, 417
Flow area goodness factor, 387
Flow excursion, 413
Flow induced vibration (FIV)
approaches to, analysis, 427
[Flow induced vibration (FIV)]
dynamical behaviour of tube arrays, 425–426
empirical nature of, 427–428
evaluation procedure, 449–451
prevention guidelines, 451–455
failure mechanisms, 425
flow induced vibration mechanisms,
acoustic resonance, 425
fluid elastic instability (FEI), 425
turbulent buffeting, 425
vortex shedding, 425
hydrodynamic forces, 426
mechanisms vs. flow mediums, 427
possible damaging effects, 424
principle, 423–424
probable regions of tube failure, 424–425
tube response curve, 425
Flow periodicity (*see* Vortex shedding)
Flow reversibility, 41–43
Fluid bed regenerative heat exchanger, 338
Fluid damping forces, 436
Fluid elastic instability
acceptance criteria, 441
analytical model, 438
Connors analysis, 437–438
design recommendations, 440–441
fluid elastic forces, 436–437
instability criteria, 440–441
quasi-static model,
stability diagrams, 441
unsteady model,
displacement mechanism, 439
velocity mechanism, 440
unsteady model, 438, 439–440
Fluid physical properties, 209
Fluid properties and allocation factors, 250–222
Fluidized bed waste heat recovery heat exchanger, 416
Fluid-structure coupling, 425, 437
Fluoroscopy, 920
Flux removal test, 1023
Formed head expansion joint design, 562–563
Formed membrane (*see* Bellows)
Forming of heads and closures, 998–1000
Fouling (*see also* Cooling water fouling; Fouling prevention and control)
costs of fouling, 395–399
effect on thermo-hydraulic performance, 393, 395
expert system, 406
fouling curves, 399
fouling data, 404
fouling model, 400–401
fouling monitoring, 405–406

[Fouling]
gas side fouling, 401
gas side fouling measuring devices, 404
vs heat transfer augmentation devices, 398
how fouling is dealt at design stage?, 405
instruments for monitoring of, 404
mechanisms
biological fouling, 403
chemical reaction fouling, 402
corrosion fouling, 402
particulate fouling, 401–402
precipitation fouling, 403
solidification fouling, 403–404
modes of fouling, 399
oversizing, 395, 405
parameters that influence fouling, 395–399
research in fouling, 405
stages of fouling, 399
TEMA fouling resistance values, 405–406
vs. type of heat exchanger
Fouling prevention and control (*see also* Fouling)
chemical cleaning, 410–412
by chemical additives, 416–417
foulant and common solvents, 411
solvent and compatible base metals, 411
cleaning techniques, 408
control of fouling from suspended solids, 417
measures to be taken at design stage, 407–408
mechanical cleaning,
off-line, 413–416
on-line, 409–410
Fracture mechanics, 932
Fracture toughness, 672
Freezing fouling (*see* Solidification fouling)
Fretting corrosion, 621
Functional requirements of materials,
brittle fracture, 671
corrosion resistance, 676–677
avoid these combinations, 676–677
favored combinations, 676
creep, 672–673
fabricability, 679
fatigue strength, 670–671
heat and corrosion, 676
resistance to temperature, 673–676
sources of material data, 677
strength, 670
toughness, 671–672
Furnace brazing,
atmospheres, 1008–1009
brazing furnaces, 1009
controlled atmosphere brazing, 1011
furnace heating, 1008
[Furnace brazing]
NOCOLOCK™ brazing, 1011–1017
procedure, 1010
vacuum brazing, 1011–1012
Furnace brazing of aluminum, 1016–1018

Galerkin method for regenerator design, 320
Galvanic cell, 580
Galvanic corrosion,
of aluminum, 771–772
area effect, 594
of brazed joint, 1034–1035
control,
in cooling water, 651
of copper, 784
description, 592
distance effect, 594
electromotive force series, 595
galvanic corrosion sources, 593
galvanic metals in sea water, 595
heat exchanger locations susceptible for, 593
magnitude, 593
of nickel, 802
of soldered joint, 1037
of stainless steels, 730
of titanium, 814
tools to determine the degree of, 595
types, 593
of zirconium, 823
Galvanic series of metals in sea water, 595
Galvanizing, 635
Gammascopy, 920
Gas tungsten arc welding of nickel, 808–809
Gas-gas heat exchanger, 18–19
Gasket materials for plate heat exchanger, 356
Gas-liquid heat exchanger, 16
General corrosion (*see* Uniform corrosion)
GEWA-T (Weilaand Werke) fins, 389
GEWA-TX fins, 389
GEWA-TXY fins, 389–390
Glass, 828–830
applications, 828
borosilicate glass, 829
composition, 829
demerits of glass material, 830
glass-lined steel, 829
heat exchangers, 829
hybrid heat exchangers, 829
mechanical properties, 829
properties, 828
resistance to chemicals, 829
Glass coil heat exchanger, 4

Graphite
drawbacks, 827
heat exchangers, 827–828
impervious graphite, 827
properties, 826–827
Grid baffle (*see* ROD baffle)
Grit cleaning of fouling, 415

Head designs
front head, 263
rear head, 263
shellside clearances, 263–265
TEMA designation for heads, 263
Heat capacity rate ratio, 30–32
Heat exchangers
choice for intended applications. 25
classification, 2–19
construction, 1
fabrication techniques, 24–25
fouling tendencies, 23
materials of construction, 20–22
maintenance aspects, 24
overall economy, 24
requirements, 25–26
selection criteria, 20–25
Heat exchanger design methodology,
computer aided thermal design, 138–140
overall structure, 139
of shell and tube exchanger, 140
subroutines, 139
corrosion allowance, 146–147
design considerations, 129
design problems
rating, 135, 137–138
sizing, 135–137, 138
design procedure, 132
fouling, 146
maldistribution, 146
performance failures, 145–146
pressure drop, 140
contraction loss coefficient, 141
expansion loss coefficient, 141
for compact heat exchangers, 143
due to flow turning and in headers, 143
in nozzles, 143–144
process specifications, 129
surface characteristics, 132
surface geometrical properties, 131–132
specification sheet,
for compact exchanger, 142
for shell and tube exchanger, 136
surface selection,
temperature fluid properties ratio method, 144
for gases, 144–145
for liquids, 145
for laminar flow, 144–145
for turbulent flow, 144–145
thermo-hydraulic design, 131–132
thermophysical fluid properties, 131
uncertainties in heat exchanger design,
additional pressure drop due to, 158
additional surface area required due to, 157
by Cho's method, 155–157
description, 149–154
determination of uncertainties, 154–157
Heat exchanger effectiveness, 30–31
Heat pipe exchangers, 342–343
Heat recovery system, 314
Heat transfer area, 288
Heat transfer augmentation (*see also* Heat transfer augmentation passive techniques)
application, 374
benefits, 374
enhancement techniques,
active techniques, 376–384
passive techniques, 384
friction factor, 385
major areas of applications, 390–391
pertinent problems, 385
fouling, 385
performance evaluation criteria, 386–388
testing methods, 385
phase change application, 388–390
air conditioning and refrigeration, 387–388
for single phase, 374
in laminar flow, 374
in turbulent flow, 374
Heat transfer augmentation passive techniques
additives for gases, 384
additives for liquids, 384
displaced enhancement devices, 380
extended surfaces, 376–380
rough surfaces, 379–380
surface tension devices, 383–384
swirl flow devices, 381–383
treated surfaces, 378–379
tube inserts, 380–381
Heat treatment of tube-to-tubesheet welding, 992–993
Heat wheel, 310
Helium mass spectrometer, 950
Helium mass spectrometer leak detection,
detector probe technique, 952
principle, 950–951
tracer probe method, 952
vacuum technique, 952

Helmhotz cavity resonator, 458–459
Herringbone trough pattern (*see* Plates)
HIC-tested A 516 steels, 660
High temperature attack, 620
High temperature resistant materials,
  alloying elements for, 674
  low alloy steels, 674
  material groups and service temperature, 674
  nickel base material, 675
  stainless steels, 674–675
  steels, 674–675
  tests to evaluate, 675–676
High theta plates, 359–360
Hitachi bent saw tooth fins, 389
Holographic interferometry, 934
Horizontal style plate, 361
Horizontal supports, 568
Hot blow, 306
Hot cracking
  of aluminium, 776
  chevron cracks, 705–706
  of copper, 793
  crater cracks, 706
  ductility dip cracking, 705
  factors responsible for, 700–702
  heat affected zone (HAZ) liquation cracking, 703–704
  microfissuring, 704
  of nickel, 797
  reheat cracking, 704–705
  solidification cracking, 702–703
  of super austenitic stainless steel, 764
  susceptible alloys, 702
  underclad cracking, 705
  weldability test, 706
Hot cracking of nickel, 807
Hot roll bonding, 842
Hot wall effect, 645
Huey test, 760
Humidity test, 1038
Hydraulic radius, 177, 317
Hydrodynamic mass (*see* Added mass)
Hydrogen assisted cracking (HAC), 656–657
Hydrogen attack, 677–679
Hydrogen cooling environments, 653
Hydraulic expansion
  by the bladder technique, 971
  by the O-ring technique, 971
Hydrogen
  effects on steel, 653
  sources of, in steel, 653–654
Hydrogen blistering, 620, 657–660
  correction of blisters, 660
[Hydrogen blistering]
  detection of blisters, 660
  susceptible materials, 657–660
Hydrogen embrittlement, 620, 656–657
  of tantalum, 825
  of titanium, 814–815
Hydrogen induced cracking
  avoiding, 693
  carbon equivalent to masses, 694–696
  preheating, 693–694
  sources, 692
  susceptible material, 692
Hydrogen induced cracking,
  prevention, 655–656
  of steels, 654–655
  testing specification, 660
Hydrogen sulfide
  in cooling water, 644
  stress cracking (HSCC), 620, 653, 656
Hydrostatic pressure testing of tubes, 690

Ideal j factor for shellside flow, 284
Identification of materials, 960
Image quality indicators (IQI), 916–917
Imaging plate, 920
Impact and fretting wear, 424, 461–462
Impingement protection, 249
Induced draft vs forced draft, 191–192
Industrial regenerators 338–343
Inhibitors, 416
  adsorption inhibitors, 893
  anodic inhibitors, 892–893
  cathodic inhibitors, 893
  copper inhibitors, 894
  descriptions, 630
  effectiveness of inhibitors, 894
  inhibitor evaluation, 894
  multicomponent systems, 893
  passivation inhibitors, 894
  precipitation inhibitors, 894
Inspection
  check list for components, 880–881
  definition, 878
  design and inspection, 878
  vs.examination, 878
  hold points and witness points, 882
  inspection guidelines, 879
  master traveller, 881
  objectives, 878
  scope for heat exchangers, 879
  third party inspection, 881–882
Instability, 425, 437
Integral roughness, 389

Integrity of vacuum furnaces, 1023
Intergranular corrosion,
of aluminum, 773
of copper, 784
description, 605
mechanism, 606
of nickel, 802–803
sensitization, 606
of stainless steels, 735–738
of superferritic stainless steel, 756–757
susceptible alloys, 605–606
test for detection of, 607
weld decay, 606
ISO 9000–1994 quality system
benefits, 786
contents of, 876–878
definition, 875
need for ISO 9000, 875–876
principles, 875
Internal micro fin tubes, 377
Inverse configuration, 42
Inverse solubility effects, 403
Iridium 194, 911
Iron and manganese bacteria, 623
Iron oxide removal, 421
Isotopes, 913

Jacketing (*see* Panelcoil heat exchanger)
j and f correlations
for bare tube bank, 193
for circular tube-fin arrangement, 194
for continuous fin on circular tube, 196–198
for flat tube array, 198
for louvred fin, 199–200
for offset strip fin, 198–199
for pin fin, 200–201
J factor (*see* Watanabe number)
J integral, 672
Jensen number, 364
Jet cleaning of fouling, 409
Joint categories, 504

K805 cladding alloy, 1036
Kirchoffs-Kelvin equation, 515
Knife line attack, 737

Labyrinth leakage, 336
Lace the tube bundle, 452
Lamella heat exchanger, 9–10
Lamellar tearing,
complementary information test for, 699–700
conditions that promote, 697–698
detection of, after welding, 700
[Lamellar tearing]
locations prone for, 698
prevention of, 698–699
Langelier saturation index (LSI), 652–653
Lap joint flange, 540
Larson-Miller parameter, 724
Laser scanner system, 920
Layer type dezincification, 607
Lead embrittlement of nickel welding, 807
Leak testing (LT),
bubble testing, 949
gas leak lake testing, 949
halogen diode detector testing, 949–950
helium mass spectrometer leak detection, 950–952
in-service examination of exchangers for leaks, 952
methods, 948–956
pressure change test, 949
purpose, 948
ultrasonic leak detection, 949
written procedure, 948
Lift force, 429
Lifting devices and attachments, 571
ligament efficiency, 523
Liquation cracking, 703 (*see also* Microfissuring)
of duplex stainless steel, 761
Liquid droplet impingement erosion, 609–610
Liquid-liquid heat exchanger, 16–17
Liquid penetrant inspection (PT),
acceptance standards, 903
applications, 899
approved material, 902
evaluation of indications, 902–903
excess penetrant removal, 902
limitations, 899
merits, 899
method
visible dye, 901
fluorescent dye, 901
penetrants, 900–902
application, 901–902
time, 901–902
post cleaning, 903
principle, 899
recent developments, 903
selection of developer, 901
standardization of light levels, 902
standards, 900
surface preparation, 902
test procedure, 901
written procedure, 900
LMTD, 22, 32, 36, 131, 269, 272, 274, 365
Local membrane stress, 500
Lock-in phenomenon, 429

Log mean temperature difference correction factor F, 22, 32–35
Logarithmic decrement of damping, 467
Longitudinal heat conduction effect on thermal effectiveness, 216–217
Longitudinal seams, 965
Longitudinal varestraint test, 706
Low alloy steels,
  classification, 714–715
  selection for pressure vessels, 713
Low carbon stainless steels, 726
Low theta plates, 359–360
LR stainless steels (*see* Low residual stainless steel),
LT (leak testing), 891

Macroorganisms, 403
Magnetic particle (MT) inspection
  acceptance standards, 909
  accessories, 909–910
  applications, 903–904
  demagnetization, 909
  equipment, 906
  evaluation of indications, 909
  examination coverage, 906
  formation of the particles pattern, 904
  inspection medium
    application, 908
  inspection method
    dry method, 908
    wet method, 908
  interpretation, 909
  limitations, 905
  magnetic particles, 908
  magnetising current, 905
  merits, 905
  magnetising technique, 906
  principle, 903
  record of test data, 909
  reference documents, 904
  surface preparation, 908–909
  test procedure, 904
  written procedure, 905
Manganese sulfides (MnS) inclusions, 597
Manipulative equipment, 997
Manual cleaning of fouling, 409
Martensitic stainless steel, 725
Mass velocity, 193
Material control, 866–867
Material procurement control, 866
Material selection (*see also* Functional requirements of materials)
  ASME code requirements, 669
  cost, 679–680
[Material selection]
  equipment design features, 680–682
  evaluation of material, 679
  failure modes in service, 680
  material tests, 679
  principle, 667–668
  for pressure boundary components, 683–684
  raw material forms, 682–684
    bolts and studs, 683
    castings, 682
    forgings, 682–683
    rods and bars, 683
  review of design, 668
  review of operating process, 668
  selection of material, 668–679
    baffles, 684
    shell, channel, covers, and bonnets, 684
    tubes, 684
    tubesheet, 684
Materials for heat exchanger construction (*see* Alloys for subzero temperatures; Aluminium and aluminium alloys; Austenitic stainless steel; Carbon steel; Cast iron; Ceramics; Copper and copper alloys; Duplex stainless steel; Ferritic stainless steel; Glass; Graphite; Low alloy steel; Martensitic stainless steel; Nickel and nickel alloys; Superaustenitic stainless steel; Superferritic stainless steel; Tantalum; Teflon; Titanium and titanium alloys; Zirconium)
Materials for hydrogen sulfide environments, 653
Maximum allowable working pressure (MAWP), 506
Mechanical cleaning of scales, 421
Mechanical design of shell and tube exchangers
  basics of mechanical design, 495–498
    design loadings, 497–498
    information required, 495–496
    mechanical design procedure, 497
    sequence of decisions, 496
  design of
    bolted flanged joints, 538–554
    cylinderical shell, 533–535
    expansion joints, 554–567
    heads/end closures, 535–538
    openings and nozzles, 565–567
    supports, 567–571
    Stress Analysis, 499
    tubesheet, 506–533
  design methods and criteria, 502–503
  key design terms, 505–506
  stress categories, 499–500
  stress classification, 500–502
  weld joint efficiencies, 504
Membrane stresses, 502

Mercurous nitrate test, 620, 790
Mesroc® cleaning system (*see* Brush and cage system)
Metal coordinators, 402, 417
Metal ion concentration cell, 603
Microbiologically influenced corrosion (MIC)
  categories of
    aerobic, 624
    anaerobic, 624
  control of, 625–626
  of copper, 624–625
  description, 622–623
  failure analyses, 626
  of industrial alloys, 624
  of mild steel, 624
  sources of microorganisms, 623, 644
  of stainless steels and weldments, 624
  susceptible metals, 623
  of titanium, 625, 815
Microfocus X-rays source, 920
Minimum free flow area, 179, 180, 182, 183
Minimum nozzle size, 249
Minimum thickness for heads, 536–537
Modal mass, 434
Mode shape, 433, 435
Modern ASTM A 387 steels, 722
Modine solder, 1028
Modular construction, 24, 349
Modular-block cylindrical exchanger, 828
Monogram, stamping of, 963
Multilayer clad aluminum brazing sheet, 1036
Multipass exchangers, 16
Multiple segmental baffles, 454
Munter wheel (*see* Heat wheel)

NACE Standard MR-01-75, 656
NACE Standard TM-02-84, 660
National standards
  British standards(BSI) 1993, 486
  DIN, German standards, 486
  ISO 1993 standards, 487
  Japanese industrial standards (JIS), 486
Natural frequencies
  of tube bundles, 463–466
  of U-tube, 466
Nelson curves, 678
NESTS™ baffle, 455
Net effective pressure, 512
Neutron radiography, 920
Nickel alloy cladding, 846
Nickel and nickel alloy designation
  INCO alloy C-280, 801
  INCO alloy G-3, 801
[Nickel and nickel alloy designation]
  INCO alloy HX, 801
  INCOLOY alloy 800, 801–802
  INCOLOY alloy 800HT, 802
  INCOLOY alloy 825, 802
  INCONEL alloy 600, 800
  INCONEL alloy 601, 800
  INCONEL alloy 617, 800
  INCONEL alloy 625, 800–801
  INCONEL alloy 718, 801
  INCONEL alloy X-750, 801
  Monel 400, 799
  Monel alloy R-405, 799
  Monel alloy 450, 799
  Monel alloy K-500, 799
  nickel 200, 798
  nickel 201, 798–799
  nickel-chromium alloys, 799–801
  nickel-copper alloys, 799
  nickel-iron-chromium alloys, 801–802
  nickel, pure nickel, 798–799
Nickel and nickel base alloys
  ASTM specification for tube, 804
  classification, 798–802
  favorable properties, 797–798
  forms of corrosion, 802, 804
  low temperature applications, 798
  magnetic properties, 802
  nominal composition of
    INCO alloys, 800
    INCONEL, 800
    nickel-copper alloys, 799
    pure nickel, 799
  product forms, 802
  product forms and specification, 802–803
Nickel welding
  considerations while welding, 805–808
  methods, 808–809
  post weld heat treatment, 809
  of precipitation hardenable alloys, 805
  of solid solution strengthened alloys, 804
Nickel flashing, 1020
Nickel steel, 9%
  edge preparation, 839
  electrodes, 839
  forming, 839
  guidelines for welding of, 839–840
  merits, 838
  post weld heat treatment, 840
  surface preparation, 839
  welding, 839
  welding problem, 839–840
Nil-ductility transition temperature (NDTT), 672

Niobium (columbium in US), 606
Nitrogen added stainless steels, 726
Nitrogen blanketing, 404
Nonconformance reports (NCR), 867
Noncorrosive flux brazing, 1011–1017
Nondestructive evaluation (*see* Nondestructive testing)
Nondestructive examination, 867
Nondestructive testing (NDT), 891
  acceptance criteria, 892
  AWS symbol for NDT, 894
  of brazed joint, 1025
  capabilities, 892
  cost, 892
  inspection equipment, 893
  methods (*see* Acoustic emission testing; Acoustical holography; Eddy current testing; Leak testing; Liquid penetrant inspection; Magnetic particle inspection; Radiographic testing; Ultrasonic testing; Visual examination)
  personnel, 892
  reference codes and standards, 893
    ASME Code Section V, 893
  selection, 892–893
    and limitations, 894
  soldered joint, 106
  written procedures, 894
Nonwetting surfaces, 397
Normal solubility, 403
No-tubes-in window design (NTIW), 452
Nozzles, 249–250, 565–567
  design loads, 567–568
  reinforcements, 566
Nuclear grade (NG) stainless steels, 735
Number of transfer units, 30, 32
Number of tube passes, 247–249
Numerical finite difference method, 320

On-line removal of iron deposits, 421
Openings, 565
  reinforcement pad, 565
    air-soap solution testing of, 565
    tell-tale hole in, 565
Operating pressure, 22, 506
Operating temperature, 22, 506
Operation cryogenics, 840
Operations list
  for drilling of tubesheets, 871
  for fixed tubesheet tube bundle assembly, 871
  for long seams/circular seams, 870
  for nozzles on shell/dish, 870–871
  for shell preparation and forming, 870
Organization, 866
Outside diameter of the tubes
Oven soldering (*see* Furnace soldering)
Overall conductance, 210
Overall heat transfer coefficient, 288
  in clean condition, 394
  in fouled conditions, 394
Overbrazing, 1023
Over design, 630
Oxidizing agents, 416
Oxyacetylene welding of Nickel, 809
Oxygen
  concentration cell, 603
  in cooling water, 643
  ingress, 397

Panelcoil heat exchanger, 6–9
Parallel flow exchanger, 13–14
Parameter, R_p, 526
Parameter Z, 523
Parameters X, 523
Parameters X_m, 526
Partial braze joint (underbrazing), 1023
Pass arrangements for flow through tubes, 247–249
Passing brushes through tubes, 413
Passivation, 586, 637, 649, 738–739
Passivity, 586
Peak amplitude of tube response, 434
Peak stress, 502
Penetrants
  fluorescent, 901
  visible, 901
pH effect on,
  corrosion, 588, 645
  erosion of tube inlet, 652
Pickling, 738
Pipes and tubes,
  ASME code requirements, 688–689
  ASTM specification for ferrous tubes, 691
  defect detection, 689–690
  mill scale, 691
  selection for heat exchangers, 689
  specification for tubes, 689
  standard testing for tubes, 690
  tubing requirements, 689
Pit producers, 598
Pitch ratio, 430, 440
Pitting corrosion
  of aluminum, 772
  of austenitic stainless steels, 730–731
  condition for pit initiation, 598–599
  in cooling water, 651
  of copper, 784
  critical pitting corrosion temperature (CCPT), 602
  description, 595

[Pitting corrosion]
detection of pits, 600
of duplex stainless steel, 760
gauging resistance to pitting, 602
mechanism, 599
morphology of pits, 600
of passive alloys, 596–599
parameters responsible for, 596
pitting index number (PRE_N), 602
pitting potential, 599–600
prevention, 600–601
of superaustenitic stainless steel, 763
of superferritic stainless steel, 756
of titanium, 815
of zirconium, 823
Pitting factor, 600
Pitting index, 602, 731
Pitting potential, 599–600
Pitting resistance equivalent number (PRE or PRE_N), 602
Plastic coatings, 635
Plates (*see also* Plate heat exchanger)
Chevron plate pattern, 355
intermating troughs, 354–355
plate materials, 355
plate pattern, 353
Plate and frame heat exchanger (*see* Plate heat exchanger)
Platecoils (*see* Panelcoil heat exchanger)
Plate-fin heat exchanger
advantages, 171
applications, 171, 172
corrugation selection, 176
economics, 172
features, 169–170
fin geometry selection
herringbone fin, 175
louvre fins, 175
offset strip fin (OSF), 174–175
pin fins, 176
plain fin, 172–173
plain-perforated fin, 173–174
flow arrangements, 172
limitations, 171–172
manufacture and inspection, 177
materials of construction, 177
mechanical design, 177
size, 171
Plate heat exchangers (*see also* Plates)
all welded type, 358
applications not recommended for, 359
benefits, 351–353
brazed type, 357
[Plate heat exchangers]
comparison with shell and tube exchanger, 353
connections, 356
connector plates, 356
construction, 347–349
corrosion, 366–367
description, 4–5
Diabon F graphite type, 358
double-wall type, 358
flow-flex tubular type, 357
flow patterns and pass arrangement, 349
fouling, 23–24, 367
frame, 356
gasket, 356
glue-free gaskets type, 358
limitations, 23, 367
nozzles, 356
plate, 353–355
semi-welded type, 357
specification Sheet, 370
standard performance limits, 351
thermo-hydraulic fundamentals, 361–364
heat transfer correlation, 362–363
pressure drop, 363–364
thermal design methods
ε-NTU approach, 365–366
LMTD method, 365
tie bolts, 356
useful data, 351
where to use, 358–359
wide gap type, 357
Plate steels
ASTM specifications, 686–687
classification, 685–688
quality description, 685
Plug type dezincification, 607
Pneumatic test
of heat exchanger, 995–996
of tubes, 690
Pneumatic testing of exchanger, 996
Polarization
diagrams, 585
measurement, 585–586
Polymerization (*see* Chemical reaction fouling)
Polythionic acid cracking, 617
Polythionic acid stress corrosion cracking (PASCC), 617, 734
Poor braze fillets, 1023
POP-A-PLUG, 613
Porcelain enamelled flat plate heat exchanger, 342
Porosity of regenerator matrix, 317
Post cleaning inspection, 410

Post weld heat treatment (PWHT) of welded joints,
ASME code requirement, 855
annealing, 853–854
defects due heat treatment, 858
effectiveness of heat treatment, 858
effects on steel quality, 854–855
heat treatment charts, 855–856
methods of PWHT, 858
NDT after PWHT, 859
normalizing, 854
objectives, 853
PWHT cycle, 856–857
quality control during, 857–858
quench and temper, 854
solution heat treatment, 854
stress relieving, 854
welding related failures, 858
PRE$_N$
austenitic stainless steel, 602, 731
duplex stainless steel, 602, 768
ferritic stainless steel, 602, 763
6% Mo superaustenitic stainless steel, 602, 763
Precracked Charpy V-notch test, 672
Pressure drop, 363–364
in tubes and pipes, 287–288
Pressure vessel steels for sour environments, 660
Primary stress, 500
bending, 500
membrane, 500
Process control, examination and inspection, 867
Prod magnetization, 906
Prod spacing, 906
PT (liquid penetrant inspection), 891
Pull through gauge, 965
PWHT, 992–993, 997, 1000
of cladding, 850
of dished ends, 1000
of shells, 997
tube-to-tubsheet welding, 992–993

Quality control and quality assurance, 861, 864–866
aims of, 864
ASME code, 868
auditing, 874
authorized inspector, 868
defined, 864
documentation, 874–875
documents of the quality system
check list, 872–873
quality control plan (QCP), 869
operation process sheet, 869–873
economics of quality assurance, 873–874
management, 863
[Quality control and quality assurance]
manual, 866, 868–869
review and evaluation procedures, 874
retention of records, 868
system elements, 866–868
Quenched and tempered steels
compositions and properties, 716–717
description, 715
joint design, 717
postweld heat treatment, 717
preheat, 717
stress relief cracking, 718
weldability, 717
welding processes, 717

Radiators
fin density vs. fouling, 165–166
mechanically bonded core, 167–168
1-row, 166–167
soldered core, 168
Radiation recuperators, 342
Radiation sources, 910–911
Radiator manufacture by soldering, 1028–1029
Radiography, 910
Radiographic testing (RT)
acceptance criteria, 919
application, 910
density of radiograph, 916
documentation, 919
examination of radiographs, 917
full radiography, 913–914
gamma rays technique, 913
general procedure, 912
identification marks, 913
image quality indicators (IQI), 916–917
location markers, 913
merits and limitations, 911
panoramic radiography with isotopes, 913
principle, 910
processing of x-rays films, 913
quality, 915–919
radiation sources, 911
recent developments in, 919–920
reference documents, 912
requirements, 912
safety, 912
sensitivity, 915
spot radiography, 915
surface preparation, 913
of weldments of pressure vessels, 913
x-rays and gamma rays, 911
x-rays clues to welding discontinuities, 917–919
written procedure, 911–912

Radioscopy, 920
Rating of a compact exchanger, 206–211
  Shah's method for rating, 211
Rating of heat exchangers
  of compact heat exchanger, 135
  inputs, 135
  of shell and tube heat exchanger, 135
  steps in rating problem, 137–138
    LMTD method, 138
    ε-NTU method, 137
Reduced frequency, 430
Reduced period, 320, 329
Reducing agents, 416
Regenerator thermal design
  correlation for j and f, 319–320
  design methodology, 334–335
  designation of regenerators, 326
  fluid bypass and carryover, 334
  Galerkin method for, 329–330
  heat capacity rate ratio, 324
  heat transfer, 325
  influence of longitudinal heat conduction, 332–333
    Romie's solution, 333
  methods, 321
    Coppage and London model, 321–325
    ε-NTUo method, 321–329
    Λ-Π method, 329–331
  Rozelos method, 331
  parameter definitions, 325–326
  solution techniques, 321
  surface geometrical properties, 317–319
  thermal effectiveness, 321
  thermo-hydraulic fundamentals
Regenerator mechanical design, 335–337
  drive for the rotor, 337
  seal design for rotary regenerator, 336
  thermal distortion and Transients, 337
Regenerators (*see also* Fixed bed regenerator; Rotary regenerator; Regenerator thermal design)
  construction material, 315
  corrosion resistance, 315
  description, 10–11, 158
  fixed bed, 307–309
  fuel savings due to preheating combustion air, 305
  gas turbine cycle with regeneration, 304
  life, 315
  recuperator, 306
  regeneration principle, 303
  rotary type, 309–314
  strength and stability, 315
  in thermodynamic systems, 314
  for waste heat recovery application, 304–305
Regenerative burner, 340
Reheat cracking, 724
Remote field slit eddy current testing, 945–947
Repassivation potential, 600
Resonance, 425
Reverse flange, 540
Reversing flow, 413
Reynolds number, 193, 210
Ring flange, 540
ROD baffle, 241, 297, 454
  heat exchanger design, 297–299
Roll bending machine, 997
Rolling-in process,
  amount of thinning of tubes, 974
  basic rolling process, 971
  criterion for rolling adequacy, 972
  expanding in double tubesheets, 978
  factors affecting rolling process, 976
  joint cleanliness, 975
  joint reinforcements by annular grooves, 978
  leak testing, 980
  leak tightness of rolled joints, 977
  length of tube expansion, 974
  mock-up test, 974
  optimum degree of expansion, 972
  rolling equipment, 971
  sequence of tube expansion, 976
  size of tube holes, 976
  step rolling, 978
  strength of rolled joints, 976–977
  tube end growth during rolling, 975
Rolling of shell sections, 961–963
Root fluxes to protect stainless steel, 750
Rotary regenerator (*see also* Regenerator),
  comparison with recuperators, 313–314
  desirable characteristics for the matrix, 312–313
  drive, 310
  for gas turbine applications, 310
  merits, 313
  operating temperature and pressure, 310
  salient features, 309
  size, 311
  surface geometry, 310
  total heat regenerators, 313
  types, 310
    Ljugstrom type, 309
    Rothemuhle type, 308, 309
Rothemuhle regenerative air heater, 11, 308
RT (radiographic testing), 891
Ryznar stability index, 642

Salt concentration cell, 582
Salt spray (fog) test, 1038
Scrapped surface exchangers, 20

Sea-cure, 754
Sealing devices, 265
Sealing strips, 265
Secondary stress, 501
Selective leaching (*see* Dealloying)
Self cleaning fluid bed exchangers, 415–416
Sensitization
  of austenitic stainless steels, 735–736, 748, 841
  of ferritic stainless steels, 757
Sequestrant, 403, 416
Sequestrant and chelate chemicals, 418
Service oriented crack, 707
Shell, 247
  longitudinal stress, 520–521
Shell and tube heat exchanger (*see also* Disk and doughnut heat exchanger; ROD baffle heat exchanger)
  baffles, 234–242
  Bell-Delaware method for rating, 275–280
  classification, 252–255
  constructional details, 229
  design methodology, 265–290
  crossflow velocity, 290–291
  expert system, 299
  heads, 263
  shellside clearances, 263–265
  shellside flow pattern, 265–269
  shellside performance, 269
  shell types, 256–262
  sizing, 270–274
  tube arrangement, 233–234
  tube bundle, 246–247
  tubes, 229–233
  tubesheet, 243–246
Shellside passes, 249
Shellside performance, 269
Shellside flow streams, 265–269
Shellside flow patterns,
  A stream, 266–267
  B stream, 267
  C stream, 267
  E stream, 267
  flow fractions for each stream, 267–269
  F stream, 267
Shellside performance, 269
Shell-to-baffle clearance, 264
Single wall single image technique, 913
Sizing of heat exchanger,
  of compact heat exchanger, 137, 212–214
  and optimization, 137
  sensitivity analysis, 137
  of shell and tube heat exchanger, 137
  size of a heat exchanger, 137
[Sizing of heat exchanger]
  steps in sizing problem, 138
    LMTD method, 138
  ε-NTU method, 138
Sizing of shell and tube heat exchanger,
  Bell's method for approximate sizing, 271–274
  calculation of surface area, 274
  design considerations, 271
  determination of shell size and tube length, 274
  estimation of overall heat transfer coefficient, 273
  guidelines, 270
  method to determine number of shells, 273
  specify the right heat exchanger, 270–271
  thermal design procedure, 271
Skin effect, 943–944
Slenderness ratio, 448
Sludge fluidizers, 419
Solder bloom corrosion, 1037
Solders, 1027–1028
Soldering of heat exchangers (*see also* Radiator manufacture by soldering: Solders; Soldering processes; Ultrasonic soldering of aluminum heat exchangers)
  of aluminum coils by flux soldering, 1029
  cleaning and descaling, 1028
  destructive testing, 1034
  discontinuities, 1034
  elements of soldering, 1026–1028
  flux residue removal, 1029
  inspection of solderd joint, 1033–1034
  joint design, 1026
  non destructive testing of soldered joint, 1034
  soldering fluxes, 1028
  tube joint, 1026
  tube-to-header solder joint, 1027
Soldering processes
  dip soldering, 1028
  furnace soldering, 1028
  torch soldering, 1028
  ultrasonic soldering, 1028, 1029–1033
Soot blowing, 410
Sopt Varestraint test, 706
Sound hologram, 933
Sour environments (*see* Hydrogen sulfide environments)
Spacers, 265
Spacers, 265
Specific pressure drop, 364
Speckle interferometry, 934
Spiral plate heat exchanger
  advantages, 369–370
  applications
  construction material, 368

[Spiral plate heat exchanger]
description, 5, 367
flow arrangements, 368
limitations, 23, 370
mechanical design, 369
thermal design, 368–369
SPIRELF system, 415
Split-flow exchanger (*see* TEMA G shell),
Sponge rubber balls cleaning system, 413–414
Spot radiography of cladding, 852
Sprayed-on epoxy coatings, 617
Stabilisation, 606
Stabilizers, 417
Stagewise inspection chart, 863
Stainless steels (*see* Austenitic; Duplex; Ferritic; Martensitic; Precipitation hardening (PH))
ASTM specification, 725
classification, 724–725
definition, 724
designations, 725
selection, 725
Stainless steel strip cladding
consideration for, 845
control of ferrite, 845
dilution, 845
heat treatment considerations, 846
inspection, 846
welder qualification, 845–846
Standards
API standard 660, 489
definition, 485
EJMA standard, 489
heat exchange institute standards, 489
TEMA standards, 487–489
types, 486–487
Standing waves frequency, 443
Stanton number, 193
Stationary regenerator (*see* Fixed bed regenerator)
Steam injection cleaning of fouling, 406
Steam side erosion of condenser, 568
Steels
carbon steel, 708
grades of steel, 708
high strength low alloy steel (HSLA), 708
low alloy steels, 708–709
Stiff borescope, 898
Storage type regenerators, 303
Strain age cracking of nickel weldments, 808
Strain on the outer fibres while forming, 963
Stress category concept,
in BS 5500, 524–525
in CODAP formula, 523
in TEMA, 518
Stress corrosion cracking (SCC)
of aluminum, 772–773
avoiding, 619–620
classification, 617
in cooling water, 652
conditions responsible for, 617–618
of copper, 788–789
description, 614–615
detection, 618
heat exchanger components susceptible to, 616–617
of nickel, 804
susceptible alloys and the environment, 618
of stainless steels, 733–735
test for, 620
theory of, 618–619
thin walled expansion joint, 616, 617
titanium, 815
tube-to-tubesheet expanded joint, 617
U-bend, 617
welded joints, 618
zirconium, 824
Stress relief cracking (SRC),
Stress-number of cycles (S-N) curve, 670
Strip baffles, 452
Structural leakage, 336
Structural mass, 433
Sulfate reducing bacteria (SRB), 623
Sulfide shape control, 698
Sulfur embrittlement of nickel welding, 807
Sulfur oxidizing bacteria, 623
Sulfureous acid cracking, 617
Superaustenitic stainless steel (*see also* 4.5% Mo superaustenitic steels; 6% Mo superaustenitic stainless steel), 762–765
applications, 764
arc welding filler metals, 764–765
corrosion resistance, 763
corrosion resistance of welds, 765–766
hot cracking, 764
molybdenum microsegregation, 764
postweld heat treatment, 765
precipitation of intermetallic phases, 764
welding problems, 764
welding processes, 765
Superferritic stainless steel
alloy composition, 754
applications, 754
corrosion resistance, 756–757
ductile-to-brittle transition temperature (DBTT), 756
fabricability, 757
PWHT, 758
weldability problems, 757
welding, 757–758

Supported tubesheet, 507
Suppression of standing waves
antivibration baffles (AVB), 457–458
detuning, 455
fin barriers, 455
helical spacers, 455
irregular lateral spacing of tubes, 455
porous baffle, 458
removal of tubes, 455
resonators, 455, 457
solid baffle, 457
surface modification, 455
Surface geometrical parameters
hydraulic diameter, 177
surface area density, 178
Surface geometrical properties, 209
Surface oxide
on copper, 793
removal on nickel, 805
Surfactant, 416
SWAAT test, 1038
Symmetry property, 41

Tack tubes, 975
Tafel equation, 585
Tantalum
corrosion resistance, 825
cost, 826
heat transfer, 826
hydrogen embrittlement, 825
performance vs. other materials, 826
product forms, 826
resistance to chemicals, 825–826
welding, 826
Taprogge system, 413
Teflon
in chemical processing industry, 830
design considerations, 831
favorable properties, 830
fluoropolymer resin development, 831
heat exchanger fabrication, 831
reactor coils, 831
shell and tube heat exchanger, 830–831
size and construction, 831
Telltale hole in clad plate, 852
TEMA X shell, 16, 79, 256, 262
TEMA designation of shells
comparison of various shells, 262
E shell, 256
F shell, 256–259
G shell, 259
H shell, 259
J shell, 259
[TEMA designation of shells]
K shell, 259
X shell, 262
TEMA standards, 16, 25, 45, 63, 134, 226, 227, 229, 248, 252, 255, 258, 259, 260, 280, 399, 424, 429, 434, 438, 440, 441, 442, 449, 457, 459, 460, 462, 478, 479, 501, 507, 517, 529, 536, 537, 542, 554, 559, 563, 600, 909, 987, 991, 995, 1002, 1005, 1006, 1018, 1022, 1024
Temper embrittlement, 707, 721–723
Temperature approach, 43
Temperature approach, in plate heat exchanger, 352
Modular construction, 349
Temperature cross, 43–45
for TEMA shells, 45
Temperature driving force, 22
Temperature effect
cooling water corrosion, 645
corrosion, 587
fouling, 396, 418
scaling, 419
Temperature meet, 438
Temperature program, 22
Tests to determine susceptibility to cracking, 706
Thermal cleaning of fouling, 410
Thermal effectiveness, 23
charts, 38–41
Thermal mixing, 360–361
Thermal relation formulas and charts for
counterflow, 46, 47, 50
crossflow
mixed-mixed, 46, 47
Schedwill's formula for N rows, 48, 50
single or multiple rows, 46, 48, 58
1 row-1 pass, 58, 59
2 rows-1 pass, 58, 60
3 rows-1 pass, 58, 61
4 rows-1 pass, 58, 61
tube rows in multipass arrangement, 52, 53, 55–57, 58, 63
2 rows-2 passes, 53, 64
3 rows-3 passes, 53, 65
4 tube rows, 4 passes, 55, 66
5 tube rows, 5 passes, 55, 67
6 tube rows, 6 passes, 57, 68
4 rows-2 pass, 57, 70
6 rows-2 pass, 57, 58, 71
unmixed-mixed, 46, 53, 54, 55, 56
unmixed-unmixed, 46, 51, 52
multipass heat exchangers, 81, 93–117
crossflow exchangers, 88–117
E shells in series,
2 x E_{1-2} 120, 126

[Thermal relation formulas and charts for]
3 x E_{1-2}, 121, 126
4 x E_{1-2}, 122, 126
5 x E_{1-2}, 123, 126
6 x E_{1-2}, 124, 126
N passes, 85, 88
two passes, 85
parallel flow, 45, 47, 48, 49
TEMA shells
E shell, 63
E_{1-2}, 73, 74
E_{1-3} counterflow arrangement, 77, 78
E_{1-3} parallel flow arrangement, 77
E_{1-4}, 73, 75
E_{1-5} counterflow arrangement, 79, 80
$E_{1\text{-}N\text{ even}}$, 73
even number tube passes, 63
multipassing on the tubeside, 63
odd number tube passes, 69
F shell, 69, 72
G shell, 72, 76
G_{1-1} 81, 82
G_{1-2} 81, 83
G_{1-4} 125, 126
H Shell, 76
H_{2-1}, 84, 86
H_{1-2}, 84, 85, 87
J shell, 76, 77
J_{1-1}, 88, 90
J_{1-2}, 88, 91
J_{1-4}, 89, 92
$J_{1\text{-}N\text{ even}}$, 89
X shell, 79
Thermal resistance monitors, 404
Thermal shock test, 1038
Thermal shock treatments, 625
Thermal wheel (*see* Heat wheel)
Thermoexcel fins, 390
Thermo-hydraulic fundamentals,
capacity rate, 27
convection resistance, 27
energy balance equation, 29
heat transfer analysis methods, 29–36
heat transfer analysis method,
functional relationship, 36
LMTD method, 32–35
ε-NTU method, 30–31
P-NTU$_1$ method, 31–32
ω-P method, 35–36
overall conductance equation, 28
thermal circuit, 27
thermal circuit variables, 27
thermal resistance due to fouling, 27
[Thermo-hydraulic fundamentals]
thermal resistance of the separating wall, 27–28
true mean temperature difference, 27
Thiobacillus thiooxidants, 625
Threshold agents, 403, 417
Threshold chemicals, 418
Threshold velocity, 612
Tie rods, 265
Titanium
ASTM/ASME specifications for mill products, 811
alloy specification, 810
fouling, 816
grades and alloys, 810–811
as PHE, 817
properties, 809–810
in refinery and chemical processing, 816–817
in surface condensers, 816
thermal performance, 816
Titanium corrosion resistance,
forms of corrosion, 813–816
hydrogen embrittlement, 814–815
resistance to chemicals and solutions, 814
surface oxide film, 811, 813
Titanium welding
to dissimilar metals, 817
filler metal, 819
heat treatment, 822
gas tungsten arc welding, 819–820
narrow groove welding, 820
gas shielding, 820
in process quality control, 821–822
in open air environment, 820
manufacturing facilities, 817–818
MIG welding, 820
precleaning and surface preparation, 818
shielding gases, 817
weld defects, 822
welding methods, 817
weldability considerations, 817
Tomography, 919
Total quality management (TQM), 876
Total resistance to heat transfer, 393
Toughness tests, 671–672
Toxic and lethal fluids, 252
Trace elements, 397
Trane bent fins, 389
Transformation property, 42
Transport processes during brazing, 1018
Tube
classification, 230
count, 232–233
diameter, 230–231
duplex tubes, 232

[Tube]
layout pattern, 233–234
length, 231–232
low finned tubes, 231
means of fabrication, 232
number of tubes, 232
pitch, 233
wall thickness, 231
types, 230
U-bend requirements, 233
wall thickness, 231
Tube arrangement,
layout, 233–234
tube pitch, 233
Tube bundle,
bundle Weight, 246
outer tube limit, 247
sealing devices, 246
spacers, 246
tie rods, 246
Tube bundle assembly, 967–969
Tube expansion, 970–980
Tube-fin heat exchanger,
applications, 162
considerations for, 161
construction materials, 163–164
with continuous fins, 164–168
enhanced fin geometry, 163
fin height, 162–163
individually finned tubes, 162
performance factors, 186–192
plain circular fins, 162
surface selection, 168–169
tube layout, 164
fouling of, 168–169
manufacturing considerations, 169
quantitative considerations, 169
selection, 160
Tube layout patterns, 430, 434
Tube longitudinal stress, 520–521
Tube material to resist fouling, 396–397
Tubesheet, 243–246
demerits
double tubesheets, 243–245
conventional, 243–245
integral, 245
tube-to-tubesheet attachment, 243
Tubesheet bending moment, 514
Tubesheet design
assumptions, 509–510
basis of fixed tubesheet design, 512
boundary restraint, 510–511
conventional double tubesheets design, 532–533
[Tubesheet design]
curved tubesheets, 531–532
effective elastic constants, 511
fixed tubesheet design,
as per ASME code, 522
CODAP, 522–523
BS 5500, 523–524
comparison of thickness formulas, 525
flanged tubesheets, 529
of floating head exchangers,
as per BS 5500, 526–528
as per CODAP, 526–528
fundamentals, 506–512
mean ligament efficiency, 511–512
modeling of the tube bundle, 510
modeling of the tube sheet, 510
as per TEMA, 515–522
rectangular tubesheet design, 529–531
thin circular plate on elastic foundation, 512
tubesheet connection with shell/channel, 506–507
U-Tube tubesheet formula,
as per BS 5500, 528
as per CODAP, 528
as per ASME Code, 528
Tubesheet drilling, 966–967
Tubesheet to shell welding, 969–970
Tubeside heat transfer coefficient, 284–287
Colburn equation, 287
Dittus-Boelter equation, 287
Sider-Tate equation, 286–287
Tube-to-baffle hole clearance, 264
Tube-to-tubesheet joining methods
brazing, 991
explosive joining, 971
hydraulic expansion, 971
rolling-in process, 971
welding, 980–990
Tube-to-tubesheet joint welding
heat treatment, 992–993
joint configuration, 981
internal bore welding, 981
leak testing, 990
methods, 980
radiographic inspection, 991
seal welded joints, 984–985
strength welded joints, 985–986
welded mock-ups, 990
welding before expanding or after, 987–988
welding process, 981–984
Tubular heat exchangers, 178–184
Turbining, 409
Turbo-B (Wolverine) fins, 390
Turbo-V fins, 390

Turbulators for fire tube boilers, 381
Turbulent buffeting
  acceptance criteria, 436
  description, 435
  frequency, 435
  as random phenomenon, 435–436
Turbulence, 434–435
Turbulent buffeting frequency, 425, 435, 446
Twin-plate heat exchanger, 357
Twisted tape insert, 381
Type 321 stainless steel, 606
Type 347 stainless steel, 606
Type II MnS inclusions, 655

U-bend support, 452
Ultrasonic calculator, 930
Ultrasonic plate tester, 924
Ultrasonic soldering pot, 1031
Ultrasonic soldering of aluminum heat exchangers
  Alcoa 571 process, 1030–1033
  materials, 1029–1030
  Reynolds process, 1033
Ultrasonic testing (UT)
  acceptance criteria, 930
  advantages, 925
  angle beam technique, 927
  applications, 923–924
  A-scan presentation, 927
  calibration, 932
  code coverage, 925
  couplant, 928
  defect location, 930
  examination coverage, 930
  examination procedure, 926–928
  limitations, 926
  probes, 928
  pulse-echo technique, 926
  recent developments, 933
  reference blocks, 931
  sensitivity and resolution, 930
  surface preparation, 927–928
  test method, 921, 923
  of welds, 928–930
  written procedure, 924–925
Ultraviolet radiation, 403
Uniform corrosion
  of aluminum, 771
  atmospheric corrosion, 590
  in cooling water, 651
  control, 590
  determination, 592
  forms, 590
  material selection for, 592
[Uniform corrosion]
  rating of metals subject to, 592
  of titanium, 813
Unfired systems, 19–20
Unified numbering system (UNS), 779
Unmixed fluid stream, definition of, 14
Unsupported tubesheet, 507
Upstream filtration, 403, 413, 625
Use of inserts, 415
Utilization factor, 330

Vacuum brazing of aluminum, 1017–1019
Vacuum brazing furnaces
  hot wall design, 1009
    cold wall design, 1009, 1019
    semicontinuous, 1010
Vacuum brazing sheet, 1019
Vacuum induction melting (VIM), 709, 754
Vacuum oxygen decarburization (VOD), 709, 754
Vapor phase organic cleaning of fouling, 412
Varestraint test, 706
Vehicle durability test, 1038
Velocity dependent damping, 437
Velocity effect
  on corrosion, 588, 645–646
  on fouling, 396
Vertical style plate, 361
Vertical vessel supports, 570–571
Vibration test, 1037
Video microscopes, 899
Viscosity correction factor, 284
Visual examination (VT)
  combined with computers, 899
  direct techniques, 895
  during welding, 897–898
  equipment, 896–897
  NDT of raw materials, 897–898
  optical Instruments, 898–899
  prerequisites, 896
  principle, 895
  reference document, 896
  remote techniques, 896
  written procedure, 896
Volume goodness factor, 387–388
Von Karman streets, 426, 428
Vortex flow direct contact heat exchanger, 339
Vortex shedding
  avoiding resonance, 430
  criteria to avoid, 432–433
  lock-in, 429
  response due to, 433–434
  single tube, 428

[Vortex shedding]
Strouhal number, 428–429
for tube arrays, 430–432
tube bundle, 429–430
Vortex shedding frequency, 428, 432, 446
VT (visual examination), 981

Washboard pattern (*see* Intermating troughs)
Watanabe number, 732
Water jet cleaning of scales, 421
Water treatment, 649
Wavy fin (*see* Herringbone fin), 175
surface geometrical relations, 177–178
Weiland flattened fins, 389
Weld decay, 606
Weld defects
acceptance levels, 891
causes of discontinuities, 888
discontinuities, 888
faults in fusion welds, 889–891
types and their significance, 888–891
Weld dilution while cladding, 844
Weld neck integral flange, 540
Weld overlaying, 843
Weld surfacing (*see* Weld overlaying)
Weldability problems (*see* Cold cracking; Hot cracking)
Welded joints, 503–505
Welded joint efficiencies, 504
Welding design
ASME code, Section IX, 884–885
grouping of base metals, 885
P numbers, 885
grouping of filler metals, 886
A numbers, 886
F numbers, 886
procedure qualification record, 887
qualifications, 886
quality, 883–884
[Welding design]
selection of consumables, 885
specifications, 886–887
symbols for welding, 884
variables affecting welding quality, 884
welder requalification, 887
Welding engineer data sheet No. 493, 1032
Welding of nozzles to shell, 966
Welding of shell, 964–965
Welding parameters
essential variables, 886
nonessential variables, 886
supplementary essential variables, 886
Welding positions and qualifications, 888
Welding quality assurance, 867
Welding related failures, 708
Welding variables (*see* Welding parameters)
Winged spacers, 265
Wisconcian process, 304
Working pressure (*see* Operating pressure)
Working temperature (*see* Operating temperature)
Wulff process, 304

X factor (*see* Watanabe number)

Yoke magnetization, 906

Zick stress, 570
Zircaloys, 823
Zirconium
alloy classification, 823
applications, 823
corrosion resistance, 823
limitations, 823
product forms, 823
resistance to chemicals, 823
welding, 824
with dissimilar metals, 825

Copyrighted Material

about the book . . .

This comprehensive reference covers all the important aspects of heat exchangers (HEs)—their design and modes of operation—and practical, large-scale applications in process, power, petroleum, transport, air conditioning, refrigeration, cryogenics, heat recovery, energy, and other industries.

Reflecting the author's extensive practical experience in industry, the ***Heat Exchanger Design Handbook***…discusses standard construction, thermo-hydraulic fundamentals and thermal design of HEs—tubular, extended surface, plate, and both rotary matrix and fixed regenerators…explains algorithms and subalgorithms derived from heat transfer and geometry optimization modules…showcases the tremendous **recent advances** in plate exchanger designs—brazed-plate, flow-flex tubular, wide gap, twin plate, double wall, graphite, and welded—and associated improvements…addresses **global and national** standards and codes…analyzes flow-induced vibration and mechanical design of shell-and-tube HEs…explores a wide spectrum of materials for HEs, corrosion behavior, and optimal fabrication methods…illustrates techniques for fabrication of shell-and-tube HEs, as well as brazing and soldering compact HEs…examines quality assurance issues for HE manufacture and NDT techniques…considers operational problems such as corrosion and fouling…and more.

Abundantly illustrated with over 400 drawings, diagrams, tables, and equations, the ***Heat Exchanger Design Handbook*** is an excellent resource for mechanical, chemical, and petrochemical engineers; process equipment and pressure vessel designers; and upper-level undergraduate and graduate students in these disciplines.

about the author . . .

T. KUPPAN is the Deputy Chief Mechanical Engineer at Indian Railways, Madras, India. The author of an article in the American Society of Mechanical Engineers' *Journal of Pressure Vessel Technology*, he has extensive experience in the design, fabrication, and performance evaluation of many types of heat exchangers. Mr. Kuppan received the B.E. (Hons) degree (1980) in mechanical engineering from Madras University, India, and the M.Tech. degree (1982) in production engineering from the Indian Institute of Technology, Madras.

Printed in the United States of America

ISBN: 0—8247—9787—6

MARCEL DEKKER, INC. NEW YORK • BASEL

ISBN:0-8247-9787-6

9 780824 797874 90000

Copyrighted Material